LINEAR COLLIDER STUDIES

Steinar Stapnes, CERN, Geneva, Switzerland
The Linear Collider Collaboration [1].

Abstract

Two major Linear Collider (LC) accelerator studies are currently on-going. The International Linear Collider (ILC) based on Super Conducting RF (SCRF) technology aims for implementation during the next 10-15 years strongly motivated by the recent Higgs discovery, while the Compact Linear Collider (CLIC), based on X-band normal conducting accelerator structures and a drive beam to provide optimised RF power to the main beams, has a post-LHC time perspective and aims towards energy frontier physics at higher energies. While the basic RF technologies are different leading to different optimisation of bunch lengths, charges and repetitions rates, many key technical challenges are in common. Several major parts of the designs, as sources, damping rings, beam delivery and final focus systems to mention a few, are covered by common or connected studies. The physics potential and main detector issues, as well as possible implementation stages are being studied in parallel for both machines. A summary of recent progress and status of a selected set of studies are given below.

ILC AND CLIC PROJECT OVERVIEW

The key parameters for ILC and CLIC at their design energies are shown in table 1. The ILC design [2] is compatible with later upgrades to 1 TeV, while a 3 TeV CLIC will be built with initial stages at ~500 GeV and ~1.5 TeV [3]. The exact energy stages are in the process of being re-evaluated and changed taking into account the Higgs energy scale now known and other developments.

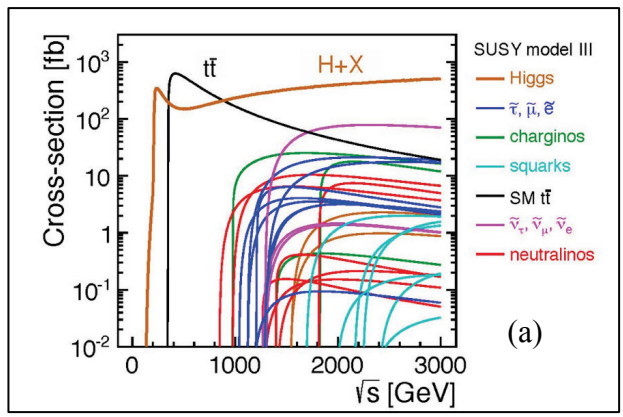
Table 1: ILC and CLIC main parameters

Parameter	ILC 500 GeV	CLIC 3 TeV
Luminosity [cm^{-2} s^{-1}]	1.8 x 10^{34}	5.9 x 10^{34*}
Accelerator length [km]	31	48.3
Acc. gradient loaded [MV/m]	31.5	100
Bunch charge [10^9 e]	20	3.72
Bunch separation [ns]	554	0.5
Number of bunches	1312	312
Repetition rate [Hz]	5	50
H./V. norm. emittance [10^{-6}/10^{-9}]	10 / 35	0.66 / 20
H./V. IP beam size [nm]	474 / 5.9	40 / 1

* Total, luminosity within 1% of peak: 58% and 32%

Physics Motivation for Future LCs

Future LCs can deliver high luminosity (~10^{34} $cm^{-2}s^{-1}$) e+e- collisions from ~100 GeV to 3 TeV. The natural first stage, at or above the 350 GeV top-pair-production threshold, gives access to precision Higgs physics through the Higgs-strahlung and WW-fusion production processes, providing absolute values of Higgs couplings to both fermions and bosons. This stage also addresses precision top physics [3]. ILC is technically mature and can provide access to very precise and model independent measurements in these areas relatively quickly. The potential of providing unique information about New Physics through such measurements [2], overlapping with and complementing LHC high luminosity running on a similar timescale, provides a strong motivation for ILC.



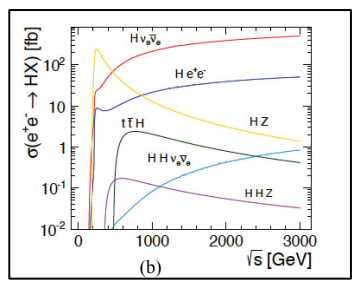


Figure 1: a) Cross-section for various physics processes at a LC as function of CoM energy. The Higgs and top studies are known opportunities, while various type of Beyond the Standard Model processes (a SUSY model in this example) are currently still speculations; b) Various types of Higgs production processes become available as the CoM energy increases, showing that slightly above 500 GeV new channels can provide important additional information.

Further LC stages open the energy frontier in earnest, potentially allowing for the discovery and direct access to New Physics phenomena as illustrated in figure 1. This stage also gives access to additional Higgs properties, such as the top-Yukawa coupling, the Higgs potential and rare Higgs decay branching ratios. LC energies of 3 TeV as aimed for by CLIC enlarges the physics potential even further, covering the complete scope for precision

Copyright © 2014 CC-BY-3.0 and by the respective authors

ISBN 978-3-95450-142-7

COMMISSIONING OF THE LOW-ENERGY PART OF LINAC4

A.M. Lombardi, CERN, Geneva, Switzerland

Abstract

The Linac4 front-end (3MeV) was first commissioned in a dedicated test stand and then moved to its final position in the Linac4 tunnel. Accelerating cavities will be added progressively over two years to allow the characterisation of the beam with a dedicated measurement line at several energy stages (3,12,30,50, 100 and finally 160MeV). This paper reports about the progress and the commissioning experience up to today.

INTRODUCTION

Linac4 is a 160 MeV H^- linear accelerator presently under construction at CERN. It will replace the present 50 MeV proton Linac2 as injector of the CERN PS Booster, as a first step of the LHC Injector Upgrade project. A sketch of Linac4 is shown in Fig. 1 and a detailed description of the layout and beam dynamics can be found in [1,2]

The pre-injector includes a source followed by a Low Energy Beam Transport at 45 keV, a Radio Frequency Quadrupole which accelerates the beam to 3MeV and a Medium Energy Beam Transport line (MEBT). The MEBT, 3.6 m in length, houses a fast chopper with the purpose of removing selected micro-bunches in the 352 MHz sequence and therefore avoid losses at capture in the CERN PSB (1MHz). Presently the preferred scheme envisages to chop out 133 bunches over 352 with a resulting average current reduced by 40%. The beam is then further accelerated to 50 MeV by a conventional Drift Tube Linac (DTL) equipped with Permanent Magnet Quadrupoles (PMQ), to 100 MeV by a Cell-Coupled Drift Tube Linac and to 160 MeV by a Pi-mode structure. The focusing after 100 MeV is provided by Electromagntic Quadrupoles (EMQ) whereas between 50 and 100 MeV by a combination of PMQs and EMQs.

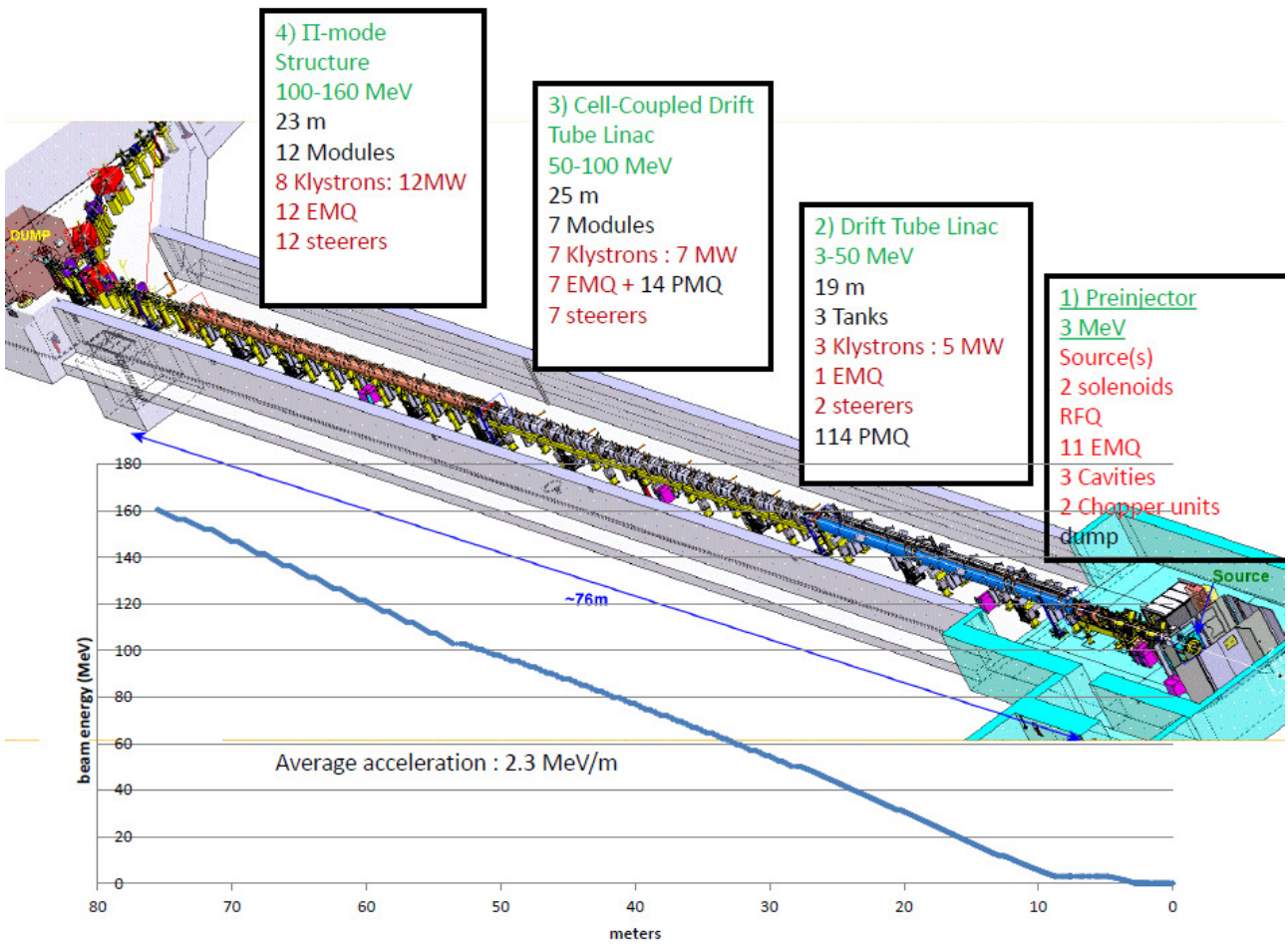


Figure 1: Sketch of Linac4.

Copyright © 2014 CC-BY-3.0 and by the respective authors

ISBN 978-3-95450-142-7

EARLY COMMISSIONING EXPERIENCE AND FUTURE PLANS FOR THE 12 GeV CONTINUOUS ELECTRON BEAM ACCELERATOR FACILITY*

M. Spata#, Jefferson Lab, Newport News, VA 23606, USA

Abstract

Jefferson Lab has recently completed the accelerator portion of the 12 GeV Upgrade for the Continuous Electron Beam Accelerator Facility. All 52 SRF cryomodules have been commissioned and operated with beam. The initial beam transport goals of demonstrating 2.2 GeV per pass, greater than 6 GeV in 3 passes to an existing experimental facility and greater than 10 GeV in 5-1/2 passes have all been accomplished. These results along with future plans to commission the remaining beamlines and to increase the performance of the accelerator to achieve reliable, robust and efficient operations at 12 GeV are presented.

INTRODUCTION

The Continuous Electron Beam Accelerator Facility (CEBAF) was initially constructed as a 5-pass 4 GeV CW machine consisting of two 1497 MHz SRF linacs connected by nine 180 degree recirculation arcs (Fig. 1). The accelerator in that configuration had the capability to provide interleaved 499 MHz beams to three experimental halls (A, B, C) with independent control of the beam intensity, energy and polarization. The North (NL) and South (SL) linacs each consisted of 20 SRF cryomodules containing eight 5-cell cavities with an average operating gradient of 5 MV/m to achieve a design energy gain per linac of 400 MeV. These so-called C20 cryomodules provided a nominal 20 MeV/cryomodule energy gain.

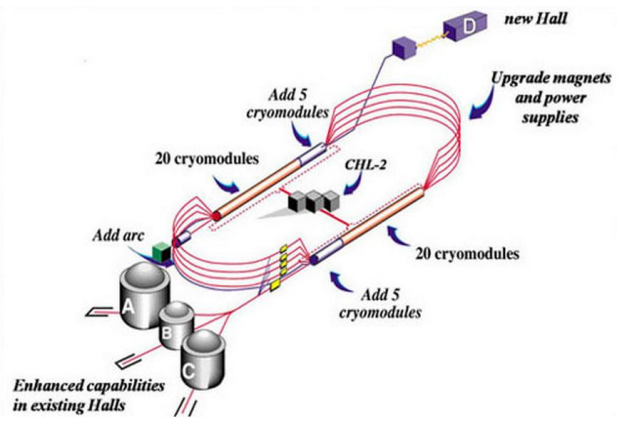


Figure 1: Schematic representation of the CEBAF accelerator showing the original configuration along with the major components of the upgrade.

*Work supported by DOE contract DOE-AC05-06OR2317 under which Jefferson Science Associates, LLC operates Jefferson Lab.
#spata@jlab.org

The original CEBAF Injector used 2-1/4 cryomodules to provide 45 MeV beam for injection into the NL. The beam was then extracted after one through five transits around the accelerator using transverse deflecting 499 MHz normal conducting RF Separator cavities [1] to selectively and simultaneously direct beams to the three experimental user facilities designated Halls A, B and C.

A cryomodule refurbishment program [2] was started in 2006 and completed in 2009 with the goal of increasing the top energy of the linacs from 400 MeV to 600 MeV. Ten of the 40 original CEBAF cryomodules with the lowest overall energy reach were sequentially removed from the accelerator to be reworked at Jefferson Lab's SRF Institute. The cryomodules were disassembled and the cavities cleaned using advanced processing techniques to eliminate field emission. The original fundamental power couplers and ceramic window designs were also modified to improve performance. The goal was to increase the average operational cavity gradient from the initial 5 MV/m to 12.5 MV/m or 50 MeV/cryomodule energy gain. The so-called C50 program was successful in enabling the facility to routinely operate at 5-pass energies approaching 6 GeV in support of the nuclear physics program.

The CEBAF 12 GeV Upgrade [3,4] is a major project funded by the Department of Energy's Office of Nuclear Physics. The project scope doubles the energy of the CEBAF accelerator by adding 5 high-performance cryomodules and their associated RF power systems in each linac, expanding the capacity of the 2k Central Helium Liquefier (CHL) to manage the additional heat load, upgrading the magnets and power supplies for the existing nine recirculation arcs, adding a 10th recirculation arc and power supply to transport the beam a 6th time in the NL to a new beamline and fourth experimental Hall D. Upgrades to the Extraction System, Beamline Instrumentation, Safety Systems and High Level Applications were also part of the accelerator scope for the 12 GeV Upgrade.

CRYOMODULE COMMISSIONING

The ten new C100 cryomodules, as well as the existing C20 and C50 cryomodules, were all commissioned between May 2013 and November 2013. The maximum accelerating voltage, cavity Q_0's and a field emission survey were recorded for each of the cavities in the system. The design specifications [5] for the C100 cryomodules are shown in Table 1. The slot length includes the warm girder assemblies between cryomodules and represents the center-to-center distance between the quadrupole magnets that make up the linac lattice. To meet the 12 GeV energy performance criteria each of the new cryomodules must make 98 MeV. The

Copyright © 2014 CC-BY-3.0 and by the respective authors

ISBN 978-3-95450-142-7

OPTIMIZING RF LINACS AS DRIVERS FOR INVERSE COMPTON SOURCES: THE ELI-NP CASE

C. Vaccarezza, D. Alesini, M. Bellaveglia, R. Boni, E. Chiadroni, G. Di Pirro, M. Ferrario, A. Gallo, G. Gatti, A. Ghigo, B. Spataro, P. Tomassini, INFN-LNF, Frascati, Italy
A. Bacci, I. Drebot, D. Palmer, V. Petrillo, A. R. Rossi, L. Serafini, , INFN-MI, Milano, Italy
A. Giribono, A. Mostacci, L. Palumbo, University of Rome La Sapienza , Italy
A. Cianchi, University of Rome Tor Vergata, Italy
C. Ronsivalle, ENEA-CRE, Frascati, Italy

Abstract

The design guide-lines of RF Linacs to fulfil the requirements of high spectral density Inverse Compton Sources for the photo-nuclear science are mostly taken from the expertise coming from high brightness electron Linacs driving X-ray FEL's. The main difference is the quest for maximum phase space density (instead of peak brightness), but many common issues and techniques are exploited, in order to achieve an optimum design and lay-out for the machine. A relevant example in this field is the design of the hybrid C-band multi-bunch RF Linacs for the ELI-NP Gamma Beam System, aiming at improving by two orders of magnitude the present state of the art in spectral density available for the gamma-ray beam produced.

INTRODUCTION

In the last two decades the crucial role played by the high brightness electron beams in the frontier fields of radiation generation and advanced acceleration schemes has been largely established. The production of high quality phase space electron beams has shown to be essential for the coherent X-rays generation in the FEL's as well to provide the matching conditions for the novel acceleration schemes based on high gradient wakefields and for the realization of bright Gamma-ray Compton sources. The characteristic brightness parameter B can be expressed as:

$$B = \frac{2I}{\epsilon_n^2} \tag{1}$$

where I (A) is the beam current and ε_n is the normalized emittance in the transverse phase space, hence high brightness means high current and a small footprint in the transverse phase space. A big effort has been devoted in these years to develop fruitful techniques of phase space control and manipulation of intense electron sources based on RF guns, equipped with laser driven photocathodes, followed by one or two accelerating sections (photoinjectors). The proper shaping of the laser pulse hitting the photocathode has been intensely studied together with the apposite properties of accelerating and focusing field in the gun and in the downstream linac sections as well.

In the first section of this paper the main aspects of the high brightness beam production in a photoinjector will be described while in the following section the phase space density optimization will be described for the ELI case. In the third section the ELI-NP Gamma Beam System design will be illustrated.

THE HIGH BRIGHTNESS BEAM EXPERIENCE

The Photoinjector Optimization

A simple emittance compensation scheme [1] based on a focusing solenoid at the exit of the RF gun, can be used in photoinjectors to control emittance growth due the space charge effects while, from the invariant envelope theory [2], a proper matching of the transverse space of the electron beam injected in the downstream accelerating sections (booster) after the gun exit can help to control the transverse emittance oscillations during the acceleration. It is shown in the paper that in the space charge dominated regime these oscillations are due to the mismatch between the space charge correlated forces and the rf focusing gradient, and to dump these oscillations the beam has to be injected into the booster under the invariant envelope condition, i.e. at the laminar envelope waist occurrence ($\sigma' = 0$), while the following condition has to be fulfilled for the accelerating gradient E_{acc}:

$$\gamma' = \frac{2}{\sigma}\sqrt{\frac{\hat{I}}{2I_0\gamma}}, \tag{2}$$

where $\gamma' \approx 2E_{acc}$, σ is the transverse rms beam size, $\hat{I}$ is the peak current, I_o=17kA is the Alfven current, and γ is the beam energy. In this way the damping of the emittance oscillations is provided but its final value at the linac exit depends on the phase of the plasma oscillations at the entrance of the booster that has to be located at a relative emittance maximum occurrence [3] in order to shift the following emittance minimum at higher energy where, taking advantage of the additional emittance compensation due to the booster, the emittance can be frozen at its lowest value at the exit of the linac. Under the conditions of invariant envelope and proper phasing of space charge oscillations [4] the final emittance is almost compensated down to the thermal emittance value given by cathode emission with an expected emittance

Copyright © 2014 CC-BY-3.0 and by the respective authors

ISBN 978-3-95450-142-7

GENERATION AND ACCELERATION OF LOW-EMITTANCE, HIGH-CURRENT ELECTRON BEAMS FOR SUPERKEKB

M. Yoshida#, N. Iida, S. Kazama, T. Natsui, Y. Ogawa, S. Ohsawa, H. Sugimoto, L. Zang, X. Zhou,
High Energy Accelerator Research Organization, 1-1 Oho, Tsukuba, Ibaraki, 305-0801, Japan
D. Sato, Tokyo Institute of Technology, 2-12-1, Ookayama, Meguro-ku, Tokyo, 152-8550, Japan

Abstract

KEK e-/e+ linac is now in a final stage of upgrade for SuperKEKB. One of the key issues is to stably generate and accelerate a low-emittance, high charge electron beam for SuperKEKB (a couple of single-bunched beams with a charge of 5 nC and a normalized emittance of 20 mm-mrad each).

REQUIREMENTS

The injector upgrade as shown in Fig. 2 is required for the SuperKEKB injection due to the small dynamic aperture and the short life time of the ring. The bunch charge must increase up to 5 times higher than KEKB and the lower normalized emittance is required around 20 mm mrad. Further the small energy spread of around 0.1 % is required in the condition of higher bunch charge for the synchrotron injection of the HER of the SuperKEKB.

Table 1: Required Parameters for SuperKEKB

	KEKB(e^+/e^-)	SuperKEKB(e^+/e^-)
Beam Energy	3.5 / 8.0 GeV	4.0 / 7.0 GeV
Bumch Charge	1.0 / 1.0 nC	4.0 / 5.0 nC
Normalized transverse Emittance (1σ)	2100 / 300 mmmrad	6 / 20 mm mrad
Energy Spread	0.1 %	0.1 %

PHOTOCATHODE RF-GUN

The initial emittance at the electron gun is determined by the space charge effect and the RF emittance. The photocathode RF-Gun is required to generate such low emittance of lower than 10 mm mrad for the high charge electron bunch of 5 nC. From the analytical calculation, the bunch length must be longer than 20 ps to obtain the charge of 5 nC and the transverse emittance of 10 mm mrad.

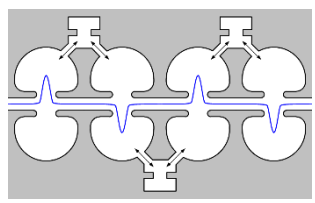
This requirement of the electron bunch charge for the SuperKEKB is slightly higher than the standard S-band RF-Gun. Further it is better to use same RF gun for the positron production with the primary electron bunch charge of 10 nC.

Thus we developed the new advanced RF gun with the following specifications for the long time stable operation of the SuperKEKB injection:

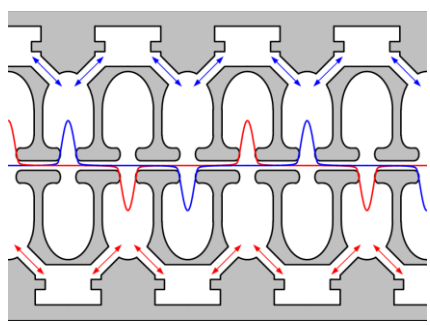
- The quasi-traveling wave side coupled cavities for the strong focusing electric field to keep the beam side against the space charge.
- The reasonable lower maximum surface electric field of 120 MV/m.
- The metal composite cathode (IrCe) with the long lifetime and reasonable high quantum efficiency.
- The ytterbium based laser system with the temporal manipulation to get the minimum energy spread.

QTW-SIDE COUPLED RF GUN CAVITY

The strong focussing field is generated by the annular coupled cavities with the narrow acceleration gap as the disk and washer (DAW) or side coupled cavities narrow acceleration gap. Conversely the narrow gap causes a long drift space as Fig.1 (a). We solved this problem to use two staggered standing wave cavities with π/2 phase difference as shown in Fig.1 (b). This acceleration field is similar to the traveling wave from the accelerated beam. We call this cavity as the quasi-traveling wave (QTW)[1]. This quasi-traveling wave RF-Gun can realize to obtain both of the higher acceleration voltage and the strong focussing field.



(a) Normal side coupled cavities.



(b) Quasi traveling wave side coupled cavities.

Figure 1: Structure of the quasi traveling wave cavity.

#mitsuhiro.yoshida@kek.jp

Copyright © 2014 CC-BY-3.0 and by the respective authors

ISBN 978-3-95450-142-7

CURRENT STATUS OF PAL-XFEL*

I. S. Ko†, J.-H. Han on behalf of the PAL-XFEL project team
Pohang Accelerator Laboratory (PAL), Pohang, 790-784, Republic of Korea

Abstract

The PAL-XFEL project aims to produce 0.1 nm coherent X-ray laser to photon beam users. In order to produce such photons, there are 10 GeV electron linac based on S-band normal conducting accelerating structures and a 150 m long out-vacuum undulator system. The project was already started in April 2011, and the 1.1 km long building is expected to be completed by December 2014. The injector test facility (ITF) which is for a test of the first 139 MeV section of the main linac has been installed and is in normal operation at the extension of the PLS linac building. In this paper, we introduce the project in general, a brief summary of site preparation and building construction, beam test results of ITF, and test results of subsystems produced by domestic manufacturers

PROJECT OVERVIEW

The Pohang Accelerator Laboratory X-ray Free-Electron Laser (PAL-XFEL) project was started in 2011. This project aims at the generation of X-ray FEL radiation in a range of 0.1 to 10 nm for users [1, 2]. The machine consists of a 10 GeV electron linac and five undulator beamlines (see Fig. 1). The linac is based on the normal-conducting S-band technology, which has been used for the 3 GeV full energy injector linac of PLS-II, the 3rd generation light source at PAL, over 20 years [3]. As Phase-1 of PAL-XFEL, one hard X-ray undulator beamline with two experiment stations and one soft X-ray undulator beamline with one experiment station are under preparation. Both undulator systems are variable-gap, out-vacuum type.

The building is under construction and to be ready by December 2014. Accelerator components will be installed from January 2015 over the year. The layout of the PAL-XFEL linear accelerator and undulator lines is shown in Fig. 2. Experiment beamline components will be installed during the same period. The machine is capable of 60 Hz operation with a single bunch initially. Main parameters of the first Phase of PAL-XFEL are summarized in Table 1. Upgrade to a 120 Hz repetition rate as well as two micro-bunches is foreseen as the next phase. A fast kicker to divide electron pulses into the two undulator beamlines is considered as future upgrade.

Accelerator commissioning will be started in winter 2015. Beam commissioning will be carried out at a repetition rate of 10 Hz for the first year of operation mainly due to the operation budget. First FEL generation is foreseen in early summer 2016. First experiment using FEL beam will be possible in summer 2016.

* Work supported by The Ministry of Science, ICT and Future Planning of the Korean Government
† isko@postech.ac.kr

Table 1: Main Parameters of PAL-XFEL Phase I

FEL wavelength	
hard X-ray	0.1 - 0.06 nm
soft X-ray	3 - 1 nm
Electron beam energy	
hard X-ray	4 - 10 GeV
soft X-ray	3.15 GeV
Bunch charge	200 pC
Repetition rate	60 Hz
# of bunches per RF pulse	1
Gun type	S-band photocathode gun
Linac type	S-band normal conducting
Linac hall length	716 m
Beam transport line	57 m
Number of beamline	
hard X-ray	1
soft X-ray	1
Undulator type	out-vacuum
Undulator hall length	
hard X-ray	246 m
soft X-ray	125 m
Number of experiment station	
hard X-ray	2
soft X-ray	1
XFEL beamline hall length	
hard X-ray	60 m
soft X-ray	74 m
Total building length	1110 m

BUILDING CONSTRUCTION

The building construction was started in autumn 2012. The 1.1 km long new machine is being built on the northern hill of the PAL campus (see Fig. 3). Soil on the site was removed until 56 m altitude from the sea level. Most of the building lies on the sedimentary bedrock. For the area where the bedrock does not reach the altitude, soft X-ray experiment hall area, soil was removed and the empty volume was replace with hard concrete.

2 m thick concrete floor was constructed for the linac and undulator tunnel area. Linac tunnel wall and roof is 2 m thick for radiation safety. Possible radiation effect was studied and checked that the residential area is safe from the radiation produced by PAL-XFEL [4]. Construction of the Iron frames for the outside building is recently finished. Flat panels are being attached to the frame. Six utility buildings are under construction along the southern side of the main building. The building construction including utilities will be ready by December 2014.

Copyright © 2014 CC-BY-3.0 and by the respective authors

STATUS OF SUPERCONDUCTING ELECTRON LINAC DRIVER FOR RARE ION BEAM PRODUCTION AT TRIUMF

R.E Laxdal, F. Ames, R.A. Baartman, I. Bylinskii, Y.C. Chao, D. Dale, K. Fong, E. Guetre, P. Kolb, S.R. Koscielniak, A. Koveshnikov, M. Laverty, Y. Ma, M. Marchetto, L. Merminga, A.K. Mitra, N. Muller, R. Nagimov, T. Planche, W.R. Rawnsley, V.A. Verzilov, Z. Yao, Q. Zheng, V. Zvyagintsev, TRIUMF, Vancouver

Abstract

A MW class cw superconducting electron linac is being installed at TRIUMF as a driver for radioactive beam production through photo-fission. The ARIEL e-linac will house five 1.3GHz nine-cell cavities in three cryomodules and accelerate up to 10mA of electrons to 50MeV. A first phase of installation will see three cavities in two cryomodules installed by the end of 2014. The injector cryomodule has been installed with cryogenic, rf and beam acceleration tests completed. The second cryomodule is installed and being prepared for first tests. The linac status is reported.

INTRODUCTION

The ARIEL project [1] will allow a three-fold increase in the RIB delivery hours for the existing ISAC I & II experimental facilities. In brief the project consists of augmenting the present 500MeV (50kW) proton driver beam from the cyclotron and associated ISAC target stations with the addition of a new electron linac driver of 50MeV (0.5MW) and a second 500MeV (50kW) proton beam driver from the cyclotron and associated two new target stations and low energy RIB delivery systems. A first stage of the ARIEL installation including a 30MeV portion of the e-Linac and electron beamlines plus new ARIEL building and infrastructure is now nearing completion. The second phase encompassing the upgrade of the e-Linac to full energy, new target stations new proton beamline and low energy RIB beamlines is now under fund request adjudication.

Accelerated electrons can be used to generate RIBs via the photo-fission process [2]. The electrons are slowed either in the target material itself or in an upstream converter material to generate bremsstrahlung photons that produce fission in the actinide target material. The fission production resonance is centered near an incident photon energy of 15 MeV such that the production yield saturates around an electron energy of 50MeV. A beam current of 10mA at 50MeV is required to produce the goal rates of 10^{13} fissions/sec in an actinide target of sufficient density. This sets the operating boundary envelope for the completed electron linac.

The electron linac is housed in a pre-existing shielded experimental hall adjacent to the TRIUMF 500MeV cyclotron that has been re-purposed as an accelerator vault. The e-linac is being installed in a staged way with stages shown schematically in Fig. 1.

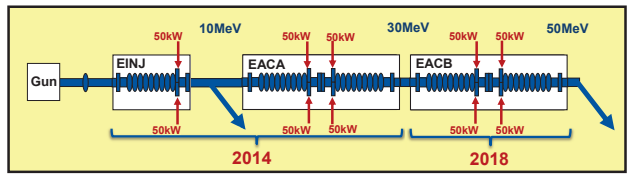


Figure 1: The stages of the e-Linac project.

A first phase consisting of a 300kV 16mA electron gun, an injector cryomodule, ICM, containing one 1.3GHz nine-cell cavity and an accelerating cryomodule, ACM1, containing two 1.3GHz nine-cell cavities plus associated beamlines is now installed and is in various stages of commissioning. This first phase is designed to accelerate cw up to 10mA of electrons at 30MeV but the initial beam dumps and production targets will only be compatible with 100kW operation. A second phase, dependent on funding, will see the addition of a second accelerating module and a ramp up in beam intensity to the full 50MeV 0.5MW capability.

ARIEL E-LINAC DESIGN

An rf frequency of 1.3GHz is chosen to take advantage of the considerable global design effort at this frequency both for pulsed machines (ILC) but also for cw ERL applications [KEK, Cornell, BerlinPro]. The linac architecture was determined by the choice of final cw beam power and the available commercial cw rf couplers at the design rf frequency of 1.3GHz. The CPI produced coupler developed with Cornell for the ERL injector cryomodule is capable of operation at 50kW cw. The cavity design allows two CPI couplers per cavity arranged symmetrically around one end delivering a total of 100kW of beam loaded power. This sets a maximum gradient per cavity at 10MV/m. A total of five cavities are required to reach 50MeV and 0.5MW beam power. It is our intention to install a future ERL ring with injection and extraction between 5-10MeV and so a single cavity off-line injector cryomodule was chosen plus two 2-cavity accelerating modules. The electron hall is shown in Fig. 2 as it would appear at the end of Phase II.

Electron Gun

The electron source [3] provides electron bunches with charge up to 15.4 pC at a repetition frequency of 650 MHz. The main components of the source are a gridded dispenser cathode in a SF_6 filled vessel, and an in-air high

Copyright © 2014 CC-BY-3.0 and by the respective authors

ISBN 978-3-95450-142-7

SINGLE-KNOB BEAM LINE FOR TRANSVERSE EMITTANCE PARTITIONING

C. Xiao, L. Groening, O.K Kester, H. Leibrock, M. Maier, and P. Rottländer,
GSI, Darmstadt, Germany
M. Chung, Ulsan National Institute of Science and Technology, Ulsan, Republic of Korea

Abstract

Flat beams feature unequal emittances in the horizontal and vertical phase space. Such beams were created successfully in electron machines by applying effective stand-alone solenoid fringe fields in the electron gun. Extension of this method to ion beams was proposed conceptually. This contribution is on the decoupling capabilities of an ion beam emittance transfer line. The proposed beam line provides a single-knob-tool to partition the horizontal and vertical rms emittances, while keeping the product of the two emittances constant as well as the transverse rms Twiss parameters ($\alpha_{x,y}$ and $\beta_{x,y}$) in both planes. It is shown that this single knob is the solenoid field strength, and now we fully understand the decoupling features.

INTRODUCTION

Beams provided from linear accelerator are generally round, and the horizontal and vertical emittances are quite equal. However, the transverse acceptance of subsequent rings might be flat. For instance, the multi-turn injection schemes using orbit bumps in one plane impose flat injection acceptances. Round-to-flat transformation requires a change of the beam eigen-emittances by a non-symplectic transformation [1].

Such a transformation can be performed by placing a charge state stripper inside a longitudinal field region as proposed in [2]. Inside such a solenoidal stripper, the transverse inter-plane correlations are created non-symplectically. Afterwards they are removed symplectically with three skew quadrupoles. A set-up providing round-to-flat transformation is shown in Fig. 1. Such a solenoidal stripper is proposed to be integrated into the existing charge state stripping and separating beam line of the GSI UNILAC [3].

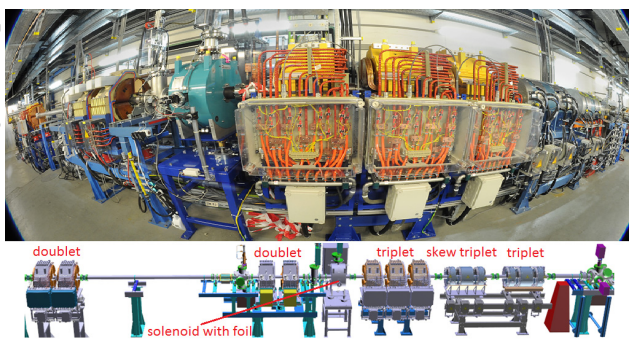


Figure 1: Emittance transfer experiment (EMTEX) beam line for demonstration of transverse rms emittance transfer.

BASIC MATHEMATICAL FOUNDATION

The four-dimensional symmetric beam matrix

$$C = \begin{bmatrix} \langle xx \rangle & \langle xx' \rangle & \langle xy \rangle & \langle xy' \rangle \\ \langle x'x \rangle & \langle x'x' \rangle & \langle x'y \rangle & \langle x'y' \rangle \\ \langle yx \rangle & \langle yx' \rangle & \langle yy \rangle & \langle yy' \rangle \\ \langle y'x \rangle & \langle y'x' \rangle & \langle y'y \rangle & \langle y'y' \rangle \end{bmatrix}. \quad (1)$$

contains ten unique elements, four of which describe the coupling. If at least one of the elements of the off-diagonal sub-matrix is non-zero, the beam is x-y coupled. The four-dimensional rms emittance ε_{4d} is the square root of the determinant of C, and the projected beam rms emittances ε_x and ε_y are the square roots of the determinants of the on-diagonal sub-matrices. Diagonalization of the beam matrix yields the eigen-emittances ε_1 and ε_2, and the transverse eigen-emittances are calculated as [4]:

$$\varepsilon_1 = \frac{1}{2}\sqrt{-tr[(CJ)^2] - \sqrt{tr^2[(CJ)^2] - 16|C|}}, \quad (2)$$

$$\varepsilon_2 = \frac{1}{2}\sqrt{-tr[(CJ)^2] + \sqrt{tr^2[(CJ)]^2 - 16|C|}}. \quad (3)$$

The four-dimensional matrix J is the skew-symmetric matrix with non-zero entries on the block diagonal of form:

$$J = \begin{bmatrix} 0 & 1 & 0 & 0 \\ -1 & 0 & 0 & 0 \\ 0 & 0 & 0 & 1 \\ 0 & 0 & -1 & 0 \end{bmatrix}. \quad (4)$$

Any symplectic transformation M obeys

$$M^T J M = J. \quad (5)$$

Eigen-emittances are invariant under symplectic transformations, and the transverse eigen-emittances are equal to the transverse rms emittances when inter-plane correlations are zero.

STRIPPING INSIDE A SOLENOID

Stripping inside a solenoid is fundamentally different from stripping between two solenoids due to the longitudinal magnetic field component and the fringe fields. In case of pure transverse field components (dipoles, quadrupoles, n-poles) there is equivalence between stripping inside this magnet and stripping between two such magnets of half lengths.

Copyright © 2014 CC-BY-3.0 and by the respective authors

MODEL AND BEAM BASED SETUP PROCEDURES FOR A HIGH POWER HADRON SUPERCONDUCTING LINAC

A. Shishlo#, ORNL, Oak Ridge, TN 37831, USA

Abstract

This presentation will review methods for experimental determination of optimal operational set points in a multi-cavity superconducting high power hadron linac. A typical tuning process is based on comparison between measured data and the results of simulations from envelope and single-particle models. Presence of significant space charge effects requires simulation and measurement of bunch dynamics in 3 dimensions to ensure low loss beam transport. This is especially difficult in a superconducting linac where use of interceptive diagnostics is usually restricted because of the risk of SRF cavity surface contamination. The procedures discussed here are based on non-interceptive diagnostics such as beam position monitors and laser wires, and conventional diagnostics devices such as wire scanners and bunch shape monitors installed outside the superconducting linac. The longitudinal Twiss analysis based on the BPM signals will be described. The superconducting SNS linac tuning experience will be used to demonstrate problems and their solution for real world linac tune-up procedures.

INTRODUCTION

The superconducting linac (SCL) of the Spallation Neutron Source (SNS) accelerates negative charged hydrogen ions from 185.6 MeV to 1 GeV providing at its exit 1.4 MW of average power. To have an acceptable level of the linac activation (less than 100 mrem/h for "hands-on" maintenance) beam loss in the accelerator should be very small. The SCL design predicted that this part of the SNS linac should be virtually free of beam loss because of a good vacuum, hydrogen instead of nitrogen as a residual gas, and a big beam pipe aperture. During the commissioning and the power ramp up in 2006 -2007, it was found that the SCL had substantially more beam loss than expected, but still at an acceptable level for the design power level of 1.4 MW. It was found that the beam loss could be reduced by an empirical "step-by-step" procedure of reducing the SCL quadrupole gradients using beam loss as a figure of merit. The design and final production gradients are shown in Fig. 1.

This seemingly counterintuitive measure to reduce beam loss in the SNS superconducting linac was explained by the discovery of an Intra Beam Stripping (IBSt) beam loss mechanism [1,2]. According to IBSt, beam loss is the result of intra-beam collisions of two H^- ions that strip the electron from one of the ions. Then the created neutral hydrogen atoms are lost on the beam pipe. Reducing the quad gradients in the SCL makes the beam transverse size bigger, reduces the beam density, and eventually reduces the collision and stripping rate in the beam. The process of increasing the transverse beam size has its limit when we start to lose ions on the beam pipe.

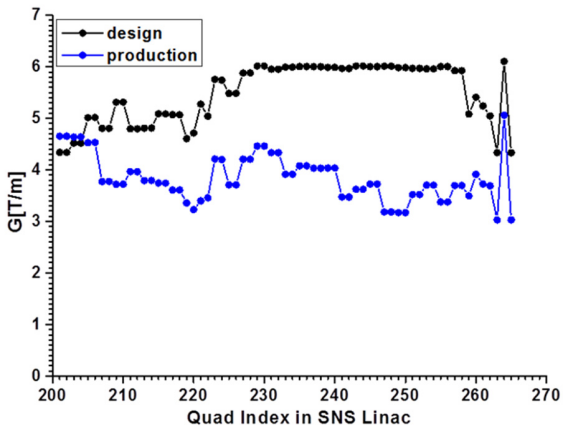


Figure 1: SCL quadrupole gradients.

The disadvantage of using the phenomenological tuning based only on beam loss is that we cannot tell if we have reached the optimal tuning and nothing else can be done. To answer this question we have to create the beam dynamics model of SCL including parameters of all RF cavities and initial conditions of the beam at the entrance of SCL. So far all attempts to build a working model and to get a "matched" beam in the SCL have failed [3]. In the present paper we will discuss work that has been done during the last two years at SNS to build such model, a possible reason why we failed before, and what we want to do in the future.

SCL TUNING PROCEDURE

The SNS superconducting linac tuning procedure is performed each time when the accelerator is turned on after an extended shutdown period (several weeks or more), and it consists of the following steps:

- Setting phases of all RF cavities. The phases are set using phase scan data. The process is discussed in details later. The amplitudes of the cavities (field gradients) are not a subject of tuning. These values are defined by the SCL group to be as high as possible and, at the same time, to provide a stable operation.
- Initial quadrupole gradient values are taken from the previous run settings. Then these values are tweaked to minimize beam loss in the SCL and the next section of the accelerator.
- SCL beam loss is further reduced by changing RF parameters in the warm linac. The parameters include all cavity phases, amplitudes, and quadrupole magnetic fields.

#shishlo@ornl.gov

Copyright © 2014 CC-BY-3.0 and by the respective authors

FIRST EXPERIMENTAL RESULTS FOR THE SUPERCONDUCTING HALF-WAVE RESONATORS FOR PXIE*

Z.A. Conway#, A. Barcikowski, G.L. Cherry, R.L. Fischer, S.M. Gerbick, M.J. Kedzie, M.P. Kelly, S-h. Kim, S.W.T. MacDonald, R.C. Murphy, P.N. Ostroumov, T.C. Reid, and K.W. Shepard, ANL, Argonne, IL 60439, USA

Abstract

The first superconducting niobium half-wave resonator operating at 162.5 MHz for the FNAL PIP-II project is complete and this paper reports the cold test results. The half-wave resonator cavities are optimized to accelerate protons/H^- from 2 to 10 MeV and build upon optimized electromagnetic designs and processing techniques developed at Argonne for the Intensity Upgrade of the ATLAS superconducting heavy ion accelerator.

INTRODUCTION

Fermi National Accelerator Laboratory (FNAL) is pursuing an ambitious plan to modernize the on-site accelerator infrastructure to provide high-intensity proton beams of >1.2 MW at 120 GeV [1], with powers approaching 1 MW at energies down to 60 GeV. The first phase of this plan was the recently completed upgrades to the Recycler and Main Injector synchrotrons for the NO*v*A experiment. The next phase, the Proton Improvement Plan (PIP-II), includes improvements to the existing Linac aimed at supporting higher intensity beam operations by enabling 15 Hz beam operations, a 50% increase in delivered protons per pulse, raising the booster energy from 400 to 800 MeV and requiring that all of the new hardware must be upgradable to continuous-wave operation in the future. These demanding requirements can be met by replacing the existing 400 MeV injector with a new 800 MeV superconducting linear accelerator injecting into the existing Booster synchrotron.

The new 800 MeV accelerator has a superconducting cryomodule containing 8 half-wave resonators (HWRs) and 8 solenoids for the acceleration of an H^- beam from 2.1 to 10 MeV. This cryomodule will be commissioned as part of a prototype front end accelerator demonstration experiment referred to as PXIE, the Project-X Injector Experiment [2]. The aim of the work presented here is to demonstrate the viability of operating HWRs in the first superconducting accelerator cryomodule of PXIE by presenting the cold test results for the first prototype.

For details of the HWR design, see reference [3], which reviews the RF optimization. In the following we discuss the design, processing and cold test results for a 162.5 MHz HWR optimized for particle velocities of $\beta \sim 0.11$.

*This material is based upon work supported by the U.S. Department of Energy, Office of Science, Office of Nuclear Physics, under contract number DE-AC02-06CH11357, and the Office of High Energy Physics, under contract number DE-AC02-76CH03000. This research used resources of ANL's ATLAS facility, which is a DOE Office of Science User Facility.

zconway@anl.gov

CAVITY FABRICATION

Design and Construction

HWR operation is proposed to be 1.7 MV of voltage gain per cavity at 2 K. The design was constrained to provide a 162.5 MHz HWR of optimum $\beta = 0.11$ with a 33 mm aperture. Given these constraints the RF optimization focused on minimizing the cryogenic load and the peak electromagnetic surface fields simultaneously. This was accomplished with an advanced design using conical inner and outer conductors. This design is electromagnetically similar to recently commissioned quarter-wave resonators which have excellent online performance [4]. The cavity is 125 cm from end-to-end and 41 cm in diameter at its largest. Table 1 gives the RF performance parameters for the HWR.



Figure 1: The 162.5 MHz, $\beta = 0.11$, niobium half-wave resonator enclosed in an integral stainless-steel helium vessel. The cavity is 125 cm end-to-end.

Table 1: HWR RF Parameters

Parameter	Value
Frequency	162.5 MHz
β	0.112
Effective Length ($\beta\lambda$)	20.7 cm
E_{peak}/E_{acc}	4.68
B_{peak}/E_{acc}	5.02 mT/(MV/m)
$G = R_sQ$	48.2 Ω
R_{sh}/Q	271.7 Ω

Copyright © 2014 CC-BY-3.0 and by the respective authors

DESIGN OF A SUPERCONDUCTING QUARTER-WAVE RESONATOR FOR eRHIC *

S. V. Kutsaev[1], S. Belomestnykh[2,3], I. Ben-Zvi[2,3], Z. A. Conway[1], M. P. Kelly[1], B. Mustapha[1], P. N. Ostroumov[1], Q. Wu[2], B. Xiao[2], W. Xu[2]

[1)] Argonne National Laboratory, Argonne, IL 60439, U.S.A.
[2)] Stony Brook University, Stony Brook, NY 11794, U.S.A.
[3)] Brookhaven National Laboratory, Upton, NY 11973-5000, U.S.A.

Abstract

The electron-ion collider project (eRHIC) at Brookhaven National Laboratory requires a 50 mA 12 MeV electron injector for the eRHIC main linac [1] and an SRF electron gun for a Coherent electron Cooling (CeC) linac [2]. The necessity to deal with long electron bunches required for both the eRHIC injector and the coherent electron cooler sets the frequency requirement of 84.5 MHz. A quarter wave resonator is an obvious choice for this frequency because of its dimensions, RF parameters and good experience with manufacturing and using them at ANL. Here we present the design and optimization of an 84.5 MHz superconducting quarter-wave cavity with accelerating voltage of 2.5 MV suitable for both machines. One QWR will be used as a bunching cavity in the injector linac, the other one as the photoemission electron source for the CeC linac. In addition to the optimization of the QWR electromagnetic design we will discuss the tuner design, approaches to cavity fabrication and processing.

INTRODUCTION

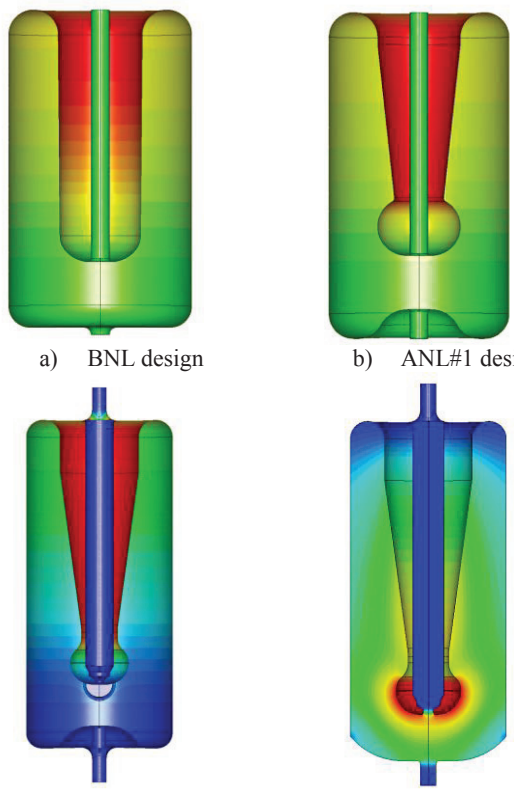
Both eRHIC injector and CeC linac have similar requirements for the front-end: they need to accelerate electron beams up to ultra-relativistic velocities (2.5 to 12 MeV), operate with a bunched beam, and require to provide beam transport of the electron bunches without significant degradation of beam emittance and energy spread [3]. These requirements limit the RF frequency of the cavities to 84.5 MHz in order to provide relatively long bunches. The other important requirement for the electron cooling linac is the capability to tune its frequency over a 78 kHz range in order to synchronize it with the heavy ion beam revolution frequency of RHIC.

One of the most efficient cavity types for such low frequencies are superconducting Quarter-Wave Resonators (QWRs) that are widely used in $\beta \sim 0.1$ part of ion linacs. Argonne National Laboratory has significant experience in building such cavities for ATLAS Upgrade Program [4], so QWRs would be a natural choice for this application because of the dimensions and highly-optimized RF parameters. Changing from a 2-gap layout to 1-gap eliminates the problem of velocity acceptance which otherwise becomes a problem for ultra-relativistic electron beams.

ELECTROMAGNETIC DESIGN

The electromagnetic design was done in CST Microwave Studio [5]. The following considerations were taken into account for the cavity design and shape optimization:

- An operating frequency of 84.85 MHz QWR to accelerate electrons in a longitudinal gap;
- A diameter of the cavity not to exceed 65 cm to fit into BNL's vertical test facility;
- 2.5 MV accelerating voltage with a peak electric field less than 40 MV/m and magnetic field less than 80 mT for reliable operation.



a) BNL design b) ANL#1 design
c) ANL#2 design d) ANL#3 design

Figure 1: Cavity electromagnetic design progress (electro-magnetic field distribution)

* Work is supported by Brookhaven Science Associates, LLC under contract No.DE-AC02-98CH10886. This material is based upon work supported by the U.S. Department of Energy, Office of Science, Office of Nuclear Physics, under contract number DE-AC02-06CH11357. This research used resources of ANL's ATLAS facility, which is a DOE Office of Science User Facility

Copyright © 2014 CC-BY-3.0 and by the respective authors

ISBN 978-3-95450-142-7

A COMPACT LINAC DESIGN FOR AN ACCELERATOR DRIVEN SYSTEM*

B. Mustapha#, S.V. Kutsaev, P.N. Ostroumov and J.A. Nolen
Physics Division, ANL, Argonne, IL 60439, USA
A. Kar, Department of Physics, Carnegie Mellon University, Pittsburgh, PA 15213, USA

Abstract

A compact linac design has been developed for an Accelerator Driven System (ADS). The linac is about 150 meters in length and comprises a radio-frequency quadrupole (RFQ) and 20 superconducting modules. Three types of half-wave cavities and two types of elliptical cavities have been designed and optimized for high performance at frequencies of 162.5, 325 and 650 MHz. The lattice was designed and optimized for operation with a peak power of 25 MW for a 25 mA – 1 GeV proton beam. The cavities RF design as well as the linac lattice will be presented along with end-to-end beam dynamics simulations for beam currents ranging from 0 to 25 mA.

COMPACT LINAC LAYOUT

Figure 1 shows a schematic layout of the proposed linac with its different sections. The linac is only 150 m in length taking advantage of the latest and successful normal conducting and superconducting RF developments at Argonne [1], especially developments of high cavity accelerating voltages [2] and compact cryomodule design [3]. For comparison, the proposed linac has half the length of the SNS linac [4] with the same 1 GeV output energy and a 25 mA CW proton beam. The key factors for a compact linac design are:

- Optimized superconducting cavity design for high voltage and low cryogenic losses.
- Superconducting solenoid focusing inside cryomodules to minimize warm transitions and consequently the number of required cryomodules.
- Cold BPMs attached to SC cavities inside the cryomodule to reduce the number of diagnostics required between cryomodules
- Horizontal and vertical steering correctors are built into the solenoids requiring no additional space for correctors along the beam-line.

With these considerations, the drift space between cryomodules is reduced, benefiting the beam dynamics from a more periodic focusing and acceleration sequence.

RF CAVITIES DESIGN

The base linac frequency is 162.5 MHz, it was mainly chosen because the CW RFQ requires less power and is more reliable in operation than at 325 MHz for example. At this frequency, half-wave (HWR) and single-spoke (SSR) resonators are more efficient for beta < 0.6 than other resonators. HWRs were chosen because of the mature fabrication and processing technologies available at Argonne. Figure 2 shows three types of half-wave resonators and two types of elliptical resonators. The cavity design frequencies are 162.5, 325 and 650 MHz. The low-β HWR is very similar to the one being constructed for the PXIE project [5] and could actually be used as is. Table 1 lists the RF performance parameters for the different cavity types and figure 3 shows the electric and magnetic field distribution in the HWR-2 and ELL-2 cavities. We can clearly distinguish between the electric and magnetic field regions. Making sure the surface fields are evenly distributed reduces their peak values.

LINAC LATTICE DESIGN

The lattice design is a very important step for any accelerator, it defines the acceleration and focusing profiles for the machine. The transition from one cavity type to the next has to be optimized based on the voltage a cavity can provide as function of the beam velocity or transit time factor. Figure 4 shows the voltage profile for the different cavities as a function of β, it also shows the transitions between cavity types. It is important to slowly ramp up the voltage for the lowest-β cavity to avoid rapid acceleration and beam blow-up. It is also important to provide sufficient and more frequent focusing in the first cryomodule to better control the space charge forces in the low-energy region, especially below 10 MeV. Table 2 gives the details of the lattice design, including cavity voltages and synchronous phases, the focusing period per section as well as the cavity, solenoid and cryomodule counts for each linac section.

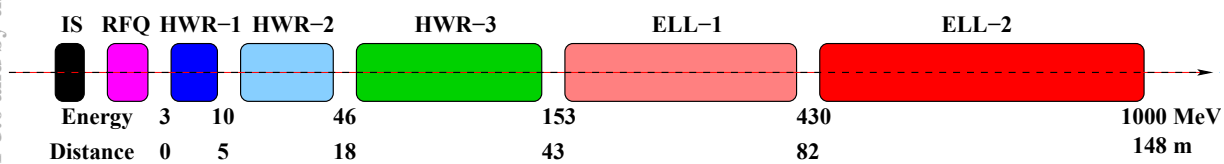


Figure 1: Layout of the proposed compact ADS linac showing the energies and dimensions of every section.

* This material is based upon work supported by the U.S. Department of Energy, Office of Science, Office of Nuclear Physics, under Contract number DE-AC02-06CH11357. This research used resources of ANL's ATLAS facility, which is a DOE Office of Science User Facility.
# brahim@anl.gov

Copyright © 2014 CC-BY-3.0 and by the respective authors

DESIGN AND DEVELOPMENT OF PULSED MODULATORS FOR RF ELECTRON LINACS

K. P. Dixit, S. Chandan, N. Chaudhary, R. B. Chavan, S. R. Ghodke, M. Kumar, H. Sarukte, A.R. Tillu, H. Tyagi, V. Yadav, K. C. Mittal & L. M. Gantayet
Accelerator & Pulse Power Division, Bhabha Atomic Research Centre, Mumbai - 400085, INDIA

Abstract

Pulsed Modulators required for RF sources, based on klystrons and magnetrons, for RF electron linacs have been designed and developed at Electron Beam Centre, BARC, Mumbai, India. Electron guns in these linacs have also been powered by pulsed modulators. Line-type modulators, as well as IGBT-based solid-state modulators have been developed for these applications. A 150 kV/100 A line-type modulator has been tested on klystron to generate 7 MW peak RF Power. Magnetron modulator has undergone testing up to ~40 kV, 165 A on resistive load. Solid-state modulator, using fractional-turn pulse transformer has been designed, developed and tested successfully on magnetron load up to output power of 1.3 MW peak. A transformerless solid-state modulator for electron gun of 6 MeV cargo-scanning linac, uses the Marx adder configuration and has been successfully tested up to 40 kV. In addition, line-type modulators for electron guns up to 85 kV have been successfully commissioned and are in operation in the linac systems. This paper describes the salient design features of these modulators, development of pulse transformers, details of test set-up and discusses the test results of these modulators.

INTRODUCTION

Industrial electron RF linacs [1], including the 10 MeV RF Linac and 3 MeV DC Accelerator, have been indigenously designed and developed at Accelerator & Pulse Power Division, BARC, India. Several industrial applications such as plastic modification, semiconductor irradiation [2] have been demonstrated with these accelerators. 6 MeV and 9 MeV linacs as x-ray sources for cargo-scanning and radiography have been built and characterized. These linacs operate in the pulsed mode, which requires the use of pulse modulators for the RF source as well as the electron guns. The design, development, testing and operation of various pulse modulators is presented in this paper.

MODULATORS FOR E-GUNS

Electron guns [3], acting as injectors to RF linacs, are powered by modulators. The ratings of these modulators are rated from 40-85kV, with peak current ranging from 1-4A. Pulse width varies between 3-10µs, while pulse repetition rates lie between 250-400 Hz, depending upon the application for which the linac is used. Both line-type and solid-state modulators have been designed and developed indigenously. A brief description is given in this section.

Line Type Modulators

An indigenously developed 85 kV line-type modulator, shown in Figure 1, has been used in the 6 MeV linac [4] as x-ray source for cargo-scanning applications. This is rated for 4 A with 6 µs pulse width and 250 Hz repetition rate. A 10-stage PFN capacitor (72 nF total), shown in Figure 1, is charged resonantly through a charging choke of 20 H. Impedance of the PFN is kept as 50Ω in order to facilitate the use of coaxial cables between the primary circuit and the pulse transformer kept at a distance of ~20m, close to the gun. Hydrogen thyratron, rated for 18kV, acts as the switch, which causes the stored energy in PFN capacitors to discharge through the 1:20 pulse transformer to obtain 85 kV at its secondary.

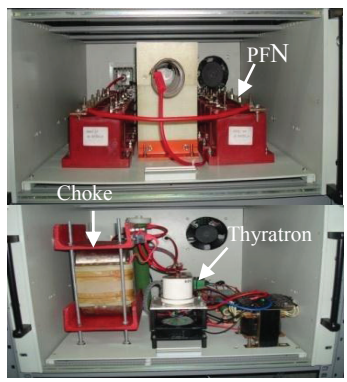


Figure 1: Primary circuit of 85 kV modulator

Solid-state Modulators

A transformerless solid-state modulator using the Marx adder configuration [5], has been designed, developed and tested. Figure 2 shows the 84-stage IGBT-based adder and the output of 40 kV, 10 µs pulse at 250 Hz rep.rate. Rise time achieved is <250 ns.

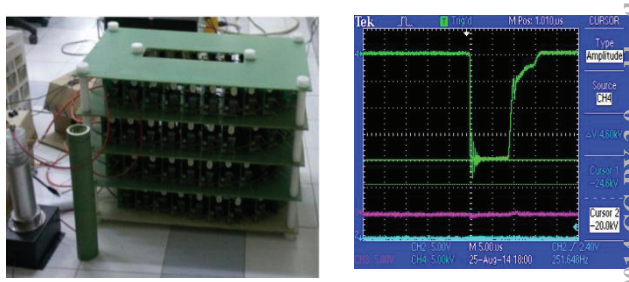


Figure 2: Marx adder (84-stage) and output of 40 kV on resistive load

Copyright © 2014 CC-BY-3.0 and by the respective authors

ISBN 978-3-95450-142-7

HIGH POWER ELECTRON ACCELERATOR PROGRAMME AT BARC

K.C. Mittal, V.T. Nimje, S. Acharya, K.P. Dixit, R.I. Bakhtsingh, M. Kumar, S.R. Ghodke
R. Rajan, D.K. Sharma, V. Yadav, D. Bhattacharjee, S. Chandan, S.P. Dewangan, A.R. Tillu,
R.B. Chavan, V. Sharma, J. Mondal, D. Jayaprakash, P.C. Saroj, R. Barnwal, N. Chaudhary,
S.K. Srivasatava, H. Tyagi, B. Nayak, S. Gade, S. Parashar, R. Patel, M. Kumar,
H. Manjunatha, R.L. Mishra, S. Nayak, H. Sarukte, S. Gond, N. Thakur, R. Tiwari,
A. Waghmare, L.M. Gantayet
Accelerator & Pulse Power Division, Bhabha Atomic Research Centre,
Mumbai - 400085, INDIA

Abstract

Bhabha Atomic Research Centre in India has taken up the indigenous design & development of high power electron accelerators for industrial, research and cargo-scanning applications. For this purpose, Electron Beam Centre (EBC) has been set up at Navi Mumbai, India. Pulsed RF Linacs, with on-axis coupled cavity configuration, include the 10 MeV Industrial RF linac, as well as 9 MeV linac and compact 6 MeV linac for cargo-scanning applications. Industrial DC accelerators include a 500 keV Cockroft-Walton machine and 3 MeV Dynamitron. Several radiation processing applications, such as material modification, food preservation, flue-gas treatment, etc. have been demonstrated using these accelerators. Cargo-scanning linacs have been successfully commissioned and are being characterized for the required x-ray output. A 30 MeV RF Linac, for research applications, such as shielding studies and n-ToF experiments, is being designed and developed. For ADS studies, a 100 MeV, 100 kW RF Linac system is proposed. This paper presents the details of the design of these accelerators, their development, current status and utilization for various applications.

INTRODUCTION

Electron beam (EB) irradiation and its applications are increasing day by day. To cater to some of these applications, such as material modifications, food preservation, flue-gas treatment, etc., a programme of indigenous design and development of high power electron beam accelerators has been taken up at BARC in the Accelerator & Pulse Power Division [1]. The Electron Beam Centre, located at Navi Mumbai, houses 2 accelerators, viz. the 10 MeV RF linac and the 3 MeV DC Accelerator. A 9 MeV linac for cargo-scanning applications has been set up at ECIL, Hyderabad. For mobile cargo-scanning applications, a 6 MeV compact linac has been developed. In the field of research, a 30 MeV RF Linac has been designed and is under developed for neutron generation. Flue-gas treatment (FGT) requires megawatt-class of DC Accelerators. A pilot EB-FGT plant with multiple DC accelerators is being configured for treating the flue gas from a captive power plant of 30 MWe. Salient features and status of these accelerators is discussed here.

RF LINACS

RF Linacs operate at 2856 MHz in the pulsed mode and are based on the on-axis coupled cavity geometry. Acceleration gradients of 18 MV/m have been achieved. Three linacs developed in this configuration are successfully operating presently.

RF Industrial Linac

The 10 MeV RF linac, comprising of 17 accelerating cells and 16 coupling cells, is ~1m long. Electron gun has a triode geometry, with indirectly heated LaB_6 cathode and produces pulsed beam of electrons with energy of 85 keV. Klystron-based source provides 6 MW RF power to establish the acceleration gradient in the linac. The 10 MeV electron beam from the linac is scanned over a length of ~800 mm with the help of a magnetic scanner. Electron beam emerges through titanium window for utilization purposes. This linac is in regular operation at 3 kW for various industrial applications [2]. Irradiation of semiconductor has resulted in the reduction of reverse recovery time from 15 to 7 μs. Photofission experiments are also being conducted using this linac facility. Other successful experiments include enhancement of softening temperature of PE, gel formation, cable irradiation, etc.

X-ray Sources Based on RF Linacs for Cargo-scanning

Two linac systems have been configured to operate as x-ray sources for cargo-scanning applications.



Figure 1: View of 6 MeV x-ray source for mobile cargo-scanning applications

Copyright © 2014 CC-BY-3.0 and by the respective authors

ISBN 978-3-95450-142-7

SF_6 GAS MONITORING AND SAFETY FOR DC ELECTRON BEAM ACCELERATOR AT EBC, KHARGHAR, NAVI MUMBAI

Suneet Kumar Srivastava , Shyam Rao Ghodke , Satyanarayan Acharya, Srutarshi Banerjee, Rajesh Barnwal, Dhruva Bhattacharjee, Nishant Chaudhary, Ramchandra B. Chavan, Kavita P Dixit, Sirisha Gade, Lalit Mohan Gantayet, Seema Gond, Israel Bakhtsingh, D. Jayaprakash, Nagesh Lawangare, Kumar Mahendra, Radhelal Mishra, Kailash Chander Mittal, Biswaranjan Nayak, Susanta Nayak, Rupesh Patel, Rehim Rajan, P C Saroj, D K Sharma, Vijay Sharma, Mukesh Kumar Srivastava, Suryaprakash Dewangan, Nitin Thakur, Rajnish Tiwari, Abhay Waghmare
Accelerator & Pulse Power Division, Bhabha Atomic Research Centre,
Mumbai - 400085, INDIA
sunsri1@rediffmail.com, ghodke_barc@yahoo.co.in

Abstract

A 3 MeV, 30kW DC Industrial electron beam accelerator has been designed, commissioned and tested at Electron beam centre, Kharghar. The accelerator has been tested up to 10 kW power level with SF_6 gas at 6 kg/cm^2. The accelerating column, high voltage multiplier column, electron gun and its power supply are housed in accelerator tank, which is filled with SF_6 gas as gaseous insulator at 6 kg/cm^2. The SF6 gas is being used due to high dielectric strength and excellent heat transfer characteristics. The SF6 gas is non toxic and non carcinogenic. The SF6 gas replaces oxygen and OSHA has established the permissible TLV of 1000ppm. The SF6 gas is being green house gas, leak tightness has to monitor in the system and leak if any should be repaired. The gas should be used, recycled and reuse and thus saving the environment. This paper describes the safety and monitoring of the SF6 gas leak, quality and precautions in 3 MeV accelerator.

INTRODUCTION

A 3 MeV, 30 kW DC Industrial electron beam accelerator has been designed, commissioned and tested at Electron beam centre, Kharghar. Fig 1 shows the schematic of the same. The multiplier column required the input voltage of 150 kV-0-150 kV at 120 kHz. The class C push pull power oscillator coverts the 10kV DC into 120 kHz, 10kV RF and air core RF transformer step up the voltage to 150kV-0-150 kV and fed to the two cylindrical shaped RF electrodes. The accelerator tank will house the high voltage multiplier columns, RF electrodes, corona shields, high voltage terminals, electron gun, accelerating tubes, heat exchanger, RF transformer etc. Normal operating pressure inside the accelerator is 6 kg/cm2 of SF6 gas. It is 7 meters long has a maximum outer diameter of shell is 2.16 meters and volume of 26 m3. The SF6 gas supply is contained in two storage tanks whose total capacity is 32 m^3 [3]. Fig 2, Fig 3, and Fig 4 shows the RF Electrodes, RF Transformer and SF_6 Gas Storage tanks respectively. SF6 gas is inert, stable, colourless, nontoxic and non-flammable gas at temperatures below 500C

It is easily liquefied at room temperatures by application of pressure. It is approximately five times heavier than air and displaces air in confine areas. It is the most suitable medium for insulation and cooling purpose. This gas is having excellent arc quenching properties.

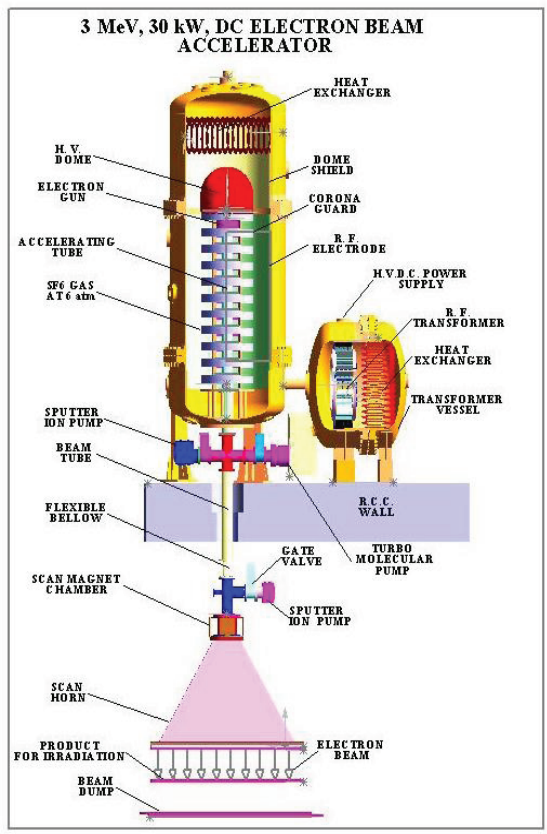


Figure 1: Schematic of 3 MeV DC Accelerator

SF6 gas when released into the atmosphere, has a relatively long life, contributes to green house. The environmental protection agency (EPA) has identified SF6 as green house gas with global warming potential 23900 times more effective than carbon monoxide and

Copyright © 2014 CC-BY-3.0 and by the respective authors

ISBN 978-3-95450-142-7

LOW CHARGE LASER ION SOURCE FOR THE EBIS INJECTOR*

M. Okamura#, T. Kanesue, J. Alessi, E. Beebe, A. Pikin, D. Raparia, CJ Liaw, J. Ritter, V. Lodestro, BNL, Upton, NY 11973, USA
Y. Fuwa, M. Kumaki, S. Ikeda, RIKEN, Saitama 351-0198, Japan

Abstract

In March 2014, we successfully commissioned a newly designed low charge high brightness laser ion source (LIS) named as "LION," which delivers various singly charged heavy ions to the electron beam ion source (EBIS) in Brookhaven National Laboratory. Since then, the LIS is used in routine operation for the RHIC accelerator complex and is providing stable, less-contaminated beams into the EBIS. The laser power density was optimized to provide singly charged ions with low material consumption rate. The nominal laser energy on the target is around 500 mJ at 1064 nm wavelength. The plasma produced by the laser is transported through a 3 m pipe to stretch the ion beam pulse length to match the EBIS's requirement, and the degradation of the beam current caused by aging of the laser flash lamps and target surface deformation can be compensated by a longitudinal magnetic field induced by a coil surrounding the pipe. A twin laser system, firing sequentially, is to extend the beam width further. The accelerated beams through the EBIS, RFQ and IH-linac showed a good performance. Also we can now provide relatively lower charge state ion beams from the EBIS, if desired, using fast injection scheme. Before introducing the LION, fast injection was not typically used, since it was difficult to get sufficient injected ion intensity. This mode will be used in the next run to maximize particle number in the relativistic heavy ion collider (RHIC) for running with Al ions.

INTRODUCTION

Since 2010, the EBIS injector has been used to provide heavy ion beams to NASA Space Radiation Laboratory (NSRL) and RHIC[1]. The injector consists of two hollow cathodes ion sources for 1+ heavy ion production, an EBIS for breeding of injected ions to high charge state, a 4 rod 300 keV/u RFQ, and a 2 MeV/u IH-DTL. In the spring of 2014, to enhance the versatility of the injector, a newly designed LIS was installed[2]. After the beam commissioning of the LIS, we have provided beams both from the LIS and the hollow cathode ion source (HCIS) for the RHIC and NSRL runs. In this paper, some operation results of the EBIS injector comparing the LIS and HCIS are reported.

LION

The new LIS was named as LION and the installed apparatus is shown in Fig. 1. The LION comprises three major parts, which are target chamber, 3m solenoid and extraction chamber. In the target chamber, a two dimensional motorized x-y motion stage is installed. In Run 14, carbon, silicon, titanium, iron, tantalum and gold plates were installed, and those beams were provided. The targets were illuminated a by QUANTEL Brilliant-B twin (850 mJ, 1064 ns, Q-switched Nd:YAG) laser system. The laser was placed on the top of the supporting frame and the laser beam was guided into the target chamber.

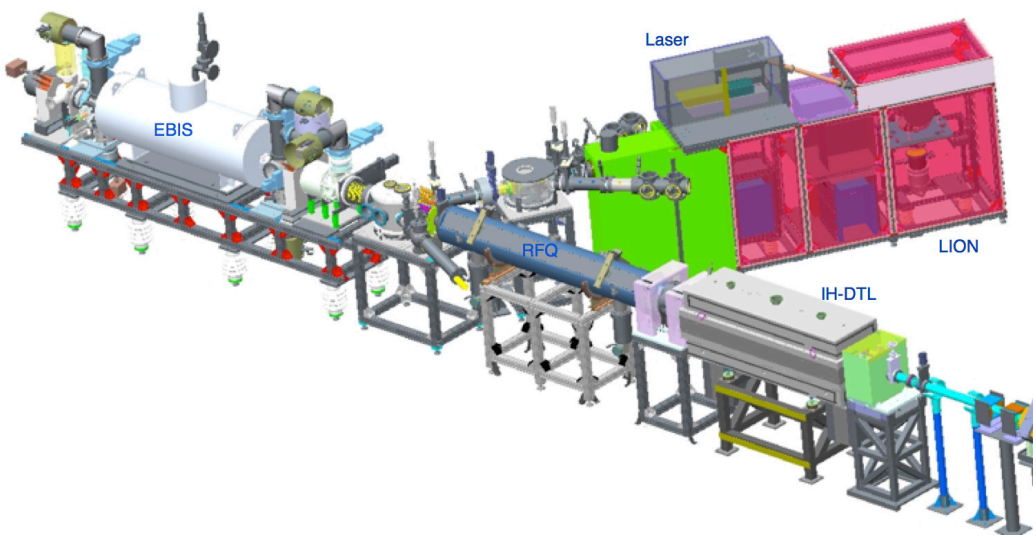


Figure 1: EBIS injector equipped with LION

*Work supported by US. Department of Energy and the National Aeronautics and Space Administration.

Copyright © 2014 CC-BY-3.0 and by the respective authors

RELIABILITY AND INTENSITY UPGRADE FOR BROOKHAVEN 200 MeV LINAC *

D. Raparia#, J. Alessi, B. Briscoe, D. Gassner, O. Gould, T. Lehn, V. LoDestro, J. Ritter, W. Shaffer, A. Zelenski, Brookhaven National Laboratory, Upton, NY 11973, USA

Abstract

Brookhaven 200 MeV H- linac has been operating for the last 44 years and providing beams to nuclear physics and isotope programs. Three linac upgrades are in progress; (a) to make machine more reliable, (b) to double the intensity by increasing the beam pulse length and, (c) to produce more uniform beam current density on the target by raster the beam on the target.

INTRODUCTION

The Brookhaven National Laboratory (BNL) 200 MeV drift tube linac (DTL) was built in 1970 [1] with following design parameters for proton: input energy 0.75 MeV, output energy 200.3 MeV, frequency 201.25 MHz, peak beam current 100 mA, beam pulse length (max) 200 μs, RF pulse length 400 μs, pulse repetition rate (max) 10 Hz. Over the 44 years of linac operations, it has gone through several improvements. The major upgrades were; (a) switch to 5 Hz operation [2], (b) change proton to H- [3], (c) addition of polarized H- source [4], (d) replacement of the Cockcroft-Walton by Radio Frequency Quadrupole (RFQ) [5], (e) new timing system [6], (f) new 12 inches pressurised coax system [6], (g) RF system improvements [6], new 50 kV power supply, eliminating of DC charge control at 60 kV, new rf control system, phase and amplitude servo redesign, (h) new polarized source OPPIS source and its upgrade, and [7,8], (i) reconfiguration of 35 keV and 750 keV transport lines [9,10,11,12,13].

At present linac provides H- beam at 200 MeV to polarized proton program for Relativistic Heavy Ion Collider (RHIC) and 66-200 MeV to Brookhaven Linac Isotope Production (BLIP). The RHIC program needs two pulses every AGS cycle (~4-5 sec), one for injection into the AGS booster and other for 200 MeV polarization measurements located in the High Energy Beam Transport line (HEBT). The rest of the pulses from high intensity source are delivered to BLIP. Requirements for these programs are quite different and they are following. (1) RHIC: 200 MeV, 600 μA beam current, up 400 μs pulse length, polarization as high as possible and emittance as low as possible, (2) BLIP: 66-200 MeV, 450 μs pulse length, current as high as possible (~45 mA), uniform beam distribution at the target, and beam losses as low as possible.

Many of subsystems of the linac are 45 yeas old and need to be replaced. Three upgrade programs; reliability, intensity, and beam raster, are in progress. Here, we will discuss only intensity and reliability upgrade program. Beam raster program will be discussed in the companion paper in this conference [14].

*Work performed under Contract Number DE-AC02-98CH10886 with the auspices of the US Department of Energy
#raparia@bnl.gov

RELIABILITY UPGRADE

Based on the down time of different systems we are upgrading following subsystems; RF system, beam loss monitors, beam current monitors, multi-wires, secondary emission monitor (profiles), control system, fast beam interrupt system. Schedules for these upgrades will depend on the availability of the funding. This summer we are starting with RF and beam loss monitor system. The major part of the linac down time is caused by linac RF system. Figure 1 shows the total down time since 1972 for the linac. The substantial reduction in down time was due to reducing repetition rate to 5 Hz in 1977 and changing to pressurized coax in 1996.

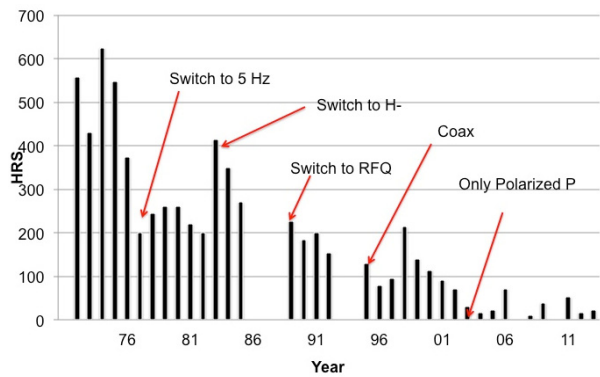


Figure 1: Total linac down time in hours since 1972 for HEP and RHIC operations.

We are replacing 5 kW Tetrode 7651, one of six tubes in amplifiers chain, by solid state amplifies. Since last year we are using similar solid-state amplifier for buncher in the 750 keV line. It is very reliable and down time for buncher is reduced to zero due to this change. We plan to replace all ten 7651-tubes with solid-state amplifies this summer. All amplifiers will be delivered by end of September 2014. Figure 2 shows the tube-based system on the right and solid-state amplifier on the left.

We are adding beam loss monitor for low energy operation of BLIP. BLIP wants to run at 66 MeV, the existing long radiation monitors are not sensitive for this low energy. We have tested (shielded with lead and cadmium) scintillator BC-400 for first three tanks and first bending magnet in the BLIP line. Figure 3 shows shielding configuration of the scintillator and Figure 4 shows location of these detectors along the linac.

Copyright © 2014 CC-BY-3.0 and by the respective authors

ISBN 978-3-95450-142-7

BEAM COMMISSIONING PROGRAM OF THE 704 MHz SRF GUN*

Wencan Xu#,1, Z. Altinbas[1], S. Belomestnykh[1,2], I. Ben-Zvi[1,2],S. Deonarine[1], L. DeSanto[1], D. Gassner[1], R. C. Gupta[1],H. Hahn[1], L. Hammons[1], Chung Ho[1], J. Jamilkowski[1], P. Kankiya[1], D. Kayran[1], R. Kellerman[1], N. Laloudakis[1], R. Lambiase[1], C. Liaw[1], V. Litvinenko[1,2], G. Mahler[1], L. Masi[1], G. McIntyre[1], T. Miller[1], D. Phillips[1], V. Ptitsyn[1], T. Seda[1], B. Sheehy[1], K. Smith[1], T. Rao[1], A. Steszyn[1], T. Tallerico[1], R. Than[1], J. Tuozzolo[1], E. Wang[1], D. Weiss[1], M. Wilinski[1], A. Zaltsman[1]

[1)] Collider-Accelerator Department, Brookhaven National Lab, Upton, NY 11973, USA
[2)] Physics & Astronomy Department, Stony Brook University, Stony Brook, NY 11794, USA

Abstract

A 704 MHz superconducting RF photoemission electron gun for the R&D ERL project is under commissioning at BNL. Without a cathode insert, the SRF gun achieved its design goal: an accelerating voltage of 2 MV in CW mode. During commissioning with a copper cathode insert, it reached 1.9 MV with 18% duty factor, which is limited by multipacting in a choke-joint cathode stalk. A new cathode stalk has been designed to eliminate multipacting in the choke-joint. At the same time, a first beam test was carried out in May this year, and dark current from the photocathode was measured in the faraday cup. The SRF cavity was tested after the beam commissioning and shows no-degradation of the performance. This paper presents recent commissioning setup, results and plans for the future beam tests.

INTRODUCTION

The R&D ERL [1] at BNL is an accelerator with high average current, up to 500 mA. It serves as test bed for future RHIC projects: eRHIC [2], Coherent-Electron-Cooling [3], and Low Energy RHIC Electron Cooler [4]. The 704 MHz half-cell SRF gun is designed to provide 0.5 A, 2 MeV electron beam. Commissioning of the SRF gun is carried out in stages: without a cathode stalk (finished in early 2013), with a copper cathode stalk (finished in fall of 2013), and beam commissioning (started in mid-2014). The SRF gun without a cathode stalk reached the design voltage of 2 MV in CW mode. During commissioning with a copper cathode stalk, strong multipacting in the quarter-wavelength choke-joint was observed and it was understood with simulation. A multipacting-free choke-joint has been designed and an order was placed its fabrication. In the meantime, first beam commissioning with the existing cathode stalk coated with alkali antimonide photoemission layer took place in May of 2014. Dark current was observed, measured and conditioned. This paper describes the SRF gun commissioning results and plans. A multipacting-free choke-joint design is addressed as well.

PERFORMANCE OF THE SRF GUN

The SRF gun cryomodule is shown in Figure 1. It is built around the 704 MHz half-cell SRF cavity, including a quarter-wavelength choke-joint cathode insert, a pair of opposing fundamental power coupler (FPC) to deliver 1 MW of RF power, a high temperature superconducting solenoid (HTSS) to compensate space charge and a room-temperature ferrite HOM damper. The gun was successfully commissioned and reached the design goal (2 MV in CW mode) without a cathode stalk insert [5]. However, multipacting occured during commissioning with a copper cathode stalk. The main reason for multipacting was caused by distortion of grooves due to BCP and high SEY in the stainless steel area. After spending some time on mutipacting conditioning, the gun was able to operate at 1.9 MV with 18% duty factor. One important parameter for the cavity operation is its field stability. The amplitude stability of 2.3E-4 (rms) and the phase stability of 0.035 degree (rms) was demonstrated.

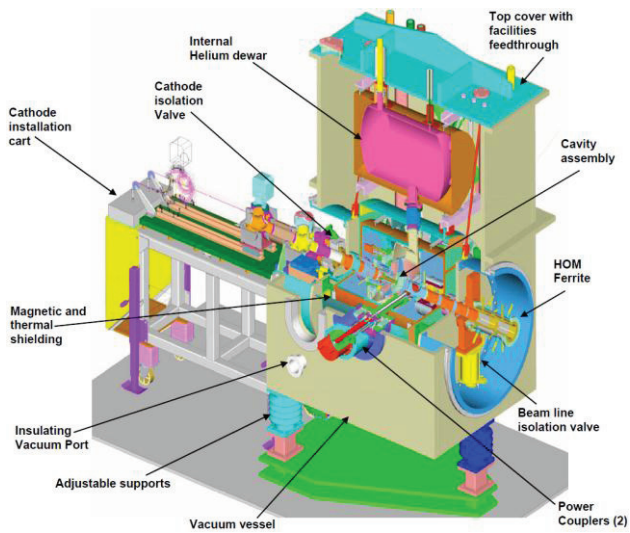


Figure 1: SRF gun cryomodule.

MULTIPACTING-FREE CATHODE STALK DESIGN

Figure 2 shows the cathode stalk to be inserted into the SRF cavity. There are two folded half-wavelength chokes or four quarter-wavelength chokes, so the stalk has four gaps. The copper cathode substrate and an inner Nb cylinder compose the first gap. The second gap (end of the first half-wavelength choke) is formed by two Nb cylinders. The third gap is composed of the outer Nb cylinder and an inner stainless steel cylinder. Two stainless steel cylinders constitute the forth gap. The Nb cylinders are part of the

Copyright © 2014 CC-BY-3.0 and by the respective authors

VERTICAL TEST RESULTS OF 704 MHz BNL3 SRF CAVITIES*

Wencan Xu#,1, S. Belomestnykh1,2, I. Ben-Zvi1,2, H. Hahn1, C. H. Boulware4, T. L. Grimm4, D. Holmes3, G. McIntyre1, R. Porgueddu1, R. Than1, D. Weiss1

1) Collider-Accelerator Department, Brookhaven National Lab, Upton, NY 11973, USA
2) Physics & Astronomy Department, Stony Brook University, Stony Brook, NY 11794, USA
3) Advanced Energy System, Inc., Medford, NY 11763, USA
4) Niowave, Inc., Lansing, MI 48906, USA

Abstract

An electron-ion collider (eRHIC) proposed at BNL requires superconducting RF cavities able to support high average beam current. A 5-cell niobium SRF cavity, called BNL3, was designed for a conventional lattice eRHIC design. To avoid inducing emittance degradation and beam-break-up (BBU), the BNL3 cavity was optimized to damp all dangerous higher-order-modes (HOMs) by employing a large beam pipes and coaxial antenna-type couplers. Additionally, the cavity was designed for an acceptable cryogenic load and peak surface RF fields. Two BNL3 cavities have been fabricated and tested at a vertical test facility at BNL. This paper addresses development of the SRF cavities for eRHIC, including SRF cavity design, fabrication and test results.

INTRODUCTION

The Collider-Accelerator Department at BNL is working on the electron-ion collider (eRHIC) [1] R&D and coherent electron cooling [2]. Both machines require high current SRF linacs with extremely good HOM damping to preserve the emittance and have a high BBU threshold. The BNL3 cavity is a 5-cell 704 MHz SRF cavity designed for the high current SRF linacs with strong HOM damping capability. The HOM damping scheme with six coaxial-line HOM dampers allows high real-estate accelerating gradient, which is very important for long linacs. The RF measurements on a copper prototype of the BNL3 cavity verified the HOM damping capability [3]. Two Nb cavities were fabricated, one by AES [4] and one by Niowave [5]. This paper describes the vertical test results of these cavities.

NB BNL3 CAVITY DESIGN

The BNL3 cavity [6] was designed with integration of HOM damping scheme. It employs a concept that uses an enlarged beam pipe to propagate Higher Order Modes (HOMs) but attenuate the fundamental mode, by choosing the diameter of beam-pipe with cutoff frequency slightly lower than the first HOM. The HOMs are damped by three coaxial-line HOM couplers (separated azimuthally by 120º) located on the enlarged beam pipe. The HOM coupler groups at the two ends of the cavity are rotated by 60º relative to each other. Compared to the BNL1 cavity in the R&D ERL at BNL [7], the BNL3 cavity improves the fundamental mode performance, resulting in the *R/Q* and geometry factor increase of about 20% and 30% respectively. By avoiding a room-temperature ferrite damper on the beam pipe, the real-estate gradient of the BNL3 cavity has improved by about 50% as compared with the BNL1 cavity. To reduce the cross-talk between neighboring cavities, tapered sections to a reduced diameter beam pipe are added on both sides of the cavity. Figure 1 shows two Nb cavities made by AES and Niowave. The BNL3-Niowave cavity has become, unintentionally, made 2 cm shorter than the AES cavity.

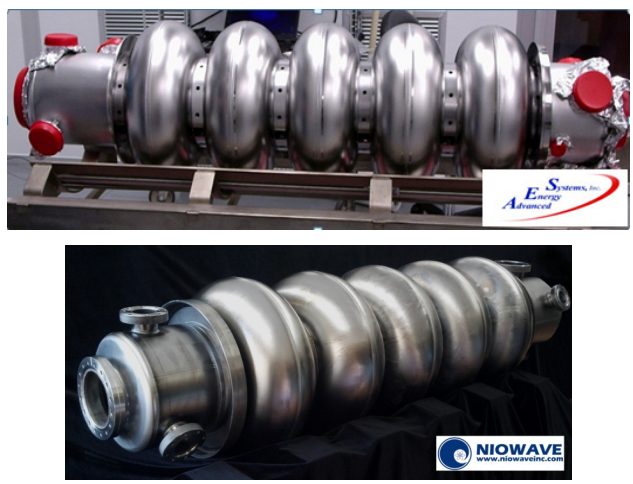


Figure 1: BNL3 cavities made by AES (top) and by Niowave (bottom).

VERTICAL TEST SETUP

Vertical tests of the BNL3 cavities were carried out at the vertical test facility in Bldg 912 at BNL. Figure 2 shows a vertical test setup. The fundamental power coupler (FPC) is located on the short-end side of the cavity. To assure critical coupling during 4 K and 2 K tests, the external *Q* of the FPC is designed to adjust in a range of 2×10^8 to 1×10^{11}, as is shown in Figure 3. The RF loss on the FPC components is minimized with a copper mask on the cavity flange. The total RF loss in the FPC (cavity flange, inner conductor and outer conductor) is

* This work is supported by Brookhaven Science Associates, LLC under Contract No. DE-AC02-98CH10886 with the U.S. DOE, and Award No. DE-SC0002496 to Stony Brook University with the U.S. DOE.
#wxu@bnl.gov

Copyright © 2014 CC-BY-3.0 and by the respective authors

ISBN 978-3-95450-142-7

HIGH ENERGY ELECTRON RADIOGRAPHY EXPERIMENT RESEARCH BASED ON PICOSENCOND PULSE WIDTH BUNCH

Quantang Zhao, Shuchun Cao, Rui Cheng, Xiaokang Shen, Zimin Zhang#,
Yongtao Zhao, IMP, CAS, Lanzhou 730000, China
Wei Gai, ANL, Argonne, IL 60439, USA
Yingchao. Du, THU, Beijing, 100084, China

Abstract

A new scheme is proposed that high energy electron beam as a probe is used for time resolved imaging measurement of high energy density materials, especially for high energy density matter and inertial confinement fusion. The first picosecond pulse-width electron radiography experiment was achieved by Institute of Modern Physics (IMP), Chinese Academy of Sciences (CAS) and Tsinghua University (THU), based on THU Linear electron accelerator (LINAC). It is used for principle test and certifying that this kind of LINAC with ultra-short pulse electron bunch can be used for electron radiography. The experiment results, such as magnifying factor and the imaging distortion, are consistent with the beam optical theory well. The 2.5 um RMS spatial resolution has been gotten with magnifying factor 46, without optimization the imaging lens section. It is found that in the certain range of magnifying factor, the RMS spatial resolution will get better with bigger magnifying factor. The details of experiment set up, results, analysis and discussions are presented here.

INTRODUCTION

The technique of charged particle radiography [1] has been developed and proved with 800 MeV protons at LANSCE of Los Alamos National Laboratory (LANL), as a diagnostic to study dynamic material properties under extreme pressures, strain and strain rate. The high spatial resolution and high energy proton microscopy also developed at ITEP and FAIR [2-4]. LANL used 30 MeV electrons to radiograph thin static and dynamic eRad with picosecond pulse-width electron bunch has been achieved by IMP, CAS and THU. The experiment objects. The spatial resolution of their imaging system is 100 um in both x and y directions [5]. A principle test of is based on the THU Thomson X-ray scattering source. The LINAC consists of RF photocathode injector and s-band accelerating tube. The RF photocathode injector provides 3 MeV, very low emittance and picoseconds pulse-width electron bunches. The highest beam energy of the LINAC is 50 MeV.

zzm@impcas.ac.cn

THE ERAD EXPERIMENT SETUP

In the eRad experiment, the beam energy is 46.3 MeV, bunch charge is about 100 pC, the emittance is about 2 mm-mrad, the beam spot size is about 3 mm, the bunch length is about 1 ps and the beam momentum divergence is less than 1%. The lens consists of two triplets. For simplicity, the lens section is not designed purposely. The quadrupoles for imaging are provided by the old ones, which have been used for focusing the beam in the Thomson scattering X-ray experiment.

The sketch of eRad experiment is shown in Fig. 1. The target vacuum cell and YAG and mirror vacuum cell are added. The electromagnetic quadrupole lens section consists of two triplets. The maximum of the magnetic field gradient is 12 T/m.

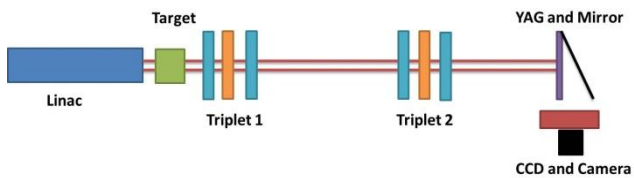


Figure 1: the sketch of the eRad based on THU linac.

The samples are electron microscopy grids, placed on the object plane. Four kinds of grids are installed in the target cell. They include 50 meshes square nickle (Ni) grid, 200 meshes square gold (Au) grid, 200 meshes square copper (Cu) grid and 75 meshes hexagon Cu grid. They are all in 25 microns thickness and 3 mm diameter. They are installed in a column, and can be moved up and down by a stepper motor. The samples pictures are shown in Fig. 2 (a). In the experiment, a criterion is set, if the 200 meshes square Au grid is imaging clearly, it is considered that the parameters of the lens section is suitable for imaging, shown in Fig. 2 (b). The other experiments can be taken under these conditions.

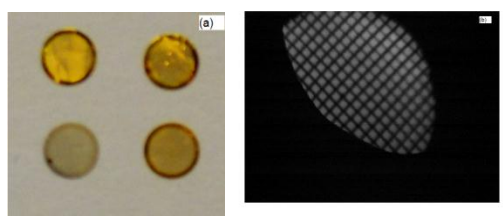


Figure 2: the picture of the samples (a) and the image of 200 mesh Au grid (b).

Copyright © 2014 CC-BY-3.0 and by the respective authors

EXTRACTING SUPERCONDUCTING PARAMETERS FROM SURFACE RESISTIVITY BY USING INSIDE TEMPERATURES OF SRF CAVITES*

M. Ge#, G. Hoffstaetter, V. Shemelin, M. Liepe, Cornell University, Ithaca, NY, 14853, USA
H. Padamsee, Fermilab, Batavia, IL, 60510, USA

Abstract

The surface resistance R_s of an RF superconductor depends on the surface temperature T_{in}, the residual resistance R_0 and various superconductor parameters, *e.g.* the energy gap and the electron mean free path. These parameters can be determined by measuring the quality factor Q_0 of a SRF cavity in helium-baths of different temperatures. The surface resistance can be computed from Q_0 for any cavity geometry, but it is not trivial to determine the temperature T_{in} of the surface when only the temperature of the helium bath is known.

Traditionally, it was approximated that the surface temperature on the inner surface of the cavity was the same as the temperature of the helium bath. This is a good approximation at small RF-fields on the surface, but to determine the field dependence of R_s, one cannot be restricted to small field losses.

Here we show the following: (1) How computer simulations can be used to determine the inside temperature T_{in} so that $R_s(T_{in})$ can then be used to extract the superconducting parameters. The computer code combines the well-known programs, the HEAT code and the SRIMP code. (2) How large an error is created when assuming the surface temperature is the same as the temperature of the helium bath? It turns out that this error can be more than 10% at high RF-fields in typical cases.

INTRODUCTION

The surface resistance R_s of superconductors under an RF-field is a function of the temperature on the RF surface. In the case of a standing-wave resonator, this is the inner surface of an SRF cavity. To determine R_s, the quality factor Q_0 has traditionally been measured in a series of the helium-bath temperatures at low RF-fields, usually around 3-5MV/m. It was typically approximated that the inner temperature was equal to the bath temperature at these low fields. By fitting superconductor parameters in an equation for $R_s(T_{in})$ to the data, quantities like the energy gap, the residual resistance, the electron mean free path *etc.* have been obtained.

Superconductivity theories [1-4] describe the performance of superconductors under low magnetic-field ($H_{RF} \ll H_c$), whether it can be extended to the high RF-fields is unclear [5, 6]. In [7], an effort has been made to empirically establish the relation between the superconducting parameters and the magnetic field by fitting $R_s(T_{in})$ curves to data that was obtained with high RF-fields. This was done up to 100-120mT on the surface, which corresponds to 25-30MV/m accelerating gradient. For such high fields, it is no longer accurate to approximate the inner temperature by the bath temperature [8-10].

This paper demonstrates a method of computing the inner temperature from the bath temperature T_{bath} and the RF-field (the peak magnetic field H_p or the accelerating gradient E_{acc})[1], so that the correct relation between the surface resistance and the inner temperature can be established at each RF-field.

This paper simulates a 120°C baked case with the energy gap 1.51 (eV×10^{-3}), corresponding to $\frac{\Delta}{kT_c} = 1.9$,[2] which error is the minimum case. But it turns out that in typical cases of the high gradient region, the superconductor parameters obtained by fitting $R_s(T_{in})$ can differ by more than 10% from those obtained by the traditional method of approximating T_{in} as the bath temperature. In the high-field region it can therefore often be important to apply the here presented, improved method.

THE FITTING METHODS OF $R_S(T)$ CURVES

The surface resistance of superconductors under RF-fields includes two parts, one is the BCS resistance R_{BCS} and the other part is the residual resistance R_0 shown in Eq. (1). Eq. (2) is the approximate expression of the surface resistance from the BCS theory [5]:

$$R_s = R_{BCS} + R_0, \quad (1)$$

$$R_{BCS} = A\left(\frac{1}{T_{in}}\right) f^2 \exp\left(-\frac{\Delta}{kT_{in}}\right). \quad (2)$$

Here, T_{in} is the temperature on inner surface, the factor A is a constant which is determined by material properties *e.g.* the electron mean free path l_e *etc.*; Δ is the energy gap; f is the resonant frequency of the cavity. Eq. (1) and (2) have been widely used for fitting $R_s(T_{bath})$ at low fields to extract the residual resistance, A, and Δ.

A better fitting method is based on the SRIMP code. The SRIMP code which incorporates the full BCS theory was written by Jurgen Halbritter [11, 12] for BCS-resistance calculations.

Traditionally, both fitting methods introduced above don't consider the temperature difference between the inside and the bath temperature. The temperature difference relates to the RF-power, hence it can be written as a function of the peak magnetic fields H_p and the surface resistance $R_s(T_{in})$ of the cavity. The ratio of the peak magnetic field H_p and the accelerating gradient E_{acc}

*Work supported by NSF award PHY-0969959 and DOE award DOE/SC00008431
#mg574@cornell.edu

[1] The ratio of E_{acc} and H_p is a constant.

[2] $\frac{\Delta}{kT_c}$ is used to express the energy gap in this paper.

Copyright © 2014 CC-BY-3.0 and by the respective authors

COOL DOWN AND FLUX TRAPPING STUDIES ON SRF CAVITIES*

Dan Gonnella† and Matthias Liepe, Cornell University, Ithaca, NY, USA

Abstract

Recent results from Cornell and FNAL have shown that cool down rate can have a strong impact on the residual resistance of a superconducting RF cavity during operation. We have studied the effect of cool down rate, gradient, and external magnetic field during cool down on the residual resistance of an EP, EP+120°C baked, and nitrogen-doped cavities. For each cavity, faster cool down and large gradient resulted in lower residual resistance in vertical test. The nitrogen-doped cavities showed the largest improvement with fast cool down, while the EP+120°C cavity showed the smallest. The cavities were also placed in a uniform external magnetic field and residual resistance was measured as a function of applied field and cool down rate. We show that the nitrogen-doped cavity was the most susceptible to losses from trapped flux and the EP+120°C cavity was least susceptible. These measurements provide new insights into understanding the physics behind the observed impact of cool down rates and gradients on the performance of cavities with differing preparations.

INTRODUCTION

New light sources such as the SLAC Linac Coherent Light Source II (LCLS-II) require the operation of SRF cavities in CW mode [1]. In order to achieve this, the cavities must have a very high intrinsic quality factor (Q_0). A major limitation on cavity performance is the ambient magnetic field present in the vicinity of the cavity during cool down through T_c. When a material transitions from normal conducting to superconducting, some of hte ambient field gets trapped in the superconductor, causing RF losses [2]. Importantly, the cool down procedure has also been shown to have a strong effect on cavity performance [3–5]. It is therefore important to understand the effect of magnetic field and cool down procedure on cavity performance in order to properly design cryomodules for future machines. Previously a study at Cornell showed that nitrogen-doped cavities are much more susceptible to increased residual resistance from trapped magnetic field and slow cool down than standard EP and 120°C baked cavities [3]. This paper discusses an expansion of this previous study in which 6 additional cavities (for a total of 8) were studied. In total, 6 nitrogen-doped cavities, an EP cavity, and an EP+120°C baked cavity were studied. These measurements provide new insights into the susceptibility to RF losses from trapped flux and its significant dependence on cavity surface preparation.

* Work supported by NSF Grants U828706 and U558307
† dg433@cornell.edu

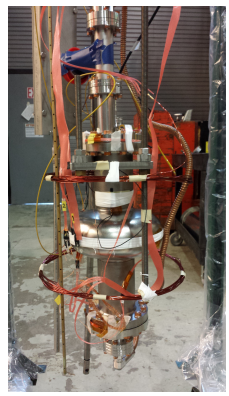


Figure 1: The experimental setup showing cavity, coil for applying magnetic field, fluxgate magnetometers, and temperature sensors.

EXPERIMENTAL METHOD

Seven single-cell 1.3 GHz ILC shaped cavities were prepared with different methods. Five of them (constructed at Cornell) were prepared with nitrogen-doping in the method outlined in [6]. The sixth cavity was prepared with nitrogen-doping at FNAL (heat treatment at 800°C in vacuum followed by 20 minutes in 20 mTorr of nitrogen followed by an additional 30 minutes in vacuum and finally a 7 μm final EP). The seventh cavity was first prepared with EP and 120°C bake and then retreated with just final EP but no 120°C bake. Each cavity was cooled through T_c in a variety of applied uniform external magnetic fields and with different cool down rates. The equipment and method is outlined in [3]. A picture of the experimental setup is shown in Fig. 1. The cavities were surrounded by a coil for applying magnetic field and affixed with three temperatures sensors, one on the bottom flange, one on the equator, and one on the top flange. A fluxgate magnetometer was also affixed to the iris just above the cell for measuring applied field and trapped flux. For each cavity and each cool down, cool down rate and gradient over the cavity were measured in addition to the trapped flux from the external field and the residual resistance (extracted from Q_0 vs temperature data with SRIMP [7]).

EFFECT OF EXTERNAL FIELD

For each cavity and cool down, the applied magnetic field and cool down rate was tuned. By adjusting these parameters, the amount of trapped flux could also be tuned. Figure 2 shows the measured residual resistance as a function of trapped magnetic flux for all eight cavities. Also included is a linear fit for each cavity. We can see that the EP and EP+120°C bake cavities have significantly less susceptibility to residual losses from trapped flux than the six nitrogen doped cavities. Moreover, the more doped a nitrogen-doped

Copyright © 2014 CC-BY-3.0 and by the respective authors

ISBN 978-3-95450-142-7

NITROGEN-DOPED 9-CELL CAVITY PERFORMANCE IN THE CORNELL HORIZONTAL TEST CRYOMODULE*

D. Gonnella†, R. Eichorn, F. Furuta, M. Ge, D. Hall, Y. He, G. Hoffstaetter, M. Liepe, T. O'Connell, S. Posen, P. Quigley, J. Sears, and V. Veshcherevich, Cornell University, Ithaca, NY, USA
A. Grassellino and A. Romanenko, FNAL, Batavia, IL, USA

Abstract

Cornell has recently completed construction and qualification of a horizontal cryomodule capable of holding a 9-cell ILC cavity. A nitrogen-doped niobium 9-cell cavity was assembled into the Horizontal Test Cryomodule (HTC) with a high Q input coupler and tested. We report on results from this test of a nitrogen-doped cavity in cryomodule and discuss the effects of cool down rate and thermal cycling on the residual resistance of the cavity.

INTRODUCTION

SLAC is currently developing a superconducting CW light source, LCLS-II. In order for economic feasibility in CW operation, superconducting RF cavities in the main linac must achieve an average intrinsic quality factor (Q_0) of 2.7×10^{10} at 16 MV/m and 2.0 K [1]. Nitrogen-doping of niobium cavities has been proposed to meet this high Q specification [2, 3]. In order to test the feasibility of these goals, a 1.3 GHz ILC shaped 9 cell cavity was dressed and placed in the Cornell Horizontal Test Cryomodule (HTC). The HTC has previously been used to test a 7 cell Cornell ERL cavity [4]. In this paper we discuss the results of the first nitrogen-doped 9 cell cavity tested in a cryomodule.

METHOD

The Cornell HTC has been modified to hold a standard 9 cell ILC cavity. A schematic of the HTC with 9 cell cavity is shown in Fig. 1. The HTC accepts a cavity that is dressed with helium tank. A high Q input coupler with $Q_L \approx 4\times10^{10}$ was used. The cavity was prepared with Nitrogen-doping at FNAL. It was given a bulk treatment of CBP and EP followed by a heat treatment at 800°C in vacuum for 3 hours followed by 20 minutes in 25 mTorr of nitrogen followed by an additional 30 minutes in vacuum. Finally it was given a final EP of 18 microns, dressed in a liquid helium tank at FNAL, and assembled in the cryomodule at Cornell.

Cavity performance was measured for a variety of cool downs. For each cool down, Q_0 vs E was measured at 1.6, 1.7, 1.8, 1.9, 2.0, and 2.1 K. Additionally, Q_0 vs E was measured for the additional TM010 modes at 2.0 K. After all of these measurements were completed, the quench field was measured at 2.0 K for all TM010 modes. For one cool down, resonance frequency vs temperature was measured during warm-up and Q_0 vs temperature was measured between 1.6 and 4.2 K. This data was used with SRIMP to extract material properties for the cavity [5, 6].

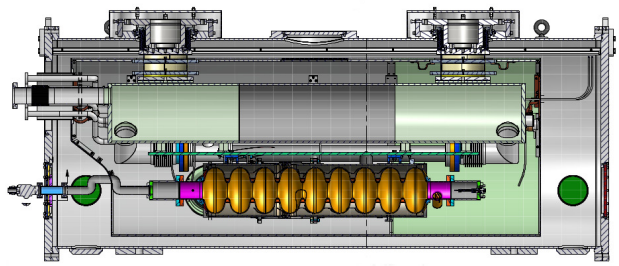


Figure 1: A schematic of the Cornell HTC with 9 cell cavity.

COOL DOWNS AND Q_0 VS E PERFORMANCE

Cool Down Dynamics

A total of four cool downs were performed (motivated by [4, 7, 8]): three fast (dT/dt>1 K/min) cool downs and one slow (dT/dt<1 K/min). The dynamics are summarized in Table 1, along with the residual resistance for each cool down. $\frac{dT}{dt}$ is the rate of cool down near T_c and ΔT_{cavity} is the largest temperature gradient across the cavity when it transitions from normal conducting to superconducting. Note that the R_{res} measured for the first fast cool down was after many quenches.

Table 1: Summary of Cool Down Dynamics

Cool Down	$\frac{dT}{dt}$ [K/min]	ΔT_{cavity} [K]	R_{res} [nΩ]
Fast 1	5	5	5 ± 1
Fast 2	7	3	4.0 ± 0.8
Slow 1	0.04	0.3	5 ± 1
Fast 3	5	20	2.7 ± 0.5

A profile of the fourth (fast 3) cool down is shown in Fig. 2. Temperature sensors were fixed inside the helium tank to the tops and bottoms of cells 1 and 5 and the top of cell 9. Additionally, two fluxgate magnetometers were attached to either side of cell 5, one to measure field perpendicular to the cavity axis, and one to measure field parallel to the cavity axis. From Fig. 2, we can see that below 100 K, the cavity cools from the bottom first (cells 1 and 5) followed by the tops of cells 1 and 5, while the top of cell 9 takes longer to cool. These large temperature gradients will induce thermal currents along the cavity and liquid helium tank and

* Work supported by the US DOE and the LCLS-II Project
† dg433@cornell.edu

Copyright © 2014 CC-BY-3.0 and by the respective authors

Nb_3Sn MATERIALS STUDIES*

S. Posen†, M. Liepe
Cornell Laboratory for Accelerator-Based Sciences and Education, Ithaca, NY 14853, USA
T. Proslier, ANL, Argonne, IL 60439, USA

Abstract

Nb_3Sn is a very promising material for use in SRF cavity applications, potentially offering significant improvements in quality factor and energy gradient compared to niobium. In order to better understand how to optimize this material for SRF applications, Nb_3Sn samples were prepared at Cornell via vapor deposition, using varying parameters in the coating process. Microscopic studies were performed with SEM/EDX, and studies were performed on bulk samples to measure secondary electron yield, energy gap, and upper critical magnetic field. The results are presented here, with discussion for how they might point the way towards reaching even higher fields in Nb_3Sn cavities.

INTRODUCTION

Nb_3Sn is a material with great potential for SRF applications, offering large potential gains in quality factor and energy gradient compared to niobium due to its large critical temperature T_c and predicted superheating field [1]. At Cornell, infrastructure has been developed to coat single cell 1.3 GHz niobium SRF cavities with Nb_3Sn using the vapor deposition technique, as described in [2]. The first cavities produced have had very promising RF performances, achieving quality factors above 10^{10} at 4.2 K and 13 MV/m [3]. In order to push performance further, it is important to better understand this material. Its superconducting behavior is determined by its properties on the length scale of the coherence length (approximately 3-4 nm) and the penetration depth (approximately 100 nm), so it must be examined on this scale in order to make correlations to its SRF properties. In this paper, we present the results of both bulk and microscopic studies of Nb_3Sn samples designed to better understand and improve the material and the fabrication process.

SEM/EDX AFTER NORMAL COATING

The standard coating process (including annealing step discussed in [3]) produces Nb_3Sn grains with size of approximately 2 μm on top of the much larger niobium grains. Figure 1 shows the Nb_3Sn surface imaged by SEM with a tilt of 52 degrees to show the texture. There are flat facets visible in many grains, as well as smooth curves, and many of the grains have what appear to be indented regions near the middle. EDX scans performed in several regions show a stoichiometry of 24±1 atomic percent tin.

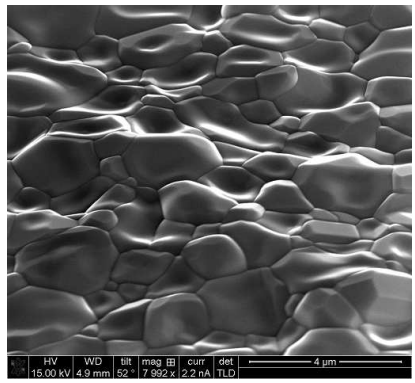


Figure 1: Nb_3Sn surface after coating with the standard recipe. The sample is tilted at 52 degrees with respect to the detector to highlight three dimensional features.

SEM/EDX WITH LG SUBSTRATES

Several small samples were fabricated for experimenting with different Nb_3Sn coating conditions, including some made from large grain niobium. After coating, these samples showed some structures not observed on fine grain niobium. SEM images show the 1-2 μm sized grains usually observed along with localized "clumps." These regions, which appear as dark areas with size on the order of 10 μm, have a lower tin content, as measured by EDX, by up to 10 atomic percent. Two images taken from samples coated without the usual nucleation agent, $SnCl_2$, are shown in Fig. 2 (these structures are also observed on LG samples when coating with $SnCl_2$).

In RF measurements of cavities, a dramatic reduction in Q-slope was observed after an annealing step was added, indicating that the grain structure may strongly influence RF properties. Therefore, studies like this are important to understand how the substrate and coating process influence the grain structure.

SEM/EDX BEFORE/AFTER HF RINSE

For the first time, a niobium cavity with an electropolished surface was coated with Nb_3Sn, and EP samples were coated with it. An SEM image is seen in Fig. 3. The sample was later given 5 cycles of HF rinsing, the same treatment given to a cavity that caused it to have strong Q-slope. SEM of the HF-rinsed surface showed unusual structures on top of the Nb_3Sn grains, which might be the source of the extra losses. EDX was used to probe the structures, but no sign of contamination was measured, and no change in atomic

* Work supported by NSF Career award PHY-0841213 and DOE award ER41628. This work made use of the Cornell Center for Materials Research Shared Facilities which are supported through the NSF MRSEC program (DMR-1120296).
† sep93@cornell.edu

Copyright © 2014 CC-BY-3.0 and by the respective authors

INPUT COUPLERS FOR CORNELL ERL*

R. Eichhorn, P. Quigley, and V. Veshcherevich†
Cornell University, Ithaca, NY 14853, U.S.A.
S. Belomestnykh, BNL, Upton, Long Island, New York, USA

Abstract

Cornell has developed two types of coaxial input couplers for the Energy Recovery Linac (ERL) Project. Both couplers are 1.3 GHz CW coaxial couplers. The coupler for ERL injector is a 65 kW CW coupler with variable coupling (Q_{ext} = 9×10^4 to 9×10^5). The coupler for ERL main linac is a 5 kW CW coupler with fixed coupling. It can be easily modified for variable coupling operation. Couplers have been tested on test stands and in cryomodules and showed good performance.

INTRODUCTION

Cornell University wants to build a hard X-ray light source driven by an Energy Recovery Linac (ERL). The proposed Cornell ERL will operate in CW at 1.3 GHz, 2 ps bunch length, 100 mA average current in each of the accelerating and decelerating beams, normalized emittance of 0.3 mm-mrad, and energy ranging from 5 GeV down to 10 MeV, at which point the spent beam is directed to a beam stop [1, 2].

Cornell has already built and commissioned a short ERL injector prototype and continues to test it and improve its performance. The injector consists of a DC photoemission electron gun, a buncher, and an accelerating cryomodule. The injector cryomodule houses five (twelve for full ERL injector) 2-cell superconducting cavities. Each cavity has two symmetrically placed coaxial input couplers.

Now Cornell is building a prototype cryomodule of the main linac. An ERL main linac cryomodule (MLC) is 9.8 m long and houses six 7-cell superconducting cavities [3]. Each cavity has a single coaxial RF input coupler.

INJECTOR COUPLER

Each 2-cell injector cavity is equipped with two symmetrically placed coaxial input couplers (Figure 1). That allows to reduce the RF power for each coupler and dramatically decrease the transverse kick from the coupler which is essential for the ERL injector.

The parameters of the injector coupler are summarized in Table 1. The design of the coupler is based on the TTF-III coupler design [4]. It was significantly modified to comply with the ERL injector requirements. The main challenges were strong coupling, wide range of coupling adjustment and high CW power. The design of the injector coupler [5] is shown in Figure 2.

The coupler has a large Pringles-shaped antenna tip, large diameter of cold coaxial line, large size of the cold ceramic window. For reducing overheating of bellows that are parts of the design, the bellows in outer conductors of the coaxial lines are subdivided in two sections with heat intercepts between the sections; the

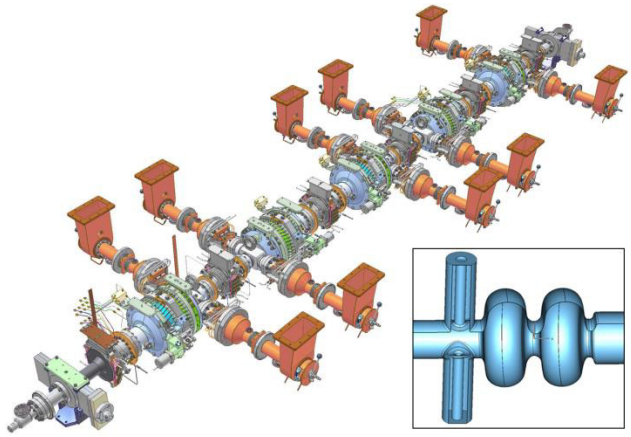


Figure 1: Injector cavities with input couplers.

Table 1: Parameters of ERL Injector Coupler

Central frequency	1300 MHz
Bandwidth	±10 MHz
Maximum CW RF power transferred to matched load	65 kW
Number of ceramic windows	2
Q_{ext} range	9×10^4 to 9×10^5
Cold coaxial line impedance	60 Ω
Warm coaxial line impedance	46 Ω
Coaxial line OD	62 mm
Antenna stroke	≥15 mm
Heat leak to 2 K	<0.2 W
Heat leak to 5 K	<3 W
Heat leak to 80 K	<75 W

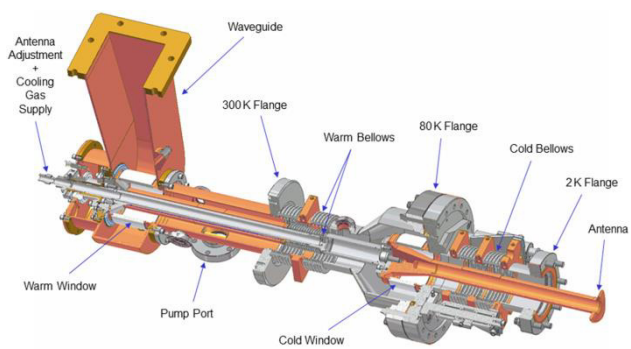


Figure 2: Injector coupler design.

* Work is supported by NSF Grants NSF DMR-0807731 and NSF PHY-1002467.
† vgv1@cornell.edu

Copyright © 2014 CC-BY-3.0 and by the respective authors

ISBN 978-3-95450-142-7

XFEL CRYOMODULE TRANSPORT: FROM THE ASSEMBLY LABORATORY IN CEA-SACLAY (FRANCE) TO THE TEST-HALL IN DESY-HAMBURG (GERMANY)

S. Barbanotti#, K. Jensch, W. Maschmann, O. Sawlanski, DESY, Hamburg, Germany

Abstract

The one hundred, 12 m long XFEL 1.3 GHz cryomodules are assembled at CEA Saclay (F) and have therefore to be transported, fully assembled, to the installation site in DESY Hamburg (D). Various studies and tests have been performed to assess and minimize the risk of damages during transport; a new transport frame and a specialised company are being used for the series transport. This paper resumes the studies performed, describes the final configuration adopted for the series transport and the results obtained for the first XFEL modules.

INTRODUCTION

An industrialization study performed on the XFEL cryomodule production and installation highlighted a critical point in the cryomodule transport between the assembly site in CEA Saclay and the installation site at DESY Hamburg.

The study reports a critical acceleration value of 1.5 g for the vertical and longitudinal directions (risks of coupler damages) and a limit value of 1 g in the transverse direction (45° inclination of the cold mass).



Figure 1: Cryomodule being prepared for transport.

A first transport frame (figure 1) was therefore designed, a test transport of an assembled cryomodule was done and a set of measurements was performed to verify the tooling and record the maximum accelerations. These tests have been reported in [1].

Since then, further transports of the XFEL prototype modules highlighted some criticality in the frame design and some modifications were necessary. A second transport frame was built and a new transport test was performed. The series transport was organised together with the shipping company and more than 10 modules have been transported to DESY up to now. This paper resumes the work done since the publication of the first results in 2009.

#serena.barbanotti@desy.de

XFEL TRANSPORT SYSTEM

The cryomodule is supported with a metallic frame consisting of two cages, one fixed to the truck and the other damped with helical coils in a compression-roll configuration connected to the cryomodule.

The supporting system includes two end-caps to lock the helium gas return pipe at the end position and to avoid transversal movement of the supporting posts.

The module is equipped with vacuum gauges to monitor the beam vacuum and 2 synchronised accelerometers to record the acceleration experienced by the module and evaluate the frame damping factor (one sensor on the fixed frame and one on the damped one).

RESULTS OF THE TRANSPORT WITH THE FIRST FRAME DESIGN

The following cryomodules were transported with the first frame: the FLASH cryomodule n. 8 (a so called TTF type 3+ module, M8) and 2 XFEL prototype cryomodules PXFEL2 and PXFEL3_1. The maximum values of the acceleration measured during the trip are summarised in table 1.

The transport of Module 8 and PXFEL3_1 present acceleration values on the inner frame below the limit of 1.5 g, while the values recorded during the transport of PXFEL3_1 triggered some further investigation (see trip summary in figure 2) [2].

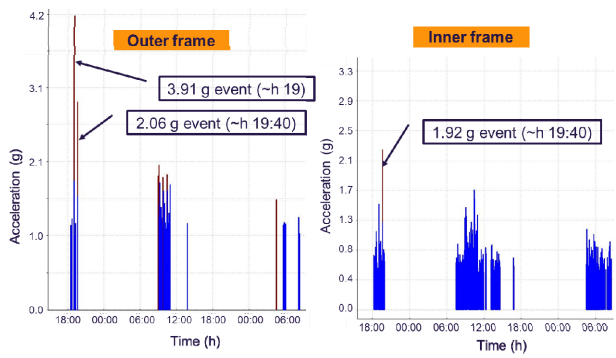


Figure 2: Event summary on PXFEL3_1.

The first event (almost 4g), although the higher-than-usual values, presents at further investigation a normal behaviour. The second event shows instead a not-so-high value on the outer frame (2.06 g), but at the same time the acceleration on the inner frame is equal to 1.92 g. The details of the vertical acceleration aZ for this event are presented in figure 3. The image shows that almost no damping happened between the inner and outer frame and

Copyright © 2014 CC-BY-3.0 and by the respective authors

ISBN 978-3-95450-142-7

X-BAND TECHNOLOGY FOR FEL SOURCES

G. D'Auria, S. Di Mitri, C. Serpico, Elettra-Sincrotrone Trieste, Italy.
N. Catalan-Lasheras, A. Grudiev, A. Latina, D. Schulte, S. Stapnes, I. Syratchev, W. Wuensch, CERN, Geneva, Switzerland.
A. Aksoy, Ö. Yavaş, Institute of Accelerator Technologies, Ankara, Turkey.
M. J. Boland, T. Charles, R. Dowd, G. LeBlanc, Y.-R. E. Tan, K. P. Wootton, D. Zhu, Australian Synchrotron, Clayton, Australia.
D. Angal-Kalinin, J. Clarke, STFC, Daresbury Laboratory Cockcroft Institute, Daresbury, UK.
M. Jacewicz, R. Ruber, V. Ziemann, Uppsala University, Uppsala, Sweden.
W. Fang, Q. Gu, Shangai Institute of Applied Physics, Shanghai, China.
E. N. Gazis, National Technical University of Athens, Greece.
C. J. Bocchetta, A. Wawrzyniak, Solaris, Jagiellonian University, Krakow, Poland.
E. Adli, University of Oslo, Norway.
G. Burt, Lancaster University, Lancaster, UK.
X.J.A. Janssen VDL ETG T&D B.V., Eindhoven, Netherlands.

Abstract

As is widely recognized, fourth generation Light Sources are based on FELs driven by Linacs. Soft and hard X-ray FEL facilities are presently operational at several laboratories, SLAC (LCLS), Spring-8 (SACLA), Elettra-Sincrotrone Trieste (FERMI), DESY (FLASH), or are in the construction phase, PSI (SwissFEL), PAL (PAL-XFEL), DESY (European X-FEL), SLAC (LCLS II), or are newly proposed in many laboratories. Most of the above mentioned facilities use NC S-band (3 GHz) or C-band (6 GHz) linacs for generating a multi-GeV low emittance beam. The use of the C-band increases the linac operating gradients, with an overall reduction of the machine length and cost. These advantages, however, can be further enhanced by using X-band (12 GHz) linacs that operate with gradients twice that given by C-band technology. With the low bunch charge option, currently considered for future X-ray FELs, X-band technology offers a low cost and compact solution for generating multi-GeV, low emittance bunches. Furthermore, X-band accelerating structures are also becoming widely used for extremely high brilliance e-sources, beam phase space manipulation and very accurate beam diagnostics.

The paper reports the ongoing activities in the framework of a collaboration among several laboratories for the development and validation of X-band technology for FEL based photon sources.

INTRODUCTION

Applications of X-band technology is rapidly expanding due to its great potential already shown in different areas of particle accelerators. Early studies on accelerating structures operating at 11.4 GHz were made at SLAC/KEK, in the last two decades of the last century (up to 2004), for the development of a TeV-scale high energy Linear Collider, and led to achieve 65-70 MV/m accelerating gradients [1]. Later, significant progress have been achieved by the CERN CLIC (Compact Linear Collider) Collaboration, that has recently demonstrated the possibility to operate 12 GHz accelerating structures with an average loaded gradient higher than 100 MV/m [2], values far beyond those reached with the present S and C band technology. These results suggest that the X-band may represent a useful solution to get very compact and cost effective linacs for multi-GeV electron beams. Considering operation at the above mentioned gradients, a 1 GeV X-band linac can be easily housed in less than 20 m, a very attractive solution even for application with a limited space availability [3]. More recently, after the successful operation of the new FEL light sources like LCLS, SACLA, FERMI, a stronger and more vigorous interest in X-band technology has arisen.

The demand for new FEL facilities is worldwide continuously increasing, spurring plans for new dedicated machines [4]. This led to a general reconsideration of costs and spatial issues, particularly for the hard X-ray sources, driven by long and expensive multi-GeV NC linacs. For these machines the use of X-band technology can greatly reduce cost and capital investment, reducing the linac length and the size of buildings. To pursue these objectives, a scientific collaboration has recently been established among several laboratories, interested in FEL developments, aimed at validating the use of X-band technology for FEL based light sources [5]. Other Institutions, like CERN, with no specific interest in FEL physics, are within the collaboration for its positive impact on the CLIC project. The specific objectives of the collaboration will include the design, assembly and high power tests of an X-band accelerating module for FEL applications, made up of two accelerating structures, RF pulse compression and a waveguide distribution systems. Special care will be given to the operating gradients, RF breakdown fault rate, alignment issues, wake fields, and operation stabilities. The overall objective of the collaboration is to support the feasibility studies of new research infrastructures and/or the major upgrading of existing ones, using X-band technology. The work program foresees a strong interaction between FEL scientists, FEL designers and accelerator experts. Starting from the FEL output specification, a fully self consistent FEL facility design will be established (in terms of

Copyright © 2014 CC-BY-3.0 and by the respective authors

ISBN 978-3-95450-142-7

PERSPECTIVES OF THE S-BAND LINAC OF FERMI

A. Fabris#, P. Delgiusto, M. Milloch, C. Serpico, Elettra-Sincrotrone Trieste S.C.p.A., Trieste, Italy
A. Grudiev, CERN, Geneva, Switzerland

Abstract

The S-band linac of FERMI, the seeded Free Electron Laser (FEL) located at the Elettra laboratory in Trieste, has reached the peak on-crest electron energy of 1.55 GeV required for FEL-2 with the present layout. Different ways are being considered to extend the operating energy of the S-band linac up to 1.8 GeV. At the same time upgrades on the existing systems are investigated to address the requirements of operability of a users facility. This paper provides an overview of the developments that are under consideration and discusses the requirements and constraints for their implementation.

INTRODUCTION

FERMI, the Italian seeded FEL facility located in Trieste, consists of two FEL lines. FEL-1, covering the wavelength between 100 and 20 nm, is already open to external users. FEl-2, covering the shorter wavelength range down to 4 nm, will be opened to external users in the next calls for proposals [1]. The linac is based on warm S-band technology and it is presently composed of fifteen 3 GHz 45 MW peak RF plants powering sixteen accelerating structures, the gun and the RF deflectors.

BRIEF OVERVIEW OF THE S-BAND RF SYSTEM OPERATION

After the conditioning periods dedicated in August 2013, the on-crest electron energy has reached 1.55 GeV [2], which means achieving the design 1.5 GeV operating energy once losses for chirp compensation and linearization by deceleration in the fourth harmonic X-band cavity are taken into account. Operating energy is actually set according to the requirements for users' experiments. The working points of the structures are fixed to the maximum gradient achievable for a reliable operation. When less beam energy is required, some of the last structures are set off-line providing the redundancy that is very useful to ensure the operation for the users. Although presently the repetition rate of the machine is 10 Hz, operation at 50 Hz of the modulators has been validated on long time period (few months). Klystron peak power is typically in the range between 32 and 36 MW. Uptime of the S-band system during users period in 2013 has been 93.5 % with klystron arcs accounting for the major number of faults.

After these first years of commissioning and operation, possible developments have been analysed to correct the major downtime sources, increase safety margins and redundancy and extend operating margins of the machine especially in terms of peak energy.

#alessandro.fabris@elettra.eu

ACCELERATING STRUCTURES

The machine is composed of three types of accelerating structures. After the gun, the first two are 3.2 m long forward travelling wave (FTW) used in the old Elettra injector. These are followed by seven 4.5 m long LIL type FTW structures, donated by CERN, and by seven 6.1 m long backward travelling wave (BTW) SLED equipped structures from the old Elettra injector.

New Accelerating Structures

The layout of the machine reserves space and availability of power outputs from the klystrons along the linac for two additional 3.2 m long structures. Being the same length of the first two structures, this gives the opportunity to replace these two structures with new ones optimised for the needs in the injector part of the linac. The structures presently in operation will be then relocated along the machine in the space available.

The new structures will be FTW, $2\pi/3$, constant gradient, disk loaded and with minimised phase and amplitude asymmetries in the coupler cells, to minimize the induced kick on the beam. The main design parameters are listed in Table 1 [3]. The structures will be built by RI Research Instruments GmbH. Delivery is planned in Spring 2015, followed by high power RF conditioning in the test stand, expected to take place in summer 2015. Considering the FERMI schedule, installation in the machine is expected in the first months of 2016. These two structures will provide additional 100 MeV to the energy budget.

Table 1: Requirements for the new accelerating structures

Parameter	Value
Working frequency	2998.01 MHz
Maximum input	25 MW
Maximum pulse duration	5 μs
Maximum repetition rate	50 Hz
Filling time	< 1.5 μs
Q factor	>13000
Target shunt impedance	> 60 MΩm^{-1}
Energy gain@16 MW	> 48 MeV
Input coupler type	symmetric 180 degree

New Accelerating Modules

The last part of the linac is based on the already available 6.1 m long BTW structures from the old Elettra injector. These structures are made up of magnetic

Copyright © 2014 CC-BY-3.0 and by the respective authors

ISBN 978-3-95450-142-7

LONGITUDINAL BEAM PROFILE MEASUREMENTS IN LINAC4 COMMISSIONING

G. Bellodi, V. A. Dimov, J-B. Lallement, A. M. Lombardi, U. Raich, F. Roncarolo, F. Zocca
(CERN, Geneva)
M. Yarmohammadi Satri (IPM, Tehran)

Abstract

Linac4, the future 160 MeV H- injector to the CERN Proton Synchrotron Booster, is presently under construction at CERN as a central step of the planned upgrade of the LHC injectors. The Linac front-end, composed of a 45 keV ion source, a Low Energy Beam Transport (LEBT), a 352.2 MHz Radio Frequency Quadrupole (RFQ) and a Medium Energy Beam Transport (MEBT) housing a beam chopper, has been installed and commissioned. Precise measurements of the longitudinal micro bunch profiles of ion beams were possible with the help of a Bunch Shape Monitor (BSM) developed at INR Moscow. These were crucial for the successful commissioning of the three RF buncher cavities mounted along the MEBT and well complemented with higher precision the information provided in parallel by spectrometer measurements.

INTRODUCTION

Linac4 commissioning started in 2013 and is progressing in stages of increasing beam energy with the aim of reaching the final 160 MeV at the end of 2015 [1]. The accelerator front-end, composed of a temporary ion source, LEBT, RFQ and MEBT line was first commissioned on a dedicated test stand at the start of 2013 [2] before being moved to its final location in the underground tunnel in summer 2013. A 10-12 mA H- beam was used for the measurements detailed below.

Longitudinal beam measurements were taken on a moveable temporary test bench installed downstream of the machine (see Fig.1). On the straight arm of the bench there are three pick-ups (BPMs) for beam position and Time-Of-Flight-based energy measurements and a Feschenko/Bunch Shape Monitor (BSM), all to be later used permanently as in-line diagnostics devices. Validation of their performance during commissioning at low energy was done with the aid of a spectrometer line branching off after the BSM and ending in a harp monitor. This was used in particular during calibration of the RF structures for measuring the beam average energy and energy spread. The precise beam longitudinal characterisation thus obtained was instrumental to a full validation of the RFQ performance and of a correct beam injection in the DTL.

DIAGNOSTICS

The positioning and separation between BPMs was chosen to ensure a resolution of ~0.1% in the average energy measurements at 3 and 12 MeV. The spectrometer arm, formed by a 28.5° bending magnet and downstream

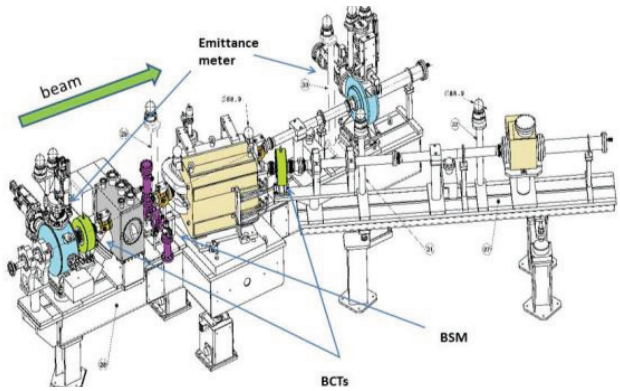


Figure 1: Test bench drawing.

Secondary Emission Monitor (SEM) grid (at ~3 m distance) has a momentum resolution of ~0.1%. The BSM installed at Linac4 was developed and built at INR Troitsk (Russia) [3]. As shown in Fig. 2, it consists of a 100 µm thick Tungsten wire which is inserted into the beam. Secondary electrons, created through the interaction of the primary beam with the wire, are accelerated away by a 9kV applied wire polarization. A fraction of the electrons travels through a slit to a deflector, to which an RF voltage of the same frequency as the bunch structure is applied. The electron beam is then steered and focused and finally amplified by an electron multiplier. The time structure of the secondary electrons being virtually identical to that of the primary H- beam, it is possible to measure the longitudinal intensity distribution by scanning through the beam pulse while changing the phase delays on the deflector. The BSM can characterize the full 400 µs pulse with a phase resolution of 1° covering the full phase range (180° at 352 MHz). The background due to stripped electrons is less than 1% of the total secondary emission from H- and the phase scan will provide one measurement point per beam pulse.



Figure 2: Photograph of the Bunch Shape monitor.

Copyright © 2014 CC-BY-3.0 and by the respective authors

ACTIVELY COOLED RF POWER COUPLER: THEORETICAL AND EXPERIMENTAL STUDIES

R. Bonomi[a,b], V. Parma[a] - [a]CERN, Geneva, Switzerland - [b] ESS, Lund, Sweden

Abstract

In cryostats for Superconducting Radio-Frequency Cavities, the heat loads introduced by the high-power RF couplers represent an important fraction of the overall static thermal budget. Working at low temperature benefits from a reduced surface resistance (low dynamic losses) but is penalized by the high refrigeration cost. The external conductor of RF coaxial couplers provides a direct conduction path from ambient to cryogenic temperature plus is heated by resistive power deposition. Heat interception is therefore essential to contain heat in-leaks: a double-walled external conductor with a properly designed gas cooling effectively reduces heat loads to the cold bath by one order of magnitude. This paper presents the thermal design of the RF power coupler of the Superconducting Proton Linac (SPL) at CERN, featuring a helium vapour cooling between 4.5 K and ambient temperature. Numerical models, which can be used as design tools for other applications, have been developed to assess efficiency and thermal performance. A full-size mock-up cooled by liquid nitrogen has been built for experimental validation. Comparison between calculations and measurements is presented and discussed.

INTRODUCTION

For superconducting (SC) cryostats devices, heat load management is fundamental to maintain low temperatures in the most efficient way. The very low operating temperature required by a SC device results in a high electrical power consumption; for example, each watt of thermal power at 2 K costs about 1'000 W electrical*.

The SPL Fundamental Power Coupler (FPC)

The SPL cryomodule (cross section in Fig. 1) is composed of four elliptical niobium 5-cells cavities, each powered by one coaxial fundamental power coupler[#] (FPC) [1]. The contribution of each FPC to the thermal budget is considerable, accounting for 97% of the static thermal load per cryomodule at 2 K *if the FPC is not cooled* [2]. As a consequence, effective FPC cooling is essential in the thermal management of the cryomodule.

Helium gas cooling, between 4.5 and 300 K, is the choice for the SPL FPC, through a double-walled external conductor where the gas flows from the cold side. Among the others, this solution is supposedly the most thermodynamically efficient, especially for very tight heat load requirements [3].

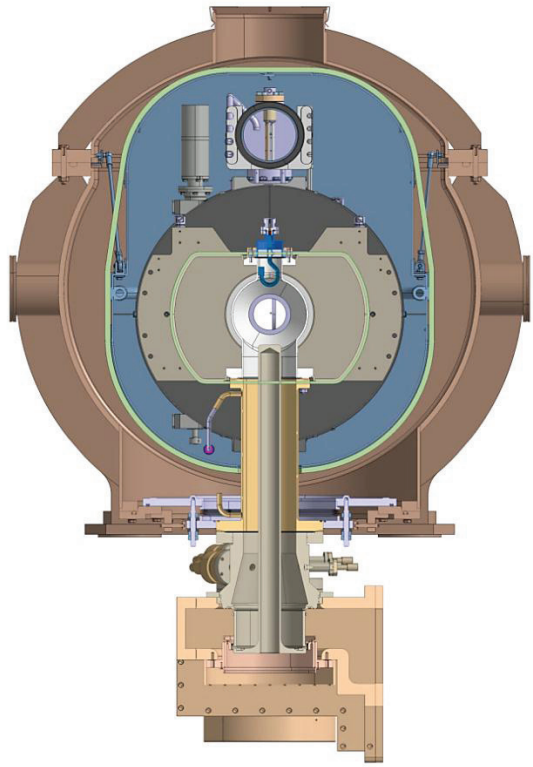


Figure 1: Cross section of the SPL cryomodule [1].

The total calculated refrigeration power required for a SPL-like FPC is reported in Table 1 for some common cooling methods. An optimised and adequately operated gas cooling (case 5) is highly effective, as it remains very close to the theoretical limit of the self-sustained cooling (case 2).

Table 1: Calculated refrigerator power for some SPL FPC cooling systems♦ (GHe: Gas Helium; boundary temperatures: 2-300 K)

Cooling Case	$P_{ref,tot}$ (kW_{el})	Ratio
(1) No cooling	12.2	15.2
(2) Self-sustained GHe cooling (19 mg/s)	0.8	1
(3) 1 heat intercept at 80K	2.8	3.5
(4) 2 heat intercepts at 9-80K	1.3	1.6
(5) 4.5K non isothermal GHe cooling (40 mg/s)	1.0	1.2

* Value obtained considering a state-of-the-art LHC-type cryogenic plant working at 15% of Carnot efficiency between 2-300 K.

[#] Design power for the SPL FPC: 1 MW peak (100 kW average).

♦ Efficiency at 50-80 K: 17 W/W (30% Carnot); efficiency at 4.5-9 K: 220 W/W (30% Carnot); efficiency at 2 K: 990 W/W (15% Carnot).
1 g/s helium at 4.5-300 K was considered equivalent to 100 W at 4.5 K [4].

Copyright © 2014 CC-BY-3.0 and by the respective authors

ISBN 978-3-95450-142-7

NEW CRITERION FOR SHAPE OPTIMIZATION OF NORMAL-CONDUCTING ACCELERATOR CELLS FOR HIGH-GRADIENT APPLICATIONS*

Kyrre Ness Sjobak† and Erik Adli (Department of Physics, University of Oslo, Norway)
Alexej Grudiev (CERN, Geneva, Switzerland)

Abstract

When optimizing the shape of high-gradient accelerating cells, the goal has traditionally been to minimize the peak surface electric field / gradient, or more recently minimizing the peak modified Poynting vector / gradient squared. This paper presents a method for directly comparing these quantities, as well as the power flow per circumference / gradient squared. The method works by comparing the maximum tolerable gradient at a fixed pulse length and breakdown rate that can be expected from the different constraints. The paper also presents a set of 120° phase-advance cells for traveling wave structures, which were designed for the new CLIC main linac accelerating structure, and which are optimized according to these criteria.

INTRODUCTION

One of the main challenges for the Compact LInear Collider (CLIC) [1] is the design of accelerating structures which are able to reach very high gradients for long enough pulse lengths to efficiently produce useful amounts of luminosity. Part of this is done by optimizing the overall design of the structure, such as its length, aperture and tapering while obeying constraints from beam dynamics and minimizing the total cost of the machine [2]. An important component of these calculations is the fast estimation of the RF parameters and breakdown constraints of a candidate accelerating structure [3]. These estimates are based on a database of pre-calculated accelerator cell geometries for a large number of different iris apertures and thicknesses [4]. The optimization of these cell geometries for maximizing the gradient for a given breakdown rate is the topic of this paper.

QUANTITIES FOR OPTIMIZATION

Traditionally, accelerating cavities where optimized using constraints on the peak surface electric field $\hat{E}$ [5], peak surface magnetic field $\hat{H}$, or more recently power flow constraints such as the averaged power flow through the cell by the iris aperture circumference P/C [6] or the peak modified Poynting vector $\hat{S}_c$ [7]. While the geometry parameters affecting $\hat{H}$ is often mostly orthogonal to the other constraints, the choice of which of the iris-dominated constraints $\hat{E}$, P/C or $\hat{S}_c$ to optimize for produces different geometries, as demonstrated in the next section.

* Work supported by the Research Council of Norway
† k.n.sjobak@fys.uio.no

However, the iris-dominated constraints can be directly compared by using the observed scaling relation [7] for the average accelerating gradient G, pulse length τ and the breakdown rate BDR

$$\frac{G^{30}\tau^5}{\mathrm{BDR}} = K \ , \tag{1}$$

where K is a scaling constant which varies between different structures. By scaling the achieved gradient G for different cavities to a set of standard conditions with breakdown rate $\mathrm{BDR}_0 = 10^{-6}$ breakdowns / pulse / structure length in meter and pulse length $\tau_0 = 200$ ns, the achievable gradient G' can be directly compared between different cavities.

Further, using FEM simulations of the accelerating mode in a given geometry, it is possible to calculate the ratios between the limiting factors and the average accelerating gradient as $\bar{E} \equiv \hat{E}/G$, $\bar{S}_c \equiv \hat{S}_c/G^2$ and also $(P/C)/G^2$. These ratios are independent of the field level. The normalized peak fields can then be applied to the re-scaled gradient G', yielding a comparison of the peak fields at a common breakdown rate BDR_0 and pulse length τ_0, as shown in Fig. 1.

From the data presented in Fig. 1 and using Eq. 1, an expression for the *breakdown index*

$$\kappa \equiv K^{1/5} = \left(\frac{G^{30}\tau^5}{\mathrm{BDR}}\right)^{1/5} = \frac{G^6\tau}{\mathrm{BDR}^{1/5}} \tag{2}$$

can be defined for each of the limiting factors. For a given geometry, three breakdown indexes κ_E, κ_{S_c} and $\kappa_{P/C}$ can thus be computed and compared with the same dimensions. A higher value of κ implies that the cell is less likely to break down due to that peak field, and for optimization purposes, the worst (smallest) breakdown index is used, such that the overall value for the cell is given as

$$\kappa = \min\left(\kappa_E, \kappa_{S_c}, \kappa_{P/C}\right) \ . \tag{3}$$

In many cases, the breakdown index is easier to interpret when converted to a maximum gradient $\hat{G}$ at the standard conditions. This can be calculated as

$$\hat{G} = \frac{\kappa^{1/6}\,\mathrm{BDR}_0^{1/30}}{\tau_0^{1/6}} \ . \tag{4}$$

For $\hat{E}$, the following scaling limit can be found

$$\kappa_E \bar{E}^6 = \frac{\hat{E}^6\tau}{\mathrm{BDR}^{1/5}} \leq \frac{\hat{E}_0^6\tau_0}{\mathrm{BDR}_0^{1/5}} \ , \tag{5}$$

where $\hat{E}_0$ is the peak field limit at standard conditions (220–250 MV/m), indicated with red lines in Fig. 1 [8]. When

Copyright © 2014 CC-BY-3.0 and by the respective authors

OVERVIEW OF THE NEW HIGH LEVEL SOFTWARE APPLICATIONS DEVELOPED FOR THE HIE-ISOLDE SUPERCONDUCTING LINAC

D. Lanaia*, M.A. Fraser, D. Voulot, CERN, Geneva, Switzerland

Abstract

The High Intensity and Energy (HIE) ISOLDE project consists of an upgrade of the ISOLDE facility at CERN. With the installation of 32 independently-phased, superconducting (SC) quarter-wave resonator cavities the energy of post-accelerated radioactive beams (RIBs) will be increased from 3 MeV/u to over 10 MeV/u. The large number of cavities will increase the number of parameters to optimise. In order to ensure a fast set-up of the machine during operation and commissioning, new software applications have been specially developed for the SC linac. The first allows the conversion of optics settings into machine settings, and vice versa. The second will aid the phasing of the cavities using beam energy measurements. The last application will automatically generate the phase and the voltage settings for the cavities in the SC linac. In this contribution we will present the new application and how the HIE-ISOLDE controls are integrated with the CERN control system.

INTRODUCTION

The HIE-ISOLDE project represents a major upgrade of the ISOLDE facility at CERN. It focuses on the installation of a 40 MV superconducting linac, comprising 32 niobium sputter-coated copper cavities, operating at 101.28 MHz. The energy of the post-accelerated beam will increase to over 10 MeV/u, when the installation is completed. A layout of the HIE-ISOLDE installation, including the chopper line and the six cryomodules can be seen in Figure 1.

The new machine will be fully integrated in the CERN control system. An upgrade of the existing software is necessary, as well as the development of new dedicated applications related to the superconducting part. Three applications are now ready to be tested and, in addition to this, a fourth application, now under study, will provide a tool to help phase the cavities by means of time-of-flight (ToF). This work will mainly focus on the new applications developed for the SC part of the machine, after an introduction to the CERN control system and the tools that it contains.

The vacuum and cryogenics controls will not be discussed. Their development belongs to the Vacuum and Cryogenics groups respectively. Only monitoring will be allowed for the cryogenics, while for the vacuum an "operator mode" is foreseen, which will allow operators to accomplish small changes to the vacuum status of the machine.

*The author acknowledges funding from the Swedish Knut and Alice Wallenberg Foundation (KAW 2005-0121) and from the Belgian Big Science program of the FWO (Research Foundation Flanders) and the Research Council K.U. Leuven.

We acknowledge as well the receipt of fellowships from the CATHI Marie Curie Initial Training Network: EU-FP7-PEOPLE-2010-ITN Project number 264330.

CERN TOOLS FOR HIE-ISOLDE

The accelerator complex at CERN includes several accelerators and hundreds of different devices, all remotely controlled. Therefore a strong and reliable control system is needed. The CERN control system is based on a so-called 3 tier architecture, see Figure 2.

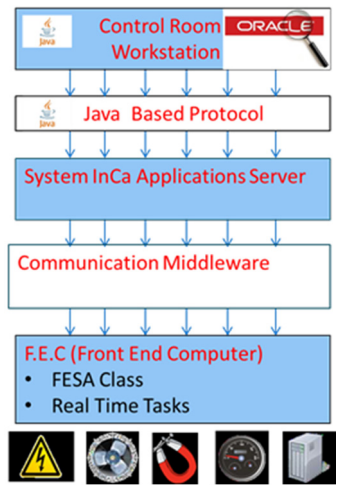


Figure 2: Three tier architecture

The first tier is the front end software application (FESA). FESA is a complete environment that provides JAVA based GUIs for the equipment specialist to design, test and develop their software [1]. A communication middleware developed in JAVA or C++ brings to the second level of the architecture: the InCA application server. InCA (Injection Control Architecture) aims at the homogenisation of the control system across the CERN complex [2]. In the top tier, running from the ISOLDE control room workstations one can find the GUIs made for generic applications, developed in JAVA by the Operation group, to control and observe the accelerator devices.

In order to support basic operation with the control system the CERN control group develops a handful of generic applications that allow runtime operation to be easily performed from any device. The ISOLDE facility mainly uses the following: Working Set (WS), Knobs, Timber, Inspector, Ramses.

The WS concept is a way to group devices together so that generic applications for display and acquisition can be viewed and controlled in a grouped way [3].

A knob can be seen as a set of properties that will be exposed via a generic viewer for a given device class/family name [4].

Timber is a tool that can extract time series data from multiple data sources simultaneously [5].

Copyright © 2014 CC-BY-3.0 and by the respective authors

CALIFES: A MULTI-PURPOSE ELECTRON BEAM FOR ACCELERATOR TECHNOLOGY TESTS

J.L. Navarro Quirante*, R. Corsini, A. Grudiev, T. Lefevre, S. Mazzoni, R. Pan, F. Tecker, CERN, Geneva, Switzerland
W. Farabolini, F. Peauger, CEA/DSM/IRFU, Saclay, France and CERN, Geneva, Switzerland
D. Gamba, JAI, Oxford, United Kingdom and CERN, Geneva, Switzerland
M.A. Khan, K. Yaqub, PINSTECH, Islamabad, Pakistan and CERN, Geneva, Switzerland
N. Vitoratou, Thessaloniki University, Thessaloniki, Greece and CERN, Geneva, Switzerland
J. Oegren, R. Ruber, Uppsala University, Uppsala, Sweden

Abstract

The Compact Linear Collider (CLIC) project aims to accelerate and collide electrons and positrons up to 3 TeV center-of-mass energy using a novel two-beam acceleration concept. To prove the feasibility of this technology the CLIC Test Facility CTF3 has been operated during the last years. CALIFES (Concept d'Accélérateur Linéaire pour Faisceau d'Electron Sonde) is an electron linac hosted in the CTF3 complex, which provides a flexible electron beam and the necessary equipment to probe both the two-beam acceleration concept and novel instrumentation to be used in the future CLIC collider. In this paper we describe the CALIFES Linac and its beam characteristics, present recent test results, outline its future program on two-beam module testing and finally discuss about possible future applications as a multi-purpose accelerator technology test facility.

INTRODUCTION

The CLIC project relies on a novel two beam acceleration concept where 12 GHz RF power produced in the deceleration of a high current (~100 A) beam is used to accelerate a low current (~1 A) beam up to an energy of 3 TeV [1]. CTF3 was constructed with the aim of addressing the key issues of the concept. The facility contains the necessary elements to produce the high current beam, so called drive beam, as well as its recombination by interleaving bunches using a delay loop and a combiner ring to multiply bunch frequency up to 12 GHz and current up to 28 A. Finally, in the CLIC Experimental Area (CLEX) the deceleration can be done in specific Power Extraction and Transfer Structures (PETS) to produce 12 GHz high power RF. Additionally, CLEX hosts the CALIFES injector (section 7.2.6 in [1]) which provides the low current probe beam that is accelerated and successfully demonstrates the two beam acceleration concept.

CALIFES LAYOUT

The main goal of the CALIFES injector (Fig. 1) is to mimic the main beam of CLIC. This probe beam is produced in a Cs_2Te photo-injector pulsed by an UV (262 nm) laser which delivers up to 270 nJ/pulse. This energy can be reduced using a hard aperture to produce a bunch charge up to 0.6 nC with a bunch frequency of 1.5 GHz [2]. Trains ranging from 1 to 300 bunches have been tested successfully. The acceleration is provided by a single klystron delivering pulses of 45 MW to power the gun, a buncher structure and two accelerating structures. Using a compression cavity the pulse peak power is increased to 130 MW during 1.2 μs, the necessary time to fill the accelerating structures. An attenuator and a phase shifter located before the gun provide flexibility tuning bunch extraction from the photo-cathode. The phase of the buncher can be independently controlled using a specially developed power phase shifter thereby operating the structure close to the zero crossing, thus shortening the bunch length via velocity bunching. The measured bunch length of 1.4 ps compared with the 6 ps of the laser shows the efficiency of the system. The whole acceleration system of the injector can provide a beam with kinetic energy up to 210 MeV with an energy spread <2%. The energy spread can be increased on purpose by changing the timing of the laser pulse versus the RF pulse to produce a train of pulses scaled in energy if needed. A system of solenoids around the accelerating cavities allow to keep the beam emittance below $10\,\pi \cdot mm \cdot mrad$; which can be measured by quadrupole scan using a quadrupole triplet and a screen downstream the last accelerating cavity. An electro-optical system and a streak camera located after the triplet, allow to measure bunch length with a 200 fs resolution. Finally a spectrometer line located downstream the injector enables energy measurements.

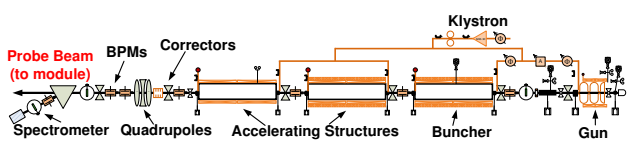


Figure 1: Layout of the CALIFES injector installed in CLEX.

This layout provides a flexible electron beam which can be used not only as CLIC probe beam, but also as a line for accelerator technology tests.

Downstream the CALIFES injector, the Two Beam Test Stand (TBTS) [3] was installed with the aim to demonstrate the two beam acceleration concept. The facility has successfully demonstrated the feasibility of the concept achieving up to 145 MV/m of gradient using one PETS and powering two X-band accelerating structures

* jl.navarro@cern.ch

ISBN 978-3-95450-142-7

Copyright © 2014 CC-BY-3.0 and by the respective authors

EXPERIMENTAL VERIFICATION TOWARDS FEED-FORWARD GROUND MOTION MITIGATION AT ATF2

J. Pfingstner*, K. Artoos, C. Charrondiere, St. Janssens†, M. Patecki‡, Y. Renier,
D. Schulte, R. Tomás, CERN, Geneva, Switzerland
A. Jeremie, LAPP, Annecy, France
K. Kubo, S. Kuroda, T. Naito, T. Okugi, T. Tauchi, N. Terunuma, KEK, Tsukuba, Japan

Abstract

Without counter measures, ground motion effects would deteriorate the performance of future linear colliders to an unacceptable level. An envisioned new ground motion mitigation method (based on feed-forward control) has the potential to improve the performance and to reduce the system cost compared to other proposed methods. For the experimental verification of this feed-forward scheme, a dedicated measurement setup has been installed at ATF2 at KEK. In this paper, the progress on this experimental verification is described. An important part of the feed-forward scheme could already be demonstrated, namely the prediction of the orbit jitter due to ground motion measurements.

INTRODUCTION

Ground motion is a severe problem for future linear colliders. The continuously misaligned quadrupole magnets induce beam oscillations, which result in emittance increase and beam-beam offset at the interaction point. If uncorrected, these effects reduce the luminosity to an unacceptable level. Different mitigation methods have been studied to reduce the deteriorating ground motion influence. Orbit feedback systems can suppress beam oscillations efficiently, if their frequencies are about a factor 20 lower than the beam repetition rate f_R (oversampling necessary for digital control to be efficient). For the remaining components at higher frequencies, additional mitigation methods have to be foreseen. Two systems have been designed and tested in the past: intra-pulse feedback systems [1] and stabilisation systems [2, 3]. Intra-train feedback systems measure the positions of the first few bunches of each beam train, in order to correct the following bunches via the utilisation of ultra-fast feedback electronics. Even though they work very efficient for the ILC, they are not sufficient for CLIC where the bunch spacing is too short to react quickly enough. Additionally, intra-train feedback systems can only be utilised at a few dedicated locations and no spatially distributed corrections can be applied. Therefore, stabilisation systems are the baseline solution for CLIC. These systems compensate mechanical motion of quadrupole magnets by stabilising each of them with a dedicated positioning structure. Stabilisation systems have shown to meet their stringent specifications, but they are costly and the individual quadrupole magnets are stabilised independent of each other.

To overcome these disadvantages a third mitigation method is presented in this paper. It is based on feed-forward control utilising vibration sensors that are positioned along the beamline. The sensor measurements are used to predict the beam orbit change due to the misalignments of the quadrupole magnets. For this prediction, a linear system model is used, which is represented by the orbit response matrix $\boldsymbol{R}_q$. As a last step, actuations of corrector magnets are computed to compensate the predicted beam motion.

The described feed-forward system has the potential of cost reduction and performance improvements compared to other systems. An analytic model and simulation studies of the feed-forward scheme has been already presented in [4] and [5], respectively. In this paper, results from an experiment at ATF2 [6] at KEK are presented. The experiment aims to demonstrate the practical feasibility of the prediction part of the overall system. Also updated simulation studies for this experiment are shown. The important demonstration of the full mitigation system is subject to future work.

SIMULATION RESULTS

Simulations have been presented in [5], in which the feasibility of the prediction of orbit jitter from vibration measurements with seismometers is evaluated. The focus was laid on the predictions of orbit changes (orbit jitter) $\Delta\boldsymbol{b}_k = \boldsymbol{b}_k - \boldsymbol{b}_{k-1}$ in all beam position monitors (BPMs), where k is the beam pulse index. Using the orbit jitter corresponds to a high-pass filtering of the orbit data $\boldsymbol{b}_k$, which suppresses low frequencies that would be corrected in a real application by an orbit feedback system. The simulations have been performed with the tracking code PLACET [7]. Realistic ground motion has been created with a ground motion generator using a model developed especially for ATF2 in [8]. Also other dynamic and static imperfections have been included, most importantly orbit jitter at the beginning of the beamline with an RMS value of 10% and 25% of the beam size in the horizontal and vertical direction, respectively.

The simulations showed that the orbit jitter due to ground motion is a factor 20 to 100 smaller than the orbit jitter from other sources. Therefore, the detection of ground motion effects seems to be very challenging. To overcome this problem a technique was developed that removes incoming, parasitic orbit jitter from other sources than ground motion. The initial technique was based on a singular value decomposition (SVD) of the BPM data, but turned out to be not

* juergen.pfingstner@cern.ch
† Also at Nikhef, Science Park 105, 1098 XG Amsterdam, The Netherlands.
‡ Also at Warsaw University of Technology, Pl. Politechniki 1, 00-661 Warsaw, Poland.

Copyright © 2014 CC-BY-3.0 and by the respective authors

ISBN 978-3-95450-142-7

DESIGN, HARDWARE TESTS AND FIRST RESULTS FROM THE CLIC DRIVE BEAM PHASE FEED-FORWARD PROTOTYPE AT CTF3*

J. Roberts (CERN, Geneva, Switzerland; JAI, Oxford, UK),
A. Andersson, P.K. Skowroński, (CERN, Geneva, Switzerland),
P.N. Burrows, G.B. Christian, C. Perry (JAI, Oxford University, UK),
A. Ghigo, F. Marcellini (INFN/LNF Frascati, Italy).

Abstract

In the CLIC two beam acceleration concept the phase synchronisation between the main beam and the RF power extracted from the drive beam must be maintained to within 0.2 degrees of 12 GHz [1, 2]. A drive beam phase feed-forward system with bandwidth above 17.5 MHz is required to reduce the drive beam phase jitter to this level [3]. The system will correct the drive beam phase by varying the path length through a chicane via the use of fast strip line kickers. A prototype of the system is in the final stages of installation at the CLIC test facility CTF3 at CERN. This paper presents results from preparations for the phase feedforward system relating to optics improvements, the development of a slow phase feedback that will be run in parallel with the feedforward system and first tests of the kicker amplifier and kickers.

INTRODUCTION

The RF power used to accelerate the main beam in the proposed linear collider CLIC is extracted from a second 'drive beam'. To ensure the efficiency of this concept a drive beam 'phase feedforward' system is required to achieve a timing stability of 50 fs rms, or equivalently a phase stability of 0.2 degrees of 12 GHz (the CLIC drive beam bunch spacing) [1, 2]. This system poses a significant hardware challenge in terms of the bandwidth, resolution and latency of the components and therefore a prototype of the system is in the final stages of development at the CLIC test facility CTF3 at CERN.

A schematic of the CTF3 phase feedforward system is shown in Fig. 1. The phase will be corrected utilising two kickers placed prior to the first and last dipole in the pre-existing chicane in the TL2 transfer line. By varying the voltage applied to the kickers the beam can be deflected on to longer or shorter paths through the chicane, thus inducing a phase shift. The goal is to demonstrate a 30 MHz bandwidth phase correction with a resolution of 0.2 degrees of 12 GHz. The required hardware consists of three precise phase monitors [4, 5] and two strip line kickers [5] designed and fabricated by INFN/LNF Frascati, and a kicker amplifier and digital processor [6] from the John Adams Institute at Oxford University. More detailed descriptions can be found in [7].

The latency of the feedforward system, including cable lengths and the latency of each component, must be below the 380 ns beam time of flight between the first monitor and the first kicker.

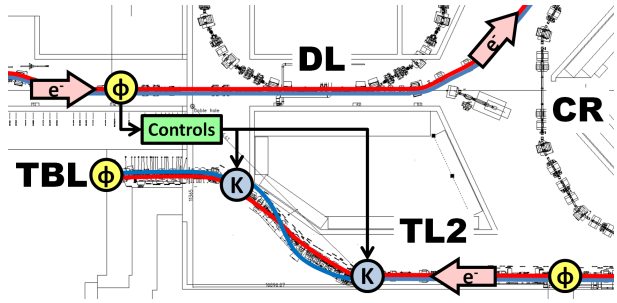


Figure 1: Simplified schematic of the phase feedforward system. Red and blue lines depict orbits for bunches arriving late and early at the first phase monitor, ϕ, respectively. The trajectory through the TL2 chicane is changed using two kickers, K.

OPTICS AND MODEL CORRECTIONS

The phase feedforward system imposes strict constraints on multiple optical parameters of the chicane and therefore an accurate model becomes critical. The key parameter for the phase feedforward system is the transfer matrix coefficient R_{52}. However, large R_{52} values drive the optics towards large horiztonal dispersion and this must be kept as low as possible and always under $|D_x| = 2.0$ m due to the large drive beam energy spread of 1% rms and 10 cm physical aperture. Additional constraints ensure the beam leaves the correction chicane on the nominal trajectory irrespective of the given kick. Fig. 2 shows the solution that has been used for the system commissioning. It limits the maximum dispersion to 1.2 m whilst yielding an R_{52} value of -0.7 m to give a correction range of $\pm 10°$.

Response matrix and dispersion measurements were completed for several variants of the optics in order to identify unambiguously and correct any errors present in the MADX model. As shown in Fig. 3 large errors in the model were immediately apparent and there were two key areas in which modifications were required. Firstly, there was a large uncertainty on the magnetic properties of a type of quadrupole reclaimed from the CELSIUS machine, with 16 out of the 27 quadrupoles in TL2 being of this type. The agreement with data was improved by increasing the strength of these magnets by 7% in the model. Secondly, in other sections of CTF3 large discrepancies in the edge focusing of the (typically above 25°) dipoles had been observed. Further

* Work supported by the European Commission under the FP7 Research Infrastructures project Eu-CARD, grant agreement no. 227579

Copyright © 2014 CC-BY-3.0 and by the respective authors

BEAM DYNAMICS STUDIES OF THE CLIC DRIVE BEAM INJECTOR

Sh. Sanaye Hajari, S. H. Shaker, IPM, Tehran, Iran; CERN, Geneva, Switzerland
S. Doebert, CERN, Geneva, Switzerland

Abstract

In the Compact Linear Collider (CLIC) the RF power for the acceleration of the Main Beam is extracted from a high-current Drive Beam that runs parallel with the main linac. The beam in the Drive Beam Accelerator is phase coded. This means only every second accelerator bucket is occupied. However, a few percent of particles are captured in wrong buckets, called satellite bunches. The phase coding is done via a sub-harmonic bunching system operating at a half the acceleration frequency. The beam dynamics of the Drive Beam injector complex has been studied in detail and optimised. The model consists of a thermionic gun, the bunching system followed by some accelerating structures and a magnetic chicane. The bunching system contains three sub-harmonic bunchers, a prebuncher and a tapered travelling wave buncher all embedded in a solenoidal magnetic field. The simulation of the beam dynamics has been carried out with PARMELA with the goal of optimising the overall bunching process and in particular decreasing the satellite population and the beam loss in magnetic chicane and in transverse plane limiting the beam emittance growth.

INTRODUCTION

The Compact Linear Collider (CLIC) is a future Multi-TeV electron-positron collider under study at CERN. In the acceleration scheme of CLIC, the RF power for the acceleration of the Main Beam is extracted from a high-current Drive Beam that runs parallel with the main linac. The Drive Beam loses its energy in special RF structures called Power Extraction and Transfer Structure (PETS) [1].

DRIVE BEAM TIME PROFILE

At the end of the Drive Beam complex the main pulse of the beam consists of 24 bunch trains of 244ns length with a bunch repetition frequency of 12 GHz.

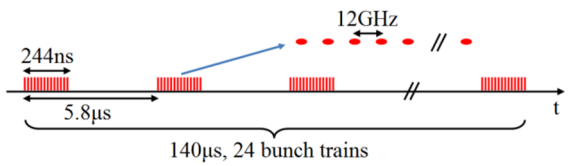


Figure 1: Drive Beam final time structure.

To achieve such a time structure the continuous beam of 5 A current from the electron gun passes through the 0.5 GHz sub-harmonic bunching system with a phase switching of 180° every 244 ns [2]. Afterwards, a 1 GHz prebuncher and buncher are used to reduce the bunch length then the beam is accelerated with 1 GHz frequency. Therefore, only every second accelerator bucket is occupied. Due to the phase switching of the sub-harmonic bunching system the main pulse is made up of even and odd bunch trains. This procedure is called phase coding. However, a few percent of particles captured in wrong buckets, called satellite bunches. These bunches have to be eliminated from the beam for reasons of efficiency and machine protection at the end of injector [1].

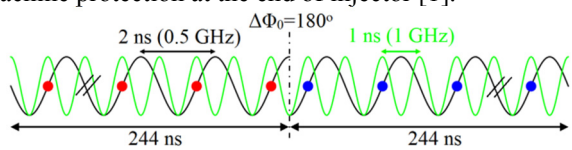


Figure 2: The phase switching and the satellite concept.

At the end of Drive Beam Accelerator a delay loop is used to combine even and odd trains to double the bunch repetition frequency and the peak current. The trains then are recombined three and four times in the following two combiner rings. Therefore, the overall multiplication of the frequency and the peak current is 24 and the final time structure (cf. Fig. 1) will be achieved.

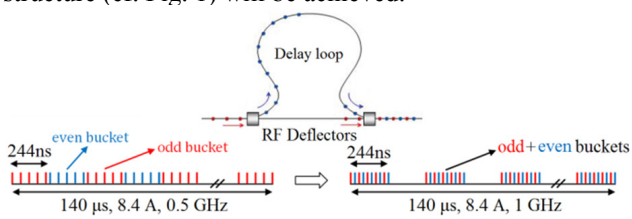


Figure 3: The bunch combination in the delay loop [1].

SUB-HARMONIC BUNCHING SYSTEM AND PREBUNCHER

The general layout of the bunching system is shown in Fig. 4. The sub-harmonic bunching system consists of three travelling wave sub-harmonic bunchers (SHB). The optimisation criteria for this system are to minimise the satellite population and together with the prebuncher to accumulate the particles as many as possible in the acceptance of the buncher.

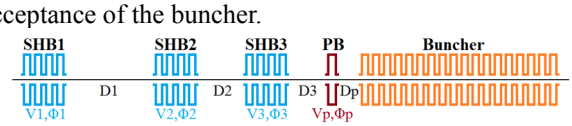


Figure 4: General layout of the bunching system.

For optimisation, we need to decide on the values of 12 parameters. For each cavity the phase, voltage and the drift space afterwards should be determined. However, beforehand we need a deep understanding of the dynamics of such a system to clarify the road map.

The principle of bunching with the sub-harmonic bunching system and the prebuncher is based on velocity modulation bunching [3]. As illustrated in Fig. 5 just after the first SHB the longitudinal phase space is convergent for the main bunch and divergent for the satellite bunch (diagram (a)). This results in bunching and debunching of

Copyright © 2014 CC-BY-3.0 and by the respective authors

BEAD-PULL MEASUREMENT METHOD AND TUNING OF A PROTOTYPE CLIC CRAB CAVITY

R. Wegner, W. Wuensch, CERN, Geneva Switzerland
G. Burt, B. Woolley, Lancaster University, UK

Abstract

A bead-pull method has been developed which measures in a single bead passage the amplitude and phase advance of deflecting mode travelling wave structures. This bead-pull method has been applied to measure and tune a Lancaster University-designed prototype crab cavity for CLIC. The technique and tuning results are described.

INTRODUCTION

The prototype CLIC crab cavity, designed by Lancaster University [1], is a multi-cell travelling wave cavity with ten regular and two single-feed coupling cells. In order to provide synchronism with the beam, the phase advance of each cell needs to be adjusted to its nominal value to correct for machining deviations, etching and assembly artefacts. This adjustment process is called tuning.

Figure 1 shows the electric field of the deflecting mode inside the crab cavity and the coordinate system used. The Brillouin diagram of the first modes in the regular cell is plotted in Fig. 2. The desired quasi-TM_{11}-mode has a phase advance of -120° per cell (backward wave) at the operating frequency of 11.994 GHz and a group velocity of ~3.3% of the speed of light c_0.

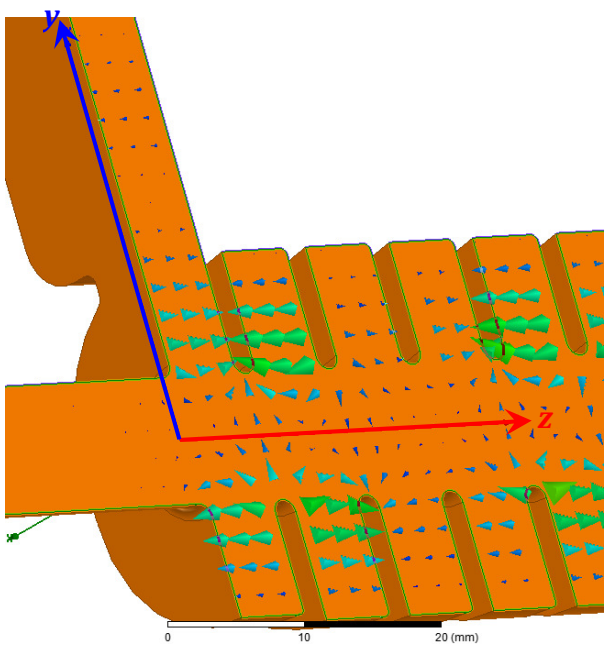


Figure 1: Electric field distribution of the deflecting quasi-TM_{11}-mode in a cross section of the crab cavity. The power is fed into the structure via the input coupler (top left). The following coordinate system is used: z is the beam axis and y is the direction of desired deflection.

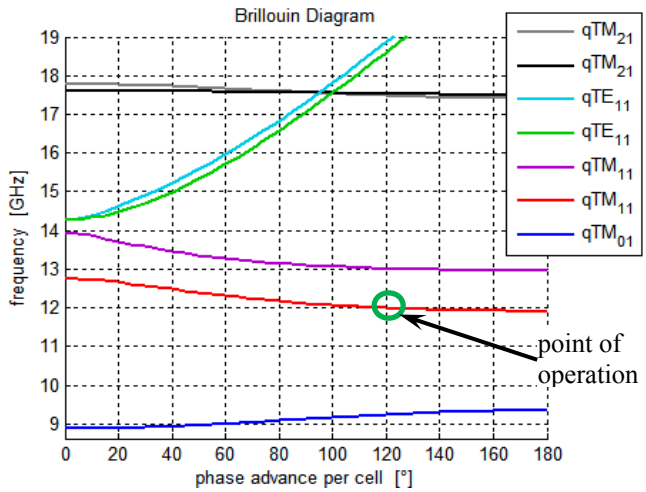


Figure 2: Mode spectrum of the first seven modes. The operating quasi-TM_{11}-mode (red) is well separated in frequency from the fundamental mode and the higher order modes, including the x-polarised quasi-TM_{11}-mode (purple).

ELECTOMAGNETIC FIELDS AND BEAD-PULL MEASUREMENTS

A charged particle is subject to the Lorentz force and inside the crab cavity it is deflected by the electric (E) and the magnetic (H) field of the operating mode. The relevant components for a deflection in y-direction are:

$$F_y = q\left(E_y + c_0\mu_0 H_x\right) = q\left(E_y + Z_{F0}H_x\right), \qquad (1)$$

assuming that the charge q travels at the speed of light in z-direction. The vacuum permeability is denoted by μ_0 and the impedance of free space by Z_{F0}.

The electromagnetic field has been measured via a bead-pull measurement – a perturbation measurement where a bead is pulled through the cavity [2]. The change of input reflection is recorded and is proportional to the weighted sum of all electromagnetic field components squared [3] at the position of the bead, assuming a small perturbation:

$$\Delta S_{11} = S_{11,\,perturbed} - S_{11,\,unperturbed}$$

$$\Delta S_{11} = \sum_{*=x,y,z} \{(e_* E_*)^2 - (Z_{F0} h_* H_*)^2\} \qquad (2)$$

The complex components e_x, e_y, e_z, h_x, h_y and h_z describe the polarisation and magnetisation effects of the bead in the local electromagnetic field. For the tuning of

Copyright © 2014 CC-BY-3.0 and by the respective authors

ISBN 978-3-95450-142-7

THERMAL LOAD AND SIGNAL LEVEL OF THE ESS WIRE SCANNER

B. Cheymol*, European Spallation Source, Lund, Sweden

INTRODUCTION

In the ESS linac [1] and in the transfer line to the target, a number of wire scanners will be installed. Due to the high power of the beam, the measurement can not be done during the production mode (2.86 ms, 62.5 mA, 14 Hz), the beam power has to reduced in order to preserve the wire integrity. Two modes will be dedicated to commissioning and specific beam studies where the insertion of interceptive devices are allowed, a slow tuning mode (*i.e.* 100 μs, up to 62.5 mA, 1 Hz) and a fast tuning mode (*i.e.* 10 μs, up to 62.5 mA, 14 Hz).

The ESS linac consists in two section, one equipped with normal conduction cavities and the second with superconducting cavities, the current layout of the ESS linac is shown in Fig. 1.

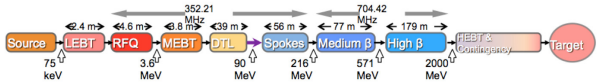


Figure 1: Current ESS accelerator baseline (2014).

In the warm linac, 4 wire scanner are foreseen to be installed in the MEBT, 4 more will be installed between the DTL tanks and one in the transition between the cold and the warm linac (LEDP).

Ideally, 4 wire scanner will be installed at the beginning of each cold section and of the HEBT in order to preform emittance measurement with the 3 gradient method.

THERMAL LOAD

Two types of wires have been considered a 33 μm carbon wire for the warm linac and a 40 μm tungsten wire for the cold linac.

Warm Linac

MEBT The maximum temperature reached by each wire scanner during a scan at 1 Hz are summarized in Tab. 1 as well as the expected beam sizes at the wire location.

Table 1: Maximum temperature with a scan at 1 Hz.

Beam sizes [mm]		T_{max} [K]	T_{max} [K]
σ_x	σ_y	50 μs	100 μs
1.85	1.45	1900	–
3	1.5	1430	2110
2.5	2.4	1240	1780
3.2	3.2	975	1350

Due to the low beam energy, the MEBT represents the worst case for the wire scanner, in addition beam density is relatively high. As shown in Tab. 1 the temperature increase for the first wire scanner is above the mechanical limit of the wire even with a reduced beam power, the wire will survive only if the pulse length is reduced to 50 μs. In this case, the maximum temperature is around 1900 K, below threshold of thermoionic emission and the limit of a carbon wire. In fast mode, the temperature is below 1400 K.

DTL The relevant beam parameters at each wire scanner location are summarized in Tab. 2. The stopping power is lower than the MEBT case and the wire can withstand a 100 μs pulse.

Table 2: Beam parameters at the DTL wire scanner location,

Position	σ_x [mm]	σ_y [mm]	Energy [MeV]
DTL1	1.7	1.2	21.29
DTL2	1.3	2	39.11
DTL3	1.8	1.6	56.81
DTL4	1.6	1.9	73.83
LEDP	2.6	1.8	89.91

WS are named according to their position.

After DTL tank 1, the expected temperature on the wire is $\approx$ 1400 K during the slow tuning mode, the temperature is decreasing with the energy and is around 700 K in the LEDP. The evolution of temperature for these two cases is shown in Fig. 2.

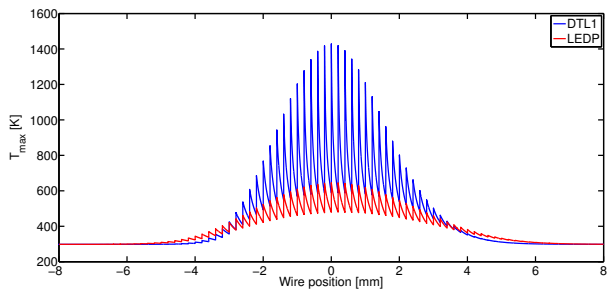


Figure 2: Maximum temperature on the wire during a scan as function of the wire position for a 21 MeV beam (blue line) and 90 MeV beam (red line).

At 90 MeV, the expected signal in case of carbon wire is weak and a tungsten wire might be considered to improve the signal level.

An estimation of the temperature has been performed for the wire scanner positioned in the LEDP in order to check the possibility of replacing the carbon wire by a 40 μm tungsten wire. During the slow tuning mode, the temperature will reach 1860 K, while during the fast tuning mode the peak temperature will be less than 1500 K. In both case, signal will not be perturbed by the thermoionic emission. Tungsten wire

* benjamin.cheymol@esss.se

Copyright © 2014 CC-BY-3.0 and by the respective authors

ISBN 978-3-95450-142-7

CONCEPTUAL DESIGN OF THE ESS DTL FARADAY CUP

B. Cheymol*, E. Lundh, European Spallation Source, Lund, Sweden

Abstract

The DTL section of the ESS linac will accelerate the beam form 3.6 MeV to 90 MeV at a peak current of 62.5 mA. It is foreseen to install after each DTL tank a Faraday cup for beam current and the beam transmission measurements during retuning phase. An energy degrader will be positioned in front of the in order to perform a low resolution phase scan of the DTL tank before injecting the beam in the downstream structure. This paper describes the preliminary studies of the Faraday cup, mainly focus on the energy degrader.

INTRODUCTION

The European Spallation Source (ESS) is a neutron source based on a 5 MW proton linac, build in Lund, Sweden. The normal conducting front end will accelerate the beam coming for the ion source up to 90 MeV, it consists in an ECR ion source, a Low Energy Beam Transport line (LEBT), a radio frequency quadrupole (RFQ), a Medium Energy Beam Transport line (MEBT) and a drift tube linac (DTL) [1].

The DTL employs a permanent magnet FODO lattice leaving empty drift tubes for diagnostics like BPMs and Beam current Transformer. The inter-tank regions will each house a wire scanner and a Faraday Cup (FC), a preliminary layout of the beam diagnostic is shown in Fig. 2.

In total 5 FC will be installed in the DTL section, they consist in a charge collector positioned downstream an energy degrader, in order to study the transmission of the beam in function of the RF phase and amplitude in the DTL cavity (see Fig. 1).

The degrader thickness is chosen to stop incoming beam with energy slightly below the cavity design output.

The cavity phase and amplitude are scanned, for each point the signal on the FC is measured and at the end of the process an acceptance can be determined by looking at he width of the signal

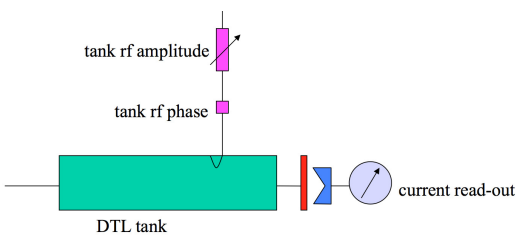


Figure 1: Schematic of the energy degrader method from phase scan measurement in the DTL, the energy degrader is represented in red and the charge collector in blue.

FARADAY CUP DESIGN

As all the other interceptive devices installed in the ESS linac, the FCs will not be able to withstand the full beam power. They will be used only during commissioning and dedicated study periods with reduced beam power, the different machine modes are shown in Tab. 1.

Table 1: ESS beam parameters during operation (left) and during retuning and commissioning phases.

	Operation	Fast mode	Slow mode
I $[mA]$	6 to 62.5	6 to 62.5	6 to 62.5
Pulse length $[\mu s]$	2860	10	100
Rep. Rate [Hz]	14	14	1

All the simulations presented in this paper have been done with the maximum beam intensity.

Beam parameters

The nominal beam parameter at the FCs location are summarized in Tab. 2.

Table 2: Beam parameters at the DTL FC location, FC are named according to their position in Fig. 2.

Position	σ_x [mm]	σ_y [mm]	Energy [MeV]
FC1	1.7	1.2	21.29
FC2	1.3	2	39.11
FC3	1.8	1.6	56.81
FC4	1.6	1.9	73.83
FC5	2.6	1.8	89.91

The beam sizes will slightly change during the RF scan of the DTL cavity, for the studies presented in this paper, average beam sizes of σ_x= 1 mm σ_y = 2 mm have been assumed for all inter tank area and for all beam energies, and also for FC5 in the case of this FC will be installed at the exit of the last tank.

Energy degrader parameters

The energy deposition on a single energy degrader is too high for the ESS beam parameters. In order to cop with the higher beam power, the energy degrader consists in two foils separated by 30 mm, an example of the geometry used in the simulation is show in Fig. 3.

For a given FC, the thickness of the first is chosen in order to let the beam goes thought if the upstream cavity is not powered. The Multiple scattering in the foil increase the beam divergence and thus reduced the beam density on the second foil. The thickness of the second foil is chosen in function of the threshold energy required for the FC.

* benjamin.cheymol@esss.se

Copyright © 2014 CC-BY-3.0 and by the respective authors

LONGITUDINAL BUNCH PROFILE MONITORING AT THE ESS LINAC

I. Dolenc Kittelmann*, ESS, Lund, Sweden
B. Cheymol, ESS, Lund, Sweden

Abstract

The European Spallation Source (ESS), which is currently under construction, will be a neutron source based on 5 MW, 2 GeV proton linac. This high intensity linac will among other beam instrumentation require longitudinal bunch profile monitors. These shall be used during the commissioning phase and start-up periods for beam dynamics optimization and beam loss reduction. The paper focuses on the preliminary studies concerning the longitudinal bunch profile monitoring at the ESS linac.

INTRODUCTION

The European Spallation Source (ESS) is a material science facility, which is currently being built in Lund, Sweden and will provide neutron beams for neutron-based researches [1]. The neutron production will be based on bombardment of a tungsten target with a proton beam of 5 MW average power. A linear accelerator (linac) [2] will be used to accelerate protons up to 2 GeV and transport them towards the target. The ESS linac will create a pulsed beam with an average pulse current of 62.5 mA, pulse duration of 2.86 ms and repetition rate of 14 Hz. The beam will be bunched at 352.21 MHz frequency in the first and 704.42 MHz in the ending part of the linac.

It is essential to have a linac equipped with a certain set of beam instrumentation during the commissioning phase and start-up periods of a linac in order to tune it for optimal beam transmission and minimal beam losses during the operation periods. An example of such an instrument is a Longitudinal Bunch Profile Monitor (LBM), which provides information about an average time structure of a bunch. This paper summarizes the current status and plans regarding the LBM system at the ESS linac.

LBM LAYOUT AT THE ESS LINAC

Four LBM devices are currently planned to be installed in the ESS linac. Their anticipated positions along the linac are marked on Fig. 1. The one-sided RMS longitudinal bunch size is expected to shrink from ~150 ps to 3 ps during the acceleration process. The intrinsic limit for the LBM methods that are based on detection of the bunch electric field at the beam pipe boundary can be estimated [3] as

$$\Delta t = \frac{R_{bp}}{\sqrt{2} v \gamma}, \qquad (1)$$

where $\Delta d = v/\Delta t$ represents the RMS value of the longitudinal charge distribution on the inner wall of the beam pipe with radius R_{bp}, which is produced by a charged particle moving with speed v. Due to the rather low Lorentz factors γ of the ESS beam the one-sided RMS bunch lengths will be far below this limit (see Fig.2). Therefore the available options to measure the bunch profiles are rather limited. The most common device used for measuring the longitudinal bunch profile in proton machines like ESS is one called Bunch Shape Monitor (BSM) proposed by A. Feschenko [4]. A typical phase resolution of this device is ~1 ° [5], which is accurate enough only for one of the 4 planned LBM devices at the ESS linac[1], namely LBM1 located in the MEBT section. However it has been recently proposed by A. Feschenko that a resolution of 0.5 ° or less could be achieved with a modernized version of the RF deflector, which should provide more symmetric electro-magnetic fields with less fringing fields at the edges [6]. As this is accurate enough for both LBM1 and LBM2 device, ESS aims for both to be a Feschenko's BSM with proposed modernized RF deflector. Depending on how well the modernized BSM resolution can be improved the LBM3 could potentially also be a BSM device. However the expected bunch lengths at the LBM4 location will be to short to be resolved even with the modernized BSM. Therefore LBM4, and potentially LBM3 as well, require development of a new device type. Additional argument for new development in the case of LBM3 follows from the study of the space charge effect on the performance of a BSM, which is the subject of the following section.

BSM AND SPACE CHARGE EFFECT

Feschenko's BSM is based on collecting the low energy Secondary Electrons (SEs) emitted from a thin wire target placed in the beam. The time structure of the primary bunch is transformed into spatial distribution of SEs through a RF modulation generated by a RF deflector. High negative voltage potential is applied to the wire to accelerate the SEs towards the RF deflector with a set of slits and an electron detector at the exit.

There are several contributions to the resolution of a BSM [5, 6]. Some can in principle be controlled by the design (e.g. contributions due to non zero wire size, due to defocusing, focusing and dispersive properties of RF deflector, etc), while others represent a natural limit and are a consequence of either the space charge (SC) of the primary bunch or the physical process of SE emission (time, velocity and direction spread of emitted SEs). The most worrying intrinsic limitations to the resolution are the time delay of SE emission and the SC effect due to the primary bunch. Here the latter is discussed for the case of the ESS linac.

The electromagnetic field of the analyzed beam disturbs the trajectory of the SEs on their way towards the RF deflector.

* irena.dolenc.kittelmann@esss.se

[1] The quoted phase resolution was determined at the linac frequency of 352.21 MHz, thus 1° corresponds to ~8 ps.

Copyright © 2014 CC-BY-3.0 and by the respective authors

ISBN 978-3-95450-142-7

DYNAMICS OF BUNCHES PARTIALLY CHOPPED WITH THE MEBT CHOPPER IN THE ESS LINAC

R. Miyamoto*, B. Cheymol, R. De Prisco, M. Eshraqi, A. Ponton, E. Sargsyan, ESS, Lund, Sweden
I. Bustinduy, ESS-Bilbao, Bilbao, Spain

Abstract

The front-end of a hadron linac typically has a transient time during turning on and off and bunches in the head and tail of a pulse from this period likely have wrong parameters and a risk to cause beam losses. A risk of losses must be avoided as possible in a high power machine so these bunches are removed with deflectors called *choppers* in the ESS Linac. From experiences of other machines, a rise time of a chopper as fast as one RF period (2.84 ns for ESS) is challenging to achieve and not necessarily needed with no ring to inject like ESS, and hence a 10 ns rise time is planned for a chopper in the medium energy beam transport of ESS. This, however, means that several bunches receive intermediate deflections and may propagate with large trajectory excursions. This paper studies dynamics of such *partially chopped* bunches in detail to ensure no significant loss is caused by them.

INTRODUCTION

The European Spallation Source (ESS) is a neutron source planned in Lund, Sweden based on a proton linac with a 2 GeV beam energy, 62.5 mA peak current, 352.21 MHz bunch frequency, 2.86 ms pulse length, and 14 Hz repetition rate, producing an unprecedented 5 MW beam power. For such a high power linac, minimization of beam losses is one of the most important and difficult challenges. Figure 1 shows the layout of ESS Linac [1]. The beam produced in the ion source (IS) is first accelerated with room temperature structures, a radio frequency quadrupole (RFQ) and drift tube linac (DTL), and then accelerated in three superconducting (SC) sections, consisting of spoke, medium-β, and high-β cavities. The linac also includes low, medium, and high energy beam transports (LEBT, MEBT, and HEBT) for characterizations and manipulations of the beam.

A conventional microwave discharge ion source used in the ESS Linac typically has a rise and fall time of tens of µs [2] and the bunches in the head and tail of a pulse, generated in this period, are likely to have wrong parameters related to the space-charge force. Though it is hard to predict behaviors of these bunches and they may or may not cause losses, it is better to remove them to avoid a risk of losses as possible. Modern hadron machines such as SNS Linac, J-PARC Linac, CERN Linac4, and RAL FETS use a system so-called *chopper*, which deflects and removes bunches together with a dedicated beam dump to manipulate the pulse structure for the ring injection [3]. Such a system can be also used for ESS to remove above mentioned bunches and the plan is to have two choppers: a slower chopper in the LEBT with a rise time of 2-3 µs removes most of these bunches



Figure 1: Schematic layout of the ESS Linac. Blue (orange) color indicates room (superconducting) temperature.

and a faster chopper in the MEBT with a rise time of 10 ns removes the remaining bunches in the 2-3 µs part.

The 10 ns rise time of the MEBT chopper is a balance between the required engineering effort and the ideal of beam dynamics. The difficulty to achieve a fast rise time lies in the switch. Fast switches on the order of 10 ns are commercially available and some are tested for a chopper of the RAL FETS [4]. On the other hand, experiences of the above mentioned machines proved that a rise time as fast as one RF period (2.84 ns for ESS) could be an engineering challenge to achieve and could require more space in the lattice. The 10 ns rise time means that several bunches receive intermediate deflections and may propagate in the linac with large trajectory excursions. Although the SNS Linac and J-PARC Linac have a similar situation and they are having no issue [5, 6], these *partially chopped bunches* are still of concern to cause losses. Therefore, the intent of this paper is to study dynamics of these bunches in detail and to ensure that they cause no significant loss and the 10 ns rise time is fast enough. ESS also uses the often quoted 1 W/m as the limit of allowed losses but it is ideal to keep an order of magnitude or so margin during the operation. Hence, it is desired that the losses due to the partially chopped bunches are limited to the level of 10^{-3} W/m or at most 10^{-2} W/m to leave a room for the bulk of the pulse. It is also desired to have losses as small as possible in the SC sections since SC structures are generally more sensitive to losses than normal temperature structures.

PARTIALLY CHOPPED BUNCH

Prior to studying the losses, this section gives a brief description of the MEBT chopper of ESS and discusses basic properties of the partially chopped bunches. The top part of Fig. 2 shows a schematic layout of the MEBT lattice, where blue boxes above (below) the central line are focusing (defocusing) quadrupoles, green boxes are buncher cavities, and red lines and triangles are the chopper and its dump. As seen in the figure, the chopper and its dump are located after the first quadrupole triplet. Hardware of the chopper is planned be similar to that of the CERN Linac4 [7]; an electric deflector with a 20 mm gap and 40 cm length is surrounded with a large aperture quadrupole. However, due to the differences

* ryoichi.miyamoto@esss.se

Copyright © 2014 CC-BY-3.0 and by the respective authors

APPLICATION INVESTIGATION OF HIGH PRECISION MEASUREMENT FOR BASIC CAVITY PARAMETERS AT ESS

R. Zeng, ESS, Lund, Sweden
W. Schappert, FNAL, Batavia, IL 60510, USA
P. Jönsson, Lund University, Lund, Sweden

Abstract

The ESS cavity control and operation methods/algorithms are challenging due to the use of long pulse, higher beam intensity, high beam power, high gradient, uncertainties in spoke cavities and high demands for energy efficiency and availability. Suitable and effective solutions could make use of modern technologies (flexible FPGA, faster CPU, bigger memory, faster communication speed, etc.), novel measuring techniques, accurate system modelling, and advanced control concept. Those possible implementations are essential to a better understanding, and thus a better operation of ESS cavity especially SRF cavities. All these concepts rely on high precision measurement of basic cavity parameters and consequent high quality data with high resolution, high precision and completeness. This paper focuses on how high precision measurement will address the challenges at ESS on the following topics: long pulse Lorentz force detuning, high precision phase and amplitude setting, heavy beam loading compensation and power overhead reduction.

INTRODUCTION

Cavity parameters discussed in this paper refer to the parameters in cavity baseband equation that reflects the fundamental static and dynamic field behaviours of a RF powered cavity with beam loading [1]:

$$\frac{dV_{cav}}{dt}+\frac{\omega_0}{2Q_L}\left(1-i\tan\varphi_D\right)V_{cav}=\frac{\omega_0}{4}\left(R/Q\right)I \quad (1)$$

where $\tan\varphi_D$ is the detuning angle,

$$\tan\varphi_D=Q_L\left(\frac{\omega_0}{\omega}-\frac{\omega}{\omega_0}\right)\approx 2Q_L\frac{\Delta\omega}{\omega}$$

In steady state, V_{cav} reaches designed value V_c, and required generator current can be written as [2]:

$$I_{gr}=\frac{2V_c}{\left(R/Q\right)Q_L}+I_b\cos\varphi_b \quad (2)$$

$$I_{gi}=-\frac{2V_c}{\left(R/Q\right)Q_L}\tan\varphi_D-I_b\sin\varphi_b \quad (3)$$

Five basic parameters are being discussed in this paper: accelerating cavity voltage V_c, synchronous phase φ_b, loaded quality factor Q_L, cavity detuning $\Delta\omega$, and R/Q.

V_c is the absolute value of the line integral of the electric field seen by the beam along the accelerating axis, which reflects the maximum achievable energy gain for beam acceleration. φ_b is, for a given particle traversing the cavity, the phase shift from RF phase at which it obtain the maximum energy gain. It is equivalent to the phase angle between beam and accelerating voltage in vector diagram. Q_L is defined as 2π times the number of RF cycles needed for stored energy to dissipate on the wall and leak out the from couplers, which measures the 'quality' of cavity resonator, conveys the information of cavity field decay rate, and determines cavity bandwidth. $\Delta\omega$ becomes a key parameter in superconducting cavity due to long RF pulse (~3.5ms) operation along with high gradient level. R/Q relates the stored energy and maximum accelerating voltage acting on the beam, which depends on only the cavity shape for a given resonant mode [3].

CAVITY DETUNING ΔΩ AND LOADED QUALITY FACTOR Q_L

Measurement/Calibration Method

While high precision measurement of single point Q_L and $\Delta\omega$ can be done by measuring decay of the cavity field, dynamic $Q_L(t)$ and $\Delta\omega(t)$ can be derived from the cavity base band differential equation (1) [4, 5]:

$$\omega_{1/2}\left(t\right)=\frac{1}{2}\frac{d\left|V_{cav}\right|^2}{dt}\Big/\left(\left|V_{for}\right|^2-\left|V_{ref}\right|^2\right) \quad (4)$$

$$\Delta\omega\left(t\right)=\mathrm{Im}\left(\left(\frac{dV_{cav}}{dt}-2\omega_{1/2}\left(t\right)V_{for}\right)\Big/V_{cav}\right) \quad (5)$$

Where $\omega_{1/2}\left(t\right)=\omega_0\left(t\right)/2Q_L\left(t\right)$. The precision of dynamic $Q_L(t)$ and $\Delta\omega(t)$ depends on how precise the measurement of cavity probe power, cavity forward power and reflected power can be. It is reported [4, 5] that better precision will be achieved if good isolation and correction of forward power and reflected power is made.

Adaptive Lorentz Force Detuning Compensation

The adaptive Lorentz force detuning compensation algorithm via piezo tuner has been developed at Fermilab to compensate for Lorentz force detuning in SRF cavities, which is promising to address the challenge of long pulse Lorentz force detuning compensation. Appropriate piezo tuner compensation waveform is automatically generated in this method, by inverting cavity response matrix obtained by applying elaborately designed stimulus signals on piezo tuner. Precisely determining the Q_L and the $\Delta\omega$ is essential in this method to acquire accurate result [5].

Copyright © 2014 CC-BY-3.0 and by the respective authors

ISBN 978-3-95450-142-7

COMMISSIONING PLAN FOR THE FRIB DRIVER LINAC *

M. Ikegami†, L. Hoff, S. Lidia, F. Marti, E. Pozdeyev, T. Russo, R. Webber, J. Wei, Y. Yamazaki
Facility for Rare Isotope Beams, Michigan State University, MI 48824, USA

Abstract

Facility for Rare Isotope Beams is a high-power heavy ion accelerator facility now under construction at Michigan State University. An overall commissioning plan for its driver linac is established with emphasis on safety, which is presented in this paper together with hazard mitigation and machine protection assumed during commissioning.

INTRODUCTION

Facility for Rare Isotope Beams (FRIB) is a high-power heavy ion accelerator facility now under construction at Michigan State University under a cooperative agreement with the US DOE [1]. Its driver linac operates in CW mode and accelerates all stable ions to energies above 200 MeV/u with the beam power on target up to 400 kW. The linac has a folded layout as shown in Fig. 1, which consists of a front-end, three Linac Segments (LSs) connected with two Folding Segments (FSs), and Beam Delivery System (BDS) to deliver the accelerated beam to target. The linac is located in a tunnel underground with the exception of two ECR ion sources and a part of LEBT (Low Energy Beam Transport) located on the ground level (not shown in Fig. 1). The beam is delivered to the linac tunnel through a vertical beam drop. LSs consist of two types of superconducting QWRs (Quarter Wave Resonators) with geometrical β of 0.041 and 0.085, and two types of superconducting HWRs (Half Wave Resonators) with geometrical β of 0.29 and 0.53. LS1, LS2, and LS3, respectively, have 14, 24, and 6 cryomodules. The total number of superconducting cavities is 330 including rebuncher cavities in FSs. A charge stripper is located after LS1. The linac has four tuning Beam Dumps (BDs), BD FS-1a, BD FS-1b, BD FS-2, and BD BDS, as shown in Fig. 1.

FRIB driver linac is substantially larger both in scale and beam power than existing facilities of a similar kind, which poses significant challenges in realizing safe commissioning. The unique layout of the linac adds additional difficulties. We present overall commissioning plan for the FRIB driver linac in this paper with emphasis on hazard mitigation and machine protection. Detailed tuning algorithms for specific operation parameters will be discussed elsewhere. The commissioning plan presented in this paper builds on a preliminary plan [2] by incorporating hazard mitigation and machine protection details.

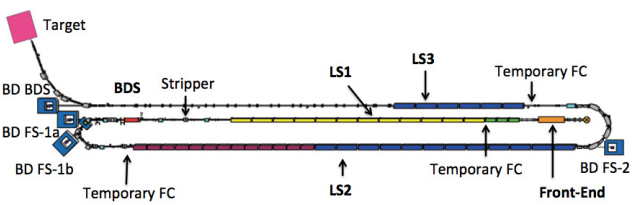


Figure 1: Schematic layout for FRIB driver linac.

GOALS FOR COMMISSIONING AND COMMISSIONING BEAMS

Although we will accelerate various ions up to uranium with the FRIB linac, ^{36}Ar and ^{86}Kr are chosen for commissioning beams. One key commissioning goal is to accelerate an Ar beam with energy exceeding 200 MeV/u. A second key goal is to detect ^{84}Se at fragment separator for secondary beams at the FRIB experimental system. To achieve the second goal, the driver linac is expected to accelerate a CW ^{86}Kr beam as a primary beam. We adopt single-charge-state beams for commissioning, although multi-charge-state beams are planned to increase the beam power in later stages. Assumed charge states for the commissioning beams are listed in Table 1.

While the FRIB linac is a CW linac, most of the tuning during the commissioning will be performed with a pulsed beam. Considering the risk of single point beam loss during the initial phase of beam commissioning, the peak current, pulse width, and repetition rate for the beam are chosen to be 50 eμA after stripping, 50 μs, and less than 1 Hz, respectively. The pulse structure is generated with a LEBT electrostatic chopper. The peak current corresponds to several % of the full intensity, which is chosen to give sufficient resolution/accuracy for beam diagnostics. The corresponding average beam power is approximately 1 W for Ar beam, which poses no radiation hazard even if it is totally lost at a single point. We refer to this pulse beam as "medium intensity short pulse beam" hereafter. The peak power for the medium intensity short pulse beam is about 20 kW in the case of Ar beam.

We need to accelerate a CW beam to achieve the second key goal for the commissioning. We plan to have a "low intensity long pulse beam" as an intermediate step from the medium intensity short pulse beam to low current CW beam. The peak current, pulse width, and repetition rate for the low intensity long pulse beam are 350 enA after stripping, 5 ms, and less than 1 Hz respectively. The corresponding average beam power is approximately 1 W for Kr beam. In the final stage of the beam commissioning for driver linac, we plan to deliver a CW Kr beam with the peak intensity of 350 enA to target for the beam commissioning

* Work supported by the U.S. Department of Energy Office of Science under Cooperative Agreement DE-SC0000661.
† ikegami@frib.msu.edu

Copyright © 2014 CC-BY-3.0 and by the respective authors

MSU RE-ACCELERATOR REA3 0.085 QWR CRYOMODULE STATUS*

T. Xu#, B. Arend, B. Bird, F. Casagrande, J. Crisp, K. Davidson, C. Dudley, A. Facco*, I. Grender, P. Gibson, L. Hodges, K. Holland, M. Johnson, S. Jones, B. Laumer, D. Leitner, A. McCartney, D. Morris, J. Ottarson, J. Ozelis, S. Miller, S. Nash, R. Rosas, R. Rose, J. Popielarski, L. Popielarski, M. Thrush, K. Saito, D. Sanderson, R. Walker, D. Wahlquist, J. Wenstrom, J. Wei, W. Wittmer, Y. Xu, Facility for Rare Isotope Beams, Michigan State University, East Lansing, MI, 48824, USA
*INFN - Laboratori Nazionali di Legnaro, Legnaro (Padova), Italy
M. Leitner, Lawrence Berkeley National Laboratory, Berkeley, CA, 94720, USA

Abstract

ReA3 β=0.085 QWR cryomodule is the third cryomodule for the superconducting LINAC of ReA3 reaccelerated beam facility, which will bring the maximum beam energy to 3 MeV/u for heavy ions. This cryomodule consists of 8 β=0.085 QWR cavities and 3 9T superconducting solenoids and operates at 4K. Qualification of cavities and FPCs and the construction of cold mass was completed in 2013. The installation of the module was completed this summer. Functioning not only as an important part of the ReA3 facility, cryomodule 3 also serves as a test bed for FRIB driver Linac and demonstrated the technology needed for FRIB CMs. Here we report the construction, installation and testing of the β=0.085 cryomodule and the development of the critical components.

INTRODUCTION

ReA is a low-energy re-accelerator facility for nuclear physics experiments at FRIB/NSCL, MSU [1,2]. ReA3 will provide a maximum beam energy of 3 MeV/u for heavy ions with this third cryomodule as shown Figure 1. Not only an important part of the ReA facility, cryomodule 3 also served as a test bed for FRIB driver LINAC cryomodules. The technical development of this cryomodule started in 2009. The detailed technical obstacles and resolution of ReA quarter-wave resonators were described by previously [3]. The final certification tests of production cavities show that cavity performance is well above the ReA design goal and even reaches FRIB 4K field requirements [3]. Currently, the fabrication and installation of the cryomodule has been finished and integrated testing is underway.

Table 1: 0.085 QWR Cavity Specification of ReA3

Parameter	ReA3 0.085 QWR
RF frequency	80.5 MHz
β_{opt}	0.085
$L_{eff}= \beta_{opt} \lambda$	317 mm
R_a/Q_0	408 Ω
E_{peak}/E_{acc}	6.2
E_{acc}	3.4 MV/m
Operating temperature	4.5 K
Q_0	>5.0E+8
Aperture	30 mm

CRYOMODULE COMPONENTS

The cryomodule is equipped with 8 β=0.085 QWR cavities. The key parameters of the cavities are listed in Table 1. Three focusing superconducting solenoids with 9 T peak field and 1.8T-m integrated strength are located after 1st 4th and 7th cavities. Each solenoid also comes with sets of vertical and horizontal dipole corrector coils. The cryomodule utilizes a local magnetic shielding scheme

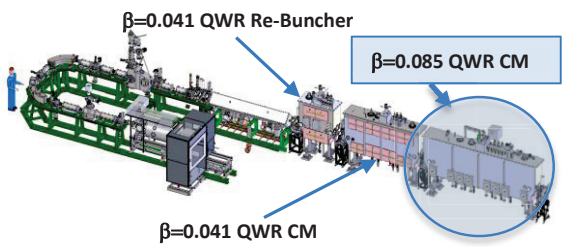


Figure 1: Isometric view of ReA3 Linac

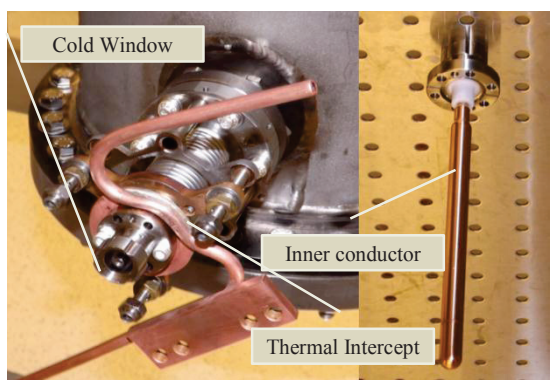


Figure 2: ReA3 β=0.085 QWR adjustable coupler

*Project funded by Michigan State University
#xuti@frib.msu.edu

ISBN 978-3-95450-142-7

Copyright © 2014 CC-BY-3.0 and by the respective authors

PROGRESS AND PLAN OF OPEN XAL APPLICATIONS FOR FRIB*

Yan Zhang#, Paul Chu, Dylan Maxwell,
FRIB, Michigan State University, East Lansing, MI 48824, USA

Abstract

FRIB driver linac will deliver all heavy ion beams up to uranium with beam energy above 200 MeV/u, maximum beam power on fragment target 400 kW for rare isotope productions. In the FRIB project, constructions of state-of-the-art low beta cryomodules and developments of advanced physics application software are important. In this paper, our major progress and the development plan of physics application software for the FRIB driver linac within the Open XAL framework are discussed, which include the FRIB linac online model, back-end database for physics applications, virtual accelerator for software testing, and several pilot physics applications. Deploying and initial testing of Open XAL and the pilot applications are currently planned for a new cryomodule at Michigan State University.

INTRODUCTION

The FRIB, Facility for Rare Isotope Beams, is currently under construction on the campus of MSU, Michigan State University. This nuclear project is funded by the Department of Energy Office of Science, MSU, and the State of Michigan. The total budget of the project is about 730 million dollars, and it will be completed in 2022 [1].

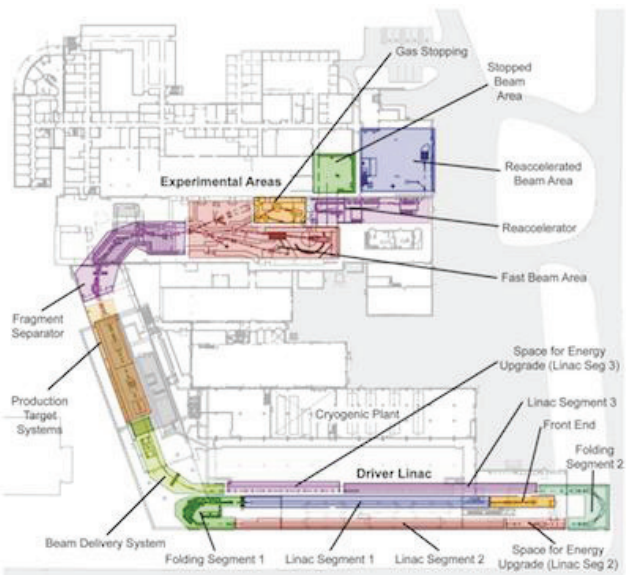


Figure 1: Layout of the FRIB

Figure 1 shows the layout of FRIB. Major components of the facility include a driver linac, a fragment target and separator, re-accelerator, nuclear experiment instruments, and several beam transport lines. The linac consists of a front end, three straight superconducting linac sections, two 180º isochronous, achromatic folding sections, and a beam delivery system. The driver linac accelerates and transports primary beams to the fragment target for rare isotope productions, and in the design, it will deliver all heavy ion beams up to uranium, beam energy above 200 MeV/u, and beam power on target 400 kW [2]. Because various ion species and different energy are necessary to a wide verity of nuclear research program, and a 90% beam availability is required – build, tuning, and operation of the world's first SRF linac for high-power heavy ion beams will be a challenge.

OPEN XAL COLLABORATION

Extended accelerator language, or XAL – a Java based accelerator physics software toolkit, has been successfully established at the Spallation Neutron Source (SNS) [3, 4]. It was later applied for Japan Proton Accelerator Research Complex linac [5], Linac Coherent Light Source [6], and some other accelerators. Because of the distinctiveness and complexity of each unique accelerator, it is difficult to build one-size-fits-all suit, however, as the similarity of accelerator structure and component, it is favourable to have a common toolkit. The Open XAL collaboration is formed to develop a common platform for accelerator modelling, control and analysis [7], participant institutes include SNS, European Spallation Source (ESS), FRIB, China Spallation Neutron Source (CSNS), TRIUMF, and Cosy Lab. Monthly meeting has been established, and there were several Open XAL workshops at SNS, FRIB, and ESS. Current status and more info about the Open XAL project can be checked online [8].

Even though XAL has been successfully applied for the SNS operation with a 1.4 MW beam power and a beam availability more than 90%, the SNS team still managed to make major contributions to the Open XAL project which benefits all other institutes: modified the software structure, reduced dependencies on third-party libraries, optimized the core, and migrated many validated physics applications into Open XAL. Most importantly, in earlier this year, it has been deployed at the SNS control room successfully; operators and physicists can use Open XAL to control and analyse the SNS accelerators [9].

The ESS team built an automation testing framework for Open XAL physics applications, benchmarked the online model against other linac models such as, the Java ESS linac model and TraceWin, and they also improved the documentation in order to ease the learning curves to the developers and to general users. They are planning to work on benchmarking and improving the space charge model, and adding new RF cavity model [10].

Because many accelerator physicists favour scripting languages, such as MATLAB and Python, for the control room testing and for fast developments, it is required to

* Work supported by the U.S. Department of Energy Office of Science under Cooperative Agreement DE-SC0000661
# zhangy@frib.msu.edu

Copyright © 2014 CC-BY-3.0 and by the respective authors

ON THE DESIGN OF HIGHER ORDER MODE ANTENNAS FOR LCLS II*

M. Awida#, T. Khabiboulline, I. Gonin, O. Pronitchev, K. Premo, N. Solyak, and V. Yakovlev,
Fermilab, Batavia, IL 60510, USA

Abstract

The upgrade of the Linac Coherent Light Source (LCLS-II) necessitates a major modification to the higher order mode (HOM) antenna of the conventional ILC elliptical 9-cell cavity. Due to the continuous wave nature of the proposed LCLS II Linac, the HOM antenna is required to bare higher RF losses. A modified design of the HOM antenna is presented in this paper ahead with a thorough thermal quench study in comparison with the conventional ILC design.

INTRODUCTION

Higher order modes (HOM) could be excited in the particle accelerator's superconducting cavities by the particle beam causing instabilities and affecting the particle accelerator performance. In this perspective it is essential to couple them away from the cavity through HOM antennas. However, the RF losses accumulated on the HOM antenna surface would induce heating and might cause the antenna surface to heat up and eventually quench if the temperature exceeded 9.2 K; the critical temperature for Niobium. The problem would even be rather more critical for continuous wave machines compared to pulsed machines.

LCLS II, a proposed coherent light source to be built at SLAC, is a continuous wave linear accelerator that would utilize state of the art superconducting cavities. HOM heating is one of the technical challenges that are facing this machine.

Given that we would like to utilize several existing ILC cavities in LCLS II project, we investigate in this paper, the possible shape modifications of the current ILC HOM antenna that could lower the RF losses (goal is reduce the losses by a factor of 5), while relatively preserving the current coupling (goal is to avoid reducing the coupling more than 10 times).

Figure 1 shows the geometry of the conventional ILC 9-cell elliptical cavity. The cavity has a power coupler and a HOM antenna (HOMc) on one side and a pick-up and a HOM antenna (HOMpu) on the other side. The front projection of the cavity is shown in Figure 2(a), depicting geometry of the HOM antennas and showing both the antennas and the f-parts. Figure 2(b) and (c) illustrate the nominal dimension of the HOM antenna and the gap size between the antenna and the f-part [1]. Possible modifications to the current ILC style of the HOM antenna are either in changing the gap size or changing the tip size.

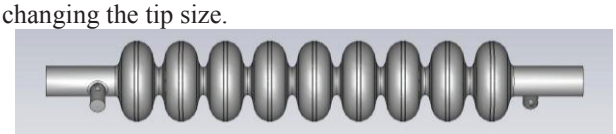


Figure 1: Geometry of the ILC Cavity.

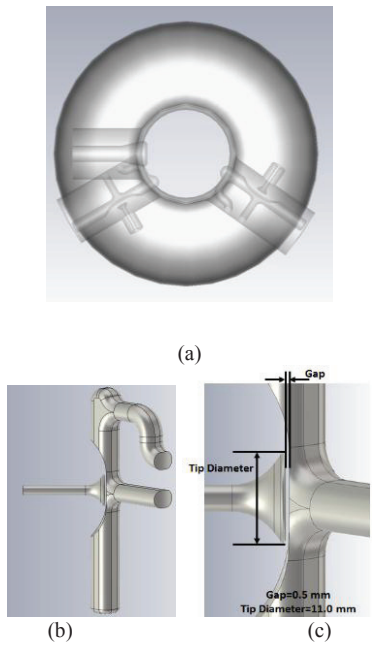


Figure 2: The geometry of the HOM coupler and antenna for the ILC cavity (a) Transparent front view of the cavity showing the HOM couplers (b) HOM antenna and f-part. (c) Dimension of HOM antenna.

ELECTROMAGNETIC ANALYSIS

In this section the electromagnetic performance of possible modified designs is reported. In this perspective, we will take the conventional ILC style antenna as a reference design and the modified versions will be evaluated based on their performance relative to this reference design as far as losses and external quality factor of the antenna. Ratios of both losses and Q_{ext} will be used as criteria of comparison.

a) Modified Design of Trimmed Antenna

Trimming the antenna should reduce the losses but will considerably change the coupling (i.e, Q_{ext}). To investigate this modification option, the geometry was simulated with a trimmed antenna. Two trimmed versions were simulated of 2.5 mm and 3.5 mm in gap size.

Figure 3(a) shows the effect of trimming the antenna on Q_{ext} for all higher order modes up to 2.5 GHz. A magnetic-magnetic (MM) boundary conditions were enforced on the pipe boundaries in all simulations. The ratio of Q_{ext} with respect to the ILC reference design (gap size=0.5 mm) is shown in Figure 3(b). Clearly, the gap size affects significantly the coupling. Ignoring the fundamental band around 1.3 GHz, the ratio of Q_{ext} is no less than 21.1, 7.4 for the trimmed version of 3.5 mm, and 2.5 mm in gap size, respectively.

Copyright © 2014 CC-BY-3.0 and by the respective authors

ISBN 978-3-95450-142-7

DIPOLE KICK DUE TO GEOMETRY ASYMMETRIES IN HWR FOR PXIE*

P. Berrutti#, T. N. Khabiboulline, V. Lebedev, V. P. Yakovlev

Fermilab, Batavia, IL 60510, USA

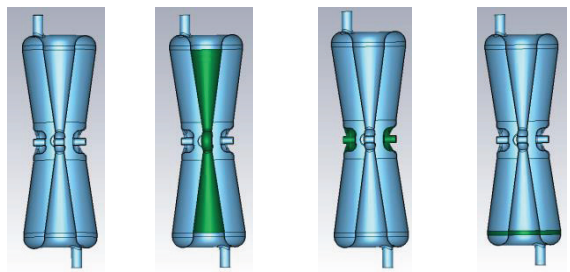
Abstract

Project X Injector Experiment (PXIE) will have a family of half wave resonators having frequency=162.5 MHz and beta optimal=0.11. During cavity production, when the niobium parts are assembled and welded together, it is fundamental to control the frequency of the accelerating mode in order to meet the specified operating value. For the HWR of PXIE the tuning will be achieved by trimming one end of the resonator only, this will introduce unwanted asymmetry in the cavity geometry leading to a dipole kick for the particles traveling through the cavity. The cavity geometry will be different from the ideal, once the cavity is assembled, because of small misalignment of the niobium parts and because of the welding shrinkage. Misalignments of the inner conductor and the beam pipes can be expected. The asymmetry due to tuning process along with production misalignments, have been simulated and the equivalent dipole kick has been calculated.

INTRODUCTION

PXIE is a CW linac to be built at FNAL, it consists of an ion source capable of delivering 5 mA (nominal) at 30 keV followed by a LEBT section, a 5 mA RFQ, a MEBT section with integrated wideband chopper. Two superconducting cryomodules are then used to accelerate the beam from 2.1 MeV, at the end of the MEBT, to 30 MeV [1]. The HWR cavities, designed and built by ANL [2][3], operating at 162.5 MHz and having optimal beta = 0.11, will bring the beam energy from 2.1 to approximately 10 MeV, and they will be placed before a section of spoke cavities SSR1 (frequency = 325 MHz and beta = 0.21). Spoke resonators are used for low and medium beta acceleration, since they have compact size at low frequency. Since coaxial resonators have an inner electrode which breaks the azimuthal symmetry, these structures show asymmetric transverse fields, even though the cavity shape is perfectly matching the ideal design [4] [5]. For a real structure there will be some misalignment due to fabrication tolerances, weld shrinkage or, in some cases, the manufacturing process will require asymmetric trimming of the Nb parts. At FNAL one family of single spoke resonators has been built and tested and the transverse field perturbation due to geometry misalignments has been study and presented in [6]. The HWR for PXIE manufacture requires an asymmetric trim of one end of the cavity, in order to match the resonance frequency of the whole structure. As a result, one could expect to have cavities with up to 3 mm (worst case) asymmetry in the half-length: distance from beam tube to top or bottom of the resonator.

In this paper a study of the effects of geometry misalignments on the HWR transverse fields is presented. The Y-Z cross-section of the cavity is shown in Fig. 1(a). Different kinds of perturbation have been taken into account: displacements of the inner electrode, highlighted in Fig. 1(b), misalignments of the beam tubes, shown in Fig. 1(c), the asymmetry due to one end trim for final frequency match, the area to be trimmed is shown in Fig 1(d). The calculation of the transverse momentum gain has been carried out by direct integration of the transverse field components and by Panofsky-Wenzel's theorem. In addition the radial component of the transverse momentum gain has been expanded into multipoles to see what kind of perturbation to the beam dynamic is present.



(a) (b) (c) (d)

Figure 1: HWR geometry Y-Z section (a), inner electrode highlighted (b), beam tubes highlight (c), area of asymmetric trimming shown in green (d).

HWR GEOMETRY MISALIGNEMENTS

The RF fields have been simulated with Comsol Multiphysics, which allows local mesh refinement on lines, surfaces and domains. This feature is crucial in order to get precise values of the field amplitudes for geometry misalignments of the order of 1 mm. The displacements induce electric and magnetic transverse fields on the Z axis: a displacement along X perturbs Ex and Hy fields, while a modification along Y axis affects Ey and Hx. For example the transverse fields on Z axis for X and Y misalignments of the electrode are plotted in Fig. 2. The transverse momentum gain induced on the particles traveling on axis can be calculated by integration of the fields:

$$\Delta \boldsymbol{P}_{\perp} c = \int_{z_i}^{z_f} (\mathbf{E} + \mathbf{v} \times \mathbf{B}) \frac{1}{\beta} e^{i\frac{kz}{\beta}} dz \qquad (1)$$

Panofsky-Wenzel's theorem gives an alternative formula:

$$\Delta \mathbf{P}_{\perp} c = \frac{i}{k} \int_{z_i}^{z_f} \nabla_{\perp} E_z \, e^{i\frac{kz}{\beta}} dz \, . \qquad (2)$$

When the inner electrode, Fig. 1(b), is displaced with respect to its ideal position the electric field on axis shows

*Work supported by D.O.E. Contract No. DE-AC02-07CH11359
#berrutti@fnal.gov

Copyright © 2014 CC-BY-3.0 and by the respective authors

ISBN 978-3-95450-142-7

TRANSMISSION EFFICIENCY MEASUREMENT AT THE FNAL 4-ROD RFQ*

J.-P. Carneiro†, F. G. Garcia, J.-F. Ostiguy, A. Saini, R. Zwaska, Fermilab, Batavia, IL 60510
B. Mustapha, P. Ostroumov, ANL, Argonne, IL 60439

Abstract

This paper presents measurements of the beam transmission performed on the 4-rod RFQ currently under operation at Fermilab. The beam current has been measured at the RFQ exit as a function of the magnetic field strength in the two LEBT solenoids. This measurement is compared with scans performed on the FermiGrid with the beam dynamics code TRACK. A particular attention is given to the impact, on the RFQ beam transmission, of the space-charge neutralization in the LEBT.

INTRODUCTION

A new injector has been in operation since 2012 on the FNAL 400 MeV Linac as a part of the Proton Improvement Plan whose primary goal is to increase the proton flux in the booster to ultimately 2.25×10^{17} protons per hour. This new injector, composed of an ion source, a Low Energy Beam Transport line (LEBT), a 4-rod Radio Frequency Quadrupole (RFQ) and a Medium Energy Beam Transport (MEBT) is presented in details in Ref. [1]. The beam transmission in the injector, from the ion source to the MEBT exit, has routinely been measured since the start of its operation ranging from 40% to 50%. This measured transmission is significantly lower than the expected one, which according to computer simulations should be close to 100%. After a brief description of the injector, this paper presents a measurement of a beam transmission at the MEBT exit as a function of the LEBT solenoid fields. This measurement is compared to numerical simulations from the code TRACK [2]. The simulations reveal that the space charge neutralization pattern, which is unlikely to be homogeneous along the LEBT, plays a crucial role in the injector transmission.

THE FNAL LINAC INJECTOR

A layout of the injector is depicted in Fig. 1. A magnetron source produces 35 keV H^- bunches of typically 100 μs long, at a repetition rate of 15 Hz with an average current ranging from 50 to 70 mA. The LEBT comprises two solenoids that match the H^- beam produced by the source into the RFQ entrance. The beam is further accelerated to 750 keV by a 4-rod RFQ operating at 201.25 MHz. At the exit of the RFQ, the MEBT matches the beam into the first Drift-Tube Linac Tank (DTL#01) using two doublets for transverse matching and an RF buncher operating at 3 MV/m for longitudinal matching. An Einzel lens operating at -37.7 kV is installed near the entrance of the RFQ to chop the first 20 μs of the pulse. A current monitor which is used in the measurement described in the next session is located 8.25 cm from the downstream face of the last MEBT quadrupole, i.e at the DTL#01 entrance. The total length of the injector line is in the order of 4 meters.

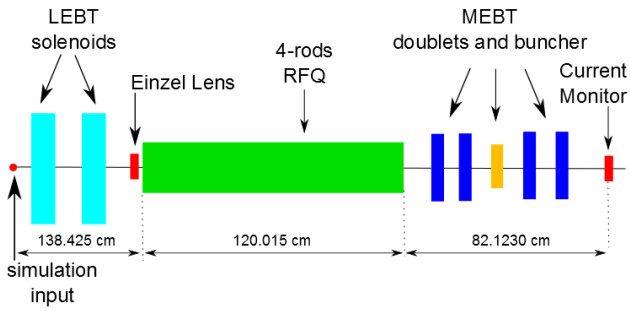


Figure 1: Layout of the FNAL Linac Injector.

TRANSMISSION MEASUREMENT

An experiment has been performed on the linac injector which consisted in varying, in a systematic way, the current in the two LEBT solenoids and measuring the beam intensity on the current monitor located at the MEBT exit. This measurement is represented in Fig. 2.

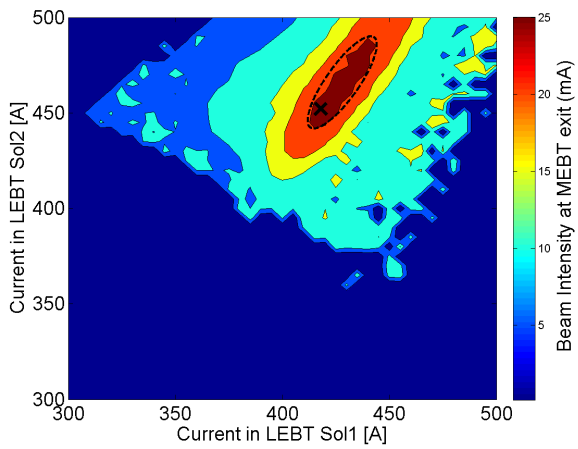


Figure 2: Measurement of the beam intensity at the current monitor located at the exit of the MEBT as a function of the LEBT solenoid currents. The cross represents the actual point of operation of the LEBT and the ellipse mimics the area of favorable transmission.

For this measurement, the LEBT solenoids have been scanned from 300 A to 500 A with a step of 5 A, all other

* Work supported by Fermilab Research Alliance, LLC under Contract No. DE-AC02-07CH11359 with the United States Department of Energy.
† carneiro@fnal.gov

Copyright © 2014 CC-BY-3.0 and by the respective authors

DEVELOPMENT OF 5-CELL BETA=0.9 650 MHz CAVITIES FOR PROJECT X*

M.H. Awida, M. Foley, I. Gonin, A. Grassellino, C. Grimm,T. Khabiboulline, A. Lunin, A. Rowe, V. Yakovlev, FNAL, Batavia, 60510, USA

Abstract

Several 5-cell 650 MHz elliptical cavities have been fabricated for the PIP-II Project [1]. Two versions of the cavities have been designed to accelerate protons of relative group velocity of β=0.9 and β=0.92 in the high energy region of the linac. In this paper, we report the development status of these cavities, summarize the results of the quality control measurements performed on five initial prototypes, and outline the VTS test results.

INTRODUCTION

The proposed design of the 0.8 GeV PIP-II SC Linac employs two families of 650 MHz 5-cell elliptical cavities with different Beta versions. The β=0.61 will cover the 177-480 MeV range and the β=0.9 will cover the 480-800 MeV range.

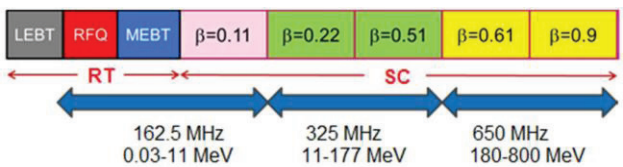


Figure 1: The PIP-II Linac Layout.

Approximately 30 medium beta and 24 high-beta cavities are currently required for the project. The low beam current for CW operation of PIP-II requires cavities to be mechanically optimized to operate at a high loaded Q and thus, low bandwidth with higher sensitivity to microphonics. The base line high-beta cavity (β=0.90) was designed for 1mA average beam current and has a potential drawback with high-Q trapped monopole modes. Recently the cavity was redesigned for β=0.92 version with increased aperture and better damping of monopole High Order Modes (HOMs), while keeping the same performance as the base line version [2]. This paper will also present the finalized mechanical design of the Helium Vessel (HV) for both the β=0.9 and β=0.92 versions of the cavities, which will be instrumental in minimizing the magnitude of df/dP. The HV in the current design is equipped with the tuner located at the end of the cavity instead of the initially proposed blade tuner located in the middle.

* Operated by Fermi Research Alliance, LLC under Contract No. DE-AC02-07CH11359 with the United States Department of Energy.

gonin@fnal.gov

HELIUM VESSEL DESIGN

The helium vessel assembly is constructed from a single 5 mm thick sheet of grade 2 titanium that is rolled and seam welded into a tube with an inside diameter of 441 mm and a length of 930 mm. The helium vessel assembly is shown in Figure 2, the same helium vessel design is common for both the β=0.9 and β=0.92 cavities. The baseline design for the β=0.9 cavity utilized a blade tuner and was later reconfigured to an end lever tuner for better efficiency of a cavity tuning. However the nine β=0.90 cavities that have been ordered already had their niobium-titanium transitions rings welded on. It is limited the ability of reducing the bellows diameter when dressing this beta version cavity. The dressing configurations for β=0.92 and β=0.90 are outlined below.

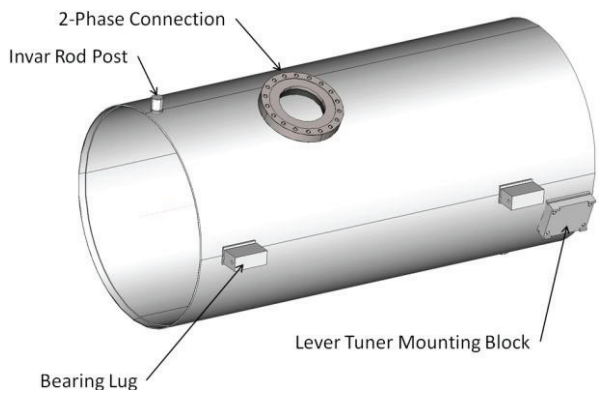


Figure 2: He Vessel Assembly β=0.9 & β=0.92

The weld joint designs on the helium vessel satisfy the American Society of Mechanical Engineers (ASME) Boiler & Pressure Vessel Code Section VIII Division 2. [3] It is important to note that the 5 mm wall thickness for the helium vessel specification was chosen not because of the ASME code, but rather to help in reducing *df/dp* coefficient by using the helium vessel for cavity stiffening.

The main coupler end and the field probe end of the helium vessel have slightly different joint designs due to the cavity installation sequence and variations in the cavity length. The main coupler end of the vessel is considered a fixed position relative to the main coupler port of the cavity, and consistency between these key features for dressed cavities is maintained. Figure 3 shows the titanium-to-titanium Tangstem Inert Gas (TIG) weld connection between the cavity and the helium vessel at the main coupler end of the β=0.92 cavity. This joint design utilizes a backing ring and satisfies the ASME

Copyright © 2014 CC-BY-3.0 and by the respective authors

ISBN 978-3-95450-142-7

TTF-III COUPLER MODIFICATION FOR CW OPERATION*

I. Gonin, T. Khabiboulline, A. Lunin, O. Prokofiev, N. Solyak, V. Yakovlev,
FNAL, Batavia, 60510, USA

Abstract

LCLS-II linac is based on XFEL/ILC superconducting technology, but CW regime of operation requires the modification of components to satisfy LCLS-II requirements. TTF-III [1] coupler is considered as a candidate for a fundamental power coupler for the 1.3 GHz 9-cell accelerating structure at the LCLS-II project [2]. In this paper we discuss the results of multiphysics analysis of the coupler working at various operating regimes. Two major modifications are proposed in order to meet the LCLS-II requirements and eliminate possible overheating: reducing the length of antenna (cold part) and increasing the thickness of a cooper plating on the inner conductor of the warm part of the coupler.

INTRODUCTION

XFEL (modified TTF-III) fundamental power coupler doesn't not meet to the following LCLS-II requirements:

- The coupler tuning range doesn't cover the required nominal Q_{ext} = 4.e7
- There is an overheating of the internal bellow in the warm section of the coupler at 7 kW CW input power and full reflection (effective power ~14 kW)

Table 1: LCLS-II Coupler Technical Specs

Item	Spec
Design	EuXFEL Coupler
Max Input Power	7 kW CW
Minimum Qext Foreseen	1e7
Maximum Qext Foreseen	5e7
Reduction in Antenna Length	8.5 mm
Range of Antenna Travel	+/- 7.5 mm
Predicted Qext Min Range Qext Max Range	3.6e6 – 4.7e6 – 7.5e6 1.0e8 – 1.1e8 – 1.5e8
Warm Section Outer Cond Plating	10 um +/- 5 um, RRR = 30-80
Warm Section Inner Cond Plating	100 um +/- 10 um, RRR = 30-80
Cold Section Outer Cond Plating	10 um +/- 5 um, RRR = 30-80
Center Conductor HV Bias	Optional
Warm and Cold e-Probe ports req	No
Warm Light Port Required	No
Motorized Antenna	Yes – max step = 50 um
RF Processing	7 kW CW with full reflection – vary reflected phase by 180 deg

Two modifications were proposed to address these problems in a frame of the TTF-III coupler R&D and test program:

- Cut the antenna at 8.5mm for increasing the nominal Q_{ext} value.
- Increase the thickness of copper plating on the internal inner conductor of the warm section from 30 μm to 100-150 μm and eliminate overheating.

The main technical specs of the LCLS-II coupler are summarized in Table 1.

MODIFICATION OF ANTENNA

The proposed solution for matching the coupler tuning range is cutting of the antenna tip by 8.5 mm. Figure 1 shows geometries of the original TTF-III (up) and the modified coupler (down) antennas respectively.

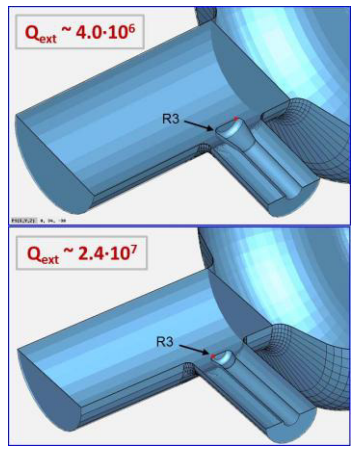


Figure 1: Original TTF-III antenna (up) and modified LCLS-II antenna (down), cut 8.5 mm, rounding is 3 mm.

The range of the antenna tuning displacement is supposed to be similar to the TTF-III coupler: ±7.5 mm. Figure 2 shows the dependence of Q_{ext} versus antenna offset from the cavity axis for the TTF-III and two proposed variants of modifications by cutting the antenna tip on 7 mm (red) and 8.5 mm (blue). Dashed line shows the nominal Q_{ext} value required by the LCLS-II specification.

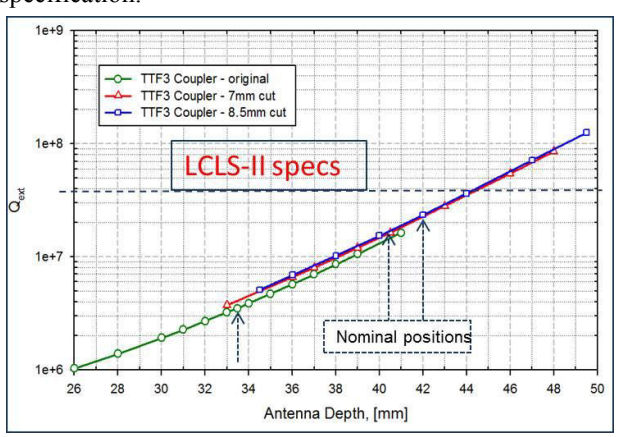


Figure 2: Q_{ext} vs. antenna depth. Green – original TTF-III coupler, red - cut 7 mm, blue – cut 8.5 mm.

* Operated by Fermi Research Alliance, LLC under Contract No. DE-AC02-07CH11359 with the United States Department of Energy.
# gonin@fnal.gov

Copyright © 2014 CC-BY-3.0 and by the respective authors

CONTINUOUS-WAVE HORIZONTAL TESTS OF DRESSED 1.3 GHz SRF CAVITIES FOR LCLS-II

A. Hocker*, C. Crawford, M. Geynisman, J. Holzbauer, A. Lunin, D.A. Sergatskov, N. Solyak, A. Sukhanov, FNAL#, Batavia, IL 60510, USA

Abstract

Fermilab's Horizontal Test Stand has recently been upgraded to provide CW RF testing capabilities in support of the LCLS-II project at SLAC. Several cavities have been tested in this new configuration in order to validate component designs and processes for meeting the requirements of LCLS-II. Areas of study included gradient and Q0 performance and their dependence on extrinsic factors, thermal performance of the input coupler and HOM feedthroughs, and microphonics and RF control. A description of the testing and the results obtained are presented.

INTRODUCTION

The Linac Coherent Light Source (LCLS)-II project [1] features a 4 GeV superconducting radiofrequency (RF) electron linac operated in the continuous wave (CW) regime. The ILC/XFEL nine-cell 1.3 GHz cavity serves as the basis for the LCLS-II dressed cavity design, with a number of elements modified to meet the needs of LCLS-II:

- A new cavity processing recipe optimized to achieve Q_0 = 2.7 x 10^{10} at a gradient of 16 MV/m [2]
- HOM feedthroughs with better heat conduction [3,4]
- Fundamental power couplers (FPC) with a higher Q_{ext} (4 x 10^7) and improved thermal conductivity
- Improved magnetic shielding to keep fields at the cavity < 5 mG
- A new helium vessel design to accommodate larger dynamic heat loads and meet mechanical and cooldown requirements
- A new tuner system for excellent resonance control and microphonics compensation

All of these design modifications need to be validated as they become available; the first two items were in hand relatively quickly and are the focus of this paper.

HORIZONTAL TEST STAND (HTS) UPGRADES

Fermilab's HTS [5] is currently dedicated to providing the testing necessary to support the above validation work. It was initially designed to test high gradient dressed cavities with high power pulsed RF. In order to measure Q_0 accurately it is necessary to use an RF coupling close to unity as opposed to a strongly overcoupled high power coupler. Therefore a number of upgrades to HTS were necessary to support low-power CW testing, including:

- A blank-off flange for the FPC port with a coaxial feedthrough and heat-intercepted cable in lieu of a high power coupler
- Installation of a low-level RF (LLRF) system with phase-locked loop control based on the system described in [6]
- Repurposing a 200 W solid state amplifier as a primary power source rather than a klystron preamplifier
- Installation of a set of Helmholtz coils around the HTS cryostat to provide three-axis cancellation of the Earth's magnetic field

The latter item is critical due to HTS's stainless steel cryostat, which provides minimal magnetic field attenuation. The average ambient field inside an ILC helium vessel and its single layer of magnetic shielding while inside HTS was measured to be approximately 45 mG at room temperature, well above LCLS-II specifications. With the addition of the cancellation coils, the room temperature magnetic field inside the helium vessel was reduced to 6 mG; see Fig. 1.

These upgrades were commissioned using cavity TB9RI026, an electropolished/120°-C-baked cavity in an

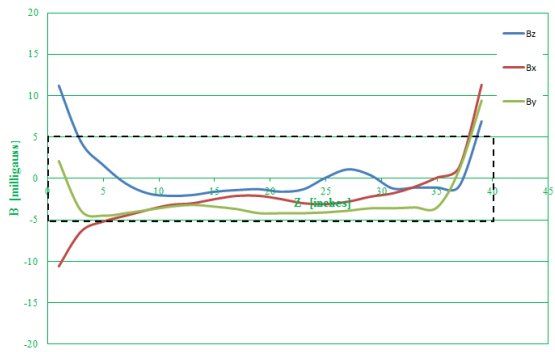


Figure 1: Room temperature magnetic field profile along the length of an ILC helium vessel/magnetic shield installed in HTS with cancellation coils turned on. The z-direction is along the cavity axis (north-south in HTS), the y-direction is vertical, and the x-direction is transverse. The dotted outline represents the LCLS-II target and the extent of the helium vessel/shielding.

*hocker@fnal.gov

Operated by Fermi Research Alliance, LLC under Contract No. DE-AC02-07CH11359 with the United States Department of Energy.

Copyright © 2014 CC-BY-3.0 and by the respective authors

ISBN 978-3-95450-142-7

RF TESTS OF DRESSED 325 MHz SINGLE-SPOKE RESONATORS AT 2 K

A. Hocker*, E. Cullerton, B. Hanna, W. Schappert, A. Sukhanov, FNAL#, Batavia, IL 60510, USA

Abstract

Fermilab has recently completed an upgrade to its spoke resonator test cryostat to enable testing of cavities in superfluid helium. Two single-spoke resonators with differing helium vessel designs have been tested in this new configuration. Gradient and Q_0 performance was studied along with microphonics control and sensitivity of the resonant frequency to pressure variations. A description of the testing and the results obtained are presented.

INTRODUCTION

Fermilab's Proton Improvement Plan (PIP)-II project (essentially equivalent to Stage 1 of Project X) includes an 800 MeV superconducting continuous-wave (CW) H^- linac that makes use of five different types of radiofrequency (RF) cavities [1]. One of these is a superconducting single-spoke resonator (SSR1) operating at a frequency of 325 MHz [2]. These cavities are first tested "bare" at Fermilab's Vertical Test Stand (VTS) before being welded inside a helium jacket. The "dressed" cavity can then be tested in a cryomodule-like environment at the Spoke Test Cryostat (STC) facility located in Fermilab's Meson Detector Building (MDB). Cavity performance at STC is evaluated in terms of maximum accelerating gradient, Q_0, and field emission in order to qualify cavities for assembly into an accelerator cryomodule.

THE STC FACILITY

Over the past year the STC was upgraded to allow operation at superfluid helium temperatures. The central component of this upgrade was a new feed can housing a Joule-Thomson heat exchanger for cooling helium to 2 K and supplying it to the cavity. This new feed can is shown in Fig. 1 and described in detail in [3].

RF power is provided by a 200 W solid state amplifier driven by a digital low-level RF (LLRF) system [4] that processes the I and Q of the cavity forward, reflected, and transmitted power signals. This system employs a phase-locked loop to keep the RF power matched to the cavity resonance when the cavity bandwidth is narrow (< 1 Hz). A Labview application serves as an interface to the LLRF system and also provides online calculations of cavity Q's and gradients.

X-rays from field emission are measured with two detectors, one on each end of the test cryostat. All cavity, RF, and cryo data are continuously archived through the dataloggers available from Fermilab's ACNET controls system.



Figure 1: The Spoke Test Cryostat with upgraded feed can.

COMMISSIONING RESULTS

The SSR1 cavity S1B-ZN-101 was used to re-establish operations at STC. This cavity was previously tested at 4.5 K at STC prior to the upgrade, and thus serves as a good benchmark for assessing 2 K operations. It was assembled in a configuration identical to its previous CW test [5], with a prototype slow tuner, fast piezo tuners, and a high-Q_{ext} input coupler.

The cavity was installed in STC and actively pumped throughout its test with a 20 L/s ion pump. It was cooled to 2 K without incident, and after tuning up the helium pressure and liquid level regulation loops RF operations began.

Measurements of the forward, reflected, and transmitted powers, along with the time constant of the decay of the cavity field after turn-off of the RF at low power, enable the determination of the cavity Q_0 and voltage at any power level. To define the accelerating gradient for the spoke cavity the convention $L = \beta\lambda = 0.203$ m was adopted, where L is the effective RF length (the geometrical β for the SSR1 cavity is 0.22). After calibrating the LLRF system in this way, the forward power was slowly increased.

*hocker@fnal.gov

#Operated by Fermi Research Alliance, LLC under Contract No. DE-AC02-07CH11359 with the United States Department of Energy.

Copyright © 2014 CC-BY-3.0 and by the respective authors

Z-SLICER: A SCHEME FOR SHAPING THE ELECTRON BEAM PROFILE IN A LINAC*

J. Thangaraj[1†], D. Crawford[1], D. Broemmelsiek[1], R. Thurman-Keup[1], C. Baffes[1], W. Wortley[2]
[1] Fermilab, IL, USA
[2]University of Rochester, NY, USA

Abstract

A train of short bunches (∼100 fs) are at a premium at accelerator facilities and their applications include terahertz (THz) generation, short bunch diagnostics, advanced accelerator R&D, etc [1].In this work we report on the design and simulation of an experiment involving a 20 MeV electron beam, that will be intercepted by a set of metallic slits inside a bunch compressor. After the mask, some electrons are scattered while other pass through un-affected. After exiting the bunch compressor, those electrons that were not affected by the slits will appear as short electron bunches. The key advantage of our scheme is its simplicity, tunability and low cost. The scheme does not require any additional hardware such as lasers, undulator, or transverse deflecting cavity. The tuning variable is only the RF-chirp. The detection of the bunching requires just a skew quad in the chicane and a transverse screen downstream.

INTRODUCTION

Among the various techniques available to generate short or modulated bunches for THz radiation generation at low energies[2, 3, 4, 5, 6], one simple way is to use a metallic-slit mask inside a dispersive section[7, 8]. In this paper, we describe Z-Slicer, a tool that is planned for installation at the Advanced Superconducting Test Accelerator (ASTA) low energy bunch compressor, which has the flexibility to generate a train of short pulses, a train of pulses of varying separation or just a slice of a bunch.

THE ASTA LINAC

The ASTA linac will employ a Cs2Te photocathode irradiated by an ultraviolet (264 nm) laser pulse of rms width 3.2 ps, producing bunch trains at a repetition rate of 5 Hz and a train frequency of 3 MHz for a 1 ms macro-pulse. The number of bunches in each train can be anywhere from 1-3000, depending on the beam charge and permit. The charge of each bunch can range from 20 pC to 3.2 nC giving an average current of 9 mA at maximum charge. The low energy beamline can have energies ranging from 20 MeV to 50 MeV.

* Fermi Research Alliance, LLC operates Fermilab under contract No. DE-AC02-07CH11359 with the U.S. Department of Energy
† jtobin@fnal.gov

Z-SLICER INSIDE THE ASTA BUNCH COMPRESSOR

The ASTA bunch compressor is a chicane style bunch compressor with the parameters listed in Table 1. The Z-Slicer will be installed at the center of the ASTA chicane. The Z-Slicer tool consists of a stepper motor controlled actuator (rotatory stage) along with a 316L stainless steel holder that has three positions. The first position can hold four blades, the second one a YAG screen with a mirror for a spot size measurement, and the final is an impedance matching cage for the beam to pass through. The bunch compressor is equipped with a skew quad just before the third dipole that allows time-dependent studies of CSR or measuring the formation of the train of pulses without resorting to radiation based detection systems, such as a streak camera, bolometer or an interferometer. The ASTA bunch compressor also has a complete plan for collection of CSR/CER for beam diagnostics and THz-based instrumentation. The ASTA bunch compressor is built and ready for commissioning with the low energy beam. A schematic of the ASTA buch compressor and the operation of the Z-Slicer is shown in Fig. 1.

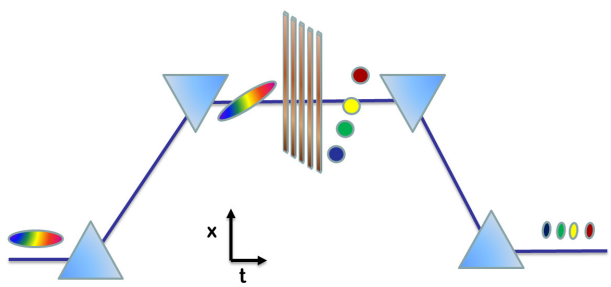


Figure 1: Schematic of the ASTA bunch compressor with the Z-Slicer.

THEORY OF OPERATION

The energy-chirped beam generated from the photoinjector after passing through the accelerating cavity is then sent to the bunch compressor. At the center of the bunch compressor, the bunch is intercepted by a slit mask which selectively scatters some of the electrons while other electrons are transmitted through the rest of the chicane. At the end of the chicane, such transversely separated beamlets are transformed into a train of short bunches longitu-

Copyright © 2014 CC-BY-3.0 and by the respective authors

STUDY AND DESIGN OF THE HIGH POWER RF COUPLER FOR THE CH-CAVITY OF THE FAIR pLINAC

F. Maimone, G. Clemente, W. Vinzenz, GSI, Planckstraße 1,64291 Darmstadt, Germany

Abstract

At GSI a proton Linac has been designed and developed in order to provide a 70 MeV proton beam for the FAIR facility. The pLINAC consists of an RFQ followed by six CH-DTL accelerating cavities and the electromagnetic field inside each cavity is generated by seven Klystrons providing up to 2.8 MW power at 325.224 MHz. The high power RF coupling between the Klystron and the accelerating CH-cavity has been studied and an inductive coupling loop has been designed. The coupler insertion inside the cavity and the rotation angle with respect to the magnetic field lines have been adjusted and the results of the analysis of the coupler positioning are presented. A prototype coupler is under construction and the measurement of RF coupling with the CH-cavity is scheduled within this year.

INTRODUCTION

In the framework of the Facility for Antiproton and Ion Research (FAIR) project a linac is under construction to inject a 70 MeV proton beam into the SIS18. The FAIR proton injector consists of a microwave based ECR proton source delivering up to 100 mA protons to be accelerated by an RFQ and a normal conducting Drift Tube Linac (DTL). The DTL is composed by three Coupled Cross-bar H-mode (CCH) cavities, providing the acceleration up to the energy of 36 MeV, followed by three Cross-bar H-mode (CH) cavities. [1] [2]

In order to prove the concept of the CCH cavity, a prototype of the second accelerating unit, from 11.5 MeV to 24.2 MeV, has been manufactured, assembled and tuned with respect to the resonance frequency and to the electromagnetic field flatness along the beam axis. [3]

The RF power system of the proton linac consists of seven klystrons providing up to 3 MW saturated power at 325 MHz, in RF pulses of 200 µs at a repetition rate of 4 Hz, to the RFQ and to the two sections where the three CCH-cavities and the three CH-cavities are grouped [4].

The RF power transport system is composed by WR2300 waveguides, circulators and waveguide WR2300 to 6 1/8" coaxial adapters. In order to provide the RF power to the accelerators, seven couplers connected to 6 1/8" coaxial lines have to be designed and machined. Concerning the DTL section, it has been decided to make use of six inductive couplers. By means of the loop coupler type, the coupling factor can be easily tuned by adjusting the penetration inside the tank and the rotation angle with respect to the magnetic field lines.

The effect on the coupling factor and on the electromagnetic properties of the RF coupler insertion and rotation inside the coupling cell has been studied. The results of this study, together with the mechanical design of the prototype of the high power RF coupler, are here presented.

RF DESIGN

The high power RF coupler has the task to transfer the RF power to the CH-cavity. In order to reduce the reflected power to the RF generator it has to provide an impedance matching between the to 6 1/8" coaxial lines impedance (50 Ω) and the cavity one. When the matching condition is fullfilled the power is fully transferred to the cavity which is said to be *critically coupled*. In such a case the external quality factor Q_{ext} is equal to the unloaded quality factor Q_o. When this condition is achieved the loaded quality factor Q_L:

$$Q_L = \frac{Q_0}{1+Q_0/Q_{ext}} = \frac{Q_0}{1+\beta} \quad (1)$$

is equal to $Q_o/2$. The conventional parameter $\beta=Q_o/Q_{ext}$ indicates wheter the cavity is undercoupled ($\beta<1$), overcoupled ($\beta>1$) or critically coupled ($\beta=1$).[5] In order to properly desing the RF inductive coupler preliminary simulations of the electromagnetic field patterns of the CCH-DTL described in [3] have been carried out with CST MWS. Figure 1 shows the electromagnetic field of the mode H_{210} having a resonance frequency f=324.356 MHz and an unloaded quality factor Q_o=14280 (by assuming a copper internal surface). The fields are normalized to have 1 J of stored energy inside the structure. The following formula is used to calulate the area A_s of the coupling loop necessary to obtain the mathing condition [5] :

$$A_S = \frac{\sqrt{100P}}{2\pi f H_0 \cos(\alpha)} \quad (1)$$

This quantity can be calculated by using the simulations results concering the magnetic amplitude H_o as a function

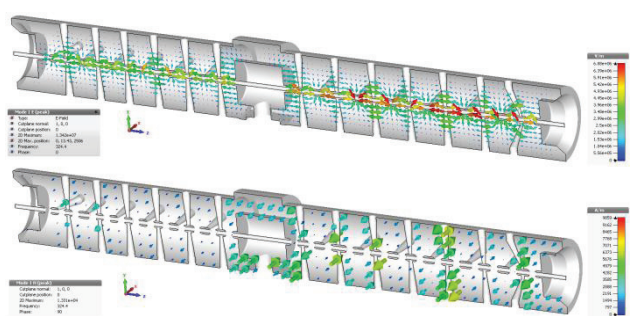


Figure 1: Electric field (up) and magnetic field (down) distribution for the H_{210} mode.

Copyright © 2014 CC-BY-3.0 and by the respective authors

ISBN 978-3-95450-142-7

STATUS OF THE GSI POSTSTRIPPER - HE-LINAC

S. Mickat, W. Barth, G. Clemente, X. Du, L. Groening, A. Orzhekhovskaya, B. Schlitt, H. Vormann, C. Xiao, S. Yaramyshev, GSI, Darmstadt, Germany
M. Droba, H. Hähnel, U. Ratzinger, R. Tiede, IAP, Frankfurt, Germany

Abstract

The High-Energy (HE) Linac is proposed to substitute the existing UNILAC post-stripper section. The post-stripper is an Alvarez DTL, which is in operation over four decades successfully. A quasi Front-to-End simulation along the UNILAC shows that by taking future upgrade options into account already, with the existing Alvarez section the FAIR requirements are not reached. Even by substituting the Alvarez section by the HE Linac the aim is not reached per se regarding the existing boundary conditions. Currently workpackages are defined together with the Institute of Applied Physics at Frankfurt University. Starting from the ion sources to the SIS18 transfer channel every section is reinvestigated for improvements in beam quality and intensity.

REVIEW OF FAIR URANIUM ACCELERATOR CHAIN

The design ion for the future Facility for Antiproton and Ion Research (FAIR) is uranium. The present GSI-accelerator complex, i.e. the linear accelerator UNILAC and the heavy ion synchrotron SIS18, are foreseen to serve as an U28+ injector for FAIR.

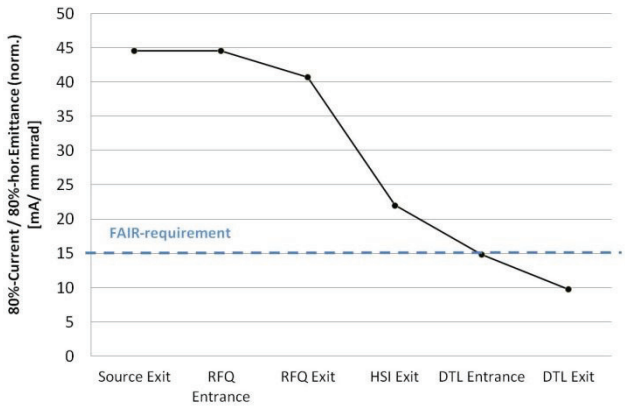


Figure 1: Beam quality along the UNILAC including future upgrade options like the Compact LEBT already with the existing Alvarez DTL [2].

In November 2013 this accelerator chain was reviewed by five external accelerator experts. The two main results are pointed:

- The input beam parameter window for the SIS18 is defined. For providing $2x10^{11}$ U28+ particles a beam current of 15 mA at a pulse length of 80 µs within a total horizontal emittance of 5 mm mrad is required [1].
- A quasi Front-to-End simulation along the UNILAC shows that by taking future upgrade options into account already, with the existing Alvarez section the FAIR requirements are not reached. Even by substituting the Alvarez section by the HE Linac the aim is not reached per se regarding the existing boundary conditions [Fig. 1].

In its report the review committee recommends the following measures [3]:

- Privilege the maintenance of beam quality instead of rf efficiency
- Establish the 3 Hz operation of uranium source
- Redesign the LEBT
- Substitute/redesign the consumed RFQ electrodes
- Optimize/redesign the matching line from RFQ to HSI IH – the MEBT

LEBT

A dedicated high current uranium ion source and LEBT is planned to fulfil the intensity requirements for FAIR [4]. This new injection line is integrated in between the two existing branches as a straight injection line without a dipole magnet (Fig. 2).

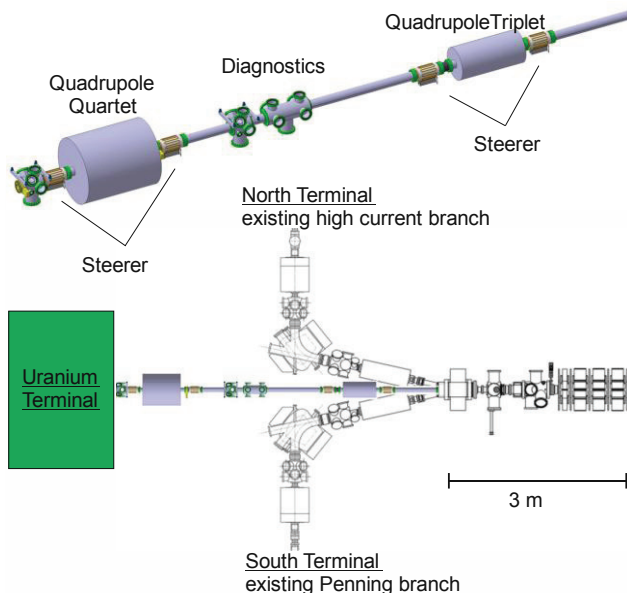


Figure 2: The existing HSI-LEBT branches together with the planned straightforward injection.

All uranium charge states, coming from the ion source, are injected into the HSI-RFQ. Only the design charge state U^{4+} is accelerated through the RFQ, while the other charge states are lost inside the RFQ mainly.

Copyright © 2014 CC-BY-3.0 and by the respective authors

ISBN 978-3-95450-142-7

FIRST RF MEASUREMENTS OF THE SUPERCONDUCTING 217 MHz CH CAVITY FOR THE CW DEMONSTRATOR AT GSI*

F. Dziuba†,[1], M. Amberg[1,3], K. Aulenbacher[3,4], W. Barth[2,3], M. Basten[1], M. Busch[1], H. Podlech[1], U. Ratzinger[1], S. Mickat[2,3]

[1]IAP University of Frankfurt, 60438 Frankfurt am Main, Germany
[2]GSI Helmholtzzentrum, 64291 Darmstadt, Germany
[3]Helmholtz Institut Mainz (HIM), 55099 Mainz, Germany
[4]KPH Mainz University, 55128 Mainz, Germany

Abstract

Presently, a superconducting (sc) 217 MHz Crossbar-H-mode (CH) cavity [1] is under construction at Research Instruments (RI), Bergisch Gladbach, Germany. Among the horizontal cryomodule and two sc 9.5 T solenoids the cavity is the key component of the cw demonstrator at GSI. To show the operation ability of sc CH cavity technology under a realistic linear accelerator environment is one major goal of the demonstrator project. A successful beam operation of the demonstrator will be a milestone regarding the continuing advanced sc cw linac project [2] at GSI for a competitive production of Super Heavy Elements (SHE) in the future. The fabrication status as well as first rf measurements at room temperature of the 217 MHz CH cavity are presented.

CW DEMONSTRATOR PROJECT

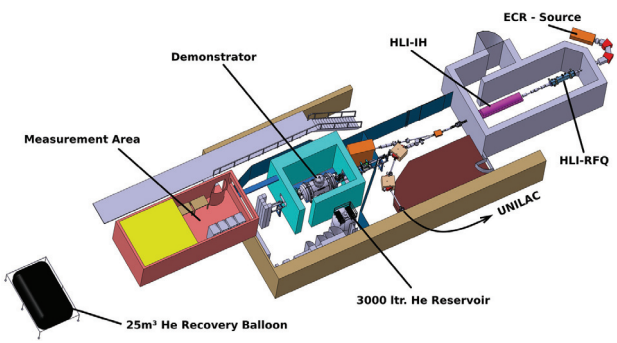


Figure 1: Future test environment at GSI using the existing HLI as an injector for the cw demonstrator.

The successful acceleration of a beam with the cw demonstrator, which consists of two sc 9.5 T solenoids and a sc 217 MHz CH cavity mounted in a horizontal cryomodule, will be a milestone realizing a new sc cw linac to keep the SHE program at GSI competitive on a high level. The 1.4 AMeV GSI High Charge State Injector (HLI) will serve as an injector to run first beam tests. Figure 1 shows the future test environment at GSI.

* Work supported by GSI, HIM, BMBF Contr. No. 05P12RFRBL
† dziuba@iap.uni-frankfurt.de

LAYOUT OF THE CAVITY

Since June 2012, the sc 217 MHz CH cavity [3] (see Fig. 2) for the cw demonstrator project is under production at Research Instruments (RI) GmbH, Bergisch Gladbach, Germany. The cavity has a design gradient of 5.1 MV/m which will be achieved by 15 equidistant arranged accelerating cells. For the related beam dynamics layout the special EQUUS (EQUidistant mUlti-gap Structure) [4] code was used. Nevertheless, the production of the cavity is almost finished. Its delivery to the IAP for first cold tests with low rf power is expected in December 2014. Table 1 summarizes all main parameters of the cavity. The cavity will be equipped with a 10 kW cw power coupler which is currently under development at the IAP, a titanium helium vessel, several flanges for surface preparation and a frequency tuning system. Figure 3 shows the current fabrication status of the cavity and the setup of the following rf measurements.

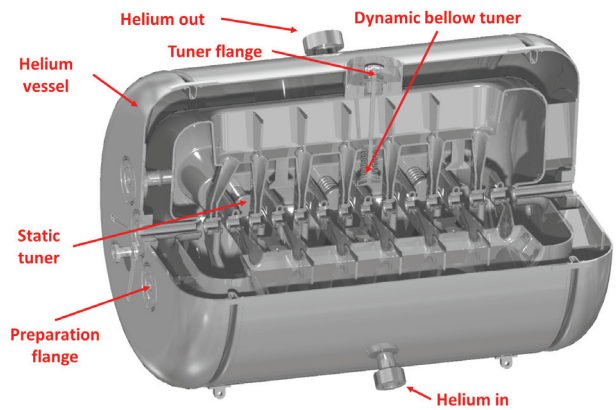


Figure 2: 3D-model of the sc 217 MHz CH cavity.

RF MEASUREMENTS

Intermediate rf measurements during the production process of the cavity have been performed at room temperature to determine the frequency shift of the static tuners in order to adjust the cavity to its design frequency successively. Furthermore, the electric field distribution on the beam axis as well as the external quality factor Q_e of preliminary couplers for cold tests with low rf power have been evaluated. To validate the performed measurements

Copyright © 2014 CC-BY-3.0 and by the respective authors

ISBN 978-3-95450-142-7

PROPOSAL OF A CONVENTIONAL MATCHING SECTION AS AN ALTERNATIVE TO THE EXISTING HSI MEBT SUPERLENS AT GSI UNILAC*

H. Hähnel†, U. Ratzinger, R. Tiede, IAP Frankfurt, Germany

Abstract

We propose a new design for the MEBT section of the High Current Injector (HSI) [1] at the GSI UNILAC as part of the planned UNILAC upgrade for the FAIR project. The existing MEBT section was designed in 1996 [2] and was based on a novel concept called the superlens (SL) which uses a magnetic quadrupole doublet lens combined with an 11-cell RFQ cavity for transversal and longitudinal focusing. In 2009 the RFQ section in front of the MEBT was upgraded [3] which led to significant changes in the RFQ output particle distribution. Recent LORASR simulations show that for high currents the superlens transmission decreases to 90 % (related to 20.75 mA U^{4+} at input). Moreover, the matching to the following IH-DTL is not ideal. This leads to further losses in the IH-DTL and to a decrease of the overall UNILAC efficiency. To reach the FAIR requirement of 18 mA U^{4+} current at the 1.4 AMeV gas jet stripper of the UNILAC within normalized transverse emittance values below 0.6 mm mrad and to provide more flexibility for varying current level operation, a new design based on two magnetic quadrupole triplet lenses and a 2-gap buncher is proposed. The design shows full transmission at 20.75 mA U^{4+} current and improved matching to the IH-DTL, leading to lossless beam transport along the IH-DTL. For improved transmission through the IH-DTL, the effect of the input phase was investigated.

PERFORMANCE OF THE CURRENT SUPERLENS MEBT

Simulations show that after the RFQ upgrade in 2009 [3] the superlens has to be operated at high currents to meet the FAIR requirements due to the losses in the superlens and following IH-DTL. Figure 1 shows that the aperture of the superlens electrodes is too small for the incoming beam which leads to significant losses of up to 10 % at full current. To investigate the matching of SL and IH-DTL, the input acceptance of the IH-DTL was determined by using the original design input distribution (ideal) and by increasing the emittance until particles were lost (acceptance). Comparison of the superlens output distribution with the IH-DTL acceptance (see Fig. 2) shows that the superlens is not ideally matched to the IH-DTL. This results in high emittance growth and in losses along the IH-DTL, leading to a total transmission of 85.7 % for the SL+IH-DTL. This corresponds to an output current behind the IH-DTL of 17.78 mA U^{4+} for an input current of 20.75 mA U^{4+}. In conclusion, the superlens has to be operated at its limit, accepting high particle losses, to reach the FAIR-requirements of 18 mA U^{4+} at the end of the HSI prestripper section.

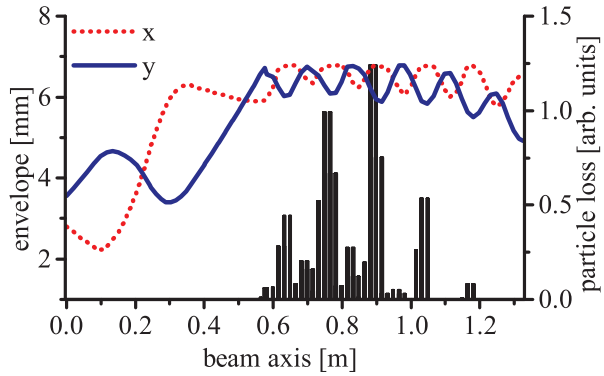


Figure 1: Loss profile of the current MEBT superlens for 20.75 mA U^{4+}. Plottet beam envelopes are 100 %, the superlens aperture is 6.8 mm.

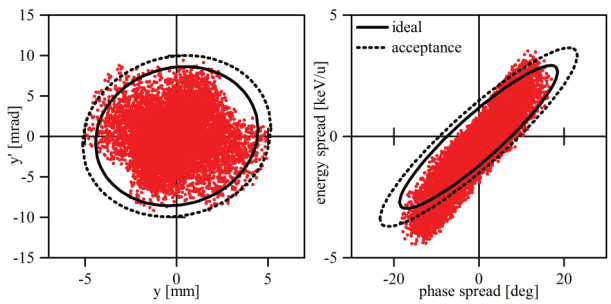


Figure 2: Output distributions of the superlens MEBT with IH-DTL acceptance ellipses.

CONVENTIONAL MATCHING SECTION

As an alternative to the current MEBT section, a conventional design (see Fig. 3) consisting of two magnetic triplet lenses and a two-gap buncher cavity is proposed. This layout allows to reuse the existing XY-steerer, the vacuum valve and the diagnostics box. It also provides some spare room for additional/redesigned components. The lenses have field gradients of 91.5 $\frac{T}{m}$ which results in 1.1 T at the magnet pole tips (for 24 mm pole aperture).

The buncher cavity is designed for 36.136 MHz, therefore a spiral cavity might be chosen due to its low diameter (0.5 m, e.g. [4]). The effective gap voltage for a beam current

* Work supported by BMBF 05P12RFRB9
† haehnel@iap.uni-frankfurt.de

Copyright © 2014 CC-BY-3.0 and by the respective authors

DEVELOPMENT OF A PEPPER POT EMITTANCE MEASUREMENT DEVICE FOR FRANZ*

B. Klump#, U. Ratzinger, W. Schweizer and K. Volk,
Institute of Applied Physics, Goethe-University Frankfurt,
60438 Frankfurt am Main, Germany

Abstract

Within the FRANZ project on the Institute of Applied Physics, University Frankfurt, a robust and simple pepper pot emittance measurement device for high beam power densities is developed. To use the device directly behind the ion source, a high robustness against HV breakdowns is necessary. This paper gives an overview on experimental setup, on the analysis method and on imaging properties of the screen. Furthermore, the implemented software-based evaluation method is shown. It concludes with a preliminary emittance measurement on the high current ion source for FRANZ.

INTRODUCTION

For emittance measurements directly behind an ion source a measuring system is required that is insensitive against high voltage breakdowns. Therefore, a robust, high voltage insensitive and simple measuring device for high beam power densities has been developed within the FRANZ project (Frankfurt-Neutron-Source at the Stern-Gerlach-Center) [1]. The basis is the pepper pot measurement method.

EXPERIMENTAL SETUP

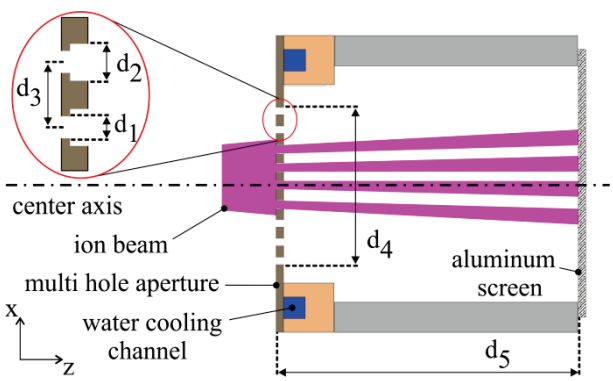


Figure 1: Collector setup.

Fig. 1 shows the schematic setup of the pepper pot emittance measurement system. The ion beam penetrates from the left side through a multi hole aperture plate with more than 700 holes with a diameter of $d_1 = 0.3$ mm, which are arranged grid-like inside a diameter of $d_4 = 60$ mm. The plate is made of wolfram-copper and is water cooled. Partial beams hit after $d_5 = 70.5$ mm a pretreated aluminum screen. The maximum measurable divergence angle is limited to 200 mrad by the contour of the boreholes. The center distance between holes on the

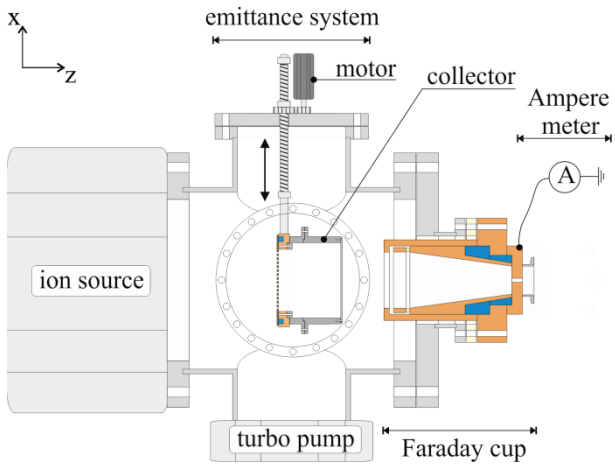


Figure 2: Experimental setup [2].

multi hole aperture d_3 is 2 mm, which ensures no overlap of the partial beams. To investigate this concept, a prototype was build and installed in a diagnostic chamber, which also contains a Faraday cup, the vacuum system and a view window. The system can be moved into the beam by a motor drive. For the investigations, the ion beam of the FRANZ ion source was used. The ion source was mounted directly on the diagnostic chamber (Fig. 2). The FRANZ ion source is a filament driven high current arc discharge volume source [2].

Beam currents and beam energies are variable in the range of 30 mA to 200 mA protons and 20 keV to 60 keV beam energy. To reduce the mean beam power on the multi hole aperture, the source discharge was pulsed with 80 Hz and 1 ms pulse length. Due to the hole diameter a spatial resolution of 0.3 mm results. The angle resolution is 0.6 mrad because of the digitalization (see below).

MEASUREMENT METHOD

Pepper Pot Principle

The ion beam is split into several partial beams due to the multi hole aperture. Those hit the pretreated surface of

*Work supported by HGS-HIRE
#klump@physik.uni-frankfurt.de

ISBN 978-3-95450-142-7

Copyright © 2014 CC-BY-3.0 and by the respective authors

R&D OF THE 17 MeV MYRRHA INJECTOR*

D. Mäder†, M. Basten, D. Koser, H. C. Lenz, N. F. Petry, H. Podlech, A. Schempp,
M. Schwarz, M. Vossberg, IAP, Goethe Universität Frankfurt, Germany
C. Zhang, GSI Helmholtzzentrum, Darmstadt, Germany

Abstract

MYRRHA is designed as an accelerator driven system (ADS) for transmutation of long-lived radioactive waste. The challenge of the linac development is the very high reliability of the accelerator to limit the thermal stress inside the reactor. With the concept of parallel redundancy the injector will supply a cw proton beam with 4 mA and 17 MeV to the main linac. The new MYRRHA injector layout consists of a very robust beam dynamics design with low emittance growth rates. Sufficient drift space provides plenty room for diagnostic elements and increases the mountability. Behind a 4-Rod-RFQ and a pair of two-gap QWR rebunchers at 1.5 MeV the protons are matched into the CH cavity section. A focussing triplet between the rebunchers ensures an ideal transversal matching into the doublet lattice. Each of the 7 room temperature (RT) CH structures has a constant phase profile and does not exceed thermal losses of 29 kW/m. The transition to the 5 superconducting (SC) CH cavities with constant beta profile is at 5.9 MeV. For a safe operation of the niobium resonators the electric and magnetic peak fields are defined below 25 MV/m and 57 mT respectively.

MOTIVATION

For the development of the MYRRHA injector and all of its components the reliabilty is a key issue [1, 2]. Based on the error studies for the current injector design an enhanced version with an optimized matching section and a doublet focusing lattice has been developed [3]. The beam emittance and particle losses regarding the error studies could be further reduced.

Failures need to be detected very fast and localized accuratley to avoid unnecessary shut downs and in case to reduce the MTTR (mean time to repair). Phase probes are placed between every cavity. Additional drift space in the rebuncher section and in the transition section to the SC cavities is reserved for beam position monitors, a faraday cup, two pairs of steering magnets, halo collimators, vacuum pumps and gate valves.

RESULTS

A Monogan M-1000 ECR ion source by Pantechnik[1] and the LEBT developed at SCK-CEN deliver the 4 mA proton beam to the following injector section shown in Figure 2 [4]. Because of the high accelerating gradients SC cavities are favourable and should be used to the greatest possible extend. Figure 1 illustrates the gap voltages and the energy gain in the CH section of the injector. In the current accelerator configuration 17.3 MeV are reached at the end of the injector.

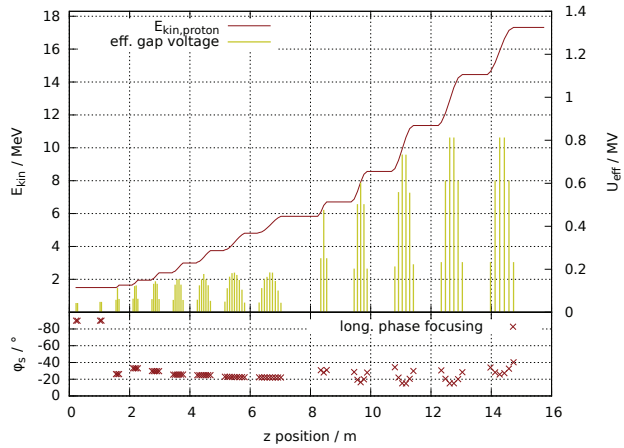


Figure 1: The kinetic proton energy after the 4-Rod-RFQ is $W_p = 1.5$ MeV and increases up to $W_p = 17.3$ MeV at the end of the CH section (upper graph, in red). The effective voltages of the gaps are plotted in yellow. In the lower graph the gap phase configuration of the RT constant phase structures and the SC constant β structures is visualized.

A few particles losses after the 4-Rod-RFQ, which don't occur in the beam simulations, can be expected empirically. To protect the clean niobium surfaces inside the SC structures, RT CH structures are used up to the transition energy of 5.9 MeV. Additionally constructing CH cavities for lower beam energies is a challange because of the slow particle velocities and the related small cell length and should be avoided for a reliable linac [5].

The CH cavities of the injector are based on the optimized geometries of the consolidated injector design [6]. They are adjusted for phase, energy and the gap number. A prototype RT CH cavitiy with a constant phase profile has been built and is currently being tested at IAP in Frankfurt [7, 8]. The 217 MHz SC demonstrator CH structure for the SHE-Linac at GSI is currently under development at IAP [9]. It is based on the design of the SC constant β CH cavities for MYRRHA with 176.1 MHz and serves as a prototype for MYRRHA, too.

Matching Section

Three different electrode modulations of the MYRRHA 4-Rod-RFQ were used for the beam dynamics of various injector designs, which were developed in the last three years. The CH section of the new injector design consists of a flexi-

* Work supported by the EU, FP7 MAX contract number 269565
† d.maeder@iap.uni-frankfurt.de
[1] http://www.pantechnik.com

Copyright © 2014 CC-BY-3.0 and by the respective authors

INVESTIGATIONS OF SPACE-CHARGE COMPENSATION IN LOW-ENERGY BEAM TRANSPORT (LEBT) SECTIONS USING A PARTICLE-IN-CELL CODE

D. Noll, M. Droba, O. Meusel, K. Schulte, U. Ratzinger, C. Wiesner,
Institute for Applied Physics, Goethe University, Frankfurt am Main, Germany

Abstract

Among the advantages of magnetostatic LEBT sections in the case of positively charged ion beams is the possibility for compensation of space charge by accumulating electrons. In the past, it has been shown that the distribution of these compensation electrons can lead to unwanted emittance growth [1]. However, the distribution of electrons especially in the presence of the magnetic fields of the focussing lenses is difficult to predict. To improve the understanding of the influence on the beam, models for the relevant processes namely residual gas ionization using realistic cross sections as well as secondary electron production on surfaces have been implemented in a particle-in-cell code. In this contribution, we will present the code used as well as first results for two model systems as an example.

MOTIVATION

Many processes can lead to the appearance of electrons in low-energy ion beams. For low-energy ion beams, the most significant of these are residual gas ionization and secondary particle emission due to beam losses.

A simple estimation of the compensation built-up time by electrons produced via residual gas ionization under the assumption that all electrons can be trapped inside the beam volume leads to

$$t_{\text{compensation}} = \frac{kT}{v_{\text{beam}} p\sigma} = \frac{I}{v_{\text{beam}} e} \nu^{-1} \qquad \nu = \frac{Ip\sigma}{ekT} . \quad (1)$$

For a proton beam at 120 keV and a residual gas pressure of $p = 10^{-5}$ mbar N_2 ($\sigma \approx 5\text{Å}^2$) at $T = 300$ K this gives a compensation time of 17 μs. The collision rate is $\nu = 8 \cdot 10^{15}\,\text{s}^{-1}\text{m}^{-1}$.

Secondary electron yields after surface impact for protons at these energies are typically in the order of a few electrons per projectile, strongly depending on surface composition and treatment. For the parameters given above and an electron yield of 2, losses have to be below 0.6% for residual gas ionization to produce more electrons than secondary emission.

For the steady-state however, electrons from residual gas ionization seem to be more relevant since these electrons are born within the beam volume. Furthermore, LEBT sections are typically designed for very low beam loss, even though this might not be the case during the built-up of space charge compensation.

For low-intensity beams, ionization of residual gas by secondary electrons is negligible because the fraction of electrons with energies high enough to lead to ionization is typically small. In the presence of electric fields from a high-intensity particle beam however, electrons can easily gain enough energy for another ionization process to take place. For this reason, the processes $e^- + X \rightarrow X^+ + 2e^-$ should be considered as well.

TEST SYSTEMS

To systematically investigate the built-up of space-charge compensation and the resulting steady-state, a number of test systems were selected.

- A 50 cm drift, 120 keV, 100 mA proton beam with $\epsilon = 100\,\text{mm} \cdot \text{mrad}$. The focussed particle beam was matched using a 2d code so that it enters and leaves the system with the same beam size and maximum divergence angle under full space charge and at 95% global space charge compensation.
- A 80 cm transport section including a solenoid at 378 mT, focussing a divergent proton beam with $\epsilon = 100\,\text{mm} \cdot \text{mrad}$ so that it leaves the system again with same beam size and maximum divergence angle under 95% global compensation.

The systems are fitted with repeller electrodes in the front and the back at negative potential about twice the beam potential in magnitude. Without these, electrons could leave

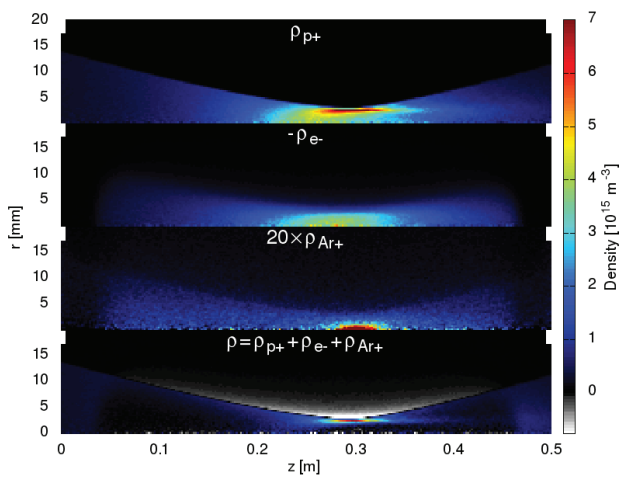


Figure 1: Proton, electron and residual gas ion particle densities in the simulation of the 50cm drift test system. The repeller electrodes at −1.5 kV are visible at the front and the back of the system.

Copyright © 2014 CC-BY-3.0 and by the respective authors

ISBN 978-3-95450-142-7

HIGH GRADIENT CH-TYPE CAVITY DEVELOPMENT FOR 10 – 100 AMeV BEAMS*

Ali Almomani and Ulrich Ratzinger, IAP, Frankfurt am Main, Germany

Abstract

The activities in pulsed linac development aim on compact designs and on an increase of the voltage gain per meter. At IAP - Frankfurt, a 325 MHz CH - cavity is under construction, where the mean effective accelerating field is expected to reach well above 10 MV/m at an energy of 12.5 AMeV corresponding to β=0.164. Within a funded project, this cavity is systematically developed. Currently, the cavity is under construction at NTG GmbH and expected to be ready for copper plating in autumn 2014. The results should give an impact on the rebuilt of the UNILAC - Alvarez section – aiming to achieve the beam intensities specified for the GSI – FAIR project. A mid - and long - term aim is the development of a compact, pulsed high current linac. The new GSI 3 MW Thales klystron test stand will be very important for these investigations. Detailed studies on two different types of copper plating can be performed on this cavity. Additionally, operating of normal conducting cavities at cryogenic temperatures will be discussed for the case of very short RF pulses.

INTRODUCTION

Progress in pulsed power solid-state amplifier development opens the path towards compact low - beta linac designs. At higher frequencies beyond 600 MHz powerful klystrons are anyway available to continue such a strategy up to ion energies of several hundred AMeV. Separated function DTL technology and strategies for a minimization of the consequences from transverse rf defocusing have been developed during the last decades of heavy ion linac development. Moreover, high effective voltage gains beyond 10 MV/m in H – mode cavities with slim drift tube geometries have been demonstrated successfully at CERN Linac3 [1].

H – Mode cavities profit very much from slim drift tubes (see Fig. 1), as they concentrate the electric field on the drift tube structure. Thus, the stored energy is reduced efficiently by a small outer drift tube diameter, reducing surface damages in case of sparking.

In case of Crossbar H – type (CH) – structures the stem structure makes a larger partial contribution to the total capacity, and therefore, the drift tube effect is not as pronounced as for the Interdigital H – type (IH), but still important.

The development of room temperature CH – cavities was discussed in [2] in more detail. This paper is focusing on the development of CH – cavities towards a high field gradient.

This aspect is important for cases, where a compact linac for low duty factor applications is needed. Also, for high current operation the high field acceleration provides the needed longitudinal focusing forces.

*This work is supported by BMBF 05P12RFRB9.

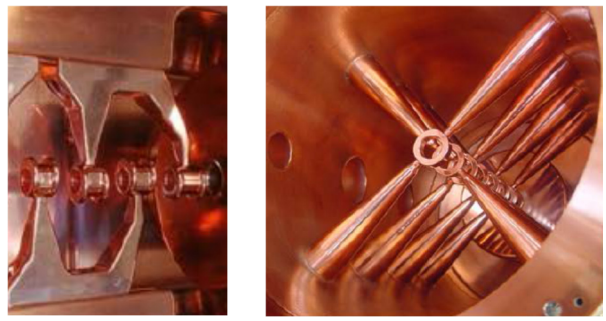


Fig. 1: IH – type (left) and CH – type (right) structure.

One main goal of this work is to prepare for the rebuilt of the high energy section of the GSI – Unilac, which will in future serve as heavy ion injector for the FAIR project.

STRUCTURE PERIOD LAYOUT

As an example how to apply this structure technology one typical lattice period is described in the following. It consists of an FDF quadrupole triplet followed by a 20 gap cavity and a DFD quadrupole triplet.

Table 1: Cavity Parameters for $^{238}U^{+28}$ Beams

Number of gaps	20
Freq. (MHz) / current (mA)	325.224 / 150
Energy range (AMeV)	12.16 – 13.71
Drift tube aperture (mm)	26
"Structure period" (mm)	2222.5
Quadrupole aperture (mm)	28
Effective pole length (mm)	145, 264, 145
Field gradients of the quadrupoles (T/m)	76, 75, 76

The transverse beam envelopes as well as the apertures are shown by Fig. 2.

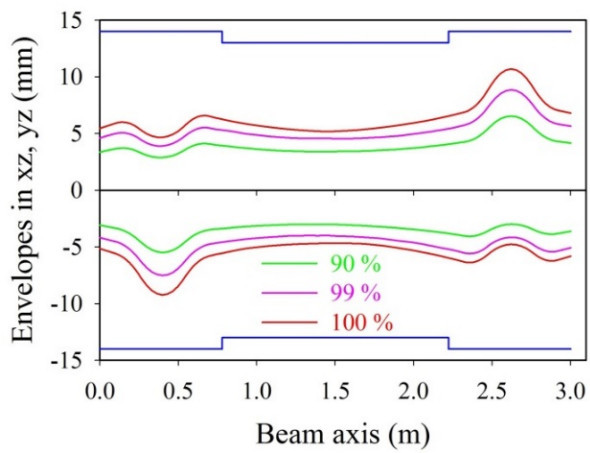


Fig. 2: Transverse beam envelopes along the 13.2 MV section for a 150 mA U28+ - beam.

Copyright © 2014 CC-BY-3.0 and by the respective authors

ISBN 978-3-95450-142-7

OPERATION OF THE LINAC AND THE LINAC RF SYSTEM FOR THE ION-BEAM THERAPY CENTER HEIDELBERG

E. Feldmeier, R. Cee, Th. Haberer, HIT, Heidelberg, Germany

Abstract

The Heidelberg Ion Therapy Center HIT is in clinical operation since 2009. It is the first dedicated European particle accelerator for medical treatment. Its central location on the campus of the Heidelberg University Hospital fits perfectly in the clinical everyday life. The accelerator complex consists of a linear accelerator and a synchrotron and is designed for protons and carbon ions, but can also provide helium and oxygen ions.

The LINAC, build in 2006, operates since 5 years in a 24/7 schema which leads to 60000 operating hours up to now. The performance with an availability of better than 99% is much higher than expected and is caused by a solid design and a well planned and foresighted maintenance.

Unavoidable failures during operation can be solved very fast with the on site experts for each section. The combination of personnel, spare parts and permanent ongoing developments is very successful.

An upgrade program for parts of the LINAC and also for the RF system is in planning to keep the up-time high and to improve the performance for further needs.

INTRODUCTION

The layout of the accelerator of the Heidelberg Ion Therapy Center HIT includes three ECR ion sources, a 7 MeV/u injector linac, a 6.5 Tm synchrotron and a high energy beam transport line to deliver beam for the four target places: Two treatment rooms with a horizontally fixed beam-line, the worlds unique heavy ion gantry and an experimental area.

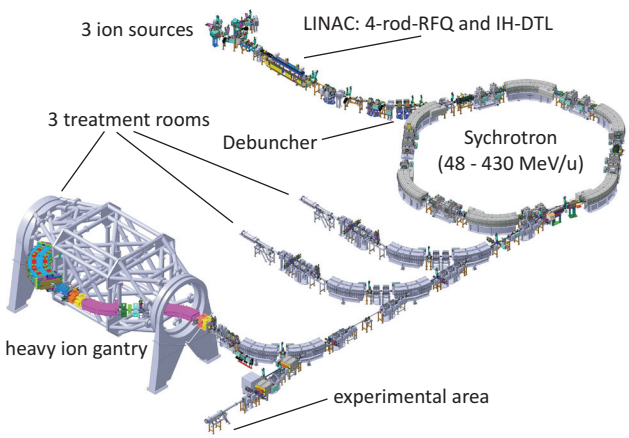


Figure 1: The accelerator of the Heidelberg Ion-Beam Therapy Center (HIT) with three ion sources, the LINAC (7 MeV/u) consisting of a 4-rod-RFQ and a IH-DTL, the synchrotron (48-430 MeV/u), the beam lines to the treatment rooms and the experimental area and the heavy ion gantry [1].

The ECR ion sources produce proton, helium, carbon and oxygen beam, of which the protons and the carbon ions are used for the medical treatment of localized tumors.

In the injector linac, beams with an AoQ of 1-3 can be accelerated to 7 MeV/u. The synchrotron accelerates the beam to an energy of up to 430 MeV/u for carbon ions, which corresponds to a penetration depth in water or human tissue of 30 cm.

LINAC AND RF SYSTEMS

The LINAC RF system shown in Fig. 2 supplies three RF cavities in front of the Synchrotron to accelerate and form the beam from the ion sources. A 4-rod-RFQ is used to accelerate the beam to 400 keV/u, focus the beam an form bunches. The following IH-DTL accelerates the beam to 7 MeV/u and the Debuncher spreads the bunches longitudinal to match the acceptance of the synchrotron. The cavities are operated at 216.816 MHz. For a beam with an $AoQ = 3$ a power for the RFQ of 200 kW, for the IH-DTL of 900 kW and for the Debuncher of 1.2 kW is needed.

The RF system (Fig. 2) consists of a common master oscillator providing the frequency. A amplifier and splitter is used to distribute the RF signal to the three power amplifiers. Dependent on the needed power, different amplifier stages of transistor and tube amplifiers are combined. The RFQ has a 8 kW transistor preamplifier and a 250 kW tube final stage. The IH-DTL has a 4 kW transistor preamplifier, a 120 kW tube stage and a 1.4 MW tube final stage [2]. The RF system for the Debuncher only uses a 4 kW transistor amplifier.

The analog PI-controller for each system corrects the amplitude and the phase of the decoupled cavity signal.

The RF system was designed by GSI in Darmstadt, Germany and build by Bertronix in Munich, Germany and the company today named Ampegon in Turgi, Switzerland.

OPERATION OF THE ACCELERATOR

The accelerator is operated more than 320 days a year in a 24/7 mode. The medical treatment takes place during the day in the time from 8am to 8pm. In the morning quality assurance measurements are done and in the evening the treatment plans for the next days are verified. The night shifts are mainly used for experiments and the adjustment of the accelerator.

The patients at HIT are treated with carbon ions or protons. The clinical dose is distributed over mostly 20 fractions with a 5+2 scheme. They are treated 5 days in a row with two days rest period, which leads to a residence time of about one month at the center.

Copyright © 2014 CC-BY-3.0 and by the respective authors

ISBN 978-3-95450-142-7

THE FAST PIEZO-BASED FREQUENCY TUNER FOR SC CH-CAVITIES*

M. Amberg †, K. Aulenbacher, Helmholtz-Institut Mainz (HIM), 55099 Mainz, Germany
M. Busch, F. Dziuba, H. Podlech, U. Ratzinger, IAP Frankfurt University, 60438 Frankfurt, Germany
W. Barth, V. Gettmann, S. Mickat, GSI Helmholtzzentrum, 64291 Darmstadt, Germany

Abstract

Superconducting structures are very susceptible to external influences due to their thin walls and their narrow bandwidth. Even small mechanical deformations caused by dynamic effects like microphonic noise, pressure fluctuations of the liquid helium bath or Lorentz-Force-Detuning can lead to resonance frequency changes of the cavity which are much larger than the bandwidth. To compensate the slow and fast resonance frequency variations during operation a compact frequency tuner prototype equipped with a stepper motor and a piezo actuator has been developed at the Institute for Applied Physics (IAP) of Frankfurt University. In this paper, the tuner design and the results of first room temperature measurements of the tuner prototype are presented.

INTRODUCTION

To guarantee a stable operation a new dynamic frequency tuner for sc CH-cavities [1] has been developed at the IAP. This tuner consists of an inner and an outer part: dynamic bellow tuners are welded into the girders of the cavity which react on frequency variations by changing their height. The tuner drive consisting of a slow stepper motor and a fast reacting piezo actuator is mounted on top of the helium vessel and provides slow and fast tuning by pushing or pulling the dynamic bellow tuner (see Fig. 1).

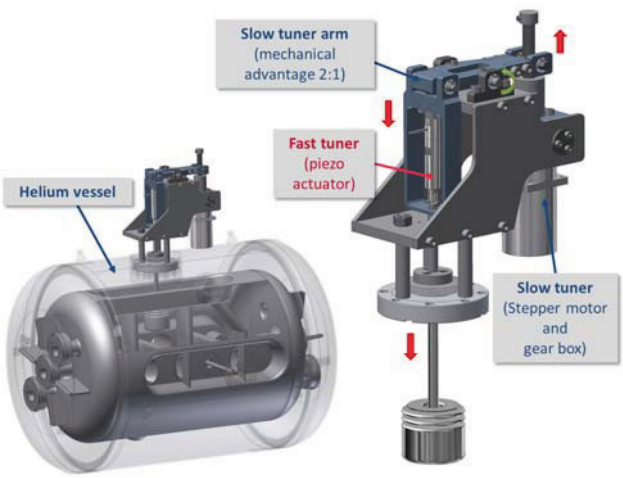


Figure 1: Tuner drive mounted on top of the helium vessel (left) and complete frequeny tuning system including the dynamic 3-cell bellow tuner (right).

DYNAMIC BELLOW TUNER

For the sc 325 MHz and 217 MHz CH-cavities [2] [3] which are currently under first tests and under construction, respectively, a new dynamic frequency tuning concept has been worked out. Additionally to the cylindrical static tuners, several dynamic capacitive bellow tuners are welded into the girders to act against slow and fast frequency variations by changing their height of up to ±1 mm. The goal of the slow tuners, driven by stepping motors, is to readjust the frequency changes caused by cavity cool-down to 4.2 K and evacuation effects. In addition, one of these slow tuners is based on a fast reacting piezo actuator to compensate frequency changes due to microphonic excitations and Lorentz Force Detuning. This tuning device including slow and fast dynamic bellow tuners is sufficient for frequency tuning during beam operation. The final design of a 3-cell bellow tuner for the sc 325 MHz CH-cavity is shown in Figure 2 [4].

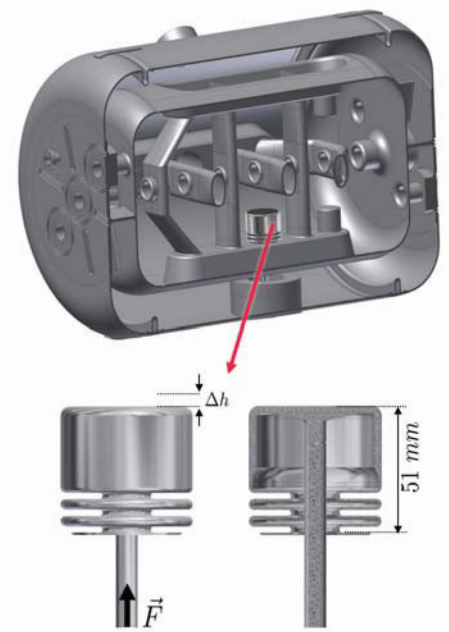


Figure 2: Dynamic 3-cell bellow tuner for the sc 325 MHz CH-cavity.

RF simulations of the sc 325 MHz CH-cavity with CST Microwave Studio [5] show that a frequency shift of around 130 kHz/mm is achievable for each of the two bellow tuners at a working point of 51 mm tuner height. To validate the RF simulation results first room temperature measurements regarding the frequency shift of the bellow tuners have been performed. Preventively, the mechanical range of the bellow tuners was limited to $\Delta x = \pm 0.15$ mm because of the

* Work supported by HIM, GSI, BMBF Contr. No. 05P12RFRBL
† amberg@iap.uni-frankfurt.de

Copyright © 2014 CC-BY-3.0 and by the respective authors

FINAL DESIGN FOR THE bERLinPro MAIN LINAC CAVITY *

A. Neumann†, J. Knobloch
Helmholtz-Zentrum Berlin, 12489 Berlin, Germany
B. Riemann, T. Weis
TU Dortmund University, Dortmund, Germany
K. Brackebusch, T. Flisgen, T. Galek, U. van Rienen
Rostock University, Rostock, Germany

Abstract

The Berlin Energy Recovery Linac Project (bERLinPro) is designed to develop and demonstrate CW LINAC technology for 100-mA-class ERLs. High-current operation requires an effective damping of higher-order modes (HOMs) of the 1.3 GHz main-linac cavities. We have studied elliptical 7-cell cavities based on a modified Cornell ERL design combined with JLab's waveguide HOM damping approach. This paper will summarize the final optimization of the end-cell tuning for minimum external Q of the HOMs, coupler kick calculations of the single TTF fundamental power coupler (FPC) as well as multipole expansion analysis of the given modes and a discussion on operational aspects.

INTRODUCTION

For the bERLinPro ERL [1] a 100 mA beam has to be accelerated and decelerated in the main linac of the recirculator from 6.5 MeV to 50 MeV and vice versa while preserving a low normalized emittance of smaller than 1 mm mrad. Effectively the linac cavities therefore experience the passage of two with respect to the TM_{010}-π mode 180 deg. phase shifted high current beams. Thus strong HOM damping is required in order to avoid beam break-up instability (BBU) [2] by the interaction with dipole-like mode patterns excited by the beam during previous passages. By that the cavity design has to be optimized for low transverse shunt impedance $R/Q_\perp$ and low external quality factors Q_{ext} regarding the HOMs, while the fundamental has to feature low peak field ratios and a high shunt impedance. This challenge was addressed by combining Cornell's mid-cell shape [3] featuring low E_{peak}/E_{acc}, thus avoiding field emission, with JLabs concept of waveguide damped cavity structures [4]. The latter has a natural cutoff frequency by the waveguide dimensions and the danger of dust propagating from ferrite-based beam tube absorbers is avoided.

Figure 1 shows a sketch of the bERLinPro demonstrator ERL and the main linac cavity design. By two Y-shaped waveguide (WG) end groups rotated by 60 deg. any HOM's polarization is covered. To even improve the propagation of the HOMs, the beam tube is enlarged from the 72 mm iris to 105 mm via a spline based nose cone transition. Table 1 summarizes the calculated RF performance of the cavity. The structure was developed and optimized within a collaboration of the universities Dortmund and Rostock with HZB. The methods applied and developed for this project are published in [5–9].

Table 1: Calculated RF parameters and operating conditions of the main Linac cavity with a TTF-III FPC and five HOM damping rectangular waveguides.

Number of cells	7
$R/Q_\parallel$	788 Ω
$f_{TM_{010}-\pi}$	1.3 GHz
E_{peak}/E_{acc}	2.08
B_{peak}/E_{acc}	4.4 mT/MVm^{-1}
Q_{ext} TM_{110} dipole	$\leq 8 \cdot 10^3$
Beam tube TE_{01} cutoff	1.596 GHz
Waveguide TE_{10} cutoff	1.576 GHz
Q_L for TM_{010}-π	$1 \cdot 10^7 - 1 \cdot 10^8$
$P_{forward}$ at $Q_L = 5 \cdot 10^7 (\Delta f = 0)$	1.4 kW

Recently [10] end-cell tuning optimizations using CST MWS's [11] swarm particle optimizer with the eigenmode solver were performed to achieve best HOM damping results while still keeping the cavity field-flat and within given limits regarding peak field ratios and $R/Q_\parallel$. The best candidate of this approach was selected for more detailed studies, presented here, in order to achieve a design ready for production.

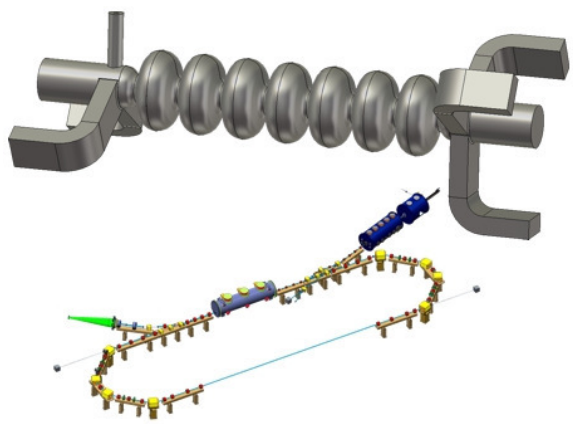


Figure 1: Scheme of the bERLinPro ERL with the main linac section within the recirculating ring. Above the linac cavity structure is shown including the FPC and five waveguides for HOM damping.

* Work supported by German Bundesministerium für Bildung und Forschung, Land Berlin, by grants of Helmholtz Association and by Federal Ministry for Research and Education BMBF under contract 05K10HRC and 05K10PEA
† Axel.Neumann@helmholtz-berlin.de

Copyright © 2014 CC-BY-3.0 and by the respective authors

ISBN 978-3-95450-142-7

BESSY VSR 1.5 GHz CAVITY DESIGN AND CONSIDERATIONS ON WAVEGUIDE DAMPING

Adolfo Velez, Jens Knobloch, Axel Neumann , Helmholtz-Zentrum Berlin, 12489 Berlin, Germany

Abstract

The BESSY VSR upgrade of the BESSY II light source [1] represents a novel approach to simultaneously store long (ca. 15ps) and short (ca. 1.5ps) bunches in the storage ring with the "standard" user optics. To this end, new high-voltage L-Band superconducting multi-cell cavities must be installed in one of the straights of the ring. These 1.5 GHz and 1.75 GHz cavities are based on 1.3 GHz systems being developed for the bERLinPro energy-recovery linac. This paper describes the baseline electromagnetic design of the first 5-cell cavity operating at 1.5 GHz as well different design approaches to ensure reliable operation.

INTRODUCTION

Simultaneous operation of long and short pulses by BESSY VSR represents a very attractive upgrade of the conventional storage ring operation concept. Nevertheless, very restrictive and challenging SRF cavity design requirements must be fulfilled in order to ensure stable operation [2]. High E_{acc} (20 MV/m) are needed and special attention must be paid to the damping of high order modes (HOMs) excited by the beam that may otherwise cause coupled bunch instabilities of the beam [3]. This paper shows the current status of the prototype design for this first 1.5 GHz cavity starting from the mid-cell to the 5 cell design including damping concepts. To this end, Q_{ext} calculations have been performed with Ansoft HFSS eigenmode solver [4] while the centre cell optimisation studies have been performed in COMSOL MULTIPHYSICS (eigenmode calculator) [5].

MID-CELL DESIGN

The first stage on a SRF high current cavity design consists on finding the centre cell parameters fulfilling RF specification and offering best possible performance. SRF requirements imposed by project boundary conditions are: a low E_{peak}/E_{acc} (<2.3), low B_{pk}/E_{acc} (<2.3 mT/(MV/m)) and large R/Q_l for TM_{010} (>95 Ω per cell). The present mid-cell design is depicted in figure 1 compared to the Cornell [6] and Jlab [7] designs. In order to avoid trapped modes the iris diameter has been set to a relatively high value (ϕ=71.34mm) and thus obtaining a high cell to cell coupling factor (K_c=3.3%) for the fundamental mode. A final set of mid-cell parameters fulfilling specifications has been obtained by performing a parametric analysis in COMSOL MULTIPYSICS with the main figures of merit (R/Q, G, E_{pk}/E_{acc} and B_{pk}/E_{pk}) as design goal (Table 1). This software has been chosen due to its good performance in 3D simulation and post-processing from 2D parameterized geometries.

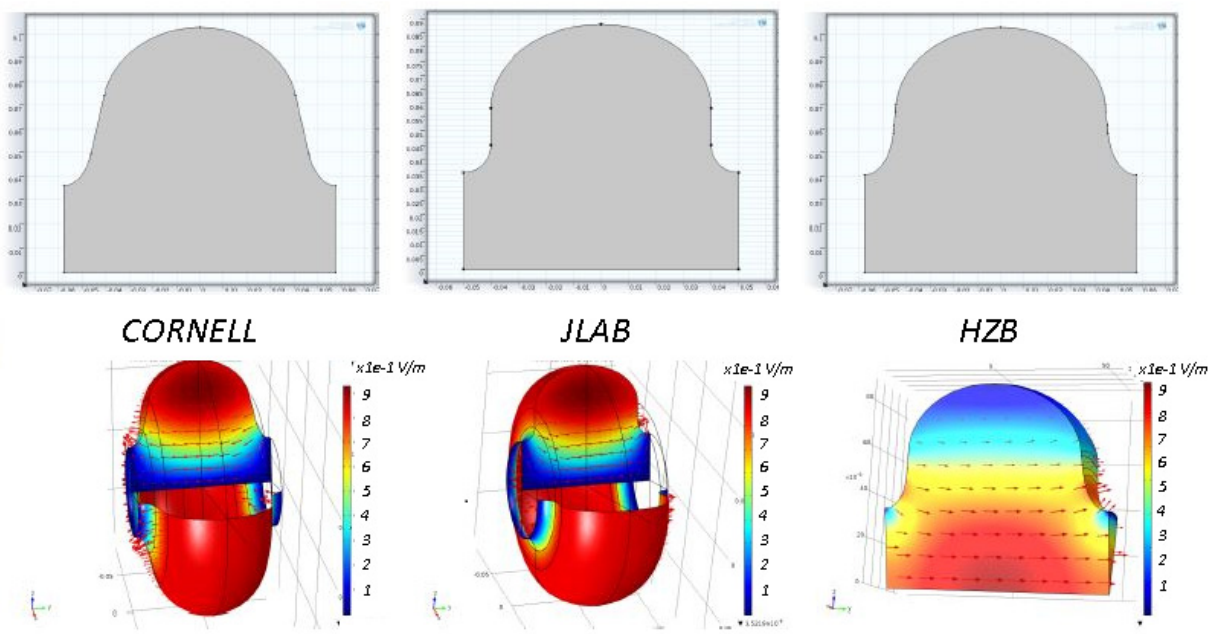


Figure 1: Layout of HZB Mid-cell geometry compared to Cornell and JLab base cell models.

Copyright © 2014 CC-BY-3.0 and by the respective authors

ISBN 978-3-95450-142-7

PRESENT STATUS OF J-PARC LINAC LLRF SYSTEMS

Z. Fang, K. Futatsukawa, Y. Fukui, T. Kobayashi, S. Michizono, KEK
F. Sato, S. Shinozaki, E. Chishiro, JAEA

Abstract

The low-level RF (LLRF) control systems have been successfully developed and improved for the J-PARC LINAC. In January 2014 the output proton energy of the J-PARC LINAC was upgraded to 400 MeV. In the past 8 years of the J-PARC LINAC operation, no heavy troubles occurred in the RF control systems. Every year we made improvements on the RF control systems, according to the operation experiences. In this paper, the present status of the J-PARC 400-MeV LINAC RF control systems will be described in details.

INTRODUCTION

The 400-MeV proton linear accelerator (LINAC) at the Japan Proton Accelerator Research Complex (J-PARC) consists of 324-MHz low-β and 972-MHz high-β accelerator sections, and it is operated at a repetition rate of 25 Hz with a beam pulse width of 500 μs. From October 2006 to May 2013, only the 324-MHz accelerator section was in operation with the proton beam energy of 181 MeV. In January 2014, the proton beam energy was successfully upgraded to 400 MeV after the installing the 972-MHz accelerator section. For the 400-MeV J-PARC LINAC, there are 48 RF stations and 64 cavities in total. For each RF station, one RF source is used to feed RF power to the RF cavities using a low level RF (LLRF) control system [1-2]. The RF signals including the RF amplitude and phase at the RF cavities are controlled by an FPGA (Field-Programmable Gate Array)-based digital feedback (FB) control system installed in a compact PCI (cPCI) [3-4]. Recently lots of improvements on LLRF control systems have been successfully carried out.

IMPROVEMENT OF TIMING DISTRIBUTION SYSTEM

All of the accelerator systems of the J-PARC are controlled basing a 12-MHz master clock produced at the Center Control Room (CCR). The 12-MHz output signal is connected to an E/O (Electro-Optical) converter and then sent to the J-PARC LINAC. Then it will be used in the RF reference generator system to produce phase-locked 312-MHz and 960-MHz LO (Local Oscillator) signals [5]. The 312-MHz and 960-MHz LO signals, as well as the reference 12-MHz signal, will be sent to each RF station at the J-PARC LINAC through a timing distribution system, and used for the feedback control systems in the cPCI. During the experiments on the feedback control systems at each RF station, we found that, there is a stable range of the reference 12-MHz signal delay setting from the LO (312-MHz or 960-MHz) signal for the cPCI operation, and this stable range is quite narrow especially for the 972-MHz feedback systems, since the RF frequency is 3 times of the 324-MHz RF systems. According to the measurement results, the jitter range between the reference 12-MHz signal and LO signal must be smaller than 150 ps for the J-PARC LINAC upgrade.

Then, an improvement of the timing distribution system has been successfully carried out for the whole J-PARC LINAC. Figure 1 shows the schematic diagram of the improved timing distribution system. As shown in Fig. 1, instead of an electrical fan-out used in the previous timing distribution system, the reference 12-MHz signal from CCR is divided by an optical coupler, and sent to each system at local station. Figure 2 shows an image of the timing distribution system at the LINAC after improvement. According to the measurement results, a good stability of the timing distribution has been successfully achieved as shown in Fig. 3. The jitter range between the reference 12-MHz signal and LO signal is smaller than 45 ps for all of the RF stations, satisfying our requirements. Owing to this improvement, a very good stability of the RF system has been successfully achieved for the long-term operation. We have never suffered from any problems caused by the timing instabilities up to now.

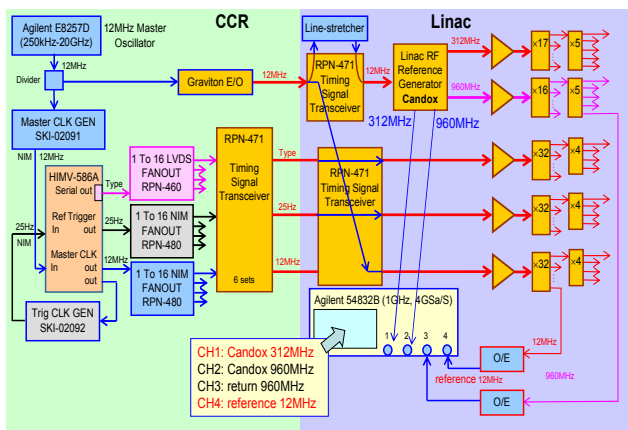


Figure 1: Schematic diagram of the improved timing distribution system.

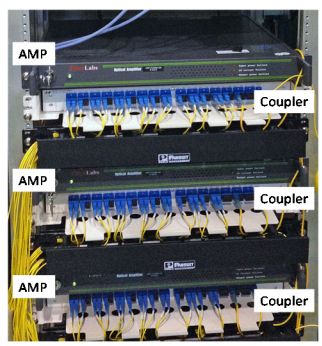


Figure 2: Timing distribution system at the LINAC after improvement.

Copyright © 2014 CC-BY-3.0 and by the respective authors

DIGITAL FILTERS USED FOR DIGITAL FEEDBACK SYSTEM AT CERL

F. QIU#, S. MICHIZONO, T. MIURA, H. KATAGIRI, D. ARAKAWA, T. MATSUMOTO,
IBARAKI,305-0801, JAPAN.

Abstract

As a test facility for the future KEK 3-GeV energy recovery linac (ERL) project, the compact ERL (cERL) features three two-cell cavities for the injector and two nine-cell cavities for the main linac. Digital low-level radio frequency (LLRF) systems have been developed to realize highly accurate RF control. In order to reduce the influence of clock jitter and to suppress the parasitic modes in the multi-cell cavities, we have developed several types of digital filters, including a first-order IIR filter, a fourth-order conjugate poles IIR filter and a notch filter. Furthermore, to design a more effective and robust controller (such as an H-infinite controller, or repetitive controller), we need to acquire more detailed system knowledge. This knowledge can be gained by using modern system identification methods. In this paper, we present the latest applications in the LLRF systems of the cERL.

INTRODUCTION

The compact energy recovery linca (cERL) is a prototype machine that was developed for the planned light source 3-GeV ERL project at KEK [1]. It is a superconducting (SC) project and is operated in the continuous wave (CW) mode. Three two-cell cavities and two nine-cell cavities were installed in the injector and main linac (ML), respectively. To achieve a low-emittance beam, the RF field fluctuation should be maintained to less than 0.1% (in amplitude) and 0.1° (in phase). The challenging requirements are satisfied by using μTCA-based digital low-level RF (LLRF) systems [2].

To suppress the parasitic modes in the nine-cell cavities of the ML in the cERL, a high-order IIR filter was proposed and implemented in the cERL. As a comparison, a second-order notch filter was also developed and applied in the system [3].

A system model is required in order to design the more effective controlling applications. Such as H-infinite multi-input multi- output (MIMO) control [4], disturbance observer controls (DOBs) [5], and repetitive controls (RCs) [6]. Modern system identification techniques provide a method for determining the mathematical model of the system.

This paper focuses on the development of a high-order IIR filter for parasitic mode suppression. Experiments on system identification in the CW mode are presented as well.

LLRF SYSTEM

The schematic diagram of the LLRF system for cERL is shown in Fig.1. The 1.3-GHz cavity probe signal is down-converted to a 10-MHz intermediate frequency (IF) signal and then processed by digital signal processing (DSP) algorithms that are implemented in an FPGA. The main functions of the algorithms include in-phase and quadrature (I/Q) detection, amplitude/phase (A/P) calibration, digital filter, feedback (FB) control, and feed forward (FF) control. The processed signal is then up-converted to an RF signal again to drive the power source of each cavity. Detailed information about this digital platform can be found in [7].

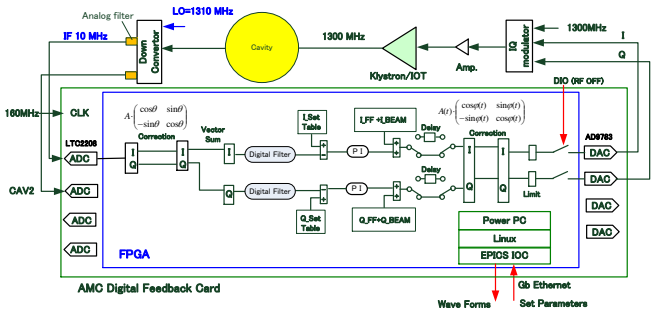


Figure 1: Schematic of the LLRF system in the cERL.

NINE-CELL CAVITY IN MAIN LINAC

Two nine-cell L-band superconducting cavities were installed in the ML of the cERL [8]. The nine-cell cavity hosts a normal RF mode and eight different parasitic modes; only the π mode is used for the beam acceleration. The parasitic modes, especially the so-called 8π/9 mode limit the feedback loop gains. For the cavity of the ML1, the location of π mode and parasitic modes is shown in Fig. 2.

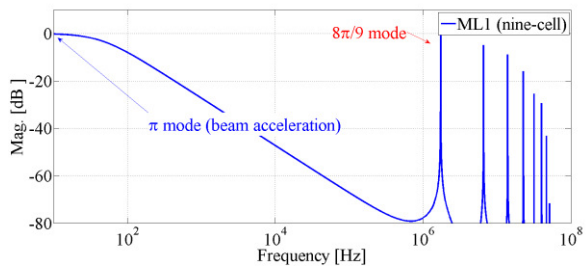


Figure 2: Bode plot of the nine-cell cavity in the ML1. The nearest parasitic mode (8π/9 mode) is located around 1.7 MHz from the π mode.

HIGH ORDER FILTER

Applying digital filters is an effective means to remove the parasitic modes. In the previous LLRF system, an IIR-type filter, which has a difference equation, as shown in (1) was selected as the main filter. It is the simplest IIR filter with only one real-pole. The filter bandwidth is proportional to the adjustable parameter α.

#qiufeng@post.kek.jp

ISBN 978-3-95450-142-7

Copyright © 2014 CC-BY-3.0 and by the respective authors

CONSTRUCTION OF AN ACCELERATOR-BASED BNCT FACILITY AT THE IBARAKI NEUTRON MEDICAL RESEARCH CENTER

M. Yoshioka#, T. Kurihara, S. Kurokawa, H. Kobayashi, H. Matsumoto, N. Matsumoto, KEK, Tsukuba 305-0801, Japan
H. Kumada, A. Matsumura, H. Sakurai, S. Tanaka, Tsukuba University, Tsukuba 305-0005, Japan
T. Sugano, T. Hashirano, Mitsubishi Heavy Industries, LTD., Mihara 729-0393, Japan
T. Nakamura, JAEA, Tokai 319-1195, Japan
F. Hiraga, Hokkaido University, Sapporo 060-8628, Japan
T. Ohba, N. Nagura, NAT, Nippon Advanced Technology CO., LTD., Tokai 319-1112, Japan
T. Nakamoto, T. Zagar, Cosylab, Tsukuba 305-0044, Japan
T. Ouchi, ATOX CO., LTD., Tokai 319-1112, Japan

Abstract

An accelerator-based BNCT (Boron Neutron Capture Therapy) facility is being constructed at the Ibaraki Neutron Medical Research Center. It consists of a proton linac of 80kW beam power with 8 MeV energy, a beryllium target, and a moderator system to provide an epi-thermal neutron flux sufficient for patient treatment. The technology choices for this present system were driven by the need to house the facility in a hospital where low residual activity is essential.

OUTLINE OF THE PROJECT

An accelerator-based BNCT facility, (hereafter, i-BNCT [1]) is being constructed at the Ibaraki Neutron Medical Research Center (INMRC) with broad a collaboration coming from universities and organizations: KEK, Tsukuba University, Hokkaido University, JAEA; and commercial enterprises: Mitsubishi Heavy Industries, NAT, ATOX and COSYLAB. It consists of a high-power proton linac of 80 kW beam power with 8 MeV energy (3MeV RFQ + 5MeV DTL), a beryllium target, and a moderator system to provide a high enough epi-thermal neutron flux for patient treatment. The main parameters of the i-BNCT are summarized in Table 1 and the layout and a block diagram are shown in Figures 1 and 2, respectively. The basis for the technology choices will be described in the next section. Presently the construction of the accelerator system has been completed and RF conditioning of the RFQ and DTL is in progress. The first phase beam commissioning will be carried out this fall with a small beam current (a few μA) by using a target without a beryllium layer and the second phase full beam commissioning is scheduled for next year with a beryllium target and moderator system to provide the epi-thermal neutron flux.

Since the INMRC is a retrofit into an existing building, the layout of the irradiation room, accelerator and klystron modulator is not optimum as can be seen in Figure 1. In particular, the design of the beam transport line optics is made complex because of the 1.8 m floor level difference between the accelerator and irradiation room.

#masakazu.yoshioka@kek.jp

Table 1: Main Parameters of the 80 kW Linac

Beam energy	8 MeV (50kV ion source, 3MeV RFQ and 5MeV DTL)
Peak current	50 mA
Repetition rate	200 Hz
Pulse Width	1 msec
RF Frequency	324 MHz (also used by the J-PARC front-end linac)

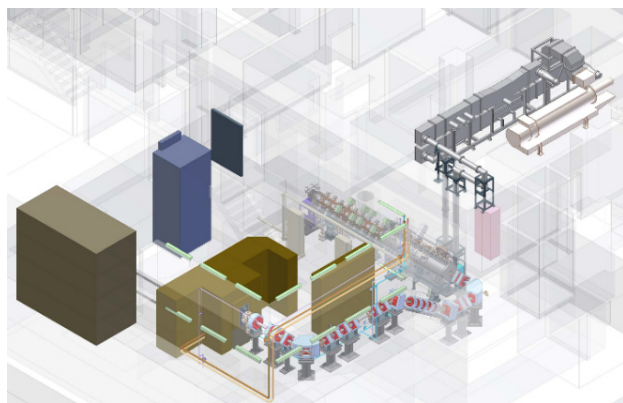


Figure 1: Layout of the i-BNCT, (left) Irradiation room, (middle) accelerator and (right) Klystron, modulator and LLRF, and magnet power supplies

TECHNOLOGY CHOICES

In order to reduce R&D requirements, the RF design of the RFQ and DTL builds on the same design as the J-PARC front-end Linac. However, in order to obtain an 80 kW beam power the duty factor of the i-BNCT is very high (20%) as compared with J-PARC (2.5%).

The technology choice of an 8 MeV Linac for the present system was driven by the need to site the facility in a hospital where low residual activity is essential. Neutron energy spectra are shown in Figure 3 for various production angles from 0 to 110 degree.

Copyright © 2014 CC-BY-3.0 and by the respective authors

ISBN 978-3-95450-142-7

ELECTRON-DRIVEN POSITRON CAPTURE SIMULATION FOR ILC

Y. Seimiya, M. Kuriki, T. Takahashi, HU/AdSM, Higashi-Hiroshima
T. Okugi, T. Omori, M. Satoh, J. Urakawa, KEK, Tsukuba, S. Kashiwagi, Tohoku U., Sendai

Abstract

ILC (International Linear Collider) is a next high-energy physics project to study the Higgs property as detail as possible and new phenomena beyond standard model. In ILC, the positron beam is produced by converting gamma rays from undulator radiations. To obtain gamma rays as undulator radiation, the electron beam for collision (more than 100 GeV) is used. This positron generation scheme is a totally new approach. From project point of view, it is desirable to have a technical backup as a replacement of the undulator scheme. We propose an ILC positron source based on the conventional electron driven scheme. In this scheme, positron beam is generated from electromagnetic shower in a heavy target material where electron beam is injected. By manipulating the beam time structure to relax the heat load on the production target, the scheme can be feasible technically. In this study, positron capture in the electron driven scheme is simulated from the positron production to the positron DR (Damping Ring), to demonstrate that an enough amount of positron can be generated and captured with a controllable heat load on the target.

INTRODUCTION

ILC is a e- and e+ linear collider for high energy physics to study an Higgs sector and new particles, such as SUSY particles. It is based on the Super-conducting accelerator with its CME (Center of Mass Energy) 500 GeV in the first phase. Technical Design Report of ILC has been published in 2013 [1]. In the report, positron is generated by undulator method. In this method, the driver electron beam passes through undulator and generates high energy gamma ray. The gamma ray impinges on Ti-alloy target and is converted to positron through pair-creation process. For an efficient conversion, the gamma ray energy is required at least more than 10 MeV, which needs 130 GeV drive electron beam energy with 10 mm undulator period. A dedicated electron beam for the positron generation is not realistic. High energy electron beam more than 100 GeV is shared between the collision and the positron generation. Therefore, time structure of the positron generation is fixed. This is a totally new approach as positron source and a demonstration of the system prior to the real construction is desirable, but it is practically difficult hence the demonstration require an accelerator comparable to ILC. In positron creation for ILC, heat load of the target is the biggest issue. In the undulator method, the target has to be rotated at 100 m/s tangential speed to avoid any damage in ultra high vacuum environment. The technology of such a rotating target is not fully established. By considering the risk control of a project, it is necessary to have a technical backup for a positron source of the ILC to reduces unknown technical risks related to this totally new approach.

Conventional positron generation, electron-driven positron source, for ILC has been proposed [2]. In this proposal, several GeV electron beam impinges on a W-Re target and positron is generated by Bremsstrahlung. This method requires several GeV electron beam and a dedicated electron driver is reasonable. The time structure of positron generation is determined freely. Heat load of the target is relaxed by stretching a pulse length of a bunch-train with 300 Hz linac. This relaxation enable rotating target speed to only 5 m/s. Possible target destruction is still the biggest issue. According to SLC experience, Peak Energy Deposition Density (PEDD) given by incident electron beam has to be less than 35 J/g [2].In this report, we study a design of the positron source to achieve enough amount of positron for ILC keeping PEDD less than the limit.

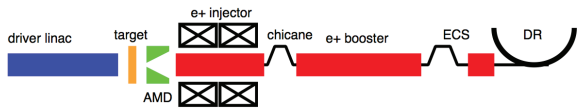


Figure 1: Layout of the ILC electron-driven positron source.

CONCEPT OF POSITRON SOURCE

ILC electron driven positron source is described in this section. The layout is shown in Fig. 1. It consists of electron linac, conversion target, AMD (Adiabatic Matching Device) for transverse momentum suppression, positron injector with focusing solenoid for positron capturing up to 250 MeV, chicane to remove electron and energy large deviated positron, positron booster up to 5 GeV, and ECS (Energy Compressor Section). Our goal is transferring an enough amount of positron to DR, whose dynamic aperture is $\gamma A_x + \gamma A_y < 0.07$ m in the transverse phase space and $z < \pm 35$ mm and $\delta < \pm 0.0075$ in longitudinal phase space, where γ is Lorenz factor, A_x and A_y are action values, and δ is relative energy deviation. As a design criteria, 50% margin on the number of positron in DR acceptance is required. Number of positron in each bunch at IP (Interaction Point) should be same as that of electron, 2.0×10^{10}. Therefore, 3.0×10^{10} positrons in the acceptance is required. The electron beam energy and bunch intensity of the driver linac is typically 6 GeV and 2.0×10^{10}, respectively. The target has typically 14 mm thickness.

Peak field of AMD is typically 5 Tesla and the field is smoothly connected to the solenoid field (0.5 Tesla) at the positron injector. AMD magnetic field is generated by Flux Concentrator, which should be similar to that designed for Super-KEKB factory at KEK, Japan [3]. The positron in-

Copyright © 2014 CC-BY-3.0 and by the respective authors

ISBN 978-3-95450-142-7

RF POWER SYSTEMS FOR THE FAIR PROTON LINAC

C. Joly, J. Lesrel#, IPN Orsay, CNRS-IN2P3 Université Paris Sud, France
E. Plechov, A. Schnase, G. Schreiber, W. Vinzenz GSI, Darmstadt, Germany

Abstract

In the framework of collaboration between the FAIR project, GSI, and CNRS, the IPNO lab is in charge of providing the high power RF components for a cavity test stand and for the planned FAIR proton Linac. This Linac will be connected to the existing GSI synchrotron SIS18 for serving as an injector for the new FAIR facility.

The 70 MeV FAIR proton Linac design contains a 3 MeV RFQ, and a DTL based on Cross-bar H-mode cavities (CH). It will operate with pulsed RF at 325.224 MHz with a width of 200 µs and a repetition rate of 4 Hz. The planned RF systems of the proton Linac will be presented as well as the description of the test stand.

The first power test results are obtained with a Thales klystron developed jointly with CNRS. Three solid state amplifiers made by SigmaPhi Electronics for the bunchers will also be described in this paper.

INTRODUCTION

The FAIR proton linac [1, 2, 3] has to provide the primary proton beam for the production of antiprotons, and will be connected to the existing GSI synchrotron SIS18.

This Linac will deliver a 70 MeV beam with 70 mA current and will operate with a pulsed RF signal at 325.224 MHz with a width of 200 µs and a repetition rate of 4 Hz. The proton Linac will consist of a RFQ and 6 DTL based on Cross-bar H-mode cavities (CH).

Three bunchers are planned for the linac. Each acceleration cavity will be fed by a single high power RF system. Its conceptual layout is shown in Fig. 1.

The RF power systems of the proton linac are composed to 7 klystrons and 3 solid state amplifiers for bunchers, and also the waveguides and coaxial components (circulators, RF loads, couplers measurements, arc detector).

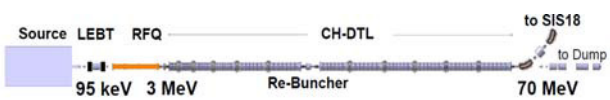


Figure 1: Layout of FAIR proton Linac.

The collaboration between the FAIR project, GSI, and CNRS began in 2010. The IPNO lab participated in the installation of the test stand at GSI, which consists of a klystron, its modulator and all components for the CH cavities test in a bunker. Meanwhile IPNO and THALES (TED) developed a klystron at 352.224 MHz with 3.1 MW peak.

#lesrel@ipno.in2p3.fr

KLYSTRON

The klystron developed in collaboration with THALES and IPNO is shown in Fig. 2. The gun is a diode type. The interaction structure has 5 cavities with the 3rd one operating close to the second harmonic. The output cavity is coupled to a coaxial window and a full height WR2300 waveguide transition. The collector and the body are at ground potential. The electromagnet consists of discrete water-cooled coils and is integrated with the klystron into a supporting frame. The tube operates in horizontal position and is equipped with a CERN type oil tank, and a built-in X-ray shielding. The high voltage module of the heater power supply is integrated into the oil tank.



Figure 2: The THALES klystron TH2181.

The klystron has been successfully tested, with a fast conditioning, and achieved performances are in agreement with predictions.

The klystron delivers 3.2 MW output peak power at saturation, with an efficiency of 52%. The cathode voltage and beam current are 115kV and 53A respectively. The corresponding beam perveance is 1.36 10^{-6} $AV^{-1.5}$.

The input power required to saturate the tube is 150 W, or a gain of 43.3 dB. The power transfer curve is given in figure 3. It is free of discontinuities and the power linearity is lower than 200 kW peak between 20% and 80% of saturated output power. The phase linearity is around 2 degree.

The gain variation is 0.16 dB over ± 0.75 MHz at -1dB below saturation (or 2.5 MW). The corresponding phase change is 92 °, which leads to a group delay of 170ns. The sensitivity of the output power and the input-output phase versus cathode voltage, are respectively 0.07 dB / kV and 6.4 ° / kV.

Copyright © 2014 CC-BY-3.0 and by the respective authors

ISBN 978-3-95450-142-7

BEAM DYNAMICS STUDY FOR RAON SUPERCONDUCTING LINAC

Hyojae Jang, Hyung Jin Kim, IBS, Daejeon, Korea
Ji-Gwang Hwang, KNU, Deagu, Korea
BongHoon Oh, POSTECH, Pohang, Korea

Abstract

Rare Isotope Science Project (RISP) in Korea is going to build an ion accelerator, RAON which can generate and accelerate various stable ions such as uranium, proton, xenon and rare isotopes such as tin, nickel. Linear accelerators of RAON adopted superconducting RF cavities and warm quadruple doublet structure. In RAON, there are two low energy linacs which can accelerate the Uranium beam from 0.5MeV/u to 17.5MeV/u, charge stripping sections and one high energy linac which can accelerate the Uranium beam up to 200MeV/u. Due to the diversity of planned ions and isotopes, their A/q range lies widely from 1 to 8. As a result, the research related with linac lattice design and beam dynamics is one of the important topics to build RAON. In this presentation the current status of RAON linac lattice design and the beam dynamics simulation results for acceleration of various ions will be described.

INTRODUCTION

A high energy ion accelerator is essential to research of nuclear, material, medical science and many other areas. In Korea, Rare Isotope Science Project (RISP) project has been going on since 2009 and its goal is to build an ion accelerator which can generate high-power ion beams and rare isotopes. [1] For generation of stable ions, electron cyclotron resonance ion source (ECR-IS) will be used and for rare isotopes, isotope separation on-line (ISOL) system will be used as ion sources. Generated ions are accelerated and bunched in low energy beam transport (LEBT), radio frequency quadrupole (RFQ), medium energy beam transport (MEBT). Superconducting linear accelerators start immediately after MEBT. They consist of two low superconducting energy linacs (SCL1 and SCL3) and one high energy superconducting linac (SCL2). The layout of RAON superconducting linear accelerators is shown in Fig. 1.

SCL1 accelerates stable ion beams while SCL3 accelerates rare isotope. Ions from low energy linac are transported to high energy linac, SCL2. Charge stripping sections are placed between SCL1 and SCL2 and between SCL3 and SCL2 to enhance the acceleration efficiency. To provide high quality ion beams, RAON adopted superconducting cavity and normal conducting quadrupole doublet structure for linac lattice. The Bunch frequency of the linear accelerator is 81.25 MHz. There are four kinds of cavities in RAON. Quarter wave resonators (QWR) will be used at the beginning of low energy linac and this section is called as SCL11 and SCL31. Half wave resonators (HWR) are going to be used for the rest of low energy linac and this section is called as SCL12 and SCL32. Two kinds of single spoke resonators (SSR) are going to be used for high energy linac (SCL2) and they are called as SCL21 and SCL22. Selected optimum betas were β_g=[0.047,0.12,0.3,0.51]. Also the transit time factors according to beta are shown in Fig. 2.

Each period in linac consists of a cryomodule containing superconducting cavities, one quadrupole doublet and a beam box for diagnostics. Layout of superconducting linac is shown in Fig. 3 and configurations of each section are summarized in Table 1. SCL3 and SCL1 are identical except that SCL3 has one less cryomodule containing four HWRs than SCL1. The number of cryomodules of four HWRs is 18 in SCL32.

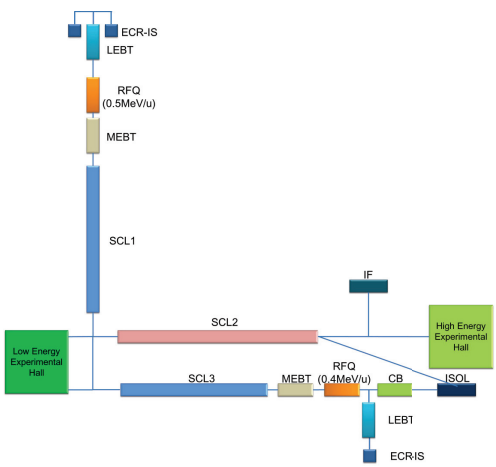


Figure 1: Layout of RAON superconducting linacs.

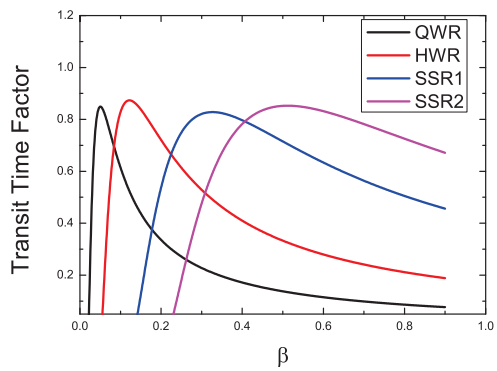


Figure 2: Transit time factors of cavities in RAON superconducting linac.

Copyright © 2014 CC-BY-3.0 and by the respective authors

ISBN 978-3-95450-142-7

THE ECT SYSTEM FOR RAON'S CAVITIES

J. Mijoung#, J. Yoochul, K. Hyungjin, IBS, Deajeon, South Korea

Abstract

The ECT system is in use for Nb surface control in many laboratories. This system can inspect Nb surface quickly using high resolution. The ECT system for RAON's cavity was made with the feature : It has 3-axis acting probe movement system, It can inspect big size of Nb sheet, which is 1m by 1m and It contain the analysis program that can show the result as 2D and 3D image as well as relative figure of surface level. The standard sample was made with various sizes of defects using the same Nb sheet that was used to make RISP cavity. The ECT system conditioning was carried out to optimize ECT operation on the frequency, the range is from 300kHz to 2MHz. The result of 900 kHz shows the strongest signal. The conditioning experiment on other parameter will be carried out in near future.

INTRODUCTION

It is very important to make high performance cavity in SRF cavity field in terms of reducing the cost as well as getting high quality beam. The quality control is necessary to make high performance cavity. There are three aspects in terms of quality control: purity, workability, and surface quality [1]. Because of this reason, many non-destructive tests were used for SRF cavity fabrication. The ECT system is one of the non-destructive inspection methods and it has been used to control surface quality of Nb in many accelerator laboratories such like FNAL, DESY and KEK [2-9]. The ECT system is for finding out surface defect such as pit, scratch, voids and cracks. It can also detect foreign material like Ta, Fe and so on. The ECT system has some advantages compared with other non-destructive inspection systems. These are: it is fast, has high resolution and easy to operate.

RISP Cavity

The goal of RISP (Rare Isotope Science Project) is to make the accelerator which can generate the 200 MeV/m beam energy based on uranium beam [10]. A total of over 550 cavities are needed to make the linac part of the RISP accelerator which was named RAON. We will use four kinds of cavities to meet the beam quality of RAON [11] and each cavity needs 3~4 Nb sheets that has the size of 1200 by 635mm. Nb sheets have similar properties with other SRF cavity material. The RRR value is larger than 300 and average grain size of Nb is finer than 64μm [12].

#mijoung@ibs.re.kr



Figure 1: Four types of SRF cavities used for RAON superconducting linac [11].

RISP ECT SYSTEM

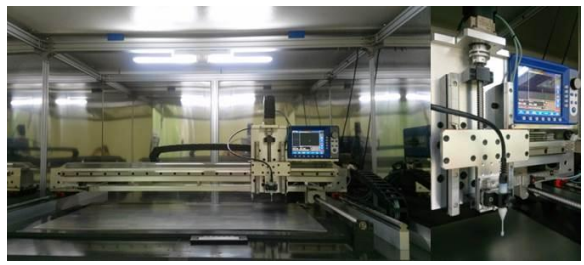


Figure 2: The ECT system for RAON's cavities.

Figure 2 shows the ECT system for RAON's cavities. It has the features as follows,

- The probe moves by 3-axis machinery system: It is more accurate than using turntable to find out the position of defect.
- The RISP ECT system can inspect about 1m by 1m large sheet.
- The probe was customized product by ZETEC, Inc.
- The ECT main body was also made by ZETEC, Inc.
- The analysis program made by FORUTEC, which is one of the domestic company in South Korea, can show the 2D and 3D result including relative surface level of the sample.

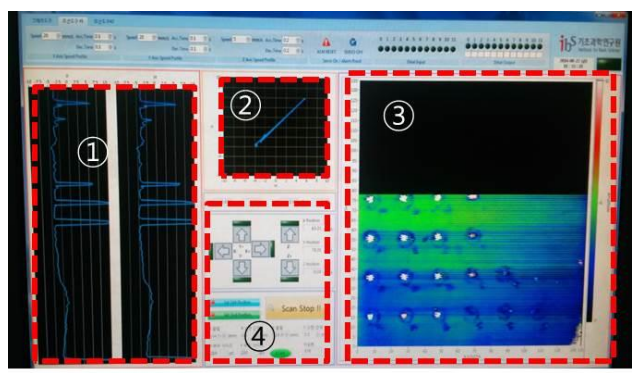


Figure 3: RISP ECT analysis program.

Copyright © 2014 CC-BY-3.0 and by the respective authors

ISBN 978-3-95450-142-7

SUPERCONDUCTING LINAC FOR THE RARE ISOTOPE SCIENCE PROJECT

H. J. Kim, H. J. Cha, M. O. Hyun, H. J. Jang, H. C. Jung,
Y. K. Kim, M. K. Lee, G.-T. Park, Institute for Basic Science, Daejeon, Korea

Abstract

The RISP (Rare Isotope Science Project) has been proposed as a multi-purpose accelerator facility for providing beams of exotic rare isotopes of various energies. It can deliver ions from proton to Uranium. Proton and Uranium beams are accelerated upto 600 MeV and 200 MeV/u respectively. The facility consists of three superconducting linacs of which superconducting cavities are independently phased. Requirement of the linac design is especially high for acceleration of multiple charge beams. In this paper, we present the RISP linac design, the prototyping of superconducting cavity and cryomodule.

INTRODUCTION

The Rare Isotope Science Project accelerator has been planned to study heavy ion of nuclear, material and medical science at the Institute for Basic Science. It can deliver ions from proton to Uranium with a final beam energy, for an example, 200 MeV/u for Uranium and 600 MeV for proton, and with a beam current range from 8.3 pμA (Uranium) to 660 pμA (proton) [1, 2]. The facility consists of three superconducting linacs of which superconducting cavities are independently phased and operating at three different frequencies, namely 81.25, 162.5 and 325 MHz.

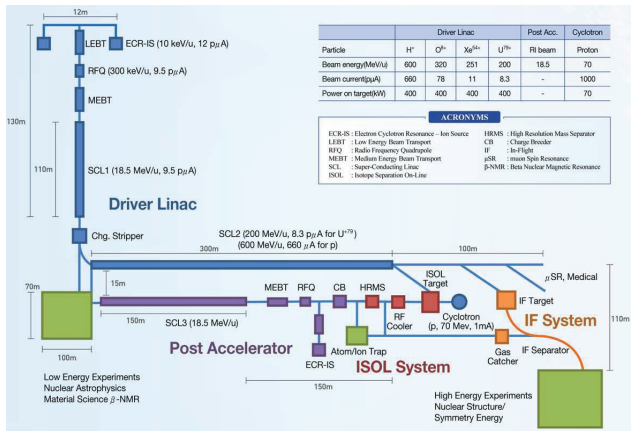


Figure 1: Layout of the RISP accelerator.

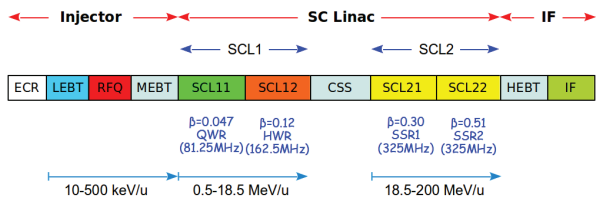


Figure 2: The RAON linear accelerator.

SUPERCONDUCTING LINAC

Lattice Design

The configuration of the accelerator facility within the rare isotope science project is shown in Fig. 1. An injector system accelerates a heavy ion beam to 500 keV/u and creates the desired bunch structure for injection into the superconducting linac. The injector system comprises an electron cyclotron resonance ion source, a low energy beam transport, a radio frequency quadrupole, and a medium energy beam transport. The superconducting driver linac accelerates the beam to 200 MeV/u. The driver linac is divided into three different sections as shown in Fig. 2: low energy superconducting linac (SCL1), charge stripper section (CSS) and high energy superconducting linac (SCL2). The SCL1 accelerates beam to 18.5 MeV/u. The SCL1 uses the two different families of superconducting resonators, i.e., quarter wave resonator (QWR) and half wave resonator (HWR). The CSS accepts beam at 18.5 MeV/u. The charge stripper strips electrons from heavy ion beams to enhance the acceleration efficiency in the high energy linac section. The SCL2 accepts beam at 18.5 MeV/u and accelerates it to 200 MeV/u. The SCL2 uses the two types of single spoke resonators, i.e., SSR1 and SSR2. The SCL2 provides beam into the in-flight fragmentation (IF) system via a high energy beam transport (HEBT). The post accelerator (SCL3) is designed to accelerate the rare isotopes produced in the ISOL (Isotope Separation On-Line) system. The SCL3 is, in principle, a duplicate of the driver linac up to low energy linear accelerator. The accelerated rare isotope beams are reaccelerated in the SCL2. Hence, the RISP accelerator provides a large number of rare isotopes with high intensity and with various beam energies [3].

For the actual SCL, machine imperfections cannot be avoided. The error comes from the misalignment of the linac elements and the limitation of manufacturing accuracy and various control errors. For instance, steering magnets are used to correct beam orbit displacements. In the baseline design of the RISP linac, steering magnets are placed where normal conducting quadrupoles are. The misalignment analysis includes all superconducting cavities and focusing elements assuming a uniform distribution. Table 1 summarizes tolerances for the lattice consisting of superconducting cavity and normal conducting quadrupole. In the misalignment and RF error analysis, charge states of 33+ and 34+ of Uranium beams are used. Effect of machine imperfection on beam envelope is shown in Fig. 3. The maximum envelope is kept well below the transverse aperture 20

Copyright © 2014 CC-BY-3.0 and by the respective authors

ISBN 978-3-95450-142-7

HELICAL WAVEGUIDES FOR SHORT WAVELENGTH ACCELERATORS AND RF UNDULATORS*

S.V. Kuzikov#, A.V. Savilov, A.A. Vikharev Institute of Applied Physics, Russian Academy of Sciences, Nizhny Novgorod, Russia

Abstract

The short wavelength accelerating structure can combine properties of a linear accelerator and a damping ring simultaneously. It provides acceleration of straight on-axis beam as well as cooling of this beam due to the synchrotron radiation of particles. These properties are provided by specific slow eigen mode which consists of two partial waves, TM_{01} and TM_{11}. The flying RF undulator introduces a high-power short pulse, propagating in a long helically corrugated waveguide where the -1st space harmonic with negative phase velocity is responsible for particle wiggling. High group velocity allows providing long interaction of particles with RF pulse. Calculations show that RF undulator with period 5 mm, undulator parameter 0.1 is possible in 1 GW 10 ns pulse at frequency 30 GHz. These RF parameters, as it was shown experimentally, are achievable by means of the relativistic BWO. The eigen mode in a helical undulator might be slow one so that the 0th harmonic phase velocity is equal to light velocity. Such wave (with non-zero longitudinal electric field) can be excited by relativistic drive bunch in a waveguide where witness bunch follows after the drive bunch, wiggles in wakefield of the drive bunch, and generates X-rays at whole waveguide length. Helical waveguides can also be used in order to channel low-energy bunches (due to longitudinal focusing field) in RF undulator of THz FEL.

HELICAL ACCELERATING STRUCTURE

An accelerating structure, based on helical corrugated waveguide has the operating normal mode consisted of the 0^{th} spatial harmonic (with positive phase velocity), which is actually the accelerating mode, and the -1^{st} harmonic (with negative phase velocity) which is responsible for particle wiggling [1]. The transverse non-synchronous field components can provide emittance control and beam focusing due to ponderomotive force. Let us consider the shape of the accelerating structure in cylindrical system of coordinates (r, z, φ) by equation:

$$r(z,\varphi) = R + a \cdot \sin(\frac{2\pi \cdot z}{d} + \varphi) . \qquad (1)$$

where R – is a waveguide radius, a and L – are amplitude and period of the corrugation. Period of the corrugation is close to $2\pi/h_{TM01}$, where h_{TM01} – is a propagation constant of the partial TM_{01} mode in smooth circular waveguide of the radius R. In the normal eigen mode the TM_{01} partial wave does not perturb transverse movement of on-axis electrons [2], the TM_{11} wave does not have longitudinal E_z component on axis.

Parameters of the 28 GHz TM_{01}-TM_{11} helical structure was optimized (R=6.1 mm, a=1.25 mm, d=8 mm) to reach maxima of the accelerating field relative to maximum of surface field, $E_a / E_s^{max} = 0.307$; and shunt impedance, R_{sh}=19 MOhm/m [1]. At acceleration gradient 100 MV/m the equivalent magnetic field is as high as 0.75 T. Field structure of the operating mode is shown in Fig. 1. The phase velocities of longitudinal component and both transverse components have opposite signs (Fig. 2).

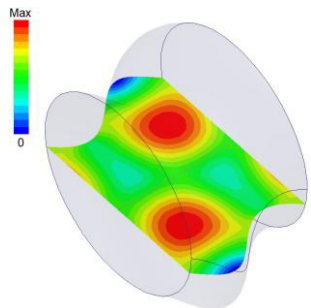


Figure 1: Module of electric field in middle plane.

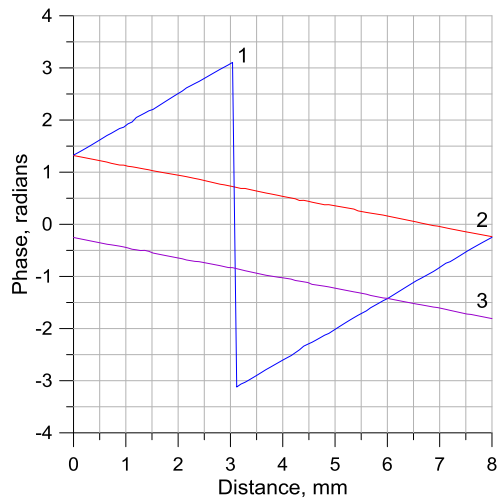


Figure 2: Phases of E_z (longitudinal) field component (curve 1) and phases of E_x (curve 2) and E_y (curve 3) field components.

The helpful feature of TM_{01}-TM_{11} helical structure is a flexible focusing of electrons due to higher space harmonics crowded to the corrugation.

*Work supported by Russian Foundation for Basic Research (grant No. 14-02-00691).
#kuzikov@apppl.sci-nnov.ru

Copyright © 2014 CC-BY-3.0 and by the respective authors

NONDESTRUCTIVE DIAGNOSTICS OF PROTON BEAM HALO AND TRANSVERSE BUNCH POSITION BY CERENKOV SLOW WAVE STRUCTURES

A.V. Gromov, M.B. Goykhman, S.V. Kuzikov#, A.V. Palitsin, Yu.V. Rodin, A.A. Vikharev,
Institute of Applied Physics, Russian Academy of Sciences, Nizhny Novgorod, Russia

Abstract

An appearance of the halo around bunch of particles is very undesirable destructive phenomenon in high-intensity proton accelerators. We suggest using built-in short BWO section in form of the corrugated metallic waveguide, in order to control particle distribution in real time. In BWO low velocity proton bunch has synchronism with slow spatial harmonic of TM_{01} wave. Fields of slow harmonic sharply grow in direction from axis to walls and rf power, generated by flying bunch of the given charge, critically depends on transverse bunch size. Results of the simulation, carried out for 20 pC proton bunch of 10 ps duration, show that in 5 GHz BWO of 30 cm length the output rf pulse of several nanosecond duration is varied from mW- level (for 1 mm transverse bunch size) to several tens of mW (for bunch of 20 mm radius). This power level is high enough to control halo appearance in each single proton bunch. The producible rf power in a BWO is also dependent on bunch deflection from axis. This effect we plan to use, in order to provide transverse bunch position monitoring by means of two additional rectangular slow wave section which have corrugations on mutually perpendicular walls.

PROTON BEAM HALO MONITOR

High-intensity proton machines like Project-X in Fermilab [1] require accurate non-destructive on-line monitoring for bunch halo. Existing methods either do not provide non-destructive basis [2-3], or work well for electron bunches only [4]. New methods for diagnostics of heavy particles are necessary.

Short proton bunch, flying in an axial corrugated waveguide, can naturally cause BWO oscillations due to Cerenkov synchronism ($v_p \approx v_{ph}$) with slow backward eigen wave of the structure [5]. Because we consider protons with moderate energies ($v_p \leq 0.5c$), the mentioned Cerenkov synchronism is possible with -1st harmonic of the TM_{01} wave which has sharply growing fields in direction from axis to wall. That is why, power level of BWO excitation essentially depends on transverse bunch size. The bigger bunch size and the longer BWO section, the higher is rf signal (assuming full bunch charge to be constant). Therefore, one can measure in real time the magnitude of BWO oscillations and to recover bunch size.

Let us consider the BWO consisted of 15 periods (each period is 20 mm) in regular part and 6 periods in tapered part of the corrugation (full length is ~30 cm), average radius is 25 mm, corrugation depth is 10 mm. Bunch parameters of the bunch used in simulations are shown in Table 1.

Table 1: Bunch parameters.

Parameters	Value
Velocity, v_p	0.5c
Charge, Q	24 pC
Bunch length, l_b	12 ps
Radial space charge distribution	uniform

Dispersion of the TM_{01} mode in the chosen corrugated waveguide (Fig. 1) has intersection with bunch dispersion line near 5 GHz. At this point slow TM_{01} wave has distinctive surface character (Fig. 2).

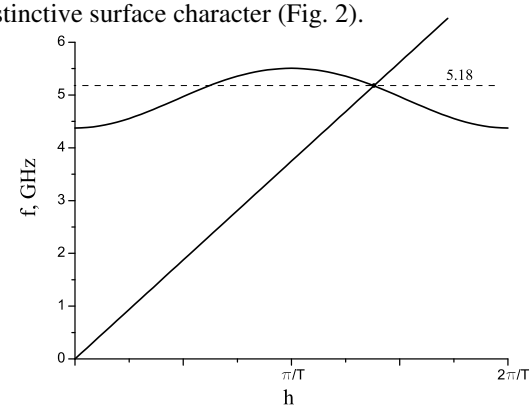


Figure 1: Dispersion curves of the operating TM_{01} eigen mode in BWO and proton bunch.

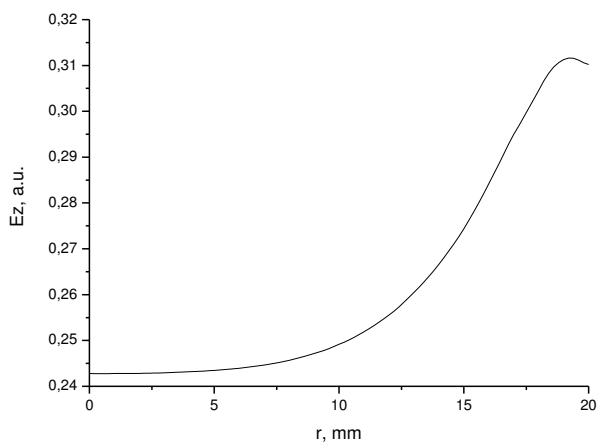


Figure 2: Longitudinal component of electric field for TM^{01} eigen mode in BWO vs. radial coordinate.

#kuzikov@appl.sci-nnov.ru

Copyright © 2014 CC-BY-3.0 and by the respective authors

ISBN 978-3-95450-142-7

ECR ION SOURCES DEVELOPMENTS AT INFN-LNS FOR THE PRODUCTION OF HIGH BRIGHTNESS HIGHLY CHARGED ION BEAMS*

D. Mascali#, L. Andò, G. Castro, L. Celona, L. Neri, S. Gammino, Istituto Nazionale di Fisica Nucleare, Laboratori Nazionali del Sud, 95123 – Catania, Italy
F. P. Romano, INFN-LNS and CNR-IBAM, Catania, Italy
C. Altana, C. Caliri, G. Sorbello INFN-LNS and Università di Catania, Catania, Italy
G. Torrisi, INFN-LNS and Università Mediterranea di Reggio Calabria, Reggio Calabria, Italy

Abstract

The design of future high-performing ECRIS will require alternative approaches in microwave-to-plasma coupling, in order to maximize the electron density at relatively low frequency and to reduce the hot electrons formation and their consequences on beam stability and on source reliability. On these purposes, different activities have been carried out at INFN-LNS in the recent past, including advanced modelling, diagnostics, and studies about alternative methods of plasma heating based on electrostatic-waves generation. A description of these activities will be presented, with special emphasis to the microwave to plasma coupling and to the plasma diagnostics. Some of the already collected results have been a basis for the design of the new AISHa source (for hadrontherapy purposes) and for the construction of an innovative prototype named Flexible Plasma Trap: on this machine we will search for new schemes of microwave launching, in synergy with the full-wave plus kinetic calculations of the wave-to-plasma interaction mechanism.

INTRODUCTION

Among the various types of ion sources developed since 1950s, Electron Cyclotron Resonance Ion Sources (ECRIS) are the best candidate to support the growing request of intense beams of multicharged ions coming from both fundamental science (nuclear and particle Physics, especially) and applied research (neutrons spallation sources, subcritical nuclear reactors, hadrotherapy facilities, material treatments, ion implantation).

Inside an ECRIS machine [1] a dense and hot plasma, made of multicharged ions immersed in a dense cloud of energetic electrons, is confined by multi-Tesla magnetic fields and resonantly heated by some kWs of microwave power in the 2.45-28 GHz frequency range. The ECRIS development path has been traced – since the years of general scaling laws definition (1980-1995) [2,3]– on the philosophy of magnetic field and microwave source frequency and power boosting. This trend is now deemed of approaching saturation due to technological constraints.

*Work supported by European Union - Seventh Framework Programme FP7/2007–2013 under Grant Agreement No. 262010-ENSAR, and by the RDH project of the V Nat. Comm. of INFN
#davidmascali@lns.infn.it

While until 2004-2005 the output currents and charge states were deemed to depend only on major plasma parameters (density and temperature), more recently some unexpected issues have come to the attention of the ECRIS community: plasma instabilities [4], local fluctuations and/or non uniform distribution of the plasma density [5], non linear response of the electron heating to the pumping wave frequency, or sensitivity to slight adjustments of the magnetic field, have been correlated with the intensity and emittance of the plasma-generated beams, showing that the parameters' space has not been fully explored, as well as the wave-to-plasma interaction in a closed resonant cavity (i.e. the ECRIS plasma chamber) with small size-to-waveguide ratio is still not fully exploited [6,7].

PLASMA HEATING IN ECRIS

The development of new generation ECRIS requires a more detailed comprehension of plasma heating processes. Recent research activity has shown that the heating process is critically dependent not only on the RF power level, but also on the fine tuning of the pumping wave frequency (frequency tuning effect [8]). Fine adjustments of the magnetostatic field profile also play a relevant role [9]. In a long-term perspective, in addition, we have considered the option of a radically different heating method of ion sources plasmas, that could be based on Electron Bernstein Waves [10].

Tuning of Frequency and B-field Profile

At INFN-LNS additional studies about frequency tuning effect have been carried out. Recently, a campaign of measurements has been carried out in collaboration with GSI-Darmstadt ion sources team [11]: it has been shown a critical variation of the plasma energy content (defined as the product of electron density and temperature $\varepsilon=n_e kT_e$) versus slight adjustments of the pumping wave frequency and magnetic field profile. Measurements about plasma spectral energy were done by means of an hyper-pure Germanium detector (HpGe) sensitive in the 30-400 keV energy range (energy resolution around 200 eV at 40 keV). The average charge state extracted from the source, namely <q>, was simultaneously evaluated: it came out that <q> was roughly connected to fluctuations of ε, the latter being so sensitive to the frequency tuning. By modifying the extraction coil current of less than 10% we slightly changed the magnetic field profile at the

Copyright © 2014 CC-BY-3.0 and by the respective authors

CONSTRUCTION OF THE MODULES OF THE IFMIF-EVEDA RFQ

A. Pepato, R. Dima, A. Prevedello, E. Udup, INFN/PD, Padova, Italy
L. Ferrari, F. Grespan, E. Fagotti, C. Roncolato, A. Palmieri, A. Pisent, INFN/L.N.L., Legnaro, Italy
A. Margotti, INFN/BO, Bologna, Italy, P. Mereu, INFN/TO, Torino, Italy

Abstract

The IFMIF project aims to produce an intense neutron flux to test and qualify materials suitable for the construction of fusion power plants. We are working on the engineering validation phase of the project (IFMIF-EVEDA) [1], which consists on the construction of a linear accelerator prototype (LIPAC) to be installed and commissioned in Rokkasho (Japan). The RFQ is composed of 18 modules flanged together for a total length of 9.8 m designed to accelerate the 125 mA D+ beam to 5 MeV at a frequency of 175 MHz. The mechanical specifications are very challenging, tight tolerances are required on the machining and on the brazing process (Fig. 1). The line is subdivided into three Super Modules of six modules each. The production of the High Energy portion has been completed and delivered, while the Low Energy one is performing the acceptance test. They were commissioned to external firms. The production of the Intermediate Energy portion has been done in house (INFN) and will be fully commissioned soon. The first modules (16, 17 and 2) were produced adopting two brazing steps, while for all the remaining ones we adopted a single brazing step [2,3,4,5]. In this paper the production status as well as the development of the brazing procedure design will be described.

THE HIGH ENERGY SUPER MODULE (SM_III)

The SM_III contract was assigned by an international tender on April 2011 to an Italian firm (CINEL S.p.A.). The SM_III production has been a full scale completion of the Module prototyping. We optimise the geometrical survey versus the CuC2 components machining as well as the brazing tooling and brazing thermal cycle with a fruitful collaboration with the firm personnel. The extensive use of the CMM continuous active scanning represented the most effective tool for the milling cycle tuning and the most effective approach for the components assembly and module qualification at the acceptance stage.

An extensive FEM analysis was mandatory for the correct understanding of the material behaviour, for the tuning of the oven parameters and for the dimensioning of the brazing tooling components. The introduction of the TZM[1] (molybdenum alloy) springs helped a lot on the soft fixation of AISI parts, while minimizing the material budget during the brazing cycles. The SM_III production has been successfully completed on May 2014 (Fig. 2).

The first two Modules (M_16 and M_17) have been brazed adopting a two-step process, while a single step brazing was used for the remaining ones, with all the advantages in terms of overall mechanical precision, costs and material properties deterioration.

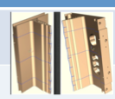
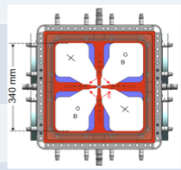
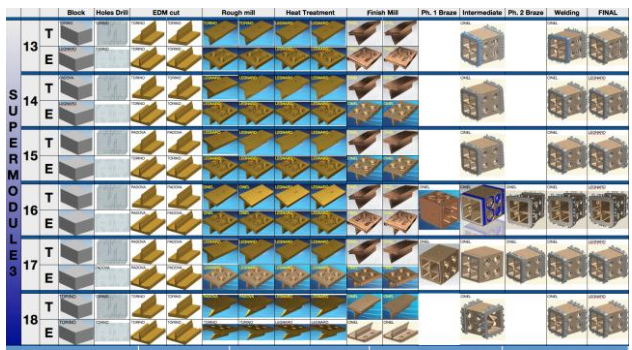
Parameter	Limit Value		Definition
Geometry of vane tip	± 10μm		Overall error of position and shape of the modulation of the vane tip with respect to the electrode reference system, as defined in the drawings.
Roughness Ra	0.7 μm		For any sample measure on any surface being part of the cavity inner surface including the modulation on the vane tip (on a single electrode or on the module, after etching and passivation)
Vane tip position with respect to beam axis	± 50 μm		Beam axis defined as the straight line going through the best fit points at the two ends of the module (w.r.t the mid planes of the four tips). The mid plane of the tip being defined by the two surfaces as indicated in the drawings.
Beam axis	± 50 um		Tolerance on distance between beam axis as defined above and the external references (small plates for supports and laser tracker reference)
Vacuum tightness of cavity and channels	10^{-9} mbar/l/s		Helium leak test of the cavity and all the channels
Pressure test of channels	5 bar		hydraulic test with dry inert gas

Figure 1: Geometrical Specification of the IFMIF-EVEDA RFQ.



Module	Limit Value	Pre-braze[MHz] fq(WG)	Post-braz[MHz] fq(WG)	Δf MHz/[μm]
M_16	± 50 μm	186.862	186.981	0.119/+17
M_17	± 50 μm	187.015	186.820	0.195/-25
M_15	± 50 μm	187.207	187.359	0.152/+22
M_18	± 50 μm	178.494	178.742	0.248/+35
M_14	± 50 μm	186.935	187,165	0.230/+30
M_13	± 50 μm	187.231		

Figure 2: SM_III production status (top); measured values of the overall frequency variations with respect to the nominal values (bottom).

The last part of the RFQ, where the RF power density is maximum, will be tested in Europe up to the operating field. A new test stand has been built at LNL, based on a 220 kW RF transmitter and of a dedicated cooling system (with separate circuits for vanes and external walls) for the

1 TZM ® –Titanium-Zirconium-Molybdenum Alloy (Plansee Group)

ISBN 978-3-95450-142-7

Copyright © 2014 CC-BY-3.0 and by the respective authors

MUNES A COMPACT NEUTRON SOURCE FOR BNCT AND RADIOACTIVE WASTES CHARACTERIZATION

A. Pisent, E. Fagotti, P. Colautti INFN/LNL, Legnaro, Italy

Abstract

At INFN LNL (Legnaro Italy) it has been built a high intensity Radio Frequency Quadrupole (RFQ) structure, able to produce a 5 MeV proton beam of 30 mA. Coupled with a Be target such a beam can generate a neutron flux of 10^{14} n/s, with a spectrum centred in the MeV region (that has been recently characterized in detail at LNL accelerators). This neutron flux can be moderated to generate a thermal or epithermal source for BNCT with very little contamination of energetic form energetic neutron and gamma.

Since the approval of MUNES project (in 2012) the high technology issues related to a compact neutron source to be installed in a Hospital environment have been faced. In particular for the powering of the accelerating structure an innovative system, completely based on solid state amplifiers, has been developed and ordered to industry. An outline of MUNES design and the status of the project will be given in the paper.

INTRODUCTION

New neutron sources are being developed for various applications (test of materials for fusion reactors, experimental oncological treatments, characterization of nuclear wastes…), based on high intensity "low energy" (up to 40 MeV) proton or deuteron linear accelerators. This kind of sources has recognized advantages respect to reactors and spallation sources for these applications.

The project MUNES (Multidisciplinary Neutron Source), aiming at the realization of an intense source of thermal-epithermal neutrons for Boron Neutron Capture Therapy (BNCT) and for the characterization of nuclear wastes, has been launched during 2012. Such neutron source is based on a high intensity linear accelerator under realization at Legnaro National Laboratory.

The accelerator is a Radio Frequency Quadrupole able to accelerate 30 mA of protons up to 5 MeV. The RFQ was developed in the last years in the framework of TRASCO project (see Fig.1). For BNCT application this CW source promises unique performances in terms of neutron flux and spectra (very low gamma and fast neutrons components) as needed for a successful therapy. For the characterization of waste barrels (mainly for the detection of very low plutonium content) a pulsed neutron beam with high pick intensity shall be used; this approach should allow to improve dramatically (at least two order of magnitude) the sensitivity to Pu content respect to the present devices based on D-T sealed tubes with an important economic impact on nuclear waste cycle.

The proposal of a neutrons source based on TRASCO RFQ for these applications has a quite long history as SPES-BNCT project [1], in close collaboration with IOV (Istituto Oncologico Veneto) and other institutions. More recently, it has been approved a trilateral collaboration between INFN, University of Pavia and SOGIN (public company for nuclear sites decommissioning) for the development of such a neutron facility at Pavia. Finally with the so-called "Progetti Premiali", the project MUNES has been selected by MIUR and funded with 5 M€, that allows a substantial step forward in the realization of the accelerator high technology part. Table 1 summarizes the main parameters of MUNES.

Table 1: MUNES main parameters

Ion source	TRIPS	Proton energy 80 keV
Accelerator type	RFQ	Radio Freq. Quadrupole
Final energy	5 MeV	
Beam current	30 mA	accelerated
Duty cycle	CW	Continous Wave
Neutron	Beryllium	Water cooled 150 kW
Neutron source intensity	~10^{14} s^{-1}	entire solid angle, Ave. neutron energy 1.2MeV
RF power	1.0 MW	
Electrical power	5 MVA	



Figure 1: TRASCO RFQ modules.

Copyright © 2014 CC-BY-3.0 and by the respective authors

ISBN 978-3-95450-142-7

ADJUSTMENT OF THE COUPLING FACTOR OF THE INPUT COUPLER OF THE ACS LINAC BY A CAPACITIVE IRIS IN J-PARC

J. Tamura*, H. Ao, K. Hirano, Y. Nemoto, N. Ouchi, JAEA/J-PARC, Ibaraki, Japan
F. Naito, K. Takata, KEK/J-PARC, Ibaraki, Japan
H. Asano, Nippon Advanced Technology Co.,Ltd., Ibaraki, Japan

Abstract

Annular-ring Coupled Structure (ACS) cavities have been installed to increase the beam energy of the Japan Proton Accelerator Research Complex (J-PARC) linac from 181 to 400 MeV in the maintenance period of 2013. Some of the pillbox type input couplers with a ceramic window to the ACS cavity have a larger coupling factor than the target value by an avoidable manufacturing error. To adjust the coupling factor, a capacitive iris was introduced in the rectangular waveguide near the coupler. As a result, it has been confirmed that the iris decreases the coupling factor to a target value without any significant increase in temperature and in a discharge rate during high-power operation.

INTRODUCTION

To increase the beam energy of the Japan Proton Accelerator Research Complex (J-PARC) linac from 181 to 400 MeV, twenty-one Annular-ring Coupled Structure (ACS) accelerating cavities, two ACS buncher cavities, and two ACS debuncher cavities have been installed in the beam transport at the downstream of the separated-type drift tube linac in the maintenance period of 2013. After the installation, RF power has been fed into the cavities. And then, the negative ion beam has been successfully accelerated to the beam energy of 400 MeV in January 2014. Figure 1 shows the diagram of the J-PARC linac accelerating structure in the 400-MeV beam operation.

The ACS cavities consist of two accelerating tanks and one bridge tank. In ACS accelerating cavities, shown in Fig. 2, one accelerating tank consists of 17 accelerating cells and 16 annular-ring type coupling cells, while one

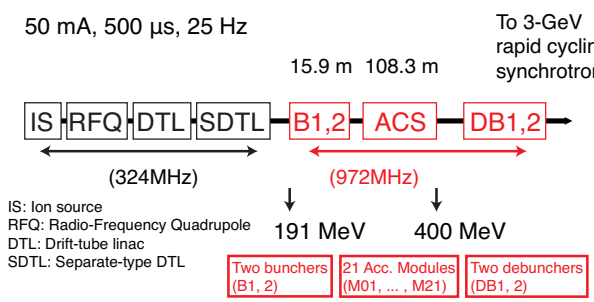


Figure 1: Diagram of the J-PARC linac accelerating structure in the 400-MeV beam operation.

* jtamura@post.j-parc.jp

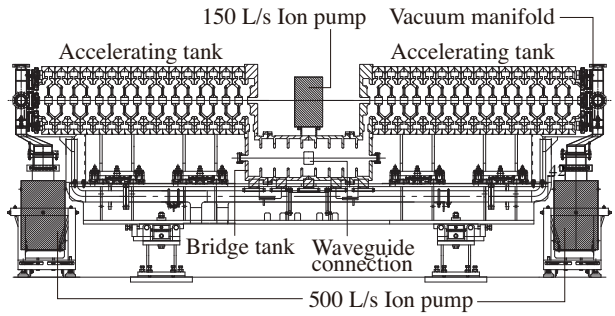


Figure 2: Accelerating cavity in the J-PARC ACS.

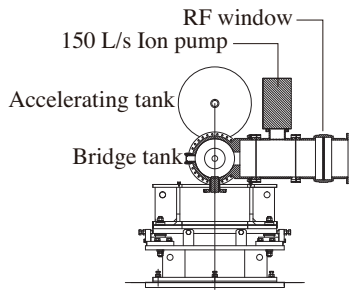


Figure 3: Bridge coupler of the J-PARC ACS.

bridge tank consists of 5 accelerating cells (excited in $\pi/2$-mode) and 4 coupling cells (unexcited in $\pi/2$-mode). The accelerating mode ($\pi/2$-mode) frequency of the cavity is tuned by the plunger tuners installed in the accelerating cells of the bridge tank. As shown in Fig. 3, an RF power from a klystron is fed into the cavity through the iris in the side of the center cell of the bridge tank [1].

Some of the pillbox type input couplers to the manufactured ACS cavity have a larger coupling factor than the target value by an avoidable manufacturing error [2]. The matching of the ACS cavity and the waveguide is decided by the configuration of the iris in the side of the center cell of the bridge tank. However, this part is difficult to be machined for tuning the coupling after the cavity fabrication is completed [3]. So we decided to correct the coupling factor by introducing a capacitive iris, shown by the purple color in Fig. 4, in the rectangular waveguide between the cavity and the RF window[1]. We aimed to adjust the VSWR of

[1]The reflection from the total load (the cavity and the RF window) is decided by the VSWR of the cavity adjusted by the capacitive iris and of the RF window [4]

Copyright © 2014 CC-BY-3.0 and by the respective authors

ISBN 978-3-95450-142-7

BEAM TEST OF A NEW RFQ FOR THE J-PARC LINAC

Y. Kondo*, T. Morishita, S. Yamazaki, T. Hori, Y. Sawabe,
JAEA, Tokai, Naka, Ibaraki, 319-1195, Japan
A. Takagi, KEK, Oho, Tsukuba, 305-0801, Japan

Abstract

We performed a beam test of a new 324-MHz 3-MeV H^- RFQ (RFQ III) for the beam-current upgrade of the J-PARC linac. RFQ III is the first RFQ developed to meet the requirement of the J-PARC linac. The peak beam current is 50mA, pulse length is 500 μs, and the repetition is 25 Hz. Prior to the installation to the accelerator tunnel in summer of 2014, we constructed a test stand for off line testing of the new ion source and RFQ. Basic performances of RFQ III such as transmission and emittances were measured. In this paper, the beam test results are presented.

INTRODUCTION

The Japan Proton Accelerator Research Complex (J-PARC) is a multi-purpose facility for particle physics, nuclear physics, materials and life science, and others. The J-PARC accelerator [1] consists of a 400-MeV linac, a 3-GeV rapid cycling synchrotron, and a 50-GeV main ring. The original design energy and peak beam current of the linac are 400 MeV and 50 mA, respectively. A four-vane-type radio frequency quadrupole (RFQ) built for the Japan Hadron Facility project was used for the initial phase linac, and the design peak beam current of this RFQ was 30 mA. To upgrade the beam current of the J-PARC linac to achieve the original design power of 1 MW (at the neutron target), a new RFQ with a design current of 50 mA has been developed [2]. This RFQ is called RFQ III, whereas the former 30-mA RFQ is called RFQ I [1]. Table 1 lists the design parameters of RFQ III.

Table 1: Design Parameters of J-PARC RFQ III.

Beam species	H^-
Resonant frequency	324 MHz
Injection energy	50 keV
Extraction energy	3 MeV
Peak beam current	50 mA
Vane length	3623 mm
Average bore radius (r_0)	3.49 mm
ρ_t/r_0 ratio	0.75 (ρ_t =2.62 mm)
Inter-vane voltage	81.0 kV
Maximum surface field	30.7 MV/m (1.72 Kilpatrick)
Nominal peak power	400 kW
Repetition rate	50 Hz
RF pulse length	600 μs
Duty	3%

RFQ III employs a conventional beam dynamics design. That is, the RFQ is divided into four sections: a radial matching section (RMS), a shaper (SP), a gentle buncher (GB), and an accelerator (ACC). Additionally, the inter-vane voltage V and the average bore radius r_0 are maintained constant except for the injection section. For the beam dynamics design of RFQ III, LINACSrfqDES [3] was used [2]. The feature that characterizes the beam dynamics in LINACSrfqDES is the equipartitioning condition, which is used to avoid the effect of parametric resonances in high current linacs [4]. This condition requires that the internal energies in the transverse and longitudinal phase spaces of the beam are same. When this condition is satisfied, there is no free energy to drive a resonance. However, the equipartitioning condition is not maintained with maintaining V constant as the particles are accelerated. Therefore, for RFQ III, we adopted equipartitioning in the GB, which is the most critical section of RFQs.

In accordance with the concepts described above, J-PARC RFQ III was designed and fabricated. Because the J-PARC linac provides a beam for user operation, the performance of RFQ III had to be confirmed by off line testing using a negative hydrogen (H^-) beam prior to replacing RFQ I. In this paper, the beam test results of J-PARC RFQ III are described.

EXPERIMENTAL APPARATUS

As mentioned in the previous section, RFQ III was tested off line prior to installation in the accelerator tunnel. To this end, an RFQ test stand (TS) was constructed on the ground floor of the J-PARC linac building. This TS allowed the use of a 50 mA beam with a duty factor of up to 25% of the nominal duty (500 μs, 25 Hz) for continuous operation, wherein the duty factor was limited by allowable radiation levels. Figure 1 shows a schematic drawing of the TS.

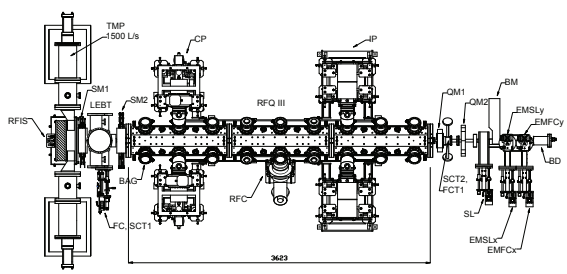


Figure 1: Schematic of the RFQ test stand (top view).

An RF driven ion source (RFIS) for the J-PARC linac upgrade [5] was employed for the RFQ testing. The plasma is driven by a pulsed 2-MHz RF power, and a 30-MHz con-

* yasuhiro.kondo@j-parc.jp

[1] Because a sparking problem occurred in RFQ I, a spare RFQ was fabricated. We call this spare one RFQ II.

Copyright © 2014 CC-BY-3.0 and by the respective authors

ISBN 978-3-95450-142-7

COMPACT TIMING SYSTEM WITH FPGA FOR SPRING-8 LINAC

H. Dewa#, H. Hanaki, S. Suzuki JASRI/SPring-8, Hyogo, JAPAN

Abstract

The SPring-8 linac is an injector for the SPring-8 booster synchrotron and the New SUBARU SR ring. The linac emits 1 GeV electron beam to these two rings at 2 Hz by time-sharing. The linac timing system synchronises the electron gun system, the pulsed rf system and the beam diagnosis system etc. It has been assembled with more than one hundred NIM modules and a lot of thin coaxial cables to connect them. To make the timing system small, simple, and reliable, we developed a prototype of compact timing system with FPGA. The developed FPGA includes circuit elements with most of the functions of the NIM modules we are using in the current linac timing system. All of gun trigger circuit in the current system were completely reproduced in it. The timing of the output signal is re-clocked with the master clocks of 500/508 MHz and the rms jitter was less than 1.7 ps. This prototype proved the possibility that the large and complex linac timing system based on NIM modules can be integrated into a small FPGA based timing system.

INTRODUCTION

The timing system of accelerator is usually large and complicated, but the time accuracy around pico seconds is also necessary. To satisfy the time accuracy, the timing systems of traditional accelerators have used NIM signal or NIM modules. But the semiconductor technologies have been advancing these days and very fast and large-scale integrated circuits have been appearing. The FPGA (Field-Programmable Gate Array) is thought to be the most suitable integrated circuit to the timing system of accelerator, because the scale is large enough and it is user-programmable and re-writable. As for the clock speed of FPGA, it was not fast enough five years ago, but the clock speed exceeds 500 MHz now and is likely available for the timing system.

As described later, the timing system of the SPring-8 linac has been also based on NIM modules. It is growing so large and complex for seventeen years' machine operation and improvements that the extension or maintenance of the system is getting difficult. For these reasons, we started to replace the current timing system to a compact timing system with FPGA. The prototype of the compact timing system is described in this paper.

CURRENT LINAC TIMING SYSTEM

SPring-8 is a synchrotron radiation research facility with an 8 GeV storage ring. The SPring-8 linac is an injector for both the SPring-8 booster synchrotron (Sy) and the 1 GeV storage ring New SUBARU (NS). The linac emits 1 GeV electron beam to these two rings at 2 Hz by time-sharing.

#dewa @spring8.or.jp

There are three kinds of timing sources, namely, the Sy timing, the NS timing and the Li timing, which were determined according to the selected beam injection route. The Sy timing is used when a beam is emitted to Sy, and the NS timing likewise. The Li timing is used for a solo operation of the linac, when the beam is injected to L2 beam dump or L3 beamline. The Sy timing signals are generated at Sy and then sent to the linac, and the NS timing signals are generated at NS as well. The Li timing triggers are independently generated at the linac.

For each timing source, three kinds of triggers such as the pre-trigger, the gun trigger, and the monitor trigger are prepared in the linac timing system. The pre-trigger is a 2 Hz trigger, distributed to two AWGs (arbitrary wave generators) for generating pulsed reference RF signal [1], an rf pulse modulator, two gun modulators and thirteen klystron modulators. The gun trigger is a continuous 1 Hz trigger, and then is selected out at the injection timing to distribute to the gun pulsers of the two electron guns [2]. The monitor trigger is also a continuous 1 Hz trigger and is distributed to the beam current monitors or the beam position monitors.

The SPring-8 linac timing system has following two special features that complicate the timing system.

1) Time-shared injection

The beam injection to Sy or NS has been time-shared since 2013 for an efficient beam injection called as "fast alternate injection". In the fast alternate injection, all of the Sy timing triggers and the NS timing triggers are switched every 0.5 second [3,4]. It is necessary to synchronize the NS timing trigger to the Sy timing trigger for time-sharing, so that all NS timing sources are generated from the Sy timing pre-trigger.

2) Irregular triggering for energy saving

The 2 Hz modulator trigger to the klystron modulators, which is generated from a pre-trigger, cannot keep the PFN voltage high enough until the discharge time of thyratron, because the PFN voltage decreases during the charging interval of 500 ms in case of 2Hz modulator trigger. For this reason, irregular 4 Hz trigger is used, where another discharge timing was added at 100 ms before the 2Hz modulator trigger for the pre-discharge of the decreasing charge stored in the PFN capacitors [3].

To complete these requirements, many kinds of NIM modules have been used, for example, fanout, AND/OR logic, majority logic, selector switch, delay/gate generator, and precise long delay using 30 bits counter. The number of NIM modules we are using is 161 and the number of NIM bin is 22 at this moment. They are so many that it is not easy to modify the circuit further more and maintain the line connections or validity of the circuit. For these reasons, we decided to develop a new compact linac timing system.

Copyright © 2014 CC-BY-3.0 and by the respective authors

ISBN 978-3-95450-142-7

EVALUATION OF BEAM ENERGY FLUCTUATION CAUSED BY PHASE NOISE

H. Hanaki #, H. Dewa, S. Suzuki, K. Yanagida, JASRI, Hyogo, Japan
T. Asaka, T. Ohshima, Riken RSC, Hyogo, Japan

Abstract

The SSB noises of the RF reference signal dominate the short-term instabilities of the RF phase of the carrier RF. This phase modulation finally results in beam energy fluctuation. This presentation gives a quantitative evaluation of the beam energy fluctuations in an electron linear accelerator caused by phase noises, comparing a theoretical analysis and experimental results. A simple model was introduced to understand how phase noises result in the relative phase difference between a beam bunch and accelerating RF fields. In the experiments, we measured the enhanced beam energy fluctuations by modulating the phase of the reference RF signals with an external signal. The interference between the accelerating RF phase modulation and the timing modulation of a beam bunch was found in the model analysis and also in the experimental results.

INTRODUCTION

Recently, it has become easier to introduce a high-precision signal generator as a master oscillator for an accelerator; hence the phase noises of a master oscillator do not dominate beam instability if a low-power RF system is carefully designed.

However, the effect of phase noises may be evaluated in the following cases. The RF sources for XFELs is generally required to satisfy the integrated phase fluctuation of less than several tens of femtoseconds [1]. A programmable arbitrary waveform generator, whose phase noise levels are larger than those of a normal type, may be required to generate a linac's reference signal synchronizing with that of a storage ring [2].

Since the SPring-8 linac has used the latter system to stabilize the beam energy, we performed the preliminary experiment to understand the beam energy variation caused by phase noises. In this experiment, we modulated the phase of the reference RF signal by external sinusoidal waves with various frequencies or noises and then observed that the resulting beam energy modulations depended on the modulation frequencies.

The motivation of this study to determine the mechanism of the beam energy variation caused by phase noise is based on the above preliminary study.

UNDERSTANDING PHASE NOISE

Interference of Phase Noise

The RF phase variations caused by phase noise seem like random phenomena. On the contrary, we can unfold even a random signal by applying the Fourier integral as an integration of an infinite number of sinusoidal waves. When we pay attention to each Fourier frequency component, this sinusoidal wave must have a constant amplitude and phase advance at least during a period of milliseconds, for example. That is, we can conclude that any sinusoidal wave of the Fourier frequency component is so stable as to show the interference because the length of the sinusoidal wave is sufficiently long in actual linacs.

In addition, since actual circuits including waveguide circuits and accelerating structures have limited frequency bandwidths, the randomness of signals is reduced according to the bandwidths.

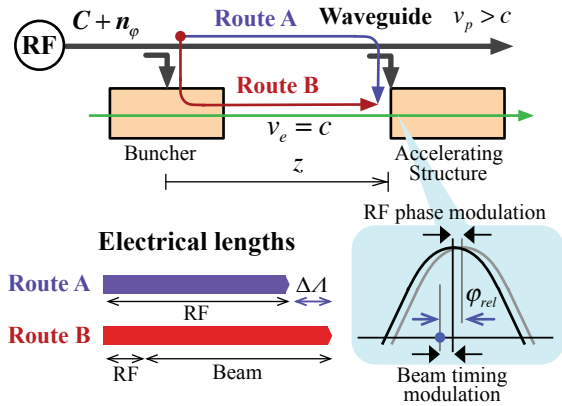


Figure 1: Simplified model of electron linac is proposed to understand the phase noise propagation. Relative phase modulation is caused by the electrical path difference $\Delta\Lambda$, which depends on the RF frequency due to the dispersion of the transmission line.

Figure 1 presents a simplified model of a normal conducting electron linac with a buncher and multiple accelerating structures. This model treats only RF phase, not RF amplitude. In this model, we assume that the phase variation is expressed as the superposition of stable sinusoidal waves as explained above. This figure shows also the electrical lengths of the routes of the accelerating RF and the electron beam bunched in the buncher cavity and a diagram to explain the relative phase deviation that results in the beam energy deviation.

If the phase velocity of the RF wave propagating in the transmission line does not depend on its frequency and is the same as the electron velocity (= c), the length difference $\Delta\Lambda$ in Fig. 1 is almost zero. Assuming that the frequency responses of the buncher and the accelerating structure are the same, the RF phase deviation observed by a beam bunch at the entrance of every accelerating structure is the same as the timing deviation of the beam. Hence the RF phase modulation caused by a master oscillator does not modulate the beam energy.

#hanaki@spring8.or.jp

ISBN 978-3-95450-142-7

Copyright © 2014 CC-BY-3.0 and by the respective authors

LATEST IMPROVEMENTS OF THE SPring-8 LINAC FOR HIGH RELIABILITY

S. Suzuki#, H. Dewa, T. Kobayashi, T. Magome, A. Mizuno, T. Taniuchi,
K. Yanagida and H. Hanaki
JASRI/SPring-8, Kouto, Sayo-cho, Sayo-gun, Hyogo, 679-5198
T. Asaka, RIKEN/SACLA, Kouto, Sayo-cho, Sayo-gun, Hyogo, 679-5498

Abstract

The 1-GeV SPring-8 linac is an injector for the SPring-8 synchrotron radiation storage ring (SR) with an 8-GeV booster synchrotron (Sy) and the 1.5 GeV NewSUBARU (NS) synchrotron radiation storage ring. In recent years, we modified the linac and NS timing system to change the beam routes every 0.5 seconds. The NS timing system was changed for synchronization with that of Sy, and the gun trigger signals were improved to be time-shared for Sy and NS. These modifications were completed successfully in 2013 and realized a no-wait injection of SR and NS. A pressurized SF_6 waveguide system was replaced with a vacuum waveguide system that included newly developed S-band vacuum circulators and isolators in FY 2013. In FY 2013, the total operation time of the SPring-8 injector linac was 4328.3 hours. The total downtime was 0.13% and as stable as the last few years ; the fault frequency was 0.22 times per day.

INTRODUCTION

The SPring-8 accelerator complex is composed of a 1-GeV electron linac, an 8-GeV booster synchrotron, and an 8-GeV storage ring. The linac injects electron beams into the booster synchrotron and the 1.5-GeV storage NewSUBARU ring of the University of Hyogo.

In the early stage of SPring-8 operation, the linac injected beams one or two times a day into each ring. In 2004, the top-up operation of the SR and the NewSUBARU ring (at 1 GeV) started to stabilize the stored currents and realized constant SR lights. At present, SR is being injected every time without depending on the filling pattern, and the stored current stability is 0.03% at 99.5 mA. The NewSUBARU ring performs the injection every six or seven seconds with a current stability of 0.01% at 300 mA.

To address the problem of aging equipment and improve the RF phase stability at the electron injector section of the SPring-8 linac, we replaced a pressurized SF_6 waveguide system with a vacuum waveguide system that included newly developed S-band vacuum circulators and isolators in FY 2013. As a result of RF conditioning and beam tuning, satisfactory beam performance was confirmed. Regular beam operation with this system started in April 2014 [1].

The data acquisition system, which was synchronized with the beam timing, has been adapted for BPM data collection. For other data, we performed conventional acquisition in 1-second cycles. However, if the beam synchronization of the monitored values of other apparatuses is carried out, we can easily investigate the cause of beam variation. Therefore, we added the data of klystron voltages, RF powers, RF phases, the magnet currents, and electron gun voltages etc. to our synchronized data acquisition system.

IMPROVEMENT OF RAPID CYCLE INJECTION SYSTEM

In the previous top-up operation, the beam direction from the linac was switched every fifteen or twenty seconds by sending command messages to network devices from the central control room. Because the commands are software-based and executed successively one by one, it took about ten seconds to complete them. To switch the beam injection routes every 0.5 seconds, we improved the timing systems of linac and NS. The NS timing system was improved to synchronize with that of Sy, and the gun trigger signals were improved to be time-shared for Sy and NS. The radiation safety system was also improved for faster alternate injection. The beam route's layout is shown in Figure 1. These improvements were successfully completed in June 2013 and realized no-wait injection of SR and NS.

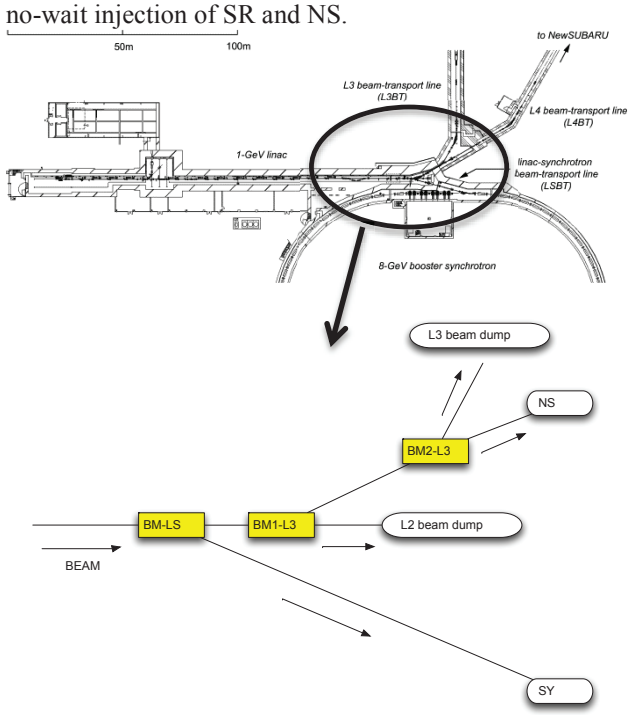


Figure 1 : Beam routes from SPring-8 linac.

shin@spring8.or.jp

Copyright © 2014 CC-BY-3.0 and by the respective authors

EMITTANCE MEASUREMENT FOR SPring-8 LINAC USING FOUR SIX-ELECTRODE BPMS

K. Yanagida*, S. Suzuki, H. Hanaki, JASRI/SPring-8, Sayo, Hyogo, Japan

Abstract

We installed four six-electrode beam position monitors at the end of the SPring-8 linear accelerator to measure the emittances and the Twiss parameters. Our method was to measure the second-order relative moments as we changed the magnetic field strengths of four quadrupole magnets, and to deduced the emittances and the Twiss parameters at the reference point. An entire calibration, which included effects up to the fifth-order moments with effective aperture radii, was essential and indispensable for precise measurements.

INTRODUCTION

For Twiss parameter matching of electron beams, emittances were measured at the end of the SPring-8 1-GeV linear accelerator (linac). Wire scanner monitors and profile monitors (PMs) had previously been utilized. However, such destructive monitors are not practical for daily operation because of frequent gain tuning in the case of signal saturation or reduction to the noise level.

In the previous works the emittances or the beam sizes were measured using non-destructive multi-electrode beam position monitors (BPMs) [1] [2]. Fortunately, a wide dynamic range signal processor has been developed in the SPring-8 linac [3], and we started a design study of a six-electrode (6E) BPM [4] for a second-order moment measurement and constructed such a system [5].

In this conference, we present the following four items, including emittance measurements, as the compilation of work related to second-order moment measurements:

- Signal difference composed of up to fifth-order moments.
- Effective aperture radius.
- Entire calibration.
- Emittance measurement by the Q-scan method.

SIGNAL DIFFERENCE FORMULAE

At LINAC2012, we proposed the entire calibration and effective aperture radius concepts [5]. The effective aperture radius was defined as a proportional coefficient between nth-order signal difference C_n (S_n) and absolute moment P_n (Q_n).

This expression was accurate when an electron beam was located within 1 mm of the BPM duct center. On the other hand, the beam positions must exceed 3 mm when the beam was swept for an entire calibration. To ensure measurement accuracy, the signal differences were modified to include more higher-order moments [6].

The signal differences were defined for the SPring-8 linac 6EBPM with circular cross-section [4] as

$$\begin{aligned}
C_1 &= \frac{V_1 - V_3 - V_4 + V_6}{V_1 + V_3 + V_4 + V_6},\\
S_1 &= \frac{V_1 + V_3 - V_4 - V_6}{V_1 + V_3 + V_4 + V_6},\\
C_2 &= \frac{V_1 + V_3 + V_4 + V_6 - 2(V_2 + V_5)}{V_1 + V_3 + V_4 + V_6 + 2(V_2 + V_5)},\\
S_2 &= \frac{V_1 - V_3 + V_4 - V_6}{V_1 + V_3 + V_4 + V_6},\\
S_3 &= \frac{V_1 - V_2 + V_3 - V_4 + V_5 - V_6}{V_1 + V_2 + V_3 + V_4 + V_5 + V_6},
\end{aligned} \tag{1}$$

where V_d ($d = 1, \cdots, 6$) is the output voltage from electrode d (Fig. 1).

C_m and S_m are expressed by nth-order absolute moments P_n and Q_n ($m \leqq n \leqq 5$) with corresponding effective aperture radius $R_{C,SmP,Qn}$ as follows:

$$\begin{aligned}
C_1 \approx& \frac{2P_1}{R_{C1P1}}\left(1 - \frac{2P_2}{R^2_{C1P2}} + \frac{4P_2^2}{R^4_{C1P2}} + \frac{2P_4}{R^4_{C1P4}}\right)\\
&+ \frac{2P_3}{R^3_{C1P3}} - \frac{2P_5}{R^5_{C1P5}},\\
S_1 \approx& \frac{2Q_1}{R_{S1Q1}}\left(1 - \frac{2P_2}{R^2_{S1P2}} + \frac{4P_2^2}{R^4_{S1P2}} + \frac{2P_4}{R^4_{S1P4}}\right)\\
&+ \frac{2Q_3}{R^3_{S1Q3}} + \frac{2Q_5}{R^5_{S1Q5}},\\
C_2 \approx& \frac{2P_2}{R^2_{C2P2}}\left(1 + \frac{2P_2}{R^2_{C2P2'}}\right) - \frac{2P_4}{R^4_{C2P4}},\\
S_2 \approx& \frac{2Q_2}{R^2_{S2Q2}}\left(1 - \frac{2P_2}{R^2_{S2P2}}\right) + \frac{2Q_4}{R^4_{S2Q4}},\\
S_3 \approx& \frac{2Q_3}{R^3_{S3Q3}}.
\end{aligned} \tag{2}$$

Each $R_{C,SmP,Qn}$ is given in Table 1.

Note that in Eq. 2, C_1 and S_1 include the second-order absolute moment, P_2. This means that C_1 and S_1 are slightly affected by the beam shape because a horizontally (vertically) long beam shape has a positive (negative) second-order relative moment, P_{g2} (Eq. 4).

P_n and Q_n can be expressed by the lengths and the arguments of a two-dimensional polar coordinates: b_G, β_G, a_{gk} and α_{gk} (Eq. 3). b_G and β_G are the components of first-order absolute moments P_1 and Q_1. a_{gk} and α_{gk} are the components of kth-order relative moments P_{gk} and

* ken@spring8.or.jp

ISBN 978-3-95450-142-7

Copyright © 2014 CC-BY-3.0 and by the respective authors

CURRENT STATUS OF THE MAINZ ENERGY-RECOVERING SUPERCONDUCTING ACCELERATOR PROJECT *

M. Dehn, I. Alexander, K. Aulenbacher, J. Diefenbach, R. Heine, C. Matejcek, F. Schlander, D. Simon
Institut für Kernphysik, Universität Mainz, Germany

Abstract

The Mainz Energy-Recovering Superconducting Accelerator (MESA) project at Johannes Gutenberg-Universtität Mainz has started in 2012 and is in full swing now. This paper presents the current status of the project with a glance on cryogenics, superconducting RF, accelerator lattice design and the normal conducting injector.

INTRODUCTION

MESA is designated for two modes of operation – an energy recovering mode (ER, 105 MeV, pseudo internal target and beam currents of up to finally 10 mA in stage 2) and an external mode (EB), with polarized electrons of up to 150 μA at 155 MeV for high precision experiments on parity violation and Weinberg angle (P2-experiment). The main parameters are listed in Table 1. Both experiments require a large range of flexibility of the accelerator and its components. From the machine point of view the P2-experiment requires extreme stability of most beam parameters which is being considered during all design phases. Meanwhile the multi-turn ER mode with the two passes is very interesting for accelerator physics. We will present the current situation, the ongoing construction works and latest conceptual developments with respect to the beginning of the commissioning of stage 1 in 2017.

Table 1: MESA operation modes

Parameter stage 1 (2)	EB	ER
Energy [MeV]	155	105
Beam current	150 μA	1 mA (10 mA)
Bunch charge [pC]	0.12	0.77 (7,7)
max. Beam power [kW]	22.5	105 (1050)

The new accelerator MESA will be built in former experimental halls of the Mainzer Mikrotron (MAMI), the present 1.6 GeV CW electron accelerator (Fig. 1). The double sided concept for MESA (see Fig. 2) with the two linac straights and vertical stacking of the return arcs was foremost presented in [1] and has been developed further since [2–4].

THE SITUATION AT THE FACILITY

Civil Works and Radiation Protection

To keep interferences with the ongoing physics programme at MAMI as low as possible the first major step

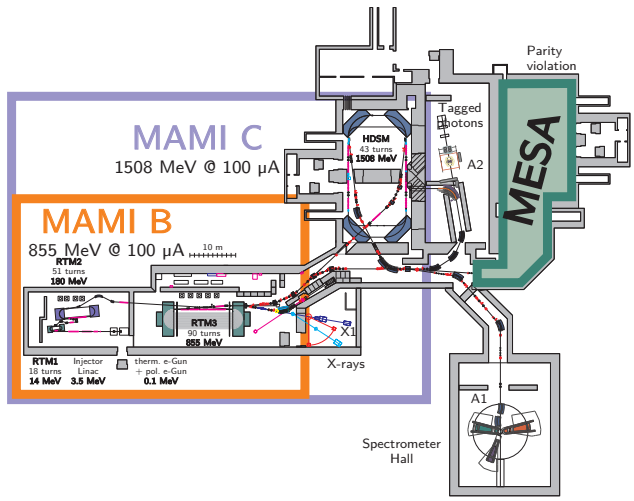


Figure 1: Floor plan of the MAMI accelerator. The space for MESA is marked in green.

was to erect a sufficient shielding between the construction site for MESA and the MAMI beam transfer lines. That should provide maximum safety even at full beam losses of 100 μA at 1.5 GeV in that area. The construction is now finished and simulations with FLUKA [5] show reasonable agreement to measured radiation doses. Hence the site will soon be deregulated and the constructions necessary for infrastructure of MESA (i.e. cooling water, the LHe supply etc.) can be started at the end of this year.

DIAGNOSTICS AND FEEDBACK SYSTEMS

The P2-experiment is of fundamental importance for the physics programme at the institute and also for the accelerator design. MESA will utilise several different beam diagnostic systems similar to the diagnostics at MAMI. At MAMI RF cavities operated at the fundamental bunch frequency (2.45 GHz) or the first or third harmonic are well established and yield CW position information or relative phases. Monitors of similar functionality can easily be manufactured in our own workshops for the frequency of MESA at 1.3 GHz.

Feedback and Feedforward Systems

Parity violating experiments like the P2-experiment measure a tiny asymmetry (here 10^{-8}) in the scattering under the reversal of the longitudinal spin polarisation of the beam (helicity reversal). In consequence, it must be monitored to what extent beam parameters change during the reversal, hence creating unwanted "helicity correlated effects"

* Work supported by the German Federal Ministry of Education and Research (BMBF) and German Research Foundation (DFG) under the Cluster of Excellence "PRISMA"

Copyright © 2014 CC-BY-3.0 and by the respective authors

THE PHYSICS PROGRAMME OF MICE STEP IV*

V. Blackmore, University of Oxford, UK
On behalf of the MICE Collaboration

Abstract

The international Muon Ionisation Cooling Experiment (MICE) is progressing toward a full demonstration of the feasibility of the cooling technology required for neutrino physics and muon colliders. Step IV will provide the first precise measurements of emittance and determine the influence of material properties on emittance reduction. The physics programme of the Step IV measurements is described in detail, along with a longer term view to demonstrating and studying (sustainable) ionisation cooling with re-acceleration.

INTRODUCTION

The front-end of a Neutrino Factory or Muon Collider will produce muons that occupy a large area of phase space. The phase-space area, or emittance, of these muons must be reduced (*i.e.* "cooled") so as to fit within the acceptance of downstream acceleration and storage systems. The expected beam produced at the front-end has a large transverse emittance, $\varepsilon_N \approx 15$–$20\,\pi$ mm.rad, and a large momentum spread of ≈ 20 MeV/c. For a Neutrino Factory, the emittance must be reduced to 2–5 π mm.rad [1], whereas more stringent requirements are placed on a Muon Collider. Conventional cooling techniques are ineffective, as the muon lifetime is short, and it is necessary to develop a new method of maximising the muon flux through an accelerator.

Ionisation cooling is the only practicable approach to reducing the emittance of a muon beam. Muons are passed through a low-Z "absorber" where they lose energy by ionising the medium. This reduces the transverse phase space area of the beam. The longitudinal momentum component must be restored in RF-cavities for sustainable ionisation cooling.

MICE STEP IV

A reduction in transverse normalised emittance is approximated by the ionisation cooling equation,

$$\frac{d\varepsilon_N}{ds} \simeq \frac{\varepsilon_N}{\beta^2 E_\mu}\left\langle\frac{dE}{ds}\right\rangle + \frac{\beta_\perp (13.6\,\text{MeV})^2}{2\beta^3 E_\mu m_\mu X_0}\,, \qquad (1)$$

where ε_N is the normalised transverse emittance, β the relativistic velocity, E_μ the energy, $\frac{dE}{ds}$ the energy lost by ionization, m_μ the mass of the muon, X_0 the radiation length of the absorber material and $\beta_\perp$ the transverse beta function at the absorber. The first term of this equation describes "cooling" by ionisation energy loss, and the second term describes "heating" by multiple Coulomb scattering. When these terms are equal, the equilibrium emittance of the cooling channel is,

$$\varepsilon_{\text{eq}} \simeq \frac{\beta_\perp (13.6\,\text{MeV})^2}{2\beta m_\mu X_0}\left\langle\frac{dE}{ds}\right\rangle^{-1}. \qquad (2)$$

The smaller the equilibrium emittance, the more efficient the cooling channel. For this purpose it is desirable to minimise $\beta_\perp$ at the absorber and maximise $X_0\langle\frac{dE}{ds}\rangle$.

The Muon Ionisation Cooling Experiment (MICE) [2] will demonstrate the performance of one "SFOFO" [3] lattice cell of the Neutrino Factory Feasibility Study 2 design [1]. The cell has a large momentum acceptance, accepting a spread of ≈ 20 MeV/c over a 140–240 MeV/c central momentum range.

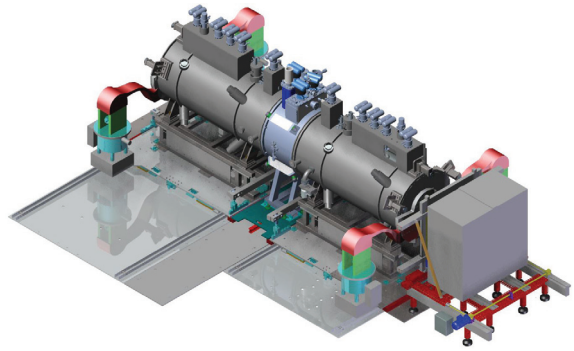


Figure 1: Layout of MICE Step IV.

Figure 1 shows the Step IV lattice section. This consists of two 4T Spectrometer Solenoids containing scintillating fibre tracker planes, either side of an Absorber Focus Coil (AFC) that can contain either liquid hydrogen (LH_2) or lithium hydride (LiH) absorbers. A variable amount of high-Z material is situated at the upstream side of the upstream Spectrometer Solenoid and provides the cooling cell with a range of input emittances. Step IV will study how material and beam properties affect emittance reduction. A further AFC module and RF system will be installed prior to MICE Step V to demonstrate sustainable ionisation cooling. Progress towards the construction of Step IV is detailed in [4].

The beam delivered by the MICE muon beam line [5] is of low intensity compared to conventional primary beams, and has been characterised during Step I [6]. MICE measures the phase space components, (x, y, p_x, p_y) of individual muons as they cross the scintillating fibre tracker planes in the up- and downstream Spectrometer Solenoids. A " beam" is constructed from these individually measured muons, and a covariance matrix calculated. In this way, MICE measures a change of emittance of $\simeq 5$ % (10% in Step V) to a relative precision of 1 %.

* Work supported by the Science and Technology Facilities Council (UK)

Copyright © 2014 CC-BY-3.0 and by the respective authors

ISBN 978-3-95450-142-7

PHYSICAL STARTING OF THE FIRST AND SECOND SECTION OF ACCELERATOR LINAK-800

V.V. Kobets, N.I. Balalykin, I.N. Meshkov, V.F. Minashkin,
V.G. Shabratov, G.D. Shirkov, A.G. Sorokin, Dubna, Russia

Abstract

The report discusses the modernization of the linear electron accelerator MEA (Medium Energy Accelerator). The aim is to develop a set of MEA based free-electron lasers, imposed a number of emission wavelengths from infrared to ultraviolet. In work presents the results of the physical starting of the first accelerating station and status of work on the second accelerating station linear electron accelerator LINAC-800, as well as start the infrared undulator. We discuss the program of work of the accelerator.

INTRODUCTION

JINR accelerator creates a stand based on electron linear accelerator LINAC-800. The linear accelerator LINAC-800 energy of 800 MeV and a pulse current up to 60 mA and a duration of 4 microseconds modernized to create a complex free-electron lasers, covering a continuous spectrum from infrared to ultraviolet. Currently launched the first accelerating section of the accelerator and the undulator infrared radiation. Preparing to launch a second accelerating station. Installed the klystron second accelerating station. Obtained by working vacuum in the waveguide path and accelerator sections.

LINEAR ELECTRON ACCELERATOR

Structural linear accelerator consists of the electronic injector and seven accelerator stations - part of LINAC-800. Linac accelerating system is 4 accelerating station (A00 - A3), including sources of RF power (klystrons with modulators), microwave - feeders and accelerating structures (panels + drift sections). Injection station A00 consists of a the gun and the buncher. Accelerating station A01 provides the short accelerating section A0BB (length 3.67 m) and the drift area DS0 / 1, combined with a portion of the analysis of the characteristics of beam (energy, current, size, position, emittance). Microwave power to the accelerating section A01 station is served by accelerating station A00. Accelerating station A02 enables two short accelerating sections A1AA and B2AA to 3.67 m with a longitudinal magnetic field and the portion of the drift DS2 / 3. Regular accelerating station A02 and A03 provide job length (7.35 m) accelerating sections (two sections of the station). The stations are separated by drift spaces (DS2 / 3 - DS4 / 5) with a length of 1.5 m. Section, composed of one station are separated by nearly identical portions of the drift (DS3 / 4 - DS5 / 6). At sites drift installed vacuum locks, vacuum pumping stations, quadrupoles, correctors beam position, current monitors, beam position and profile.

The structure of the electron injector includes an electron gun, a chopper, and prebuncher and buncher (Fig. 1).



Figure 1: The electron injector.

Its main element is a triode type the electron gun with a permanent high voltage at the cathode, "grounded" the anode and the gate electrode [1]. It is placed in a tank filled with sulfur hexafluoride (SF6) under pressure about 6 atmospheres. Electron-optical system of the gun control electrode formed by and a system of 15 the anodes with forced resistive (R = 200 MW) distribution of the potential (of the order of 30 kV on the gap). At first focusing the anode supplied with a DC voltage, adjustable between 12 - 30 kV. The source ICT (Insulating Core Transformer) provides a cathode voltage -400 kV with the stability of 10-4 - 10 -5 [2]. The source is placed in the tank with the insulating gas under a pressure of about 6 atm. The stability of high voltage with an additional unit "ICT 400 kV Stabilizer". Voltage is applied to the high-voltage oil-filled the gun in a coaxial cable with a diameter of 6 cm at a pressure of 2-3 bar oil. Cable core - bifilyar on which the tank to the console electronics with high voltage power is supplied to the cathode electronics unit 110 B, f = (U 50 Hz).

THE KLYSTRON MODULATOR

The modulator linear type consists of a pulse transformer and 40 the block pulse shapers. Each of these blocks is performed by a printed circuit and able to generate a pulse amplitude of 2 kV duration of 50 microseconds. The magnetic core of the pulse transformer is made up of several cores, each of which has a coil connected to two blocks of the pulse generator. In the secondary winding of the transformer pulses are summed. In this scheme, the

Copyright © 2014 CC-BY-3.0 and by the respective authors

ISBN 978-3-95450-142-7

COMPACT PROTON INJECTOR FOR SYNCHROTRONS

A.D. Kovalenko, A.V.Butenko, JINR, Dubna, Russia
A.A. Kolomiets, A.S. Plastun, ITEP, Moscow, Russia

Abstract

Compact proton linac comprising two sections of different RFQ structures was designed. The first section is conventional RFQ with output energy 3.5 MeV whereas the second one is RFQ with spatial periodic RF quadrupole focusing. The linac output energy is about 9 MeV. The both structures operate at frequency of 352 MHz. The total length of machine is less than 6 m. The output pulsed beam current is of 40 mA. The design is suitable for NICA injection complex and proton superconducting medical synchrotron.

INTRODUCTION

The design of proton linac was carried out in accordance with the NICA mega-project program at JINR [1]. There are two purposes to design of simple, reliable and compact proton machine: 1) proton injector for the Nuclotron (or it's booster) and 2) proton injector for medical synchrotron based on the Nuclotron-type technology [2,3]. The main parameters specified for the design are presented in Table 1.

Table 1: Linac parameters

Output beam energy, MeV	3.5…8.0
Pulse duration, microseconds	5…15
Average beam pulse current, mA	5.0…15.0
Pulse repetition rate, Hz	1…2

The particle energy range specified above can be reached with the use of well known scheme of a proton linac. The scheme comprise of a front end – RFQ structure operating at 325 – 433 МГц and the main accelerator part based on much more effective accelerating structures, nevertheless at the same frequency. The RFQ section provides bunch formation and acceleration of the particles up to an energy of 2.5…3.0 MeV. The accelerating structure of the most advanced proton linacs, such as SNS [4], J-PARC [5], Linac4 [6], followed after the RFQ, is the Alvarez-type one with permanent magnet quadrupoles. Compact linear accelerator has been proposed by the AccSys Company for the market also follows to the above mentioned scheme [7]. The list of beam parameters specified above is not full, because one should keep in mind also a number of other very important characteristics of any device aimed at application in medical treatment procedure, namely: high reliability, simple engineering design based on standard elements as much as possible, easy handling with low number of personal. Despite of a wide recognition, the scheme meets a lot of difficulties due to complexity of its manufacturing and high cost.

The goal of our paper is to demonstrate that a compact proton linac for the considering application area can be built using only RFQ structures.

LINAC SCHEME

The proposed injector scheme is shown in Figure 1. Injector consists of proton source (pS), matching channel (LEBT), conventional RFQ (RFQ1) and spatially – periodic RFQ (RFQ2). Design of all injector parts was aimed at providing compact and inexpensive linac with high transmission, which keeps initial beam brilliance and provides relatively small longitudinal output emittance.



Figure 1: General layout of the injector.

LEBT

Conventional LEBT function is beam transport from ion source to RFQ input and transverse matching with RFQ input. LEBT layout of compact injector is shown in Fig.2. It includes buncher and 4 quadrupole static lenses. RFQ input radial matcher is also shown in the picture because it is functionally part of matching channel.

Radial matcher is designed using optimizing computer code to reduce beam convergence at RFQ1 input and reduce beam envelope inside static lenses to minimize beam distortion in LEBT. Matcher has 12 $\beta\lambda/2$ cells. Twiss parameters at RFQ input are given in Table 2.

Table 2: Matched beam parameters at RFQ input

Beam current, mA	α	β, mm/mrad
10	0.10	0.032
20	0.11	0.038
30	0.12	0.042

Initial cell length at chosen frequency $\beta\lambda/2 = 4.4$ mm. Thus, it is a problem to design conventional drift tube buncher. A short RFQ structure consisted of 2 modulated cells with modulation coefficient $m = 1.2$ and of 6 cell input and output radial matchers is used as a buncher in our LEBT design. Transverse beam envelopes inside the LEBT are shown in Figure 2.

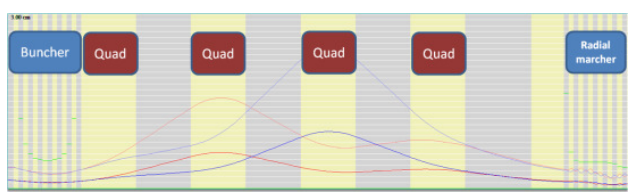


Figure 2: LEBT layout and simulated envelopes

Copyright © 2014 CC-BY-3.0 and by the respective authors

ISBN 978-3-95450-142-7

DESIGN OF THE 4 MeV RFQ FOR THE HELIUM BEAM IRRADIATOR*

Hyeok-Jung Kwon#, Yong-Sub Cho, Han-Sung Kim, Kyung-Tae Seol, Young-Gi Song,
KOMAC/KAERI, Gyeongju, Korea

Abstract

A radio frequency quadrupole (RFQ) is considered as a main accelerator of the helium beam irradiation system for the power semiconductor in Korea Multipurpose Accelerator Complex (KOMAC) The RFQ was designed to accelerate the He2+ beam up to 4 MeV with 10 mA peak beam current. We chose a vane type RFQ with 200 MHz operating frequency. The RFQ will be operated with the frequency tracking mode supplied by the digital low level RF control system. In this paper, the design of the 4 MeV RFQ is presented and the beam irradiation system including RF system, control system, utility system, is discussed.

INTRODUCTION

Power semiconductors are widely used in power converter and inverters and need to have higher voltage and current ratings with high frequency. It is necessary to reduce the switching loss in addition to the conduction loss in order to achieve the above requirement. There are several methods to enhance the switching characteristics such as gold diffusion, irradiation of gamma ray and irradiation of particle beam (for example electron or proton). Recently, irradiation with helium beam is under research for the complimentary method with the existing one.

A RFQ for helium beam is proposed by KOMAC for the purpose of the irradiation to semiconductor [1]. At first, the energy of the system was proposed as 3 MeV but we increased the energy up to 4 MeV in consideration that the penetration depth in the silicon is more than 15um and 1 MeV/u system has more application fields. The requirements of the irradiation system are summarized in Table 1.

Table 1: Requirements of the Helium Beam Irradiation System

Parameter	Value
Particle	Helium
Target	Silicon
Penetration depth	15um
Wafer size	8 inch
Dose	1×10^{14} / cm^2
Uniformity	± 3%
Production rate	500 wafers / day

The energy of the RFQ was determined from the possible penetration depth of the helium into the silicon. The calculation by using SLIM code showed that 4 MeV helium beam can penetrate 18um into the silicon. The average current was determined by the required dose and production rate. The irradiation time was less than 10 seconds when the average beam current was 0.1 mA. The specifications of the accelerator based on the above requirements are summarized in Table 2. The system consists of ion source, low energy beam transport (LEBT), RFQ, medium beam energy transport (MEBT), target system, RF system, vacuum system, beam diagnostics, control system and utilities including cooling water system and electricity. The block diagram of the system is shown in Fig. 1. The red dots include the main hardware system and the blue dots include the ancillary system.

Table 2: Specifications of the Accelerator

Parameter	Value
Particle	$^4He^{2+}$
Beam energy	4 MeV
Peak beam current	10 mA
Beam duty	0.1%

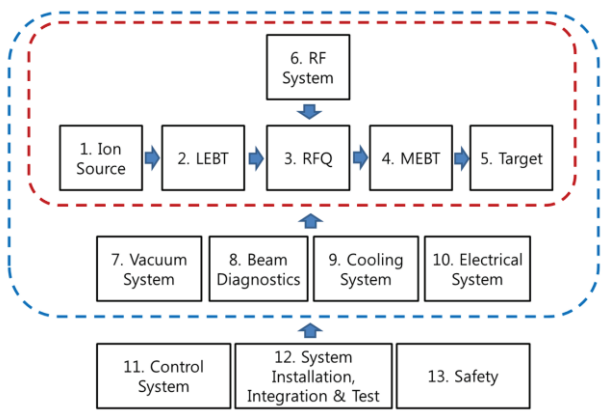


Figure 1: Block diagram of the helium irradiation system

SYSTEM DESIGN

Ion Source

The 2.45 GHz microwave ion source will be used as an ion source. The same type ion source has been used for KOMAC 100 MeV proton linear accelerator for 3 years. One of the characteristics of the microwave ion source of KOMAC 100 MeV proton accelerator is such that it uses single solenoid for system compactness. But the microwave ion source will be modified to have two solenoid magnets to produce mirror fields in order to facilitate the $^4He^{2+}$ production and enhance the confinement. Also the extraction geometry will be

*Work supported by the MEST in Korean Government
#hjkwon@kaeri.re.kr

Copyright © 2014 CC-BY-3.0 and by the respective authors

FAULT TOLERANCE AND CONSEQUENCES IN THE MYRRHA SUPERCONDUCTING LINAC*

F. Bouly#, LPSC, Université Grenoble-Alpes, CNRS/IN2P3, Grenoble, France
J.-L. Biarrotte, CNRS/IN2P3, IPN Orsay, France
D. Uriot, CEA-Saclay, Gif-sur-Yvette, France

Abstract

The MYRRHA project aims at the construction of an ADS demonstrator in Mol (Belgium) which requires a proton flux with a maximum power of 2.4 MW (600 MeV-4 mA). Such a continuous wave beam will be delivered by a superconducting linac which must fulfil very stringent reliability requirements. In this purpose, the accelerator design is based on a fault-tolerant scheme to enable rapid failures mitigations. We here review beam dynamics studies on the RF fault-tolerance capability of the MYRRHA linac and the resulting impact on the R&D.

INTRODUCTION

MYRRHA (Multi-purpose Hybrid Research reactor for High-tech Applications) is a new fast spectrum nuclear facility which is planned to be built at SCK-CEN in Mol (Belgium) [1]. This 100 MW_{th} nuclear reactor is especially designed to demonstrate the ADS (Accelerator Driven System) concept for the transmutation of high level radioactive wastes. To operate, the sub-critical reactor requires a continuous wave (CW) proton beam, with a maximum power of 2.4 MW (600 MeV - 4 mA).

Initiated during previous EURATOM programmes (PDS-XADS and EUROTRANS), the conceptual design of this ADS-type accelerator had been consolidated in the frame of the MAX project (EURATOM FP7) [2]. It is a superconducting linac fed by a 17 MeV injector (details in [4] and [5]). The 17-600 MeV MYRRHA main linac is composed of an array of independently-powered superconducting (SC) cavities. Three different cavity families are used to cover the energy range: a first section with 352.2 MHz Spoke 2-gap cavities (β_{opt}=0.37) and two following sections with 704.4 MHz 5-cells elliptical cavities (β_{opt}=0.51 & 0.70). In the MEBT (Medium Energy Beam Transfer line), between the injector and the main linac, three 352.2 MHz spoke cavities can be used as bunchers. All these choices result of longitudinal beam dynamics optimisations and are more detailed in [6].

This linac was designed to provide large transverse and longitudinal acceptances. The versatility of such design was performed to reach the exceptionally high level of reliability required to operate an ADS. Indeed, frequently-repeated beam interruptions can induce high thermal stresses and fatigue on the reactor structures. In addition, beam interruptions might trigger safety reactor shutdowns that could also significantly affect the ADS availability [7]. Therefore, the number of beam interruption will have to remain extremely low: the current maximum limit is set to 10 beam interruptions, longer than 3 seconds, per 3-month operating cycle. It leads to a global accelerator MTBF (Mean Time Between Failures) of ~ 250 hours [8]. To achieve such a reliability level, the linac design is based on a redundant and a fault-tolerant scheme to enable the rapid mitigation of RF failures.

FAULT-TOLERANCE SCHEME

The followed reliability guidelines for the MYRRHA linac design is: to provide a robust beam optics with operation margins, to elaborate an efficient maintenance scheme with on-line reparation if possible, and to dispose of a maximum redundant elements for failure compensation. For the 17 MeV injector the adopted philosophy is parallel redundancy: by providing a second hot stand-by spare injector able to quickly resume beam operation in case of failure in the main one [9].

In the main 17-600 MeV linac the fault compensation scheme is based on serial redundancy. The present adopted strategy is to use a local compensation method to compensate RF failures (cavities and their associated control and power systems): the faulty cavity (respectively cryomodule) is compensated by acting on the RF gradient and the phase of the 4 nearest neighbouring cavities (respectively cryomodules) operating de-rated (i.e. not already used for compensation).

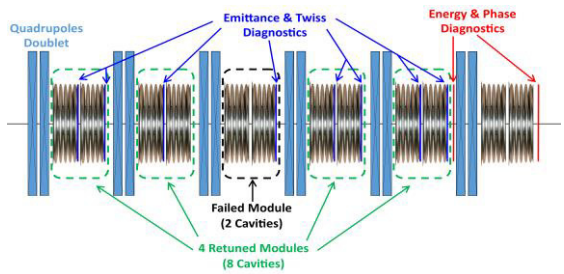


Figure 1: Principle of the local fault compensation method. Example of the retuning strategy used in TraceWin for the failure compensation of one cryomodule in the medium energy section (β_{opt}=0.51).

This retuning scheme can only be achieved by providing significant RF power and gradient overhead throughout the 3 superconducting sections. In the present design, this operation margin in terms of acceleration capability has been chosen to 30% (details in [6, 8]). As a consequence, the operating accelerating gradients (E_{acc}) of the MYRRHA cavities have been chosen on the conservative side to enable these compensation procedures. The average operating point of the SNS β=0.61 cavities in 2008 [10]

* Work supported by the EAEC/EURATOM FP7 under grant agreement n°269565 (MAX project).
#frederic.bouly@lpsc.in2p3.fr

Copyright © 2014 CC-BY-3.0 and by the respective authors

3D MODE ANALYSIS OF FULL TANKS IN DRIFT-TUBE LINACS

Sergey S. Kurennoy, LANL, Los Alamos, NM 87545, USA

Abstract

Drift-tube linacs (DTLs) are usually designed and analyzed in axisymmetric approximation, cell by cell, using 2D codes such as Superfish and Parmila. We have developed 3D models of full DTL tanks with CST Studio to accurately calculate the tank modes, their sensitivity to post-coupler positions and tilts, tuner effects, and RF-coupler influence. Such models are important for the LANSCE DTL where each of four tanks contains tens of drift tubes and tank 2 has as much as 66 cells. We perform electromagnetic analysis of the DTL tank models using MicroWave Studio (MWS), mainly with eigensolvers but also in time domain. A similar approach has already been applied for thermal analysis of the LANSCE DTL but only with short tank models [1]. The full-tank analysis allows tuning the field profile of the operating mode and adjusting the frequencies of the neighboring modes within a realistic CST model. The MWS-calculated RF fields can be used for beam dynamics and thermal modeling. Here we present beam dynamics results for the LANSCE DTL from Particle Studio.

INTRODUCTION

The drift-tube linac (DTL) structure, proposed by Alvarez in 1946, became the most popular type of proton linacs for many decades. The DTL structure employs long cylindrical resonators (tanks) operating in TM_{010} mode and containing a sequence of drift tubes (DTs) installed along the beam axis. The DTL accelerators achieve their best efficiency for particle velocities approximately from 10% to 35% of the speed of light, i.e. $\beta = v/c$ = 0.1-0.35. At the Los Alamos Neutron Science Center (LANSCE), the 201.25-MHz DTL covers a wider velocity range, from β = 0.04 to 0.43 (proton energies 750 keV to 100 MeV), with the efficiency decreasing at both ends. The LANSCE DTL consists of four DTL tanks; some parameters are listed in Table 1, where N_{DT} is the number of full DTs and N_{pc} is the number of post-couplers in the tank.

Table 1: LANSCE DTL Design Parameters [2]

Parameter	Tank1	Tank2	Tank3	Tank4
Energy in, MeV	0.75	5.39	41.33	72.72
β, in-out	0.04	0.107	0.287	.37-.43
Length L, m	3.26	19.688	18.75	17.92
N_{DT}	30	65	37	29
N_{pc}	0	65	37	29
Aperture r_b, cm	0.75	1-1.5	1.5	1.5
Grad. E_0, MV/m	1.6-2.3	2.4	2.4	2.5
Aver. ZT^2, MΩ/m	26.8	30.1	23.7	19.2

DTL TANK MODELS

We have built 3D models of the four DTL tanks in the CST Studio [3] using CST geometrical macros and tank element dimensions from the LANSCE database. The CST model of tank 2 (T2) is illustrated in Fig. 1. This is the longest DTL tank that contains 65 full DTs and two half-DTs on the end walls. The full DTs are supported by vertical stems. The tank cavity of radius 45 cm is shown in Fig. 1 as the blue-gray cylinder, which is assumed to be surrounded by perfect conducting walls for field calculations. Two upper insets show side views near the tank entrance (blue) and its exit (green). The stabilizing post-couplers (gray) with rotating tabs alternate positions in the horizontal plane; they can be seen better in the end view of the tank in the right-bottom inset.

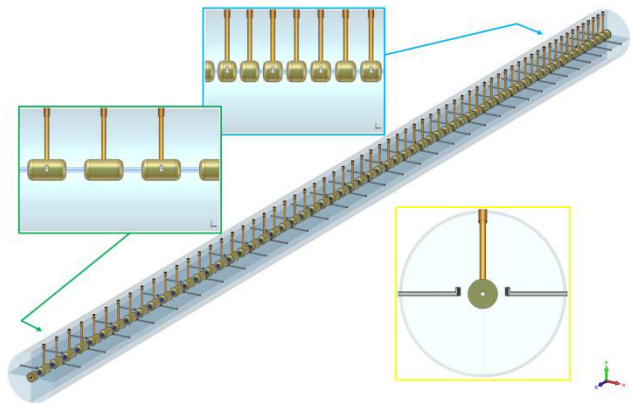


Figure 1: CST model of the DTL tank 2.

The CST model of tank 4 (T4) with 8 frequency slug tuners (cyan) is shown in Fig. 2. The left inset enlarges details: the bellows near the stem connection to the cavity wall are modeled as metal cylinders; the blue line through DT apertures indicates the beam axis.

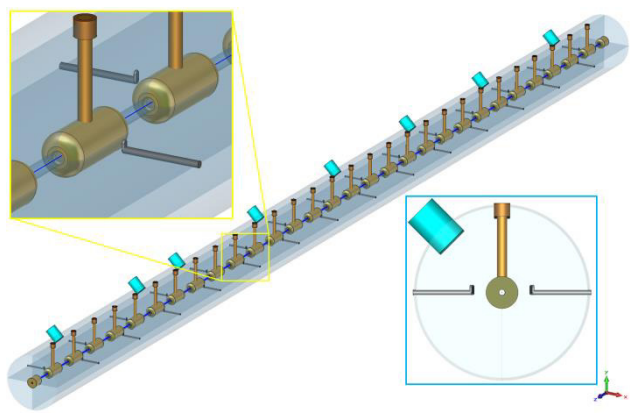


Figure 2: CST model of tank 4 with frequency tuners.

Unlike long tanks 2 to 4, the relatively short tank 1 (T1) does not have post-couplers. One the other hand, the

Copyright © 2014 CC-BY-3.0 and by the respective authors

ISBN 978-3-95450-142-7

RESULTS FROM THE INSTALLATION OF A NEW 201 MHz RF SYSTEM AT LANSCE *

J. T. M. Lyles#, C. Arnold, W. Barkley, J. Davis, A. Naranjo, M. Prokop, D. Rees, G. Sandoval,
AOT Division, Los Alamos National Laboratory, Los Alamos, NM
D. Baca, R. Bratton, R. Summers, Compa Industries, Los Alamos, NM

Abstract

The LANSCE RM project is restoring the linac to it's original high power capability after the power grid tube manufacturer could no longer provide triodes that could consistently meet our power requirements. High duty factor Diacrodes® now supply RF power to the largest DTL tank. These tetrodes reuse the existing infrastructure including water-cooling systems, coaxial transmission lines, high voltage power supplies and capacitor banks. The power amplifier system uses a combined pair of LANL-designed cavity amplifiers using the TH628L Diacrode® to produce as much as 3.5 MW peak and 420 kW of mean power. A digital low-level RF control system was developed to complement these new linear amplifiers. Design and testing was completed in 2012, with commercialization following in 2013. The first installation is commissioned. The two remaining high power RF systems for tanks 3 and 4 will be replaced in subsequent years using a hybrid old/new RF system until the changeover is complete. Features and operating results of the replacement system are summarized, along with observations from the rapid-paced installation project.

RF SYSTEM GOALS

The LANSCE drift tube linac (DTL) uses four Alvarez cavities powered at 201.25 MHz, to accelerate both protons (H^+) and negative hydrogen ions (H^-) from 0.75 to 100 MeV before injection into a coupled-cavity linac (CCL). Pulsed RF power must be capable of 12% duty factor (DF). DTL cavity 2 has the highest energy gain of ~36 MeV, requiring a peak RF power of 3.3 MW. Significant average power is required for the largest three room temperature cavities with 120 pulses/sec of ~1 mS length. This is in contrast to the high-peak/low-average power machines at 200 MHz proton injector linacs at Fermilab, CERN, RAL and BNL. Over the past 25 years, manufacture of reliable RF amplifier triodes operating at this high average power has been unpredictable. Both premature loss of cathode emission and ceramic cracking have repeatedly occurred in the tubes.

In 2006, the operating point of the power amplifiers had to be reduced in order to hold operating costs on budget (for all-too-frequent tube replacements) and prevent excess downtime. This led to the decision to operate LANSCE at half of its original duty factor to maintain acceptable beam availability. A primary goal of the LANSCE Risk Mitigation project has been to replace the original 201.25 MHz amplifiers with modern power amplifier (PA) circuits having higher average power capability. Another goal has been to modernize the low level RF controls, to improve operational efficiency and replace obsolete components. In addition, end-of-life klystrons for the CCL are being replaced with forty-five new CPI VA862A1 1.3 MW klystrons [1].

Gridded Tube Cavity Amplifier

A previous report [2] explained the reasoning behind the choice of the TH628L Diacrode® as the active device for this application. Combining the outputs of two PAs (fig. 1) provides suitable headroom in peak and average power, allowing the tubes to operate at ~55% of their rating. Increased amplifier reliability and tube lifetime will result from this pairing.

The caveat for gridded tubes is that a matching cavity amplifier circuit must be developed around a chosen device. This may require that the tube manufacturer or an independent producer commercialize this complex unit into an amplifier system. An acceptable solution may also have the amplifier designed by the laboratories, as was done here, although development costs must be weighed against industrialization of this technical effort. The PA was developed by our team, with assistance from the Thales Product Engineering Dept.

The common-grid configuration uses a full wavelength double-ended coaxial line output circuit, in order to double the power available over a traditional single-ended tetrode. Progress on the mechanical and electrical design of the PA, supporting electronics and intermediate power amplifier (IPA) are discussed elsewhere [3][4][5]. Months of testing in 2012-13 ran up to 2.5 MW peak power at 12% duty factor. The amplifier was tested at the 3 MW operating point to demonstrate design capability and to test the cathode emission capabilities of the tube. It will operate at < 1.85 MW at LANSCE. Testing has continued for over 8500 hours using six different Diacrodes®, while also testing the remaining components for the installation.

A tender for manufacturing the LANL-designed PA was issued in 2012 and the work was subsequently awarded to Continental Electronics Corporation [6]. Three PAs were delivered in 2013 and tested at LANL. Additional units are being manufactured for delivery in 2014 along with a commensurate quantity of Diacrodes® from Thales Electron Tubes. Three IPAs have been produced by Betatron Electronics, Inc., and tested at LANL. This unit uses a Thales TH781 tetrode and a matching TH18781 cavity amplifier from Thales. One IPA drives two final

* Work supported by the United States Department of Energy, National Nuclear Security Agency, under contract DE-AC52-06NA25396
# jtml@lanl.gov

ISBN 978-3-95450-142-7

Copyright © 2014 CC-BY-3.0 and by the respective authors

VERTICAL ELECTRO-POLISHING OF NB NINE-CELL CAVITY USING CATHODE WITH VARIABLE-GEOMETRY WINGS

K.Nii#, V.Chouhan, Y. Ida, T. Yamaguchi, MGI, Himeji, Japan
K. Ishimi, MGI, Kashiwa, Japan
H. Hayano, S. Kato, H. Monjushiro, T. Saeki, M. Sawabe, KEK, Tsukuba, Japan

Abstract

Marui Galvanizing Co. Ltd. has been studying on Vertical Electro-Polishing (VEP) of Nb nine-cell superconducting accelerator cavity for the mass-production and cost-reduction of Electro-Polishing (EP) process in collaboration with KEK. And we invented our original cathode named "i-cathode Ninja"® which has four Al wing-shape parts per one cell for nine-cell cavity VEP. We thought that these parts can realize uniform distributions of both electric current and EP solution flow at inner surface of cavity. In this article, we will report the first fabrication of VEP facility for nine-cell cavity and VEP results using this cathode.

INTRODUCTION

Electro-polishing (EP) is the most effective method to realize high acceleration gradient of Superconducting Radio-Frequency (SRF) cavity. So far, horizontal electro-polishing (HEP) have been adopted mainly for cavity EP [1-2]. In addition to this, vertical electro-polishing (VEP) is studied actively [3-4]. Marui Galvanizing Co. Ltd., decided to focus on the VEP because of the benefit for mass production (for example space-saving, no cavity rotation). For VEP, we invented our original cathode with variable-geometry wings named "i-cathode Ninja"® [5]. Using this cathode, we have studied single-cell cavity and coupon cavity VEP in collaboration with KEK [5-7]. However, 9-cell cavity is required for linier accelerator production (for example international linier collider (ILC)). Therefore we started to study 9-cell cavity VEP. To realize high performance VEP, more sensitive control of temperature and bubbles are required. In addition, larger and safer facility also is needed. In this article, we report the first fabrication of 9-cell cavity VEP facilities and the results of 1st 9-cell cavity VEP using "i-cathode Ninja"®.

I-CATHODE "NINJA" ®

The schematic view of the "i-cathode Ninja"® which we invented is shown in Fig.1.

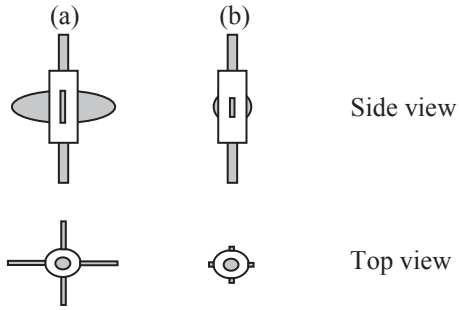


Figure 1: Schematic view of "i-cathode Ninja"®. (a) unfolded status. (b) retracted/folded status.

The most important feature is that it has four wing-like shaped aluminum parts at the center of all cavity cells. Compared with rod type cathode,

(1) The wings work as a baffle plate in the cell of cavity for the flow of electrolyte, and the uniform distribution of electrolyte can be achieved.
(2) The wings make the distance between the cathode and the equator shorter in the cell and realize the uniform distance distribution between cathode and anode.

There are two benefits to use "i-cathode Ninja"® . Then this cathode has a retractable structure of flexible wings and can be folded and unfolded by simple action.

9-CELL VEP FACILITY

Fig.2 shows the pictures of 9-cell cavity VEP facility. And Fig.3 shows the schematic view of 9-cell cavity VEP facility.



Figure 2: (Left) Picture of 9-cell cavity VEP facility. (Right) Picture of 9-cell cavity.

#keisuke_nii@e-maui.jp

ISBN 978-3-95450-142-7

Copyright © 2014 CC-BY-3.0 and by the respective authors

ION BEAM ACCELERATION IN NEUTRON TUBE

V.I.Rashchikov, NRNU(MEPHI), Moscow, Russia
A.S.Plastun, ITEP, Moscow, Russia

Abstract

Deuteron beam acceleration in ion-optic system of gas-filled neutron tubes was investigated. PIC code SUMA [1-2] used for computer simulation of ionization and knock on processes and there influence on deuteron beam parameters. When deuteron and ionized particles space charge self-field forces become the same order of magnitude as external one, virtual cathode may occurs. It is happens because of injected from ion source deuterons cannot overcome their own space charge potential wall and move in transverse direction. However, electrons, produced by ionization, are trapped within the deuteron beam space charge potential wall and decrease it significantly. Thus, space charge neutralization of deuteron beams by electrons, may considerably increase target current and, as a result, output neutron flow. Moreover, own longitudinal electric field rise near the target leads to reduction of accelerating electrode – target potential wall, which was made to prevent knock on emission from the target. As a result, additional knocked on electrons may appear in the region and should be taken into account. The data obtained were compared with experimental results.

COMPUTER SIMULATION

To design neutron tube with assigned flow value and other parameters such as size, service life and so forth, preliminary computer simulation should be fulfilled. PIC code SUMA was used for ion optic system modeling and investigation of ionization processes influence on deuteron beam dynamics and output data of gas-filled neutron tubes. As a sample typical gas-filled pulse neutron tube has been studied (see Fig. 1).

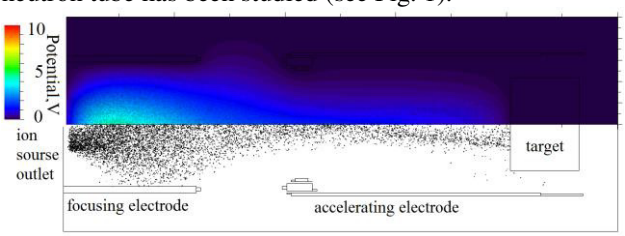


Figure 1: Deuterons distribution (lower) and their self-field potential (upper) in neutron tube.

Accelerated electrode is under -85kV potential, target -83kV, focusing electrode is grounded.

Preliminary ion source deuteron beam parameters has been obtained experimentally. For this purpose alone Langmuir probes, multi-electrode energy analyzer and Faraday cup were used. We obtain following deuteron beam parameter: longitudinal energy 1.7±0.4 keV, current ~150μA for initial gas pressure $0.5 \cdot 10^{-3}$ Torr. Moreover, some beam density distribution measurement were fulfilled. Nevertheless, it was not enough data for computer simulation. Therefore, the attempt to solve inverse problem was made. As the result to be obtained the experimental deuteron current density distribution on target shown on Fig. 2*a* was used.

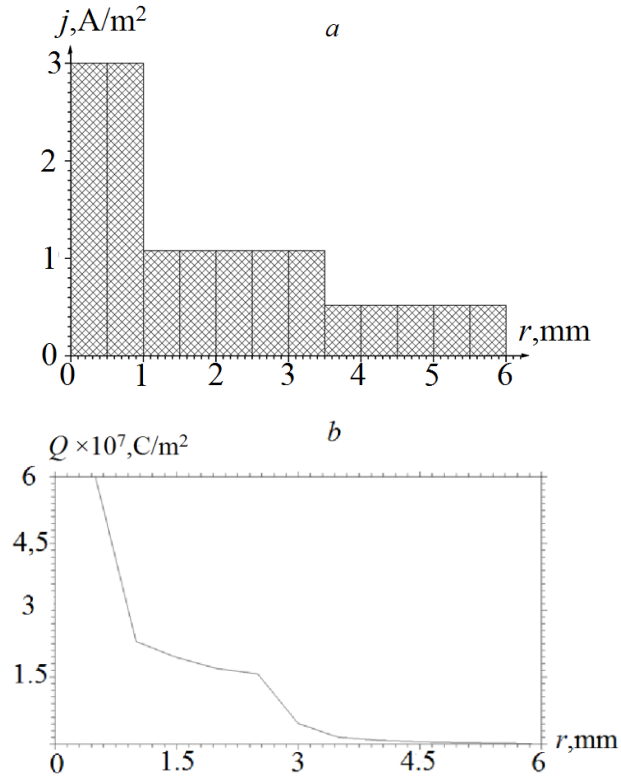


Figure 2: Current density (experimental, *a*) and charge distributions (simulation, *b*) on the target.

Experimental data were rebuild from target depth erosion and target sputtering calculation.

Computer simulation shows that for the following input beam data, experimental and calculated distributions are closed to each other: longitudinal energy 1.9±0.1 keV and transverse energy distribution ~120 eV, current ~150μA (see Fig.2*b*).

Passing through the gas, deuteron beam produce plasma, which consist of electron and slow ion. Their densities under considered gas pressure range approximately equal each other (see Fig. 3.) [3].

Copyright © 2014 CC-BY-3.0 and by the respective authors

ISBN 978-3-95450-142-7

MULTIPACTING PREDICTION FOR THE 106.1 MHz QUARTER WAVE RESONATOR

M.A. Gusarova, I.I. Petrushina, E.A. Savin, A.N. Stolbikova, V.L. Zvyagintsev
National Research Nuclear University «MEPhI»
Kashirskoye sh. 31, 115409, Moscow, Russia

Abstract

The results of the numerical simulations of multipacting in the 106.1 Mhz Quarter Wave Resonator (QWR) are presented. The influence of the cavity geometry and inner surface properties on the discharge possibilities is studied. In this paper we compare CST PS and MultP-M 3D simulation results for multipacting in the cavity.

INTRODUCTION

In this paper different geometries of the Quarter Wave Resonators from the ISAC-II project are overviewed. These geometries are presented on the Fig.1. [1]

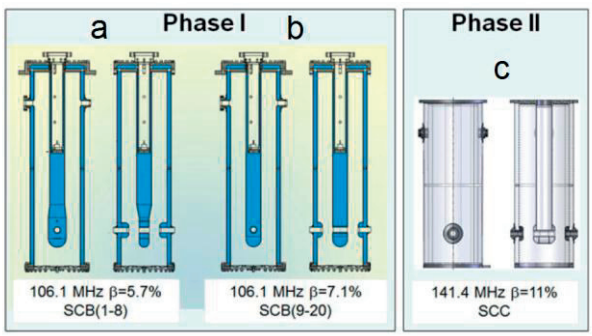


Figure 1: ISAC-II superconductive Quarter Wave Resonators.

The detailed results of the calculations comparing with the experiment data of the multipacting threshold for the 141.4 MHz cavity were presented in paper [2]. Simulations were carried out using 3D code MultP-M [3]. The good corresponding between this simulations and experimental data vas obtained.

But at the time of calculations in view of MultP-M features and limitations and also without opportunity to carry out calculations in the different code, only 141.4 MHz geometry and partially 106.1 MHz at β=7.1% geometry were calculated. QWR 106.1 MHz at β=5.7% construction was impossible to simulate in view of inner conductor constructing complexity. The MultP-M code upgrade that was held in 2013 allowed us to construct and calculate QWR 106.1 MHz at β=5.7% geometry. The information about code upgrade was presented on the IPAC'14 conference [3].

MULTP-M SIMULATIONS

On the Fig.2 the electric field distribution on the cavity (Fig. 1.a) axis is presented.

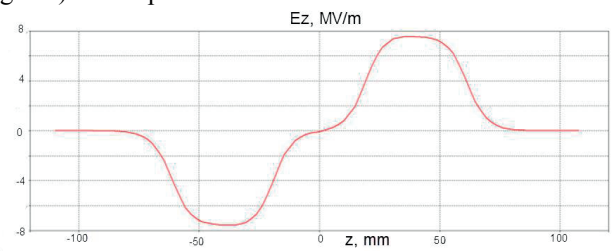


Figure 2: Electric field distribution throw the z axis for the Fig 1.a geometry; Ezmax=7,85 MV/m.

Using (1) and (2) relationship we can obtain that 1 of the normalize field value corresponds to the 0,4091 MV/m of the accelerating field.

$$U = \left|\sum_{j=0}^{n-1}\left[(Ez_j) * e^{\frac{i*k*j*dz}{\beta}} dz\right]\right| \quad (1)$$

$$E = \frac{U}{L} \quad (2)$$

Calculations results in the wide range of the accelerating field value for the three types of geometries are presented on the Fig.3 where one unit of the normalized field corresponds to the 0.4091 MV/m of the accelerating field. For the geometry on the Fig.3.c the result of the research [2] was used. Calculations were carried out for the 100 initial particles and the calculation time was corresponded to the 10 RF periods. Dependences of the increase in the number of particles in structure with the different accelerating field levels are presented on the graphs below.

Obtained graphs shows that despite the fact, that the range of the dangerous levels for the structure (c) is wider than for the (a) and (b) geometries, this geometry show the smallest particles number increasing during 10 RF periods.

Let's consider the initial range of the field levels. On the Fig.4 the dependences of the particle number increasing in the structure in the different accelerating field levels: in the 0 – 0.03 range. The calculation was considered for the 1000 particles, calculation time corresponded to 10 RF periods.

Copyright © 2014 CC-BY-3.0 and by the respective authors

ISBN 978-3-95450-142-7

BEAM DYNAMICS OF MULTI CHARGE STATE IONS IN RFQ LINAC

Y. Fuwa#, Kyoto University, Kyoto, Japan and RIKEN, Saitama, Japan
S. Ikeda, Tokyo Institute of Technology, Kanagawa, Japan and RIKEN, Saitama, Japan
M. Kumaki, Waseda University, Tokyo, Japan and RIKEN, Saitama, Japan
T. Kanesue, Brookhaven National Laboratory, Upton, NY 11973, USA
M. Okamura, Brookhaven National Laboratory, NY 11973, USA
Y. Iwashita, Kyoto University, Kyoto, Japan

Abstract

Laser ion source with DPIS (Direct Plasma Injection Scheme) is a promising candidate for a pre-injector of a high-brightness accelerator. In DPIS, high current ion beam is extracted from laser plasma at the entrance of an RFQ linac. Therefore, without LEBT (Low Energy Beam Transport) where the space charge effect is severe, ions are injected directly into the RFQ linac and high brightness ion beam can be accelerated. However, the injected beam consists of ions with various charge states. The unneeded ions cause space charge force and consume energy of RF field, emittance growth and excess beam loading occurs. In this research, we study the beam dynamics of ions with various charge states in an RFQ. Using the result of computer simulations, a set of 100 MHz 4-rod RFQ vanes, which accelerates Al 12+ ion among various charge states of aluminium ions from 8.9 keV/u to 180 keV/u, is newly designed and fabricated for beam acceleration test with beams from laser ion source.

LASER ION SOURCE WITH DPIS

Laser ion source is one of the promising candidates for a front end of future high power heavy ion accelerators [1]. The acceleration of relatively light ion nucleus (such as carbon, aluminum, iron) from laser ion source with DPIS is successfully demonstrated [2,3,4].

Although laser ion source with DPIS can provide high brightness ion beams, ions in laser plasma are provided in thermal process and their charge state distribution is broad. For example, to produce Al^{12+} ions in laser ion source, almost same number of Al^{11+} and Al^{13+}, and relatively small number of other ions with lower charge states are provided. Therefore, extracted beam into RFQ have various charge states ions, and ions other than those who have designed charge state would be accelerated. These unneeded ions consume RF power and strengthen space charge effect. These phenomena would be critical issue in operation of RFQ with space charge dominant region. Furthermore, if these unneeded ions are accelerated by RFQ and subsequent front-end accelerators, they must be aborted by some analyzer magnets in beam transport line after MEBT. However, in high power beam operation, such abort section provides excess radiation. Therefore, an RFQ that accelerates only designed charge state ions has advantages for future high power accelerator front-ends.

CHARGE STATE SELECTIVE ION BEAM ACCELERATION

The ions injected into RFQ have different kinetic energies depending on their own charge states, because they are extracted from same electric field. Therefore, ions whose charge state is enough lower than designed charge-to-mass ratio would not captured and just drift to the exit of RFQ tank, because the electric force is too small for an ion to be captured in an RF bucket, which might be absent entirely. However, ions whose charge states are higher or comparable with the designed charge to mass ratio would be captured by RF bucket and accelerated in RFQ.

To design an RFQ linac that accelerate only ions with a designed charge state, beam behavior of ions with various charge states are simulated with various cell parameters. We choose Al^{12+} ion as the design particle. To demonstrate beam acceleration with a 100 MHz 4-rod RFQ tank in Brookhaven National Laboratory, simulation conditions are set as shown in Table 1. In our simulation, Al^{11+}, Al^{12+}, and Al^{13+} are tracked. In order to study various vane parameters, we simplify the beam simulation condition; beams are tracked only in the longitudinal direction, space charge effect is ignored, and electric field in all cells is described by two-term potential function.

As first simulation, we apply the conventional RFQ design with adiabatic bunching section [5]. However, RFQs with such designs would accelerate Al^{13+} and capture rate of Al^{13+} is almost same number as that of Al^{12+}. It is because RFQ linacs with the adiabatic bunching section has large longitudinal acceptance.

Second, we don't apply the adiabatic bunching section, and introduce pre-buncher section and drift section in RFQ linac. In this case, pre-bunch section consisting of a few number of cells with modulation are located at the beginning part of RFQ to rotate longitudinal phase. In subsequent cells, modulations of vane suddenly vanish, and beams are bunched due to their velocity differences. Selecting the length of this drift section, ions with different charge states can be bunched in different phases, because their initial energies depend on their charge states and their phase slip factors are different. At the region where this phase difference to be 180 degree, the modulation of vane is gradually increased and Al^{12+} would be captured. However, our simulation shows that, with this pre-buncher scheme, capture rate of Al^{12+} is less

#fuwa@kyticr.kuicr.kyoto-u.ac.jp

Copyright © 2014 CC-BY-3.0 and by the respective authors

ISBN 978-3-95450-142-7

SNS LINAC UPGRADE PLANS FOR THE SECOND TARGET STATION *

J. Galambos#, D. Anderson, M. Howell, S. Kim, M. Middendorf, M. Plum, A Shishlo
ORNL, Oak Ridge TN, 37831 USA

Abstract

The Second Target Station (STS) upgrade proposal for the Spallation Neutron Source (SNS) [1] adds a short pulse, long wavelength neutron scattering station. In order to provide world-class neutron intensity at the additional station, the SNS linac beam power capability is doubled, to 2.8 MW. This will be accommodated by a 38% increase in the operational beam energy to 1.3 GeV and a 42% increase in beam current. The beam energy increase will be provided with the addition of 7 additional cyromodules and supporting RF equipment in space provided during the original SNS construction. Improving the ion source and reducing the chopping fraction will provide the beam current increase. Increases in the RF and high voltage modulator systems are needed to accommodate the additional beam loading. Initial plans are presented.

INTRODUCTION

In order to double the intensity per pulse delivered by the SNS accelerator, we plan to increase the linac beam energy from the present 940 MeV to 1.3 GeV and to increase the average macro-pulse beam current from 27 mA to 38 mA. The repetition rate will remain at 60 Hz, and the macro-pulse length will remain at 1 ms. All linac pulses will still be time-compressed in the SNS storage ring to support short-pulse neutron source generation, however one-sixth (10Hz) of the extracted pulses from the ring will be redirected towards the new target station.

In the following sections we describe the linac improvements required to support this power upgrade, and the general plans to implement these improvements. High-level STS linac parameters are listed in Table 1, along with operational parameters from the recent 1.4 MW operation in June 2014.

BEAM ENERGY INCREASE

Provisions to accommodate a beam energy upgrade were provided in the original SNS construction. There are 9 empty plots at the end of the superconducting RF linac section in the tunnel, and space for the accompanying high power RF in the high-energy end of the RF equipment "klystron gallery" that parallels the linac.

Table 1: Machine parameters to support the STS power upgrade

	1.4 MW Operation	STS / 2.8 MW
Final energy (MeV)	940	1300
Average macro-pulse current (mA)	27	38
Peak macro-pulse current – RFQ exit (mA)	34.6	48
Un-chopped fraction	0.78	0.80
Repetition rate (Hz)	60	60
Macro-pulse length (ms)	0.97	1.0
High beta cryomodules	12	19

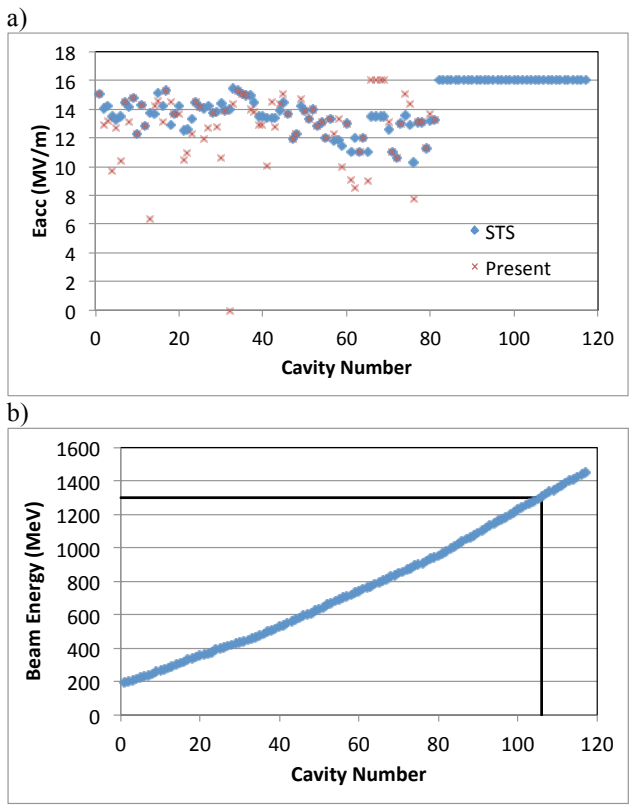


Figure 1: a) Cavity gradients for the SNS superconducting linac (SCL), b) the energy vs. cavity along the SCL.

* ORNL is managed by UT-Battelle, LLC, under contract DE-AC05-00OR22725 for the U.S. Department of Energy.
# jdg@ornl.gov

Copyright © 2014 CC-BY-3.0 and by the respective authors

PLASMA PROCESSING OF Nb SURFACES FOR SRF CAVITIES*

P. V. Tyagi#, R. Afanador, M. Doleans, S-H. Kim, C. McMahan
SNS, ORNL, Oak Ridge, TN, USA

Abstract

Field emission is one of the most critical issues to achieve high performances of niobium (Nb) superconducting radio frequency (SRF) cavities. Field emission is mainly related to contaminants present at top surface of SRF cavities that act as electron emitters at high gradient operation and limit the cavity accelerating gradient. An R&D program at the Spallation Neutron Source (SNS) is in place [1, 2] aiming to develop an in-situ plasma processing technique to remove some of the residual contaminants from inner surfaces of Nb cavities and improve their performance. The plasma processing R&D has first concentrated on removing hydrocarbon contamination from top surface of SRF cavities. Results from the surface studies on plasma processed Nb samples will be presented in this article and showed the removal of hydrocarbons from Nb surfaces as well as improvement of the surface workfuntion (WF).

INTRODUCTION

Plasma cleaning R&D for niobium (Nb) superconducting radio frequency (SRF) cavities is currently being pursued at the Spallation Neutron Source (SNS), Oak Ridge National Laboratory. The first objective of the plasma processing R&D is to develop an in-situ cleaning technology for SNS high beta (HB) cryo-modules [1, 2]. SNS HB cavities are presently limited by electron emission (field emission) during operation at high accelerating gradients and operating below their designed accelerating gradient. Organic contaminants located in different adsorption sites at top surface of SRF cavities can be responsible for the field emission and degradation of the cavity performance. In-situ plasma processing appears to be a promising technology for in-situ removal of such organic contaminants from top surface of SRF cavities. Plasma cleaning of carbonaceous contaminants is already being used extensively in the semiconductor industry and has shown its potential to clean organic contaminants.

Plasma ignition in the plasma reactor is accomplished by applying appropriate RF field level for the desired gas composition and working pressure. The gas discharge creates a plasma containing reactive species in the processing volume. In multicell SRF cavities, plasma ignition can be controlled by exciting a cavity with a combination of different resonant modes of the cavity while a continuous gas flow is maintained [2, 3]. The reactive species formed in the plasma react with the organic contaminants present at top surface, forming volatile compounds which are pumped out through the vacuum system. Plasma processing of SRF cavities at SNS utilizes the gas mixture of neon (Ne) and oxygen (O_2) where Ne is the primary gas to generate and tune the plasma in a cavity [3] and O_2 is used as a cleaning agent for organic contaminants. Plasma generated reactive species of O_2 reacts with the organic contaminants and oxidizes them into the volatile compounds which are then pumped out. In order to study plasma chemistry during the plasma processing, residual gas analyzer (RGA) can be utilized and provide direct measurement of the partial pressure of the volatile by-products from the plasma reaction. To assess the effect on the field emission after the plasma processing, we utilized a scanning kelvin probe (SKP) which measures the surface workfunction (WF) [4,5]. The surface WF is particularly important for our application as it is directly related to the field emission via Fowler-Nordheim law (see Eq. 1) [6].

$$j \propto \frac{E^2}{\phi} \exp\left(\frac{-a \times \phi^{\frac{3}{2}}}{E}\right) \qquad (1)$$

Where, j is current density, E is electric field and ϕ is work function. In practice, E is not the ideal surface electric field but is a surface enhanced electric field, E= βE (β>1), where β is known as field enhancement factor. It can be seen from Eq. 1 that increasing the work function helps reducing the field emission current. Thus, cleaning contaminants with lower work function than the natural cavity top surface is desirable. SKP is an ideal tool to measure the changes in work-function after the plasma processing. In this article, we present plasma processing studies of Nb samples using RGA and SKP.

PLASMA PROCESSING

Plasma Reactor

A barrel type plasma reactor made of Pyrex glass was used for the plasma processing of Nb samples. The glass reactor has an inlet and outlet port for the process gases and to connect vacuum system. The reactor assembly is located inside a microwave system which operates at 2.4 GHz with a maximum power of 500 Watts. The complete plasma reactor was provided from SPI supplies [7]. Fig. 1 shows the picture of the microwave plasma reactor.

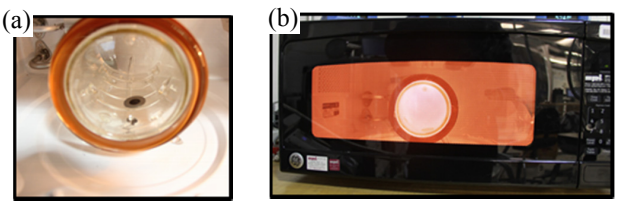


Figure 1: Microwave plasma processing. (a) contaminated Nb sample in the plasma reactor (b) plasma ignited in the microwave plasma reactor.

The process gases were introduced in the reactor via a gas manifold to control the gas flow and mixture. An additional nitrogen (N_2) line was also available for venting the reactor when exchanging the samples. The outlet line of the plasma reactor was connected to the vacuum system and to an RGA.

*Work supported by SNS through UT-Battelle, LLC, under contract DE-AC05-00OR22725 for the U.S. DOE.
#tyagipv@ornl.gov

ISBN 978-3-95450-142-7

Copyright © 2014 CC-BY-3.0 and by the respective authors

MULTIPOLE AND FIELD UNIFORMITY TAILORING OF A 750 MHz RF DIPOLE *

A. Castilla[1,2,3†], J. R. Delayen[1,2].
[1]Center for Accelerator Science, Old Dominion University, Norfolk, VA 23529, USA
[2]Thomas Jefferson National Accelerator Facility, Newport News, VA 23606, USA
[3]Universidad de Guanajuato (DCI-UG), Departamento de Fisica, Leon, Gto. 37150, Mexico

Abstract

In recent years great interest has been shown in developing rf structures for beam separation, correction of geometrical degradation on luminosity, and diagnostic applications in both lepton and hadron machines. The rf dipole being a very promising one among all of them. The rf dipole has been tested and proven to have attractive properties that include high shunt impedance, low and balance surface fields, absence of lower order modes and far-spaced higher order modes that simplify their damping scheme. As well as to be a compact and versatile design in a considerable range of frequencies, its fairly simple geometry dependency is suitable both for fabrication and surface treatment. The rf dipole geometry can also be optimized for lowering multipacting risk and multipole tailoring to meet machine specific field uniformity tolerances. In the present work a survey of field uniformities, and multipole contents for a set of 750 MHz rf dipole designs is presented as both a qualitative and quantitative analysis of the inherent flexibility of the structure and its limitations.

INTRODUCTION

Recently, several studies regarding the rf dipole design have been presented, including analysis on the multipole components for some applications [1, 2]. However, the present work is intended to provide a point of comparison on *to what extent* the parameters in the rf dipole geometry can be manipulated to tailor specific multipole components on the electromagnetic field in order to achieve the parameters required in different application. We take as a case of study the 750 MHz rf dipole, originally designed as a crab cavity corrector for the Medium Energy Electron-Ion Collider (MEIC) at Jefferson Lab [3], for which the multipole components and uniformity of the fields are crucial factors in the beam emittance conservation, this being the main motivation for the present analysis. Nevertheless this does not exclude its possible applications to linear accelerators as luminosity corrector, beam separator or assisting in longitudinal diagnostics, among others.

The 750 MHz rf dipole crab cavity design operates in the lowest mode and has been built and tested in the vertical testing area both at Niowave, Inc. and Jefferson Lab [4], a computer render of the geometry is presented in Fig. 1 and its properties are enlisted in Table 1.

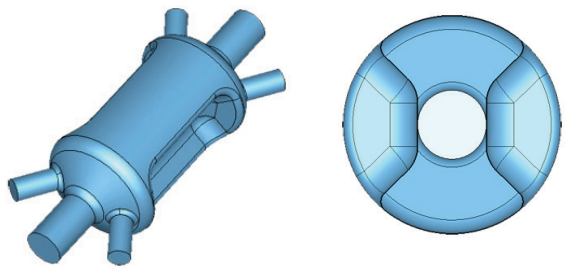


Figure 1: 750 MHz rf dipole design with flat parallel loading elements (left) and its cross section (right).

Table 1: Properties of 750 MHz Crab Cavity Rf Dipole Structure

Parameter	750 MHz	Units
$\lambda/2$ of π mode	200.0	mm
Cavity length	341.2	mm
Cavity radius	93.7	mm
Bars width	63.0	mm
Bars length	200.0	mm
Bars angle	45	deg
Aperture diameter -d	60.0	mm
Deflecting voltage -V_T^*	0.20	MV
Peak electric field -E_P^*	4.45	MV/m
Peak magnetic field -B_P^*	9.31	mT
B_P^*/E_P^*	2.09	$\frac{\text{mT}}{\text{MV/m}}$
Energy content -U^*	0.068	J
Geometrical factor	131.4	Ω
$[R/Q]_T$	124.2	Ω
$R_T R_S$	1.65	$\times 10^4 \Omega^2$

At E_T^*= 1 MV/m

PARAMETERIZATION

The rf dipole does not have a longitudinal electric field on axis, and the deflecting/crabbing kick is mainLy given by the tranverse electric field, which is concentrated in the parallel loading elements region. Therefore the field uniformity and its multipole components can be modified by introducing an outwards curvature to the flat parallel bars to reduce transversal variations of the fields. For the present study we

* Authored by Jefferson Science Associates, LLC under U.S. DOE Contract No. DE-AC05-06OR23177. This research used resources of the National Energy Research Scientific Center, supported by the Office of Science under U.S. DOE contract No. DE-AC02-05CH11231.
† acastill@jlab.org

Copyright © 2014 CC-BY-3.0 and by the respective authors

C-BAND LOAD DEVELOPMENT FOR THE HIGH POWER TEST OF THE SWISSFEL PULSE COMPRESSOR

A. Citterio, R. Zennaro, J. Stettler
Paul Scherrer Institute, Villigen

Abstract

The SwissFEL C-band Linac will have 26 RF modules, each one consisting of a solid-state modulator and a 50 MW klystron that feeds a pulse compressor and four two meters long accelerating structures. The pulse compressor is of the Barrel Open Cavity type (BOC). A first prototype was successfully produced and high-power tested, reaching for full power klystron operation a peak power of 300 MW. For testing this BOC at maximum RF power, a broadband load was designed and built, based on a ridge waveguide design and high permeability stainless steel. Based on the experience gained at CERN for CLIC X-band high power loads, the RF design of the load was optimized to ensure high losses for a quite large range of magnetic steels. Test pieces were realized in three different magnetic steels to choose the best suited material commercially available.

This paper reports about the RF design, material study, production and impressive high power results of this C-band load.

POWER SPECIFICATION AND MATERIAL STUDY

High power loads commercially available in C-band frequency are usually specified to absorb maximum peak power in the range of 25 to 50 MW, according to the technology – dry or water loads – and the adopted RF design. Same loads can support average powers as large as 15 kW.

During the high power test of the BOC prototype performed in 2012 [1], the phase jump operation mode produced, for 50 MW power klystron, a compressed pulse of 300 MW peak power and 12 kW average power. In order to keep the waveguide setting of the high power test as simple as possible, no splitting of the power out of the BOC was carried out, using instead only one load to dissipate this so large peak power. For that a new load was studied to fulfill the power specifications of the C-band pulse compressor of the SwissFEL, having as major constraint high power losses in a compact RF design.

Similar constraints were at the base of the development of a new X-band high power load designed in the context of the R&D CLIC studies [2]. Here a magnetic lossy material such as the stainless steel AISI430 with magnetic permeability $\mu = 6$ h/m, together with a design based on a multiple ridge waveguide, allowed to fabricate a load 0.89 meter long. Because the power losses per unit length in waveguide scale with the frequency f like $f^{1.5}$ [3], assuming for the AISI430 the same permeability at 5712 MHz, a dry load as long as 2.55 m was needed to get the same total power losses in C-band. The problematic machining of such a long piece, together with the unknown μ value of AISI430 at C-band, pushed for the study of a new dry load both in terms of lossy materials and RF design.

Figure 1 shows, before welding, sections of three resonant 5712 MHz standing wave cavity pieces, made of three different magnetic steels with unknown permeability: AISI430, AISI431 and AISI420.



Figure 1: Sections of the cavity test used to determine the best magnetic steel for the load.

Low-power measurements of each cavity allowed to know the β coupling and the unloaded quality factor Q_0 for the three magnetic steels. Then the β and Q_0 measured values were used to obtain the ratios μ/σ between permeability and conductivity by means of the corresponding simulated curves, like in Figure 2.

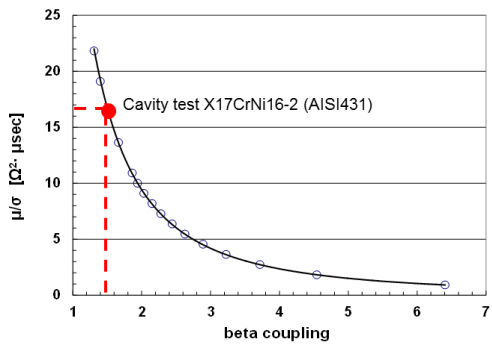


Figure 2: Simulated curve of the ratio μ/σ versus the β coupling. The red circle represents one of the tested material, the magnetic steel AISI431.

The final results of the three magnetic steels taken into account are summarized in Table 1. All the three tested materials are very similar. Because of the lower Q_0 and larger μ/σ ratio, the first choice was the AISI430, the same material as in [2], but its poor availability in the market led to accept the AISI431 as the magnetic steel for the C-band load.

Copyright © 2014 CC-BY-3.0 and by the respective authors

ISBN 978-3-95450-142-7

MEASUREMENTS AND HIGH POWER TEST OF THE FIRST C-BAND ACCELERATING STRUCTURE FOR SwissFEL

R. Zennaro, J. Alex, A. Citterio, J.-Y. Raguin
Paul Scherrer Institut, Villigen

Abstract

The SwissFEL project is based on a 5.8 GeV C-band Linac which is composed of 104 accelerating structures with a length of 2 m each. Due to the absence of dimple tuning no local frequency correction is possible and hence ultra-precise machining is required. The paper reports on both low level and high power RF test of the first nominal structure produced. The required mechanical precision has been reached and the structure has been successfully power tested to a gradient larger than 50 MV/m, well above the nominal level of 28 MV/m. The measured dark current and break down rates are well in the specifications.

INTRODUCTION

Each of the 104 accelerating structures consists of two RF couplers and of 111 regular cells, the dimensions of which shall ensure operation with a $2\pi/3$ phase advance per cell at 5712 MHz. To reduce the RF power losses, each regular cell has rounded outer walls. The cell-to-cell coupling irises have an elliptical cross-section to minimize the peak surface electric fields. The main feature of the designed structure is the optimization of the cell-to-cell iris and cell radii to produce in each regular cell an *identical* accelerating gradient at the operating frequency. The developed methodology for achieving such RF field characteristics is presented in [1].

The temperature stabilisation of the structure is performed with eight azimuthally distributed water channels integrated into each cell. However, due to a change of the nominal inlet temperature of the water – 30°C instead of 40°C – the dimensions of the cells were updated accordingly. The updated dimensions of the first, middle and last cell at 20°C are given in Table 1. The resulting new numerical RF mode parameters are presented in Table 2. The Qs, given at 30°C, are 94 % of the values computed with SUPERFISH.

Table 1: Dimensions for the first, middle and last cells.

	Av. iris radius (mm)	Cell radius (mm)
First cell	7.232	22.429
Middle cell	6.480	22.197
Last cell	5.458	21.936

Table 2: RF mode parameters for the middle and last cell – Q at 30°C and corrected.

	v_g/c (%)	r/Q (kΩ/m)	Q
First cell	3.08	7.24	10223
Middle cell	2.17	7.84	10183
Last cell	1.21	8.68	10139

The first two meter structure, labelled "L0" is composed by cups and couplers produced by the company VDL; the brazing was performed in PSI [2,3]. It is the first of four structures produced up to now (August 2014), but it is the only one power tested to almost twice the nominal gradient.

COLD RF MEASUREMENTS

The RF measurements of L0 in frequency domain show a very good matching, -30.2 dB for the nominal 120° phase advance at 5711.960 MHz, only 40 kHz below the nominal frequency (5712 MHz). The S_{21} measurement provides an average Q_0 of 10820 in agreement with the value computed with SUPERFISH and without correction. The bead pulling in Figure 1 shows a small standing wave component.

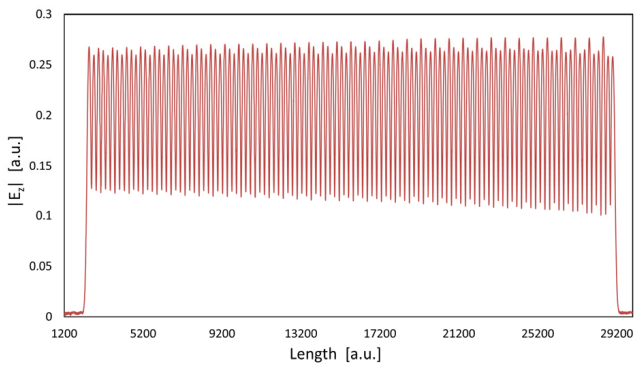


Figure 1: Electric field in the L0 structure.

A special tuning code has been developed at PSI in collaboration with INFN LNF capable to calculate the individual frequency error of each cell, with the exception of the input coupler, from the bead pulling data [4]. The computed error vector for L0 is shown in Figure 2. The output coupler has a frequency error of almost 2 MHz.

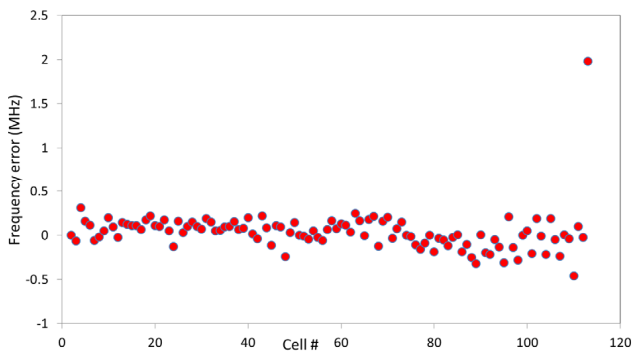


Figure 2: Individual cell frequency error in L0.

The design of the output coupler was re-optimized to remove the residual standing wave component. The

Copyright © 2014 CC-BY-3.0 and by the respective authors

ISBN 978-3-95450-142-7

BEAM DYNAMIC DESIGN OF A 100 mA, 162.5 MHz HIGH-CURRENT LINAC *

F.J. Jia, Y.R. Lu, Z. Wang, W.L. Xia, K. Zhu, X.Q. Yan, J.E. Chen
State Key Lab of Nuclear Physics and Technology, Peking University, Beijing 100871, China
W.P. Dou, Y. He
Institute of Modern Physics, China Academy of Science, Lanzhou 730000, China

Abstract

The beam dynamic design of a 100 mA, 162.5 MHz Radio Frequency Quadrupole (RFQ) is presented in this paper. The RFQ will accelerate protons from 85 keV to 3 MeV under the operation mode of continuous-wave (CW). The code PARMTEQM is used to carry out the beam dynamics design and the transmission efficiency has been optimized and improved to more than 99%. In the design of this high-current linac, the space charge effect is analyzed as it can cause emittance growth, nonuniform particle density distribution and resonance effect. The electrode structure parameters generated by PARMTEQM also be adopted by the code of Toutatis to verify the result's veracity.

INTRODUCTION

Radio Frequency Quadrupole (RFQ) accelerators are widely used as injectors in the high-current linacs. Because of their remarkable capability of simultaneously focusing, bunching and accelerating the low-energy particles with high transmission and minimum beam emittance growth, many RFQ projects have been done in the world.

With the beam intensity increases from a low level to high, the particles' interaction, which is called space charge effect, become stronger and stronger. It will cause emittance growth, energy spread, beam halo, etc. These bad effects caused by space charge interaction will significantly reduce the beam quality and transmission efficiency. Due to the challenges exist in high-current linac, although many RFQ projects have been done worldwide, just a few projects have been ambitious to step into the range of more than 100 mA's RFQ design.

While, as high-current linear accelerator has wide application field such as neutron radiography, cancer therapy and the experiment of ion irradiation, many scientific research institutions put focus on the research of it now. To have deep research about high-current linacs, a new scientific research project was proposed by Institute of Modern Physics of Chinese Academy of Science and Peking University recently. The project aims to research about a new type RFQ with beam current up to 100 mA. This RFQ will adopt a new type of 4-vane with window structure. Deeper research work about high-current linacs will be done in this project. The basic beam dynamics design parameters of this RFQ are listed in Table 1.

*Work supported by the 973 program (No. 2014CB845503) and the NSFC (Grants No. 11079001)
#Corresponding author: yrlu@pku.edu.cn; fangjianjia@pku.edu.cn

Table 1: Basic Parameters

Parameters	Value	Unit
Particle	Proton	
Type	4-vane with window	
Frequency	162.5	MHz
Peak Beam Current	100	mA
Output Energy	3	MeV
Input Transverse Emittance (Norm., RMS)	0.2	π·mm·mrad
Beam Duty Factor	100	%

BEAM DYNAMIC DESIGN

The dynamic simulation was carried out by the code of PARMTEQM in this project. It was developed at Los Alamos National Laboratory (LANL) and has been widely applied to the design of many RFQs.

In this project, the beam intensity reaches 100 mA. Learning from the dynamic design and the practical running results of the ≥100 mA RFQ projects such as LEDA [1], IPHI [2], JAERI BTA[3], FRANZ [4] in the world we can see that the phenomenon of accelerator's instability and low transmission is very common in high-current linac. To ensure the RFQ's high beam transmission efficiency and the stability of the operation, the dynamic parameters were optimized carefully and modulate slowly during the beam dynamic design of this project.

Design Strategy

The strong space charge effect will affect the beam transport in the low energy part prominently. Therefore the input energy should not be too low. Whereas, too high input energy will make the manufacture of ion source too difficult. And as this project requires the RFQ work in CW mode, the inter-vane voltage cann't be set too high or too low either. To keep enough radial focusing and longitudinal accelerating strength, and to reduce the power consumption and RF sparking risk, the voltage value should be set reasonably. Compared with other high-current RFQ project in the world, the input energy and inter-vane voltage of this RFQ was chosen as 85 keV and 80kV respectively.

The Four-Section Procedure [5] beam dynamics design method, developed by LANL, has been adopted and proved by various RFQ projects in the world. This method

Copyright © 2014 CC-BY-3.0 and by the respective authors

CONSTRUCTION OF THE NEW AMPLIFIERS FOR THE RIKEN-LINAC

K. Suda, E. Ikezawa, O. Kamigaito, N. Sakamoto, K. Yamada
RIKEN Nishina Center for Accelerator-Based Science, Wako, Saitama 351-0198, Japan
Y. Touchi, Sumitomo Heavy Industries, Ltd., Niihama, Ehime, 792-8588, Japan

Abstract

New tetrode based amplifiers have been constructed for the RIKEN heavy-ion linac, so called RILAC, replacing 36-year-old amplifiers to improve their reliability as a main injector for the RIBF accelerator complex. The RILAC is a DC machine and their frequency are tunable between 18 to 40 MHz so as to be capable of accelerating heavy ions with mass-to-charge (m/q) ratios up to 28. The new rf amplifier is based on a tetrode THALES/SIEMENS RS2042SK coupled with a tetrode THALES/SIEMENS RS2012CJ with a grounded grid circuit. The maximum output power is 150 kW with a frequency ranging from 18 to 40 MHz. The amplifier was originally designed for RIKEN Ring Cyclotron. Since we have many experiences with this type of amplifier, some modification to avoid exciting the parasitic modes which might damage the cavity and/or the amplifier itself. Their construction started in April 2013 and installation was performed in January 2014. After the installation their commissioning has been successfully made. Beam services started in March 2014, and the new amplifiers were operated without any troubles.

RIKEN HEAVY-ION LINAC (RILAC)

The RIKEN heavy-ion linac, RILAC [1], consists of six variable frequency cavities (tanks) constructed in 1978 (Fig. 1). It accelerates various kinds of ions up to 4 MeV/u by varying RF frequency from 18 to 40 MHz. Beam service started since 1981. Since 2002, by adding six booster cavities, intense beams up to 6 MeV/u are provided for experiments such as super heavy element (SHE) synthesis. RILAC is also used as an injector for RI Beam Factory (RIBF) since 2006.

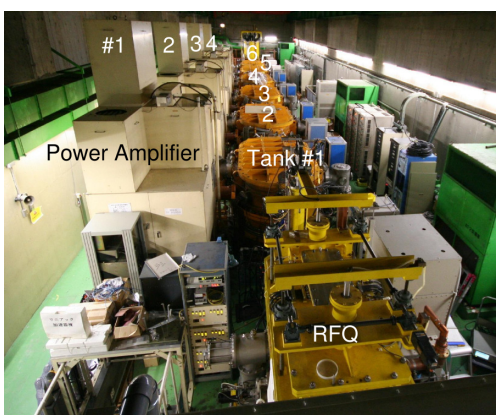


Figure 1: RILAC tanks and power amplifies.

POWER AMPLIFIER FOR RILAC

There are six power amplifiers for RILAC tanks. The prototype of amplifier was constructed in 1977, prior to the construction of tanks, and the amplifier was used for tank #1. Other five amplifiers were constructed in 1978. The #5 and #6 amplifiers were upgraded in 1999 for SHE experiments. Three final-stage plate DC power supply were upgraded at the same time; one power supply is used for two amplifiers. In recent years, several troubles occurred, such as water leaks from a pin hole on cooling pipe, and damage of socket for tetrode caused by a insufficient contact between socket and tetrode. The contact is shallow and a careful alignment is necessary. Such troubles deteriorated the reliability of the RF systems. Therefore, in FY 2013, amplifiers for #1 and #2 were upgraded (Fig. 2). The upgrade project started in April 2013. Installation of two amplifiers started in January 2014, and dummy load and power tests were performed in February 2014. Beam service using the new amplifier started in March 10 th, 2014 on schedule.

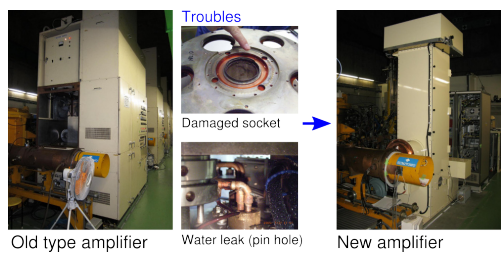


Figure 2: Old power amplifier, its troubles, and a new amplifier constructed in FY2013.

CIRCUIT DIAGRAM OF AMPLIFIER

The new amplifier for RILAC #1 and #2, as well as for #5 and #6 is based on a tetrode RS2042SK coupled with a tetrode RS2012CJ from THALES/SIEMENS with a grounded grid circuit, which was originally designed for RIKEN Ring Cyclotron (RRC) [2]. The maximum RF input power of 0.01 W(10 dBm) is amplified by a pre-, driver- and, final-stage amplifiers up to 1, 15, and 150 kW, respectively. A frequency range is from 18 to 40 MHz. The circuit diagram of the amplifier is shown in Fig. 3. In 14 years operation of the amplifier for RILAC #5 and #6, we have experienced several parasitic modes, which might damage the tank and/or the amplifier itself. One is caused by a coupled oscillation between the 99-MHz G1-G2 resonance of RS2042SK and the output circuit including a feeder line to the tank. The other example is the 7th harmonic mode observed in RILAC #5 shown in Fig. 4. In order to avoid such parasitic modes, we have installed a 50 kW dummy load at plate STUB.

Copyright © 2014 CC-BY-3.0 and by the respective authors

ISBN 978-3-95450-142-7

DEVELOPMENT ACTIVITIES OF ACCELERATOR INSTRUMENTS FOR SACLA

Y. Otake#, T. Asaka, T. Inagaki, C. Kondo, H. Maesaka, T. Ohshima, T. Sakurai, K. Togawa,
RIKEN SPring-8 Center, 1-1-1 Kouto, Sayo-cho, Sayo-gun, Hyogo, 679-5148, Japan
H. Ego, S. Matsubara, JASRI, 1-1-1 Kouto, Sayo-cho, Sayo-gun, Hyogo, 679-5148, Japan

Abstract

The X-ray free-electron laser (XFEL), SACLA, is constantly operated for user experiments aimed at new science. However, experimental users demand further experimental abilities to XFEL facilities, such as many experiment chances by using multi-X-ray beamlines, much better repeatability of experimental conditions and further intense high-energy X-rays. To equip SACLA with these abilities in the future, we developed a 2π /3 quasi-constant gradient accelerating structure with an acceleration gradient of over 50 MV/m in order to adapt operation for generating the intense high-energy X-rays. A high-voltage power supply to charge the PFN of a klystron modulator, a klystron and an accelerating structure were also developed in order to upgrade a machine repletion cycle to 120 pps from the present 60 pps, since 120 pps is more suitable to increase the beam repetition to one of the multi-beamlines. To meet the further experimental repeatability realized by stable timing, such as a pump-probe experiment, an optical-fiber length control system in order to mitigate timing drift below 1 fs was developed. A highly precise cavity temperature control system in an injector cavity for below ± 2 mK (p-p) was also realized for the experimental repeatability. The performances of the above-mentioned instruments were experimentally tested to be sufficient for our demands of 50 MV/m, 120 pps, 1 fs and ± 2 mK (p-p).

INTRODUCTION

An X-ray Free-electron laser (XFEL) based on a linac, such as the SPring-8 angstrom compact laser, SACLA [1], is already operated for regular user experiments and almost single user machine; therefore it is a very expensive machine. Furthermore, experiment users usually demand intense and high-energy X-ray beams. To countermeasure the above-mentioned issue, X-ray multi-beamlines driven by one linac in order to accelerate a further high-energy electron beam are the solution. It is because that the high-energy electron beam allows us to increase X-ray flux and its energy in an undulator beamline, if the K value of the undulator is fixed to be a certain value. In the case of SACLA, we have plan to construct a new beamline of BL2 [2].

The next important issue is stability of the XFEL, because it guarantees repeatability of experimental results. Perturbation sources to the instability of the XFEL linac are mainly environmental condition changes, such as a temperature, humidity and vibration around accelerator instruments. In the case of SACLA, there is still X-ray laser intensity instability affected from the environmental condition changes. The perturbations, as which triggers the instability not satisfying a temporal stability demand of about 50 fs in rms, [3] mainly affect the rf phase and amplitude of injector cavities.

As solutions of the above-mentioned issues, we conducted development of a high-acceleration gradient and high rf-pulse repetition-rate linac for future XFELs [4]. Of course, our requirements to the acceleration gradient and the rf pulse repetition rate are as much as possible. However, there are empirically confirmed technical-limitations, such as the cooling capacity of instruments and a natural cavity surface breakdown limit in vacuum. Furthermore, we do not want to drastically change the present rf source conditions, such as an output rf power of 50 MW generated by the existing high-power pulse klystron, because the change demands much money and time consuming effort. Hence we set an acceleration gradient of 50 MV/m and an rf pulse rate of 120 pps, as our immediate targets, to overcome SACLA's performances of 40 MV/m and 60 pps. These targets should be attained by using the present rf source with minor modification.

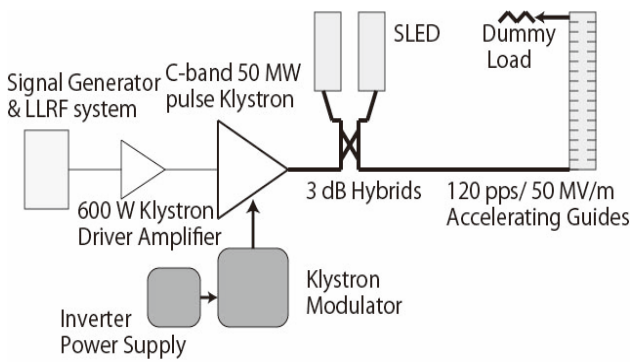


Figure 1: Experimental set-up of the 120 pps C-band acceleration unit.

Since the environmental condition perturbations mainly affect the rf phases of cavities along bunch compression process from the injector to three bunch compressors in SACLA, we developed a control system achieving highly stabilized a cooling water temperature of within several mK for an acceleration cavity and a 19 inch rack for a low-level rf (LLRF) system to reduce the effects from the perturbations [5]. Furthermore, an optical fiber length control to reduce effects from temperature and humidity changes to the low-level rf system of SACLA were also developed [6]. They were produced for

#otake@spring8.or.jp

Copyright © 2014 CC-BY-3.0 and by the respective authors

DEVELOPMENT OF 3 MeV PROTOTYPE RFQ STRUCTURE FOR HIGH INTENSITY PROTON LINAC FOR ISNS

S.C.Joshi, G.V. Kane, N.K.Sharma, A.Chaturvedi, S.Raghavendra, K.K.Das, S.K.Chauhan, S.V. Kokil and B.Oraon

Raja Ramanna Centre for Advanced Technology (RRCAT), Indore, India

Abstract

Raja Ramanna Centre for Advanced Technology (RRCAT) has taken up a program on R&D activities for a 1 GeV, high intensity superconducting H- ion/proton linac for spallation neutron source programme. Front end of the linac will consist H- ion source, LEBT and 3 MeV Radio Frequency Quadrupole (RFQ). RFQ has been designed and fabricated to validate the design and manufacturing procedures. RFQ structure length of 3.49 meter has been divided in three segments for machining. Three segments have been machined and assembled for low power RF characterization. Frequency and field tuning exercise for the assembled RFQ structure is being carried out. The paper presents engineering design, fabrication issues and tuning studies carried on prototype structure.

INTRODUCTION

Four vane 3MeV RFQ has been designed to accelerate H^- ion beam from 50 keV to 3 MeV for 20mA beam current and a prototype has been fabricated. Prototype structure development involves engineering design, vacuum design, fabrication and assembly. RFQ has been designed for a duty factor of 1.25%. Important physics design parameters for RFQ [1] are listed in the table below.

Table1. Design parameters of RFQ

Design Parameters	Values
Input Energy	50 keV
Output Energy	3 MeV
Peak beam current	20 mA
Particle	H^- Ion
Operating Mode	Pulsed
Duty Factor	1.25%
Frequency	325 MHz
Structure	4-vane type
Total Length	3.49 m
Peak Power loss	300 kW
Material	OFE Copper

THERMAL DESIGN OF RFQ

The RF power loss in the structure will results in thermal deformations and RFQ structure will detune from its designed operating frequency. Therefore thermal stability of the structure is the main concern of engineering design. The thermal analysis of RFQ has been carried out for a maximum duty factor of 10 % where average power loss is taken as 42 kW. The power loss for the thermal analysis has been considered 40% more than the power loss calculated by SUPERFISH to compensate for the deviation in ideal surface conditions, theoretical electrical conductivity and joints etc. 12 mm circular cross section was selected for cooling channel considering machining feasibility. Studies were performed to optimize cooling channel locations and flow velocities for effective cooling of RFQ structure. Thermal analysis result reveals that using optimized parameters, the temperature gradient in RFQ structure is restricted within 1.2 deg C. The thermal induced frequency shift of 32 kHz was observed. 2D Thermal – structural - high frequency electromagnetic coupled sequential analysis has been performed to evaluate the effect of cooling water temperature on RFQ frequency. The analysis will help in thermal management of RFQ to control frequency detuning during operation.

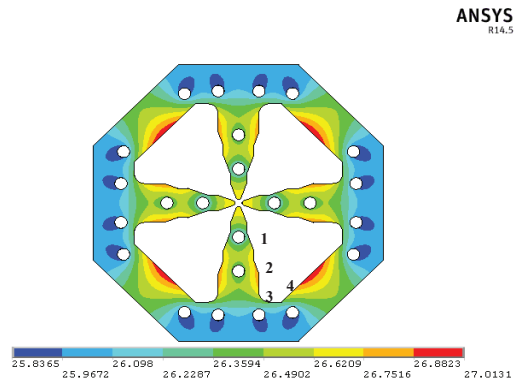


Figure 1: 2D Temperature distribution for RFQ

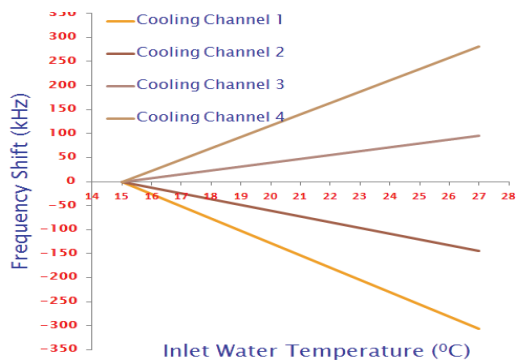


Figure 2: Effect of cooling water temperature on RFQ frequency.

Copyright © 2014 CC-BY-3.0 and by the respective authors

ISBN 978-3-95450-142-7

COMPARISON OF NORMAL CONDUCTING HIGH ENERGY ACCELERATING STRUCTURES FOR A MODERATE OPERATING FREQUENCY *

V. Paramonov †, INR of the RAS, Moscow, 117312, Russia

Abstract

The progress in the CERN Linac 4 project confirms the very attractive possibility for single frequency high intensity high energy normal conducting hadron linac. The important part of such linac is the accelerating structure for high energy part. The set of parameters, such as dimensions, RF efficiency, field stability, cooling capability, vacuum conductivity, is considered and compared for possible accelerating structures at operating frequency 352 MHz are in proton energy range up to 600 MeV.

INTRODUCTION

For the high energy part of normal conducting intense hadron linac the Coupled Cell Structure (CCS) is used. For operating frequency $f_0 = 352.2MHz, \lambda = 85.12cm$ application of such well known and proven CCS's as the Side Coupled Structure (SCS), the Annular Coupled Structure (ACS) and the Disk And Washers (DAW) is not practical due to enormously large transverse dimensions $2R_c \sim 1.5\lambda$. Structures with the smaller outer diameter $2R_c \sim 0.7\lambda$ look realistic. During TRISPAL project, see [1], LEP-type structure was suggested to take the beam to high energy part. Also consideration of the compact On Axis Coupled (OAS) structure was rejected due low value of the effective shunt impedance Z_e for low β and possibility of multipactor in coupling cells. This suggestion is successfully developed now and realized in the Pi Mode Accelerating Structure (PiMs) for Linac 4, [2]. The small transverse dimensions has also the Cut Disk Structure (CDS), [3]. Below PiMS and CDS parameters are compared for proton energy range from $50MeV$ to $600MeV$.

PARAMETERS COMPARISON

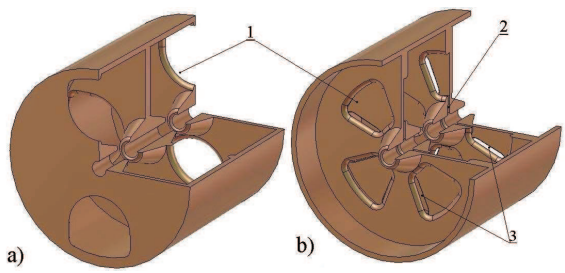


Figure 1: The considered structures, PiMS (a) and CDS (b). 1 - coupling windows, 2- coupling CDS cell, 3 - slots 'To Look Through' (TLT) between CDS cells.

The considered structures are shown in Fig. 1.

Cells Parameters

For both structures the dimensions of Drift Tube (DT) are essential. Especially interesting is the value of a cone angle θ for DT. In PiMS the dimensions of coupling windows are well matched with DT dimensions and cone angle is fixed to $\theta = 20^o$, [4]. For the energy range from $160MeV$ to $600MeV$ this value is conserved to provide appropriate dimensions of coupling windows for the higher value of the coupling coefficient k_c. As it is known well, the optimal for the maximum of Z_e, length of accelerating gap l_g depends on θ. All time in simulations below for each θ the optimal l_g value was used. Also structures were compared for the same aperture radius.

In CDS another concept of coupling is realized, [3], and there are no essential relationships between θ and k_c. Plots of some CDS parameters in the dependence on θ value are shown in Fig. 2. Blue and green lines corresponds to proton energy $100MeV$ and $400MeV$, respectively. With θ increasing to $\theta \geq 25^o$ there is visible Z_e decreasing, especially for higher energy, and the rise in the cell diameter, Fig. 2a,b. In Fig. 2c,d are shown plots for the maximal temperature rise dT_{max}, which is realized at the DT tip, and the corresponding increasing in the DT length, dz_{max}. (See below about CCS cooling). With the small $\theta \sim (15^o \div 20^o)$ we have the thin long DT, especially for higher energies. For design simplification, inside DT body there are no cooling channels. Simultaneously, near DT pedestal (in both structures) the

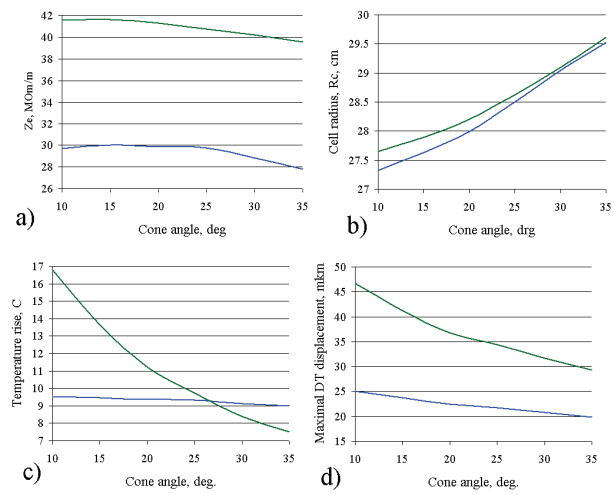


Figure 2: The plots of $Z_e(\theta)$, (a), $R_c(\theta)$, (b), $dT_{max}(\theta)$, (c), $dz_{max}(\theta)$, (d) for CDS.

* Work supported by IHEP contract N 0348100096313000178
† paramono@inr.ru

Copyright © 2014 CC-BY-3.0 and by the respective authors

UNTRAPPED HOM RADIATION ABSORPTION IN THE LCLS-II CRYOMODULES*

K. Bane, C. Nantista#, C. Adolphsen and T. Raubenheimer, SLAC, Menlo Park, CA 94025, USA,
A. Saini, N. Solyak and V. Yakovlev, FNAL, Batavia, IL 60510, USA

Abstract

The superconducting cavities in the continuous wave (CW) linacs of LCLS-II are designed to operate at 2 K, where cooling costs are very expensive. One source of heat is presented by the higher order mode (HOM) power deposited by the beam. Due to the very short bunch length–especially in L3 the final linac–the LCLS-II beam spectrum extends into the terahertz range. Ceramic absorbers, at 70 K and located between cryomodules, are meant to absorb much of this power. In this report we perform two kinds of calculations to estimate the effectiveness of the absorbers and the amount of beam power that needs to be removed at 2 K.

INTRODUCTION

While the use of superconducting accelerating cavities in large particle accelerator facilities offers many advantages in areas such as RF efficiency and feasible beam parameter ranges, a major expense of operating such a machine is the power required of the cryogenic plant. Care must be taken to minimize both static and dynamic heat loads. One element of the latter, particularly relevant in a high-current, short bunch, CW facility like LCLS-II, is higher-order-mode (HOM) electromagnetic field power generated by the beam in passing through the cavities and beamline elements.

LCLS-II will run with a CW megahertz bunch train of initial current 62 μA, but eventually upgradable to 0.3 mA. HOM heat load is of particular concern in the 20 cryomodules of the L3 linac region, after the second bunch compressor, where the rms length of the 300 pC bunches will be only $\sigma_z = 25$ μm. The main generators of HOM power are the 35 mm radius irises of the nine-cell periodic L-band accelerator cavities, though other features, such as inter-cavity bellows and beam pipe radius transitions between regions, play a role. For a quantitative treatment of generated HOM (or more accurately wakefield) power in LCLS-II see [1,2].

HOM coupler ports incorporated in the end pipes of the cavities provide damping against build-up of higher-order cavity mode fields. Since the spectrum of excited HOM power extends well beyond the beam pipe cutoff, annular ceramic RF absorbers are included in the drifts between the 8-cavity cryomodules in the hope of absorbing much of this untrapped wakefield radiation.

In what follows, we describe and compare two attempts to theoretically characterize the relative HOM power lost in the different cryogenic environments (2 K, 70 K) by assessing the effectiveness of the HOM absorbers. We would like as much of the power as possible to be lost in the 70 K absorbers rather than in the NC beam pipes and bellows between the cavities, for which heat is removed by the 2 K cooling system. The first method uses a numerical, S-matrix approach, and the second involves an analytical diffusion-type calculation. This topic was previously addressed for the European XFEL project using a ray tracing method and the diffusion approach presented here [3]. Also, the S-matrix calculation has been previously applied to the ILC cryomodules [4]. We focus here on the maximum average beam current.

S-MATRIX APPROACH

Most of the LCLS-II linac can be seen as a periodically repeated sequence of cryomodule elements joined at their 39 mm-radius beam pipe ports. This periodic unit consists of eight nine-cell ILC-type cavities, each followed by a bellows, a long beam pipe drift (through the quad), an absorber and a shorter drift section. The absorber, a suspended ring of ceramic recessed in a pillbox diameter step, has an integrated bellows, which we treat as part of the same element.

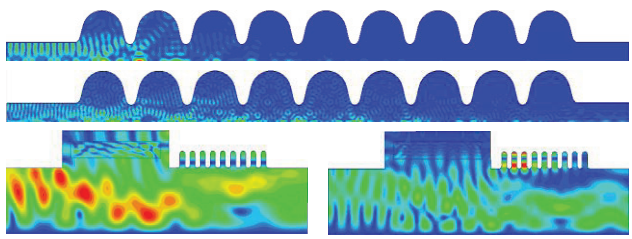


Figure 1: Geometries and field plots from HFSS S-matrix calculations: cavity and absorber at 12 & 20 GHz.

At a number of discrete frequencies, 4, 8, 12, 16, 20 and 40 GHz, we used the field solver HFSS [5] to calculate the scattering matrix for each element (cavity, bellows, drifts and absorber) for all TM_{0n} monopole modes propagating in the beam pipe at each respective frequency. The niobium cavities were modelled as perfect conductors. The bellows and drift pipes were assumed to be copper (or copper plated), for which an electrical conductivity in this temperature and frequency regime, ranging from $1.97–0.914\times10^9/\Omega$m between 4–40 GHz, was calculated according to

$$\sigma_{Cu,eff}(\omega) = (\omega Z_0/2c)\,\mathrm{Re}\left(\mathcal{Z}_{Cu,eff}(\omega)\right)^{-2}, \qquad (1)$$

where Z_0 is the impedance of free space and $\mathcal{Z}_{Cu.eff}$ is the surface impedance from Eq. (6) below for the extreme anomalous skin effect [6]. We also considered the case where the bellows and drifts are stainless steel, for which

*Work supported by the U.S. Department of Energy under contract DE-AC02-76SF00515.
nantista@slac.stanford.edu

ISBN 978-3-95450-142-7

Copyright © 2014 CC-BY-3.0 and by the respective authors

WAKEFIELD EFFECTS OF THE BYPASS LINE IN LCLS-II*

K.L.F. Bane§, T. Raubenheimer, SLAC, Menlo Park, CA 94025, USA

INTRODUCTION

In LCLS-II [1], after acceleration and compression and just before entering the undulator, the beam passes through roughly 2.5 km of 24.5 mm (radius) stainless steel (SS) pipe. The bunch that passes through the pipe is extremely short with an rms of 8 μm for the nominal 100 pC case. Thus, even though the pipe has a large aperture, the wake that applies is the short-range resistive wall wakefield.

The LCLS-II bunch distribution is approximately uniform and therefore, for short bunches, the wake induced voltage is characterized by a rather linear variation. For self-seeding operation, however, longer bunches are desirable. An important question is, what constraints do the bypass line wakes place on the bunch length? In this note we calculate the wake, discuss the confidence in the calculation, and investigate how to improve the induced chirp linearity and/or strength. Finally, we also study the strength and effects of the transverse (dipole) resistive wall wakefield. Selected beam and machine parameters are given in Table 1.

Table 1: Selected Beam and Machine Properties in the Bypass of LCLS-II That are Used in Our Calculations. The longitudinal bunch distribution is approximately uniform. Note that the nominal bunch charge is 100 pC, also with $I = 1$ kA.

Parameter name	Value	Unit
Charge per bunch, Q	300	pC
Beam current, I	1	kA
Rms bunch length, σ_z	25	μm
Beam energy, E	4	GeV
Maximum repetition rate, f_{rep}	1	MHz
Bypass pipe radius, a	2.45	cm
Bypass pipe length, L	2.5	km
Average β function β_x	260	m

WAKE OF BYPASS LINE

The point charge (dc) resistive wall wake in a round, metallic pipe is given by [2]

$$W_\delta(s) = \frac{Z_0 c}{\pi a^2}\left(\frac{1}{3}e^{-s/s_0}\cos\frac{\sqrt{3}s}{s_0} - \frac{\sqrt{2}}{\pi}\int_0^\infty dx\frac{x^2 e^{-sx^2/s_0}}{x^6+8}\right) \quad (1)$$

with s (> 0) the distance the test particle follows behind the drive particle, $Z_0 = 377\ \Omega$, c the speed of light, and a the beam pipe radius. The characteristic distance over which the wake falls to zero, $s_0 = (2a^2/Z_0\sigma_c)^{1/3}$, with σ_c the conductivity of the walls.

For the LCLS-II bypass line $a = 2.45$ cm and for SS $\sigma_c = 1.4\times10^6\ \Omega^{-1}\text{m}^{-1}$. Thus $s_0 = 132\ \mu$m. A plot of the total wake of the bypass is given in Fig. 1.

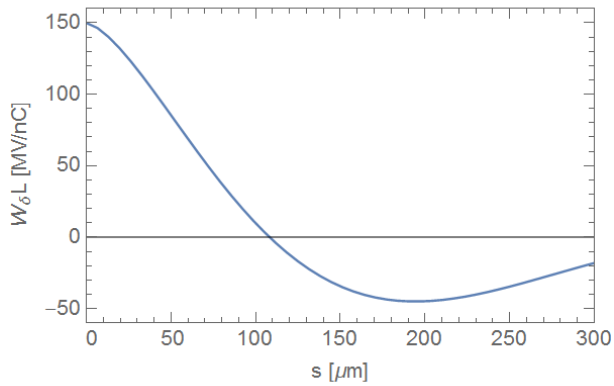


Figure 1: Point charge wake of LCLS-II bypass beam pipe.

The bunch shape in the LCLS-II bypass line is approximately uniform. For a uniform bunch distribution the induced relative energy variation is given by

$$\delta_w(s) = -\frac{eIL}{cE}\int_0^s W(s')\,ds' \qquad 0 \le s \le \ell\,, \quad (2)$$

with I the beam current, L the pipe length, E the beam energy, with the head of the bunch at $s = 0$ and the tail at $s = \ell$. The induced energy variation for the bypass line, assuming a uniform bunch with $I = 1$ kA, is plotted in Fig. 2. The head of the bunch is at $s = 0$, and the extent of three charge scenarios is indicated by color coding. The bunch reaches to $\ell = 2\sqrt{3}\sigma_z = Qc/I = 30, 90, 150\ \mu$m for the cases $Q = 100, 300, 500$ pC, respectively. We note that δ_w, for the 100 pC case, introduces a linear chirp of $\sim -10^{-4}\ \mu\text{m}^{-1}$, for the 300 pC case the chirp has curvature in the bunch tail, and for the 500 pC case the chirp at the tail actually changes sign.

A linear induced chirp is desirable, since it is of the correct sign to help remove surplus chirp left over from the last bunch compressor (to "dechirp" the beam). But the curvature at the tail of the 500 pC case is not desirable, since it will leave a non-correctable energy variation in the tail of the bunch. Because of this result, the 500 pC scenario has been dropped as a mode of operation for the LCLS-II.

How could one improve the situation for the 500 pC case? To have the chirp be rather linear for this case, one could *e.g.* increase s_0 by coating the inside of the bypass pipe with a metal that is a poorer conductor than SS. For example, to have the curvature of the chirp be the same or better than

* Work supported by Department of Energy contract DE–AC02–76SF00515.

§ kbane@slac.stanford.edu

Copyright © 2014 CC-BY-3.0 and by the respective authors

BRIDGING THE GAP BETWEEN CONVENTIONAL RF ACCELERATION AND LASER DRIVEN ACCELERATION*

M.V. Fazio#, S.G. Tantawi, V.A. Dolgashev
SLAC National Accelerator Laboratory, Menlo Park, CA 94025, USA

Abstract

For decades conventional RF accelerators have been built and operated with ever increasing capability thru a few tens of gigahertz in frequency. More recent research takes advantage of the continuing development of high peak power short pulse lasers to drive accelerator structures at optical frequencies. This jump from RF to optical frequencies skips four orders of magnitude in wavelength. With recent experiments that demonstrate high gradients in metallic structures at millimeter wavelengths one is compelled to consider the viability of new approaches for acceleration in the millimeter-wave to terahertz regime. This paper will explore some of these possibilities.

INTRODUCTION

The traditional approach to linear collider design involves a series of choices aimed at producing an average beam power of about 10 MW. The basic choices are operating frequency and normal or superconducting structures. Normal conducting X-band structures are chosen in the hope of achieving high gradient operation and superconducting structures are selected in search of a reliable high efficiency system. Next comes the decision on power source options, which can be klystrons, with or without pulse compression systems, or two beam systems with klystrons used to produce the drive beam. Finally the modulator system is selected. For normal conducting accelerators this is usually a very high voltage modulator with its very inefficient pulse compression system, or a long pulse modulator for superconducting or two beam colliders. The end result is an overall system that is very expensive, inefficient, and not well suited to future expansion.

A multi-faceted approach is being explored for enabling an efficient, cost-effective design. This integrated approach tries to optimize the entire accelerator system that includes the accelerator structure, the RF source, and the modulator. This is accomplished by building on a basic physics understanding of high-gradient phenomenon in normal conducting structures, developing efficient novel structure designs that can be normal or superconducting, transformational RF sources based on low voltage operation, and intelligent modulators with feedback loops to recover energy from both the RF source and the accelerator structures. Finally, we are expanding our frequency range under investigation to the millimeter-wave to terahertz region (100 GHz to 1 THz) because of its potential for extremely high gradients that makes operation at these frequencies worthy of consideration.

The following discussion is focused on the high frequency operation aspect, additionally motivated by the fact that accelerator developers have largely ignored this spectral region. This is partly due to the fact that powerful RF sources are not available at these frequencies with which to power accelerators. While RF accelerator technology has been developed as high as X-band with some experimental devices up to 17 GHz, the remainder of the RF spectrum has been skipped over in favour of laser-driven accelerators four orders of magnitude higher in frequency. The availability of high power lasers developed for commercial applications has made laser-driven acceleration a very active research area.

MILLIMETER-WAVE STRUCTURES

A recent preliminary experiment was conducted using the SLAC FACET Facility's 20 GeV electron beam as the driver to excite a millimeter-wave structure and examine the RF breakdown characteristics. The traveling wave structure consisted of two copper slabs with a machined slow-wave structure as shown in Fig. 1.

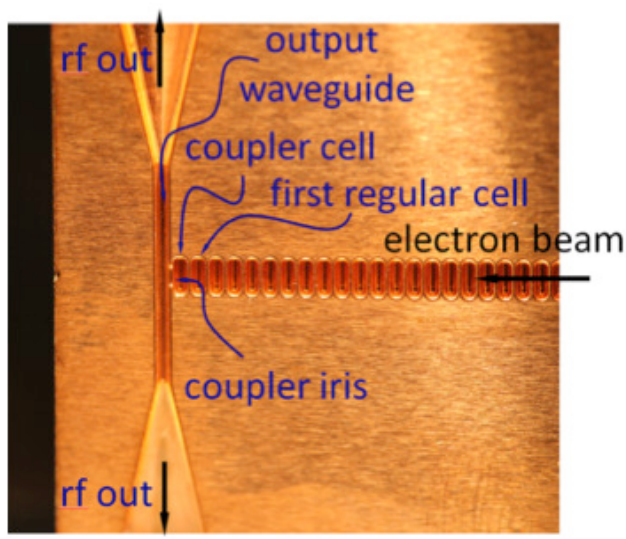


Figure 1: W-band 116 GHz traveling wave structure. Two such slabs are used on either side of the drive beam.

The structure consists of 112 cells. In the experiment the two slabs are placed on either side of the drive beam. The beam transfers RF energy to the structure as it passes through and the wave grows as it travels down the structure. Both the spacing between the slabs and the

*Work supported by the US DOE under contract DE-AC03-76SF00515
mfazio@slac.stanford.edu

Copyright © 2014 CC-BY-3.0 and by the respective authors

STATUS OF THE FETS PROJECT

A. Letchford, M. Clarke-Gayther, M. Dudman, D. Faircloth, S. Lawrie, STFC RAL ISIS, UK
C. Plostinar, STFC RAL ASTeC, UK
S.Alsari, M. Aslaninejad, P. Savage, Imperial College of Science and Technology, UK
J. Pozimski STFC RAL, UK & Imperial College of Science and Technology, UK
G. Boorman, A. Bosco, S. Gibson, Royal Holloway University of London, UK
R. D'Arcy, S. Jolly, University College London, UK
J. Back, University of Warwick, UK

Abstract

The Front End Test Stand (FETS) under construction at RAL is a demonstrator for front end systems of a future high power proton linac. Possible applications include a linac upgrade for the ISIS spallation neutron source, new future neutron sources, accelerator driven sub-critical systems, high energy physics proton drivers etc. Designed to deliver a 60mA H-minus beam at 3MeV with a 10% duty factor, FETS consists of a high brightness ion source, magnetic low energy beam transport (LEBT), 4-vane 324MHz radio frequency quadrupole, medium energy beam transport (MEBT) containing a high speed beam chopper and non-destructive laser diagnostics. This paper describes the current status of the project and future plans.

FRONT END TEST STAND

FETS was originally conceived as a chopper beam test facility but has since expanded its objectives to become a generic test stand for high power proton accelerator front end technologies. Applications include but are not limited to ISIS upgrades, future Spallation Neutron Sources, a Neutrino Factory, Muon Collider, Accelerator Driven Sub-critical Systems and Waste Transmuters.

FETS has been extensively described elsewhere [1][2]. It consists of an H- ion source, magnetic low energy beam transport (LEBT), 324 MHz 4-vane Radio Frequency Quadrupole accelerator (RFQ), medium energy beam transport and chopper line (MEBT) and comprehensive diagnostics. The rest of this paper describes the status and future plans for each component of the test stand.

ION SOURCE

FETS uses a Penning Surface Plasma Source (SPS) [3]. A programme of continuous development over many years has resulted in source performance which is very close to the demanding FETS specification [4].

Recent developments include new sector magnet poles design to allow higher fields with less aberration [5], a new high voltage extraction power supply capable of 25 kV at the full 10% duty factor [6] and a redesigned downstream post-acceleration system which results in a considerably less divergent beam entering the LEBT. The beam emittance is now ~0.35 π mm mrad, still higher than the ideal value but much reduced over earlier values.

LEBT

The FETS LEBT consists of three identical magnetic solenoids with maximum on axis field of 0.4 T. Previous studies had shown high beam currents of up to 60 mA at the end of the LEBT with a reasonably small rms-emittance. However, large offsets of ~10mm in position and ~10 mrad in angle were observed in both transverse planes. These were traced to a lack of repeatability in mounting the ion source assembly following source changes or maintenance. An improved datum and alignment system has largely corrected this and although a perfect alignment cannot be achieved due to the length of ~2 m, minor offsets can be corrected with the dipole steerers integrated into the solenoids.

An extensive parametric evaluation of the LEBT has shown that a well aligned, well matched beam can be delivered to the RFQ injection point [7][8].

RFQ

The FETS RFQ is a 324 MHz, 4-vane type with a final energy of 3 MeV and a total length of ~4.0m. It employs a bolted, braze-free construction with a 3D O-ring for the vacuum seal and RF finger contacts [9]. The 4m long cavity consists of 4 sections each made up of 2 major and 2 minor vane segments.

Manufacturing of the RFQ is well advanced [10]. Following delivery of the first section to RAL, inspection showed a manufacturing error resulting in a transverse and longitudinal shift of the vane modulations. This error was traced to a changed datum setting in the 5-axis CNC machine. Although simulations showed that the effect on the beam dynamics would have been acceptable the resulting resonant frequency shift cannot be compensated for. Fortunately the internal surfaces can be re-machined and both major and minor vane segments recovered. Machining of sections 2, 3 & 4 is almost completed.

Resonant frequency measurements of section 1, including the error, showed good agreement with modelling confirming the inspection results. The first bead pull measurements on section 1 with tuneable end flanges have started.

MEBT

The beam optics design of the Medium Energy Beam Transport has been fixed for some time [11]. The first part

Copyright © 2014 CC-BY-3.0 and by the respective authors

ISBN 978-3-95450-142-7

A LINAC-BASED APPROACH TO MODELLING AN ORBIT SEPARATED CYCLOTRON

C. Plostinar, G. Rees, STFC/ASTeC, Rutherford Appleton Laboratory, UK

Abstract

An orbit separated cyclotron (OSC) is a new type of accelerator intended as a proton driver for Accelerator Driven Subcritical Reactors (ADSRs) [1]. A ring has been designed based on the new concept that accelerates a proton beam from 500 MeV to 1 GeV in four turns using multi-cell superconducting cavities in each period. From a beam dynamics point of view, the ring can be considered as a "wrapped-up" linac at four times the ring circumference. In this paper we present beam dynamics modelling details when using 3D linac codes and cavity field maps. We conclude that the versatility of codes such as TraceWin [2], allows detailed machine modelling and improved design procedures that take into account various aspects including orbit distortion caused by transverse deflecting fields in the cavities.

THE ORBIT SEPARATED CYCLOTRON

Accelerator Driven Sub-critical Reactors require proton drivers with a high degree of reliability capable of delivering MW level beam powers. As machine availability is paramount to limit thermal stress damage in the neutron target, new accelerator designs have been proposed as alternatives to conventional accelerators. One recent proposal is the Orbit Separated Cyclotron (OSC). Its underlying goal is to improve reliability by reducing accelerator units and increasing redundancy.

An OSC uses superconducting multi-cell RF cavities in each period and combined function magnets resulting in a spiral beam orbit with only several turns. The magnets have a common yoke, but separated poles for each orbit. Each magnet is subdivided for triplet focusing with adjustable gradients, bending angles and bending radii. Although the beam energy changes in every period, synchronous acceleration is achieved by using orbit length adjustments, reverse bending, and harmonic number jumps. A schematic layout of an OSC arc is shown in Figure 1. A detailed description of the OSC concept is given in [1] and [3].

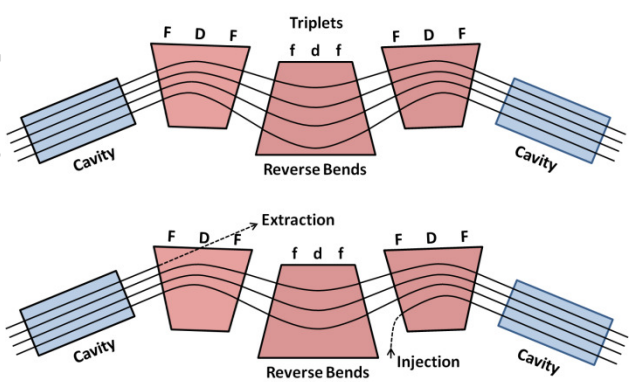


Figure 1: Schematic layout of a typical OSC arc (top), as well as the injection and extraction section (bottom).

Using the OSC concept, a 10 MW acceleration scheme has been designed as a potential ADSR proton driver. The accelerator uses a 250 MeV linac followed by two OSC rings. The first ring accelerates the beam to 500 MeV, while the second to the final energy of 1 GeV (Figure 2). The accelerator operates in CW mode and the beam current is 10 mA. An RF frequency of 324 MHz is used throughout.

ACCELERATOR MODEL

The second OSC ring is further detailed. It has four turns with separated orbits. This is sufficient to double the beam power from 5 to 10 MW. Each turn uses eight superperiods, with cavities placed in each long straight section (eight in total). For comparison, employing the linac for the same energy and power interval, would require four times more superconducting cavities. The average length of a superperiod is ~20 m, while the average ring radius is ~25 m. A schematic ring layout is shown in Figure 2.

From a beam dynamics point of view, an OSC can be regarded as a wrapped-up linac and therefore a linac-based modelling approach has been adopted. Simulation

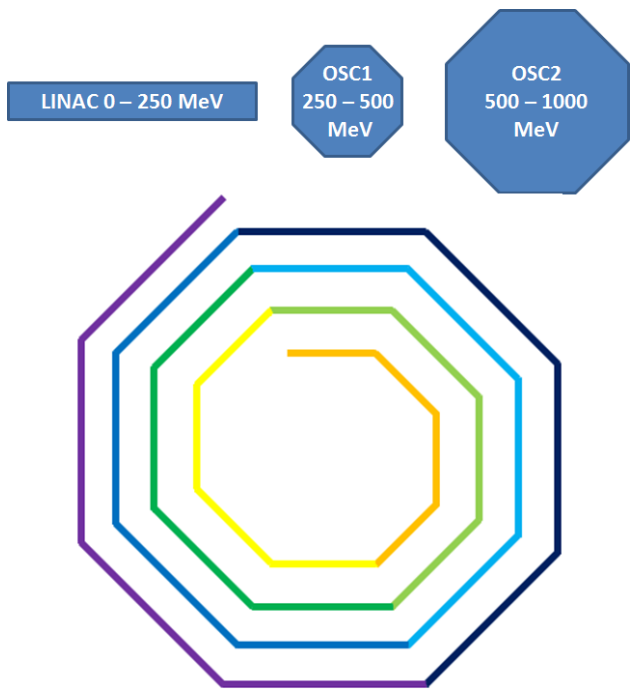


Figure 2: Potential 10 MW accelerator chain (top) and details of the four-turn OSC2 (0.5-1.0 GeV). Colours represent groups of four equal length periods.

Copyright © 2014 CC-BY-3.0 and by the respective authors

DEVELOPMENT OF A MICRO-PULSE ELECTRON GUN BASED UPON PI-MODE DUAL-CAVITY*

L. Liao, M. Zhang, Q. Gu, M. Zhao,
SINAP, CAS, Shanghai 201800, China

Abstract

The concept of a novel micro-pulse electron gun (MPG) based upon π-mode dual-cavity is proposed and analyzed in this paper, and we termed it as dual-cavity micro-pulse electron gun (D-MPG) as compared to single-cavity standard MPG. From simulations, it is clear that the D-MPG is capable of yielding dozens of ampere peak currents and a few ps bunch length. Thought the mechanism for dual cavity is not fully understand, the D-MPG has demonstrate the potential to be the injectors for FEL and THz radiation facilities. Also it is a good candidate to replace the thermal cathode for industrial and medical accelerator system because of the cost-effective of the D-MPG.

INTRODUCTION

The highest brightness mainly relies on the injectors and in particular by the electron gun performance, hence the conceive of the electron gun is of paramount importance. Up to now, the injectors aimed at high quality electron beams are characterized by the following conditions: high gradient cathode field and high cost laser system. However, the high cost of injectors make it a obstacle for wide use around the world. The need for cost-effective gun system has driven the development of the micro-pulse electron gun (MPG) [1-3]. Since the multipacting effect is typically one of major cause of power consumption in the RF devices or failure of ceramic windows, there are many works studied to suppress its adverse effect [4-8]. Also the multipacting effect was found to have amplification function in the cavity [9], the micro-pulse electron gun demonstrate the potentialities of this function by resonant electrons to saturation [1-3]. The concept of micro-pulse electron gun describe a new kind of RF gun as a positive application of multipacting in the cavity.

In this paper, a novel dual-cavity micro-pulse electron gun (D-MPG) as compared to standard MPG is proposed. The standard MPG is widely studied for its simply structure, but it is imperative to note that because of the phase focusing mechanism as will discussed later, the width of micro-pulse is limited by this mechanism. In this point, the standard MPG is hard for further development, so the conceive of dual cavity is necessity. Combined with GaP as the cathode and anode material, the π-mode dual-cavity allows much longer gap distance as well as the cavity voltage, which help to boost the energy high enough to reduce the effect of space charge force. As a result of dual-cavity, it can be shown that the D-MPG give rise to electron beams with a few ps width, which is much better than the standard MPG.

* Work supported by National Basic Research Program of China (973 Program) (Grant No. 2011CB808300)

DUAL-CAVITY DESIGN

D-MPG Simulations

The working principle of MPG can be illustrated as below: The initial electrons in the cavity traverse from cathode to anode by means of their interaction with electromagnetic fields, and they impact the anode after odd multiple of half period and generate secondary electrons. The secondary electrons travel in the opposite direction from anode to cathode. Triggered by the initial electrons, the secondary electrons traverse back and forth between the electrodes until saturation so a series of micro-pulses are expected to export through the grid electrodes.

According to standard MPG, the quality of micro-pulse is confined by the phase focusing mechanism:

$$0 \le \theta_0 \le \arctan(2/N\pi) \quad (1)$$

It can be shown from Eq. (1) that only the electrons which belongs to a small range would survive in the cavity after a few periods, which can be termed as the self-bunching process. As the characteristic of MPG, the pulse is bunched in the cavity and steady output at saturation, that is the reason for the name "micro-pulse gun" . The Eq. (1) predict the width of pulse, which is about 9% of the period of RF field, and in the 2.856 GHz case, the value is found to be about 31.5 ps at the base of the pulse. It is important to note that the full width at half maximum (FWHM) of the pulse is about 15 ps, which results in good agreement with the results from reference [2]. Unfortunately, This width is limited to a constant value and hard to low further. The scale of width is preferable for the industrial accelerator systems, but not for the FEL or some kind of units which need sub-ps width beam quality.

So how to decrease the pulse width is the purpose of this paper, in what follows we will represent the dual-cavity structure in the MPG, namely D-MPG. The working principle of D-MPG is a little different from that of standard MPG, while the time for electrons to fly from one electrode to another electrode is even multiple of half period. For the reasons as will discussed below, this structure will provide a possibility to increase the quality of beams.

The D-MPG simulations were carried out by

Copyright © 2014 CC-BY-3.0 and by the respective authors

MEASUREMENTS OF CAVITY MISALIGNMENT BY BEAM INDUCED HOM EXCITED IN 9-CELL SUPERCONDUCTING CAVITIES

A. Kuramoto#, The Graduate University for Advanced Studies [Sokendai], Tsukuba, Japan
H. Hayano, KEK, Tsukuba, Japan
N. Baboi, DESY, Hamburg, Germany

Abstract

Detection of cavity misalignment in the ILC superconducting cavities inside of the cryomodules can be done by using beam induced Higher Order Modes (HOM). It is beneficial to identify possible source of emittance growth by cavity misalignment.

Beam pipe modes which are localized in both ends of the cavity and TE111 1/9 pi mode which is localized in the center of the cavity are focused in this research. Deviations of these electrical centers from beam trajectory reference indicate cavity misalignment and bending. We measured beam-induced HOM in STF cavities of the STF accelerator at KEK in 2012 – 2013 [1] and TESLA cavities of FLASH at DESY in 2013 [2]. We could identify beam pipe modes and TE111 1/9 pi mode in STF cavities and TESLA cavities at around 2.1 GHz and 1.6 GHz, both of which were very small signals. In addition, we have measured beam induced HOM signals at FLASH in May 2014. We discuss this measurement in this paper.

Furthermore the electrical centers of these beam pipe mode are studied by stretched wire method, beads perturbation method and simulations by HFSS 12 [3]. The results of these measurements and simulations are also summarized.

BEAM INDUCED HOM MEASUREMENT

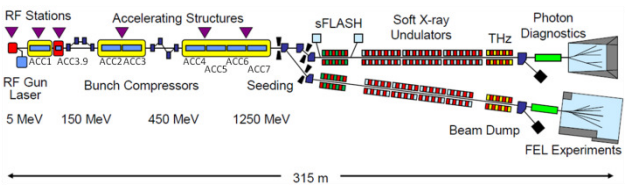


Figure 1: Layout of FLASH accelerator [4].

We measured beam induced HOM at FLASH twice. At the first measurement, some dipole-like modes, the one believed to be beam pipe modes, are found for the 8th TESLA cavity (Cav8) in the 7th cryomodule (ACC7) in September 2013.

In the second experiment, we measured beam induced HOM in the 8th TESLA cavity (Cav8) in the 5th cryomodule (ACC5).

We changed electron beam orbit by using two dipole magnets which are H3DBC3 and V3DBC3 located at upstream of ACC4. Estimated beam positions in the middle of ACC5Cav8 are plotted in Fig.2. These beam positions are estimated from two beam position monitors (BPM) located at upstream and downstream of ACC5.

Ignoring beam orbit changes due to Q magnet switched on, and assuming that beam positions are strongly correlated to dipole magnets setting value even though beam passed out of range BPM linearity, beam orbits are calculated with linearly passing between two BPM.

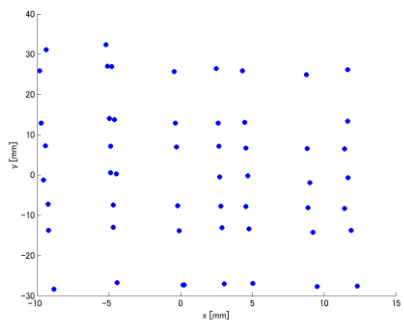


Figure 2: Beam Positions used in beam induced HOM measurements.

A layout of measurement setup is shown in Fig.3. One cavity has two HOM couplers. HOM signal picked up by each HOM coupler was divided twice. We measured the one of signal divided by the first splitter. The other signal was measured by the other measurement group. Two high pass filters (VHF-1500+) which cut off the main RF power whose frequency is 1300 MHz were added before the second splitter were connected. Then HOM signal were divided again for two different frequencies. Branch 1 for TE111-1 consisted of a band pass filter (BPF) from 1605 to 1785 MHz and two amplifiers (ZX60-1614LN-S) whose gain is 14 dB and noise figure is 0.5 dB from 1217 to 1620 MHz. Then branch 2 for beam pipe modes consisted of a BPF from 2100 to 2210 MHz and an amplifier (ZRL-2400LN) whose gain is 28 dB and noise figure is 1.2 dB. Finally, both branches were connected to an oscilloscope (TDS7404). One waveform data taken by the oscilloscope has 200 k points with 5 GSa/s.

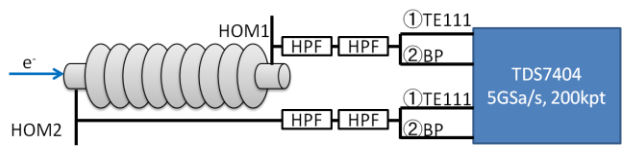


Figure 3: Measurement Setup.

Spectrums of TE111-1 and beam pipe mode (BP) are described as FFT of waveform data in Fig.4-1 and Fig. 5-1.

#kuramoto@post.kek.jp

Copyright © 2014 CC-BY-3.0 and by the respective authors

SUPERCONDUCTING ACCELERATING CAVITY PRESSURE SENSITIVITY ANALYSIS AND STIFFENING

J. Rodnizki*, Yakir Ben Aliz, Asher Grin, Zvi Horvitz, Amichay Perry, Leonid Weissman (Soreq NRC, Yavne), Kirk Davis (JLAB, Newport News, Virginia), Jean Roger Delayen (ODU, Norfolk, Virginia)

Abstract

The Soreq Applied Research Accelerator Facility (SARAF) design is based on a 40 MeV 5 mA light ions superconducting RF linac. Phase-I of SARAF delivers up to 2 mA CW proton beams in an energy range of 1.5 - 4.0 MeV. The maximum beam power that we have reached is 5.7 kW. Today, the main limiting factor to reach higher ion energy and beam power is related to the HWR sensitivity to the liquid helium coolant pressure fluctuations. The HWR sensitivity to helium pressure is about 60 Hz/mbar. The cavities had been designed, a decade ago, to be soft in order to enable tuning of their novel shape. However, the cavities turned out to be too soft. In this work we found that increasing the rigidity of the cavities in the vicinity of the external drift tubes may reduce the cavity sensitivity by a factor of three. A preliminary design to increase the cavity rigidity is presented.

INTRODUCTION

Phase-I of the Soreq Applied Research Accelerator Facility (SARAF) proton/deuteron linac is currently operational at Soreq Nuclear Research Center [1]. Phase-I of the linac has been built in order to study and prove novel acceleration technologies for intense CW beams. The SARAF Prototype Superconducting Module (PSM) houses six 176 MHz Half Wave Resonators (HWR) and three Super Conducting (SC) 6T solenoids. The PSM was designed and built by Accel/RI [2] (Fig. 1). The PSM accelerates protons and deuterons from 1.5 MeV/u to 4 and 5 MeV [1], respectively. The HWR nominal design goal was 850 kV for a 4 mA ion beam at β_{opt}=0.09. The HWRs were found to be highly sensitive to the coolant liquid helium pressure fluctuations. The measured HWRs sensitivity to helium pressure, 60 Hz/mbar, is an order of magnitude larger than currently designed similar shape cavities. Reducing the cavity sensitivity to the helium liquid coolant pressure fluctuations may enable SARAF Phase-I to reach a CW proton beam current and energy of 4 mA and 4 MeV, respectively.

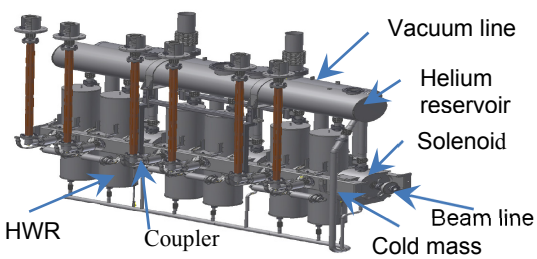


Figure 1: The inner parts of the 2.5 m long PSM.

*Jacob@soreq.gov.il

The 3 mm thick, single wall, bulk Nb superconducting cavity is assembled in a SS liquid helium (LHe) vessel (Fig. 2,3,4). The Nb cavity and the SS vessel are connected by bellows in the beam, vacuum and coupler ports.

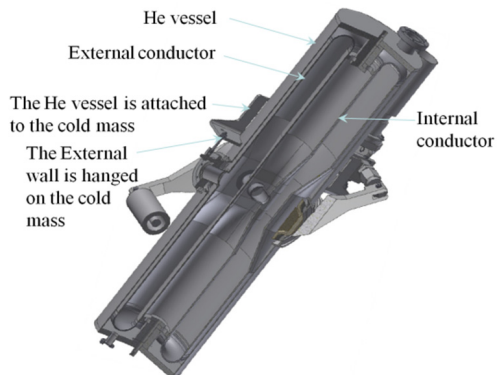


Figure 2: The HWR liquid helium vessel with the superconducting HWR assembly.

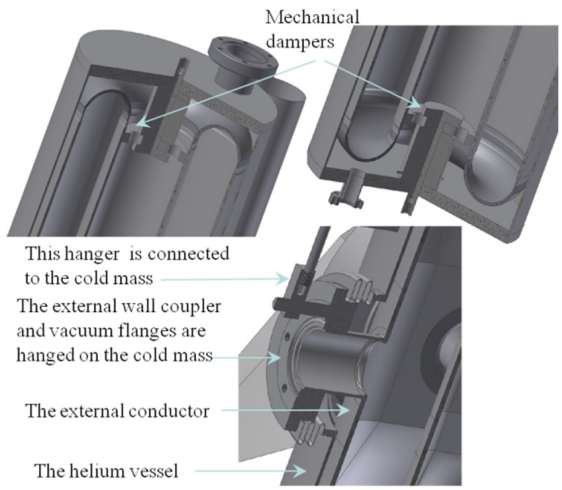


Figure 3: The top and bottom mechanical dampers fix the horizontal position of the HWR internal wall. The mechanical hanger fixes the position of the external wall, coupler and vacuum SS flanges.

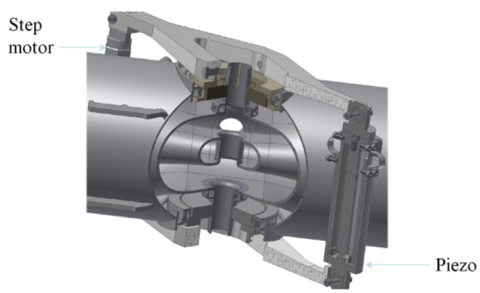


Figure 4: The piezo and step motor mechanical tuning system that controls the HWR resonance frequency [3].

Copyright © 2014 CC-BY-3.0 and by the respective authors

ISBN 978-3-95450-142-7

EXACT SOLUTIONS OF THE VLASOV EQUATION IN MAGNETIC FIELD *

O.I. Drivotin, D.A. Ovsyannikov, St.-Petersburg State University, St.Petersburg, Russia

Abstract

Stationary self-consistent distributions for charged particle beam in magnetic field are considered. These distributions can be regarded as formal solutions of the Vlasov equation which is formulated in the covariant form.

COVARIANT FORM OF THE VLASOV EQUATION

Dynamics of a charged particle beam can be described as dynamics of all individual particles composing it. Another model of the beam dynamics is the Vlasov equation which is an integro-differential equation for density of the particle distribution in the phase space.

Let us formulate the Vlasov equation in covariant form following the works [1,2]. Firstly, let us specify a reference frame and introduce the phase space $\mathcal{M}$ as the tangent bundle of the configuration space associated with given reference frame [3,4]. If particles always lie on the same surface S in the phase space, or distribution density does not depend on some coordinate, then the phase space $\mathcal{M}$ can be taken as coresponding subspace of the initial phase space.

Define the particle distribution density in the phase space (phase density) [1, 2] as such differential form $n(t,q)$ of degree p that for any open subdomain $G \subset \mathcal{M}$

$$\int_D n = N_G. \tag{1}$$

Here N_G is a number of particles in G, t is the time, $q \in \mathcal{M}$. If particle lie in some open subdomain of $\mathcal{M}$, then $p = \dim \mathcal{M}$, $D = G$. If all particles lie on some surface S in the phase space, then $p = \dim S$, $D = S \cup D$. The latter case includes as a particular case a set of point-like particles. In this case, the phase density is a form of degree 0, i.e. a scalar function, and integration over D is the summation over all particles lying in G.

In all cases the Vlasov equation can be written in the form [1,2]

$$n(t+\delta t, F_{f,\delta t}q) = F_{f,\delta t}n(t,q). \tag{2}$$

Here $F_{f,\delta t}q$ denotes Lie dragging along vector field f [4], which is defined by the dynamics equation $dq/dt = f$, and depends on an external field and the self field.

Consider the case when particle distribution is described by the form of maximal degree. Assume that its single component $\tilde{n}$ is continuously differentiable on phase coordinates. Ho do this component change at some point q of the phase space depending on the time t?

Let the phase density at some instance t at a point q be equal to $n(t,q)$. At the instance $t+\delta t$ in this point, it will be equal to $n(t+\delta t,q) = F_{f\,\delta t}n(t, F_{f\,-\delta t}q)$, as the phase density change according to equation (2). Introduce the derivative of a differential form on the parameter t as a form which components are derivatives of corresponding components on t. Then we obtain the Vlasov equation in the form

$$\frac{\partial n}{\partial t} = \lim_{\delta t \to 0} \frac{n(t+\delta t,q) - n(t,q)}{\delta t} = -\mathcal{L}_f n(t,q). \tag{3}$$

Here $\mathcal{L}_f n(t,q)$ denotes the Lie derivative of the phase density along the vector field f. Components of the Lie derivative of a differential form of degree p can be written in the form

$$(\mathcal{L}_f T)_{i_1\ldots i_p} = \frac{\partial T_{i_1\ldots i_p}}{\partial q^k} f^k + \frac{\partial f^j}{\partial q^{i_1}} \cdot T_{j\,i_2\ldots i_p} + \tag{4}$$

$$\ldots \frac{\partial f^j}{\partial q^{i_p}} \cdot T_{i_1\ldots i_{p-1}\,j} \tag{5}$$

(summation is meant on coincident indices).

LONGWISE UNIFORM BEAM

Consider stationary longitudinally uniform axially symmetric beam in a uniform longiduninal magnetic field [7-13]. Uniformity means that phase distribution does not depend of longituninal coordinate z. Assume also that longitudinal velocities v^z of all particles are the same. Then we can consider particle distribution in 4-dimensional phase space. Axial symmetry means that the phase density and density in the configuration space do not depend of azimuthal angle φ. Then electric field potential U depends only on radial coordinate r : $U = U(r)$. In this case, particle dynamics equations give the first integrals of motion M and H in the form

$$M = r^2(\dot{\varphi} + \omega_0) = const, \tag{6}$$

$$H = \dot{r}^2 + \omega_0^2 r^2 + M^2/r^2 + 2\varepsilon U(r) = const. \tag{7}$$

Here $\omega_0 = eB_z/(2m\gamma)$, $\varepsilon = e/(m\gamma^3)$, e and m are charge and mass of a particle, B_z is $z-$component of the magnetic flux density, γ is the Lorentz factor.

Assume that function $\omega_0^2 r^2 + M^2/r^2 + 2\varepsilon U(r)$ is strictly convex. Then $\varphi, M,$ and H define a particle trajectory. Therefore φ, M, H, and the phase of the trajectory θ can be taken as particle coordinates in the phase space. Additionally assume that particles are evenly distributed on phases of a trajectory. It means that trajectory segments corresponding to equal time intervals contain equal number of particles. This assumption provides the stationarity of the distribution.

As distribution is uniform on φ and θ, consider two-dimensional supspace with coordinates M and H as the

* Work supported by St.-Petersburg State University grant #9.38.673.2013

Copyright © 2014 CC-BY-3.0 and by the respective authors

DESIGN PROGRESS OF THE MYRRHA LOW ENERGY BEAM LINE

R. Salemme, L. Medeiros Romão, D. Vandeplassche, SCK•CEN, Mol, Belgium
D. Uriot, CEA-DSM/IRFU/SACM, Saclay, France
J.-L. Biarrotte, CNRS-IN2P3/IPNO, Orsay, France
M. Baylac, D. Bondoux, F. Bouly, J.-M. De Conto, E. Froidefond,
LPSC, Université Grenoble-Alpes, CNRS/IN2P3, Grenoble, France

Abstract

The MYRRHA project, a flexible spectrum neutron irradiation facility, is designed according to the Accelerator Driven System (ADS) reactor concept. The MYRRHA driver consists of a high power superconducting proton linac. A prototype of the front end injector is being built up into a test platform conceived to experimentally address its design issues. Currently, the ECR proton source has been industrially procured. LPSC Grenoble designed the subsequent Low Energy Beam Transport (LEBT) section. Right before the RFQ, a short section hosts an electrostatic beam chopper producing carefully controlled beam interruptions. In this paper the status of the LEBT design with the associated beam instrumentation is reviewed. Future experimental plans including LEBT beam characterization and optimization of the beam transmission are presented.

INTRODUCTION

The MYRRHA project, proposed by SCK•CEN, aims to demonstrate the feasibility and operability of a safe and efficient transmuter reactor, comprising a subcritical core fed by an external spallation neutron source, in turn obtained by an high intensity proton beam delivered by a superconducting linac. The specifications set on the MYRRHA accelerator are typical for ADS [1, 2]: in particular, the issue of reliability is considered the main design challenge and concerns all the R&D activities [3]. In the framework of the RFQ@UCL R&D program [4], a test platform of the MYRRHA Linear Accelerator Front-End is being built-up to experimentally address the injector design through prototyping. The program is a collaborative effort of SCK•CEN, the Cyclotron Resources Center (UCL/CRC), the CNRS/IN2P3 laboratories IPN Orsay (IPNO) and LPSC Grenoble, the IAP Frankfurt laboratory. Currently, the 30 keV proton source industrial procurement has been achieved with the successful production of a stable beam. The subsequent Low Energy Beam Transport (LEBT) line has been engineered and designed by LPSC and entered the construction phase in late 2013. First beam tests are scheduled for late 2014 in Grenoble.

THE ION SOURCE

The proton source has been procured by Pantechnik (France). The design choice is an Electron Cyclotron Resonance (ECR) ion source at 2.45 GHz. A specific flat magnetic confinement configuration is provided by two Permanent Magnets (PMs), while tapered axial RF injection up to 1.2 kW is adopted. Beam is extracted from the plasma chamber by a multi-stage cascade of polarized electrodes. The source extraction box is equipped with a Einzel electrostatic focusing lens, which can be used to adjust the beam size in case of excessive beam divergence at this stage. During the acceptance tests, the source has been capable to deliver a 30 keV proton beam up to 16 mA (DC), with a vertical beam emittance of $\sim 0.1\pi$·mm·mrad RMS norm. at 5 mA H^+. The total beam production efficiency has been estimated around 84% (comprising HV losses), with particular ionization efficiency of ~63% for H^+. Long test runs (24 hours) showed a good beam stability, with brief recovery time in case of electrical discharges. Preliminary investigations on the influence of the Einzel lens on the transverse beam emittances are currently performed. The goal is to optimize the extraction settings in view of the future LEBT line commissioning.

THE MYRRHA LEBT

The MYRRHA LEBT layout is based on a short magnetic solution and is designed to maximize the proton beam quality injected into the RFQ by considering the Space Charge Compensation (SCC) effects of the beam. At the same time, this solution helps to fulfill the ADS reliability requirements, minimizing beam trip risks due to HV breakdowns and beam losses [5].

The overall length of the line, from the plasma chamber extraction hole to the RFQ rods, is around 2.8 m. The beam transport and focusing is assured by a pair of solenoid magnets with integrated dipole steerers. The first set is placed as close as possible to the ion source so as to limit the beam size at this stage. The second is situated at the end of the line and allows a net beam species separation. A magnetic model of the magnet set has been created in OPERA 3D. A nominal axial magnetic field B_0= 0.25 T at the center of the solenoid is obtained through a total of 48900 At generated by 496 hollow copper turns. Two separate inner windings produce an additional transverse component for dipole corrections (H&V) up to 12.5 mrad. The inner solenoid diameter (including steerers' coils) is 158 mm, a good compromise to minimize geometrical aberrations potentially leading to emittance growth. Particular care was taken in limiting stray magnetic fields to a maximum of 3.3 mT on the solenoid axis at 300 mm from its center. Solenoid magnets are currently under industrial procurement from

Copyright © 2014 CC-BY-3.0 and by the respective authors

ISBN 978-3-95450-142-7

FABRICATION AND MEASUREMENTS OF 500 MHz SUPERCONDUCTING DOUBLE SPOKE CAVITY*

HyeKyoung Park[2,1#], C. S. Hopper[1], J. R. Delayen[1,2]
[1] Center for Accelerator Science, Old Dominion University, Norfolk, VA 23529, USA
[2] Thomas Jefferson National Accelerator Facility, Newport News, VA 23606, USA

Abstract

A 500 MHz β_0=1 double spoke cavity has been designed and optimized for a high velocity application such as a compact electron accelerator at the Center for Accelerator Science at Old Dominion University [1] and the fabrication was recently completed at Jefferson Lab. The geometry specific to the double spoke cavity required a variety of tooling and fixtures. Also a number of asymmetric weld joints were expected to make it difficult to maintain minimal geometric deviation from the design. This paper will report the fabrication procedure, resulting tolerance from the design, initial test results and the lessons learned from the first β_0=1 double spoke cavity fabrication.

ELECTROMAGNETIC DESIGN

A superconducting double spoke cavity was optimized to minimize the peak surface fields while maximizing the shunt impedance. It was designed to operate at 4.2K to lower the operating cost. Table 1 shows the radio frequency (RF) and geometric properties of the cavity design.

Table 1: Properties of β0=1 Double Spoke Cavity [1]

Parameter	Value	Units
Frequency	500	MHz
Cavity diameter	416	mm
Cavity length	805	mm
Aperture diameter	50	mm
R/Q	675	Ω
QR_s	174	Ω
E_p/E_{acc}	3.7	-
B_p/E_{acc}	7.6	mT/(MV/m)
B_p/E_p	2.05	mT/(MV/m)

†Reference length=$3\beta_0\lambda/2$

* Work supported by U.S DOE Award No. DE-SC0004094. Authored by Jefferson Science Associates, LLC under U.S. DOE Contract No. DE-AC05-06OR23177. The U.S. Government retains a non-exclusive, paid-up, irrevocable, world-wide license to publish or reproduce this manuscript for U.S. Government purposes.
# hkpark@jlab.org

FABRICATION

The double spoke cavity was divided into symmetric sections in order to reduce the number of forming dies and weld joints. A total of four forming dies were made: spoke half, end cap, 50 mm ID beam pipe, and 40 mm ID ancillary port. The outer cylindrical conductor half was rolled in multiple steps instead of using forming dies. The radius was verified by a template. Figure 1 shows the formed spoke half and end cap.



Figure 1: Formed spoke half and end cap.

The spoke halves were trimmed and welded along with a beam pipe to form a spoke subassembly. Then, the spoke base, where it joins the outer cylindrical conductor, was trimmed. Figure 2 is the complete spoke subassembly being measured on the coordinate measuring machine (CMM). A total of 152 points were measured, the best fit model was constructed, and compared with the cavity model. Figure 2 also shows the results.

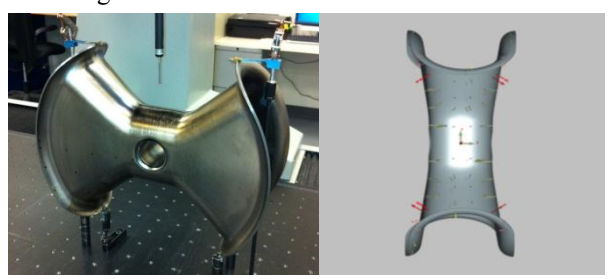


Figure 2: Welded spoke and CMM results showing deviations from the cavity model.

The forming die of the spoke half was within .13 mm (.005 inch) of the design profile. However, the spoke assembly showed a spring back with a maximum deviation of 2.8 mm (.111 inch). The deviation was symmetric about the central plane.

The openings for the spoke base in the cylindrical conductor halves were machined while the cylinder was held in a fixture. The machined profile is perpendicular to the surface, which makes the cut cross section uniform 1/8 inch throughout. This provides a uniform butt weld joint with a constant electron beam parameter during welding. Figure 3 shows the weld fit-up of the spoke

Copyright © 2014 CC-BY-3.0 and by the respective authors

ISBN 978-3-95450-142-7

STUDIES OF CSR IN THE JEFFERSON LAB FEL DRIVER WITH IMPLICATIONS FOR BUNCH COMPRESSION*

C. Tennant#, D. Douglas, R. Li
Thomas Jefferson National Accelerator Facility, Newport News, VA 23606, USA
C.-Y. Tsai
Virginia Polytechnic Institute and State University, Blacksburg, VA, 24061, USA

Abstract

The Jefferson Laboratory IR FEL Driver provides an ideal test bed for studying a variety of beam dynamical effects. Recent studies focused on characterizing the impact of coherent synchrotron radiation (CSR) with the goal of benchmarking measurements with simulation. Following measurements to characterize the beam, we quantitatively characterized energy extraction via CSR by measuring beam position at a dispersed location (a direct measure of extracted energy) as a function of bunch compression. In addition to operating with the beam on the rising part of the linac RF waveform, measurements were also made while accelerating on the falling part. For each, the full compression point was moved along the backleg of the machine and the response of the beam (distribution, extracted energy) measured. Initial results of start-to-end simulations using a 1D CSR algorithm show remarkably good agreement with measurements. A subsequent experiment established lasing with the beam accelerated on the falling side of the RF waveform in conjunction with positive momentum compaction (R_{56}) to compress the bunch. The success of this experiment motivated the design of a modified CEBAF-style arc with control of CSR and microbunching effects.

BACKGROUND

Virtually all existing high energy linac-driven FELs compress bunch length through use of off-crest acceleration on the rising side of the RF waveform followed by transport through a magnetic chicane. Though effective to some degree, this approach has at least three flaws:

1) It is difficult to correct aberration effects, particularly phase space distortion due to RF curvature. Typically harmonic RF is invoked in response, at considerable expense and with the difficulties attendant to the use of high frequency resonant cavities.
2) Acceleration on the rising side of the RF waveform exacerbates some aspects of longitudinal space charge (LSC) induced degradation of beam quality, resulting in reduced peak current when interacting with coherent synchrotron radiation (CSR) effects.
3) Chicanes necessarily create a parasitic compression of the bunch during the final compression process and expose the (somewhat over-compressed) bunch to interaction with coherent transition radiation from the end of the penultimate dipole of the compressor.

It is possible to avoid all of these deficiencies by using acceleration on the falling side of the RF waveform and using a bunch compressor with $R_{56} > 0$ [1].

INTRODUCTION

Recent studies at the Jefferson Lab IR FEL Upgrade Driver focused on characterizing the impact of CSR with the goal of benchmarking measurements with simulation. The Driver is an energy recovery based linear accelerator used to condition an electron beam for high average power lasing in the infrared. Electrons are generated in a DC photocathode gun (135 pC), accelerated to 9 MeV and injected into the linac where they are further accelerated up to 130 MeV through three cryomodules. The spent electron beam is recirculated and phased in such a way that the beam is decelerated through the linac on the second pass. Nominal acceleration occurs off-crest at –10° to impart a phase-energy correlation across the bunch. The first- and second-order momentum compactions of the first Bates-style recirculation arc are set so that, in conjunction with the downstream chicane, the bunch is rotated upright at the wiggler and phase space curvature is eliminated. Following the undulator, the longitudinal phase space must be rotated back by 90° to energy compress the beam.

MEASURED EFFECT OF CSR

The experimental program consisted of characterizing the effects of CSR for two different longitudinal matches: accelerating on the rising (falling) side of RF waveform together with a negative (positive) momentum compaction for compression.

Accelerating 10° Before Crest

Measurements were made to quantify the effect of parasitic compressions on beam quality through the first Bates bend. With the nominal energy chirp the beam experiences 3 parasitic compressions. Quadrupole scans were performed at several locations around the machine and repeated with the linac cross-phased. Cross-phasing refers to switching the accelerating phase of only the middle cryomodule (which has the same gradient as the two outboard cryomodules combined) to the falling side of the RF waveform. Upon exiting the linac the energy

*Authored by Jefferson Science Associates, LLC under U.S. DOE Contract No. DE-AC05-06OR23177, the Office of Naval Research and the High Energy Laser Joint Technology Office. The U.S. Government retains a non-exclusive, paid-up, irrevocable, world-wide license to publish or reproduce this manuscript for U.S. Government purposes.
#tennant@jlab.org

Copyright © 2014 CC-BY-3.0 and by the respective authors

SIMULATIONS FOR THE HIGH GRADIENT, LOW EMITTANCE SUPERGUN RF PHOTOINJECTOR

A. Cahill, A. Fukasawa, J. Rosenzweig, UCLA, Los Angeles
B. Spataro, INFN, Frascati
A. Valloni, CERN, Geneva, Switzerland
L. Failace, RadiaBeam Technologies, Los Angeles

Abstract

A new S-Band photoinjector is being developed at UCLA that will feature a large accelerating gradient at 160 MeV/m creating a beam with approximately 6.5 MeV at the exit. Because of the large accelerating gradient and other considerations, such as cooling and manufacturing, the new Supergun will be coupled into using a coaxial method, rather than side coupling. With the large accelerating gradient we hope to create very low emittance beams on the order of 0.025 mm mrad. These beams can then be used for a number of purposes, mainly for high quality beams used in FELs. Electric simulations have been done using HFSS and Superfish. Heating and mechanical simulations were done using Ansys. Finally, beam simulations were completed with GPT.

INTRODUCTION

One of the large problems in creating suitable electron beams for X-Ray FELs such as LCLS is creating a low emittance beam inside the undulator. If the emittance of the electron beam is larger than the emittance of the photons [1], where the emittance of a photon is $\epsilon = \frac{\lambda}{4\pi}$, then the actual 3D gain length will be larger than the calculated 1D gain length. Due to Louisville's theorem [2] the normalized emittance of an electron beam can only increase along the beamline under energy conserving processes. To solve this the emittance directly following the photoinjector should be minimized. For a 1nm output the emittance is already 0.079 mm mrad, therefore we would require that the electron beam be <0.1 mm mrad. To accomplish this a S-Band BNL/SLAC/UCLA style1.5 cell RF photoinjector was chosen. S-Band was chosen, as opposed to a 11.424 GHz system, due to availability of klystrons. The other consideration is that the breakdown of approximately 240 MV/m in an X-band system compared to 160 MV/m in S-Band is not a large enough increase, particularly when considering the X-band system would likely have a starting phase further from peak voltage, to warrant the increase in complexity for machining and energy supply [3]. A coaxial coupling method was chosen for a few reasons: the focusing solenoid can be placed further upstream to maximize emittance compensation effects, the symmetric nature of the coupling minimizes multipole fields, and the cooling of the gun is more effective since there is no port attached to the full cell [4]. In the following we show a design for a photoinjector useful in low charge and low emittance settings.

RF DESIGN

The RF design was initially done with the 2D code Poisson Superfish [5], then it was finished in the 3D code HFSS from Ansys. The initial cell was chosen to be 0.4 times the distance light travels in half a period of 2.856 GHz. After this the full cell length was chosen so that the electrons would leave the cell as the RF reaches a zero crossing. This can be done using a particle tracking code, in this case GPT [6], where the length is varied until there is no deceleration on the electron beam at the end of the photoinjector. This photoinjector design is able to bring the electron beam to 6.4 MeV. An Elliptical shape was used to decrease the field increase on irises. The outer radii of the cells are chosen so that each cell resonates at the correct frequency. These are then modified slightly so that the fields are balanced between the cells and the entire cavity rings at the correct frequency, in this the fields are even to within 98%. The iris radius was chosen to be small to increase the shunt impedance, and since the gun will not run in a pulsed beam setting, wake fields will not be important to dynamics. The input is designed after the doorknob coupler used in a variety of coaxial designs, namely the Flash gun at DESY [7]. There are two ports on this design, one is an open waveguide and the other is a tunable short. The choice of using one open port rather than two was to avoid the complexity of building a waveguide system to split the incoming RF power that could also add asymmetries into the system. All of the geometry was chosen initially to critically couple the power in, $\beta = 1$ where β is the coupling constant. The β of teh cavity can be calculated by finding the VSWR of the system. If the caivy is under coupled then $VSWR = \frac{1}{\beta}$, and $VSWR = \beta$ when the cavity is overcoupled [8]. It is easy to tell if the cavity is under or over coupled by calculating the Smith chart of the system. This choice of coupling will be examined in the next section.

COUPLING CONSIDERATIONS

From the superfish calculations we can get the quality factor Q, and the shunt impedance per unit lenght Z. Choosing the klystron pulse to be 25MW and to have 1μs of fill time then the final voltage at that microsecond can be calculated [9].

$$E0 = \sqrt{\frac{4\beta Z P_{in}}{L(1+\beta)^2}}\left(1 - e^{\frac{-t\omega_0(1+\beta)}{2Q}}\right)$$

Copyright © 2014 CC-BY-3.0 and by the respective authors

ISBN 978-3-95450-142-7

R&D EFFORTS FOR ERLS

R. Eichhorn
CLASSE, Cornell University, Ithaca, NY 14853, USA

Abstract

Even though the first conceptual idea of an energy recovery linac (ERL) dates back almost 50 years, it took many years to foster the interest in these unique devices. The last few years have seen extensive R&D for ERLs, with several prototype facilities now under construction or in operation. The article reviews the world-wide progress made towards the construction of a large scale energy recovery linac with some focus on the Cornell ERL R&D program that has reached major achievements recently.

INTRODUCTION

The original paper from Tigner dates back to 1965 [1], where he suggested that a beam, being accelerated to a certain energy is decelerated again after interaction, with the energy being recovered in the RF field of the accelerating cavity (see Fig. 1).

At first sight, the concept seems to be a smart way to increase the efficiency of particle accelerators. As we know of today, the energy recovery linac concept if far more as it allows you to combine the advantages of a synchrotron with these of a linear accelerator.

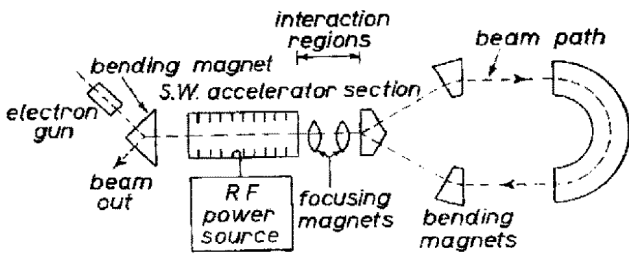


Fig. 3.

Figure 1: The concept of an Energy Recovery Linac (ERL), taken from the the first publication [1].

While todays storage rings usually are operated at high currents (several 100 mA) with high bunch repetition rates (sometimes GHz), the beam parameters are less favourable for future applications: the bunch length of those machines is more in the order of 10 ps, the energy spread is mostly fixed around 10^{-3} relative and moreover, the equilibrium emittance is determined by the ring lattice.

Linear accelerators can provide beams with excellent energy spread (sometimes below 10^{-4}), the bunch length is tunable down to the 100 fs region and they can provide small emittance beams being mainly defined by the emittance of the particle source. However, their limitation comes from the operating cycle being pulsed: linacs have usually low average currents (but can have high peak currents), and, when pushed towards cw operation, they become a huge power consumer.

Energy recovery linacs now allow you to combine the beneficial parameters of both machines. As the energy of the beam is almost fully recovered there are now power limits on the duty cycle- which allows you to ramp up the average current- assuming one is able to provide the beam by a source. As a matter of fact, an energy recovery linac, which is based on superconducting RF, is a very interesting option for future synchrotron radiation sources [2]. They open up new paths for future x-ray science as they are able to deliver defraction limited photon beams that can hardly be achieved with existing machines.

The basic principles of ERL operation were demonstrated in the late 1980's [3] and first applied to a low-energy dedicated machine at the Thomas Jefferson National Accelerator Facility (JLab) in the last half of the 1990's [4]. Since then, the last few years have seen extensive R&D for ERLs, with several prototype facilities now under construction or in operation. They address the challenges of ERL operation, which mainly fall into three categories: generating high current and high charge bunches, getting and conserving small emittance beams and ensuring a highly efficient acceleration with superconducting cavities while keeping beam driven excitations (BBU) controlled and small.

In addition, possible applications of ERL concepts have expanded which includes light source design, beam cooling applications and collider or thin target applications for nuclear physics.

ERL FACILITIES

FEL/ERL @ JLab

Jefferson Lab has been pioneering in ERL operation. Since the late 90' the JLab FEL has been pushing the limits, achieving ultra-fast (~150 fs), ultra-bright (10^{23} photons/s/mm^2/mrad^2/0.1%BW) laser beams. Being the first high current ERL the machine produced a 14 kW average power IR beam.

The electron energy can be up to 135 MeV with up to 135 pC pulses at a repetition rate of 75 MHz. Currently, proof of principle experiments are conducted to simulate high-power ERL operation with an internal gas target to address dark light search. In order to controlling power

#r.eichhorn@cornell.edu

Copyright © 2014 CC-BY-3.0 and by the respective authors

THE MAX IV LINAC

S. Thorin, J. Andersson, F. Curbis, , M. Eriksson, O. Karlberg,
D. Kumbaro, E. Mansten, D. Olsson, S. Werin, MAX IV Laboratory, Lund, Sweden

Abstract

The MAX IV linac will be used both for injection and top up into two storage rings, and as a high brightness injector for a Short Pulse Facility (SPF). The linac has also been designed to handle the high demands of an FEL injector. In the storage ring injection mode, the linac is operated at 10 Hz with a thermionic RF gun and the electron bunches are kicked out from the linac at either 3 GeV or 1.5 GeV to reach the respective storage ring. For the Short Pulse mode the linac will operate at 100 Hz with a high brightness photo cathode gun. Compression is done in two double achromats with positive R56 and the natural second order momentum compaction, T566, from the achromats is used together with weak sextupoles to linearise longitudinal phase space, leaving no need for a linearising harmonic cavity. The achromat design for bunch compression produces very short, high peak power electron pulses, while minimizing emittance increase. In this paper we present the MAX IV linac design and the status of commissioning which started in March 2014.

BACKGROUND

The MAX IV facility [1] is the successor of the MAX-lab accelerators at Lund University and include two storage rings, a full energy linac and a Short Pulse Facility (SPF). The rings will be operated at 1.5 and 3 GeV. The SPF will be a single pass spontaneous linac lightsource, producing sub-ps spontaneous X-ray pulses. The injector will be flexible enough to drive both injection and top-up for the storage rings, and produce high brightness pulses for the SPF. The long term strategic plan for the facility include an X-ray FEL, and the linac was developed to be fully prepared to handle the high demands for an FEL driver.

Currently the linac system is completely installed and under commissioning while the storage ring building is being finalized and magnet delivery has commenced.

MAX IV LINAC GENERAL DESIGN

For injection and top up to the storage rings a thermionic gun with a pulse train chopper system is used. In high brightness mode we use a 1.6 cell photo cathode gun capable of producing an emittance of 0.4 mm mrad at a charge of 100 pC [2]. The gun will be operated together with a kHz Ti:sapphire laser at 263 nm. The same laser will be used for timing and synchronisation of the whole accelerator.

The acceleration is done in 39 warm S-band linac sections together with 18 RF units, each consisting of a 35 MW klystron and a solid state modulator. The klystrons are operated at the lower power of 25 MW which reduces the operational cost and gives a total redundancy in energy of 0.6 GeV. The RF power will be doubled with a SLED.

The three first RF units are driven individually by a low level RF system, and the main drive line for the remaining 15 RF units is controlled by extracting power from the last of these LLRF stages. The RF phase can be set individually in the first three stages and power can be set individually for all RF units. The MDL is situated inside the linac tunnel and is attached to the linac in such a way that it will follow the length variations of the linac and help keep the phases stable.

The lattice in the main linac is made with few magnets for simplicity and reduction of vibration sensitivity. Matching is done before each bunch compressor, and the beam is focused with one triplet before each injection extraction point. This means that only 6 quads are used through the whole main linac, about 200 m. This restrictive use of quads leads to a simple, stable and cost effective lattice, that is easy to operate and tune.

The beam is kicked out for injection into the storage rings at 1.5 and 3 GeV. Bunch compression is done in double achromats at 260 MeV and at full energy, 3 GeV, after extraction to the storage ring. A schematic view of the layout can be seen in figure 1. BC2 is not only used for bunch compression, but also works as a beam distributor for a few beamlines. This is done by letting all electrons pass through the first achromat, and then chose where, in a long transport, to extract the bunch in the second, compressing achromat.The second exit is used for the Short Pulse facility in the current MAX IV plan. The first exit achromat would be used to lead the beam into the linac extension for a possible FEL.

SELF LINEARISING BUNCH COMPRESSORS

The two magnetic double achromats used as bunch compressors in the MAX IV linac has a positive R56 unlike the commonly used magnetic chicane which has a negative R56. The energy chirp needed for compression is done by accelerating the electrons on the falling slope of the RF voltage. Both types of bunch compressors naturally have a positive T566 and in the case of a BC with positive R56 this has a linearising effect on the longitudinal phase space. We can thus choose the optical parameters in the achromat to get optimal linearisation without needing to have a harmonic linac for this purpose [3].

A sextupole is used in the center of each achromat to minimize the second order dispersion at the end. This sextupole is rather weak and could be compared with the chromaticity compensating sextupoles in a storage ring. These sextupoles are also used to tweak the linearisation through the bunch compressor. The natural T566 of the double achromats is

Copyright © 2014 CC-BY-3.0 and by the respective authors

ISBN 978-3-95450-142-7

THE NEW LCLS-II PROJECT: STATUS AND CHALLENGES*

John N. Galayda# (representing the LCLS-II Collaboration), SLAC National Accelerator Laboratory, Menlo Park, California, USA

Abstract

The LCLS-II was an upgrade of the LCLS which essentially replicated the LCLS in another tunnel using the middle 1/3 of the SLAC S-band linac. In August 2013, the project was doubled in scope and redirected towards providing MHz-rate x-ray pulses from 0.2 to 5.0 keV while still supporting the ongoing program at the LCLS. The new accelerator is now based on a 4.0 GeV SCRF linac installed in the front of the SLAC linac tunnel. Key features of the LCLS-II linear accelerator are described, so that LCLS-II can be responsive to the July 2013 recommendation of DOE BESAC for a fully coherent, CW FEL with photon energies up to ~5 keV.

INTRODUCTION

The Linac Coherent Light Source (LCLS) [1,2] started as a 1992 proposal to employ the third kilometer of the 3 km SLAC linac to create an x-ray free-electron laser. This proposal was followed by a comprehensive design study and numerous workshops on the scientific potential of an x-ray free-electron laser. In 2000, the US Department of Energy (DOE) Office of Science officially recognized the need to build such a facility. Groundbreaking took place in 2006 and the LCLS produced first x-rays in April 2009. Since then, LCLS has become a major scientific user facility hosting thousands of experimenters per year at one of the six x-ray experiment stations that share the single x-ray source. The high energy of the LCLS copper linac has enabled LCLS to produce very intense x-ray pulses with >2 mJ concentrated in a few 10's of femtoseconds. SLAC began planning an expansion of the facility very soon after operations began. LCLS was designed to support several options for expansion which have been developed in various degrees since 2010 [3,4,5]; some of these options have been developed into mature concepts. By July 2013, SLAC had prepared a complete design for adding two x-ray sources in a new tunnel. The second kilometer of the SLAC linac was to be dedicated to these two sources, while the original LCLS linac would continue to serve the LCLS undulator. In July 2013, the DOE Basic Energy Sciences Advisory Committee concluded [6] that duplicating the 120Hz repetition rate of the SLAC linac in LCLS-II would limit the scientific reach of the facility; a pulse repetition rate in the kHz to MHz range would be necessary to meet future needs. This advice prompted SLAC to propose a sweeping change to the LCLS-II project.

During August and September of 2013, the project was re-planned [7]. Rather than use another portion of the SLAC linac, LCLS-II will construct a new 4 GeV CW superconducting linac in the first kilometer of the SLAC linac tunnel. Two new undulator x-ray sources will be installed in the existing LCLS undulator hall. A soft x-ray (SXR) source (200-1,300 eV) will occupy an area reserved for a future undulator during construction of LCLS, and the original fixed-gap LCLS undulator will be replaced by a new variable-gap hard x-ray (HXR) source. Both undulators will be configured to receive electrons simultaneously from the new superconducting linac. In addition, the HXR source will be configured so that it may be switched to receive >14 GeV electrons from the LCLS "copper" (Cu) linac at 120 Hz. In this configuration, the HXR source can produce a beam of coherent x-rays, extending the spectral coverage of the facility to 25 keV.

THE LCLS-II PROJECT COLLABORATION

A collaboration of six institutions has been formed to design and construct LCLS-II. Thomas Jefferson National Accelerator Facility (JLAB) will design and acquire the cryogenic refrigeration system and assemble half of the 1.3 GHz cryomodules. Fermi National Accelerator Laboratory (FNAL) will design and acquire the helium distribution system and 3.9 GHz modules. FNAL will also make the necessary design changes to 1.3 GHz modules and assemble ½ of the cryomodules. Lawrence Berkeley National Laboratory (LBNL) is responsible for design/performance optimization and fabrication of the 187 MHz photocathode electron gun as well as the 53 undulator magnets required for the two x-ray sources. Argonne National Laboratory (ANL) will support the FNAL cryomodule effort and provide aluminium vacuum chambers for the undulators. Cornell University is a collaborator in the effort to achieve major improvements in performance of the superconducting cavities. Cornell is also conducting theoretical and experimental studies of the capabilities of its DC gun design, an alternative choice for the LCLS-II injector. SLAC, the host laboratory for the project, is responsible for overall design and integration of the facility, including the installation of the linac. SLAC will also design and construct the electron beam transport systems, controls, and x-ray optics. This collaboration, an extraordinary concentration of US accelerator expertise, has made it possible to transform the LCLS-II project in a matter of months. The collaboration has a goal of producing first x-rays using the superconducting linac by September 2019.

*Work supported by US DOE Contract DE-AC02-766SF00515
#galayda@slac.stanford.edu

Copyright © 2014 CC-BY-3.0 and by the respective authors

HIGH-POWER INDUSTRIAL ACCELERATOR ILU-14 FOR E-BEAM AND X-RAY PROCESSING

V. Bezuglov, A. Bryazgin#, K. Chernov, B. Faktorovich V. Gorbunov, E. Kokin, M. Korobeynikov, A. Lukin, I. Makarov, S. Maximov, A. Panfilov, V. Radchenko, E. Shtarklev, A. Sidorov, V. Tarnetsky, M. Tiunov, V. Tkachenko, A. Vlasov, L. Voronin, Budker INP, Novosibirsk, Russia

Abstract

Growing interest to product irradiation by E-beams and X-rays calls for dedicated industrial electron accelerators. Budker INP has developed ILU-14 radio-frequency pulsed linear accelerator capable of providing 100 kW beam at 7.5–10 MeV. The accelerator has fast removable X-ray converter and can operate both in e-beam and X-ray processing modes. The machine utilizes a low frequency (176 MHz) SW accelerating structure. ILU-14 accelerator was developed as turnkey equipment. Technical details and test results are presented.

INTRODUCTION

At Budker INP, a product line of ILU type electron accelerators with beam power up to 50 kW and energy up to 5 MeV has been developing since 1970; tens of the accelerators operate in many countries over the world. The RF power systems for all these machines are based on the self-exiting generators using the low-cost reliable vacuum tubes (GI-50A triodes made in Russia) with pulse power no less than 2 MW. These RF systems do not need precise frequency adjustment of the accelerating structure and generator. It results in relatively simple design of both accelerator control system and generator that allows us to considerably decrease the machines total and maintenance costs and improve their reliability.

The ILU-8 machines with energy range 0.8–1 MeV local shielding are mainly used for treatment of wires, tubes, and films. The ILU-6 machines with energy up to 2.5 MeV have been used for industrial treatment of big wires since 1983. The ILU-10 machines operate at the energy of 5 MeV and can be supplied with X-ray converters [1].

At present, there are the market needs for accelerators with electron energy up to 10 MeV. To produce a new product line covering all the energy and power ranges (up to 10 MeV and 100 kW), a concept of module-type ILU-14 accelerator with new 176 MHz modular accelerating structure has been developed at Budker INP [2]. 5 MeV accelerator prototype (called ILU-12) was successfully tested at Budker INP stand in early 2007. In 2010, 7.5 MeV of the output electron energy was obtained on modified prototype with two power inputs, that corresponds to the designed accelerating rate of the 10 MeV ILU-14 accelerator. ILU-14 machine can meet the growing demands of the industry. The energy range of 7.5–10 MeV allows that machine to treat the products in the EB mode with energies up to 10 MeV and also operate in X-ray generation mode with energy of 7.5 MeV.

The penetration depth of X-rays generated by ILU-10 at the energy of 5 MeV is 35 g/cm^2, that is practically close to the penetration depth of the gamma rays emitted by the cobalt source. The irradiation facility based on the ILU-10 or ILU-14 accelerator with removable X-ray converter can treat the full spectrum of the products that are treated by cobalt sources.

ILU-14 ACCELERATOR

Budker INP can produce high-performance, easy in use and control linear accelerators based on standard RF generator and modulator modules, developed and available in the Institute. The output parameters of such accelerators are defined by the number of generator modules and accelerating structure sections used, and can cover wide range of the output beam energy and average power.

Table 1 presents the main parameters of ILU-14 accelerator, which can operate in two regimes with different output electron energies. The generator is based on standard equipment used in ILU type accelerators (GI-50A triodes, modulator etc.).

Table 1: ILU-14 Accelerator Parameters

Parameter	7.5 MeV regime	10 MeV regime
Generator tube	5xGI-50A	5xGI-50A
Maximal energy	7.5 MeV	10 MeV
Average power	100 kW	100 kW
Energy spread	8 %	7.7 %
Acc. structure efficiency	84 %	71 %
Repetition rate	50 Hz	50 Hz
Total efficiency	29%	25%

Operating Principles

Figure 1 presents ILU-14 accelerator block diagram. The accelerator contains the 176 MHz accelerating structure, self-excited generator based on five GI-50A tubes with the pulsed power of 6 MW (maximal power up to 8 MW), modulators for RF feeding of the tubes, triode RF gun, beam output system, and (optional) an X-ray converter.

Copyright © 2014 CC-BY-3.0 and by the respective authors

ISBN 978-3-95450-142-7

BEAM COMMISSIONING OF THE 100 MeV KOMAC LINAC*

Yong-Sub Cho#, KOMAC/KAERI, Gyeongju, Korea

Abstract

The operation of the 100 MeV proton linear accelerator for multipurpose application started in July, 2013 at Korea Multipurpose Accelerator Complex (KOMAC), Korea Atomic Energy Research Institute (KAERI). Also, the operation of the two beam lines, one for 20 MeV beam and the other for 100 MeV beam, started in order to supply proton beams to users. The accumulated operation time was 2,290 hours and the proton beam was supplied to 937 samples in 2013.

INTRODUCTION

After the successful commissioning and getting the operation license of the facility, KOMAC started its 100 MeV proton beam service at July, 2013 [1]. The facility consists of a 100 MeV proton linac including a 50 keV injector, a 3 MeV radio frequency quadrupole (RFQ), and a 100 MeV Drift Tube Linac (DTL), and 20 MeV and 100 MeV beam lines. 100 MeV linac and beam lines are installed in the first floor of the accelerator building, high power RF components including klystrons, circulators and cooling systems are installed in the second floor and the modulators for the klystrons are installed in the third floor. The KOMAC site is shown in Figure 1. As shown in the Figure, ion beam application building and roads are under construction.



Figure 1: KOMAC site

KOMAC 100 MEV PROTON LINAC

The main parameters of the linac are summarized in Table 1. The injector of the KOMAC accelerator consists of a microwave ion source with the extraction voltage of 50kV, and a low energy beam transport (LEBT) for matching proton beams into the RFQ. The LEBT consists of 2 solenoids and 2 steering magnets. The ion source can work in cw (continuous wave) and pulsed modes. The peak beam current is 20 mA.

*This work was supported by Ministry of Science, ICT & future Planning of the Korean government

#choys@kaeri.re.kr

The 20-MeV part of the linac consists of a 3-MeV RFQ and a 20-MeV DTL. The peak beam current and the maximum beam duty are respectively 20 mA and 24%. The RFQ is a four vane type with the resonant coupling and dipole rods for field stabilization. The total length of the RFQ is about 3.2 m. The 20 MeV DTL includes four tanks which are driven by a klystron. The FFDD lattice was adopted for the 20-MeV DTL with pool-type quadrupole magnets.

The 100-MeV part of the linac consists of 7 DTL tanks. The maximum beam duty is 8% and the peak beam current is 20 mA. In this part, each klystron drives a DTL tank. The focusing lattice is also FFDD with quadrupole magnets whose integrated field is 1.75 T. The 100 MeV linac installed inside the tunnel is shown in Figure 2 [2][3][4].

Table 1: Parameters of KOMAC Linac

Parameters	Value
Frequency	350 MHz
Beam Energy	100 MeV
Operation Mode	Pulsed
Max. Peak Current	20 mA
Pulse Width	<1.33 ms (< 2.0 ms for 20 MeV)
Max. Beam Duty	8% (24% for 20 MeV)
Max. Beam Power	160 kW (96 kW for 20 MeV)

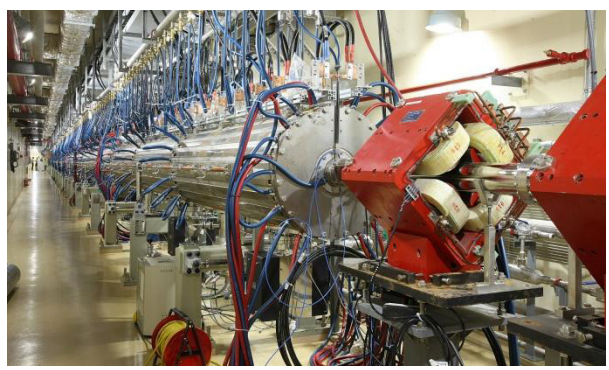


Figure 2: 100 MeV proton linear accelerator

The KOMAC accelerator facility can provide 20 MeV and 100 MeV proton beams to users. The 100 MeV beam line starts from the end of the linac. The 20 MeV beam line extracts proton beams in the middle of the linac. In order to install a 45 degree bending magnets for 20 MeV beam extraction and a beam matching system into the next DTL tank, we installed a medium energy beam transport (MEBT) system after the 20 MeV DTL. Among the 10 beam lines originally designed, KOMAC now opens two beam lines, one for 20 MeV beam (TR23) and the other for 100 MeV beam (TR103). In future, we will

Copyright © 2014 CC-BY-3.0 and by the respective authors

ISBN 978-3-95450-142-7

COMMISSIONING OF ENERGY UPGRADED LINAC OF J-PARC

Kazuo Hasegawa #
Accelerator Division of J-PARC, JAEA and KEK, Tokai-mura, Ibaraki-ken, 319-1195, Japan

Abstract

To realize a full potential of the J-PARC facility (1 MW at 3 GeV and 0.75 MW at 30 GeV), the J-PARC linac is upgraded from 181 MeV to 400 MeV by using an Annular-ring Coupled Structure linac (ACS). The ACS modules and peripheral system were installed and commissioned from summer of 2013. The results of beam commissioning and user operation are reported here.

INTRODUCTION

J-PARC, which stands for Japan Proton Accelerator Research Complex, consists of a 400 MeV linac, a 3 GeV rapid cycling synchrotron (RCS), a 30 GeV Main Ring synchrotron (MR) and related experimental facilities[1]. A proton beam from the RCS is injected to the Materials and Life Science Experimental Facility (MLF) for neutron and muon experiments. The MR has two beam extraction systems. One is a fast extraction for the neutrino beam line for the Tokai-to-Kamioka (T2K) experiment, and the other is a slow extraction for the Hadron Experimental Facility.

The goal of the J-PARC project is to deliver a 1 MW beam from the RCS and 0.75 MW beam from the MR. To achieve the goal, a step-by-step approach for the linac is taken: energy upgrades from 181 MeV to 400 MeV, and then, a peak current upgrades from 30 to 50 mA[2]. The energy upgrade project actually started in March 2009. The tunnel and the building had been designed and constructed for 400 MeV linac from the beginning of J-PARC project.

A radioactive material leak accident occurred at the Hadron facility in May 2013 and all the J-PARC operations were suspended[3]. As of April 2013, the beam power for MLF users was 300 kW and the maximum beam powers of the MR for the T2K experiment and the Hadron facility were 240 kW and 15 kW, respectively.

During the long shutdown period in summer of 2013, new accelerating modules and peripherals for the energy upgrade were installed, as scheduled before the accident, and beam commissioning started in December. The user operation for the MLF was resumed in February 2014.

LINAC SYSTEM

The configuration of the energy upgraded J-PARC linac is shown in Fig. 1. The linac consists of a negative hydrogen ion source, a 3 MeV RFQ (Radio Frequency Quadrupole linac), a 50 MeV DTL (Drift Tube Linac), a 191 MeV SDTL (Separated-type DTL) and a 400 MeV Annular-ring Coupled Structure linac (ACS). RF frequencies are 324 MHz for low β section (RFQ, DTL and SDTL) and 972 MHz for high β section (ACS), respectively.

By the time of the energy upgrade, after the SDTL section was a beam transport line. The last two SDTL cavities were installed in the beam line as debuncher cavities where no acceleration was expected. Therefore, the injection energy to the RCS was 181 MeV instead of 191 MeV.

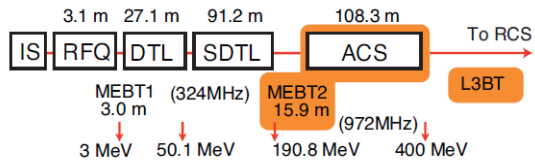


Figure 1: The configuration of the energy upgraded J-PARC linac.

ANNULAR-RING COUPLED STRUCTURE LINAC (ACS)

Development of ACS

The ACS is one of coupled cavity linacs, for example, a side-coupled structure (SCS), operated in a π/2 mode[4]. Comparing to the SCS, the ACS has an axial symmetry around a beam axis and has several advantages. It has a smaller transverse kick field component and can be obtained a smooth surface with an ultra-precision lathe machining. Shunt impedance and a coupling factor are comparable to those of the SCS.

Since the coupling cavity of the ACS is nearly coaxial, it has many modes above the coupling modes. This is one of the reasons why its development has not been succeeded. Improvement of the symmetry by increasing the number of coupling slots has solved the mixing of these modes to the coupling modes. In this way, the 1296 MHz ACS cavity for Japan Hadron Project at KEK was successfully developed and power tested[5]. The structure size of the 972 MHz ACS, which is used for the J-PARC linac, is much bigger based on a simple frequency ratio of 1.3, and it is very hard to machining and handling. We have successfully modified the cavity shape to reduce the size of the 972 MHz ACS to that of the 1296 MHz one[6].

Figure 2 shows an illustration of the ACS accelerating module. The ACS module consists of one lower bridge tank with 9 cells and two upper accelerating tanks with 17 cells. Focusing doublet Q magnets are placed between the accelerating tanks and also between the modules. Movable tuners for the frequency adjustment are attached in an excitation cell of the bridge tank. Twenty-one ACS

#hasegawa.kazuo@jaea.go.jp

Copyright © 2014 CC-BY-3.0 and by the respective authors

ISBN 978-3-95450-142-7

DTL CONSTRUCTION STATUS OF CSNS PROJECT

H.C. Liu[1,2#], S.N. Fu[1,2], J. Peng[1,2], S. Wang[1,2]
[1] China Spallation Neutron Source (CSNS), Institute of High Energy Physics (IHEP), Chinese Academy of Sciences (CAS)，Dongguan 523803, China
[2] Dongguan Institute of Neutron Science (DINS), Dongguan 523808, China

Abstract

The 324MHz Alvarez-type Drift Tube Linac (DTL) for the China spallation neutron source will be used to accelerate the H^- ion beam. It can provide 15mA peak current beam with energy gain from 3 to 80MeV. It consists of four independent tanks, of which the average length is about 8.6 m. Each tank is divided into three short unit sections for ease of fabrication and assembly. A hollow coil based electromagnet is accommodated in each drift tube for its compact structure. So far, the machining of all 12 tanks is completed; nine of those tanks are successfully electroplated. The ultimate vacuum and RF properties tests are successfully performed. The fabrications of 63 drift tubes for the first tank are also finished and about to install in CSNS site. The fabrication and test details are presented in this paper.

INTRODUCTION

The China Spallation Neutron Source (CSNS) Linac mainly consists of an H^- ion source, a LEBT, a 3 MeV RFQ, a MEBT and an Alvarez-type Drift Tube Linac (Figure 1) [1]. It will be constructed and tested until 2016.09. Main components of DTL are now under construction. We are scheduled to start the installing of 1st tank from September this year.



Figure 1: CSNS Linac layout.

DTL TANK

The tank is a vacuum vessel that provides a mechanically stable platform for the array of drift-tube assemblies, post couplers, and slug tuners. The tank also provides support and interfaces to the RF system, the cooling system and the vacuum pumping system. Each tank is equipped with 2 movable tuner and 12 fixed tuner equally distributed over the bottom of tank body. There are twelve straight water cooling channels embedded into the tank out-wall. An iris waveguide coupler was used to feed the power due to its simple structure, good power handling capability, small frequency perturbation in the cavity. The tank will operate in a sufficiently high vacuum for RF environment by using two 1000L/s ion pumps and 1 turbo-molecular pump for each unit tank (Figure 2).

liuhc@aps.anl.gov

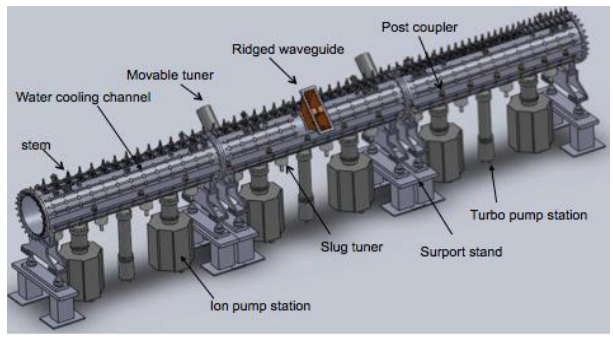


Figure 2: general drawing of DTL tank.

Tank Fabrication

For ease of fabrication, each DTL tank assembly is divided into 3 unit sections which can be bolted together to form one long assembly. Each tank section is approximately 3 meter long and is fabricated from 20# carbon steel. The machining of CSNS DTL tank is finished and the mechanical dimensions of each tank are measured. The length tolerance is -0.1to -0.3mm and the radius tolerance is within ± 0.1mm.The measured holes position precision is less than ± 0.1mm.



Figure 3: Tank fabrication.

Tank Copper Plating

Each DTL tank section was Copper plated to increase the electrical conductivity of the tank RF surfaces. The inner surface of the tank is copper plated in 200-250 μm thickness (Figure 4). We polished mechanically the surface after plating in order to satisfy the Ra 0.4 μm roughness. Up to now, 9 out of 12 CSNS DTL tanks have been electroplated. Including preparation and post treatment, each tank section is plated in approximately three weeks.

Copyright © 2014 CC-BY-3.0 and by the respective authors

ISBN 978-3-95450-142-7

LARGE SCALE TESTING OF SRF CAVITIES AND MODULES*

J. Świerblewski#, IFJ PAN, Kraków, Poland

Abstract

Series production of superconducting RF cavities, superconducting quadrupole packages and accelerator cryomodules for the European XFEL is in full swing. Mid 2014 approximately. 400 cavities will be tested, the testing of quadrupole packages will be almost finished, and regular module testing will be established. Thus this talk will emphasize the quasi industrial testing of these components, including a good overview about the used unique AMTF infrastructure.

INTRODUCTION

Currently the European X-ray Free Electron LASER (XFEL) [1] is under construction at DESY in Hamburg. The laser will produce high-intensity ultra-short X-ray flashes. Brightness of these flashes will be incomparably greater than the best conventional X-ray source. With this unique device all scientists around the world and also users from industry can explore new research opportunities [2].

Poland is one of twelve countries (Denmark, France, Germany, Greece, Hungary, Italy, Poland, Russia, Slovakia, Spain, Sweden and Switzerland) participating and financing the construction of XFEL.



Figure 1: XFEL cavities installed into the insert.

A team of physicists, engineers and technicians from the Henryk Niewodniczanski Institute of Nuclear Physics Polish Academy of Sciences (IFJ PAN) performs the tests of all superconducting cavities, superconducting magnets and accelerator modules as a Polish in-kind contribution for the XFEL.

IFJ PAN is responsible for preparation, conditioning and testing of 840 superconducting cavities (Fig. 1), 103 superconducting magnets (Fig. 2), 103 current leads and 103 accelerating cryomodules [2].

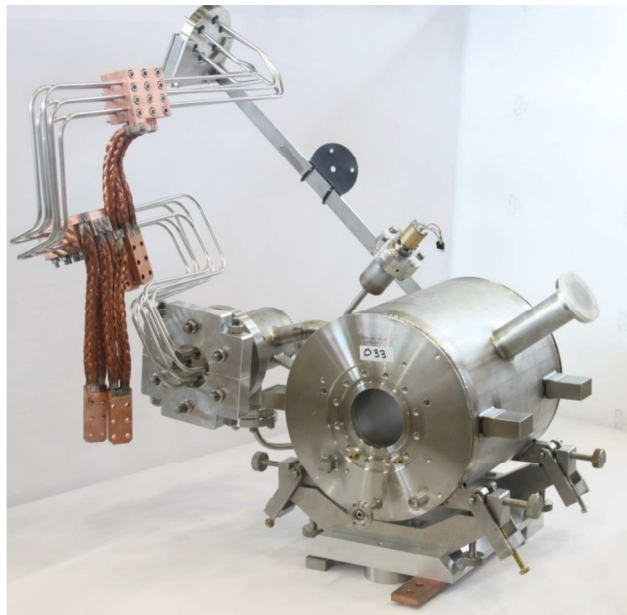


Figure 2: Superconducting magnet with current lead

INFRASTRUCTURE

The "Accelerator Module Test Facility" – AMTF hall at DESY in Hamburg is dedicated to perform the acceptance tests for superconducting cavities and accelerator cryomodules (Fig. 3).



Figure 3: Inside view of the AMTF hall – cryomodules.

*The research leading to these results has received funding from the European Union Seventh Framework Programme (FP7/2007-2013) under grant agreement no 283745 (CRISP)

jacek.swierblewski@desy.de

Copyright © 2014 CC-BY-3.0 and by the respective authors

Nb_3Sn – PRESENT STATUS AND POTENTIAL AS AN ALTERNATIVE SRF MATERIAL*

S. Posen† and M. Liepe
Cornell Laboratory for Accelerator-Based Sciences and Education, Ithaca, NY, USA

Abstract

Nb_3Sn is a material that has the potential to have a transformative impact on SRF linacs. Due to its large critical temperature of approximately 18 K, Nb_3Sn cavities can have far smaller surface resistances at a given temperature than standard Nb cavities. This could significantly reduce the costs for infrastructure and power in cryoplants for large CW linacs. In addition, the predicted superheating field of Nb_3Sn is approximately double that of Nb, potentially doubling the maximum energy gradient. This would significantly decrease the size and cost of high energy linacs. In this work, we present recent progress in research and development for this promising material.

INTRODUCTION

Niobium is an excellent SRF material, and relatively easy to fabricate particle accelerator cavities with, but it has significant limitations. Let us consider two applications relevant to the linac community. The first is low duty factor, high energy SRF linacs, which require many cavities operating at high accelerating gradients E_{acc}. For example, the ILC design calls for approximately 16,000 cavities in a 31 km linac [1]. The maximum gradient of a state-of-the-art cavity has an accompanying peak surface magnetic field B_{pk} close to the superheating field B_{sh} of niobium, a fundamental limit. The only way to reach significantly higher gradients—and thereby decrease the number of cavities needed in such an SRF linac—is to use an alternative material with a larger B_{sh} than niobium.

The second application to consider is high duty factor (or CW), medium energy linacs, such as LCLS II. The BCS surface resistance R_{BCS} scales with the cavity temperature T and the material's critical temperature T_c approximately as

$$R_{BCS} \sim e^{-T_c/T} \tag{1}$$

so these these machines generally operate near 2 K to keep the surface resistance R_s manageable. However, the high duty factor means that the dynamic load is quite large, necessitating the use of large cryogenic plants, which cost on the order of 100 million USD and require megawatts of power to operate. Because the heat dissipated by a cavity scales as $P_{diss} \sim R_s E_{acc}^2$, the cost optimum energy gradient tends to be relatively small, well below the B_{sh} limit [2, 3]. An alternative material with a smaller R_{BCS} at a given temperature than niobium could increase the cost optimum E_{acc}, allowing fewer cavities to be used. Alternatively, it could allow the cavities to be operated at a higher temperature, simplifying the cryoplant, reducing its capital cost and its power requirements.

Nb_3Sn, an alternative SRF material, is predicted to have a B_{sh} of ~400 mT [4], approximately twice that of niobium. At B_{pk}=400 mT, an ILC-style cavity would reach $E_{acc} \approx$100 MV/m, compared to the maximum field for a niobium cavity, ~50 MV/m. The T_c of Nb_3Sn, 18 K, is also about twice that of niobium, which means that (taking into account the exponential dependence of R_s on T_c shown in Eqn. 1) it has a far smaller R_{BCS} at a given temperature. The comparison of different preparations in Table 1 shows that even with the preparation methods recently developed for very high Q_0 niobium surfaces (the quality factor Q_0 is determined by a global average of the surface resistance given by G/R_s, where G is a geometry-dependent constant), Nb_3Sn with small R_{res} has approximately the same Q_0 at 4.2 K as niobium has at 2 K, but the cryogenic efficiency is approximately 3.6 times higher at 4.2 K [5] and the cryoplant can be simpler without having to support subatmospheric helium. These dramatic increases in both B_{sh} and Q_0 at a given temperature illustrate the potential of Nb_3Sn to improve SRF linacs.

Table 1: Approximate Q_0 for 1.3 GHz TeSLA or 1.5 GHz CEBAF Cavities Prepared in Different Ways If Residual Resistance Is Small (for description of N-doping, see [6])

Preparation	Max Q_0, 4.2 K	Max Q_0, 2 K
Nb, EP+120 C bake	6×10^8	2×10^{10}
Nb, EP/bake/HF rinse	6×10^8	3×10^{10}
Nb, N-doped	6×10^8	$4 - 8 \times 10^{10}$
Nb_3Sn, vapor diffusion	6×10^{10}	$> 10^{11}$

On a smaller scale, Nb_3Sn cavities could be used in low energy industrial applications. In these situations, it may not be cost-effective to have a supply of superfluid liquid helium to keep Nb cavities in the $Q_0 \sim 10^{10}$ regime. The higher T_c of Nb_3Sn would allow low-loss operation with atmospheric liquid helium at 4.2 K or perhaps gas or supercritical helium at higher temperatures. This could have applications in flue gas and wastewater treatment, isotope production, and border security.

After many years of development, state-of-the-art niobium cavities can now achieve high-Q_0 operation close to B_{sh}. Achieving this with Nb_3Sn will be the ultimate goal of R&D into this alternative material, to which comparatively little effort has been dedicated to date. This paper will present recent progress towards this goal.

* Work supported by NSF Career award PHY-0841213 and DOE award ER41628.
† sep93@cornell.edu

Copyright © 2014 CC-BY-3.0 and by the respective authors

ISBN 978-3-95450-142-7

CRYOGENIC PERFORMANCE OF A NEW 72 MHz QUARTER-WAVE RESONATOR CRYOMODULE*

Z.A. Conway#, G.L. Cherry, R.L. Fischer, S.M. Gerbick, M.J. Kedzie, M.P. Kelly, S-h. Kim, S.W.T. MacDonald, R.C. Murphy, P.N. Ostroumov, C.E. Peters, M.A. Powers, T.C. Reid, J.R. Specht, ANL, Argonne, IL 60439, USA

Abstract

The Argonne National Laboratory ATLAS accelerator's Intensity and Efficiency Upgrade project has been successfully finished [1]. This upgrade substantially increases beam currents for experimenters working with the existing stable and in-flight rare isotope beams and for the neutron rich beams from the Californium Rare Isotope Breeder Upgrade. A major portion of this project involved the replacement of three existing cryomodules, containing 18 superconducting (SC) accelerator cavities and 9 SC solenoids, with a single cryomodule containing 7 SC 72.75 MHz accelerator cavities optimized for ion velocities of 7.7% the speed of light and 4 SC solenoids all operating at 4.5 K. This paper reports the measured thermal load to the 4 K and 80 K coolant streams and compares these results to the pre-upgrade cryogenic system.

INTRODUCTION

A major objective of the ATLAS Intensity and Efficiency Upgrade was replacing three existing split-ring resonator cryomodules with a single Quarter-Wave Resonator (QWR) cryomodule. This intensity upgrade was motivated by experimental needs which require higher currents for both stable and exotic beams to isolate and investigate previously unstudied uncommon-isotopes. The split-ring cryomodules steer the beam and limit the total transmission through the ATLAS linac and must be replaced to achieve the increased intensity goal [1]. The new SC QWRs were built with tilted drift tube and reentrant nose faces, reducing beam steering to negligible levels and improving the overall transmission through this portion of the accelerator [1]. The QWR cryomodule constructed at Argonne National Laboratory (ANL) contains 7 72.75 MHz, $\beta = 0.077$, QWRs and 4 superconducting 9 T solenoids, all of which operate at 4.5 K. The cryomodule occupies 5.2 meters of beam-line and provides a total voltage gain of 17.5 MV (2.5 MV per cavity, roughly twice any other cavity operating in this velocity regime) [2] with a total measured 4.5 K heat load of 33+10/-5 W.

A second upgrade goal was the reduction of the 4.5 K thermal load in the section of the ATLAS linac where the new QWR cryomodule is located. Reducing the 4.5 K load was accomplished through two measures: (1) reducing the number of cryomodules in the ATLAS linac by replacing 3 old cryomodules with a single new one and (2) replacing and installing new, more efficient, liquid helium transfer lines and distribution boxes. This paper reports on the upgraded 4.5 K and 80 K loads present in ATLAS.

In the following the 72.75 MHz QWR cryomodule design, and measured thermal loads are discussed. This is followed by a comparison of the results to the previous split-ring cryomodule performance. The new QWR cryomodule was first cooled to 4.5 K in December 2013 and has been in full-time use supporting ATLAS operations since March 2014. This has given us ample time to characterize the cryomodule performance and the results presented here represent the highest measured thermal-loads; e.g., with all cavities operating at 2.5 MV.

QWR CRYOMODULE

Cryomodule cold-mass hanging from the lid is shown in Figure 1. The intensity upgrade cryomodule is a modified version of our previous box-type cryomodule which has been in operation since 2009 [3]. Argonne box cryomodules implement current state-of-the-art techniques such as separate cavity and insulating vacuum systems, surface processing and clean handling to achieve and preserve record single-cavity test performance [2, 4], and a design which enables the clean assembly to be complete and hermetically sealed prior to installing the "dirty" subsystems of the cryomodule. The cryomodule structure has been described in great detail in [5].

The cryomodule 4.5 K cryogenic system is gravity fed where each of the 7 QWR and 4 solenoids is attached to a common helium distribution manifold. All penetrations through the cryomodule 80 K thermal shield are baffled or covered such that the solid angle for room temperature surfaces viewing 4.5 K surfaces is minimal (a few square inches for the entire cryomodule) and much of the reflective path between room temperature and 4.5 K is coated with high-infrared-emissivity blackened surfaces [6]. Further reducing the 4.5 K heat load are the low-emissivity 80 K and 4.5 K surfaces which are either aluminized mylar or electropolished stainless steel. Finally, all of the connections to 4.5 K are very low-conductivity. This is accomplished by using very thin stainless steel walls (e.g., the beam-line gates valves and the helium manifold safety pressure relief) or by taking advantage of the acoustic impedance mismatch between titanium and stainless steel at low temperature to increase the contact impedance between these materials (e.g., the cold-mass hangers). The calculated 4.5 K static thermal load is 15 W

*This material is based upon work supported by the U.S. Department of Energy, Office of Science, Office of Nuclear Physics, under contract number DE-AC02-06CH11357. This research used resources of ANL's ATLAS facility, which is a DOE Office of Science User Facility.
zconway@anl.gov

Copyright © 2014 CC-BY-3.0 and by the respective authors

ISBN 978-3-95450-142-7

COMMISSIONING OF THE 72 MHz QUARTER-WAVE CAVITY CRYOMODULE AT ATLAS*

M.P. Kelly#, Z.A. Conway, S.M. Gerbick, M.R. Hendricks, M. Kedzie, S.H. Kim, S. MacDonald, R.C. Murphy, P.N. Ostroumov, T. Reid, S.I. Sharamentov, G. Zinkann,
ANL, Argonne, IL 60439, U.S.A.

Abstract

A cryomodule of seven 72 MHz superconducting (SC) quarter-wave cavities optimized for ions with v/c=0.077 has been commissioned in the ATLAS heavy-ion accelerator at Argonne. The new module, with the new CW RFQ injector [1], provide ATLAS the capability to deliver much higher beam currents with low beam losses for nuclear physics experiments using stable or rare isotope beams or neutron rich beams from the Californium Rare Isotope Breeder. The goal for the cryomodule, to provide a large accelerating voltage of 17.5 MV (2.5 MV/cavity) with no detectable beam losses, was been met during the first month of commissioning. To date, cavities and primary subsystems, including 4 kW nominal RF couplers and pneumatic tuners, are operating as designed with full availability. For V_{ACC}=17.5 MV (ave. E_{PEAK}=40 MV/m) field emission is small and RF losses to 4.5 K helium are 5 Watts/cavity, about half of the planned value. Cavity fields continue to be gradually increased beyond the nominal design values. The limit due to cavity quench is at least V_{ACC}=3.75 MV per cavity. The good RF performance stems primarily from combination of RF design and cavity processing. Effective voltages are 2½ times higher than those of other operational cavities for this v/c. We report here on the recent online test results and important technical features.

INTRODUCTION

SC two-gap quarter-wave cavities, with intrinsic properties of high shunt impedance, large aperture, and wide particle velocity acceptance have been the cavity of choice for heavy-ion linacs with beam velocities near β=0.1 for more than four decades. Rapid advance in SRF cavity performance and new requirements, such as for high-intensity CW ion beams, have not changed these basic considerations. In fact, quarter-wave cavities combined with the latest techniques provide the best means to reduce low-beta linac footprint and cost and, permit high reliability needed for high-intensity/high-power applications [2,3].

Key technical features of the new ATLAS 72 MHz quarter-wave cavity and cryomodule, some of which are known widely but not practically implemented until now, include:

* This material is based upon work supported by the U.S. Department of Energy, Office of Science, Office of Nuclear Physics, under contract number DE-AC02-06CH11357. This research used resources of ANL's ATLAS facility, which is a DOE Office of Science User Facility.
#mkelly@anl.gov

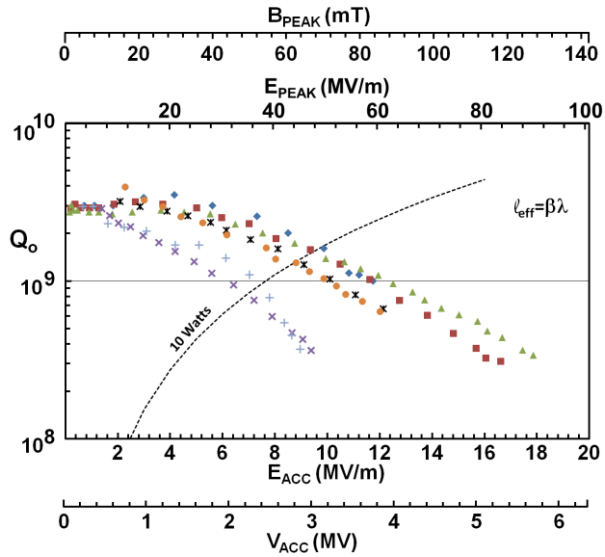


Figure 1: Measured online performance data for seven quarter-wave cavities at T=4.5 Kelvin.

- The first use in any TEM-mode cavity (quarter- or half-wave) of tapered inner and outer conductors [4].
- Electropolishing on the completed quarter-wave cavity with stainless steel helium jacket.
- Tilted drift-tubes formed into the niobium to cancel the beam steering from on-axis magnetic fields over a wide velocity range [5].
- Centering of the central conductor to 100 microns during fabrication to nearly eliminate the effect of resonant, *i.e.* pendulum mode, microphonics.
- 'In-situ' maintenance on the clean cavity string while maintaining performance with E_{PEAK}≥40 MV/m.

RF PERFORMANCE

The approach for ATLAS cavities has never been to design to a gradient 'spec', but to provide the maximum capability to ATLAS with available funding. The 72 MHz cavity, β_{OPT}=0.077, provides at least 60% of the peak voltage over the range 0.05<v/c<0.2. Higher cavity accelerating voltages, therefore, add directly to the list of beam/energy combinations available to the over 400 active ATLAS users. This is particularly important for higher beam intensities (≥100 eμA) where only the new steering-corrected cavities are practical.

Figure 1 shows measured online performance curves from June 2014, after five months of operation in the ATLAS tunnel. Performance has not changed measurably during this time. The measured accelerating gradient,

Copyright © 2014 CC-BY-3.0 and by the respective authors

4 K ALIGNMENT OF SUPERCONDUCTING QUARTER-WAVE CAVITIES AND 9 T SOLENOIDS IN THE ATLAS INTENSITY UPGRADE CRYOMODULE*

S.H. Kim#, Z.A. Conway, W.G. Jansma, M.J. Kedzie, M.P. Kelly, and P.N. Ostroumov,
ANL, Argonne, IL 60439, USA

Abstract

The superconducting cavities and, especially, the magnets in high intensity ion linacs need to be aligned to the beam with typical transverse tolerances of ±0.25 mm and ±0.1 degrees at temperatures of 1.8 – 4.5 K. This is necessary to limit the emittance growth and minimize the beam losses. A new cryomodule with 7 superconducting quarter-wave resonators and 4 superconducting solenoids has been installed and is now operated at the Argonne Tandem Linear Accelerator System (ATLAS). We developed the techniques necessary to assemble the superconducting components in this cryomodule at room temperature so that they are aligned to the beam axis at 4.5 K. We achieved transverse alignment tolerances of <0.2 mm RMS. In this paper, we will present the details of the alignment hardware, procedures and results.

INTRODUCTION

Several new high-intensity hadron linear accelerators which require low-beta (β = v/c < 0.5) superconducting cavity resonators and superconducting magnets are being built and proposed, e.g., the Proton Improvement Project (PIP-II) at Fermi National Accelerator Laboratory, Argonne Tandem Linear Accelerator System (ATLAS) Intensity Upgrade at Argonne National Laboratory, and the International Fusion Materials Irradiation Facility Project. These and other high-intensity accelerators aim at achieving beam currents of several to hundreds of milliamps. Emittance growth and beam losses <1 W/m, to limit activation of the accelerator components [1], require alignment errors of the superconducting magnets to be less than 250 μm RMS and 0.1° with relaxed tolerances for the superconducting cavities [2,3]. Achieving this high alignment accuracy is non-trivial for components which should be assembled at room temperature but operated at 2-4.5 K in cryomodules. The alignment procedure must take into account the mechanical displacement of components due to thermal contraction and vacuum/pressure loading to obtain the desired accuracy at the operating temperature and pressure. One example of alignment techniques in such cryomodules is the low-CTE invar rod and the sliding cavity support to decouple longitudinal thermal motion of the cavity jacket from the fixture attached to the helium gas return pipe used in the TESLA Test Facility (TTF) cryomodule [4].

At Argonne we have recently commissioned a superconducting cavity cryomodule with 7 β=0.077 superconducting quarter-wave cavities and 4 superconducting 9 T solenoids contained in a single 5.2 meter long cryomodule [5,6]. In this cryomodule, the solenoids are required to be aligned to the beam at 4.5 K with transverse tolerances of 0.25 mm RMS as shown in Table 1 and the tolerances of the cavities are 4 times looser than the solenoids. In this paper, we present the alignment hardware used for satisfying these alignment tolerances, procedures of alignment and measurement, and alignment results measured at 4.5 K.

Table 1: Alignment tolerances of the solenoids in the ATLAS Intensity Upgrade Cryomodule

Coordinate	Alignment Tolerance
X/Y	0.25 mm RMS
Z	1 mm RMS
Pitch/Yaw/Roll	0.1° RMS

ALIGNMENT HARDWARE

The cavities and solenoids are loaded and aligned on the spanning titanium rail system, called strongback as shown in Fig. 1, which is suspended from the cryomodule lid [6]. Each cavity and solenoid mounts on top of the strongback with its own kinematic-alignment hardware. Details of this hardware are as shown in Fig. 2. The brackets are firmly attached to the solenoids and cavities and 3 balls, which are a part of the Kelvin type kinematic coupling [7], are attached to the brackets. The counter parts of the kinematic coupling are “ring”, “vee”, and “flat” [7]. The first two are attached on the runner which sits on the rail and vertically and horizontally movable by the adjustable screws during room temperature fine alignment. On the other side of the runner where the “flat” coupling sits on the rail the vertical position is adjusted by the screws and stainless steel shims.

ALIGNMENT PROCEDURES

The cavities and solenoids are aligned warm to an axis, which is translated from the cold beam axis by 3.0 mm vertical and 0.4 mm horizontal, to compensate for the expected thermal contraction of the cold mass and deflection of the titanium strongback due to the deflection of the hangers attachment points on the cryomodule lid

*This material is based upon work supported by the U.S. Department of Energy, Office of Science, Office of Nuclear Physics, under contract number DE-AC02-06CH11357. This research used resources of ANL’s ATLAS facility, which is a DOE Office of Science User Facility.
#shkim121@anl.gov

Copyright © 2014 CC-BY-3.0 and by the respective authors

ISBN 978-3-95450-142-7

AN IN-FLIGHT RADIOACTIVE ION SEPARATOR DESIGN FOR THE ATLAS FACILITY*

B. Mustapha#, C.R. Hoffman, B.P. Kay, B.B. Back, J.A. Nolen and P.N. Ostroumov
Physics Division, ANL, Argonne, IL 60439, USA

Abstract

An in-flight radioactive beam separator, named AIRIS, is being designed to enhance the radioactive beam capabilities of the ATLAS facility at Argonne. In order to serve all the experimental areas while maintaining the stable beam capabilities, the separator design is of a broadband type. This design allows the selected radioactive beam to return to the ATLAS beam line while stable beams continue on the same straight line when the separator is turned off. The separation is performed in two steps. The first is magnetic in a chicane made of four magnets and four multipoles, while the second uses an rf sweeper taking advantage of the time separation between the beam of interest and potential contaminants including the primary beam tail. We report here on the progress of the AIRIS design effort with special emphasis on the performance of the rf sweeper.

AIRIS LAYOUT AND DESIGN PARAMETERS

An efficiency and intensity upgrade of the ATLAS accelerator facility at Argonne has just been successfully completed [1]. Most of the stable beams will see their intensities increased by one to two orders of magnitude. To take advantage of this intensity upgrade and to enhance the existing radioactive beam capability at ATLAS [2], a new in-flight radioactive beam production and separation system is being designed. The new system will consist of a production target placed at the end of ATLAS followed by a two-step ion separator. The first step is magnetic called AIRIS while the second consists of an RF sweeper or chopper to take advantage of the time separation of the selected beam from potential contaminants including the tail of the primary beam, which could be orders of magnitude more intense. Figure 1 shows how AIRIS and the rf sweeper will be integrated into the ATLAS facility following the last accelerating module. The main constraint on the AIRIS design is to preserve stable beam operation by moving the target out and using AIRIS as a zero-degree transport line. For this purpose, AIRIS should have the same beam axis as ATLAS and the existing beamline. The developed design is of broadband type [3, 4] made of 4 rectangular dipoles and four quadrupoles. Table 1 lists the most recent AIRIS design parameters.

Table 1: AIRIS Design Parameters

Parameter	Value
Total chicane length, m	6.6
Angular acceptance, mrad	75
Dispersion at mid-plane, mm/%	1.2
Dipole bend angle, deg	22.5
Dipole radius, m	1
Dipole full gap, cm	8
Max. dipole field, T	1.8
Quadrupole length, cm	30
Quadrupole full aperture, cm	16
Max. quad. field at pole-tip, T	1.1

AIRIS INTEGRATION INTO ATLAS

As shown in figure 1, AIRIS will be installed downstream of the last ATLAS cryomodule and upstream of all experimental areas to maximize the use of ATLAS beams. In the original configuration, the rf sweeper was located just downstream of AIRIS in front of the first switching magnet. Due to space limitations in the ATLAS tunnel, the rf sweeper was moved downstream of the switching magnet preventing one or two experimental areas from taking advantage of the time separation provided by the sweeper. As we will show later, the new sweeper location has a significant advantage by providing a much better time separation due to the longer beam path between AIRIS and the sweeper.

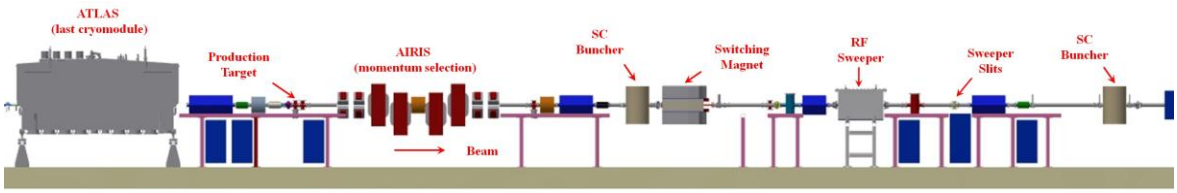


Figure 1: Integration of AIRIS and the RF sweeper into the ATLAS facility following the last accelerating module.

* This material is based upon work supported by the U.S. Department of Energy, Office of Science, Office of Nuclear Physics, under Contract number DE-AC02-06CH11357. This research used resources of ANL's ATLAS facility, which is a DOE Office of Science User Facility.
# brahim@anl.gov

Copyright © 2014 CC-BY-3.0 and by the respective authors

COMPLETION OF EFFICIENCY AND INTENSITY UPGRADE OF THE ATLAS FACILITY*

P.N. Ostroumov#, Z.A. Conway, C. Dickerson, S. Gerbick, M. Kedzie, M.P. Kelly, S. Kim, Y. Luo, S. MacDonald, R. Murphy, B. Mustapha, R.C. Pardo, A. Perry, T. Reid, S.I. Sharamentov, K.W. Shepard, J. Specht and G. Zinkann,
Argonne, IL 60439, U.S.A

Abstract

The ANL Physics Division has completed a major upgrade of the ATLAS National User Facility by successfully installing a new RFQ and cryomodule. The new normal conducting CW RFQ, capable of providing 295 keV/u beams of any ion with m/q ≤7, was fully integrated into ATLAS and has been in routine operation for more than a year. The RFQ doubled the efficiency of beam delivery to experiment targets and opened the possibility to accelerate much higher intensity beams. Recently, the new cryomodule containing 7 high-performance 72.75 MHz superconducting quarter-wave resonators and 4 superconducting solenoids was successfully commissioned with beam. New design and fabrication techniques for these resonators resulted in record accelerating voltages during the beam commissioning. From the very beginning, the new cryomodule provided 17.5 MV accelerating voltage which has been gradually raised by increasing the available input RF power and improving LLRF system. The new cryomodule, which replaced 3 old split-ring cryomodules, is also essential for high intensity stable beams. Results of beam commissioning and operation of ATLAS with the new RFQ and cryomodule are presented.

INTRODUCTION

Starting in the 1990's, the ATLAS heavy ion linac included 48 MHz SC resonators capable of accelerating pre-bunched ions with an initial velocity of 0.008c. Due to the high velocity gain in the first 4 SC resonators, a significant distortion of both transverse and longitudinal emittance occurred and resulted in low beam transmission through the linac. To address this issue, we have developed and built a CW RFQ capable of accelerating any ion from proton to uranium from 30 keV/u to 295 keV/u. The first cryomodule of ATLAS's Positive Ion Injector (PII) was significantly modified for operation with the new RFQ: the first three SC resonators were removed and the fourth is operated in a re-bunching mode.

While split-ring resonators are successfully operated at ATLAS with low-intensity ion beams, they exhibit a fundamental limit in the acceleration of high-intensity beams due to RF steering. Therefore we are planning to replace all ATLAS split-ring resonators with QWRs. Five years ago we commissioned a new cryomodule containing seven 109 MHz β_{OPT}=0.15 QWRs to provide an additional 15 MV of voltage. Now, we have developed, built and commissioned a new cryomodule consisting of seven SC β_{OPT}=0.077 QWRs operating at 72.75 MHz and four 9-Tesla SC solenoids. The SC solenoids include return coils to minimize stray magnetic fields. As a result of this innovative design, no extra magnetic shielding is required inside the cryomodule. The new high-performance cryomodule replaced three existing split-ring cryomodules increasing the intensities of accelerated ion beams available for experiments.

LEBT AND MEBT

The Low Energy Beam Transport (LEBT) is composed of electromagnetic quadrupoles and two 90° bending magnets to provide a small beam size (≤20 mm in diameter) in the multi-harmonic buncher (MHB). In conjunction with the installation of the RFQ, we have decided to build a new beam matching section between the MHB and RFQ using 3 electrostatic doublets and a triplet. The latter is directly attached to the front flange of the RFQ resonator. Fig. 1 shows matched beam envelopes in the MHB-RFQ section.

The RFQ is connected to the first PII cryomodule through a short bellows section. The Medium Energy Beam Transport (MEBT) is situated within the available space inside the cryomodule where the first three SC cavities were removed. The MEBT includes four SC solenoids, electrostatic X-, Y-steerers and a SC cavity operating as a re-buncher. The RFQ forms an axially-symmetric beam, and the transverse matching with SC solenoids is straightforward.

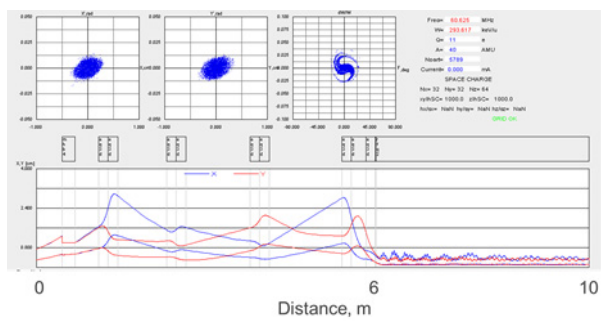


Figure 1: TRACK screenshot with the beam phase space plots after the RFQ and beam full, rms envelopes in the MHB and RFQ section.

* This material is based upon work supported by the U.S. Department of Energy, Office of Science, Office of Nuclear Physics, under contract number DE-AC02-06CH11357. This research used resources of ANL's ATLAS facility, which is a DOE Office of Science User Facility.
#ostroumov@anl.gov

Copyright © 2014 CC-BY-3.0 and by the respective authors

ISBN 978-3-95450-142-7

DESIGN OF RELATIVISTIC MAGNETRON FOR HIGH POWER MICROWAVE GENERATION

Romesh Chandra, Sandeep Singh, Ankur Patel, S. R. Ghodke, Archana Sharma
Accelerator & Pulse Power Division, Bhabha Atomic Research Centre, Mumbai, 400085, India

Abstract

A Linear Induction Accelerator based upon magnetic storage, utilising magnetic switches has been made and it is capable of providing a 400 kV diode voltage, 4 kA beam current for 100 ns pulse duration with 100 Hz repetition rate. It operates in a very high repetition rate due to the use of magnetic switches in it. The lesser shot to shot variation make this system ideal for a Relativistic Magnetron operation, where a huge dependence of output power on applied voltage and applied current is observed. A relativistic magnetron with axial extraction is analytically designed and simulated for this system. This relativistic magnetron is expected to give a power of 100 MW per pulse when operated in its full rating. The design features of this relativistic magnetron are presented here. This magnetron was designed for an output microwave frequency of 2.52 GHz.

INTRODUCTION

Pulse power systems are widely used for High Power Microwave (HPM) generation, Flash X-rays (FXR) production and intense electron beam applications. The applications include circuit vulnerability testing, dynamic radiography of fast moving objects via FXR and colouring of precious gems using electron beams [1].

In the recent developments in pulse power techniques for HPM generation, Relativistic Magnetrons have shown the best efficiency amongst all the available high power microwave devices [2]. Relativistic magnetron basically consists of coaxially coupled cavities in which a high magnetic field (0.2 T to 0.6 T) is applied perpendicular to the electron beam trajectory. This applied magnetic field is just enough to restrict the electrons within the interaction region between the cavities and the cathode. The minimum value of the magnetic field that can be applied for a given geometry at a particular accelerating voltage of electrons is given by Hull Cut-off condition. The maximum value of the magnetic field is given by Buneman and Hartree relation [3].

Based upon the extraction method of the HPM from the cavities, relativistic magnetrons can be divided into two subcategories, one is with radial extraction and another is with axial extraction. In the magnetrons based upon the radial extraction, a radial slot is made in one of the cavities and HPM is extracted through a waveguide and is radiated in the medium through an antenna. In the axial type of extraction system a portion of HPM is extracted through each of the cavities axially and is then radiated through an antenna. Since normally magnetrons are operated in π-mode which has zero group velocity, HPM extraction made through tapered cavity antenna.

A Relativistic magnetron based upon axial extraction method has been designed and developed for linear Induction Accelerator-400 (LIA-400).

RELATIVISTIC MAGNETRON

Design of the magnetron was done using Charged particle simulation technique (CST) simulation software.

LIA-400 System

A repetitive pulse power system was developed which is based on the magnetic pulse compression (MPC) technique and inductive voltage adders (IVA) similar to LIA-200 developed earlier in BARC [4]. The advantage of these types of systems is that these systems have high rep rate and a better shot to shot variability compared to those spark gap switch based systems. [5].

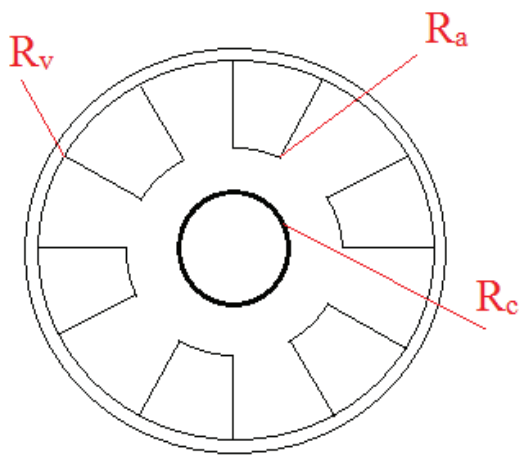


Figure 1: Simulated structure of the magnetron.

Simulation

Simulations were performed with the help of CST MS and CST PIC to get the frequency domain behaviour of this device. The simulation structure is given in fig.1. The values of R_c, R_a and R_v are 10 mm, 21.1 mm and 41.5 mm respectively. The length of the magnetron structure is 75 mm and is inside to the plane of the paper. Initially Eigen mode simulation was performed to get the Eigen modes of the six coupled cavities as shown in fig. 2. In all the modes obtained for the magnetron operation, π-mode operation with frequency 2.52 GHz was chosen because it is the only frequency which is non-degenerate. The electric field directions inside the cavity are shown in fig.3 for π-mode.

Copyright © 2014 CC-BY-3.0 and by the respective authors

ISBN 978-3-95450-142-7

MULTI GIGAWATT HIGH CURRENT PULSED ELECTRON ACCELERATOR TECHNOLOGY DEVELOPMENT PROGRAM AT BARC

Archana Sharma, Romesh Chandra, S. Mitra, Sandeep Singh, Vishnu Sharma, K. Senthil, Ankur Patel, S. R. Ghodke, A. Roy, P. C. Saroj, Ritu Agarwal, T. S. Kolge, Hitesh Choudhary, Ranjeet Kumar, M. Danish Beg, K. C. Mittal and L. M. Gantayet[1]
Accelerator and Pulse Power Division, Bhabha Atomic Research Centre, Mumbai India-400085
[1]Beam Technology Development Group, Bhabha Atomic Research Centre, Mumbai India-400085

Abstract

High current intense electron beams were investigated earlier for Flash X-rays and nuclear electromagnetic pulse generation. Starting with moderate parameters of 200 kV, 6 kA, 60 ns pulsed electron beam source from a system named Kilo Ampere Linear Injector (KALI-75) our latest development is KALI-30 GW system rated for 1 MV, 30 kA, 80 ns.

First repetitive pulse LINAC without spark gap switching was developed as Linear Induction Accelerator (LIA-200) for technology demonstrations at 100 Hz. Also a repetitive Marx generator coupled reflex triode system to operate at 10 Hz. Next to this series of development LIA-400 has been developed to a capacity of 400 kV, 4 kA, 100 ns, 300 Hz. To make these pulse power systems applicable for big LINAC projects like nToF studies or ADS program, a high current electron gun has also been developed to give 100 A, 2 ns,10 Hz pulses.

INTRODUCTION

High current intense electron beams were investigated earlier for fusion related studies followed by high power microwaves (HPM), Flash X-rays (FXR) and nuclear electromagnetic pulse (NEMP) generation. In these systems, relativistic electron beams (REB) are produced by high voltage pulse power systems terminated to a suitable electron gun diode. In changing global scenario, numerous applications of repetitive pulsed power systems have been experimentally demonstrated to meet industrial and inter-disciplinary R&D activities.

KALI SYSTEMS

The design and development of high voltage pulsed electron accelerator program in Bhabha Atomic Research Centre has been initiated in early 1970s. Starting with moderate parameters of 200 kV, 6 kA, 60 ns pulsed electron beam source from a system named Kilo Ampere Linear Injector (KALI)-75. Latest development is KALI-30 GW system rated for 1 MV, 30 kA, 80 ns. During this development many involved technologies were developed viz. Compact pulse transformers (air core and amorphous core based), Unipolar and bipolar Marx generators, to create impulse from DC charging. For shaping the output pulse across the load, various kinds of pulse forming lines (PFL) such as castor oil/transformer oil or demineralized (DM) water filled coaxial PFL, Blumlein and strip forming lines have been adopted. For efficient energy transfer and low rise time (<10 ns), fast switching of 100s



Figure 1: KALI 30 GW System.

of kV and 10s of kA current, solid state switches cannot be utilized. Hence coaxial high pressure spark gaps and trigatron electrodes are implemented. During system development, in-situ pulsed diagnostics for the measurement of fast rising current using self integrating Rogowski coil were developed and for voltage measurements aqueous voltage dividers from 100s of kV to a few MV regimes were developed. In APPD, BARC single shot systems are developed in successive up gradation of output peak power of these KALI systems with a suffix of pulse energy in joule such as KALI-75 J, KALI-200 J, KALI-1000 J and KALI-5000 J. All these systems were based on spark gap switches and interval between two pulses is 5-10 minutes [1, 2]. It is very critical to control pre-pulse by choosing appropriate design [5] to generate REBs of desired parameters [6]. The KALI 30 GW system image is shown in Fig.1. Figure 2 shows the output voltage and current pulse of KALI 30 GW system.

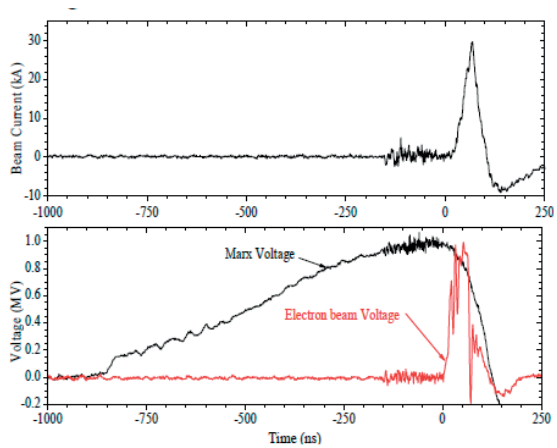


Figure 2: Electron beam current (above) and Marx voltage and Diode Voltage for KALI 30 GW system.

Copyright © 2014 CC-BY-3.0 and by the respective authors

OPERATION AND IMPROVEMENTS OF THE ALBA LINAC

R. Muñoz Horta, JMª Gómez Cordero, F. Pérez
ALBA Synchrotron, Cerdanyola del Vallès, Barcelona, Spain

Abstract

The ALBA Light Source pre-injector is a 100 MeV electron Linac which started operation in July 2010. Since then, several improvements have been made to the Linac system to enhance the beam stability and the operation reliability with special focus to top-up mode operation requirements. A description of the modifications applied to the RF system and an overview of the different modes of injection are presented. Also operational experience in decay mode and in the recently implemented top-up mode are reported.

THE ALBA LINAC



Figure 1: The ALBA Linac

ALBA is a third generation synchrotron light source whose injector consists of a 100 MeV linac and a Booster that accelerates the beam up to the full energy, 3 GeV. The ALBA storage ring has a circumference of 268.8 m and provides a photon beam to 7 beamlines [1]. The ALBA pre-injector is a Thales linac installed and commissioned in 2008 [2].

The beam at the linac is generated at 90 keV by a thermionic gun in multi or single bunch. The beam is then sent to a three stage bunching system consisting of a sub-harmonic pre-buncher cavity resonant at 500 MHz (PB1), a 3GHz pre-buncher (PB2) and a 22-cells standing wave buncher (BU). The energy of the beam at the buncher exit is of 16 MeV. Two identical travelling wave constant gradient accelerating sections (AS1 and AS2) increase further the energy up to a maximum of 125 MeV. However, the linac is routinely operated at 110 MeV. The beam emittance in both planes is of 15 mm.mrad.

The ALBA linac is driven by two Thales TH2100 klystrons that deliver 5μs pulses at a frequency of 3GHz. They generate a maximum output of 35MW at a repetition rate of 3 Hz.

TOP-UP OPERATION

Until recently, ALBA has been operating for users performing two injections to the Storage Ring (SR) per day to the present nominal current level of 120 mA. In June 2014 ALBA offered to users its first operation in top-up mode, where frequent injections keep the average storage ring current within few per cent variation [3].

Currently a two-third storage ring filling pattern is used, in which 320 out of the 448 buckets of the SR are filled with electrons. For this fill the linac is operated in multi-bunch mode, delivering trains of 32 bunches per injection. At present, top-up mode injections are performed every 20 minutes. At each injection the linac delivers 10 shots to refill de SR with 1mA of current. In this way, the current is distributed between all the full buckets of the SR.

Linac single bunch injection in top-up mode is being implemented and expected to be offered to users in 2015. This injection mode will allow us to select and to inject on the less populated bunches, thus keeping a more uniform distribution of electrons among the buckets [4].

LINAC STABILITY

The ALBA Linac is running reliably since started its operation in 2010. At the early stages of the linac operation we experienced that the thermionic gun filament heating process and the thermalization of the klystron components (gun components and low level RF) need a stabilization period of 36 hours to have good energy and charge stability at the linac beam.

The linac beam is also sensitive to fluctuations of the air and cooling water temperatures of the linac bunker and of the service area, where the klystrons and the racks with instrumentation are located. Air temperature fluctuations of 0.7ºC p-p on the linac bunker produce beam charge oscillations of 0.15 nC. After that the temperature of the linac bunker is kept at 23±0.2 ºC. On the service area the temperature is also of 23ºC, but with a day-night temperature variation of about 1ºC.

Instabilities of the linac beam position are observed from time to time at the exit of the bunching stage, where the first YAG screen is located. The instabilities follow the pattern shown in Figure 2. The beam position drifts for several minutes (in x and/or y-direction) until it suddenly shifts. These instabilities are typically small, with shifts of less than 1mm, and do not disturb operation. However, sporadically, the instabilities are amplified and affect as well to the linac charge, which also oscillates following the same pattern. The source of the instabilities is still under investigation.

Copyright © 2014 CC-BY-3.0 and by the respective authors

ISBN 978-3-95450-142-7

STATUS ON AIRIX RESTART

A.Georges, J.Beaubernard, V.Bernigaud, L.Buche, Y.Collet, S.Combacon, G.Grandpierre, B.Gouin, J.Kranzmann, J.Magnan, L.Magnin, D.Pierre, F.Poulet, R.Nicolas, Y.Tailleur, JL.Verstraete, CEA Valduc, Is sur Tille, FRANCE

Abstract

The Airix accelerator has been moved from Moronvilliers to Valduc to be part of the EPURE facility. Airix has been refurbished and restarted. This paper presents the first results and quantification of performances at its new location.

AIRIX MOVE

Airix is a linear induction accelerator with a 4 MeV beam injector and 64 induction cells. A more complete description is available in [1, 2]. It is used for hydrodynamics experiments.

Following the creation of the French-British shared experimental facility EPURE at Valduc, France, the Airix machine has been moved from its previous location in Moronvilliers, France to this new facility, where it will provide a 1st radiographic axis.

AIRIX REFURBISHMENT

Main Systems

This move has been used to address and upgrade a number of technological issues:

- replacement of sulfur hexafluoride by pressurized dry air gaseous medium for the main switches of accelerating cells drivers [3],
- replacement of high voltage rubber-based cables and high voltage connections between the drivers and the cells [3],
- oil change in accelerating cells
- replacement of thyratron switches
- redesign of the drifting and focusing space at the end of the accelerator to accommodate for the new building characteristics and norms.

Ancillary Systems

This move has also been the occasion to improve upon the performances of ancillary systems:

- upgrade of the vacuum system, with faster pumping times and locally improved levels of secondary vacuum or some measurements systems,
- alignment and beam position monitors, with positioning and testing systems with higher precision. Those systems have kept their original designs [4].
- refurbishment of the command-control system and data acquisition system
- modernization of the imaging systems,
- installation of a high performance safety system

The machine has also been hardened against the effect of a seismic event in accordance with building regulations for this experimental facility.

AIRIX RESTART

Initial Testing

In accordance with the plan, systems have been transferred and individually tested for a year before being run together. On schedule, Airix has been completely restarted on April 1st 2014.

Production

Since then, the machine has delivered more than 1000 electron beams for adjustment and optimization of parameters. Up to 20 X-ray beams per day have been produced reliably by conversion of the electron beams.

AIRIX PERFORMANCES

On a usual day of operations, Airix will display very stable characteristics.

Electrical Performances

The beam injector has been fitted with a 50 mm cathode (2 mm recess) [5]. The beam current, for an amplitude range of 800 A to 2 kA, will present a peak to peak amplitude jitter of 10 A and for pulse duration of 100 ns (at 10% of the maximum voltage) a rms timing jitter (1σ) of 1 ns. Since the objective is to obtain a flat top, we also gauge the stability of the 60 ns pulse plateau at less than 1% (cf. Figure 1).

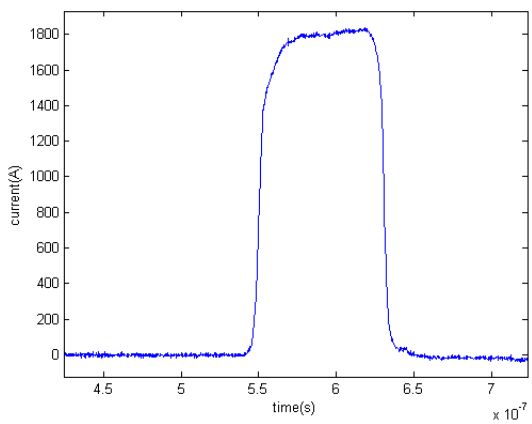


Figure 1: beam current input pulse shape

The voltage sensors of the emission diode have been calibrated by a parallel time-resolved electron spectrometry measurement. Energy spread remains very

Copyright © 2014 CC-BY-3.0 and by the respective authors

ANALYSIS OF SYSTEMATIC AND RANDOM ERROR IN SRF MATERIAL PARAMETER CALCULATIONS*

S. Meyers †, S. Posen, M. Liepe, Cornell University, Ithaca, NY 14853, USA

Abstract

To understand the relationship between an RF cavity performance and the material on its surface, one must look at various parameters, including energy gap, mean free path, and residual resistance. Though SRIMP fits for seven parameters, three parameters are eliminated using measurement and literature values, and the uncertainty of the fit of the remaining four parameters is further reduced by synthesizing two 3-parameter fits, each from a different data set. To study random error, Monte Carlo simulations were performed of ideal data with added noise; for systematic error, contour plots of normalized residual sum of squares (RSS) of the polymorphic fit on inputted data were generated.

INTRODUCTION

SRF researchers are currently developing new methods, such as nitrogen doping of niobium cavities, and new materials, such as Nb_3Sn, to improve cavity performance. In particular, nitrogen doping is being developed for SLAC's Linac Coherent Light Source II (LCLS II), which will require hundreds of niobium cavities [1]. Nitrogen doping has been found to significantly increase quality factors Q_0, which would significantly reduce associated infrastructure and energy costs for the cryogenic plant [2]; however, the reasons behind this increase in quality factor are not completely understood. In order to gain a deeper understanding of this increase in performance, material parameters and associated uncertainty must be reliably extracted. Similarly, reliable extraction of material parameters of Nb_3Sn can yield insight into this new material. Limitation mechanisms in Nb_3Sn-coated cavities are not yet well understood, so it is imperative to be able to compare critical fields of the material with onset fields for these limitations, but reliable material parameters are needed in order to calculate the critical fields. Furthermore, it is important to characterize Nb_3Sn because its parameters vary widely depending on preparation methods (e.g., temperatures and times); thus, knowledge of its parameters can be used to optimize preparation methods.

For both nitrogen-doped Nb and Nb_3Sn, the parameters of interest are critical temperature, T_c, energy gap, $\frac{\Delta}{k_B T_c}$, intrinsic coherence length, ξ_0, London penetration depth, λ_L, mean free path, ℓ, residual resistance, R_0, and penetration depth at f_0, λ_0. Data on superconducting materials of interest were taken by two different methods: measurement of the quality factor as a function of temperature and measurement of the cavity frequency (f) as a function of temperature. Given either set of data, superconducting parameters can then be obtained by fitting to a model. In this study, J. Halbritter's SRIMP program was used [3], which takes input arrays of temperatures and uses BCS theory equations to compute surface resistance R_s (where $R_s = G/Q_0$, where G is a geometry-dependent constant) and penetration depth λ, which respectively are related to Q_0 and f, for given values of T_c, $\frac{\Delta}{k_B T_c}$, ℓ, λ_L, and ξ_0. Using these 5 parameters, fits can then be made by the addition of constant offsets R_0 and λ_0. However, because T_c can be measured, and ξ_0 and λ_L extracted from the literature, the 7-parameter fit can be reduced to a 4-parameter fit. Furthermore, both sets of data can be fit concurrently to obtain ℓ and $\frac{\Delta}{k_B T_c}$: since λ_0 can be extracted only from the f vs. T data set, and R_0 only from the Q vs. T data set, the sloppiness of the fit can be further reduced by using, rather than one 4-parameter fit based off one data set, two 3-parameter fits—one from each data set—in conjunction with one another. Fitting only f vs. T or Q vs. T yields large uncertainty in material parameters, because either measurement is sensitive to parameters the other is less sensitive to. One of the aims of this paper is to show how the given methods of obtaining parameters such as $\frac{\Delta}{k_B T_c}$ and ℓ minimize their associated uncertainty, and to present a comparison of how the different parameters of interest affect the uncertainty of the fit. Sample fits of Q vs. T and f vs. T data, using the final extracted values for the 7 parameters of interest, are shown in Fig. 1.

METHODS

In order to separately understand the effects of systematic error and random error on the parameters of interest, two methods were used. To look at systematic error from fitting, a range for $\frac{\Delta}{k_B T_C}$ and ℓ were iterated through; the SRIMP-based polymorphic fit was then applied to the data with all values fixed except for constant offsets R_0 or λ_0, depending on which data set was being fitted. The resulting residual sum of squares (RSS) value was saved for each iteration, and a contour plot of RSS, normalized to the minimum, as a function of $\frac{\Delta}{k_B T_c}$ and ℓ was generated. Each call of the polymorphic fitting function used MATLAB's built-in fminsearch function [6] to optimize R_0 or λ_0 after every iteration of the program had run, the resulting array of RSS values was normalized to the global minimum. Because such a contour plot was generated for each of the two data sets, the results from each plot could be synthesized to generate a "combined" contour plot by averaging the normalized RSS values from each data set, and then normalizing these combined RSS values to the minimum.

Monte Carlo simulations were used to analyze and understand random error. SRIMP was used to generate artificial data sets of both types, λ and R_s, from input material param-

* Work supported by NSF Career award PHY-0841213 and DOE award ER41628.

† sjm342@cornell.edu

Copyright © 2014 CC-BY-3.0 and by the respective authors

ISBN 978-3-95450-142-7

QUALIFICATION OF THE TITANIUM WELDS IN THE E-XFEL CRYOMODULE AND CE CERTIFICATION

S. Barbanotti#, H. Hintz, K. Jensch, R. Klos, W. Maschmann, A. Matheisen, A. Schmidt,
DESY, Hamburg, Germany
C. Boulch, J.P. Charrier, C. Cloué, C. Madec, O. Napoly, J.L. Perrin, Y. Sauce, T. Trublet,
CEA/DSM/Irfu, Saclay, France

Abstract

The CE stamping of the one hundred 1.3 GHz cryomodules for the European XFEL Linac is a main step in the process of the certification of the entire Linac as pressure equipment. Stringent requirements on materials and the quality of the welds of the pressurised components need to be satisfied to obtain the stamp. This paper summarizes these requirements, describes the process developed to qualify each module and summarises the rework campaign on the cavity helium vessels made necessary to obtain the required quality for a reliable and safe accelerator.

INTRODUCTION

The European XFEL linac has to fulfil for operation the requirements of the "Betriebsicherheitsverordung" (German implementation of the European Directive 2009/104/EC "use of work equipment"). In Hamburg, where the linac will be installed and brought into operation, this means that the linac needs for operation the approval from the "Amt für Arbeitsschutz (AfA, HH)" (office for work safety).

The AfA does not verify the facility itself; the certification (e.g. CE marking) is done via a notified body (in the XFEL case, the TÜV Nord [1]). The CE marking is the manufacturer's declaration that the product meets the requirements of the applicable EC directives. For the XFEL, this means that the cold linac has to be conform to the Pressure Equipment Directive PED (97/23/EC) [2].

XFEL CRYOMODULE CERTIFICATION

The cold XFEL linac is an assembly of 100 cryomodules, ~ 100 sets of bellows for the cryomodule connections, string connection boxes and End/Feed caps with relief valves. Bellows, boxes and caps have a declaration of conformity to the PED or are already CE marked at the delivery, while the cryomodules are marked during the assembly process under DESY responsibility at CEA-Saclay.

Each XFEL cryomodule is an assembly, made of the following PED-relevant sub-components: 8 cavities, 1 quadrupole, 7 titanium bellows, 1 end connection, 1 quadrupole pipe and 1 cold mass (also an assembly of cooling pipes and heat exchangers). Each component is independently certified as "part of pressure equipment" by a notified body or by DESY (as an approved manufacturer according to AD2000 HP0 and EN3834).

#serena.barbanotti@desy.de

At Saclay, the cavity string (figure 1) is assembled and the helium circuit is welded together; these processes need to be approved by the manufacturer DESY and by the notified body. This means strict requirements on the material employed, on the welding techniques and on the non-destructive tests to be performed on the weld seams. It also implies that all the operations (welding and non-destructive tests) have to be performed by certified and well trained personnel.

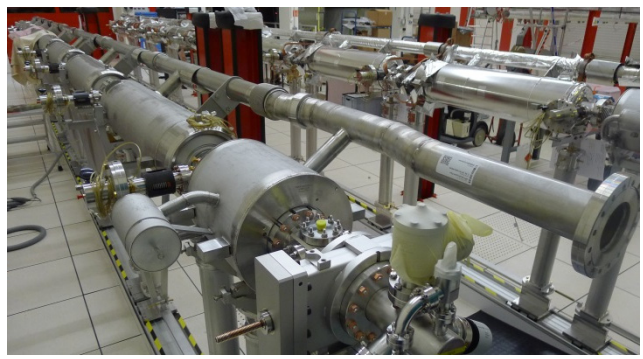


Figure 1: Two assembled cavity strings with welded helium circuit.

Material Requirements

In the choice of material, the easiest solution is to require the manufacturer of the components to be certified for producing according to the PED. Otherwise, additional examinations/certifications on the pipes and bellows are required. As an example, if the producer is PED certified the pipes can be delivered with an EN10204 3.1 certificate, while if he is not, an EN10204 3.2 certificate from an external authority is required.

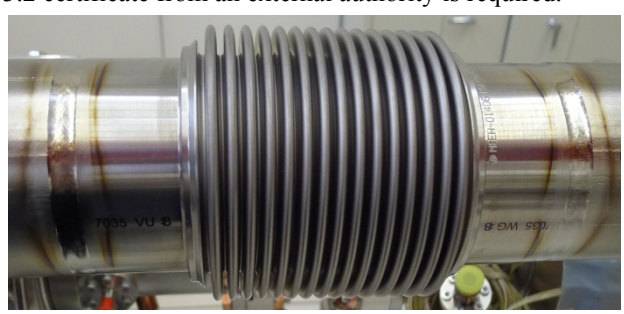


Figure 2: Example of a Ti76 weld

Welding

The PED relevant helium circuit welds performed during module assembly are:

Copyright © 2014 CC-BY-3.0 and by the respective authors

ISBN 978-3-95450-142-7

BEAM DYNAMICS SIMULATION FOR FLASH2 HGHG OPTION

Guangyao Feng#, Igor Zagorodnov, Torsten Limberg, Martin Dohlus, Winfried Decking,
Yauhen Kot, Jörn Boedewadt, Matthias Scholz, Sven Ackermann, DESY, Hamburg, Germany
Kirsten Hacker, Technische Universität Dortmund, Germany
Tim Plath, University of Hamburg, Germany

Abstract

The free electron laser (FEL) facility at DESY in Hamburg (FLASH) is the world's first FEL user facility which can produce extreme ultraviolet (XUV) and soft X-ray photons. In order to increase the beam time delivered to users, a major upgrade named FLASH II is in progress. The electron beamline of FLASH2 consists of diagnostic and matching sections and a SASE undulator section. A seeding undulator section will be installed in the future. FLASH2 will be used as a seeded FEL as well as a SASE FEL. In this paper, some results of beam dynamics simulation for the SASE option are given at first which includes parameters selection for the bunch compressors, RF parameters calculation for the accelerating modules and beam dynamics simulation taking into account the collective effects. Beam dynamics simulation for a single stage HGHG option is based on the work for the SASE option. Electron bunches with low uncorrelated energy spread and small energy chirp are obtained after parameters optimization. The FEL simulation results show that 33.6 nm wavelength FEL radiation with high monochromaticity can be seeded at FLASH2 with a 235 nm seeding laser.

INTRODUCTION

In order to increase the beam time, a major upgrade of FLASH, FLASH II, is in progress [1]. As the extension of FLASH, the beamline of FLASH2 has been constructed in a separate tunnel. A seeding undulator section will be installed in the FLASH2 beamline. The layout of the undulator sections will allow for different seeding schemes, like HHG, cascaded HGHG scheme and several combinations of those [2]. In this paper, parameters selection for the bunch compressors, RF parameters calculation for the accelerating sections and beam dynamics simulation taking into account the space charge, CSR and longitudinal cavity wake field effects are introduced for the SASE option. Based on the work for the SASE option, beam dynamics simulation and FEL simulation for a single stage HGHG option are presented. The injector, the main linac, the bunch compressors, the FLASH2 arc section and the beamline between the modulator and the radiator are studied with help of codes ASTRA [3] and CSRTack [4]. Code Genesis 1.3 [5] is used to simulate the physics in the undulator sections.

LAYOUT OF FLASH

The schematic layout of FLASH facility and the magnets distribution in the FLASH2 arc section are shown in Figure 1.

The injector of FLASH consists of a photo cathode RF gun, an L-band accelerating section (ACC1) [6] and a third harmonic accelerating section (ACC39) [7]. There are two accelerating sections, L1 (ACC2, 3) and L2 (ACC4, 5, 6, 7), in the main linac. Two bunch compressor chicanes are installed in horizontal plane along the main linac. The first compressor BC2 is placed downstream of ACC39. It is a C-type chicane which consists of four dipole magnets. The second compressor BC3 is located after ACC3 which has an S-type structure [8, 9].

Behind the main linac, three fast vertical kickers and a DC Lambertson-Septum are installed which can distribute the electron bunches either to the dogleg section of FLASH1 or to the FLASH2 arc section. In the extraction arc of FLASH2, there are four horizontal bending magnets and the arc section is achromatic in horizontal plane. The vertical dispersion caused by the kickers is closed with two vertical bending magnets at the end of the extraction arc. The first order R_{56} parameter becomes zero at the exit of the last dipole magnet [10]. Besides the SASE undulator, a seeding undulator section will be installed in the FLASH2 beamline.

BEAM DYNAMICS SIMULATION FOR SASE

At the entrance of the SASE undulator section, bean bunches with high peak current, small slice emittance and low energy spread are needed to get FEL radiation with short gain length. In the beam dynamics simulation for the SASE option, the peak current of 2.5 kA is used and the beam energy after the main linac is 1.0 GeV. The nominal energies before BC2 and BC3 are fixed as follows: E_1=145.5 MeV, E_2=450 MeV.

The transformation of the longitudinal coordinate in the i^{th} bunch compressor is described by

$$s_i = s_{i-1} - \left(R_{56i}\delta_i + T_{566i}\delta_i^2 + U_{5666i}\delta_i^3\right) \quad i = 1, \dots, N$$

where R_{56i}, T_{566i} and U_{5666i} are the momentum compaction factors in the i^{th} compressor. δ_i is the relative energy deviation. For the fixed values of RF parameters and momentum compaction factors, the global compression function can be defined as

$$C_N = \frac{1}{Z_N}, Z_N = \frac{\partial s_N}{\partial s}$$

where, the function $C_N(s)$ describes the increase of the peak current in the slice with initial position s and $Z_N(s)$ is the inverse global compression function. For the linear compression in the middle of the bunch, the first and the second derivatives of the global compression can be set to zero. Considering the relation between the derivative of the global compression and the derivative of the inverse

guangyao.feng@desy.de

Copyright © 2014 CC-BY-3.0 and by the respective authors

A NEW TYPE OF WAVEGUIDE DISTRIBUTION FOR THE ACCELERATOR MODULE TEST FACILITY OF THE EUROPEAN XFEL

V.Katalev#, S.Choroba, DESY, Hamburg, Germany
A.Seliverstov, S.P.A.FERITE Ltd., St.Petersburg, Russia
E.Apostolov, MicroPlus-Apostolov Ltd., Sofia, Bulgaria

Abstract

In order to test 100 superconducting accelerator modules within two years three test benches have been created in the accelerator module test facility (AMTF) to achieve the rate of one cryomodule per week. Each RF station of the test facility consists of a 5 MW RF station, at 1.3 GHz, 1.37 ms pulse width and 10 Hz repetition rate, with a waveguide distribution system. Each waveguide distribution supplies RF power to eight cavities, four times a pair of cavities. The distribution allows for a maximum power of 1 MW per cavity when the distribution is switched to a mode supplying power to only four cavities. A new type of 1 MW isolator and a new compact 5 MW power divider have been developed to achieve that goal.

Several cryomodules have been already successfully tested with this setup. We present the waveguide distribution for this test stand and describe the performance of the different elements.

REQUIREMENTS FOR THE AMTF WAVEGUIDE DISTRIBUTION

The AMTF [1] waveguide distribution should meet several specific sometimes conflicting requirements. On one side the distribution should have a compact size since there is only limited space in the AMTF shielding tunnel. On the other side it should supply high pulse RF power to the individual cryomodule cavities with high flexibility by only one power klystron. In addition the waveguide distribution has to protect the klystron against reflected power from superconducting cavities.

The three basic requirements are:

- Power per cavity:
  1 MW max pulse power
  2.2 kW max average power
- One 5 MW klystron as RF power source
- The waveguide distribution layout must allow for a free access to the cavity couplers for local clean room installation.

In order to satisfy these conditions specific waveguide components, such as a 1 MW isolator and a 5 MW power divider have been developed and integrated in the waveguide distribution. A 3D-view of the AMTF waveguide distribution is shown in Fig.1.

During maintenance of RF station the klystron has to be connected to two dummy loads. Therefore a mechanical waveguide switch is installed which allows for quick connection of the klystron and the loads.

#valery.katalev@desy.de

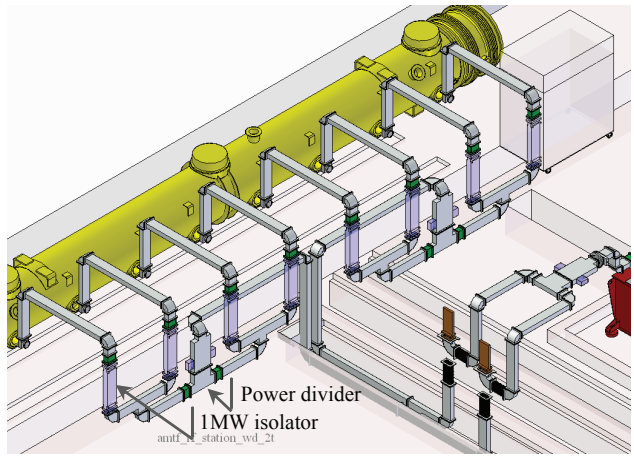


Figure 1: 3D-view of the AMTF waveguide distribution.

1 MW ISOLATOR

In order to protect the klystrons in the XFEL tunnel against reflected power the Y-junction circulators with matched and four port phase shift circulators with two matched load are used. For the AMTF waveguide distribution the isolators could not be used since the Y-junction circulators are limited in power and phase shift circulators are too big. Therefore a new type of a 1 MW isolator has been developed by the Company “FERRITE” from St. Petersburg, Russia. The new FWHI3-27A type isolator uses the nonreciprocal energy absorption in the ferrite elements by ferromagnetic resonance for waves with circular polarization. An overview of the device (without magnetic system) is shown in Fig.2.

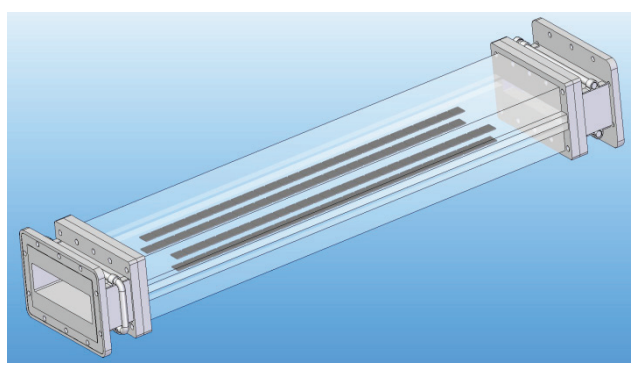


Figure 2: View of the S.P.A.FERRITE 1 MW isolator.

In this device the reflected power is absorbed in the ferrite material itself and not in an external matched load. The special type of the ferrite, its shape and location as well as the design of water cooling system allows to increase the average power. The magnet system uses a

Copyright © 2014 CC-BY-3.0 and by the respective authors

ISBN 978-3-95450-142-7

RF TUNING OF A S-BAND HYBRID BUNCHER FOR INJECTOR UPGRADE OF LINAC II AT DESY

Y.C. Nie#, C. Liebig, M. Hüning, M. Schmitz, DESY, Hamburg, Germany

Abstract

LINACII at DESY currently provides 450 MeV electrons for the synchrotron radiation source PETRAIII. The injector upgrade of it aims to improve its reliability and mitigate the radiological activation due to electron losses at hundreds of MeV. Therefore, a 2.998 GHz hybrid buncher has been developed and will be installed in between a pre-buncher and LINAC II. It comprises a 1-cell standing-wave (SW) section for rapid acceleration and a 13-cells travelling-wave (TW) section for further bunching and acceleration. This paper focuses on its RF tuning procedure. The tuning strategy combines a non-resonant bead-pull measurement of complex electric field and a linear model for local reflection coefficient calculation. The tuning result is satisfying. Field unflatness of the TW section has been improved from ±9% to ±4%, and field in the SW section has been enhanced significantly. By using ASTRA simulation, it has been verified that the residual detuning of the structure is acceptable in view of beam dynamics performance.

INTRODUCTION

LINAC II at DESY accelerates electron bunches to 450 MeV before they are injected into PIA and DESY II. DESY II provides 6.0 GeV beam for the third generation radiation source PETRA III [1]. Moreover, LINAC II has promising potential to provide 800 MeV electron bunches for the Helmholtz distributed ARD facility SINBAD [2]. A new injector of LINAC II has been constructed and is being tested in parallel to the old injector. In the new injector, the old DC diode gun was replaced by a triode gun, and a hybrid buncher was inserted after the pre-buncher to mitigate the radiological activation problem due to electron loss at hundreds of MeV. The detailed upgrade plan can be found in [1]. The performance of the new injector has been verified by using ASTRA simulations [3, 4].

In this paper, we focus on the RF tuning of the 2.998 GHz hybrid buncher, one of the most critical components in the new injector. A hybrid structure combines the advantages of both SW regime and TW regime. The detailed RF design of the hybrid buncher was reported in [1]. The structure and the simulated electric field using CST Microwave Studio [5] of the hybrid buncher are shown in Fig. 1. Each cell can be tuned by the deformation of the cylindrical holes in the outer wall, the so called tuners. All the tuning holes can only be pressed inwards the cavity gently by hammering a copper rod with a spherical head, and the deformations can hardly be recovered. It means that we can only increase the structure's frequency during tuning. So the buncher was manufactured at a frequency several MHz lower than the operating frequency of 2.998 GHz.

The most used tuning strategy was derived from a non-resonant perturbation theory of C. Steele [6] and a linear model of T. Khabiboulline et al [7]. They were used for the overall bead-pull measurement of the complex electric field, and the derivation of each cell's (local) reflection coefficient, respectively. Such a method has been complemented during its applications to the tuning of the 12 GHz X-band TW accelerator of CLIC at CERN [8], and the 5.712 GHz C-band prototype for SPARC photo-injector upgrade [9], etc. We used the similar method, while paying special attention to enhancing the field in the SW cell to ensure its beam capturing capability.

TUNING PRINCIPLE

According to the non-resonant perturbation theory, the relationship between the reflection coefficient and the electric field can be expressed by the following equation at a given frequency $\omega=2\pi f$:

$$2P_i \Delta S_{11} = 2P_i (S_{11p}-S_{11a}) = -j\omega k E_a^2 , \quad (1)$$

where P_i is the input power, S_{11p} is the reflection coefficient in the presence of a perturbing object, S_{11a} is the value in the absence of it, k is a constant depending on the electric property and the geometry of the perturbing object, and E_a is the electric field at the perturbed position. It means that the field amplitude is proportional to the square root of the amplitude of ΔS_{11}, and its phase is half to the phase of ΔS_{11}.

Required tuning for each TW cell can be represented in terms of local reflection coefficient, which can be derived via T. Khabiboulline's linear model. In the center of a cell, the field can be considered as a superposition of forward and backward waves, provided that the cavity is lossless. For a regular TW n-th cell, its local reflection S_{11}^n can be calculated approximately by:

$$S_{11}^n = \frac{B_n - B_{n+1} e^{-j\varphi n}}{A_n} , \quad (2)$$

where A_n is the forward wave in the n-th cell, B_n and B_{n+1} are the backward waves in the n-th and $(n+1)$-th cells, respectively, and φ_n is the phase advance between $(n+1)$-th and n-th cells. They can be calculated from the measured complex field. Normally φ_n is close to the nominal phase advance $\varphi_0 = 2\pi/3$. For better distinguish, the local reflection coefficient calculated using φ_0 is denoted by $S_{11}^{n(0)}$. In principle, if the imaginary part of S_{11}^n

#yuancun.nie@desy.de

Copyright © 2014 CC-BY-3.0 and by the respective authors

TESTING OF THE FIRST PART OF SERIES PRODUCTION 10MW MBKS FOR THE XFEL PROJECT

V. Vogel, L. Butkowski, S. Choroba, A. Cherepenko, J. Hartung, V. Kachaev, R. Wagner.
DESY, 22607 Hamburg, Germany

Abstract

At present more than half of 27 of 10 MW horizontal multi-beam klystrons (MBK) manufactured by two companies for the European XFEL project have been delivered to DESY. After delivery each klystron is connected to the connection module (CM), a HV oil tank with integrated HV connector, voltage and current monitors and a coaxial filament transformer, tested on the test stand and, if necessary conditioned. After this the klystrons are ready for installation in the underground linear accelerator tunnel. Two MBKs are already installed at the injector area of the XFEL. For the European XFEL project MBKs which can produce RF power of 10 MW, at RF frequency of 1.3 GHz, 1.5 ms pulse length and 10 Hz repetition rate, were chosen as RF power sources. During the incoming test the most important parameters of the MBK such as bandwidth, filament power, perveance, gain at different cathode voltage, phase stability and sensitivity to the solenoids current setting are measured and documented. In this paper we will give an overview of the test procedure, summarize the current test results and give a comparison of the most important parameters for several tubes.

INTRODUCTION

Two companies, "Thales" with MBK TH1802 [1] and "Toshiba" with MBK E3736H [2], started klystrons delivery for the European XFEL project in 2012. By the end of 2014 DESY should have MBKs for all 27 RF station of the XFEL. The main parameters of the MBKs are given in Table 1.

Table 1: Main parameters of L-band MBK for XFEL

Parameters	Design value	Test value
Output power (MW)	10	9.9-10.5
RF pulse length (ms)	1.5	1.5
Efficiency (%)	> 63	63-68
Repetition rate (Hz)	up to 30	10
Average RF power (kW)	150	155
Collector power (kW)	300	270
Max drive power (W)	<200	<200
Bandwidth (MHz)	3	>3

All klystrons delivered in DESY were first connected to a connection module, CM, that had been produced by BINP Novosibirsk [3, 4 and 5] and then conditioned and tested in one the MBK test stands [6, 7 and 8]. The average time of conditioning and testing for the TH1802 is about 330 hours and for the E3736 about 280 hours. The tubes were conditioned up to full RF power and full RF pulse length with a repetition rate of 10 Hz. Figure 1 shows the top view of the test stands. Figure 2 shows one of klystrons with CM and HV cable inside of the test chamber. During acceptance test of MBK, in addition, two HV cables "NEXAN" with "PFISTERER 3S" connector were tested for about 11,000 hours. The test didn't show any sign of degradation or increasing level of partial discharge.

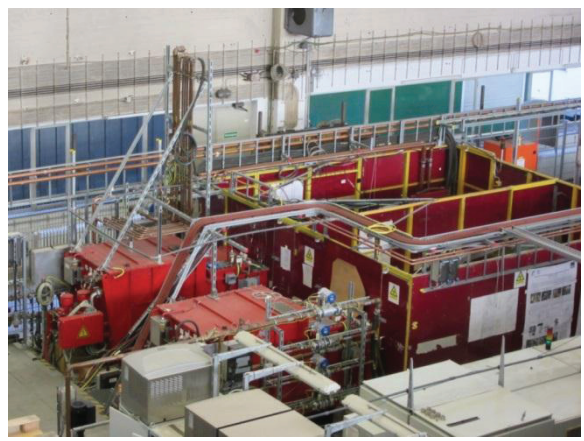


Figure 1: MBK test stands at DESY Hamburg

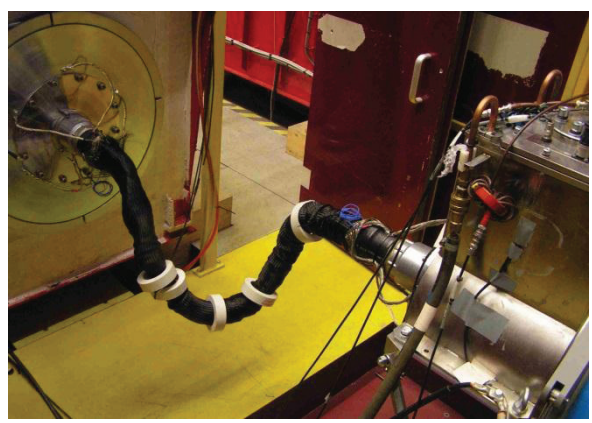


Figure 2: HV connection between pulse transformer and MBK, connectors' type "PFISTERER 3S"

Copyright © 2014 CC-BY-3.0 and by the respective authors

ISBN 978-3-95450-142-7

PROGRESS ON ESS MEDIUM ENERGY BEAM TRANSPORT

I. Bustinduy*, J.L. Muñoz, D. Fernández-Cañoto, O. González, S. Varnasseri, A. Ghiglino, R. Vivanco, F. Sordo, M. Magan, P. Gonzalez, N. Garmendia, L. Muguira, Z. Izaola, I. Madariaga, I. Rueda, ESS-Bilbao, Spain
A. Ponton, R. Miyamoto, M. Eshraqui, ESS, Sweden

Abstract

The considered versatile ESS MEBT is being designed to achieve four main goals: First, to contain a fast chopper and its correspondent beam dump, that could serve in the commissioning as well as in the ramp up phases. Second, to serve as a halo scraping section by means of various adjustable blades. Third, to measure the beam phase and profile between the RFQ and the DTL, along with other beam monitors. And finally, to match the RFQ output beam characteristics to the DTL input both transversally and longitudinally. For this purpose a set of eleven quadrupoles is used to match the beam characteristics transversally, combined with three 352.2 MHz CCL type buncher cavities, which are used to adjust the beam in order to fulfil the required longitudinal parameters. A thorough study on the optimal input beam parameters will be discussed. Quadrupole design update will be presented along with new RF measurements over the buncher prototype. Finally, updated results will be presented on the chopper and beam-dump system.

LAYOUT

During last year the ESS linac cost was reevaluated, in order to cope with the cost objective, final energy of the linac was reduced and both gradients and beam current were increased [1]; as a consequence important modifications were introduced to the linac design that affected MEBT section. RFQ output beam energy increased from 3 MeV to 3.62 MeV, and beam current under nominal conditions was increased from 50 to 62.5mA. From the envisaged layout [2] most affected systems were: quadrupole, buncher and chopper and beam-dump.

Fig. 2 shows the updated layout, where a quadrupole triplet is still used to focus the beam out of the RFQ. After leaving the chopper and beam-dump, the beam expands. Another triplet is used to focus the beam before entering the space for diagnostic devices. The last set of four quadrupoles is used to obtain DTL periodic transverse solution; accompanied by three CCL type buncher cavities for the longitudinal plane. In both cases, a good compromise in the focusing is required to prevent beam excursions to non-linear field regions, while avoiding over-focused bunches that would enhance inner space-charge repulsive forces [3].

Required Inputs for MEBT

In order to improve MEBT performance, a systematic approach was conducted to seek best input beam. 2 different sets of potential RFQ outputs were used as input of the ESS warm linac. MEBT focusing elements were used to match the beam to the required DTL periodic solution, and different beam parameters were evaluated at the end of the warm linac section.

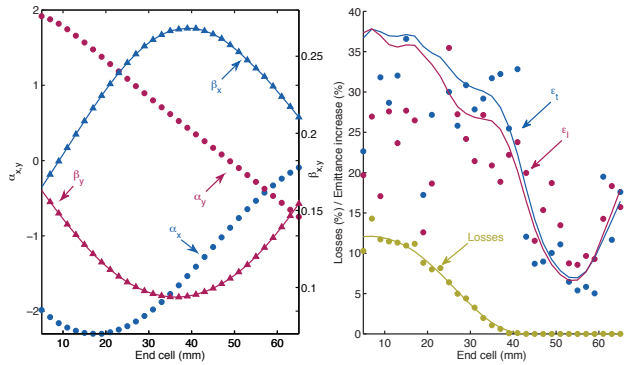


Figure 1: **Left:** Generated inputs from RFQ. **Right:** Output parameters at the end of ESS warm linac.

In order to produce the possible inputs, different end-cell and transition-cell lengths were adopted. Fig. 1 shows the particular case where end cell length adopts different values. This figure shows the combination of Courant-Snyder parameters ($\alpha_{x,y}, \beta_{x,y}$) employed at the input distribution (left frame), and the results obtained at the end of the warm linac in terms of transmission and transverse emittance increase respect to RFQ output distribution. Different simulations prove that lower values of α are desirable as input for this lattice. In the particular simulations presented in Fig. 1, this corresponds to end-cell values between 50 and 60mm. Therefore, it is recommended that RFQ includes a transition cell to obtain a symmetric output beam.

BUNCHER CAVITY

A prototype for the 352.2 MHz CCL type buncher cavity [2] was machined in stainless steel, characterised using a tridimensional metrology system (see Fig. 3) and thoroughly characterised by means of an RF bead pull system. Although, metrology report confirmed that machining in the lower ends of the cavity were substantially out of specs; in the critical nose-cone region, metrology report shows that surface flatness was within tolerances (92 μm), but distance between them was found to be 14% off its expected value. Such problem was solved using a pre-calibrated corrector ring. This ring was latter used in the RF bead pull measurement campaign. For this RF characterisation, three different dielectric beads were employed (Macor, Glass, Teflon). The form fac-

* ibon.bustinduy@essbilbao.org

Copyright © 2014 CC-BY-3.0 and by the respective authors

ISBN 978-3-95450-142-7

BEAM TESTS AT THE CLIC TEST FACILITY, CTF3

R. Corsini, S. Döbert, J.L. Navarro Quirante, T. Persson, P. Skowronski, F. Tecker, CERN, Geneva, Switzerland, W. Farabolini, CEA/DSM/IRFU, Saclay, France and CERN, Geneva, Switzerland
D. Gamba, John Adams Institute, Oxford, United Kingdom and CERN, Geneva, Switzerland

Abstract

The CLIC Test Facility CTF3 has been built at CERN by the Compact Linear Collider (CLIC) International Collaboration, in order to prove the main feasibility issues of the two-beam acceleration technology on which the collider is based. After the successful completion of its initial task, CTF3 is continuing its experimental program in order to give further indications on cost and performance issues, to act as a test bed for the CLIC technology, and to conduct beam experiments aimed at mitigating technological risks. In this paper we discuss the status of the ongoing experiments and present the more recent results, including improvements in beam quality and stability.

INTRODUCTION

The Compact Linear Collider (CLIC) [1] is one of the two machine design studies being pursued by the Linear Collider Collaboration. Essential for the verification of key issues of the CLIC design is the work carried out at the CLIC Test Facility CTF3 [2], located at CERN. In particular, CTF3 was built in order to demonstrate the following two main issues:

1. Drive Beam Generation: efficient generation of a high-current electron beam with the correct time structure needed to generate 12 GHz RF power. CLIC relies on a novel scheme of fully-loaded acceleration in normal conducting travelling wave structures, followed by beam current and bunch frequency multiplication by using RF deflectors for injection in a series of delay lines and rings. CTF3 is using a 120 MeV e^- linac followed by a stretching chicane, a 42 m Delay Loop (DL) and an 84 m Combiner Ring (CR) in order to produce a 30 A Drive Beam with 12 GHz bunch repetition frequency. The Drive Beam can be sent to an experimental area (CLEX) where it is used for deceleration and two-beam experiments.

2. RF power production and two-beam acceleration: in CLIC the needed 12 GHz high power RF is obtained by decelerating the high-current Drive Beam in travelling wave resonant structures, called PETS (Power Extraction and Transfer Structures). Such power is transferred efficiently to high-gradient accelerating structures, operated at 100 MV/m. In CLEX, one line (the Test Beam Line, TBL) is used to decelerate the Drive Beam in a string of PETS. The Drive Beam can be alternatively sent to another beam line (the Two-Beam Test Stand, TBTS), where a PETS is used to power one or more structures and further accelerate a 200 MeV electron beam provided by a dedicated injector, CALIFES.

CTF3 was build, installed and commissioned in stages. The commissioning of the Delay Loop, Combiner Ring and transfer lines connecting them and delivering the beam to CLEX was completed in 2009, together with the CALIFES probe beam injector. In autumn of 2009, the first full recombination with the DL and CR together was also achieved. In 2010 the nominal power production from the PETS was obtained, and the first two-beam test was performed, reaching a measured gradient of 100 MV/m. In 2011 a gradient of 145 MV/m was reached in two-beam tests and the PETS ON/OFF mechanism was successfully tested. In 2012 and 2013 the Drive Beam stability and the overall performances of the facility were improved and a 23 A Drive Beam was decelerated by 35% of its initial energy in a string of 12 PETS structures.

RESULTS OF THE FIRST 2014 RUN

The first CTF3 run in 2014 lasted from mid-February to the end of June. A summer shut-down started after that in order to allow for modulator/klystron maintenance and the installation of a full-fledged CLIC Two-Beam module in CLEX. The complex is now restarting gradually its experimental activity, as detailed later in the paper. The main areas of activity during the first run are summarized below.

Improvements in Drive Beam Generation

Most of the experimental activity was dedicated to improvements in the reliability, repeatability and stability of the Drive Beam generation.

The main problem in the previous runs was the availability of the travelling-wave tubes (TWTs) used to power the 3 sub-harmonic bunchers (SHB) of the drive beam injector. Most of the time in 2013 the injector was operated with only two or even a single SHB cavity, severely limiting the overall performance. A consolidation campaign took place during the 2013-2014 shut-down, reconfiguring the power supply/control units, and one new design TWT prototype from a different manufacturer has been procured. During the 2014 run the uptime for all TWTs was then close to 100%. Only one of the tubes showed gradual signs of aging (as expected from its 12000 hours of operation, well above the nominal lifetime of 6000 hours) and its power gradually decreased over time. We had been able to compensate for this behaviour during operation, and the tube will be substituted with a spare before the next run.

Other improvements were obtained in repeatability by implementing several tools and procedures [3] and additional feed-back loops [4]. An online dispersion measurement has been used extensively in operation and the feed-backs include now an injector feed-back, beam-loading and energy feed-backs.

Copyright © 2014 CC-BY-3.0 and by the respective authors

ISBN 978-3-95450-142-7

DIAGNOSTICS AND ANALYSIS TECHNIQUES FOR HIGH POWER X-BAND ACCELERATING STRUCTURES

A. Degiovanni, S. Doebert, W. Farabolini, I. Syratchev, W. Wuensch, CERN, Geneva, Switzerland
J. Giner-Navarro, IFIC and University of Valencia, Spain
J. Tagg, National Instruments Switzerland, Ennetbaden, Switzerland
B. Woolley, Lancaster University, Lancaster, United Kingdom

Abstract

The study of high gradient limitations due to RF breakdowns (BD) is extremely important for the CLIC project. A series of diagnostics tools and analysis techniques have been developed in order to monitor and characterize the behaviour of accelerating structures under high power operation in the first CERN X-band klystron-based test stand (Xbox-1). The data collected during the last run on a TD26CC structure [1] are presented in this paper. From the analysis of the RF power and phases, the location of the breakdowns inside the structure could be determined. Other techniques based on the field emitted dark current signals collected by Faraday cups placed at the two extremities of the structure have also been investigated. The results of these analyses are reported and discussed.

INTRODUCTION

CERN has constructed and is operating a klystron-based X-band test stand, called Xbox-1, dedicated to the high-gradient testing of prototype accelerating structures for CLIC and other applications such as FELs [2]. A TD26CC structure was high-power tested in the Xbox-1 test stand from July to December 2013. The conditioning process was computer controlled using the newly-developed algorithm described in [2].

The accelerating structure was instrumented and interlocked for BD with incident, transmitted and reflected RF signals, Faraday cups and vacuum [1]. A photograph of the experimental setup is shown in fig. 1.

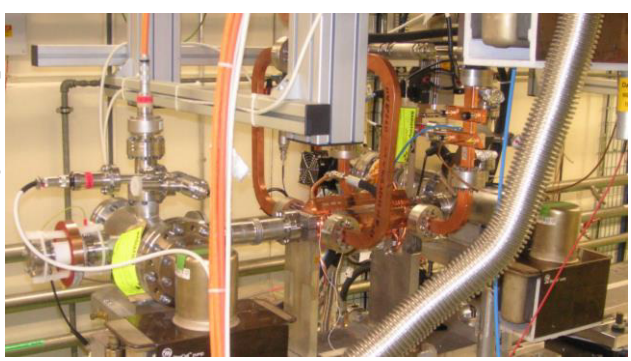


Figure 1: TD26CC structure installed in X-box1.

During breakdowns, a strong field reflection and charge emission can be measured. The data collected during breakdown events have been analysed in order to determine the breakdown location and to characterize the behaviour of the structure [3, 4]. The difference in timing between the transmitted and reflected signals or the echo between incident and reflected signals method can be used for breakdown cell localization. The emergence of a so-called "hot cell" can then be determined by looking at the distribution of breakdowns along the structure. Such information provides very important feedback for fabrication, conditioning and even the RF design of the structure [5]. For example a concentration of breakdowns could occur due to field profile along the structure.

The results of a breakdown position analysis obtained during the last run of the TD26CC structure are presented in this paper.

DIAGNOSTICS AND ACQUISITION SYSTEM

RF signals are sampled via 50 dB high power directional couplers and then propagated via N-type coaxial cables to an electronics crate. The signals are then split and sent to log detectors and IQ demodulators. The voltage outputs from the log-detectors are then digitized with 250 MHz Analogue to Digital Converters (ADCs) installed on a National Instruments PXI crate for acquisition and control. The IQ signals are converted to digital signals by 1 GHz ACQIRIS cards and then sent to the PXI crate. Power and phase of the signals are reconstructed from the IQ signals.

The dark current pulses are collected by Faraday cups placed in the downstream (DC1) and upstream (DC2) directions along the structure's beam axis and then digitized with a 250 MHz ADC. The Faraday cup signals are terminated in 50 Ohms.

The acquisition system stores pulse shapes of breakdown pulses with the previous two normal pulses (for comparison), as well as the pulse shapes of a normal pulse every minute, in order to monitor the behaviour of the accelerating structure. Typical incident, transmitted and reflected power signals, as well as Faraday cup signals during normal operation and for breakdowns are compared in Fig. 2.

As it is visible in Fig. 2, during a breakdown the transmitted power drops, while the reflected power signal increases. The dark current signals increase by a factor 100-1000, saturating the ADCs.

Copyright © 2014 CC-BY-3.0 and by the respective authors

DESIGN OF A HIGH CURRENT ELECTRON SOURCE FOR THE CLIC DRIVE BEAM INJECTOR

S. Doebert, N. Chritin, CERN, Geneva, Switzerland
J. Gardelle, B. Cassany, B. Cadilhon, K. Pepitone, CEA/CESTA, Bordeaux, France

Abstract

The drive beam injector for CLIC needs to deliver a 4.2 A electron beam for a duration of 140 μs with a repetition rate of 50 Hz. The shot to shot and flat top current stability has to be better than 0.1% to guarantee the beam stability required for CLIC. Based on the experience with the CTF3 injector, a thermionic high voltage gun with a gridded cathode has been designed together with a sub-harmonic bunching system to achieve these requirements. The grid will allow controlling the current and eventually feed back on the flat top shape. The gun will operate at 140 kV and an emittance of 14 mm mrad can be obtained. The paper describes the design approach and the results of the systematic electromagnetic simulations to optimize the gun. Care was taken during the mechanical design of the gun to obtain a modular design allowing adjusting for different beam currents and cathode sizes.

INTRODUCTION

In the two beam acceleration scheme of the Compact Linear Collider (CLIC) the drive beam serves as the power source for the main linac [1]. This drive beam is a low energy, high current beam where the beam power is extracted locally by deceleration and directly fed into the main linac. Therefore the beam stability of the main beam is critical to obtain the desired luminosity determined by the stability of the drive beam. This dependence put severe stability requirements on the drive beam injector. In CLIC the drive beam is generated from a 140 μs long DC electron beam, bunched at a sub-harmonic frequency of 500 MHz and then accelerated with an rf frequency of 1 GHz. The sub-harmonic bunching is used to phase code the beam to enable beam combination using rf deflectors and a series of combiner rings. In the end the long bunch train gets combined to 24 sub-trains which are each 240 ns long and have a 12 GHz bunch repetition rate. The average beam current gets increased from 4.2 A to 100 A during this process (see [1] for more details).

The drive beam injector consists of a thermionic gun, three sub-harmonic buncher cavities, a pre-buncher, a travelling wave buncher and fully loaded accelerating structures [2, 3]. A sketch of the drive beam front end is shown in Fig. 1. This paper concentrates on the electron source itself, which has to deliver a beam with the following parameters. The current needed from the gun to obtain 4.2 A average current or a bunch charge of 8.4 nC after bunching is about 5 A according to the injector simulations. Nevertheless a certain flexibility to increase the current should be taken into account for the gun design. The high average current and long pulse length is a major challenge for the cathode-grid assembly while the required current stability puts severe constraints on the high voltage power supply. The high voltage will be supplied by a solid state modulator currently under development in collaboration with CEA/CESTA.

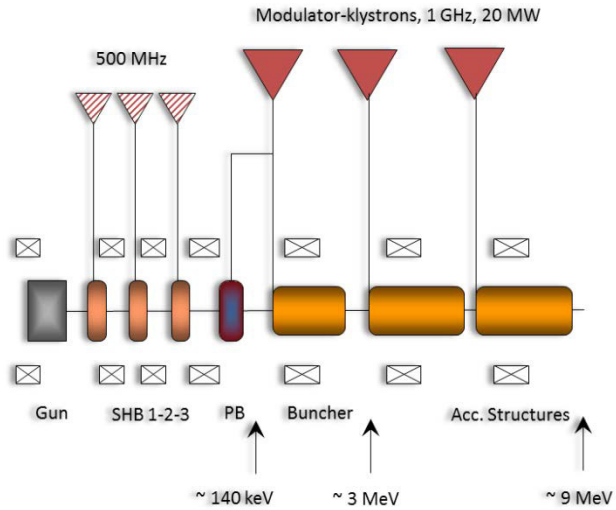


Figure 1: Layout of the CLIC drive beam injector front end. From left to right: Thermionic gun, 500 MHz sub-harmonic bunchers, 1 GHz pre-buncher, 1 GHz travelling wave buncher and two 1 GHz accelerating structures.

Table1: Main electron source parameters

Gun voltage	140 kV
Beam current	5 to 7 A
Pulse length	140 μs
Repetition rate	50 Hz
Emittance (rms)	< 20 mm mrad
Shot to shot charge variation	0.1%
Flat top charge variation	0.1% after correction
Average beam power	4.9 kW

ELECTRON GUN DESIGN

The electromagnetic design of the CLIC drive beam gun was done in collaboration between CEA/CESTA and CERN. The emphasis of the study was to obtain a focusing electrode geometry which allows operating the gun in a wide range of currents without compromising too much on the emittance of the generated beam. The design is based on the assumption that a commercial cathode grid assembly can be used. The grid is essential because it allows regulating the current of the gun and eventually could be used to correct the shape of the generated current pulse independent of the high voltage. We studied two different cathode assemblies produced by CPI/Eimac [4]

Copyright © 2014 CC-BY-3.0 and by the respective authors

ISBN 978-3-95450-142-7

UNDERSTANDING THE ERROR TOLERANCES REQUIRED TO AUTOMATICALLY PHASE THE HIE-ISOLDE LINAC

M.A. Fraser*†, S. Haastrup, J.C. Broere, D. Lanaia, D. Valuch, D. Voulot, CERN, Geneva, Switzerland

Abstract

The broad experimental programme at ISOLDE, CERN means that the same radioactive beam species and energy are rarely studied twice and the cavities of the linac must be scaled or re-phased for each experiment. A software application was developed to automatically re-phase the cavities of the HIE-ISOLDE superconducting linac to the beam from computed settings. The application was developed to expedite both machine set-up in normal operation and in scenarios involving cavity failures. A beam dynamics error study will be presented in order to better understand the challenges facing the automatic phasing routine. The effects of a variety of different errors on the efficacy of the phasing application were studied, leading to a specification of the tolerances required for the calibration of the rf system and the accuracy of the survey system that monitors the positions of the cavities.

INTRODUCTION

The High Intensity and Energy (HIE) linac upgrade will provide post-accelerated radioactive ion beams of better quality at energies over 10 MeV/u to the ISOLDE user community at CERN. The linac is discussed in more detail in other contributions to this conference [1, 2] and further details on the HIE-ISOLDE project can be found in [3, 4].

The tuning of linear accelerators comprised of independently phased cavities is usually carried out with beam-based measurements. The changing beam energy is measured in response to phase shifts of the rf power feeding the cavities as they are turned on sequentially. This procedure can become time-consuming when large numbers of cavities are considered and when the settings must be adjusted for different beam species with different mass-to-charge (A/q) states, as will be the case in the operation of the HIE-ISOLDE linac. The number of cavities will increase from 7 to 35 after the upgrade of the Radioactive ion beam EXperiment (REX) post-accelerator. Therefore, in developing a software tool to calculate and set automatically the cavity phases, we are motivated by reducing the time required to set-up the linac in both normal operational circumstances and in failure scenarios when the performance of a cavity (or several cavities) drops or goes offline. In principle, one could manually set-up the machine with a set of intermediate charge states or 'pilot' beams and scale the linac settings to the mass-to-charge state of each isotope requested by the experimental programme, as must necessarily be done for fixed-velocity linacs and is presently done at REX. However, by tuning the superconducting linac in this way one can neither exploit the maximum accelerating voltage nor react quickly to cavity failures; a single cavity dropping offline would require that all downstream cavities are manually retuned. The re-phasing of the ISAC-II linac at TRIUMF has been successfully carried out using computed values [5]. In these proceedings we investigate the effects of each error source on the beam quality delivered to the experiments. This work builds on tests already carried out at REX where it was identified that further error studies were needed to understand the tolerances required for successfully phasing the extra cavities accompanying the HIE-ISOLDE upgrade [6].

* The author acknowledges co-funding by the European Commission as a Marie Curie action (Grant agreement PCOFUND-GA-2010-267194) within the Seventh Framework Programme for Research and Technological Development.

† mfraser@cern.ch

HIE-ISOLDE LINAC RF SYSTEM

The rf system, shown schematically in Figure 1, has been designed to minimise phase errors between cavities with the automatic cavity phasing concept in mind. An rf reference line distributing the 101.28 MHz master oscillator signal will run alongside the accelerator and for each cavity the reference signal will be extracted by a directional coupler and sent along with the cavity's pick-up signal via a standard cable bundle to the LLRF controller; all phase signals should be subject to similar drift effects [7]. The reference phase signals will be used to normalise the pick-up signals from the cavities. The absolute phase on the reference line is known from calibration with an expected accuracy of a few degrees, but in any case an initial beam-based calibration of the rf system is foreseen to check and correct any phase errors in the system. The beam-based calibration checks will require accurate beam dynamics simulations and diagnostics in order to identify the phase errors.

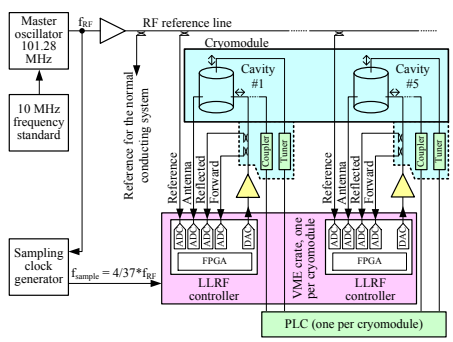


Figure 1: Schematic of HIE-ISOLDE rf system design.

SOFTWARE APPLICATIONS

A software application was written in object-oriented `C++11` to simulate the longitudinal beam dynamics in the HIE-ISOLDE linac. In a first step, the cavities were mod-

Copyright © 2014 CC-BY-3.0 and by the respective authors

EFFECT OF BEAM-LOADING ON THE BREAKDOWN RATE OF HIGH GRADIENT ACCELERATING STRUCTURES*

J.L. Navarro Quirante†, R. Corsini, A. Degiovanni, S. Doebert, A. Grudiev, G. McMonagle, S. Rey, I. Syratchev, F. Tecker, L. Timeo, W. Wuensch, CERN, Geneva, Switzerland
O. Kononenko, SLAC National Accelerator Laboratory, Menlo Park, USA and CERN
A. Solodko, JINR, Dubna, Russia and CERN, Geneva, Switzerland
J. Tagg, National Instruments, Switzerland
B. Woolley, Lancaster University, Lancaster, UK and CERN, Geneva, Switzerland
X.W. Wu, Tsinghua University, Beijing, P.R.China and CERN, Geneva, Switzerland

Abstract

The Compact Linear Collider (CLIC) is a study for a future room temperature electron-positron collider with a maximum center-of-mass energy of 3 TeV. To efficiently achieve such high energy, the project relies on a novel two beam acceleration concept and on high-gradient accelerating structures working at 100 MV/m. In order to meet the luminosity requirements, the break-down rate in these high-field structures has to be kept below 10 per billion. Such gradients and breakdown rates have been demonstrated by high-power RF testing several 12 GHz structures. However, the presence of beam-loading modifies the field distribution for the structure, such that a higher input power is needed in order to achieve the same accelerating gradient as the unloaded case. The potential impact on the break-down rate was never measured before. In this paper we present an experiment located at the CLIC Test Facility CTF3 recently proposed in order to quantify this effect, layout and hardware status, and discuss its first results.

INTRODUCTION

The CLIC project [1] aims to collide electrons and positrons accelerated in two opposing linacs using normal conducting high-gradient accelerating structures. The main limitation for the achievable gradient is the RF breakdown effect which results in luminosity loss due to the transverse kick on the beam. In order to limit luminosity loss due to this effect to less than 1%, a maximum breakdown rate of $3 \cdot 10^{-7}$ BD/(pulse·m) is specified for CLIC at 3 TeV, at the nominal gradient of 100 MV/m [1]. During the last years an extensive program has been carried out to understand and control the RF breakdown rate in prototype CLIC accelerating structures. Results [2] demonstrate that such low breakdown rates are achievable.

In contrast, all breakdown high-gradient tests so far have been performed without the presence of an accelerated beam inside the structure. CLIC is designed to run with a high RF-to-beam efficiency (the fraction of RF power converted to beam kinetic energy), reaching around 30%. This high level of beam loading is accomplished with the high beam current of approximately 1A, which unavoidably modifies the longitudinal field profile (Fig. 1).

The effect of the changing field profile on the breakdown behaviour is hard to predict. While the whole-structure breakdown rate varies approximately with electric field as E_{acc}^{30} when input power is varied [2], the longitudinal dependency of the breakdown rate with the surface electric field is linear [3]. In order to experimentally measure the effect of beam loading on breakdown rate, an experiment is running at CTF3 using a 12 GHz klystron connected to a CLIC prototype accelerating structure loaded by the drive beam of the facility.

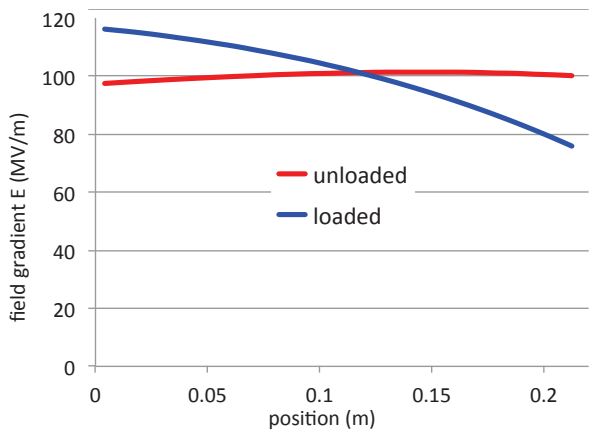


Figure 1: Longitudinal field gradient profile for an unloaded (red line) and 1.2 A of beam loaded (blue line) CLIC travelling wave structure at 100 MV/m average gradient.

EXPERIMENT LAYOUT

CTF3 was built to probe the main feasibility issues of the two beam acceleration concept [1]. In the past, a dogleg line branching off midway the drive beam linac was used to divert the beam and send it through an RF generating Power Extraction and Transfer Structure (PETS) to produce 30 GHz RF power conveyed to CTF2 [4]. The line has been reused to install a 24 cell CLIC prototype accelerating structure (Fig. 2) connected to a 12 GHz RF source. The iris radius of the structure cells are tapered to reduce the group velocity and provide a constant distribution of the unloaded gradient (Fig. 1). The forward, reflected and transmitted RF powers are sampled by logarithmic detectors and measured by the

* Funding for accelerating structure provided by the Swiss National Science Foundation Grant 135012.
† jl.navarro@cern.ch

Copyright © 2014 CC-BY-3.0 and by the respective authors

ISBN 978-3-95450-142-7

COMMISSIONING OF THE CERN LINAC4 WIRE SCANNER, WIRE GRID AND SLIT-GRID MONITORS AT 3 AND 12MeV

Uli Raich, F. Roncarolo*, F. Zocca, CERN, Geneva, Switzerland

Abstract

The CERN LINAC4 has been fully commissioned up to 3 and 12 MeV. The H^- beam transverse profile distributions were measured by both wire grids and wire scanners. A slit-grid system located on a temporary diagnostics bench was used to characterize the transverse emittance during the three different stages of commissioning: at the exit of the RFQ, at the exit of the MEBT line and at the exit of the DTL1 tank. The wire signal is a balance between the negative charge deposited by the stripped electrons from the H^- and the charge lost due to secondary emission. Optimal settings were found for the repelling plates used to suppress secondary emission, which were confirmed by electromagnetic simulations. In addition, suppression of the secondary emission due to the beam space charge was observed. The benefit of changing the wire scanner geometry in order to minimize the cross-talk between horizontal and vertical wires is also discussed.

INTRODUCTION

As part of the CERN LHC injector chain upgrade, Linac4 will accelerate H^- ions from 45 keV to 160 MeV. The ion source, the LEBT line, the RFQ and the MEBT line have been installed and commissioned in the Linac4 tunnel. The first DTL tank has been installed and has successfully accelerated the first beam to 12 MeV. While the 3 MeV beam commissioning has been completed, the 12 MeV commissioning is still on-going. In this paper the performance of the wire devices used to characterize the beam transverse profile is discussed, in particular with respect to the biasing electrodes used to suppress secondary emission and to repel secondaries produced by the temporary commissioning beam dumps. The performance of the LEBT wire grids (at 45 keV), of the MEBT wire scanners (at 3 MeV) and of the slit-grid emittance meter of the movable test bench are presented. The emittance meter has been used for the 3 MeV beam characterization and will soon be used for the beam at 12 MeV as well.

LEBT SEM GRIDS

The wire grid in the LEBT consists of two planes, one for the horizontal profile and one for the vertical profile, each composed of 24 wires with a pitch that varies from 1mm in the middle of the grid to 3 mm and then 5 mm while getting closer to the frame. All wires are 40 μm diameter gold-plated tungsten wires. At the energy of 45 keV, the H^- ions are stopped in the wires as their range is only about 0.2 μm. The current signal generated on the wire is given by the positive charge (+1) of the proton stopped, the negative charge of the stripped electrons (which can be as large as -2 if they are not back-scattered) and the positive charge due to the secondary electron emission generated by the proton entering the wire surface. The secondary emission yield of a 45 keV proton in tungsten is about 3.5, when calculated with the well-known Sternglass formula [1]. According to this

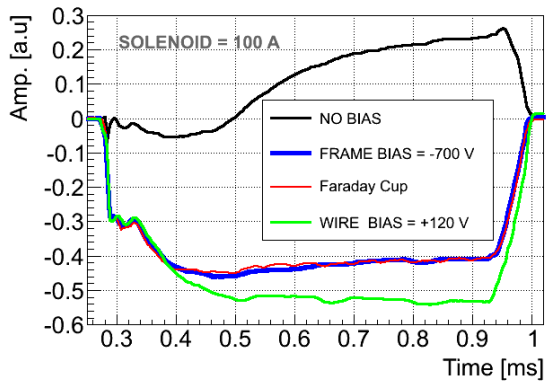


Figure 1: Central wire signal vs time with no bias, frame bias=−700 V and and wire bias=120 V.

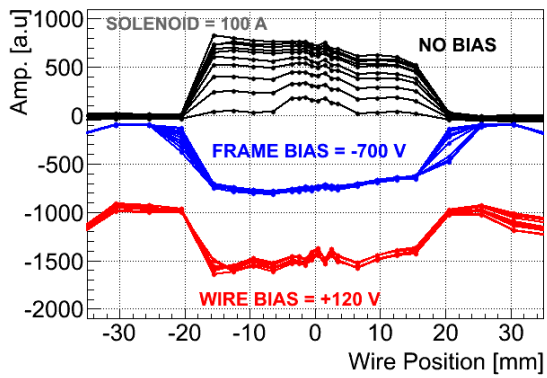


Figure 2: Beam profiles with no bias, frame bias=−700 V and and wire bias=120 V. For each case, different lines correspond to sampling at different times along the linac pulse.

estimate, even if the stripped electron back-scattering coefficient is not known, the wire signal is expected to be positive, owing to the strong contribution of secondary emission. The experimental results are actually more complicated than this simplified model. The calculation does not take into account the effect of secondary emission suppression due to the negative space charge of the H^- beam. Space charge suppression of secondary electron emission is a well-known phenomenon described in literature [2, 3], and looks as it plays a key-role in the wire signal generation for the Linac4

* federico.roncarolo@cern.ch

Copyright © 2014 CC-BY-3.0 and by the respective authors

ISBN 978-3-95450-142-7

TRANSVERSE PROFILE AND EMITTANCE MEASUREMENTS WITH A LASER STRIPPING SYSTEM DURING THE CERN LINAC4 COMMISSIONING AT 3 AND 12 MeV

E. Bravin, T. Hofmann, Uli Raich, F. Roncarolo*, F. Zocca, CERN, Geneva, Switzerland
J. K. Pozimski, Imperial College of Science and Technology, London
G. Boorman, A. Bosco, S. M. Gibson, K. Kruchinin Royal Holloway, University of London, Surrey
C. Gabor, STFC/RAL/ASTeC, Chilton, Didcot, Oxon

Abstract

The CERN LINAC4 beam commissioning at 3 MeV was completed in early 2014 and the one at 12 MeV is ongoing. A novel system for measuring the transverse beam profile and emittance, based on low power laser stripping and H0 detection using a diamond detector, was successfully tested at these two energies. The measurement results agree with the operational slit-grid method within a few percent in terms of both transverse profile and emittance. After describing the general system setup, this remarkable achievement is discussed in detail together with the present limitations, which will be addressed in order to design a laser based emittance monitor for the LINAC4 top energy of 160 MeV.

INTRODUCTION

The CERN LINAC4, that will accelerate H^- ions from 45 keV to 160 MeV, is in the beam commissioning phase at low energy [1]. The transverse profiles will be measured at different energies along the acceleration with wire scanners and wire grids [2]. Presently, wire grids and wire scanners are also foreseen to be used at 160 MeV to reconstruct the transverse emittance via either the *quadrupole scan* or the *three-profile* method.

However, wire scanners and wire grids are interceptive devices which implies: i) partial or complete stripping of the electrons from the H^- ions and subsequently beam losses because of the opposite polarity of the thus created protons and ii) their use will be allowed only for a reduced beam pulse length (e.g. 40 mA, 100 μs beam pulse) in order to avoid wire damage

These issues can be overcome with a modern transverse beam measurement system based on a pulsed laser that strips the H^- outer electron (the binding energy is about 0.75 eV) while selecting tiny slices of the beam (see Fig. 1). The un-stripped H^- ions are bent away by a downstream dipole, while the neutral H^0 drift on a straight path toward a strip-detector. Like in a conventional slit-grid system, the H^0 profile measurement during a laser scan allows the transverse phase space to be reconstructed. The stripped electrons can be extracted at the laser location by a weak dipole field and counted by a Faraday cup-like detector in order to reconstruct the transverse profile.

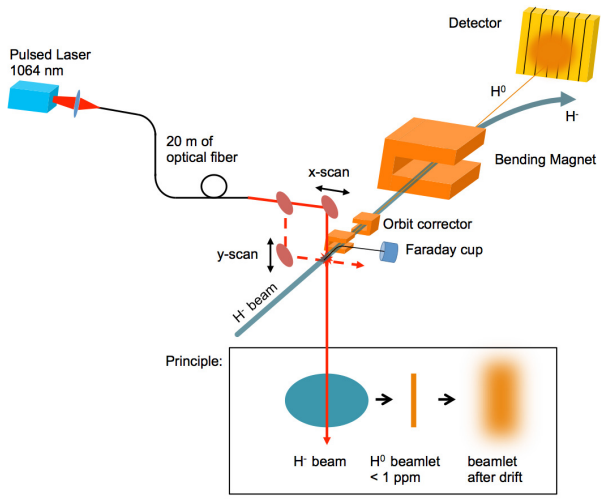


Figure 1: Laser emittance meter concept.

3MeV AND 12MeV SETUP

During the LINAC4 commissioning at 3 and 12 MeV, the transverse emittance of the beam was measured with the classical slit-grid system installed on a temporary diagnostic bench [3] that was placed at first after the MEBT and then after the first DTL tank. In order to advance with the final system design before having the possibility of tests at 160 MeV, the same test bench was equipped with a laser prototype system (see Fig. 2). The system consisted of a rack-mounted laser source (Q-switched, diode pumped [4]) coupled to an optical fiber (5 m and 10 m for the two different locations) delivering the laser beam to a focusing and scanning system. The laser was scanned in the vertical plane through the H^- beam via a view port mounted on the vacuum vessel also hosting the slits of the operational slit-grid emittance meter. A polycrystalline diamond strip detector was installed 3.3 m downstream just before the emittance meter wire grids, after the spectrometer dipole. For this first test, no stripped electrons detection was foreseen. As shown in Table 1, during each H^- pulse, lasting about 300 μs, the laser was pulsing at 60 kHz (i.e. a laser pulse every 16 μs) and amplified to about 0.5 kW peak power.

* federico.roncarolo@cern.ch

Copyright © 2014 CC-BY-3.0 and by the respective authors

ISBN 978-3-95450-142-7

SPACE CHARGE COMPENSATION IN THE LINAC4 LEBT FOR THREE INJECTED GAS TYPES

Cristhian A. Valerio-Lizarraga, UNISON, Sonora, México, CERN, Geneva, Switzerland
R. Scrivens. CERN, Geneva, Switzerland
N. Chauvin CEA Saclay, France

Abstract

The space charge of unbunched, high intensity beams can be compensated by the trapping of charged particles in the potential well of the beam. The source of these secondary charge particles can be the residual gas in the beam line. The effect is important in the Low energy beam transport (LEBT) regions. At CERN's Linac4, the LEBT transports a pulsed 45keV H- beam, which is compensated by the positive ions, created by collision of the beam with the neutral gas in the beam pipe. The rise time and amount of compensation may be varied by the density of neutral gas and the type of gas used (through the cross-section for ion production and the mass of the resulting ion). In this paper we present measurement results for the transport of the beam at the Linac4 LEBT with the addition of hydrogen, nitrogen and krypton gases into the line, and compare them with simulations of the beam dynamics including the effect of compensating positive ions. The H- beam is provided by a cesiated 2MHz RF ion source with an external solenoidal antenna, operating with 600 us pulses at 0.8Hz repetition rate.

INTRODUCTION

The Linac4 LEBT transports a high intensity H- beam at 45 keV, extracted from the source, to match the RFQ under strong space charge conditions. It is preferable to reduce the space charge using the Space charge compensation effect[1] (SCC).

The SCC effect occurs when the secondary particles created from ionization of the residual gas are trapped by the beam potential and decreases the overall beam potential. Changing the type of gas could affect the dynamics of the SCC. Some experiments have shown that the rms beam emittance of the beam can be improved by using this technique [2].

Measurements were done at the Linac4 Ion Source Test Stand [3], using the first section of the Linac4 LEBT with a solenoid and emittance meter[4]. The pressure inside the LEBT can be varied by the injection of different gases, and compared to beam simulations of the region including the SCC.

EXPERIMENTAL LAYOUT

The Linac4 ion source used in the experiment is a 2MHz RF volume source enhanced with cesium for surface negative ion production, designed and built at CERN[5]. It delivered a 35 mA H- beam at 45 keV with pulses of 600 µs spaced by 1.2 s. The first section of the LEBT (Fig. 1) consists of one solenoid, two steerer magnets for beam trajectory correction, a Faraday cup and a slit-grid emittance meter. The signals from the measurement grid were sampled with an ADC with a resolution of 6 µs. The emittances reported in this paper have been calculated by integrating the signals over a time period of 200 µs, starting 300 µs after the first observed beam from the source.

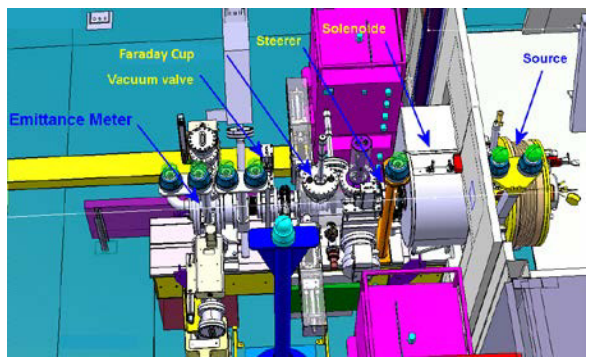


Figure 1: Experimental Setup Distance between the emittance meter and source 1.308 m

From the LEBT entrance, the solenoid start position is 50 mm, the Faraday cup at 876 mm and the emittance meter at 1308 mm. The beam pipe has an aperture radius of 50 mm, the solenoid has a maximum integrated magnetic field of 0.13 Tm. An integrated solenoid field of 0.089 Tm was used during the measurements.

The flux of H_2 gas from the source leads to a minimum pressure $1x10^{-6}$ mbar of H_2 in the LEBT, from here on referred to as the baseline pressure. A gas injection system was used to control the LEBT gas type and pressure and therefore the degree and speed of SCC.

For the experiments reported here, injection of hydrogen, nitrogen and krypton gases have been used; H_2 is used for H- production and therefore it should not have any detrimental effect on its performance; N_2 is safe and easy to pump; and Kr has been seen in other experiments [1] to be very effective for space charge compensation.

The measurements of the beam phase-space emittance were made as a function of the gas pressures.

SIMULATIONS OF THE EXPERIMENT

The modelling and simulation of the source and beam extraction system [5] has been made with the code IBSimu[6]. First the beam is tracked in the extraction system taking into account the full space charge, as the SCC is supressed by the electric field in the extraction system.

Copyright © 2014 CC-BY-3.0 and by the respective authors

TRANSVERSE EMITTANCE MEASUREMENTS OF THE REX-ISOLDE BEAMS IN PREPARATION FOR THE HIE-ISOLDE COMMISSIONING

D. Voulot#, M.A. Fraser, D. Lanaia‡, T. Olsson, CERN, Geneva, Switzerland

Abstract

The transverse emittance at the output of the REX-ISOLDE normal conducting linac has been measured at different energies in order to characterise the beam at injection to the future HIE-ISOLDE superconducting linac. The measurements were done with low intensity stable beams in order to avoid compensation effects in the electron beam ion source (EBIS) and obtain representative measurements of the radioactive ion beam emittance. Emittances were measured using a slit-grid emittance meter and compared with results obtained with a quadrupole-scan (three-gradient) method. An analysis of the background suppression is presented and possible source of errors for both type of measurements are discussed.

INTRODUCTION

REX-ISOLDE is operational since 2001 and has been delivering radioactive ion beams (RIB) at energies up to 3 MeV/u for a large physics programme [1]. With the extension of the charge-breeding performance for ions with large A and the increasing number of isotopes available at ISOLDE, an energy upgrade was necessary to make full use of the available beams. The new High Intensity and Energy (HIE-ISOLDE) superconducting linac will be installed downstream the existing linac and extend the energy range to 5.5 and eventually 10 MeV/u for ions with mass-to-charge ratios below 4.5 keeping full flexibility and improving the beam quality [2] [3]. The accurate measurement of the transverse emittance of the accelerated beams is essential to assess the performance of the linac and the quality of the delivered beams. It is also a key parameter for the design of the HIE-ISOLDE linac.

Due to the low intensity nature of the RIBs typically accelerated at REX-ISOLDE, a stable pilot beam extracted from the rest gas of the EBIS charge breeder is normally used to set-up the linac. These beams have a typical intensity of 10-100 epA and should represent well the beam characteristics of the charge-bred beams. The stable beam intensity can be increased by injecting gas directly in the electron beam region of the source but this has the disadvantage of degrading the EBIS beam emittance through electron beam compensation. For this reason the beam intensity was practically limited to 500 epA – 1000 epA which is very challenging for the classical slit-grid emittancemeter employed here. For this reason a number of steps were taken to ensure that the effect of background data point and offsets were appropriately treated. The results were also compared with emittance measurements obtained with alternative methods in particular a quadrupole scan method.

MEASUREMENTS AND DATA TREATMENT

The transverse emittances were measured with a commercial slit-grid emittance-meter (NTG Neue Technologien GmbH, Germany) with a slit of 0.2 mm width separated from the grid by a 1 m drift distance. The grid is made of two sets (X and Y) of 30 wires 0.2 mm in diameter with 2 mm spacing. The minimum step size of the slit is 10 µm and the grids can be moved in steps of 250 µm to improve the angular resolution.

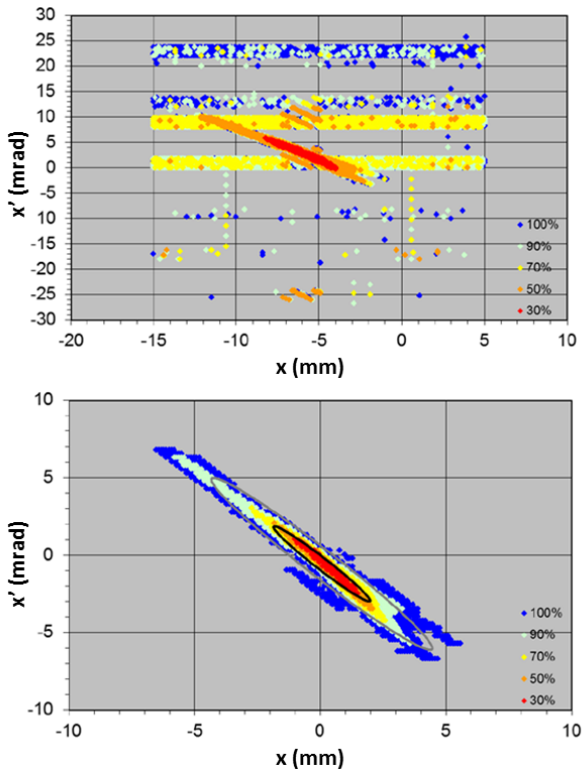


Figure 1: Emittance scan of a 2.85 MeV/u beam of Ne5+, raw data (top), emittance plot after background suppression (bottom)

The emittance-meter was placed downstream the normal conducting linac. Beams of mass to charge ratio equal to 4*, either Ne5+ from the EBIS rest gas or He+ from gas injection, were used. The beams had a repetition

‡ The author acknowledges the receipt of a fellowship from the Marie Curie Initial Training Network CATHI.
#voulot@cern.ch

* The REX-ISOLDE linac can accelerate beams with A/q in the range 2-4.5

Copyright © 2014 CC-BY-3.0 and by the respective authors

ISBN 978-3-95450-142-7

TRANSVERSE BEAM PROFILE MEASUREMENTS IN THE LINAC4 MEDIUM ENERGY BEAM TRANSPORT

M. Yarmohammadi Satri*, G. Bellodi, V. Dimov, J.B. Lallement, A. Lombardi, U. Raich, F. Roncarolo, F. Zocca, CERN, Geneva, Switzerland

Abstract

Linac4 is a 160 MeV H^- linear accelerator presently under construction at CERN. It will replace the present 50 MeV proton Linac2 as injector of the proton accelerator complex as part of a project to increase the LHC luminosity. The Linac4 front-end, composed of a 45 keV ion source, a Low Energy Beam Transport (LEBT), a 352.2 MHz Radio Frequency Quadrupole (RFQ) which accelerates the beam to 3 MeV and a Medium Energy Beam Transport (MEBT) housing a beam chopper, has been commissioned in the Linac4 tunnel. The MEBT is composed of three RF cavities and 11 quadrupole magnets to match the beam from the RFQ to the next accelerating structure (DTL) and it includes two wire scanners for beam profile measurement. In this paper we present the results of the profile measurements and we compare them with emittance measurements taken with a temporary slit-and-grid emittance measurement device located after the MEBT line.

INTRODUCTION

Linac4 is part of the CERN LHC injector upgrade [1], it accelerates H^- ions to 160 MeV in an 80 m long accelerator housed in a tunnel 12 m underground. It consists of a 45 keV RF volume source, a two-solenoid Low Energy Beam Transport (LEBT), a 352.2 MHz Radio Frequency Quadrupole (RFQ) accelerating the beam to 3 MeV, a Medium Energy Beam Transport (MEBT) line (Fig. 1), a 50 MeV Drift Tube Linac (DTL), a 100 MeV Cell-Coupled Drift Tube Linac and a Pi-Mode Structure bringing the beam to the final energy of 160 MeV. The ion source, the RFQ and the MEBT line have been commissioned in the Linac4 tunnel between October 2013 and March 2014, with a temporary diagnostic bench shown in Fig. 2.

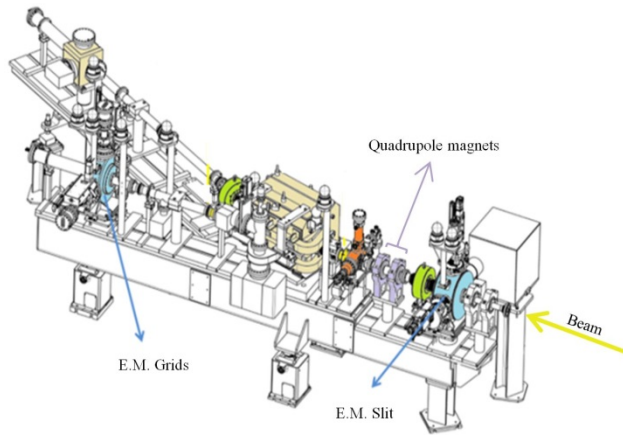


Figure 2: The 3 MeV temporary diagnostics bench.

The diagnostics permanently installed in the MEBT is minimal and consists of two beam current transformers and two wire scanners (WS), whereas a full suite of diagnostics, including a slit-and-grid emittance device (EM), a spectrometer, a Halo monitor, a Bunch Shape Monitor (BSM), and several position monitors are available on the temporary diagnostic bench [2].

The WSs are made of two 33µm carbon wires which travel through the beam in variable steps (0.07 mm minimum) and acquire the horizontal and vertical profiles over several pulses. The WSs measurements are time resolved in 4 µs slices, thus allowing observation of the profile along the beam pulse (100-400 µs). The emittance meter consists of a slit-and-grid system for a direct sampling of the horizontal and vertical phase space. The slits (with 300 µm aperture) are near the output plane of the MEBT and the grids are placed about 3 m downstream. A system of two quadrupoles allows changing the phase advance between the slits and the grids. In this paper we report the results of the transverse measurements in the MEBT and a comparison with the corresponding beam dynamics simulations.

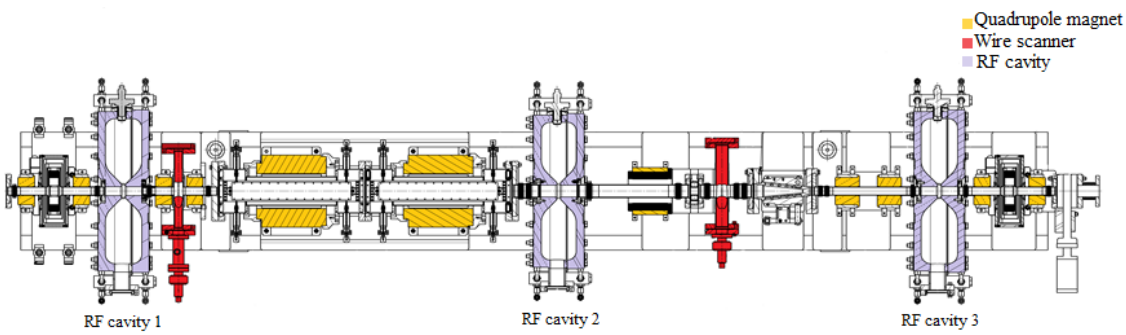


Figure 1: The 3 MeV MEBT line.

* Home Institute: IPM, Tehran, Iran

Copyright © 2014 CC-BY-3.0 and by the respective authors

ISBN 978-3-95450-142-7

ACCURACY DETERMINATION OF THE ESS MEBT EMITTANCE MEASUREMENTS

B. Cheymol*, A. Ponton, European Spallation Source, Lund Sweden

Abstract

The European Spallation Source MEBT will be equipped with a full set of diagnostics in order to characterize the bean properties before the injection in the DTL. The 6D phase space of the beam shall be characterize during the commissioning of the normal conducting as well as on regular basis during retuning phase of the machine.

In this paper we will discuss the accuracy of the transverse emittance measurement that will be performed with the slit-grid method. The slit geometric parameters have been determined in order to achieve the required resolution and sensitivity. Scattering effects at the slit have been considered to determine the emittance measurement accuracy.

INTRODUCTION

The European Spallation Source (ESS) [1] is a neutron source based on a 5 MW proton linac, build in Lund, Sweden. The normal conducting front end will accelerate the beam coming for the ion source up to 90 MeV, it consists in an ECR ion source, a Low Energy Beam Transport line (LEBT), a radio frequency quadrupole (RFQ), a Medium Energy Beam Transport line (MEBT) and a drift tube linac. At the exit of the RFQ, the beam has an energy of 3.63 MeV, with a current of 62.5 mA and nominal pulse length and repetition rate of 2.86 ms and 14 Hz respectively.

One of the function of the MEBT is to fully characterize the beam at the exit of the RFQ [2], the lattice and the beam envelopes are shown in Fig. 1, a preliminary layout of the beam diagnostics has been proposed (see Fig. 2). The slit and grid system will installed in reserved drift space for beam diagnostic downstream the second triplet.

The space available for the beam diagnostics after the second triplet is less than 350 mm (flange to flange) and might not be sufficient to meet the performance requirement for emittance measurement with the slit and grid system. The distance between the slit and grid has to be increased to provide enough angular resolution, therefore the slit has to be positioned between 2 quadrupoles, in this case the distance between the slit and the grid is increased to 400 mm. A bipolar power supply might be requested for the quadrupole positioned between the slit and the grid, primarily to suppress any remanent magnetic field which can lead to perturbation in the emittance measurement., in addition bipolar power supply might be useful for emittance measurement by increasing the rotation of the beamlet in the phase space.

For the studies presented in this paper, the nominal Twiss parameters at the slit location have been used, they are summarized in Tab. 1.

* benjamin.cheymol@esss.se

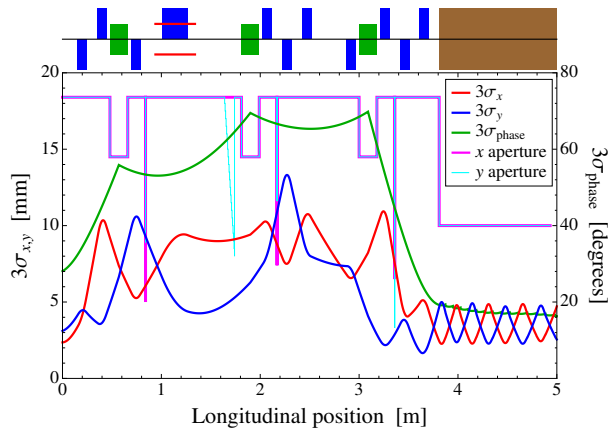


Figure 1: Schematics layout of the MEBT lattice (top), beam envelopes (3 σ), and apertures. In the schematic, blue boxes are quadrupoles, green boxes are buncher cavities, red lines are chopper plates. (courtesy of R. Myamoto).

Table 1: Nominal Courant-Snyder parameters 70 mm upstream the slit location .

Parameter	H plane	V plane
$\varepsilon_{norm.}$ [$\pi.mm.mrad$]	0.282	0.256
β [m/rad]	2.25	5.76
α	-5.37	13.62

GENERAL ARCHITECTURE OF THE SLIT AND GRID SYSTEM

The mechanical design of the slit is constraint by the space available between 2 quads and the necessity to absorb the beam power. The slit is not able to absorb the nominal beam power, during emittance scan the pulse length as well as the repetition rate has to be reduced to 50 μs and 1 Hz respectively. From the studies done for the LINAC4 emittance meter [3], graphite seems to be the best candidate for the slit material.

The slit has to be inclined w.r.t the beam axis in order to spread the energy deposition on a larger surface, the angle can not be less than 45 degrees due to space limitation.

The SEM grids will be equipped with 50 μm tungsten wires. The pitch of the grid is 500 μm, despite this small distance between the wire, the resolution is not sufficient for the beam parameters considered. The resolution can be increased to 100 μm by moving the grids by small step for a given slit position. A metallic foil will be positioned downstream and will be polarized in order to reduce the cross talk between wires.

Copyright © 2014 CC-BY-3.0 and by the respective authors

ISBN 978-3-95450-142-7

PRELIMINARY FUNCTIONAL ANALYSIS OF ESS SUPERCONDUCTING RADIO-FREQUENCY LINAC

C. Darve, N. Elias, J. Fydrych, D. Piso, European Spallation Source, Lund, Sweden

Abstract

The European Spallation Source (ESS) is one of Europe's largest planned research infrastructures. This collaborative project is funded by a collaboration of 17 European countries and is under design and construction in Lund, Sweden. Three families of Superconducting Radio-Frequency (SRF) cavities are being prototyped, counting the spoke resonators with a geometric beta of 0.5, medium-beta elliptical cavities (b_g=0.67) and high-beta elliptical cavities (b_g=0.86). The 5 MW, 2.86 ms long pulse proton accelerator has a repetition frequency of 14 Hz (4 % duty cycle), and a beam current of 62.5 mA. The cavities and power couplers are assembled into cryomodules, which are operating using RF sources, cryogenic and water-cooling. This document describes the process of the ESS SRF cryomodule operation, their functions, referred to the operational modes and the different interfaces present in this system.

INTRODUCTION

The choice of SRF technology is a key element in the development of the ESS accelerator. Three types of superconducting cavities are being fabricated; the 56 m long section of spoke cavities operates at 352.21 MHz whereas the 77 m long section medium-beta and 179 m long section high-beta elliptical cavities operate at 704.42 MHz. All the SRF cavities operate in saturated He II bath at 2 K, whilst their power couplers require cooling by helium vapour at the range from 4.5 K to 300 K. The SRF linac accelerates the proton beam from 96 MeV as input energy of the 13 spoke cryomodules, to 216 MeV at the inlet of the 9 medium-beta elliptical cryomodules and to full energy at 2.0 GeV outlet of the 21 high-beta elliptical cryomodules. The ESS linac is fully segmented and cavities are grouped into cryomodules; with two spoke cavities and four elliptical cavities per cryomodule.

Within the framework of the ESS-CEA-IPNO cooperation agreement, technology demonstrators are being designed, fabricated and tested for the spoke and the elliptical cavities and cryomodules. Those demonstrators will validate the technologies to be implemented for the ESS SRF linac series production.

The fabrication, the test, the assembly and the operation of each SRF cavities and cryomodule components shall comply with ESS requirements. The disciplines covered by the requirements are described elsewhere [1].

The operating modes for the cool-down, warm-up, emptying and cold stand-by will be validated during the commissioning phase of the ESS tunnel [2]. The SRF linac operating conditions are derived from the requirements and shall be verified for each operating modes. System, sub-systems, interfaces, process variables, local interlocks, alarms and control state diagrams are being identified. The choice of the control hardware, the electronics and SRF accelerator components must comply with industrialisation abilities. Operating modes need to be defined. Once they are properly defined, it is possible to define in detail the controls architecture to identify the processes. The integration of these local control systems into the Integrated Control System (ICS) will be done using ESS standard controllers and EPICS (Experimental Physics and Industrial Control System) controls framework. The states diagrams for the process control logic are obtained using the operating modes definition. This logic will be implemented in PLCs.

This paper describes the preliminary functional analysis of the process (operating modes and transitions between them) and the interfaces with other systems like cryo-distribution system (CDS), vacuum, RF, utilities and control system.

PROCESS AND SRF CRYOMODULE FUNCTIONAL ANALYSIS

Cryomodule Functionality

The proton acceleration is provided along the beam line by individual control of the spoke and elliptical cavities electro-magnetic field. The cavity helium tank bath temperature and pressure, the power coupler antenna water-cooling can be controlled independently from one cryomodule to the next one. Only the beam vacuum is common to all cryomodules and regulated separately.

The helium provided by the accelerator cryogenic plant (ACCP) is delivered to the cryomodules through the CDS. It consists of the cryogenic distribution line (CDL) running alongside the linac for transfer, which supply/return from/to the valve boxes [3], interfacing with each individual cryomodule. Each valve box is equipped with a set of valves allowing for warming up the linked cryomodule while keeping the rest at cryogenic conditions. The CTL provides the cryomodules with supercritical helium at 4.5 K and 0.3 MPa. During cool-down and filling, the helium is expanded to 0.14 MPa whilst during nominal operation the required 2 K temperature level is created by pre-cooling the 4.5 K helium in a heat exchanger and throttling in a Joule-Thompson (JT) valve, being the vapors pumped back by cold compressors in the ACCP at 31 mbar. The heat exchangers and JT valves are located in the valve boxes for the spoke SRF section and in the cryomodules for the elliptical SRF section [4]. The regulation of the thermal operating conditions of SRF cavities, is performed by a control loop acting upon cryogenic controlled valves and dedicated process variables.

Copyright © 2014 CC-BY-3.0 and by the respective authors

ISBN 978-3-95450-142-7

BEAM CURRENT MONITOR SYSTEM OF THE EUROPEAN SPALLATION SOURCE

H. Hassanzadegan, M. Donna, A. Jansson, H. Kocevar, A. Nordt, ESS, Lund, Sweden
U. Legat, Cosylab, Ljubljana, Slovenia
M. Werner, DESY, Hamburg, Germany

Abstract

The Beam Current Monitor system of the ESS will be primarily used for beam current and charge measurements in absolute and differential modes. Moreover, it will provide a fast input to the Beam Interlock System, initiating a trigger to shut the beam off upon high beam loss detection. As the BCM system will be needed at an early stage for Linac commissioning, it needs to work successfully under non-optimal conditions, ex. short pulse and low current beams. It is planned to install in total 20 AC Current Transformers and one Fast Current Transformer along the Linac. The FCT will have a larger bandwidth and it will be used to measure the performance of the fast chopper of the Medium Energy Beam Transport with a rise time of 10 ns. A prototype based on a commercial ACCT and EPICS-integrated MTCA.4 electronics has been set up and successfully tested with an emulated beam. The ACCT signal has been FPGA processed to compensate for the offset and droop as well as filtering and synchronization to an external trigger. This paper gives an overview of the design and test results of the prototype ACCT system with an outlook to future modifications before installation in the ESS Linac.

INTRODUCTION

The Beam Current Monitor (BCM) system of the ESS Linac will be based on AC Current Transformers (ACCTs). Table 1 gives a summary of the beam and ACCT specifications. It is planned to install in total 20 ACCTs along the ~600 m Linac with a higher concentration of the sensors in the low-energy part. This is mainly to address issues regarding fast detection of high beam losses and initiating a trigger to stop beam operation in areas where Beam Loss Monitors (BLMs) cannot be successfully used.

It is also foreseen to include one Fast Current Transformers (FCT) in the BCM system. The FCT will have a significantly larger bandwidth compared to the ACCTs and it will be mainly used to measure the performance of the Medium Energy Beam Transport (MEBT) chopper with a rise time of 10 ns approximately.

The BCM system can be used to measure the pulsed beam current as well as the per-pulse and cumulative beam charge. The readout data can be presented to the end-user in numerical and graphical formats.

The ESS Machine Protection System (MPS) requirements mandate that a differential beam current shall be measured at several locations along the Linac. In this case, the readout current from two ACCTs need to be compared with each other and in case the difference exceeds a certain threshold, a request to stop beam operation will be sent to the Beam Interlock System (BIS) with a total response time of 10 µs from detection to having inhibited beam operation.

The ACCT electronics will be installed in the klystron gallery, which will extend in parallel to the Linac tunnel over most of the Linac length. In order to achieve a good signal-to-noise ratio for the ACCT output, care should be taken to use short and well-shielded cables for signal transmission to the ACCT front-end electronics in addition to a good grounding system with a low voltage difference between the tunnel and klystron gallery grounds. Moreover, some electronics developments are currently being done for differential signal transmission to the ACCT crate where the signals are digitized and FPGA processed.

MTCA.4 standard has been chosen at ESS as a prototyping platform for systems requiring high-performance electronics including the ACCT. A decision on the final electronics platform is expected in Sep. 2014. A demo MTCA.4 system has been used for digitizing the ACCT signal, FPGA processing and integration into the ESS EPICS control system. The ACCT data is communicated to the user through EPICS Input/Output-Controller (IOC) and Channel Access (CA).

It is planned to commission the Low Energy Beam Transport (LEBT) ACCT in the second half of 2015.

This article gives an overview of the current status of the ACCT project with the focus being mainly on the electronics with an outlook to future improvements.

Table 1: ESS Beam and ACCT Specifications

Max beam energy	2	GeV
Pulse repetition rate (nominal)	14	Hz
Pulse duration (nominal)	2.86	ms
Beam current (nominal)	62.5	mA
Beam current (min)	6.25	mA
Bunch frequency	352	MHz
BCM quantity	21	
ACCT accuracy (nominal beam)	+/-1	%
ACCT resolution (nominal beam)	1	%
ACCT response time (incl. elect.)	1 – 2	µs
Beam pipe diameter	60, 100	mm

Copyright © 2014 CC-BY-3.0 and by the respective authors

ISBN 978-3-95450-142-7

DESIGN OF THE PHASE REFERENCE DISTRIBUTION SYSTEM AT ESS

R. Zeng, O. Persson, H. Hassanzadegan, J. Jurns, M.R.F. Jensen, A. Sunesson, ESS, Lund, Sweden
K. Strniša, Cosylab, Ljubljana, Slovenia

Abstract

PRDS (Phase reference distribution system) at ESS will provide phase reference signals for all LLRF systems and BPM systems with low phase noise and low phase drift. Phase stability requirement is currently 0.1° for short term (during pulse), 1° for long term (days to months). There are 155 LLRF systems, 165 BPM (Beam Position Monitor) systems, and 4 BSM (Bunch Shape Monitor) systems in total at current ESS accelerator design.

INTRODUCTION

PRDS (Phase reference distribution system) will provide phase reference signals for all LLRF systems and beam instrumentation systems such as BPMs (Beam Position Monitors) and BSMs (Bunch Shape Monitors) with low phase noise and low phase drift. Phase stability requirement is currently 0.1° for short term (during pulse), 1° for long term (days to months). There are 155 LLRF systems, 165 BPM systems, 4 BSMs in total at current ESS accelerator design. Figure 1 shows the numbers of LLRF systems and BPM systems in different accelerator sections in current ESS design [1].

PRDS at ESS consists of RF reference signal delivery sub-system, temperature control sub-system, air pressure sub-system, and data acquisition and drift calibration sub-system, by referring mainly the PRDS system implemented at SNS [2].

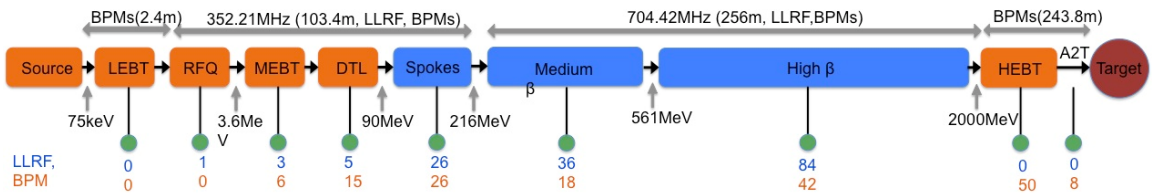


Figure 1: BPM and LLRF system number distribution at ESS.

RF REFERENCE SIGNAL DELIVERY

Topology

RF reference signal delivery topology is chosen as follows at current PRDS design: Master Oscillator (MO) locates in between 352.21MHz section and 704.42MHz section in klystron gallery. Two transition lines will transport RF signals from master oscillator in klystron gallery to main line in tunnel. Two main lines carrying RF frequency 352.21MHz and 704.42MHz goes all the way along the tunnel, with local distribution lines tapping out from each tap (here tap is directional coupler) reach as close as possible to cavity probe cable and BPM/BSM probe cables. Each cavity or BPM/BSM will be assigned a local distribution line, which is bundled together with the cavity probe signal sending to LLRF rack, or bundled together with four probe signals from BPM/BSM sending to BPM/BSM rack. The schematic diagram of phase reference line topology is shown in figure 2 [3].

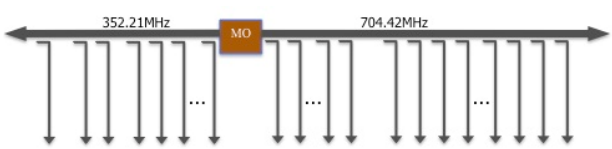


Figure 2: System topology diagram for PRDS.

Main Line

Coaxial rigid transmission lines is chosen as delivery medium due to strong radiation environment in accelerating tunnel, while the main line has to be put in tunnel in order to compensate the phase drift from tunnel to klystron gallery. Optical fibres are first ruled out, due to that they are generally sensitive to radiation, leading not only radiation-induced attenuation, but also radiation-induced refractive index changes [4].

Dielectric filled coaxial cables suffer as well from radiation-induced attenuation and radiation-induced dielectric constant change. It is reported that [5, 6], for PTFE (or Teflon), mechanical properties affected mainly by total absorbed radiation dose, while dielectric properties affected more by dose rate. The experiment made in ORNL half century ago [7] indicated that both polyethylene filled cable and Teflon filled cable experience dielectric constant change, and polyethylene cable showed bigger attenuation than Teflon cable, which is the opposite of radiation effect on their mechanical properties. Dielectric constant change is especially crucial for phase reference distribution, as even small change in dielectric constant will result in significant phase change for 704.42MHz RF signal running on a 300m long cable. Thus, air filled coaxial rigid transmission line with few dielectric

Copyright © 2014 CC-BY-3.0 and by the respective authors

ISBN 978-3-95450-142-7

BEAM PHYSICS CHALLENGE IN FRIB DRIVER LINAC*

Y. Yamazaki#, N. Bultman, A. Facco*, Z. He, M. Ikegami, M. Johnson, S. Lidia, F. Marti,
E. Pozdeyev, K. Saito, J. Wei, X. Wu, Y. Zhang, Q. Zhao, FRIB, MSU, East Lansing, MI 48824, USA
*INFN - Laboratori Nazionali di Legnaro, Legnaro (Padova), Italy

Abstract

The Facility for Rare Isotope Beams (FRIB) driver linac at MSU provides CW beams of all the stable ions (from protons to uranium) with a beam power of 400 kW and a minimum beam energy of 200 MeV/u in order to produce a wide variety of rare isotopes for nuclear physics study. The low beam emittances, both transverse and longitudinal, are key performance requirements, together with beam stability. These are required for efficiently separating one isotope from another, the reason for choosing this linac configuration. Multi-charge states (five charge states for the uranium case) are accelerated for maximizing the beam current, while keeping the low emittances. The efficient acceleration of high beam currents from 0.5 MeV/u through the superconducting linac is, needless to say, one of the biggest challenges. The beam power is more than 200 times higher than existing similar SC heavy ion linac. In particular, the SC cavities are difficult to protect from heavy ion beam damage, which can be more than 30 times larger locally than a proton beam with the same beam power. Other challenges peculiar to the FRIB linac will be presented, together with possible solutions.

INTRODUCTION

The Facility for Rare Isotope Beams (FRIB) driver linac at Michigan State University [1] is the first heavy ion accelerator aiming to join the beam power front as shown in Fig. 1 with a beam power of 400 kW and a beam energy over 200 MeV/u. The Chart like Fig. 1 was first used at J-PARC [2] to show "Proton Beam Power Front" throughout the wide range of the beam energy, where both SNS and J-PARC were challenging to push the front from an order of 100 kW to 1 MW. The Proton Beam Power Front is nothing but the technology front to control the beam loss rate within a certain radioactivity level a few hours after stopping the beam operation, that is, the hands on maintenance is possible afterwards. Therefore, one of the technological challenges of the SNS and J-PARC was to suppress the beam loss rate by an order of magnitude from the existing accelerators.

Figure 1 was extended one from the proton accelerators to the heavy ion ones. It should be noted that the PSI cyclotron had already marked the beam power of 1 MW, when the SNS and J-PARC started their construction. The beam loss control issue at cyclotrons is different from that at synchrotrons. For the former, the beam loss at extraction limits the beam power, while that at injection is the main issue for the latter. This is the reason for the different beam power front. The heavy ion beam power front may have different technical implication.

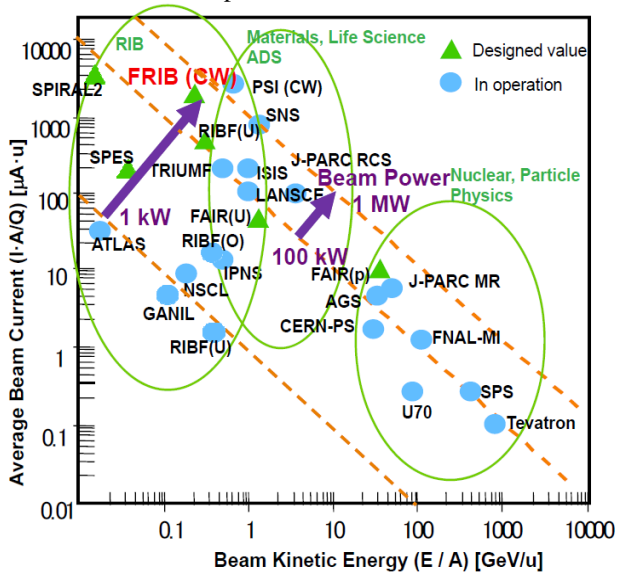


Figure 1: Average hadron beam power versus beam energy.

This article presents what we learned from design study and development for the FRIB driver linac, and what will be outcome from its completion for the future prospects of the world wide accelerator physics and technology.

REQUIREMENTS FOR FRIB DRIVER LINAC

It is needless to say that any particle accelerator for scientific study should be designed so as to maximize the scientific output economically and efficiently. The FRIB is aiming for a large number of prominent scientific research results, studying rare isotopes, in particular, to be produced by nuclear fragmentation process. For that purpose, it is important to produce not only a large number of rare isotopes, but also to efficiently and precisely separate one isotope from another. Isotopes produced by the nuclear fragmentation process are separated by means of time of flight technique as well as a series of magnet systems referred to as a fragment separator [3]. Then, not only the high beam power, but also the low beam emittances are crucial both longitudinally and transversely. It is thus oversimplification to judge the accelerator performance only by its beam power. And of course, high availability and reproducibility are important for efficient experiments.

Table 1 numerically summarizes the required beam quality. These parameters are only feasible with a linac. This is the reason why we chose the relatively expensive linac scheme. Another requirement is to make a full use of

*Work supported by the U.S. Department of Energy Office of Science under Cooperative Agreement DE-SC0000661.
#yamazaki@frib.msu.edu

Copyright © 2014 CC-BY-3.0 and by the respective authors

PXIE RFQ BEAD PULL MEASUREMENTS*

P. Berrutti#, T. N. Khabiboulline, V. Poloubotko, G. Romanov, J. Steimel, V. Yakovlev,
Fermilab, Batavia, IL 60510, USA,
D. Li, J. Staples, Lawrence Berkeley Lab, Berkeley, CA 94720

Abstract

The Project X Injector Experiment (PXIE) radio frequency quadrupole (RFQ) is being built for Fermilab by Berkley laboratory (LBNL). This RFQ will be placed after the low energy beam transport (LEBT) and before the medium energy beam transport (MEBT). The RFQ will operate at 162.5 MHz in CW regime; its function is to accelerate and focus particles coming from the LEBT at 30 keV, and to deliver a beam at 2.1 MeV to the MEBT. In order to make sure that the RFQ meets the specifications of field flatness and frequency the field in the vanes should be measured using bead pull technique and tuned according to specifications. FNAL created a new single wire bead pull set up for the RFQ of PXIE. The measurements are used to find the electrical centre of the structure, then the amplitude of the electromagnetic field in all the sectors of the RFQ; and the tuning will be based on these measurements. This paper describes the bead pull experimental set up, the software developed for this particular application and the measurements taken.

INTRODUCTION

PXIE is a CW injector experiment of the new multi MW linac to be built at Fermilab [1]. The project is composed of a H^- ion source, a low energy beam transport (LEBT) section, a radio frequency quadrupole (RFQ), medium energy beam transport (MEBT) and two cryomodules of superconducting cavities for a final beam energy of 30 MeV. All the components will operate in CW regime having 100% duty cycle. The main RFQ parameters are reported in Table 1.

Table 1: Main RFQ Parameters

Input energy [keV]	30.00
Output energy[MeV]	2.10
Frequency [MHz]	162.50
Vane-vane voltage [kV]	60.00
Vane Length [cm]	444.60
RF Power [kW]	100.00
Beam Power [kW]	10.50
Duty factor	100%

The RFQ is being built at LBNL and is the product of collaboration between FNAL and LBNL [2] [3]. It consists of four modules that will be attached together to form the whole structure. Figure 1 shows the full RFQ 3D model. Once the RFQ is constructed, the electric centre, field profile on axis, and quadrant symmetry can be measured with a bead pull technique.

*Work supported by D.O.E. Contract No. DE-AC02-07CH11359
#berrutti@fnal.gov

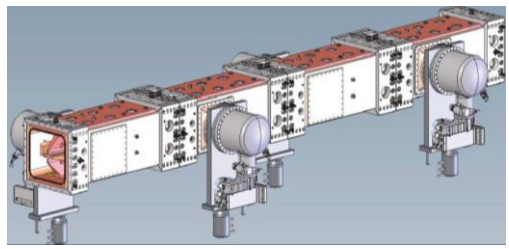
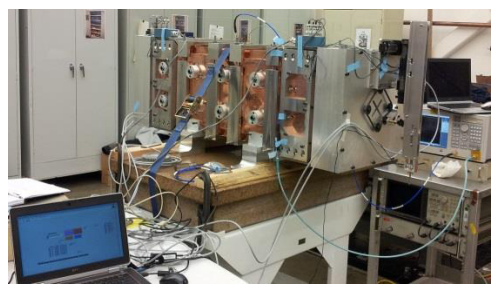


Figure 1: PXIE RFQ 3D model.

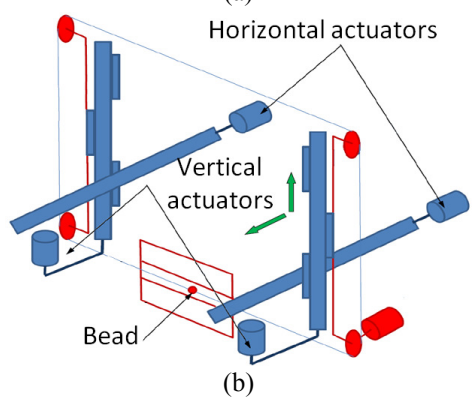
This paper reports the results of the bead pull measurements taken on the dry fit of a single RFQ module before brazing. The main focus is to verify RF simulations and machining tolerances. Once RFQ construction is complete, in early 2015, tuning and final measurements will be taken using this bead-pull setup.

MEASUREMENT SET UP

A common measurement set up for RFQ bead pull uses 4 lines, a separate line for each quadrant. The set up used for the measurements of PXIE RFQ module consists of one line capable of moving into any quadrant.



(a)



(b)

Figure 2: (a) measurement set up on module 2 at LBNL, (b) schematic of the bead pull system for PXIE RFQ.

The measurement apparatus and its schematic are presented in Figure 2; the main advantages of using such a sophisticated set up are:

- Reduction of number of lines necessary.

Copyright © 2014 CC-BY-3.0 and by the respective authors

ISBN 978-3-95450-142-7

TEST STAND FOR 325 MHz POWER COUPLERS*

S. Kazakov#, V. Poloubotko, B.M. Hanna, T. Khabiboulline,
O. Pronitchev, V.P. Yakovlev, FNAL, Batavia, IL 60510, USA

Abstract

325 MHz superconducting Single Spoke Resonators (SSR1) will be utilized in the Project X Injector Experiment (PXIE). Fermilab has developed the main coupler that will supply 2 kW CW RF power to each cavity. Fermilab developed and designed a special test stand where the couplers will be tested and design properties confirmed. This paper describes the design of the coupler test stand and preliminary results of the tests.

INTRODUCTION

The PXIE [1] accelerator includes one cryomodule with eight 325 MHz SSR 1 cavities. Each cavity requires 2 kW RF power in CW mode for 1 mA of H- beam. In future upgrades beam currents of up to 5 mA are desired in which case RF power for SSR 2 cavities (which is not a part of PXIE) will be 18 kW, CW. To satisfy all upgrade plans, couplers must be able to operate at 25 kW power at any reflection [2]. Before installing to superconducting (SC) cavity, a coupler must be tested and conditioned. For this purpose a test stand was designed and built. There are some requirements the test stand must meet. First, the tests should be done under vacuum to check the multipactor properties of the couplers; the couplers must be free of multipacting. Second, the performance of SC cavities is very sensitive to dust particles. After conditioning the couplers, they will be installed directly onto cavities without any additional cleaning procedure. Thus disassembly of the test configuration should not create or spread dust particles. To satisfy this demand a configuration with 'untouchable' antennas was chosen: during assembling/disassembling and testing, coupler antennas have no mechanical contacts with other parts.

TEST CAVITY STRUCTURE

After considering several options, the structure presented in Figure 1 was chosen. Two couplers are connected through this test cavity. The test cavity is a coaxial half wave resonator with two lateral conductors. These lateral conductors are hollow and the coupler antennas fit inside them. Diameter of the inner conductor of the resonator is 1 inch and the diameter of the outer conductor is 6 inches. These sizes eliminate multipactor in the operating range of power and provide for low losses. A low loss allows us to make the outer conductor of stainless steel. Both the inner and lateral conductors are made of copper. Figure 2 illustrates a simulated pass band for the test cavity. Wide pass band allows us to avoid spatial tuning accessories. Simulated losses are 0.22% (-9.5E-3 dB).

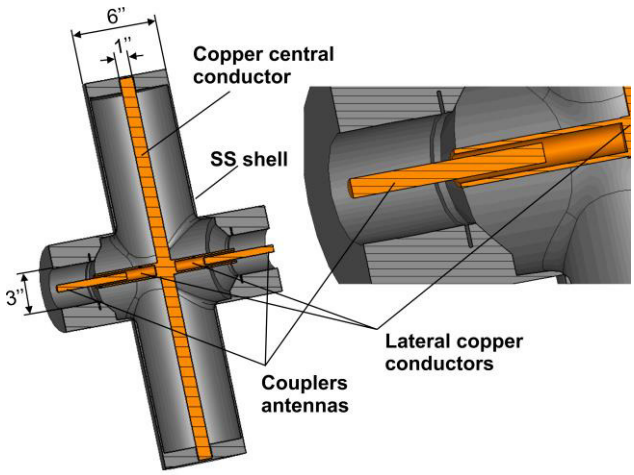


Figure 1: Structure of test cavity.

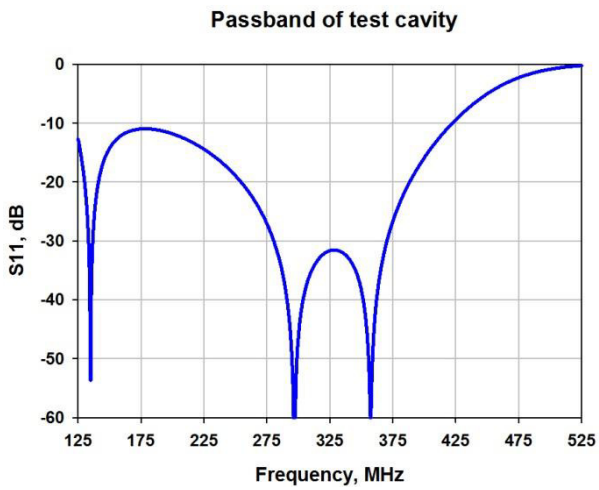


Figure 2: Pass band of test cavity.

MOVEABLE SHORT

To allow us to test couplers at arbitrary reflections, a movable short was designed. This is illustrated in Figure 3.The plunger is electrically isolated from the inner and outer conductors. There are slots between the plunger and walls which allows us to move the plunger without sparking. The inner volume of the plunger works like a choke providing good isolation (full reflection) between volumes in front and behind the plunger. From simulations the power leakage beyond the plunger is -50

* Work supported by DOE
# skazakov@fnal.gov

Copyright © 2014 CC-BY-3.0 and by the respective authors

SSR1 TUNER MECHANISM: PASSIVE AND ACTIVE DEVICE*

D. Passarelli†, FNAL, Batavia, IL 60510, USA - University of Pisa, Italy
L. Ristori, FNAL, Batavia, IL 60510, USA

Abstract

In this paper we present the methodology adopted in designing the mechanism responsible for controlling the resonant frequency of Single Spoke Resonators of first type (SSR1). Such device is capable of compensating the effects of external perturbations, such as pressure fluctuations and microphonics, on the frequency of SSR1. The compensation is achieved through active responses via an actuation system and passive responses which are inherent to the elastic behavior of the overall system. The first experiences in the design, assembly, QA and testing are reported.

INTRODUCTION

The SSR1 cryomodule for the project PXIE [1] contains superconducting cavities with very narrow bandwidth in operating condition at 2 K. Due to that, a particular effort is needed to keep the resonant frequency of the cavity at its nominal value of 325 MHz. Even tough the cavity receives an inelastic tuning before the cooldown from room temperature to 2 K, there is a range of uncertainty of the final frequency that has to be adjusted by the tuner (coarse tuning). On top of that, there are other external noises generally known as microphonic that disturb the resonant frequency of the cavity in operation. The tuner is also used to minimize and possibly cancel that effect (fine tuning).

The tuning device for the SSR1 cavities of generation 3 (SSR1-G3) [2] has to operate only on one of the beam-pipe regions of the cavity and only generates forces directed towards the cavity (push only). The resonant frequency of the cavity is modified by adjusting the spacing between the cavity end-wall and the spoke. Controlling this gap allows to maintain the frequency near the nominal value of 325 MHz.

An expansion joint (bellows) structurally connects the Nb-cavity to the He-vessel to facilitate the tuning. The axial stiffness of the bellows is negligible compared to the stiffness of the Nb-cavity of $k_{cav} = 30\,\mathrm{N\,\mu m^{-1}}$. The geometry and structure of the He-vessel is such that it accommodates the tuner's supports on the cylindrical shell, where the reacting forces during the tuning do not affect the high sensitive zones of the SRF cavity.

SPECIFICATIONS

The architecture and efficiency of the tuner must be such that the range of the RF frequency change has to be at least of 135 kHz and 1 kHz, while operating in coarse and fine tuning mode, respectively. The cavity has a sensitivity at the beam-pipe of $\frac{df}{dL} = 540\,\mathrm{kHz\,mm^{-1}}$. Thus, the displacement at the beam pipe has to be of $x_{BPc} \geq 250\,\mu\mathrm{m}$ in coarse tuning mode and $x_{BPf} \geq 1.85\,\mu\mathrm{m}$ in fine tuning mode. Moreover the tuner's stiffness seen by the cavity (passive stiffness) must be greater than $30\,\mathrm{kN\,mm^{-1}}$ in order to have a system with a pressure sensitivity $\frac{df}{dp} \leq 25$ Hz/Torr.

The reliability of a frequency-tuning system is always of great concern. The actuators are prone to failures if not integrated and operated carefully. Failure of the tuning system has an immediate impact on the accelerator complex. Due to the concerns on reliability, the system shall be designed to allow the replacement of the actuating devices in case of failure or deterioration. Maintenance operations shall be simplified where possible considering the system will be serviced manually through access ports in the vacuum vessel of the cryomodule.

CONCEPTUAL DESIGN

Based on the performance of the first SSR1 tuner [3] and other R&D activities, it was decided to develop a lever mechanism actuated by a Phytron stepper motor assembly and Noliac piezos (Table 1) to meet the PXIE specifications.

Table 1: Performance of Phytron Stepper Motor Assembly and Noliac Piezo-electric Actuators to be Used

Parameter	Value
Stepper motor with gear box	
Max force	1300 N
Resolution	0.1 µm
Piezo	
Stroke (x_f) at 293 K	68 µm
Stroke (x_f) at 20 K	15 µm
Max operating force	2700 N
Min operating force	840 N

Figure 1 shows the scheme of the double lever mechanism that allows the coarse and fine tuning of the cavity. A main arm hinged at one end and connected to the actuation system at the other end has a probe that tunes the cavity physically pushing on the beam pipe. The actuation system consists of a stepper motor held by a bracket and connected to a second arm. This arm is hinged at the other end and keeps the piezos in series with the motor.

Figure 2 shows the scheme of forces applied to the tuner components by the stepper motor (F_m), piezos (F_p) and Nb-cavity (F_c). Assuming that the losses in the system (i.e. friction) are negligible compared to the force for tuning the cavity, a good estimation of the range of force applied at the tuner's probe, F_c, during the tuning is calculated in eq. 1. The mechanical advantage at the motor and piezos is

* Work supported by D.O.E. Contract No. DE-AC02-07CH11359
† donato@fnal.gov

ISBN 978-3-95450-142-7

Copyright © 2014 CC-BY-3.0 and by the respective authors

STUDY OF BEAM-BASED ALIGNMENT FOR THE LCLS-II SC LINAC*

A. Saini#, N. Solyak, V. Yakovlev FNAL, Batavia, IL 60510, USA
T. Raubenheimer, SLAC, Stanford, CA 94309, USA

Abstract

The Linac Coherent Light Source (LCLS) is an x-ray free electron laser facility. The proposed upgrade of the LCLS facility is based on construction of 4 GeV superconducting (SC) linac. The achievable performance of linac is determined by beam sensitivity to various component errors. In this paper we review misalignment tolerances of LCLS-II SC linac and discuss possible beam-based alignment algorithm to meet these tolerances.

INTRODUCTION

The proposed upgrade of Linac Coherent Light Source (LSLS) –II [1] is based on construction of SC linear accelerator (linac) which will operate in continuous wave (CW) regime. It will use TESLA [2] accelerating structure to accelerate the electron beam from kinetic energy of 0.75 MeV to 4000 MeV. The SC linac is segment into five sections in order to include warm sections which are designed for specific purpose such as laser heating, diagnostic and bunch compressions. Number of elements and operational parameters in each section are summarized in Table 1. In order to deal with technological constraints and beam dynamics issues, beam optics of SC linac is continuously evolving. Thus, number of elements and operational parameters shown in Table 1 may differ than those have been presented elsewhere [3].

Table 1: Configuration of Each Section in SC Linac

Linac section	Phase (deg)	Gradient (MV/m)	No. of CM's	Avail. cavities	Energy (MeV)
L0	~0	14.78	1	8	0.75-95
L1	-21.0	13.43	2	16	95-303
HL	-165	13.25	3	12	303-250
L2	-21	14.56	12	96	250-1600
L3	0	14.46	18	144	1600-4000

GENERAL

One of the primary accelerator design and operation objectives for LCLS-II SC linac is the preservation of beam emittance along the linac. The principal source of emittance dilution in a linac is typically misalignment of beam line elements. Transverse misalignments of quadrupoles introduce undesired dispersion while transverse misalignments of cavities cause excitation of wake fields that produce transverse kick to the beam. A tilted cavity results in time dependent transverse kick to the beam. Misalignment of cryomodule (CM) may also happen in linac and it is introduced a sort of correlated misalignment of elements in the cryomodule. All these effects associated with misalignment of elements lead to beam emittance dilution along the linac. Thus, preservation of ultra-small emittance requires stringent tolerances on alignment of beam line elements. These alignment tolerances are far beyond that which can be achieved using traditional mechanical and optical techniques. Beam based alignments or correction algorithms are used in modern accelerator to compensate emittance dilution.

In this paper, we present studies performed to understand linac performance in presence of misalignments of beam line elements and review effectiveness of orbit correction algorithm to meet these tolerances.

MISALIGNMENT TOLERANCES

On the basis of experience gained from existing facilities and studies performed for proposed SC linear accelerator facilities such as XFEL, ILC, TESLA etc., a set of alignment requirements for beam line elements in SC linac of LCLS-II facility is generated and specified in Table 2.

Table 2: RMS Alignment Tolerances of Elements in SC Linac of LCLS-II Facility [4]

Error Source	w.r.t	1 RMS tolerances
Cavity X.Y offset	CM	0.5 mm
Quadrupole X,Y offset	CM	0.5 mm
BPM X, Y offset	CM	0.5 mm
Cryomodule X,Y offset	Linac	0.3 mm
Cavity Z offset	CM	2.0 mm
Quadrupole Z offset	CM	2.0 mm
BPM z offset	CM	2.0 mm
Cryomodule Z offset	Linac	2.0 mm
Cavity Tilt	CM	0.5 mrad
Quadrupole tilt	CM	3 mrad
BPM tilt	CM	3 mrad
Cryomodule tilt	Linac	0.05 mrad
Cavity Roll	CM	10.0 mrad
Quadrupole Roll	CM	3.0 mrad
BPM roll	CM	3.0 mrad
Cryomodule Roll	Linac	2.0 mrad

Effects of misalignments of components in LCLS-II SC linac are studied using beam dynamics code LUCRETIA [5]. Simulation is performed for 300 pC bunch charge. The major portion of linac is composed with L2 and L3 sections. Therefore, those sections determine requirement

*Work supported by Fermi Research Alliance, LLC under Contracts No. De-Ac02-07CH11359 with the DOE, USA.
#asaini@fnal.gov

Copyright © 2014 CC-BY-3.0 and by the respective authors

PROGRESS ON EUCLID SRF CONICAL HALF-WAVE RESONATOR PROJECT*

E. Zaplatin, Forschungszentrum Juelich, Germany,
C. Boulware, T. Grimm, A. Rogacki, Niowave, Inc, Lansing, MI, USA,
A. Kanareykin, Euclid TechLabs, Ohio, U.S.A
V. Yakovlev, FNAL, Geneva, IL, U.S.A

Abstract

Project X is a high-intensity proton accelerator complex proposed at Fermi National Accelerator Laboratory. Euclid TechLabs is involved through the design of a conical Half-Wave Resonator (cHWR) with a frequency of 162.5 MHz optimized for protons at β=v/c=0.11. The novel design considers both the superconducting resonator and helium vessel together to minimize the dependence of the resonant frequency on external loads. A unique cavity side-tuning option is also under development.

Niowave, Inc. builds and operates commercial superconducting accelerators for electrons, and as such, was able to propose a complete cavity production procedure including preparation of technical drawings, processing steps and resonator high gradient tests.

Here we present the procedure of the cavity and helium vessel fabrication, cavity preparation and initial experimental results.

INTRODUCTION

The very first investigations of the conical Half-Wave Resonator were made in the frame of the COSY Linac project [1]. The recent cavity developments [2-3] integrated the conceptual design of the cHWR with its liquid helium vessel, minimizing the sensitivity of the resonant frequency to fluctuations in helium pressure.

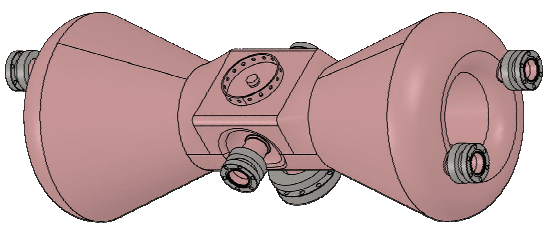


Figure 1: cHWR modified design.

To use the outer conductor walls for cavity tuning deformations effectively, the central part of cHWR is made asymmetric with a planar surface on one side. This planar surface is used for tuning by deformation (Fig. 1). This optimization of the central resonator section was made without compromising the cavity performance. The cavity RF parameters are shown in Table 1.

*Work supported by the DOE SBIR Program, contract # DE-SC0006302

The side tuning procedure results in tune sensitivity up to 80 kHz/mm with acceptable stresses 350 MPa/mm. There is nearly no dependence on the resonator frequency slow tuning.

Table 1: Conical HWR Parameters

frequency	MHz	162.5
$\beta = v/c$		0.11
R_aperture	mm	18
$\beta\lambda$	mm	202.94
R_cavity **)	mm	90
G	Ohm	36.36
R/Q	Ohm	119
E_{pk} / E_{acc} *)		5.1
B_{pk} / E_{acc} *)	mT/MV/m	7.1
B_{pk} / E_{pk}	mT/MV/m	1.39
tune	kHz/mm	-87
*) $L_{eff} = N_{gaps} * \beta\lambda/2$, where N_{gaps}=2 – number of gaps		
**) Cavity radius in center		

CAVITY FABRICATION

Niowave, Inc. proposed a series of cavity and helium vessel modifications to simplify their manufacturing without affecting the main resonator mechanical stability parameters [3]. The modified cold mass design calculations (cavity and helium vessel) confirmed that the total effect of external pressure on all cavity and liquid helium vessel walls results in nearly complete compensation of the frequency shifts caused by cavity and vessel wall deformations (df/dp is close to zero).

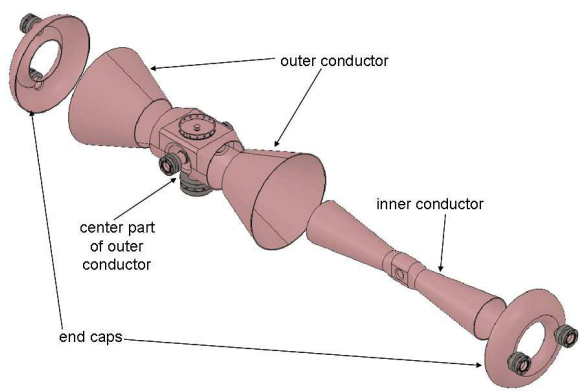


Figure 2: Cavity assembly.

Copyright © 2014 CC-BY-3.0 and by the respective authors

ISBN 978-3-95450-142-7

HIGH CURRENT PROTON BEAM OPERATION AT GSI UNILAC

W. Barth[1,2], A. Adonin[1], P. Gerhard[1], M. Heilmann[1], R. Hollinger[1], W. Vinzenz[1], and H. Vormann[1]
[1]GSI Helmholtzzentrum, 64291 Darmstadt, Germany
[2]HIM, Helmholtzinstitut, 55099 Mainz, Germany

Abstract
A significant part of the experimental program at FAIR is dedicated to pbar physics requiring a high number of cooled pbars per hour [1]. The primary proton beam has to be provided by a 70 MeV proton linac followed by two synchrotrons. The new FAIR proton linac [2] will deliver a pulsed proton beam of up to 35 mA of 36 µs duration at a repetition rate of 4 Hz. The recent GSI heavy ion linac (UNILAC) is able to deliver world record uranium beam intensities for injection into the synchrotrons, but it is not dedicated for FAIR relevant proton beam operation. In an advanced machine investigation program it could be shown, that the UNILAC is able to provide for sufficient high intensities of CH_3-beam, cracked (and stripped) in a supersonic nitrogen gas jet into protons and carbon ions. This advanced operational approach results in up to 2 mA of proton intensity at a maximum beam energy of 20 MeV, 100 µs pulse duration and a rep. rate of 4 Hz. Recent linac beam measurements will be presented, showing that the UNILAC is able to serve as a proton FAIR injector for the first time, while the performance is limited to 17% of the FAIR requirements.

INTRODUCTION

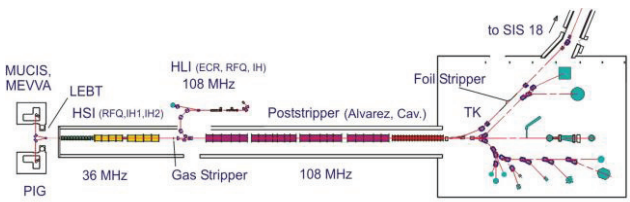


Figure 1: Schematic overview of the GSI UNILAC and experimental area.

Besides two ion source terminals and a low energy beam transport system (LEBT) the High Current Injector (HSI) [1] of the UNILAC (Fig. 1) comprises a 36 MHz IH-RFQ (2.2 keV/u up to 120 keV/u) and an IH-DTL, consisting of two separate tanks, accelerating the beam up to the final HSI-energy of 1.4 MeV/u. After stripping and charge state separation the Alvarez DTL provides for beam acceleration up to $\beta = 0.155$. In the transfer line (TK) to the synchrotron SIS 18 a foil stripper and another charge state separator system can be used. To provide the highest heavy ion beam currents (15 emA, U^{28+}), as required for the FAIR project, the GSI-HSI must deliver up to 18 mA of U^{4+} ions [3]. Highly charged heavy ion beams as well as protons, both with high average intensities (but low pulse intensities), from an ECR ion source of CAPRICE-type are accelerated in the High Charge State Injector (HLI) comprising an RFQ and an IH-resonator to 1.4 MeV/u. The HLI as well as the HSI serve in a time-sharing mode for the main drift tube linac.

The new FAIR proton linac has to provide the high intensity primary proton beam for the production of antiprotons. It will deliver a 70 MeV beam to the SIS18 with a repetition rate of 4 Hz. The room temperature linac will be located north of the existing UNILAC complex. The main beam parameters are listed in Table 1.

Table 1: Main Parameters of the FAIR Proton Linac [2]

final energy	70 MeV
pulse current	70 mA
protons per pulse	$7 \cdot 10^{12}$
repetition rate	4 Hz
transv. beam emittance	4.2 µm (tot. norm.)
RF-frequency	325.224 MHz

The use of RF-coupled CH-cavities (<35 MeV) and single CH-cavities (35-70 MeV) is proofed to be advantageous for a compact and efficient linac design (Fig. 2). Commissioning of the new proton linac is envisaged for end of 2018.

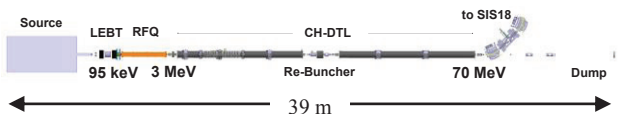


Figure 2: Layout of the FAIR-proton linac.

Recently an advanced investigation program at the existing UNILAC was successfully pushed to deliver high intensity proton beams (up to the UNILAC space charge limit) for a dedicated experimental program at SIS18. In this frame CH_3^+-beam operation with a MUlti Cusp Ion Source (MUCIS) was established. Besides efforts were made for careful machine optimizations in all UNILAC sections, aiming in a high proton beam transmission and highest beam brilliance.

Special focus of investigation efforts was the gas stripper- and charge seperator-section performance, where the molecules are cracked into protons and carbon ions and the separated high brilliance proton beam is matched to the Alvarez-DTL. proton beam acceleration and succesful transport via the 120m transfer line to the SIS18 depends mainly on the accurate set up of the RF-controls of the Alvarez high power supplies, operated at very low RF-power.

Copyright © 2014 CC-BY-3.0 and by the respective authors

ISBN 978-3-95450-142-7

IN SITU MEASUREMENT OF MECHANICAL VIBRATIONS OF A 4-ROD RFQ AT GSI

P. Gerhard*, L. Groening, K.–O. Voss, GSI, Darmstadt, Germany

Abstract

A new 4-rod CW Radio Frequency Quadrupole RFQ was commissioned at the High Charge State Injector HLI at the UNILAC in 2009. It is in operation since 2010 [1,2]. At high rf amplitudes strong modulations of the rf reflection emerge, with a modulation frequency of approximately 500 Hz. They are attributed to mechanical oscillations of the rods, excited by the rf pulse. The high fraction of reflected rf power severely limits the pulse length and amplitude achievable. The frequency control is challenging due to the amplitude of the modulation and its variation with rf power level. Stable operation is hard to achieve. As these modulations could so far only be seen *during* the rf pulse by means of rf measurements, a direct observation of the mechanical vibrations was desirable. Such measurements have been conducted using a commercial laser vibrometer, allowing the investigation of the mechanical behavior of the RFQ *in situ* and independent of the presence of rf power. This paper gives a short introduction of the method, presents some important results and a comparison with rf measurements. Possible countermeasures are discussed.

INTRODUCTION

Fast modulations of the reflected rf power were already observed long ago at the first HLI RFQ [3], but with the new RFQ the impact on the operation became unacceptable. A number of investigations based on rf measurements were conducted. They all suffered from the fact, that the measurements were restricted to the timespan of the rf pulse. Another rf independent approach was required. The idea of using a laser, which could be directed into the cavity through a vacuum window, to monitor the movement of the RFQ electrodes, lead to the application of a laser vibrometer, which allows for remote, fast measurement of the movement of any (reflective) surface.

PRINCIPLE OF MEASUREMENT

The Polytec OFV-525 laser vibrometer exploits the Doppler effect of a laser beam reflected by the surface of interest. The laser beam is split into a probe and a reference beam. The Doppler frequency shift of the reflected light with respect to the reference beam, which is proportional to the velocity of the movement, is determined by a laser interferometer. In order to define the direction of movement relative to the vibrometer, the reference beam light frequency is modulated. The displacement of the surface, and hence the amplitude of the vibration, can either be measured directly by a second operation mode of the vibrometer, or calculated from the velocity data. In principle, only oscillations in the direction of the laser beam can be monitored. For more details about the principles of vibrometry refer to [4].

By pointing the laser through a vacuum window onto e. g. the back edge of a rod between two mounting bridges, we were able to measure the vibration of the rods*in situ* for different operational states. The laser beam was pointing at the electrode at about 30° (60°) with respect to the principle axes of the electrode. This allowed for the measurement of oscillation modes along both axes. The vibrometer was placed on top the RFQ, and the laser beam was guided into the cavity by a motorized mirror. The beam spot was monitored by a video camera. By this, also other parts of the structure like the coupling loop, could be examined. Reference data were taken in order to exclude any perturbation of the vibrometer by the rf, X-rays, vibration of the mounting or the vacuum window.

RESULTS

In Fig. 1, measurements without rf, but with vacuum pumps and cooling water running, are shown as frequency spectra of the vibration velocity (black and red dashed curves, ten times enhanced). The vacuum pumps and other devices

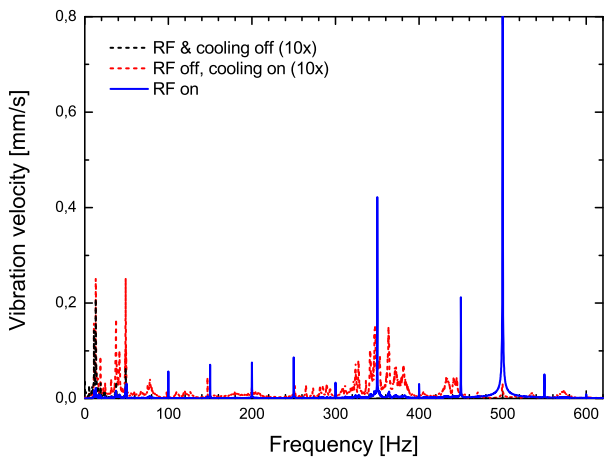


Figure 1: Frequency spectra of the measured vibration velocity. Black: Vacuum pumps running, cooling water and rf switched off. Red: With cooling water. Blue: With RF on at 50 Hz pulse repetition rate. (Black and red are 10x enhanced.)

lead to vibrations of the electrode rods in the range from a few to about 100 Hz, with noticeable signals around 12 and at 50 Hz. Switching on the cooling water, which runs directly through the electrodes and other parts of the structure, adds a broad background up to 600 Hz, with higher amplitudes between 300 and 400 Hz and below 50 Hz.

* p.gerhard@gsi.de

ISBN 978-3-95450-142-7

Copyright © 2014 CC-BY-3.0 and by the respective authors

RF SYSTEM DEVELOPMENT FOR THE NEW 108 MHz HEAVY ION HIGH-ENERGY LINAC AT GSI

B. Schlitt, M. Hoerr, A. Schnase, G. Schreiber, W. Vinzenz, GSI, Darmstadt, Germany

Abstract

The GSI heavy ion linac UNILAC is in operation successfully since about 40 years. A replacement of the post stripper section is proposed to provide heavy ion beams for the future FAIR facility. Design studies for a new 108 MHz high-energy (HE) linac optimized to accelerate high brilliance and high current ion beams up to U^{28+} for synchrotron injection are in progress. Thus, the UNILAC will be converted into a short-pulse accelerator, the RF duty cycle being reduced from around 30 % to ≤ 2 %. To feed the future HE linac and to prepare for the FAIR commissioning, a major modernisation of the existing post stripper RF systems is planned from 2015 to 2017. Besides, the development of a new 1.8 MW cavity amplifier prototype was started recently, based on the widely-used THALES tetrode TH 558SC promising an availability for at least 25 years. New 120 –150 kW solid state driver amplifiers will replace the existing tube drivers. A digital LLRF system designed by industry was integrated into an existing amplifier driving a single gap resonator and was tested including ion beam tests. An overview of the RF system design and of the planned upgrades is reported including some results of the d-LLRF tests.

INTRODUCTION

For the upcoming new FAIR facility at GSI [1] all ion beams heavier than protons will be provided by the existing GSI accelerator complex used as injector system, comprising the heavy ion linear accelerator UNILAC [2] and the subsequent synchrotron SIS18.

The UNILAC started operation in 1975 [3]. Whereas the original Wideröe pre-stripper linac was replaced by a high-current injector in 1999, the 108 MHz post stripper linac with five Alvarez tanks followed by ten single-gap resonators as well as the corresponding RF systems are still in operation since the earliest days of the machine. The UNILAC provides ion beams up to uranium for various experiments at the output of the linac at variable energies and high duty cycles as well as high current beams with highest magnetic rigidities for injection into the SIS18. Up to three ion species with different beam currents, magnetic rigidities, and pulse lengths are accelerated in a pulse-to-pulse time-sharing mode with varying requirements for each pulse at 50 Hz pulse repetition rate and RF pulse lengths up to > 6 ms, corresponding to a max. RF duty cycle of > 30 % [4].

The Proposed High Energy Linac

Due to an increasing number of diverse types of failures at the linac cavities and due to operation limitations, a replacement of the post stripper linac by a new high-energy (HE) linac and an extensive modernisation of the RF systems were proposed to assure reliable operation and the beam quality required for FAIR [5][6]. The new HE linac will serve the needs as a FAIR injector linac, with fixed end energy, short RF pulses (≤ 2 ms), and low duty cycle (≤ 2 %, max. 10 Hz RF pulse repetition rate). Demands for ion beams with high duty cycle and variable energies in the MeV/u regime, e.g. for the super-heavy element program, will be met by a proposed independent superconducting cw linac.

Two different HE linac options are currently studied for acceleration of ion beams up to 15 mA U^{28+} from 1.4 MeV/u to 11.4 MeV/u (85 MV total acceleration voltage) [6]: an IH type drift tube linac comprising six cavities or a conventional Alvarez DTL. Both options are based on the same operation frequency of 108.4 MHz as of the present linac. Each accelerating structure will be fed by an individual RF system with a maximum pulse power of 1.6 – 1.8 MW. Besides the cavity losses, a significant beam load up to 1.3 MW for the complete HE linac is considered.

MODERNISATION OF THE EXISTING POST STRIPPER RF SYSTEMS

Currently, five pulsed high power amplifiers (HPA) equipped with RS 2074HF tubes feed the five Alvarez tanks. A maximum pulse power around 1.7 MW can be achieved for duty cycles up to about 20 % [4]. The HPA stages are fed by four 1 MVA plate power supplies connected directly to the 20 kV power network.

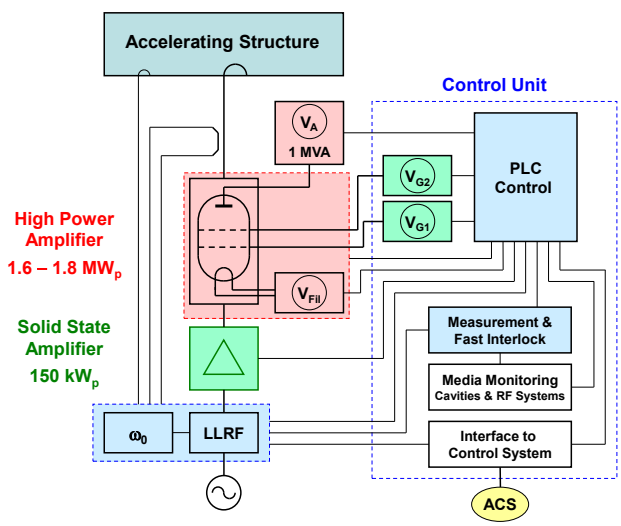


Figure 1: Simplified block diagram of the post stripper RF systems after modernisation (ACS ≡ Accelerator Control System).

Copyright © 2014 CC-BY-3.0 and by the respective authors

ISBN 978-3-95450-142-7

ADVANCED BEAM MATCHING TO A HIGH CURRENT RFQ

S. Yaramyshev, W. Barth, L. Dahl, P. Gerhard, L. Groening, M. Maier, S. Mickat,
A. Orzhekhovskaya, B. Schlitt, H. Vormann, GSI, Darmstadt, Germany

Abstract

The High Current Injector (HSI) of the heavy ion linac UNILAC at GSI comprises the transport lines, the RFQ and two DTL tanks. Beam matching to the RFQ acceptance with a magnetic quadrupole quartet has been worked out manually during commissioning and operation of the machine. Due to a strong overlapping of the field from neighbouring quadrupole lenses, a standard optics calculation does not provide for the required reliability. Advanced beam dynamics simulations have been done with the macroparticle code DYNAMION. The superposition of the measured magnetic fields of each quadrupole was taken into account. The quadrupole settings were optimized using the Monte-Carlo method. Two solutions have been found in accordance with the general theory of particle optics. Beam dynamics simulations with new quadrupole settings show an increased particle transmission through the RFQ. The results of numerical study have been confirmed during experimental campaigns. An improved performance of the whole HSI has been demonstrated. The proposed algorithm and a comparison of the measured data with result of simulations are presented.

INTRODUCTION

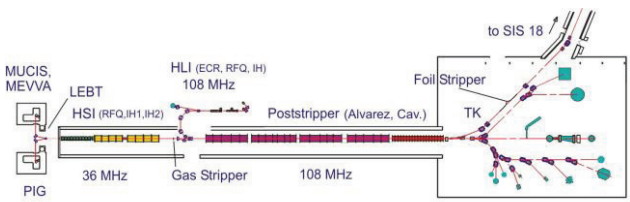


Fig. 1: Schematic overview of the GSI UNILAC and experimental area.

Besides two ion source terminals and a low energy beam transport system (LEBT) the High Current Injector of the GSI UNILAC (Fig. 1) comprises a 36 MHz RFQ accelerating the ion beam from 2.2 keV/u up to 120 keV/u and a short RFQ adapter (Superlens). The IH-DTL, consisting of two separate tanks, accelerates the beam up to the energy of 1.4 MeV/u. After stripping and charge state separation the Alvarez DTL provides for beam acceleration up to 11.4 MeV/u. The transfer line (TK) to the synchrotron SIS 18 is equipped with a foil stripper and charge state separator system. Several upgrade measures have been realized for UNILAC since the last years. Nevertheless, the beam intensity and brilliance are still a factor of five below FAIR requirements [1]. Besides hardware upgrade, further improvement of the UNILAC performance strongly requires for an optimum beam matching to each accelerating-focusing section.

HIGH CURRENT HSI-RFQ ACCEPTANCE

Assuming low beam current and smooth approximation, a local normalized acceptance V_k for each RFQ cell can be calculated from the Floquet functions, which are the solution of the Mathieu-Hill equation for particle motion:

$$V_k = \nu_f \frac{a^2}{\lambda}, \quad \nu_f = \frac{1}{\rho^2},$$ where ρ is a module of the Floquet function, a - aperture of the cell, λ - wave length of the operating frequency; ν_f can be treated as a minimum of the phase advance μ on the focusing period.

The low current HSI-RFQ acceptance (Fig. 2) has been also evaluated from results of dedicated beam dynamics simulations. The acceptance area (approx. 400 mm*mrad) and orientation correspond well to the calculated minimum of the local acceptance along the channel.

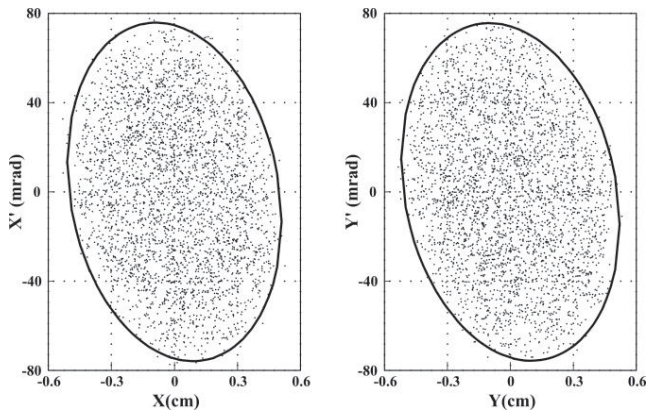


Figure 2. Low current HSI-RFQ acceptance

In case of significant beam current, the values of μ and ν_f decrease (tune depression). Quantitavely it can be calculated using the Coulomb parameter, which combines parameters of the beam and accelerating channel [2].

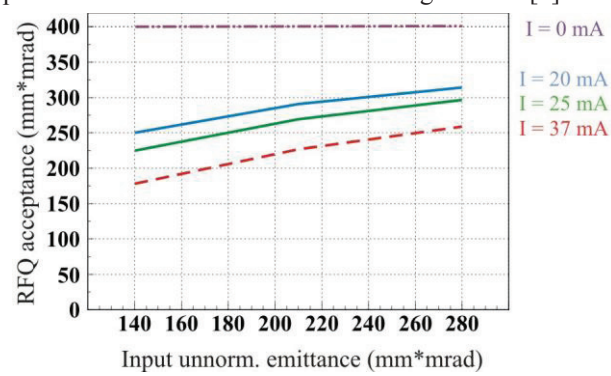


Fig. 3: "High current" acceptance of the HSI-RFQ (unnormalized) as a function of the input beam current and emittance.

Copyright © 2014 CC-BY-3.0 and by the respective authors

DEVELOPMENT OF A 217-MHz SUPERCONDUCTING CH-STRUCTURE*

M. Basten†, M. Busch, F. Dziuba, D. Mäder, H. Podlech,
IAP Frankfurt University, Frankfurt am Main, Germany
M. Amberg, K. Aulenbacher, Helmholtz-Institut Mainz (HIM), Mainz, Germany
W. Barth, S. Mickat, GSI-Helmholtzzentrum, Darmstadt, Germany

Abstract

To compete in the production of Super Heavy Elements (SHE) in the future a 7.3 AMeV superconducting (sc) continuous wave (cw) LINAC is planned at GSI. The baseline design consists of 9 sc Crossbar-H-mode (CH) cavities operated at 217 MHz. Currently an advanced cw demonstrator is under design at the Institute for Applied Physics (IAP) at Frankfurt University. The purpose of the advanced demonstrator is to investigate a new concept for the superconducting CH structures. It is based on shorter CH-cavities with 8 equidistant gaps without girders and with stiffening brackets at the front and end cap to reduce pressure sensitivity. One major goal of the advanced demonstrator is to show that the new design leads to higher acceleration gradients and smaller E_p/E_a values. In this contribution first simulation results and technical layouts will be presented.

INTRODUCTION

At the moment the demonstrator for the sc cw-LINAC at GSI is under construction and its successful beam operation will be the first milestone realizing the new sc cw-LINAC at GSI [1]. The advanced demonstrator which is presented here will be the second milestone for the sc LINAC at GSI. The sc LINAC will consist of the demonstrator as first cavity and 5 additional cryomodules with 2 CH-cavities per cryomodule [2, 3]. The design of the advanced demonstrator will be used for all 10 cavities in the sc cw-LINAC after the demonstrator. The cavity is designed and optimized for high power applications, consists of 8 accelerating cells and has a design gradient of 5 MV/m. Its frequency is the second harmonic of the High Charge Injector (HLI) at GSI, Darmstadt. Table 1 shows the main parameters of the sc 217 MHz CH-cavity and Figure 1 shows the Layout of the sc 217 MHz CH-cavity.

DRIFT TUBE DESIGN

The superconducting cavity for the advanced demonstrator has to reach high electric fields and high accelerating gradients. Without drift tubes the electric field on the beam axis is dropping rapidly in the first and last gap (Figure 2). To increase the field in the first gaps several simulations with

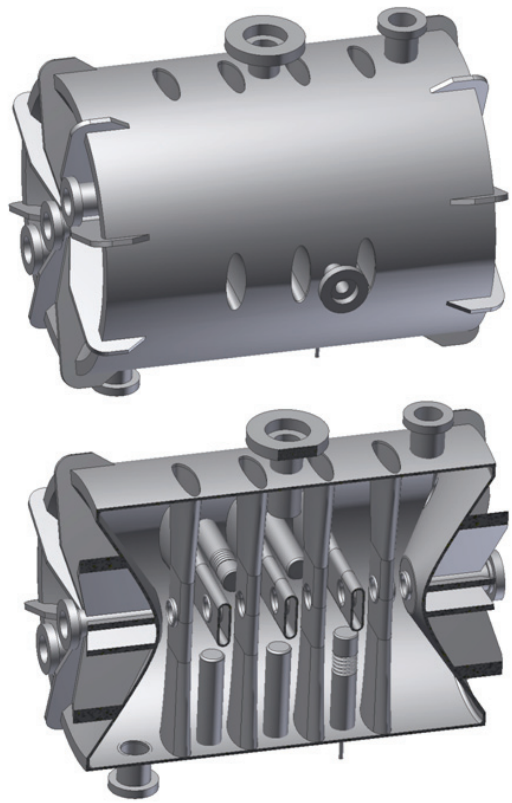


Figure 1: Layout of the sc 217 MHz CH-cavity.

CST-Microwave-Studio have been performed to determine the optimum drift tube length for the different gaps [4]. Figure 2 shows the electric field on the beam axis without drift tubes and with optimized drift tubes. The electric field in the first and last two gaps could be increased significantly wich results in higher accelerating gradients and better E_p/E_a values.

The optimized drift tubes in gap 1 and 8 are 7 mm and in gap 2 and 7 2.5 mm long as shown in Figure 3

BUFFERED CHEMICAL POLISHING

One of the most important conditions for sc cavities is a good surface preparation without contamination wich can be achieved by the so called buffered chemical polishing (BCP). Two BCP treatments of at least 100 μm are planned for the sc CH-cavity after fabrication. Each processing step will change the frequency of the cavity so several CST-

* Work supported by HIM, GSI
† Basten@iap.uni-frankfurt.de

ISBN 978-3-95450-142-7

Copyright © 2014 CC-BY-3.0 and by the respective authors

A REBUNCHING CH CAVITY FOR INTENSE PROTON BEAMS*

M. Schwarz†, C. Claessens, M. Heilmann, O. Hinrichs, D. Koser,
D. Mäder, O. Meusel, H. Podlech, U. Ratzinger, A. Seibel
IAP, Goethe-Universität Frankfurt am Main, Germany

Abstract

The Frankfurt Neutron Source at the Stern-Gerlach-Zentrum (FRANZ) will provide ultra-short neutron pulses at high intensities and repetition rates [1]. The facility is currently under construction at the Goethe-University in Frankfurt am Main (Germany).

A 5-gap CH rebuncher (see Table 1 and Fig. 3) is installed behind a coupled RFQ/IH-DTL combination at the end of the LINAC section between two magnetic quadrupole triplets (see Fig. 1). It will be used for varying the final proton energy around 2 MeV as well as for focusing the bunch longitudinally to compensate huge space charge forces at currents up to 200 mA at the final stage of extension.

High current beam dynamic simulations have been performed. They include benchmarking of different beam dynamic codes like LORASR [2] and TraceWin [3], as well as validating the results by measurements. Detailed examination of multipole field impact, due to the cavity's geometry, together with error tolerance studies and thermal simulations are also performed. Furthermore, this CH rebuncher serves as a prototype for rt CH cavities at MYRRHA (see Fig. 2), an Accelerator Driven System in Belgium for transmutation of high level nuclear waste [4]. After copper plating the cavity, RF conditioning will start soon.

In the following, the results regarding the electric quadrupole components will be presented.

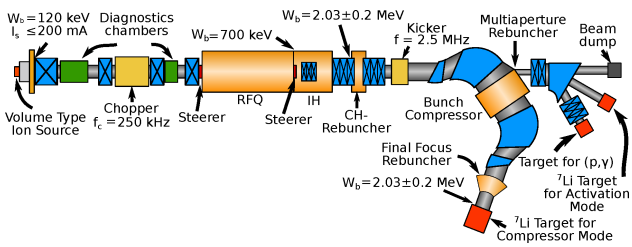


Figure 1: Schematic figure of FRANZ.

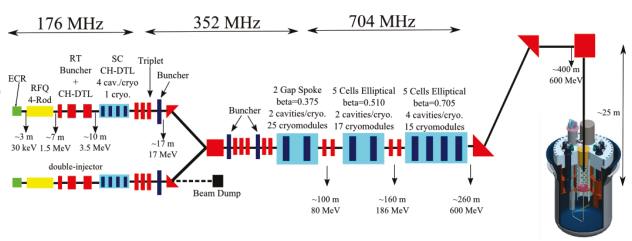


Figure 2: Schematic figure of the MYRRHA accelerator [5].



Figure 3: 3D model cross sectional view in CST MWS [6] *(left)* and picture of drift tubes and crossed stems *(right)*.

Table 1: Specifications of the CH Cavity

Parameter	Unit	Value
β		0.065
Frequency	MHz	175
Gaps	#	5
Total length	mm	462
Cavity inner diameter	mm	332
Aperture diameter	mm	24
Wall thickness	mm	40–52
Dynamic tuner	#	1
Static tuner	#	1
U	kV	295
U_{eff}	kV	245
Q_0 [1]		13500
Z_{eff} [1]	MΩ/m	58
P [1]	kW	2.9

MULTIPOLE COMPONENTS

The geometrical shape of CH structures with crossed neighbouring stems leads to a deformation of the electric fields inside the accelerating gaps. In addition to its dependence on the time t respectively the RF-phase φ_{RF}, the longitudinal position z and the distance to the beam axis r, the electric field varies with the azimuth angle φ: $\vec{E}(r, \varphi, z, t)$. The deviation of the colour contours from a circle to an elliptical geometry in Fig. 4 illustrates this asymmetry.

Former studies of drift tube linacs dealing with these asymmetries can be found for single- and multi-spoke cavities in [7]– [10] and for quarter-wave resonators in [11]. Initial studies on CH structures were published in [12] and [13]. In the following, the findings and results achieved so far will be further specified and extended, especially in relation to beam dynamics issues.

Figure 4 shows E_z along several straight lines parallel to the beam axis. When looking at the curves for $r = 11.9$ mm

* Work supported by the EU, FP7 MAX, Contract No. 269565
† schwarz@iap.uni-frankfurt.de
[1] simulated CST MWS value, normalized with the desired voltage.

Copyright © 2014 CC-BY-3.0 and by the respective authors

IMPROVEMENTS OF THE LORASR CODE AND THEIR IMPACT ON CURRENT BEAM DYNAMICS DESIGNS

R. Tiede, D. Mäder, N. Petry, H. Podlech, U. Ratzinger, C. Zhang#,
IAP, Frankfurt University, Germany

Abstract

LORASR is a multi-particle tracking code optimized for the beam dynamics design of 'Combined Zero Degree Structure (KONUS)' lattices, which can benefit from an adapted input file structure and code architecture. Recent code developments focused on the implementation of tools for machine error studies and loss profile investigations, including also steering correction strategies. These tools are a stringent necessity for the design of high intensity linacs. Thus, the abilities of the present LORASR release allow performing a manifold of checks and optimizations before finalizing the layouts of KONUS-based or conventional linacs. Two representative examples are the MAX-MYRRHA Injector and the GSI FAIR Facility Proton Linac, both under development with strong participation of IAP, Frankfurt University.

This paper presents the status of the LORASR code development with focus on the new features and illustrates the impact on current designs by examples taken from the above-mentioned projects.

MACHINE ERROR TYPES IMPLEMENTED IN LORASR

The LORASR beam dynamics code [1] [2] is maintained and continuously improved at IAP, Frankfurt University. Recent code development focused on the implementation of tools for defining random machine errors, in order to study their effect on the beam dynamics in linacs. The error types implemented so far are described in the following table.

Table 1: Error Type Definitions Available in LORASR

Error Type	Typical Range
Transverse displacements Δx, Δy	≤ 0.1 mm
Lens rotations $\Delta\Phi_x$, $\Delta\Phi_y$, $\Delta\Phi_z$	$\Delta\Phi_{x,y} \leq 5$ mrad $\Delta\Phi_z \leq 10$ mrad
Voltage variations $\Delta U_{i,j}$ of single gaps (i) and whole cavities (j)	$\Delta U_i / U_i \leq 5$ % $\Delta U_j / U_j \leq 1$ %
Cavity rf phase variations $\Delta\phi_j$	$\Delta\phi_j \leq 1$ deg

Typical reasons for the occurrence of such errors are failures during the manufacturing, alignment and tuning of the components (*static errors*) or fluctuations (rf source instabilities, mechanical vibrations) during the operation (*dynamic errors*).

Consequently, in LORASR the error settings can be defined explicitly, as well as statistically distributed.

Manual input is adequate when data from measurements is available (e.g. quadrupole alignment listings or measured gap voltages). In this case, single runs are performed in order to investigate the effects of one particular set of error parameters.

In case of randomly generated error settings many runs (100 to 1000 typically) are needed for good statistics. In LORASR, the random errors are Gaussian distributed and truncated at the 2σ-width. A "batch" processing mode has been implemented: the user defines the number of runs and the starting seed. Results from each run are stored to separate files (sets of runs on different PCs are also possible).

Moreover, an elementary steering correction strategy has been implemented. Steerers are treated as ideal elements with no field limitation.

ERROR ANALYSIS TOOLS AVAILABLE IN LORASR

When operated in the batch mode as described in the previous chapter, LORASR stores all relevant data (error settings and results) of each run in separate files. Thus, all needed information is available for post processing by any statistical software application.

Nevertheless, several error analysis tools related to the collected data were implemented directly to LORASR. The corresponding new plots are as follows:

- Loss profile plots for single runs (Figure 1), as well as for all runs (showing the averaged losses).
- Plot of the maximum beam envelope compounded from all runs, together with the envelope of the nominal case (Figure 2, top; Figure 3).
- Probability distribution of the maximum aperture filling factor (Figure 2, bottom).
- Distribution of the additional relative emittance growth, compared to the nominal run.

In Figure 1 a single run loss profile plot is shown exemplary. The plotted loss profile (= loss rate) is defined as follows:

$$\frac{(dN/N_0)}{dz} = \frac{fraction\ of\ locally\ lost\ particles}{path\ length\ of\ local\ losses} \left[\frac{1}{m}\right] \quad (1)$$

This quantity with the unit 1/m is not very descriptive, but it is independent of the beam current setting and the related plot provides a realistic representation of the distribution of losses along the beam line. Knowing the initial beam current and the bunch energy along the beam line, the loss rate can be easily converted into a current loss rate dI/dz [A/m] or into the beam power loss rate dP/dz [W/m].

Current affiliation: GSI Helmholtzzentrum, Darmstadt, Germany

Copyright © 2014 CC-BY-3.0 and by the respective authors

ZERO-CURRENT LONGITUDINAL BEAM DYNAMICS

J-M. Lagniel, GANIL, Caen, France

Abstract

In linacs, the longitudinal focalization is done by nonlinear forces and the acceleration induces a damping of the phase oscillations. The longitudinal beam dynamics is therefore complex, even when the nonlinear space-charge forces are ignored. The three different ways to study and understand this zero-current longitudinal beam dynamics are presented and compared.

THREE WAYS TO STUDY THE LONGITUDINAL BEAM DYNAMICS

As schematically illustrated by Fig. 1, there are three different methods traditionally used to compute the longitudinal beam dynamics in linacs.

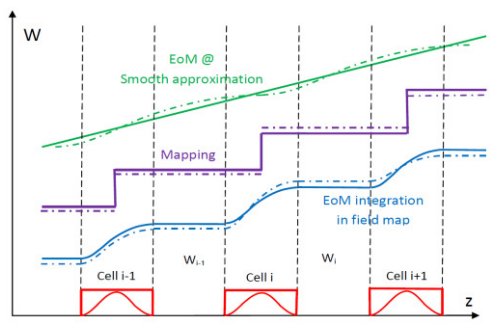


Figure 1 : Schematic representation of the energy evolution with the 3 methods used to compute the longitudinal dynamics : integration of the EoM in field maps (blue), mapping from cavity to cavity (violet), from the EoM obtained in smooth approximation (green).

The first method, by far the most accurate but computer-time consuming, consists in integrating the equation of motion (EoM) (1) using field maps giving the amplitude of the rf accelerating field $E_z(r,z)$.

$$dW = q\,E_z(r(z),z)\,\cos\left(\frac{2\pi z}{\beta(z)\lambda}+\Phi_0\right)dz$$
$$d\phi = \omega_{rf}\,dt = \frac{2\pi}{\beta(z)\lambda}\,dz \qquad (1)$$

The second method consists in computing the evolution of the particle energies using the so-called Panofsky equation (2) [1] which gives the total energy gain produced by an accelerating gap or a cavity.

$$\Delta W = q\,\bar{E}L_c\,\mathrm{T}_{r,\beta}\cos(\Phi_0) \qquad (2)$$

In (2), q is the particle charge, $\bar{E}$ the accelerating field mean value, L_c the gap or cavity length, $\mathrm{T}_{r,\beta}$ the Transit Time Factor (TTF) and Φ_0 the rf phase when the particle crosses the gap or cavity center. The exact value of the TTF is given by (3) which shows that all the information concerning the field value along the particle trajectory and the evolution of the particle "velocity" $\beta(z)$ have been transferred into the TTF.

$$\mathrm{T}_{r,\beta} = \frac{1}{\bar{E}L_c}\int_{-L_c/2}^{+L_c/2} E_z(r(z),z)\,\cos\left(\frac{2\pi z}{\beta(z)\lambda}\right)dz - \frac{\mathrm{tg}\,(\Phi_0)}{\bar{E}L_c}\int_{-L_c/2}^{+L_c/2} E_z(r(z),z)\,\sin\left(\frac{2\pi z}{\beta(z)\lambda}\right)dz \qquad (3)$$

Using (3) the computation of the particle energy evolution is even more complicated than using (1); the practical use of the Panofsky equation often used for linac designs requires therefore several approximations.

The first approximations consist in assuming that the accelerating field $E_z(r(z),z)$ seen by the particle is an odd function of z and that the evolution of the particle radial position and velocity can be neglected. In this case the second integral of (3) vanishes and the TTF can be expressed as a function of the particle radial position ($\bar{r}$) and "velocity" ($\bar{\beta}$) at the entrance of the gap or cavity (4).

$$\mathrm{T}_{\bar{r},\bar{\beta}} = \frac{1}{\bar{E}L_c}\int_{-L_c/2}^{+L_c/2} E_z(\bar{r},z)\,\cos\left(\frac{2\pi z}{\bar{\beta}\lambda}\right)dz \qquad (4)$$

Under the form (4), the use of an analytical expression of the accelerating field distribution $E_z(\bar{r},z)$ allows a fast computation of the TTF, then a fast computation of the particle energy evolutions using (2).

Eq. (4) has nevertheless the redhibitory drawback to produce non symplectic transformations inducing large spurious emittance growths [2]. The only way to build a simple symplectic mapping (5) is to use the synchronous particle TTF ($\mathrm{T}_{\bar{r}=0,\ \bar{\beta}=\beta_s}$) for any particle, then to neglect the effect of the particle velocity spread on the TTF. The error introduced by all these approximations can be very significant in the case of superconducting linacs with large energy gains per cavity and large energy spreads.

$$\delta W_i = \delta W_{i-1} + qE_0L_i\,\mathrm{T}_{\beta_{si}}\left[\cos\left(\Phi_{si}+\delta\varphi_i\right)-\cos\Phi_{si}\right] \qquad (5\text{-}1)$$

$$\delta\varphi_i = \delta\varphi_{i-1} - \frac{2\pi L_i}{m_0c^2\lambda\,\beta_{s\,i-1}^3\gamma_{s\,i-1}^3}\,\delta W_{i-1} \qquad (5\text{-}2)$$

The third method used to compute and understand the longitudinal dynamics consists in considering a continuous longitudinal focalization (smooth approximation). In this case the mixing of (5-1) and (5-2) leads to the second order differential equation (6) which describes the particle phase oscillations around the synchronous particle. In (6) σ_{0l} is the zero-current longitudinal phase advance per unit of length and K_{dp} is the damping coefficient which will be discussed later on.

$$\frac{d^2\delta\varphi}{dz^2} + K_{dp}\frac{d\delta\varphi}{dz} + \sigma_{0l}^2\left[\frac{\cos\Phi_s-\cos(\Phi_s+\delta\varphi)}{\sin\Phi_s}\right] = 0 \qquad (6)$$

Copyright © 2014 CC-BY-3.0 and by the respective authors

RF INPUT POWER COUPLERS FOR HIGH CURRENT SRF APPLICATIONS

V.F. Khan, W. Anders, A. Burrill, J. Knobloch, O. Kugeler, A. Neumann,
Helmholtz Zentrum Berlin, Germany
H. Wang, Thomas Jefferson Laboratory, Newport News, VA 23606, USA

Abstract

High current SRF technology is being explored in present day accelerator science. The bERLinPro project is presently being built at HZB to address the challenges involved in high current SRF machines with the goal of generating and accelerating a 100 mA electron beam to 50 MeV in continuous wave (cw) mode at 1.3 GHz. One of the main challenges in this project is that of handling the high input RF power required for the photo-injector as well as booster cavities where there is no energy recovery process. A high power co-axial input power coupler is being developed to be used for the photo-injector and booster cavities at the nominal beam current. The coupler is based on the KEK–cERL design and has been modified to minimise the penetration of the coupler tip in the beam pipe without compromising on beam-power coupling (Q_{ext} ~10^5). Herein we report on the RF design of the high power (115 kW per coupler, dual couplers per cavity) bERLinPro (BP) coupler along with initial results on thermal calculations. We summarise the RF conditioning of the TTF-III couplers (modified for cw operation) performed in the past at BESSY/HZB. A similar conditioning is envisaged in the near future for the low current SRF photo-injector and the bERLinPro main linac cryomodule.

INTRODUCTION

Super conducting (SC) energy recovery linac (ERL) machines are being explored in various laboratories not only to be used as a particle collider but also as a potential candidate for the next generation light sources. A brief listing of the current SRF ERL projects around the world is presented in [1]. The bERLinPro [2] project is envisaged to circulate a 100 mA, 50 MeV electron beam accelerating through SC cavities at 1.3 GHz. One of the main aspects of the bERLinPro project is to circulate the high current beam whilst preserving the beam quality. Another important feature is handling of the high cw RF power of 230 kW per cavity in the photo-injector as well as booster cavities where there is no energy recovery process. In the initial stages, the photo-injector and booster cavities will be tested at a low current of 5 μA and 4 mA. Hence at these stages the TTF-III couplers modified for cw operation [3] at 10 kW (low power) will be utilised for the injector cavity. Whereas for the nominal final 100 mA current operation a high power coupler, referred to as bERLinPro (BP) coupler is being developed [4-5]. The RF design of the BP coupler is based on the cERL-KEK [6-7] coupler design. The RF conditioning of the cw TTF-III couplers is envisaged at HZB for the SRF photo-injector in the near future. As the similar test has been performed at BESSY/HZB in the past, we briefly mention those results in the next section. The following section describes the high power BP coupler design along with the initial thermal calculations. We summarise the present results and future plans in the final section.

LOW POWER COUPLER

The original RF parameters of the TTF III coupler for XFEL are: peak input power 250 kW, pulse length 1.3 ms and repetition rate 10 Hz [8]. This implies the average power ~3.2 kW. In travelling wave (TW) operation at room temperature the coupler's designed temperature rise is about 25-30 K/kW. In order to test the TTF III couplers at cw operation, RF conditioning tests were performed in collaboration with DESY, Cornell, HZB and HZDR at Rossendorf (at room temperature) and BESSY/HZB (room and SC temperatures) [3]. A detailed design of the TTF III input power coupler and test stand are presented in Fig. 1.

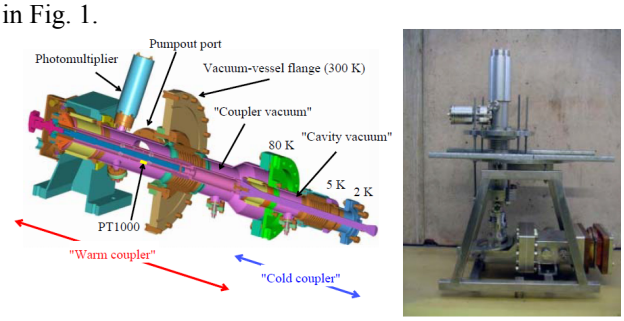


Figure 1: The TTF III coupler (left) and test stand (right).

The experimental set up at BESSY/HZB's HoBiCaT test facility and various tests performed are presented in [3]. In order to test the coupler at a higher average cw power, a modification was done to the inner conductor to improve the power dissipation. The TTF III coupler relies only on conduction cooling; hence its power handling capability is limited to 5 kW. To improve the cooling of the inner conductor, a tube was introduced to allow a room temperature air flow at 20 litre/min. This increases the power handling capability up to 10 kW. The coupler was tested at 4 kW power at room temperature. The cold test was limited to 2 kW power due to severe outgassing leading to arcing in the RF load (which was placed in the vacuum). In both the warm and cold tests the temperature rise was about 29 K/kW [3]. The bERlinPro photo-injector (initial stage 4 mA) and main linac cavities need 10 kW power/cavity dependent on the actual level of microphonics. Hence dual TTF III couplers per cavity

Copyright © 2014 CC-BY-3.0 and by the respective authors

ISBN 978-3-95450-142-7

COMMISSIONING RESULTS OF THE 2ND 3.5 CELL SRF GUN FOR ELBE

A. Arnold#, M. Freitag, P. Murcek, J. Teichert, H. Vennekate, R. Xiang, HZDR, Dresden, Germany
P. Kneisel, G. Ciovati, L. Turlington, JLAB, Newport News, USA

Abstract

As in 2007 the first 3.5 cell superconducting radio frequency (SRF) gun was taken into operation, it turned out that the specified performance has not been achieved. However, to demonstrate the full potential of this new type of electron source, a second and slightly modified SRF gun II was built in collaboration with Thomas Jefferson National Accelerator Facility (TJNAF).

We will report on commissioning and first results of the new gun, which includes in particular the characterization of the most important RF properties as well as their comparison with previous vertical test results.

INTRODUCTION

At the superconducting (SC) electron linear accelerator of the ELBE radiation facility [1] a new superconducting electron photo injector has been installed in May 2014. This new SRF gun II is replacing the previous one which had been in successful operation from 2007 until April 2014. Although SRF gun I could not reach the design specifications, it was successfully operated for R&D purposes and also some dedicated user experiments at ELBE accelerator had been done [2].

For SRF gun II a new niobium cavity has been built, treated and tested at JLab [3]. At the same time a new cryomodule has been designed and built at HZDR [4]. In November 2013, the cavity was shipped to HZDR and assembled into the cryomodule. About half a year later, the gun was installed into the ELBE accelerator hall and since June 2014 it is under commissioning for first RF and beam tests.

The main goal of SRF gun II is to achieve medium average current (1 mA) and low emittance (1 mm mrad) at a moderate bunch charge (77 pC) as well as to test new semiconductor cathodes.

COLD MASS DESIGN

The design of the new cold mass for SRF gun II is shown in Figure 2. Most of the components are identical to the previous SRF gun I [5]. The 1.3 GHz Nb cavity, for example, consists of three TESLA cells and a specially designed half-cell. Another superconducting cell, called choke filter, prevents leakage of the RF field into the cathode support system. The normal conducting (NC) photocathode is installed in this system, which is isolated from the cavity by a vacuum gap and cooled with liquid nitrogen. This design allows the application of NC photocathodes with high quantum efficiency (QE) such as Cs_2Te.

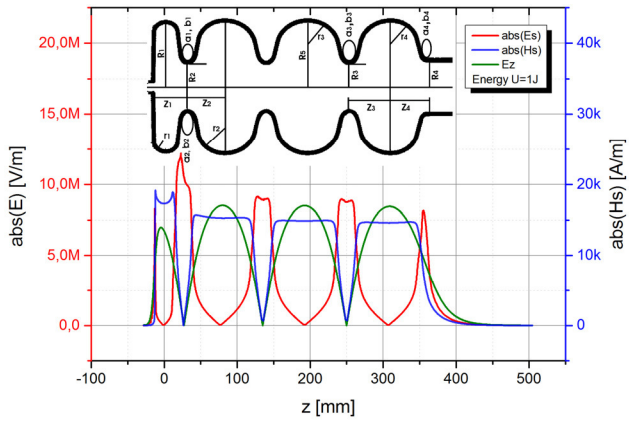


Figure 1: Electric and magnetic surface field as well as on-axis electric field distribution of the accelerating mode normalized to 1J stored field energy.

New is the integration of a SC solenoid in the cryomodule. Compared to the NC solenoid of SRF gun I which was placed downstream the gun, the new design is much more compact and the distance to the cavity is smaller. The SC solenoid is placed on a remote-controlled x-y table to align its center to the electron beam axis. Additional μ-metal shields hold the solenoid remanence field and the stepper motors fields near the cavity on a 1 μT level. Details of the SC solenoid design and testing are published in [6].

Table 1: Updated Design Parameters for 3.5 Cell Cavity

stored energy, U	34.8 J
quality factor, Q_0	10^{10}
dissipated power, P_c	28.5 W
geometry factor, G	224 Ω
normalized impedance, r	167.5 Ω
acceleration voltage, V_{acc}	9.75 MV
acceleration gradient, E_{acc}	19.5 MV/m
$E_{z,max}/E_{acc}$	2.56
B_{peak}/E_{acc}	7.4 mT/(MV/m)

The cavity itself differs in an improved half-cell stiffening and in a slightly changed on-axis electric field distribution. In contrast to the original design, the field in the half cell was increased from 60% to 80% compared to the field strength in one of the three TESLA like cells.

#a.arnold@hzdr.de

Copyright © 2014 CC-BY-3.0 and by the respective authors

CHOPPER OPERATION FOR THE TANDEM SCRAPERS AT THE J-PARC LINAC

K. Futatsukawa#, T. Kobayashi, Z. Fang, Y. Fukui, S. Michizono, KEK, Ibaraki, Japan
K. Hirano, F. Sato, S. Shinozaki, JAEA, Ibaraki, Japan

Abstract

In the J-PARC linac, the energy upgrade to 400 MeV by the installation of Annular-ring Coupled Structure (ACS) cavities was successfully achieved in 2013. In the next stage, we schedule the current upgrade by improving the front-end in this summer. Then, the heat load of a scraper to irradiate the kicked beam by the RF deflector increases and its surface is predicted to be damaged. Therefore, we are preparing the tandem scrapers to suppress the heat load. The half of the kicked beam leads to a scraper and the residual is to the other. Its chopping operation will be achieved by rotating the phase of the RF deflector in the periodic cycles by the low-level RF (LLRF) system. We are preparing the device for the phase rotation and the MPS unit. This will be investigated this system on October and utilized from the user operation of 50 mA on April, 2015.

INTRODUCTION

In the J-PARC linac, the energy of the injection beam to RCS was upgraded from 181 MeV to 400 MeV by the installation of 25 additional ACS modules and 25 new 972-MHz RF systems in the shutdown of 2013 [1]. The 400-MeV acceleration was successfully achieved on January 17th, 2014 and the user operation with the 400 MeV injection energy started from February 17th [2, 3].

In the next step, the upgrade of the beam current is scheduled in order to achieve the design power of 1 MW by improving the front-end, an ion source, a RFQ and a 3 MeV Medium Energy Beam Transport (MEBT1), in the summer shutdown of 2014. The beam current after this upgrade is supposed to be 50 mA and it is three times than that of the present. One of grave concerns for this upgrade is the thermal durability of a scraper to stop the wasted beam for the increment of the heat load. The present scraper had a dent of 1 mm on the surface caused by merely the operation of 17 mA [4]. Therefore, we are preparing the tandem scrapers to reduce the damage as shown in Fig. 1. The half of the kicked beam leads to a scraper and the residual is to the other. Its chopping operation will be achieved by rotating the phase of the RF deflector in the periodic cycles by the LLRF system.

The beam of 50 mA is predicted to irradiate the beam pipe by the simulation of the beam dynamics [5]. Therefore, the chopper cavity with an expanded gap and beam pipes was developed and installed [6]. Additionally, since the beam halo is predicted to spread longitudinally to increase the current, the deflected field by the present RF source, 30 kW, does not have enough to dissipate the remaining beam [7].

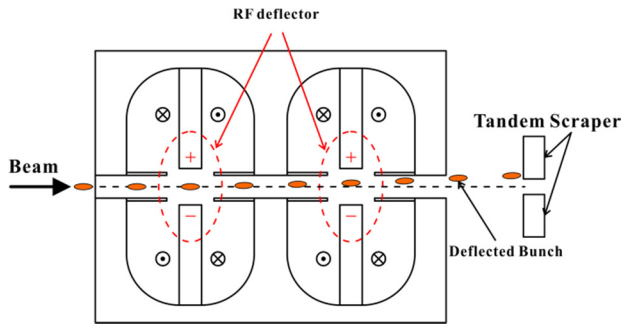


Figure 1: A RF deflector and tandem scrapers. The phase of the RF deflector is quickly rotated by 180 degrees to guide the wasted beam to each scraper.

DESIGN CONCEPT

We are preparing two methods of the phase rotation, by a macro-pulse with 25 pps and by an intermediate-pulse with 1.227 MHz.

The phase rotation in the period of macro-pulses will be realized using the IQ modulator in cPCI. When a phase-rotated trigger of $25/2 = 12.5$ Hz is inputted to the IO module of cPCI, the phase of the DAC output is rotated by the software. This method is convenient and hardly causes the problems. On the other hand, the less effect to suppress the transitional temperature's increment of scrapers is expected in comparison with that of the phase rotation by an intermediate-pulse.

For the phase rotation in the period of intermediate-pulses, two approaches are prepared. One is implemented through the introduction of hardware, which is called a "chopper controller", as shown in Fig. 2 (a). In this case, the chopper controller has two functions, producing the chopping RF with the comb-like structure and rotating the phase, when inputting the normal pulsed RF. The development of new chopper controller with the function to rotate the phase by an intermediate-pulse is required for us. Although there is a lack of the flexibility, this approach inhibits the possibilities of some problems like a rotated-timing error. The other's principle is shown in Fig.2 (b). It is achieved using the IQ modulator of cPCI as same as the rotation by a macro-pulse. In this approach, we do not have to develop hardware since we just improves the software of the LLRF system. Because the phase is rotated in cPCI and the chopping RF is produced in the chopper controller, we have to tune the timing in both instruments. We are slightly concerned this instrument's difference causes a critical trouble.

#kenta.futatsukawa@kek.jp

ISBN 978-3-95450-142-7

Copyright © 2014 CC-BY-3.0 and by the respective authors

NEW SRF FACILITY AT KEK FOR MASS-PRODUCTION STUDY IN COLLABORATION WITH INDUSTRIES

Hitoshi Hayano
High Energy Accelerator Research Organization (KEK), Tsukuba, Japan

Abstract

The building construction of new SRF facility next to the superconducting RF test facility (STF) in KEK has started from 2014 for the mass-production study of SRF accelerators in collaboration with industries. This new building has a dimension of 80m x 30m, and the plan is to install clean room for cavity string assembly, cryomodule assembly tools, cryogenic system, vertical test facility, cryomodule test facility, input coupler process facility, cavity electro-polish (EP) facility, and control rooms in it. The purpose of this new SRF facility is to establish a close collaboration between SRF researchers and industries in order to prepare for the upcoming large-scale future SRF project, ILC [1]. This paper describes the infrastructure detail and the plan to utilize future SRF accelerator.

INTRODUCTION

The STF in KEK is the facility to demonstrate the ILC Main Linac accelerator technology and to have experience of high current and high beam power superconducting accelerator operation. In STF underground tunnel, the STF accelerator construction and installation has been started from 2009. We conducted several experiments, such as S1-Global cryomodule experiment [2], and Quantum-beam experiment for a compact high-flux X-ray generation [3]. The Quantum Beam accelerator part is now used to the STF accelerator, as an injector. At the downstream of an injector, ILC-type cryomodule, CM-1 and a half size cryomodule CM-2a were installed and waiting for cool-down test.

Since the STF facility does not have enough space to assemble the full-size cryomodule, so the full-size cryomodule has been assembled using the accelerator tunnel underground. Once it has built and equipped, no more full-size cryomodule is assembled in the STF.

In order to prepare ILC mass-production of cavities and cryomodule, and to equip ILC testing function of cavities and cryomodule, a new SRF facility to accommodate cavity testing, cryomodule assembly and testing is desired. By using new funding of "International Science Center of Innovation 2013" of MEXT (Ministry of Education, Culture, Sports, Science and Technology in Japan), a new SRF facility "Superconducting Accelerator Development hall" has been started its building construction and equipment fabrication. This new SRF facility has a function of development of ILC cavity test and ILC cryomodule assembly, test for a model equipment of ILC mass-production support function.

NEW BUILDING

The location of the new building, should be next to the STF building for close connection of SRF accelerator development and operation. Joint work and easy access of people, joint operation of helium cryogenics system are the main reason. There is open space in the 30m north of the STF. The building construction has been started by cut out trees and making the land flat. Satellite view of the new SRF facility location and the STF is illustrated in figure 1.



Figure 1: Satellite view of the new SRF facility building location and the STF, ATF.

The size of the new facility is 80m long (east-west) and 30m width (north-south) and 12.5m height. This dimension is determined to accommodate minimum number of required equipment and to have maximum space from available funds. Birds view (from south-east) of the new SRF facility building is illustrated in figure 2.



Figure 2: Birds view of the new SRF facility building.

Copyright © 2014 CC-BY-3.0 and by the respective authors

ISBN 978-3-95450-142-7

STATUS AND RECENT MODIFICATIONS TO 324-MHz RF SOURCE IN J-PARC LINAC

M. Kawamura#, Y. Fukui, K. Futatsukawa, F. Naito, KEK/J-PARC, Ibaraki, Japan
E. Chishiro, T. Hori, F. Sato, S. Shinozaki, K. Hasegawa, JAEA/J-PARC, Ibaraki, Japan

Abstract

This paper describes the present status of and the recent modifications to the 324-MHz RF source in the J-PARC linac. The recovery from the Great East Japan Earthquake Disaster, the status of the 324-MHz klystrons, the failure of 3 high-voltage transformers (HVTRs), and the discharge suppression for the anode-modulators are described.

INTRODUCTION

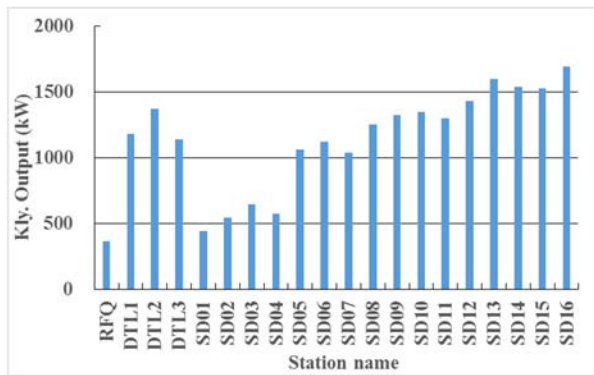
The J-PARC (Japan Proton Accelerator Research Complex) linac [1] began 400-MeV operation on January 17th of this year [2]. The linac comprises two RF sources: a 324-MHz RF and a 972-MHz RF source. The 324-MHz RF source, which is primarily composed of 20 klystrons and the power supply systems for these klystrons, has been in operation since 2006. The majority of the 324-MHz RF source components have total operating times of over 35,000 hours. This paper will give a brief overview of the present status of this system, along with a summary of recent modifications necessitated by various external and internal factors, such as the Great East Japan Earthquake Disaster and the recent 400-MeV upgrade.

PRESENT STATUS

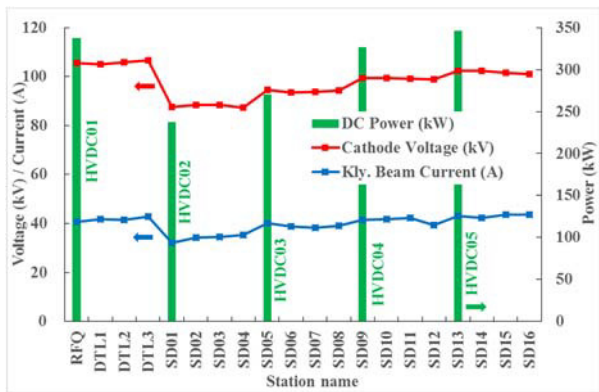
From November 2006 [3] to May 2013, the output energy of the J-PARC linac was 181 MeV. The 324-MHz RF source of the 181-MeV linac [4] was composed of 20 klystrons (TOSHIBA, E3740A [5]) and the power supply systems for these klystrons consisted of 6 high voltage DC power supplies (HVDC01-06) and 20 anode-modulators (one anode-modulator connected to one klystron). Four HVDCs, numbered HVDC01 - HVDC04, connected four anode-modulators and klystrons. In addition, three anode-modulators and klystrons (stations SDTL13, 14, 15) were linked by HVDC05, and HVDC06 connected one anode-modulator and one klystron (DeBuncher01 station).

Between August and November 2013, the linac was upgraded from 181 MeV to 400 MeV. The 324-MHz RF source was adjusted to comprise 20 klystrons, 20 anode-modulators (stations RFQ, DTL1-3, SDTL01-16), and 5 high voltage DC power supplies (HVDC01-05). HVDC05 was then composed of four anode-modulators and klystrons (SDTL13, 14, 15, 16) and HVDC06 was relocated to the 972-MHz RF source.

At present, the typical operational conditions of the 324-MHz RF source are as follows: the repetition rate is 25 pps, the RF pulse width is 600 μs, and the power supply pulse width is 700 μs. Figure 1 shows the measured values of the klystron output powers, the cathode voltages and the beam currents of the klystrons, and the HVDC powers, when negative hydrogen ion beams of 15 mA and 500 μs are accelerated. Similar neutrino, neutron and muon experiments are scheduled to take place in June 2014.



(a)



(b)

Figure 1: The measured values of the 324-MHz RF source. (a) The klystron output powers. (b) The cathode voltages and the beam currents of the klystrons, and the HVDC output powers.

RECENT MODIFICATIONS

In this section, modifications made to the 324-MHz RF source since September 2010 are primarily described. (Revisions and performance up to August 2010 have been described in ref. [4].)

Recovery from Earthquake Disaster

A large earthquake with a magnitude of 9.0 struck north-eastern Japan on March 11, 2011 (the Great East Japan Earthquake Disaster). The J-PARC is located in Tokai-mura, Ibaraki-ken, which is approximately 200 km from

#masato.kawamura@kek.jp

ISBN 978-3-95450-142-7

Copyright © 2014 CC-BY-3.0 and by the respective authors

VORTEX-PENETRATION FIELD AT A GROOVE WITH A DEPTH SMALLER THAN THE PENETRATION DEPTH*

Takayuki Kubo†,
KEK, High Energy Accelerator Research Organization, Tsukuba, Ibaraki 305-0801, Japan

Abstract

Analytical formula to evaluate the vortex-penetration field at a groove with a depth smaller than penetration depth is derived, which can be applied to surfaces of cavities or test pieces made from extreme type II superconductors such as nitrogen-doped Nb or alternative materials like Nb_3Sn or NbN.

INTRODUCTION

The vortex-penetration field B_v is the field at which a vortex overcome the Bean-Livingston barrier [1] and start to penetrate into the superconductor (SC). B_v of extreme type II SC, where the penetration depth λ is much larger than the coherence length ξ, can be evaluated in the framework of the London theory. Materials that attract much attentions in the field of SC accelerating cavity such as dirty Nb like nitrogen-doped Nb and alternative materials like Nb_3Sn or NbN are all categorized into this class. For an SC with an ideal flat surface, B_v is given by $B_v = \phi_0/(4\pi\lambda\xi) \simeq 0.7B_c$, where ϕ_0 is the flux quantum and B_c is the thermodynamic critical magnetic field. Actually, experiments shows fields can not reach such a level. More realistic assumption, such as surface irregularities, should be incorporated.

In this paper we consider a groove with a depth δ smaller than λ as a simple example of a surface irregularity, which assume irregularities on cavity surfaces or test pieces made from extreme type II SC such as a nitrogen-doped Nb or alternative materials. B_v at this type of irregularity has not been obtained so far, in spite of the fact that there are many studies on B_v at a surface irregularity [2, 3, 4, 5].

MODEL

Let us consider a groove shown in Fig. 1(a). Gray and white regions represent the SC and the vacuum, respectively. Surface, groove and applied magnetic-field are perpendicular to the x-y plane. The half width of the groove and the slope angle are given by R and $\pi(\alpha-1)/2$, respectively, and thus the depth is given by $\delta = R\tan[\pi(\alpha-1)/2]$, where $1 < \alpha < 2$. The depth is assumed to satisfy $\xi \ll \delta \ll \lambda$.

FORCES ACTING ON A VORTEX AND THE VORTEX-PENETRATION FIELD

Suppose a vortex is at the position $(x,y) = (0, \delta+\xi)$, inside the bottom of groove. This vortex feels two distinct forces: (i) $\mathbf{F}_\mathrm{M}$ a force from a Meissner current due to an external field and (ii) $\mathbf{F}_\mathrm{I}$ a force due to an image antivortex that is introduced to satisfy the boundary condition of zero current normal to the surface. The former and the latter draw the vortex to the inside and the outside of the SC, respectively. The vortex-penetration field is a field at which these competing forces are balanced.[1]

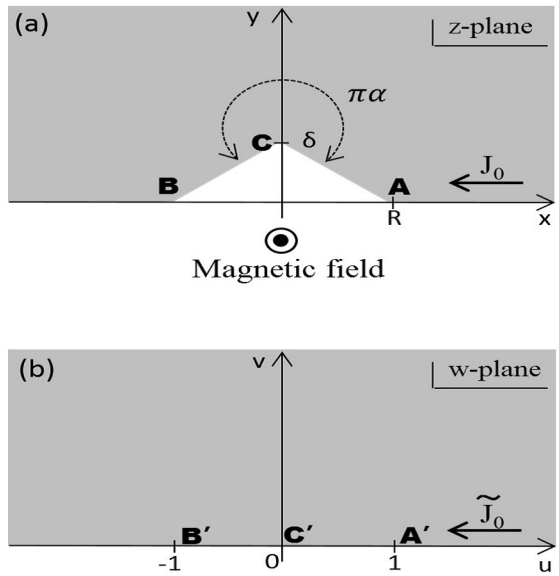


Figure 1: (a) Groove with a depth that is smaller than the penetration depth of the material and (b) its map on the w-plane.

Force Due to an External Field

An external magnetic-field pushes a vortex into the superconductor by a force $\mathbf{F}_\mathrm{M} = \mathbf{J}_\mathrm{M} \times \phi_0\hat{\mathbf{z}}$, where $\mathbf{J}_\mathrm{M}$ is a Meissner screening-current, $\phi_0 = 2.07 \times 10^{-15}$ Wb is the flux quantum and $\hat{\mathbf{z}}$ is the unit vector parallel to the z-axis. To evaluate $\mathbf{F}_\mathrm{M}$, we evaluate $\mathbf{J}_\mathrm{M}$ as follows. $\mathbf{J}_\mathrm{M}$ satisfies $\mathrm{div}\,\mathbf{J}_\mathrm{M} = 0$ and one of the Maxwell equations, $\mathbf{J}_\mathrm{M} = \mathrm{rot}\,\mathbf{H}$, where the magnetic field $\mathbf{H}$ plays the role of the vector potential of $\mathbf{J}_\mathrm{M}$. For our two-dimensional problem, $\mathbf{H}$ can be written as $\mathbf{H} = (0, 0, -\psi(x,y))$, and $\mathbf{J}_\mathrm{M}$ is given by $\mathbf{J}_\mathrm{M} = \mathrm{rot}\,\mathbf{H} = (-\partial\psi/\partial y, \partial\psi/\partial x, 0)$. On the other hand, since λ is assumed to be much larger than the typical scale of the model, the London equation is reduced to $\mathrm{rot}\,\mathbf{J}_\mathrm{M} = -\triangle\mathbf{H} = \mathbf{0}$, which allows us to introduce a scalar potential of $\mathbf{J}_\mathrm{M}$. For our two-dimensional problem the scalar potential can be written as $\phi(x,y)$, and $\mathbf{J}_\mathrm{M}$ is given by $\mathbf{J}_\mathrm{M} = -\mathrm{grad}\,\phi = (-\partial\phi/\partial x, -\partial\phi/\partial y, 0)$. Since

* The work is supported by JSPS Grant-in-Aid for Young Scientists (B), Number 26800157
† kubotaka@post.kek.jp

[1] Detailed reviews are given in Ref. [6, 7].

Copyright © 2014 CC-BY-3.0 and by the respective authors

STUDIES ON WAKE FIELD IN ANNULAR COUPLED STRUCTURE

Yong Liu, Kenta Futatsukawa, Tomofumi Maruta (KEK/JAEA, Ibaraki-Ken)
Akihiko Miura (JAEA/J-PARC, Tokai-mura)

Abstract

LINAC injector of J-PARC (Japan Proton Accelerator Research Complex) was recently successfully upgraded from 181 MeV to 400 MeV, applying a type of coupled cavity linac (CCL) structure ACS (Annular Coupled Structure). It was warmly discussed since very beginning on the wake field in the ACS cavities, where there are CCL modes with the same number as that of cells within ~50 MHz, possibly resonating with high intensity proton/H- beams. One of the most important effects from the wake field is the influence on the ACS phase scan. Analytical and simulation studies, as well as the countermeasures were prepared before the energy upgrade. Fortunately we found that detuning of the ACS was unnecessary, which helped to save much work in the commissioning. In addition we got chance to make experiment studies. It was also discussed why the wake field is not so serious as we expected at the very beginning.

INTRODUCTION

The Japan Proton Accelerator Research Complex (J-PARC) is a high-intensity proton accelerator, which consists of a linac[1], as shown in Fig.1, a 3GeV synchrotron (rapid cycling synchrotron, RCS), and a main ring synchrotron (MR).

The J-PARC linac consisted of a 3 MeV RFQ, 50 MeV DTL (Drift Tube Linac) and 181/190 MeV SDTL (Separate-type DTL) before 2013. It was upgraded to 400 MeV in Jan., 2014, with 42 (21 coupled pairs) new annular-ring coupled structure (ACS) [2] installed during the summer shutdown in 2013.

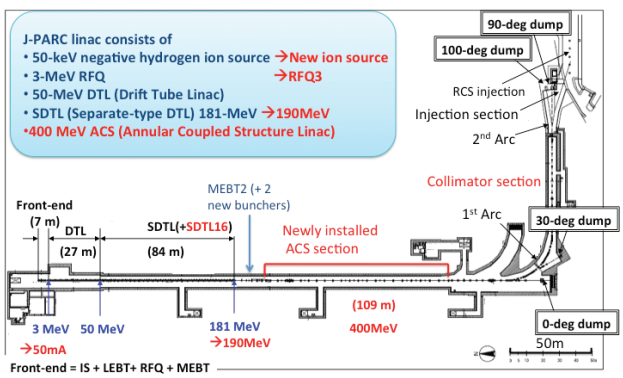


Figure 1: Layout of J-PARC linac.

The present nominal operation current is 15mA, with designed peak current of 30 mA applied for beam studies. A new RF ion source and a new RFQ (RFQ3) are being installed in the summer shutdown this year with designed current of 50mA. The commissioning is scheduled in this October.

ACS is a type of normal conducting coupled cavity linac (CCL) structure, optimized for efficient acceleration for mid-beta high-power pulsed hadron beams. ACS cavities used for acceleration at J-PARC have $N_g = 17$ gaps. Every two ACS cavities are coupled by a bridge coupler and fed by one Klystron, as shown in Fig. 2.

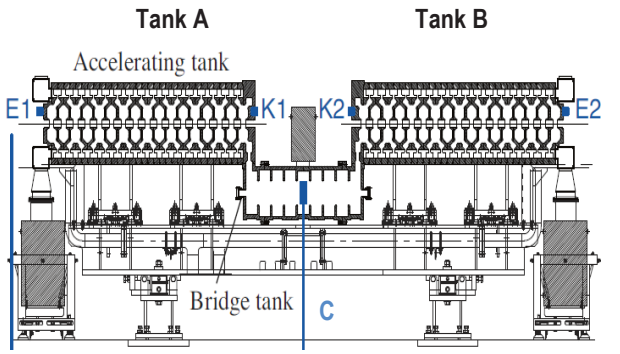


Figure 2: Sketch of J-PARC ACS cavity for acceleration.

As a property of CCL, J-PARC ACS has $N_{mode} = 2N_g - 1$ resonant modes in the cavity within frequency range of ~ ± 2.5 % near the acceleration mode (π/2-mode), which can be resonant to the beam with MW-level of peak power. Shunt impedance of J-PARC ACS is ranged in 36~45 MΩ/m. In the very beginning of J-PARC wake field of ACS aroused discussions. One major worry is the effect by the wake field on ACS phase scan, which is used to set each cavity voltage and phase as design. Beam needs to pass through several downstream idle cavities to get enough flight distance for energy measurement. Wake field decelerates the beam, and could affect the measurement.

In the previous studies it was proposed to detune the downstream idle ACS cavities in the phase scan measurement [3]. It will be enormously time-consuming for the commissioning and hardware preparation.

In our recent studies it is found that the ACS wake field is not sensitive to the incoming beam energy within the phase scan range, although it is ineligible. The phase scan curves are mainly moved conformably, so that the ACS detuning could be fortunately avoided. This conclusion has been verified in the commissioning.

Another motivation for further wake field studies came from the observation of free oscillation of ACS after power off. The properties of ACS modes except for the main one were not interesting during ACS preparation. The wake field is the only way to learn these features.

#yong.liu@kek.jp

Copyright © 2014 CC-BY-3.0 and by the respective authors

ISBN 978-3-95450-142-7

STUDY OF THE ACS CAVITY WITHOUT A BRIDGE CAVITY

Fujio Naito*, KEK/J-PARC Center, Tokai, Japan
Koji Takata, KEK, Tsukuba, Japan
Hiroyuki Ao, Nobuo Ouchi, Kazuo Hasegawa, Kouichiro Hirano, Takatoshi Morishita
JAEA/J-PARC Center, Tokai, Japan

Abstract

One module of the Annular-ring Coupled Structure (ACS) linac, which has been installed in the linac tunnel of J-PARC to increase the beam energy up to 400 MeV, is composed of two accelerating tanks which are coupled by a bridge cavity. Although the bridge cavities can simplifiy the handling of the multi-tank system of the coupled cell linac, it is possible to feed the RF power into the each of tank directly with the power divider and the phase shifter instead of the bridge cavity. The rf properties of the ACS linac without a bridge cavity has been studied by using the low power model. The study results are summarized below.

INTRODUCTION

Japan Proton Accelerator Research Complex (J-PARC) is a high-intensity proton accelerator facility [1]. The linac of J-PARC uses the annular-ring coupled structure (ACS) linac as a CCL to accelerate the H^- ion beam from 191 to 400-MeV. One ACS module shown in Fig. 1 is composed of two accelerating tanks which are coupled by the bridge cavity. We can use the bridge coupled tanks as one cavity from the viewpoint of rf system.

As each of the tanks has 17 accelerating cells, one module has 34 accelerating cells. In this manner the bridge cavity simplifies the handling of the multi-tank system [2]. Figure 2 shows the cross sectional view of the ACS module.

The resonant frequency of the ACS is 972MHz.



Figure 1: An ACS module for J-PARC linac.

Although the bridge cavity system is useful to connect the multi-accelerating tanks like the side coupled linac of FNAL in USA [3], it is also possible to feed the RF power into the each of tanks directly without the bridge cavity. In this case, each of the ACS tanks must have the power input port independently. Furthermore the waveguide system requires

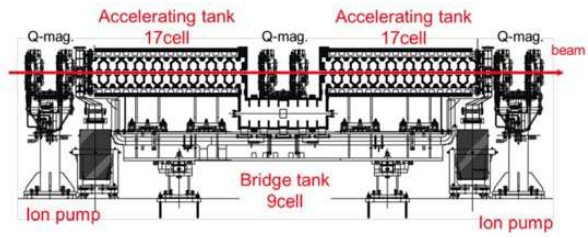


Figure 2: Cross section of an ACS module [1].

the power divider and the phase shifter. (The latter has been realized in the RF system for the SDTL of J-PARC as described in the appendix.)

Merits of the ACS without a bridges are as follows;

1. A cavity assembling become much easier;
2. An alignment of the tank is much easier;
3. Cavity installation is much easier;
4. RF power load of the input coupler decreases.

Demerits are as follows;

1. A number of cavity to be tuned doubles;
2. A phase shifter and a power divider are required.

This paper describes the study to realize the ACS system without bridge cavity.

ACS WITHOUT A BRIDGE CAVITY

When the ACS accelerating tank has no bridge cavity, it must have the extra port for the RF power input. Probably the power input cell is located at the canter of the tank as shown in Fig. 3 to make a power droop minimum.

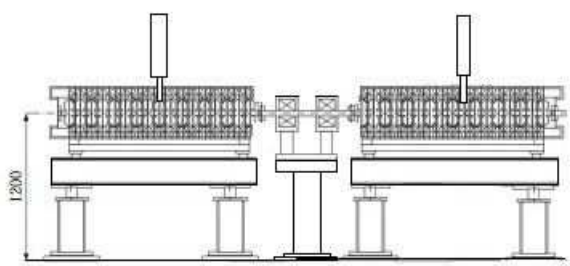


Figure 3: Schematic view of ACS without a bridge cavity.

Since the accelerating cell which has an iris to couple the wave-guide can not have the annular-ring coupling cell, the cell has the side coupled structure with a mirror symmetry for the middle plane of the gap. The neighboring accelerating cell is a hybrid cell which has a side coupled and an annular-ring coupled structure.

* fujio.naito@kek.jp

Copyright © 2014 CC-BY-3.0 and by the respective authors

THE FIRST BEAM RECIRCULATION AND BEAM TUNING IN THE COMPACT ERL AT KEK

S. Sakanaka, M. Adachi, S. Adachi, M. Akemoto, D. Arakawa, S. Asaoka, K. Enami, K. Endo, S. Fukuda, T. Furuya, K. Haga, K. Hara, K. Harada, T. Honda, Y. Honda, H. Honma, T. Honma, K. Hosoyama, K. Hozumi, A. Ishii, X. Jin, E. Kako, Y. Kamiya, H. Katagiri, H. Kawata, Y. Kobayashi, Y. Kojima, Y. Kondo, O.A. Konstantinova, T. Kume, T. Matsumoto, H. Matsumura, H. Matsushita,S. Michizono, T. Miura, T. Miyajima, H. Miyauchi, S. Nagahashi, H. Nakai, H. Nakajima, N. Nakamura, K. Nakanishi, K. Nakao, K. Nigorikawa, T. Nogami, S. Noguchi, S. Nozawa,T. Obina, T. Ozaki, F. Qiu, H. Sagehashi, H. Sakai, S. Sasaki, K. Satoh, M. Satoh, T. Shidara,M. Shimada, K. Shinoe, T. Shioya, T. Shishido, M. Tadano, T. Tahara, T. Takahashi, R. Takai, H. Takaki, T. Takenaka, Y. Tanimoto, M. Tobiyama, K. Tsuchiya, T. Uchiyama, A.Ueda, K. Umemori, K. Watanabe, M. Yamamoto, Y. Yamamoto, Y. Yano, M. Yoshida,
High Energy Accelerator Research Organization (KEK), Tsukuba, Ibaraki 305-0801, Japan
R. Hajima, S. Matsuba, R. Nagai, N. Nishimori, M. Sawamura, T. Shizuma,
Japan Atomic Energy Agency (JAEA), Tokai, Naka, Ibaraki 319-1195, Japan
M. Kuriki, Y. Seimiya, Hiroshima University, Higashihiroshima, Hiroshima 739-8530, Japan
E. Cenni*, the Graduate University for Advanced Studies (Sokendai), Tsukuba, Ibaraki, Japan
J.-G. Hwang, Kyungpook National University, Daehakro, Bukgu, Daegu 702-701, Korea
A. Valloni, CERN, Geneva, Switzerland

Abstract

To demonstrate overall technologies for the energy-recovery-linac(ERL)-based light source, we constructed the Compact ERL (cERL) during 2009-2013. In March, 2014, we succeeded in recirculating the CW beams of 6.5 μA in the cERL; the beams were successfully transported from the gun to the beam dump under energy recovery operation in the main linac. We report our experience on commissioning the cERL, as well as the results of initial measurements of beam properties.

INTRODUCTION

Superconducting(SC)-linac-based light sources [1,2], which can produce ultra-brilliant photon beams in CW operation, are attracting worldwide attention. In Japan, we have been conducting R&D efforts towards the energy-recovery-linac(ERL)-based light source [3] since 2006. To demonstrate overall technologies for the ERL, we constructed the Compact ERL (cERL) [4] at KEK during 2009-2013. Basic configuration and the principal parameters of the cERL are shown in Fig. 1 and Table 1.

In the cERL, high-brightness CW electron beams are produced using a 500-kV photocathode DC gun. The beams are accelerated to a nominal energy of 5 MeV in a SC injector module, and merged into the main linac (ML) where the beams are accelerated to a nominal energy of 35 MeV. The beams are then transported through a recirculation loop, decelerated in the main linac, and dumped. A major challenge in the cERL is the production and transportation of low-emittance and high-current beams which are required for the ERL light source.

The injector of the cERL was constructed in Japanese fiscal year 2012, and it was completed in April, 2013. Commissioning of the injector [5] was conducted from April to June in 2013 with a total beam-operation time of 202 hours. During this period, we successfully produced low-emittance beams from a GaAs photocathode, and accelerated them to a typical total energy of 6.1 MeV.

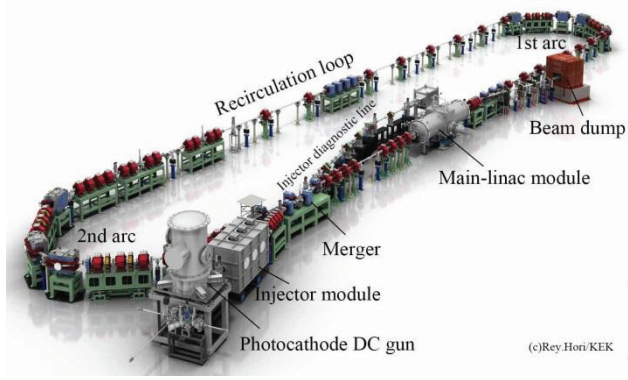


Figure 1: Illustration of the Compact ERL.

Table 1: The principal parameters of the cERL

Nominal beam energy E	35 MeV
Nominal injector energy E_{inj}	5 MeV
Beam current I_0 (initial goal)	10 mA
Normalized emittance ε_n	< 1 mm·mrad
RF frequency	1.3 GHz

From July to November in 2013, we constructed the recirculation loop including magnets, girders, vacuum

* Present address: Institute for Chemical Research, Kyoto University

Copyright © 2014 CC-BY-3.0 and by the respective authors

ISBN 978-3-95450-142-7

HIGH PRECISION MANUFACTURING FOR LINACS*

F. Mirapeix#, J. Añel, HTS, Mendaro, Spain
A. Urzainki, J. Presa, J. Amores, DMP, Mendaro, Spain

Abstract

A big effort in R&D focused to the LINAC devices together with the know-how already deployed through emblematic projects, places DMP in the state of the art of the extreme precision mechanics. This mechanic culture makes DMP a natural partner in early stages of design or driver of a comprehensive solution, optimizing industrial risks, quality and due date. Surface roughness below 1 nanometer, figure errors better than 50 nanometers in OFE copper enhances lifetime and performance of many devices for LINACs. Research in joining techniques and combining several alternative technologies to traditional machining, improves figure stability and makes complex cooling systems possible.

INTRODUCTION

DMP is well known as provider for high precision machining. Established as a reliable partner in high technology, HTS (High Technology Solutions) completes the cycle from engineering to design. Different kinds of products have been developed together for LINACs.

Some of the technical goals achieved in the ultra high precision manufacturing field for accelerating structures are highlighted in this paper.

ULTRA HIGH PRECISION

Overview

The field of ultra high precision requires considerable experience, not only in frequently used materials like aluminium or steel but also in titanium, invar, OFE copper, armco, nimonic, alumina, etc. Ultra high precision can only be achieved in a fully controlled process where room temperature must be rigorously controlled with accuracy within ±0.1 K in order to avoid any distortion due to thermal dilatation. Computer numeric control (CNC) machines for lathing, milling, grinding and electric discharge machining (EDM) must enable dynamic control as a function of the temperature of the piece being machined and the temperature of the spindle. All manufactured pieces must be 3D scanned in house to enable a closed loop between different steps. High precision and ultra low probing force (0.001 N) 3D coordinate measuring machine (CMM) with accuracy below 0.3 µm are used to validate devices in a clean environment. Higher forces will damage the pieces above the specifications; the next picture shows the impact of a low force head, with a 0.8 mm Ø stylus over a OFE Cu flat surface.

Correspondent author: fmirapeix@hights.es

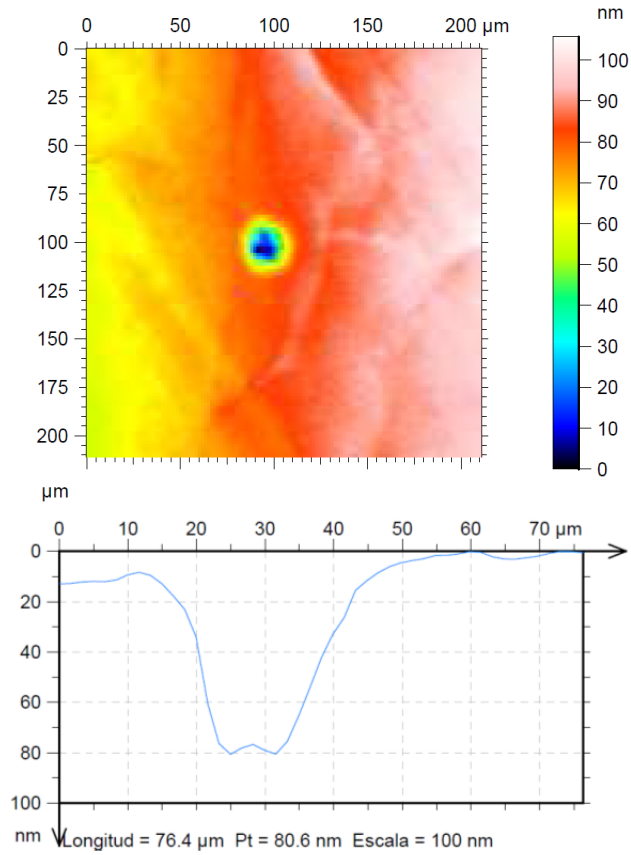


Figure 1: Impact on flat OFE copper of a 3D CMM 0.8 mm Ø stylus. The result is a crater 80.06 nm in deep.

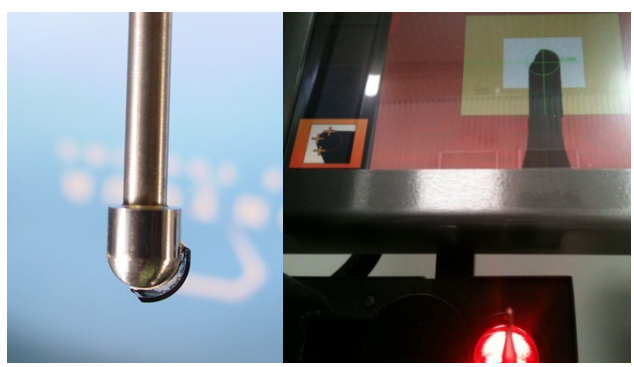


Figure 2: Image of a diamond tool and a laser waviness measuring system.

Other kind of devices combining interferometry and confocal techniques are also necessary for high precision non-contact measurements (resolution below 0.1 nm).

Copyright © 2014 CC-BY-3.0 and by the respective authors

ISBN 978-3-95450-142-7

HIGH GAIN FEL WITH A MICRO-BUNCH STRUCTURED BEAM BY THE TRANSVERSE-LONGITUDINAL PHASE SPACE ROTATION

M. Kuriki*, Y. Seimiya, HU/AdSM, Higashihiroshima
R. Kato, ISIR, Osaka
H. Hayano, K. Ohmi, KEK, IBaraki
S. Kashiwagi, Tohoku University, Sendai

Abstract

FEL is one of the ideal radiation source over the wide range of wavelength region with a high brightness and a high coherence. Many methods to improve FEL gain has been proposed by introducing an active modulation on the bunch charge distribution. The transverse-longitudinal phase-space rotation is one of the promising method to realize the density modulation as the micro-bunch structure. Initially, a beam density modulation in the transverse direction made by a mechanical slit, is properly transformed into the density modulation in the longitudinal direction by the phase-space rotation. That results the longitudinal micro-bunch structure. The micro-bunch structure made with this method has a large tunability by changing the slit geometry, the beam line design, and the beam dynamics tuning. A compact FEL facility based on this method is proposed.

INTRODUCTION

In recent years, an extremely short bunch electron beam generation by employing short pulse laser and photo-cathode is one of the hottest topic in electron linac. The temporal scale is less than 1 ps and is approaching to as (1.0×10^{-18}) level. The extremely short electron beam is useful as a driver of coherent radiation, a probe to fast phenomena, etc. As we mentioned already, such short pulse electron beam is usually generated by photo-cathode technology with a short pulse laser. In this case, however, the time structure of the generated bunch is limited by temporal response of the cathode (some material has a long tail in the electron emission). Although once we succeeded the generation, we have to fight against de-bunching phenomena by space-charge effect. In this article, we discuss a totally different approach to generate such extremely short bunch. In addition, we also propose to generated a micro-bunch structure which enhances the coherent radiation effectively.

In our approach, a moderate brightness electron beam is generated by ordinal photo-injector technology, i.e. a short pulse in order of several ps with a photo-cathode and boosted up to more than 100 MeV. By a bunching method, the bunch is shorten down to 1 ps full width. Such kind of bunch can be generated by employing ordinal technologies. Figure 1 shows EEX (Emittance EXchange) beam line which rotates the beam in X-Z phase-space. A part of bunch is clipped by a mechanical slit which limit the spatial distribution of the bunch in transverse space as shown figure. The transverse spatial modulation by the slits is transferred to the longitudinal modulation by the X-Z phase space rotation as shown in the figure. If the slit is a narrow single slit, an extremely short bunch can be obtained. If the slit is equi-distant multi-slits, a micro-bunch structure in the longitudinal space is obtained.

* mkuriki@hiroshima-u.ac.jp

PHASE SPACE ROTATION

Here, we explain the foundation of the X-Z rotation with EEX beam line. The phase-space rotation is initially proposed for optimization for efficient FEL[1][2]. Transfer matrix of the first dogleg in X-Z phase space is given by

$$\mathrm{M}_D(\eta,\xi,L) = \begin{bmatrix} 1 & L & 0 & \eta \\ 0 & 1 & 0 & 0 \\ 0 & \eta & 1 & \xi \\ 0 & 0 & 0 & 1 \end{bmatrix}, \quad (1)$$

where L is the length of the dogleg, η and ξ are dispersion and momentum compaction of the dogleg. η and ξ are given with geometry of the dogleg as

$$\eta = S_1 \frac{\sin\alpha}{\cos\alpha^2} + 2\frac{D}{\sin\alpha}\left(\frac{1}{\cos\alpha} - 1\right) \quad (2)$$

$$\xi = S_2 \frac{\sin\alpha^2}{\cos\alpha^3} + 2\frac{D}{\sin\alpha - \alpha}, \quad (3)$$

where D and S_1 are pole length of a bending magnet and its interval, α is the bending angle. The transfer matrix of the TM_{210} cavity is given in the thin-lens approximation as

$$\mathrm{M}_C(k) = \begin{bmatrix} 1 & 0 & 0 & 0 \\ 0 & 1 & k & 0 \\ 0 & 0 & 1 & 0 \\ k & 0 & 0 & 1 \end{bmatrix}, \quad (4)$$

Particle transfer through EEX beam line is given by product of these matrices as

$$\mathrm{M}_{EX}(\eta,\xi,L,k) = \mathrm{M}_D\mathrm{M}_C\mathrm{M}_D, \quad (5)$$

and a matching condition give as

$$1 + \eta k = 0, \quad (6)$$

greatly simplifies the result given as

$$\mathrm{M}_{EX} = \begin{bmatrix} 0 & 0 & -L/\eta & \eta - L\xi/\eta \\ 0 & 0 & -1/\eta & -\xi/\eta \\ -\xi/\eta & \eta - L\xi/\eta & 0 & 0 \\ -1/\eta & -L/\eta & 0 & 0 \end{bmatrix}, \quad (7)$$

Copyright © 2014 CC-BY-3.0 and by the respective authors

ISBN 978-3-95450-142-7

COMMISSIONING OF THE MAX 700 MHz TEST STAND*

J-L. Biarrotte#, M. El Yakoubi, F. Chatelet, N. Gandolfo, C. Joly,
J. Lesrel, H. Saugnac, CNRS/IN2P3, IPN Orsay, France
A. Bosotti, R. Paparella, P. Pierini, INFN/LASA, Milano, Italy
F. Bouly, LPSC, Université Grenoble-Alpes, CNRS/IN2P3, Grenoble, France
I. Martin-Hoyo, ADEX, Madrid, Spain.

Abstract

The MYRRHA project aims at the construction of an Accelerator Driven System demonstrator. The criticality will be sustained by an external spallation neutron flux produced thanks to a 600 MeV high intensity proton beam. This beam will be delivered by a superconducting linac which must fulfil very stringent reliability requirements. Under the MAX (MYRRHA Accelerator eXperiment) program, which aims at pursuing the R&D activities on the ADS-type accelerator, a 700 MHz Cryomodule was developed. The main goal of this test stand is to dispose of a facility to carry out "real scale" reliability oriented studies on a RF Superconducting cavity of the high-energy linac section. This module holds a 5-cell elliptical cavity equipped with its blade cold tuning system and its coaxial power coupler. The experimental work undertaken at IPN Orsay, has allowed to fully qualify the module in machine configuration (high RF power, at 2K), including assessment of the tuning system and measurement of microphonics spectrums. During this study the dynamic behavior of the fast tuning system of the cavity was also measured. We review here the obtained results and lessons learnt by operating this module.

INTRODUCTION

MYRRHA (Multi-purpose Hybrid Research reactor for High-tech Applications) is a new fast spectrum nuclear facility which is planned to be built at SCK-CEN in Mol (Belgium) [1]. This 100 MW_{th} nuclear reactor is especially designed to demonstrate the ADS (Accelerator Driven System) concept for the transmutation of high level radioactive wastes. To operate, the sub-critical reactor requires a continuous wave (CW) proton beam, with a maximum power of 2.4 MW (600 MeV - 4 mA). In addition to the high beam power, one has to consider that frequently repeated beam interruptions can induce high thermal stresses and fatigue on the reactor structures, the target or the fuel elements, with possible significant damages especially on the fuel claddings. Therefore the accelerator will have to be extremely reliable. The present tentative limit for the number of allowable beam trips is 10 unexpected interruptions longer than 3 seconds per 3-months operation cycle.

In this purpose, the accelerator design is based on a redundant and fault-tolerant scheme to enable the rapid mitigation of RF failures [2]. The conceptual design of this ADS-type accelerator had been recently consolidated in the frame of the MAX project (EURATOM FP7) [3]. It is composed by a 17-600 MeV superconducting main linac [4] with independently-powered spoke and elliptical cavities, fed by a redundant 17 MeV injector [5].

In the continuation of the work initiated within the FP6 EUROTRANS programme [6], a prototypical cryomodule of the medium-energy section of the MYRRHA proton linac has been developed, built and fully tested in "accelerator-like" configuration, and a few reliability-oriented experiments have been performed in view of the foreseen MYRRHA fault-recovery procedures [2].

THE MAX CRYOMODULE 700 MHz TEST STAND

Jointly developed by INFN Milano and IPN Orsay, the MAX prototypical cryomodule is composed of the following elements: a MYRRHA-type/TRASCO β=0.5 elliptical superconducting cavity [7], as illustrated in Figure 1, a slow mechanical Cold Tuning System (CTS), a fast piezo-based CTS, a high-power coupler, a 80 kW IOT operating at 700 MHz, a digital Low Level RF (LLRF) feedback system coupled to the CTS control loop, a cold valve box and all cryogenic circuits (2K, 4K, coupler supercritical cooling loop).

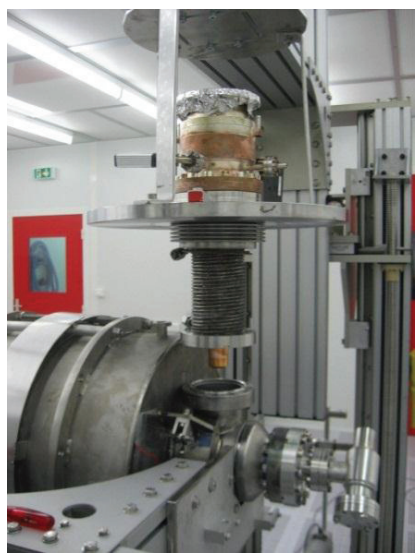


Figure 1: 5-cell SRF elliptical β=0.5 cavity being connected to its high-power RF power coupler in clean room.

*Work supported by the EURATOM FP7 MAX project (GA n°269565)
#biarrott@ipno.in2p3.fr

Copyright © 2014 CC-BY-3.0 and by the respective authors

THE MYRRHA SPOKE CRYOMODULE

H.Saugnac, J.L. Biarrotte, S. Blivet, P. Duchesne, N. Gandolfo, J. Lesrel, G. Olry, E. Rampnoux, D. Reynet, IPNO, Orsay, France

Abstract

In the framework of the MAX project, dedicated to the detailed study of the MYRRHA facility LINAC, the engineering study of the 'Spoke' cavities cryomodule, situated in the low energy superconducting section, has been achieved. The beam optics study, highly constrained by strong reliability requirements, leads to a modular cryomodule composed of two beta=0.37, 352 MHz, single bar 'Spoke' cavity cooled at 2K. The power coupler design, not studied in detail under the MAX project, is directly taken from a 20 kW continuous wave 352 MHz coupler designed and successfully tested in the framework of the previous EUROTRANS and EURISOL projects. The cold tuning system is identical to the one designed for the ESS 'Spoke' cavities. We present in this paper, the RF, the mechanical and the thermal design of the complete cryomodule as well as the optimization and simulations of its individual components (Cavity, Cryostat, Tuning System...).

INTRODUCTION

The proton superconducting LINAC for MYRRHA [1] (600 MeV, 5 mA) consists in 4 sections [2]. The low beta (0.37) section from ~17 MeV to ~100 MeV is comprised of cryomodules housing two single Spoke cavities cooled at 2K [6]. A beta = 0.47, from ~ 100 MeV to ~ 200 MeV, and a beta = 0.65 from ~ 200 MeV to ~ 600 MeV, sections are comprised of cryomodules housing 4 elliptical Cavities. The detailed study of the complete spoke cryomodule and its constituting components (Cavities, Cold Tuning System, Power Coupler, Cryostat...), achieved in the framework of the European MAX [3] project is described below.

SPOKE CAVITY DESIGN

Two Spoke cavities designed for the MYRRHA Cryomodule are currently under manufacturing. We describe below the studies done for the RF and mechanical optimizations.

RF Design

The RF design [7] was conducted taking into account the feedback experience on the manufacture and the tests results of two spoke cavities designed at IPNO. The main manufacturing issue concerns the spoke-bar geometry.

In a first single spoke cavity prototype a cylindrical shape at the magnetic field area was chosen to simplify the manufacture. It leads to high peak magnetic field not acceptable for the specifications for the MHYRRA LINAC. On a second triple spoke prototype a racetrack shape at the spoke bar cavity body connection leading to good theoretical RF parameters was manufactured. The 3D welding for this connection is difficult to manage and because of a lack of experience for this kind of manufacturing we conservatively avoid to choose this solution for the MAX Spoke Design.

A conical shape at the spoke bar/cavity body connection was chosen. It leads to acceptable RF parameters according to the MAX specifications and reduce the manufacturing difficulties. At the E field area (cavity central part) a racetrack shape giving good theoretical RF performances and easy to manufacture is chosen.

The electro-magnetic optimization leads, keeping Beta = 0.37 and the frequency of the first TM_{010} at 352 MHz, to minimize the peak surface electric field over accelerating gradient ratio (E_{pk}/E_{acc}) and the peak surface magnetic field over the accelerating gradient ratio (B_{pk}/E_{acc}). The goal is E_{pk}/E_{acc} < 4.4 and B_{pk}/E_{acc} (mT/MV/m) < 8.3. The accelerating gradient values for the Spoke section of MHYRRA are $E_{acc\ max\ nominal}$ = 6.2 MV/m for nominal operation and $E_{acc\ max\ fault\ tolerance}$ = 8.2 MV/m when the cavity is used in fault recovery mode [4]. It leads to a maximal surface magnetic field of 68 mT, and a maximal surface electrical field of 36 MV, which for spoke cavities, gives a sufficient margin and fulfill the reliability constrains of the MHYRRA accelerator.

Table 1: RF Parameters

Parameters	Value
Optimal beta	0.37
Vo.T [MV/m] @ 1 Joule & optimal beta	0.693
E_{pk}/E_{acc}	4.29
B_{pk}/E_{acc} [mT/MV/m]	7.32
G [Ohm]	109
r/Q [Ohm]	217
Q_o @ 2K for R_{res}=20 nΩ	$5.2\ 10^9$
P_{cav} for Q_o=$2\ 10^9$ & 6.4 MV/m [W]	9.35
L_{acc}= beta $_{optimal}$. c . f [m]	0.315m

The Electro-Magnetic design was performed using the 'CST Micro Wave Studio 2012' numerical code (see Table 1). A quarter of the cavity was simulated using border conditions on the magnetic planes with tetrahedral mesh elements (10 000 Tetrahedrons were used). Only the first mode (TM010) was calculated for the optimization that was performed by playing on a dozen of geometrical parameters.

Copyright © 2014 CC-BY-3.0 and by the respective authors

ISBN 978-3-95450-142-7

DESIGN AND ANALYSIS OF SLOW TUNER IN THE SUPERCONDUCTING CAVITY OF RISP*

Myung Ook Hyun, Hoe Chun Jung, Hyung Jin Kim
Rare Isotope Science Project (RISP), Institute of Basic Science (IBS), Daejeon, Korea

Abstract

Superconducting cavity is one of the most complex systems from the view of mechanical engineering, which is installed and operated in the superconducting linear accelerator. In order to operate SC cavity properly and precisely, superconducting cavity needs many sub-systems, including power coupler for applying RF power inside cavity, and liquid helium jacket for cooling cavity until reaching to the superconducting conditions. And, also cavity needs frequency tuning system for adjusting operating frequency when RF frequency of cavity is changed with outer disturbances such as liquid helium fluctuation, mechanical deformation due to vacuum condition of cavity. Generally, this tuning system is called as a tuner. There are two types of tuner, one is slow tuner which operates with motor, and the other is fast tuner which operates with piezo-electric actuator. This paper describes about design process and analysis results about slow tuner.

DESIGN OBJECTIVES

For tuning superconducting cavities, a tuner should generate high force and operate with proper speed. To decide specification of slow tuner, first we setup our tuning target as quarter wave resonator (QWR) type cavity. Next, we consider other tuner's specification for operation conditions of our slow tuner [1]. Table 1 shows the specifications of other research group's tuner [2].

Table 1: Specification of Other Tuners

	CEBAF Upgrade	RIA 0.47	SNS 0.61	TESLA 500
Cavity Frequency (MHz)	1497	805	805	1300
Lorentz Detuning (Hz)	324	1600	470	434
Coarse Range (kHz)	±400	950	±245	±220
Tuning Method	Tension	N/A	Comp.	Tension Comp.

QWR cavity's resonant frequency is 81.25 MHz, comparably lower than other cavities. Therefore, we can setup our target as similar as above specification, because these are higher specification thus we surely can control our cavity with high specification, if we can make our slow tuner satisfying above specification. Consequently, we setup coarse tuning rage as ±100 kHz, and tuning method as compression only due to its easiness and robustness as well.

CONCEPT DESIGN

At the design stage, we first decided some design constraints with cavity designers. Cavity designers want to operate slow tuner along the beam direction, not to other position, because adjusting cavity's inner gap is the most efficient than others. Figure 1 shows concept design of slow tuner for QWR cavity.

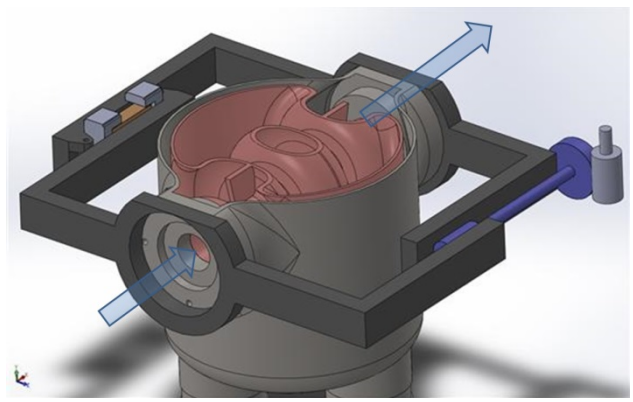


Figure 1: Layout of Slow Tuner for QWR Cavity.

Blue arrow represents the beam direction, and black structure is slow tuner. Right side of slow tuner is worm-worm wheel components which reduce operating speed and increase transferred force. Red structure is cavity and gray structure is liquid helium jacket. From cavity and liquid helium jacket design, cavity's beam port flange is connected with jacket body so that pulling or pushing beam port flange is most effective for tuning resonant frequency of cavity.

There are many tuning mechanisms in other tuners, like simple lever [3], complex lever [4, 5], or compliant mechanism [6]. Through many considerations, we decided to use lever mechanism because it is very easy to operate.

Copyright © 2014 CC-BY-3.0 and by the respective authors

ISBN 978-3-95450-142-7

SURFACE TREATMENT FACILITIES FOR SCRF CAVITIES AT RISP

J. Joo#, D. Jeon, M. J. Joung, Y. Jung, H. J. Kim, M. Lee, IBS, Daejeon, Korea

Abstract

Rare isotope science project (RISP) is engaged in the fabrication of four types of superconducting RF cavities. The surface treatment is one of the important processes of superconducting RF cavity fabrication. New superconducting RF cavity processing systems have been designed and developed for the etching of niobium in buffered chemical polish at RISP. The safety precautions used in protecting the operator from the acids used in the etchant and from the fumes given of during the process are discussed. All of the new hardware will be located in RISP Munji superconducting cavity test facility.

INTRODUCTION

The heavy-ion Accelerator complex, RAON, has been constructing in Daejeon, Korea [1]. Four different types of superconducting niobium cavities for RAON have been developed: Quarter Wave Resonator (QWR), Half Wave Resonator (HWR), Single Spoke Resonator 1 (SSR1) and Single Spoke Resonator 2 (SSR2). The cleanliness of the inner surface of cavities is an essential condition for the successful performance [2]. In the preparation of superconducting niobium cavities for testing at cryogenic temperature, surface damage and contamination caused by mechanical deformation are must removed by chemical etching. This is followed by a high pressure water rinse (HPWR) of the inside of the cavity to remove any chemical stain or niobium salts that remain following the chemical etching. After the HPWR the cavity is dried in a class 100 cleanroom to keep the cavity is particulate free prior to attachment of vacuum components and RF test probes. In addition, following a particularly aggressive chemical etching commonly referred to as buffered chemical polishing (BCP), where 100-150 μm of material is removed, the cavity is baked at 600-1200 °C in a high vacuum furnace for hydrogen degasing from the bulk niobium.

FACILITY DESCRIPTION

RISP Munji superconducting cavity test facility contains chemical processing room, ultrasonic cleaning, wet cleanroom for HPWR and heat treatment room for high vacuum furnace. Each specific area to be mentioned below has its own purposed, optimum size and class. Chemical processing room has 9 x 8 m^2 and is set a class 1000 cleanroom. Ultrasonic cleaning area has 5 x 3 m^2 and is set a class 1000 cleanroom. HPWR area has 3 x 3 m^2 and is set a class 100 cleanroom. Heat treatment room has 14 x 10 m^2 and is set a class 1000 cleanroom. DI water supply system is also installed inside cavity process area. The layout of surface treatment area in RISP Munji superconducting cavity test facility is shown in Figure 1.

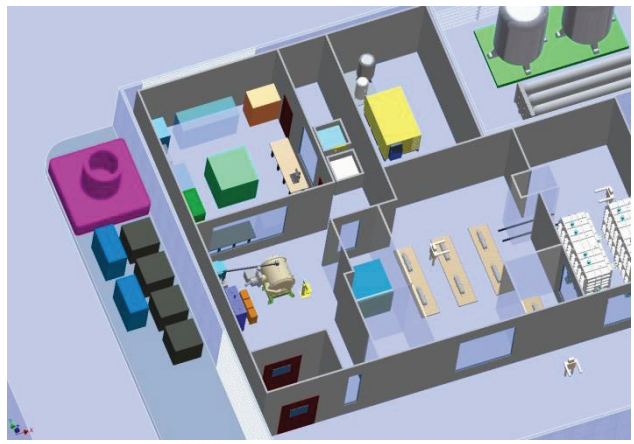


Figure 1: 3-dimensional view of the surface treatment facilities

BCP Cabinet

Chemical etching is accepted worldwide as a method to remove mechanically damaged and contaminated surface from superconducting cavities. There are two major approaches to chemical etching used for superconducting cavity production: BCP [3] and electrochemical polishing (EP) [4].

In RISP, BCP is chosen as a chemical treatment because BCP has been widely understood. Mixture of 1 part HF (49%), 1 part HNO_3 (69%) and 2 parts H_3PO_4 (85%) are used in BCP. The BCP cabinet is currently under construction. The BCP cabinet, manufactured by VITZRO TECH, is designed to accommodate a cavity that is 1000mm long, 250mm in diameter. The BCP cabinet, shown in Figure 2, is designed with safety as a first consideration [5]. The chemical storage tank can hold 100 liters of acid.

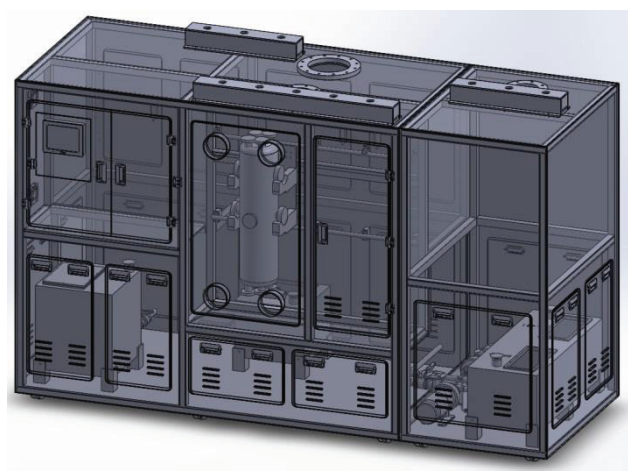


Figure 2: Perspective view of BCP cabinet for RISP cavities

#joojd@ibs.re.kr

ISBN 978-3-95450-142-7

Copyright © 2014 CC-BY-3.0 and by the respective authors

RAON CRYOMODULE DESIGN FOR QWR, HWR, SSR1 AND SSR2*

Woo Kang Kim#, Heetae Kim, Min Ki Lee, Young Kwon Kim, Gunn-Tae Park and Hyung Jin Kim

Rare Isotope Science Project, Institute for Basic Science, Daejeon 305-811, Republic of Korea

Abstract

The accelerator called RAON which will be built in Korea has four kinds of superconducting cavities such as QWR, HWR, SSR1 and SSR2, operating at 2 K and 4.5 K. The current status of design for the QWR, HWR, SSR1 and SSR2 cryomodules are reported. The issues included in the paper are thermal and structural design results of the components such as support and thermal shield in the cryomodules. The cryomodule hosts the superconducting cavities in high vacuum and thermally insulated environment in order to maintain the operating temperature of superconducting cavities. It also keeps the cavities in a good alignment to the beam line. It has an interface for supplying RF power to cavities between cold and warm components. The whole configuration of the integrated system is also presented. This paper presents the detailed design of the cryomodule.

INTRODUCTION

The superconducting driver linac accelerates the beam up to 200 MeV/u [1]. The driver linac hosts low energy superconducting linac (SCL1) and high energy superconducting linac (SCL2). The SCL1 accelerates beam up to 18 MeV/u. The SCL1 uses the two different cryomodules such as QWR and HWR which have superconducting cavity. The SCL2 has SSR1 and SSR2 cryomodule, which accelerates beam up to 200 MeV/u

In this report, we show the cryomodule design for QWR, HWR, SSR1, and SSR2. The deformation simulation for SSR1 and SSR2 is performed.

CRYOMODULE DESIGN

The parameters and requirement for the superconducting driver linac are shown in Table 1. Table 1 summarizes the design parameter of cryomodules. In order to construct SCL1 and SCL2, we need to make 22 QWR, 13 HWR1, 19 HWR2, 23 SSR1, and 23 SSR2. The drive frequencies for cavity in QWR, HWR, and SSR are 81.25 MHz, 162.5 MHz, and 325 MHz, respectively. Fig. 1 represents the components of SSR2 cryomodule. The SSR2 cryomodule consists of vacuum chamber, magnetic shield, thermal shield, cryogenic pipe lines, and support. The cryogenic pipe lines are located inside of the thermal shield. The thermal shield is installed inside of magnetic shield. The magnetic shield is installed in the vacuum chamber.

Table 1: Design parameters of cryomodules

Note	No	Frequency
QWR	22	81.25 MHz
HWR1	13	162.5 MHz
HWR2	19	162.5 MHz
SSR1	23	325 MHz
SSR2	23	325 MHz

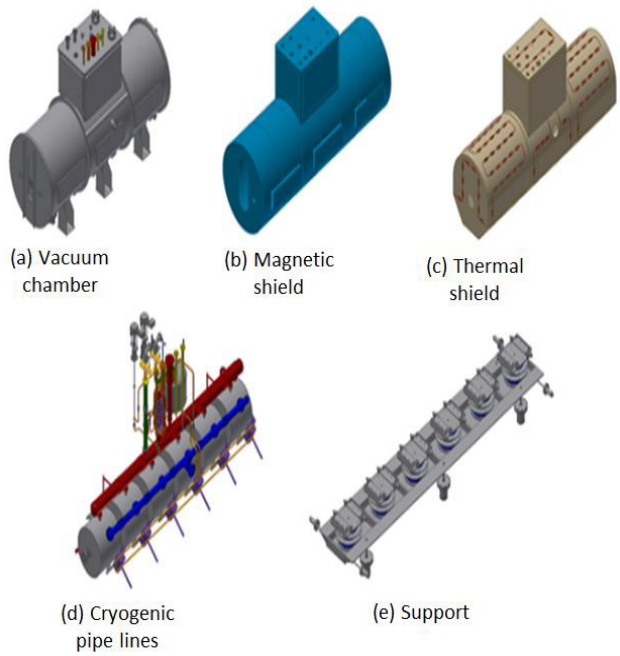


Figure 1: Components of SSR2 cryomodule

Thermal Shields

In order to reduce the radiation heat from room temperature to the 2 K cold mass, the copper thermal shields cooled by liquid helium are adopted between the cold mass assembly and the vacuum chamber. The thickness of the shields is 3 mm. The shields comprise two end plates and two side plates with liquid helium cooling pipe soldered onto them. The shields are designed to assemble and disassemble easily for the purpose of changing the cavities.

*Work supported by the Rare Isotope Science Project of Institute for Basic Science funded by the Ministry of Science, ICT and Future Planning (MSIP) and the National Research Foundation (NRF) of the Republic of Korea under Contract 2013M7A1A1075764.

kwko11045@ibs.re.kr

Copyright © 2014 CC-BY-3.0 and by the respective authors

RAON SUPERCONDUCTING RADIO FREQUENCY TEST FACILITY CONSTRUCTION*

Heetae Kim#, Yoochul Jung, Jaehee Shin, Seon A Kim, Woo Kang Kim, Gunn-Tae Park, Sangjin Lee, Young Woo Jo, Shinwoo Nam, and Dong-O Jeon

Rare Isotope Science Project, Institute for Basic Science, Daejeon 305-811, Republic of Korea

Abstract

Superconducting Radio Frequency (SRF) test facility for RAON is under construction process. It consists of cryogenic system, clean room for cavity process and assembles vertical test, horizontal test, and the radiation shield. The cryoplant has 330 W (4.5 K equivalent) which supplies 4.5K supercritical helium to the cavity test and cryomodule test bench. Clean rooms are for cavity process and assemble whose class is from 10 to 10000. The layout for the vertical and horizontal test bench is shown and the radiation shield for the test bench is shown to reduce X-ray coming from cavity. To estimate the thickness of concrete, radiation simulation is performed.

INTRODUCTION

Properties of superfluid fog were studied [1-3]. Size effect of thermal radiation [4, 5] and the effective temperature for non-uniform temperature distribution were investigated [6, 7]. Thermal analysis was studied for cryogenic system design [8]. To accomplish Rare Isotope Science Project, the construction of superconducting radio frequency test facility is important.

In this report, we show schematic design of Superconducting Radio Frequency (SRF) test facility, which includes cryoplant, clean room for cavity process and assembles, vertical test bench, horizontal test bench, and radiation shield to protect X-ray coming from the test.

SRF TEST FACILITY

Superconducting Radio Frequency (SRF) test facility for RAON is under construction process. The SRF test facility consists of cryogenic system, clean room for cavity process and assembles vertical test bench, and horizontal test bench. Fig. 1 shows the layout of SRF test facility. The remodelling area for the facility is 1482 m^2 and most of utilities such as air compressor, process cooling water, deionized (DI) water system, and transformer will be reused. The total electric power to run the facility is about 2500 kW. Clean room includes buffered chemical polishing (BCP), high pressure rinsing (HPR), high vacuum furnace, cavity assemble place, etc. Cryogenic system consists of cold box, dewar, compressors, pumps, oil removal system, distribution line, etc. The power of cryoplant is 330 W (4.5 K equivalent), which supplies 4.5 K supercritical helium to cavity and cryomodule test bench. The supercritical helium of 4.5 K is supplied to cryostat, and the cavity test can be performed at 2 K while the liquid helium is being pumped to cool down.

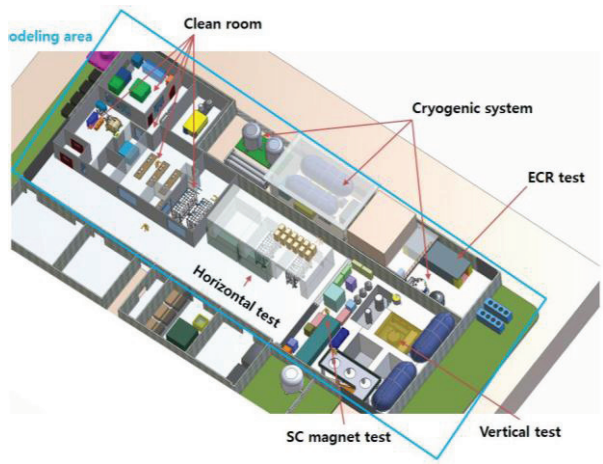


Figure 1: Layout of SRF test facility.

Cryogenic System

Fig.1 shows the layout for cryogenic system. Cryogenic system consists of cold box, liquid helium dewar, compressors, pumps, oil removal system, distribution line, and helium gas bag. Two cryoplants having 330 W and 200 W are used in order to supply liquid helium for

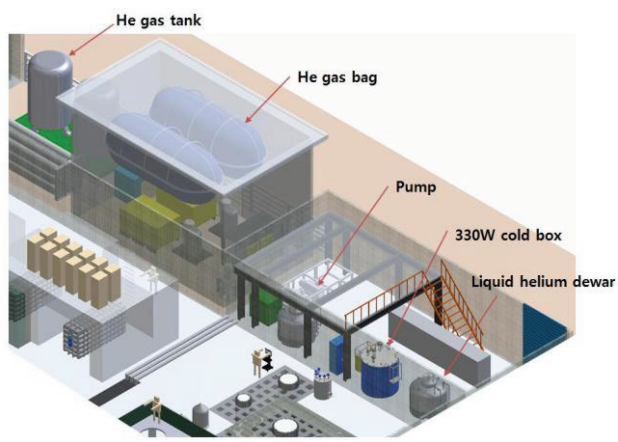


Figure 2: Layout for cryogenic system.

*Work supported by the Rare Isotope Science Project of Institute for Basic Science funded by the Ministry of Science, ICT and Future Planning (MSIP) and the National Research Foundation (NRF) of the Republic of Korea under Contract 2013M7A1A1075764.
kimht7@ibs.re.kr

ISBN 978-3-95450-142-7

Copyright © 2014 CC-BY-3.0 and by the respective authors

THE FABRICATION OF THE $\beta = 0.12$ HWR AT RISP

G.T. Park*, H. Kim, W.K. Kim, Y. Jung and H.J. Cha
Rare Isotope Science Project (RISP), Daejeon, Korea

Abstract

The fabrication of the $\beta = 0.12$ half wave resonator (HWR) at RISP is complete. In this paper, we describe the fabrication process in detail: the material inspection, forming, machining, buffered chemical polishing (BCP) for the parts, the electron beam welding (EBW), and the clamp-up test followed by the final welding.

INTRODUCTION

At RISP, a driver linac contains a SCL1-2 section consisting of the HWR's that accelerates the low-medium velocity ions. Earlier study on the beam dynamics determined the operation condition of the HWR as $\beta = 0.12, f = 162.5$ MHz with the accelerating voltage $V_{acc} \sim 1.2$ MV.

In this paper, we report our progress on the fabrication of the HWR. The fabrication is complete now and the cavity is waiting to be processed and vertically tested. The vertical test can verify the performance of the cavity and also show some characteristic anomalies, i.e., the severe reduction of the Q_0 value leading mostly to the quench at the lower gradient than targeted. The causes for the quenches most likely trace back to the imperfections during the fabrication process. For example, a poor welding in the strong current region of the cavity reduces the *RRR* value causing the early quench through the thermal instability. A failure to do vacuum furnacing is well known to cause the hydrogen Q-disease. These all trace back to the contamination of the RF surface. Thus it is utmost importance to maintain the defect-free RF surface within skin depth of about 50 nm. The important fabrication processes are summarized in Fig. 1.

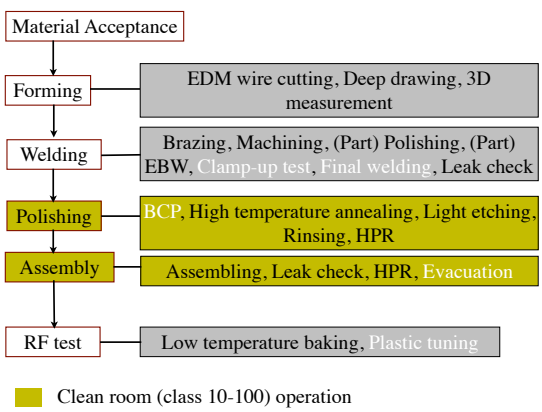


Figure 1: The fabrication process.

MATERIAL INSPECTION

The 3 mm niobium sheet is purchased from Wah-Chang Inc. Its important material properties are summarized in Table 1. The high *RRR* is crucial to deter the quench by

Table 1: The Material Properties of the Niobium Obtained

Material properties	Value
RRR value	>300
Grain size	<4 ATM
Recrystallization	100%

delivering the heat to the helium with the high thermal conductivity λ, which in turn comes from high *RRR* value, with the relation given as

$$\lambda(T = 4\,\mathrm{K}) = \frac{RRR}{4}. \quad (1)$$

The grains must be small and uniform in size for a high formability. In addition, to spot the rust the de-ionized water dipping test is done for 24 hours (Fig. 2).



(a) The DI water dipping test (b) The rust

Figure 2: The DI water dipping test.

FORMING

The niobium sheets were cut by the EDM wire cutting and deep drawn to form the parts. The niobium has very good formability and ductility with little spring back and does not work harden. The parts were pressed while controlling the pressure, velocity and hold time of the punch to avoid the tears or wrinkles (Fig. 3).

NIOBIUM TO STAINLESS STEEL BRAZE TRANSITION

The helium vessel was designed to be stainless steel L316 (non-magnetized after the welding) with the thickness of 3 mm and encloses the 10 mm outside the bare cavity. Since the stainless thermally contracts more than the niobium in cool down, it could deform the cavity. So we introduced the bellows to the coupling ports at the upper and lower toroids

* gunnpark@ibs.re.kr

Copyright © 2014 CC-BY-3.0 and by the respective authors

ISBN 978-3-95450-142-7

TUNING AND FIELD STABILIZATION OF THE CERN LINAC4 DRIFT TUBE LINAC

M.R. Khalvati*, CERN, Geneva, Switzerland and IPM, Tehran, Iran
S. Ramberger, CERN, Geneva, Switzerland

Abstract

The Drift Tube Linac (DTL) for the new linear accelerator Linac4 at CERN will accelerate H^--beams of up to 40 mA average pulse current from 3 to 50 MeV. The structure consists of three cavities. The first cavity (Tank1) is a 3.9 m long tank containing 38 drift tubes, 10 fixed tuners, 2 movable tuners and 12 post-couplers, operating at a frequency of 352.2 MHz and an average accelerating field of 3.1 MV/m. This paper reports on the results and procedures used for the low–power tuning, stabilization and power coupler tuning carried out on the first Linac4 DTL tank. The upgrade of the bead pull measurement system and twists to the well-known tilt sensitivity technique are discussed.

INTRODUCTION

The low power RF tuning and field stabilization of Tank1 of the Linac4 DTL has been accomplished. Considerable improvements on the precision of the electric field measurement system have been undertaken as errors could affect tuning and stabilization. In the present work the peak field method is used to extract the average axial electric field E_0 [1]. This method allows reducing the relative standard deviation down to 0.25% in our measurement setup, compared to typically 1..2% in the traditional direct integration method. In an analytical approach the initial set of tuner lengths has been found, bringing fields and frequency close to target. Small individual changes in tuner length lead to the desired field flatness of around ±1.3%. Post-couplers (PCs) are used to stabilize the fields inside the structure. The PC lengths are found by minimizing the tilt sensitivity (TS) slope. The paper reports a modification of the traditional procedure of TS measurements which overcomes a deliberate limitation in the mechanical options for applying a perturbation [1]. By simulation, a good agreement between these two approaches has been found. The TS slope has been reduced 28-fold using PCs.

BEAD PULL MEASUREMENT

The purpose of tuning of the Linac4 DTL cavity is to reach the operating frequency with uniform average electric field in all accelerating cells. Beam dynamics simulation show that the maximum acceptable error in average accelerating field between cells is ±2% [2]. The measurement system thus needs to achieve an accuracy that is a good factor better than that. In this work, the well-established bead pull measurement technique is employed for measuring the axial electric field along the structure [3].

In the current setup, a metallic bead of 6 mm length and 0.8 mm diameter on a thin plastic wire traveling at constant speed along the cavity axis causes a frequency perturbation that can be quantified according to the Slater perturbation theorem as

$$\frac{\Delta f}{f} = \frac{\Delta W_m - \Delta W_e}{U} \tag{1}$$

where ΔW_m and ΔW_e are the changes in the stored magnetic and electric energies respectively and U is the total stored energy.

The wire tension is adjusted such that the effect of wire sag on measurements gets less than 0.1%. Instead of a direct measurement of the variation of the resonance frequency, the phase shift is sampled every 0.002 ms at a constant excitation frequency f_0 and the phase shift is converted to frequency shift using

$$\frac{\Delta f}{f_0} = \frac{tan(\Delta\varphi(f_0))}{2Q} \tag{2}$$

where Q is the loaded quality factor [4]. The average axial electric field E_{0i} for the i^{th} cell can be calculated by direct integration over the localized electric field distribution $E(z)$.

More accurate values E_{0i} can be obtained by comparing measurements with SUPERFISH simulations using the peak field method [1]. The change in stored energy due to the bead located at the field maximum and the field integral are found in single cell SUPERFISH simulations from the electric field along the axis of the cavity. The peak field coeffient for the bead located at the centre of the i^{th} cell gap is defined as

$$pfc_i = \frac{1}{E_{0i}^2 L_i^2} \int_{z-l/2}^{z+l/2} E(z)^2 dz \Big|_{z=\text{gap center}} \tag{3}$$

where l is the bead length.

The values pfc_i are insensitive to any variation in cavity shape outside the gap area. The measured average axial field is $E_{0m}^i \propto (\Delta\varphi_m^i / pfc_i)^{0.5}/L_i$ Where $\Delta\varphi_m^i$ is the measured maximum phase-shift, and L_i the lengths of the i^{th} cell. Finally, the measured E_{0i} are normalized to 1. The peak field method has further advantages compared to direct integration. First, the effect of the bead length is taken into account intrinsically. Secondly, wire slippage that is difficult to tackle does not particularly affect measurements. Wire slippage usually causes sudden bead movements by few steps – usually less than 4 steps in our setup – which ,when uncompensated, leads to a reduction in the measurement accuracy in direct integration. In our bead pull measurement setup, the reproducibility has been determined to be around ±1.5% for direct integration compared to ±0.25% for the peak field method.

* khalvati@ipm.ir

ISBN 978-3-95450-142-7

Copyright © 2014 CC-BY-3.0 and by the respective authors

SPATIALLY PERIODIC RF QUADRUPOLE LINAC

A.A. Kolomiets *, A.S. Plastun #, ITEP, Moscow, Russia

Abstract

Spatially-periodic RF quadrupole structure is proposed as second section of front end of ion linac. It consists of conventional drift tubes and RF quadrupoles. Quadrupoles are 4-vane segments with nonzero electric potential on the longitudinal axis. Thus the accelerating electric field is formed between drift tubes and RF quadrupoles. Moreover accelerating field can be provided even inside the RF quadrupoles. It allows building structures with different focusing lattices and provides high energy gain.

INTRODUCTION

Modern ion linacs have Radio Frequency Quadrupole structures (RFQ) for initial beam formation and acceleration to energy of several MeV. Drift Tube Linac (DTL) with magnetic quadrupole focusing is the most common solution for following acceleration. This scheme allows us to design effective front ends for high energy linacs and linacs with of several MeV for medical or industrial applications as well.

Several accelerating structures with drift tubes and RF focusing have been proposed to build compact, efficient and inexpensive ion linacs in this energy range. They are well known as spatially periodic structures with RF quadrupoles [1, 2]. In spite of inherent merits of these structures and their successful operation over the years, they are not widespread. This can be explained by complexity of their mechanical design, complicated RF design and tuning, more complicated beam dynamics design due to stronger coupling of transversal beam motion with longitudinal one comparing with conventional DTL structures.

This paper presents simple and flexible realization of spatially periodic RF quadrupole focusing structure with considerably reduced disadvantages mentioned above.

FOCUSING LATTICE

Energy gain of a conventional RFQ is limited by transverse motion of particles defined by vane geometry and inter-vane voltage due to limited maximum field at vane surface. Voltage increase leads to reducing of focusing strength and vice verse. Spatial period of focusing structure have to be enlarged to provide both good focusing strength and high energy gain of linac with RF quadrupole focusing [3]. One more realization of spatially periodic RF quadrupole structure proposed in the paper is shown in Figure1.

* kolomiets@itep.ru
# asplastun88@gmail.com

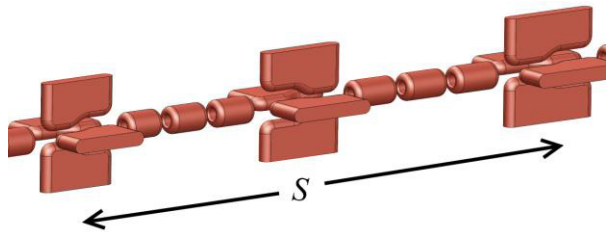


Figure 1: Spatially periodic RF quadrupole lattice.

The structure consists of 4-vane segments separated with a number of conventional drift tubes. The main difference of the structure from well known ones is different transversal displacements of vertical and horizontal vanes of RF quadrupole. It means that there is nonzero electric potential on the quadrupole axis that forms accelerating gap between quadrupole and drift tubes.

Unlike known spatially periodic structures with quadrupoles integrated into the accelerating period the proposed structure provides more freedom of choice for quadrupole length. In case when quadrupole is longer than accelerating period it is possible to form accelerating gap inside RF quadrupole varying displacements of vanes along the quadrupole as it is shown in Fig.1.

If all vertical quadrupole electrodes have the same potential sign the alternating focusing can be provided for focusing period length $S = N\,\beta_z\lambda$, $N = 1, 3, 5, \ldots$, $\beta_z = v_z/c$ – normalized velocity of ion beam, λ – wavelength of RF field. Case $N = 1$ and RF quadrupole length $L = \beta_z\lambda/2$ corresponds to spatially homogeneous RFQ. Other cases present variations of spatially periodic focusing structures. General properties of these structures are considered in smooth approximation in this paper.

Smooth Approximation

Phase advance μ of particle transverse motion per focusing period of a structure with RF focusing depends on phase of RF field φ when particle is in the center of quadrupole, i.e. $\mu = \mu(\varphi)$. Table 1 shows some possible focusing lattices without taking RF defocusing effect into account. The relation $\mu(\varphi)$ can be approximated as:

$$\mu = \mu_0 + \Delta\mu\cos 2\varphi, \qquad (1)$$

here μ_0 and $\Delta\mu$ are mean and spreading values of phase advance μ during RF period (see Fig.2). Analysis of transverse motion using smooth approximation has shown that:

- Focusing gradient G decreases with N for a given value of transverse phase advance or μ_0 increases with N for a given gradient G,

Copyright © 2014 CC-BY-3.0 and by the respective authors

3 BPM STUDY AT PAL ITF

M. Znidarcic, Instrumentation Technologies, Solkan, Slovenia
Changbum Kim, So-Jeong Lee, PAL, Pohang, Kyungbuk, Korea

Abstract

Pohang Accelerator Laboratory (PAL) is building the 4th generation X-ray free electron laser (XFEL) machine. To examine the efficiency of various diagnostic devices an injector test facility (ITF) was constructed. The last part of the ITF is dedicated for evaluation of beam position measurement devices. A "3-BPM-study" was done with 3 Libera Single Pass E BPM modules that were connected to the 3 equidistantly positioned stripline sensors. The aim of the test was to measure the performances of the Libera Single Pass E devices with beam conditions similar to the real pal XFEL machine.

INTRODUCTION

The Pohang Accelerator Laboratory X-ray Free-Electron Laser (PAL-XFEL) project started in 2011. The final machine will consist of a 10-GeV electron linac based on S-band normal conducting accelerating structures and five undulator beamlines. The goal of the project is the production of 0.1 nm coherent X-ray laser to photon beam users.

An injector test facility (ITF) for the Pohang Accelerator Laboratory X-ray free electron laser has been constructed to demonstrate the performance of sub-systems far in advance of the PAL-XFEL construction. One of the subsystems is also a BPM system with feed-forward calculation and magnet control capability.

In February 2014 extensive testing was carried out at the PAL ITF facility. Three Libera Single Pass E BPMs (Electron Beam Position Processors) were efficiently implemented in a PAL ITF control system and connected to three dedicated stripline sensors. Extensive two day testing session followed.

LIBERA SINGLE PASS E

Libera Single Pass E (see Fig. 1) system is based on uTCA modular technologies with IPMI platform management. The system is therefore developed on multiple AMC modules, with each module covering different functionalities [1].



Figure 1: Libera Single Pass E front panel.

On the top layer, Libera Single Pass E provides the MCI with a development package and Command Line utilities for open interaction in different control systems. This interface was developed to facilitate the integration of Libera Single Pass E into the accelerator's control system software. On top of the MCI, various adaptors to different control systems can be implemented (EPICS, Tango, etc.).

Data Processing

The data processing is initiated by the external event signal. The short signal from the detector is first shaped by the analog front-end filtering, designed in relation to the accelerator parameters.

Through the configuration of various software parameters, Libera Single Pass E offers processing of various beam types (flavors). After the hardware trigger signal which announces the arrival of the bunch, the search of the bunch signal is started. The bunch signal is detected in comparison with the threshold parameter, then a useful part of the signal is defined with the pre-trigger and post-trigger parameters. The sum of the pre-trigger and post-trigger defines the processing window. The signal energy is calculated from the signal as defined by the processing window. After calculating the four signal amplitudes – Va, Vb, Vc and Vd – the beam position is calculated using formulas for X and Y. Four options can be used for position calculation:

- Diagonal pickup orientation – Linear formula
- Diagonal pickup orientation – Polynomial formula (3rd order)
- Orthogonal pickup orientation – Linear formula
- Orthogonal pickup orientation – Polynomial formula (3rd order):

Typical Measuring Performances

Measurement performance mostly depends on the Libera front-end configuration [2]. Its parameters are set in accordance with other accelerator parameters. The standard type of Libera Single Pass E, used during the testing session at PAL ITF, implements 500 MHz SAW filters with 10 MHz bandwidth. At operational beam charges, the position measurement resolution is close to 1 μm for a single-bunch beam structure (see Fig. 2).

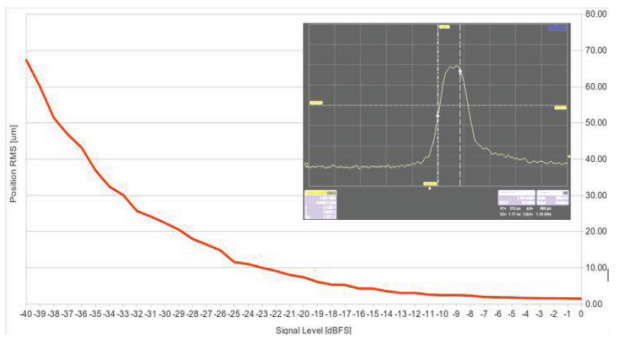


Figure 2: Measurement performance versus input signal level (0 dBFS = 5 V peak).

Copyright © 2014 CC-BY-3.0 and by the respective authors

ISBN 978-3-95450-142-7

DEVELOPMENT AND OPERATIONAL ASPECTS OF Nb QWR BASED HEAVY ION LINAC SYSTEM AT IUAC DELHI

S.Ghosh, B.K.Sahu, A.Rai, P.Patra, A.Pandey, J.Karmakar, G.K.Chaudhari, D.S.Mathuria, R.N.Dutt, B. Karmakar, S.S.K.Sonti, K.K.Mistri, R.Kumar, S.K.Suman, R.Joshi, A.Sarkar, J.Chacko, A.Chowdhary, S.Kar, S.Babu, M.Kumar, J.Antony, R.Ahuja, J.Sacharias, P.N.Prakash, T.S.Datta, and D.Kanjilal
Inter University Accelerator Centre (IUAC), Aruna Asaf Ali Marg, New Delhi, India
A. Roy, Variable Energy Cyclotron Center, Kolkata, India

Abstract

The superconducting linac of IUAC consists of five cryostats containing 27 niobium quarter wave resonators. Since last few years, energized ion beams from linac are being delivered routinely for scheduled experiments. In a recently concluded linac operation, all the resonators installed in the five cryostats were used in the acceleration and delivery of the ion beam on the target with an energy gain of 8 MeV/q and a time width of ~ 180 ps. Recently, an improved mechanical damping mechanism has been implemented and piezo actuator based tuning mechanism have replaced the gas based tuner of most of the resonators. Other new developments e.g. automatic phase locking of the resonators and auto beam tuning of the complete linac are being currently pursued.

INTRODUCTION

The project of superconducting (SC) linac of Inter University Accelerator Centre (IUAC) started in collaboration with Argonne National Laboratory (ANL) and first twelve quarter wave resonators (QWR) along with the prototype resonators were built at ANL [1]. Subsequently, the facilities to build SC QWR were developed at IUAC and the remaining resonators were fabricated in-house [2]. In figure 1, a schematic of the linac at IUAC is shown.

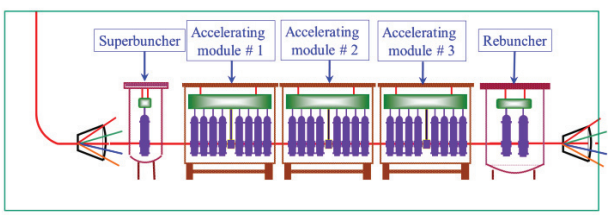


Figure 1: The schematic of SC linac of IUAC.

During the initial period of linac operation (2004-2007), multiple problems were faced. The major problems were to generate higher accelerating fields (≥ 4 MV/m) and to phase lock the resonators at those fields with nominal RF power (~100-120 W). Due to the large stored energy in our QWR and presence of ambient microphonics in the cryostat, the power requirement to lock the resonators at higher fields has gone up to ~300 W, which caused serious operational problems in the past [3]. To tackle these problems, the buffer volume of liquid Helium at the top of the resonators was increased [3], SS-balls were used as the vibrational damper [4], and the non-coaxiality of the central conductor with respect to the outer niobium cylinder was corrected. Recently, piezo actuator has been used as the mechanical tuner [5]. The piezo-tuner seems to be a marvellous tool not only to correct the slow frequency drift more efficiently than the existing gas based tuner but also to damp the vibration of the mechanical tuner bellows reducing a particular mode of microphonics. All the recent improvements along with the latest results during the last linac operation are presented in this paper.

REMAINING FEW HURDLES IN LINAC OPERATION

During the last linac operation, out of 22 accelerating QWRs, the number of resonators achieving accelerating fields (at 6 W helium power) above 4 MV/m, between 3-4 MV/m, between 2-3MV/m and < 2 MV/m are 3, 15, 2 and 2 respectively. To improve the accelerating fields of the resonators, conventional routine procedures are applied on them. The QWRs have undergone more number of electropolishing cycles than usually required, their RF surfaces are cleaned with 18MΩ-cm de-ionized water in an ultrasonic cleaner and they are subjected to couple of hours of helium conditioning in addition to RF pulse conditioning.

Since last few years, efforts are dedicated to bridge the gap between the electric field achieved during Q-measurement at 6 W of helium power and during phase locking [6] of the SC resonator. The major reason behind the inability to phase lock a SC resonator with ≤ 120 watts (up to 120 W was proved to be safe for our system in long term operation) is the requirement of large stored energy [0.11J/(MV/m)^2] and the presence of large amount of microphonic vibration coupled to the resonator. The vibration present in the cryostat ambience can contribute to different modes of vibration in the resonator, e.g. (a) the central conductor of the resonator can act as a pendulum and start vibrating at its own natural frequency of ~ 60 Hz, (b) the slow tuner bellows can vibrate at a frequency of ~ 30 Hz, (c) the thin sheet of all parts of the niobium resonator can vibrate at a frequency of a few Hz due to pressure fluctuation of liquid helium etc. In addition, some other higher order cryogenic excitation modes may also be

Copyright © 2014 CC-BY-3.0 and by the respective authors

THE COUPLERS FOR THE IFMIF-EVEDA RFQ HIGH POWER TEST STAND AT LNL: DESIGN, CONSTRUCTION AND OPERATION

Enrico Fagotti, Loris Antoniazzi, Mauro Giacchini, Francesco Grespan, Maurizio Montis, Antonio Palmieri, Andrea Pisent, Carlo Roncolato (INFN/LNL, Legnaro (PD))

Abstract

In order to assess the critical aspects of the IFMIF-EVEDA RFQ construction procedure and operation, it was decided to perform a High Power Test of a subset of the RFQ consisting in its last 550 mm three modules (out of 18) plus a Prototype Module, 390 mm long, used as RF plug. These modules are going to be tested at full power in CW of INFN LNL Labs, in the so-called RFQ High Power Test Stand. For such a purpose, a RF tube-based amplifier capable of 220 kW CW output power at the operational frequency of 175 MHz was purchased from an Italian company. A critical component of this test is the RF power coupler. Therefore INFN-LNL developed a design of two identical water-cooled loop antenna couplers, built with OFE copper and vacuum sealed with a commercially available 6"1/8 Alumina planar window. These couplers were tested separately on an aluminium coupling cavity. In particular one of them acts as a power feeder, while the other one, connected with a 200 kW water-cooled load, acts as a receiver. In this paper, the main aspects of the design, construction and tests performed on the couplers and coupling cavity will be described.

HIGH POWER COUPLER DESIGN AND CONSTRUCTION

The High Power Coupler is designed to be critically coupled with the 2 meter long RFQ, in conditions of minimum acceptable Q_0 value of Q_{0min}=9000 (ideal Q_0=15000)[1]. Moreover, it must be properly cooled in order to manage its RF losses induced by the high power feeding the RFQ (up to 220 kW) and travelling on the RF coaxial line. The design of the loop therefore has a coaxial inner radius R=20 mm, an insertion depth of 29 mm and a thickness of 8 mm. The coupling was verified both with analytical calculations and with HFSS simulations. Should the Quality Factor be higher, a rotating flange can accomplish a proper change of the coupling. The power dissipated in the loop is about 100 W for an input power of 200 kW. The coupler and RF window are two separate devices coupled with a standard 6-1/8 IEC coaxial interface. In particular, the Coupler material is copper OFHC, and the water heat exchange coefficient is maintained near 10000 W/m^{2}K on the whole heat exchange surface: water velocity is above 2.5 m/s both in the external and internal spiral and in the loop. The coupler inner connection is used to remove power from the RF window.

In Fig.1 the power density of the coupler is shown, for an input power of 200 kW. With this power density, thermo-structural simulations have shown that the temperature in the copper bulk does not exceed 45ºC, for a water flux of 15 l/min, and that all the thermal-induced stresses are far below from the safe engineering limits (70 MPa).

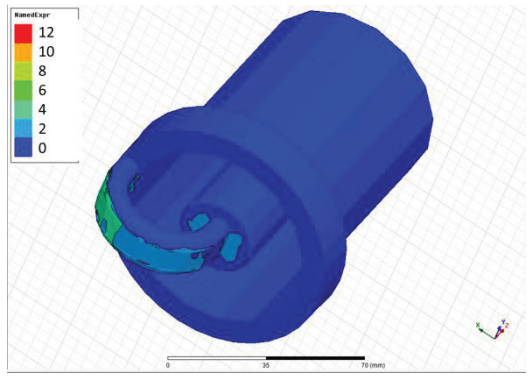


Figure 1: RF power density in the loop.

As far as the construction procedure is concerned, the coupler is made of OFE copper. Demineralized water cooling path is a double-spiral in the outer and inner conductors connected through double-channel in the loop (Fig.2).

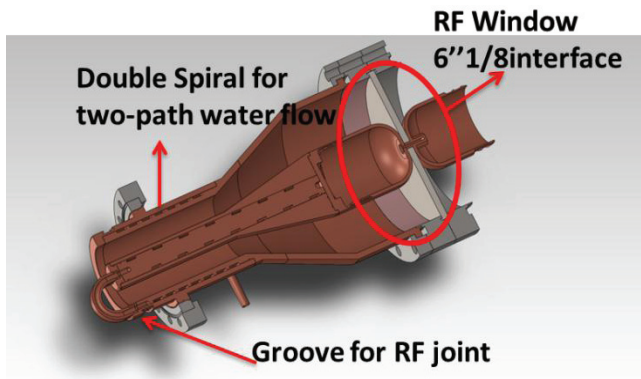


Figure 2: Coupler assembly in its final configuration.

The construction procedure foresees three brazing steps. In the first step, the cooling spirals are brazed separately on inner and outer conductors and also the SS flange seats and the water tubes are brazed on the copper bulk. In the second step, the plugs are brazed at both ends of the inner conductor and the outer conductor with cooling spiral is brazed with the tapered coaxial. Finally, in the third step the inner and outer conductors are brazed to the loop, and the assembly is completed. After both the first and the second brazing step, machining is required and brazing defects can be eventually recovered.

Copyright © 2014 CC-BY-3.0 and by the respective authors

ISBN 978-3-95450-142-7

RECENT PROGRESS OF BEAM COMMISSIONING AT J-PARC LINAC

T. Maruta*, K. Futatsukawa, Y. Liu, T. Miyao, KEK / J-PARC, Tokai, Japan
A. Miura, H. Sako, JAEA / J-PARC, Tokai, Japan
M. Ikegami, FRIB, East Lansing, MI 48824-1321, USA

Abstract

To recover the beam energy to the original design of 400 MeV, the J-PARC linac was conducted large upgrade in year 2013. The main upgrade is the installation of annular-ring coupled structure (ACS) cavities at SDTL downstream. The first beam commissioning after the upgrade was started at December 16, 2013. And then we successfully realized 400 MeV acceleration at January 17, 2014. The user operation had been stably operated from February 16 to the end of June with the peak current of 15, which is equivalent to the beam power of 300 kW at the extraction of 3 GeV Rapid Cycling Synchrotron (RCS). In this paper, we discuss the progress of beam commissioning.

INTRODUCTION

The J-PARC linac is comprised from a 50 keV negative hydrogen (H^-) ion source (IS), a 3 MeV Radio Frequency Quadrupole (RFQ), a 50 MeV Drift Tube Linac (DTL) and an 191 MeV Separate-type DTL (SDTL) and a 400 MeV Annular-ring coupled structure (ACS) as shown in Fig.1 [1]. The beam transport sections are placed from RFQ to DTL (MEBT1), from SDTL to ACS (MEBT2) and ACS to 3 GeV RCS (L3BT), respectively. The RF frequency is 324 MHz for RFQ to SDTL and threefold higher frequency of 972 MHz for ACS. In the beam commissioning of linac alone, three beam dumps are available. The 0 degree dump (0BD) is on the extended line of straight section, the 30 degree dump (30BD) line is branched in the middle of the 1st arc section and the 100 degree dump (100BD) locates in the middle of the 2nd arc section.

The construction of the J-PARC linac is separated to two stages. In the first stage, beam energy is 181 MeV by installing IS to SDTL in the beam line. SDTL is designed for the acceleration to 191 MeV. The last two cavities, however, are placed in L3BT to divert them into debuncher cavities. The operation of the J-PARC linac was started in 2008 at beam current of 5 mA. Since then, we continuously conducted the beam commissioning to improve the beam quality and to increase the beam power. The peak current of the user operation was finally achieve to 15 mA, which is equivalent to 300 kW at the extraction of 3 GeV RCS [2]. For the construction of the second stage, ACS had been developed in parallel with user operation. With a significant effort of the R&D and fabrication, ACS is successfully installed on the beam line in year 2013.

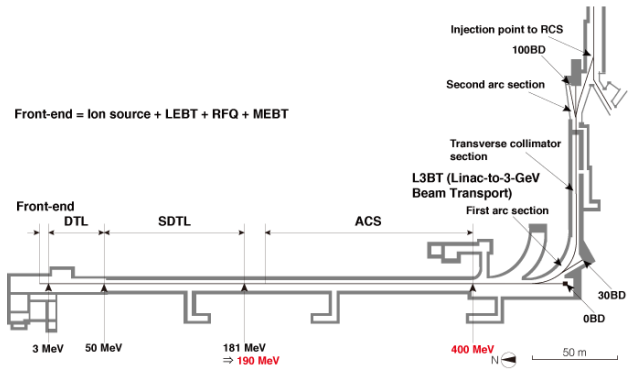


Figure 1: Outline of the J-PARC linac. In the initial stage, the linac had been operated at 181 MeV by the installation of IS to SDTL on the beam line as shown in black character. The ACS accelerator was installed at second stage to extend the beam energy to 400 MeV (red).

BEAM COMMISSIONING AFTER THE ACS INSTALLATION

The linac beam commissioning was started on December 16, 2013, and it continues till January 30, 2014. The main purpose of the beam commissioning is the establishment of 400 MeV acceleration, tuning of 15 mA beam for user operation and tuning of 25 mA beam for high power test.

Achievement of 400 MeV Acceleration

After the front-end (from the IS to MEBT1) tuning, we started the tuning of RF cavities. RF amplitude and driving phase for each cavity is determined by a phase scan method [3] one by one from upstream. The output beam energy from a cavity is calculated by time-of-flight method. We place phase detectors (FCTs) to measure the flight time. When a beam bunch passes thought the upstream (downstream) FCT at the phase of ϕ_1 (ϕ_s), the flight time in the phase coordinate system is calculated as

$$\Delta\phi = \phi_2 - \phi_1 + 360 \times n, \quad (1)$$

where n is number of turns and it is estimated from the distance of two FCTs. It is around 21 for the FCT pairs in SDTL, and around 17 for the paris in ACS. The phase scan is conducted with peak current of 5 mA. Because the output beam energy varies during a phase scan, the beam could be lost on the way to a beam dump due to the mismatch of transverse focusing power. In addition, an unexpected beam loss may occur in the upgraded ACS section. We choose 5 mA beam to minimize the beam loss even when such situation happens. It is the lowest peak current for the J-PARC linac to operate stably. The phase scan of DTL and

* tmaruta@post.j-parc.jp

Copyright © 2014 CC-BY-3.0 and by the respective authors

ISBN 978-3-95450-142-7

HIGH-POWER TEST RESULTS OF THE RFQ III IN J-PARC LINAC

T. Morishita#, Y. Kondo, T. Hori, S. Yamazaki, K. Hasegawa, K. Hirano,
H. Oguri, JAEA, Ibaraki-ken, JAPAN
A. Takagi, T. Sugimura, F. Naito, KEK, Ibaraki-ken, JAPAN

Abstract

The RFQ III, which is designed for 50mA beam acceleration from 0.05MeV to 3MeV, has been fabricated and the high-power test has started at April 2013 at the test station in the J-PARC. The high-power conditioning reached to the 120% of the nominal peak power with 1.5% (600μs, 25Hz) RF duty. Then, the beam acceleration test has started. In Jun. 2014, continuous beam operation for one month has been demonstrated.

INTRODUCTION

The J-PARC accelerator comprises an injector linac, a 3-GeV Rapid-Cycling Synchrotron (RCS) and a 50-GeV Main Ring. The beam energy of the linac has been upgraded from 181MeV to 400MeV in 2013. For the beam current upgrade, the new frontend (RF ion source, RFQ, chopping system) installation is scheduled in summer 2014 for 1MW operation at RCS. We performed the beam operation at the test station and measured parameters of the beam accelerated by the RFQ III. The results of the high-power conditioning and the stability of the RFQ with beam are described.

RFQ III AND TEST STATION

The beam dynamics design is described in Ref. [1]. The RFQ III is a Four-vane type cavity. To reduce the dipole mode mixing, the dipole stabilization rods (DSRs) are inserted from the endplates. The frequency separation from the nearest dipole mode is 4.6MHz. The mechanical and the RF properties of the RFQ III cavity are in Refs. [2, 3].

The nominal RF power and RF duty of the RFQ III are 400kW and 3%, respectively. The cavity is driven by one loop-type input coupler, of which coupling is adjusted to 1.8 for the beam loading. Vacuum system for the RFQ cavity consists of three cryogenic pumps (2700L/s for hydrogen), three ion pumps (400L/s for nitrogen), a B-A gauge, a cold cathode gauge, and a residual gas analyzer at the test station.

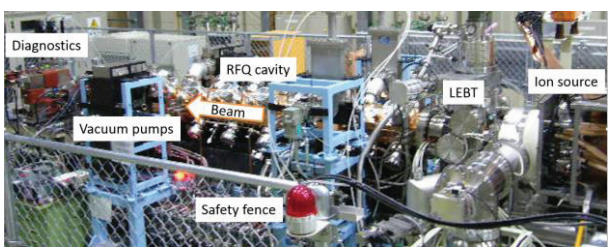


Figure 1: Photograph of the test station.

The test station (Fig. 1) consists of the ion source, two solenoids in the low-energy beam transport (LEBT), the RFQ, and the diagnostics with beam dump. The ion source is RF driven cesium seeded type, which can extract more than 60 mA, 50keV negative hydrogen beam with the pulse width of 1ms and the repetition rate of 25Hz. The diagnostics section has two quads, a bending magnet, and an emittance measurement system. After the accelerated beam parameter measurement, the emittance measurement system was replaced to the scraper irradiation test chamber. Then, the RFQ conditioning with beam was performed in parallel with the scraper irradiation test for one month.

HIGH-POWER TEST RESULTS

Conditioning

Before the beam operation, the high-power conditioning has performed at the test station in Apr. 2013. The vacuum pressure reached to 6e-6Pa before the high-power conditioning. At the beginning of the high-power conditioning, the RF pulse width was taken as 30μs with 25Hz repetition. Figure 2 shows the history of the high-power conditioning. The tank level was gradually increased and reached to the 110% of the design tank level after ten hours conditioning. Then, the RF pulse width was extended to 50μs. After 20 hours conditioning, the tank level reached to 110% of the design level with RF width of 600μs. At that time, the RF trips (mainly due to the abnormal RF reflection from the cavity) occurred a few times per hour, however, it was improved to a few times per day. Then, we started the beam acceleration test [4].

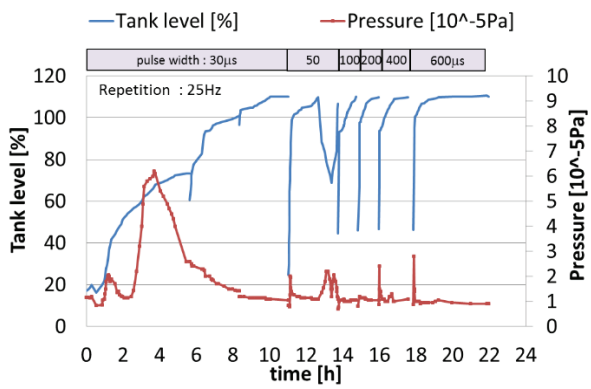


Figure 2: History of the high power conditioning. The blue and red curves show the tank RF level and vacuum pressure in the RFQ cavity, respectively.

The vacuum pressure was less than 1e-5Pa with high-power RF. At the beginning of this conditioning, there were two outgassing region near the RF tank level of 30% and 70% as shown in Fig.2. After this conditioning, vacuum pumping continued and the beam test has

#takatoshi.morishita@j-parc.jp

ISBN 978-3-95450-142-7

Copyright © 2014 CC-BY-3.0 and by the respective authors

LUE-200 LINAC. STATUS & DEVELOPMENT

A.P. Sumbaev#, A.S. Kayukov, V.V. Kobets, V.F. Minashkin, V.G. Pyataev, V.G. Shabratov, V.A. Schvets, V.N. Shvetsov, JINR, Dubna, Russia

Abstract

The general scheme and current status of an electron linac with an S-band travelling wave (f = 2856 MHz) accelerating structure – a driver for a pulsed neutron source (IREN) at the Frank Laboratory of Neutron Physics of the Joint Institute for Nuclear Research - are presented. The parameters of the accelerating system and the measured parameters of the electron beam – pulse-beam current, duration of the current pulse, repetition rate, electron-energy spectrum, and loading characteristics of the accelerating structure - are given. The beginning of the implementation of the project of the second stage of the IREN facility, which forms the basis for the development of the accelerator aimed at increasing its beam power, is reported. Technical solutions underlying the modernization of the accelerator's electrophysical systems are discussed: accelerating system, RF power supplies, and modulators.

INTRODUCTION

In January, 2009, at the Frank Laboratory of Neutron physics of JINR the physical start-up of the first stage of the **I**ntense **Re**sonance **N**eutron source (IREN) for fundamental and applied investigations in neutron nuclear physics in a neutron energy range from eV to hundreds of keV was carried out [1]. The conceptual scheme of the neutron source is based on the electron linac with an S-band travelling wave (f = 2856 MHz) accelerating structure. The scheme of the linac with a beam energy up to 200 MeV (Fig. 1) and average beam power of ~ 10 kW, consisting of two accelerating sections which was suggested by the Budker Institute of Nuclear Physics [2], is realized in two stages. At the first stage a full-scale accelerator consisting of one accelerating section with constant impedance, which is powered by one klystron with the SLED RF-power multiplication system, was created [3]. The first electron beam was obtained in June 2008, and the first neutrons were produced in the IREN target in December 2008. In February 2009 the regular operation of the accelerator started at a repetition rate of 5-10 Hz, and in May 2010 it began at a rate of 25 Hz. All in all, by the middle of 2014 the accelerator operated in experiments for more than 4200 h.

CURRENT STATUS OF THE FIRST STAGE OF THE LINAC

At the first stage of the linac one accelerating section is powered by one TH2129 klystron with a nominal pulse power of 20 MW. Thus, the design beam power was reduced to ~ 3 kW. In the course of the realization of the project the parameters of the linac were changed. The repetition rate of the operation of the accelerator was reduced to 25 Hz, and in order to increase the resolution power of the time-of-flight neutron spectrometers, the beam pulse duration was decreased from 250 ns to 100 ns. The average power of the electron beam was 0.13 kW for a beam with a current of 1.5 A and 0.2 kW for a beam with a current of 2.5 A. Table 1 presents the initial design characteristics of the linac, the design characteristics corrected for the assembly with one accelerating section powered by klystrons of different power, and the characteristics of the linac obtained at the first stage in a regular operating mode.

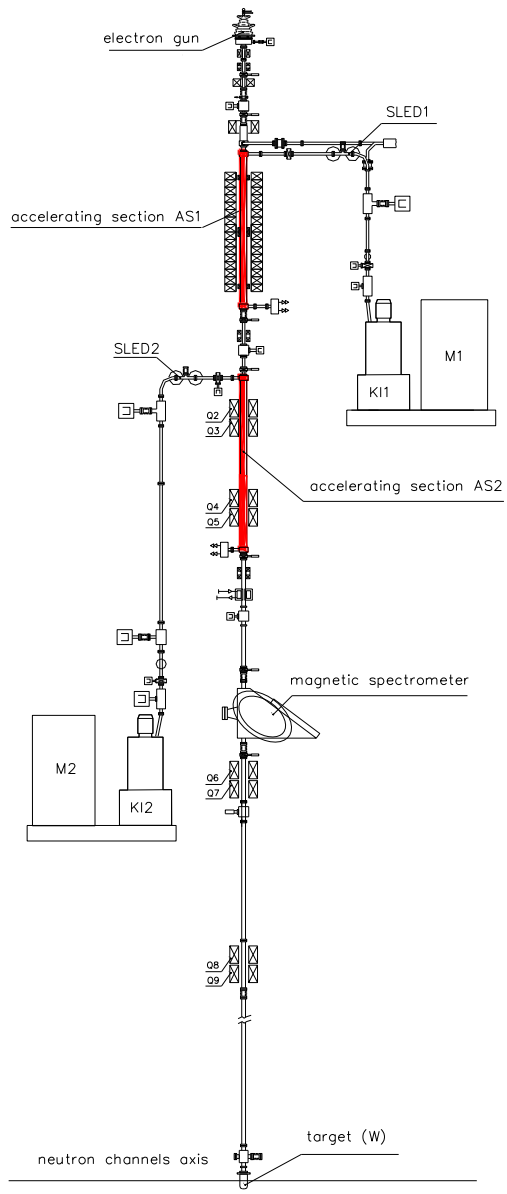


Figure 1: Scheme of the accelerator development.

Copyright © 2014 CC-BY-3.0 and by the respective authors

ISBN 978-3-95450-142-7

100-MeV PROTON BEAM PHASE MEASUREMENT BY USING STRIPLINE BPM*

Han-Sung Kim#, Hyeok-Jung Kwon, Yong-Sub Cho, KAERI, Daejeon, Korea

Abstract

In Korea Multi-purpose Accelerator Complex (KOMAC), a 100-MeV proton linac, which is composed of a proton injector based on the microwave ion source, 3-MeV RFQ with a four-vane type and 100-MeV DTL with electromagnetic quadrupoles has been developed and currently provides the proton beam to users for various applications. To increase the beam power up to the design value, several improvements are required including the fine adjustment of the RF set-point during the operation. A stripline BPM is used for the beam phase measurement, where the pickup signals from four electrodes are combined by using the RF combiner, then mixed with 300 MHz LO reference signal resulting in 50 MHz IF signal which is processed by digital IQ demodulation method. In this paper, the details of the beam phase measurement setup and results will be presented.

INTRODUCTION

A 100-MeV proton linac in KOMAC has been provided the proton beam for various users and applications including basic research and the industrial uses since July, 2013. The KOMAC accelerator consists of a 50-keV proton injector, a 3-MeV RFQ and a 100-MeV DTL. The DTL section is composed of total 11 tanks and one of unique feature of the DTL is that there are MEBT and dipole magnets to extract the 20-MeV beam for low energy beam applications [1].

The average beam power is gradually increased by lengthening the beam pulse width with higher repetition rate. To further increase the beam power, it is important to adjust the RF set points precisely such as the RF amplitude and phase in each accelerator sections [2].

The RF phase can be measured by using the beam position monitor (BPM). The proton linac at KOMAC has total 10 stripline-type BPMs, which are located between each DTL tank as shown in Fig. 1. The layout for the beam current transformers for measuring the beam current and the beam loss monitors based on scintillation detector is also shown in Fig. 1.

STRIPLINE BEAM POSITION MONITOR

Design and Fabrication

To measure the RF phase, we designed, fabricated and installed the stripline BPM [3]. The design of the BPM was performed based on the Microwave Studio code and Superfish code. Two different types of the stripline BPMs were used in KOMAC proton accelerator. One is for the linac and installed between DTL tanks and the other is for beamlines to measure the beam position. Table 1 shows the design parameters of the BPMs both the linac BPM and the beamline BPM; the differences are mainly due to the different aperture size. The fabricated BPM is shown in Fig. 2.

Low Power Performance Test

We performed the low power RF test for the BPM to check the design and fabrication of the BPM on the test bench. We used a probe wire with 3 mm in diameter which is connected to the RF signal generator to simulate the beam.

The design value of the coupling between the beam and each electrode of BPM is 30 dB at 350 MHz and 23 dB at 700 MHz. The measured values showed some scattered distribution with maximum error of about 3%. These scattered data are considered mainly due to difference between the physical center and the electrical center.

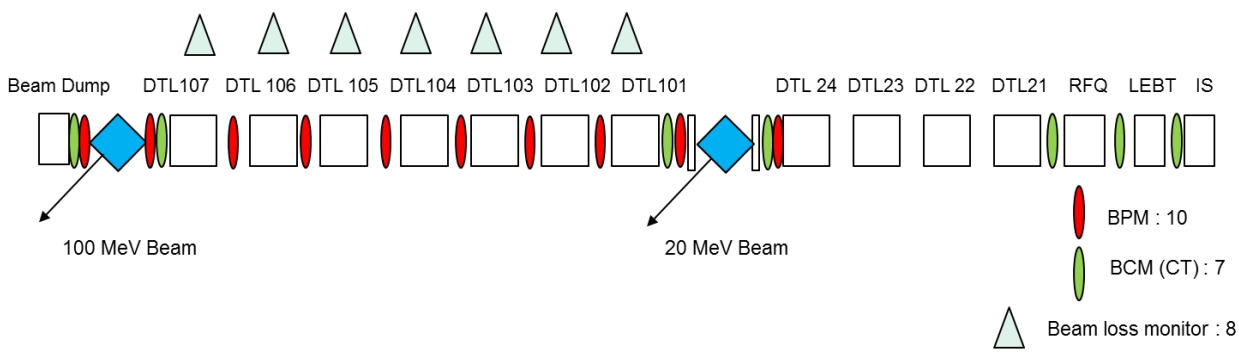


Figure 1: Layout of beam position monitors, beam current monitors and beam loss monitors along the linac.

*Work supported by Ministry of Science, ICT & Future Planning.
#kimhs@kaeri.re.kr

Copyright © 2014 CC-BY-3.0 and by the respective authors

OPERATION OF THE VERSATILE ACCELERATOR DRIVING THE LOW POWER ADS GUINEVERE AT SCK•CEN

M. Baylac#, A. Billebaud, P. Boge, D. Bondoux, J. Bouvier, S.Chabod, G. Dargaud, E. Froidefond, E. Labussière, R. Micoud, S. Rey, LPSC, Univ. Grenoble-Alpes, CNRS/IN2P3, Grenoble, France
A. Kochetkov, J. Mertens, F. Van Gestel, C. Van Grieken, B. Van Houdt,
G. Vittiglio, SCK•CEN, Mol, Belgium
F. Lecolley, J.-L. Lecouey, G. Lehaut,
N. Marie, LPC Caen, ENSI Caen/Univ. Caen, CNRS-IN2P3, Caen, France

Abstract

GUINEVERE is a low power accelerator driven system (ADS) consisting of a versatile neutron source, GENEPI-3C, driving the fast sub-critical core, VENUS-F, in SCK•CEN (Belgium). GENEPI-3C is an electrostatic accelerator generating 14 MeV neutrons by bombarding a 250 keV deuteron beam onto a tritium target located within the reactor core. This accelerator produces alternatively continuous beam (up to 1 mA DC), possibly chopped with fast and adjustable interruptions, or short and intense deuteron bunches (~25 mA peak, 1 µs). This paper presents the facility and assesses the 2 years of coupled operation of the accelerator to the reactor.

INTRODUCTION

The Generator of Uninterrupted Intense NEutrons at the lead VEnus Reactor (GUINEVERE) facility is devoted to experimental studies of Accelerator Driven System feasibility. It aims to investigate on-line reactivity monitoring, sub-criticality determination, which are major safety issues, and operational procedures [1]. It is based on a low power facility representing an ADS demonstrator: an experimental reactor of SCK•CEN (Belgium) modified into a fast lead core, VENUS-F, is coupled to a versatile accelerator driven neutron source developed by CNRS/IN2P3 (France). The accelerator operates in pulsed or continuous beam mode, the latter being more representative of a powerful system. GUINEVERE provides a unique facility in Europe for fast sub-critical reactor physics investigations. The facility, under operation for the experimental program for more than 2 years, has led to the first physics results. After presenting the facility, this paper assesses the coupled operation and discusses the sensitivity of the reactor to the accelerator operation.

REACTOR CORE

For sub-critical operation, the VENUS-F reactor is loaded with 93 square fuel assemblies (FA). Each FA is composed of uranium metal highly enriched in ^{235}U (30%) and solid lead rodlets acting as a fast system coolant. The core is composed by a cylindrical arrangement of FA (~800 mm in diameter, 600 mm in height), surrounded by axial and radial lead reflectors [1]. The central core region is left empty to host the terminal section of the accelerator beam line. This insertion channel holds a small lead buffer surrounding the beam pipe supporting the target. The reactor is equipped with 6 safety rods and 2 control rods. Rods are located as close as possible to the centre without interfering with the vertical structure of the accelerator.

ACCELERATOR FACILITY

The Generator of Neutrons Pulsed and Intense-3C (GENEPI-3C) is an electrostatic accelerator producing and transporting a deuteron beam onto a tritium target located at the core center, creating 14 MeV neutrons by T(d,n)^{4}He reactions. The machine is fully presented in reference [2].

To fulfill the requirements of the experimental program, this machine produces alternatively (cf Table 1):

- short and intense deuteron pulses with adjustable repetition rate,
- continuous (DC) beam, possibly chopped with adjustable programmable interruptions.

Table 1: Beam specifications

Pulsed mode Beam bunches	**DC interrupted mode** With beam interruptions
I peak ~25 mA	I mean: ~50 µA – 1 mA
Rate: 10 Hz- 5kHz	Interrupt. rate: 0.1 – 200 Hz
Width ~ 0.7 µs	Interrupt. duration: ~20 µs – 10 ms
Reproducibility ~1%	Interrupt. transition duration ~1 µs

Deuteron beams with different time structures and intensities are generated by a unique duoplasmatron ion source. The main differences between pulsed and DC beam modes, concern source efficiency and beam transport. The ion source and electrodes sit within a high voltage platform and connect to the 250 kV accelerating

*Work supported by FP6 IP-EUROTRANS, FP7 FREYA & MAX and the PACEN program form CNRS
#baylac@lpsc.in2p3.fr

Copyright © 2014 CC-BY-3.0 and by the respective authors

ISBN 978-3-95450-142-7

VERTICAL ELECTRO-POLISHING OF NB SINGLE-CELL CAVITY USING CATHODE WITH VARIABLE-GEOMETRY WINGS AND ITS RESULTS OF VERTICAL TEST

K.Nii#, V.Chouhan, Y. Ida, T. Yamaguchi, MGI, Himeji, Japan
K. Ishimi, MGI, Kashiwa, Japan
H. Hayano, S. Kato, H. Monjushiro, T. Saeki, M. Sawabe, KEK, Tsukuba, Japan
P. Carbonnier, F. Eozénou, C. Servouin, CEA/DSM/IRFU, France
C. Madec, L. Maurice, CEA/IRFU, Gif-sur-Yvette, France

Abstract

Marui Galvanizing Co. Ltd. has been studying Vertical Electro-Polishing (VEP) on Nb single-cell superconducting accelerator cavity with the goal of mass-production and cost-reduction of Electro-Polishing (EP) process in collaboration with KEK and CEA saclay. And we invented our original cathode named "i-cathode Ninja"® which has four Al wing-shape parts for single-cell cavity VEP. We thought that these parts can realize uniform distributions of both electric current and EP solution flow at inner surface of cavity. Using this cathode, we performed various tests of VEP with Nb single-cell cavities. In this article, we will report results of VEP using "i-cathode Ninja"® and 1AC3 Nb single-cell cavity form CEA Saclay for vertical test.

INTRODUCTION

Electro-polishing (EP) has been used for the final surface treatment to improve acceleration gradient of Superconducting Radio-Frequency (SRF) cavity. So far, horizontal electro-polishing (HEP) have been adopted mainly for cavity EP [1-2]. In addition to this, vertical electro-polishing (VEP) is studied actively [3-4]. Marui Galvanizing Co. Ltd., decided to focus on the VEP because of the benefit for mass production (for example space-saving, no cavity rotation), and we started the study on the VEP process in the collaboration with KEK and CEA Saclay. For cavity EP, we thought that uniform anode-cathode distance and diffusion of flesh electrolyte in the whole cavity are most important factor. To realize these, we invented the VEP using cathode with variable-geometry wings named "i-cathode Ninja"®. [5]. Once, we have performed the 1st-3rd VEP of single-cell cavity using this cathode and reported these results [5]. Now, coupon cavity VEP has been performed for parameter investigation and surface analysis [6]. And 9-cell VEP setup preparation and VEP study have been performed [7]. In this article, we report the results of VEP using "i-cathode Ninja"® and 1AC3 single-cell cavity from CEA Saclay for vertical test.

#keisuke_nii@e-maui.jp

I-CATHODE "NINJA" ®

The schematic view of the "i-cathode Ninja"® which we invented is shown in Fig.1.

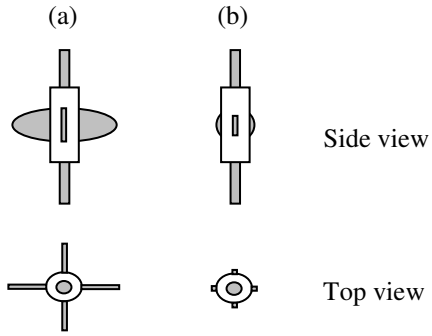


Figure 1: Schematic view of "i-cathode Ninja" ®. (a) unfolded status. (b) retracted/folded status.

The most important feature is that it has four wing-like shaped aluminum cathodes at the center of cavity cell. Compared with rod type cathode,

(1) The wings agitate electrolyte in the cell of cavity and flesh electrolyte goes around the equator.
(2) The wings make the distance between the cathode and the equator shorter in the cell and realize the uniform distance distribution between cathode and anode.

There are two benefits to use "i-cathode Ninja" ®. Then this cathode has a retractable structure of flexible wings and can be folded and unfolded by simple action.

1ST 1AC3 SINGLE-CELL CAVITY VEP

Fig.2 shows pictures of VEP setup and single-cell cavity of this experiment.



Figure 2: (Left) Picture of single-cell VEP system. (Right) Picture of single-cell cavity.

Copyright © 2014 CC-BY-3.0 and by the respective authors

ISBN 978-3-95450-142-7

THE BEAM ENVELOPE CONTROL IN SC LINAC FOR THE PROTON RADIOTHERAPY

I.A. Ashanin, S.M. Polozov, A.V. Samoshin, National Research Nuclear University MEPhI (Moscow Engineering Physics Institute), Moscow, Russia

Abstract

Proton cancer therapy is conventionally based on normal conducting synchrotrons and cyclotrons. The high electrical power consumption and especial devices necessary to energy variation are main problems of such facilities. Superconducting linacs based on short identical independently phased cavities have a seriously progress and it's development allow to propose their using for medical application. High accelerating gradient and small capacity losses nearly 10^{-4} W/m are main advantages in advance of normal conducting facilities, the energy variation can be realized by means of RF field amplitude and phase variation in a number of cavities. Besides linac structures are lack of unwieldy magnetic system, simplicity of input and output of particles and high current densities.

The parameters choose and the optimization for SC linac structure with energy up to 240 MeV and envelope control will discuss in this paper. The simulation was done using BEAMDULAC-SCL code [1]. The study of beam dynamics will direct to realize the energy variation in range 150-240 MeV with beam quality preservation.

INTRODUCTION

There are some conventional parameters of the facilities for the proton cancer therapy: the energy of the beam about 240 MeV with the possibility of the wide regulation, possibility of control of beam envelope up to 6 mm and intensity of the beam at about 10^9 particles per second.

The proton beam usually receives using proton synchrotrons or cyclotrons [2]. But it can be also received in a linac. The main limitation till recent times was a low acceleration rate that provides to the high length of accelerator. Nowadays progress in SC linacs development allows solving this problem. SC linacs have some significantly preferences. It's a very high rate of energy gain for the period of the structure that allows reducing of the facilities length and low requirement in RF power feeding. In addition power-intensive magnets are not necessary. And also the possibility of easily beam energy variation by means of a number of the resonator turn-off (deeply variation) or RF field phase in last resonators (slow variation).

A proton linac based on SC independently phased cavities up to energy 240 MeV is an possible variant for medical application [3].

Beam focusing can be provided with help of SC solenoids following each cavity or with help of RF focusing [4]. Using a solenoid into focusing period will allow the separate control of the transverse and longitudinal beam dynamics.

Beam dynamics and beam envelope control in such structure will be discussed in this paper. The methods of energy variation in range 150-240 MeV will discuss.

STRUCTURE CHARACTERISTICS

With a large number of resonators it is advisable to divide them into several groups, consists of geometry identical resonators. Certainly, in this accelerating system will always violate the synchronism principle, when the synchronous particle velocity equal to the phase velocity of the accelerating wave during acceleration. A slipping of the particles relative to the accelerating wave is in evidence. The slipping value must not exceed acceptable value if not the acceleration rate will rapidly reduced and beam longitudinal stability worse. The number of resonators should be limited and the number of groups should be minimal [5].

So in this study the phase slipping factor was limited by 18%. Accordingly the accelerator will be divided into four groups of cavities with geometric velocity of cavities β_g = 0.09, 0.18, 0.31 and 0.49 respectively. The geometrical velocity β_g of the RF wave is constant for any group of cavities and the number of such groups in linac should be minimized to reduce the accelerator cost. Therefore the first two groups consist of the cavities has two accelerating gaps and the third and the fourth would consist of three gap cavities (see Fig. 1). Values of length of solenoid were assigned 0.2 m and length of gap 0.1 m at the all accelerator length.

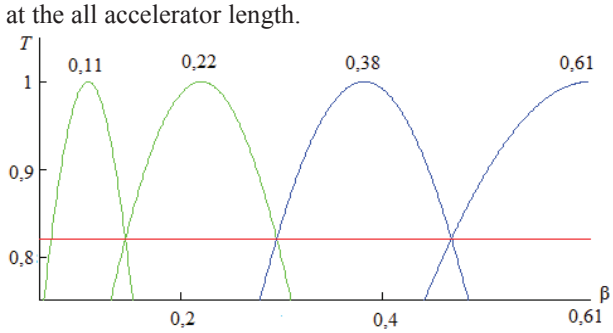


Figure 1: Slipping factor value depending on β.

TRANSVERSE MOTION STABILITY ANALYSIS AND BEAM ENVELOPE CONTROL

Transverse motion stability and beam dynamics analysis results for the first part having the beam energy range from 2.4 to 10.4 MeV will considered bellow. The accelerating field for each cavity is equal 3.21 MV/m, the

Copyright © 2014 CC-BY-3.0 and by the respective authors

ISBN 978-3-95450-142-7

STORAGE RING AS A LINAC BEAM MONITOR – ITS OPERATION AND CONTRIBUTION TO THE STABLE TOP-UP INJECTION

Y. Shoji#, NewSUBARU/SPring-8, University of Hyogo, Japan
T. Asaka, H. Dewa, H. Hanaki, T. Kobayashi, Y. Minagawa, A. Mizuno, T. Shinomoto, S. Suzuki, Y. Takemura, T. Taniuchi, and K. Yanagida, SPring-8, JASRI, Japan

Abstract

We have used the electron storage ring, NewSUBARU, as a beam monitor of the SPring-8 linac. The time and transverse profiles of the injected linac beam in the ring are recorded in a frame of a dual-sweep streak camera. A measurement through synchrotron oscillation or betatron oscillation periods gives multi-dimensional beam structure. We report how we use the system and its contribution to the stable beam injection of the ring.

INTRODUCTION

The SPring-8 linac [1] has been operated as an injector to the electron storage ring, NewSUBARU (NS) [2]. A fine parameter tuning is required for the stable top-up injection, because of a small ring acceptance and a radiation safety regulation. In the tuning process, a single shot linac beam monitor has been a powerful diagnostic to understand what is happening at the injection because the linac beam has shot-by-shot fluctuation.

We used the storage ring as a linac beam monitor. The dual sweep streak camera, set at the beam-line of the storage ring, recorded profiles of the injected linac beam for many revolutions in one camera frame. These images enabled reconstruction of multi-dimensional linac beam parameters. The measurement took place at least once after every long shut down. It functioned as a final check of the linac beam tuning before user operations.

The measurements gave better understanding of the injection process and is also a strong driving force for the improvements of the linac beam quality.

PARAMETERS OF DAILY OPERATION

Fig. 1 shows the layout of the SPring-8 linac, the booster synchrotron, and NS storage ring. Table 1 shows the main parameters for the linac. The pulse width of the linac beam is normally 1 ns, which contains 3 linac bunches. The rf synchronization system between the linac and the ring [3] enables an injection to a single rf bucket of the ring with rf frequency of 500 MHz.

The listed transverse emittance was the average of many shots, measured by Q-scanning at the beam transport line. The longitudinal parameters were obtained from the measurements described in this report [4]. The listed bunch length and the energy spread were the average of 10 shots.

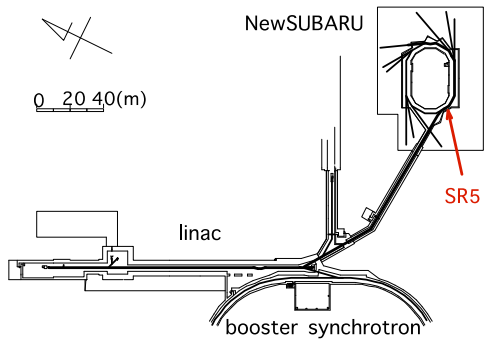


Figure 1: Layout of the 1 GeV SPring-8 linac, the booster synchrotron, and the NewSUBARU storage ring.

Table 1: Main Parameters of the Linac

Electron energy	1 GeV
Rf frequency	2856 MHz
Common pulse rate	1 Hz
Common pulse width	1 ns
FWHM Bunch length; front/middle	10 ps / 14ps
Full energy spread; front / middle	0.4% / 0.6%
Transverse emittance (HWHM^2)	100 π nmrad.

MEASUREMENTS USING STREAK CAMERA

How to Use Dual Sweep Image

Fig. 2 shows dual sweep images of the injected linac beam obtained at different three operation cycles. A time profile at the injection timing gives the bunch structure in a macro pulse, and its evolution with time shows the synchrotron oscillation in the ring. Fig. 3 is the mountain view of the time profile obtained from the middle image of Fig. 2. The time profile at after 1/4 of synchrotron oscillation period gives the energy profile of the injected linac beam.

Fig. 4 shows the results obtained in these 7 years. It shows the improvement of the energy spread of the linac beam, which is now small enough for the injection. The number of bunches (gate pulse width) was not fixed because it was optimized for the pulse charge to the booster synchrotron.

shoji@lasti.u-hyogo.ac.jp

Copyright © 2014 CC-BY-3.0 and by the respective authors

RF CHARACTERISTICS OF 20K CRYOGENIC 2.6-CELL PHOTOCATHODE RF-GUN TEST CAVITY*

T. Sakai#, T. Tanaka, K. Nakao, K. Nogami, M. Inagaki, K. Hayakawa, Y. Hayakawa, LEBRA, Nihon University, Funabashi, Japan
T. Shintomi, ARISH, Nihon University, Tokyo, Japan
T. Takatomi, M. Yoshida, M. Fukuda, J. Urakawa, KEK, Ibaraki, Japan

Abstract

A cryogenic C-band photocathode RF-gun operating at 20 K is under development at LEBRA in Nihon University. The RF-gun is of the BNL-type 2.6-cell pillbox cavity with the resonant frequency of 5712 MHz. The 6N8 high purity OFHC copper (corresponding to RRR-3000) is used as the cavity material. From the theoretical evaluation of the anomalous skin effect, the quality factor Q of the cavity at the operating temperature of 20 K has been expected to be approximately 60000. The cavity basic design and the beam bunching simulation were carried out using Poisson Superfish and General Particle Tracer (GPT). Machining and diffusion bonding of the RF-gun cavity was carried out in KEK. After diffusion bonding the Q_0 value of the π-mode resonance at the room temperature (23.5 °C) was approximately 11440.

INTRODUCTION

A C-band photocathode RF gun is under development for future use in the compact accelerator developed at KEK [1] as a high brightness X-ray source. As a basic design the RF gun cavity consists of 2.6-cell pillbox-type π-mode structure and operates at 5712 MHz under low temperature of 20 K. The electron beam is extracted by using a cryogenically-cooled copper RF cavity, which can be driven with considerably low RF power compared to those in room temperature RF guns. A low power test cavity has been designed with Poisson Superfish [2] for basic understanding of the RF properties at low temperature. The simulation of the beam bunching was performed using General Particle Tracer (GPT) [3]. This paper reports the results of the beam simulation and the low power RF properties measured at room temperature.

LOW-TEMPERATURE PROPERTIES FOR HIGH PURITY OXYGEN FREE COPPER

The dimensional variation ratio of higher purity oxygen free copper (OFHC copper (UNS C10100/C10200)) was obtained from the linear expansion coefficient data in the database of National Institute of Standards and Technology (NIST) (temperature range from 4 to 300 K) [4]. The deduced dimensional change in the cavity between room temperature and 20 K is 0.33428%. In addition, the linear expansion coefficient at around 20 K is around 1/100 of that in the room temperature. This means that the temperature dependence of the cavity resonant frequency is very low. The temperature dependence of the thermal conductivities in different OFHC copper Residual Resistivity Ratios (RRR) were also obtained from the NIST database, which is shown in Fig. 1 for the OFHC copper material of RRR-50 to 500. Fig. 1 suggests that the thermal conductivity at around 20 K is expected to be more than 10 times larger compared with that in room temperature by using a high purity OFHC copper exceeding RRR-500. Therefore, an RF gun cavity made of high purity OFHC copper has a possibility of stable pulsed operation at around 20 K.

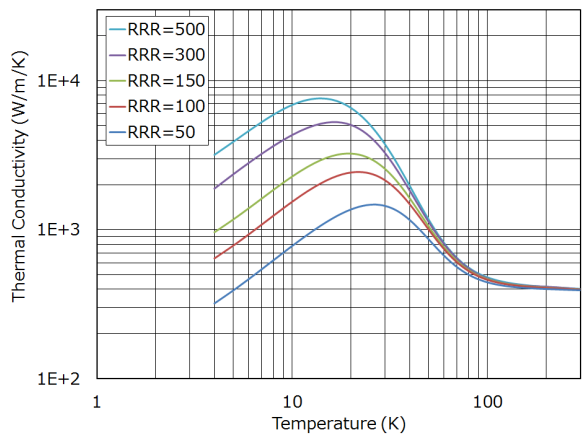


Figure 1: Thermal conductivity of coppers with different residual resistivity ratio (RRR-50 to 500)

CAVITY CHARACTERISTICS

The surface resistance of the RF cavity is an important parameter which determines the wall RF loss and the Q value, and is dominated by the skin depth in room temperature domain. However, the electron mean free path in material is extremely long compared to the skin depth in low temperature region, which causes a higher surface resistance than that is predicted by the skin depth. This behavior is known as the anomalous skin effect. The behavior of the surface resistance at 5712 MHz was calculated on the basis of the Reuter's theory of the anomalous skin effect [5], which is shown in Fig. 2 together with the result of calculation of the normal skin effect for comparison. As seen in Fig. 2, the surface resistance of the cavity at 20 K is reduced to

* This work was supported by Photon and Quantum Basic Research Coordinated Development Program from the Ministry of Education, Culture, Sports, Science and Technology, Japan.
# sakai@lebra.nihon-u.ac.jp

Copyright © 2014 CC-BY-3.0 and by the respective authors

ISBN 978-3-95450-142-7

HOM AND IMPEDANCE STUDY OF RF SEPARATORS FOR LCLS-II*

S. U. De Silva#, B. R. P. Gamage, R. G. Olave, J. R. Delayen, G. A. Krafft, T. Satogata
Old Dominion University, VA 23529, USA

Abstract

The LCLS-II upgrade requires an rf spreader system to guide bunches into a switchyard delivering beam to two undulators and the primary beam dump. The beam pattern therefore needs a 3-way beam spreader. An rf deflecting cavity concept was proposed that includes both superconducting and normal conducting options. We characterize the higher order modes (HOM) of these rf separator cavities and evaluate beam dynamics effects due to potential HOM excitation. This study includes both short term wake and multi-bunch effects.

INTRODUCTION

The LCLS-II upgrade includes a superconducting linac that will deliver an electron beam with energy of 4 GeV to one of three destinations of the SXR undulator, the HXR undulator and the beam dump. The beam switching and transporting system that separates the beam therefore, requires a three-way beam spreader [1]. Among the options considered for the beam separation are fast magnet kicker systems or a set of rf separator cavities.

An rf separator system operating at a frequency of 325 MHz is required to provide a transverse voltage of 4.0 MV that deflects the beam in vertical direction with a separation of 1 mrad [1].

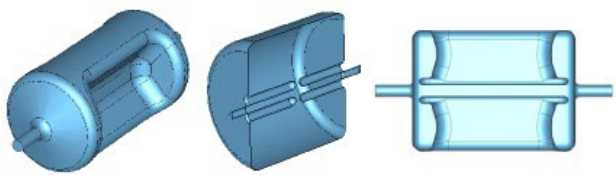


Figure 1: The three rf separator designs: superconducting rf-dipole design (left), normal conducting 4-rod design (center) and normal conducting rf-dipole design (right).

Three preliminary cavity options have been studied, including a superconducting rf-dipole design and two normal conducting designs: the 4-rod design, and normal conducting version of the rf-dipole design [2]. The design requirement of 4.0 MV can be achieved with one superconducting rf-dipole cavity, or by 6 cavities for each of the normal conducting cavity options.

The LCLS-II linac is expected to accelerate an electron beam with an average beam current of 0.02 mA consisting of very short bunches and high bunch repetition rate. The operating beam parameters are shown in Table 1.

The beam may generate single pass beam effects including both transverse and longitudinal effects. This paper presents the higher-order mode properties with further analysis of longitudinal and transverse impedances for the superconducting rf-dipole cavity.

*Work supported by the U.S. Department of Energy under contract DE-AC02-76SF00515
#sdesilva@jlab.org

Table 1: Operational Electron Beam Parameters

Parameter	Nominal Value	Range	Units
Electron energy (E_f)	4.0	2.0-4.0	GeV
Electron bunch charge (Q_b)	0.1	0.01-0.5	nC
Bunch repetition rate (CW) (f_b)	0.2	0-1	MHz
Average current (I_{avg})	0.02	0.001-0.3	mA
Peak current (I_{pk})	1000	500-1500	A
rms bunch length (σ_z)	8.3	0.6-52	μm

LOM AND HOM PROPERTIES

The lower-order mode (LOM) and higher-order modes (HOM) are determined for the three rf-separator cavities using CST Microwave Studio and compared to the values obtained from Omega3P package of the SLAC ACE3P suite [3]. The modes are categorized as accelerating modes and transverse modes with a net deflection in the horizontal and vertical directions, respectively.

Superconducting RF-Dipole Cavity

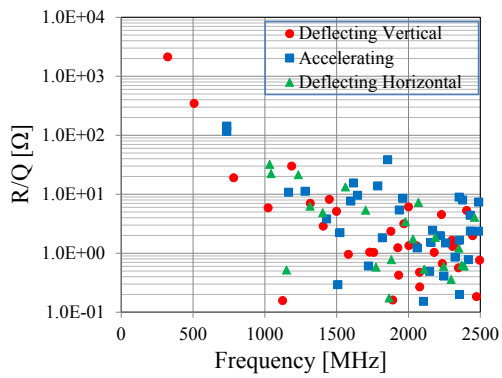


Figure 2: Mode spectrum of the superconducting rf-dipole cavity.

The HOM spectrum of the superconducting rf-dipole design is shown in Fig. 2. The fundamental deflecting mode is the lowest mode with no lower-order modes existing in the rf-dipole geometry where the [R/Q] values decrease as a function of the mode frequency.

Copyright © 2014 CC-BY-3.0 and by the respective authors

ISBN 978-3-95450-142-7

CRYOGENIC TESTING OF HIGH-VELOCITY SPOKE CAVITIES*

C. S. Hopper†, HyeKyoung Park, and J. R. Delayen
Center for Accelerator Science, Department of Physics,
Old Dominion University, Norfolk, VA, 23529, USA and
Thomas Jefferson National Accelerator Facility, Newport News, VA 23606, USA

Abstract

Spoke-loaded cavities are being investigated for the high-velocity regime. The relative compactness at low-frequency makes them attractive for applications requiring, or benefiting from, 4 K operation. Additionally, the large velocity acceptance makes them good candidates for the acceleration of high-velocity protons and ions. Here we present the results of cryogenic testing of a 325 MHz, β_0 = 0.82 single-spoke cavity and a 500 MHz, β_0 = 1 double-spoke cavity.

INTRODUCTION

High-velocity single- and multi-spoke cavities have been suggested for applications including high energy proton accelerators [1] and the acceleration of electrons in compact light sources [2, 3]. To this end, we have designed, fabricated (along with Niowave, Inc.), and cryogenically tested a single-spoke cavity with a geometric β_0 = 0.82 and operating at 325 MHz and a double-spoke cavity with a β_0 and operating frequency of 1.0 and 500 MHz, respectively. Table 1 shows some of the rf properties for these cavities. The reference length is $\beta_0\lambda$ and $3\beta_0\lambda/2$ for the single- and double-spoke cavity, respectively, while E_{acc} = 1 MV/m for both.

Table 1: RF Properties

Parameter	325 MHz Single	500 MHz Double
β_0	0.82	1.0
E_p/E_{acc}	3.6	3.7
B_p/E_{acc} [mT/(MV/m)]	6.0	7.6
R/Q [Ω]	449	675
$Q \cdot R_s$ [Ω]	182	174

CAVITY FABRICATION AND PROCESSING

The 325 MHz single-spoke cavity was designed at ODU while the fabrication was done at Niowave, Inc. A 150 μm bulk BCP and 30 μm light etch was also performed by Niowave, Inc. In between these processing steps, a 600° C heat treatment was preformed at FermiLab. When the cavity arrived at Jefferson Lab, a 3-pass high pressure rinsing with deionized water at 1250 psi followed by class 100 cleanroom assembly and 25 hour 120° bake were all carried out.

The 500 MHz double-spoke cavity was designed at ODU while the complete fabrication, processing, and cryogenic testing were done at Jefferson Lab. The fabrication details can be found in [4]. The processing was similar to that described above. A bulk BCP removing 150 μm was initially done. This was done in two steps- 75 μm was removed, the cavity was rotated 180° within the BCP cabinet, and the remaining 75 μm was removed. The cavity thickness (between the spokes, at the center) is measured in real time to ensure accurate removal. The BCP mixture had a volume ratio 1:1:2, which gave an etch rate of roughly 0.5 μm per minute, at this particular point. The complicated geometry of the double-spoke cavity resulted in more material being removed from the end cap regions.

The 500 MHz double-spoke cavity then received a heat treatment of 600° for 10 hours, followed by a light etch of 10 μm, manual high pressure rinsing through the cleaning ports and three passes through the beam ports in the HPR cabinet, finishing with a low-temperature bake of 120° for 48 hours.

HIGH POWER TESTING

The cryogenic testing of both cavities was carried out at Jefferson Lab which houses the Vertical Test Area (VTA). While calibrating the cables, a low power amplifier (1 W) was used and a 500 W amplifier was used to drive the cavities during the high power tests. The VTA operates with a closed cycle LHe supply capable of cooling from 300 K to 4 K in a matter of hours. The 4 K test is then performed and the dewar is refilled and cooled from 4 K to 2 K. During this cool down, frequency and Q_0 measurements are taken in order to determine the residual resistance. Finally, the 2 K tests are carried out.

Gradient Measurements

A fixed-length input coupler installed in one of the cleaning ports was used for both tests. The 325 MHz single-spoke cavity was calibrated to have a Q_{ext} of 6×10^9 while that of the 500 MHz double-spoke cavity was 1×10^{10}. In both cases, the pickup probe Q_{ext} was roughly 2×10^{11}.

The initial tests of the 325 MHz single-spoke cavity exhibited soft multipacting barriers which were predicted quite accurately by TRACK3P (within the SLAC ACE3P code suite [5]). Below 2.5 MV/m, strong multipacting was expected and it was indeed observed, as shown in Fig. 1. After a relatively short amount of processing, it was found that these barriers could be eliminated.

* Work supported by U.S DOE Award No. DE-SC0004094
† chopp002@odu.edu

ISBN 978-3-95450-142-7

Copyright © 2014 CC-BY-3.0 and by the respective authors

QUASI NONLINEAR PLASMA WAKEFIELD ACCELERATION EXPERIMENTS

S. K. Barber, G. Andonian, B. D. O'Shea, J. B. Rosenzweig, Y. Sakai, O. B. Williams, UCLA, Los Angeles, CA 90095,USA
M. Ferrario, INFN/LNF, Frascati, Italy
P. Muggli, MPI, Munich, Germany

Abstract

It is generally agreed that the best way forward for beam driven plasma wakefield acceleration (PWFA) is in the nonlinear or blowout regime. In this regime the expulsion of the plasma electrons from the beam occupied region produces a linear transverse focusing effect and position independent longitudinal accelerating fields, which can, in principle, produce high quality beams accelerated over many meters. However, certain aspects of a linear plasma response can be advantageous, such as the possibility for resonant excitation of wakefields through the use of pulse trains. Exploiting advantages of both linear and nonlinear PWFA may be achievable through the use of low emittance and tightly focused beams with relatively small charge. In this case the beam density can be greater than that of the ambient plasma while simultaneously having a smaller total charge than the plasma electrons contained in a cubic plasma skin depth allowing for blowout in the region of the beam while simultaneously maintaining a quasi linear response in the bulk plasma. Recent experiments at the Accelerator Test Facility at Brookhaven National Lab have been aimed at probing various salient aspects of this regime and are presented here.

INTRODUCTION

Plasma based acceleration schemes promise to revolutionize the field of accelerator physics in a way that would permit a continued push into the high energy frontier as a well as provide a path to the development novel radiation sources such as a compact XFELs. With a wide variety of technical and physical challenges, there is much theoretical and experimental work devoted to optimizing such schemes. Generally speaking, the focus is on operations in the nonlinear regime, which provides a conceptually neat way of accelerating beams at high gradients while preserving high quality phase spaces. There are, however, certain aspects of the linear regime that would prove useful in many instances; namely, the ability to resonantly excite the wakefields.

The quasi nonlinear regime [1] provides a delicate compromise between the two regimes, allowing for blowout and accompanying ideal accelerating and focusing fields without the expense of a plasma response which can be driven resonantly. In this regime, the beam density exceeds that of the ambient plasma leading to blowout. At the same time, the normalized charge, defined as $\tilde{Q} \equiv N_b k_p^{\,3} / n_0$ (where N_b is the total number of beam electrons, k_p is the plasma wavenumber and n_0 is the plasma density) is kept below one. A low $\tilde{Q}$ mitigates strong nonlinear effects such as wavebreaking and amplitude dependent periodicity of the wake. While simulations have demonstrated the feasibility of operating in this regime, there is to date little experimental evidence.

Recently, an experimental program at the Accelerator Test Facility at Brookhaven National Lab (ATF BNL) has begun[2]. The aim of these experiments is to verify certain aspects of the quasi nonlinear regime. In particular, the goals of these experiments are twofold: using electron pulse trains observe resonant wakefield excitation and observe strong focusing/guiding of a matched pulse train through the plasma. The latter will be the focus of the present paper.

EXPERIMENTAL RESULTS

The ATF at BNL is well suited for this experiment as a number of beam-plasma interaction experiments have already been performed there [3-5]. Furthermore, they have demonstrated a masking technique to generate electron pulse trains with adjustable separations [6]. These experiments, however, have been always been performed with $n_b << n_0$. In order to perform experiments in the QNL regime the focusing capabilities at ATF need to be augmented to get transverse beam sizes on the order of a few microns instead of ~100 microns, increasing the beam density by a factor of ~400.

Accordingly, a permanent magnet quadrupole triplet was installed [7]. With an effective focal length of ~8 cm at 60 MeV and assuming a typical normalized emittance for ATF of 2 mm-mrad, it is reasonable to anticipate RMS transverse spot sizes of ~5 microns. Combined with a peak current of ~100 A, these beams will have densities with $n_b \geq 2\times10^{16}$ cm^{-3}. Beyond simply making small spot sizes at the interaction point, it is desirable to match the beam to the plasma, which for a 10^{16} cm^{-3} requires a beta function of ~1 mm.

In order to measure these electron beam parameters, a high-resolution optical transition radiation (OTR) imaging system is used. This system includes a 10 micron Ti foil placed in the focal plane of a Schwarschild objective. The collected light is directed out of vacuum to a CCD with an imaging lens providing 2 micron resolution. The objective and foil are mounted to a longitudinal stage making it possible to image the transverse spot size over a range of 50 mm along the beam path, more than sufficient to

Copyright © 2014 CC-BY-3.0 and by the respective authors

SwissFEL C-BAND LLRF PROTOTYPE SYSTEM

A. Hauff, M. Brönnimann, I. Brunnenkant, A. Dietrich, F. Gärtner,
Z. Geng, M. Jurcevic, R. Kalt, S. Mair, A. Rezaeizadeh, L. Schebacher,
T. Schilcher, W. Sturzenegger, PSI, Villigen, Switzerland

Abstract

The SwissFEL is driven by more than 30 RF stations at different frequencies (S-, C-, X-band). To control the RF a new, in-house developed digital Low Level RF (LLRF) system measures up to 24 RF signals per station and performs a pulse-to-pulse feedback at a repetition rate of 100 Hz. The RF signals are down-converted to a common intermediate frequency. The state-of-the-art digital processing units are integrated into the PSI's EPICS controls environment. Emphasis has been put on modularity of the system to provide a well-defined path for upgrades. Thus the RF front-ends are separated from the digital processing units with their FMC standard interfaces for ADCs and DACs. A first prototype of the LLRF system consisting of the digital back-end together with a C-band RF front-end was installed in the SwissFEL C-band test facility.

In this report the performance of the prototype system has been compared with the LLRF system requirements for SwissFEL. The critical parameters are high intra-pulse phase and amplitude resolutions, good channel-to-channel isolations, very low phase-to-amplitude modulation and a negligible temperature drift.

INTRODUCTION

SwissFEL is a free-electron X-ray source where 5.8 GeV are required for laser wavelengths down to 1 Å. In its baseline design two electron bunch will be accelerated within one RF pulse. The electron bunch length will be 25 fs (rms) and the spacing between them amounts 28 ns [1].

The Low Level Radio Frequency (LLRF) system is designed to control one RF station. Depending on the location along the machine the LLRF system controls the accelerating fields of up to 4 RF structures. The modular system consists of a common digital processing unit and a frequency dependent RF front-end which converts the different RF frequencies to a common intermediate frequency (IF). A first prototype system was developed with an RF front-end at C-band frequency.

Table 1: SwissFEL RF parameters

Parameter	Value
C-band frequency:	5.712 GHz
Repetition rate:	100 Hz
RF pulse length:	0.02 – 5 µs
Amplitude stability:	1.8e-4 rel. (rms)
Phase stability:	0.036 deg (rms)
Channel-to-channel drift:	0.1 deg / day

Figure 1 shows the topology of one C-band RF station where the reference RF signal is modulated by a vector modulator, amplified by one klystron and fed into four C-band accelerating structures. The input signal before and after the structure is measured and a vector sum is calculated which is required for a pulse-to-pulse feedback.

The RF tolerances for a C-band RF station are summarized in Table 1. The phase tolerances can be divided into the individual components by assuming that the jitter contribution is uncorrelated and equally distributed amongst the subsystems (vector modulator, pre-amplifier, klystron):

$$(\sigma_\phi)_{vecMod} = (\sigma_\phi)_{preAmp} = (\sigma_\phi)_{kly} = \sqrt{((\sigma_\phi)^2_{total} - (\sigma_\phi)^2_{ref.})/3}$$

For the C-band system the phase tolerance of the vector modulator results in a phase tolerance of the vector modulator of 0.017 deg (rms).

LLRF SYSTEM

The modular 24-channel LLRF system can be split in three groups of components: analog front-end, data converter and digital back-end. The advantage of this modular approach is the well-defined upgrade possibility of individual sub-systems. It also provides flexibility for troubleshooting.

Analog Front-End

The analog front-end consists of a vector modulator, a local oscillator (LO), clock generation, and a multi-channel down-converter. Their design is mainly driven by the required space for the components. The circuit for LO and clock generation and the vector modulator are placed in one 19" chassis with a height of one rack unit while the multi-channel down-converters are placed in a separate 19" chassis. An optical reference system with an optical-to-electrical converter node placed in the LLRF rack will provide a 5712 MHz reference input signal with an integrated jitter of less than 10 fs (10 Hz – 10 MHz).

In the LO unit, the reference signal is divided by 144 to result in the desired intermediate frequency (IF) of 39.667 MHz, which is then mixed with the 5712 MHz reference signal. The extraction and amplification of the upper mixing product provides the required LO signal of 5751.667 MHz at +10 dBm. Along the frequency divider chain the ADC and DAC clock signals of 238 MHz (24th sub-harmonic) are extracted.

Copyright © 2014 CC-BY-3.0 and by the respective authors

ISBN 978-3-95450-142-7

STUDY OF A C-BAND TW ELECTRON GUN FOR SwissFEL

M. Schaer *, A. Citterio, P. Craievich, L. Stingelin, R. Zennaro
Paul Scherrer Institut, 5232 Villigen, Switzerland

Abstract

For a future upgrade of the SwissFEL facility, the replacement of the S-band standing wave electron gun by a C-band standing wave, or traveling wave gun is investigated. The full model of the C-band TW gun is calculated with HFSS and is characterized by an almost vanishing group velocity in the first cell to increase the field at the cathode. ASTRA simulations predict that in the case of the C-band SW gun, a two times higher peak current of ~ 40 A can be generated while still preserving the low normalized slice emittance of ~ 0.2 μm at 200 pC, due to the higher electric field on cathode and improved magnetic focusing. This would help to halve the overall beam compression factor, relax the phase stability requirement of S- and X-band systems operated off-crest for compression and decrease the gain curve in the micro bunch instability. Compared to the SW gun, a TW gun provides a more homogeneous acceleration and does not require any circulator. In this study, the preliminary RF design and beam performance of a C-band TW gun is presented and compared to a pure C-band SW gun presently under design at Paul Scherrer Institut and to the operating S-band SW gun.

INTRODUCTION

The baseline design of the SwissFEL injector [1] foresees a 2.6-cell S-band standing wave (SW) gun as electron source. Recent studies [2] have shown the potential of a 5.6-cell C-band SW gun to double the transverse brightness at the end of the injector. One drawback of SW guns is the need for a high power circulator in order to protect the klystron from the reflected power. Unfortunately, such C-band circulators are commercially not available yet and their design can not be solved with a straightforward rescaling of the device [3]. However, if a traveling wave (TW) gun with a similar performance as that of a conventional SW gun can be designed, the need for a circulator is eliminated, representing an important advantage for the technical realization of the device.

In this paper the feasibility and several advantages of this approach are demonstrated by presenting a preliminary RF design with the corresponding beam dynamics simulations. In particular, the presented design shows the potential of having a very short filling time in the order of 40 ns. Considering in addition that the maximum surface electric field at the iris is smaller than that at the cathode due to the TW nature of this design, the maximum achievable accelerating gradient at the cathode can potentially increase compared to a SW solution.

* mattia.schaer@psi.ch

RF DESIGN

The main motivations for designing a gun in C-band for the SwissFEL injector are the confidence with the C-band technology being developed at PSI and the higher gradient which can be achieved at higher frequencies.

In this paper, the feasibility of an injector based on a photo-cathode RF TW gun is adressed. Fig. 2 shows the electric field computed by HFSS for the full cavity model composed by one coaxial input coupling cell containing the cathode, 18 regular cells with 60° phase advance and one coaxial output coupling cell. The main RF parameters of the cavity are summarized in Tab. 1. The on-axis longitudinal electric field $|E_z|$ of this TW gun as compared to that of a SW gun [2] is also plotted (Fig. 2, bottom). Furthermore, a zoom of the cathode region is provided (top right) to show an off-axis field enhancement at the cathode of 20 %, which still represents an open issue to be improved.

Table 1: RF Cavity Parameters.

Frequency f_0	5.712 GHz
Phase advance / cell $\Delta\phi$	60°
Regular cell length L_c (1)	8.7 mm
# of cells	20
RF Length L	~ 180 mm
Filling time τ_L	39 ns
Group velocity v_g	$0.015 \cdot c$
Q (2)	5720
R/Q (2)	9128 Ω/m
Nominal cathode gradient	135 MV/m
Nominal input power	120 MW
Cavity attenuation S_{21}	1.06 dB

(1) $\lambda_0 = c/f = 52.485$ mm.

(2) From the eigenmode solution with losses of the regular cell.

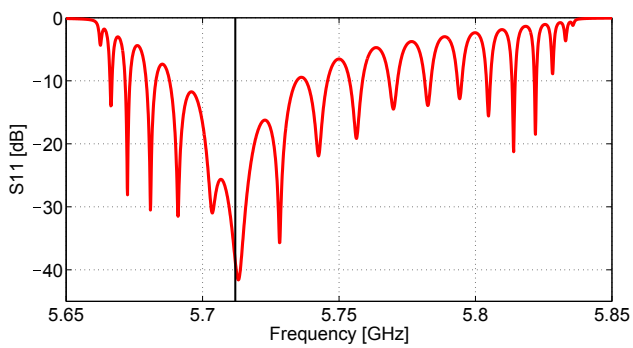


Figure 1: RF frequency spectrum of the TW gun of Fig. 2. The operating American C-band (5.712 GHz) is indicated.

Copyright © 2014 CC-BY-3.0 and by the respective authors

HIGH RF POWER TEST OF COUPLED RFQ-SFRFQ CAVITY*

W. L. Xia, Z. Wang#, Y. R. Lu&, K. Zhu, J. Zhao, F. J. Jia, S. L. Gao, J. E. Chen,
IHIP, SKLNPT, Peking University, Beijing, China

Abstract

A new combined accelerator that couples radio frequency quadrupole (RFQ) and separated function radio frequency quadrupole (SFRFQ) in a single cavity has been designed and manufactured. Recently, the performance of the cavity under high RF power was tested with an upgraded RF power source. The inter-vane voltages of both RFQ section and SFRFQ section were measured by using high purity germanium detector and the corresponding measurement system. The measured shunt impedance is about 546.9 kΩ·m, which means the cavity needs 19.5 kW for the designed inter-vane voltage of 65 kV. The results are well consistent with the cavity design.

INTRODUCTION

Based on the simulations and experiments of the former ISR-1000 RFQ and SFRFQ structure [1-4], we have been exploring the feasibility of coupling the two different structures in a single cavity. The coupled structure combines both the advantage of RFQ for better beam acceptance of low energy ions and the advantage of SFRFQ for higher accelerating efficiency, and will significantly shorten the length of the accelerator for the same beam energy gain in RFQ. The beam matching between RFQ and SFRFQ were realized and shown in the dynamic analysis [5] not only for the transverse emittance also for the longitudinal synchronous phase and beam energy. Thus, the coupled RFQ-SFRFQ (CRS) cavity can accelerate 5 mA He^+ beam from 7.5 keV/u to 201.2 keV/u in 2.5 m cavity. Fig. 1 shows the schematic drawing of the CRS linac [6]. The design parameters of CRS cavity are listed in Table 1.

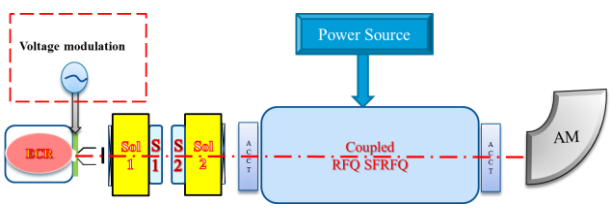


Figure 1: Layout of CRS linac.

Recently, the CRS cavity has been manufactured and tested under low RF power. Based on the measured RF features of the cavity, such as frequency, Q value and electric field distributions, we adjusted the conditions of an upgraded RF power source and set up a measurement system for high RF power test of CRS cavity.

*Work supported by NSFC, Grant No. 11075008, 11079001 and 11175009.
#wangzhi@pku.edu.cn;
&yrlu@pku.edu.cn

Table 1: Main Design Parameters of CRS Cavity

	RFQ	SFRFQ
Frequency (MHz)	25.5	25.5
Inter-vane Voltage (kV)	65	65
Current (mA)	5	5
Duty Factor	1/6	1/6
Input Energy (keV/u)	7.5	105.7
Output Energy (keV/u)	105.7	201.2
Cells Number	33	10
Length (m)	1.48	1.00

CRS STRUCTURE

Because of the low operating frequency, four-rod structure in RFQ section was adopted. The two sections use the same shape supporting rings, considering the capacitance between SFRFQ electrodes is larger than that between RFQ electrodes, we have shortened the distance between the supporting rings in SFRFQ section to maintain the similar RF features of the two sections. Based on the electromagnetic simulation and optimization, the final structure was determined. The cavity has been manufactured and assembled as shown in Fig. 2, the electrodes connect to 14 supporting rings, the eight for the RFQ and another six for the SFRFQ section. The transition region, where RFQ electrodes directly connect to SFRFQ electrodes, should maintain good electrical conductivity so that the two sections will be resonated in the single cavity.

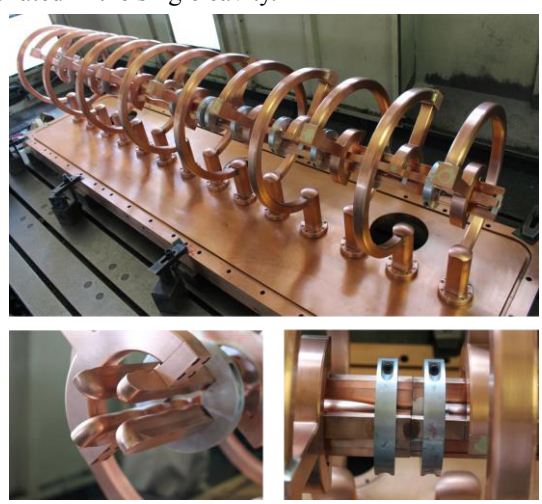


Figure 2: Structure of CRS cavity.

Copyright © 2014 CC-BY-3.0 and by the respective authors

STATUS OF THE FERMI II RF GUN AT SINCROTRONE TRIESTE

L. Faillace#, R. Agustsson, P. Frigola, A. Verma
Radiabeam Technologies LLC, Santa Monica CA, USA

Abstract

Radiabeam Technologies, in collaboration with UCLA, presents the development of a high gradient normal conducting radio frequency (NCRF) 1.6 cell photoinjector system, termed the Fermi Gun II, for the Sincrotrone Trieste (ST) facility. Designed to operate with a 120MV/m accelerating gradient, this single feed, fat lipped racetrack coupler design is modeled after the LCLS photoinjector with a novel demountable cathode which permits cost effective cathode exchange. Full overview of the project to date, installation, high-power RF conditioning and initial electron beam emittance measurements at Sincrotrone Trieste will be discussed along with basic design, engineering and manufacturing.

INTRODUCTION

Radiabeam is currently involved in the development of new technology aimed at high average power operation for a NCRF electron gun system, the FERMI II RF Gun, for the Sincrotrone Trieste facility operating at the frequency of 2.99801GHz.

The gun design was originally based on the UCLA-University of Roma-INFN-LNF [1] high repetition rate photoinjector for SPARX project, which was based on the LCLS [2,3] version and using a larger radius of curvature in the rounding of the input coupler irises, and by including an enhanced cooling channels system in the most highly dissipative regions in the structure. This basic design was re-optimized by request of ST to use a replaceable cathode for easy exchange of different material samples with a repetition rate >50Hz.

RF GUN DESIGN

The RF design of the Gun has been performed by using the codes SuperFish [4] and HFSS [5]. Figure 1 shows half structure of the RF gun with surface electric field distribution calculated by HFSS. RF power is fed through one waveguide only (top one); the waveguide located 180deg. opposite the input one, a dummy waveguide, forbids the propagation of the electromagnetic field that is below its cutoff value (i.e. the dummy waveguide has a width much smaller than the input one). The main purpose of the second waveguide is to cancel the field dipole component.

faillace@radiabeam.com

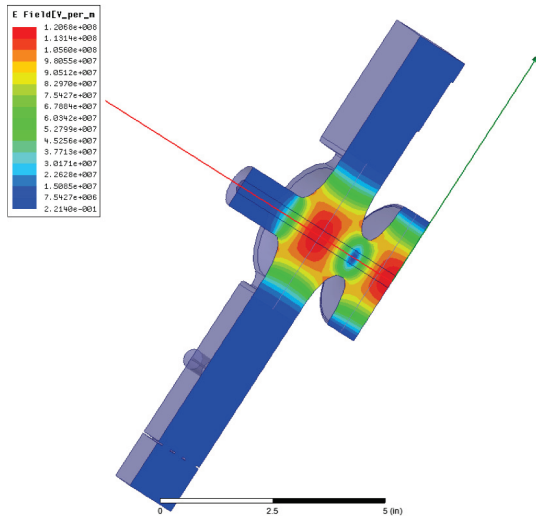


Figure 1: 3D model used for HFSS simulation. Surface electric field is shown.

Cell Design

The RF cavity shape, as proposed, has several innovative electromagnetic features, including Z-coupling and enhanced cell-to-cell coupling to produce higher mode separation, elliptical irises to reduce surface electric field, symmetric couplers for dipole mode minimization, racetrack geometry to minimize quadrupole field components. In contrast to the LCLS gun, which has these features, it is externally fed only by one side, avoiding the need of a power splitter and making the whole assembly much more compact, easier to handle and cost efficient.

In order to calculate the maximum surface electric field, we normalize the on-axis field to 120 MV/m at the cathode. The peak field on the iris is found to be 102 MV/m, below the breakdown safety threshold.

Per usual procedure, a first pass on the RF design was made with SUPERFISH and then HFSS was used to provide a complete picture of the RF performance, including mode frequencies, field balance, quality factor *Q,* shunt impedance and external coupling.

The design parameters achieved in simulation through this process are summarized below in Table 1.

Copyright © 2014 CC-BY-3.0 and by the respective authors

COMMISSIONING OF VERTICAL TEST STAND FACILITY FOR 2 K TESTING OF SUPERCONDUCTING CAVITIES AT RRCAT

S. C. Joshi, S. Raghvendra, S. Suhane, M. Kumar, P. Mohania, A. Chauhan, P. Fatnani, P. Shrivastava, P. K. Kush and P. D. Gupta, Raja Ramanna Centre for Advanced Technology, Indore, INDIA

Abstract

Raja Ramanna Centre for Advanced Technology (RRCAT) has developed a 2K vertical Test Stand (VTS) facility for characterization of Superconducting RF (SCRF) cavities, under Indian Institution Fermilab Collaboration (IIFC). The VTS is used for qualifying bare SCRF cavities for their required performance by measuring quality factor and cavity accelerating gradient at a cryogenic temperature of 2 K. The VTS facility comprises of a large size liquid helium (LHe) cryostat, cryogenic system, RF power supply, control and data acquisition system and radiation monitoring system. It will facilitate testing of superconducting cavities of different frequencies ranging from 325 MHz low beta to 650 MHz / 1.3 GHz medium and high beta cavities. The helium vessel has an inner diameter of 923 mm and an overall depth of 4860 mm with a capacity to store up to 2900 litres of liquid Helium. The engineering design and fabrication of VTS cryostat was carried out in accordance with ASME B&PV code.

The cryostat is installed inside a vertical pit in the cryogenic test building. It is equipped with facilities for supply of liquid nitrogen and liquid helium and vacuum system for pumping out helium gas to lower the temperature of liquid helium bath down to 1.8 K. A 500 W, 1.3 GHz RF system has been indigenously developed to supply required CW power for testing of the SCRF cavities. The VTS facility has now been commissioned and its performance validation has been successfully carried out by benchmarking it with respect to the facility at the Fermilab, USA.

INTRODUCTION

The VTS facility at RRCAT is designed to test superconducting cavities ranging from 325 MHz low beta to 1.3 GHz/ 650 MHz medium and high beta cavities at their operating frequencies in a 2K LHe bath [1]. The cryostat can accommodate six 1.3 GHz nine-cell cavities or two 650 MHz five-cell cavities in a single cool down. Presently, a 40 litres/hour capacity liquid helium plant is being utilized for testing of cavities. The facility will be upgraded with a new plant with a liquefaction rate of 145 litres/ hour by the end of this year [2]. The VTS cryostat assembly is installed below the ground level in a pit. A 500 W, 1.3 GHz RF system along with its low level RF (LLRF) control & data acquisition system has been developed for testing of the SCRF cavities. A system of radiation shielding comprising of internal radiation shield and movable external radiation shielding lid shall ensure that ionizing radiation exposure levels are maintained below prescribed levels.

MAJOR SYSTEMS OF VTS FACILITY

VTS Cryostat and Insert Assembly

VTS cryostat assembly comprises of an ASME Code stamped stainless steel liquid helium vessel (LHe) suitable for 2K liquid helium and suitable process tubing for flow of liquid helium & liquid nitrogen. The helium vessel and tubing are thermally shielded with a LN2 cooled thermal shield to reduce the cryostat's overall static heat load at 2K. The assembly of LHe vessel and thermal shield is housed in a stainless steel insulating vacuum vessel. The cryostat has an overall dimension of diameter 1370mm and length of 5420mm. A schematic of the cryostat assembly is shown in Figure 1.

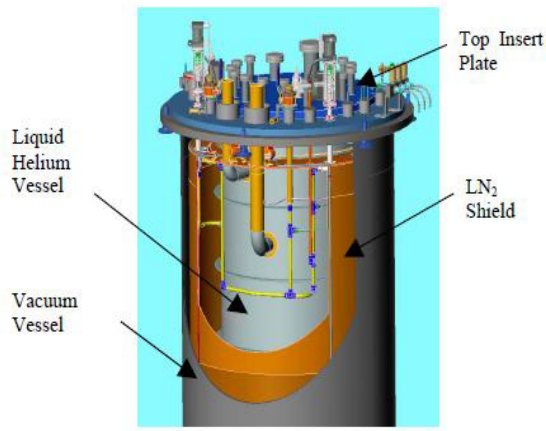


Fig 1. Schematic of VTS Cryostat Assembly

The VTS insert assembly supports the cavity in the liquid helium bath during the RF testing and provides penetrations for RF cables, diagnostics, vacuum line etc. It also provides thermal shielding for the liquid helium bath.

The engineering design of the cryostat was carried by RRCAT in collaboration with Fermilab [3]. Fabrication of the cryostat vessels was carried out by an US based vendor in strict accordance with ASME BP&V code under joint supervision of engineers from RRCAT and Fermilab [4].

Magnetic Shielding

To avoid trapping of magnetic flux which may degrade the SRF cavity quality factor, the cavity must be

Copyright © 2014 CC-BY-3.0 and by the respective authors

ISBN 978-3-95450-142-7

DESIGN STUDIES FOR MEDIUM AND HIGH BETA SCRF CAVITIES FOR INDIAN SPALLATION NEUTRON SOURCE*

Arup Ratan Jana and Vinit Kumar#
Materials and Advanced Accelerator Sciences Division
RRCAT, Indore 452013, India

Abstract

There is a plan to build a 1 GeV H- linac for the proposed Indian Spallation Neutron Source (ISNS) at Raja Ramanna Centre for Advanced Technology (RRCAT), Indore. The medium and high energy section of the ISNS linac will consist of $\beta_g = 0.61$, as well as $\beta_g = 0.9$, 650 MHz, 5-cell superconducting radiofrequency (SCRF) cavities, for which detailed design studies have been performed. During our design study, we have evolved a generalized procedure for the optimization of geometrical parameters of multi-cell elliptic SCRF cavities. Studies on higher order modes supported by the cavity, and its effect on beam dynamics, as well as on cryogenic heat load have been performed. Finally, studies have been performed to minimize the effect of Lorentz Force Detuning (LFD). The paper discussed these calculations and initial beam dynamics studies.

INTRODUCTION

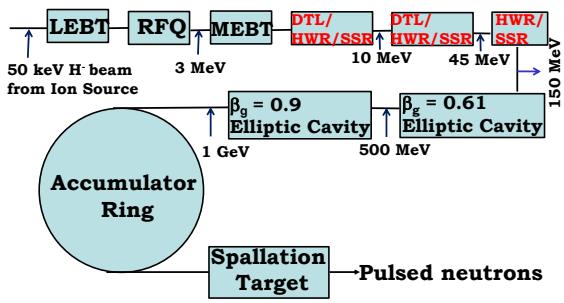


Figure 1: A schematic of the accelerator for ISNS.

It is proposed to build a spallation neutron source at Raja Ramanna Centre for Advanced Technolgy (RRCAT) in India for experimental studies of condensed matter physics and various engineering applications [1]. A schematic configuration of the injector linac and the accumulator ring that will produce ~ 1 μs pulses of 1 GeV proton beam is shown in Fig. 1. Physics design studies of various accelerators and beam transport lines have commenced at RRCAT. In this paper, we describe our recent design studies of Superconducting Radiofrequency (SCRF) cavities. Operating frequency of the SCRF cavities is chosen as 650 MHz in order to utilize the indigenously developed solid state RF power sources at this frequency. Based on the calculations of transit time factor in the operating range of beam energies, for different values of geometric beta (β_g) of cavities, we have opted for two families of SCRF cavities: 5-cell, $\beta_g = 0.61$ cavities to accelerate the particles from 150 MeV to 500 MeV, followed by 5-cell, $\beta_g = 0.9$ cavities to further accelerate the particles to 1 GeV. In the next section, we describe the electromagnetic design of SCRF cavities. This is followed by discussion of Lorentz Force Detuning (LFD) studies and initial results of beam dynamics studies.

*Work supported by Department of Atomic Energy, Govt. of India
#vinit@rrcat.gov.in

ELECTROMAGNETIC DESIGN STUDIES

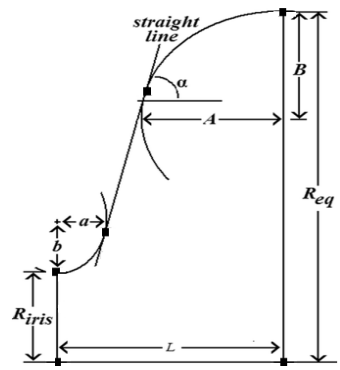


Figure 2: Schematic of the half-cell of an elliptic cavity.

We first discuss the optimization of the geometrical parameters of an SCRF cavity. Figure 2 shows the cross section of the half-cell, which is obtained by joining two elliptical arcs by a common tangent, and is described by seven parameters – iris ellipse radii a and b, equator ellipse radii A and B, iris radius R_{iris}, equator radius R_{eq}, and half-cell Length L. Since the cavity operates in π mode, $L = \beta_g\lambda/4$, where λ is the free space wavelength corresponding to the operating RF frequency. Choice of R_{iris} is made to ensure that it is just enough to provide the required cell-to-cell coupling, while not affecting the shunt impedance significantly. The maximum feasible value is chosen for the cavity wall angle α since it results in reduced heat loss on the cavity wall. In our design, these values are 85° and 88° for $\beta_g = 0.9$ and 0.61 cavities respectively. The required resonant frequency is achieved by tuning R_{eq}. The remaining three independent geometrical parameters are optimized to minimize the value of E_{pk}/E_{acc} and B_{pk}/E_{acc}, where E_{pk} and B_{pk} are the peak electric and magnetic fields respectively on the cavity surface, and E_{acc} is the average acceleration gradient in the cavity. In our generalized design procedure, we first put the constraint $a/b = A/B = 1$, and plot E_{pk}/E_{acc} and B_{pk}/E_{acc} as a function of B, as shown in Fig. 3, using the computer code SUPERFISH [2]. The

Copyright © 2014 CC-BY-3.0 and by the respective authors

ISBN 978-3-95450-142-7

COMISSIONING OF BNP INJECTION COMPLEX VEPP-5

P.Logatchev, A.Levichev, A.Starostenko, D. Nikiforov, F.Emanov, Y.Maltseva, A.Petrenko, D. Bolkhovityanov, I. Pivovarov, K. Astrelina, A. Makeev BINP, Novosibirsk, RUSSIA.

Abstract

The VEPP-5 Injection Complex [1] will supply BINP RAS colliders with electron and positron beams. Primary launch have been performed: electron and positron beams were obtained, injection to damping ring have been done, as well as storage of electrons and positrons. Now both transport channel to the electron/positron colliders VEPP-2000 and VEPP-4M are fully assembled and therefore test extractions of electron beam with energy of 360 MeV into beam lines to users are being performed. Main users require a reliable and trouble proof source of particles, thus reliability and stability of operation are a paramount tasks.

INTRODUCTION

VEPP-5 Injection Complex consists of 270 MeV driving electron linac, 510 MeV positron linac and dumping ring (See Fig.1). Both linear accelerators are based on four accelerating modules, each one feeds by one SLAC klystron (5045). Two first modules have three accelerating structures and second two — four structures. First accelerating structures of both linacs have an enhanced average acceleration gradient of 20 MeV/m and other regular sections up to 17–20 MeV/m. Both linacs can operate up to 50 Hz repetition rate. Dumping ring stores and cools down both electron and positron beams (See Figure 3). It is equipped by 50 Hz injection system.



Figure 2: Linear accelerators

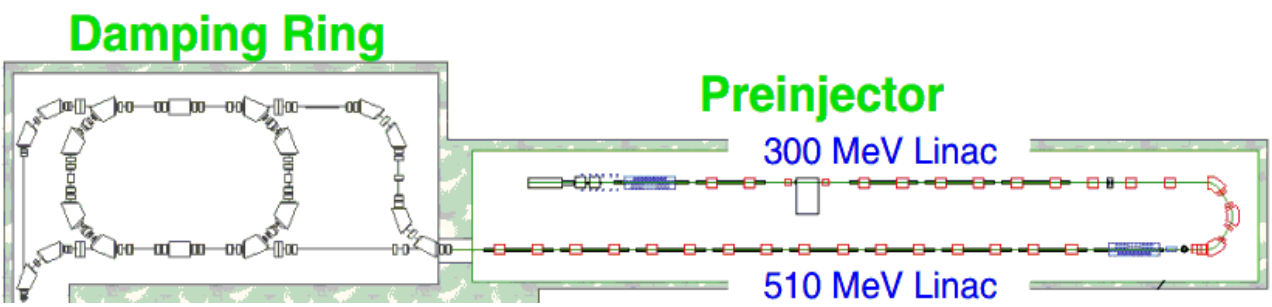


Figure 1: Injection complex



Figure 3: Damping ring

Table 1: Designed Parameters of Injection Complex

Maximum Beam Energy (MeV)	510
Max. number of electrons in the beam	$2 \cdot 10^{10}$
Max. number of positrons in the beam	$2 \cdot 10^{10}$
Energy spread in the beam (%)	0.07
Longitudinal beam sigma (mm)	4
Vertical emittance (mm mrad)	0.005
Horizontal emittance (mm mrad)	0.023
Dumping times vert./horis. (ms)	17/11
Extraction rate (Hz)	1

Designed parameters of VEPP-5 Injection Complex are presented in Table 1. At the parameters listed above Injection Complex will be able to cover all needs of BINP e+ e- colliders for nearest future. This will greatly improve the VEPP-2000 and VEPP-4M performance, because of significant increase of positron production rate and will help to reach their maximum luminosity of these colliders.

Copyright © 2014 CC-BY-3.0 and by the respective authors

ISBN 978-3-95450-142-7

LIMITATIONS FOR ACCELERATION OF INTERMEDIATE MASS PARTICLES WITH TRAVELLING WAVE STRUCTURE

V. Paramonov *, INR of the RAS, Moscow, 117312, Russia

Abstract

The Disk Loaded Waveguide (DLW) is the mostly used high frequency structure for acceleration of lightweight particles electrons in the high energy range. DLW parameters are considered for the lower frequency range and lower particle velocity. Physical and technical restrictions for DLW application for the low particles velocity are analyzed. Basing on particularities of acceleration with traveling wave, deep optimization of DLW cells dimensions, the choice of optimal operating phase advance for each DLW section and combination of forward and backward wave modes, it looks possible to create the simple, cost effective acceleration system for intermediate particles acceleration in the moderate velocity range, in some parameters overcoming accelerating system with RF cavities in the standing wave mode.

INTRODUCTION

Due to relative simplicity of manufacturing and sufficient RF efficiency DLW is widely used for acceleration of electrons with $\beta \approx 1$ and the structure is well studied for this case. But the same features stimulate consideration of DLW application for acceleration of more heavy particles - muons and protons. For this task DLW parameters should be considered for lower β and for different modes of operation to define the technical and the physical limitations for DLW application.

DLW PARAMETERS

The distribution of the longitudinal electric field E_z in the DLW aperture for Travelling Wave (TW) operation is the sum over spatial harmonics, [1]:

$$E_z(r,z) = \sum_{-\infty}^{+\infty} E_n I_0(k_{sn} r) e^{-ik_{zn}z}, k_{zn} = \frac{\theta + 2n\pi}{d_p}, \quad (1)$$

$$k_{sn}^2 = k_{zn}^2 - k^2, k = \frac{2\pi}{\lambda},$$

$$d_p = \frac{\beta\lambda\theta}{2\pi}, n = 0, \quad d_p = |\frac{\beta\lambda(\theta - 2\pi)}{2\pi}|, n = -1.$$

where E_n is the amplitude of the n-th spatial harmonic, $I_0(k_{sn}r)$ is the modified Bessel function, λ and θ are the operating wavelength and the operating phase advance, β is the particle velocity. The length of the cell d_p is defined from the synchronism with appropriate spatial harmonic.
Usually the main harmonic $n = 0$ is used for acceleration. This case DLW has a positive dispersion and operates in Forward Wave (FW) TW mode. Acceleration with the first nearest spatial harmonic $n = -1$ is also possible. There are a lot of papers with proposals, but for $\beta \sim 1$ it loses in RF efficiency, because $|E_0| > |E_{-1}|$. Until now just one practical application, using DLW with the first harmonic $n = -1$ is known with the interesting results for particles focusing, [2]. Such case DLW operates in Backward Wave (BW) TW mode and has a negative dispersion.

Parameters of the DLW structure were calculated and

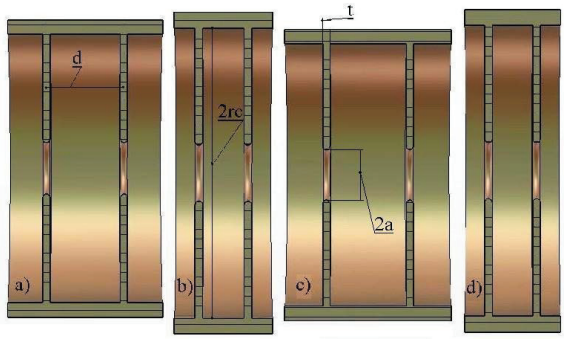


Figure 1: The DLW geometry for FW operation $\beta = 0.90, \theta = 90^0$, (a), $\beta = 0.41, \theta = 120^0$, (b) and BW operation, $\beta = 0.41, \theta = 120^0$, (c), $\beta = 0.20, \theta = 120^0$, (d).

stored in the data library in the same procedure, as described in [3] by using fast and precise 2D FEM codes. Examples of the considered shapes of DLW cells are shown in Fig. 1 for different β and θ combinations. For more details of the data library storage see [4]. Simulations of the DLW parameters were performed assuming the L-band operating frequency $f_0 = 1296MHz$ and for another f_0 value parameters can be recalculated by using well known scaling relations.
The magnitude of the n-th spatial harmonic E_n is related with the flux of RF power P_t as:

$$\frac{E_n}{\sqrt{P_t}} = \sqrt{\frac{2\pi Z_{en}}{\lambda|\beta_g|Q}} \sim f_0, \quad (2)$$

$$Z_{en} = \frac{|\int_{d_p} E_z(0,z)e^{ik_{zn}z}dz|^2}{P_s d_p} \sim f_0^{\frac{1}{2}},$$

$$\alpha = \frac{\pi}{\lambda|\beta_g|Q} \sim f_0^{\frac{3}{2}},$$

where Z_{en} is the value of the effective shunt impedance per unit of length for the n-th harmonic, P_s is the power of RF losses in the cell surface and α is the attenuation.
The main parameter for the DLW structure is the group velocity β_g, which depends mainly on the aperture radius a

* paramono@inr.ru

ISBN 978-3-95450-142-7

Copyright © 2014 CC-BY-3.0 and by the respective authors

ROUGHNESS TOLERANCES IN THE UNDULATOR VACUUM CHAMBER OF LCLS-II*

K.L.F. Bane§, G.V. Stupakov, SLAC, Menlo Park, CA 94025, USA

INTRODUCTION

When a bunch passes through the LCLS-II undulator, the wakefields induced in the vacuum chamber will add energy variation along the bunch, which can negatively impact the FEL performance. The wakefield of the vacuum chamber is primarily due to the resistance of the walls and the roughness of the surface. To minimize the impact of the wakes, one would like a wall surface smooth enough so that the roughness component of the wake is a small fraction of the total wake. In LCLS-I, with an undulator chamber of the same material (aluminum) and of roughly the same aperture, the roughness tolerance specified as an rms slope of the surface, $(y')_{rms}$ = 10–15 mr, was difficult to achieve [1]. The goal of the present study is to understand the consequences to LCLS-II of loosening the roughness specification by a factor of two to 30 mr.

The vacuum chamber within the undulator of LCLS-II will be primarily extruded aluminum with a racetrack cross-section: the aperture can be described as a rectangle of 12 mm by 5 mm (x by y), with added semicircular sides. (In addition, there are short breaks at the quads with a different shape and a larger aperture.) The impedance is essentially the same as for two parallel plates separated vertically by a distance of 5 mm. In this note we calculate the total wake effect of the resistive wall plus a model of roughness. The roughness model we use consists of small, shallow, sinusoidal corrugations [2]. We choose this model because measurements of samples of polished aluminum, similar to that to be used for the undulator chamber, find that the typical roughness is shallow [3]. Note that this model does not generate a so-called "synchronous mode" wake, which applies in the case of small *steep*, periodic corrugations [4, 5].

The calculation of the short-range wake of a resistive pipe has been done before [6], as has the case of a pipe with small, shallow corrugations [7]; in this report we properly combine the two effects. We first consider a round model of the chamber aperture, and then move to the flat geometry. Selected beam and machine properties in the undulator region of LCLS-II, that are used in our calculations, are given in Table I. The bunch charge, Q = 300 pC, is the largest charge envisioned. For the nominal case, Q = 100 pC, the current will also be uniform with I = 1 kA. More details can be found in Ref. [8].

ROUND VACUUM CHAMBER

Consider a round chamber of radius a, with wall resistance and small (in amplitude), shallow sinusoidal corrugations that represent the wall roughness. While in some cases the beam impedance can be calculated as a sum of the impedances due to resistance and that due to wall roughness, in general such summation of impedances is not correct. A more general approach is based on the concept of surface impedance [9] defined as the ratio of the longitudinal electric field and the azimuthal magnetic field at the wall, $\zeta = -(E_z/Z_0 H_\phi)|_{r=a}$, where Z_0 = 377 Ω. Denoting $\zeta_{rw}(k)$ as the wall resistive surface impedance and $\zeta_{ro}(k)$ as the surface impedance due to roughness we can write the beam impedance $Z(k)$ as

$$Z(k) = \frac{Z_0}{2\pi a}\left(\frac{1}{\zeta_{rw}(k)+\zeta_{ro}(k)} - \frac{ika}{2}\right)^{-1}, \qquad (1)$$

with wave number $k = \omega/c$, where ω is frequency and c is speed of light. The resistive wall surface (ac) impedance $\zeta_{rw}(k)$, is given by [10]

$$\zeta_{rw}(k) = (1-i)\sqrt{\frac{k(1-ikc\tau_c)}{2Z_0\sigma_c}}, \qquad (2)$$

with σ_c the dc conductivity and τ_c the relaxation time of the metallic walls. The roughness surface impedance [7]

$$\zeta_{ro}(k) = \frac{1}{4}kh^2\kappa^{3/2}\left(\frac{\sqrt{2k+\kappa} - i\sqrt{2k-\kappa}}{\sqrt{4k^2-\kappa^2}}\right); \qquad (3)$$

here the wall profile radius r is assumed to vary sinusoidally with longitudinal position z: $r = h\cos\kappa z$. For the model to be valid we require the oscillations to be small and shallow, *i.e.* $\kappa a \ll 1$ and $h\kappa \ll 1$. Note that Eq. 1 implies that at low frequencies the two contributions to the impedance simply add: $Z(k) \approx (Z_0/2\pi a)[\zeta_{rw}(k) + \zeta_{ro}(k)]$; however, in general this is not true. Once the impedance is known, then the wake is obtained by the inverse Fourier transform:

$$W_\delta(s) = \frac{c}{2\pi}\int_{-\infty}^{\infty} Z(k)e^{-iks}dk, \qquad (4)$$

with s the distance the test particle is behind the driving particle, and a positive value of W_δ indicates energy loss.

Table 1: Selected beam and machine properties in the undulator region of LCLS-II that are used in our calculations.

Parameter name	Value	Unit
Charge per bunch, Q	300	pC
Beam current, I	1	kA
Rms bunch length, σ_z	25	μm
Beam energy, E	4	GeV
Maximum beam power, P_b	120	kW
Vacuum chamber half aperture, a	2.5	mm
Vacuum chamber length, L	130	m

* Work supported by Department of Energy contract DE–AC02–76SF00515.

§ kbane@slac.stanford.edu

Copyright © 2014 CC-BY-3.0 and by the respective authors

DESIGN OF NOVEL RF SOURCES TO REDUCE THE BEAM SPACE-CHARGE EFFECTS*

Massimo Dal Forno**, Sami G. Tantawi, Ronald D. Ruth, Aaron Jensen,
SLAC National Accelerator Laboratory, CA 94025, USA

Abstract

Traditional rf sources, such as Klystrons, TWT require a magnet (such as a solenoid) in order to maintain the electron beam focusing, compensating the particle repulsion caused by space charge effects. We designed a novel rf source with an alternative approach that reduces beam space charge problems. This paper shows the design of the device, with a new formulation of the Childs Law, and the mode-beam stability analysis. The electron beam interaction with the cavity fields has been analyzed by means of particle tracking software and the maximum efficiency of the output cavity has been evaluated.

INTRODUCTION

Traditional klystrons rf sources work with a focused electron beam that propagates along one preferred direction, interacting with several cavities and elements. To keep the beam focused, those devices require additional focusing elements (such as solenoids that provide a focusing magnetic field) in order to compensate the particle repulsion caused by space charge effects. In this paper we want to propose an alternative klystron design in which the electrons are allowed to propagate in them natural expansion according to the space charge forces. This approach leads to design multidimensional rf sources. If the beam is generated by a spherical cathode, it will expand in the radial direction (considering a spherical coordinate system centered in the cathode center). In this ideal case, the transversal space charge forces are fully balanced (where the transverse dimension is orthogonal to the propagation of each electron). No magnet is required to compensate space charge effects.

We started the klystron design with a cylindrical device that is the easiest case to analyze. The electrons are generated by a cylindrical cathode and equally propagates in the radial direction. The cavities are coaxial resonators endowed by beampipe apertures to let the electrons pass through (Fig. 1). In this novel cylindrical klystron design, the space charge repulsion forces are fully balanced in the φ direction (Indicated in Fig. 1(a)). Moreover less magnetic field will be required to keep the beam focused, since remnant space charge effects acting in the other directions will fast decay when the beam is expanding.

This paper shows the cylindrical klystron fundamentals, a new formulation of the Child's Law and the coaxial mode

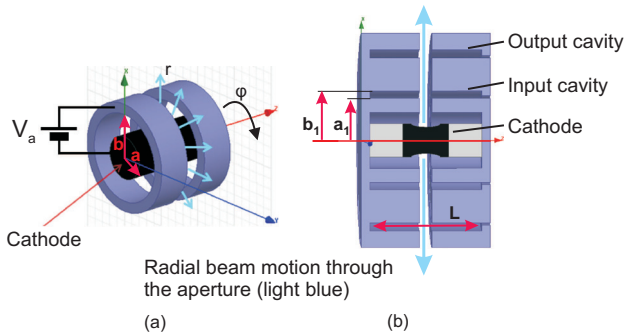


Figure 1: Cylindrical cathode with expansion of electrons (a), Cylindrical klystron with two coaxial resonators (b).

stability in presence of electrons. The electron beam interaction with the cavities has been analyzed with an in-house developed particle tracking software in order to evaluate the efficiency of the output cavity.

CATHODE CHILD'S LAW

We developed a formula in order to have an analytical esteem of the space charge limited current generated by the cylindrical cathode of Fig. 1(a), approximated by a cylindrical diode composed of two concentric cylinders. This problem was addressed by Langmuir and Blodgett [1], Page and Adams [2], Degond et. al. [3, 4]. In our design, we need an expression where the distance between the two cylinders are comparable to the radius of the inner one. Our expression that represents the current is:

$$I_a = \frac{\sqrt{8}\pi V_0}{\eta}\left(\frac{V_a}{V_0}\right)^{3/2}\frac{L}{a}\frac{1}{d^2}\left(\frac{4}{9}+\frac{16}{45}d+o(d)\right) \quad (1)$$

where $V_0 = 0.511MV$ is the electron rest voltage, $\eta = \sqrt{\frac{\mu_0}{\epsilon_0}} \approx 377\,\Omega$ is the free space impedance, a is the radius of the inner cylinder, b is the radius of the outer cylinder, $d = b/a$, L is the length of the cathode. I_a and V_a are the anodic current and voltage, respectively. This expression is used to design the cylindrical cathode.

MODES STABILITY ANALYSIS

In this section we propose a method to evaluate the stability of a single cavity crossed by a DC electron beam. A single cavity can behave like an oscillator self-bunching the electron beam. This happens when the noise or other effects start bunching the electron beam, and the electron beam modulation releases energy to the cavity. The induced electromagnetic field could contribute to further

* Work supported by the US DOE under contract DE-AC03-76SF00515.
** dalforno@slac.stanford.edu

Copyright © 2014 CC-BY-3.0 and by the respective authors

ISBN 978-3-95450-142-7

R&D OF X-BAND ACCELERATING STRUCTUREFOR COMPACT XFEL AT SINAP

W. C. Fang#, M. Zhang, J. H. Tan, Q. Gu, Z. T. Zhao, SINAP, Shanghai, China
W.Wuensch , A. Grudiev, A. Latina, D. Schulte, S.Stapnes, CERN, Geneva, Switzerland
G. D'Auria, S. Di Mitri, C. Serpico, Elettra-Sincrotrone Trieste, Italy
A. Aksoy, Ö. Yavaş, Institute of Accelerator Technologies, Ankara, Turkey
M. Boland, J. McKinlay, Synchrotron Light Source Australia, Clayton, Australia
J. Clarke, D. Angal-Kalinin, STFC, Daresbury Laboratory Cockcroft Institute, Daresbury, UK
R. Ruber, T. Ekelof, V. Ziemann, Uppsala University, Uppsala, Sweden
E. Gazis, A. Charitonidis, National Technical University of Athens, Greece
C. J. Bocchetta, A. Wawrzyniak, Solaris, Jagiellonian University, Krakow, Poland

Abstract

One compact hard X-ray FEL facility is being planned at SINAP, and X-band high gradient accelerating structure is the most competitive scheme for this plan. X-band accelerating structure is designed to switch between 65MV/m and 80MV/m, and carries out 6.5GeV and 8GeV by 130 meters linac respectively. In this paper, brief layout and simulation of compact XFEL will be introduced, and in particular the prototype design of dedicated X-band acceleration RF system is also presented.

INTRODUCTION

Recently, FEL has been being developed to new era with great success, in particular LCLS[1], SACLA[2] were successful to carry out first lasing and user operation. Since further R&D of FEL technology, FEL facility is led to tendency of compact facility, and it makes it more feasible and acceptable.

Compact linac based on high gradient technology is one effective and crucial way to carry out compact FEL facility. Recently FEL facility are based on L-band (EuroXFEL), S-band (LCLS) and C-band (SACLA, SwissFEL), and the accelerating gradient is ranged from 20MV/m to 40MV/m [3], which also make facilities more compact step by step, however higher gradient is required for future compact facility, such as X-band high gradient technology. SLAC, CERN and KEK have developed X-band for several ten years, and have reached gradient higher than 100MV/m in the condition of experiment lab [4]. Based on present status of X-band accelerating structure, 80MV/m could be stable operation gradient, and it can make linac half scale of C-band linac, so that it's only about 200 meters required for 8 GeV linac for FEL facility.

Recently one hard X-ray FEL facility is being planned at SINAP, and one 6.5 GeV or 8GeV linac is required for FEL radiation. Since length of our campus is about 600 meters, and linac should be limited to be less 200 meters, so that the 65MV/m or 80MV/m gradient is required for 6.5 GeV or 8GeV respectively, and X-band high gradient technology is the first selection for hard X-ray FEL plan. In this paper, the brief layout and simulation of hard X-ray FEL is introduced, and prototype of X-band RF system is presented.

BRIEF LAYOUT OF FEL PLAN AT SINAP

Shanghai photon science centre is being planned, and there will be two FEL facilities built in the same campus of Shanghai Synchrotron Radiation Facility (SSRF) in future, which is shown in Figure 1.

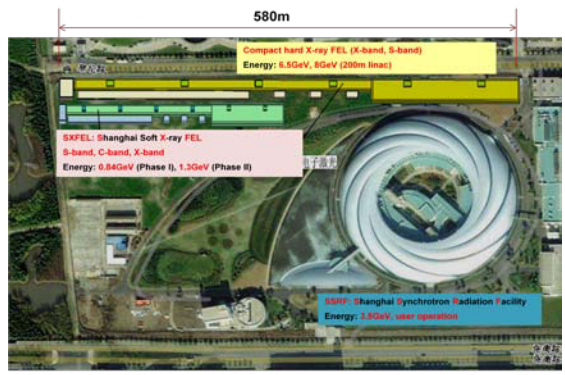


Figure 1: Layout of Shanghai photon science centre

Shanghai Soft X-ray FEL facility(SXFEL) is the test facility of future hard X-ray FEL facility, and its linac is composed of S-band and C-band accelerating structure in first step, and the total energy can reach 800MeV, as shown in Figure 2. In second step X-band RF system will replace C-band RF system for energy upgrading to 1.3MeV, and X-band accelerating structure will be operated at 80MV/m.

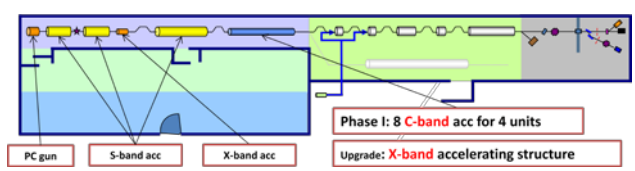


Figure 2: Layout of Shanghai Soft X-ray FEL

#fangwencheng@sinap.ac.cn

ISBN 978-3-95450-142-7

Copyright © 2014 CC-BY-3.0 and by the respective authors

ECHO-ENABLED TUNABLE TERAHERTZ RADIATION GENERATION WITH A LASER-MODULATED RELATIVISTIC ELECTRON BEAM*

Dazhang Huang†, Zhen Wang, Qiang Gu, Zhentang Zhao
SINAP, Shanghai, 201800, China.
Dao Xiang
Key Laboratory for Laser Plasmas (Ministry of Education), Department of Physics and Astronomy
Shanghai Jiao Tong University, Shanghai 200240, China.

Abstract

A new scheme to generate narrow-band tunable Terahertz (THz) radiation using a variant of the echo-enabled harmonic generation is analyzed. We show that by using an energy chirped beam, THz density modulation in the beam phase space can be produced with two lasers having the same wavelength. This removes the need for an optical parametric amplifier system to provide a wavelength-tunable laser to vary the central frequency of the THz radiation. The practical feasibility and applications of this scheme is demonstrated numerically with a start-to-end simulation using the beam parameters at Shanghai Deep Ultraviolet Free-Electron Laser facility (SDUV). The central frequency of the density modulation can be continuously tuned by either varying the chirp of the beam or the momentum compactions of the chicanes. The influence of nonlinear RF chirp and longitudinal space charge effect have also been studied in our article. We also briefly discuss how one may retrieve the beam longitudinal phase space through measurement of the THz density modulation.

INTRODUCTION

As been widely used in radar, security, communication, medical imaging etc, THz radiation has drawn a lot of attention all over the world. A lot of studies have been done on the generation of THz radiation. Accelerator-based free electron laser (FEL) technology, such as the 4^{th} generation light source, can produce radiation with high intensity, high peak power and coherence, which might be a great candidate for the generation of THz radiation. In recent years, a new scheme of employing the echo effect previously observed in hadron accelerators was proposed [1] and experimentally tested [2] to generate high harmonics of FEL radiation, and the bunching coefficients of this scheme was also analyzed in detail [3] to give us clearer picture of the mechanism behind it. Providing the advantages of the echo-enabled harmonic generation FEL such as compact size, tunable frequency, etc., a method of using two lasers to modulate the electron beam to generate density modulation at THz frequency has been proposed and analyzed in Ref. [4, 5]. In this scheme, the relativistic electron beam is firstly sent into a modulator to interact with a laser with the wave number k_1. Then the beam is transmitted into the following modulator to interact with another laser with the wave number k_2. The energy modulation will be converted into density modulation when the beam passes through a dispersion section. In this situation, the density modulation at wave number $k = nk_1 + mk_2$ can be achieved, where n and m are non-zero integers. By varying the wavelength of those two lasers and the parameter of dispersion, one can vary the central frequency of the beam density modulation conveniently. In this scheme, an optical parametric amplifier (OPA) is needed to provide two different lasers (e.g. 800 nm and 1560 nm in this scheme) to modulate the electron beam respectively.

As briefly mentioned in [5], one may generate the continuously tunable density modulation with two lasers having the same wavelength, which is different from the scheme mentioned above, if there is a chicane between the two modulators, similar to the echo-enabled harmonic generation scheme. A chirped electron beam is modulated in the modulator at wave number k_0. The wave number of the beam density modulation will be compressed to $k_1 = C_1 k_0$ and its high harmonics when the beam passes through the first dispersion section with small R_{56}. Then the beam will be sent into another same modulator to interact with a laser at the same wave number k_0. After the beam passing through the second dispersion section, the energy modulation is converted into density modulation at the final wave number $k = nC_1C_2k_0 + mC_2k_0$, where n and m are non-zero integers. It is easy to find out that one may vary the final frequency of density modulation continuously by varying the chirp of the beam or R_{56} of the first dispersion section.

GENERATION OF DENSITY MODULATION IN THEORY

As introduced in Sec. I (more details, see Ref. [4]), the layout of the scheme to generate THz density modulation in a relativistic electron beam with two different lasers at wave numbers k_1 and k_2 is shown in Figure 1(a1), which consist of two modulators and a dispersion section. The beam is modulated by two different lasers at wave numbers k_1 and k_2 when the beam passes through two modulators respectively. After the beam passes through the dispersion

* Work supported bythe Major State Basic Research Development Program of China (2011CB808300) and National Natural Science Foundation of China (NSFC), grant No. 11275253 and 11327902
† huangdazhang@sinap.ac.cn

ISBN 978-3-95450-142-7

Copyright © 2014 CC-BY-3.0 and by the respective authors

OPTIMIZATION OF BEAM PARAMETERS IN APF CHANNEL*

V. Altsybeyev, D. Ovsyannikov, SPbSU, Saint-Petersburg, Russia

Abstract

A new approach based on mathematical optimization methods to obtain a synchronous phase sequence in APF linacs is suggested. The optimization problem of intensity deuteron beam parameters is discussed. As an example, the results of beam dynamics simulations are presented.

INTRODUCTION

Linear accelerators with alternating-phase focusing (APF) are admitted to be of considerable practical importance. They have found wide application in fundamental nuclear research as the initial stage in high-energy accelerators. At present there is a significant progress in the development of APF accelerators and H-resonators [1-6]. To design an initial stage of accelerator complex, such parameters as the size of linac, beam current, beam transmission, effective emittance and so on should be considered. Improvement of these parameters may be achieved by using different optimization techniques. So, design of linear accelerator on the base of optimization approach has wide practical significance.

INITIAL APF PARAMETERS

The main initial parameters of designed APF accelerator are presented in Table 1.

Table 1: Initial parameters

Input ion energy, MeV	3.45
Output ion energy, MeV	14.2
Operating frequency, MHz	433
Accelerating wave amplitude kV/cm	110
Charge number $Z=q/q_{proton}$	1
Mass number $A=m/m_{proton}$	2
Beam current, mA	10
Transversal emittance (XdX,YdY), cm·mrad	0.029π
Longitudinal emittance, keV·ns/u	1.55π
Energy spread, %	± 1

DESIGN TECHNIQUE

At the same time today we have a well-developed mathematical theory of the multiparameter optimization which can be applied to beam [7-21] and plasma dynamics [22, 23]. By using simple mathematical models at the first stage of the accelerator designing we can generate the main accelerator parameters, which determine the main characteristic of the beam. In the case of APF structure it is a synchronous phase sequence φ_S generation by using analitic representation of quality functional gradient.

The next step is to evaluate the geometry of the resonator, the lenght and aperture radii of the drift tubes and so on. Also we should realize, that using simple beam dynamics models may give an inaccurate result. So, we should conduct the final correction of accelerator parameters. In this paper we use genetic algorithm for correction lenght of accelerating cells.

GRADIENT OPTIMIZATION

The standing wave approximation of accelerating field allows to accept the following mathematical model of beam dynamics in the equivalent traveling wave [1, 2].

Let us consider the beam dynamics in following variables: β_S is the velocity of synchronous particle, $\psi=\varphi-\varphi_S$ is the phase deviation, $p=\gamma_S-\gamma$ is the energy deviation, S_{11}, S_{21}, S_{22} are the elements of the matrix $G=\begin{pmatrix} S_{11} & S_{21} \\ S_{21} & S_{22} \end{pmatrix}$, that describe dynamics of the initial ellipse G_0 in the radial plane (η,κ) where $\eta=r/\lambda$ is the radial position of particle and $\kappa=d\eta/d\tau$ (where $\tau=ct/\lambda$ is an independent variable). When

$$\frac{d\beta_S}{d\tau}=(\alpha/2)\sqrt{1-\beta_S^2}\cos(\varphi_S(\tau)), \quad (1)$$

$$\frac{d\psi}{d\tau}=\frac{2\pi(\beta_S-\beta)}{\beta_S}p, \quad (2)$$

$$\frac{dp}{d\tau}=(\alpha/2)\beta(\cos(\varphi_S(\tau))-\cos(\varphi_S(\tau)+\psi)), \quad (3)$$

$$\frac{dG}{d\tau}=-A^TG-GA, \quad (4)$$

$$A=\begin{pmatrix} 0 & 1 \\ Q & 0 \end{pmatrix}, \quad Q=\frac{(\alpha/2)\pi(1-{\beta_S}^2)^{3/2}}{\beta_S}\sin(\varphi_S(\tau)+\psi).$$

Where $\alpha=q\lambda E_{max}/(m_0c^2)$ is the accelerating wave amplitude parameter, $\varphi_s(\tau)$ is the synchronous phase function defined by the value $\varphi_s^{(i)}$ of each i-th accelerating cell.

To solve the problem of reducing the loss of particles and decrease of beam radius it is possible to take the following functional

$$I(u)=\int_{M_{T,u}}(c_1F_1(\psi(T))+$$

*Work supported by St. Petersburg State University, 9.38.673.2013
altsybeyev@gmail.com

Copyright © 2014 CC-BY-3.0 and by the respective authors

OPTIMIZATION OF THE RF CAVITY OF THE MEDICAL PURPOSE ELECTRON LINAC BY USING GENETIC ALGORITHM *

S.W. Shin, Department of Energy Science,
Sungkyunkwan University, Gyeonggi-do, Republic of Korea
J.S. Chai#, College of Information & Communication Engineering,
Sungkyunkwan University, Gyeonggi-do, Republic of Korea

Abstract

A compact electron linear accelerator for the medical application has been developing at Sungkyunkwan University. Due to this electron linac is attached on the robot arm or gantry, it should be compact enough to be held by the structure. An X-band technology has been used to meet the requirements for the compact linac. Because the particle accelerator is complex and sensitive machine to design it takes a lot of time to get a good performance accelerator. In this research, a special technique named single-objective genetic algorithm for the optimization process has been applied to achieve a better RF cavity design by changing various geometric parameters.

INTRODUCTION

Because X-band electron accelerator has a better mobility than the C-band or S-band electron linac, it is mainly used at the medical treatment machine such as Stereotactic Radiosurgery (SRS), Intraoperative radiation therapy (IORT) or cyberknife where mobility and compactness is needed.

To develop a dual-head gantry radiotherapy machine using X-ray, a compact 6 MeV electron linac using X-band technology has been developing at Sungkyunkwan University.

GENETIC ALGORITHM

Due to the particle accelerator is composed of a complex structure where many components are controlled simultaneously, it is not easy to achieve a guaranteed best design. It can be reached by putting a lot of time into an optimization process but it is not a good way. There are lots of optimization techniques to help designers to get a good quality machine. Among them the genetic algorithm (GE) is a good candidate for the accelerator field where the non-linear problem is dominant. The genetic algorithm adapted a nature's biological evolution mechanism such as mating (including selection and competition), mutation and generation. Because each individuals of the each population is generated randomly, diversity of this algorithm is very wide so that it is easy to find a global maximum (minimum) point for the optimization problem. Another advantage of the genetic algorithm is its calculation speed. As a generation goes by, it converges to the local maximum (minimum) point very quickly. That is why genetic algorithm is suitable to the accelerator field where non-linear problem is dominant.

OPTIMIZATION PROCESS

We adapted a π/2 - mode nose-cone introduced structure to increase the transit time factor (TTF) for the high beam acceleration efficiency. The Poisson/Superfish [1] has been used to design a single cell of the RF cavity.

General Layout of the RF cavity

Optimization process was done by changing several geometric parameters of the RF cavity: Nose cone angle, Outer corner radius, Inner corner radius, Outer nose cone radius, Inner nose cone radius while a length of the RF cavity (to get the synchronism between RF phase and beam), a gap distance between two nose cones (trade-off between high transit time factor and minimum distance for the electrical breakdown happen), a septum thickness (fabrication issue) are fixed. A Fig. 1 shows a general layout of the RF cavity sing cell.

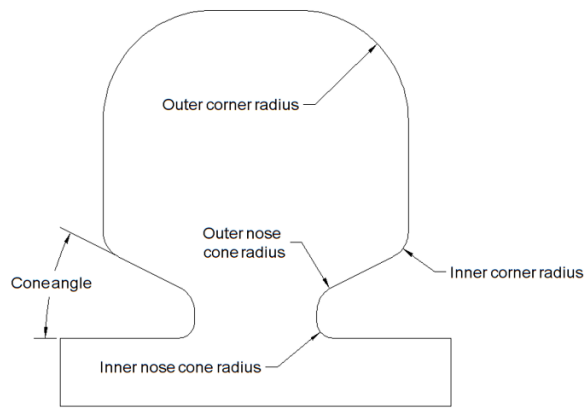


Figure 1: Layout of the RF cavity single cell.

Table 1: Parameters and Constraints for the Optimization Process

Parameters	Constrains
Cone angle	0 ~ 60 °
Outer corner radius	0 cm ~ 5 cm
Inner corner radius	0 cm ~ 1.5 cm
Outer nose cone radius	0.25 cm ~ 1.5 cm
Inner nose cone radius	0.25 cm ~ 1.5 cm

#jschai@skku.edu

Copyright © 2014 CC-BY-3.0 and by the respective authors

ISBN 978-3-95450-142-7

BEAM DYNAMICS CALCULATIONS AND MAGNET DESIGN FOR FUTURE MEASUREMENTS OF TRANSVERSE BEAM BREAK-UP AT THE S-DALINAC*

F. Hug#, M. Arnold, L. Jürgensen, T. Kürzeder, N. Pietralla, M. Schilling,
TU Darmstadt, Darmstadt, Germany

Abstract

The superconducting electron accelerator S-DALINAC at TU Darmstadt produces c.w. electron beams of up to 90 MeV. The S-DALINAC consists of a SC 14-MeV injector linac, a SC main linac and two recirculation paths. Currently a third recirculation is in its final design phase and will be constructed end 2014 in order to achieve an energy of 130 MeV in future. The main linac houses eight 20-cell SRF cavities operating at 3 GHz and 2 K. Due to the occurance of transverse beam break-up, the highest stable beam current obtained so far amounts to 5 µA only, which is below the design beam current of 20 µA but sufficient for the nuclear physics experiments carried out in Darmstadt since 1991 [1]. In this work we will present beam-dynamics calculations and newly designed magnets for planned experiments at the S-DALINAC in order to benchmark different strategies of increasing the threshold current for beam break-up.

INTRODUCTION

The Superconducting DArmstadt LINear Accelerator (S-DALINAC) is delivering electron beams for nuclear- and astrophysical experiments at the University of Darmstadt since 1987 [2]. It has been designed for producing beams of either unpolarized or polarized electrons [3] up to energies of 1 to 130 MeV with beam currents from several pA up to 60 µA in single pass mode or 20 µA in recirculating mode using up to two recirculation beamlines. Due to the limited cooling power of the cryo plant in conjuction with a too low quality factor of the superconducting cavities the total beam energy in c.w. mode is limited to 90 MeV currently [4]. In order to reach the design energy of 130 MeV in future an additional third recirculation will be operational in spring 2015 [5]. The current layout of the S-DALINAC is shown in Fig. 1.

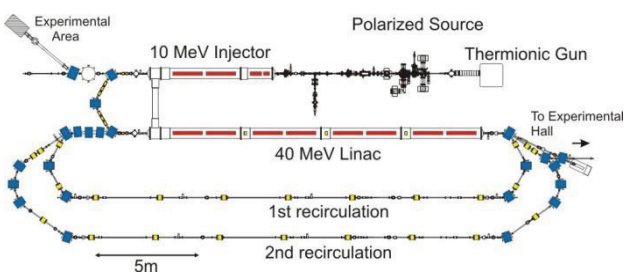


Figure 1: Floor plan of the S-DALINAC.

*Work supported by BMBF through 05K13RDA
#hug@ikp.tu-darmstadt.de

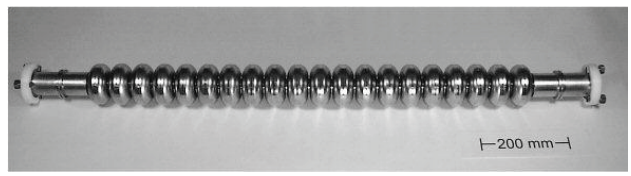


Figure 2: S-DALINAC 20 cell cavity. .

For acceleration of the beam ten 20 cell superconducting elliptical cavities (see Fig. 2) with a quality factor of $Q_0 \approx 10^9$ and a maximum accelerating gradient of 5 MV/m are used while the operation frequency of the cavities is 3 GHz. By recirculating the beam up to two times, later three times, the maximum energy of 130 MeV can be achieved. In the adjacent experimental hall this beam can be used for several experiments such as electron scattering in two electron spectrometers or experiments with tagged photons. For these experiments an energy spread (rms) of $1 \cdot 10^{-4}$ as well as a very low γ-ray background are required.

OPERATIONAL EXPERIENCE

The S-DALINAC is the first superconducting and recirculating cw accelerator for electrons which has been put into operation in Europe [2]. The injector has been constructed in 1987 while the complete accelerator started operation in 1991 and has been used for experiments in nuclear, astro- and radiation physics since then. A great success has been the observation of a first infrared laser beam at the free electron laser (FEL) in 1996 [6]. For achieving an FEL operation the peak current of the electron beam needed to be increased to 2.7 A at a pulse length of some ps and an operation frequency of 600 MHz [4]. Originally it was thought of operating the S-DALINAC as an ERL as well when using the FEL but the challenges of operating this first European FEL had been high enough even without trying the ERL mode.

BBU AT THE S-DALINAC

One reason for this has been the occurance of instabilities due to the high peak current of the electron bunches – a first observation of transverse beam break up (BBU) at the S-DALINAC. This BBU occurs at a relative low threshold current of some µA due to the design of the 20-cell accelerating cavities which have not been optimized for suppressing any higher order modes (HOMs).

The occurance of beam break up also limits the

Copyright © 2014 CC-BY-3.0 and by the respective authors

HIGH POWER SOLID-STATE AMPLIFIERS. NEW DEVELOPMENTS AND TECHNOLOGY COMPARISON *

G. B. Sharkov[1], A. I. Botyachkova[1,2], E.V. Ivanov[1], N. G. Kalugin[1], A.A. Krasnov[1], K. K. Naraianamurtkhi[1], K.I. Nikolskiy[1], S. A. Polikhov[1], I.N. Rezanov[1], A.Y. Smirnov[1], P.M. Yazev[1]
[1] Siemens Research Center, Moscow, Russia
[2] National Research Nuclear University (MEPhI) Chemical Physics Department

Abstract

We present a newly developed compact and cost effective SSPA with megawatt range output power and scalable architecture. System components test results are discussed. A comparison of the state-of-the-art vacuum tube and solid-state technologies of RF power amplifiers for scientific accelerators is given.

INTRODUCTION

The last year's developments in the field of high power high frequency solid-state transistors lead to the expansion of solid-state technology on the RF amplifiers market. Developing Si, SiC, GaN, GaAs LDMOS, FET transistors [1] allow building not only the drivers for vacuum tubes, but to substitute the entire RF systems [2]. The general trend on the market is to reduce the Total Cost of Ownership (TCO) which brings in system, operating, and construction costs. The typical TCO breakdown for 10 years operation of thirty amplifiers at 50% wall plug efficiency is shown in Table 1. The operation costs have so large impact on TCO that the increase of the efficiency by ~10% can compensate the whole procurement cost.

Table 1: Total Cost of Ownership. Breakdown for Thirty 800 kW Amplifiers Working for 10 Years

Cost	Role in TCO
Procurement cost	14%
Construction cost	14%
Operation costs	69%
Service costs, spare parts, % from procurement	1%
Costs of downtime	1%
R&D and labour	1%

Particular market segments demand different ways to reduce these costs. While PET cyclotrons, lasers and plasma sources require high persistence against reflected waves, the broadcast market needs high signal purity and linearity. The construction costs driven by the footprint of PA's is a significant share of the cost books of such projects as large light and neutron sources, HEP Linacs. The reduction of TCO can be achieved using following approaches:

1. Reduction of procurement price using novel high power cost effective solid-state technologies;
2. Reduction of construction costs using more compact devices;
3. Reduction of service costs by icreasing MTBF and reduction of spares costs;
4. Increase of system availability (downtime costs) by reduction of MTTR;
5. Reduction of energy costs by increase of PA's efficiency;
6. Reduction of R&D, labor costs for high qualified RF specialists providing turnkey solutions.

For us this lead to the following responses on abovementioned market demands:

1. Standardization of amplifier architecture and subsystems for different applications;
2. Modular structure;
3. Usage of fast connectors for fast module maintenance;
4. Ability to work at full power and nominal efficiency with several broken RF power modules;
5. Efficient and compact RF power combination from numerous transistors in few (one/two) steps;
6. All-in-one solution with power supply, LLRF, control system, cooling etc. onboard.

SYSTEM ARCHITECTURE

Driven by these tasks the system concept has been developed and being validated through building a solid-state microwave generator prototype with technical requirements according ESS low-β section specification. The system structure is presented on Fig. 1. It consists of a 19-inch cabinets with a docking station for several RF generating modules, the power combiner with RF switches for failed RFM disconnection, power supply and capacitor blocks to feed the RF modules with electrical energy required for the pulse, the control system and cooling system.

The system has versatile modular structure allowing fast module change. The idea behind it is to reduce the efforts needed to build the generator for a new specification. To do so the system should be easy scalable in output power. It can be done by using mechanical standard with RF modules/cabinets which can be easily added to the system, e.g. 19'' cabinets with standard racks. The redesign for a new frequency should affect the redesign of the RF module and the power combiner only.

*Work supported by:
Skolkovo Foundation, Russia. www.sk.ru

Copyright © 2014 CC-BY-3.0 and by the respective authors

ISBN 978-3-95450-142-7

ANALYSIS OF NEW HIGH-Q_0 SRF CAVITY TESTS BY NITROGEN GAS DOPING AT JEFFERSON LAB*

A. D. Palczewski†, R. L. Geng, and C. E. Reece
Thomas Jefferson National Accelerator Facility, Newport News, VA 23606, USA

Abstract

In order to refine systematic understanding and establish confident process control, Jefferson Lab has joined with partners to investigate and thoroughly characterize the dramatically higher Q_0 of 1.3 GHz niobium cavities first reported by FNAL in 2013[1]. With partial support from the LCLS-II project, JLab has undertaken a parametric study of nitrogen doping in vacuum furnace at 800 °C followed by variable depth surface removal in the 5 - 20 µm range. Q_0 above 3×10^{10} are typical at 2.0 K and 16 MV/m accelerating field. We report observations from the single cell study and current interpretations. In addition to the parametric single cell study, we also report on the ongoing serial testing of six nitrogen-doped 9-cell cavities as baseline prototypes for LCLS-II.

INTRODUCTION

JLab is collaborating with FNAL and Cornell to expedite the development and exploitation of methods to produce dramatically lower-loss SRF cavities using the nitrogen doping technique discovered by FNAL[2-6]. The LCLS-II project[7] is eager to take advantage of these developments to minimize cryogenic capital and operating costs. JLab's contribution to this effort centers on systematic processing and test of a set of single-cell 1.3 GHz cavities, followed by a "production-style" run treating six existing new TESLA-style 9-cell cavities to assess any performance and yield issues.

The envisioned parametric study included two rounds of matrix testing of 9 single cell cavity where the exposure to nitrogen would be held constant in each round and the post nitrogen annealing time and electropolishing (EP) would be varied. This matrix was performed twice; first with a 2 min exposure of nitrogen with 5, 10 and 15 µm EP removal and second with 20 min exposure with 10, 15 and 20 µm EP removal. These two sets of data along with auxiliary side tests would be performed before a fixed-recipe serial test of six 9-cell cavities in order to understand the yield associated with integrating N doping into a standard production process.

To date, Jefferson Lab has performed over 25 nitrogen doping/EP cycles on 18 SRF cavities and 30 vertical cryogenic tests including cavities outside the LCLS-II funded scope [8]. The matrixed studies showed the ability to dope an SRF cavity and control the EP removal to gain a lower BCS resistance and create a cavity which has a rising Q_0 with gradient is straightforward and easier than initially envisioned. We have found with any doping used at ~25 mTorr, the EP window is over 15 µm wide which yields $Q_0 \geq 3.3\times10^{10}$ performance of the 1.3 GHz cavities at E_{acc} = 16 MV/m at 2.0 K.

The unforeseen complications within the systematic study turned out not to be within the doping or subsequent EP removal, but rather controlling the environmental conditions, both cooling profiles (spacial thermal gradients) and remnant magnetic fields to not mask the improvements due to nitrogen doping.

800°C HEAT TREATMENT – NITROGEN ABSORPTION

To date there have been over 60 cavities nitrogen doped at FNAL, JLab and Cornell combined. All the doping consists of about the same procedure with any minor changes coming from the nitrogen injection systems. The heat treatments begin with a standard ILC/XFEL 800 °C heat treatment for three hours to remove hydrogen from the bulk, followed by addition of low pressure nitrogen ~20 mTorr and a nitrogen diffusion period. For the six 9-cell LCLS-II baseline testing cavities, the JLab doping was decided to be an 800°C anneal for three hours, a 20-minute nitrogen doping with a controller set point of 20 mTorr (26 mTorr average pressure) with no active pumping and a 30-minute anneal after pumping out the nitrogen. The nomenclature for the doping is 800°C_A180_N20@26mTorr_A30. Including the ramp up and cooldown, the full cycle time for a 9-cell nitrogen doping run is approximately 18 hours (This includes the vacuum pump-down time). During the nitrogen injection all vacuum valves are closed and the nitrogen is injected through a 0.2 L/min orifice with a computer-controlled Brooks 4850 mass flow controller with feedback from the furnace convectron. An example of the temperature profile (red curve) and furnace pressure (blue curve) are shown in Fig. 1.

During doping, nitrogen gas is injected into the furnace until the set point is reached; because of the relatively high flow of the controller and long piping lengths, the controller overshoots the set point by approximately 10 mTorr. The valve closes and the cavity absorbs the N_2 until the pressure drops below the set point. At this time the flow is turned back on. This creates asymmetric saw-tooth in the furnace pressure (Fig. 2, red curve) with short pulses of gas (Fig. 2, black curve). This injection and decay profile (dp/dt) allows us to calculate the absorption rate (Fig. 2, blue curve) as well as the total amount of nitrogen absorbed by the cavity. This is illustrated in Fig. 2 for the 20 minute nitrogen injection of AES031 – 9 cell TESLA-shaped cavity. Using the flow from the

*Authored by Jefferson Science Associates, LLC under U.S. DOE Contract No. DE-AC05-06OR23177. The U.S. Government retains a non-exclusive, paid-up, irrevocable, world-wide license to publish or reproduce this manuscript for U.S. Government purposes
†ari@jlab.org

Copyright © 2014 CC-BY-3.0 and by the respective authors

DESIGN STUDIES WITH DEMIRCI FOR SPP RFQ

B. Yasatekin*, G. Turemen, Ankara University, Ankara, Turkey
A. Alacakir, TAEK-SANAEM, Ankara, Turkey
G. Unel, UCI, Irvine, California, USA

Abstract

To design a Radio Frequency Quadrupole (RFQ) is a onerous job which requires a good understanding of all the main parameters and the relevant calculations. Up to the present there are only a few software packages performing this task in a reliable way. These legacy software, though proven in time, could benefit from the modern software development tools like Object Oriented (OO) programming. In this note, a new RFQ design software, DEMIRCI is introduced. It is written entirely from scratch using C++ and based on CERN's OO ROOT library. It has a friendly graphical user interface and also a command line interface for batch calculations. It can also interact by file exchange with similar software in the field. After presenting the generic properties of DEMIRCI, its compatibility with similar software packages is discussed based on the results from the reference design parameters of SPP (SNRTC Project Prometheus), a demonstration accelerator at Ankara, Turkey.

INTRODUCTION

A new project in the form of a computer code, written in C++, called DEMIRCI[1] [1] is started to explore the potential of the modern concepts such as object oriented programming and ROOT environment [2]. This tool helps the designer to create an RFQ model which would achieve certain goals such as a final target energy or a fixed total accelerator length in a fully graphical environment. It calculates a large number of design and beam dynamics parameters such as energy at the end of the cavity, power dissipation and cavity quality factor for each cell. It also allows the designer to visualize a large set of parameters change along the RFQ. Another property of this tool is the interoperability with similar software in the field, either directly using the user interface or by simple exchange of plain text files.

DESIGN PROCEDURE

The classical procedure used in designing 4-vane RFQs has been around since LANL designed the first proof of principle (PoP) device. This procedure is known as the "LANL Four Section Procedure (FSP)" method [3]. According to this method, the RFQ is divided into 4 sections named as radial matching section (RMS), shaper section, gentle buncher section and acceleration section.

The potential between the electrodes of a single RFQ cell is given [4] by

$$U(r,\theta,z) = \frac{V}{2}\left[\sum_{m=1}^{\infty} A_{0m}\left(\frac{r}{r_0}\right)^{2m}\cos(2m\theta) + \sum_{m=0}^{\infty}\sum_{n=1}^{\infty} A_{nm} I_{2m}(nkr)\cos(2m\theta)\cos(nkz)\right] \quad (1)$$

where r and θ are spherical coordinates for which z represents the beam direction, V is the inter-vane voltage, k is the wave parameter given by $k \equiv 2\pi/\lambda\beta$, with λ being the RF wavelength and β being the speed of the ion relative to the speed of light. Also, r_0 is mean aperture of the vanes, I_{2m} is the modified Bessel function of order 2m and the A_{nm} are the multipole coefficients whose values depend on the vane geometry.

New Design Procedure

The parameters needed to define an RFQ can be divided into two categories: the ones which can be a function of RFQ length and the ones which are constant for a given RFQ. The resonant frequency (f), the initial ion energy (E_{in}), the input beam current (I) and the braveness factor (in terms of the Kilpatrick value) can be cited as examples to the latter. The four parameter vectors falling into the first category are: the synchronous phase (ϕ), the cell modulation (m), the minimum bore radius (a) and the inter-vane voltage (V). This last one, together with R/ρ could be kept constant along the RFQ length to simplify the design and manufacture.

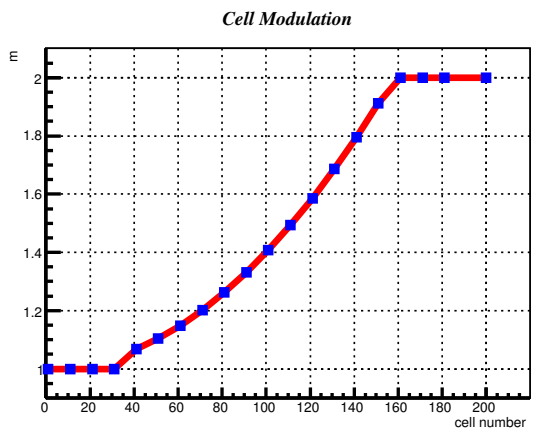


Figure 1: Cell modulation (m) versus cell number. m is a typical RFQ parameter which changes with cell number. The meaning of blue squares and red line is explained in the text.

In case of DEMIRCI, a typical parameter's variation along the RFQ can be seen in Fig. 1. The points represented by

* byasatekin@ankara.edu.tr
[1] meaning "blacksmith" in Turkish

Copyright © 2014 CC-BY-3.0 and by the respective authors

ISBN 978-3-95450-142-7

OBSERVATION OF >GV/M DECELERATING FIELDS IN DIELECTRIC LINED WAVEGUIDES*

B. O'Shea†, O. Williams, G. Andonian, J. Harrison, S. Hakimi, K. Fitzmorris, J. Rosenzweig
University of California, Los Angeles, CA 90095, USA
M. Hogan, V. Yakimenko, SLAC, Menlo Park, CA 94025, USA

Abstract

Recent experimental measurements of the energy lost to wakefields in a dielectric lined waveguide are presented. These measurements demonstrate average decelerating gradients on the order of >1 GV/m, for two different structures. The measurements were made at the Facility for Advanced aCcelerator Experimental Tests (FACET) at SLAC National Laboratory using sub-millimeter diameter fifteen-centimeter long quartz fibers of annular cross section. The unique extremely short, high charge, ultra relativistic beam at FACET (200 fs, 3 nC, 20 GeV) allows the use of dielectric wakefield structures of unprecedented size and length. In addition to experimental results, we support conclusions with simulation and theoretical work. This measurement builds on a large body of work previously performed using dielectric wakefield structures in an effort to provide high gradient accelerating structures for tomorrows linear colliders.

INTRODUCTION

Accelerator physicists are looking for technologies to increase the average gradient in new systems past the present limit of ~20 MVm^{-1} in traditional room temperature copper structures [1]. The end goal of such research is not only reduction in size of present and future accelerating complexes, from kilometers [2] to a kilometer or less, but for the creation of high energy, compact beam sources that pave the way for the next generation of radiation sources which operate in bands heretofore difficult to access, such as terahertz [3–5] and x-rays [6].

Such possible gradient increasing modalities include systems that produce modest increases in gradients, such as superconducting radio frequency structures at ~50 MVm^{-1} [1], and ones that produce massive gains in gradients, such as plasmas at ~100 GVm^{-1} [7]. An additional intermediate option is the use of dielectric lined waveguides, or Dieletric Wakefield Accelerators (DWA), capable of supporting fields on the order of ~5 GVm^{-1} [8]. We discuss here recent experiments designed to measure the decelerating gradient in cylindrical dielectric lined waveguides. Such measurements allow an estimate of the accelerating gradient behind the wake driving bunch to be made and allow studies of the effects of beam breakup instabilities [9]. We show here measured decelerating gradients of the GVm^{-1} level, which exceed previous measurements by two orders of magnitude [10, 11].

* Work supported by grant HDTRA1-10-1-0073.
† boshea@physics.ucla.edu

EXPERIMENT

The experiment presented here threads an electron beam through a hollow, cylindrically symmetric dielectric structure [12]. As the beam passes through the dielectric structure it couples to the modes supported in the structure that have non-zero longitudinal electric field, $E_z \neq 0$. The experiment is conducted in two parts that allows the characterization of the beam-structure interaction. First, the radiation generated in the structure is spectrally characterized, which allows a description of the structure's reaction to the beam. Second, the average beam energy is measured both with and without the structure in the beam so that the beam's reaction to the structure can be described. A diagram of the experiment can be found in Figure 1.

Table 1: Structure Parameters divided by transverse geometry, a and b are in μm.

ρ_{in}/ρ_{out} = a/b	**450/640**	**400/600**	**200/300**
Length [cm]	10	15	15
λ [μm] (TM_{01})	760	760	430
$E_0[\frac{V}{m}]$	0.047	0.053	0.124

The structures used in this experiment are metal coated SiO2 and Quartz ($\epsilon_r = 3.8 - 3.9$) optical fibers of annular cross section with hollow inner channel of radius a and outer diameter of radius b. The dielectric thickness is the difference between these two radii. Other structure parameters can be found in Table 1. The fibers are purchased uncoated and unspooled, so as not to unintentionally introduce bends in the final product. The fibers are then cleaned and a small adhesion facilitating layer of aluminum is vacuum deposited to around 30 nm thickness. After aluminum, copper is vacuum deposited to 500 nm thickness followed by a sulfate base electroplating bath that increases the copper thickness to 20 μm. Finally the structures are cut to length using a diamond saw to produce the flat surfaces shown in Figure 2.

FACET

While we will show later that the fields in the structure approach several GVm^{-1} it is still desirable to achieve as large of an energy shift as possible after passing through the structure. To that end the high energy beam available at the Facility for Advanced aCcelerator Experimental Tests (FACET) at SLAC National Laboratory provides naturally long beta functions, thus extending the interaction without the need of a focusing channel to keep the beam in the structure. In addition to high beam energy, FACET offers

Copyright © 2014 CC-BY-3.0 and by the respective authors

ISBN 978-3-95450-142-7

CONSTRUCTION AND RF CONDITIONING OF THE CELL-COUPLED DRIFT TUBE LINAC (CCDTL) FOR LINAC4 AT CERN*

A. Tribendis#, Y. Biryuchevsky, E. Kenzhebulatov, Y. Kruchkov, E. Rotov, A. Zhukov, BINP, Novosibirsk, Russia
M. Naumenko, RFNC-VNIITF, Snezhinsk, Russia
Y. Cuvet, A. Dallocchio, J.F. Fuchs, F. Gerigk, J.M. Giguet, T. Muranaka, J. Hansen, E. Page, B. Riffaud, N. Thaus, M. Tortrat, M. Vretenar, R. Wegner, CERN, Geneva, Switzerland

Abstract

This paper reports on the construction experience of the Linac4 CCDTL, which took place in two Russian institutes in the framework of three ISTC projects in close collaboration with CERN. The tanks were constructed at VNIITF, Snezhinsk, while the drift tubes and supports were made at BINP, Novosibirsk. All structures were then assembled and tuned at BINP before shipment to CERN where the high-power conditioning took place. The tuning principles, quality checks and conditioning results are presented.

INTRODUCTION

Linac4, a new 86 m long 160 MeV H- accelerator [1] under construction at CERN, will replace the 50 MeV proton Linac2 as an injector to the PS Booster. This is an essential step towards higher luminosity of the LHC.

Linac4 consists of accelerating structures of different types. After the H- source a 45 keV beam is accelerated in an RFQ *(Radio Frequency Quadrupole)* structure up to the energy of 3 MeV. The RFQ is followed by a DTL *(Drift Tube Linac)* structure where particles are accelerated up to 50 MeV. After that the beam enters a CCDTL *(Coupled Cavity DTL)* where its energy is further increased up to 104 MeV. Finally the beam passes through the PIMS *(PI-Mode Structure)* section and reaches its output energy of 160 MeV.

All Linac4 structures operate at 352.2 MHz.

At low energies an Alvarez type DTL with quadrupoles housed in the drift tubes is a standard choice due to its good transverse focusing ability. For Linac4 permanent magnetic quadrupoles (PMQs) are used, which allows reducing the size of the drift tubes and thus increasing the RF efficiency but makes it impossible to change the transverse focusing once the machine is in operation. A CCDTL structure is used as soon as it becomes possible to place quadrupoles between subsequent accelerating cavities rather than inside drift tubes. The advantages of this approach are: i) drift tube diameter is small and thus the RF efficiency is high, ii) although EMQs are used only between the modules while PMQs are installed between the cavities within a module, the simulations showed that this provides sufficient flexibility for transverse beam dynamics, iii) the quadrupoles that need to be positioned quite precisely relative to the beam axis can be aligned on the supports independently from the cavities thus significantly relaxing the tolerances of the drift tube positioning. At higher energies the CCDTL is replaced by the PIMS for the sake of high effective shunt impedance.

The CCDTL structure consists of separate accelerating cavities (tanks) with drift tubes. Accelerating cavities are connected by single cell off-axis coupling cavities (or "cells"). An accelerating cavity has 2 drift tubes, that is 3 accelerating gaps per cavity. Quadrupoles are placed between the accelerating cavities. The cavities are grouped in modules, each module containing 3 accelerating cavities with 2 coupling cells in between (fig. 1). Each module is driven by a klystron amplifier through a coupling iris in the bottom of the middle tank. In total 7 modules are needed for Linac4 occupying about 25 m of its length.

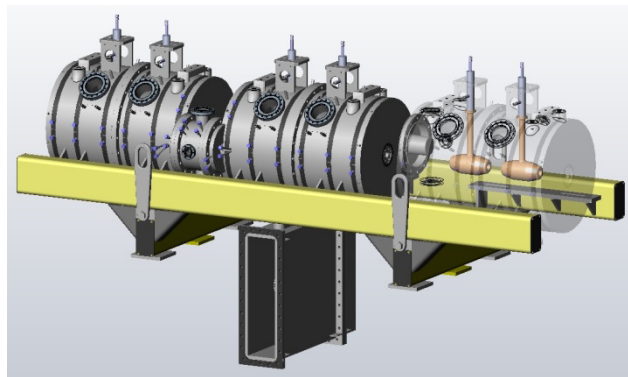


Figure 1: CCDTL module.

Linac4 will be the first operating machine, where a CCDTL is used to accelerate beam.

WORK DISTRIBUTION

The original concept of a CCDTL came out from LANL in 1994 [2]. In 2000 CERN started considering the CCDTL concept for the intermediate energy range of Linac4, although at lower frequency than at LANL. After investigating a scaled (1:3) model in aluminium, CERN designed and built in 2004-2005 a 352.2 MHz CCDTL prototype consisting of 2 half-tanks with a single drift tube in each one and a coupling cell in between. The prototype was successfully tested at high power at CERN in 2006 [3].

*Work supported by the ISTC under the contracts 2875, 3888, 3889
#A.G.Tribendis@inp.nsk.su

Copyright © 2014 CC-BY-3.0 and by the respective authors

PHASE LOCKED MAGNETRONS FOR ACCELERATORS

A.C. Dexter
Engineering Department, Lancaster University, Lancaster, LA1 4YR, UK
and Cockcroft Institute, Daresbury, Warrington UK

Abstract

Magnetrons offer lower capital costs and higher efficiencies than klystrons, however are natural oscillators rather than amplifiers. This paper reviews techniques and issues for applying high efficiency L band magnetrons to long pulse, high intensity proton linacs. Reference is made to a proof of principle experiment whereby the phase of an SRF cavity was accurately controlled when energised by a magnetron.

INTRODUCTION

Early split ring anode magnetrons as described by Elder in 1926 [1] were operated both as amplifiers and oscillators. A magnetron is characterized by a d.c. electric field applied between a cylindrical cathode and a surrounding anode with a d.c. magnetic field that is transverse to the electric field. The development of high current cathodes in the years just prior to 1939 [2] allowed the first high power magnetron to be developed in 1940 [3]. The resonant circuits that were previously outside the vacuum envelope became solid copper anode blocks to dissipate heat from the impacting electrons.

By 1943 the electronic behaviour of the cavity magnetron and its equivalent circuit were well understood. Reike's contribution in Collin's book [4] identifies the fundamental electrical quantities for the magnetron as the d.c. magnetic field B, the RF output power P_{out}, the frequency f, the load impedance Z_L , the d.c. current I_{dc} and the d.c. voltage V_{dc} applied between the anode and the cathode.

Frequency Pulling

The pulling characteristic of a magnetron is a map of how its frequency is perturbed by a load. It can be understood by representing the magnetron as a negative resistance oscillator as depicted in Fig. 1.

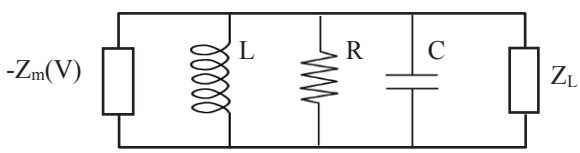


Figure 1: Equivalent circuit for a magnetron.

In Fig. 1 the values of L and C are chosen to give the operating mode frequency of the magnetron and the impedance that the anode resonator presents to the electronic current. The value of R is chosen to give the correct Ohmic heating in the RF circuit. The negative impedance $-Z_m$ represents the mechanism by which the electrons generate RF in the resonant anode structure. The value of Z_m depends primarily on the RF field in the anode structure, the d.c. current I_{dc} and the magnetic field B. Define the RF voltage V as the instantaneous RF voltage between anode vane tips. The magnitude of the steady state RF voltage is then achieved after I_{dc} has adjusted itself to make

$$\mathrm{Real}\{-Z_m(V, I_{dc}, B)+Z_L\}+R=0 \qquad (1)$$

The circuit of Fig. 1 dictates the general form of the Magnetron Rieke diagram as illustrated in Fig. 2. The figure shows that reflecting power back to the magnetron with a $\pm 90^o$ phase shift increases or decreases the magnetron frequency respectively. It should be noted that reflecting power in phase or 180° out of phase will change the power output. The outer circle in Fig. 2 represents a reflection coefficient of 0.8. Reflecting 10% of the power back to the magnetron changes the output by 8% and this can be plus or minus depending on the phase of the reflection. The skewing of the constant frequency lines in this figure are probably as a consequence of the anode being cooler and hence smaller at lower power levels.

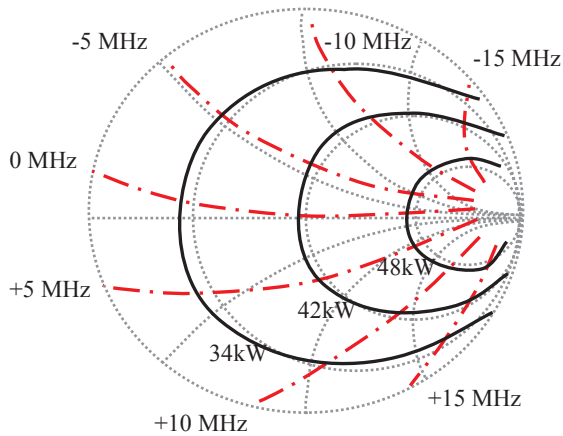


Figure 2: Rieke Diagram re-drawn from Collins [4] for a type 725A Pulsed X band magnetron, B = 0.55T, Peak anode current = 10A.

Injection Locking

The magnetron pulling characteristic enables phase locking with an injected signal. If the magnetron's phase falls behind or moves in front of the injection signal's phase then the magnetron sees a complex impedance that moderates its frequency. This moderation acts to move the magnetron's phase back to the injection signal's phase. Prior to the development of circulators the phase of two magnetrons could be locked to a third magnetron using 3dB hybrid splitters [5]. Varian repeated this experiment by phase locking two high power X band magnetrons to a TWT with 13dB of gain for ~ 9μs pulses.

Copyright © 2014 CC-BY-3.0 and by the respective authors

ISBN 978-3-95450-142-7

HIGH POWER RF SOURCES FOR THE ESS RF SYSTEMS

M.R.F. Jensen, G. Göransson, C. Marrelli, C. Martins, R.E. Montaño, A. Sunesson, R. Yogi, R. Zeng, European Spallation Source ESS AB, Lund, Sweden
A. J Johannson, Lund University, Lund, Sweden

Abstract

The RF systems for ESS will consist of around 150 high power RF sources and will deliver 125 MW peak power to the proton beam during the 2.86 ms pulse with an average power of 5 MW. The two RF frequencies, 352 and 704 MHz, the different power requirements along the linac and the sources currently available strongly influence the choice of RF technology. This talk will focus on the high power RF solutions for the main parts of the linac. We present an overview of the available technology along with the first test results of the main sources. Additionally, we will present the preliminary design of a new 1.2 MW multi-beam super power IOT being designed together with industry for the high beta section of the linac.

THE EUROPEAN SPALLATION SOURCE

The European Spallation Source, located in Lund, Sweden, has entered the construction phase of a project to construct the world's most powerful neutron source. The facility is based around a proton linac and will deliver its first neutrons in 2019 and is expected to be fully operational with 22 instruments by 2025.

The linac will accelerate the proton beam to 2 GeV with a peak beam current of 62.5 mA. The RF systems will be pulsed at 14 Hz and during each pulse will deliver a peak power to the beam of 125 MW. The linac is divided up into different sections with accelerating technologies to match the increasing beam energy. The main RF systems are Radio-Frequency-Quadropole (RFQ), Medium-Energy-Beam-Transport (MEBT), Drift-Tube-Linacs (DTL), Spoke Cavities (SPK), Medium-Beta (MB) and High-Beta Elliptical Cavities (HB).

The main power requirements are listed in Table 1.

Table 1: Beam Power Requirements for the Accelerating Sections

	Total Peak Beam Power (MW)	Number of RF Stations	Frequency (MHz)
RFQ	1.60*	1	352
DTL	11.0*	5	352
SPK	8.02	26	352
MB	21.9	36	704
HB	89.4	84	704
Totals	132	152	

*Note that for the RFQ and the DTL the RF power includes the power lost in the cavity.

In addition to the power required for the beam, the RF sources must be capable of being operated with sufficient overhead for the LLRF to maintain the correct cavity voltage and phase. The RF plan and design currently assume a power overhead of up to 25% for feedforward and feedback systems, to compensate for microphonics, Lorentz detuning, beam loading, power supply ripple etc. Additionally, 5% power loss is assumed for the RF distribution system including losses in the transmission lines, circulators and mismatches. Please refer to [1] for details of the design of the phase reference line.

THE HIGH POWER RF SOURCES

The power level and frequency restricts the high power RF sources available for each section of the linac and in addition each section will need drive amplifiers and for the medium energy beam transport (MEBT) section, three high power amplifiers required for the buncher cavities.

The solid state and tube based RF amplifiers will be placed in a surface building along the length of the underground tunnel which will house the accelerating structures and proton beam. The RF gallery is split up into sections, with each section typically offering access to eight cavities through a common, connecting shaft, which will house waveguides from up to eight amplifiers and contain the cabling required in the tunnel. Figure 1 shows a preliminary representative section showing the layout of klystrons, the RF distribution system, racks for controls and one modulator for up to 4 klystrons for the medium and high beta part of the linac. To minimise the floor space, the 704 MHz klystrons will be placed vertically.

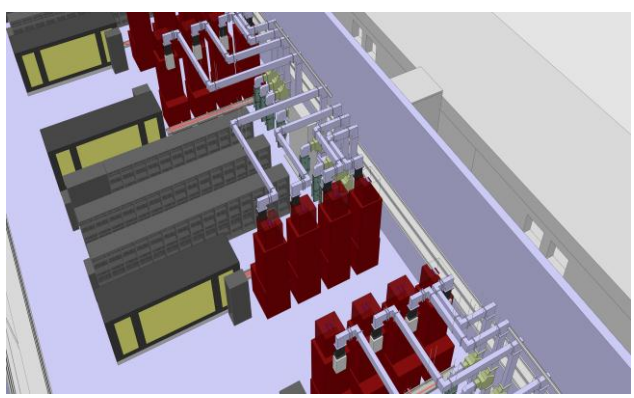


Figure 1: Preliminary typical layout in the RF gallery.

352 MHz, 2.8 MW Klystron

The RFQ and DTL sections of the linac each require high power klystrons with a peak power capability of 2.1 MW and 2.9 MW respectively including overhead and transmission losses. At this power level and frequency the

Copyright © 2014 CC-BY-3.0 and by the respective authors

ISBN 978-3-95450-142-7

LOW LEVEL RF FOR SRF ACCELERATORS

J. Branlard*, DESY, Hamburg, Germany
for the DESY LLRF group

Abstract

Low level radio frequency (LLRF) systems are a fundamental component of superconducting RF accelerators. Since the release of the MicroTCA standard (MTCA.4), major developments in MTCA.4-based LLRF systems have taken place. State-of-the-art LLRF designs deliver better than 10^{-4} relative amplitude and 10 mdeg phase stability for the vector sum control of SRF cavities. These developments in LLRF systems architecture and technology, driven by research institutes and supported by the industry are of highest importance for the European XFEL, but also for other SRF-based projects such as LCLS-II and the ESS, as well as for the next generation accelerators with 10^{-5} and mdeg regulation requirements.

INTRODUCTION

Low level radio frequency (LLRF) control and systems have been around for as long as particle accelerators have existed, so one can legitimately ask if there is something left to be demonstrated in this field. The final goal has not changed since the early days: control the accelerating field in amplitude and phase with the required precision and stability. With the advent of FPGAs, digital LLRF systems have gradually replaced their analog counterpart. The evolution of technology has changed the implementation of LLRF systems and opened new doors, in effect spreading the field of applications. Increasing FPGA capabilities and very fast analog-to-digital converters have changed the way designers approach LLRF systems, always pushing further and extending its role within the accelerator control. Every new generation accelerator pushes the limit of the beam control stability requirements. State of the art accelerators require RMS amplitude and phase stability of 0.01% and 0.01 deg. LLRF systems should prepare for the next challenge: 10^{-5} amplitude and millidegree phase stability requirements.

Details on the architecture of the XFEL LLRF system can be found in [1–3]. This paper presents instead an overview of some of the many facets of a LLRF system for superconducting RF (SRF) accelerators, with examples taken from the LLRF system developed using the micro telecommunications computing architecture (MTCA.4) [4] for the European X-ray free electron laser (XFEL) accelerator. In particular, the interface and contributions of the LLRF to other sub-systems are presented. The second part of this contribution focuses on special challenges posed to the LLRF system, relevant for large scale SRF accelerators.

* julien.branlard@desy.de

INTERFACES TO LLRF

RF Power Sources

The very next component in the RF signal chain at the output of the LLRF system is the high power RF amplification and distribution: pre-amplifiers, klystrons, solid state amplifiers or inductive output tubes followed by a waveguide distribution including power directional couplers, circulators and phase shifters. While the responsibility of the LLRF system lies in delivering the proper accelerating drive signal, the impact of all down stream subcomponents should be taken into account. In most cases, amplitude and phase klystron linearization is necessary to optimize the controller performance, implemented as look up tables [5] or by polynomial interpolation [6], as a middle layer server or directly in the FPGA of the LLRF controller.

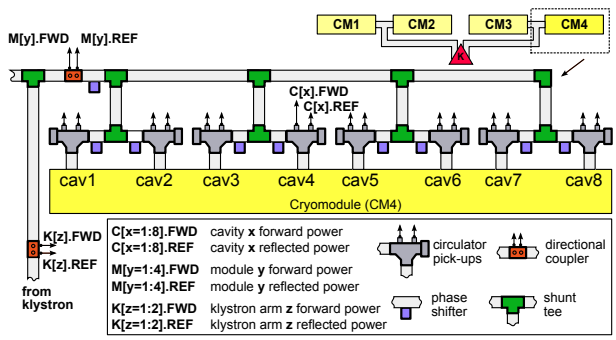


Figure 1: XFEL waveguide distribution showing forward and reflected power pick-ups.

The waveguide power distribution can be fixed or dynamically adjustable, for optimal cavity field control. Phase shifters are typically mounted along the waveguides, to control the incoming waveform phase, for individual cavities, or for group of cavities. Motorized phase shifters and motorized hybrid splitters allow for a tunable power distribution, providing an additional knob to control the cavity forward power (slow control). This also has a direct impact on the reflections and cross talks between cavities which can clearly be seen from the LLRF system. Directional couplers used along the waveguide distribution are important monitoring points (Fig. 1). The directivity of these couplers affects the waveform detection. Forward and reflected power signals can then be efficiently decoupled within the LLRF system. For the XFEL, the forward and reflected power waveforms (P_{FWD} and P_{REF}) are digitized by dedicated MTCA.4 boards and then centralized into the main LLRF controller [7]. The main controller then performs a complex linear combination of P_{FWD} and P_{REF} to decouple the waveforms, effectively removing the cross-coupling induced by the directivity of the circulator pick-ups. These calibrated P_{FWD} and

Copyright © 2014 CC-BY-3.0 and by the respective authors

ISBN 978-3-95450-142-7

CHOPPING HIGH-INTENSITY ION BEAMS AT FRANZ

C. Wiesner*, M. Droba, O. Meusel, D. Noll, O. Payir, U. Ratzinger, P. Schneider,
IAP, Goethe-University, Frankfurt am Main, Germany

Abstract

The accelerator-driven Frankfurt Neutron Source FRANZ is under construction at the science campus of Frankfurt University. Its Low-Energy Beam Transport (LEBT) line also serves as test stand for transport and chopping experiments with high-intensity ion beams. The high-current proton source was tested successfully with dc currents above 200 mA. The LEBT section consisting of four solenoids and a 250 kHz, 120 ns chopper was successfully commissioned using a helium test beam at low beam currents. Transport simulations including space-charge compensation and measurements are discussed. Simulations and experimental results of the novel LEBT chopper using a Wien-filter type field array and pulsed electrode voltages of up to ±6 kV will be presented.

INTRODUCTION

The "Frankfurt Neutron Source at the Stern-Gerlach-Zentrum" (FRANZ) is under construction in the experimental hall of the *Institut für Angewandte Physik* (IAP) at Frankfurt University [1, 2]. It will deliver neutrons in the energy range of 1 keV to 500 keV, which are especially suited for nuclear astrophysics experiments [3].

The neutrons are produced via the ^{7}Li(p,n)^{7}Be reaction channel, thus requiring a driver linac delivering a 2 MeV primary proton beam.

Figure 1: Overview of the Frankfurt neutron source FRANZ.

In the main operation mode, the so-called Compressor Mode, a pulsed high-intensity beam is required for the energy-dependent measurements of neutron capture cross-sections using the time-of-flight method.

ION SOURCE

The primary high-intensity proton beam is generated by an arc discharge driven volume type ion source [4]. Since the ion source cannot be pulsed at the required repetition rate of 250 kHz, it will be operated in dc mode while the beam pulses will be shaped by a chopper in the LEBT section. The design proton current is 50 mA in a first stage, with possible upgrades up to 200 mA.

At the moment, the ion source is undergoing a detailed test program at a dedicated ion source test stand. A proton beam current density of 480 mA/cm^2 was achieved during dc operation using a total arc power of 9.7 kW. For an emission opening radius of 4 mm, a proton current of 240 mA was extracted at 50 keV beam energy. By manipulating the plasma properties, the percentage of the undesired hydrogen fractions, H_2^+ and H_3^+, can be reduced to less than 10 % [5]. First beam emittance measurements show an 89 %-rms emittance of $\epsilon_{\text{rms, norm}} = 0.08$ mm·mrad at 52 keV energy and at a normalized beam current of 85 mA [6]. For the future FRANZ operation, a relatively high initial beam energy of 120 keV was chosen to reduce space-charge effects.

LEBT SECTION

In the LEBT line, transverse focusing is provided by four solenoids, allowing space-charge compensated beam transport. An overview of the LEBT section is given in Fig. 3.

The first two solenoids match the beam into the chopper while the remaining two inject the beam into the Radio-Frequency Quadrupole (RFQ). The vertically moveable high-power Faraday Cup, installed at the Diagnostics Chamber 1, is used to measure the beam current and, if required, to stop the beam. The beam pulses that are shaped by the chopper can be measured with a fast Beam Current Transformer (BCT) installed between Solenoids 3 and 4. In addition, a rotating vacuum chamber developed especially for this beamline can be used for beam tomography [7].

Detailed numerical investigations of the LEBT show an efficient matching of the 50 mA dc beam into the acceptance of the RFQ [8]. For these simulations, a fixed space charge compensation of 95 % in front of the chopper and of 0 % behind it was assumed. However, new simulation tools considering a more realistic time-dependent electron production from residual gas ionization and secondary electron production at the metallic walls are under investigation [9].

Figure 2 shows the present status of the LEBT section.

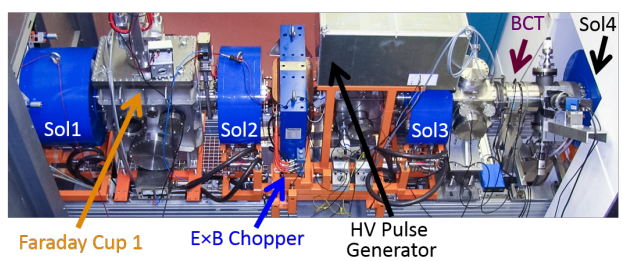


Figure 2: FRANZ LEBT section after assembly.

* wiesner@iap.uni-frankfurt.de

ISBN 978-3-95450-142-7

Copyright © 2014 CC-BY-3.0 and by the respective authors

PHASE-I PROTON / DEUTERON LINAC BEAM OPERATION STATUS

A. Kreisel, L. Weissman, A. Arenshtam, Y. Ben Aliz, D. Berkovits, Y. Buzaglo, O. Dudovich, Y. Eisen, I. Eliyahu, G. Feinberg, I. Fishman, I. Gertz, A. Grin, S. Halfon, Y. Haruvy, T. Hirsh, D. Hirschmann, Z. Horvitz, B. Kaizer, D. Kijel, Y. Luner, I. Mor, J. Rodnizki, G. Shimel, A. Shor, I. Silverman, D. Vartsky and E. Zemach,

Soreq NRC Yavne 81800, ISRAEL

Abstract

Phase I of the Soreq Applied Research Accelerator Facility, SARAF, is under operation at the Soreq Nuclear Research Center. The status of Phase I main components is reported, as well as beam operation experience accumulated over the recent two years. The latter includes operation of high power CW protons beams on beam dumps and special targets, and experiments with low-intensity deuterons beams. Recent and future improvements in the current facility performance are discussed.

INTRODUCTION

Phase-I of the SARAF linac is composed of a 20 keV/u ECR ion source and LEBT [1], a 176 MHz, 4 m long, 250 kW, 4-rod RFQ [2], a 65 cm long MEBT and a 4.5 K superconducting module housing 6 β_0=0.09 bulk Nb HWRs, 0.85 MV each and three 6T solenoids in a separated vacuum, 2.5 m long cryostat [3]. SARAFPhase-I routinely accelerates CW and pulsed protons and pulsed deuterons beams.

Significant new experience in beam operation has been accumulated during the recent two years. The main objective was learning how to deliver high power beams to the state of art beam dumps and targets, including the first proton irradiation of a liquid lithium target.

In this period we improved some of the accelerator subsystems, enabling more stable operation of the facility and several basic science experiments. The main limiting factors were lack of a target room, insufficient engineering resources and poor quality of the electrical network. These problems are being addressed and gradually solved: a new powerful 750 kW UPS system was procured and installed, a first target room is being designed and new personnel are being hired. These improvements will enable a significant increase in beam-on-target hours.

In this paper we report on the SARAF accelerator subsystems status, as well as experience in beam operations that has been accumulated since the recent reports [4-8].

STATUS OF MAIN COMPONENTS

EIS/LEBT

The SARAF ECR ion source has been in operation during recent years with minimal maintenance. Once a year the boron nitride parts are being replaced to avoid source instability. We have experienced several failures connected to magnetron operation. A test bench was built in the lab in order to test the magnetron electronics

First experience with the slow LEBT chopper and plans regarding the fast LEBT chopper were discussed in [9]. Introduction of the chopper would allow for a more flexible working range of the beam duty cycle. At present the beam intensity ramping is done by manipulation of LEBT parameters. Measuring of CW beam profiles with a non-destructive residual gas profiler monitor [10] showed that such a ramping method leads to variation in the beam optics during ramp. Introduction of the chopper will improve beam tuning and the beam ramping procedure.

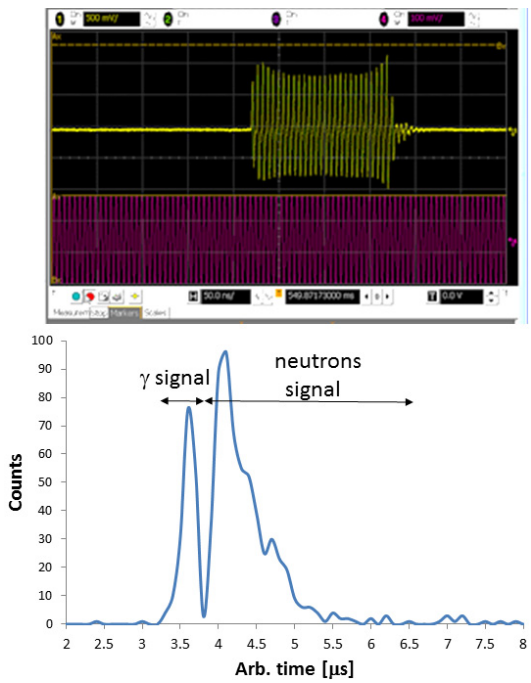


Figure 1: Layout of papers Top. A 160 ns beam pulse from the slow chopper. Pulse measured by BPM pick-ups. Bottom. A measured TOF neutrons spectrum generated with 4 MeV proton pulses on lithium target.

The shortest time of the chopping voltage obtained with the slow chopper is approximately 200 ns corresponding to approximately 160 ns beam pulse (Fig. 1). Simulations show that such a beam pulse length will allow measurement of neutron energy using the time-of-flight (TOF) technique. The first test for feasibility of TOF technique was successful. In this test a 0.5 mA, 4 MeV proton pulses were sent to the liquid lithium target (see

Copyright © 2014 CC-BY-3.0 and by the respective authors

ISBN 978-3-95450-142-7

STATUS OF THE RAON HEAVY ION ACCELERATOR PROJECT

Dong-O Jeon# and Hyung Jin Kim representing the RAON
Institute for Basic Science, Daejeon, Republic of Korea

Abstract

Construction of the RAON heavy ion accelerator facility is under way in Korea to build the In-flight Fragment (IF) and Isotope Separation On-Line (ISOL) facilities to support cutting-edge researches in various science fields. At present prototyping of major components are proceeding including 28 GHz ECR ion source, RFQ, superconducting cavities, magnets and cryomodules. Superconducting magnets of 28 GHz ECR ion source are fabricated and tested. First article of prototype superconducting cavities are delivered that were fabricated through domestic vendors. Prototype HTS quadrupole is under development. Progress report of the RAON accelerator systems is presented.

INTRODUCTION

The RAON facility will be a unique facility that has the 400 kW In-flight Fragmentation (IF) facility and the 70 kW Isotope Separator On-Line (ISOL) facility providing wider range of rare isotope beams for users.

The driver accelerator for the IF facility is a superconducting linac that can accelerate up to 200 MeV/u in case of uranium beam and up to 600 MeV for proton beam delivering more than 400 kW of beam power to the IF target and various other targets. The driver for the ISOL facility is an H^- 70-MeV 1 mA cyclotron that delivers 70 kW beam power to the ISOL target. The cyclotron has dual extraction ports with thin carbon foils for charge exchange extraction of H^- beam.

The rare isotope beams generated by the ISOL system is re-accelerated by a chain of post accelerators: RFQ, MEBT and superconducting linac SCL3 up to 18.5 MeV/u. The RI beams can be delivered to the low energy experimental hall or can be injected through P2DT to the SCL2 to accelerate to higher beam energy. The schematic layout of the RISP facility is shown in Fig. 1.

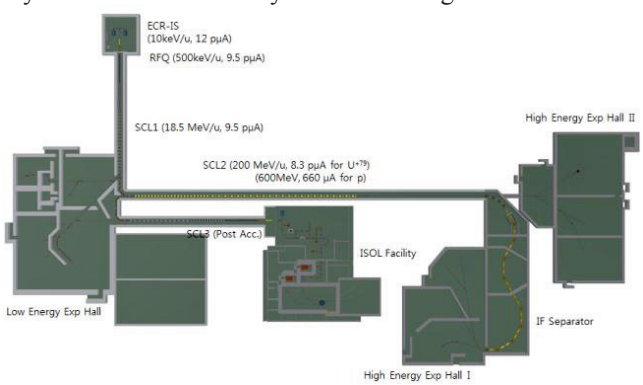


Figure 1: Plot of the RAON facility layout.

#jeond@ibs.re.kr

To meet the diverse needs, the RISP design is optimized to provide various high intensity stable ion beams and radioactive isotope (RI) beams from proton to uranium for domestic and international users.

Construction of the RAON heavy ion accelerator facility has begun December 2011. The assessment of the conceptual design has followed and design changes were introduced [1]. Detailed design of the accelerator systems has progressed, and prototyping of critical components and systems have been materialized. In this paper, the status of the RAON accelerator systems is presented along with prototyping progress.

THE DRIVER LINAC

The RAON has two linear accelerators; one is the driver linac and the other is the linac as post-accelerator. The driver linac delivers beams to In-flight Fragment (IF) facility and is designed to accelerate high intensity stable ion beams from uranium to proton. Driver linac consists of 28 GHz ECR ion sources, LEBT, RFQ accelerating beam to 0.5 MeV/u, MEBT, low energy superconducting linac (SCL1) accelerating uranium beam to 18 MeV/u, Charge Stripper Section (CSS) for charge state increase and collimation, and high energy superconducting linac (SCL2) accelerating uranium (proton) beam to 200 MeV/u (600 MeV). The driver linac is designed to deliver 400 kW beam power with uncontrolled beam loss less than 1 W/m to IF target and other targets. Figure 2 shows the diagram of the RAON driver linac.

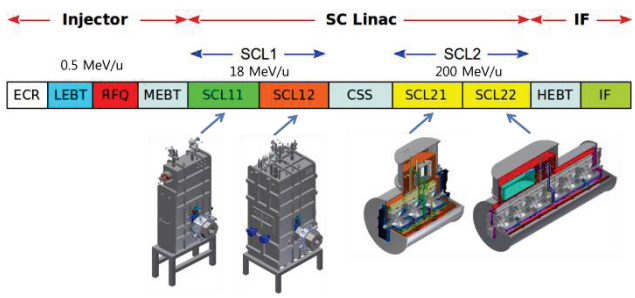


Figure 2: Diagram of driver linear accelerator of the RAON. Driver linac consists of four types of cryomodules and transverse focusing is provided by normal conducting quadrupole doublets as shown in the figure. For diagnostics, there are beam boxes located between quadrupole doublets.

Injector

The injector consists of 28 GHz superconducting ECR ion source (ECR IS), Low Energy Beam Transport (LEBT), Radio Frequency Quadrupole (RFQ) and Medium Energy Beam Transport (MEBT). For ECR IS, superconducting magnets and dual high power RF sources

Copyright © 2014 CC-BY-3.0 and by the respective authors

ISBN 978-3-95450-142-7

CW HEAVY ION ACCELERATOR WITH ADJUSTABLE ENERGY FOR MATERIAL SCIENCE*

S. V. Kutsaev, B. Mustapha, J. Nolen and P. N. Ostroumov
ANL, Argonne, IL 60439, U.S.A.

Abstract

The proposed eXtreme MATerial (XMAT) research facility at ANL's Advanced Photon Source (APS) combines medium-energy heavy-ion accelerator capability with the high-energy X-ray analysis to enable rapid in situ mesoscale bulk analysis of ion radiation damage in advanced materials and nuclear fuels. The XMAT facility requires a CW heavy-ion accelerator with adjustable beam energy in the range of 300 keV/u to 1.25 MeV/u. Such an accelerator has been developed and comprises of an ECR ion source, a normal conducting RFQ and four multi-gap quarter-wave resonators (QWRs) operating at 60 MHz. This paper presents the linac design and the multi-physics design of the RFQ and the QWRs. The design includes a beam transport system capable of focusing ions into a 20-micron diameter spot on the target.

INTRODUCTION

Many technological areas in our life benefit from using new materials. Materials and our ability to design and fabricate them are undergoing a dramatic revolution leading to improved costs, safety, efficiency, and reduced waste. Active development of nuclear energetics requires new materials to be used in nuclear reactors to increase their life time, enhance accident tolerance, improve burn-up operation, and enable advanced reactor designs. Material properties deteriorate due to micro-structural defects caused by protons and neutrons and can include bubbles, voids, precipitates, solute segregation, grain boundaries, helium cavities, amorphization etc. These can lead to consequences such as void swelling or cracking [1]

XMAT FACILITY

The traditional approach of performing neutron irradiation in test reactors, followed by post-irradiation testing and examination, is extremely time consuming as it takes years to reach the required dose. To expedite the required experimental time down to hours or days, a dedicated facility XMAT (Fig.1) is being developed at Argonne National Laboratory. Combining the capabilities of a heavy-ion linac and the brightest X-ray source in the western hemisphere– the Advanced Photon Source (APS), the facility will enablematerial scientists to:

- Accelerate heavy ions to energies about 1 MeV/u for sample irradiation. These energies correspond to those of fission products in nuclear reactors.
- Deliver mixed beams with the same charge-to-mass ratio (e.g. $^{86}Sr^{15+}$ and $^{132}Xe^{23+}$) to model the simultaneous damage by fission fragments.
- Separate damage and interstitial effects since the ion energy deposition and implantation probability peaks are offset in distance [2]
- Provide ~10 μm beam penetration into samples to avoid surface effects, which otherwise interfere with real damage effects [3]
- Provide high damage doses (~25 dpa/hour) that will allow rapid material screening.
- Benefit from using high-energy, focusable X-rays to enable 3 dimensional meso-scale in situ study of radiation damage. Such experiments will allow observing and understanding the physics of radiation damage.

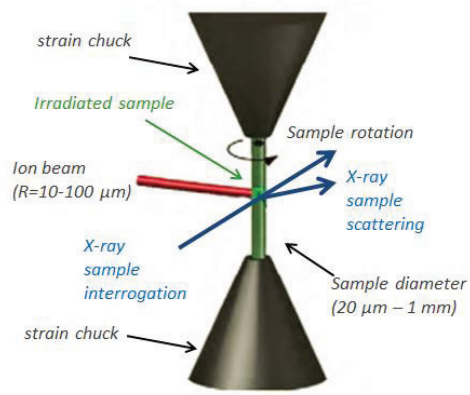


Figure 1: XMAT beamline scheme.

This paper presents the results of a pre-conceptual design and analysis of a continuous wave (CW) linear accelerator capable of delivering 1.2 MeV/u ion beams with mass-to-charge ratio of 5 and less.

HEAVY ION ACCELERATOR

The proposed heavy-ion linac design, presented in Figure 2, is capable of accelerating particles with A/Q=5 to 1184 keV/u (1200 keV/u for $^{238}U^{50+}$ ions). Heavy ions of any species from protons to uranium are extracted from an Electron-Cyclotron-Resonance (ECR) ion source and then delivered to a 4-meter RFQ where they are bunched and accelerated to 300 keV/u. The beam is then re-bunched in a 4-gap quarter wave resonator (QWR) and accelerated to the final energy in four normal conducting continuous wave (CW) multi-gap QWRs. Finally, the beam comes through a 100 micron slit and is focused into a 30 micron spot on the target using superconducting solenoids in the microbeam forming section.

* This material is based upon work supported by the U.S. Department of Energy, Office of Science, Office of Nuclear Physics, under contract number DE-AC02-06CH11357. This research used resources of ANL's ATLAS facility, which is a DOE Office of Science User Facility

Copyright © 2014 CC-BY-3.0 and by the respective authors

COST OPTIMIZED DESIGN OF HIGH POWER LINACS

M. Eshraqi*
European Spallation Source, Lund, Sweden

Abstract

The research accelerators are growing in energy and power which translates to an increase in their cost, and also size when the conventional acceleration techniques are used. On the other hand, handling megawatts of power requires a design that is robust and respects the known criteria in beam physics to avoid losses in excess of one part in a million. Traditionally cost increases with power and quality of the accelerator and beam. In this paper, using the ESS linac as an example, this tradition is challenged and ways to reduce the cost while neither quality nor power is compromised are presented.

INTRODUCTION

The applications of the hadron linacs are becoming more and more diverse, from the very low power medical accelerators to the high power irradiation and spallation accelerators. Even when these linacs are used as injectors to rings, their power, complexity and cost is a considerable percentage of the total project cost [1]. While some of the design rules of high current linacs are irrelevant to low current accelerators, there are still several similarities in their design, architecture and optimization. The output energy and power of each of these accelerators is imposed to the design team through its goals and applications. Having a defined, limited budget, the linac should be redesigned and optimized several times to meet the goals, and all these should happen considering the fixed dates in the project. The risk factor should be added as another dimension to this triangle of scope, cost and schedule. While no one intends to take a higher risk, the constraints defining the base of this pyramid tend to push the risk higher and cut the margins. During the design and optimization one should consider reasonable mitigation schemes for these risks that are cost and schedule neutral. The goal of this paper is to share the experiences gained in the design and optimization of the ESS linac, specially those acquired during cost scrubbing.

HADRON LINACS

Some examples of recent hadron accelerators and their application are listed below.

European Spallation Source [2] is a spallation neutron source which produces neutrons through bombardment of neutron rich nuclei with high energy protons. The high flux of moderated, slow, neutrons is used to study the structure of e.g. biological substances. The Spallation Neutron Source, SNS [3] in Oak Ridge, US, uses a 1 MW superconducting linear accelerator as the main accelerator. The aging research reactors and the public resistance against new research nuclear reactors plus the pulsed structure of neutron flux out of spallation sources has made them even more attractive in recent years [3–5].

Neutrino beams [6] are produced using an intense beam of protons to create pions that upon decay produce muons and muon neutrinos as secondary particles. The oscillation of these muon neutrinos into other types of neutrinos will be detected at a detector far from the generation point to determine parameters that determine these oscillations. On a recent staged proposal, the muons could be captured, cooled and accelerated in a muon decay ring for a neutrino factory that could later be extended up to a muon collider [7].

Accelerator driven systems [8, 9] also called accelerator driven subcritical nuclear reactors or hybrid reactors as well as transmutation facilities [10] are being designed to produce cleaner and safer energy and transmute the long lived nuclear waste to short lived waste. Both of these applications need a multi-megawatt class accelerator in the GeV range. However, the fail/trip rate of these accelerators is orders of magnitude tighter than the existing accelerators. Though technically these machines are not insuperable, they are not yet economically very attractive, reducing the accelerators' construction and operation cost might affect that balance.

RULES OF THUMB ON LINAC DESIGN

When designing a high power hadron linac, one should consider few guidelines. The zero current phase advance per focusing period should not exceed 90° in any of the transverse or longitudinal planes. Having a zero current phase advance per focusing period above $\sigma_0 > 90^\circ$ would cause envelope instabilities even at low beam currents [11]. The second important parameter is the average zero current phase advance, $k_0^2 \propto F$, where F is the external force on the beam. Having a smooth phase advance along the linac guarantees that the space charge equilibrium within the beam will not be altered abruptly at the transitions. Such abrupt changes in the focusing channel, either transverse of longitudinal, could increase the emittance [12] and depopulate the core of the beam.

For high intensity accelerators the tune depression (η), the ratio of phase advance with current (σ) to zero current

* mohammad.eshraqi@esss.se

ISBN 978-3-95450-142-7

Copyright © 2014 CC-BY-3.0 and by the respective authors

SUPERCONDUCTING RF DEVELOPMENT FOR FRIB AT MSU*

K. Saito#, N. Bultman, E. Burkhardt, F. Casagrande, S. Chandrasekaran, S. Chouhan, C. Compton, J. Crisp, K. Elliott, A. Facco, A. Fox, P. Gibson, M. Johnson, G. Kiupel, B. Laxdal, M. Leitner, S. Lidia, D. Morris, I. Malloch, D. Miller, S. Miller, D. Norton, R. Oweiss, J. Ozelis, J. Popielarski, L. Popielarski, A. Rauch, R. Rose, T. Russo, S. Shanab, M. Shuptar, S. Stark, N. Usher, G. Velianoff, D. Victory, J. Wei, G. Wu, X. Wu, T. Xu, Y. Xu, Y. Yamazaki, Q. Zhao, W. Zheng,
FRIB, Michigan State University, 640 South Shaw Lane East Lansing, MI 48824, USA
K. Hosoyama, KEK, 1-1 Oho, Tsukuba-shi, Ibaraki-ken, 305-0801, Japan

Abstract

The Facility for Rare Isotope Beams (FRIB) is a high intensity, heavy ion SRF CW linac for nuclear science. FRIB SRF cryomodule design addressed four critical issues: high performance, stable operation, easy maintainability, and low cost construction, each presenting a unique challenge. FRIB SRF system design and R&D are almost complete. This paper presents unique R&D done in past 2-3 years for FRIB.

FRIB PROJECT

FRIB is a Department of Energy (DOE) joint project operated at MSU and obtained CD3-B approval in August 2014. Conventional facilities construction began in March 2014. The accelerator system construction will begin in October 2014, and will be completed in 2022 (CD4). A new SRF highbay has been constructed for SRF mass-production, and technical equipment is being installed [1].

Fig. 1 shows FRIB machine configuration in the tunnel, which consists of three folded linac segments with a total length about 500 m. It accelerates from proton to uranium up to 200 MeV/u, with beam power of 400 kW on the target. FRIB is the intensity frontier machine for heavy ions - for example it accelerates ^{238}U to $5{\cdot}10^{13}$ /s, 250 times greater than ATLAS. FRIB applies SRF technology from low β(v/c) =0.041 to medium β=0.53 acceleration sections. FRIB cryomodules include two cryogenic circuits, 2K for cavities and 4.5K for solenoid operation [2].

FRIB SRF SCOPE

FRIB uses two types of SRF cavities: Quarter Wave Resonators (QWR) for β=0.041 and 0.085, both operated at 80.5 MHz, and Half Wave Resonators (HWR) for β=0.285 and 0.53, both operated at 322 MHz. Fig. 2 illustrates these four cavities. RF parameters are summarized in Table 1. The operating gradients are ~5.5 MV/m @ $Q_O = 2x10^9$ for the QWRs and ~7.5 MV/m @ $Q_O = 9x10^9$ for the HWRs. These performance levels are a challenge compared to existing heavy ion linacs. However, advanced cavity design with a lower B_p/E_{acc} and operation at 2K can achieve these goals. The required number of cavities are 12 for β=0.041, 88 for β=0.085, 72 for β=0.285, and 144 for β=0.53. In total, 333 cavities are required. All four cavity families have been prototyped and their

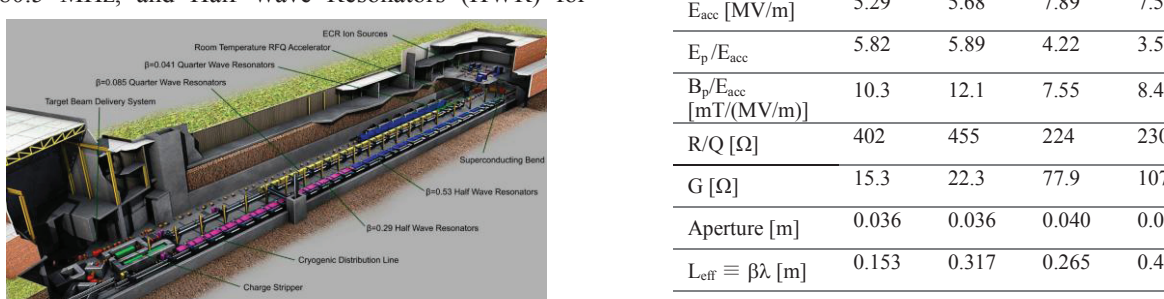


Figure 1: Linac configuration in FRIB tunnel.

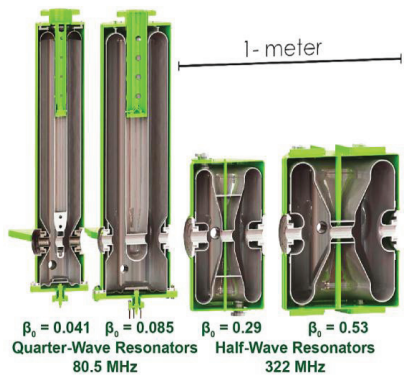


Figure 2: FRIB SRF cavity families

Table 1: RF Parameters for FRIB Cavities

Cavity Type	QWR	QWR	HWR	HWR
β_0	0.041	0.085	0.285	0.53
f [MHz]	80.5	80.5	322	322
V_a [MV]	0.810	1.80	2.09	3.70
E_{acc} [MV/m]	5.29	5.68	7.89	7.51
E_p/E_{acc}	5.82	5.89	4.22	3.53
B_p/E_{acc} [mT/(MV/m)]	10.3	12.1	7.55	8.41
R/Q [Ω]	402	455	224	230
G [Ω]	15.3	22.3	77.9	107
Aperture [m]	0.036	0.036	0.040	0.040
$L_{eff} \equiv \beta\lambda$ [m]	0.153	0.317	0.265	0.493
Lorenz detuning [Hz/(MV/m)^2]	< 4	< 4	< 4	< 4
Specific Q_O @VT	$1.4x10^9$	$2.0x10^9$	$5.5x10^9$	$9.2x10^9$

* Work supported by the U.S. Department of Energy Office of Science under Cooperative Agreement DE-SC0000661.
# Saito@frib.msu.edu

Copyright © 2014 CC-BY-3.0 and by the respective authors

STATUS OF THE HIE-ISOLDE LINAC

W. Venturini Delsolaro, L. Alberty, L. Arnaudon, K. Artoos, J. Bauche, A. P. Bernardes, J. A. Bousquet, E. Bravin, S. Calatroni, E. D. Cantero, O. Capatina, N. Delruelle, M. Elias, F. Formenti, M. A. Fraser, J. C. Gayde, S. Giron, J. N. Jecklin, Y. Kadi, G. Kautzmann, Y. Leclercq, P. Maesen, V. Mertens, E. Montesinos, V. Parma, D. D. Ramos, G. J. Rosaz, K. M. Schirm, E. Siesling, D. Smekens, A. R. M. Sublet, M. Therasse, D. Valuch, G. Vandoni, E. Vergara, D. Voulot, L. R. Williams, P. Zhang.

CERN, Geneva, Switzerland

Abstract

The HIE-ISOLDE project aims at increasing the energy of the radioactive beams (RIB) of REX-ISOLDE from the present 3 MeV/u up to 10 MeV/u for A/q up to 4.5. This will be accomplished by means of a new superconducting linac, based on independently phased quarter wave resonators using the Nb sputtering on copper technology, and working at 101.28 MHz. The focusing elements are superconducting solenoids providing 13.5 T^2m field integral. These active elements are contained in a common vacuum cryostat. The presentation will cover the status of advancement of the HIE-ISOLDE linac technical systems. The performance of the superconducting elements will be presented, together with the assembly work of the cryomodule in clean room and the planned qualification tests in the horizontal test facility at CERN.

INTRODUCTION

The superconducting post accelerator for the HIE-ISOLDE project [1] entered gradually the construction phase in 2013 after an R/D stage which had taken off in 2009 with the formal approval by CERN. The staging and the schedule of the project were reviewed at the beginning of 2014: the present plan foresees to deliver beams up to 4.2 MeV/u for the heaviest species in autumn 2015 with a single high-beta cryomodule. A second cryomodule will then be installed during the winter shutdown 2015/2016 bringing the energy to 5.5 MeV/u for all the radionuclides available at ISOLDE. This will complete phase 1, making Coulomb excitation studies possible up to A/q=4.5. A second phase will consist in adding two more high-beta cryomodules, thus doubling the available accelerating voltage. Finally, in phase 3, two low-beta cryomodules would be installed, replacing some normal conducting structures of the present REX-ISOLDE. This will allow varying continuously the energy between 0.45 and 10 MeV/u together with an improved beam quality. A detailed description of the optics and beam dynamics design choices for the linac can be found in [2]. The design minimized the longitudinal space for the 40 MV linac, optimizing transmission and emittance growth.

The high-beta cryomodules house five superconducting Quarter Wave Resonators (QWR) based on Nb/Cu technology [3], [4], and a superconducting solenoid for beam focusing, while their low-beta counterparts will contain six QWR and two SC solenoids.

Following the examples of ISAC-2 in TRIUMF [5] and of ALPI in INFN-LNL [6], the active elements are installed in common vacuum cryostats, i.e. the beam vacuum and the insulation vacuum are in common.

Normal-conducting steerers, alignment equipment and beam instrumentation are located in-between the cryomodules, together with the vacuum systems and valves which create a vacuum sector of each cryomodule.

As we write, all the main contracts for the procurement of the linac hardware are running, and intense work is ongoing at CERN to produce the superconducting cavities, carry out acceptance tests and prepare the infrastructure and the assembly of the cryomodules in clean room conditions. This paper offers a snapshot of the main activities one year before the scheduled commissioning of the HIE-ISOLDE linac with beam.

GENERAL INFRASTRUCTURE

The long shutdown of the CERN accelerators in 2013-2014 was used to upgrade the general infrastructure of the existing ISOLDE facility to the needs of HIE-ISOLDE with minor disruptions to the physics programs. The entire ISOLDE water-station has been replaced first and became operational in time for the 2014 low energy run of ISOLDE. Two new buildings were added to the complex to house the HIE-ISOLDE services.

The Compressor building contains the now fully installed and tested water cooling systems supplying REX-ISOLDE, the warm elements of the HIE-ISOLDE High Energy Beam Transfer lines (HEBT) as well as the different power convertors and RF amplifiers with demineralized water. Regarding the cryogenics system, the two He tanks are in place outside the building, and the installation of the overhauled ALEPH compressor units is ongoing. The ALEPH Cold Box is being renovated and

Copyright © 2014 CC-BY-3.0 and by the respective authors

ISBN 978-3-95450-142-7

SUPERCONDUCTING CAVITIES AND CRYOMODULES FOR PROTON AND DEUTERON LINACS

G. Devanz, CEA-Irfu CEA-Saclay, Gif-sur-Yvette 91191, France

Abstract

We review the recent advances in the design plans and test results of the superconducting structures for proton (ESS) and deuteron linacs (SPIRAL2, IFMIF). A variety of RF resonators is used for these purposes, from multicell elliptical cavities for the acceleration of pulsed proton beams to half and quarter wave resonators for CW deuteron beams. The increase in beam power with respect to previous generations of linacs brings new challenges to cavities and RF couplers. Test results of the available SRF prototypes and cryomodules of the aforementioned projects will be presented.

EUROPEAN SPALLATION SOURCE

The European Spallation Source ESS will be built in Lund, Sweden. It is based on a 2 GeV, 62.5 mA superconducting (SC) pulsed proton linac [1]. It is composed of a spoke resonator section running at 352.21 MHz which brings the proton beam energy up to 220 MeV, followed by two 704.42 MHz elliptical cavity sections. The first one, based on 6-cell β=0.67 cavities accelerates the beam to 570 MeV. The higher energy section is using 5-cell β=0.86 cavities to increase the proton energy to 2 GeV. Each SC cavity is fed by an independent RF power source. Nominal RF parameters for the ESS cavities are summarized in table 1.

Table 1: RF Operation parameters of ESS cavities

	Spoke	Medium β	High β
Frequency (MHz)	352.21	704.42	704.42
Nominal E_{acc} (MV/m)	9	16.7	19.9
Qo at Nom. E_{acc}	1.5 10^9	>5.10^9	>5.10^9
βg	0.50	0.67	0.86
RF peak power (kW)	335	1100	1100
FPC Q_{ext} (x10^5)	2.85	7.5	7.6

Helium for cavity cooling is supplied at 4.5K by the common cryogenic transfer line (CTL). Each cryomodule (CM) is fed through a valve box and jumper connection. He-II is produced at the CM level using a heat exchanger and JT valve, vapour being pumped out. The operation temperature of SRF cavities is 2 K. All CM types use a 40 K shield and MLI for thermal radiation insulation. A common characteristic of all types of CMs is the use of single, room temperature window power couplers (FPC), connected to the cavities using rigid double-wall outer conductors which ensure thermal insulation using He counter flow. Cold tuning systems combining slow and fast tuning capability are used on all cavities to cope with pulsed operation. The cold magnetic shielding surrounds the He jacket of cavities. The current phase of the CM and cavity development consists in designing and building technical demonstrators of each type of CM. A collaboration between ESS, CEA-Irfu and IN2P3-IPNO is performing this tasks. Important decisions concerned the maximum allowable pressure (PS) of CMs: it was chosen sufficiently low for minimizing licensing constraints of He vessels, while conserving operation margins.

Spoke Cavities and Cryomodules

Two β=0.5 double spoke resonators are housed in each of the 13 CMs (fig. 1) designed by IPNO [2]. Besides achieving low peak surface field and tunability, the cavity design [3] must conserve a sufficient mechanical resistance of the end caps and spoke bars for sustaining pressure and leak tests at room temperature. The Ti He jacket is free of any bellow and contributes to the stiffening of the resonator. In the framework of the European pressure vessel directive PED PS was chosen at 0.8 barg for the CM. The He vessel of the spokes can thus be classified as "§ 3.3" i.e. required to be designed using sound engineering practice only.



Figure 1: Double spoke ESS cryomodule.

They are supported by antagonists tie rods directly from the vacuum vessel, four radial and one axial pairs. The alignment mechanism allows adjusting the resonator position even in the operating conditions. Currently, the manufacturing of three prototypes is close to completion.

Elliptical Cavity Cryomodules

The cryomodule design is performed by IPNO in collaboration with CEA-Irfu. Medium and high β CMs have the same design and physical length. The design of the vessel, thermal shield and cavity support is described

Copyright © 2014 CC-BY-3.0 and by the respective authors

ISBN 978-3-95450-142-7

AN 800 MeV SUPERCONDUCTING LINAC TO SUPPORT MEGAWATT PROTON OPERATIONS AT FERMILAB*

Paul Derwent, Steve Holmes, Valeri Lebedev#, Fermilab, PO box 500, Batavia, IL 60510, USA

Abstract

Active discussion on the high energy physics priorities in the US carried out since summer of 2013 resulted in changes in Fermilab plans for future development of the existing accelerator complex. In particular, the scope of Project X was reduced to the support of the Long Base Neutrino Facility (LBNF) at the project first stage. The name of the facility was changed to the PIP-II (Proton Improvement Plan). This new facility is a logical extension of the existing Proton Improvement Plan aimed at doubling average power of the Fermilab's Booster and Main Injector (MI). Its design and required R&D are closely related to the Project X. The paper discusses the goals of this new facility and changes to the Project X linac introduced to support the goals.

PIP-II DESIGN CRITERIA

A number of approaches based on upgrades to the existing Fermilab accelerator complex can be taken to achieve beam power on the LBNF target in excess of 1 MW. The challenge is to identify a solution that provides an appropriate balance between minimization of near-term costs and flexibility to support longer-term goals. In order to constrain consideration to a modest number of options the following criteria were applied to possible solutions [1]:

- The plan should support the delivery of 1.2 MW from the MI to the LBNF target at energies between 80-120 GeV;
- The plan should provide support to the currently envisioned 8 GeV program, including Mu2e, g-2, and the suite of short baseline neutrino experiments;
- The plan should provide a platform for eventual extension of beam power to LBNF to >2 MW;
- The plan should provide a platform for eventual development of a capability to support multiple rare processes experiments with high duty factor beams, at high beam power.

The primary bottleneck limiting beam power to the LBNF target is related to the existing Linac and Booster. Performance is limited to about 4.4×10^{12} protons per Booster pulse by beam loss – primarily driven by the incoherent tune shift due to space-charge at the 400 MeV injection. The secondary bottleneck is the slip-stacking of twelve Booster pulses in the Recycler presently resulting in ~5% beam loss. This loss needs to be reduced for operation at larger beam power.

An ideal facility meeting the above criteria would be the pairing of a new linac with a modern rapid cycling synchrotron capable to accelerate a beam current large enough to avoid slip-stacking. Taking into account the limited acceptance of the Recycler such choice requires an injection energy of about 2 GeV. However cost limitations do not allow us to implement such plan in one step, consequently, requiring a staged approach to the upgrade of the FNAL accelerator complex.

To address the most immediate needs we propose to replace the existing 400 MeV linac by a new 800 MeV super-conducting (SC) linac. To further reduce the cost of the new machine we plan to reuse the existing Tevatron cryogenics infrastructure. Its limited cooling power requires SC linac operation in the pulsed regime. The increased injection energy should allow Booster operation with ~1.7 times larger Booster beam current. To be compatible with CW operation we limit the SC linac beam current to 2 mA. That requires an increase in number of injection turns from 12 to ~300. Although it looks as a quite large increase this number of injection turns is still about 3 times lower than used for injection to the SNS and an analysis shows that it does not present outstanding problems. To further increase the proton flux in the Booster we plan to increase its repetition rate from 15 to 20 Hz. That should also result in a decrease of the beam loss during slip-staking in Recycler. Such a cost effective approach addresses an increase of beam power required by the LBNF and creates a wide range of possibilities for future upgrades. Table 1 presents main parameters of new facility.

Table 1: Main PIP-II Parameters

Parameter	Value	Unit
Linac beam energy	800	MeV
Linac beam current	2	mA
Linac pulse duration	0.55	ms
Linac/Booster pulse repetition rate	20	Hz
Linac upgrade potential	CW	
Booster Protons per Pulse (extract.)	6.5×10^{12}	
Booster Beam Power at 8 GeV	160	kW
MI Cycle Time @ 120 GeV	1.2	s

SC LINAC

The linac was described in details in the Project X Reference Design Report (RDR). Here we point out the main features and deviations from it [2, 3]. Figure 1 shows the structure of the linac. A room temperature (RT) section accelerates the beam to 2.1 MeV and creates a desired bunch structure for injection into the

* Work supported by Fermi Research Alliance, LLC, under Contract No. DE-AC02-07CH11359 with the United States Dep. of Energy
#val@fnal.gov

Copyright © 2014 CC-BY-3.0 and by the respective authors

ISBN 978-3-95450-142-7

CRYOGENIC PLANTS FOR SRF LINACS

D. Arenius, JLab, Newport News, VA 23606, USA

Abstract

Helium cryogenic plants are a key utility for SRF linac applications. Due to their custom design and long delivery times, they are consistently on project critical path to meet SRF based project technical, schedule, cost and design safety goals requirements This paper outlines an overview of the most common considerations in their development.

INTRODUCTION

The SRF cryogenic plant consists of a modified 4.5K plant coupled with vacuum pumping to lower the operating temperature below 4.5K Common temperatures include 3.5K, 2K, and 1.8K. For plants less than 500W, this is commonly done with ambient temperature vacuum pumps For plants greater than 500W a combination of cold centrifugal and warm vacuum pumps or all cold centrifugal pumps when loads are greater than 2kW.

FUNCTIONAL DESCRIPTIONS

Warm Helium Gas Compressor System

A simplified modified schematic for the 4.5K cold box warm helium oil flooded screw compressors is presented in figure 1. The compressor system based on the Ganni Cycle is designed to maintain constant high efficiency with 20% to 100% 4.5K cold box load variation. The high pressure (HP) and medium (MP) stages compress the 4.5K cold box recycle flow (turbine bypass flow). The low pressure (LP) stages compress return flows cold compressor or other cryogenic loads, that must operate at 100 kPa, into the variable inter stage pressure between the HP and MP compressors.

All of the compressor stage is equipped with bypass valves controlled by its suction pressure. The valves, with the exception of the LP bypass, remain closed unless an extreme off design low suction pressure set point is encountered. The high pressure (HP) and medium pressure (MP) compressor stages are allowed to find their own natural operating pressures based on the charge pressure of the system and their natural tendency to automatically maintain a pressure ratio of 2.5 to 3.5.

For small variations in load during steady state operation, the compressor system charge pressure is self regulating due to the positive displacement compressor design. With increasing load return flow from the LP compressor stage, the charge pressure of the MP and HP stages increases, producing more refrigeration as the discharge pressure.

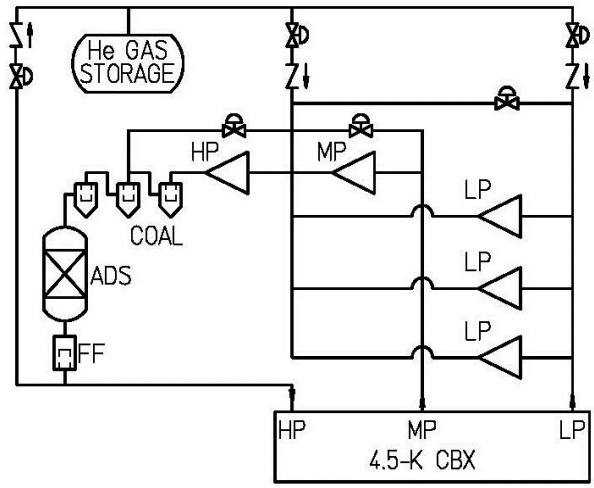


Figure 1: Simplified Warm Helium Compressor System increases at constant pressure ratio. With decreasing load return flow, the charge pressure of the MP and HP stages decreases. Multiple low pressure compressors are provided to process the large cold compressor flow rate during pump down and normal operation of the linac.

There are also secondary positive effects for this design approach. Since the system provides a fairly constant compressor discharge volumetric flow with variable pressure, the compressor oil removal coalescers and charcoal absorber vessels have constant volumetric flow which maintains oil removal performance at the calculated design. In addition, the operation of the compressors with reduced pressures and increased efficiency has shown an increase of time before major compressor maintenance is required. This time has increased to 74,000 hours from an industry standard of every 35,000 hours.

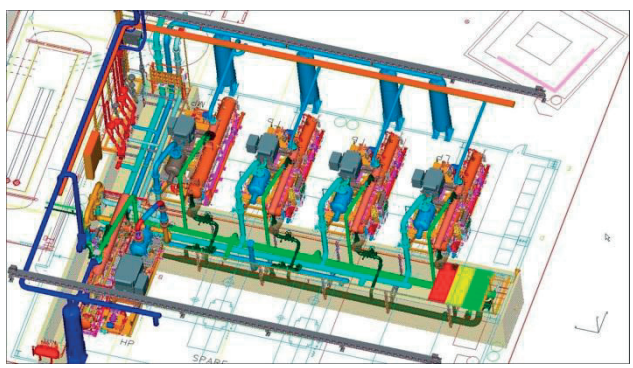


Figure 2: Typical Warm Helium Compressor Layout.

Copyright © 2014 CC-BY-3.0 and by the respective authors

ISBN 978-3-95450-142-7

SPIRAL2 CRYOMODULE PRODUCTION RESULT AND ANALYSIS

P.-E. Bernaudin, R. Ferdinand, GANIL, Caen, France
P. Bosland, C. Marchand, Irfu, Saclay, France
D. Longuevergne, G. Olry, IPN-O, Orsay, France
Y. Gómez Martínez, LPSC, Grenoble, France

Abstract

The production and qualification of the SPIRAL2 cryomodules are close to the end. Their performances are now well established. This paper will explain the path followed to the good achievements, and show some statistical analyses to be used for future projects. How far can we push the performances? What cryogenics consumption shall we take as design values?

INTRODUCTION

The SPIRAL 2 [1] linac is based on superconducting (SC), independently-phased resonators. In order to allow the required broad ranges of particles, intensities and energies (see table 1), it is composed of two families of short cryomodules developed by CEA/Irfu (Saclay) and IN2P3/IPN-O (Orsay) teams. The first family is composed of 12 quarter-wave resonators (QWR) with β_0=0.07 (one cavity/cryomodule), and the second family of 14 QWR at β_0=0.12 (two cavities/cryomodule). Resonance frequency is 88.0525 MHz and maximum gradient in operation of the QWRs is $E_{acc} = V_{acc}/\beta\lambda$ = 6.5 MV/m. Developed by IN2P3/LPSC (Grenoble), the RF power couplers shall provide up to 12 kW CW beam loading power to each cavity. The transverse focusing is ensured by means of warm quadrupole doublets located between each cryomodule, in so-called "warm sections" also equipped with beam diagnostic and vacuum equipments.

Table 1: Beam specifications.

Particles	H^+	$^3He^{2+}$	D^+	ions	ions
Q/A	1	3/2	1/2	1/3	1/6
Max. I (mA)	5	5	5	1	1
Min. energy (MeV/A)	0.75	0.75	0.75	0.75	0.75
Max energy (MeV/A)	33	24	20	15	9
Max. beam power (kW)	165	180	200	45	54

PRESENT STATUS

SPIRAL2 Phase 1 project status

SPIRAL2 Phase 1 project is presently in installation phase. Construction phase is close to the end, and reception operations of the building are almost finished.

The sources and most of the low energy beam lines have been installed. All supporting frames for the accelerators are in place and cabling operations are proceeding smoothly. Linac components installation will start as soon as the linac tunnel is dust cleaned.

First beam inside the linac is scheduled for mid-2015.

Cryomodules status

Low beta cryomodules are assembled and tested at Irfu in Saclay. Out of twelve cryomodules, eight have been tested and qualified. Clean room assembly of the remaining four ones has begun this summer; the last one shall be delivered during the first quarter of 2015.

High beta cryomodules are assembled and tested at IPN-O in Orsay. Five out of seven cryomodules have been successfully qualified. Assembly of the sixth cryomodule is well advanced and the last two cryomodules are scheduled for delivery in GANIL before the end of the year.

Power couplers for both families are prepared and conditioned at LPSC in Grenoble. All power couplers but spare ones have been processed.

CAVITIES AND CRYOMODULES DESIGN

SPIRAL2 cryomodules design has been extensively described in previous papers [2][3]. Both models are short cryomodules (one or two cavities per cryomodule) with no focusing element inside. Due to beam dynamics requirements, cryomodules are very compact. Cavities are bulk niobium QWR.

Cavity body is cylindrical and stem is conical, with toroid-shaped stem-to-body top. Helium jacket doesn't cover the bottom part of the cavities. Cavity is working at 4.5 K; copper, thermal screen is cooled at 60 K using 15 bar He gas. Insulation vacuum and beam vacuum are separated.

Power coupler is of fixed type, located on the bottom of cavities. Couplers are similar for both types of cavities. Coupling factor is optimized for each family of cryomodules (5.5 10^5 for low beta cavities and 1.1 10^6 for high beta cavities), considering the peak intensities of the various particles to be accelerated through the linac.

Both families of cavities are prepared using standard BCP chemical treatments, followed by 18 MΩ water high pressure rinsing (HPR) in clean room. None has been heat cured against 100 K effect.

Low-beta cryomodules specificities

Low beta cavities are closed by a removable bottom plate, intended to ease HPR cleaning of these small cavities. This plate is made out of OFHC copper (see reference [2]).

Tuning system is mechanical. Deformation of the cavities by squeezing its outer body perpendicularly to the beam axis provides a 13 kHz tuning range.

Copyright © 2014 CC-BY-3.0 and by the respective authors

RESULTS FROM THE LCLS X-BAND TRANSVERSE DEFLECTOR WITH FEMTOSECOND TEMPORAL RESOLUTION

Y. Ding, F.-J. Decker, V. A. Dolgashev, J. Frisch, Z. Huang, P. Krejcik, H. Loos, A. Lutman, A. Marinelli, T. J. Maxwell, D. Ratner, J. Turner, J. Wang, M.-H. Wang, J. Welch, and J. Wu
SLAC National Accelerator Laboratory, Menlo Park, CA 94025, USA
C. Behrens
DESY, 22607 Hamburg, Germany

Abstract

An X-band RF transverse deflector composed of two 1-m-long X-band deflecting structures has been recently commissioned at the Linac Coherent Light Source (LCLS) at SLAC National Accelerator Laboratory. Located downstream of the FEL undulator, this device provides electron beam longitudinal phase space diagnostics in both time and energy which enables reconstruction of the X-ray FEL power profiles with an unprecedented resolution. This talk reports on the progress of this new LCLS X-band transverse deflector, first usage experience and measured results.

INTRODUCTION

Over the past several years, great progress has been made in the realization of high power X-ray free-electron lasers (FELs) [1–4]. The typical pulse duration from these sources can vary from several hundred femtoseconds down to a few femtoseconds, which enables ultrafast time-resolved X-ray studies with atomic spatial resolution. However, tremendous challenges remain in diagnosing such X-ray pulses with femtosecond temporal resolution. The measurement of X-ray pulses on the femtosecond time scale is a hot topic in the past years and several techniques have been recently studied (see a review paper [5]).

We previously proposed characterizing the X-ray temporal structure by measuring the lasing footprint left on the "parent" of the X-ray pulse: the electron beam [6]. An X-band radio-frequency (rf) transverse cavity (XTCAV) is adopted in conjunction with an electron beam energy spectrometer to measure the electron beam longitudinal phase space (time-energy) downstream of the FEL undulator. Since the lasing process in an FEL induces both electron energy loss and energy spread growth, the output electron longitudinal phase space can indicate the X-ray pulse information. Recently demonstrated at LCLS [7], this approach is simple and robust. It provides a single-shot measurement and is non-invasive to the FEL operation. The achieved temporal resolution is ~1 fs rms at soft X-ray energy and ~4 fs rms at hard X-ray energy. We discuss the XTCAV status and summarize recent experimental results at LCLS in this paper.

DIAGNOSTIC METHOD AND LAYOUT

In the FEL process, the interaction between an electron beam and an electromagnetic wave causes electron energy loss and energy spread increase. For example, at LCLS, the typical FEL-induced electron energy loss at saturation is more than 10 MeV [2]. By measuring the electron longitudinal phase space in FEL-on and FEL-off conditions, we can retrieve the time-resolved electron beam energy loss or energy spread increase due to the FEL lasing process. In this way the x-ray temporal profile can be obtained if the FEL slippage effect is small. The key point is to design a transverse deflector with high temporal resolution. In the deflecting mode, the time variation of the transverse fields is used to create a temporal-spatial correlation in the electron bunch phase space. The resulting image on a downstream screen forms a "streak" of the electron bunch, from which the pulse duration and temporal profile can be obtained [8,9]. The resolution is determined by the deflector frequency and voltage, together with beam properties (detailed discussion can be found in the supplementary materials of ref. [7]). By choosing an X-band frequency (11.424 GHz), it produces a faster, stronger transverse sweep of the beam, improving the temporal resolution over previous deflector designs such as S-band deflectors.

The sketch in Fig. 1 shows the implementation of the deflecting system at the LCLS. Two 1-m long X-band rf deflecting structures provide a 45 MeV/c nominal time-dependent horizontal kick to the beam [10]. The pre-existing, vertical-bend dipole magnet is used to measure the electron energy spectrum. A camera monitors the downstream cerium-doped yttrium aluminum garnet (Ce:YAG) crystal screen, capturing the transverse beam image. In this arrangement, the horizontal dimension of the measured image represents time while the vertical dimension represents energy.

Once the electron longitudinal phase space is measured, we can retrieve the X-ray temporal profile by comparing the lasing-off and lasing-on electron phase space. The electron current profile, time-sliced mean energy, and sliced energy spread are then computed to calculate the photon power profile. As mentioned earlier, the FEL lasing induces both electron energy loss and energy spread growth. By conservation of energy, we can first relate changes in the mean slice energy to instantaneous FEL power. Namely, the energy loss by each time slice of the electron bunch is given to the instantaneous power of the co-propagating FEL pulse as

$$P(t) = [\langle E\rangle_{FELoff}(t) - \langle E\rangle_{FELon}(t)] \times I(t)/e. \quad (1)$$

Copyright © 2014 CC-BY-3.0 and by the respective authors

ISBN 978-3-95450-142-7

SPIRAL2 BUNCH EXTENSION MONITOR

R. Revenko, J-L. Vignet, GANIL, Caen, France

Abstract

Superconducting linacs require beam diagnostics to quantify the time extension of the bunch for a proper beam adaptation. Bunch extension monitor (BEM) should provide measurements with required resolution and minimal disturbance of beam properties, have a broad dynamic range of beam intensity and should be easy to use for accelerator routine operation. The design of BEM should take into account operation at the vicinity of cryomodules and satisfy imposed requirements for this. BEM measures the x-rays resulting of the bunch interaction with a tungsten wire. Developed prototype of detector was successfully tested with ions beams. Test for detector background conditions at vicinity of cryomodule was carried out and results are presented.

INTRODUCTION

The SPIRAL2 project [1] is based on a multi-beam LINAC driver in order to allow both ISOL and low-energy in-flight techniques to produce RIB. A superconducting light/heavy-ion LINAC with an acceleration potential of about 40 MV capable of accelerating 5 mA deuterons up to 40 MeV and 1 mA heavy ions up to 14.5 MeV/u is used to bombard both thick and thin targets. These beams could be used for the production of intense radioactive beams. The production of high intensity RIB of neutron-rich nuclei will be based on fission of uranium target induced by neutrons, obtained from a deuteron beam impinging on a graphite converter (up to 10^{14} fissions/s) or by a direct irradiation with a deuteron, ^{3}He or ^{4}He beam.

The LINAC [2] consists of two families of superconducting cavities placed in 12 cryomodules of type A and 7 cryomodules of type B where cryomodules are separated by 20 warm sections equipped by two quadrupoles and one diagnostic box. The LINAC is operated at frequency 88,0525 MHz that corresponded to 11.26 ns period between neighbour bunches. Expected phase extension is 60˚ (±2σ) or ~1,6 nsec for bunch length. The LINAC can operate at continuous or pulsed mode with period of macropulse varied at range from 100 µsec to 1 sec.

Proper LINAC adjustment is necessary for obtaining maximal intensity and luminosity on the target. Phase synchronization for each acceleration section is necessary and information about spatial beam distribution is required. While the beam transverse profile will be measured by pick up monitors (BPM) information about bunch longitudinal distribution will be obtained using a bunch extension monitor (BEM). These diagnostic detectors will be installed in firsts five warm sections placed in gaps between superconducting acceleration cavities.

BEM DESCRIPTION

The bunch extension monitor [3] is a non-interceptive beam diagnostic detector. Principe of operation is based on registration of photons emitted from thin tungsten wire placed into the beam of LINAC. Comparing to beam diagnostics based on secondary electrons emission the BEM is not using applied potential on the wire and thus measurements do not produce distortion of the beam optics. Also all BEM components should meet to UHV requirements due to operation under vacuum below 10^{-8} mbar and satisfy to required cleanness conditions to prevent cavity pollution.

BEM Design

The BEM mechanics consists of two parts: x-ray detector and system for wire insertion. These parts are mounted two flanges of diagnostic box of warm section (see Fig. 1).

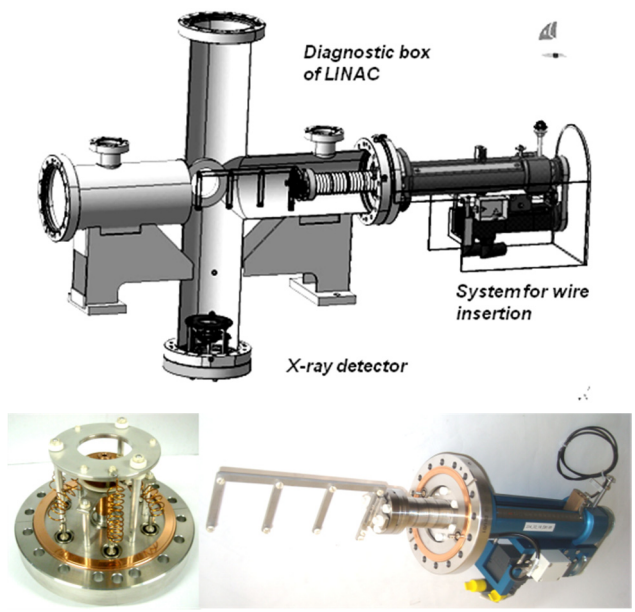


Figure 1: General view of BEM installation on diagnostic box of LINAC (top) and photo of BEM components (bottom).

The system for wire insertion permits to displace and position the tungsten wire into the beam with precision better than 100 µm. It is equipped with three wire holders on stainless steel frame. Tungsten wires of 150 microns diameter are placed on diagonal inside each holder. Wires of neighbouring BEMs are placed in perpendicular

Copyright © 2014 CC-BY-3.0 and by the respective authors

ISBN 978-3-95450-142-7

ALLISON SCANNER EMITTANCE DIAGNOSTIC DEVELOPMENT AT TRIUMF

A. Laxdal, F. Ames, R. Baartman, W. Rawnsley, A. Sen, V. Verzilov, G. Waters - TRIUMF*, Vancouver, BC, Canada
R.F. Paris - University of Ottawa, Canada
M. Kownacki - University of Simon Fraser, Canada
R. Hariwal - Inter-University Accelerator Centre, New Delhi, India

Abstract

TRIUMF has developed Allison scanners to measure the transverse emittance of both low intensity hadron beams at 10^4 pps (1.6 fA) and high intensity electron beams at 10 mA for a dynamic range of 10^{13} in intensity. The devices give high-resolution transverse emittance information in a compact package that fits in a single diagnostic box. This paper discusses the design and performance of the operating devices, and the technologies introduced. For clarity it is divided in two main parts: the first part deals with the low intensity emittance scanner and the second part with the high intensity emittance scanner.

ALLISON SCANNER - CONCEPTUAL DESIGN

The Allison type emittance scanners [1] are high-resolution scanners, which consist of a front slit, deflecting plates, a rear slit, and a Faraday cup in a single unit that is stepped across the beam with a stepper motor. At each stepper position, the beamlet selected by the front slit is swept across the rear slit with the deflecting plates and the transmitted current measured as a function of deflecting plate voltage by the Faraday cup: see Figure 1.

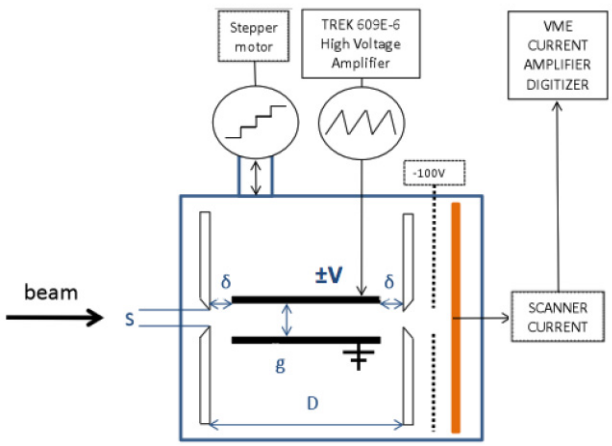


Figure 1: Emittance scanner schematic

The maximum analyzable angle, limited by particles striking the plates is given by the geometry:

$$x_m' = \pm 2g/(D + 2\delta)$$

For non-relativistic particles, the voltage across the plates was derived by Allison et al [1]. The phase-space area resolution is given by s^2/D.

PART I – LOW INTENSITY EMITTANCE

Introduction

A low intensity emittance scanner was needed for the radioactive ion beams in the ISAC facility at TRIUMF. The initial ISAC (Isotope Separator Accelerator) emittance scanner was an Allison type emittance scanner [1], which was installed in the LEBT section after the mass separator in 1998, when the beamline was built. This emittance scanner contains a Faraday cup that can measure below 1 pA. However, since the typical beam's phase space area of 30 mm-mrad is a thousand times larger than the scanner resolution of s^2/D=0.03 mm-mrad, it is not practical to analyze beams of less than 1nA. Since most of the beams delivered to the ISAC experiments are much below 1nA, a device capable of measuring emittances for low intensity radioactive beams and help characterize the ion beam created is necessary. An upgraded scanner was designed, installed and tested in 2013.

Design

In the new design the Faraday cup at the end of the emittance scanner is tilted and a channeltron (Channel Electron Multiplier) is incorporated: see Figure 2.

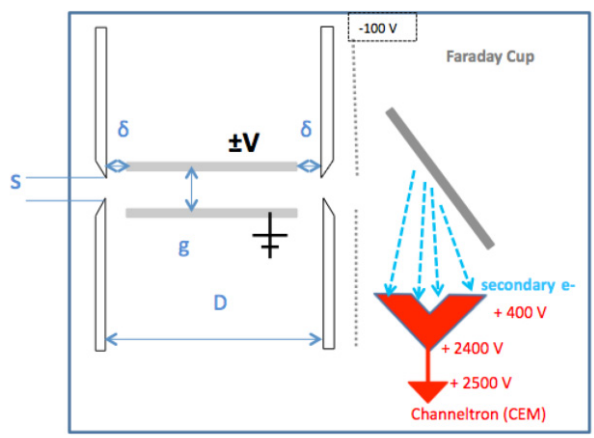


Figure 2: Emittance scanner with CEM schematic

Dimensions g, D, δ, s are given in Table 1. The power supply of the electrostatic plates is a KEPCO power supply with a maximum voltage of ±1,000 V.

* TRIUMF receives federal funding via a contribution agreement through the National Research Council of Canada. ARIEL & e-linac construction are funded by BCKDF and CFI

Copyright © 2014 CC-BY-3.0 and by the respective authors

ISBN 978-3-95450-142-7

OPERATIONAL EXPERIENCE WITH CW HIGH GRADIENT AND HIGH Q_L CRYOMODULES*

T. Allison, R. Bachimanchi, E. Daly, M. Drury, C. Hovater$, G. Lahti, C. Mounts, R. Nelson, T. Plawski, Jefferson Lab, Newport News, Virginia 23606, USA

Abstract

The Continuous Electron Beam Accelerator Facility (CEBAF) energy upgrade from 6 GeV to 12 GeV includes the installation of ten new 100 MV cryomodules (80 cavities). The superconducting RF cavities are designed to operate CW at an accelerating gradient of 19.3 MV/m with a Q_L of 3×10^7. The RF system employs single cavity control using new digital LLRF controls and 13 kW klystrons. Recently, all of the new cryomodules and associated RF hardware and software have been commissioned and operated in the CEBAF accelerator. Electrons at linac currents up to 10 μA have been successfully accelerated and used for nuclear physics experiments. This paper reports on the commissioning and operation of the cryomodules and RF system.

INTRODUCTION

In January of 2014 ten new eight cavity high gradient cryomodules (designated as C100) were operated for the first time in the CEBAF accelerator. The cryomodule design is a culmination of the lessons learned from three preproduction high gradient cryomodules and the original 42 CEBAF cryomodules [1]. To meet the 12 GeV energy goals the cryomodules must have an energy gain of 98 MeV. With that as a performance must, the cryomodule and cavities were designed to achieve 108 MV. Each cryomodule consists of eight 7-cell elliptical cavities. The cavities are tuned to 1.497 GHz, and individually controlled by both a mechanical stepper motor and a Piezo tuner (PZT).

Additionally the RF system is completely new for these cryomodules [2, 3]. Each cavity is powered and controlled by a single klystron and LLRF system. The klystrons produce 12 kW of linear power and up to 13 kW saturated. Four high voltage power supplies power two klystrons at a time. The eight klystrons are self protected with their interlocks as part of the high power amplifier system. The RF controls use a traditional heterodyne scheme and digital down conversion at an intermediate frequency. Each cavity field and resonance control PI algorithm is contained in two FPGAs. One FPGA is in the field control chassis, controlling a single cavity. The resonance control chassis contains the other and controls up to eight cavities. The RF controls are unique incorporating a digital self excited loop (SEL) to quickly recover cavities. Controls and interfaces for both the HPA and the LLRF are provided through EPICS.

RF SYSTEM/CRYOMODULE COMMISSIONING

RF System Commissioning

The RF systems and cryomodules were installed and commissioned between 2011 and 2013, while the CEBAF accelerator was off for the energy upgrade. Typically they are commissioned in series, first with the RF systems and then followed by cryomodule commissioning.

The RF power systems (circulators and waveguide directional couplers) were commissioned by powering the klystrons up to their saturated power level of 13 kW. The LLRF system (field control chassis (FCC), stepper motor chassis, cavity interlocks, Piezo amplifier and heater controls) was simultaneously tested and calibrated [3]. The new digital RF control has made testing much simpler and easier since it replaces the RF sources and analog phase lock loops used in the past.

Cryomodule Commissioning

All cavity/cryomodule performance aspects were tested in the CEBAF tunnel as part of commissioning [4]. Typical measured values include Qo, Qext and max gradient. In addition to the maximum operable gradient, the limiting factor (Quench, heat load or administrative limit) is also determined for each cavity. Finally, all eight cavities are run together to ensure they can operate at their maximum operable gradients without interfering with adjacent cavities in the cryomodule. Figure 1 compares the installed maximum gradients of the new cavities to the vertical test data [4]. Table 1 shows the installed energy gain of each cryomodule [5].

Once the cryomodule commissioning is complete, the RF control system PI gain settings are optimized and the cavity gradient calibrations are uploaded with calibration values in to the EPICS control system

* Authored by JSA, LLC under U.S. DOE Contract DE-AC05-06OR23177. The U.S. Govt. retains a non-exclusive, paid-up, irrevocable, world-wide license to publish or reproduce this for U.S. Govt. purposes.

$ hovater@jlab.org

Copyright © 2014 CC-BY-3.0 and by the respective authors

COOLING OF HIGH PRESSURE INSULATING GAS FOR 3 MeV DC ACCELERATOR: AN ALTERNATE APPROACH

Shyam Rao Ghodke#, Rajesh Barnwal, Mahender Kumar, Susanta Nayak, Vijay Sharma, Suneet Kumar Srivastava, Satyanarayan Acharya, Kavita Pramod Dixit, Israel Bakht Singh, D. Jayaprakash, Rehim Rajan, Dharmendra Kumar Sharma, Suryaprakash Dewangan, Kailash Chander Mittal, Lalit Mohan Gantayet
Bhabha Atomic Research Centre, Mumbai, India – 400085

Abstract

3 MeV Accelerator is working inside the 'Electron Beam Centre' (EBC) building at Kharghar, Navi Mumbai. Generally in DC and Pelletron accelerators Nitrogen/SF_6 gas is taken out from accelerator tank and it is cooled by separate heat exchanger and blower unit outside the accelerator tank. In our alternate approach we have designed fan/blower to work under high pressure inside accelerator tank. Fans are designed to work in high pressure SF_6 environment at 7 bar absolute pressure with 42 kg/m^3 SF_6 gas density. Fan through air over radiator type finned tube heat exchanger, installed inside accelerator tank. Fan speeds are controlled through variable frequency drive. Two numbers of such assemblies are fabricated, installed and tested in Nitrogen and SF_6 gas environment at different pressure and variable fan speed. Performances are recorded and plotted in graphical form. These cooling systems are shown excellent performance in last five years. Paper will discuss about design of cooling system, cooling calculation of fan, fabrication of fan and heat exchanger, 5 TR chiller unit, variable frequency drive, fan performance etc.

INTRODUCTION

3 MeV Accelerator is an electrostatic accelerator in which terminal is floating at a voltage of 3 MV and the accelerator tank is at ground potential. From voltage gradient point of view there is two geometries, coaxial cylindrical and spherical geometry. Design calculations show that SF_6 is the most suitable medium for insulation [7,8] and cooling purpose. Apart from excellent electrical properties, SF_6 has good chemical stability, thermal properties and nontoxic. The Accelerator tank is the main body of the Accelerator, which will house HV multiplier columns, RF electrodes, corona shields, HV terminals, electron gun, accelerating tubes, heat exchangers along with blower, RF transformer etc. All of high voltage components require SF_6 gas insulation and efficient cooling. Hence there is a need of SF_6 gas and its cooling system. Operating pressure of SF_6 gas inside the accelerator tank is 6 bar (g). On line dew point measurement system is connected in accelerator tank. SF6 gas handling system not discussed in this paper. [1, 2, 3, 4, 5, 6]

#ghodke_barc@yahoo.co.in

DESIGN OF SF_6 GAS COOLING SYSTEM

The Aim of SF6 gas cooling system is to cool SF6 gas inside accelerator and RF transformer tanks with the help of water-SF6 gas heat exchange process. This system is mainly comprises of 1.5" and 1" SS pipe line, radiator type heat exchanger and blower combination, 5 TR chiller unit, cooling tower, pressure transmitter, temperature sensors, safety interlocks, flow meter, flow transmitter, Variable frequency drive, pressure gauges and other instrumentation.

The blower has been designed and commissioned to achieve desired heat transfer under 6 bar (g) with 42 kg/m^3 density of SF_6 gas. Standard high pressure finned tube bundle with header have been selected as per the area available inside the accelerator tank. Heat exchanger assembly is made of such four numbers of bundles and makes an enclosure of size 800 x 800 x 100 mm (Figure 2 and 4). Blower is fabricated from ASTM A 240 Gr 304L stainless steel plates and it is assembled inside this enclosure and throw SF_6 gas centrifugally outward direction. Two sets of heat exchanger and blower combination along with 2 and 3 HP motors has been installed and tested for desired flow rate, pressure drop and motor current/wattage (table-1). Blower has dynamically balanced to minimize the vibration.

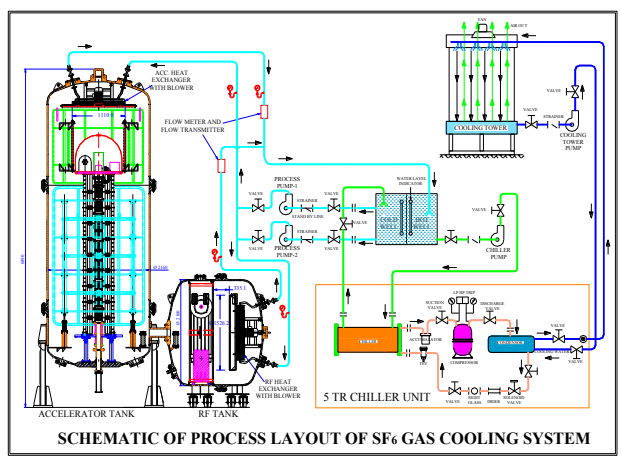


Figure 1: SF_6 Gas Cooling System

Copyright © 2014 CC-BY-3.0 and by the respective authors

ISBN 978-3-95450-142-7

DESIGN, DEVELOPMENT AND INITIAL RESULTS OF SOLID STATE MAGNETRON MODULATOR

Abhijit R. Tillu#, Shiv Chandan, Kavita Pramod Dixit, Kailash Chander Mittal, Hemant Sarukte
Accelerator & Pulse Power Division, Bhabha Atomic Research Centre,
Mumbai - 400085, INDIA

Abstract

A prototype solid state pulse modulator based on Induction Adder Topology has been designed and is currently being tested on an S Band Pulsed magnetron rated for 3.2MW Peak RF Power. After successful lab tests the modulator is intended for use in cargo scanning and radiography applications. Currently the topology consists of 4 nos. of single turn primaries driven independently at voltages not more than 1000V. The secondary encircles all the four primaries to generate the desired pulsed voltage across the magnetron. The designed output pulse parameters are 50kV, 120A, 4 micro s, at a pulse repetition rate of 250 pps. The paper describes the design and development of the Epoxy Cast Pulse transformer and the Low Inductance Primary Circuit. The rise time measured was < 400ns, and the reverse voltage at the end of the pulse was less than 12kV (at 43k V pulse). The testing was done at low PRF, on two different magnetrons having different operating points to demonstrate fairly good impedance independent operating characteristic of the magnetron modulator. Initial test results on the Resistive load and Magnetron load will also be discussed.

INTRODUCTION

Various low power linear electron accelerators designed for cancer treatment, radiography, cargo scanning and related applications use pulsed magnetrons as RF Source. The magnetrons are typically rated for 3.2MW peak RF Power and 3kW average RF Power. 1000's of such machines are available worldwide. The pulse modulators required to power these magnetrons are traditionally Line type-modulators. Though these modulators are very rugged, they are being replaced by Solid state modulators due to various reasons which are elaborated in various references [1, 4, 5, 6]. The paper describes a solid state magnetron modulator being developed in our lab. The output specifications towards with the modulator is designed are listed in Table 1.

The design of the modulator is based on Induction Adder Topology, also referred to as Split Core topology or Matrix Adder Topology [1, 3, 4]. The topology has been chosen over other solid state topologies mainly because it is much compact as compared to other competing topologies, and the gate drives and control logic need not be floating at HV.

tillu@barc.gov.in

Table 1: Output Pulse Specifications

Output Pulse Voltage	-52kV
Peak Current	120A
Pulse width	4µs (flat top)
Rise time	<400ns
Backswing	< 5kV
Pulse Droop	< 1%
Pulse to Pulse Stability	<1%
Max Pulse Repetition Rate	250 pps

DESIGN

The peak electrical power delivered to the magnetron per pulse is ~6MW. The modulator is designed for at-least 8MW of pulse power. There Split core pulse transformer has four primaries independently driven by their respective power modules. Each module is a 1kV pulse source implemented as shown in fig 1. The IGBT used is a 1700V, 2400A IGBT (ABB make 5SNA 2400E170100). The 200µF/1100V energy storage capacitor is implemented by two Vishay make Axial type Metalized polypropylene Capacitors GLI 1100-100A. The electrical connections between the IGBT, Capacitors and diode are implemented by low Inductance strip line geometry.

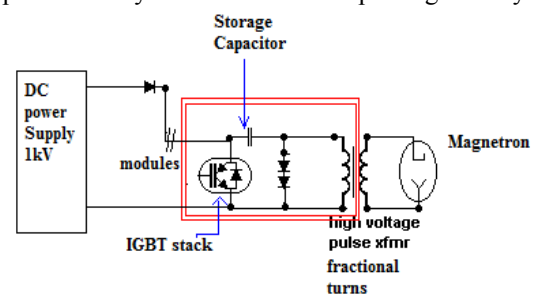


Figure 1: Conceptual schematic of the Pulse Modulator.

The split core pulse transformer also referred as fractional turns transformer has four primaries, each implemented by using a single turn foil winding of 0.3mm thick Copper. The secondary consists of 14 turns of SWG16. The secondary is in bifilar type, so as to allow filament heating power to the magnetron. There are 8 turns of Reset winding on the secondary, implemented by using SWG14 enamelled copper wire. The entire secondary is adequately screened and epoxy potted, so as to allow Oil Free construction of the pulse transformer. The pulse transformer core uses 4 pairs of Amorphous Cut C cores (2605SA1). Each core is excited by its own primary. The cores are arranged such the transformer is in E type configuration. The modelling in CST EM Studio is shown in Fig 2. The estimated flux swing is ~ 1,5T. Hence the cores are biased at ~ 0.75T, so as to get the best

Copyright © 2014 CC-BY-3.0 and by the respective authors

ISBN 978-3-95450-142-7

A NEW HIGH CURRENT AND SINGLE BUNCH INJECTOR AT ELSA

Manuel Schedler, Philipp Hänisch, Wolfgang Hillert, Dennis Proft, Jens Zappai
ELSA, University of Bonn, Germany

Abstract

At the Electron Stretcher Facility ELSA of Bonn University, an increase of the maximum stored beam current from 20 mA to 200 mA is planned for the stretcher ring.

In order to keep the desired duty cycle of the post acceleration mode at about 80 % a new high current injector operating at 3 GHz has been built. It provides an electron beam with an energy of 20 MeV and a beam current of 800 mA in pulsed operation. A prebuncher, travelling wave buncher system and an energy compressing system are installed in order to enhance the beam acceptance of the linac and to reduce the energy spread in order to achieve an improved injection efficiency into the booster synchrotron.

For studying accelerators impedances and beam instabilities the linac is able to produce single bunches with a pulse current of 2 A which will be accumulated in the stretcher ring.

THE ELECTRON STRETCHER ACCELERATOR – ELSA

Future hadron physics experiments at the Electron Stretcher Facility ELSA require an increase of the accelerator's beam current by one order of magnitude. Electrons are produced at either Linac 1 using a thermal electron gun or at Linac 2 even providing a beam of polarized electrons. The adjacent booster synchrotron accelerates the electrons to an energy of typically 1.2 GeV, operating at mains frequency of 50 Hz. The stretcher ring accumulates several shots of the booster synchrotron and offers acceleration to a maximum energy of 3.2 GeV, applying a fast energy ramp of 6 GeV/s. On flattop energy, the electrons are slowly extracted over a few seconds to the hadron physics experiments using resonance extraction methods. Afterwards, the stretcher ring is prepared for the next injection process by ramping down the magnets [1]. An overview of the accelerator facility and the hadron physics experiments is given in Fig. 1.

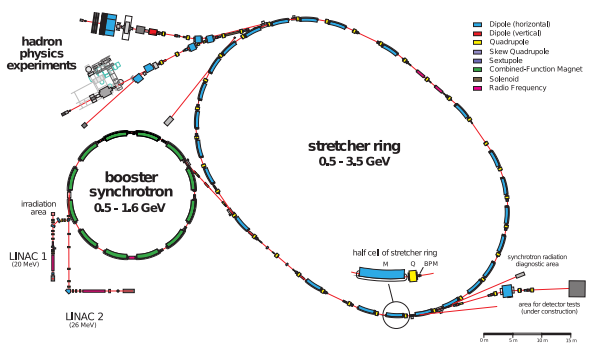


Figure 1: The Electron Stretcher Accelerator Facility ELSA.

To keep the duty cycle at reasonable values of about 80 % when operating with high intensities, the injection current has to be increased significantly. For this purpose, the Linac 1 is upgraded to high current mode. To achieve a maximum booster injection efficiency, a bunching section and energy compressing has been installed at Linac 1. In addition, it will provide a single bunch capable operation mode, which can be used for single bunch instability studies in the stretcher ring. To successfully accumulate electrons in a single bucket in the stretcher ring, a new FPGA based timing system has been developed.

MAIN OVERVIEW OF LINAC 1

A thermal electron gun is used to generate electrons with an energy of 90 keV, followed by a 500 MHz sub-harmonic prebuncher and a 3 GHz travelling wave buncher. The main linac structure accelerates the electrons to 20 MeV [2]. To reduce the energy spread and thereby enhance the booster injection efficiency which is mainly limited by it's energy acceptance, an energy compressing system has been setup behind the main linac structure.

The generated electron beam can either be filled into the booster synchrotron or can be used for material irradiation at the linac's test area.

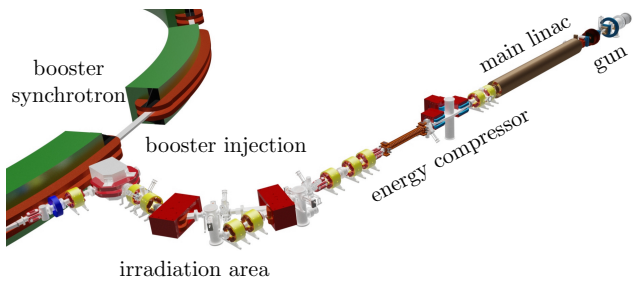


Figure 2: Overview of the new single bunch and high current injector Linac 1, the transfer line to the booster synchrotron, and the irradiation area.

THE ENERGY COMPRESSING SYSTEM

The energy spread of the electron beam produced by the main accelerating structure amounts to $\Delta p/p = 5 \cdot 10^{-2}$ whereas the energy acceptance of the adjacent booster synchrotron is about one order of magnitude smaller [3].

In order to optimize the injection efficiency into the booster synchrotron, the energy spread of the electron beam of Linac 1 has to be reduced by one order of magnitude. Even using the multi-stage bunching process of the injector, the energy spread has to be further reduced after acceleration in the main linac. This is achieved by adding an energy compressing system.

Copyright © 2014 CC-BY-3.0 and by the respective authors

ISBN 978-3-95450-142-7

UNIFORM CURRENT DENSITY FOR BLIP TARGET AT BROOKHAVEN 200 MeV LINAC *

D. Raparia, B. Briscoe, P. Cerniglia, R. Connolly, C. Cullen, D. Gassner, R. Hulsart, R. Lambliase, V. LoDestro, L. Mausers, R. Michnoff, P. Thieberger, M. Willinski, Brookhaven National Laboratory, Upton, NY 11973, USA

Abstract

Most of the beam from the Brookhaven 200 MeV linac is used for Brookhaven Linac Isotope Production (BLIP). The average current from the linac is up 130 μA and there is a plan to increase the average current in future. To produce uniform current distribution on the BLIP target, we have tried octupoles in the past but it did not produce uniform beam as calculated due to x-y coupling present in the linac.

A beam painting scheme in circular fashion involving two orthogonal dipoles with 90 degrees phase leg at 5 kHz will provide desire current density at the target. This paper discuss beam optics of the BLIP transport line and beam footprint on the target with given constrains.

INTRODUCTION

The Brookhaven National Laboratory (BNL) 200 MeV drift tube linac (DTL) was built in 1970 [1] with following design parameters for proton: input energy 0.75 MeV, output energy 200.3 MeV, frequency 201.25 MHz, peak beam current 100 mA, beam pulse length (max) 200 μs, RF pulse length 400 μs, pulse repetition rate (max) 10 Hz. Over the 44 years of operations, it has gone through several improvements to increase the average current and reliability of the linac.

At present linac provides H^- beam at 200 MeV for the polarized proton program for Relativistic Heavy Ion Collider (RHIC) and 66-200 MeV for Brookhaven Linac Isotope Production (BLIP). The RHIC program needs two pulses every AGS cycle (~4-5 sec), one for injection into the AGS booster and other for 200 MeV polarization measurements located in the High Energy Beam Transport line (HEBT). The rest of the pulses from high intensity source are delivered to BLIP. Requirements for these programs are quite different and they are following. (1) RHIC: 200 MeV, 500 μA beam current, up 400 μs pulse length, polarization as high as possible and emittance as low as possible, (2) BLIP: 66-200 MeV, 450 μs pulse length, current as high as possible (~45 mA), uniform beam distribution at the target, and beam losses as low as possible.

TRANSPOT LINE TO BLIP

Layout of the BLIP line is shown in Figure 1 and 2. The total length of the line is 33.5 meters. BLIP line has 10 quadrupoles, two dipoles, two octupoles, eight steering magnet (three horizontal, five vertical), four current transformers, three multi-wires, eight collimators (temperature interlock), ten beam pipe temperature monitors (temperature interlock) and two 0.012 inch thick Be and AlBeMet windows. Following the DTL first two pulse quadrupoles are common for HEBT and BLIP line and rest of eight quadrupoles are dc. First 7.5 degrees dipole is pulse to select beam to BLIP or AGS booster pulse-by-pulse basis and second 22.5 degrees dipole is dc. Beam pipe diameter is increased long the length to prevent vacuum failures. There are several different size of collimator as shown in the Figure 1 and 2 equipped with thermocouples to monitor and inhibit the beam in case of overheating. There are 10 places temperature monitor (thermocouples) along the BLIP line capable of interrupting the beam. The octupoles are located after the 2nd dipole as shown in Figure 2 to flatten the beam profile at the BLIP Target.

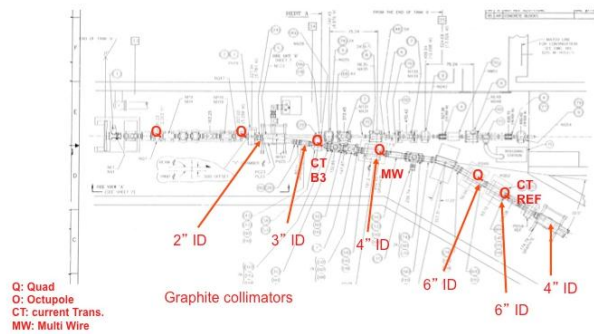


Figure 1: Layout-1 of the BLIP line showing quadrupoles (Q), octupoles (O), dipole magnet (D) and profile monitors.

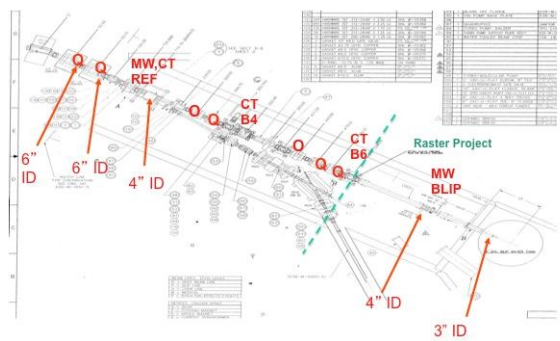


Figure 2: Layout-2 of the BLIP line showing quadrupoles (Q), octupoles (O), dipole magnet (D) and profile monitors

*Work performed under Contract Number DE-AC02-98CH10886 with the auspices of the US Department of Energy
#raparia@bnl.gov

Copyright © 2014 CC-BY-3.0 and by the respective authors

A PROTOTYPE 1 MEV X-BAND LINAC FOR AVIATION CARGO INSPECTION

M. Jenkins*, G. Burt, B. Hall, Lancaster University Cockcroft Institute, UK
P.K. Ambattu, BITS Pilani, India
P. Corlett, P. Goudket, A. Goulden, P McIntosh, K. Middleman,
Y. Saveliev, R. Smith, A. Wheelhouse, ASTeC, Daresbury Laboratory, UK
P. Hindley, C. Hill, N. Templeton, T. Hartnett, S. Griffiths,
B. Martlew, M. Hancock, Daresbury Laboratory, UK
S. Andrews, T. Cross, C. Weatherup, e2v, UK

Abstract

Aviation cargo Unit Load Device (ULD) containers are typically much smaller than standard shipping containers, with a volume of around 1 m^3. Standard 3 to 6 MeV X-ray screening linacs have too much energy to obtain sufficient contrast when inspecting ULD's, hence a lower 1 MeV linac is required. In order to obtain a small physical footprint, which can be adapted to mobile platform applications a compact design is required, hence X-band technology is the ideal solution. A prototype 1 MeV linac cavity has been designed by Lancaster University, manufactured by Comeb (Italy) and tested at STFC Daresbury Laboratory using an e2v magnetron, modulator and electron gun. The cavity is a bi-periodic $\pi/2$ structure, with beam-pipe aperture coupling to simplify the manufacture at the expense of shunt impedance. The design, manufacture and testing of this linac structure is presented.

INTRODUCTION

Inspection of aviation cargo Unit Load Device (ULD) containers is increasing in frequency due to security concerns. Due to the size of a ULD, typically 1 m^3, existing cargo scanning linacs are unable to be used due to the energy of the X-rays produced. Current X-ray screening linacs were designed to scan shipping containers which are constructed from steel and have a volume of at least 33 m^3 which means that high energy X-rays are required to traverse the container. ULD's are normally constructed from aluminium which combined with the much smaller volume of the container means that a 1 MeV linac is required. As a mobile scanner is desired a compact design is necessary which means that X-band technology is ideal.

Prototyping of an X-band 1 MeV linac is underway. The linac has been designed by Lancaster University and STFC Daresbury Laboratory. The RF design was done at Lancaster University which was then passed to STFC Daresbury Laboratory who completed the mechanical design. This structure was then manufactured by Comeb and initial RF testing was conducted at the Cockcroft Institute. The linac is now being installed on a beam line at Daresbury Laboratory to be test using an e2v magnetron, modulator and electron gun.

* michael.jenkins@cockcroft.ac.uk

CAVITY DESIGN

The cavity was designed as an X-band $\pi/2$ bi-periodic structure in order to meet the requirements of industry who would produce commercial systems for scanning ULD containers. X-band technology was chosen to produce a physically small linac which not only ensures the linac is compact but the shielding is also compact. In order to increase the cavity stability a $\pi/2$ standing wave mode was selected, as this mode has the largest frequency separation to the next nearest mode which minimises the affect of perturbations. $\pi/2$ mode structures have every 2nd cell unfilled resulting in a much lower accelerating gradient. In order to increase the accelerating gradient, which reduces the cavity length, a bi-periodic cell design was chosen for this project (see Fig. 1).

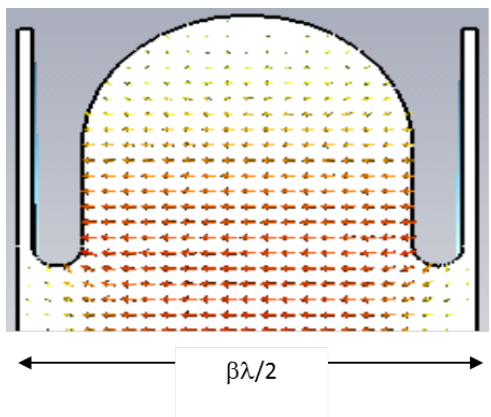


Figure 1: A single cell in a bi-periodic standing wave cavity.

The energy of the electron beam adds extra complication to the RF design. The electron gun which is connected to one end of the cavity produces 17 keV electrons which are non relativistic. This means that the relativistic β of the electron beam changes along the length of the linac. The rate of change in β depends on the accelerating gradient, the electric field amplitude must be chosen before optimising the cavity design. For this application an accelerating gradient of 30 MV/m was chosen which resulted on a structure with 8 accelerating cells. The length of these cells were then optimised by tracking the electron beam in ASTRA [1].

Copyright © 2014 CC-BY-3.0 and by the respective authors

ISBN 978-3-95450-142-7

PROTOTYPE DEVELOPMENT OF THE CLIC CRAB CAVITIES

G. Burt, A. Dexter, M. Jenkins, C. Lingwood, B. Woolley, Lancaster University, UK
Praveen Kumar A.V., BITS Pilani, Pilani campus, India
A Grudiev, G. Riddone, A. Solodko, I. Syratchev, R. Wegner, W. Wuensch, CERN, CH
P. Goudket, C. Hill, P. McIntosh, N. Templeton, ASTeC, Daresbury Laboratory, UK.
V. Dolgashev, SLAC, USA

Abstract

CERN's Compact linear collider (CLIC) will require two crab cavities to align the beams to provide an effective head-on collision with a 20 mdeg crossing angle at the interaction point. An X-band RF system has been chosen for the crab cavities.

Three prototype cavities have been developed in order to test their high power performance. The first cavity has been made by UK industry, while the second cavity has been made using the same process as the CLIC main linac in order understand potential differences in RF breakdown behaviour between deflecting and accelerating cavities. The third cavity incorporates wake-field-damping waveguides on each cell which will eventually contain RF absorbers. This paper details the design, manufacture and preparation of these cavities for testing and a report on their status.

INTRODUCTION

CLIC [1] will require a set of crab cavities to align the bunches to provide an effective head on collision in the presence of the finite crossing angle. These cavities will be X-band travelling wave dipole structures. While the voltage required is quite small a large group velocity is desired to minimise beam-loading effects. Due to very tight phase specifications (18 mdeg) both structures must be driven by a single klystron without a pulse compressor hence to keep the power required below 15 MW the group velocity is limited to 3% of the speed of light [2].

A programme of prototyping and testing these structures has been undertaken, with three structures currently being manufactured and tested. The first cavity was an early prototype designed to be very similar to the SLAC LCLS deflector [3] , and was to be tested at SLAC. The purpose of this cavity was to understand breakdown limits in dipole cavities, with the structure being autopsied (cut apart after testing to inspect damage caused by breakdown). This structure would also be made by UK industry to develop local capabilities. The second cavity was made with the structure geometry chosen for the CLIC crab cavity. This structure would be made in close collaboration with CERN, utilising CERN facilities and expertise to compare results between accelerating and deflecting structures made by the same manufacturer to the same standards. The third cavity also includes the damping waveguides, however they will not be loaded with SiC absorbers, as the purpose of this prototype is to test the breakdown performance of the waveguide loading on the cells.

CAVITY #1

The first cavity was manufactured by Shakespeare Engineering in the UK. Shakespeare has experience in manufacturing high power RF components but not accelerator cavities hence this cavity was seen as strategically important to build local capability. The structure is fed from the RF source using a dual-fed waveguide coupled through an iris to a TE11-like coupling cavity, which is then coupled to the TM11-like structures. This type of coupler was developed at SLAC for accelerating structures to reduce surface electric and magnetic fields and used in deflectors to reduce unwanted multipole components and mitigate manufacturing risks. A prototype cavity was delivered in 2013, shown in Fig. 1, and its S-parameters were measured. The scattering parameters were found to be very close to simulations. Unfortunately this cavity developed a significant vacuum leak and hence has been returned for repair.

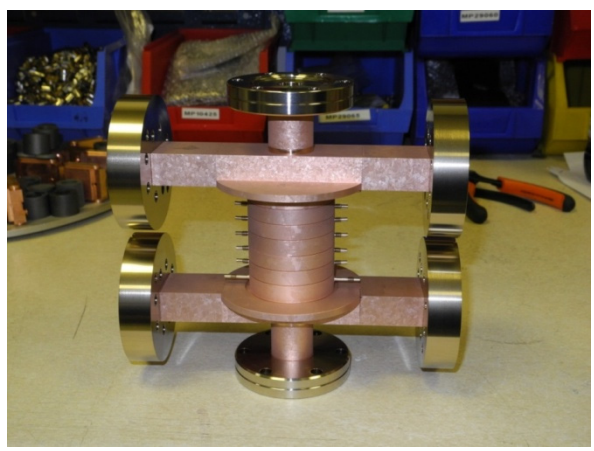


Figure 1: Cavity #1, manufactured by Shakespeare Engineering.

CAVITY #2 DESIGN

The second cavity was designed to use the same cell geometry as the CLIC crab cavity and a similar coupler. Dipole cavities have two polarisations, vertical and horizontal. While the horizontal polarised mode is used for deflecting the vertical polarised mode, the so called same order mode (SOM), can be excited by the beam leading to large unwanted defections. In order to reduce the effect of this mode on the beam, the highest impedance is designed to be at 13 GHz which is a half integer resonance with the beam. To achieve this without increasing peak surface electric and magnetic fields a racetrack shape is chosen.

Copyright © 2014 CC-BY-3.0 and by the respective authors

ISBN 978-3-95450-142-7

CATALOGUE OF LOSSES FOR THE LINEAR IFMIF PROTOTYPE ACCELERATOR

N. Chauvin*, P.A.P.Nghiem, D. Uriot, CEA, IRFU, F-91191 Gif-sur-Yvette, France
M. Comunian, INFN/LNL, Legnaro, Padova, Italy
C. Oliver Amoros, CIEMAT, Madrid, Spain

Abstract

One of the activities of the EVEDA (Engineering Validation and Engineering Design Activities) phase of the IFMIF (International Fusion Materials Irradiation Facility) project consists in building, testing and operating, in Japan, a 125 mA/9 MeV deuteron accelerator, called LIPAc, which has been developed in Europe.

For the accelerator safety aspects, a precise knowledge of beam loss location and power deposition is crucial, especially for a high intensity, high power accelerator like LIPAc. This paper presents the beam dynamics simulations allowing to estimate beam losses in different situations of the accelerator lifetime: starting from scratch, beam commissioning, tuning or exploration, routine operation, sudden failure. Some results of these studies are given and commented. Recommendations for hot point protection, beam stop velocity, beam power limitation are given accordingly.

INTRODUCTION

For a high power megawatt class accelerator, any loss, even a tiny proportion of the beam, can be harmful. A careful and detailed loss study is thus necessary for various loss scenarios. That should be analysed for all the different stages of the accelerator lifetime, from its starting up, beam commissioning through routine operation, as well as for the various accidental breakdowns. Such a catalogue will be useful, or even necessary in the definition of safety procedure, limitations and recommendations, aiming at protecting personnel or facilities.

The linear IFMIF prototype accelerator (LIPAc) is being constructed in Europe and will be assembled in Japan [1]. This machine aims at accelerating a 125 mA D^+ continuous beam at 9 MeV. The general layout of LIPAc is recalled in Fig. 1, where beam energy and power for each subsystem are also given (for more details see Ref. [2]).

The LIPAc very high c.w. beam intensity implies that almost the whole accelerator is concerned by a high power beam which ranges from 0.012 to 1.125 MW. Indeed, it is common to consider that it is safe enough to use the lowest duty cycle and the lowest beam intensity during beam commissioning or exploration. But in the present case, as the ion source is optimised for providing a 140 mA continuous beam, the lowest duty cycle for which the beam is still stable is 10^{-3}; furthermore, the nominal beam intensity implies a very high space charge regime so that any beam tuning with too low intensity will not be representative because of much lower space charge effects.

In the following, the protocol of loss simulations is discussed, then some loss results are presented in a few loss scenarios and finally, consequences on safety measures are drawn.

LOSS STUDY PROTOCOL

In the following, the losses are given in power deposition (Watt). They are obtained with the nominal (maximum) current of 125 mA continuous wave. From that, losses can be reduced if needed, by reducing consequently the duty cycle and even the current if necessary. Theoretically, because space charge effects decrease with intensity, losses at lower current are less than what can be inferred by a linear relation. But as a precaution, it is wise to deduce losses at lower current with a simple linear transformation.

The double issue is to define as exhaustively as possible all the typical loss situations in the accelerator lifetime and to define the procedure to simulate and estimate them. The following stages have been identified: (A) Ideal machine; (B) Starting from scratch; (C) Beam commissioning, tuning, exploration; (C) Routine operation; (E) Sudden failure.

Stage A: Ideal Machine

"Ideal" means here nominal machine parameters and tunings, without any error. That should correspond on the real machine to a completely satisfying situation, once all the accelerator components are perfectly fabricated and aligned, or else corrected at the source, and the beam has been idealy tuned. Losses in such conditions should be minimum; we cannot hope to have less. These are minimum and permanent losses that have to be withstood. They are obtained by a start-to-end simulation without any error for the nominal tuning [3].

Stage B: Starting From Scratch

In this condition, no correction has yet been applied, while we can expect that: (1) The accelerator components have been fabricated and aligned as specified, within the already defined tolerance ranges. (2) The tunable parameters (accelerating and focusing fields and gradients) are set at their optmized values given by beam dynamics simulation. We must however expect that the real beam behavior is not exactly the same as simulated one (the IFMIF very high space charge regime has never been experimentally observed). This simulation-reality difference can be roughly estimated as equivalent to field and gradient variations in a ±10%

* Nicolas.Chauvin@cea.fr

Copyright © 2014 CC-BY-3.0 and by the respective authors

STATUS OF THE FAIR PROTON SOURCE AND LEBT

N. Chauvin*, O. Delferrière, P. Girardot, Y. Gauthier, J.L. Jannin, A. Lotode,
A. Maugueret, N. Misara, J. Neyret, F. Senée, C. Simon, O. Tuske,
CEA, IRFU, F-91191 Gif-sur-Yvette, France
R. Berezov, J. Fils, P. Forck, R. Hollinger, V. Ivanova, C. Ullmann, V. Vinzenz
GSI, D-64291 Darmstadt, Germany

Abstract

The unique Facility for Antiproton and Ion Research – FAIR will deliver stable and rare isotope beams covering a huge range of intensities and beam energies. A significant part of the experimental program at FAIR is dedicated to antiproton physics that requires an ultimate number $7\text{x}10^{10}$ cooled pbar/h. The high-intensity proton beam that is necessary for antiproton production will be delivered by a dedicated 75 mA/70 MeV proton linac.

The injector section of this accelerator is composed by an ECR source, delivering a pulsed 100 mA H^+ beam (4 Hz) at 95 keV and a low energy beam transport (LEBT) line required to match the beam for the RFQ injection. The proposed design for the LEBT is based on a dual solenoids focusing scheme. A dedicated chamber containing several diagnostics (Alisson scanner, Wien filter, SEM grid, Iris, Faraday Cup) will be located between the two solenoids. At the end of the beam line, an electrostatic chopper system is foreseen to inject 36 µs long beam pulses into the RFQ.

The status of LEBT simulations, design and fabrication of the FAIR proton injector will be presented.

INTRODUCTION

In the next years, the new international accelerator facility FAIR, one of the largest research projects worldwide, will be built at GSI.

In the final construction, FAIR consists of eight ring colliders with up to 1,100 meters in circumference, two linear accelerators and about 3.5 km of beam pipes. The existing GSI accelerators together with the planned proton-linac (p-linac) will be used as injector for the new facility. The double-ring synchrotron will provide ion beams of unprecedented intensities at high energy in order to produce intense secondary beams (unstable nuclei or antiprotons) [1].

An important part of the experimental program at FAIR is dedicated to antiproton physics. For various experiments up to 7×10^{10} of cooled pbar/h are required. Taking into account the pbar production and cooling rate, the chain of accelerators composed by a proton linac and the two synchrotrons SIS18 and SIS100 has to provide 2×10^{16} protons/h [1].

The 70 MeV/70 mA linac is currently under design and construction. This accelerator is composed by an ECR source, a LEBT, a 3 MeV RFQ and a DTL based on CH-cavities [2].

* Nicolas.Chauvin@cea.fr

The design, the fabrication and the commissioning of the FAIR proton-linac source and LEBT is performed in the framework of a Germany-France collaboration. The present paper will present an overview of the status of this apparatus which is currently under construction at CEA/Saclay.

ION SOURCE & LEBT REQUIREMENTS

The purpose of the FAIR p-linac source & LEBT is to produce a 100 mA/95 keV proton beam and to transport and match it for its injection into the next accelerating section, which is a RFQ. The main beam parameters that are required are summarized in Table 1.

Table 1: FAIR p-linac Ion Source & LEBT Requirements

Parameters	Value
Specie	Proton
Energy	95 keV
Intensity	100 mA
Time structure	Pulsed at 4 Hz
Energy spread	< 60 eV
Final emittance	$\leqslant 0.33\ \pi$ mm.mrad
α Twiss parameter	$0.27 \leqslant \alpha \leqslant 0.59$
β Twiss parameters	$0.037 \leqslant \beta \leqslant 0.046$ mm/π.mrad

FAIR PROTON LINAC ION SOURCE AND LEBT LAYOUT

General Layout

A scheme of the general layout of the FAIR p-linac source and LEBT is given on Fig. 1. The main components (ion source, beam line and beam diagnostics) are more precisely described in the following sections.

Ion Source

The design of the FAIR p-linac 2.45 GHz ECR ion source is based on the SILHI source [3]. It will be operated in pulsed mode, by pulsing the injected RF power. The repetition rate will be fixed at 4 Hz while the length of the beam pulses extracted from the source will be a few milliseconds.

The axial magnetic field will be provided by 2 coils, identical to the SILHI ones, which are independently tunable in term of current and position. The magnetic field on the axis is generally adjusted to obtain the first ECR zone (B_{ECR} = 0.0875 T) located just at the RF input in the plasma chamber while the second one takes place in the extraction system

Copyright © 2014 CC-BY-3.0 and by the respective authors

NITROGEN TREATED CAVITY TESTING AT CORNELL*

Dan Gonnella†, Minqi Ge, Fumio Furuta, Matthias Liepe, Cornell University, Ithaca, NY, USA

Abstract

Recent results from Cornell, FNAL, and TJNAF have shown that superconducting RF cavities given a heat treatment in a nitrogen atmosphere show higher Q_0 at operating gradients at 2.0 K than standard SRF cavities. Here we present on recent results at Cornell in which five single cell cavities and three 9-cell cavities were tested after receiving various nitrogen-doping treatments. Cavity performance was correlated with treatment, and samples treated with the cavities were analyzed with SIMS. These results provide new insights into the science behind the excellent performance that is observed in these cavities.

INTRODUCTION

New light sources such as LCLS-II at SLAC require CW SRF cavity operation. In order to operate the machine in this mode, high intrinsic quality factor (Q_0) must be achieved in the medium field region. The LCLS-II specification is a Q_0 of 2.7×10^{10} at 16 MV/m and 2.0 K [1]. Until recently, this goal was very ambitious, however with the introduction of nitrogen doping, quality factors on this order and above can now be repeatedly achieved. Nitrogen doping consists of heat treating SRF cavities in a low pressure nitrogen atmosphere resulting in some nitrogen diffusion into the niobium. It has been shown that this process has the ability to completely remove the medium field Q slope usually seen in SRF cavities and even causes an anti-Q slope where the Q will increase between ~ 5 and ~ 20 MV/m [2, 3]. An effort is currently underway at Cornell, FNAL, and TJNAF to study the effect of nitrogen doping on single and 9 cell cavities for LCLS-II [4]. In this paper we discuss the current progress on this subject at Cornell.

CAVITY TREATMENT AND TESTING

Five single-cell 1.3 GHz ILC shaped cavities (constructed at Cornell) and 3 ILC 9 cell cavities were given the same doping treatment. This consisted of a bulk VEP (~ 100 µm), followed by a de-gas in UHV furnace at 800°C in vacuum, followed by 20 minutes in a nitrogen atmosphere (pressure profile shown in Fig. 1), followed by an additional 30 minutes in vacuum. After doping, a nitride layer forms on the surface (this will be clear from SIMS data which will be discussed in a later section). This nitride layer must be removed before testing. Each cavity was given a final VEP to remove this nitride layer and to change the doping level of the RF surface layer. The five single-cells were given different amounts of material removal in order to study how the cavity performance evolves with material removal. The 9 cells were given final EP in order to achieve the best performance. The removal amounts are summarized in Table 1.

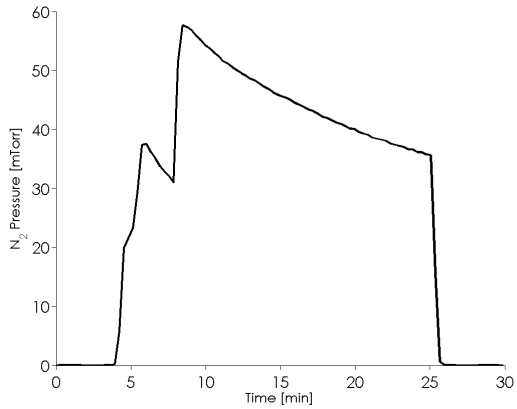


Figure 1: The nitrogen pressure profile during the heat treatment of TE1-1, 2, and 3.

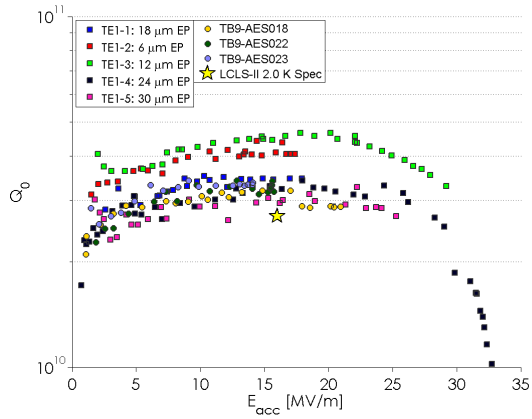


Figure 2: Q_0 vs E_{acc} performance and 2.0 K for all eight cavities. Errors are 20% on Q_0 and 10% on E_{acc}

For each cavity, the following was measured: Q_0 vs temperature, resonance frequency vs temperature (during warm-up), and Q_0 vs E_{acc} at 1.6, 1.7, 1.8, 1.9, 2.0, and 2.1 K. This extensive Q_0 vs E_{acc} data was used to extract the residual (temperature independent) and BCS (temperature dependent) resistances and their field dependence.

CAVITY PERFORMANCE

The 2.0 K Q_0 vs E_{acc} performance for each of the eight cavities is shown in Fig. 2. The LCLS-II 2.0 K specification of 2.7×10^{10} at 16 MV/m is also shown.

We can see from Fig. 2 that all the single-cell cavities easily meet the LCLS-II spec. Cavities 1 and 2 are the only single-cells to quench below 20 MV/m (a phenomenon seen in many other nitrogen-doped cavities [2, 3, 5]). The

* Work supported by the US DOE and the LCLS-II Project
† dg433@cornell.edu

Copyright © 2014 CC-BY-3.0 and by the respective authors

BEAM-BASED HOM STUDIES OF THE CORNELL ENERGY RECOVERY LINAC 7-CELL SRF CAVITY*

D.L. Hall†, A. Bartnik, M.G. Billing, R.G. Eichhorn, G.H. Hoffstaetter, M. Liepe
C. Mayes, P. Quigley, V. Veshcherevich
Cornell Laboratory for Accelerator-Based Sciences and Education (CLASSE),
Ithaca, NY 14850, USA

Abstract

The 1.3 GHz 7-cell SRF cavity for the Cornell ERL main linac is optimized for high beam current ERL operation with injected CW beam currents of 100 mA. Beam stability at 100 mA requires very strong damping of the Higher-Order-Modes (HOM) in the cavity by HOM beamline absorbers at the ends of the cavity. To verify the optimized design of the cavity and the HOM damping scheme, a prototype 7-cell main linac cavity was installed into the Cornell Horizontal Test Cryomodule (HTC), and inserted into the beamline of the Cornell ERL high current photo-injector. A beam-based method was then used to search for the presence of dangerous HOMs. Individual HOMs were excited using a charge-modulated beam, after which their effect upon an unmodulated beam was observed using a BPM. Data collected was used to calculate the R/Q and Q of observed HOMs. Results show that no dangerous dipole modes were found to be present in the HTC. In addition, measurements of the temperature rise of the HOM absorber rings during high current CW beam tests were consistent with simulations, indicating that the optimized main linac cavity is capable of operating at the specified current of 100 mA in an ERL configuration.

INTRODUCTION

In the interest of building an Energy Recovery Linac (ERL), Cornell has designed and constructed 1.3 GHz 7-cell cavities that have been optimised for operation in an ERL [1]. The cavities must be capable of sustaining 100 mA of beam current at 2 ps bunch length while operating at 16 MV/m in CW with a quality factor Q_0 of at least 2×10^{10} at a bath temperature of 1.8 K. A prototype 7-cell ERL cavity tested in a cryomodule obtained a record 1.8 K Q_0 of $(6.2 \pm 0.6) \times 10^{10}$ at 16 MV/m [2, 3], exceeding the required efficiency specifications by a factor of 3.

In this paper we present results from two separate yet linked experiments performed on the prototype 7-cell cavity test in [2] using beam provided from the Cornell ERL high-current Injector Cryomodule (ICM). The first of these qualified the monopole HOMs and the power dissipated in the HOM loads located at either end of the cavity. This experiment was also used to investigate the possible advantages of coating the beampipes near the HOM loads with copper to reduce the dynamic heat load from resistive losses in the beampipe walls. The second experiment was a beam-based HOM search used to search for any HOMs that might potentially cause BBU instabilities when operated at 100 mA in an ERL configuration.

EXPERIMENTAL PROCEDURE

To test the cavity with beam, it was installed into Cornell's Horizontal Test Cryomodule (HTC). The cryomodule was equipped with all the accessories that are expected to be used in the final ERL Main Linac Cryomodule: HOM loads at either end of the cavity, a high-current input coupler and an RF field probe for HOM diagnostics. The cavity was installed in the beamline of the ERL injector, directly after the ICM.

HOM Load Heating

The first experiment, to qualify the power dissipation and heat load on the HOM loads during beam operation, involved measuring the temperature increase of the 80K HOM load cooling system at different beam currents. The injector was operated at two different beam currents, 25 mA and 40 mA, using both a 3.4 ps and 2.7 ps long bunch. As the beam was passed through the centre of the cavity, the increase in temperature of the 80 K cooling loop that cooled both of the HOM loads was measured. A cross-section diagram of the cavity and its attached HOM loads illustrating the regions of interest for measurement is shown in Fig. 1. Using heaters installed in the HOM load near the 80 K cooling coil, this raise in temperature was calibrated to provide a relation between the temperature rise of the 80 K system, ΔT, and the power dissipated in the HOM loads, P_{load}. Using the

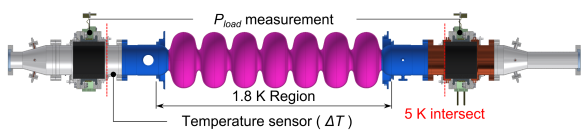


Figure 1: A cross-section diagram of the cavity and attached HOM loads, one of which has had its beampipes coated with copper. The 1.8 K region extends just beyond the cavity, and is separated from the HOM load 80 K system by the 5 K intersect. The power dissipated in the HOM loads is measured using the combined 80 K cooling system of the loads. A temperature sensor mounted between the 5 K and 1.8 K regions on the HOM load with steel beampipes measures the temperature rise of the steel beampipe under beam loading.

* Work supported by NSF Grant DMR-0807731
† dlh269@cornell.edu

ISBN 978-3-95450-142-7

Copyright © 2014 CC-BY-3.0 and by the respective authors

SAMPLE PLATE STUDIES USING A HIGH FIELD TE CAVITY WITH THERMOMETRY MAPPING SYSTEM*

D.L. Hall†, C.D. Burton, M. Liepe
Cornell Laboratory for Accelerator-Based Sciences and Education (CLASSE),
Ithaca, NY 14850, USA

Abstract

A TE-Mode sample plate cavity capable of sustaining peak fields of >90 mT on the surface of a 10 cm diameter sample plate has been developed and tested at Cornell. A thermometry mapping system composed of 40 Allen-Bradley resistors, mounted on the outside of the sample plate, is capable of measuring the surface resistance of the sample with a resolution of 1 nΩ and a spatial resolution of 0.5 cm. In this paper we present the design and expected performance of this high field TE cavity, and show data taken with a sample plate of niobium as well as results from tests qualifying the performance of the thermometry mapping system.

INTRODUCTION

As the fundamental limits of bulk niobium are explored and attained, Cornell has been developing TE mode sample host cavities for the purpose of studying alternative materials such as Nb_3Sn and MgB_2. These cavities are designed to accommodate a flat, circular sample plate that can be easily removed for inspection following a test. Furthermore, the addition of a Thermometry Mapping (T-Map) system allows for studies of isolated areas on the sample plate that are subject to higher losses.

In this paper we will present results from a test done using a niobium sample plate, which is necessary for correct calibration of the T-Map system for use with other materials and different niobium preparations. The design process of the cavity will be briefly touched upon, as well as the experimental procedure. Furthermore, results from an experiment to qualify the accuracy of the T-Map system will also be shown. Finally, plans for further work will be discussed.

Cavity Design

The cavity presented and discussed in this paper is the third iteration in the design process carried out at Cornell. The first two, a pillbox-style cavity and a mushroom-style cavity are described in further detail in [1, 2]. Photographs of these two cavities, as well as the latest BOB-style design, are shown in Fig. 1.

The latest BOB-style cavity has been designed using insight gained from studies on thermal runaway quenches [2], which is the limiting factor in the pillbox and mushroom-style designs due to their higher operating frequency of 6 GHz. Comparatively, the BOB design operates at 4 GHz, pushing back the limit imposed by thermal runaway occurring due to frequency-dependent losses in the cavity walls. Using a genetic optimisation algorithm and the solver code CLANS [3], the BOB-style was developed to have a maximum field on the sample plate of approximately 120 mT before a quench due to thermal runaway occurs on the walls of the cavity. The cavity design is expounded further in [4,5].

Figure 1: The three generations of TE-mode cavities, from left to right: A) The pillbox cavity, B) the mushroom cavity, C) the latest BOB style cavity.

T-Map System

The T-Map system is composed of 40 (upgradeable to 56) Allen-Bradley 100 Ω 1/8 W carbon-composite resistors which are mounted on a Teflon disc that is attached to the reverse (LHe) side of the sample plate during operation. A photograph of the T-Map is shown in Fig. 2. Once calibrated using a niobium sample plate prepared with the same recipe as the cavity, the T-Map is capable of detecting areas of increased surface resistance with resolution of 1 nΩ and a spatial resolution of 0.5 cm.

Figure 2: A photograph of the T-Map, which is mounted to the LHe side of the sample plate. The system is composed of 40 Allen-Bradley resistors, which can be upgraded to 56 by adding another layer of resistors to the outer ring.

* Work supported by NSF Grant DMR-0807731
† dlh269@cornell.edu

ISBN 978-3-95450-142-7

Copyright © 2014 CC-BY-3.0 and by the respective authors

LOW KICK COUPLER FOR SUPERCONDUCTING CAVITIES*

R. Eichhorn, C. Egerer and V. Veshcherevich†
Cornell University, Ithaca, NY 14853, U.S.A.

Abstract

Results from the high current, low emittance photo injector at Cornell revealed that even with two opposing input couplers, the beam emittance is affected by the coupler kick. As a result, a coupler with low transverse kick is proposed for use in superconducting accelerating cavities. In this coupler, a rectangular waveguide transforms into a coaxial line inside the beam pipe. The geometry of the coupler is tuned to minimize the transverse kick that is important for linear accelerators with low emittance. The coupler can be used in ERL injectors or other linacs for high brightness light sources.

INTRODUCTION

The proposed Cornell Energy Recovery Linac (ERL) [1] and other new ultra high brightness synchrotron light sources need high quality low emittance electron beams. That means that beam has to be formed by electron gun and accelerated with minimal destructive effects. The starting part of the accelerator, the injector, produces the strongest effect on the beam due to low beam energy.

The input coupler of superconducting cavities is usually an antenna type coupler attached to a side port in the beam pipe near the cavity. Due to axial asymmetry of this design, electromagnetic fields in the vicinity of the coupler have transverse components and produce a transverse kick to the electron beam. That leads to the emittance dilution of the beam.

To reduce this effect, the injector cavities of Cornell ERL are equipped with two identical input couplers symmetrically placed on two sides of the beam pipe [2]. That design eliminates the dipole transverse kick. However, there exist quadrupole field components and this quadrupole focusing distorts the beam [3].

Therefore we consider a possibility to build a new coupler which produces axially symmetric fields and generates very low transverse kick to the beam. That coupler has a tube inside the beam pipe which forms a coaxial line with the beam pipe. This coaxial line is coupled to a power transmission line. Couplers of that type were designed, built and used for S-DALINAC superconducting cavities in early 90s [4]. In that design the coaxial transmission line was coupled to the coaxial line in the beam pipe by movable antenna. Later similar couplers were considered at DESY [5] and FNAL [6].

Unfortunately, these designs were not perfect. For practical sizes of the beam pipe, two modes can propagate in the beam pipe coaxial line: a fully axially symmetric TEM mode and a dipole TE_{11} mode. The TE_{11} mode is excited in the coaxial line due to asymmetric coupling to the transmission line. This dipole mode produces a transverse kick to the beam.

During the early study of ERL injector design, a symmetric coupler inside the beam pipe of small diameter was considered [7]. In such a case, the TE_{11} mode could not propagate along the coaxial line of that smaller size. Unfortunately, this was not compatible with the HOM and BBU requirements set by the linac design.

A similar solution was also found at Darmstadt, operating at 3 GHz The idea was to use a rectangular waveguide instead of a coaxial transmission line to and to optimize the geometry of the field transformer between the waveguide and the beam pipe coaxial line for minimizing the excitation of the TE_{11} mode [8].

SYMMETRIC COUPLER FOR ERL INJECTOR CAVITY

Figure 1 shows the model of the ERL injector cavity with the Darmstadt type of symmetric coupler. The

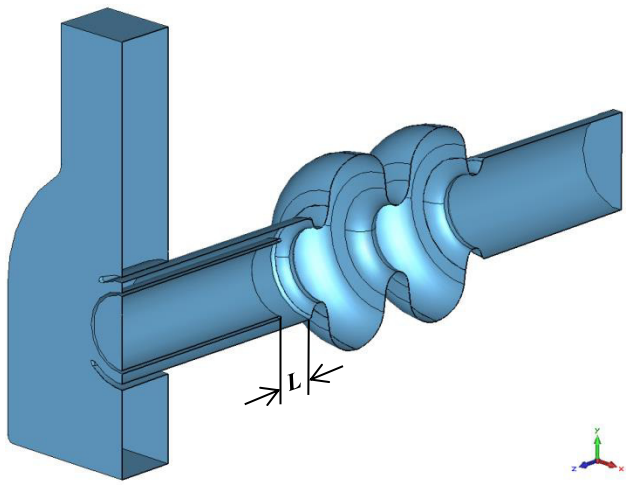


Figure 1: 2-cell cavity with the symmetric coupler.

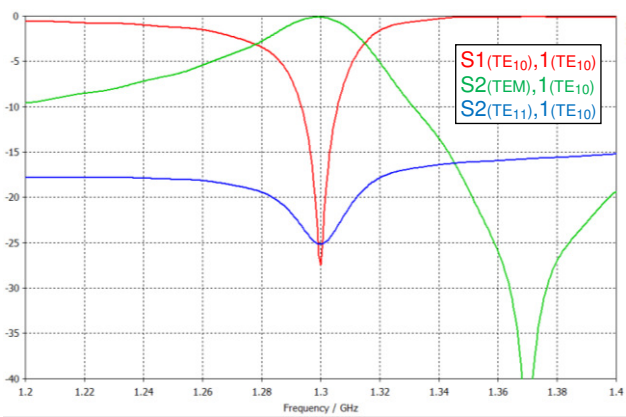


Figure 2: Calculated S-parameters of the coupler waveguide-to-coax field transformer (in dB).

* Work is supported by NSF Grants NSF DMR-0807731 and NSF PHY-1002467.
† vgv1@cornell.edu

Copyright © 2014 CC-BY-3.0 and by the respective authors

ISBN 978-3-95450-142-7

ANALYSIS OF THE RF TEST RESULTS FROM THE ON-GOING CAVITY PRODUCTION FOR THE EUROPEAN XFEL*

Detlef Reschke#, Sebastian Aderhold, Vladimir Gubarev, Jörn Schaffran, Nicholas Walker,
DESY, Hamburg, Germany
Laura Monaco, INFN Milano, LASA, Milano, Italy
Yasuchika Yamamoto, KEK, Tsukuba-shi, Japan

Abstract

The main Linac of the European XFEL will consist of 100 superconducting accelerator modules, operated at an average design gradient of 23.6 MV/m. The fabrication by industry (which includes chemical surface preparation) of the required 800 superconducting cavities is now in full swing, with approximately 400 cavities having been delivered to date. In this interim report, we present an analysis of the RF acceptance tests amassed so far.

INTRODUCTION

The 17.5 GeV SRF linac for the European XFEL is currently under construction by a consortium consisting of several European institutes [1]. A cryomodule production rate of one eight-cavity-module per week requires an average cavity production and vertical acceptance testing rate of at least eight per week. Testing is performed in a dedicated facility at DESY (AMTF) [2,3]. As of July 31, 2014, approximately 380 of the 800 series XFEL TESLA-type 1.3 GHz SRF cavities have been produced, and have each undergone at least one vertical acceptance test at AMTF. Vertical and module testing is performed by a team from IFJ-PAN Krakow as an in-kind contribution. This report presents the current statistics of the cavity results at this half-way stage in the production, including the performance of the cavities as received from industry and the impact of retreatment cycles performed in the DESY infrastructure. Finally, the first complete module test results will be reported.

XFEL CAVITIES AND VERTICAL ACCEPTANCE TEST AT AMTF

Production Overview

Series production of the 1.3 GHz TESLA cavities is equally divided between E. Zanon Spa. (EZ), Italy, and Research Instruments GmbH (RI), Germany. Production includes both mechanical fabrication and surface preparation [4]. The 800 series cavities required for XFEL (400 per vendor) are delivered complete with a helium tank, ready for vertical testing in AMTF at DESY. Each vendor also produces an additional 12 cavities without helium tank for the ILC-HiGrade programme [5], which are used as a quality control tool as well as for further R&D. Both vendors must exactly follow well-defined specifications for the mechanical fabrication and surface treatments, but no RF performance guarantee is required. The surface preparation at both vendors starts with a bulk EP followed by 800° annealing, but for the final surface treatment two alternative recipes are in use: EZ applies a final chemical surface removal ("Flash-BCP"); RI applies a final electrochemical surface removal (EP). All cavities are fully equipped with their HOM antennas, pick-up probe and a High-Q input coupler antenna with fixed coupling. The procedures before and after the vertical acceptance test are described in [6].

Vertical Testing Rates

In order to achieve the desired testing rate of at least eight cavities per week, the vertical acceptance tests are made using two independent test systems, each consisting of an independent bath cryostat and RF test stand. Each test cryostat accepts an "insert" which supports up to four cavities, greatly increasing the efficiency of cool-down / warm-up cycles. The test infrastructure has been in full operation since October 2013 and has achieved an average greater than 9 vertical tests per week (see Fig. 1). Assuming realistic rates for necessary retesting of cavities (e.g. after retreatment, see below), all vertical acceptance tests of the 824 cavities will be finished within the current project schedule (end of 2015).

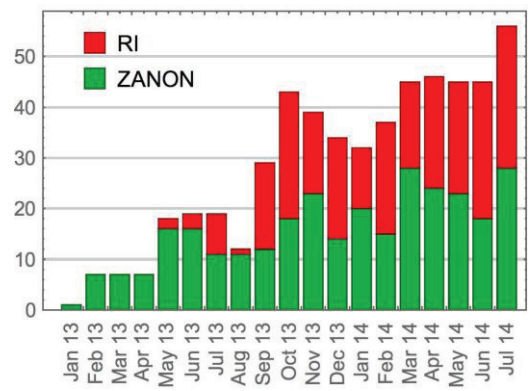


Figure 1: Trend of the vertical test rate

The vertical acceptance tests follow a standardised procedure, which includes the measurement of the unloaded Q-value (Q_0) versus the accelerating gradient E_{acc} at 2 K, as well as the frequencies of the fundamental modes. For each point of the $Q_0(E_{acc})$-curve, X-rays are measured inside the concrete shielding above and below the cryostat. No general administrative gradient limit is

*The research leading to these results has received funding from the European Union Seventh Framework Programme (FP7/2007-2013) under grant agreement no 283745 (CRISP)

detlef.reschke@desy.de

Copyright © 2014 CC-BY-3.0 and by the respective authors

ISBN 978-3-95450-142-7

EFFICIENCY OF HIGH ORDER MODES EXTRACTION IN THE EUROPEAN XFEL LINAC

A. Sulimov, J. Iversen, D. Kostin, W.-D. Moeller, D. Reschke, J. Sekutowicz, J.-H. Thie
(Deutsches Elektronen-Synchrotron, DESY, Notkestrasse 85, 22607 Hamburg, Germany),
D. Karolczyk, K. Kasprzak, S. Myalski, M. Wiencek, A. Zwozniak
(Instytut Fizyki Jądrowej PAN, IFJ-PAN, ul. Radzikowskiego 152, 31-342 Kraków, Poland)

Abstract

The serial production of components for the European XFEL linac was started in 2011 and reached the planned level of 8 cavities (1 module) per week in 2013. The measurements of High Order Modes (HOM) characteristics under cryogenic conditions (2K) are being done at the Accelerating Module Test Facility (AMTF) by the IFJ-PAN Team in collaboration with DESY groups.

More than 50 % of the cavities have been already produced and 30 % of the whole amount were measured during either cavity vertical tests or module tests.

We present first statistics of these measurements and analyze the efficiency of HOM extraction.

HOM DAMPING REQUIREMENTS

The most important high order modes for XFEL cavities are presented in figure 1 [1].

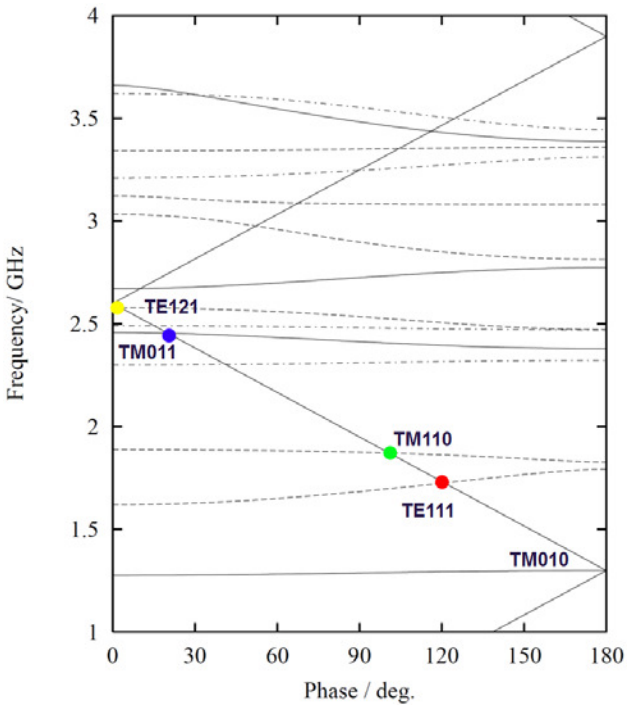


Figure 1: Dispersion curves for monopole (solid line), dipole (dashed line) and quadrupole (dash-dotted line) modes. The dots mark the most critical HOM.

The most critical modes, which could be generated by the beam, are marked with points. The two first dipole modes: TE111 (red) and TM110 (green) are usually used for beam diagnostics as beam position monitors [2]. The second monopole TM011 (blue) does not cause a critical beam perturbation, but increases the cryo losses in the linac due to a very high value of $R_{sh}/Q = 155$ Ohm, only 6 times less than the shunt impedance of fundamental TM010 pi-mode, where $R_{sh}/Q = 1010$ Ohm. The third dipole mode TE121 (yellow) is the most dangerous one for the beam dynamics [3]. Unfortunately it is very difficult to identify it without a beam. So, only three HOM pass-bands are used for XFEL cavities quality control (see figure 2).

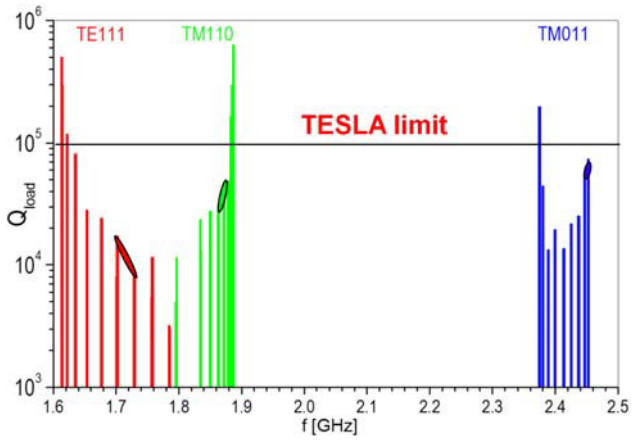


Figure 2: Example of $Q_{load}(f)$ for TE111, TM110, TM011.

The HOM damping requirements for cavities in the TESLA project [4] were also used for the European XFEL. Typically it is planned to analyze only Q_{load} values for the strongest modes (marked with black ovals in figure 2):

- TE111 (both polarizations of modes 6 and 7),
- TM110 (both polarizations of modes 4 and 5),
- TM011 (mode 9).

All values for Q_{load} have to be lower than 10^5.

The first two dipole modes for all XFEL cavities always fulfill this requirement.

Thus, special attention in this article will be given to the second monopole measurements.

STATISTICS

Before the XFEL cavities serial production was started, HOM couplers' orientation and configuration were designed in order to achieve optimal efficiency for HOM damping, corresponding to TESLA project requirements.

The zero-mode for TM011 has the highest frequency (9^{th} peak in the spectra) and is labeled as TM011_9.

The measurement results of Q_{load}(TM011_9) for 9-cell TESLA shape cavities under cryo conditions at DESY are presented in figure 3.

Copyright © 2014 CC-BY-3.0 and by the respective authors

ISBN 978-3-95450-142-7

AFFORDABLE SHORT PULSE MARX MODULATOR*

Robert Phillips, Gerard DelPriore, Dr. Marcel P.J. Gaudreau, PE, Michael Kempkes,
Diversified Technologies, Inc., Bedford, MA 01730, USA
Dr. Jeffery Casey, Rockfield Research, Inc., Las Vegas, NV 89135, USA

Abstract

Under a U.S. Department of Energy grant, Diversified Technologies, Inc. (DTI) is developing a short pulse, solid-state Marx modulator. The modulator is designed for high efficiency in the 100 kV to 500 kV range, for currents up to 250 A, pulse lengths of 0.2 to 5.0 µs, and risetimes <300 ns. Key objectives of the development effort are modularity and scalability, combined with low cost and ease of manufacture. For short-pulse modulators, this Marx topology provides a means to achieve fast risetimes and flattop control that are not available with hard switch or transformer-coupled topologies.

INTRODUCTION

Under a DOE SBIR grant and based on research begun under the Next Generation Linear Collider (NLC) program, high energy, short-pulse modulators are being re-examined for the Compact Linear Collider (CLIC) and numerous X-Band accelerator designs. At the very high voltages required for these systems, however (Table 1), all of the existing designs are based on pulse transformers, which significantly limit their performance and efficiency. There is not a fully optimized, transformer-less modulator design capable of meeting the demanding requirements of very high voltage pulses at short pulsewidths.

MARX GENERATOR

A Marx generator is a system with energy storage capacitors which are charged in parallel at low voltage and discharged in series to provide high voltage output (Figure 1). This is a legacy idea, practiced for decades using resistor charging networks and spark-gaps for discharge. Constrained by the limits of closing switches, such systems required pulse forming networks and crowbars, with their attendant limitations.

The Marx topology allows a new degree of freedom unavailable to other architectures – DTI can intentionally underdamp the series snubbing within the pulse circuit. This cannot be done conventionally – the reactive overshoot endangers the load. In a Marx, we can compensate for the overshoot by initially firing only a subset of the switches – thus "sling-shotting" the leading edge faster than otherwise possible. We can tune the number and timing of subsequent module firings to counter the reactive ringing, and hold a flattop pulse to the desired voltage and accuracy.

Similarly, additional modules may be added to fire sequentially later in the pulse to compensate for capacitor droop. This is a critical enabling technology motivating Marx use for long-pulse accelerators (such as ILC), and yields valuable optimization even for very short-pulse systems. The reduction of capacitor size afforded by this flexibility further reduces parasitic capacitance, and thus reduces equipment size and cost while increasing power efficiency.

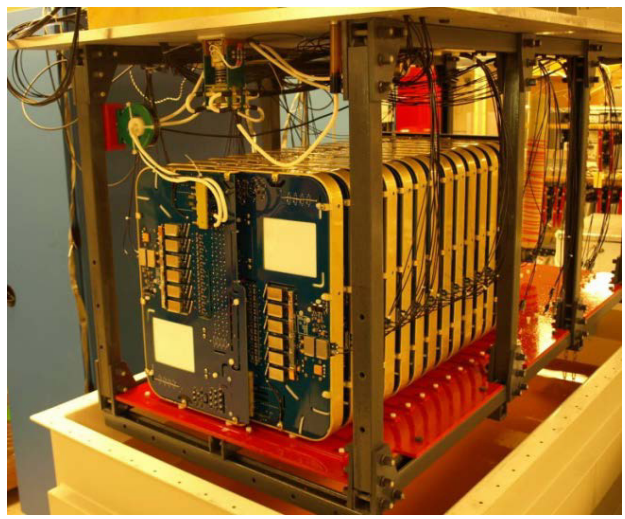


Figure 1: The Yale Marx 500 kV modulator charges many stages in parallel at low voltage, then discharges in series at high voltage. Each 12.5 kV, 250 A "flat pack" module is identical, providing for low fabrication and assembly cost.

DESIGN BENEFITS

Reduced Module Costs

Through the use of PC board trace shielding and RF cans in sensitive areas of the circuit, we were able to co-locate controls directly on the board within reasonable proximity to pulsed current sections of the same board. By exposing the IGBTs directly to the oil, we can cool the devices effectively while eliminating machined parts and hardware, further reducing the module parts count, associated materials, and assemly costs. Since the flat-pack design significantly reduces voltage gradients from module to module within the Marx bank, the only significant need for corona and field reduction geometry is at the interface between the Marx bank stack and the walls of the tank. We anticipate more than a four-fold reduction in module mechanical costs, with the potential for additional reductions in manufacturing costs, compared to earlier designs.

*Work supported by U.S. Department of Energy SBIR Award DE-SC0004251

Copyright © 2014 CC-BY-3.0 and by the respective authors

RF DESIGN AND LOW POWER MEASUREMENTS OF A NOSE CONE SINGLE GAP BUNCHER CAVITY

O. González#, N. Garmendia, P. González, L. Muguira, J. L. Muñoz, A. Zugazaga, I. Bustinduy
ESS Bilbao, Bilbao, Spain

Abstract

A nose-cone single-gap buncher cavity for the Medium Energy Beam Transport (MEBT) has been fully designed, manufactured and measured under low-power conditions at ESS-Bilbao. In this work, the main steps of the design process are first reviewed. Second, the cavity is thoroughly measured and characterized by means of an automatic test procedure based on the bead-pull technique. Third, the simulated and measured figures of merit are compared. Specifically, the results for the resonant frequency, the coupling and quality factors, the electric field profile, the R over Q ratio, the transit time factor and the tuning range are carefully analysed.

INTRODUCTION

In the framework of the ESS-Bilbao project, a nose-cone single-gap buncher cavity for the Medium Energy Beam Transport (MEBT) has been designed with the aid of the commercial simulator COMSOL [1]-[3]. The cavity geometry has been optimized in order to maximize the effective shunt impedance (RT^2) while both fulfilling the specifications imposed by the MEBT beam dynamics design (Table 1) and avoiding the electrical discharge or multipacting. The latter is achieved by limiting the peak surface electric field (*Kilpatrick* limit). The optimization procedure followed as well as the final cavity geometry and its figures of merit can be found in [1].

Although copper was assumed as the material for the designed cavity, a first prototype has been manufactured and measured in stainless steel (figure 1) which includes: a vacuum port (A), two tuning ports (B and D), a RF coupler port (C), a pick-up port (E), a blind cover port (F) and a cradle (G). At a later stage, a copper plating technique will be applied to the cavity.

BEAD-PULL TEST BENCH

The cavity has been measured and characterized by means of an automatic test procedure based on the bead-pull technique fully developed at ESS-Bilbao.

Table 1: Cavity Specifications

Parameter	Value	Unit
Frequency	352.2	MHz
Particle Energy	3	MeV
Effective Voltage (V_0T)	140	kV
Bore diameter (aperture)	30	mm
Cavity length (L)	126	mm
Peak electric field (*Kilpatrick*)	27.5 (1.48)	MV/m

#ogonzalez@essbilbao.org

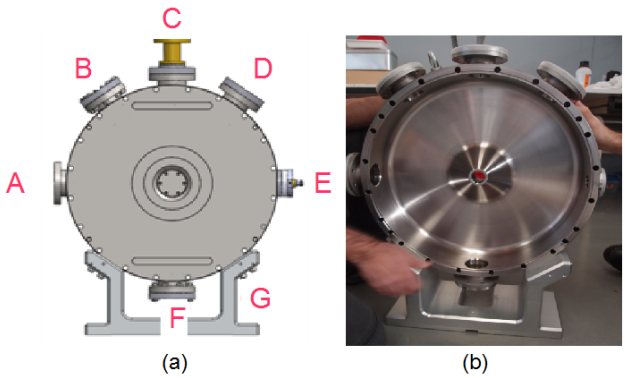


Figure 1: (a) Designed and (b) manufactured cavity.

Theory

The bead-pull technique [4,5] is based on the perturbation theory which states that when a small dielectric bead is introduced into a cavity, it causes a frequency shift given by

$$\frac{\Delta\omega}{\omega} = -F\frac{\omega E_0^2}{PQ_0}, \qquad (1)$$

where F is the form factor, ω is the resonant frequency, E_0 is the absolute electric field, P is the dissipated power and Q_0 is the unloaded quality factor. The form factor F only depends on the material and geometry of the bead.

Moreover, the characteristic impedance or ratio "R over Q", which exclusively depends on the cavity geometry and not on the material properties, can be computed as [5]

$$\frac{RT^2}{Q_0} = \frac{1}{F\omega}\left[\int_{-L/2}^{L/2}\sqrt{\frac{\Delta\omega}{\omega}}\,e^{\frac{j\omega z}{\beta c}}\,dz\right]^2, \qquad (2)$$

where z is the longitudinal axis of the cavity, β is the normalized velocity and c is the speed of light.

Design and Measurement Procedure

Figure 2 shows the test-bench implemented to carry out the measurements. It includes: 1) a cradle to support the

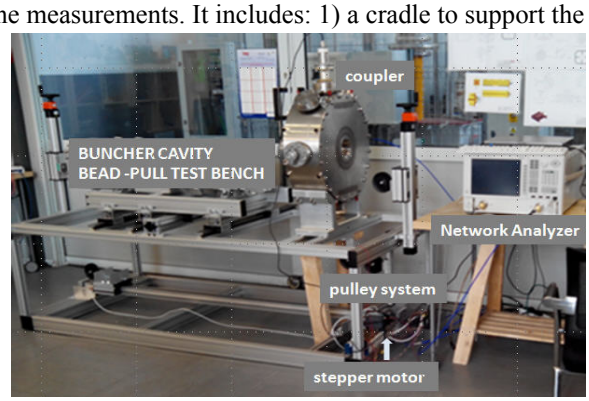


Figure 2: ESS-Bilbao bead-pull test bench design.

Copyright © 2014 CC-BY-3.0 and by the respective authors

ISBN 978-3-95450-142-7

COMMISSIONING OF THE LINAC4 LOW LEVEL RF AND FUTURE PLANS

P. Baudrenghien, J. Galindo, G. Hagmann, J. Noirjean, D. Stellfeld, D. Valuch, CERN, Geneva, Switzerland

Abstract

Linac4 is a new 86-m long normal-conducting linear accelerator that will provide 160 MeV H^- to the CERN PS Booster (PSB), and replace the present 50 MeV proton Linac2. The Low Level RF (LLRF) system has to control the RFQ, two choppers, three bunching cavities, twenty two accelerating cavities and one debuncher in the transfer line to the PSB. To optimize the transfer into the 1 MHz PSB bucket, the machine includes fast choppers (synchronized with the PSB RF) and a voltage modulation of the last two cavities that will provide Longitudinal Painting for optimum filling. The commissioning in the tunnel with beam has started in October 2013. So far the part consisting of the RFQ, the three bunching cavities, and the first DTL is operational. The rest of the machine will be progressively commissioned till end 2015. The paper presents the LLRF system. First results from the commissioning (with a prototype regulation system) are shown and the more sophisticated algorithms under development are presented.

PRESENTATION OF LINAC4 RF

The Linac4 machine will pulse at a 2 Hz maximum repetition rate, with a 400 µs maximum beam pulse length and 40 mA DC current. The machine operates at 352.2 MHz RF. The klystron-powered RFQ (3 MeV) is followed by a Medium Energy Beam Transfer line (MEBT), that includes three bunching cavities (pillbox geometry) powered by solid-state amplifiers (30 kW). The beam is then accelerated to 160 MeV by a succession of three Drift Tube Linacs (DTL), seven Cell-Coupled DTLs (CCDTL) and twelve PI Mode Structures (PIMS). A debunching cavity is inserted in the transfer line to the PSB. Except for the three bunchers, the RF power is generated by 1.3 MW and 2.8 MW klystrons. The 2.8 MW models are used with DTL2 and 3 (2 MW required power) and in other instances where they feed two cavities (1 MW per cavity). To make the beam density uniform in the PSB receiving bucket, longitudinal painting is implemented by modulating the accelerating field in the last two PIMS cavities, with a 40 µs period [1]. Given the 10 µs filling time of the PIMS, precise tracking of the voltage and phase will be a challenge. The target cavity voltage is a flat function for all cavities except the last two PIMS (triangular voltage modulation, constant phase) and the debuncher (constant voltage, triangular phase modulation). The LLRF consists of a **tuning system** that keeps the cavity at the tune that minimizes the required power (function of voltage, beam current and stable phase), and a **fast regulation** (Cavity Loops) that modifies the generator drive to keep the cavity field at the desired value.

TUNING SYSTEMS

The required power is minimized when the cavity is detuned such that generator current and cavity voltage are in phase. During each pulse, the cavity voltage (V) and the forward signal from a coupler at the cavity entrance (C_{fwd}) are demodulated to generate baseband I-Q pairs at 44.025 M-samples per second (MSps). They are then filtered and decimated (CIC decimators [2]) reducing the rate to 2.75 MSps. The cross-product is computed* and, after further filtering and decimation, the error data are passed to a DSP (ADSP-21369). The DSP normalizes the error signal to make tuning speed independent of the magnitude of cavity voltage and, at the end of the RF pulse, sends a correction to the motor piloting a plunger (except for the RFQ that is tuned by regulating the cooling water flow).

FIELD REGULATION

The loop delay from LLRF drive to the antenna signal (measured by the LLRF), is around 1 µs. That includes generator and circulator group delay, waveguide to cavity, and cable delay in the antenna signal path. Allowing 200 ns for processing in the LLRF, the closed-loop delay amounts to 1.2 µs. Fig.1 shows the regulation loops. We have four main sub-systems (shaded areas in Fig.1).

The RF is switched on 100 µs before injection. The **Cavity Filling Ramp** raises the cavity voltage in 50 µs.

The **Linear Quadratic Gaussian regulator** (LQG [3]) is then switched on and stabilizes the field in the remaining 50 µs until the beam batch is injected. Although we cannot measure the *present* cavity voltage, we can estimate it because the cavity response is well known and the generator drive is generated by the LLRF, and therefore known as well (except for the generator noise). The *optimal* estimator is the Kalman Predictor [3], a model of the cavity response with delay, driven by the same drive as the generator. The (delayed) cavity voltage measurements are used to update the predictor's estimates, and correct for the inexact model and the unknown noise sources. The measurement noise is caused by the imperfect demodulation. The process noise is mainly caused by the generator and beam loading.

* The cross-product is proportional to the sine of the phase angle:

$$V \times C_{fwd} = V_I\, C_{fwd,Q} - V_Q\, C_{fwd,I} = \sqrt{V_I^2 + V_Q^2}\ \sqrt{C_{fwd,I}^2 + C_{fwd,Q}^2}\ \sin\psi$$

Copyright © 2014 CC-BY-3.0 and by the respective authors

ISBN 978-3-95450-142-7

DESIGN AND BEAMLOADING-SIMULATIONS OF A PRE-BUNCHING CAVITY FOR THE CLIC DRIVE BEAM INJECTOR *

M. Dayyani Kelisani, H. Shaker, IPM, Tehran, Iran; CERN, Geneva, Switzerland
S. Doebert, CERN, Geneva, Switzerland

Abstract

The CLIC project is developing a multi-TeV center-of-mass electron-positron collider based on high gradient, room-temperature accelerating structures and a novel two-beam RF power generation scheme. The RF power for the CLIC accelerating structures is provided by the so-called drive beam, which is a low energy, high current electron beam. The drive beam will be generated from a high current (up to 5 A) pulsed (0.142 ms) thermionic electron gun and then followed by a bunching system. The bunching system is composed of three sub-harmonic bunchers operating at a frequency of 499.75 MHz, a pre-buncher and a traveling wave buncher both operating at 999.5 MHz. The pre-buncher cavity, which has a great importance on minimization the satellite population, should be designed with special consideration of the high beam loading effect due to the high current beam crossing the cavity. In this work, we report on RF design, analytical beam loading calculations and simulations for the CLIC drive beam injector pre-buncher cavity.

INTRODUCTION

The beam dynamics study of the CLIC drive beam injector shows that the presence of a pre-buncher cavity before the traveling buncher has a great importance in minimization of satellite population [1]. This pre-buncher cavity will be operated at a frequency of 999.5 MHz and zero crossing RF phase. The length and acceleration voltage for this cavity are indicated from beam dynamics optimization to be 50 mm and 60 kV respectively [1]. Since the 5 A electron beam which is crossing this cavity is a periodic bunched beam with a frequency of 499.75 MHz, it will induce an additional voltage in the cavity which is referred to as the beam loading voltage V_b [2]. Therefore, in our cavity we would have two different sources for the total induced cavity voltage (V_c), the external generator (V_g) and the beam loading voltage (V_b). Figure 1 shows the different type of cavity voltages and their superposition in a complex phasor diagram. We supposed that when the beam has arrived in the cavity centre, the generator voltage is out of phase by θ with respect to the beam while the beam loading voltage is out of phase by 180 ° with respect to the beam. From this diagram, we can determine the cavity voltage (V_c) and its phase relative to the beam (φ) as following:

$$V_c e^{i\varphi} = V_g e^{i\theta} + V_b e^{i\pi} \quad (1)$$

For the cavity design itself, it is ideal to have a cavity with coupling factor equal to one and higher values for shunt impedance and quality factor to minimize the input power. However, in presence of beam loading effect, any inappropriate selection for these values can result in very huge beam loading voltage and then higher necessary generator input power. In this work, we first want to calculate analytically the beam loading voltage and then try to find an optimum structure to have minimum necessary input power.

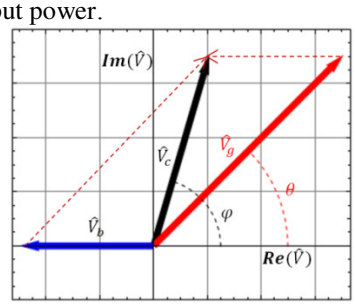


Figure 1: superposition of different cavity voltages in Complex plane as phasors.

BEAM LOADING CALCULATIONS

When a bunch of particles is crossing a cavity, the total bunch energy change is equal to [4]:

$$\Delta\varepsilon_b = q_b V_0 T F_b, \quad (2)$$

where q_b, T, F_b and V_0 are bunch charge, transit time factor, bunch form factor and electric field integral on the cavity axis respectively. To explain the beam loading effect in a simple way, we consider an empty thin lens cavity that is crossed by a beam composed of several identical point like bunches marked with numbers: 1, 2, ... respectively. Since the current has a sinusoidal time dependence with the beam frequency of ω_b, so according to Fourier transformations it can produce several harmonic electromagnetic field components. The n-th harmonic has a frequency of $\omega_n = n\omega_b$ [3]. Only one of these components, which has a very close frequency to the cavity resonant frequency ω_r, can be exited dominantly. To have a steady state in presence of a generator this frequency should be equal to generator frequency ω. Now we suppose at $t = 0$, the first bunch induces a voltage $-v_1$ in the cavity. From this time up to the arriving of the second bunch, the induced voltage inside the cavity ($\hat{V}^{(1)}(t)$) is equal to $-v_1 e^{(i\omega-\frac{1}{\tau_f})t}$. Where τ_f is the cavity filling time [4]. In addition, this bunch can interact with self-induced field and changes its energy by $\Delta\varepsilon^{(1)}$ which is equal to $\frac{1}{2}q_b\Re\{\hat{V}^{(1)}(0)\}$ [2]. Also according to conservation of energy, the electromagnetic energy stored inside the cavity from this

Copyright © 2014 CC-BY-3.0 and by the respective authors

ISBN 978-3-95450-142-7

ELECTROPOLISHING SIMULATION ON FULL SCALE RADIO FREQUENCY ELLIPTICAL STRUCTURES

Leonel Marques Antunes Ferreira, CERN, Geneva, Switzerland
Hannah Rana, Jamie Andrew Shirra, Loughborough University, Leicestershire, England

Abstract

This paper describes a methodology to simulate the electropolishing of a full scale radio frequency (RF) accelerating elliptical cavity through data acquired by means of a rotating disc electrode (RDE) in a three electrode set-up. The method combines laboratorial data from the RDE with computational simulation performed with Comsol Multiphysics® either for the primary and secondary current distribution as well as to account for the local effect of hydrodynamic perturbations. The results are compared with experimental data from the electropolishing of niobium 704 MHz five cell cavity from the Superconducting Proton Linear Accelerator (SPL) R&D project at CERN.

INTRODUCTION

The existing electropolishing installation at CERN is a vertical setup, where cavities are assembled upright whilst the electrolyte is circulating upwards inside them [1].

Previous work on the subject of computationally modelling electropolishing has involved efforts to optimise cathode geometry in an attempt to achieve uniform electropolishing, however this work only took into account primary and secondary current distribution where temperature and bath velocity were assumed constant [2]. Besides geometry optimisation, it allowed defining the minimum potential at which the cavity inner surface is under limiting current condition; for this specific surface finishing, it means that the polishing rate is mainly dependent of the electrolyte velocity and temperature.

The fluid dynamics of the process, however, has not been addressed in the previous work. Being able to study the electrolyte flow, and further, quantify its velocity at specific points inside the cavity would enable optimisation of the electropolishing process; such as the chosen electrolyte inlet flow or the cathode geometry and this to achieve a more uniform material removal all through the cavity surface. Of particular pertinence is the desire to ascertain a correlation between the electrolyte velocity within the cavity and current density value. In order to achieve it, a known electrode geometry has been used to supply the necessary data; the RDE. Under limiting current conditions, the main advantage of the RDE is that the convective-diffusion equation (see Eq. 1) can be solved and its solution is known as the Levich equation (see Eq. 2). This equation gives a direct relationship between electrode angular velocity and current.

$$\frac{\partial C_j}{\partial t} = -D_j \nabla^2 C_j - \nu . \nabla C_j \qquad (1)$$

$$j = 0.62 n F A D_0^{\frac{2}{3}} \omega^{\frac{1}{2}} \nu^{-\frac{1}{6}} C_0^* \qquad (2)$$

METHODOLOGY

The method described hereafter assumes that the entire surface to be processed is under limiting current. It can be resumed to two main steps: fluid dynamics simulation and conversion of electrolyte velocity data from simulation into current density.

Fluid Dynamics Simulation

The fluid dynamics simulation was made through COMSOL Multiphysics®. The used geometry included the cathode defined by the optimisation of primary and secondary current distribution simulation on a five cell cavity and the cavity itself (see Fig. 1). From the fluid dynamics simulation, it was possible to acquire data that defined a boundary layer through the cavity length. This

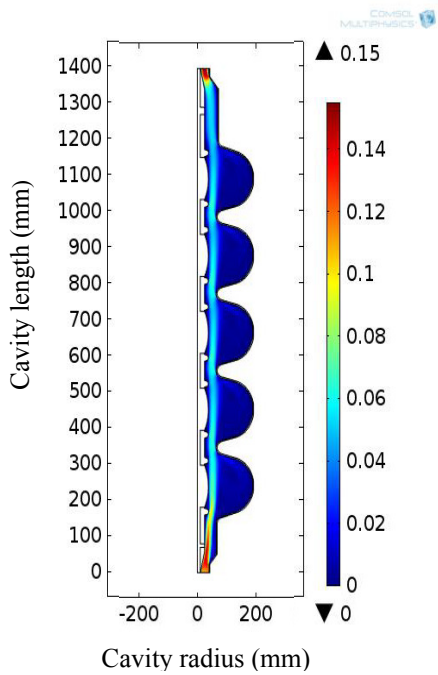


Figure 1: Electrolyte speed (m/s) distribution in an axisymmetric cut of a SPL five cell cavity assembled with its cathode.

Copyright © 2014 CC-BY-3.0 and by the respective authors

ISBN 978-3-95450-142-7

STATUS OF THE DESIGN STUDY FOR 10 MHz POST-ACCELERATED RADIOACTIVE ION BEAMS AT HIE-ISOLDE

M.A. Fraser*†, R. Calaga, CERN, Geneva, Switzerland

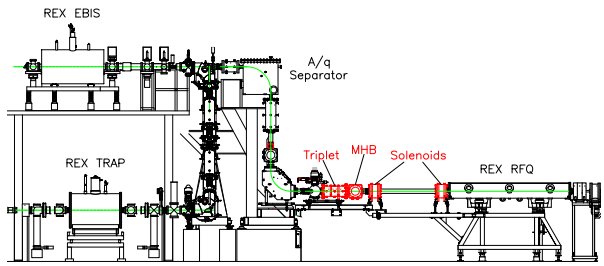
Abstract

A ten-fold increase in the bunch spacing of post-accelerated radioactive ion beams (RIBs) has been requested by several research groups at ISOLDE, CERN in order for experiments to use time-of-flight particle identification and background suppression techniques. It is proposed to bunch externally into the existing REX (Radioactive ion beam EXperiment) RFQ at a sub-harmonic frequency of 10.128 MHz to produce the desired ~ 100 ns bunch separation with minimal loss in transmission. The status of a beam dynamics design study carried out to meet this request will be presented in the framework of the HIE-ISOLDE linac upgrade at CERN.

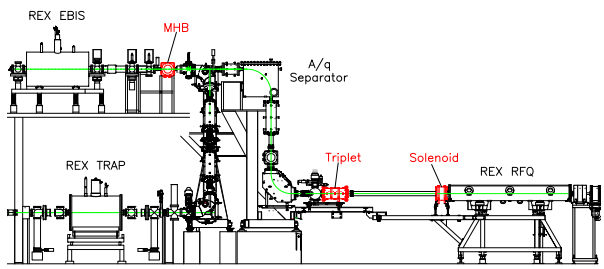
INTRODUCTION

An increased bunch spacing of approximately 100 ns has been requested by several research groups targeting experimental physics at HIE-ISOLDE [1]. It is planned to install a multi-harmonic buncher (MHB) initiating the formation of the longitudinal emittance outside of the RFQ at a sub-harmonic frequency 10 times lower than its 101.28 MHz resonant frequency. This will extend the bunch spacing to 98.7 ns permiting time-of-flight particle identification and background suppression techniques to be used by the experiments. It is foreseen to install the bunching system during the final stage of the HIE-ISOLDE linac upgrade. The layout of the HIE-ISOLDE linac including the bunching and chopping system is shown schematically in Figure 2; more information about the project can be found in [2–4]. The MHB system can be switched off with no impact on the delivery of 101.28 MHz beams.

For low-current applications where space-charge forces are not important, a discrete buncher located either internally or externally to an RFQ accelerator can be used to reduce both the length of the RFQ and the longitudinal emittance [5]. Several nuclear physics accelerator laboratories have employed this design approach, e.g. ANL with the ATLAS upgrade RFQ [6] and TRIUMF with the ISAC RFQ [7]. In most cases the RFQ electrodes are designed without an adiabatic bunching section and an external MHB is placed upstream of the RFQ. In our case we plan to retrofit an existing RFQ that already has electrodes with an adiabatic bunching section. The chosen 10.128 MHz fundamental MHB frequency is similar to the frequencies of both the ANL and TRIUMF systems but the ratio between the RFQ and MHB frequencies is much larger: at HIE-ISOLDE the ratio is a factor of 10, compared to factors of 5 and 3 for the other systems, respectively. The two different layout options being considered are shown in Figure 1.



(a) A: MHB placed after the REX A/q-separator



(b) B: MHB placed before the REX A/q-separator

Figure 1: Pre-buncher layout options: new components highlighted in red.

PRE-RFQ BUNCHING

A single-gap, grid-less MHB similar to those employed at ANL and TRIUMF was studied to avoid the transmission losses (~ 20 %) associated with gridded bunchers that are unacceptable for the acceleration of rare RIBs. More details on the optimisation of the MHB electrode geometry can be found in [8]. The feasibility of the MHB-RFQ bunching system at HIE-ISOLDE has been validated with an MHB mixing the first four harmonics of 10.128 MHz. The transmission and rms longitudinal emittance is shown in Figure 3 as a function of the upstream distance (L) of the MHB and the effective voltage (V_0) of its first harmonic. The iso-contour lines of transmission in Figure 3a indicate that the optimum focal point of the buncher is located 29 cm inside the RFQ at the position on the electrodes where the adiabatic bunching section starts. The longitudinal emittance delivered by the RFQ can be significantly reduced as the drift distance between the RFQ and MHB is increased. Transmissions of up to ~ 80 % can be expected with ~ 15 % of the beam spilling out of the main bunch and populating the nine 101.28 MHz satellite bunches, see Figure 4. In

* The author acknowledges co-funding by the European Commission as a Marie Curie action (Grant agreement PCOFUND-GA-2010-267194) within the Seventh Framework Programme for Research and Technological Development.

† mfraser@cern.ch

Copyright © 2014 CC-BY-3.0 and by the respective authors

PLANS FOR AN ERL TEST FACILITY AT CERN

E. Jensen, O. Brüning, R. Calaga, K. Schirm, R. Torres-Sanchez, A. Valloni (CERN),
K. Aulenbacher (U Mainz), A. Bogacz, A. Hutton (JLAB), M. Klein (U Liverpool)

Abstract

The baseline electron accelerator for LHeC and one option for FCC-he is an Energy Recovery Linac. To prepare and study the necessary key technologies, CERN has started – in collaboration with JLAB and Mainz University – the conceptual design of an ERL Test Facility (ERL-TF). Staged construction will allow the study under different conditions with up to 3 passes, beam energies of up to about 1 GeV and currents of up to 50 mA. The design and development of superconducting cavity modules, including coupler and HOM damper designs, are also of central importance for other existing and future accelerators and their tests are at the heart of the current ERL-TF goals. However, the ERL-TF could also provide a unique infrastructure for several applications that go beyond developing and testing the ERL technology at CERN. In addition to experimental studies of beam dynamics, operational and reliability issues in an ERL, it could equally serve for quench tests of superconducting magnets, as physics experimental facility on its own right or as test stand for detector developments. This contribution will describe the goals and the concept of the facility and the status of the R&D.

INTRODUCTION

Coupled to a vigorous R&D program on high-field magnets and high-gradient accelerating structures, CERN has started Design Studies to prepare the technologies that will be in demand for a future "ambitious post-LHC accelerator project"[1]. Since normal-conducting RF is limited to pulsed operation at high gradients, superconducting RF (SRF) clearly is a key technology for future large particle accelerators.

SRF has made remarkable progress over the last decades, notably towards the ILC, but recently interesting new ideas indicate further potential (nitrogen doping, Nb_3Sn coating …). R&D to fully exploit this potential requires facilities to fabricate and test prototypes, ultimately probing also the interaction with a particle beam. The planned ERL-TF could serve this purpose.

The Large Hadron electron Collider (LHeC) is a proposed electron proton collider that uses one of the LHC 7 TeV proton beams and collides it with a 60 GeV electron beam [2]. The LHeC may potentially be an interesting intermediate project for bridging the transition from the LHC and HL-LHC era to a future 'ambitious post LHC accelerator project', allowing for interesting complementary physics including DIS to probe the inner structure of protons and Higgs production via vector boson fusion, and would in particular fully develop the interesting technology of ERLs at large. At the same time, it employs the same SRF technology that takes centre stage of the R&D program for an "ambitious post-LHC accelerator project" and could eventually even serve as a lepton pre-injector for a post-LHC machine.

GOALS OF THE ERL-TF

Test Facility for SRF Cavities and Cryomodules

As mandated by the European Strategy, CERN has started strengthening its know-how, facilities and competencies in SRF technology. This will be needed to maintain the existing LHC systems (401 MHz), to upgrade it to HL-LHC (401 MHz crab cavities and 802 MHz harmonic system study), to design, fabricate and operate new SRF systems (e.g. HIE-ISOLDE at 101 MHz) and to further develop the technology for future applications. One of these R&D directions concerns the SPL and ESS. In this framework short 704 MHz, 4-cavity cryomodules with 5-cell cavities were designed and built – they are presently under test. Another direction is the initial design phase for the FCC [3], for which again 401 MHz and 802 MHz systems are considered. Primarily for reasons of compatibility with LHC, HL-LHC and FCC, the LHeC study has opted for the same frequency, 802 MHz.

For most of these projects and studies, the proposed ERL-TF would serve as training ground for scientists, engineers and technicians; it would have relevant parameters, including the possibility to study operational aspects with full power and beam interaction, but without perturbing the important physics exploitation of the LHC and its injector chain. Under conditions described below, the facility may be reconfigured to test cavities/cryomodules at other frequencies, notably 704.4 MHz (SPL, ESS) and 1,300 MHz (ILC, European XFEL).

Study of a High-Energy, Multi-Pass ERL

Another important goal of the proposed ERL-TF is to study fundamental questions in the behaviour of an ERL itself. Important beam dynamics aspects will require experimental verification simultaneous acceleration and deceleration, acceptable spent beam quality or the limits of energy recovery, just to name a few.

Study Injector and Electron Gun

An important part of the study is the injector and the electron gun, which should provide 350 pC bunches at a rate of 36 MHz. The preferred option would be a photo injector, but other options are currently also considered. A booster would accelerate the electron beam to at least 5 MeV (66 kW beam power) – ongoing simulations will indicate whether this energy has to be increased to better cope with space charge effects. Note that the frequency is

Copyright © 2014 CC-BY-3.0 and by the respective authors

ISBN 978-3-95450-142-7

MAGNETIC CHARACTERIZATION OF FAST-PULSED QUADRUPOLE MAGNETS FOR LINAC4

M. Buzio, S. Kasaei*, O. Crettiez, L. Fiscarelli, V. Della Selva,
J. Garcia Perez, J. B. Lallement, CERN, Geneva, Switzerland

Abstract

Linac4, currently being built at CERN, includes 24 quadrupole magnets characterized by narrow apertures and fast excitation cycles which make accurate magnetic measurements challenging. This paper describes the method used for the measurement, which is a combination of techniques based on stretched wire, rotating and fixed search coils. We show how these different instruments can be used in a complementary way to derive information on different aspects of the magnetic behaviour, such as the impact of hysteresis and dynamic eddy current effects. We summarize the results of the series measurement campaign, which include field strength, harmonic components, and the offset and orientation of the magnetic axis. Finally, we discuss the relevance of these measurements as their impact to the operation of the linac.

INTRODUCTION

This paper is mainly concerned with a series of 24 electromagnetic quadrupoles (EMQ), currently being installed in the inter-tank regions of Linac4 at CERN (see Fig. 1 and Table 1) [1, 2]. Due to their small size these magnets must be air-cooled, which entails cycling with fast ~5 ms pulses. The combination of a small aperture and possible large dynamic effects due to eddy currents and iron hysteresis makes the measurement a challenge. In the following, we discuss the measurement method and the main results obtained. More details are given in [3].

Table 1: Main Intertank EMQ Parameters

Parameter	Value
Aperture ∅ (mm)	54
Good Field Region ∅ (mm)	36
Nominal peak current (A)	67.4
Nominal integrated gradient (T)	1.83
Integrated gradient tolerance	±0.5%
Stable flat-top duration (μs)	400
Harmonic error tolerance ($\|c_n\|$, n=3 to 10)	1%
Axis offset radial tolerance (mm)	0.1
Roll angle tolerance (mrad)	1
Yaw and pitch tolerance (mrad)	2

* samira.kasaei@cern.ch, also with IPM, Institute for Research in Fundamental Sciences. Tehran

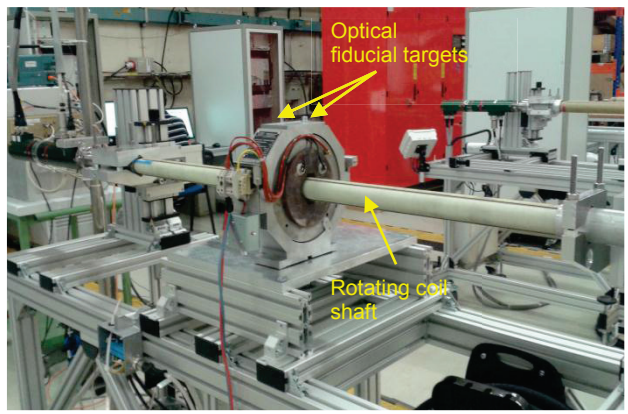


Figure 1: An EMQ on the rotating coil bench.

MEASUREMENT SETUP

Since no single instrument is available at CERN to measure all field parameters, we combined different measurement techniques. We used primarily a single stretched wire (SSW) system [4] as our established reference, together with a LEICA laser tracker LTD500, for magnetic axis fiducialization and integral field strength of the whole series in AC excitation mode at 12 A. A rotating coil system [5], more accurate but more resource-intensive, was used on a few sample units to check harmonic field content in nominal (dynamic) conditions and at 20 A DC, that is the maximum allowable for short periods. The coil shaft was kept fixed to measure dynamic effects with a fast National Instruments 6366 USB DAQ and to check the correlation with SSW in AC mode. Finally, a so-called AC mole [6] was used to measure the pitch and yaw angles. Nominal excitation was achieved using a CERN-developed prototype MAXIDISCAP capacitive discharge power supply [7].

EDDY CURRENT EFFECTS

The very high peak $\dot{B} \approx 300$ T/s in the iron yoke might give rise to substantial eddy current effects, in spite of the 0.5 mm thin laminations. These effects have been measured as explained in [8] by means of a fixed integral coil. The results are given in Fig. 2, which shows the profiles of the excitation current and of the integrated gradient, scaled to coincide at the end of the flat-top. The gradient has been corrected for integrator drift due to input voltage offset. Their difference ΔI, which is representative of the non-linearities, shows clearly an

Copyright © 2014 CC-BY-3.0 and by the respective authors

ISBN 978-3-95450-142-7

LINAC4 TRANSVERSE AND LONGITUDINAL EMITTANCE RECONSTRUCTION IN THE PRESENCE OF SPACE CHARGE

J.B. Lallement, G. Bellodi, V.A. Dimov, A.M. Lombardi, M. Yarmohammadi Satri*,
CERN, Geneva, Switzerland

Abstract

Linac4 is a pulsed, normal-conducting 160 MeV H^- linear accelerator presently under construction at CERN. It will replace the present 50 MeV Linac2 as injector of the proton accelerator complex as part of a project to increase the LHC luminosity. The 3 MeV front end, composed of a 45 keV ion source, a Low Energy Beam transport (LEBT), a 352 MHz Radio Frequency Quadrupole (RFQ) at 3 MeV and Medium Energy Beam Transport (MEBT) housing a beam chopper, and the first Drift Tube Linac (DTL) tank at 12 MeV have been commissioned during the first half of 2014. The transverse and longitudinal emittance reconstruction technique in the presence of space charge, which will be used for the next commissioning stages and permanently during the Linac operation, was successfully tested and validated. The reconstruction method and the results obtained at 3 and 12 MeV are presented in this paper.

INTRODUCTION

The Linac4 commissioning started in 2012 at a dedicated test stand [1] where the 3 MeV front-end was installed before it was moved to its final location, inside the Linac4 tunnel, and re-commissioned during the period October 2013 – March 2014. The first tank of the DTL, which accelerates the H^- ions beam to 12 MeV, is now being commissioned. Commissioning stages at the energies of 50, 100 and 160MeV will progressively follow.

Temporary measurement benches will be installed after each stage. Two different benches are foreseen: one for the low energy stages (3, 12 MeV) and another for the higher energies (50, 100 MeV). The low energy bench, see Fig.1, houses a slit-and-grid emittance measurement device, a Bunch Shape Monitor (BSM) [2] and a spectrometer magnet. The high energy bench, Fig.2, houses 2 quadrupoles, a BSM, 2 Beam Phase Monitors (BPM) and 3 profile monitors (3 horizontal and 3 vertical Secondary Emission Monitors Grids). The high energy bench comprises neither a spectrometer magnet nor a direct emittance measurement device for the sake of compactness. Cross-checks between direct and indirect methods are foreseen at the low energy bench in order to validate the design of the high energy bench. In particular the cross-checks of the direct and indirect method to obtain the transverse and longitudinal emittance of the beam are the main subject of this paper.

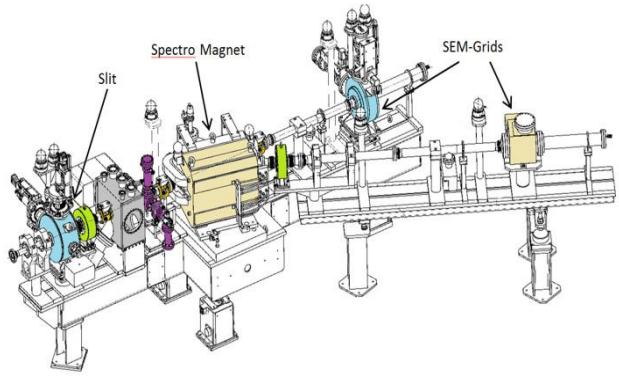


Figure 1: The low energy diagnostic bench.

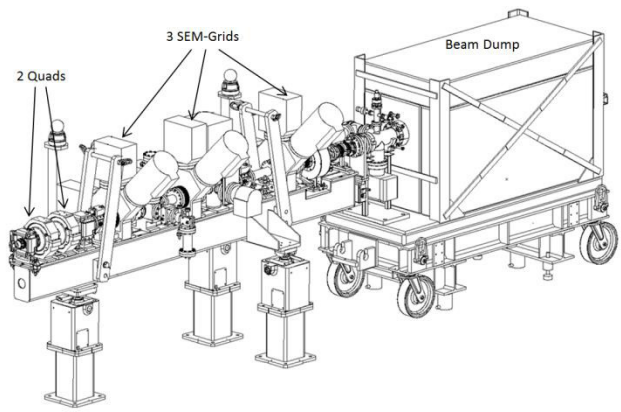


Figure 2: The high energy diagnostic bench.

THE FORWARD METHOD

The forward method is a technique which aims at reconstructing the emittance of a particle beam from profile measurements in presence of space charge [3]. It can be used both in the transverse and the longitudinal planes. For sake of clarity we will explain in detail the case of transverse emittance reconstruction.

The forward method consists of two steps as it combines a classical reconstruction technique [4] and an iterative process based on multiparticle code simulations.

In the first step, the beam size is measured at different locations with profile monitors, at least three, ideally separated with drift spaces with no focusing element in between. The beam size can also be measured on a single profile monitor with three different settings of an upstream quadrupole with well known transfer function. The transport matrices from the reconstruction point (quadrupole for the three-gradient method, first profile monitor for the three profiles method) to the profile monitor(s) being known, the emittance ε, and the Twiss

* Home institute : IPM, Teheran, Iran

Copyright © 2014 CC-BY-3.0 and by the respective authors

ISBN 978-3-95450-142-7

TOOLBOX FOR APPLYING BEAM-BASED ALIGNMENT TO LINACS

A. Latina, D. Pellegrini, J. Pfingstner, D. Schulte, CERN, Geneva
E. Adli, University of Oslo, Oslo

MOTIVATION

The performance of future linear colliders such as CLIC or ILC [1, 2] will depend critically on beam-based alignment (BBA) techniques and feedback systems, which will play a crucial role in transporting the beams through the linacs of such machines with minimal emittance growth. The complexity of such techniques is dramatically magnified by the number of correctors and monitors involved in the calculations, where figures go easily beyond the thousands. With such large numbers of parameters, corrections techniques based on human intervention and operators' touch, are not a viable option.

Powerful sets of automatic beam-based alignment techniques have been studied during the last years, and their effectiveness has been accurately assessed with computer simulations. In recent times, the authors of this paper have performed consistent and extensive experimental tests of BBA on real linacs. The main objectives of these tests were at least two: 1) trying to address the effectiveness of such techniques in real operational environments, and 2) trying to establish how far one can go with an automatic application of such procedures, aiming at requiring minimal human intervention.

Tests of BBA have been performed at the FACET linac at SLAC [3], and at Fermi@Elettra in Trieste [4]. The results in terms of emittance preservation have been very promising, as it has been documented elsewhere [5]. To enhance the automatisation potential and simplify the operational procedures, powerful tools have been developed and equipped with a graphical user interface (GUI). The GUI allows the user to access all the parameters that control the beam-steering procedures.

Using these tools, it is possible to apply orbit, dispersion, and wakefield correction, separately or simultaneously, while tracking the response matrices, monitoring the relevant observables, and recording on disk the results for post-processing the data. These tools have been used and consolidated in real experiments, and allowed to span a significant fraction of the large parameters space. These tools as well as some of the experimental results are presented in this paper.

INTRODUCTION

Beam-based alignment algorithms have been designed to ensure beam transmission with minimal emittance growth in linacs. Two such techniques are Dispersion-Free Steering (DFS) and Wakefield-Free Steering (WFS), which optimise the trajectory and simultaneously minimise the residual dispersion and wakefields. Details on the DFS and WFS procedures can be found in [5, 6], where it is shown that the combined application of dispersion and wakefield correction can be computed using the following system of equations:

$$\begin{pmatrix} & \mathbf{b} \\ \omega_d & (\boldsymbol{\eta}-\boldsymbol{\eta_0}) \\ \omega_w & (\mathbf{b}_w-\mathbf{b}) \\ & \mathbf{0} \end{pmatrix} = \begin{pmatrix} & \mathbf{R} \\ \omega_d & \mathbf{D} \\ \omega_w & \mathbf{W} \\ \beta & \mathbf{I} \end{pmatrix} \boldsymbol{\theta}.$$

In this equation $\mathbf{R}$, $\mathbf{D}$ and $\mathbf{W}$ are respectively the orbit, the dispersion and the wakefield response matrices; $\mathbf{I}$ is the identity matrix; and $\boldsymbol{\theta}$ is the vector of correctors, i.e. the *unknowns* of the system. On the left-hand side $\mathbf{b}$, $\mathbf{b}_w$, $\boldsymbol{\eta}$, and $\boldsymbol{\eta_0}$ are the observables: $\mathbf{b}$ is the vector of BPM readings for the beam in nominal conditions; $\mathbf{b}_w$ is the vector of BPM readings for the WFS test-beam with different charge; $\boldsymbol{\eta}$ and $\boldsymbol{\eta_0}$ are respectively the measured and the target dispersion for the DFS. These quantities must be measured at each step of correction. The other parameters are: ω_d is a weighting factor for the dispersion correction, ω_w is a weighting factor for the wakefield correction, β is a regulatory parameter to condition the system. In theory, the weighting factors ω can be estimated using the formula:

$$\omega_{d,w}^2 = \frac{\sigma^2_{\text{bpm offset}} + \sigma^2_{\text{bpm precision}}}{2\sigma^2_{\text{bpm precision}}},$$

as given in [7]; in practice an empirical fine tuning of these parameters is needed to achieve best performance.

The solution to this system of equations can be found using a least-square method. One may rewrite the system as

$$\mathbf{A}\Delta x = \theta,$$

where $\mathbf{A}$ represents the response matrices, and Δx represents the difference between the measured observables and their target values, the solution is the set of correctors θ that minimises:

$$\|\mathbf{A}\Delta x - g\,\theta\|$$

where g is the correction gain.

The matrices $\mathbf{R}$, $\mathbf{D}$ and $\mathbf{W}$ need to be measured experimentally, using a System-Identification Algorithm as described in [8], prior to the BBA correction. The application of the BBA correction occurs at a later moment, and is subject to the values of the free parameters. Two MATLAB tools have been created to control these two phases of the correction procedure: the first is called SysID, and the second BBA.

Copyright © 2014 CC-BY-3.0 and by the respective authors

DECELERATION MEASUREMENTS OF AN ELECTRON BEAM IN THE CLIC TEST FACILITY 3

R. L. Lillestøl* and S. Döbert, CERN, Geneva, Switzerland,
E. Adli, University of Oslo, Norway

Abstract

The Test Beam Line at the CLIC Test Facility 3 at CERN is a proof-of-principle of the future CLIC decelerators, which will extract a large amount of beam energy for acceleration of the main CLIC beams. The current beamline consists of a FODO lattice with 13 Power Extraction and Transfer Structures (PETS). We discuss beam deceleration measurements of up to 37 %, taking into account effects from the bunch length and the bunch phase. The 12 GHz phase is reproduced based on measurements in a PETS with an uncombined beam. The spectrometer measurements are also compared to predictions based on the beam current and on the produced rf power in the PETS, as well as particle tracking simulations with the Placet code.

INTRODUCTION

In the Compact Linear Collider (CLIC) design, in order to reach efficient acceleration of the main beam the acceleration energy is extracted from a low-energy, high-current drive beam [1]. The energy will be extracted in 24 decelerator sectors which are 1 km long, and which consist of FODO lattices with Power Extraction and Transfer Structures (PETS). 90 % of the beam energy will be extracted and converted to 12 GHz power, and it is vital to understand the dynamics of the strongly decelerated drive beam.

At CERN, the CLIC Test Facility 3 (CTF3) was built to verify key concepts of the CLIC two-beam scheme [2]. The facility is essentially a small drive beam complex, where the electron beam is interleaved by up to a factor 8, in order to produce the low-energy, high-current beam needed by the experiments. One of the main experiments in the facility is the Test Beam Line (TBL), which is the first prototype decelerator. Here, the ~120 MeV electron drive beam is decelerated through a line of PETS, and the produced rf power is measured and dissipated in loads.

Most of the previously reported results have been produced with a beam current of up to 14 A [3]. In this paper, however, we discuss data taken with the full bunch combination scheme of the CTF3, that allowed a beam current of 21 A delivered to the TBL. This dataset includes 88 consecutive bunch trains.

EXPERIMENTAL SETUP

Being a prototype decelerator, the TBL consists of a FODO lattice with PETS in between the quadrupoles. The lattice of the beamline is shown in Figure 1. Currently 13 PETS are installed in the beamline, and at nominal conditions each of these can produce 135 MW of 12 GHz power. The power amplitude is measured with Schottky diodes. In addition, one PETS is also measured with IQ demodulators, which provide information about the rf phase. As will be seen later, phase information is important in order to fully understand the power production and beam deceleration. The produced power is attenuated by a total of around 90 dB before entering the measurement electronics, and the attenuation chain must be calibrated piecewise. This leads to a large systematic error on the absolute power measurement, which is estimated to a maximum of 0.8 dB (20 %).

The quadrupoles in the FODO lattice are mounted on precision movers made by CIEMAT [4], that allow efficient steering and the use of beam-based alignment routines. The bunch trajectory is measured by inductive pickup wall-current monitor BPMs, and these are also used for beam current diagnostics. The BPMs were designed and constructed by IFIC and UPC [5], and have a resolution of 5 µm. A novel segmented dump spectrometer at the end of the beamline provides time-resolved, single-shot energy measurements with a precision of 1 % [6]. The spectrometer at the beginning of the beamline is of a simpler type and contains a single slit. Optical Transition Radiation (OTR) screens are used for measuring the transverse beam distribution.

HIGH RF POWER PRODUCTION

The rf power produced in a PETS scales as [7]

$$P \propto I^2 F^2 \{\lambda(z)\}, \tag{1}$$

where I is the beam current and $F\{\lambda(z)\}$ is the charge distribution form factor. When the charge distributions of the individual bunches are equal and Gaussian, and relatively short compared to the bunch separation [3], we can write $F\{\lambda(z)\} = F_\mathrm{b}(\sigma_z)\,\Phi(\{\phi_n\})$. Here $F_\mathrm{b}(\sigma_z)$ is the single-bunch form factor, dependent on the bunch length σ_z, and $\Phi(\{\phi_n\})$ is the multi-bunch form factor,

$$\Phi(\{\phi_n\}) = \frac{1}{N_\mathrm{b}} \sum_{n=1}^{N_\mathrm{b}} e^{i\phi_n}, \tag{2}$$

where N_b is the number of bunches that contribute to the field build-up in a PETS (37 in the case of the TBL), and ϕ_n is the phase of each bunch.

When the bunch phase is constant, as it should be in CLIC, $\Phi(\{\phi_n\})$ evaluates to one. In the CTF3, however, the bunch phase changes over the bunch train due to the injector setup. This leads to a multi-bunch form factor less than one, and consequently a reduced power production and energy extraction. The calculated value along the bunch train for the

* reidar.lunde.lillestol@cern.ch

Copyright © 2014 CC-BY-3.0 and by the respective authors

ISBN 978-3-95450-142-7

CERN LINAC4 DRIFT TUBE LINAC MANUFACTURING AND ASSEMBLY

S. Ramberger*, P. Bourquin, A. Cherif, Y. Cuvet, A. Dallocchio, G. Favre, J.-F. Fuchs, J.-M. Geisser, F. Gerigk, J.-M. Giguet, J. Hansen, M. Polini, S. Sgobba, N. Thaus, M. Vretenar, CERN, Geneva, Switzerland

Abstract

The manufacturing of the Linac4 Drift Tube Linac (DTL) components has been completed and the assembly of the structures is in its final stages. 3 tanks of 3.9 m, 7.3 m, and 7.3 m, designed to accelerate a 40 mA average pulse current H^--beam from 3 to 50 MeV, are being assembled from 2, 4 and 4 segments of about 2.0 m length, containing each from 22 drift tubes at the low energy end, down to only 6 at the high energy end. Due to its peculiar design avoiding adjustment mechanisms on the drift tube, tight tolerances have to be maintained in the production. This paper discusses the assembly stages that are used to achieve the tolerances over the full length of the structures. Metrology results on the assembled DTL Tank1 confirm the required precision.

INTRODUCTION

The mechanical design of the DTL has been undertaken with reliability and ease of assembly in mind from the beginning. A list of basic design decisions lead to a straightforward design that is implemented with the required quality assurance procedures in order to make sure that the final RF, vacuum and beam parameters can be achieved. All parts have been followed in production with metrology verifications so that the required positioning tolerances of drift tubes and their permanent magnet quadrupoles (PMQs) are obtained in the completed assembly, and that the quality of inner surfaces and interfaces provide the required vacuum and RF environment.

The manufacturing of the main Linac4 DTL components has been completed and assembly is currently on-going in the CERN workshops (Fig. 1). The first DTL tank has been completed and installed in the Linac4 tunnel, and it has successfully undergone first beam tests. Each of the four segments of Tank3 has been assembled individually and they are currently being assembled together.

Table 1: Linac4 DTL Mechanical Design Parameters

Parameter	Tank 1 / 2 / 3
Drift tubes per tank	38 / 41 / 29
Number of segments	2 / 4 / 4
Length of tank	3.90 / 7.34 / 7.25 m
Tuners per tank	12 / 20 / 17
Post-couplers per tank	12 / 20 / 29

MECHANICAL DTL DESIGN

The main body is made of self-supporting 304L stainless steel cylinders of 50 mm thickness doing away with any additional tank reinforcement. The material thickness is sufficient for integrating cooling channels, flanges and inter-segment interfaces without the need for welding except for the RF ports; this choice keeps deformation of the tank segments to a minimum. A maximum length of 2 m was chosen in order to facilitate the procurement of the raw material, to allow manufacturing with standard industrial equipment, and to ease the assembly with drift tubes.

Girders have been designed in EN AW-5083 aluminium to follow the shape of the tank segments. They are aligned by a groove in the tank segment providing precise vertical and lateral positioning. Their main purpose is to position drift tubes precisely along the tank. Drift tubes have been designed without the requirement for wires descending the stem as beam instrumentation and steering magnets are in areas on the beam adjacent to the tanks. PMQs in vacuum are used as focusing elements in the drift tubes. Before installation their outgassing rate is checked. Precise manufacturing of drift tubes is reported in [1].

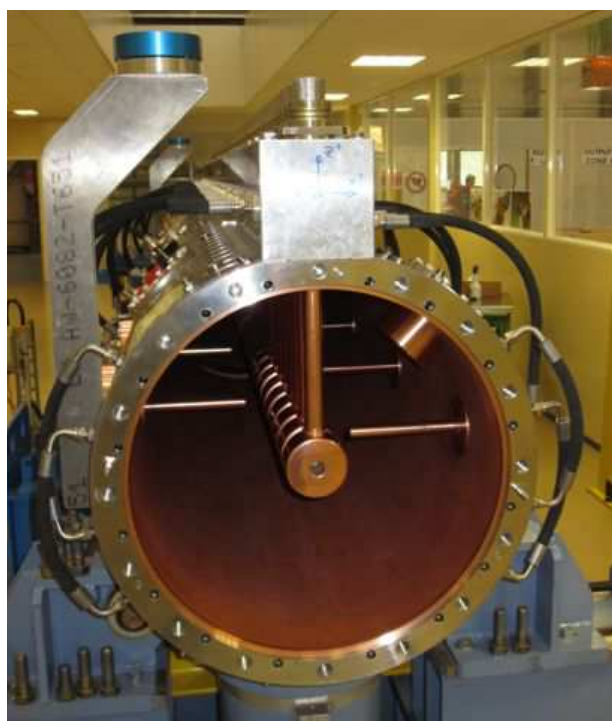


Figure 1: DTL Tank1 assembled.

* Suitbert.Ramberger@cern.ch

ISBN 978-3-95450-142-7

Copyright © 2014 CC-BY-3.0 and by the respective authors

COMMISSIONING AND OPERATIONAL EXPERIENCE GAINED WITH THE LINAC4 RFQ AT CERN

C. Rossi, L. Arnaudon, P. Baudrenghien, G. Bellodi, O. Brunner, J. Hansen, J.B. Lallement, A.M. Lombardi, J. Noirjean, CERN, Geneva, Switzerland
M. Desmons, A. France, O. Piquet, CEA, Gif-sur-Yvette, France

Abstract

The installation of Linac4 has started in 2013 with the 3 MeV Front End, aiming at delivering a fully commissioned 160 MeV H^- beam by 2016. During summer 2013, a first prototype version of the H^- ion source and the Low Energy Beam Transport lines have been installed in the Linac4 tunnel followed shortly by the Radiofrequency Quadrupole accelerator (RFQ), operating at the RF frequency of 352.2 MHz, which accelerates the ion beam to the energy of 3 MeV. The RFQ, which had already been commissioned at the 3 MeV Test Stand, was this time driven by a fully digital LLRF system. This paper reports the result of the bead-pull field check performed after the installation in the tunnel, the experience gained during recommissioning and the results of field characterization as a function of the water temperature in the RFQ cooling channels, showing how the accelerating field can be adjusted by simply tuning the different cavity modules.

INTRODUCTION

After the successful commissioning and operation at the 3 MeV Test Stand between February and June 2013 [1], the Linac4 RFQ was moved to its final position in the Linac4 tunnel (Figure 1) where bead-pull measurements were repeated before the start of operation.

This time the RFQ was driven by a completely new and fully digital LLRF system and integrated in the control environment of the Linac4.

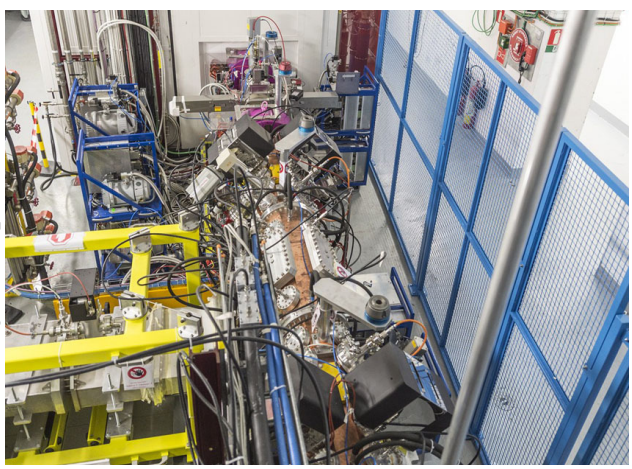


Figure 1: The Linac4 RFQ in the Linac4 tunnel.

The tunnel set up included a prototype ion source, a Low Energy Beam Transport line (LEBT), the RFQ and a Medium Energy Beam Transport followed by a temporary diagnostics bench. The source produced about 20 mA of H^- beam at 45 keV, with an emittance exceeding the RFQ acceptance. A transmission of 75% through the RFQ is expected with this source.

The RFQ operational parameters and the measured characteristics of the beam during the commissioning phase in the Linac4 tunnel are summarized in Table 1.

Table 1: RFQ and Beam Parameters at 3 MeV

Parameter	Value	Unit
Operating frequency	352.2	MHz
Total dissipated RF Power (with beam)	430	kW
Beam current	13	mA
Beam pulse length	400	μsec
Beam energy (input)	45	keV
Beam energy (output)	3	MeV
Beam transmission with present source emittance	75	%

Due to the large emittance of the beam from the source prototype, which exceeds the RFQ design acceptance, the measured transmission is poor; however it is coherent with the results from the simulations.

The installation of the ion source in its final version should bring the transmission of the RFQ to the design value of 95%.

RFQ RECOMMISSIONING AND BEAM TESTS

After the successful commissioning of the 3 MeV Front End at the dedicated Test Stand, the RFQ was moved to its final position in the Linac4 tunnel at the end of June 2013 (Figure 2).

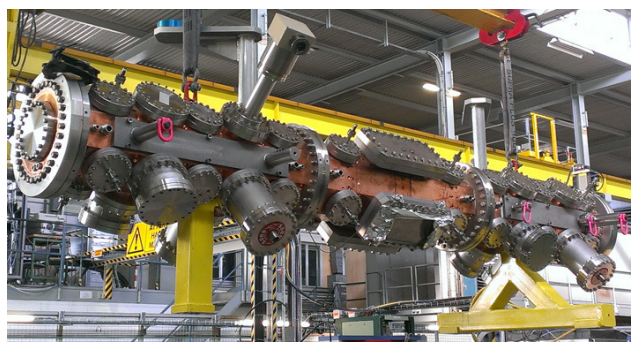


Figure 2: The Linac4 RFQ being moved from the 3 MeV Test Stand to the Linac4 tunnel.

Copyright © 2014 CC-BY-3.0 and by the respective authors

ISBN 978-3-95450-142-7

THE DRIFT TUBE WELDING ASSEMBLY FOR THE LINAC4 DRIFT TUBE LINAC AT CERN

I. Sexton, A. Cherif, Y. Cuvet, G. Favre, J-M. Geisser, F. Mirapeix (DMP, Spain),
S. Ramberger, S. Sgobba, T. Tardy,
CERN, Geneva, Switzerland

Abstract

The fabrication of the Linac4 Drift Tube Linac (DTL) required the welding assembly of 108 drift tubes (DT) which has been undertaken at the CERN workshop. The design of the DTL is particular in that it was purposely simplified to avoid any position adjustment mechanism for drift tubes in the tank. In consequence, drift tubes have been designed with tight tolerances and parts have been assembled with an optimised welding procedure. Two re-machining stages have been introduced in order to compensate for welding distortions. This paper discusses the various assembly stages with a view on the final precision that has been achieved.

INTRODUCTION

The Drift Tube Linac [1] for the new linear accelerator Linac4 at CERN will accelerate H^- ions of up to 40 mA average pulse current from 3 to 50 MeV. It is designed to operate at 352.2 MHz and at duty cycles of up to 10 %. Permanent magnet quadrupoles (PMQs) are used as focusing elements. The three DTL cavities are equipped with 38, 41 and 29 copper DTs respectively (see Fig. 1). The design aims at reducing the complexity of the mechanical structure doing away with adjustment mechanisms like screws or bellows for drift tube positioning [2]. In consequence, DTs have been designed with tight overall tolerances in the order of 100 µm. The Electron Beam Welding (EBW) technology has been chosen to minimise welding distortion and limit heat input that could damage the PMQ. The duration of the project starting from R&D to the end of the assembly stage was eight years (2005 to 2013).

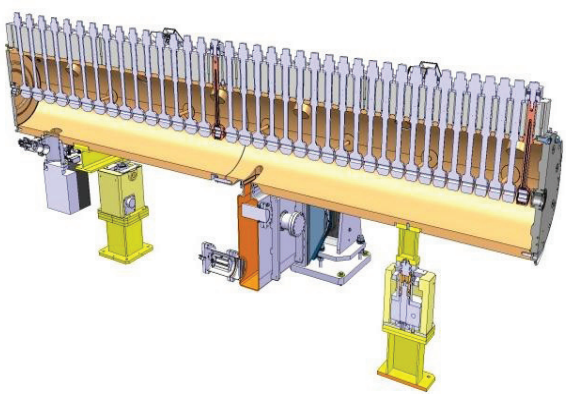


Figure 1: View of a DTL tank equipped with 38 DTs.

MATERIAL

High quality 3D forged OFE copper (99.99 % min. Cu) in half-hard temper was used, having a fine (max. 90 µm) and homogeneous grain size, low content of oxygen (5 ppm) and specific limits in ppm for sixteen additional elements. The main benefits are improved weldability, better mechanical stability, and increased yield strength allowed by the half-hard temper. Ready weldability by EBW was proven. Welding tests were performed with 3D forged OFE copper conform to ISO standard 13919-2, level B, with limited risk of porosity inducing so-called virtual leaks for the vacuum system.

The raw material (multidirectional forged and for some components finished by ring rolling) complies with the stringent requirements of CERN specifications in terms of composition, microstructure, tensile properties, hardness and ultrasonic examination criteria. The ultrasonic (frequency 4 MHz) testing procedure and acceptance criteria, which include a stringent requirement imposing a maximum acceptable loss in ultrasonic back wall echo equal to 20 % screen height, allow a fine and homogeneous microstructure to be indirectly guaranteed on all supplied forgings.

MANUFACTURING OF COMPONENTS

Nearly 1000 components are required to manufacture 108 DTs. Each DT is unique and is assembled using nine components (see Fig. 2) with four EB welds.

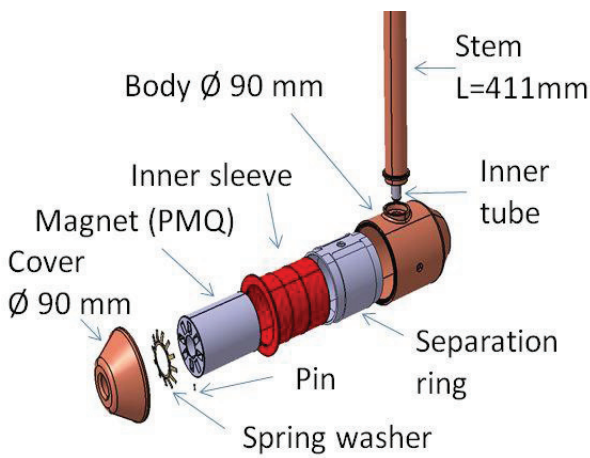


Figure 2: View of the DT's nine components.

Copyright © 2014 CC-BY-3.0 and by the respective authors

ISBN 978-3-95450-142-7

ELECTRON BEAM WELDING AND VACUUM BRAZING CHARACTERIZATION FOR SRF CAVITIES

N. Valverde Alonso, S. Atieh, I. Aviles Santillana, S. Calatroni, O. Capatina, L. Ferreira, F. Pillon, M. Redondas Monteserín, T. Renaglia, K. Schirm, T. Tardy, A. Vacca, CERN, Geneva, Switzerland

Abstract

In the framework of the SPL R&D effort at CERN, development design efforts study the joining of dissimilar metals: bulk niobium for the superconducting RF cavities and stainless steel (316LN) or titanium alloys (Ti-6Al-4V and Nb55Ti) for the cryostats. Joining techniques of electron beam welding (EBW) and vacuum brazing are particularly important for these applications. These processes have been used in the accelerator community and developed into generally accepted "best practice". Studies were performed to update the existing knowledge, and comprehensively characterise these joints via mechanical and metallurgical investigations using modern available technologies. The developed solutions are described in detail, some currently being applied uniquely at CERN.

INTRODUCTION

One of the main objectives of the SPL R&D effort at CERN is to develop 704 MHz bulk niobium β=1 elliptical cavities operating at 2 K with an accelerating gradient of 25 MV/m and to test a string of four cavities in a cryo-module [1]. The 5-cell cavities are made up of bulk niobium (RRR>300) and are equipped with SS flanges. The half-cells are shaped by spinning and assembled together with the cut-off tubes via EB welding.

VACUUM BRAZING

Stainless steel (316LN) Conflat flanges are joined to the niobium cavity by vacuum brazing. This technique was developed at CERN [2] and it has been proven as a successful solution for many years. The main challenges to attain a sound joint are shown here.

Procedure

The Nb tube and the stainless steel flange are machined for vacuum brazing with a 20 µm gap between them for its correct filling once the Cu brazing filler metal (BFM) is in molten state. In addition, one or two grooves (depending on the thickness of the flange) have to be machined in the flange where the Ø1 mm Cu-OFE will be placed. A SS insert has to be introduced inside the Nb tube to ensure that thermal expansion mismatch between Nb and SS does not increase the 20 µm clearance at brazing temperature. Brazing is performed under vacuum (10^{-5} mbar) at a temperature slightly above the melting temperature of the copper for a short period of time (< 5 min). Once finished, the insert is machined away.

Validation Campaign 1

For the first validation campaign, a Nb tube of 100 mm internal diameter (ID) and 2.2 mm wall thickness was brazed to a SS (316LN) DN100 flange. The brazed joint was submitted to the same processes to which the cavity will be, consisting of a hard electropolishing (200 µm material removal), heat treatment (600 ºC/ 24h) and a light electropolishing (20 µm material removal). Between those steps, ultrasonic examination and leak test were performed to check the soundness of the joint. In addition, thermal shocks in liquid nitrogen and a shear test reaching 30 kN (10 times higher than the mechanical stresses that the joint will suffer during operation) were accomplished. Fig. 1 shows a metallographic observation of a cross section of the brazed joint after the test campaign.

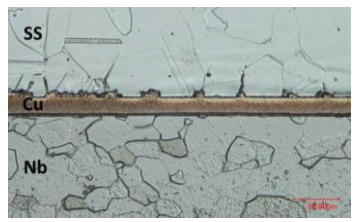


Figure 1: Metallographic observation of the brazed joint stainless steel (316LN) - niobium with copper as BFM.

Scanning electron microscopy (SEM) and energy disperse x-ray spectroscopy (EDS) analyses (detailed in [1]) showed a layer rich in chromium and iron in the niobium - copper interface, displaying brittle rupture surfaces after fractographic analysis. Nevertheless the shear test has proven they do not jeopardize the mechanical integrity of the cavity. This test campaign proved that for the dimensions above described, the brazing procedure gives a robust joint which fulfills the requirements for the SPL cavities.

Validation Campaign 2

The second campaign was intended to study the consequences on the brazed joint when submitting the assembly to a chemical polishing treatment. During fabrication of the SPL cavities, Nb pieces have to be chemically polished within 8 hours before EBW to avoid the readily formed oxide layer getting inside the weld seam [3]. For this campaign, Nb and SS plates were brazed and cut into 10 samples. They were introduced in the chemical polishing bath (40% HF, 60% HNO_3, 85% H_3PO_4 (1:1:2)) with different conditions of temperature and time. They were microscopically observed afterwards in order to determine the amount of

Copyright © 2014 CC-BY-3.0 and by the respective authors

ISBN 978-3-95450-142-7

A COMPACT HIGH-FREQUENCY RFQ FOR MEDICAL APPLICATIONS

M. Vretenar, A. Dallocchio, V. A. Dimov, M. Garlasché, A. Grudiev, A. M. Lombardi, S. Mathot, E. Montesinos, M. Timmins, CERN, Geneva, Switzerland

Abstract

In the frame of a new program for medical applications, CERN has designed and is presently constructing a compact 750 MHz Radio Frequency Quadrupole to be used as injector for hadron therapy linacs. The RFQ reaches an energy of 5 MeV in only 2 meters; it is divided into four standardized modules of 500 mm, each equipped with 12 tuner ports and one RF input. The inner quadrant radius is 46 mm and the RFQ has an outer diameter of 134 mm; its total weight is only 220 kg. The beam dynamics and RF design have been optimized for reduced length and minimum RF power consumption; conventional construction technologies have been adopted, to favour a future industrial production. The multiple RF ports are foreseen for using either 4 solid-state units or 4 IOT's as RF power sources. Although hadron therapy requires only a low duty cycle, the RFQ has been designed for 5% duty cycle in view of other uses. This extremely compact and economical RFQ design opens several new perspectives for medical applications, in particular for PET isotopes production in hospitals with two coupled high-frequency RFQs reaching 10 MeV and for Technetium production for SPECT tomography with two RFQs followed by a DTL.

INTRODUCTION

The Radio Frequency Quadrupole (RFQ) is the low-energy accelerator of choice for science, but it is so far only rarely used for medical and industrial applications. In spite of the RFQ high current, excellent beam quality, loss-free operation and minimum shielding, cyclotrons are preferred outside of the scientific environment because of their lower cost and because they have been industrialised since a long time, a large expertise being available in cyclotron construction, operation and maintenance.

RFQ technology however has considerably progressed in recent years in terms of beam dynamics design, of RF design and tuning techniques, and of availability and reliability of construction techniques. Moreover, RF frequencies in the 700-800 MHz range, about twice the maximum used in existing RFQs, are now considered as reachable, with the effect of reducing RFQ dimensions and construction costs thus opening new perspectives in the applications of RFQs outside of the scientific world.

The first challenge in this respect comes from the medical field: the request for proton therapy accelerators is rapidly growing, but at the same time there is a strong push towards reducing the accelerator size and cost. Along this line, the design and prototyping of compact proton therapy linear accelerators operating at 3 GHz is rapidly progressing [1, 2].

For proton therapy linacs, cyclotrons are far from ideal injectors because of the strict requirements in terms of input beam emittance into the 3 GHz structure; the RFQ instead can easily deliver the required beam characteristics, provided that it operates at a sub-harmonic of 3 GHz. Along this line, a study published in the TERA Green Book already in 1995 included a 750 MHz RFQ as injector for a proton therapy linac [3]; this RFQ project was later abandoned because of the technological challenges well beyond the experience of the time.

RFQ DESIGN

In the frame of its new program for medical applications, CERN has started the design and construction of a compact, low-cost RFQ as injector for a proton therapy linac, adapting to the modern technologies the previous TERA design and building on the experience from the construction of the Linac4 RFQ [4]. The frequency of 750 MHz has been retained after an analysis showing that it is close to an optimum: lower frequencies increase the RFQ length, while higher frequencies make difficult the realisation of the first very short cell.

In order to keep a sufficient beam acceptance at high frequency, the aperture must remain of the same order as in lower frequency RFQs; the related advantage is that machining tolerances remain achievable with conventional tools, but disadvantages are the small cross-section (Fig. 1) and the fact that the RF efficiency cannot profit of the increase in frequency. Additionally, the high RF frequency imposes a limitation to the length of the RFQ: to adjust the RF voltage without using complex and expensive stabilising mechanisms, the RFQ must be shorter than about 5 λ, or 2 meters.

In this RFQ design, a number of innovative design solutions have been adopted to minimise cost and to favour a future industrialisation; the RFQ is highly modular, made of 4 identical segments of 500 mm length.

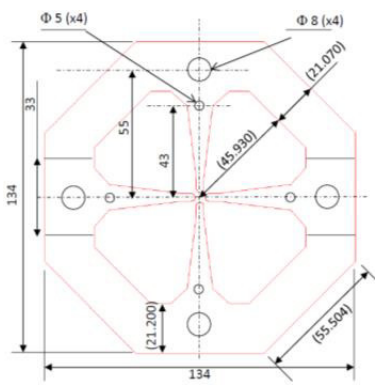


Figure 1: RFQ cross-section.

Copyright © 2014 CC-BY-3.0 and by the respective authors

ISBN 978-3-95450-142-7

THE ACCELERATOR CRYOPLANT AT ESS

P. Arnold, J. Fydrych, W. Hees, J. Jurns, X. L. Wang, J. G. Weisend II
European Spallation Source ESS
P.O. Box 176, SE-22100 Lund, Sweden

Abstract

The European Spallation Source (ESS) is a neutron science facility funded by a collaboration of 17 European countries currently under design and construction in Lund, Sweden. Cryogenic cooling is vital particularly for the linear accelerator, producing a 5 MW beam of 2.0 GeV protons to strike a rotating tungsten target. [1] The cryogenic section of the linac comprises cryomodules with superconducting RF cavities that require helium cooling at 2.0 K, shield cooling at ~40 K and liquid helium for power coupler cooling. An extensive cryogenic distribution system connects the cryomodules with the linac cryoplant. With estimated electricity consumption of up to 3 MW this plant will be one of the major power consumers at ESS. Turndown modes and the intrinsic uncertainties regarding heat loads drive the need for high plant efficiency not only during full load operation but also at reduced performance. Together with flexibility and reliability over a long operation period these are the key challenges that will be addressed in this paper.

CRYOPLANT SET-UP

The Accelerator Cryoplant (ACCP) is split into a warm and a cold section, located in the ACCP compressor building and the coldbox building respectively. The ACCP interfaces an extensive cryodistribution system (CDS) that comprises one valve box including a 2K heat exchanger per connected cryomodule.

The simplified block diagram in Figure 1 shows the main components of the ACCP, consisting primarily of

- The warm compressor station circulating helium at the flows and pressures required by the ACCP cold section,
- Helium gas treatment comprising bulk and final oil removal and a gas dryer,
- Gas management panel for process control,
- One coldbox containing all required equipment to provide the specified cooling,
- An ambient heater to assist warm-up of the system or the cool-down of single cryomodules.

The above-mentioned equipment forms part of one single procurement by ESS. All other equipment required to run the ACCP, particularly warm helium storage, a liquid helium (LHe) storage tank, the CDS or the recovery system will be separate procurements or in-kind contributions to ESS.

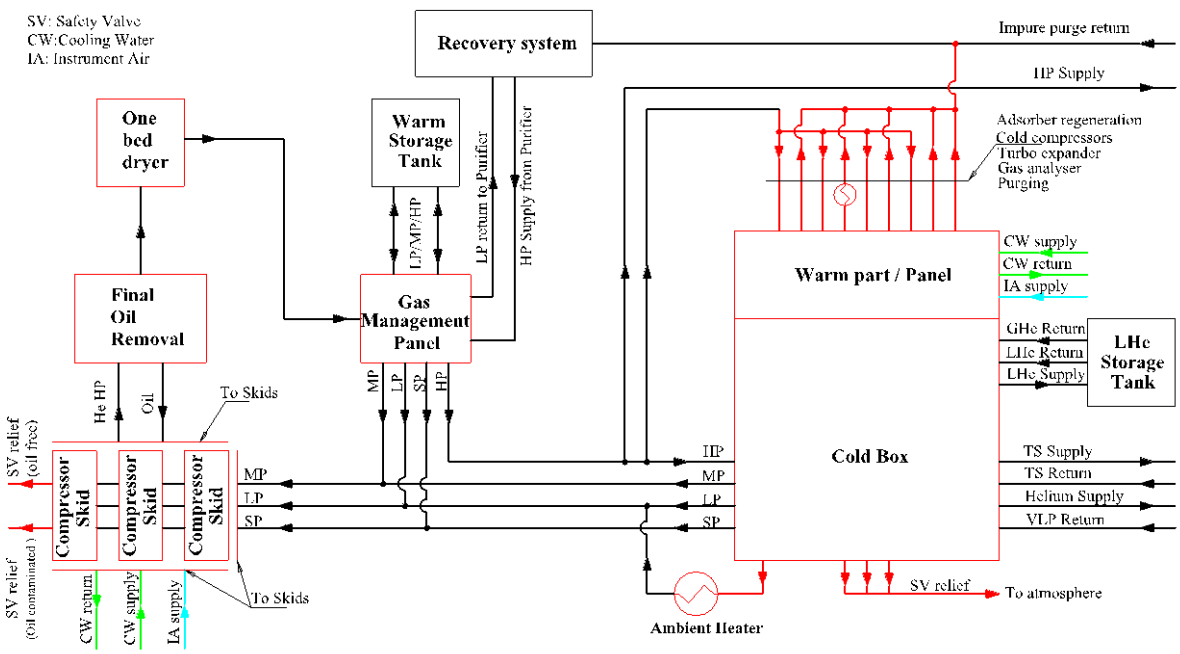


Figure 1: Simplified Block Diagram of the ACCP

ISBN 978-3-95450-142-7

Copyright © 2014 CC-BY-3.0 and by the respective authors

ERROR STUDY ON THE NORMAL CONDUCTING ESS LINAC

R. De Prisco*, ESS, Lund, Sweden and Lund University, Lund, Sweden
M. Eshraqi, R. Miyamoto, E. Sargsyan, ESS, Lund, Sweden
A. Karlsson, Lund University, Lund, Sweden

Abstract

One of the preliminary, but important test to evaluate the robustness of the accelerator design is performing the statistical error study by introducing realistic tolerances on the machine components.

In this paper the guidelines to define the tolerances and the correction system are summarized in order to validate the design. Firstly statistical studies have been performed in order to define the sensitivity to single errors and to fix the tolerances. Then all errors, within the previous defined tolerances, are applied with the correction system to evaluate the beam quality and to check if the system guarantees a radiologically safe operation.

INTRODUCTION

The European Spallation Source (ESS) uses a LINear ACcelerator (LINAC) to deliver the high intensity proton beam to the target station. The normal conducting ESS LINAC accelerates a proton beam of 62.5 mA from 0.075 MeV to 89.68 MeV at 352.21 MHz. The pulses are 2.86 ms long with a duty cycles of 4%. Permanent Magnet Quadrupoles (PMQs) in the DTL are used as focusing elements in a FODO lattice. The average beam power is 5 MW with a peak beam power at target of 125 MW.

SPACE CHARGE ROUTINE

The first crucial point to accurately describe the space charge effect of the high current LINAC is to choose a proper space charge routine. For these studies the PICNIC routine is chosen because, by applying the errors, the assumption of cylindrical symmetry on the bunch shape can not be guaranteed [1].

The second crucial point is the choice of the mesh size in the beam and the particle number. There is an optimum mesh size respect to which a larger mesh size deteriorates the resolution whereas a smaller mesh size induces a small number of particle per cell and, consequently, statistical noise. For these studies the mesh size is 15 both in transverse and in longitudinal planes. The number of particles is 1 million.

ERROR STUDY STRATEGY

The normal conducting ESS LINAC is composed of three structures: Radio Frequency Quadrupole (RFQ), Medium Energy Beam Transport (MEBT), Drift Tube Linac (DTL).

For each section, at first, each error is applied individually to evaluate the emittance growth sensitivity. At this stage the errors are analyzed without the correction steerers. *In a very preliminary approach* the additional emittance growths, due to the individual errors, in the $k-$plane, $\Delta\epsilon_k$ (with respect to the emittance growths in the case without error in the same plane, $\epsilon_{\text{out, NO ERR, }k}$) can be considered as independent variables. With this hypothesis a rough value of the total squared additional emittance growth, for the case in which all errors are applied simultaneously, can be approximated by the sum of the squared individual additional growths. This calculation is useful to fix a preliminary acceptable limit for each error.

The additional emittance growth is defined as:

$$\Delta\epsilon_k = \frac{\epsilon_{\text{out, ERR, }k} - \epsilon_{\text{out, NO ERR, }k}}{\epsilon_{\text{out, NO ERR, }k}}, \qquad (1)$$

where $\epsilon_{\text{out, ERR, }k}$ is the output emittance in presence of errors in the $k-$plane.

In the second step all the errors are applied simultaneously with the corrector steerers. A fine tuning on the tolerances is done in order to have the total additional emittance growth limited to 10 % per structure and the losses less than 1 W/m everywhere. Finally a steerer study is done for the DTL by varying their number, position and strength in order to reduce further the losses.

Each case is simulated using 1000 linacs.

ERROR DEFINITIONS

It is possible to separate the errors in two categories: *static* and *dynamic* in time. To the static category belong: quadrupole transverse position, dx, dy, rotation, $d\phi_x$, $d\phi_y$, $d\phi_z$, and gradient, dG, errors; structure to structure alignment, dx_T, dy_T, errors; field amplitude, dE_0, and phase, $d\phi_s$, error; klystron field, dE_k, and phase, $d\phi_k$, error. The klystron field, $dE_{k,d}$, and the phase, $d\phi_{k,d}$, jitter error belong to the dynamic category.

RFQ AND MEBT

The beam is generated at the RFQ input with a gaussian distribution truncated at 4σ. The nominal RFQ output distribution is saved and used in the MEBT and global error studies. The main beam parameters at the RFQ output and the tolerances for the RFQ and MEBT are reported in [2]. The effective gap voltage of the three bunchers in the MEBT are tuned to match the Twiss input DTL parameters. The MEBT output Twiss parameters and, in parentheses, their difference, in percentage, from the input ideal Twiss Parameters of the DTL are reported in Table 1.

By introducing in the MEBT the tolerances defined in [2] it is possible to define the variation interval for each output beam parameter. The intervals are reported in the Table 2.

* renato.deprisco@esss.se

Copyright © 2014 CC-BY-3.0 and by the respective authors

ISBN 978-3-95450-142-7

BENCHMARK OF BEAM DYNAMICS CODE DYNAC USING THE ESS PROTON LINAC

E. Tanke, M. Eshraqi, R. Miyamoto, A. Ponton, R. de Prisco, E. Sargsyan, ESS, Lund, Sweden
S. Valero, Consultant, retired from CEA-Saclay, Paris, France

Abstract

The beam dynamics code DYNAC was benchmarked using the European Spallation Source (ESS) Proton Linac. The code contains three space charge routines, including a 3D version. For beam dynamics, it contains a numerical method, capable of simulating a multi-charge state ion beam in accelerating elements (i.e. cavities) as well as an analytical method, capable of modelling protons, single charge state heavy ions and non-relativistic electrons. The benchmark includes comparisons of both methods with the beam dynamics models in use at ESS. As the analytical method used in DYNAC is fast, it is a prime candidate for use as an online beam simulation tool.

INTRODUCTION

The high current (62.5 mA) beam of protons is accelerated up to 2.0 GeV in a sequence of normal conducting and superconducting accelerating structures in the ESS linac. The accelerated protons are to be used for the bombardment of neutron rich nuclei in the target to produce a high flux of pulsed spallation neutrons. The 5 MW proton linac delivers beams to the target in long pulses of 2.86 ms with a repetition rate of 14 Hz, corresponding to a duty cycle of 4 %. Such beam powers are unprecedented and extensive simulations are needed to make sure that the loss levels are well controlled (<1W/m) and do not prevent hand-on maintenance of the accelerator components.

It is important that beam dynamics simulations for such a linac be tested with independent codes to eliminate unknown bugs in the codes, though each code has undergone careful debugging.

THE ESS LINAC

The ESS linac [1] is composed of a normal conducting front-end, consisting of an ion source, Low Energy Beam Transport (LEBT), Radio Frequency Quadrupole (RFQ), Medium Energy Beam Transport (MEBT) and Drift Tube Linac (DTL). The front-end is followed by a Super Conducting Linac (SCL). Each section, starting from the RFQ, is briefly described below.

RFQ

The 4.55 m long ESS RFQ is a four-vane structure, which bunches and accelerates the beam from 0.075 to 3.62 MeV. The transverse radius of curvature of the vane tips is constant along the RFQ length. The inter-vane voltage varies from 80 to 120 kV along the RFQ length.

MEBT

The MEBT consists of eleven quadrupoles and three bunching cavities to keep the beam focused and matched to the following DTL. To achieve a proper matching, the MEBT also includes diagnostics devices to characterize the beam positions and profiles in all three planes.

DTL

The DTL accelerates the beam from 3.62 to 89.68 MeV in 5 tanks. Permanent Magnet Quadrupoles (PMQs) perform the transverse focusing in a FODO lattice. The "empty" drift tubes are equipped with steerers and beam diagnostics.

SCL

The SCL consists of cryomodules arranged in three sections: the spoke section, the medium and the high beta elliptical sections. Quadrupole pairs that are placed before each cryomodule provide the transverse focusing along the SCL. Thirteen pairs of double spoke cavities with an optimal beta of 0.5 are housed in 13 cryomodules. Nine cryomodules house the medium beta 6-cell elliptical cavities with a geometric beta of 0.67, arranged in groups of four cavities. The high beta section, providing more than 70% of the total energy gain contains 84 five-cell elliptical cavities with a geometric beta of 0.86, also arranged in groups of four.

SIMULATION CODES

DYNAC

The original version of DYNAC [2] was developed by CERN, in collaboration with CEA Saclay. In that version a set of accurate quasi-Liouvillian beam dynamics equations was introduced for accelerating elements, applicable to protons, heavy ions and non-relativistic electrons.

Since then, a numerical method has been added capable of simulating both single and multi-charge state ion beams in accelerating elements. Other additions are an RFQ model and more recently the description of the Radial Matching Section has been improved. Sextupoles, quadrupole-sextupoles, and electrostatic devices as well as the capability of second order calculations for a multi-charge state beam have been added.

DYNAC contains three space charge routines, including a 2D (modified SCHEFF) and a 3D (HERSC) version. The modified SCHEFF routine can perform space charge calculations for a multi-charge state beam with separated bunches.

Copyright © 2014 CC-BY-3.0 and by the respective authors

ISBN 978-3-95450-142-7

ESS NORMAL CONDUCTING LINAC STATUS AND PLANS

A. Ponton*, B. Cheymol, M. Eshraqi, R. Miyamoto, R.de Prisco, E. Sargsyan, ESS AB, Lund, Sweden
G. Bourdelle, M. Desmons, A. France, O. Piquet, B. Pottin, N. Sellami,
CEA-Irfu, Gif-sur-Yvette, France
I. Bustinduy, P. González, J. L. Muñoz, I. Rueda, F. Sordo, ESS-Bilbao, Bilbao, Spain
L. Celona, S. Gammino, L. Neri, INFN/LNS, Catania, Italy
M. Comunian, F. Grespan, A. Pisent, , C. Roncolato, INFN/LNL, Legnaro, Italy
P. Mereu, INFN/Sezione di Torino, Torino, Itlay

Abstract

Efficient and low loss beam acceleration in the European Spallation Source (ESS) linear accelerator (linac) gives rise to specific technical challenges in the normal conducting (nc) section. The nc linac creates high current proton beams, produces the macro and micro structures (formation of the pulse and bunches respectively) of the beam and accelerates the latter up to 90 MeV before injection in the superconducting (sc) linac. Design and construction of the different components of the nc linac are part of a broad collaboration involving experts of various labs in Europe. Beam commissioning of the warm linac in the ESS tunnel is foreseen at the beginning of 2019.

INTRODUCTION

The ESS aims at becoming the world's most powerful neutron source at the end of the decade. The spallation neutrons are produced by a 5 MW proton beam hitting a solid, rotating tungsten target [1]. The acceleration of the proton beam up to a final energy of 2 GeV is ensured by a ~ 400 m Radio-Frequency linear accelerator (RF linac) whose main characteristics are 14 Hz repetition rate, 62.5 mA peak beam current and 2.86 ms beam pulse length. The layout of the ESS linac can be seen in Fig. 1.

The linac [2] is composed by a sequence of nc structures followed by sc cavities hosted in cryomodules [3]. The nc part of the linac, while giving only 5 % of the power to the beam, has to produce very high quality beams before injecting into the sc linac. The layout of the nc linac and the main technical challenges will be explained. The design and the construction of the warm linac as part of a broad European collaboration is presented in the following. Status and plans for construction and installation will finally be given.

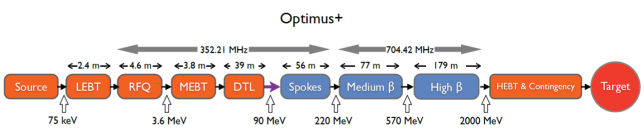


Figure 1: Layout of the ESS linac.

LAYOUT AND TECHNICAL CHALLENGES

General Layout

The proton beam is *produced and accelerated* to 75 keV in a Microwave Discharge Ion Source (MDIS) which is followed by a dual solenoid Low Energy Beam Transport line (LEBT) [4] *transporting and matching* the beam into the Radio-Frequency Quadrupole (RFQ). The latter *accelerates to* 3.62 *MeV, focuses and transforms the beam pulse in a train of bunches* at 352.21 MHz [5] to allow rf acceleration in the subsequent structures. The beam is then *transported* through the Medium Energy Beam Transport line (MEBT) [6] and *matched* into the Drift Tube Linac (DTL) [7]. The DTL finally *focuses and accelerates* the beam up to 90 MeV in 5 tanks of 8 m each.

In order to allow efficient matching with acceptable and controllable beam loss during operation, the LEBT and the MEBT, even given the reduced space available, are equipped with a set of diagnostics for current, energy and phase space measurements [8].

Technical Challenges

The main goal of the warm linac is to inject high quality proton beams with a given time structure and sufficient energy in the sc linac.

The required peak beam current on target is 625 mA. As a result, proton transport through the warm linac is very challenging due to *high space charge forces* acting on the beam. In particular, performing the injection of the matched beam into the RFQ requires to understand theoretically and experimentally how much the ionization of the residual gas by the proton beam reduces the space charge of the beam itself: the so-called space charge compensation (scc) process. In addition, reducing the development of halo is mandatory to avoid hazardous losses, which must remain below 1 W/m at high energy, therefore requiring good beam matching between sections since mistmatch is known to be one of the main mechanisms of halo production. The RFQ is also foreseen to perform efficient bunch capture with negligible production of longitudinal tail that potentially transfers into transverse halo and losses. In the MEBT collimator strategy is being studied to intercept part of the transverse halo [9]. Challenges in terms of beam performances are summarized in Tab. 1 (see [10] for a deeper analysis).

* aurelien.ponton@esss.se

Copyright © 2014 CC-BY-3.0 and by the respective authors

ISBN 978-3-95450-142-7

ESS LINAC BEAM MODES

E. Sargsyan, R. Miyamoto, ESS, Lund, Sweden

INTRODUCTION

The ESS Linac will ultimately deliver 5 MW of beam power to the target with a long-pulse structure of 2.86 ms and 14 Hz repetition rate, which are essential for the production of long-wavelength neutrons [1]. Ten different beam power levels are requested for the operation. In order to preserve the required time structure of the beam, different beam power levels will be produced by reducing the beam current in ten regular steps using an iris with an adjustable aperture in the Low Energy Beam Transport (LEBT). Low current and low emittance beams may as well be useful for the beam commissioning of the Linac. This paper describes the generation and the beam dynamics of different beam modes in the ESS Linac.

GENERATION OF BEAM MODES

The different beam currents are generated in the LEBT by adjusting the aperture of the iris placed between the solenoids, collimating the required beam fraction. The beam is matched to the Radio Frequency Quadrupole (RFQ) with two solenoids. All simulations are done using TraceWin and Toutatis codes [2].

LEBT

Beam modes with a beam current from 6.3 mA up to the nominal 62.5 mA at the target will be produced in ten regular steps. Table 1 lists the relevant design parameters of the ESS Linac without considering eventual errors. The schematic layout of the LEBT is presented in Fig. 1.

Table 1: Design Nominal Parameters of the ESS Linac

Parameter	Value	Unit
Source output beam current	65	mA
Source output norm. RMS emittance	0.2	π.mm.mrad
Space charge compensation in the LEBT	≥95	%
LEBT beam transmission	100	%
RFQ input norm. RMS emittance	0.25	π.mm.mrad
RFQ beam transmission	≥97	%
MEBT-to-target beam transmission	100	%
Beam current at the target	62.5	mA

The field strength of the solenoids and the iris aperture radius for each beam mode are calculated through an iterative process, while matching the beam to the corresponding RFQ input beam parameters in each step. To simplify the calculations, a fixed RFQ transmission of 97% has been assumed for all beam currents. For beam currents below the nominal this will introduce only a small error of up to 3% in the beam current at the target. Taking into account the overall efficiency of the Linac, beam currents from 6.5 mA to 65 mA shall be produced at the RFQ input. We will be referring to the beam currents at the RFQ input in the rest of the document.

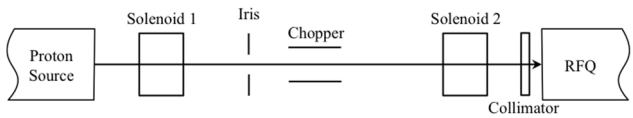


Figure 1: LEBT schematic layout.

A uniform space charge compensation of 95% along the LEBT has been assumed in the simulations, except in the collimator with the repelling electric field at the RFQ entrance. Field strength of solenoids for different beam modes is presented in Fig. 2. The beam current and the RMS emittance at the RFQ input as a function of the iris aperture radius are presented in Fig. 3. The beam size for different beam modes in the LEBT is presented in Fig. 4.

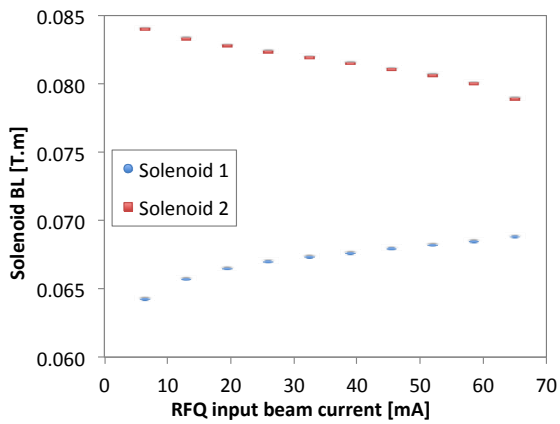


Figure 2: Field strength of the LEBT solenoids.

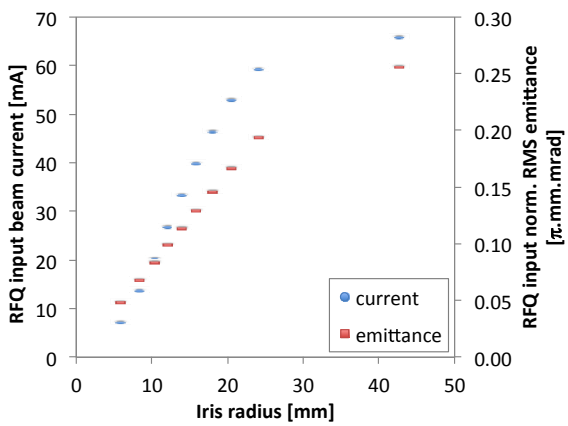


Figure 3: RFQ input beam current and RMS emittance.

Copyright © 2014 CC-BY-3.0 and by the respective authors

ISBN 978-3-95450-142-7

SRF HIGHBAY TECHNICAL INFRASTRUCTURE FOR FRIB PRODUCTION AT MICHIGAN STATE UNIVERSITY*

L. Popielarski#, F. Casagrande, C. Compton, T. Elkin, A. Fila, P. Gibson, M. Hodek, L. Hodges, M. Leitner+, I. Malloch, C. Nguyen, R. Oweiss, J. Ozelis, J. Popielarski, C. Thronson, D. Victory, T. Xu
Facility for Rare Isotope Beams, Michigan State University, East Lansing, MI, 48824, U.S.A.

Abstract

Abstract: Michigan State University (MSU) is establishing a new 2,500 m^2, high bay building to house the Superconducting Radio Frequency (SRF) infrastructure for the Facility for Rare Isotope Beams (FRIB) production requirements. The construction has been completed and beneficial occupancy began in May 2014. The new SRF highbay includes over 373 m^2 of cleanroom and chemistry facility space, automated cavity etch tools, ultra pure water systems, cold mass component inspection area, hydrogen degassing furnace, SRF testing capabilities for three vertical test Dewars and two horizontal cryomodule test caves with a dedicated helium refrigeration system. The status of the design, installation and commissioning will be presented.

INTRODUCTION

The SRF technical infrastructure is operated by the FRIB SRF Department, which has developed and will mass-produce four types of SRF cavities, coldmasses, and cryomodules for the FRIB linac. The linac requires a total of 330 certified cavities for installation into 49 cryomodules.

The SRF highbay will house all FRIB SRF-related activities except for cryomodule assembly, which will occur elsewhere. This infrastructure will support the FRIB baseline SRF cavity processing requirements [1]. Detailed coldmass component processing and testing workflows have been developed to define equipment requirements and optimize the work center layout (Fig. 1).

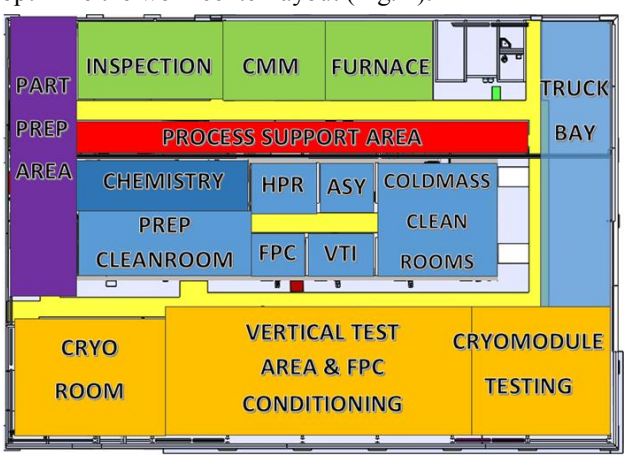


Figure 1: SRF highbay work center layout.

* This material is based upon work supported by the U.S. Department of Energy Office of Science under Cooperative Agreement DE-SC0000661
# lpopiela@frib.msu.edu
+ now at Lawrence Berkeley National Laboratory, Berkeley, CA, 94720, U.S.A.

Coldmass production will require 36 months, with an average process rate of 12.5 cavities per month. It is assumed 20% of the cavities will be reprocessed. This rate, coupled with maintenance downtime considerations, yields a required throughput of one cavity per weekday.

The SRF highbay was completed in 13 months, in May 2014. The highbay includes a 30 ton overhead crane, four 1.5 m diameter x 4.9 m deep Dewar shafts, and a roof structure designed to handle the load of eight 113.6 m^3 helium gas storage tanks.

PROCESSING FACILITY

Cleanrooms

The new 372 m^2 SRF cleanrooms were designed using lean manufacturing principles to streamline work flow and minimize cross-contamination by creating separate work centers for each major activity. Critical procedures including final rinsing and cavity and coldmass assembly are performed in an ISO 5. Less critical processes take place in an ISO 6 area. A central walkway minimizes interference between work centers, which are divided by transparent air return walls increasing visibility and flexibility for expansion. The layouts (Fig. 2) are identified as follows: 1) ante room, 2) part washing 3) power coupler assembly, 4) insert hatches, 5) coldmass pump down and leak checking, 6) coldmass assembly, 7) cavity drying and assembly, 8) high pressure rinse, 9) chemistry room pass through and 10) chemical etching room.

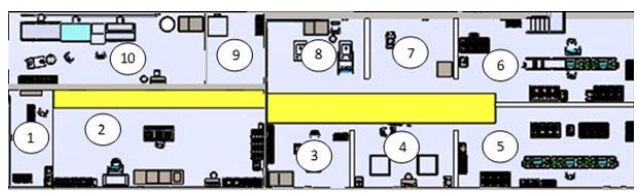


Figure 2: Cleanroom layout.

The new cleanroom has passed all vendor and independent certification tests and is fully commissioned. Processing work is now ongoing in the new cleanroom.

Chemistry Facility

The SRF cavity chemical etching facility includes state-of-the-art process equipment designed for safe and reliable performance. Sophisticated safety interlocks and alarms were implemented to eliminate the possibility of exposure to buffered chemical polish (BCP) or toxic chemical vapors. The process equipment (Fig. 3) is composed of an SRF cavity etching cabinet optimized for the FRIB cavity designs, a chemical fume hood capable of storing three 200 L drums of BCP, a niobium parts etching fume hood

Copyright © 2014 CC-BY-3.0 and by the respective authors

DESIGN OF A COMPACT LEVER SLOW/FAST TUNER FOR 650 MHz CAVITIES FOR PROJECT X*

E. Borissov, I. Gonin, T. Khabiboulline, Y. Pischalnikov, V. Yakovlev, FNAL, Batavia, 60510, USA

Abstract

Fermilab is developing 5-cell elliptical 650 MHz β=0.6 and β=0.9 cavities for project X [1].

A compact fast/slow lever tuner intended for both types of cavities has been developed for final tuning of the resonance frequency of the cavity after cooling down and to compensate the resonance frequency variations of the cavity during operation coming from liquid helium pressure fluctuations. The updated helium vessel (presented at this conference) is equipped with the tuner located at one of the end of the cavity. The tuner design and results of ANSYS analysis of their properties are presented.

INTRODUCTION

One of the important parts of the mechanical design of a helium vessel-cavity assembly is a compact fast/slow tuner for final tuning of the resonance frequency of the cavity after cooling down and to compensate frequency detuning due to helium pressure fluctuations and Lorentz force detuning.

TUNER REQUIREMENTS

The cavity operational and test requirements are summarized in Tab. 1.

Table 1: Cavity Operational Requirements

Parameter	Value
Frequency	650MHz
Bandwidth	45Hz
Operating node	CW
Operating gain per cavity	17.7 MeV
Maximum Gain per cavity	> 21 MeV
Sensitivity to He pressure fluctuations	< 15 Hz/mbar
Field Flatness dressed	> 90%
Operating temperature	2.0 K
Operating Pressure	30 mbar
MAWP	2 bar (RT), 4 bar (2K)
RF power input per cavity	up to 100 kW (CW)
Cavity longitudinal stiffness	< 10^4 N/mm
Tuning sensitivity	> 180 kHz/mm

In order to accomplish the requirements for frequency range and resolution, the tuning systems for cavities of narrow bandwidths shall integrate a coarse/slow and a fine/fast mechanism engaged in series. The former normally utilizes a mechanical system which applies forces between the He vessel and cavity flange to squeeze or stretch the cavity. An electromechanical actuator is the system (stepper motor/gear box & spindle) to convert rotation from the stepper motor to linear stroke. An electromechanical system actuates the coarse tuner with large stroke capability but limited resolution. Fine/fast tuners usually contain piezo-electric actuators with limited stroke but virtually infinite resolution. The fine/fast tuning system allows integration of active compensation of cavity frequency detuning due to helium pressure fluctuations or by Lorentz forces or other external perturbations (microphonics).

The coarse tuner is predominantly used to consistently achieve the resonant frequency during cool-down operations and to take up mechanical lash in the tuner mechanism. The range necessary to compensate for the cool-down uncertainties is estimated to be 50 kHz. In the event that a cavity must be detuned as a result of a malfunction, the coarse tuning system must be able to shift the frequency away from resonance by at least 100 bandwidths (equal to ≈45 kHz) so that the beam is not disturbed. To take up mechanical lash in the tuner mechanism additional deformation of the cavity is needed, corresponding to a 20 kHz frequency shift. The total frequency shift is 70 kHz. The requirement on the tuning range considered a safety margin of 2.0. The cavity tuning sensitivity is 180 kHz/mm. The coarse tuner should be able to change the cavity length by ~0.8 mm.

The required accuracy of the frequency tuning is 4 Hz (or ~20 nm in cavity length). Based on the parameters of different manufactured SRF cavity tuning systems one can conclude that it will be a big challenge for any type of coarse mechanical tuning system to deliver this level of precision. Taking into account backlash & hysteresis of the cavity/slow tuner system, the requirement on the resolution of the coarse tuning system was set to 10 Hz. One can conclude that the coarse tuning system alone (without assistance from a fine/fast tuner) can't deliver the required cavity tuning accuracy (2Hz).
Also it is conservatively assumed that the coarse system cannot be operated during beam acceleration; it is thought

Copyright © 2014 CC-BY-3.0 and by the respective authors

ISBN 978-3-95450-142-7

DESIGN OF 162.5 MHZ CW MAIN COUPLER FOR RFQ*

S. Kazakov#, O. Pronitchev, V. Poloubotko, T. Khabiboulline, J. Steimel, V.P. Yakovlev
FNAL, Batavia, IL 60510, USA

Abstract

Project X Injector Experiment (PXIE) at Fermilab will utilize a 162.5 MHZ CW RFQ accelerating cavity. The design of a new main coupler for PXIE RFQ is reported. Two identical couplers will deliver approximately 100 kW total CW RF power to RFQ. A unique feature of the coupler allows the application of a DC bias for multipactor suppression. Results of RF and thermal simulations, along with mechanical design, are presented.

INTRODUCTION

A multi-MW proton facility (PIP-II) has been proposed at Fermilab. A prototype of the PIP-II front end, PXIE, is planned to validate the conceptual design. PXIE will supply a 25 MeV 50 kW beam, and will include an H- ion source, a CW RFQ and two superconducting RF cryomodules providing up to 25 MeV energy gain at an average beam current of 1 mA (upgradable to 2 mA) [1]. The ion source will deliver up to 10 mA of H- at 30 keV to the RFQ. The 162.5 MHz RFQ (Fig. 1) accepts and accelerates this beam to 2.1 MeV. The RFQ is designed to dissipate ~80 kW of RF power under nominal operating conditions. To reduce coupler power demands, two power couplers will be integrated with the RFQ [2].

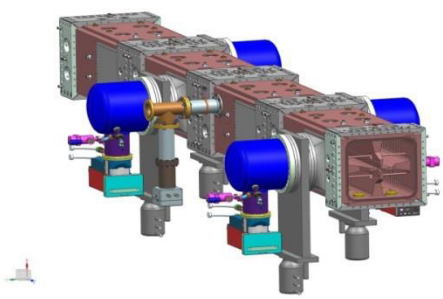


Figure 1: CAD view of RFQ

Table 1: RFQ Parameters

Parameter	Value
Ion type	H-
Beam current	1-10 mA
Beam energy	0.03-2.1 MeV
Frequency	162.5 MHz
Duty factor (CW)	100%
Total RF power	≤ 130 kW
Number of couplers	2

* Operated by Fermi Research Alliance, LLC under Contract No. DE-AC02-07CH11359 with the United States Department of Energy.
#skazakov@fnal.gov

RFQ COUPLER

Requirements

Parameters of the RFQ (Table 1) define requirements for the two couplers. They are listed in Table 2.

Table 2: Coupler Requirements

Parameter	Value
Frequency	162.5 MHz
Operating power	75 kW
Coupling type	Loop
Output port diameter	~3"
Input impedance	50 Ohm

Coupler Structure

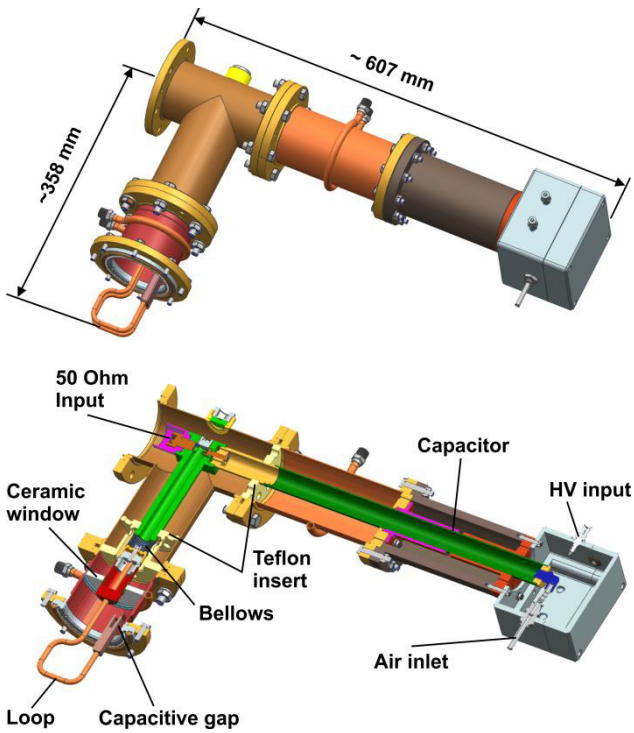


Figure 2: Main dimensions and internal structure of RFQ coupler.

Fig. 2 presents a schematic of the coupler, showing its main dimensions and internal structure. The coupler includes an alumina ceramic window with 77 mm outer diameter, 28.6 mm inner diameter and 6 mm thickness. The coupling loop consists of two parallel 1/4" copper

Copyright © 2014 CC-BY-3.0 and by the respective authors

ISBN 978-3-95450-142-7

STATUS OF 325 MHz MAIN COUPLERS FOR PXIE*

S. Kazakov#, O. Pronitchev, B.M. Hanna, V. Poloubotko, T. Khabiboulline,
L. Ristori, V.P. Yakovlev, FNAL, Batavia, IL 60510, USA

Abstract

The Project X Injector Experiment (PXIE) at Fermilab will include one cryomodule with eight 325 MHz single spoke superconductive cavities (SSR1). Each cavity requires approximately 2 kW CW RF power for 1 mA beam current operation. A future upgrade will require up to 8 kW RF power per cavity. Fermilab has designed, procured and tested two prototype couplers for the SSR type cavities. Status of the 325 MHz main coupler development for PXIE is reported.

INTRODUCTION

A multi-MW proton accelerator facility based on an H- linear accelerator using superconducting RF technology, PIP II, is being developed at Fermilab to support the intensity frontier research in elementary particle physics. The PIP-II [1] baseline design includes two types of 325 MHz superconducting cavities, single spoke resonators, SSR1, with a β=0.22 and single spoke resonators, SSR2, having β of 0.47. The first cryomodule consists of eight SSR1 cavities and will be installed in PXIE at Fermilab [2]. Both type of cavities have a similar design and are equipped with the same size power coupler flanges. This will allow us to use the same design for power couplers that feed the RF power to both types of cavities. Power consumption of the cavities for both projects varies from 2 kW to 8 kW thus the 325 MHz power couplers should operate up to 10 kW in the CW regime. This paper presents the RF design and optimization, production and tests of this coupler.

COUPLER STRUCTURE

The coupler structure is presented in Figure 1. The parts inside the vacuum include a 3 inch stainless steel tube with 0.4 mm wall thickness, 0.5 inch copper antenna and 6 mm thickness ceramic window. The stainless steel pipe has no copper coating and the ceramic window is coated with TiN.

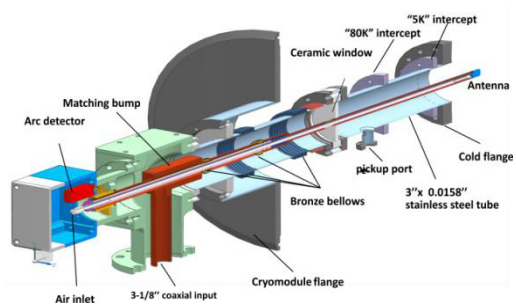


Figure 1: Structure of 325 MHz main coupler.

The copper antenna is cooled with dry air. The coupler has two thermal interceptors at "5K" and "80K". The parts that are not in a vacuum consist of copper tubes with Ni bellows coated with copper. Here, the inner conductor has a bigger diameter then the antenna to match the ceramic window. This design allows us to apply a high voltage (HV) bias in order to suppress any possible multipactor.

Three experimental couplers were fabricated. Figure 2 presents a coupler on a test bench for low power measurements and tuning. Figure 3 presents the coupler pass band after tuning; the pass band is about 20 MHz (~ 6%) at the level of S11 < -20dB.

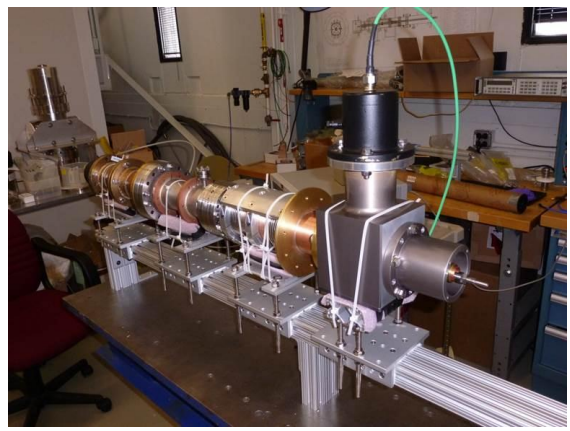


Figure 2: Coupler at test bench for tuning.

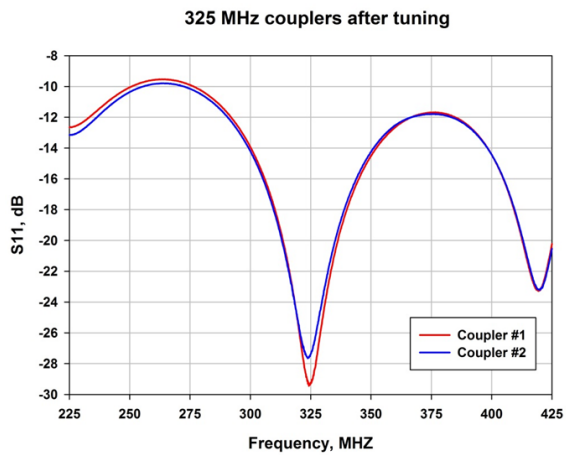


Figure 3: Pass band of couplers after tuning.

DC BLOCK

In order to apply HV bias, the internal conductor of the coupler has to be isolated from the internal conductor of the rf coaxial waveguide. For this purpose a so called DC block was designed .The structure of the DC block is presented in Figure 4. Both input and output of the DC

* Work supported by DOE
#skazakov@fnal.gov

Copyright © 2014 CC-BY-3.0 and by the respective authors

ISBN 978-3-95450-142-7

DESIGN OF A QUASI-WAVEGUIDE MULTICELL DEFLECTING CAVITY FOR THE ADVANCED PHOTON SOURCE*

A. Lunin#, T. Khabiboulline, I. Gonin, V. Yakovlev, FNAL, Batavia, IL, 60510, USA
A. Zholents, ANL, Argonne, IL 60439, USA

Abstract

This paper reports the electromagnetic design of a 2815 MHz Quasi-waveguide Multicell Resonator (called QMiR) being considered as a transverse RF deflecting cavity for the Advanced Photon Source's (APS) Short Pulse X-ray project. QMiR forms a trapped dipole mode inside a beam vacuum chamber while High Order Modes (HOM) are heavily loaded. It results a sparse HOM spectrum, makes HOM couplers unnecessary and allows simplifying the cavity mechanical design. The form of electrodes is optimized for producing 2 MV of deflecting voltage and keeping low peak surface electric and magnetic fields of 54 MV/m and 75 mT respectively. Results of detailed EM analysis, including HOM damping at the actual geometry of beam vacuum chamber, will be presented.

INTRODUCTION

The superconducting radio frequency (SRF) multi-cell trapped mode cavity is proposed for an implementation in the Short Pulse X-ray (SPX) upgrade of Argonne APS [1]. The number of Synchrotron Radiation (SR) facilities over the world is a multiple of tenth and is growing up quickly [2]. Generating short x-ray pulses in a SR facility is in high demand for research in condensed matter physics, materials science, biology and medicine. Proposed technique is based on a beam deflection resulting a correlation between the longitudinal position of an electron within the bunch and its vertical momentum. It allows obtaining a sub-picosecond X-ray pulse without a reduction of a bunch length with existing particles accelerators.

Historically a simple pill-box type resonator with an optimized elliptical shape, operating in the dipole electric TM11 mode was used for beam deflection. Despite its simple geometry and a good surface cleaning capability, there are few major drawbacks: a) the TM11 mode is not the lowest mode in the cavity spectrum, b) number of Low Order Modes (LOM) and HOM couplers are required for damping unwanted resonances, c) such cavities have large transverse dimensions. Thus, there are difficulties with cryostat design that complicate cavity operation. Recently alternative solutions based on the transverse TE11 magnetic mode and TEM lines were proposed for the deflection of charged particles [3, 4]. Both approaches resulted in significantly smaller cavity design compared to the conventional TM11 elliptical cavity and eliminate the presence of LOM modes. However, these new conceptions are still comprised of a closed resonant volume with a dense eigenfrequency spectrum and therefore require auxiliary couplers for damping coherent HOM excitation.

Thus, there is a need for a simple and compact superconducting structure for beam manipulation applications. Such a structure has to provide a high transverse kick, have a minimum number of auxiliary couplers and must be able to operate with high beam current.

CAVITY EM DESIGN

It is known that localized imperfections in a regular waveguide will cause a so called "ghost modes" to appear [5, 6]. Ghost modes are trapped to the vicinity of imperfections, with resonant frequencies lower than a waveguide cut-off limit, and usually are treated as a parasitic factor limiting the beam intensity. Instead we try to use this phenomenon for good in our design of the QMiR cavity. Since multiple electrodes immersed into a waveguide form a trapped mode resonator, the transverse EM-field components of the TE dipole mode allow creating a kick and effectively deflecting charged particles passing through the cavity. Because such a cavity is open, i.e. has no end walls, it helps significantly in reducing the maximum quality factors of HOMs and, thus, avoiding complicate HOM couplers and simplifying a cavity mechanical design in overall.

Table 1: Design parameters for the APS deflecting cavity

Parameter	Value
Frequency	2.815 GHz
Optimal beta	1.00
Nominal Kick Voltage	2 MV
Beam aperture	12 mm x 30 mm
Max surface E_{pk}	54, (< 55) MV/m
Max surface B_{pk}	75, (< 80) mT
G-Factor	130 Ω
R/Q, Operating mode	1040 Ω
R_m*F, Monopole modes	<0.44 MΩ * GHz
R_t, Horizontal mode	<1.3 MΩ/m
R_t, Vertical mode	<3.9 MΩ/m

* Operated by Fermi Research Alliance, LLC, under Contract DE-AC02-07CH11359 with the U.S. DOE
#lunin@fnal.gov

Copyright © 2014 CC-BY-3.0 and by the respective authors

STUDY OF COUPLER'S EFFECT IN THIRD HARMONIC SECTION OF LCLS-II SC LINAC*

A. Saini#, A. Lunin, N. Solyak, V. Yakovlev FNAL, Batavia, IL 60510, USA
T. Raubenheimer, SLAC, Stanford, CA 94309, USA

Abstract

The Linac Coherent Light Source (LCLS) is an X-ray Free Electron Laser (FEL) facility. The proposed upgrade of the LCLS facility is based on construction of 4 GeV superconducting (SC) linac which will use two stage bunch compression scheme to achieve ultra-short bunches with high peak current. In order to reduce non-linear effects in the first bunch compressor, third harmonic section is utilized to linearize longitudinal phase space of the beam. However, transverse phase space of beam may get distorted due to coupler RF kicks and coupler wake kicks resulting from the rotational asymmetry of 3.9 GHz cavity in presence of power and higher order modes (HOMs) coupler. In this paper, we discuss coupler's effects and analyse resulting emittance dilution in third harmonic section. Local compensation of coupler kicks using different orientations of cavities is also addressed.

INTRODUCTION

The LCLS-II [1] is a proposed high repetition rate FEL facility to be built at SLAC. It is primarily based on SC linac that will be capable to perform the acceleration of electron beam with the repetition rate of 1 MHz from kinetic energy of 0.75 to 4000 MeV in continuous wave (CW) mode. The SC linac is segment into five sections in order to include warm sections which are designed for specific purpose such as laser heating, diagnostic and bunch compressions. These sections are named as L0, L1, HL, L2 and L3. All sections except HL are composed of 9-cell 1.3 GHz SC TESLA like cavities [2]. HL section consists of 9-cell, 3.9 GHz SC cavities [3]. Number of SC cavities and their nominal operational RF parameters in each section are summarized in Table 1. In order to deal with technological constraints and beam dynamics issues, beam optics of SC linac is continuously evolving. Thus, operational parameters of SC linac shown here (Table 1) may differ than those have been presented elsewhere [4].

In order to generate high brightness coherent light in the range of X-ray, ultra short bunches with high peak current are required in undulator section. Therefore, bunch compression scheme is used to perform linear transformation of longitudinal phase space that reduces bunch length and increases energy spread. However, accelerating section prior to bunch compressor introduces non-linear distortion in longitudinal phase space due to acceleration of beam close to crest of sinusoidal RF field.

*Work supported by Fermi Research Alliance, LLC under Contracts No. De-Ac02-07CH11359 with the DOE, USA.
#asaini@fnal.gov

Table 1: Configuration of each section in SC Linac.

Linac section	Phase (deg)	Gradient (MV/m)	No. of CM's	Avail. cavities	Energy (MeV)
L0	~0	14.78	1	8	0.75-95
L1	-21.0	13.43	2	16	95-303
HL	-165	13.25	3	12	303-250
L2	-21	14.56	12	96	250-1600
L3	0	14.46	18	144	1600-4000

It limits the minimum bunch length that can be obtained in bunch compressor. Non-linear distortion in longitudinal phase space may also be amplified in bunch compressor and it can drive some undesirable collective effects that ultimately influence quality and brightness of X-rays produced in undulator section. Thus, it is essential to cancel non-linear distortion in longitudinal beam phase space prior to a bunch compressor.

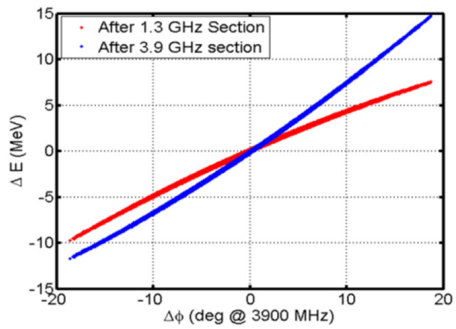


Figure 1: Longitudinal phase space before (red) and after (blue) third harmonic section of LCLS-II SC linac.

It has been studied elsewhere [5] that a short section, using RF accelerating field operating at higher harmonics of field in primary accelerating section, can compensate non-linear distortion up to second order. Nine cell, 3.9GHz (3rd harmonics of 1.3 GHz cavity) SC cavity is used in harmonic section (HL) of LCLS-II SC linac. Figure 2 shows longitudinal phase space of beam at upstream (in red) and downstream (in blue) of HL section. One can easily observe linearization of longitudinal profile after HL section. However, transverse profile of beam may get distorted due to coupler's RF and wake kicks. In this paper, we address impacts of coupler kicks and their local compensation using different orientations of cavity in HL section of LCLS-II SC linac.

COUPLER RF KICK

The third harmonic cavity is developed at FNAL and each 9-cell cavity is equipped with two HOM couplers

Copyright © 2014 CC-BY-3.0 and by the respective authors

HIGH POWER DENSITY TEST OF PXIE MEBT ABSORBER PROTOTYPE

A. Shemyakin #, C. Baffes, Fermilab*, Batavia, IL 60510, USA

Abstract

One of the goals of the PXIE program at Fermilab [1] is to demonstrate the capability to form an arbitrary bunch pattern from an initially CW 162.5 MHz H- bunch train coming out of an RFQ. The bunch-by-bunch selection will take place in the 2.1 MeV Medium Energy Beam Transport (MEBT) [2] by directing the undesired bunches onto an absorber that needs to withstand a beam power of up to 21 kW, focused onto a spot with a ~2 mm rms radius. Two prototypes of the absorber were manufactured from molybdenum alloy TZM and tested with a 28 keV DC electron beam up to the peak surface power density required for PXIE, 17W/mm^2. Temperatures and flow parameters were measured and compared to analysis. This paper describes the absorber prototypes and key testing results.

PXIE ABSORBER CONCEPT AND PROTOTYPING

The PXIE MEBT chopper concept [2] assumes that broadband kickers direct the undesired bunches onto an absorber by shifting them from the "unperturbed' trajectory by 6 rms beam sizes (Fig.1A). The absorber concept [3] features a grazing angle of incidence (29mrad) that decreases the peak absorbed surface power density to 17 W/mm^2; longitudinal segmentation to relieve thermally-induced stresses (Fig.1B); and molybdenum alloy TZM as the choice for the absorbing surface. The power density estimate assumes that 25% of the beam power is reflected.

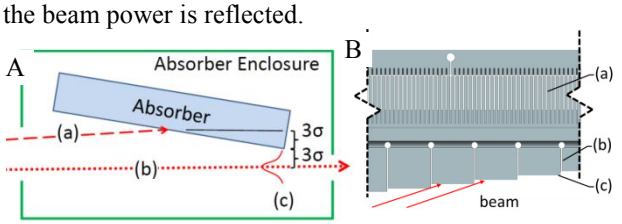


Figure 1: Concept the MEBT absorber. A- separation scheme with (a) chopped beam, (b) passed beam, (c) 6σ shift between the chopped and passed beams. B- absorber concept features: (a) cooling microchannels, (b) stress relive slits, (c) shadowing steps (magnitude exaggerated).

In this design concept, longitudinal heat transfer is interrupted by stress relief slits, and heat flows primarily transversely. Therefore, the risks related to the high surface power density can be addressed with a short prototype. Two such prototypes were manufactured and tested with an electron beam at a dedicated test stand.

* Operated by Fermi Research Alliance, LLC, under Contract DE-AC02-07CH11359 with the U.S. DOE
# shemyakin@fnal.gov

TEST STAND

At the stand (Fig.2), the prototypes were heated by an 27.5keV, typically 0.19A electron beam. The beam size was adjusted by solenoids, and it was positioned by dipole correctors.

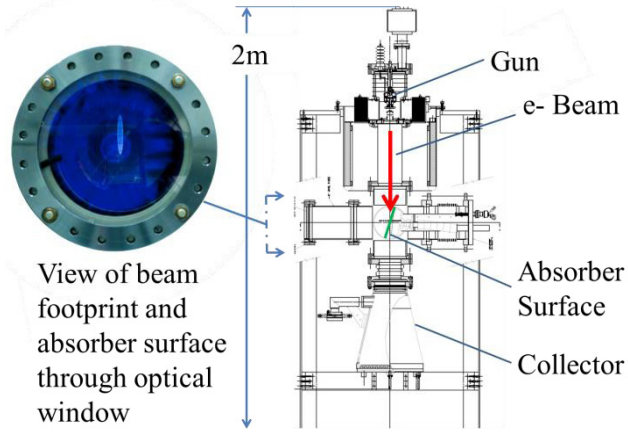


Figure 2: The test stand and OTR beam image

The coolant temperature and flow were measured while the beam was directed either to the prototype or into an effective beam collector. Comparison of caloriemetry in these cases showed that a significant portion of the beam power (~55%) was reflected or carried away in secondary electrons, so the power absorbed in the prototype was ~2.4kW.

The images of the prototype surface were recorded by a TV camera through a quartz viewport. The beam interaction with the surface produces a visible light with intensity proportional to the beam current, which was interpreted as Optical Transition Radiation (OTR). At elevated surface temperatures, the images were dominated by thermal radiation. Recording images with optical filters of different central wavelength allowed separating the broad band OTR signal from typically longer wavelength thermal radiation. While the former provided information about the beam profile, the latter helps to estimate the surface temperature (see details in Ref. [4]). Neutral filters (1% and 10%) were used to increase the dynamic range.

PROTOTYPE I

The absorbing surface of the first prototype (Fig.3) was manufactured from a monolithic TZM. Coolant flows transversely through the absorber body in 300μm wide cooling channels fabricated by EDM. A more comprehensive description of the Prototype I is given in Ref. [4], [5].

Over several months of testing, the beam size was decreased until the peak power density expected for PXIE of 17W/mm2 was achieved over one "fin", a fin being an area of the surface bordered by stress relief slits. In this

Copyright © 2014 CC-BY-3.0 and by the respective authors

ISBN 978-3-95450-142-7

STATUS OF THE WARM FRONT END OF PXIE

A. Shemyakin#, M. Alvarez, R. Andrews, C. Baffes, A. Chen, B. Hanna, L. Prost, G. Saewert, V. Scarpine, J. Steimel, D. Sun, Fermilab*, Batavia, IL 60510, USA
D. Li, LBNL, Berkeley, CA 94720, USA
R. D'Arcy, UCL, London, UK, WC1E 6BT, UK and Fermilab

Abstract

A CW-compatible, pulsed H^- superconducting linac is envisaged as a possible path for upgrading Fermilab's injection complex. To validate the concept of the front-end of such a machine, a test accelerator (a.k.a. PXIE) is under construction. The warm part of this accelerator comprises a 10 mA DC, 30 keV H^- ion source, a 2m-long LEBT, a 2.1 MeV CW RFQ, and a 10-m long MEBT that is capable of creating a large variety of bunch structures. The paper will report commissioning results of a partially assembled LEBT, status of RFQ manufacturing, and describe development of the MEBT, in particular, of elements of its chopping system.

INTRODUCTION

A proposal to upgrade Fermilab's injection complex suggests building a CW SRF H^- linac, which at its initial stage, known as the Proton Improvement Plan –II (PIP-II) [1], will be used in a pulsed mode. Front end components crucial for CW operation will be tested at an accelerator called, for historical reasons, PXIE [2]. PXIE consists of an H^- ion source; a Low Energy Beam Transport (LEBT); a CW 2.1-MeV RFQ; a MEBT; two SRF cryomodules (HWR and a SSR1); a High Energy Beam Transport (HEBT); and a beam dump (Fig.1). This paper describes the status of various components.

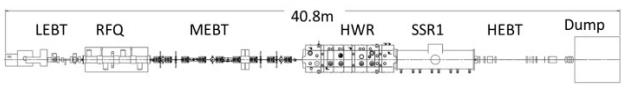


Figure 1: PXIE beamline layout.

LOW ENERGY BEAM TRANSPORT

The LEBT [3] is being commissioned in a straight configuration as depicted in Fig.2 (eventually, it will include a dipole magnet bend). It consists of an H^- volume-cusp ion source [4], 3 solenoids, a chopper assembly and diagnostics.

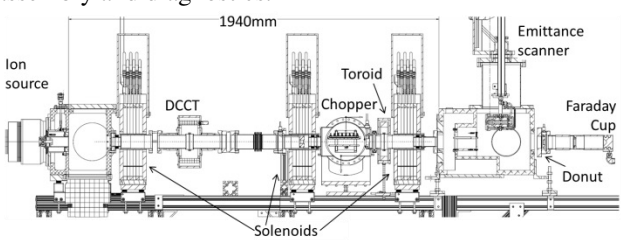


Figure 2. Mechanical schematic of the LEBT.

Each solenoid has a pair of built-in dipole correctors. Vacuum chambers of the first two solenoids contain electrically isolated diaphragms to control the beam neutralization and estimate beam position in combination with the correctors. The beam current is monitored by a DCCT, a current transformer (toroid), and a Faraday cup at the end of the line. Varying the potential of the ion source extraction electrode creates pulsed beam with a pulse length of 0.01 ms – 16 ms at 10 Hz.

All LEBT components, except the chopper, have been recently installed and are operational. Chopper installation is planned for the fall of 2014.

Transverse emittance is measured by an Allison emittance scanner, developed in collaboration with SNS. The scanner operates in both pulse and DC modes. It was commissioned with a one-solenoid LEBT configuration, and some results are shown in Fig. 3.

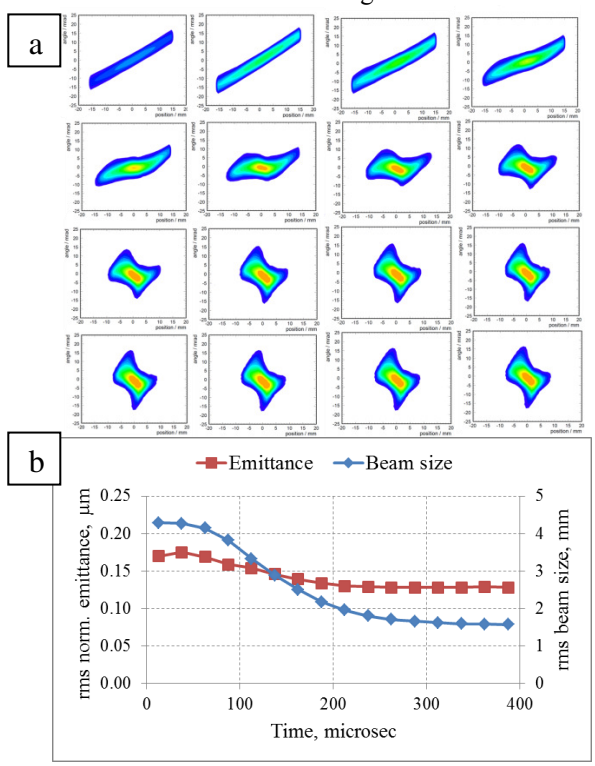


Figure 3: Evolution during a 0.4 ms, 5mA beam pulse. a-phase portraits in 25 μs temporal bins. Vertical axis is ±25mrad, horizontal ±20 mm. The same color represents the same phase density on all plots. b- rms, norm. beam emittance and rms beam size for the same set.

The measured beam emittance is within the ion source specifications and, at low currents, is in agreement with

* Operated by Fermi Research Alliance, LLC, under Contract DE-AC02-07CH11359 with the U.S. DOE
# shemyakin@fnal.gov

Copyright © 2014 CC-BY-3.0 and by the respective authors

RESULT OF COLD TESTS OF THE FERMILAB SSR1 CAVITIES

A. Sukhanov*, M. Awida, P. Berrutti, E. Cullerton, B. Hanna, A. Hocker,
T. Khabiboulline, O. Melnychuk, D. Passarelli, R. Pilipenko, Yu. Pischalnikov,
L. Ristori, A. Rowe, W. Schappert, D. A. Sergatskov
Fermilab†, Batavia, IL 60510, USA

Abstract

Fermilab is currently building the Project X Injector experiment (PXIE). The PXIE linac will accelerate a 1 mA H^- beam up to 30 MeV and serve as a testbed for validation of Project X concepts and mitigation of technical risks. A cryomodule of eight superconducting RF Single Spoke Resonators of type 1 (SSR1) cavities operating at 325 MHz is an integral part of PXIE. Ten SSR1 cavities were manufactured in industry and delivered to Fermilab. We discuss tests of nine bare SSR1 cavities at the Fermilab Vertical Test Stand (VTS). Recently, one of the SSR1 cavities was welded inside a helium jacket. Results of the test of this cavity in the Fermilab Spoke Test Cryostat (STC) are shown. We report on the measured performance parameters of SSR1 cavities achieved during the tests.

INTRODUCTION

The Proton Improvement Plan (PIP)-II project (essentially equivalent to Stage 1 of Project X) is under development at Fermilab [1]. In order to validate the concept of Project X and mitigate technical risks, Fermilab is designing and building the Project X Injector Experiment (PXIE), which will accelerate a 1 mA beam of H^- ions up to 30 MeV [2]. The final stage of acceleration in PXIE is performed by a cryomodule of eight superconducting RF Single Spoke Resonators of type 1 (SSR1) operating at 325 MHz [3]. For the PXIE application, SSR1 cavities are required to have 2.4 MeV maximum energy gain per cavity, corresponding to the accelerating gradient $E_{\rm acc} = 12$ MV/m, and to have a quality factor $Q_0 \geq 5 \times 10^9$. The assembled cavity, jacketed in a helium vessel with tuner, is required to have a frequency sensitivity to LHe pressure variations of less than 25 Hz/Torr.

Results of high gradient tests of two prototype SSR1 cavities have been reported elsewhere [4]. Another ten SSR1 cavities have been recently manufactured by C.F. Roark [5] and delivered to Fermilab. Details of SSR1 design, manufacturing and mechanical measurements are reported in [6]. We present results of the cold tests of nine SSR1 bare cavities in VTS and one jacketed cavity in STC [7].

CAVITY TESTING AT VTS

The preparation of bare cavities for VTS tests including assembly and installation of instrumentation has been reported elsewhere [8].

The typical sequence for a VTS test is as follows. At the initial stage multipactor (MP) conditioning is performed at 4.4 K. With 150 W of RF power available at VTS, it usually takes from 3 to 8 hours to process most of the MP "barriers". The first production SSR1 cavity was not baked at 120 C before the cold test. Strong MP was observed, which did not completely process away even after 20 hours of conditioning. The cavity was warmed up and baked. In the subsequent cold test all MP was processed in just 3 hours. We incorporated a 48 hour-long 120 C bake as the final step of cavity preparation for cold test. Figure 1 shows the typical behavior of SSR1 cavity during MP conditioning. Strong multipactors were observed at 4.5 and 6.5 MV/m. It took 3.5 hours to clear MP in cavity S1H-NR-107, while in the first test of another cavity, S1H-NR-108, 6.5 MV/m MP was present even after 9 hours of processing. We also observed mild field emission during this test. The cavity was warmed up, re-rinsed and baked at 120 C and then re-tested. During the second test of this cavity all MP barriers were cleared after 4 hours of conditioning.

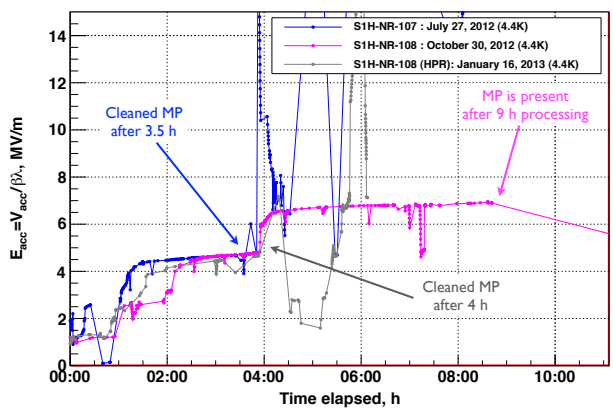


Figure 1: Multipactor processing.

After MP conditioning the cavity is cooled down from 4.4 to 2 K. During cool-down the cavity is usually kept on resonance at low field (2–3 MV/m) and measurements of the cavity frequency shift Δf *vs* LHe bath pressure and of Q_0 *vs* T are performed. Measurement of the slope parameter df/dp of the bare cavity is important for the validation of the computer model, used for the optimization of the sensitivity of the jacketed cavity to the LHe bath pressure variations. Data on the temperature dependence of Q_0 can be used to fine tune the cavity processing procedure.

Results of measurements of the resonance frequency shift Δf as a function of LHe bath pressure are shown in Fig. 2 for two cavities in four separate tests. The curve of Δf *vs*

* ais@fnal.gov
† Operated by Fermi Research Alliance, LLC under Contract No. De-AC02-07CH11359 with the United States Department of Energy.

ISBN 978-3-95450-142-7

Copyright © 2014 CC-BY-3.0 and by the respective authors

A REVIEW OF EMITTANCE EXCHANGER BEAMLINES: PAST EXPERIMENTS AND FUTURE PROPOSALS*

J. Thangaraj†, Fermi National Accelerator Laboratory, Batavia, IL, USA

Abstract

Emittance exchangers (EEX) are advanced phase space manipulation schemes where the transverse phase space of the electron beam is exchanged with the longitudinal phase space. The first experimentally demonstrated concept of the emittance exchange at the A0 photoinjector at Fermilab used a transverse deflecting cavity (TDC) sandwiched between two doglegs. This paper briefly reviews the history of the emittance exchange beamline experiments from a low charge beam without RF chirp to a high charge beam with RF chirp including collective effects such as coherent synchrotron radiation. The paper concludes by discussing future emittance-exchange schemes that have been proposed and proposes two additional schemes that can be implemented in existing modern linacs. As an example, we present an improved emittance exchanger scheme that uses a TDC sandwiched between two chicanes. The significant advantage of this scheme is that it allows the use of the expensive transverse deflecting cavity for diagnostics and still allows the flexibility to use the existing beamline either as a bunch compressor or an emittance exchanger

INTRODUCTION

More than a decade ago, a scheme for exchanging the transverse phase space of the beam with the longitudinal phase space of the beam in a linac was proposed [1]. The original scheme proposed using a transverse deflecting mode cavity placed at the center of a four-dipole chicane. In this scheme, the exchange was not exact: some residual coupling existed even for an ideal zero-length cavity. Another configuration that did an exact exchange of the emittance was then suggested in [2]. This is shown in Fig. 1. In this scheme, the deflecting mode cavity was sandwiched between two doglegs assuming an ideal deflecting mode cavity i.e. the thick-lens effect was not taken into account. The final rms emitances after the emittance exchange beam line can be written as follows:

$$\varepsilon_{x,out}^2 = \varepsilon_z^2 + (\tfrac{17\lambda^2}{40D})^2\langle x'^2\rangle\left[\langle z^2\rangle + \alpha^2 D^2\langle\delta^2\rangle + 2\alpha D\langle z\delta\rangle\right]$$

$$\varepsilon_{z,out}^2 = \varepsilon_x^2 + (\tfrac{17\lambda^2}{40D})^2\langle x'^2\rangle\left[\langle z^2\rangle + \alpha^2 D^2\langle\delta^2\rangle + 2\alpha D\langle z\delta\rangle\right]$$

where αD is the longitudinal dispersion, x', z, and δ are the incoming x-angle, longitudinal position, and energy spread of the beam, respectively, λ is the wavelength of the cavity and D is the dispersion of a single dogleg. In a practical emittance exchange beamline, the thick lens effect of the cavity is always present and so the outgoing emittance is coupled with the incoming emittance to some degree. An experimental implementation of such a scheme was done at the A0 photoinjector facility at 15 MeV [3]. The experiment showed near-ideal exchange at a lower charge. At higher charges, other effects such as the coherent synchrotron radiation (CSR) effects, and space-charge effects start becoming important. CSR studies of the emittance-exchange beamline were reported in [4] . The study pointed out that the bunch length of the beam after the emittance exchange decreased when operated with an RF chirp. Note, this is not only due to the matching of the longitudinal dispersion but also due to the compensation of the thick-lens effect of the deflecting mode cavity. We briefly mention the R-matrix formalism to understand the advantage of the chirped-beam.

Chirping to Reduce the Thick-Lens Effect on the Cavity

The complete R-matrix (x, x', z, δ) of the emittance exchanger, including the finite length of the cavity, can be written as follows:

$$\begin{pmatrix} 0 & \frac{Lc}{4} & \frac{-(4L+Lc)}{4\eta} & \eta-\alpha\frac{4L+Lc}{4} \\ 0 & 0 & \frac{-1}{\eta} & -\alpha \\ -\alpha & \eta-\alpha\frac{4L+Lc}{4} & \frac{\alpha Lc}{4\eta} & \frac{\alpha^2 Lc}{4\eta} \\ \frac{-1}{\eta} & \frac{-(4L+Lc)}{4\eta} & \frac{\alpha Lc}{4\eta^2} & \frac{\alpha Lc}{4\eta} \end{pmatrix}$$

where α is the bending angle of the dipoles, Lc is the length of the deflecting cavity, η is the dispersion of a dogleg, and L the length of the dogleg. When the RF-chirp is set to $\frac{-1}{\alpha\eta}$, the R-matrix is instead written as:

$$\begin{pmatrix} 0 & \frac{Lc}{4} & \frac{-1}{\alpha} & \eta-\alpha\frac{4L+Lc}{4} \\ 0 & 0 & 0 & -\alpha \\ -\alpha & \eta-\alpha\frac{4L+Lc}{4} & 0 & \frac{\alpha^2 Lc}{4\eta} \\ \frac{-1}{\eta} & \frac{-(4L+Lc)}{4\eta} & 0 & \frac{\alpha Lc}{4\eta} \end{pmatrix}$$

As can be seen in the above matrix, both the R_{33} and R_{43} elements are reduced to zero from the original matrix due to the chirp. To first order, this leads to a reduction in the bunch length and the energy spread after the emittance exchanger. In the transverse plane both the R_{13} and R_{23} terms are also reduced due to the chirp indicating possible reduction in beam size and beam divergence as well. A positive side-effect of using a chirped beam is the decrease in the x' after the cavity. Recall that after the cavity, $\Delta x' = \kappa\Delta z$, κ where is the strength of the deflecting cavity set to $\frac{-1}{\eta}$ for EEX. So if we reduce the bunch length at the cavity by adding energy chirp, the beam divergence after the cavity is also reduced

* Fermi Research Alliance, LLC operates Fermilab under contract No. DE-AC02-07CH11359 with the U.S. Department of Energy

† jtobin@fnal.gov

Copyright © 2014 CC-BY-3.0 and by the respective authors

Z-SHAPER: A PICOSECOND UV LASER PULSE SHAPING CHANNEL AT THE ADVANCED SUPERCONDUCTING TEST ACCELERATOR*

J. Thangaraj†, D. Edstrom, A. H. Lumpkin, J. Ruan, Fermilab, IL, USA
B. Beaudoin, University of Maryland, College Park, MD, USA

Abstract

Many accelerator applications require a longitudinally-shaped electron beam profile for studies ranging from THz generation to dielectric wakefield acceleration. An electron beam profile can be shaped through many techniques in both electron beam generation, such as with a DAZZLER or in ellipsoidal pulse generation, and beam transport, using an emittance exchanger or linearizing harmonic cavity. Shaping of a UV pulse with length on the order of picoseconds was demonstrated using alpha-BBO crystals in the Advanced Superconducting Test Accelerator (ASTA) drive laser using this relatively economical solution to effect a predictable and tunable longitudinal bunch shape, profiles have been generated and observed using a Hamamatsu C5680 streak camera, and the results are compared with the analytical theory.

INTRODUCTION

Particle beams are not ideal even under the best of laboratory conditions. The e-beam at ASTA is no exception [1]. There are always fluctuations in the beam density and beam energy. Thus, efforts to model and understand these fluctuations have long been a focus of intense beam research. Typically, these fluctuations appear due to various factors external to the bunch dynamics such as cathode roughness, laser jitter, RF fluctuations and other limitations in the instruments. Recent experiments have shown that a hightbrightness beam along a linac can also be a source of modulations both in energy (introduced primarily by longitudinal space charge impedance) and in density (generated by compression using dispersive elements) [2]. Such effects can adversely affect the beam quality and can create havoc to accelerator operations primarily beam diagnostics. One possible way to understand the effects of such modulation is to deliberately introduce perturbations on the e-beam and study the evolution of the beam along the linac. Shaping electron bunches can be done several ways. To have precise control over the longitudinal bunch profile, shaping is best done by shaping the photocathode drive laser. Ultra-short (fs - ps) laser shaping is a separate field of R&D and a wide variety of techniques are possible. Typically, such techniques are done in the IR and are at kHz repetition rate [3]. For modern accelerators based on superconducting technology, UV pulse shaping based on α-BBO crystal is a cheap, compact, power-efficient technique that is also scalable to MHz repetition rates [4–6]. In this paper, we briefly review the theory behind the technique, describe our experimental results and conclude with a proposal for future experiments.

THE ASTA LASER

The ASTA drive laser is a diode-pumped laser system using either a Yb-Fiber Amplifier seed or a Time Bandwidth Nd:YLF seed at 1054 nm with single-pass amplifiers and conversion stages. The laser (λ = 263 nm) is currently able to deliver UV (100 microseconds limited by permit) to the photocathode at 3 MHz and can deliver up to $\sim$ 5μJ per pulse for up to 3000 pulses in a pulse train. The laser is able to generate up to 81.25 MHz allowing for flexibility through future upgrade. With the measured average QE of 1%, the amount of laser energy is sufficient to generate the ASTA requirement. The schematic of the laser is shown in the Fig. 1 below.

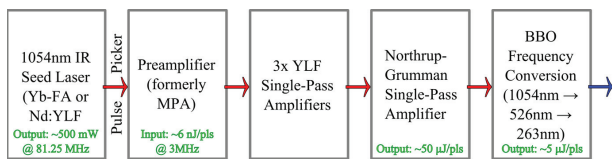


Figure 1: Schematic of the ASTA drive laser system.

THEORY OF PULSE SHAPING

Materials that exhibit anisotropy in the refractive indices for two different polarizations of the incident light are called birefrigent crystals. In such crystals, a temporal separation between the ordinary ray (perpendicular to the optical axis) and the extraordinary ray (parallel to the optical axis) occurs as the light travels through the crystal. The separation is proportional to the group velocity mismatch due to the two different indices of refraction. A very important point to note is that the group index of refraction $n_g = n - n\frac{dn}{d\lambda}$ should be used in this calculation. Therefore, the time separation between the pulses after passing through a crystal of length L can be written as $\delta t = L\frac{\delta n_g}{c}$. In practical units, $\frac{\delta t}{L}$ is equivalent to delay per unit length of the crystal. For an α-BBO crystal at λ =263 nm, the theory along with appropriate Sellenmeir equation predicts a delay of 0.864 ps/mm. Therefore, the distance between the two outgoing pulses is fixed by the length of the crystal which is not a free parameter during the experiment. An illustration for α-BBO is shown in Fig. 2. The pulse length of the individual pulse remains unaffected as the group velocity dispersion along the polarization direction is small. The flexibility of this technique stems from the fact that by rotating the crystal on the plane perpendicular to the direction of propagation,

* Fermi Research Alliance, LLC operates Fermilab under contract No. DE-AC02-07CH11359 with the U.S. Department of Energy
† jtobin@fnal.gov

Copyright © 2014 CC-BY-3.0 and by the respective authors

EFFECT OF CAVITY COUPLERS FIELD ON THE BEAM DYNAMICS OF THE LCLS-II INJECTOR*

A. Vivoli†, A. Lunin, A. Saini, N. Solyak, FNAL, Batavia, IL 60510, USA
D. Dowell, Z. Li, T. Raubenheimer, J. F. Schmerge, T. Vecchione, F. Zhou,
SLAC, Menlo Park, CA 94025, USA
D. Filippetto, R. Huang, C. Papadopoulos, H. Qian, S. Virostek, R. Wells,
LBNL, Berkeley, CA 94720, USA
A. Bartnik, I. Bazarov, B. Dunham, C. Gulliford, C. Mayes,
CLASSE, Cornell University, Ithaca, NY 14853, USA

Abstract

LCLS-II is a new light source based on a continuous wave (cw) superconducting linac to be built at SLAC. The Injector section of the linac creates the elecron beam and accelerates it up to about 100 MeV. The couplers of the accelerating cavities produce an asymmetric field resulting in a beam offset and, most importantly, in a significant transverse emittance dilution, if not compensated. In this paper we describe the simulations of the LCLS-II injector taking into account the cavity couplers effect and some mitigation techniques to reduce its impact on the beam quality.

INTRODUCTION

The Linac Coherent Light Source II (LCLS-II) project consists in a linac-based, seeded, free electron laser (FEL) with high repetition rate (up to 1 MHz) and broad photon energy range (0.2 KeV-5.0 KeV) to be built in the next few years [1]. The linac will be cw superconducting, working at an RF frequency of 1.3GHz and accelerating the beam up to an energy of 4 GeV. In order to deliver a very high quality beam to the undulators, attention should be paied to the study of the beam dynamics in the Injector [2], comprehensive of beam generation and acceleration up to about 100 MeV. Among the effects that can possibly produce emittance growth at such low energy, consideration is given to the effect of the cavity couplers on the accelerating field. The accelerating structures employed in the Injector are the 1.3 GHz 9-cell TESLA cavities, which have an upstream higher order mode (HOM) power coupler, for damping of higher-order mode power, a fundamental power coupler, to power the cavity, and another HOM coupler downstream, as shown in Fig. 1.

These couplers results in an axially asymmetric field, that produces an offset of the beam and emittance dilution. Analytic calculation of the RF kicks in these cavities have been carried out [3] with the parameters of the LCLS-II design. In this paper we present the results of tracking simulations and emittance growth estimations from tracking code TraceWin [4], after a preliminary benchmark with tracking code Astra [5] is performed to establish the validity of the results.

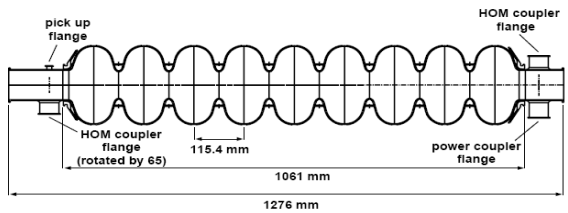


Figure 1: Schematic of the TESLA cavity showing the power and HOM couplers.

SIMULATIONS OF 1-DIMENSIONAL CASE

The study of the RF couplers contribution to the emittance growth was treated independently from the optimization of the layout for the Injector [6]. The latter was done using Astra with 1-dimensional (1D) field maps of the cavities (the values of longitudinal electric field at different points of the longitudinal axis). The study presented here was done taking one of the not optimized lattices under study (layout 1), and replacing the 1D field maps with 3D field maps calculated with Ansoft HFSS and CST Microwave Studio at Fermilab [3], for the Injector design values of Q_{ext} and V_{acc}. The lattice used for the study consists of RF gun, solenoid 1, buncher, solenoid 2 and a cryomodule containing 8 equally spaced cavities. A schematic layout of the injector is reported in Fig. 2.

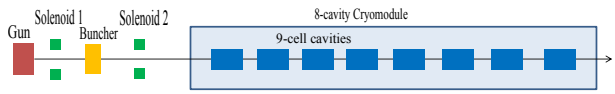


Figure 2: Schematic layout of the injector lattice used in the simulations.

The same 1D field maps of the cavities were used as input to Astra and TraceWin, each code then expanded the field assuming cylindrical symmetry. For simplicity TraceWin simulations concerned only the cryomodule: a first simulation with Astra was run up to around 5 cm from the start of the first cavity, then the output distribution was extracted in

* Work supported by Fermi Research Alliance, LLC under Contract No. De-AC02-07CH11359 with the United States Department of Energy.
† vivoli@fnal.gov

Copyright © 2014 CC-BY-3.0 and by the respective authors

RF DESIGN OF A NOVEL S-BAND BACKWARD TRAVELLING WAVE LINAC FOR PROTON THERAPY

S. Benedetti#, TERA, Novara, Italy and EPFL, Lausanne, Switzerland
A. Degiovanni, A. Grudiev, W. Wuensch, CERN, Geneva, Switzerland
U. Amaldi, TERA, Novara, Italy

Abstract

Proton therapy is a rapidly developing technique for tumour treatment, thanks to the physical and dosimetric advantages of charged particles in the dose distribution. Here the RF design of a novel high gradient accelerating structure for proton linacs is presented. The design discussed hereafter represents an unicum thanks to the accelerating mode chosen, a 2.9985 GHz backward travelling wave mode with 5π/6 phase advance, and to the RF design approach. The prototype has been designed to reach an accelerating gradient of 50 MV/m, which is more than twice that obtained before [1]. This would allow a shorter linac potentially reducing cost. The complete 3D RF design of the full structure for beta equal to 0.38 is presented.

INTRODUCTION

A collaboration between the TERA Foundation and CLIC has been established to study a novel linear accelerator for proton therapy. The main goal of the collaboration is to transfer the knowledge acquired by the CLIC group, mostly in terms of RF design, high-gradient limitations and linac optimization, to a medical linac. As a result, a low-β structure with an expected accelerating gradient of 50 MV/m has been designed, double that of the gradient reached in equivalent linacs. This design result (high-power tests have not been made yet) is based on a novel RF design approach, which will be discussed in detail in this paper. The KT – Knowledge Transfer – group of CERN has funded the construction of a first prototype of the structure, which will be produced and tested at high power at the beginning of 2015.

This accelerating structure is part of the TULIP project, a single room facility for proton therapy with the unique feature of having a linac mounted on a rotating gantry [2]. In this perspective, the high gradient structure hereafter presented remarkably improves the compactness and lightness of the rotating mechanism, with benefits in terms of cost and reliability.

REGULAR CELL DESIGN

The electromagnetic coupling between cells has been accomplished magnetically by means of magnetic *coupling holes* at the periphery of the cells. N*ose cones* are added to enhance the electric field near the axis and thus the transit time factor for the low beta structure. The regular cell geometry is shown in Fig. 1.

stefano.benedetti@cern.ch

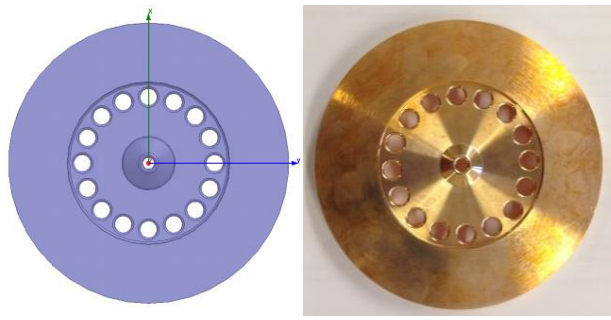


Figure 1: Regular cell design; 3D model (left) and copper piece (right) used in the creep test.

A local field quantity which predicts the high gradient performance of an accelerating structure is the modified Poynting vector S_c, defined in [3]. It has a limiting value of about 4MW/mm^2 at a pulse length of 200 ns and for a breakdown rate (BDR) of 10^{-6} bpp/m (BDs per pulse per meter). This limit is used in the design of the linac (which is approximately 6 m long) in order to have less than one BD per treatment session. By re-scaling these data to the pulse length typical of medical linacs, i.e. 2.5 μs flat-top, a limit quantity of S_c/E_a^2 – where E_a is the average accelerating gradient – lower than $7\cdot10^{-4}$ A/V has been found.

The goal of the regular cell design has been to minimize the value of S_c and at the same time the amount of RF power for a given accelerating field, i.e. the quantity:

$$\mu \equiv \frac{P_w}{E_a^2}\cdot\frac{S_c}{E_a^2} = \frac{v_g}{\omega}\cdot\frac{S_c/E_a^2}{R'/Q}, \qquad (1)$$

where ω is the angular RF frequency, R' is the effective shunt impedance per unit length and Q is the quality factor of the cell. Eq. (1) equally weights the dissipated power and the modified Poynting vector; thus, minimizing μ one obtains for a given power the highest accelerating gradient with a low BD risk.

The optimum is found when Eq. (1) is minimized simultaneously on the nose, where the electric field is maximum, and on the coupling slot, where the magnetic field is maximum, as shown in Fig. 2.

A parametric study has been performed varying the cell gap, cone angle and phase advance per cell. The thickness of the iris has been carefully studied as well. The thinner the iris, the higher the shunt impedance is, but also the lower the mechanical resistance of the structure and the

Copyright © 2014 CC-BY-3.0 and by the respective authors

B*ERL*inPro SRF GUN NOTCH FILTER INVESTIGATIONS*

E. Zaplatin, Forschungszentrum Juelich, Germany,
J. Knobloch, A. Neumann, Helmholtz-Zentrum Berlin, Germany

Abstract

B*ERL*inPro is an ERL project currently under construction to demonstrate energy recovery with a high-brightness, short pulse beam and very low beam loss [1]. These goals place stringent requirements on the SRF cavity (1300 MHz, β=1) for the photo injector, which has to deliver a small emittance 100 mA beam with at least 1.8 MeV kinetic energy while limited by fundamental power coupler performance to about 230 kW forward power.

The SRF gun cavity features 1.4 λ/2 cell resonator with a normal-conducting CsK_2Sb cathode. To prevent RF power propagation from the cavity cells down the cathode stalk and to reduce its component heating a high-frequency notch filter was investigated. We present results of different schemes of choke-cell combinations to optimize the filter parameters. The goal for the filter design was RF power attenuation better than -30 dB in the required frequency range.

INTRODUCTION

SRF guns represent a merging of the well-established normal conducting RF (NCRF) technology and superconductivity. Different approaches are being applied to overcome additional difficulties encountered in the SRF gun development as compared to NCRF guns. One of the main problems is that a cathode expected to have a limited lifetime. Hence, it is advantageous to stick to a technical design of the SRF gun where the cathode can be easily and quickly removed and substituted by a fresh one.

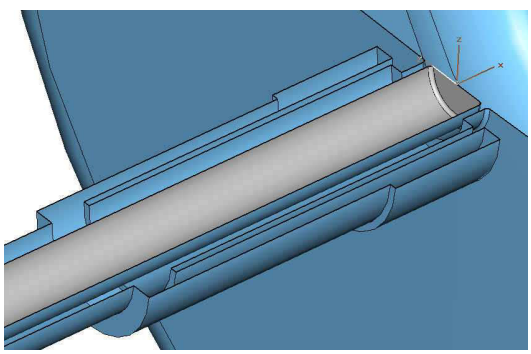


Figure 1: External coaxial quarter-wave length chokes design.

In projects with removable cathodes there is a risk for RF power leaking out of the cavity along the cathode channel (i.e., the mechanical gap between the cathode and the gun cell body that build a coaxial RF line). For this reason, different types of choke filters to reject the accelerating mode's RF power.

In signal processing, a band-stop filter or band-rejection filter or notch filter is a filter that passes most frequencies unaltered, but attenuates those in specific range to very low levels. A notch filter, usually a simple LC circuit, is used to remove or greatly reduce a specific interfering frequency. Series and parallel resonant circuits can be used to construct the band-pass and band-stop filter circuits.

This paper will briefly review the RF designs of the coaxial quarter wave chokes, the resonant choke cell and their combination to achieve the most effective RF power attenuation (better than –30 dB) in the wide frequency notch filter bandwidth.

GUN CAVITY WITH COAXIAL CHOKE STRUCTURE

The quarter wave choke, as shown in Fig. 1, represents a resonance quarter wavelength coaxial transmission line connected in parallel with a gun cathode line. Such systems were implemented, for example, in BNL's photoinjector [2]. Having zero input impedance such choke shunts the cathode line and prevents the distribution of RF power from the cavity along the cathode line. This substantially reduces the cathode heating.

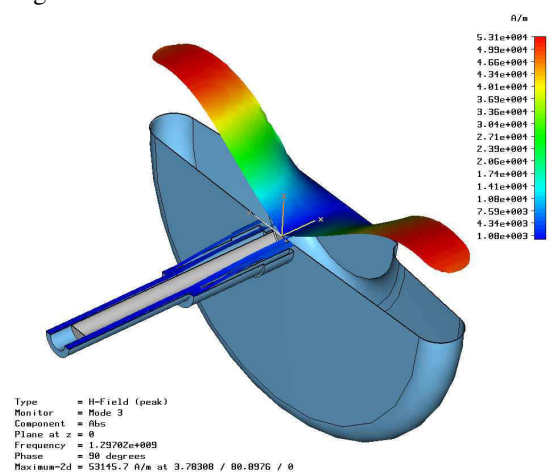


Figure 2: Magnetic field distribution in half-cell and external coaxial quarter-wave length choke.

The magnetic field distribution in half-cell and external quarter wave choke is shown on Fig. 2. There are two options of the quarter wave choke design – external (Fig. 3a) relative to the cathode line and internal (Fig. 3b). The S_{21}-parameter defining the efficiency of the choke (Fig. 4)

*Work supported by Bundesministerium für Bildung und Forschung and Land Berlin

ISBN 978-3-95450-142-7

Copyright © 2014 CC-BY-3.0 and by the respective authors

BEAM DIAGNOSTICS LAYOUT FOR THE FAIR PROTON LINAC

T. Sieber#, M. Almalki, C. Dorn, J. Fils, P. Forck, R. Haseitl, W. Kaufmann, W. Vinzenz, M. Witthaus, B. Zwicker, GSI, Darmstadt, Germany
C. Simon, CEA-Saclay, Gif-sur Yvette, France

Abstract

The planned proton Linac for FAIR (Facility for Antiproton and Ion Research) will be – additionally to the existing GSI UNILAC – a second injector for the FAIR accelerator chain. It will inject a 70 MeV, (up to) 70 mA proton into the SIS18.

The beam diagnostics system for the proton Linac comprises nine current transformers for pulse current determination and fourteen BPMs for position, mean beam energy and relative current measurement. SEM-Grids and stepping motor driven slits will be used for profile as well as for emittance measurements. A wire based bunch shape monitor is foreseen, additionally a bending magnet will be used for longitudinal emittance determination during commissioning.

Presently main efforts are conducted concerning the BPM system. Detailed signal simulations with the finite element code CST are performed. An electronics board using digital signal processing is evaluated by detailed lab-based characterization and beam-based measurements at the UNILAC. In this paper we present the general layout and status of the diagnostics system as well as key results from our measurements and simulations.

INTRODUCTION

The FAIR [1] facility, which is currently under construction at GSI/Darmstadt, is designed to provide antiproton and ion beams of worldwide unique intensity and quality for fundamental physics research.

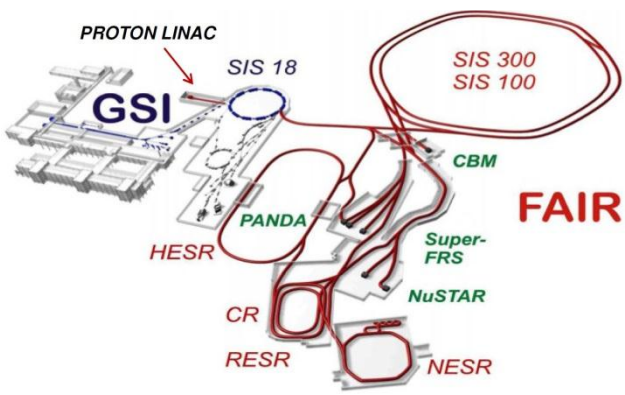


Figure 1: Layout of the FAIR facility.

The accelerator of FAIR comprises two injector Linacs, the existing UNILAC (including a separate high charge state injector) and the new proton Linac. Both Linacs inject into the SIS18 synchrotron, which is again an injector for the SIS100, the central accelerator component of FAIR.

Several upgrade steps of the UNILAC have already been performed or are currently under progress to match the beam requirements at FAIR. While the UNILAC can provide a unique variety of ions for nuclear and atomic physics, the proton Linac will provide the beam for the antiproton production chain. It will consist of an RFQ followed by two 10m sections of Cross Bar H-drifttube accelerators (CH structures). The first section includes six CH modules, which are pairwise rf-coupled. The second section consists of three separate modules, each one having its own klystron.

The proton Linac will deliver a beam current up to 70 mA at a macropulse length of 36 µs and a typical bunch length of 100 ps. The design energy is 70 MeV [2,3]. Figure 2 shows a schematic of the proton Linac, including beam diagnostics.

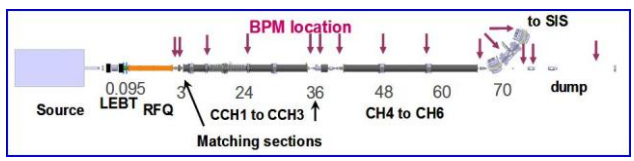


Figure 2: The FAIR proton Linac, showing the positions of the BPMs and particle energies.

BEAM DIAGNOSTICS LAYOUT

The beam diagnostics system of the p-Linac will be - due to the compact structure of the two CH sections - concentrated in the LEBT, behind the RFQ (rebuncher section) and in a diagnostics/rebuncher beamline between the CH sections. Behind the accelerator, beam diagnostics elements are placed in the transfer line to the SIS18 as well as in a straight line in the beamdump. An exception to this rule are the Beam Position Monitors (BPMs). Four of them will be installed between the CH modules, together with the magnetic triplet lenses.

Fourteen BPMs in total will be used for measurement of position, energy and relative current. The pulse current will be determined by nine current transformers. Secondary electron emission (SEM)-Grids and slits will be used for profile and emittance measurements. For determination of longitudinal emittance a wire based bunch shape monitor is foreseen in combination with a bending magnet (during commissioning).

In the LEBT charge state analysis will be performed with a Wien Filter, while the emittance is measured with an Allison scanner. Table 1 shows the diagnostics system at one glance.

#T.Sieber@gsi.de

Copyright © 2014 CC-BY-3.0 and by the respective authors

ACCELERATION OF INTENSE FLAT BEAMS IN PERIODIC LATTICES

L. Groening, C. Xiao, GSI, Darmstadt, Germany
I. Hofmann, TU-Darmstadt, Darmstadt, Germany

Abstract

Recently a scheme for creation of flat ion beams from linacs has been proposed to increase the efficiency of multi-turn-injection. The proof of principle experiment shall be performed at GSI in Summer 2014. Since the scheme requires charge stripping, it may be necessary to perform the round-to-flat transformation prior to acceleration to the final energy of the linac. This requires preservation of the beam flatness during acceleration along the drift tube linac. This contribution is on simulations of acceleration of flat beams subject to considerable space charge tune depression. It is shown that the flatness can be preserved if the transverse tunes are properly chosen and if mismatch along inter-tank sections is minimized along the DTL.

MOTIVATION

GSI is currently constructing the Facility for Antiproton and Ion Research (FAIR). The existing UNILAC [1] will serve as injector of primary beams. As reference ion serves $^{238}U^{28+}$ to be delivered by the UNILAC with pulsed electrical current of 15 mA at the injection into the subsequent synchrotron SIS18. The latter applies the horizontal multi-turn injection scheme. As a consequence the injection acceptances in the transverse planes differ, i.e. they are, in terms of normalized total emittances, about 1.0 mm mrad in the horizontal plane and about 3.0 mm mrad in the vertical plane. Although the injection acceptance is flat, the beams delivered from linacs are usually round. Round-to-flat transformation of linac ion beams should be an appropriate tool to significantly increase injection efficiency into flat-injection-acceptance accelerators.

FLAT BEAM GENERATION

A round-to-flat adapter for linacs has been proposed in [2, 3] and was recently tested with beam at GSI [4]. The adapter comprises a charge state stripping foil installed in the center of a solenoid followed by a skew quadrupole triplet. Stripping inside the solenoid changes the transverse eigen-emittances [5] of the beam and creates inter-plane correlations. Skew quadruplets remove these correlations while leaving the eigen-emittances unchanged. The adapter has the very convenient feature, that it provides at its exit beams with constant Twiss parameters β and α in all planes, while the transverse emittance ratio ϵ_y/ϵ_x can be varied just through the solenoid field strength [6].

As the reference ion for FAIR is $^{238}U^{28+}$, the adapter must be installed where the charge state $^{238}U^{28+}$ is created by gaseous stripping of a $^{238}U^{4+}$ beam at 1.4 MeV/u. This gaseous stripper is installed prior to GSI's Alvarez type DTL. Accordingly, stripping prior to the DTL imposes the challange to accelerate an intense beam of unequal transverse emittances without significant degradation of the beam quality, i.e. transmission, emittance ratio, and absolute emittance values.

ACCELERATION ALONG SYMMETRICALLY FOCUSING DTL

The Alvarez type DTL of GSI's UNILAC (Fig. 1) accelerates all ions from protons to uranium from 1.4 MeV/u to 11.4 MeV/u. It comprises five rf-tanks. Along each tank

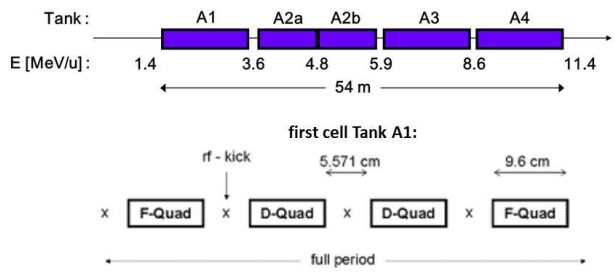


Figure 1: Scheme of the DTL (top) and its first cell (bottom).

transverse symmetric FFDD-focusing is applied, i.e. the two undepressed tunes are equal in the horizontal and the vertical plane. Emittance growth mitigation along the first tank by proper 3d-envelope matching including space charge has been demonstrated experimentally [7]. However, the inter-tank sections just apply DFD-focusing without any longitudinal focusing. Accordingly, each of the four inter-tank sections is a seed of emittance growth from envelope mismatch. The design of the DTL is from the 1970ies and space charge forces were not an issue at that time. Previous works [7] have shown that beams being space charge equivalent to 15 mA of $^{238}U^{28+}$ are accelerated with minimized emittance growth if the transverse zero current phase advance $\sigma_{\perp 0}$ of 70° is applied. The undepressed longitudinal phase advance of 44° is given by the synchronous phase of -30° along the first three tanks and -25° along the last two tanks. In the following we assume 15 mA of beam current and as initial normalized longitudinal rms-emittances in front of the DTL 0.052 deg mrad, referring to the rf-frequency of 108 MHz and to relative momentum spread.

Firstly, the sensitivity of the periodic solution w.r.t. the amount of flatness (transverse emittance ratio) was investigated. For emittance ratios ranging from 1 to 8 the periodic solutions have been calculated including space charge. They are listed in Tab.1. The dependence of the periodic solution from the amount of flatness is quite weak implying that re-matching of the envelope Twiss parameters β and α in all three planes for each transverse emittance ratio can be skipped in practice. This feature together with

Copyright © 2014 CC-BY-3.0 and by the respective authors

STATUS OF THE SPP RFQ PROJECT

G. Turemen*, B. Yasatekin, Ankara University, Ankara, Turkey
H. Yildiz, Istanbul University, Istanbul, Turkey
A. Alacakir, TAEK-SANAEM, Ankara, Turkey
G. Unel, UCI, Irvine, California, USA

Abstract

The SPP project at TAEK will use a 352.2 MHz 4-vane Radio Frequency Quadrupole (RFQ) to accelerate $H+$ ions from 20 keV to 1.5 MeV. With the design already complete, the project is at the test production phase. To this effect, a so called "cold model" of 50 cm length has been produced to validate the design approach, to perform the low power RF tests and to evaluate possible production errors. This study will report on the current status of the low energy beam transport line (LEBT) and RFQ cavity of the SPP project. It will also discuss the design and manufacturing of the RF power supply and its transmission line. In addition, the test results from some of the LEBT components will be shown and the final RFQ design will be shared.

INTRODUCTION

SANAEM[1] Prometheus Project aims to construct a proton beamline including an ion source, a Proof Of Principle (POP) RFQ and the appropriate diagnostic stations [1]. The POP machine has the humble requirements of accelerating 1 mA of beam current to an energy of 1.5 MeV. The entire system is to be designed and built in Turkey, with the main goal of training young accelerator physicists and RF engineers on the job and to involve the local industry in accelerator component construction. The project design and construction is planned to last for 3 years, and it is to start operation by the end of 2015.

STATUS OF THE SPP BEAMLINE

The SPP project will construct an ion source, a low energy beam transport (LEBT) section including diagnostics at keV level, an RFQ receiving power from an RF Power Supply Unit (PSU) via a transfer line, a MeV level diagnostics and finally a beam dump. The RFQ operating frequency will be 352.2 MHz. The beamline will be sitting on a locally designed and built pedestal. The cooling for the RF components, ion source, magnets and the cavity will be provided by a 40 kW closed loop chiller. The chiller and the pedestal supporting the ion source and two solenoid magnets are installed in the experimental area.

Ion Source, LEBT and Diagnostic Stations

The ion source and LEBT design was discussed extensively elsewhere [2]. Here we mostly report on the ongoing construction and installation processes. The ion source, as well as the first (Sol-M) of the two LEBT solenoids (Sol-M and Sol-L) are installed together with the vacuum and cooling connections as it can be seen on Fig. 1. While waiting the delivery of the "measurements box", current and stability tests are performed with a simple Faraday cup (FC) for two different ion source configurations (RF antenna and DC filament). Also the stability (magnetic field) tests are done for LEBT solenoids. Measured time required for Sol-M and Sol-L to reach steady state are approximately 111 and 105 minutes respectively.

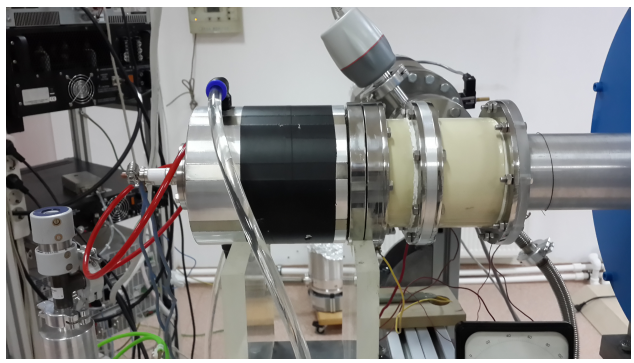


Figure 1: Ion source during the tests.

The measurements box will be located between the two solenoids and it will contain a FC, a pepper-pot filter for emittance measurements and a scintillator screen. All components will be motor controlled such that they can be pushed in and out of the beam independently. Figure 2 shows the measurement box and its components in parking position.

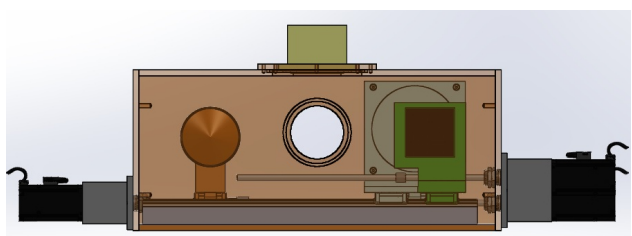


Figure 2: Measurement box design.

SPP RFQ Design Studies

Two different RFQs of various properties, designed with LIDOS [3] and cross checked with DEMIRCI [4] and TOUTATIS [5] software packages, are shown in Table 1. The property of primary importance will be the RFQ length as by the time of this note, no brazing furnace of appropriate length is available in Turkey. Therefore while waiting for

* gorkem.turemen@ankara.edu.tr
[1] SANAEM is one of the two research centers of TAEK, Turkish Atomic Energy Agency.

Copyright © 2014 CC-BY-3.0 and by the respective authors

ISBN 978-3-95450-142-7

COLD POWER TESTS OF THE SC 325 MHz CH-CAVITY*

M. Busch†,1, F. Dziuba[1], H. Podlech[1], U. Ratzinger[1], M. Amberg[2]
[1]IAP Frankfurt University, 60438 Frankfurt am Main, Germany
[2]Helmholtz-Institut Mainz (HIM), 55099 Mainz, Germany

Abstract

At the Institute for Applied Physics (IAP), Frankfurt University, a superconducting 325 MHz CH-Cavity has been designed and built and first tests have successfully been performed. The cavity is determined for a 11.4 AMeV, 10 mA ion beam at the GSI UNILAC. Consisting of 7 gaps this resonator is envisaged to deliver a gradient of 5 MV/m. Novel features of this structure are a compact design, low peak fields, improved surface processing and power coupling. Furthermore a tuner system based on bellow tuners attached inside the resonator and driven by a stepping motor and a piezo actuator will control the frequency. In this contribution measurements executed at 4.2 K and 2.1 K at the cryolab in Frankfurt will be presented.

INTRODUCTION

Various international projects demand high beam power, quality and availability, e.g. MYRRHA (**M**ulti Purpose H**Y**brid **R**esearch **R**eactor for **H**igh-Tech **A**pplications) [1] and the planned GSI/ HIM advanced s.c. cw Heavy Ion Linac [2]. For the low-β region of such linacs the superconducting CH-cavity has proved to be an appropiate structure being characterized by a small number of drift spaces between adjacent cavities compared to conventional low-β ion linacs [3]. Additionally the KONUS beam dynamics, which decreases the transverse rf defocusing and allows the development of long lens free sections, yields high real estate gradients with moderate electric and magnetic peak fields. At the Institute for Applied Physics, Frankfurt University, a new cavity operating at 325.224 MHz, consisting of 7 cells, β = 0.16 and an effective length of 505 mm (see table 1) has been designed [4] and measured after fabrication and processing at Research Instruments [5].

Table 1: Specifications of the 325 MHz CH-Cavity

β	0.16
frequency [MHz]	325.224
no. of cells	7
length ($\beta\lambda$-def.) [mm]	505
diameter [mm]	352
E_a (design) [MV/m]	5
E_p/E_a	5
B_p/E_a [mT/(MV/m)]	13
G [Ω]	66
R_a/Q_0	1260
R_aR_s [$k\Omega^2$]	80

* Work supported by GSI, BMBF Contr. No. 06FY7102
† busch@iap.uni-frankfurt.de

MEASUREMENT SETUP

At the cryolab of the IAP a measurement setup comprising a vertical cryostat has been installed for various test purposes (see Fig. 1) allowing power measurements at 4 K and 2 K, respectively. The vaporized Helium can be extracted via a port to a recovery system or the cryostat can be pumped out by a roots pump to achieve 2 K (see Fig. 4). The CH-cavity has been provided with four low-temperature probes, 40 **T**hermo-**L**uminescence-**D**osimeter (see Fig. 2) to record field emission events and two piezos for microphonic excitation and detection. Figure 3 shows the equipment for the measurements particularly the 500 W broadband amplifier (left) and the control system (centered).

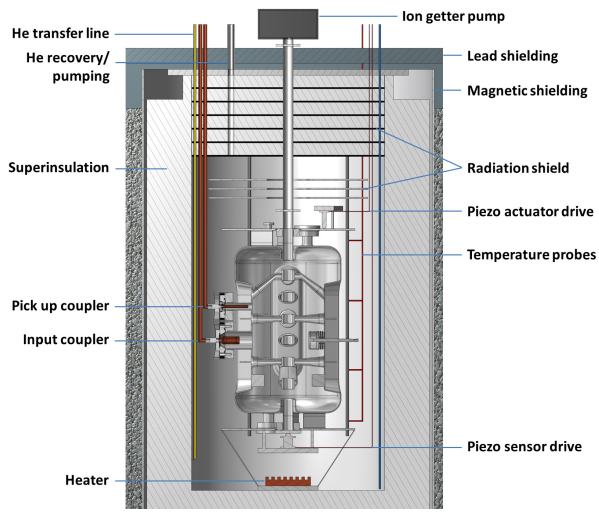


Figure 1: Schematic layout of the vertical croystat setup.

PERFORMANCE RESULTS

After one week of conditioning low multipacting barriers and achieving a pressure of $6 \cdot 10^{-10}$ mbar measurements up to the quench of the cavity have been performed. Figure 4 pictures five different Q vs. E curves beginning with the first test in January 2013 (black curve) [6] with an unprocessed surface and encountering field emission at low fields. The second curve (red) boasts an improvement of the field gradient due to HPR but reveals a Q-value of 10^8 leading to the conjecture of Q-disease. After another thermal cycle with fast cool-down to 4 K ($> 1\,K/min$) the performance improved significantly (blue curve) to gradients up to 8.5 MV/m resulting in voltages of 4.2 MV. Next step was to warm up and bake the cavity at 120°C for 72 h subsequently. The following measurement (purple curve) indi-

Copyright © 2014 CC-BY-3.0 and by the respective authors

ISBN 978-3-95450-142-7

STATUS AND OUTLOOK OF THE 325 MHz 4-ROD RFQ *

B. Koubek†, H. Podlech, A. Schempp, J. S. Schmidt
IAP, Goethe University, Frankfurt, Germany

Abstract

In order to built a Radio Frequency Quadrupole (RFQ) at 325 MHz for the FAIR proton linac, a 4-rod structure has been investigated. The RF design, especially the dipole and fringe fields and higher order modes, have been studied with simulations. A prototype has been built and power tested to verify the simulation results and investigate the high power performance. This paper summarizes the results of the research concerning the 325 MHz 4-rod RFQ and gives an overview about the next steps in this project.

INTRODUCTION

The highest frequency 4-rod RFQs are operating is at 216 MHz. An example is the MedAustron RFQ presented in [2]. At higher frequencies the asymmetries of the 4-rod structure may cause problems in the RF behavior. For example a dipole field overlaying the quadrupole field of the electrodes can lead to a vertical displacement of the beam axis. Usually this effect can be neglected, but it becomes relatively stronger on frequencies above 300 MHz. Also potential disturbing higher order modes (HOMs) need to be investigated at this frequency. In addition a general improvement of the performance of 4-rod RFQs can be achieved through investigations of the fringe fields. Based on these improvements a prototype was built and power tested. Eventually the 4-rod RFQ was compared to other RFQ resonators in terms of operation at 325 MHz.

SIMULATIONS

Dipole

The dipole field is a disturbing field overlaying the quadrupole field component and can shift the beam axis in vertical direction. This field is caused by asymmetries of the 4-rod structure. These asymmetries are resulting from the electrodes mounted at different heights. By comparing one RF cell of a 4-rod RFQ with capacitively shortened Lecher Wires in Fig. 1, the upper electrodes are loaded with to a larger potential than the lower ones. This effect becomes relatively more significant at higher frequencies and hence smaller stem sizes. The basic idea to suppress the dipole field is to align the current paths respectively the charge transport of the left and right side of each stem. This can be done by the stem shape to provide space that magnetic fields can be established and increase the charge transport at the appropriate side of the stem. In addition all other main parameters of 4-rod RFQs have been investigated to study their influence on the dipole field.

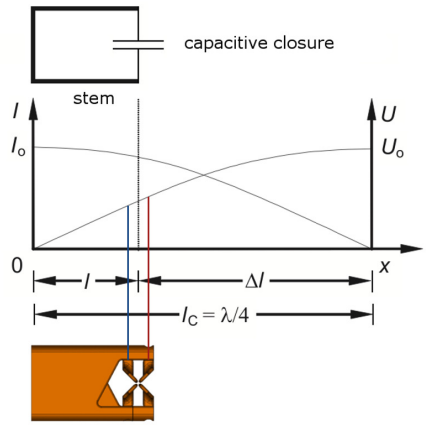


Figure 1: Comparison of a 4-rod RFQ with capacitively shortened Lecher wires.

As an example in Fig. 2 one variation of an angular cutting of the inner stem shape is shown. At one side of the stem the space sorrounding a stem arm is enlarged. The charge transport on the left and right side of the RFQ is balanced and leads to a compensation or even overcompensation of the dipole field. Several other ways of cutting variation were investigated in simulations [1]. Through this investigation a dipole free 4-rod RFQ could be designed and the results have been successfully proven with a prototype.

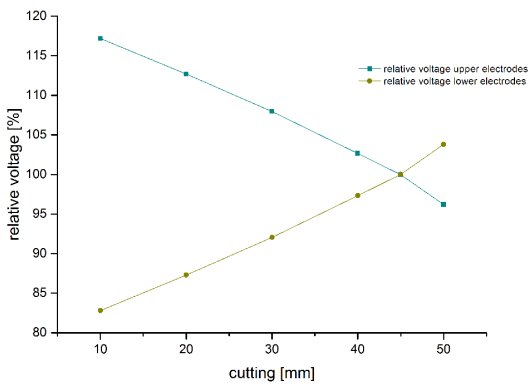


Figure 2: Adjustment and overcompensation of the dipole field by the variation of the angular cutting.

HOMs

If higher order modes (HOMs) are close to the operating modes frequency they might be excited as well and can disturb the operating mode. Usually HOMs are not critical

* Work supported by BMBF & GSI
† koubek@physik.uni-frankfurt.de

Copyright © 2014 CC-BY-3.0 and by the respective authors

ALTERNATIVE COMPACT LEBT DESIGN FOR THE FAIR INJECTOR UPGRADE*

K. Schulte†, M. Droba, S. Klaproth, O. Meusel, D. Noll, U. Ratzinger
Institute for Applied Physics, Goethe-University Frankfurt a.M., Germany
S. Yaramyshev, GSI Helmholtzzentrum für Schwerionenforschung GmbH, Darmstadt, Germany

Abstract

In order to provide high intensity and brightness of the uranium beam for the planned FAIR project, the existing High Current Injector (HSI) at GSI has to be upgraded [1]. A part of the upgrade program is the design and construction of a compact straight injection line into the 36 MHz Radio Frequency Quadrupole of the HSI. As an alternative to a conventional LEBT design consisting of magnetic systems such as solenoids or quadrupoles, the application of Gabor lenses has been investigated.

The focusing force of the Gabor lens is created by the space charge of an electron cloud, confined by crossed magnetic and electric fields inside the lens volume. Therefore, the Gabor lens combines strong, electrostatic focusing with simultaneous space-charge compensation. In previously performed beam transport experiments at GSI a prototype Gabor lens has been tested successfully. Furthermore, the operation and performance of such a device in a real accelerator environment has been studied.

In this contribution an alternative LEBT design will be discussed and an improved Gabor lens design will be presented.

INTRODUCTION

The application of Gabor lenses as an ion optics system has been studied for a long period by different research groups. Due to its strong electrostatic focusing force in combination with the space-charge compensation of high-intensity ion beams the Gabor lens could find effective and relatively low cost application in the low energy beam transport section (LEBT) of heavy linear accelerators [2].

However, the experiments at the Institute for Applied Physics (IAP) in Frankfurt were limited to low intensities and low masses of the provided ion beam. For the first time a prototype Gabor lens was successfully tested with a space-charge dominated 2.2 keV/u Ar^+-beam at GSI in mid-2012 [3].

As a consequence of the previously performed beam transport experiments, the suitability of Gabor lenses as a compact LEBT for the transport of an uranium beam using the example of the existing GSI HSI-Frontend was numerically investigated. Furthermore, a technically improved Gabor lens, which would meet the requirements was designed and a control system to automatically adjust the focusing strength is under development.

* Work supported by HIC for FAIR
† Schulte@iap.uni-frankfurt.de

ION BEAM FOCUSING USING GABOR LENSES

There are several effects that lead to an emittance growth, which shall be discussed for Gabor lens focusing in general.

Chromatic aberrations have a strong influence on the imaging quality since the focal length of the lens is energy dependent and therefore sensitive to variations in beam energy [3]. However, the energy spread of the beam right after the ion source is negligible and usually doesn't contribute to an emittance growth.

Spherical aberrations in case of the Gabor lens differ from conventional, magnetostatic ion optics in the radial trend of the focusing force i.e. the space-charge field of the nonneutral plasma decreases towards its edge. As the beam passes this nonlinear part of the electric field that results from the Debye drop-off of the plasma cloud, aberrations in form of a negative s-shape in the phase space occur (see Fig. 1). This

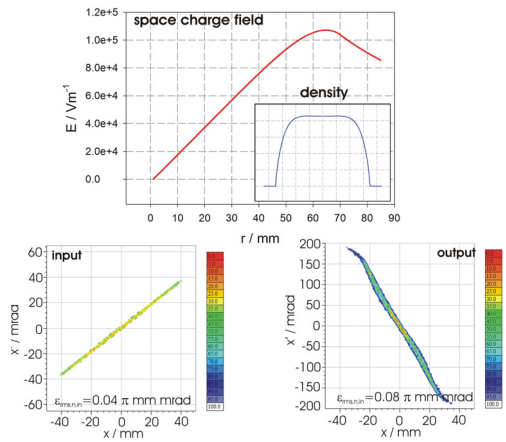


Figure 1: Example of spherical aberrations as a result of beam ions passing the nonlinear part of the electric space-charge field.

effect has a major contribution to an emittance growth.

Besides these well-known effects, an emittance growth is also observed when plasma instabilities arise if the Gabor lens is operated in a regime far from its working point for the electron confinement

$$\Phi_A = \frac{e \cdot R_p^2 \cdot \left(1 + 2 \cdot ln\left(\frac{R_A}{R_p}\right)\right) \cdot B_z^2}{8 \cdot m_e} \quad (1)$$

where Φ_A is the anode potential, R_p the ground radius, R_A the anode radius and B_z the confining magnetic field.

Accordingly, this effect does not contribute if the lens is operated appropriately.

Copyright © 2014 CC-BY-3.0 and by the respective authors

PROPOSAL OF A 325 MHz LADDER-RFQ FOR THE FAIR PROTON-LINAC *

M. Schütt[1], U. Ratzinger[1], R. Brodhage[2]
[1]Institut für Angewandte Physik
Johann Wolfgang Goethe Universität
Frankfurt, Germany
[2] GSI, Darmstadt, Germany

Abstract

Within the scope of the research programm with cooled antiprotons at FAIR a new proton Linac is proposed and beeing designed. The currently operating injectors HLI and HSI are especially designed for high mass to charge ratios but do not deliver enough beam current for the operation with protons, which necessitates a new beam injector optimized for protons. In the low energy section a new RFQ has to be designed working at a frequency of 325 MHz and at an rf duty factor up to $2 \cdot 10^{-3}$. It will accelerate protons from 95 keV to 3 MeV. Basically there are three design options for the RFQ. A 4-Rod, a 4-Vane and a Ladder-type RFQ, which is discussed in this paper. First of all it has neglectable dipole components. The ratio between the electic dipole and quatrupole field is lower than one percent [1]. Furthermore the manufacturing at reasonable costs and production time looks promising. In the following the new layout both from a mechanical and manufacturing point of view as well as a RF tuning concept are shown.

INTRODUCTION

The idea of the Ladder-RFQ firstly came up in the late eighties [2, 3] and was realized successfully for the CERN Linac3 operating at 101 MHz [4] and for the CERN antiproton decelerator ASACUSA at 202 MHz [5]. Within the 4-ROD design the challange is to minimize dipole components and to have geometrical dimensions which are suitable for a mechanical manufacturing and assembling. At frequencies above 250 MHz the 4-Vane-type RFQ is used so far. Many versions for low and high duty factors have been realized successfully until now. Draw backs are the high costs per meter, the compplexity oas well as the challenging RF tuning procedure of that structure: The dipole modes tend to overlap with the quadrupole mode. Safe beam operation conditions are resulting in ambitions mechanical vane tolerances. In the proposed ladder-RFQ version, the stems show an extended height which increases the resonance frequency and which results in an homogeneous current flow towards the mini-vanes. The mini-vanes are embedded via precisely machined carrier rings into the copper shells (see fig.2). To proof the mentioned advantages and realizability of the Ladder RFQ a prototype was designed and beeing built. The result are shown in this paper.

* Work funded by BMBF 05P12RFRB9

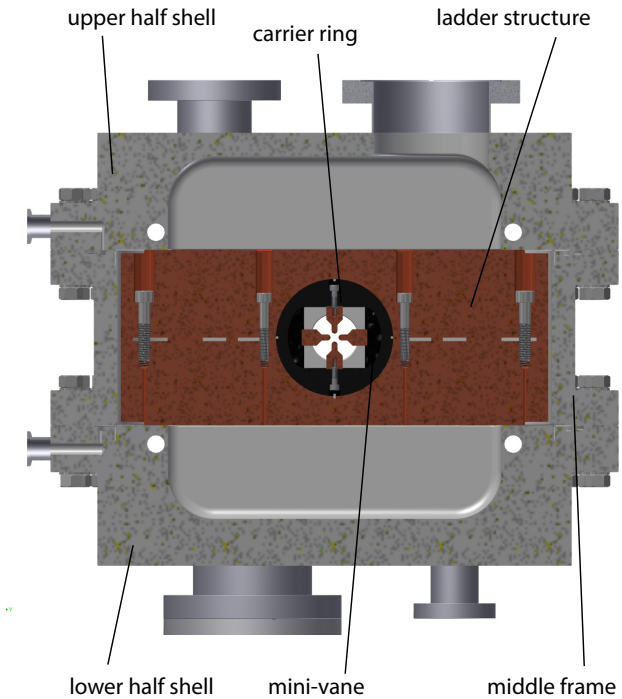


Figure 1: Sectional view through the ladder-structure. The copper carrier-rings (for a better view coloured in black) guarantee the electrode positioning as well as the RF contact.

MECHANICAL LAYOUT

The mechanical design consists of an inner copper ladder structure mounted into an outer stainless steel tank. The tank is devided into a base plate carrying the resonating inner structure, an intermediate part and the cover plate. The base will carry and adjust the position of the resonating structure. Furthermore its task is to provide a vacuum at the level of 10^{-8} mbar. The rf is mainly determined by the resonating structure, while the dimensions of the tank have no significant influence to the frequency.
To lower the wall losses it is foreseen to copperplate the lower and upper half shells. The inner resonating structure consists of two symmetric half shells (see fig.4) made of massive copper. They press and grout the carrier-rings in between. The diameter of the precisely thrilled hole will be slightly shmaller than the carrier-rings ensuring an optimal rf-contact. Both half shells have significantly reduces contact surface areas to imporve the pumping speed and the

Copyright © 2014 CC-BY-3.0 and by the respective authors

bERLinPrO BOOSTER CAVITY DESIGN, FABRICATION AND TEST PLANS

A. Burrill#, W. Anders, A. Frahm, F. Göbel, J. Knobloch, A. Neumann,
Helmholtz-Zentrum Berlin, Berlin Germany
G. Ciovati, P. Kneisel, L. Turlington, Jefferson Laboratory, Newport News, VA, USA

Abstract

The bERLinPro project, a 100 mA, 50 MeV superconducting RF (SRF) Energy Recovery Linac (ERL) is under construction at Helmholtz-Zentrum Berlin for the purpose of studying the technical challenges and physics of operating a high current, c.w., 1.3 GHz ERL. This machine will utilize three unique SRF cryomodules for the injector, booster and linac module respectively. The booster cryomodule will contain three 2-cell SRF cavities, based on the original design by Cornell University, and will be equipped with twin 115 kW RF power couplers in order to provide the appropriate acceleration to the high current electron beam. This paper will review the status of the fabrication of the 4 booster cavities that have been built for this project by Jefferson Laboratory and look at the challenges presented by the incorporation of fundamental power couplers capable of delivering 115 kW. The test plan for the cavities and couplers will be given along with a brief overview of the cryomodule design.

INTRODUCTION

Helmholtz-Zentrum Berlin (HZB) is in the process of building a high average current Energy Recovery Linac (ERL) at the site in Adlershof, Berlin Germany.[1, 2] The ERL will utilize all superconducting RF cavities for the generation and acceleration of an electron beam of up to 100 mA average current with a beam energy of 50 MeV in continuous wave (c.w.) operation. Figure 1 shows the layout of the ERL, which is made up of a 1.4 cell SRF photoinjector with normal conducting photocathode, a 3 cavity booster cryomodule to increase the low energy beam from 2 MeV to 6 MeV, and a 3 cavity linac cryomodule which will be used to accelerate and decelerate the 6 MeV beam to 50 MeV and then back to 6 MeV again. This ERL is designed to study the operation of a high current, low emittance electron beam from an SRF photoinjector, and is being built in order to explore the operation of such a machine and the challenges that come from recirculation of a 5 MW beam. The ERL will be operated in several different modes which include operation with bunch charges ranging from a few pC to 77 pC and repetition rates that range from low repetition rate burst modes up to c.w. operation at 1.3 GHz, the fundamental mode of the cavities. This wide range of operating conditions will place great demands on many of the components of the ERL, and will test the limits of the SRF cavities, in particular the photoinjector and the booster cavities, due to the high beam loading condition and the greater than 200 kW that needs to be delivered to each cavity.[3-5]

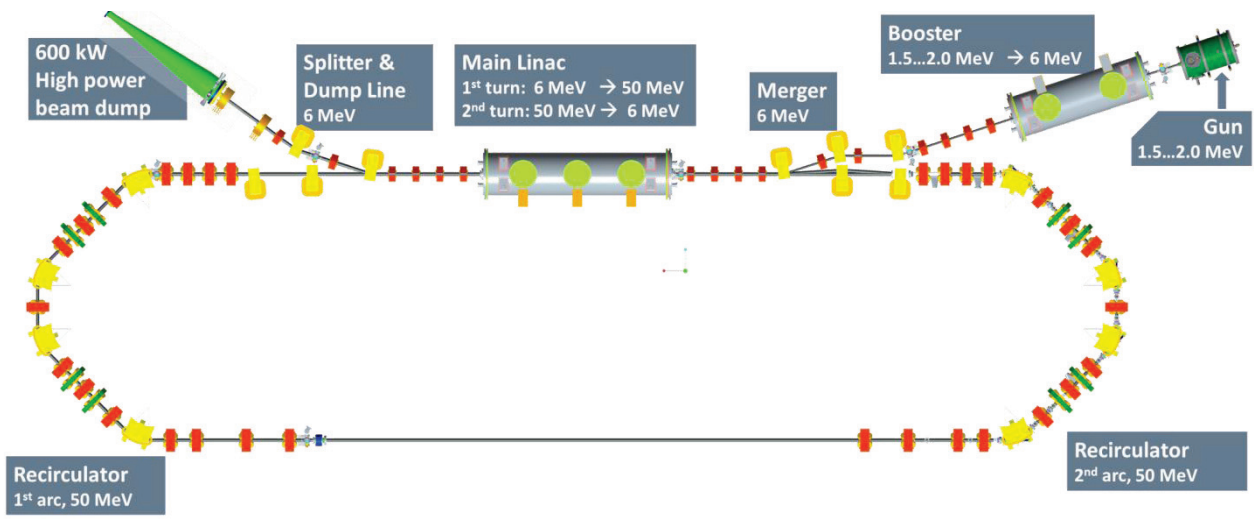


Figure 1: The bERLinPro Energy Recovery Linac machine layout.

#aburrill@helmholtz-berlin.de

ISBN 978-3-95450-142-7

Copyright © 2014 CC-BY-3.0 and by the respective authors

CAVITY EXCITATION OF THE CHOPPED BEAM AT THE J-PARC LINAC

K. Futatsukawa#, KEK, Tsukuba, Ibaraki, Japan

Abstract

In the J-PARC linac, the beam energy injected into Rapid-Cycle Synchrotron (RCS) was upgraded up to 400 MeV by the installation of 25 Annular-ring Coupled Structure (ACS), in 2013. The initial frequency of RCS was shifted to 1.227 MHz in order to change the velocity of the injection beam. In the linac, the beam is chopped as the comb-like structure with this frequency by the RF deflector. This chopped beam excited the post-coupler mode (PC1) of DTL2 and caused the instability of the RF field. Therefore, the property of this beam excitation was investigated. Additionally, the frequency components of the beams with some thinned structures to tune the beam power and to perform the commissioning were observed to manage the risk of other mode excitation.

INTRODUCTION

J-PARC is one of the highest intensity proton accelerator facilities in the world. It consists of a H^- linac, a 3-GeV Rapid Cycling Synchrotron (RCS), and, a 30-GeV Main Ring synchrotron (MR). The accelerated beam is provided for the wide-ranging applications such as materials and life science, particle and hadron physics, and so on [1].

In the J-PARC linac, the energy of the injection beam to RCS was upgraded from 181 MeV to 400 MeV by the installation of 25 additional Annular-Coupling Structure linac (ACS) modules and 25 new 972-MHz RF systems in the shutdown of 2013 [2]. The 400-MeV acceleration was successfully achieved on January 17th, 2014 and the user operation with the 400-MeV injection energy started from February 17th [3, 4]. In this energy upgrade, the velocity (β) of the injection beam was shifted from 0.55 to 0.71.

In the normal operation of the present J-PARC linac, the width of a macro-pulse is 500 μsec and the repetition rate is 25 Hz. This macro-pulse has the internal structure like a comb, which called an "intermediate-pulse", by the RF deflector to synchronize the initial frequency of RCS. This frequency ($f_{initial}$) is expressed as

$$f_{initial} = \frac{\beta c}{L/N}. \quad (1)$$

Here L, N and βc are circumference (=348 m), number of bunches (=2 in the typical operation) in RCS and the velocity of the injection beam, respectively. Therefore, the frequency of an intermediate-pulse was shifted from 0.939 MHz to 1.227 MHz to upgrade the injection energy. Figure 1 shows the pulse structure of the J-PARC linac.

#kenta.futatsukawa@kek.jp

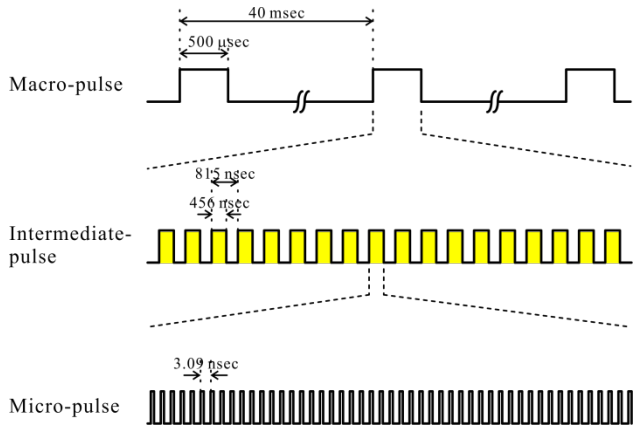


Figure 1: Pulse structure of the J-PARC linac. The frequency of an intermediate-pulse was shifted to 1.227 MHz (815 nsec) due to the energy upgrade of the linac.

DTL2 PC1 EXCITATION

RF properties for the low-level measurement

The second Alvarez-type DTL (DTL2), which consists of 42 full-size drift tubes, 42 post-couplers and 10 fixed tuners, accelerates the H^- beam from 20 to 37 MeV. In order to achieve the stabilized-uniform of the filed distribution for the accelerating mode (TM_{010}), the post-couplers were tuned [5]. Figure 2 shows the dispersion curve of DTL2 for the low-level measurement. The frequency difference of the first post-coupler mode (PC1) from 324 MHz, δf, was −1.2419 MHz.

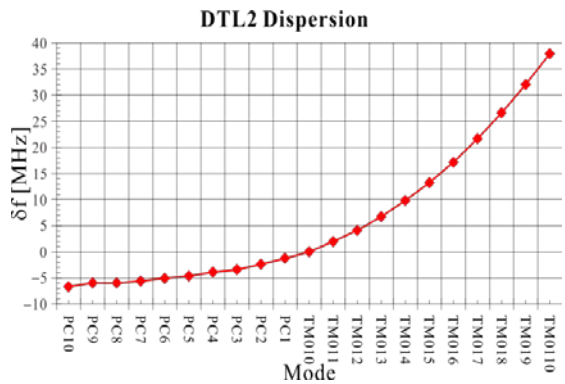


Figure 2: Dispersion curve of DTL2. The frequency of the PC1 mode is δf=−1.2419 MHz against that of TM_{010}.

Excitation by chopped beam

Figure 3 shows the result of the Fast Fourier Transform (FFT) analysis for a pickup signal of DTL2 with the chopped beam by the frequency of 1.227 MHz. Two peaks except for the driven frequency, 324 MHz, by a

Copyright © 2014 CC-BY-3.0 and by the respective authors

ISBN 978-3-95450-142-7

SUPERCONDUCTING NANO-LAYER COATING WITHOUT INSULATOR*

Takayuki Kubo†
KEK, High Energy Accelerator Research Organization, Tsukuba, Ibaraki 305-0801 Japan

Abstract

The superconducting nano-layer coating without insulator layer is studied. The magnetic-field distribution and the forces acting on a vortex are derived. Using the derived forces, the vortex-penetration field and the lower critical magnetic field can be discussed. The vortex-penetration field is identical with the multilayer coating, but the lower critical magnetic field is not. Forces acting on a vortex from the boundary of two superconductors play an important role in evaluations of the free energy.

INTRODUCTION

The multilayer coating is an idea for pushing up the field limit of superconducting (SC) accelerating cavity [1]. According to the recent theoretical studies [2, 3, 4, 5], differences among the vortex-penetration fields of semi-infinite SC, SC thin film and multilayer SC are due to those of current densities or slopes of magnetic-field attenuation which are proportional to the force pushing a vortex into SC. For the case that a penetration depth of the SC layer is larger than that of the SC substrate, the current density or the slope of magnetic-field attenuation in the SC layer is suppressed, and the vortex-penetration field of the SC layer is pushed up.

A combination of SC materials with different penetration depths is essential, but the insulator layer seems to be unnecessary. In this paper, the SC nano-layer coating without insulator layer is studied. First the magnetic-field distribution is computed. Then a set of forces acting on a vortex is derived, which is different from that of the multilayer coating model, because of the existence of the boundary of two SCs as shown in Fig. 1. By using the forces, the vortex-penetration field and the lower critical magnetic field are discussed.

MAGNETIC-FIELD DISTRIBUTION

Let us consider a model with an SC layer with a penetration depth λ_1 and a coherence length ξ_1 formed on an SC substrate with a penetration depth λ_2 and a coherence length ξ_2. All layers are parallel to the y-z plane and then perpendicular to the x-axis. The magnetic field is applied parallel to the layers. We assume the SC layer thickness d is larger than their coherence lengths ($d \gg \xi_1, \xi_2$). The proximity effect between the two SCs. is neglected.

The variational approach is an easy way to understand how the magnetic-field and the current density distribute in the system. Defining magnetic-fields in the SC layer and SC substrate as $B_1(x)$ and $B_2(x)$, respectively, current densities in the SC layer and SC substrate are given by $J_1(x) = -\mu_0^{-1} dB_1/dx$ and $J_2(x) = -\mu_0^{-1} dB_2/dx$, respectively. Then the total energy of the system as a functional of B_k ($k = 1, 2$) is given by

$$E[B_k] = \int dydz \sum_{k=1}^{2} \int_{L_{k-1}}^{L_k} dx \left(\frac{B_k^2}{2\mu_0} + \frac{\mu_0}{2} \lambda_k^2 J_k^2 \right), \qquad (1)$$

where $L_0 \equiv 0$, $L_1 \equiv d$, $L_2 \equiv \infty$. Variation of the above functional vanishes when conditions

$$\frac{d^2 B_k}{dx^2} = \frac{B_k}{\lambda_k^2}, \qquad (2)$$

$$B_1(d) = B_2(d), \qquad (3)$$

$$\lambda_1^2 \frac{dB_1}{dx}\bigg|_d = \lambda_2^2 \frac{dB_2}{dx}\bigg|_d, \qquad (4)$$

are satisfied. Eq. (2) is the London equation in each SC layer. Eq. (3) and (4) are the continuity condition of the magnetic field and the vector potential, respectively. The above formalism can be easily generalized to an n SC-layer system ($n \geq 3$).

Solving the above equations, we obtain

$$B_1(x) = B_0 \frac{\cosh \frac{d-x}{\lambda_1} + \frac{\lambda_2}{\lambda_1} \sinh \frac{d-x}{\lambda_1}}{\cosh \frac{d}{\lambda_1} + \frac{\lambda_2}{\lambda_1} \sinh \frac{d}{\lambda_1}}, \qquad (5)$$

$$B_2(x) = B_1(d) e^{-\frac{x-d}{\lambda_2}}, \qquad (6)$$

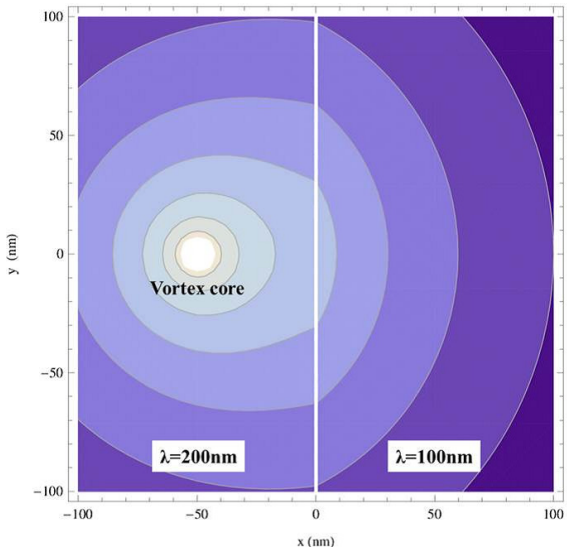


Figure 1: A contour plot of the magnetic field around a vortex core near a boundary of two semi-infinite SCs. The boundary is indicated by a vertical white-line on $x = 0$. Penetration depths of left and right SCs are 200 nm and 100 nm, respectively.

* The work is supported by JSPS Grant-in-Aid for Young Scientists (B), Number 26800157.
† kubotaka@post.kek.jp

Copyright © 2014 CC-BY-3.0 and by the respective authors

DEVELOPMENT OF SUPERCONDUCTING SPOKE CAVITY FOR ELECTRON ACCELERATORS*

T. Kubo†, T. Saeki, KEK, High Energy Accelerator Research Organization, Tsukuba, Ibaraki, Japan
E. Cenni, H. Fujisawa, Y. Iwashita, H. Tongu, Kyoto University, Uji, Kyoto, Japan
R. Hajima, M. Sawamura, Japan Atomic Energy Agency, JAEA, Tokai, Ibaraki, Japan

Abstract

A 325 MHz superconducting spoke cavity for the electron acceleration is under development to realize a compact industrial-use X-ray source with the laser-Compton scattering. Optimum designs of the spoke cavity have been searched by using the genetic algorithm, and multipactor simulations are currently in progress to finalize the detailed design. In parallel to the design-optimization efforts, studies toward fabrication processes are also being carried out. In this paper, progresses made so far and a current situation are briefly reviewed.

INTRODUCTION

In order to realize an industrial-use laser-Compton scattering compact X-ray source [1], a superconducting cavity [2] for electron acceleration is currently under development [3]. We adopted a 325 MHz superconducting spoke cavity. The spoke cavity has a small diameter around half the wavelength, namely, half a diameter of the elliptic cavity, and make it possible to reduce RF frequency f_{RF} with keeping its compactness. By setting f_{RF} to 325 MHz, Bardeen-Cooper-Schrieffer resistance ($\propto f_{\mathrm{RF}}^2$) is reduced [4], and a cavity dissipation at 4 K nearly equals to that of 1.3 GHz elliptic cavity at 2 K. In this paper, efforts for optimizations of cavity design by electromagnetic-field calculations and multipactor simulations are briefly introduced. Attempts to fabricate the spoke cavity, which have just begun, are also presented.

CAVITY DESIGN

In order to design a spoke cavity, we adopted the genetic algorithm (GA) known as a method of multi-objective optimization [3]. Objectives to be minimized are $g_E \equiv E_{\mathrm{peak}}/E_{\mathrm{acc}}$ and $g_B \equiv B_{\mathrm{peak}}/E_{\mathrm{acc}}$, where E_{acc}, E_{peak} and B_{peak} are the accelerating field, the peak electric-field and the peak magnetic-field, respectively. The definition of E_{acc} is given by

$$E_{\mathrm{acc}} \equiv \frac{\left|\int E_z(z) e^{-i\frac{2\pi z}{\lambda}} dz\right|}{\frac{\lambda}{2} N_{\mathrm{gap}}}, \qquad (1)$$

where E_z is the electric-field along the beam axis, $\lambda = c/f_{\mathrm{RF}}$, and N_{gap} is a number of gap, which equals to a number of spoke +1. The electromagnetic field calculations were carried out by using CST MW studio (MWS). The procedure

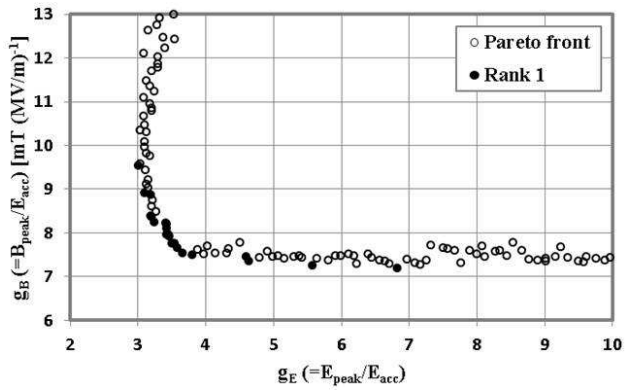


Figure 1: Pareto front shown on the g_E-g_B plane. Each symbol corresponds to an individual.

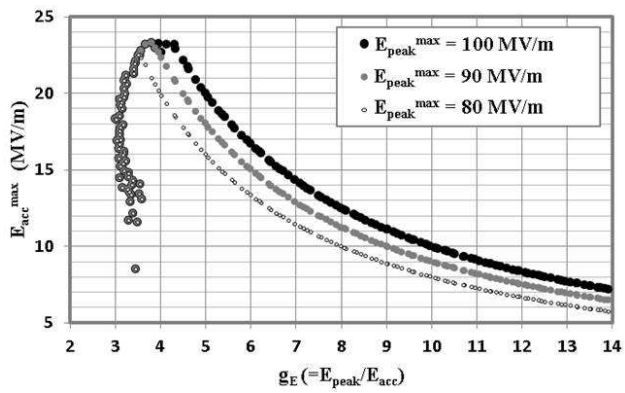


Figure 2: E_{acc}^{max} of individuals on the Pareto front as functions of g_E, where $B_{\mathrm{peak}}^{\mathrm{max}} = 175$ mT is assumed. Black dots, gray dots and circles correspond to E_{acc}^{max} under assumptions $E_{\mathrm{peak}}^{\mathrm{max}} = 100, 90, 80$ MV/m, respectively.

is as follows. (i) Generate an initial set of binary data representing geometries of spoke cavities. Binary data and corresponding cavities are called the chromosomes and the individuals, respectively. (ii) Create individuals by decoding chromosomes, and calculate the objectives g_E and g_B. (iii) Evaluate each individual by counting a number of individuals superior to itself (the rank based fitness assignment method), and select parents of the next generation from individuals with better evaluation value or based on a probability varying according to the evaluation value. (iv) Create chromosomes of children from selected parents with uniform crossover method, and mutate them with a fixed probability. (v) Repeat (ii)-(iv) until the improvement of evaluation

* The work is supported by Photon and Quantum Basic Research Coordinated Development Program from the Ministry of Education, Culture, Sports, Science and Technology, Japan.
† kubotaka@post.kek.jp

Copyright © 2014 CC-BY-3.0 and by the respective authors

FAST TUNER PERFORMANCE FOR A DOUBLE SPOKE CAVITY

N. Gandolfo, S. Bousson, S. Brault, P. Duchesne, P. Duthil, G. Olry, D. Reynet, IPN, Orsay, France
C. Darve, M. Lindroos, ESS, Lund, Sweden

Abstract

IPN Orsay is developing the low-beta double Spoke cavities cryomodule for the ESS. In order to compensate resonant frequency variations of each cavity during operation, a deformation tuner has been studied and two of them have been built. The typical perturbations are coming from LHe saturated bath pressure variations as well as microphonics and Lorentz force detuning (LFD). In this paper, the tuner performance of the double Spoke cavity is presented.

INTRODUCTION

The ESS spoke cryomodule is designed to include two cavities. These cavities require a tuning solution to prevent several kinds of undesirable shift and perturbations well identified to interfere with the resonant frequency during beam operation. The largest ones come from manufacturing, preparation and cooling down phases and can shift the resonant frequency. While it is possible to anticipate them, a relatively small incertitude still exists within a range of few tens of kilohertz. Another type of perturbations will come from RF high field which generates Lorentz forces on the cavity walls thus shifting the resonant frequency very quickly at each beam acceleration pulse. In order to compensate these two very different types of perturbations, a deformation tuner has been designed including an association of one stepper motor for a large tuning stroke capability and two piezoelectric actuators for the fast tuning compensation. The tuning principle is to apply a pulling force on one cavity wall from four fixation points of the LHe tank to the beam tube flange (Fig. 1).



Figure 1: View of the tuner equipping the ESS double spoke cavity.

TEST SETUP

Since the double spoke cavity is still under construction, a sequence of room temperature tests has been planned with the tuner on a triple spoke cavity (Fig. 2) which nearly meets the same relevant mechanical parameters (Table 1).

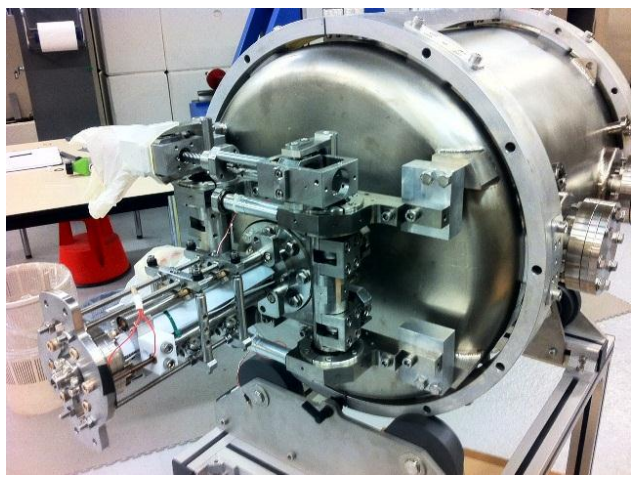


Figure 2: Photo of the tuner assembled on a triple spoke cavity.

Table 1: Cavities parameters

	Wall stiffness	**Sensitivity**
Triple spoke (computed)	19 kN/mm	166 kHz/mm
Triple spoke (measured)	16.2 kN/mm	151 kHz/mm
Double spoke (computed)	20 kN/mm	128 kHz/mm

Since two prototypes have already been built, some characterization steps have been conducted twice in order to compare performances of each tuner on the same cavity.

SLOW TUNER CHARACTERIZATION

Slow Tuner Range

Maximum cavity elongation (for ESS double Spoke cavity) at low temperature without exceeding the niobium elastic limit has been evaluated at 1.28 mm (Fig. 3).

Copyright © 2014 CC-BY-3.0 and by the respective authors

ISBN 978-3-95450-142-7

TROUBLESHOOTING AND PERFORMANCES OF TYPE-B SPIRAL2 SERIES CRYOMODULE

D. Longuevergne, F. Chatelet, C. Commeaux, N. Gandolfo, D. Grolet, C. Joly, J. Lesrel, R. Martret, G. Michel, G. Olry, L. Renard, A. Stephen, P. Szott
IPNO, UMR 8608 CNRS/IN2P3 - Université Paris Sud, France.

Abstract

SPIRAL2 aims at building a multi-purpose facility at GANIL in Caen, France [1]. It will be dedicated to nuclear physics studies, including the production of rich-neutrons isotopes. The multi-beam linear accelerator is composed of superconducting accelerating modules operating at 4.5K and warm focusing magnets. IPN Orsay is in charge of the seven high energy (Type-B) accelerating modules, each hosting two superconducting 88 MHz quarter-wave resonators made of bulk Niobium operating at an accelerating gradient of 6.5 MV/m (β=0.12). The first Type-B series cryomodule has been validated in April 2013. Since then, four additional cryomodules have been validated in a row showing a very high-quality and reliable assembly procedure. Some of encountered problems (tuner hysteresis, magnetic shielding,…) and associated solutions will be presented. Moreover, a comparison of cavity performances between vertical cryostat and cryomodule tests will be done.

INTRODUCTION

The superconducting linac is now in its installation phase [2]. Five cryomodules out of seven of the high beta section have been validated in a row in terms of cryogenic and RF performances since April 2013. This systematic validation, proof of the high quality of cavity preparation and assembly procedure, is following a very long and intense period of troubleshooting (first series cryomodule tested in October 2010).

First, several issues caused a significant degradation of the cavity performances compared to these obtained in vertical cryostat. Magnetic shielding, cavity and power coupler preparations had to be enhanced in order to meet the requirements meaning less than 10W (Qo > 1.37 E+09 at 4.2K) of RF dissipations at the operating gradient of 6.5 MV/m and a maximum gradient of at least 8 MV/m.

Secondly, the innovative tuning system by movable superconducting plunger had to be improved mechanically. Indeed, while tested at cryogenic temperature, a significant hysteresis was measured on the cavity frequency when the plunger was moved by the stepper motor.

After a summary of the performances of the five validated cryomodule, all issues encountered as mentioned previously will be explained as well as the technical solution applied.

CRYOMODULE TESTING

This section will describe most of RF tests done to perform the cryomodules validation.

Power Coupler Conditioning

The Spiral2 power couplers have been designed at LPSC in Grenoble, France. These are cleaned and assembled at LPSC and RF conditioned in standing wave at room temperature up to 20 kW in CW [3] before shipping to IPN Orsay for cryomodule assembly.

Once the cryomodule fully assembled and ready for cool down, RF tests begin with two RF conditioning of the power couplers in open loop, first at room temperature and then at 4.2 K, out of cavity resonance (usually 88.0 MHz) and at a power up to 6 kW in CW. All couplers show in a very reproducible way multipacting events (vacuum deterioration and current measured on a polarized pick-up antenna installed close to the ceramic windows) for low forward power between 80 and 150 W. This behaviour is very similar to what is observed at LPSC. Once conditioned with increasing duty cycle (1, 5, 10, 25, 50% and CW), nothing else has to be reported.

Cavity RF Conditioning

The cavity RF conditioning starts first with the processing in closed loop (self-oscillating loop) of low-level multipacting barriers between 10 and 30 kV/m and another between 1 and 1.3 MV/m. These are usually processed within an hour by RF pulses of 1 kW at around 5 Hz at a duty cycle below 5 %. Some X-rays events of tens of µSv/h and helium flow bursts are measured while processing the 1 MV/m barrier.

For all cavities tested in cryomodules, the accelerating gradient has been ramped up in CW up to 6.5 MV/m with no difficulties.

Cavity Calibration

Cavity calibration consists in evaluating coupling factor of the power coupler (Q_{ext}) and the pick-up antenna (Qt) in the cavity thanks to equations (1) and (2). This is done in three different ways (See figure 1 and 2) in order to cross-check the value of the pick-up coupling factor already evaluated during the previous vertical test:

(1) Measurement of S11 and S21 parameters with a network analyser at room temperature (cavity is under-coupled). Because of the difference between the Qo of the warm cavity (~ 4500) and the external coupling Q_{ext}, S11 and S21 are very small (respectively of the order of - 0.1 dB and - 90 dB). Even-though the error bars are quite significant, this measurement is a good way to check RF connections before cooling down.

(2) Measurement of S11 and S21 parameters with a network analyser at 4.2 K (cavity is over-coupled). This second way is the most precise way to evaluate the

Copyright © 2014 CC-BY-3.0 and by the respective authors

ISBN 978-3-95450-142-7

PROTOTYPING PROGRESS OF SSR1 SINGLE SPOKE RESONATOR FOR RAON

H. J. Cha#, H. C. Jung, G. T. Park, M. O. Hyun, H. J. Kim, D.-O Jeon,
IBS/RISP, Daejeon, South Korea

Abstract

We report the current status of prototyping of the SSR1 cavity (β = 0.3 and f = 325 MHz) for Korean heavy ion accelerator RAON. Simulation results on target frequency for vertical test of the cavity prototype are presented. Clamp-up tests for the cavity assembly are in progress.

INTRODUCTION

The RAON, an advanced heavy ion accelerator for basic sciences and multiple applications, is under construction in Daejeon, South Korea [1]. Based on the on-going technical designs, the prototyping for four different types of superconducting cavities (QWR [2], HWR [3], SSR1 [4], and SSR2) is in progress. In particular, the SSR1 cavities before the SSR2 section can reaccelerate the stable isotope heavy ion beams from the HWR cavities (β = 0.12) after the QWR section to higher energy (β = 0.3) with the resonant frequency of 325 MHz.

After completing the fabrication of the SSR1 cavity prototype, it will be qualified through vertical tests. Therefore, the target frequency considering the resonant frequency shifts by the followings: final electron beam welding (EBW) of an outer conductor with end walls, buffered chemical polishing (BCP), evacuation for ultra-high vacuum of the cavity, cooling to the temperature of 4 K and 2 K, and liquid helium (LHe) pressure acting on the cavity at the temperature should be determined before final trimming of the outer conductor and then EBW with end walls. The electromagnetic (EM) analyses with mechanical simulations will be given in the next section. In addition, the present status of clamp-up tests performing before final EBW is briefly introduced.

DETERMINATION OF TARGET FREQUENCY FOR VERTICAL TEST

The CST MWS and the CST MPhysics codes were utilized for predicting the target frequency of the SSR1 prototype. Figure 1 shows the variation of resonant frequency with respect to the width of the cylindrical outer conductor. Both sides of the outer conductor are simultaneously trimmed by the same length as shown in the inset. The positive sign at horizontal axis represents the decreasing width of the outer conductor and the negative one does the increasing that. Zero distance means the original design value of the outer conductor width. The slope was calculated to be -407.5 kHz/mm. It can be applied to the estimation of the resonant frequency shift by final EBW. Considering the shrinkage of 0.6 mm at each side in the case of niobium (Nb), the frequency shift by the EBW is -244.5 kHz.

#hjcha@ibs.re.kr

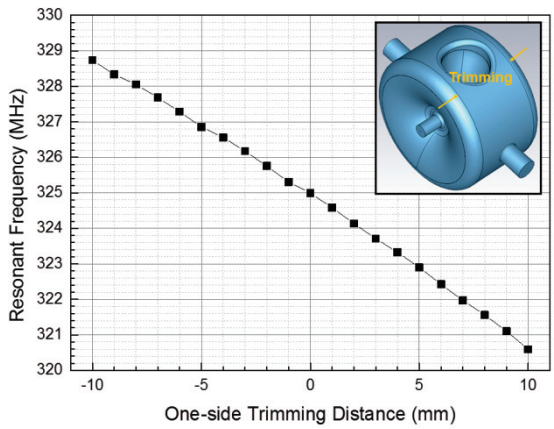


Figure 1: Variation of resonant frequency with changing the width of the outer conductor of the SSR1 cavity.

Figure 2 shows the variation of resonant frequency with respect to the BCP depth. Zero depth also means the original cavity design. The inset shows the simulation results in the narrower depth range. In both cases, it is expected that some fluctuations are caused by the limited mesh numbers. The frequency shift per unit depth calculated from linear fits of the data points is approximately -150 ~ -202 Hz/μm. For determining the target frequency, -150 Hz/μm was used.

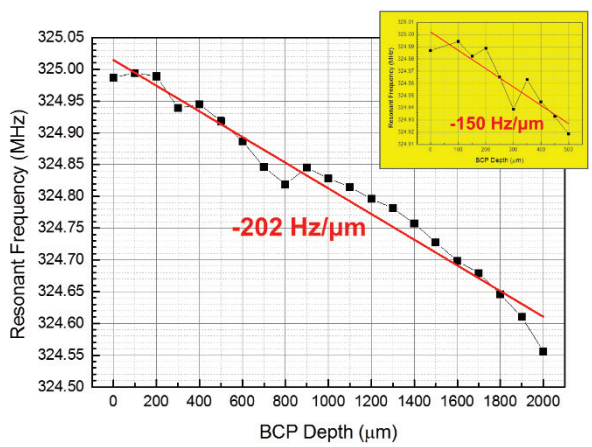


Figure 2: Variation of resonant frequency with changing the BCP depth of the SSR1 cavity.

Copyright © 2014 CC-BY-3.0 and by the respective authors

ISBN 978-3-95450-142-7

CYCLOTRON-UNDULATOR COOLING OF ELECTRON BEAMS

I.V. Bandurkin, S.V. Kuzikov#, A.V. Savilov, Institute of Applied Physics, Russian Academy of Sciences, Nizhny Novgorod, Russia

Abstract

We propose methods of fast cooling of an electron beam, which are based on wiggling of particles in an undulator in the presence of an axial magnetic field. We use a strong dependence of the axial electron velocity on the oscillatory velocity, when the electron cyclotron frequency is close to the frequency of electron wiggling in the undulator field. The abnormal character of this dependence (when the oscillatory velocity increases with the increase of the input axial velocity) can be a basis of various methods for fast cooling of moderately-relativistic (several MeV) electron beams.

NON-RADIATIVE UNDULATOR COOLING

Fast development of the technique of photo-cathode electron photoinjectors has resulted in creation of compact and accessible sources of moderately-relativistic (several MeV) dense (~1 nC in a ps pulse) bunches [1-3]. Methods for decrease of the energy spread (cooling) are actual from the point of view of various applications of such beams, including free-electron lasers (FEL) [4-6]. However, cooling methods are developed now basically for electron beams of significantly higher energies [7,8]. As for a moderately-relativistic high-dense short electron bunches, the strong Coulomb interaction of the particles results in a requirement for a short (~ 1 m and even less) length of a cooling system. Therefore, in this situation, the cooling system should possess resonant properties, namely, a strong dependence of parameters of the particles inside the cooling system on their input energies.

In this letter, we propose to provide cooling by the use of electron wiggling in a circular polarized "cooling" undulator in the presence of an axial magnetostatic field zB_0 (Fig. 1). If the bounce-frequency of electron oscillations in the undulator, $\Omega_u = V_\parallel h_u$ is comparable with the electron cyclotron frequency, $\Omega_c = eB_0/\gamma mc$ (here $V_\parallel$ is the electron axial velocity, h_u is the undulator wavenumber, and $\gamma = 1/\sqrt{1-(V/c)^2}$ is the relativistic electron mass factor). In this situation, the velocity of undulator oscillations V_u depends strongly on the initial axial velocity.

Non-radiative "axial" cooling is based on the fact that the axial velocity spread is the only factor important for the FEL operation. This spread can be decreased due to its "transformation" into the spread in the velocity of electron rotation in the cooling system. Electrons move along axial magnetic field and enter the cooling undulator with the adiabatically growing field in the input section, where each electron gets its own rotatory velocity (Fig. 1a). If at the input of the system every particle possesses only the axial velocity $V_0 = \overline{V} + \delta V$, then the axial velocity in the regular region of the undulator is determined by the energy conservation law: $V_\parallel^2 \approx V_0^2 - V_u^2$. Thus,

$$V_\parallel^2 \approx \overline{V}^2 + 2\overline{V}\delta V - V_u^2(\overline{V}) - \alpha\delta V . \qquad (1)$$

If $\alpha = \partial V_u^2/\partial V_\parallel = 2\overline{V}$, then the spread in $V_\parallel$ disappears. This condition is independent of the initial spread, δV. Evidently, we should use the range of parameters, where $\partial|V_u|/\partial V_\parallel > 0$ (Fig. 1 d), so that the initial axial velocity excess, δV, is compensated by the greater rotatory velocity, V_u.

If such a cooling system is used in a FEL, then the operating FEL undulator designed to produce optical radiation can be placed inside the regular section of the cooling undulator (Fig. 1 a). Another way is to "switch off" the field of the cooling "undulator" sharply (Fig. 1 b). Then, forced undulator oscillations of the particles are just transformed into free cyclotron oscillations with the same rotatory velocities, $V_\perp = V_u$ (and the same axial velocities).

Let us consider the equation for the transverse momentum of a particle moving in the axial uniform magnetic field, $\mathbf{B}_0 = \mathbf{z}B_0$, and in the quasi-periodical field of the undulator, $B_+ = B_x + iB_y = B_u(z)\exp(ih_u z)$:

$$\frac{dp_+}{dz} = i\frac{\Omega_c}{c}\frac{p_+}{V_\parallel} + ih_u K(z)\exp(ih_u z) . \qquad (2)$$

Here, $p_+ = p_x + ip_y$, $\mathbf{p} = \gamma\boldsymbol{\beta}$, $\boldsymbol{\beta} = \mathbf{V}/c$, and $K(z) = -eB_u/h_u mc^2$ is the undulator factor (the normalized transverse electron momentum, $K = \gamma V_u/c$); its dependence on the coordinate describes smooth entrance of the particles into the undulator. At the beginning, where $K = 0$, there exists a "parasitic" transverse electron motion due to free cyclotron oscillations, $p_+(0) = \gamma_0\beta_{\perp 0}\exp(i\theta_c)$. The initial spread in the transverse velocity is described by the uniform distribution of $\beta_{\perp 0}$ over the interval $0 < \beta_{\perp 0} < \overline{\beta}_{\perp 0}$. As for the axial velocity spread, it is described by uniform distribution of $\beta_{\parallel 0}$ in the interval

#kuzikov@appl.sci-nnov.ru

ISBN 978-3-95450-142-7

Copyright © 2014 CC-BY-3.0 and by the respective authors

THE PROTON INJECTOR FOR THE EUROPEAN SPALLATION SOURCE

L. Celona#, L. Ando, G. Castro, S. Gammino, D. Mascali, L. Neri
Istituto Nazionale di Fisica Nucleare, Laboratori Nazionali del Sud, 95123 Catania, Italy
G. Torrisi, INFN-LNS and Università Mediterranea di Reggio Calabria, Reggio Calabria, Italy

Abstract

The update of the design of the PS-ESS source and of its LEBT has been carried out in 2013 and the construction is now ongoing. The Ion Source will be able to provide a proton beam current larger than 74 mA to the 3.6 MeV RFQ. Several innovative solutions have been implemented in the redesign phase in order to cope with high-reliability/high-performance requirements of the ESS project. A flexible magnetic system will allow to investigate alternative configurations for future beam current upgrade of the machine, based on the formation of a denser plasma. New set-ups have been also explored for beam extraction, transport and chopping. Calculations have shown that space charge compensation up to 95 % is needed to preserve the low emittance in the low energy beam transfer line (LEBT). In order to obtain the optimal proton beam pulse rise and fall time we propose a LEBT chopping configuration that permits hundred nanosecond rise and fall times despite the LEBT compensation needs few microseconds. Some hints about numerical modelling efforts at LNS will be also given.

INTRODUCTION

The European Spallation Source will be one of the most advanced technological tools for scientific and industrial development in Europe in the next decades. A linear accelerator is going to be built for the production of 2 GeV protons to be used for neutron production via nuclear spallation. Neutrons will be finally used for fundamental science and applied research.

INFN-LNS is responsible of the design and construction of the accelerator front-end, including the high intensity proton source (PS-ESS, Proton Source for ESS) and the Low Energy Beam Transport line.

Recently, the decision of the ESS board to upgrade the source and LEBT requirements, made more challenging the machine design both in terms of proton current (+25% increase from 50 to 62.5 mA on target) and beam ripple minimization (±3.5%). In order to cope with the new requirements, several solutions have been adopted thus making the source a flexible machine fulfilling the project expectations.

More in detail, the maximum extracted beam current from the ion source shall exceed 90 mA, with a proton fraction above 80 %, this way producing a nominal beam pulse of 74 mA. Besides the nominal current, the injector (ion source + LEBT) is requested to deliver different levels of peak proton beam current, between 10 and 100% of the maximum one, under stable conditions. Stringent conditions are also given in terms of fast tuning of the machine, and easy/fast startup operations (16 hours, 32 hours after vacuum breaks), requiring specific efforts to be paid to vacuum issues and mechanical assembly. The pulsed beam length shall exceed 3 ms but less than 6 ms, with particular attention to the beam ripple: the level of ± 3.5 % averaged over the flat top of the pulse (200 μs time average) is quite critical for weeks of operation, thus requiring an extensive period of test in nominal conditions in the last part of 2015. The extraction voltage is fixed at 75 kV within 0.01 kV of setting accuracy and 100 eV steps allowed for fine proton energy tuning up to ± 5 keV from the nominal value, in order to optimize energy matching with RFQ.

Concerning the emittance, the source is designed for fulfilling a transverse output emittance requirement of (less than) 0.20 π.mm.mrad RMS normalized; assuming a 25 % emittance growth in the LEBT, the maximum value before the RFQ entrance must be less than 0.25 π.mm.mrad.

Variable beam current are requested to be delivered by the IS-LEBT to the RFQ, without major modifications of the source parameters, in order to keep the emittance plot unchanged. The requirements go from 6.5 mA to 70 mA with a step size of 6.3 mA, meaning that a specific item into the LEBT (an iris) must be inserted for selecting different portions of the beam. At the LEBT output, the length of the nominal beam pulse will lie in range 2.9 ms – 3 ms, guaranteed by an on-purpose developed chopping system. During this time, Twiss parameter should be adapted for RFQ matching.

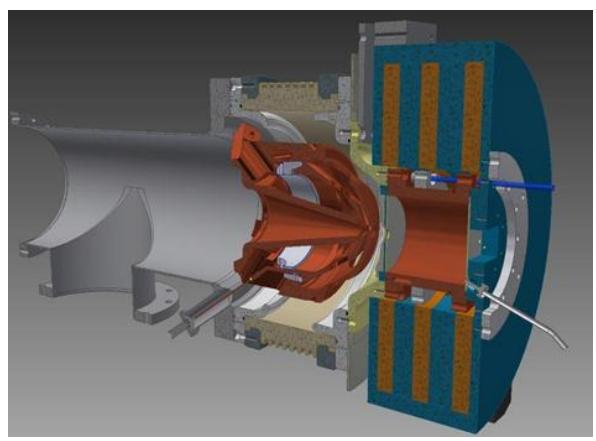


Figure 1: The PS-ESS source.

#celona@lns.infn.it

Copyright © 2014 CC-BY-3.0 and by the respective authors

ESS DTL ERROR STUDY

M. Comunian, F. Grespan, A. Pisent, INFN/LNL, Legnaro, Italy.

Abstract

The Drift Tube Linac (DTL) of the European Spallation Source (ESS) is designed to operate at 352.2 MHz with a duty cycle of 4% (3 ms pulse length, 14 Hz repetition period) and will accelerate a proton beam of 62.5 mA pulse peak current from 3.62 to 90 MeV. The error study is decisive to define the DTL manufacturing tolerances and to evaluate its robustness. In this paper the DTL performances are shown.

INTRODUCTION

The DTL of the high power linac of the European Spallation Source has been changed, respect to 2013 design, to meet the new linac optimized parameters, with higher current and final energy of the DTL [1]. The high reliability and availability of the accelerator requires short repair times and sets a loss limit for hands-on maintenance of the machine to 1 W/m above 30 MeV, on beam losses. Another limit on the tolerances on the nominal DTL design is coming from the maximum amount of emittance growth admitted in the DTL of 10% for all the planes, on top on the emittance evolution without errors [2].

ERRORS STUDY STRATEGY

The DTL nominal parameters are reported in Table 1.

Table 1: DTL beam parameters

Parameter	Value
Input Tran. Norm. RMS Emit.	0.28 mmmrad
Input Long. Norm. RMS Emit.	0.39 mmmrad (=0.15 MeVdeg)
Input current	62.5 mA

Table 2: DTL main requirements

Parameter	Value
Emit. Growth definition	$\Delta\varepsilon=(\varepsilon_{out}-\varepsilon_{in})/\varepsilon_{in}$
Maximum emittance growth	$\Delta\varepsilon$ <20%
Losses (above 30 MeV)	< 1W/m

For the statistical error studies a Gaussian input beam distribution cut at 3σ has been used, this is used to overestimate the errors beam sensitivity. Each error has been studied individually to check the single sensitivity respect to the parameter. The simulation program used is TraceWin with the space charge routine picniR (20x40 as mesh) and 50 000 macroparticles. The statistical number of DTLs generated is 500 for each single error with a uniform distribution. A final check with all the errors applied has been done. The DTL input is considered at 20 mm before the input flange on the first cell with the first PMQ, to start in a zone without fields. To simulate machine operation, the steeres are optimized for each given error set run, considering a finite resolution on the BPM. A set of sensitivity on PMQ position with and without steeres has been considered to check the steeres advantage and relax the PMQ position tolerances.

ERRORS INVESTIGATED

The errors examined, as single error and for all the planes, are:

- Input beam:
  - Emittance change
  - Current jitter
  - Position and divergence
  - Mismatch
  - Energy jitter
- PMQ:
  - Position with and without Steeres
  - Rotation
  - Gradient
  - Ageing: PMQ gradient degradation
  - Multipoles and dipoles.
- DTL RF:
  - E0 Field flatness cell by cell
  - Sync. Phase, i.e. DT relative position
- DTL tanks:
  - Klystron RF phase and amplitude
  - Relative position
- Global:
  - All the input beam errors
  - All PMQ, RF and tanks errors

These sets of errors permit to define the mechanical tolerances for machining, welding, positioning, powering of the Drift Tube and the input beam characteristics needed from the MEBT. The errors applied are uniformly distributed between plus and minus maximum of the defined range. Each tank is fed by one klystron and therefore all the errors caused at that level are coupled. Synchronous phase and field amplitude errors in each cell are determined by the shape and position of drift tubes and are uncoupled.

The observable used as output of the errors study is the final emittance and the presence of losses. The maximum admitted final transverse/longitudinal RMS emittance is 0.328/0.441 mmmrad with a 17% and 13% emittance growth respect to the input emittance without errors for the Gaussian input beam distribution. The transverse acceptance of the DTL is 13.4 mm.mrad; this is a large

Copyright © 2014 CC-BY-3.0 and by the respective authors

ISBN 978-3-95450-142-7

ESS DTL DESIGN AND DRIFT TUBE PROTOTYPES

F. Grespan, M. Comunian, A. Pisent, M. Poggi, C. Roncolato, INFN/LNL, Legnaro, Italy
P. Mereu, INFN Torino, Torino, Italy

Abstract

The Drift Tube Linac (DTL) for the ESS accelerator will accelerate protons up to 62.5 mA average pulse current from 3.62 to 90 MeV. The 5 tanks composing the DTL are designed to operate at 352.21 MHz in pulses of 2.86 ms long with a repetition rate of 14 Hz. The accelerating field is around 3.1 MV/m, constant in each tank. Permanent magnet quadrupoles (PMQs) are used as focusing element in a FODO lattice. The empty drift tubes accommodate Electro Magnetic Dipoles (EMDs) and Beam Position Monitors (BPMs) in order to implement beam corrective schemes. A complete set of Drift Tubes (DTs) is under construction that is BPM, EMD and PMQ types. These prototypes are aimed to validate the design with the involved integration issues of the various components, as well as the overall technological and assembly process. This paper presents the main mechanical choices and the status of the prototyping program of the DTs.

INTRODUCTION

The ESS linac redesign, decided in 2013 to meet the budget, had the consequence of increasing the beam current from 50 mA to 62.5 mA [1]. Since the previous 4-tanks DTL design was optimized for 50 mA beam loading at the limit of the RF coupler capability, the physical design DTL has been reviewed. Nevertheless most of the engineering choices are confirmed [2,3].

The DTL input constraints kept for this design are:

- Tank length < 8 m (9.3 λ) for RF stability. Each tank composed by 2 m long stainless steel modules.
- Total Power per tank = ($P_{Superfish}$ × 1.25 + Beam Power) ≤ 2.2 MW to maintain the design of CERN RF window [4].
- Intertank = 1 βλ between flange inner surfaces.

In addition to the beam current, the DTL transition energies have been changed:

- Input Energy from 3 MeV to 3.62 MeV. It allows simplifying the first DTs that are the most challenging, with weaker requirements on quadrupole integrated field and the possibility of longer PMQs, as well as the advantage of better shunt impedance and lower surface field level.
- Final energy > 88 MeV. It allows improving the matching point to the Superconducting section in terms of phase advance and acceleration efficiency. Since the constraints on RF power per tank and the tank length are maintained, this extra energy will be reached with 5 DTL tanks. The cost and space of the extra DTL tank could be compensated by the removal of a few spoke cryomodules [5].

Table 1: Summary of ESS DTL Properties

Tank	1	2	3	4	5
Cells	61	34	29	26	23
E_0 [MV/m]	3.00	3.16	3.07	3.04	3.13
E_{max}/E_k	1.55	1.55	1.55	1.55	1.55
φ_s [deg]	-35,-25.5	-25.5	-25.5	-25.5	-25.5
L_{Tank} [m]	7.62	7.09	7.58	7.85	7.69
R_{Bore} [mm]	10	11	11	12	12
L_{PMQ} [mm]	50	80	80	80	80
Tun. Range [MHz]	±0.5	±0.5	±0.5	±0.5	±0.5
Q0/1.25	42512	44455	44344	43894	43415
Optimum β	2.01	2.03	2.01	1.91	1.84
Beam Det [kHz]	+23	+20	+20	+18	+18
P_{cu} [kW] (no margin)	870	862	872	901	952
E_{out} [MeV]	21.29	39.11	56.81	73.83	89.91
P_{TOT} [kW]	2192	2191	2196	2189	2195

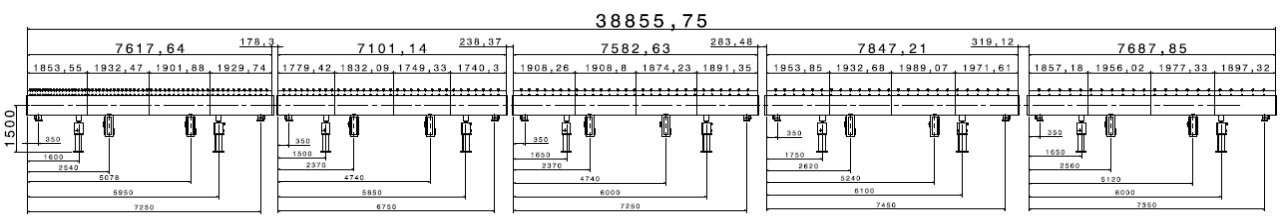


Figure 1: DTL overview.

Copyright © 2014 CC-BY-3.0 and by the respective authors

HIGH POWER CONDITIONING OF ANNULAR-RING COUPLED STRUCTURES FOR THE J-PARC LINAC

H. Ao*, J. Tamura, Y. Nemoto, T. Ito, H. Oguri, N. Ouchi, J-PARC, JAEA, Ibaraki, Japan
Z. Fang, K. Futatsukawa, K, Nammo, T. Sugimura, J-PARC, KEK, Ibaraki, Japan
H. Asano, Nippon Advanced Technology Co. Ltd, Ibaraki, Japan

Abstract

For the energy upgrade of the J-PARC linac, 25 annular-ring coupled structure modules were fabricated and installed to a beam line. In the high-power conditioning process of these modules, we faced the issue of the unstable operation of a module No. 4. Eventually this issue was naturally resolved, however the cause of this issue was uncertain. To address the cause, we investigated the records of its vacuum pressure with attention to the fluctuations of the vacuum pressure. This result indicates that the pressure fluctuation correlates with operation stability.

INTRODUCTION

Annular-ring coupled structure (ACS) has been developed for the energy upgrade of the J-PARC linac from 181 to 400 MeV [1, 2]. The ACS is a kind of coupled-cavity linac operated in $\pi/2$ mode, for example, a side-coupled structure (SCS). Comparing the SCS, the ACS has the advantage of an axial symmetry around the beam axis, which realizes a negligible small dipole component of an accelerating field and smooth surface finishing with a ultra-precision lathe. Figure 1 shows the mechanical structure and the electric field pattern of the ACS.

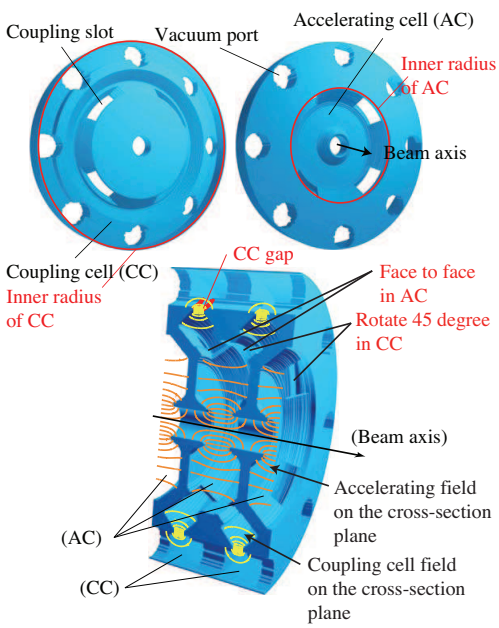


Figure 1: Structure and electric field of the J-PARC ACS [2].

For the energy upgrade, 25 ACS modules have been fabricated in total. The configurations of the J-PARC linac before and after the energy upgrade are shown in Fig. 2. From a

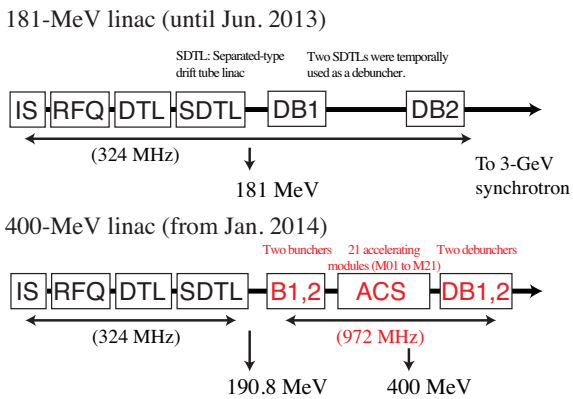


Figure 2: Configuration of the J-PARC linac.

summer maintenance period in 2013, these ACS modules were sequentially installed to a beam line. After that we started the high-power conditioning of the ACS modules. Most of ACS modules have not been powered before an installation, thus there were some troubles and issues in a conditioning process. This report focuses on a one of the most serious issues of this conditioning process: the instability of a module No. 4 (M04).

CONDITIONING HISTORY OF M04

The conditioning history of M04 is shown in Fig. 3. It should be noted that this module had been already conditioned up to 1.6 MW before the installation. This module could be, therefore, quickly and successfully conditioned more than 2 MW with a short pulse length of 50 µs at first, and then it was reconditioned from 0 aiming at 2 MW with a long pulse length of 600 µs, which is the design pulse length of the ACS [3]. The pulse repetition frequency was 25 Hz, which was constant through this conditioning.

After 27 hours later from starting the conditioning, input power was suddenly limited by the interlock due to RF power reflection. Figure 4 shows the detail around the interlock at t =28 hours 35 minutes. As shown in Fig. 4, an RF interlock by power reflection occurred just before 28 hours 35 minutes. Just after this incident, the input power was successfully recovered to a previous power level of 1600 kW. However, in the following interlock incidents, the input power could not be recovered to the same level. Consequently, the input power gradually decreased to approximately 500 kW, which is less than 1/3 of an achieved power level of 1600 kW.

* hiroyuki.ao@j-parc.jp

ISBN 978-3-95450-142-7

Copyright © 2014 CC-BY-3.0 and by the respective authors

LONGITUDINAL MEASUREMENT OF ANNULAR-RING COUPLED STRUCTURE LINAC IN J-PARC

T. Maruta*, Y. Liu, KEK / J-PARC, Tokai, Japan
A. Miura, JAEA / J-PARC, Tokai, Japan

Abstract

The measurement of the longitudinal specification is a good method to inspect the tuning accuracy of RF cavities, an RF amplitude and a driving phase. The J-PARC linac was conducted a large modification in year 2013 to recover the beam energy to the original design of 400 MeV. The main upgrade is the installation of annular-ring coupled structure (ACS) cavities at SDTL downstream. The 400 MeV acceleration is successfully realized on January 17, 2014, and then we measure the longitudinal specifications. In this paper, we discuss the measurement results.

INTRODUCTION

After the beam energy upgrade, the J-PARC linac is comprised from a 50 keV negative hydrogen (H^-) ion source (IS), a 3 MeV radio frequency quadrupole (RFQ), a 50 MeV drift tube linac (DTL), an 191 MeV separate-type DTL (SDTL) and a 400 MeV annular-ring coupled structure (ACS) linac [1] as shown in Fig.1. ACS is a variation of coupled cavity linac with emphasis on the axial symmetry of the RF field [2]. The RF frequency of ACS is 972 MHz which is threefold frequency jump from SDTL. The ACS downstream is a beam transport section (L3BT) to a 3 GeV rapid cycling synchrotron (RCS). L3BT consists of the straight section, the first arc section, the collimator section, the second arc section and the injection section. Two debuncher cavities are placed in L3BT. The first debuncher (DB1) is located in the straight section and it is for the correction of the momentum centroid jitter. The second one (DB2) is at the downstream of first arc section and it is for the optimization of the momentum spread at the RCS injection. There are three beam dumps for a beam commissioning of the linac alone. Each beam dump are branched from the middle of L3BT. Most downstream dump is the 100 degree beam dump (100BD) and it is branched from the second arc section.

The first beam commissioning after the ACS installation had been conducted on December to January. We successfully realized 400 MeV acceleration on January 17. Because it is first time to accelerate by ACS, we need to confirm the property of ACS and to estimate the RF tuning accuracy of cavities. It motivated us to measure the ACS longitudinal properties after the realization of 400 MeV acceleration.

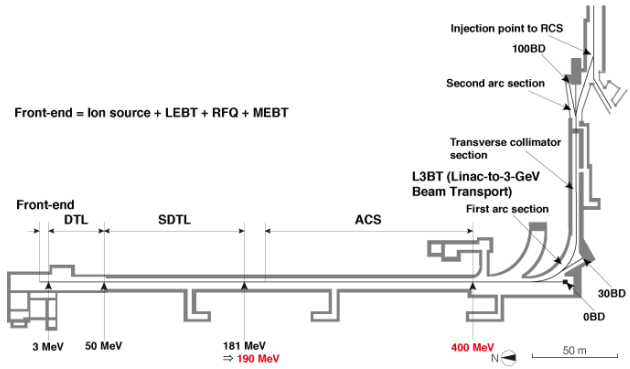


Figure 1: Outline of the J-PARC linac. In the initial stage, the linac had been operated at 181 MeV by the installation of IS to SDTL on the beam line as shown in black character. The ACS accelerator was installed at second stage to extend the beam energy to 400 MeV (red).

SIMULATIONS

Longitudinal Acceptance

This acceptance is calculated by 3D particle-in-cell code, IMPACT [3]. In the simulation, the initial particles are launched at the ACS entrance distributed over a sufficiently wide area to cover the entire acceptance in the longitudinal phase space. Then, we track these particles to the ACS exit without space charge. In the simulation, we adopt the Lorentz integrator with the step width of around $\beta\lambda/100$. Here, β and λ denote the particle velocity scaled by the speed of light and the RF wave length, respectively. No error is assumed. To eliminate the particles outside the bucket, we set an energy threshold at 396 MeV. We choose particles above the energy threshold at the ACS exit, and then find their initial positions at the ACS entrance to obtain the longitudinal acceptance. The area filled with pale blue dots in Fig. 2 shows the simulated acceptance for ACS. The horizontal axis in this figure is the beam injection phase to ACS with respect to the design synchronous phase ($\Delta\phi_s$). The vertical axis is the injection beam energy with respect to the design injection beam energy (ΔE). As seen in this figure, the acceptance is distributed from -30 to 60 deg in $\Delta\phi_s$ and from -2.7 to 2.4 MeV in ΔE, respectively.

Secondly, we evaluate the longitudinal beam distribution at the ACS entrance. The particle simulation is performed from the exit of RFQ to the entrance of ACS. The output distribution from PARMTEQM [4] is taken as the initial distribution [5]. In the simulation, we adopt the same integrator and the integration step width as the acceptance evaluation. However, the space charge effect is taken into account this time. We employ 100,000 macro-particles and $32 \times 32 \times 64$ meshes in the space-charge calculation, but no error is assumed. The longitudinal beam distribution at the ACS entrance is superimposed with red dots on the acceptance plot in Fig. 2.

* tmaruta@post.j-parc.jp

Copyright © 2014 CC-BY-3.0 and by the respective authors

ISBN 978-3-95450-142-7

INSTALLATION AND PERFORMANCE CHECK OF BEAM MONITORS FOR ENERGY UPGRADED J-PARC LINAC

A. Miura#, N. Ouchi, H. Oguri, K. Hasegawa
J-PARC Center, Japan Atomic Energy Agency, Tokai, Ibaraki, 319-1195, JAPAN
T. Maruta, Y. Liu, T. Miyao,
J-PARC Center, High Energy Accelerator Research Organization, Oho, Tsukuba, 305-0801, JAPAN
M. Ikegami
FRIB, Michigan State University, East Lansing, MI 48824-1321, USA

Abstract

An energy upgrade project has started in the J-PARC Linac since 2009. In the upgraded project, beam energy in the Linac has increased from original 181 MeV to 400 MeV using the additional 21 Annular-ring Coupled Structure Linac (ACS) cavities. The new beam monitors as the beam current monitors, the phase monitors, the beam position monitors and the transverse profile monitors (wire scanner monitors) were designed and fabricated. Till the end of November, 2013, all beam monitors were completely installed. From the middle of December, we started the beam commissioning to achieve the beam energy as 400 MeV, as well as to confirm the beam monitor functioning. We achieved the 400 MeV beam acceleration at the middle of January, 2014 using newly installed beam monitors. This paper describes the beam monitor installation and the beam commissioning results of beam monitor functioning.

INTRODUCTION

The Japan Atomic Energy Agency (JAEA) and the High Energy Accelerator Research Organization (KEK) have been organizing the Japan Proton Accelerator Research Complex (J-PARC) project at the JAEA Tokai site since 2001 [1]. The beam commissioning of the Linac started in 2006 and a 181-MeV beam was injected into the downstream 3-GeV rapid-cycling synchrotron (RCS). Since the beginning of J-PARC, user operation has successfully continued with the exception of a 10-month interval due to the Tohoku earthquake occurred at 2011. In parallel with the 181-MeV beam operation, a 400-MeV energy-upgrade project began in 2009. New Annular-ring Coupled Structure Linac (ACS) cavities had been developed [2] and the beam monitors had been designed and fabricated for the energy-upgrade project. During the summer shutdown, we installed the newly fabricated ACS cavities and related devices. Continuously we started the beam commissioning in December 2013.

NEW BEAM MONITOR LAYOUT OF 400 MeV LINAC BEAM LINE

The J-PARC Linac originally consists of a 50-keV negative hydrogen ion source, 3-MeV RFQ (Radio Frequency Quadrupole Linac), 50-MeV DTL (Drift Tube Linac), and 181-MeV SDTL (Separated-type DTL) [1]. We had two SDTL-type debunchers allocated at an ACS section and L3BT (Linac to 3-GeV RCS Beam Transport) in the original beam line. In the energy-upgrade project, we replaced the two original debuncher cavities to the end of the SDTL section as the 16th acceleration module of SDTL cavities. We installed new ACS-type bunchers for the longitudinal matching between the SDTL and the ACS cavities, because the operating frequency is 972 MHz of the ACS with three-fold frequency jump from that of the SDTL.

A number of beam monitors have been used in the original beam line, such as: the beam position monitor (BPM), beam current monitor (slow current transformer, SCT), beam phase monitor (fast current transformer, FCT), transverse profile monitor (wire scanner monitor, WSM) and beam loss monitor (BLM) [3].

Periodical layout of beam monitors in each ACS module is shown in Fig. 1. One module consists of two

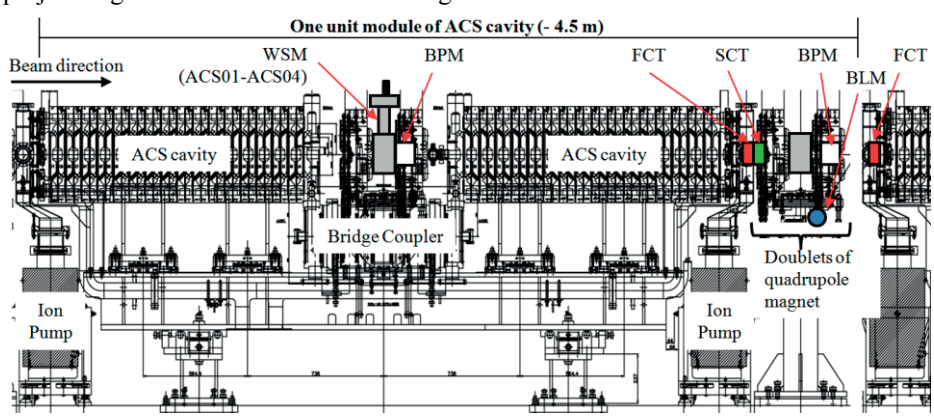


Figure. 1: Periodical beam monitor layout of all ACS cavities. MEBT2 is the second Medium Energy Beam Transport between SDTL and ACS section.

#akihiko.miura@j-parc.jp

ISBN 978-3-95450-142-7

Copyright © 2014 CC-BY-3.0 and by the respective authors

DEVELOPMENT OF SLOW NEUTRON ACCELERATOR FOR REBUNCHING PULSED NEUTRONS

S. Imajo, Department of Physics, Kyoto University, Kyoto 606-8502, Japan.
Y. Iwashita, Y. Fuwa, R. Kitahara, ICR, Kyoto University, Uji, Kyoto, 611-0011, Japan
H. M. Shimizu, M. Kitaguchi, Department of Physics, Nagoya University,
Chikusa, Nagoya, 464-8602, Japan
K. Mishima, ICEPP, University of Tokyo, Bunkyo, Tokyo 113-0033, Japan
T. Ino, KEK, Tsukuba, Ibaraki, 305-0801, Japan

Abstract

Nowadays most measurements of the neutron electric dipole moment (EDM) are carried out with ultra cold neutrons (UCN), whose kinetic energies are lower than about 300 neV, and with a small storage bottle to reduce the systematic errors. In such experiments highly dense UCNs are desired. The pulsed spallation neutron source can produce such UCNs. However, the pulsed UCNs with broad velocities diffuse in guide tubes. It becomes an advantage to focus and rebunch UCNs temporally upon the bottle by controlling their velocities in neutron EDM experiments at those facilities. Low energy neutrons can be accelerated or decelerated by the technique of the AFP-NMR method with the RF magnetic field and the gradient magnetic field. We demonstrated such accelerator in ILL. We have been developing the advanced apparatus which makes it possible to handle the UCNs of the broader energy range.

INTRODUCTION

The time-reversal symmetry is broken directly if a neutron has electric dipole moment (EDM). Furthermore, the existence of large EDM is the evidence of new physics. The physics beyond the standard model like supersymmetry theory predicts several orders of magnitude larger neutron EDM than the prediction of Standard model, which is 10^{-30} to 10^{-32} e $\cdot$ cm. Therefore the searches of the neutron EDM is being carried out. At present the upper limit is 2.9×10^{-26} e $\cdot$ cm (90% C.L.) [1].

In EDM experiment, polarized ultracold neutrons (UCNs), whose kinetic energies are lower than 300 neV, are stored in an experimental bottle. The spin rotation of UCN is measured by the Ramsey resonance technique after strong electric field is applied to the bottle. The bottle should be small in order to decrease the systematic error due to nonuniform magnetic field. Highly dense UCNs are desired in order to decrease statistical error. In future, such UCNs will be produced with the spallation neutron source and the superthermal converter.

We are proposing to construct such source at J-PARC by using its linac beam and to carry out EDM searches [2]. The peak power of the beam will become 20 MW at RCS 1 MW operation and extremely highly dense UCNs can be produced. However, the source produces pulsed UCNs and the pulse diffuses widely during transport according to their own velocity distribution.

We are developing a neutron accelerator named "UCN rebuncher" in order to control the velocity of UCN and to focus UCNs on the entrance of the bottle [3].

UCN REBUNCHER

Figure 1 shows the principle of the neutron acceleration using the magnetic field. A neutron has the magnetic moment $\boldsymbol{\mu}$ and it obtains the magnetic potential energy $-\boldsymbol{\mu} \cdot \boldsymbol{B}$ in the magnetic flux density $\boldsymbol{B}$. The absolute value of the energy is about 60 neV per 1 Tesla. If the neutron spin is flipped in the magnetic field, the variation of the kinetic energy by the field is not canceled when the neutron escapes out of the field. Hence the kinetic energy of an UCN can be controlled by flipping its spin in the suitable magnetic flux density [4, 5]. The controlled UCNs will be focused on a certain point temporally with suitable acceleration or deceleration.

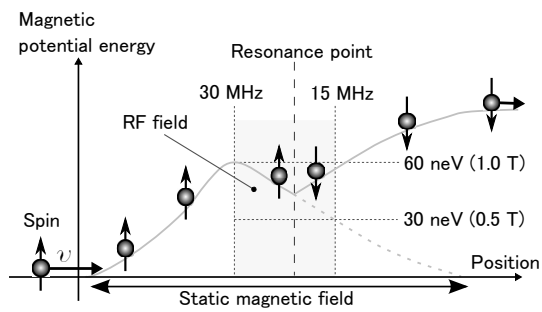


Figure 1: The principle of the neutron acceleration.

The spin is flipped by the adiabatic fast passage (AFP) NMR method. In the method a RF magnetic field is applied to neutrons in a gradient magnetic field. The spin flip occurs around the magnetic flux density B given by the Larmor frequency f, that is $\mathrm{B} = hf/2|\mu|$, where h is the Planck constant and μ is the neutron magnetic moment parallel or antiparallel with B. The flipping ratio depends on

Copyright © 2014 CC-BY-3.0 and by the respective authors

ISBN 978-3-95450-142-7

COMBINED SYSTEM OF OPTICAL INSPECTION AND LOCAL GRINDER

Y. Iwashita, ICR, Kyoto University, Uji, Kyoto, JAPAN
H. Hayano, T. Kubo, K. Wtanabe, Y. Yamamoto, KEK, Ibaraki, JAPAN

Abstract

Optical inspections on superconducting accelerating tubes have been playing an important role on improving their accelerating gradients. Instead of treatments on whole cavity inner surfaces to eliminate the found defects on the surfaces, the local grinding method succeeds to remove them efficiently. A combined system of the optical inspection and the local Grinding machines are fabricated.

INTRODUCTION

Superconducting (Sc) technology is getting popular for accelerating cavities. The fabrication cost is one of the big aspects for the Sc cavities to be applied for wide applications. Since the ILC project needs more than 16000 9-cell cavities, their production yield had been a big issue before the high resolution optical inspection technique was developed. The high resolution optical inspection system revealed the physical sources of the reduced performances, which enabled us to pursuit further investigations such as replica technique and curing the defects on the surface (see Fig.1) [1,2,3,4,5,6].



Figure 1: The High Resolution Cavity Camera (Ver.5)

EFFECTIVENESS OF REPAIR

Figure 2 shows typical defects that degrade the cavity performances. Many of them usually appear on the EBW seam area. While these defects are localized, the weakest cell performance limits the whole 9-cell cavity. The local grinding technique cures the local defects instead of the deep Electro-Polish (EP) process to entire cavities, which usually takes a few weeks for the process. Example of the local repair for MHI-08 is shown in Fig.3, where two defects limited the gradient and one of them appeared after EP [8,9]. The defects were removed by the local grinding and light EP was performed. Figure 4 shows the improvements of the Q-slope. Accelerating gradient 16

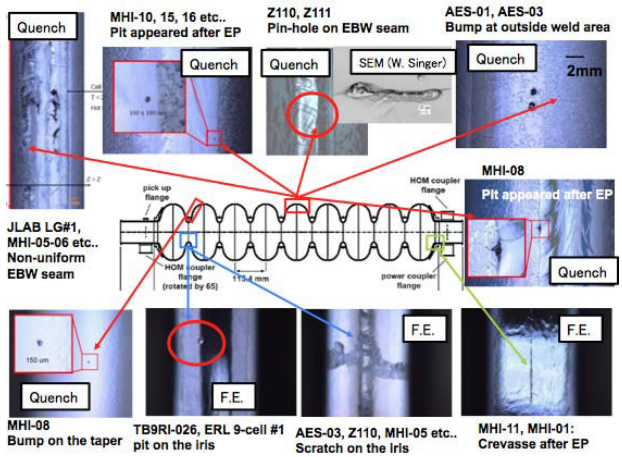


Figure 2: Defects against performance.

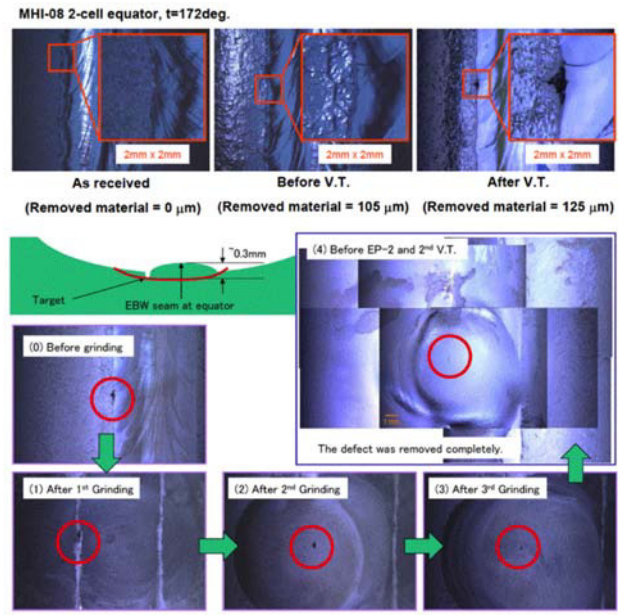


Figure 3: Example of local repair: MHI-08.

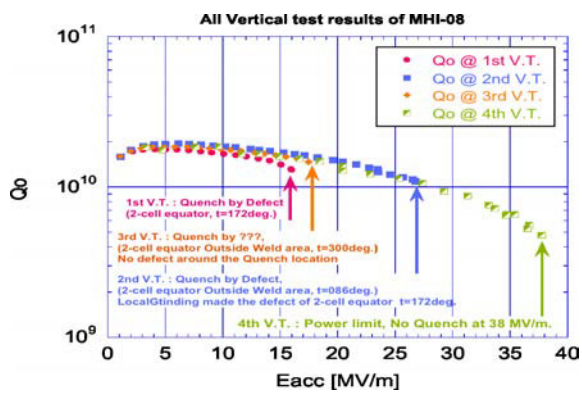


Figure 4: The Q-slope curves of MHI-08 over the repair.

Copyright © 2014 CC-BY-3.0 and by the respective authors

ISBN 978-3-95450-142-7

THE HEAVY ION LINAC AT THE NICA PROJECT

A.V.Butenko, V.S.Aleksandrov, E.E.Donets, E.D.Donets, D.E.Donets, A.I.Govorov, V.V.Kobets, A.D.Kovalenko, K.A.Levterov, V.A.Monchinsky, I.N.Meshkov, V.A.Mikhailov, A.O.Sidorin, G.V.Trubnikov, Dubna, Russia, T.V.Kulevoy, D. Liakin ITEP, Moscow, Russia, H.Hoeltermann, U.Ratzinger, A.Schempp, H.Podlech BEVATECH OHG, Frankfurt, Germany.

Abstract

The **N**uclotron-based **I**on **C**ollider f**A**cility (NICA) project at JINR (Dubna) has a goal to set up experimental studies of both hot and dense strongly interacting baryonic matter and spin physics. The experiments will be performed in collider mode and at fixed target [1]. The first part of the project program requires heavy ion collisions generation of $^{197}Au^{79+}$ nuclei. The new linear accelerator for the heavy ions – HILAc (Heavy Ion Linear Accelerator) as the injector for the Nuclotron Booster ring is under construction presently. The progress and the main characteristics of the 3.2 MeV/u linear accelerator HILAc are presented.

INTRODUCTION

NICA facility is aimed to perform at JINR wide program of fundamental and applied researches with the ion beams from p to Au at energy from a few hundred MeV/u up to a few GeV/u. The beams at required parameters will be delivered by two superconducting synchrotrons – the Booster (magnetic rigidity is 25 Tm) and the Nuclotron (45 Tm) equipped with an existing injector – linac LU-20 with new ion sources: SPP (Source of Polarized Particles), LIS (Laser Ion Source) [2].

As the injector for the designed Booster ring the new heavy ion linear accelerators for the $^{197}Au^{+31}$ beams with new ESIS type ion source Krion-6T (for high charge state heavy ions) is under construction. Status and the progress of the heavy ion injector for the Nuclotron Booster project are presented.

HEAVY ION SOURCE

Construction and assembly of Krion-6T were completed in 2013 and full-scale tests in reflex mode of operation had been started at a test bench. After reaching of 5.4 T of the solenoid magnetic field in a robust operation (the design value is 6 T) the $Au^{30+} \div Au^{32+}$ ion beams have been produced at intensity of about $6 \cdot 10^8$ particles per pulse. The required ionization time is 20 ms [3]. Obtained parameters are close to required for HILAc operation.

Thereafter the source was optimized for production of ions with charge to mass ratio of $q/A \geq 1/3$ in order to provide complex test of all its systems at operation on existing injection facility. In May 2014 the source was installed at high-Voltage (HV) platform of the LU-20 fore-injector (Fig. 1) and used during Nuclotron run #50 in June. The main goal for future two years is to reach the project parameters of KRION-6T for Au^{31+} beam.

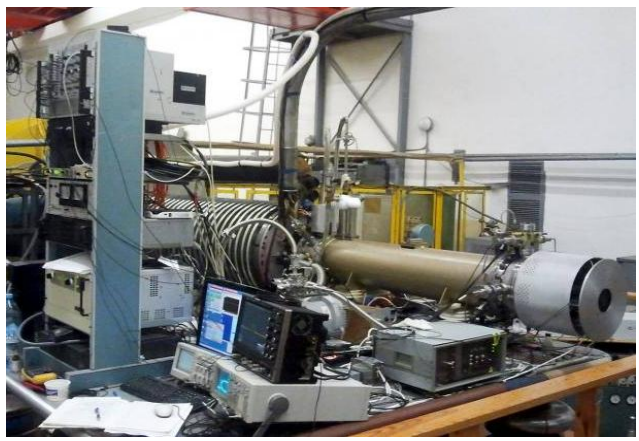


Figure 1: Krion-6T at high-voltage platform of LU-20 fore-injector. The Nuclotron Run #50.

LOW ENERGY BEAM TRANSFER CHANNEL

The ion source is situated on high-voltage platform (up to 150 kV). The LEBT channel (Fig. 2) begins from electrode with potential U0, after which a DN 250 vacuum valve is installed. In initial part of channel (IPC) the focusing electrodes with potentials U1 and U2 are located. IPC ends the tube with potential, falling off from U3 up to 0. Two solenoids, placed after initial part, form beam at the input of RFQ.

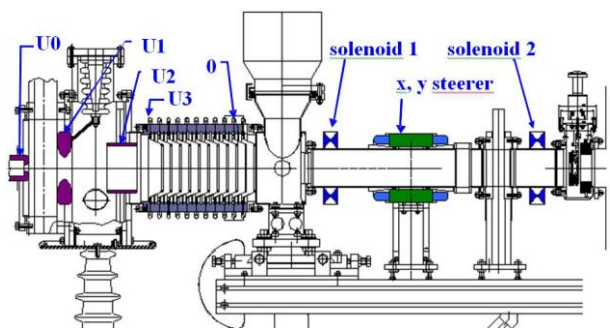


Figure 2: LEBT cannel scheme.

Electrostatic field inside IPC and magnetic field of solenoids are calculated by the POISSON program [4]. Optimization of channel parameters to achieve required beam parameters at the RFQ entrance was performed by MCIB04 code [5]. The code takes into account the aperture of the channel and the effects of the space charge of the multi-component beam. Two different variants of possible initial charge state spectrum of the gold beam are taken into account.

The phase planes of different charge states of the gold beam at RFQ entrance after optimization are shown

Copyright © 2014 CC-BY-3.0 and by the respective authors

ISBN 978-3-95450-142-7

DESIGN STUDY OF SUPERCONDUCTING LINEAR ACCELERATOR FOR UNSTABLE ION BEAM IN RISP

Ji-Gwang Hwang, Chanmi Kim, Yumi Lee, Eun-San Kim*
Kyungpook National University, Daegu, Korea
Hye-Jin Kim, Bong Hyuk Choi, Ilkyoung Shin, Hyojae Jang, Hyung Jin Kim, Dong-O Jeon
Institute for Basic Science, Daejeon, Korea

Abstract

A post accelerator of RAON can accelerate unstable and stable ion beams up to 16.5 MeV/u for $^{132}Sn^{16\sim20+}$ and 16.0 MeV/u for $^{58}Ni^{8+}$, which has a ratio of mass to charge, A/q, of 8.3. The unstable ion beam such as $^{132}Sn^{20+}$ produced by an ISOL system has the large transverse and longitudinal emittances. Hence an acceptance and envelope of the post accelerator should be optimized for safety operation. The beams accelerated by the post accelerator were transported by a post-to-driver transport (P2DT) line which consists of a charge stripper, two charge selection sections. Then the beams are accelerated up to 200 MeV/u in the high energy linac. In this paper, we will show a criteria for the design of the post accelerator and results of beam tracking simulation from the exit of the ISOL system to the end of the high energy linac.

INTRODUCTION

The linear accelerator with a superconducting technology for heavy ion beams named as a RAON (Rare isotope Accelerator Of Newness) was launched to examine the numerous facets of basic science, such as nuclear physics, astrophysics, atomic physics, life science, medicine and material science [1]. The unstable ion beams was produced by a ISOL based ion source and it was accelerated up to 16.5 MeV/u for ^{132}Sn ion beams and 16.0 MeV/u for ^{58}Ni ion beams with a high repetition rate of 81.25 MHz. The electrons of the ion beam are stripped by the charge stripper to increase the acceleration efficiency at the high energy linear accelerator and it is transported to high energy linear accelerator through the post-to-driver transport (P2DT) beam line. The schematic layout is shown in Fig. 1.

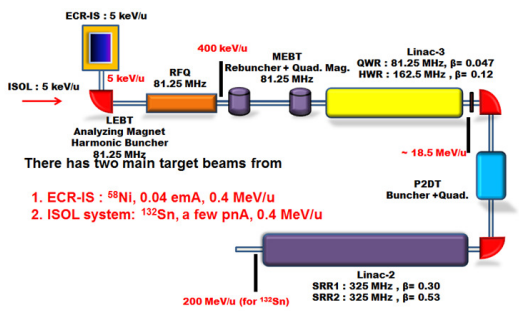


Figure 1: The schematic layout of the post linac.

TRACKING SIMULATION OF THE POST LINAC FOR ^{132}SN ION BEAM

In order to demonstrate the beam quality in the post linac, the particle tracking simulation from the low-energy beam transport (LEBT) line to the end of the high energy linac was performed with 500k macro-particles. The $^{132}Sn^{20+}$ beam was produced by the ISOL system with the energy of 5 keV/u and it was accelerated up to 400 keV/u by the RFQ accelerator. The initial particle coordinates of the macro-particles were obtained using the tracking simulation from the LEBT to MEBT by the codes TRACK and PARMTEQ. The distribution at the entrance of the post linac is shown in Fig. 2.

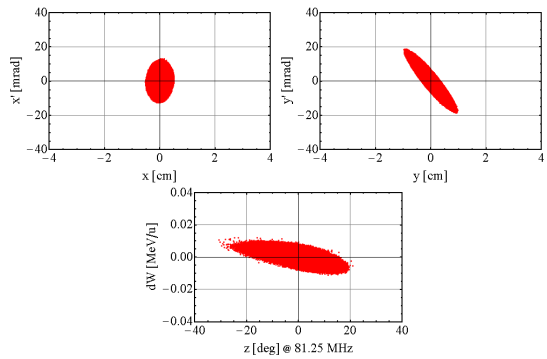


Figure 2: The particle distributions of $^{132}Sn^{20+}$ on 6D phase space at the entrance of the post linac.

The beam energy, rms horizontal and vertical emittances, and longitudinal emittance are 0.405 MeV/u, 0.282 mm-mrad, 0.287 mm-mrad and 0.464 keV/u-ns, respectively.

In order to suppress many instabilities which can cause the particle loss in the linac such as the envelope instability, parametric resonance and the space charge effect, the zero current phase advances, σ_0, is set to lower than 90° [2]. A low phase advance per period, and consequently a smooth focusing, has some costs in terms of beam dimensions, but guarantees the stability of envelope oscillations [3]. The ratio between the zero current transverse and longitudinal phase advance, ϕ_z/ϕ_x and ϕ_z/ϕ_y, were also almost kept between 1.0 and 1.5 except the matching section to vanish the effect of the parametric resonance [2]. Figure 3 shows

* eskim1@knu.ac.kr

ISBN 978-3-95450-142-7

Copyright © 2014 CC-BY-3.0 and by the respective authors

RF COAXIAL RESONATOR FOR INVESTIGATING MULTIPACTOR DISCHARGES ON METAL AND DIELECTRIC SURFACES

M. EL Khaldi, W. Kaabi, P. Lepercq, Y. Peinaud
LAL, ORSAY, France

Abstract

Multipactor discharge is a phenomenon in which electrons impact one or more material surfaces in resonance with an alternating electric field. The discharge can occur for a wide range of frequencies, from the MHz range to tens of GHz, and in wide array of geometries if the impacted surface has a secondary electron emission (SEE) yield larger than one. The discharge can take place on a single surface or between two surfaces. A novel coaxial resonator to investigate two-surface multipactor discharges on metal and dielectric surfaces in the gap region under vacuum conditions has been designed and tested. The resonator is ~ 100 mm in length with an outer diameter of ~ 60 mm (internal dimensions). A pulsed RF source delivers up to 30 W average power over a wide frequency range 650-900 MHz to the RF resonator. The incident and reflected RF signals are monitored by calibrated RF diodes. An electron probe provides temporal measurements of the multipacting electron current with respect to the RF power. These experiments were successful in identifying multipacting and allowed us the evaluation of a home made sputtered titanium nitride (TiN) thin layers as a Multipactor suppressor.

INTRODUCTION

A multipactor discharge is a phenomenon in which electrons impact one or more material surfaces in resonance with an alternating electric field [1]. Two main conditions must be met in order to develop a multipactor discharge between two material surfaces. First, electrons traversing the gap must impact the electrode near the time the E-field reverses the direction. Second, electrons must impact the surface with enough energy to create electron multiplication by secondary emission, i.e. δ (E) $\geq$1. The discharge is sustained by the population of electrons that remain in phase with the RF electric field. Because the discharge is sustained by secondary electrons, multipactor discharges typically occur under vacuum conditions.

Multipactor discharges are considered detrimental to RF systems in most applications. The discharges can cause vacuum window failure, limit the delivery of RF power, detune resonant cavities, damage high power RF sources, and cause a local pressure rise due to the desorption of surface gases[2]. As mentioned, multipactor (MP) is often an undesirable phenomenon, and avoidance can be critical in the operation of certain systems, it can be avoided in several ways. A general cure against multipacting is to avoid the resonant conditions by either a proper choice of the geometry of the device [3, 4] or by coating the critical areas with a material with a lower secondary yield [5,6]. This way the effect of multipacting can be significantly reduced, but very often the MP phenomenon cannot be removed.

Titanium nitride (TiN) coating is used as a proven anti-multipacting coating for inter-cavity coupling slots, RF vacuum windows and RF coupling loops. Several experimental investigations have been performed at DESY and LAL-Orsay, aimed at reducing secondary electron emission and multipactor effects by TiN layers generation on dielectric or metal surfaces [7, 8].

We propose here an experiment facility for investigating two-surface multipactor discharges on dielectric and metal surfaces. The compact apparatus consists of a RF coaxial resonator in a high vacuum system (~ 10^{-8} mbar). The RF resonator is ~ 100 mm in length with an outer diameter of ~ 60 mm (internal dimensions), powered with a pulsed RF source delivering up to 30W average power. These experiments were successful in identifying multipacting and allowed us the evaluation of a homemade sputtered titanium nitride (TiN) thin layers as a Multipactor suppressor.

COAXIAL RESONATOR MULTIPACTOR EXPERIMENT

The RF coaxial resonator is ~ 100 mm in length with an outer diameter of ~ 60 mm (internal dimensions). The resonator's dimensions were chosen because of the available laboratory equipment. It is made out of stainless steel whose inner walls plated with copper and equipped with 4 ports: on the top, a small coaxial line penetrates the upper center electrode to provide a direct measure of the multipacting current, the bottom port for the pumping system, and two horizontal ports for RF coupling. Both RF antennas have the same coupling in order to maintain the symmetry of the central electric field. The RF antennas and diagnostics are accessed with vacuum feedthroughs. The flanges are also fabricated from stainless steel. Several pairs of center electrodes have been made from Cu, Al, and Stainless steel (S.S). One electrode sample holder made out of Cu was developed for investigating multipactor discharges on different material surfaces (Alumina ceramic (97.6% Al_2O_3), TiN coated Alumina). The dielectric samples have the square shape with a 10 mm edge length and 1 mm thickness. The vacuum system allows low pressures of ~ 10^{-8} mbar.

A pulsed RF source delivers up to 30 W average power over a wide frequency range 650-900 MHz to the RF resonator. The pulse width and repetition rate used were 50 ms and 4Hz, respectively (20% duty cycle). The RF circuit is straightforward and illustrated in Fig.1.

Copyright © 2014 CC-BY-3.0 and by the respective authors

3D EFFECTS IN RFQ ACCELERATORS

Sergey S. Kurennoy, LANL, Los Alamos, NM, USA

Abstract

RFQ accelerators are usually designed and modeled with standard codes based on electrostatic approximations. Recent examples show that this approach fails to accurately predict the performance for 4-rod RFQs: 3D RF effects near the vane ends can noticeably influence the beam dynamics. The same applies to any RFQ where the quadrupole symmetry is broken, e.g., 4-vane RFQ with windows. We analyzed two 201.25-MHz 4-rod RFQs – one recently commissioned at FNAL and a new design for LANL – using 3D modeling with CST Studio. In both cases the manufacturer CAD RFQ model was imported into CST. The electromagnetic analysis with MicroWave Studio was followed by beam dynamics modeling with Particle Studio. For the LANL RFQ with duty factor up to 15%, a thermal-stress analysis with ANSYS was also performed. The simulation results for FNAL RFQ helped our Fermilab colleagues fix the low output beam energy. The LANL RFQ design was modified after CST simulations indicated insufficient tuning range and incorrect output energy; the modified version satisfies the design requirements.

INTRODUCTION

Radio-frequency quadrupole (RFQ) accelerators are now ubiquitous in front ends of modern ion linacs. Usual RFQ design codes, e.g., Parmteq [1], rely on electrostatic field approximations that are well justified for classical 4-vane RFQs with perfect quadrupole symmetry. On the other hand, many modern RFQs contain elements that break this symmetry. RFQ vane modulations introduce perturbations that create a longitudinal accelerating field, which is the basic idea of the RFQ. The vane-modulation effects are accounted in analytical field representation in the codes or can be calculated by solving an electrostatic problem. However, additional RF field effects can be introduced by asymmetric elements like vane windows in split-coax designs or stem supports in 4-rod RFQs. Such effects are more complicated and can't be easily taken into account in electrostatic calculations, even in 3D, but can influence beam dynamics in some cases. We discuss 3D RF effects in two 4-rod RFQs that we have recently analyzed in details [2, 3] with CST Studio [4].

RFQ MODELS

Having an accurate model of the RFQ cavity is important for its EM analysis. For both RFQs considered, a CAD model from the manufacturer Kress GmbH was imported into CST. The model was further simplified by removing details unessential for EM calculations. The RFQ cavity outer walls were also removed, leaving only the resonator vacuum volume in the CST model. The outer boundaries are assumed perfect-conducting for EM simulations. The resulting model for the new LANL RFQ is shown in Fig. 1. The RFQ vacuum vessel, in light-blue, is 175-cm long and contains 24 stems. The tuners between the adjacent stems (Fig. 1, bottom) are at different heights. They are adjusted in the CST model to make the inter-vane voltage flat, see Ref. [3].

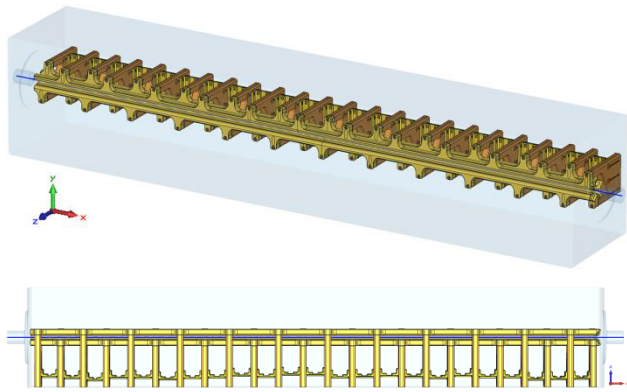


Figure 1: CST RFQ model (top) and its side view.

ELECTROMAGNETIC ANALYSIS

We studied the RFQ models using the CST MicroWave Studio (MWS). The mode frequencies and RF fields were calculated by the AKS eigensolver that provides more accurate surface approximations. In the latest CST version of 2014 the CAD import has been improved, which may allow using its more efficient tetrahedral eigensolver. The calculated RF fields have some interesting features. The first one is the presence of the longitudinal electric field in the end gaps that separate the vane ends from RFQ cavity walls. These end-gap bumps are illustrated in Fig. 2 for the FNAL 4-rod RFQ, cf. [5].

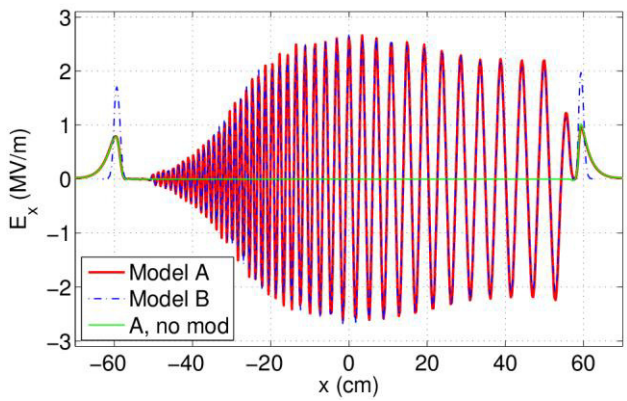


Figure 2: On-axis longitudinal field in FNAL RFQ.

Two models of the FNAL RFQ were studied [2]: model A with wide beam pipes attached to the RFQ cavity and model B with narrow beam pipes. The RFQ accelerating field (the oscillating part of the curves in Fig. 2) is produced by the vane modulation. The longitudinal field

Copyright © 2014 CC-BY-3.0 and by the respective authors

ISBN 978-3-95450-142-7

VERTICAL ELECTROPOLISHING OF Nb COUPON CAVITY AND SURFACE STUDY OF THE COUPON SAMPLES

V. Chouhan#, Y. Ida, K. Nii, T. Yamaguchi, MGI, Himeji, Japan
K. Ishimi, MGI, Kashiwa, Japan
H. Hayano, S. Kato, H. Monjushiro, T. Saeki, M. Sawabe, KEK, Tsukuba, Japan

Abstract

We have been carrying out vertical electropolishing of 1.3 GHz niobium (Nb) cavities for the ILC for 2 years. In this article we present results of investigation on vertical electropolishing (VEP) of a single cell Nb coupon cavity containing 6 Nb disk coupons located at beam pipes, irises and equator positions of the cavity. VEP were performed using our newly developed unique cathode called Ninja-cathode and a conventional rod cathode in order to observe and compare surface quality and the homogeneity of EP on the entire surface of the single cell cavity. Coupon currents for each coupon were measured to study EP phenomenon at different positions of the cavity. The surfaces of the coupons were analyzed with surface analytical tools like XPS.

INTRODUCTION

1.3 GHz niobium (Nb) superconducting RF cavities with a target field gradient of >35 MV/m and with a high Q value were adopted for the international linear collider (ILC). Rough surface and surface contamination remaining after the surface treatment degrade cavity performance. To achieve a good performance of cavities, surface treatments of the cavities play an important role. Electropolishing was considered as a promising technology for surface treatment of Nb superconducting RF cavities. Marui Galvanizing Co Ltd, Japan started vertical electropolishing (VEP) of Nb cavities in collaboration with KEK. We challenged to make a VEP system using PVC materials for the first time to aim drastic cost reduction. Moreover we are using our patented "Ninja" cathode of an especial shape having 4 retractable wings. The effect of the wings in agitation was demonstrated by flowing colored liquid having the same viscosity as EP solution in a transparent cavity [1]. In this article we show a comparison of results of two VEP experiments performed using the "Ninja" cathode and a conventional rod cathode.

VEP EXPERIMENTS

VEP experiments were carried out for a coupon cavity which was prepared with totally 6 holes on the beam pipes, irises and equator positions. The equator position contains two holes. 8 mm ϕ disk coupons which were electrically isolated from the cavity were fixed in these holes. The isolation allowed us to measure EP current from individual coupon. The cavity also contains 4 view ports on the top iris, bottom iris and equator. These view ports are used for in-situ observation and video recording especially for H_2 bubble attacks on the top and bottom irises. After the VEP the coupons are detached from the cavity and surfaces of these coupons are analyzed. These coupons provide us detail information of the inner surface at different positions of the cavity.

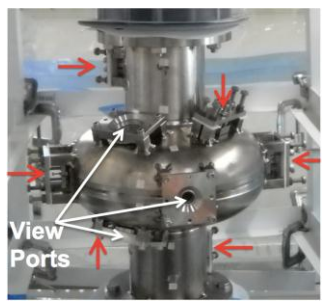


Figure 1: Nb coupon cavity with 6 Nb disk type coupons at beam pipes, irises and an equator shown by arrows.

Table 1: VEP Conditions for the Ninja and Rod Cathodes

Parameters	Ninja	Rod
H_2SO_4:HF	9:1	9:1
Electrolyte flow direction	Bottom to top	Bottom to top
Electrolyte flow rate (l/min)	5	5
Cathode rotational speed (rpm)	1	-
Applied voltage (V)	9-11	9
Target current density (mA/cm^2)	25	25-30
EP time (hours)	2.5	2.5
Cavity surface temperature (°C)	17.5-23	24.5-27

The coupon cavity was VEPed with the Ninja cathode and a rod cathode keeping the same parameters for both VEPs. All the VEP parameters are shown in Table 1. Electrolyte was circulated from bottom to top direction with a flow rate of ~5 l/min. During VEP the Ninja 4 wings cathode was rotated at 1 rpm for adequate agitation of the electrolyte. The flow rate and the cathode rotational speed were selected after several VEP experiments done with the Ninja cathode under different conditions. In order to cool the surface of the cavity during VEP we prepared a cooling system consisting of two hoses for passing the cool air from air coolers to the cavity surface. Each hose has equidistant holes to blow cool air uniformly on the beam pipes and irises for cooling. The cooling system maintained the cavity surface temperatures under 27 °C with variation of ~5 °C at different positions of the cavity. Both VEP experiments were performed for 2.5 hours for a target cavity removal thickness of 50 µm in average.

#vchouhan@e-maui.jp

Copyright © 2014 CC-BY-3.0 and by the respective authors

STATUS OF SUPERCONDUCTING CAVITY AND CRYOMODULE DEVELOPMENT AT MHI

T.Yanagisawa, H.Hara, K.Sennyu, N.Ikeda
Mitsubishi Heavy Industries, Ltd, Mihara, Hiroshima, 729-0393, Japan

Abstract

MHI's activities for superconducting accelerator are reported. MHI have supplied several 9-cell cavities for STF (R&D of ILC project at KEK) and have been considering production method for stable quality and cost reduction. And we had fabricated and installed cryomodules for STF and ERL R&D. These activities are reported in detail.

INTRODUCTION

MHI has supplied a 1.3GHz superconducting cavity for the STF project (STF is a project at KEK to build and operate a test linac with high-gradient superconducting cavities, as a prototype of the main linac systems for ILC.) for several years [1, 2]. The cavities from MHI-12 to MHI-26 reached Eacc= 35.2MV/m on average. This average Eacc achieves the ILC target, 35MV/m. (see Table 1 and Figure 1) And we have developed new techniques for improvement of productivity and for cost reduction for ILC.

On the other hand, MHI has supplied the cryomodules for KEK's superconducting projects including STF[3]. (see Figure 2) The details of cavity manufacturing techniques and cryomodule for STF are described below.

Table 1: Cavity Production List

Project	Customer	Production year	Cell number	Quantity	Remarks
STF	KEK	2005-2014	9	26	MHI-1 to MHI-26
		2013-	9	4	MHI-27 to MHI-30 (under fabrication)
ERL		2009-2010	2	3	For injector of KEK c-ERL project
		2010-2011	9	2	For main ring of KEK c-ERL project
ILC R&D	MHI	2009	9	1	[MHI-A] Deep drawing for HOM cup LBW for stiffener and flange
		2010	2	1	[MHI-B] Seamless dumbbell, Auto buffing
		2012	9	1	[MHI-C] LBW for baseplate Welding all equator line in succession
		2014	9	1	[MHI-D] Nb Gr-2 flange Welding all equator line in succession (4 cavities／1 batch)

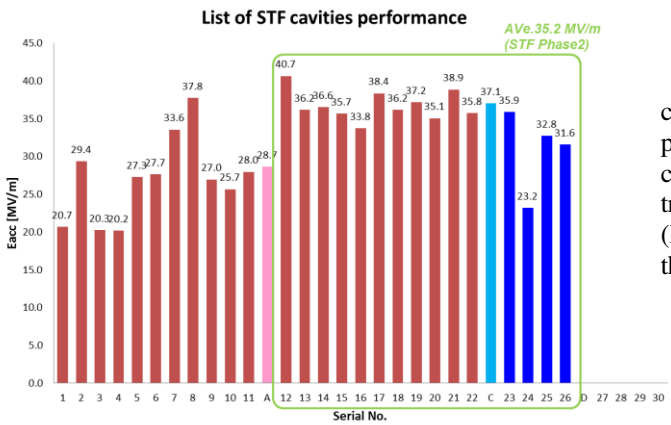
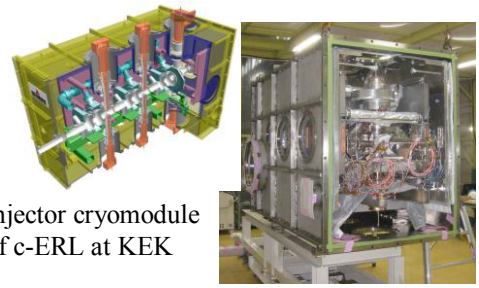
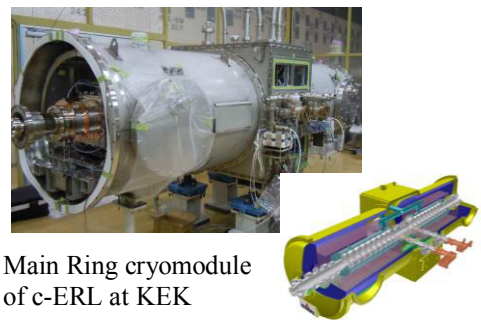


Figure 1: List of STF cavities performance.



(a) Injector cryomodule of c-ERL at KEK



(b) Main Ring cryomodule of c-ERL at KEK

Figure 2: Cryomodules

MANUFACTURING TECHNIQUES OF CAVITY

Nb Gr-2 Flange

The flanges of Cavity are generally made by Nb-Ti alloy because of the welding quality with niobium and the hardness for vacuum seal. MHI has developed to use the Niobium for cavity flanges. (see Figure 3) This way causes the reduction of number of parts and number of welding.

MHI tested three kind of niobium made by Heraeus.

- ASTM Gr-2 Nb with surface hardening treatment
- ASTM Gr-2 Nb (No treatment)
- RRR300 Nb with surface hardening treatment

After the annealing same as cavity and the thermal cycle test using liquid Nitrogen, three material flanges passed the helium leakage test. From point of view of commercial availability, ASTEM Gr-2 Nb (No treatment) was adopted. MHI has fabricated R&D cavity (MHI-D) using niobium flanges. Hereafter we will check the effect of cavity performance.

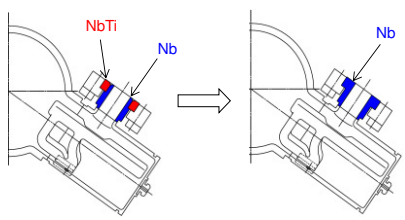


Figure 3: Cavity flange

Copyright © 2014 CC-BY-3.0 and by the respective authors

ISBN 978-3-95450-142-7

RESULT OF MHI 2-CELL SEAMLESS DUMB-BELL CAVITY VERTICAL TEST

K.Okihira, H.Hara, F.Inoue, K.Sennyu, N.Ikeda,
Mitsubishi Heavy Industries, Ltd, Mihara, Hiroshima, 729-0393, Japan
E.Kako, High Energy Accelerator Research Organization, Tukuba, Ibaraki, 305-0801, Japan
R.Rimmer, R.L.Geng, Jefferson Laboratory, Newport News, VA 23606, USA.

Abstract

MHI have supplied several 9-cell cavities for STF (R&D of ILC project at KEK) and have been considering production method for stable quality and cost reduction, seamless dumb-bell cavity was one of them. We had fabricated a 2 cell seamless dumb-bell cavity for cost reduction and measured RF performance in collaboration with JLab, KEK and MHI. Surface treatment recipe for ILC was applied for MHI 2-cell cavity and vertical test was performed at JLab. The cavity reached Eacc=32.4MV/m after BCP and EP. Details of the result are reported.

INTRODUCTION

MHI has supplied a 1.3GHz superconducting cavity for the STF project (STF is a project at KEK to build and operate a test linac with high-gradient superconducting cavities, as a prototype of the main linac systems for ILC.) for several years [1]. In a recent Vertical Test at KEK, some cavities reached Eacc= 31.5MV/m in first VT, and MHI-12 was also over 40MV/m. At the moment 19 new cavities for STF the Phase2 project involving MHI-12 and conforming to the high pressure gas safety law in Japan have been manufactured and 4 cavities are under testing (see Table 1 and Figure 1). On the other hand, we have developed new techniques for improvement of productivity and for cost reduction for ILC. The MHI-B as the first proto-type cavity using seamless dumb-bell cavity was fabricated and vertical tests were carried out at JLab. The details of MHI-B cavity are described below.

Table 1: Production list

Project	Customer	Production year	Cell number	Quantity	E_{acc} max at VT (MV/m)	Q_0 at operating (final) Eacc	Remark
STF Phase1	KEK	2005	9	4	29.4	2×10^{10}	MHI-1～4
ERL R&D		2006	1	2	31	9×10^{9}	
		2007	9	1	25	5×10^{9}	
		2007	2	1	43.7	3.4×10^{9}	pick up antenna
		2008	2	1	40.9	3.3×10^{9}	
		2009	9	1	28	7×10^{9}	
cERL		2009～2010	2	3	33.4	6.1×10^{9}	
		2010～2011	9	2	25	1.2×10^{10}	@20MV/m
STF Phase1.5		2007	9	2	27.7	5×10^{9}	MHI-5,6
		2008		3	37.8	4.8×10^{9}	MHI-7～9
		2009		2	28	5.1×10^{9}	MHI-10,11
STF Phase2		2010～2014	9	15	40.7	6.2×10^{9}	MHI-12～
		2013～		4	under testing		MHI27～
ILC R&D (MHI R&D)	-	2009	9	1	28.7	1×10^{10}	MHI-A
		2011	2	1	32.4	9×10^{9}	MHI-B
		2012	9	1	37.1	5.2×10^{9}	MHI-C
		2014	9	1	under testing		MHI-D

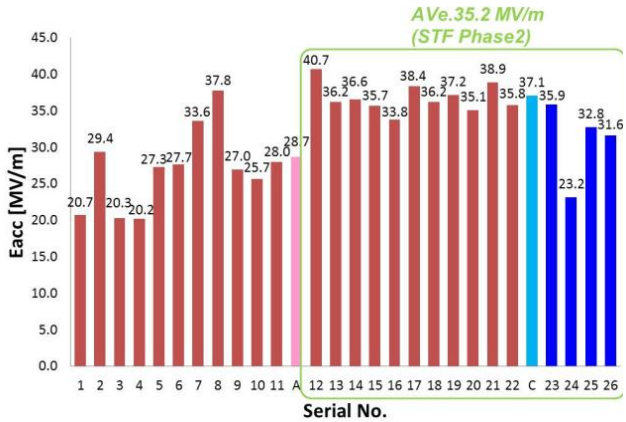


Figure 1: List of STF cavities performance.

FABRICATION OF MHI-B CAVITY (R&D)

MHI-B cavity was manufactured to establish seamless dumb-bell [2][3] as shown figure 2. This cavity was performed several testing at JLab to inspect the influences to cavity performance by seamless dumb-bell.

Feature of MHI-B

- Number of cell is two.
- No welding seam on iris (seamless dumb-bell).
- Finishing for inner surface of dumb-bell is automatic buffing by robot.
- Cell's design is the same as STF cavity



(a) (b)

Figure 2: (a) Over view of MHI-B cavity, (b) Seamless dumb-bell.

Seamless Dumb-Bell

Figure 3 shows the flow of forming for seamless dumb-bell. The quality of inner surface of dumb-bell depends on the condition of the seamless pipe. The seamless pipe was made by deep drawing.

Copyright © 2014 CC-BY-3.0 and by the respective authors

ISBN 978-3-95450-142-7

ON NONLINEAR DYNAMICS OF A SHEET ELECTRON BEAM

H.Y. Barminova, MEPhI, Moscow, Russia

Abstract

The dynamics of a charged particle beam is studed in the frame of Vlasov theory in the case of non-hollow nonuniform spatial distribution. The nonstationary model based on a beam behaviour description by means of kinetic function dependent on the integrals of the particle motion is presented. The cases of strong and weak nonlinearities are considered.The results of numerical and analitical calculations are discussed.

INTRODUCTION

For a lot of accelerator physics problems the investigation of a charged particle beam dynamics by means of the simple mathematical models is attractive tool because it allows to obtain the knowledge of the beam behaviour with most physical generality. Frequently these models are involved into programm packages which calculate the beam envelopes or particle trajectories. First such a model was proposed by I. M. Kapchinsky and V. V. Vladimirsky (KV-model) in 1959 [1]. This model allows to describe both the charge-dominated and emittance-dominated beams in the case of quasistationary beam propagation. KV-model gives a full kinetic beam description due to the assumption that the kinetic distribution function is a function of particle motion integral and hence automatically satisfies to Vlasov equation. Yarkovoy's model [2] may be considered as a development of KV-model. It allows to describe nonstationary 2D-beams without axial symmetry. Subsequent development of 2D- and 3D-models is presented, for instance, in papers [3-6]. All the models mentioned above describe the beam with linear own forces that corresponds to uniform charge density in a transverse beam cross-section in the case of continuous beam or in a bunch volume in the case of bunched beam. The models that take into account the nonuniform charge density were proposed, as example, in [7-11]. In papers [9-11] only self-similar beam oscillations are under consideration, in contrast to papers [7, 8], where the particle distributions are not stationary.

The present paper studies a charged particle beam with parabolic current density profile. The aim is to predict a behavior of the beam envelope with time. The model is used which doesn't require the particle distribution to be stationary.

MODEL DESCRIPTION AND NUMERICAL CALCULATIONS

Let us consider, for example, a quasistationary relativistic intense electron beam, the own charge of the beam being neutralized. For the mathematical simplicity let us suppose the sheet geometry of the beam. Since as a rule the beam lifetime is significantly more than the time of transition processes in the beam one can describe the beam behaviour by means of a smooth function R(z), where R(z) – the beam tranverse size, z – longitudinal coordinate. In the case of the continuos beam with uniform charge density KV-invariant [1] may be written as:

$$I = (R'x - Rx')^2 + \frac{\varepsilon_0 x^2}{R^2} \qquad (1)$$

Where x' is the derivative of x with respect to z, R' – the derivative of R with respect to z, ε_0 - the beam rms emittance squared, x – the transverse coordinate.

Let us consider the beam with the charge density distribution n(x,z), which falls down with x as parabola and reaches zero at the beam boundary. It is a good approximation for the density distribution of the real non-hollow continuous beam:

$$n(\mathrm{x},\mathrm{z}) = a_0(z) - a_2(z)x^2 \qquad (2)$$

Hence we obtain that the particle transverse motion is described by the equation

$$x'' = -\alpha_1(z)x + \alpha_3(z)x^3. \qquad (3)$$

Here $\alpha_1(z) = \mathrm{k}\, a_0(z), \alpha_3(z) = \mathrm{k} a_2(z)/3$, $k = 4\pi e^2/\mathrm{mc}^2$

For equation (3) the integral I as analogue of KV-invariant (1) may be constructed with the help of the next relation:

$$x'(\mathrm{x},\mathrm{z},\mathrm{I}) = \sum_{k=0}^{\infty} a_k(z,I)x^k \pm \Big(\sum_{k=0}^{\infty} b_k(z,I)x^k\Big)^{1/2} \qquad (4)$$

Let us substitute (4) in (3) and neglect all summands with 5$^{\text{th}}$ power and higher. Then let us introduce a kinetic distribution function as:

$$f(I) = 2\mathrm{n}_0\sigma(1 - I).$$

Copyright © 2014 CC-BY-3.0 and by the respective authors

LOW DOSE X-RAY RADIATION SOURCE FOR ANGIOGRAPHY BASED ON CHANNELING RADIATION PRINCIPLE

T.V. Bondarenko, Yu.D. Klyuchevskaya, S.M. Polozov, National Research Nuclear University MEPhI (Moscow Engineering Physics Institute), Moscow, Russia

Abstract

Angiography is one of the most reliable and contemporary procedure of the vascular system imaging. X-ray spectrums provided by all modern medical angiographs are too broad to acquire high contrast images and provide low radiation dose at the same time. The new method of narrow X-ray spectrum achieving is based on the idea of channelling radiation application. The X-ray filters used in this method allows eliminating the high energy part of the spectrum and providing dramatic dose reduction. The scheme of the facility including the X-ray filter is discussed. The results of the spectrum analysis for the channelling radiation source are shown including the data for electron beam trajectories inside the diamond crystal investigation.

INTRODUCTION

Angiography nowadays is the state of the art medical imaging technique used to visualize the inside, or lumen, of blood vessels and organs of the body, with particular interest in the arteries, veins and the heart chambers. X-ray sources in angiography applications are based on X-ray tubes. These sources are well explored and provide high rates of radiation intensity. The main drawback of the tube is wide bandwidth of the generated radiation spectrum. Monochromatic radiation source application can result in better imaging, and, moreover, lower irradiation dose can be applied to a patient.

Large scale accelerators as synchrotrons, storage rings, energy recovery accelerators or LINACs can be only used to produce synchrotron and undulator radiations. Compton scattering needs comparatively smaller accelerator but high power laser and high accuracy control system are strongly requested. Very high CW currents up to tens of Amperes are necessary to excite the characteristic X-ray of La or Ba emitters having considerable photon flux. Channeling radiation source, one of the most powerful radiation emitters by relativistic electrons in crystals is discussed below as a possible alternative of these techniques [1].

For the angiography and radiography procedure one needs a conventional total flux of $2 \cdot 10^7$-$2 \cdot 10^9$ photons/mm^2/s and irradiated area about 43x43 cm^2 [2]. The lower end of photon energy is estimated as 33.2 keV for angiography (the key energy to hit the peak value of iodine contrast mass attenuation). The X-ray monochromatic peak energy can be varied by means of the metal of crystal target variation of electron beam energy tuning. A standard therapy LINAC produced by one of the leading manufacturers can be used. Incoherent bremsstrahlung in a crystal is a serious problem that results in rather high irradiation dose. Any solution to suppress it is strongly desirable.

X-RAY SOURCE SCHEME

The monochromatic X-ray source based on the channelling radiation generated by the electrons moving inside the oriented crystals is discussed [3]. The principal scheme of the source is presented on the Figure 1. The electron beam (2) is generated in the electron source (1) and accelerated to ultra-relativistic energies in the LINAC (3) that is not considered in the work. After that electrons pass through the aligned crystal (4) placed inside the goniometer (12) and generated the monochromatic channeling X-ray radiation and broadband bremsstrahlung. The deflecting magnet (5) is used to lead the electron beam to the beam dump (11). The X-ray pass through the polycapillary optics (10) and the radiation with energy lower that 40 keV (9) is filtered and deflected to the patient (7), the rest of the radiation is propagated straightforward to the X-ray dump (6). The radiation is then detected with the panel detector (8). The electron beam deflection is done in order to eliminate the possibility of the polycalillary optics damage. The scheme of the polycapillary optics using allows to fix the main problem of such a facility – broadband bremsstrahlung spectrum that leads to unnecessary dose enhancement that is obtained by the patient. The policapillary optics is the most reliable for filtering of the high energy X-ray radiation with efficiency about 60% at the 17 keV energy level and about 40% at 33 keV level.

RADIATION FROM CRYSTALL

The channeling is the process of the electron movement inside the crystal between the crystallographic planes (in case of the planar channeling) or near the crystallographic axis (in case of the axial channeling). We investigate the planar channeling in the crystal along the <110> plane of the diamond (Figure 2). The electron dynamics in the crystal is evaluated using the BEAMDULAC-CR [4] code. The investigation is held using the classical approach of the electron propagation in the transverse potential field inside the crystal.

The electrons dynamics in the crystal shows that electron beam should have the divergence around 10 mrad and energy spread in order of 1% to eliminate the dechanneling (travelling of the electrons from one channel to another) of the electrons. Several calculations were held to estimate the dechanneling effect. The overall amount of dechanneled particles is presented on the Figure 3.

Copyright © 2014 CC-BY-3.0 and by the respective authors

ISBN 978-3-95450-142-7

SIMULATION OF THE ELECTRON BEAM DYNAMICS IN THE BIPERIODICAL STRUCTURE

Yu.D. Kliuchevskaia, T.V. Bondarenko, S.M. Polozov, National Research Nuclear University MEPhI (Moscow Engineering Physics Institute), Moscow, Russia

Abstract

A biperiodical accelerating structure (BAS) with operating frequency 27 GHz for the 6 MeV compact radiotherapy electron accelerator is considered. The operating frequency 27 GHz allows to significantly reducing the facility sizes, unlike the S-, X- and C-band operating linacs. The optimal geometrical parameters of BAS necessary for π/2 mode were defined by means of accelerating and coupling cell tuning. The BAS coupler was also simulated. Results of the electron beam dynamics analysis in designed structure are also discussed.

INTRODUCTION

Electron accelerators are becoming more widely used in the fundamental and applied scientific researches, in the medicine, industry and ecology. Compact electron accelerators uses for industrial and medical purposes [1]. The possibility of compact electron accelerator energy of about 6 MeV design is, suitable for use in medical therapy system and operating at the high frequency of 27 GHz. The beam dynamics simulation was conducted for accelerating structure based on biperiodical accelerating system (BAS) with all disk loaded waveguide (DLW) and beam dynamics in such structure. High operating frequency 27 GHz is the feature of such facility development which is much higher than the standard frequency used for the applied purpose accelerators (2856, 2898 or 5712 MHz). It makes possible to sufficiently reduce the size of the accelerator. Compact size of such accelerators allows using it for medical application. The main part of the installation is a biperiodical accelerating structure based on disk loaded waveguide (DLW) at the frequency of 27 GHz.

The beam dynamics analysis in the designed models of structures was carried out using BEAMDULAC-BL code [2].

BEAM DYNAMICS IN THE BAS

The beam dynamics will be investigated in the buncher and in the main section, the optimal parameters will choose. Optimization was conduct by varying of different parameters such as the amplitude of the accelerating RF field and the length of the bunching section.

It is offered to divide structure into two sub-sections (bunching and main accelerating section). In a buncher the continuant bunch reduces to rather short bunches, which also more accelerates to the energy, allowing injecting them in the main section without losses. In a buncher the phase velocity and amplitude of an electric field monotonically increase and in the main accelerating section they are constant.

It was shown that the electron beam can be effectively bunched and accelerated to the energy of 6 MeV in a BAS operating at 27 GHz. The total current transmission coefficient for the full structure reaches 72 %. The beam envelope can be effectively controlled. Energy spectrum, beam envelope and transverse velocity distribution, beam cross-section, longitudinal emittance for the buncher and the main section are shown in the Fig. 1-4.

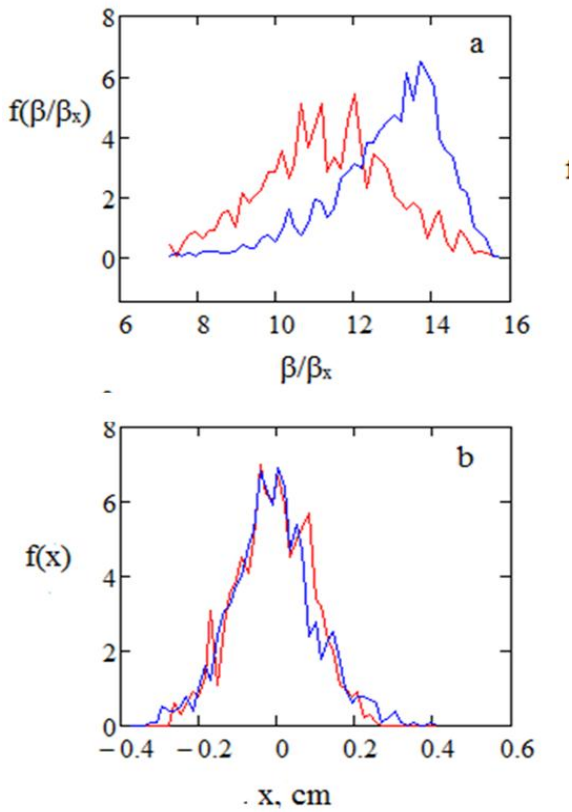


Figure 1: Energy spectrum (a) and (b).

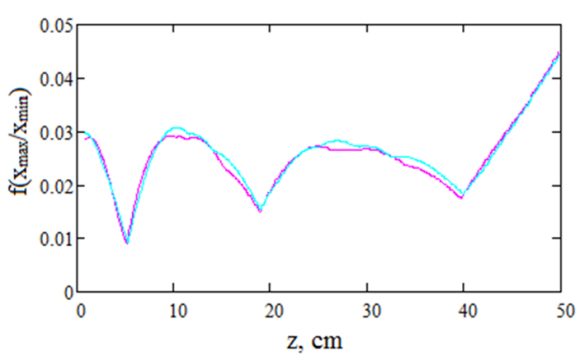


Figure 2: Beam envelope.

Copyright © 2014 CC-BY-3.0 and by the respective authors

BEAM DYNAMICS SIMULATION FOR THE 1 GeV HIGH POWER PROTON LINAC

V.S. Dyubkov, S.M. Polozov, A.V. Samoshin, National Research Nuclear University MEPhI - Moscow Engineering Physics Institute, Moscow, Russia
T.V. Kulevoy, National Research Nuclear University MEPhI - Moscow Engineering Physics Institute and Institute of Theoretical and Experimental Physics, Moscow, Russia
G.N. Kropachev, Institute of Theoretical and Experimental Physics, Moscow, Russia

Abstract

The design of high energy and high power proton linacs for accelerating driven systems (ADS) is one of the accelerator technology frontiers. Such linacs are under developing in EU, Japan, PRC but not discussed in Russia previous ten years. The driver linac and the breeder conceptual designs were funded by the Ministry of Science and Education of Russian Federation in 2013. The 2 MeV RFQ linac was proposed as the first accelerating section. A number of RF focusing sections types (by RF crossed lenses, modified electrode profile RFQ, axi-symmetrical RF focusing) were discussed for medium energies. The conventional modular scheme linac based on spoke-cavities and 5-cell elliptical cavities was designed for higher energies. The results of beam dynamics simulation in this linac will present.

INTRODUCTION

The designing of a high-power proton linac for 1.0 GeV was performed by collaboration of MEPhI, ITEP and Kurchatov institute researchers in 2013. Such linac is useful for spallation neutron sources and drivers for accelerator driven system (ADS). Operation in the CW mode is preferable for an ADS linac. Accelerator-driver design was done more that ten years ago in the Russian Federation last time. This project was supported by the Ministry of Science and Education of the Russian Federation. The conceptual design of the linac is presented in Fig. 1.

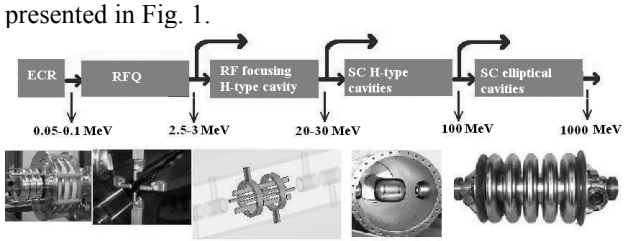


Figure 1: The linac general layout

The linac will consist of an RFQ, RF focusing section(-s) and SC modular configuration sections. Several different types of RF focusing linacs were discussed for the medium energies. There are RF crossed lenses [1], modified electrode profile RFQ [2], axi-symmetrical RF focusing (ARF) [3] and the short SC cavities system was also discussed. The conventional modular scheme linac [4] based on spoke-cavities and 5-cell elliptical cavities were designed for higher energies. The linac layout have three intermediate energy beam lines which can be used by step-by-step linac construction to different experiments with neutron production targets or for radiation testing of reactor construction materials..

BEAM DYNAMICS SIMULATION IN RFQ

Beam dynamics simulation in RFQ section was done using the BEAMDULAC-RFQ code [5] and is detail discussed in ref. [6]. The CW RFQ linac section operates at 162 MHz and accelerates the beam to 2 MeV. It should be noted that accelerating potential between the RFQ electrodes will limited by 1.5-1.7 of Kilpatrick criterion value for the CW mode (~130-150 kV for 100-200 MHz band). The accelerating channel consists of three regions as was proposed in [7-8]: the dynamic matcher, the gentle buncher and the main accelerating region. The main RFQ channel parameters are the following: operating frequency 162 MHz, channel length 2400 mm, matcher length 160 mm, buncher length 1100 mm, synchronous phase on main accelerating region 36 º, maximal electrodes modulation 2.25, maximal aperture size (on matcher start) 9 mm, maximal aperture size in main accelerating region 5.5mm, injection energy 0.047±1 % MeV, injection transverse emittance 2π mm·mrad output energy 2.0MeV. It was shown that for the injection energy (47 keV) and the electrode potential (120 kV) current transmission decreases very slowly with injection current growth: ~96 % for zero current and ~94 % with 20 mA

BEAM DYNAMICS IN MEDIUM ENERGY RANGE

The different types of RF focusing sections as RF crossed lenses, modified electrode profile RFQ and axi-symmetrical RF focusing were studied for medium energy region with short SC cavities system. Brief results of beam dynamics simulation were presented in [9].

RF Crossed Lenses

A method of ion focusing in linac by RF decelerating fields of crossed lenses (RFCL) [1] permits to obtain energy-independent focusing strength and high acceleration rate. The crossed lens (CL) is a set of plane electrodes with rectangular apertures such that the apertures in the neighbouring electrodes are rotated 90º each other (see Fig. 2).

The ratio of sides for the rectangular apertures equals 3 (chosen under $a/b<<1$) then an electrical field component directed along the slit is negligible as compared with a component across the slit. Within the considered method

Copyright © 2014 CC-BY-3.0 and by the respective authors

ISBN 978-3-95450-142-7

STUDY ON POLISHING METHOD OF Nb SURFACE BY PERIODIC REVERSE CURRENT ELECTROLYSIS WITH ALKALI SOLUTION*

M. Umehara, Nomura Plating Co, ltd., Osaka Japan
T. Saeki, H. Hayano, KEK, Tsukuba, Japan

Abstract

Currently, electropolising method is thought to be the best method for the final surface preparation of superconducting RF cavity to obtain high gradient. In this conventional electropolising method, the electrolyte is the mixture of fluoric and sulfuric acids. Therefore, the operation of this method is dangerous, and the equipment becomes expensive because all parts should be made of high density polyethylene or fluorocarbon resin to avoid metallic parts which suffers from corrosion by electrolyte. Moreover, sulfur is produced as byproduct in the electropolishing process and this causes degradation of cavity performance. In order to overcome these drawbacks, we studied new polishing method of Nb surface by periodic reverse current electrolysis with alkali solution which causes no sulfur and allows the usage of metallic parts to realize cost effective equipment. In the study, we performed experiment of Nb coupons by this new method and obtained as good surface roughness as conventional electropolishing method. In this article, we report the details of the study.

INTRODUCTION

Final surface preparations of niobium (Nb) superconducting radio frequency (SRF) cavities play a critical role in order to achieve high performance of cavity. Electropolishing with sulfuric acid (H_2SO_4) and fluoric acid (HF) is thought to be the best final surface preparation method to achieve higher gradient of SRF cavity and it has already been conventional technology around the world as the standard [1]. Development of electropolishing method that does not use fluoric acid is desired in the mass-production of SRF cavities in the future project like ILC, because the electrolytic solution used in this method is very dangerous for the operator due to toxic gases (ex. H_2S, SO_x) generated in the operation and then the complex instrumentation and operation are required for the safety which increase the cost. In addition, it is reported that sulfur is produced as byproduct in the process and this causes degradation of cavity performance [2]. Equation (1) shows the chemical reaction which creates sulphur as byproduct.

$$xH_2S + SOx \rightarrow xH_2O + (x+1)S \quad (1)$$

Then the development of electropolishing method without containing sulfur is also desired. In such situation, Faraday Inc. and FNAL have studied the periodic reverse (PR) electropolishing method with diluted H_2SO_4 for the superconducting RF cavity [3]. In the PR method, the sign of applied voltage is periodically switched to positive and negative in the electropolishing process. Typical periodic reverse current in the process is shown in Fig. 1. In the plating process, this method has been widely used and applied in industries in order to obtain uniform thickness of plating.

In this paper, we report PR electropolishing method with NaOH solution. We selected NaOH as electrolyte for the following reasons. 1) If NaOH solution is used, it is possible to fabricate apparatus with metal instead of fluorine resin. 2) The NaOH solution has chemically simple composition and then it is easy to monitor the contamination and also the prediction of reaction is easy. 3) It is known that Nb and Nb oxide dissolve in NaOH solution.

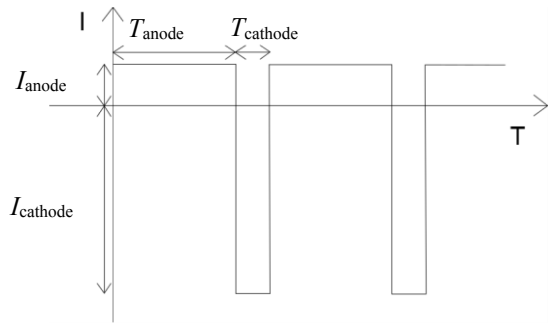


Figure 1: Typical periodic reverse current.

EXPERIMENTAL DETAIL

Experimental Setup

The experimental setup for the coupon test of PR method is shown in Fig. 2. Nb coupon is anode and Pt mesh is cathode. Specification of power source is as follows; I_{anode}=0-40 A, T_{anode}=10-99.9 ms, $I_{cathode}$=-100-0 A, $T_{cathode}$=0.1-2.0 ms. Water bath is used to control the temperature. We used EDX for the surface analysis of Nb and ICP for analysis of Nb in the solution, respectively. In addition, a laser/optical microscope is used for surface observation and a stylus-type roughness-meter is used to measure the surface roughness.

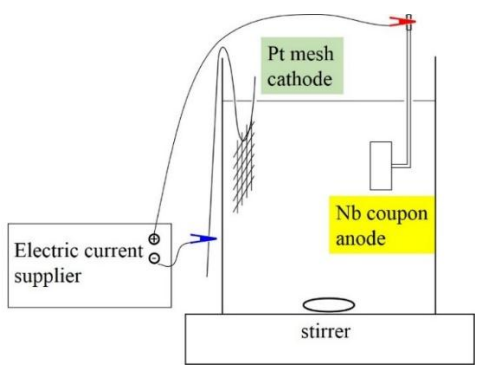


Figure 2: Schematic of the experimental apparatus.

Copyright © 2014 CC-BY-3.0 and by the respective authors

ISBN 978-3-95450-142-7

STATUS OF NEW 2.5 MeV TEST FACILITY AT SNS

A. Aleksandrov, M. Champion, M. Crofford, K. Ewald, Y. Kang, A. Menshov,
M. Middendorf, S. Murray, T. Rosebery, R Saethre, M. Stockli, A. Webster, R. Welton,
A. Zhukov ORNL, Oak Ridge, TN 37830, USA

Abstract

A new 2.5MeV beam test facility is being built at SNS. It consists of a 65 keV H- ion source, a 2.5MeV RFQ, a beam line with various beam diagnostics and a 6 kW beam dump. The facility is capable of producing one-ms-long pulses at 60Hz repetition rate with up to 50mA peak current. The commissioning with reduced average beam power is planned for fall 2014 to verify operation of all systems. The full power operation is scheduled to begin in 2015. The status of the facility will be presented as well as a discussion of the future R&D program.

INTRODUCTION

The Integrated Test Stand Facility (ITSF) consists of an H^- ion source, a Low Energy Beam Transport (LEBT), a Radio Frequency Quadrupole Accelerator (RFQ), a Medium Energy Beam Transport (MEBT), a high power beam stop and support systems. Functionally these systems replicate the SNS Front End systems to ensure relevance of the results obtained on the ITSF for the SNS Front End. The current layout of ITSF is shown in Fig. 1.

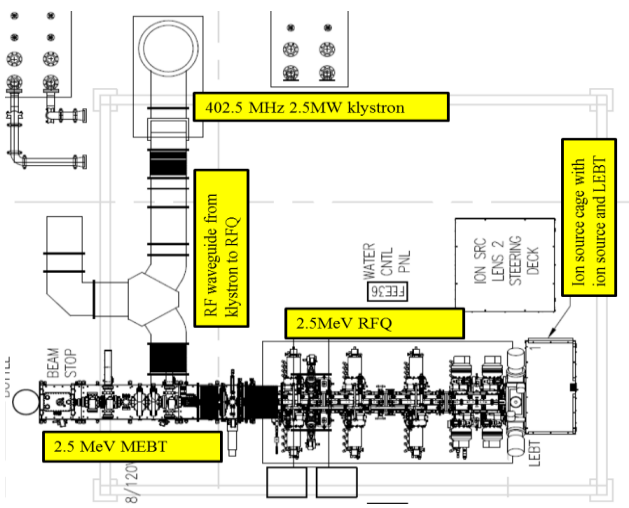


Figure 1: Current layout of the SNS Integrated Test Stand Facility.

The main goals of the ITSF are:

- Verifying operation of the SNS spare RFQ with full power beam test
- Providing a platform for testing existing equipment and developing new equipment for improving SNS reliability and power capability.
- Providing a platform for conducting R&D for novel accelerator physics and technological concepts related to high intensity hadron beam generation, acceleration, manipulation and measurement.
- Providing proton beams for a short pulse neutron source for the SNS Second Target Station moderator development.

This document provides a general description and status of the ITSF major systems.

ION SOURCE AND LEBT SYSTEMS

Ion Source

The H^- Ion source is identical to the ion source used at the SNS Front End with identical or similar support systems [1]. The developmental External Antenna Ion source will also be tested on this test stand [2].

LEBT

Several LEBT configurations are considered for the ITSF:

- An electrostatic LEBT that is identical to the baseline SNS Front End LEBT The main purpose of this LEBT is to verify operation of the spare RFQ.
- An experimental 2-solenoid magnetic LEBT with chopper. The main purpose of this LEBT is to explore the possibility of incorporating a fast chopper into a magnetic LEBT with neutralized beam. If successful, this development can lead to a 2-source magnetic LEBT design suitable for a high reliability high current Front End [3].

A schematic view of the ion source and electrostatic LEBT that is currently in use is shown in Fig. 2.

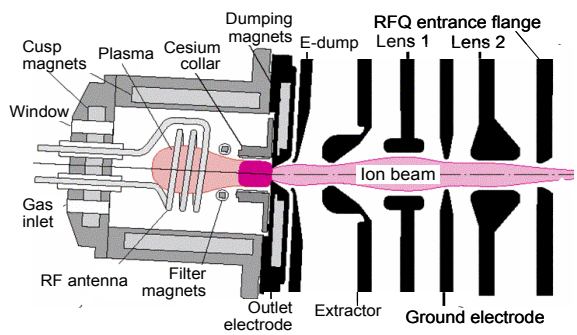


Figure 2: Schematic view of the H^- ion source and electrostatic LEBT

RFQ

The SNS spare RFQ [4] with associated support systems is used in the ITSF. When the spare RFQ is moved to the SNS Front End, the old SNS RFQ will be

Copyright © 2014 CC-BY-3.0 and by the respective authors

ISBN 978-3-95450-142-7

HISTORY OF CRYOMODULE REPAIRS AT SNS

M. Howell#, R. Afanador, B. DeGraff, M. Doleans, D. Douglas, B. S. Hannah, S-H. Kim, C. McMahan, T. Neustadt, S. Ottaway, J. Saunders, P.V. Tyagi, D. Vandygriff
ORNL, Oak Ridge, TN 377831, USA

Abstract

The operation of the Superconducting linear accelerator (SCL) has matured and now averages less than one trip per day. The availability of the SCL including radio-frequency systems, high voltage converter modulators, controls, vacuum and other support systems over the last three years is approximately 98%. The SNS has been in operation for ten years including the commissioning period. In support of achieving the stability of operation, multiple cryomodule repairs have been performed. Repairs to cryomodules have included instruments, helium leaks, valve actuators, cavity tuners, insulating vacuum repairs and upgrades, power supplies, higher order mode (HOM) feedthroughs, coupler windows, and coupler cooling components. Performance degradation has been experienced in multiple cavities. This has been corrected by thermal cycling the cryomodules with the affected cavities. Only two cavities have displayed slight permanent degradation that could not be corrected by thermal cycling. Repairs made to the SNS cryomodule will be detailed in this paper.

INTRODUCTION

The Spallation Neutron Source contains a superconducting linear accelerator which consists of eleven medium beta and twelve high beta cryomodules. The strategy to maintain high availability while operating at high power has multiple elements. The first and foremost step was to gain understanding of the machine during commissioning and initial operations such that the machine could be set up in a reliable manner while delivering beam. Due to the limited final linac output energy, each cavity is set at a maximum stable gradient based on the collective limiting gradients achieved through a series of SRF cavity/cryomodule performance tests at SNS, rather than setting uniform gradients as designed [1]. The second step in the strategy is to make systems as simple as possible while developing adequate diagnostic and protection schemes. This enables the operations staff to quickly diagnose issues and prevents permanent damage to the machine. Because simplicity is emphasized in the system design, the turnover from the system experts to the operations staff was facilitated. Good communication between the system experts and the operations staff is a critical component to the long term successful operation of the machine. Another key element of the strategy to maintain high availability at high power is to keep some energy margin. This allows operating flexibility during operation and serves to minimize down time during neutron production. One cavity is operated at zero energy gain so that it can be utilized in the event that another cavity has to be reduced in gradient. The final step to this strategy is to perform proactive and preventative maintenance. When the performance of a cryomodule is impacted, a repair plan is developed for that cryomodule. It is determined whether that repair can be completed within the tunnel (such as thermal cycling) or if the cryomodule needs to be transported to the cryomodule repair facility (such as coupler replacement). After determining the location for conducting the necessary repair, the cryomodule is evaluated for ancillary repairs and maintenance activities that correct deficiencies and enhance the cryomodule operation.

REPAIR HISTORY

Statistics for cryomodule repair at SNS have been maintained and recorded since 2007. A variety of repairs on cryomodules have been performed. These repairs can be broken into two categories; repairs that require thermal cycling of the cryomodule and repairs that do not require thermal cycling. Issues that require thermal cycling include helium leaks, cavity performance degradation, inoperable or unstable tuner, cable problems, excessive power coupling to the HOM, and coupler window leaks. Issues that do not require thermal cycling include instrumentation damage, faulty valve actuator, power supply failures, and coupler cooling system adjustments. A pie chart depicting the repairs performed at SNS since 2007 is included in Fig. 1.

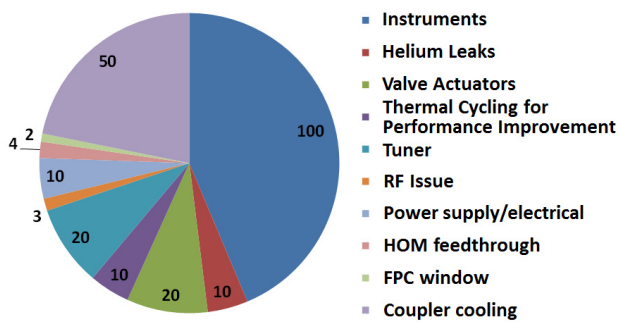


Figure 1: Number of SNS Cryomodule Repairs.

With all of the repairs that have been completed, it was necessary to perform thermal cycles of the cryomodules. Since 2007, there have been 34 instances of cryomodules being thermally cycled.

The number of repairs does not necessarily indicate the severity associated with the repair. The most significant repairs conducted that affected cryomodule performance are thermal cycling due to performance degradation, tuner repairs, HOM feedthrough removal, coupler replacement, and the repair of helium leaks due to failures in the cold

* This work was supported by SNS through UT-Battelle, LLC, under contract DE-AC05-00OR22725 for the U.S. DOE
# howellm@ornl.gov

Copyright © 2014 CC-BY-3.0 and by the respective authors

MULTIPACTING OPTIMIZATION OF A 750 MHz RF DIPOLE*

A. Castilla[1,2,3†], J. R. Delayen[1,2]
[1]Center for Accelerator Science, Old Dominion University, Norfolk, VA 23529, USA
[2]Thomas Jefferson National Accelerator Facility, Newport News, VA 23606, USA
[3]Universidad de Guanajuato (DCI-UG), Departamento de Fisica, Leon, Gto. 37150, Mexico

Abstract

Crab crossing schemes have been proposed to re-instate luminosity degradation due to crossing angles at the interaction points in next generation colliders to avoid the use of sharp bending magnets and their resulting large synchrotron radiation generation, highly undessirable in the detector region. The rf dipole has been considered for a different set of applications in several machines, both rings and linear colliders. We present in this paper a study of the effects on the multipacting levels and location depending on geometrical variations on the design for a crabbing/deflecting application in a high current (3/0.5 A), high repetition (750 MHz) electron/proton collider, as a matter to provide a comparisson point for similar applications of rf dipoles.

INTRODUCTION

Multipacting conditioning and processing is one of the principal limitations of the performance of rf structures. It consists of the emission of large amounts of secondary electrons by the rf cavity walls due to incident primary electrons. This can lead to localized and resonant trajectories sustained by the primary electrons, reaching impact energies correspondent to a secondary emission yield (SEY) greater than the unit, causing a cascade effect that can incur severe problems, such as low achievable gradients in the structure, bunch instabilities, and quenches by thermal breakdown in the case of superconducting structures [1]. Due to its complexity and random nature, this non-relativistic phenomenon has been for a long time an important case of study that needs to be assessed in order to further improve the operation and performance of current and future particle accelerators.

The SEY changes for different material and is surface condition dependent [2], therefore the impact energy bandwith $(E_{II} - E_I)$ to have multipacting condition (i. e. $\delta > 1$) varies from case to case, see Fig. 1. In the case of pure and clean Nb, the range of impact energies for the multipacting condition is $E_I > 150$ eV, and $E_{II} < 2000$ eV. The multipacting barriers are known to be either soft and easily processed and cleaned or hard multipacting barriers that cannot be removed by processing and may need redesigning the cavity geometry in order to properly operate.

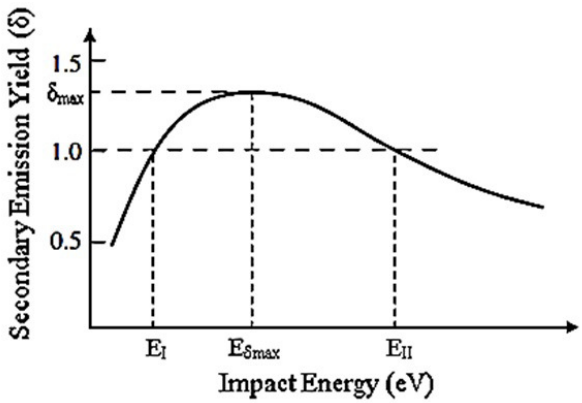


Figure 1: Secondary emission yield as a function of the particles' impact energy.

750 MHz RF DIPOLE DESIGN

The 750 MHz rf dipole was designed as a compact superconducting crab cavity for a luminosity correction scheme at the interaction points (IPs) of Jefferson Lab's Medium Electron-Ion Collider (MEIC) with crabbing voltages from $V_T = 1.3$MV to 1.8 MV for the case of electrons. However, multiple applications of such device in linear colliders such as beam spreader or high polarization corrector are under study and development [3, 4]. The rf dipole operates as a deflector/crabber in its lowest mode (TE-like) and the electric and magnetic oscillating fields for this mode are shown in Fig. 2, and its parameters are enlisted in Table 1.

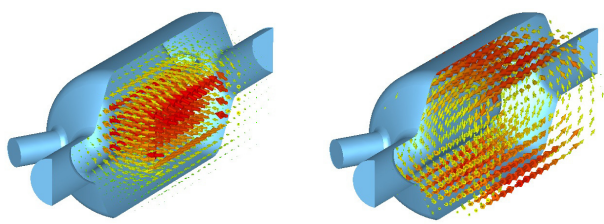


Figure 2: 750 MHz rf dipole longitudinal cross section with the electric (left), and magnetic (right) fields for the fundamental mode.

METHODOLOGY

We used the extrusion length of the endcaps (see Fig. 3) as a varying parameter to study the optimization of the multipacting conditions for the 750 MHz rf dipole, keeping all the other geometrical parameters fixed with exception of the cavity radius that was used to correct the resonant fre-

* Authored by Jefferson Science Associates, LLC under U.S. DOE Contract No. DE-AC05-06OR23177. This research used resources of the National Energy Research Scientific Center, supported by the Office of Science under U.S. DOE contract No. DE-AC02-05CH11231.
† acastill@jlab.org

ISBN 978-3-95450-142-7

Copyright © 2014 CC-BY-3.0 and by the respective authors

ARCHITECTURE DESIGN FOR THE SwissFEL LLRF SYSTEM

Z. Geng#, M. Brönnimann, I. Brunnenkant, A. Dietrich, F. Gärtner, A. Hauff, M. Jurcevic, R. Kalt, S. Mair, A. Rezaeizadeh, L. Schebacher, T. Schilcher, W. Sturzenegger, PSI, Villigen, Switzerland

Abstract

The SwissFEL under construction at the Paul Scherrer Institut (PSI) requires high quality electron beams to generate X-ray Free Electron Laser (FEL) for various experiments. The Low Level Radio Frequency (LLRF) system is used to control the klystrons to provide highly stable RF field in cavities for beam acceleration. There are more than 30 RF stations in the SwissFEL accelerator with different frequencies (S-band, C-band and X-band) and different types of cavities (normal conducting standing wave cavities or traveling wave structures). Each RF station will be controlled by a LLRF node and all RF stations will be connected to the real-time network in the scope of the global beam based feedback system. High level applications and automation procedures will be defined to facilitate the operation of the RF systems. In order to handle the complexity of the LLRF system, the system architecture is carefully designed considering the external interfaces, functions and performance requirements to the LLRF system. The architecture design of the LLRF system will be described in this paper with the focus on the fast networks, digital hardware, firmware and software.

INTRODUCTION

The layout of SwissFEL is depicted in Figure 1 [1]. The accelerator of SwissFEL consists of an S-band RF Gun, two S-band Booster sections, an X-band RF station and 3 C-band accelerator sections. To achieve the high beam stability, the RF jitters with respect to the electron beam for different RF stations should be within the tolerances listed in Table 1 [2].

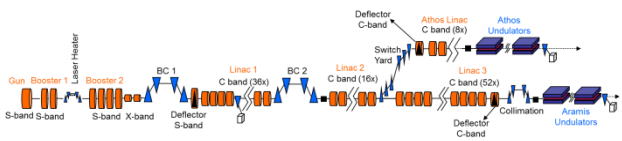


Figure 1: Layout of SwissFEL.

Table 1: RF Stability Requirements for SwissFEL

RF Station	Phase Tolerance	Voltage Tolerance
S-band	0.018 degS	0.018 %
C-band	0.036 degC	0.018 %
X-band	0.072 degX	0.018 %

The LLRF system is introduced to control all the RF stations to provide low noise RF phase and amplitude actuations and precise RF signal detections. Pulse-to-pulse feedbacks will be applied on amplitude and phase at up to 100 Hz (designed repetition rate of the SwissFEL RF system) to achieve the RF stabilities. Drift calibration is required on critical RF signals used for feedback to improve the long-term stability of the system. Automation tools are also required to help the operators to easily setup and operate the RF stations.

VIRTUAL RF STATION

From the view point of the beam physicists, some RF stations can be modelled as a Virtual RF (VRF) station and the output of it is presented by the vector sum of the individual RF stations. The VRF stations with multiple RF stations are listed in Table 2.

Table 2: VRF Stations with Multiple RF Stations

VRF Station	Comment
VRF Booster 1	With 2 S-band RF stations
VRF Booster 2	With 2 S-band RF stations
VRF Linac 1	With 9 C-band RF stations
VRF Linac 2	With 4 C-band RF stations
VRF Linac 3	With 13 C-band RF stations
VRF Athos	With 2 C-band RF stations

The physics applications for beam energy change or beam based feedback will adjust the vector sum amplitude and phase of the VRF stations via the VRF station controllers provided by the LLRF system. The VRF station controllers then determine the amplitude and phase of individual RF stations according to the predefined optimization algorithms. The VRF station controllers will also compensate the failed RF station by increasing the output powers of other RF stations in the same section if possible.

Four control nodes will be defined as VRF station controllers along the accelerator of SwissFEL (see Figure 2). Optical fiber links will be used to interconnect the beam based feedback controller, the VRF station controllers and the individual RF station controllers to support pulse-to-pulse controls, while the Ethernet network with Channel Access protocol will be used as redundancy to improve the robustness of the communications.

HARDWARE ARCHITECTURE DESIGN

The architecture of the LLRF hardware for an individual RF station control is depicted in Figure 3.

The VME based digital hardware is selected because it is well supported by the PSI Control Systems Section. A general carrier board, IFC1210 [3], with a Xilinx Virtex-6 FPGA, a dual-core PowerPC CPU and two HPC FMC slots is used as the general computation platform. The FMC board ADC3110 [4] with 8 AC coupled 250MSPS 16-bit ADC channels is used as the IF digitizer, and DAC3113 with 2 250MSPS 16-bit DAC channels is used

#zhegiao.geng@psi.ch

Copyright © 2014 CC-BY-3.0 and by the respective authors

THE SwissFEL RF GUN: MANUFACTURING AND PROOF OF PRECISION BY FIELD PROFILE MEASUREMENTS

Urs Ellenberger, Heinrich Blumer, Markus Bopp, Alessandro Citterio, Hansrudolf Fitze, Max Kleeb, Ludwig Paly, Markus Probst, Jean-Yves Raguin, Alfred Scherer, Lukas Stingelin
Paul Scherrer Institut, 5232 Villigen PSI, Switzerland

Abstract

The high brightness electron source for SwissFEL is an in-house built 2.6 cell normal-conducting RF gun which is scaled to the RF frequency of 2'998.8 MHz. The RF gun is capable of operating at 100 Hz repetition rate and produces electron bunches at the exit of the RF gun of an energy of 7 MeV. Key features of the RF gun are described and how they have been implemented in the manufacturing process. RF field measurements of the RF gun are presented to account for the mechanical precision reached after manufacturing. The RF gun has been thoroughly tested in the SwissFEL injector test facility.

INTRODUCTION AND OVERVIEW

The high brightness electron source that will drive SwissFEL has been completed at PSI and thoroughly tested recently. The photocathode of the gun is illuminated with a short-pulse laser synchronized to the RF frequency, so that electrons are emitted when the RF field on the photocathode reaches an optimum value. It is a dual-feed S-band 2.6 cell standing wave cavity which combines the advantages of two existing electron guns, namely the CTF3 RF gun [1] at CERN and the LCLS gun [2] at SLAC. The SwissFEL gun replaces the CTF3 RF gun which operated in the 250 MeV SwissFEL Injector Test Facility (SITF) until May 2014. The new SwissFEL gun can be characterized hereafter [3]:

- The backplane of the RF gun has a hole where a cathode plug can be inserted through a load-lock system [4]
- The RF field is symmetrically feeded in the middle cell which also has a racetrack design. This suppresses dipole and quadrupole components of the accelerating field in the last cell of the gun.
- A peak-accelerating gradient of 100 MV/m in the cavity leads to a low slice emittance by minimizing space charge effects during the first centimeters.
- Reduced mechanical stress due to heat load reduction is required for 100 Hz operation at a maximum gun gradient of 120 MV/m. The waveguide-to-cell coupling irises are optimized for a coupling coefficient $\beta = 2$ and, because of the pulse-heating, for a maximum temperature rise lower than 50°C.
- Surface electric fields are minimized by the elliptical profile of the cell-to-cell irises. The iris thickness was adjusted to ensure a large mode separation in frequency spectrum.

Figure 1 shows a cross section of the new SwissFEL gun with the symmetric RF connection (splitter).

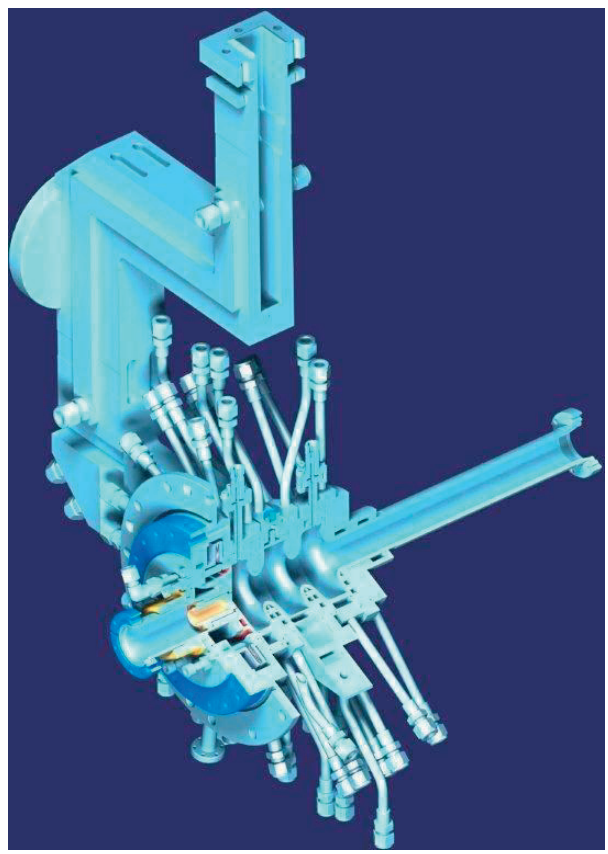


Figure 1: Cross section of 2.6 cell SwissFEL gun and of splitter.

The manufacturing of the new RF gun at PSI has to conform to stringent requirements to achieve a stable process for an economical industrial small series production for one or more guns (if required):

- Target precision of single copper parts of +/- 5 µm with a surface roughness R_a of 25 nm.
- Perpendicularity of less than 50 µm for all parts and for the gun during the whole manufacturing process.
- No mechanical tuning of the three cells of the gun would be required after brazing.
- Tuning operations are anyway possible by acting on the temperature of the cooling water and on the cathode positioning by means of the cathode plug.

Copyright © 2014 CC-BY-3.0 and by the respective authors

ISBN 978-3-95450-142-7

PKU 2.45 GHz MICROWAVE DRIVEN H- ION SOURCE PERFORMANCE STUDY*

T. Zhang[1], S. X. Peng[1], H. T. Ren[1], Y. Xu[1], A. L. Zhang[2], J. F. Zhang[1]
J. Zhao[1], Z. Y. Guo[1], J. E. Chen[1]
[1] State Key Laboratory of Nuclear Physics and Technology and School of Physics, Peking University, Beijing 100871, China
[2] School of Physics, University of Chinese Academy Sciences, Beijing 100049, China

Abstract

In a high intensity volume-produced H- ion source, H- ion production processes are great affected by electron temperature and gas pressure distribution within the discharge chamber. The H-/e ratio within an extracted H- ion beam is much depended on the electron absorption within the extraction system. At Peking University (PKU), lots of experiments were carried out for better understanding H- processes and electron dump on our 2.45 GHz microwave driven Cs-free permanent magnet volume-produced H- source. Detail will be given in this paper.

INTRODUCTION

Theoretically, H^- ion is produced in two step processes in a volume source. First, hydrogen molecules H_2 impact with fast electrons heated by microwave and vibrated to excitation state H_2*. Secondly, slow electrons interact with excited molecules H_2* and dissociate the attachment, the processes could be expressed as following:

$$e(fast) + H_2 \rightarrow H_2^* + e + h\upsilon \quad (1)$$

$$\mathrm{e(slow)} + H_2^* \rightarrow H + H^- \quad (2)$$

The energy of fast electron should above 20eV to excite the H_2 to highly rovibrationally excited molecules H_2*($4 \leqslant v \leqslant 9$) [1]. Increasing microwave power could help enhance electron temperature by ionizing gas to plasma. Enhancing the possibility of electron collision with H_2 molecule and reducing H^- loss by collision with H atoms or molecules, these could be adjusted by changing the pressure within the chamber.

H^- is fragile because its electron affinity is only 0.75 eV and it is easy to be destroyed by fast electron. The filter field keeps the destructive hot electrons away from the extraction region to reduce the H^- loss in this area. Design an appropriate filter magnetic field is very important to H^- ion production.

In order to increase H^-/e ratio, the electron in the extracted beam must be dumped properly. The electron can be dumped in the collar, in the gap between the plasma electrode and ground electrode, or behind the ground electrode [2].

The 2.45 GHz microwave-driven pure volume H^- source under development could help us understand the principle of volume H^- source and enhance the performance of H^- source by optimum the structure of 2.45 GHz microwave H^- ion source. It could be a reliable and efficient H^- source for high beam power accelerator.

The significant influence of operation pressure on beam current and electron dump field on H^-/e ratio had been found during a series of experiments, the parameter of the microwave power was also adjusted, performance of PKU H^- source was improved significantly. The negative ion source is working in pulsed/CW mode without caesium (Cs). A 15 mA pure H^- ion beam had been produced at 50 keV by this developing source. The initial design of ECR ion source can be found in ref.3.

EXPERIMENT SETUP

This microwave driven H^- ion source can briefly divides into microwave matching part, source body and beam extraction system. The source body is physically separated into three sections with different function. The first section is the primary ionization chamber (ECR zone) where high temperature electrons heated by microwave interact with molecules and generate excited H^2*. The second part is a filter region for electron separation by a transversal magnet field, the field is created by the filter magnet inside the source. The magnetic strength is about 300 Gs. The third section is the H^- formation region where H^- is generated. A cylinder with a tantalum lining is installed as a collar. As mentioned in reference [2], collar system has many unique abilities that benefit the H^- ion generation. A dipole magnet embedded in plasma electrode was used for electron bending.

The 2.45 GHz microwave driven pure volume effect H^- ion source test was done on ion source test bench of PKU [4]. The IS test bench consists of a compact 2.45 GHz PKU PMECR ion source with its microwave system, a tri-electrode extraction system, a vacuum chamber for beam diagnostic device and a 90 degree dipole analysis magnet with a Faraday cup (FC2). In the vacuum chamber, a Faraday cup (FC1) and a multi-slit single-wire (MSSW) beam emittance monitor are installed. Fig.1 shows the layout of the IS test bench.

In order to adjust the strength of e-dump field, different length of magnets which were put on the top of the ion source were added to adjust the e-dump field. There are three groups I, II, III with different strength of e-dump field 30 Gs, 40 Gs, 55 Gs respectively. The results that pure H^- current was almost the same for three

Copyright © 2014 CC-BY-3.0 and by the respective authors

PERFORMANCE OF NEW INJECTOR RILAC2 FOR RIKEN RI-BEAM FACTORY

N. Sakamoto*, M. Fujimaki, N. Fukunishi, Y. Higurashi, O. Kamigaito,
H. Okuno, K. Suda, T. Watanabe, Y. Watanabe, K. Yamada,
Nishina Center, RIKEN, Wako, Japan
R. Koyama, SHI Accelerator Service Ltd., Tokyo

Abstract

New injector called RILAC2 [1] was designed and constructed to provide intense uranium beams with A/q≈7 with an energy of 0.67 MeV/u which are injected to the succeeding ring cyclotron, RIKEN Ring Cyclotron, called RRC [2]. After the last LINAC conference where the commissioning of the RILAC2 was reported [3], some modifications and improvements with RILAC2 have been made aiming at stable operation. Recently, transmission efficiency and stability of the beams have been improved and the average beam current more than 20 pnA for uranium 345 MeV/u acceleration has been realized. In this paper the modifications and improvements of the RILAC2 together with the present performance are reported.

ACCELERATION OF U, Xe BEAMS AT RI-BEAM FACTORY

RIBF Accelerators

The layout of the RIBF is shown in Fig.1. The accelerator complex consists of cascading four ring cyclotrons and three injectors [4]. The RIBF provides the world's most intense uranium beams with an energy of 345 MeV/u at the moment. Though the goal intensity is 1 pμA the beam currents of very heavy ions like uranium and xenon are still low. The mission of the new injector project is to raise the situation of low intensities. For the RILAC2, as an injector, beam quality is also required to match to the acceptance of the RRC so as to minimize beam losses at the succeeding cyclotrons.

Figure 1: Schematic of RIBF.

RILAC2

The schematic of the RILAC2 and the RRC is shown in Fig.2. The main accelerator part of the RILAC2 consists of an RFQ and three drift tube linacs which operate in c.w. mode. The RFQ is based on the four-rod structure and the cavities of the DTLs are based on quarter wave length structure (QWR) which operate at a frequency of 36.5 MHz i.e. second harmonic of the beam frequency. The performance of the cavities has been reported in Ref. [3] and their amplitude and phase stabilities of the rf field satisfy a requirement of $|\Delta V/V| \leq \pm 0.1\%$ and $|\Delta\phi| \leq 0.1°$, respectively. Intense uranium beams with mass to charge ratio of 7 ($^{238}U^{35+}$) are produced by a superconducting ECR-ion-source (SC-ECRIS) [5] which utilizes superconducting coils for mirror and sextupole field and injection of two different frequency power sources of 18 GHz klystron and 28 GHz gyrotron. The energy of the extracted beams is 3.24 keV/u. The d.c. beams from the ion source are bunched by pre-buncher that is operated at a frequency of 18.25 MHz and injected into the RFQ and the DTLs and are accelerated to 0.67 MeV/u. The amount of the unbunched part of the beam is about 20%. The beams provided by RILAC2 are bunched and compressed again using a double-rebuncher system (B7 and S6 rebuncher) into the phase acceptance of the succeeding booster cyclotron RRC which accelerates the uranium ions to 11 MeV/u. Since the RRC is not equipped with a flat-top acceleration system, its phase acceptance is very small. According to the criterion in Ref. [6], the resoluton of the energy gain by the cyclotron rf cavity is required to be better than 10% of the inverse of the turn number that is 250 in this case to have a sufficient turn separation. This means that the injection beam phase stays within ±0.24 ns with an rf frequency of 18.25 MHz. For cyclotrons, a beam energy deviation causes a radial shift of the beam and results in sizable beam loss at the extraction device.

Beam Service

The beam services utilizing RILAC2 since the last LINAC conference are listed in Table 1 together with logged beam currents at U10(the exit of the ion source), S71(before injection into the RRC), A02a (extracted from the RRC), and G01 located at the exit of the final-stage-booster called SRC [7] when the maximum beam current at the G01 was obtained. Owing to the K-value upgrade of the fRC [8], the installation of the new gas stripper [9] and the rotating beryllium disk stripper [10], the acceleration efficiency from A02a to G01 has been greatly improved.

* nsakamot@ribf.riken.jp

Copyright © 2014 CC-BY-3.0 and by the respective authors

ISBN 978-3-95450-142-7

DESIGN OF A NEW SUPERCONDUCTING LINAC FOR THE RIBF UPGRADE

K. Yamada*, K. Suda, N. Sakamoto, O. Kamigaito,
RIKEN Nishina Center, Wako, Saitama 351-0198, Japan

Abstract

An upgrade plan for the RIKEN Radioactive Isotope Beam Factory is under discussion, the objective being to significantly increase the uranium beam intensity. In the upgrade plan, the existing RIKEN ring cyclotron (RRC) will be replaced by a new linac, mainly consisting of superconducting (SC) cavities. The new linac is designed to accelerate heavy ions with a mass-to-charge ratio of ~7 (e.g., $^{238}U^{35+}$) up to an energy of 11 MeV/u in the cw mode. A conceptual design of the SC section was devised based on a first-order approximation for the transverse and longitudinal motions. The rf design of the SC cavity was tested using CST Microwave Studio. Further study on the SC cavity, including mechanical considerations, is underway using ANSYS. We also report a preliminary design of the cryostat.

INTRODUCTION

The beam intensity of the Radioactive Isotope Beam Factory (RIBF) [1] at the RIKEN Nishina Center has been rapidly increased owing to continuous efforts in the past few years [2, 3]. Among its various heavy-ion beams, the uranium beam is one of the most important, because the in-flight fission of uranium ions can produce intense neutron-rich radioactive isotope (RI) beams far from the stability line on the nuclear chart. The maximum intensity of the uranium beam has recently reached 25 pnA (≈10^{11} pps) at 345 MeV/u by introducing a new 28-GHz superconducting electron cyclotron resonance (ECR) ion source [4, 5], the new injector linac RILAC2 [6, 7], and a new charge stripping system [8,9] and by optimization of operational parameters. The intensity of the uranium beam is to be increased to >50 pnA in the next few years using the present acceleration system.

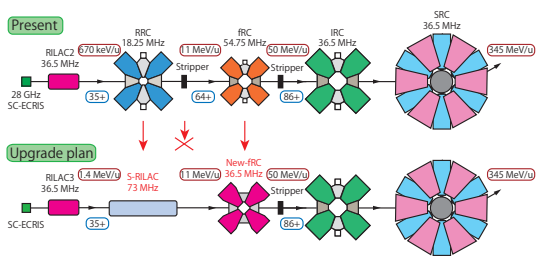


Figure 1: Present (upper drawing) and proposed (lower drawing) accelerator chains for the uranium beam at the RIBF. The final beam energy is 345 MeV/u. The radio frequencies, stripping energies, and charge states are indicated.

* nari-yamada@riken.jp

Recently, an upgrade plan for the RIBF has been proposed with the objective of expanding its capabilities to study nuclear reaction mechanisms with RI beams. The intensity of the uranium beam mentioned above is, however, insufficient to meet this demand; it should be at least an order of magnitude higher than the maximum achievable intensity with the present RIBF accelerators. The difficulty in the present acceleration scheme shown in the upper drawing of Fig. 1 mainly stems from the two-stage charge strippers located at 11 and 50 MeV/u, respectively, which yields a maximum total stripping efficiency of only 5%. In addition, the low acceleration voltage of the RIKEN ring cyclotron (RRC), which is about 280 kV/turn at an operating frequency of 18.25 MHz for uranium acceleration, causes beam losses at the extraction point of the RRC because of the significant influence of space-charge effects.

Therefore, we proposed the new acceleration scheme shown in the lower drawing of Fig. 1. In the upgrade plan, the fixed-frequency ring cyclotron (fRC) will be replaced by a new cyclotron [10] that will be designed to accept U^{35+} ions without charge stripping at 11 MeV/u, and the RILAC2+RRC will be replaced by a new linac injector, mainly consisting of superconducting (SC) cavities, to improve the transmission efficiency of the high-current beam. By making these modifications, we aim to increase the beam intensity by at least one order of magnitude compared to the achievable beam intensity with the present accelerator chain. To evaluate the feasibility of the new linac injector, we initiated a design study of the SC linac in fiscal year 2013 [11].

OVERVIEW OF THE NEW LINAC INJECTOR

A layout plan of the new linac is shown in Fig. 2. Heavy ions with a mass-to-charge ratio (m/q) of ~7 (e.g., $^{238}U^{35+}$ and $^{124}Xe^{19+}$) are designed to be accelerated up to 1.4 MeV/u by a short room-temperature (RT) section, and they are boosted up to 11 MeV/u with the succeeding SC section in the cw mode. The beam energy at the border of the RT and SC sections was chosen so that the SC section could be covered by a single structure of a quarter-wavelength resonator (QWR) with two acceleration gaps.

The rf of the SC-QWR was chosen to be 73 MHz, which is twice that of the RT section, and the gap voltage was assumed to be 800 kV. Because a broad range of velocities had to be covered, the gap length g and the length d between the gap centers of the SC-QWR were optimized to minimize the number of QWRs in the section [11]; we have determined the length as d = 160 mm and a total cavity number of 56.

Copyright © 2014 CC-BY-3.0 and by the respective authors

ISBN 978-3-95450-142-7

STABILIZATION OF BEAM PERFORMANCE DUE TO IMPROVEMENT OF THE PRECISE TEMPERATURE REGULATION SYSTEM OF THE SACLA INJECTOR

T. Asaka#, T. Hasegawa, H. Maesaka, Y. Otake, K. Togawa,
RIKEN SPring-8 Center, Sayo-cho, Sayo-gun, Hyogo 679-5148, Japan

Abstract

The acceleration field of the rf cavities of an injector in SACLA have to be precisely controlled in order to generate a stable electron beam for x-ray free-electron laser (XFEL) users. To maintain the rf voltage and the phase in each cavity, the temperatures of all cavities were kept within 28±0.04˚C by a precise temperature regulation system, which was equipped with the pulse-width modulation (PWM) AC heater with the on-off control. The beam position in the injector was affected by slight leakage magnetic fields from the AC heater elements and those cables. We replaced the existing (PWM-AC-type) precise temperature regulation system with a new system (DC-type) for each rf cavity in the injector in order to remove the leakage magnetic field of the heater current. Additionally, a thermometer module with the high resolution of 0.001˚C was installed into the new system. Consequently, the temperature variation of the rf cavities was maintained within 28±0.004˚C. The beam position jitter in an undulator was reduced to less than one-third, and the laser position variation was suppressed to within 20 μm.

INTRODUCTION

Toward increasing and stabilizing the x-ray laser intensity of SACLA to efficiency progress user experiments, we have made numerous improvements in the 8-GeV linear accelerator since beam commissioning [1]. It is also important to improve the pointing stability, which is nearly one-tenth of the beam size. The stability of laser intensity of less than 10% (rms) is required from our design [2]. The stability of the laser intensity, however, was not sufficiently stable to adopt the design value for user experiment in the period of the beam commissioning [3].

At that time, the laser intensity became low within a few hours without the tuning of the linear accelerator. One of the causes of the laser intensity drift was the peak current drift of an electron beam. Furthermore, a fluctuation of the laser intensity for the short-term had a strong correlation with the beam position jitters.

The exact locations of the causes of those beam intensity drift and fluctuation were investigated by the measurements of a beam energy and a beam position in the individual sections (injector, magnetic bunch compressor: BC1, BC2 and BC3) of the 8-GeV linear accelerator, as shown in Fig. 1. By the investigation, it was found that the causes of the beam characteristics variations were in the injector. The causes of the variations were described as the following [4].

- The beam energy drift after the injector was caused by the slight phase drifts of the rf cavies in the injector, as a velocity bunching section.
- The beam position after the injector had a periodic variation of 2 Hz in a short-term.

To mitigate these beam variations in the injector, we determined the root causes of these variations, and carried out the countermeasures, as described below.

The rf phase drift was caused by the temperature change of the rf cavity although the temperature of the rf cavities were maintained within 28±0.04˚C by a precise temperature regulation system (PTRS). The temperature stability was not sufficiently. Therefore, we replaced the conventional thermometer module with a high-resolution thermometer module in the PTRS.

The beam position jitters in the short-term, at which was a periodic fluctuation of 2 Hz, was synchronized with the current period of the pulse width modulation (PWM) for the AC heater of the PTRS. We thought, a periodic tiny leakage magnetic field from the AC heater element or its cable could make a periodic fluctuation of the beam position. Therefore, we upgrade the existing PTRS to a new PTRS system without any periodical on-off control of the heater current. Continuous current control for the heater by using a DC power supply to be installed in the new PTRS stabilized the temperatures of individual rf cavities in the injector.

In this paper, the performances of the existing PTRS and the new system are shown first. Mitigation of the beam position jitters with the new PTRS system is also described.

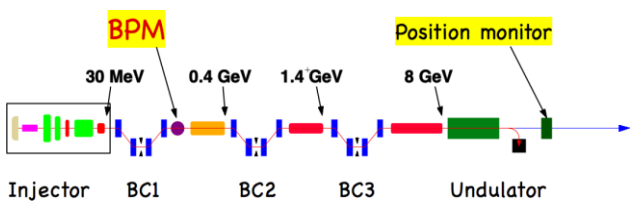


Figure 1: Schematic view of the 8-GeV linear accelerator and undulator section in SACLA.

IMPROVEMENT OF THE PRICISE TEMPERATURE-REGULATION SYSTEM

Existing Precise Temperature-regulation System

The existing PTRS was designed to maintain a temperature variation of the rf cavity within 28±0.1˚C.

#asaka@spring8.or.jp

ISBN 978-3-95450-142-7

Copyright © 2014 CC-BY-3.0 and by the respective authors

STATUS OF RADIO-FREQUENCY (RF) DEFLECTORS AT RADIABEAM

L. Faillace#, R. Agustsson, J. Hartzell, A. Murokh, S. Storms
RadiaBeam Technologies, 1717 Stewart St, Santa Monica CA, USA

Abstract

Radiabeam Technologies recently developed an S-Band normal-conducting Radio-Frequency (NCRF) deflecting cavity for the Pohang Accelerator Laboratory (PAL) in order to perform longitudinal characterization of the sub-picosecond ultra-relativistic electron beams. The device is optimized for the 135 MeV electron beam parameters. The 1m-long PAL deflector is designed to operate at 2.856 GHz and features short filling time and femtosecond resolution. At the end of 2012, we delivered an X-band Traveling wave RF Deflector (XTD) to the ATF facility at Brookhaven National Lab. The device is optimized for the 100 MeV electron beam parameters at the Accelerator Test Facility (ATF) at Brookhaven National Laboratory, and is scalable to higher energies. The XTD is designed to operate at 11.424 GHz, and features short filling time, femtosecond resolution, and a small footprint. The XTD is currently being assembled at ATF for high-power operation and conditioning results will be reported soon.

INTRODUCTION

Some of the most compelling and demanding applications in high-energy electron beam-based physics, such as linear colliders [1], X-ray free-electron lasers [2], inverse Compton scattering (ICS) sources [3,4], and excitation of wakefields in plasma for future high energy physics accelerators [5,6] now require sub-picosecond pulses. Thus, improvement in resolution and capabilities of fast longitudinal diagnostics is needed.

RadiaBeam has recently developed and delivered an S-Band Traveling wave Deflecting mode cavity to be utilized for direct longitudinal phase space measurements of compressed electron beams at the Pohang Accelerator Laboratory X-ray SASE-FEL [7] as well an X-band deflector for BNL-ATF. Both deflectors take advantage of the well-established cell machining in S-Band as well as our version of the SLAC-modified procedure for surface preparation for high RF power operation.

RF/THERMAL DESIGN

PAL Deflector Design

The 3D RF design was performed with HFSS [8]. The PAL deflector is a disc-loaded traveling-wave (TW) structure operating in the TM_{11} mode at 2.856 GHz. Two coupler cells allow the input and output of the RF power provided by a standard WR284 metallic waveguide.

faillace@radiabeam.com

The main deflecting cells, stacked in between the couplers, have a pillbox-like shape, each with holes located perpendicular to the deflection plane for the separation of the two dipole-mode field polarizations. The cell-to-cell phase shift is 120 degrees. The final full PAL deflector consists of an overall number (couplers plus main cells) of 28 cells. The main RF parameters for the L=1m long PAL deflector is listed in Table 1. The total deflecting voltage is equal to 8.5 MV, assuming an input RF power value of 10MW. Very good agreement was found between the simulated and the measured values.

Table 1: PAL Deflector RF Parameters.

RF Parameter	**Value**
2π/3-mode frequency f	2.856 GHz
Transverse Shunt Impedance r_T	28.7 MΩ/m
Unloaded Q	13,400
Attenuation α	0.15 m^{-1}
Group Velocity v_g	0.014 c
Kick/√Power	2.7 MeV/√MW
Length L	1 m

Thermal simulations were carried out with Ansys [9]. We only inserted a cooling channels system, very compact, for frequency/temperature stabilization. The result shown in Figure 1 refers to the case of an average RF power of 1kW. Due to the low temperature gradient (<3deg) across the structure, no internal channels were necessary.

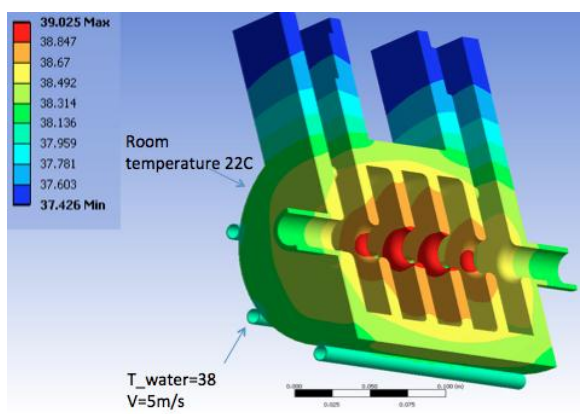


Figure 1: Thermal simulation of the PAL deflector model for 1kW average RF power.

Copyright © 2014 CC-BY-3.0 and by the respective authors

INJECTOR SYSTEM FOR THE IR-FEL AT RRCAT

L. Faillace#, R. Agustsson, RadiaBeam Technologies, Santa Monica, CA USA
K. K. Pant, A. Kumar, FEL Lab and MAASD, RRCAT, Indore, India

Abstract

An infrared (IR) free-electron laser (FEL) has been proposed to be built at the Raja Ramanna Centre for Advanced Technology (RRCAT). RadiaBeam is currently involved in the design of the RRCAT FEL's injector system. The injector will deliver an electron beam with a variable energy (from 15 up to 25 MeV) and up to 1.35 nC at 36.6 MHz repetition rate. We show here the beam dynamics of the beam transport through the injector as well as the RF design and mechanical model of the system.

INTRODUCTION

RRCAT's injector system, for the proposed IR-FEL [1], consists of a 90 keV electron gun modulated at 36.6 MHz and a sub-harmonic prebuncher (SHPB) operating at 476 MHz. The rest of the injector system, as specified in the tender, is required to accelerate to energy in the range of 15-25 MeV while maintaining good beam parameters and high transmission. The high transmission requirement necessitates the use of a fundamental frequency pre-buncher (PB). This is followed by an accelerating buncher (AB), operating with a fixed RF power, to bring the beam energy to 4 MeV ($\beta \approx 1$). The subsequent main linac can then accelerate the beam to a final energy between 15 and 25 MeV by varying input power and phase. The main linac will be a standard SLAC-type 3 m traveling wave accelerating section; this will allow for the option to accelerate to higher energies in the future (50 MeV or higher). A diagram of the proposed system is shown in Figure 1.

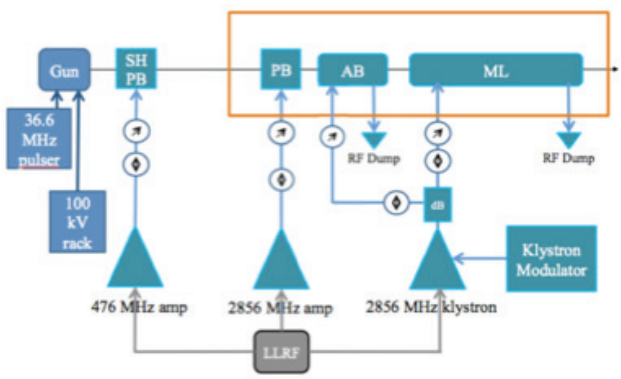


Figure 1: Diagram of proposed injector system for the RRCAT IR-FEL.

INJECTOR SYSTEM DESIGN

In order to begin the process of the injector system design, the first step is to develop the basic design of the three RF structure: the pre-buncher, the accelerating buncher, and the main linac. The design of the main linac is already complete, as we will be using a standard SLAC section. The main output beam parametrs after the Linac are given in Table 1.

Table 1: Main Output Beam Parameters.

Parameter	Value
Energy Gain	15-25 MeV
RMS energy spread	≤ 0.5 %
Charge per micropulse	≥ 0.75 nC
Micropulse Width	10-12 ps FWHM
Transverse RMS norm. emittance	≤ 30 mm-mrad
Transverse RMS beam size	≤ 2 mm

RF Design

The RF design of the PB and AB was performed by using SUPERFISH and HFSS for 2D and 3D simulations, respectively. The main RF parameters of the cavities are given in Table 2.

Table 2: Main RF Parameters.

	SHPB	PB	AB	ML
Geometry	Re-entrant SW cavity	Re-entrant SW cavity	12-cell TW cavity	3m SLAC section
Frequency	476 MHz	2.856 GHz	2.856 GHz	2.856 GHz
Shunt Impedance	170 MΩ/m	1.2 MΩ	50 MΩ/m	57 MΩ/m
Cavity Voltage	±30 kV	±38 kV	4MV	15-25 MV

Beam Dynamics

The initial beam dynamics simulations were performed with PARMELA using the field input files generated in the RF design. The goal was to transport as much beam as possible (≥ 60%) through the system while maintaining

faillace@radiabeam.com

ISBN 978-3-95450-142-7

Copyright © 2014 CC-BY-3.0 and by the respective authors

DEVELOPMENT OF SUPERCONDUCTING CAVITIES AND RELATED INFRASTRUCTURE FOR HIGH INTENSITY PROTON LINAC FOR SPALLATION NEUTRON SOURCE

S. C. Joshi, S. Raghavendra, V. K. Jain, A. Puntambekar, P. Khare, J. Dwivedi, G. Mundra, P. K. Kush, P. Shrivastava, S. B. Roy, P. R. Hannurkar and P. D. Gupta
Raja Ramanna Centre for Advanced Technology, Indore, India

Abstract

Raja Ramanna Centre for Advanced Technology (RRCAT) has taken up a program on R&D activities of a 1 GeV, high intensity superconducting proton linac for a spallation neutron source. The proton linac will require a large number of superconducting Radio Frequency (SCRF) cavities ranging from low beta spoke resonators to medium and high beta multi-cell elliptical cavities at different RF frequencies. A dedicated facility is being set up for development of multi-cell superconducting cavities and their performance characterization. 1.3 GHz single-cell SCRF niobium cavities have been developed to establish the fabrication procedure. These cavities has exhibited high quality factor with an accelerating gradients up to 37 MV/m. A novel technique of laser welding of 1.3 GHz niobium cavity has been developed and demonstrated performance comparable to electron beam welded cavity. A dedicated facility for SCRF cavity forming, machining, electron beam welding, RF characterization, cavity tuning and cavity processing is being set up. To characterize a SCRF cavity at 2K, a vertical test stand has been developed and a horizontal test stand has been designed.

INTRODUCTION

Raja Ramanna Centre for Advanced Technology (RRCAT) has taken up a program on R&D activities of a 1 GeV, high intensity superconducting proton linac for a spallation neutron source for research in the areas of condensed matter physics, materials science, chemistry, biology and engineering. The major sub-systems of the spallation neutron source would comprise of a 1 GeV high power superconducting pulsed H- linac, an accumulator ring, spallation target and beam lines. The first step towards realizing these long term objectives is to develop capabilities to build superconducting linac that can reliably and efficiently deliver a high intensity H-/ proton beam of 1 GeV energy. RRCAT has taken up R&D activities for the development of a 1 GeV superconducting pulsed H- linac for Indian spallation neutron source (ISNS) [1].

A program for setting-up of a infrastructure facility for development of SCRF cavity at RRCAT was approved. The facilities include SCRF cavity forming, machining, electron beam welding, RF characterization, cavity tuning and cavity processing has been set up at RRCAT. The cavity processing includes centrifugal barrel polishing, electro-polishing, thermal processing and high pressure rinsing. A dedicated building has been constructed to house this infrastructure and clean rooms for assembly and testing of cavities. Few 1.3 GHz and 650 MHz cavities have been fabricated and tested, showing excellent performance. A prototype blade tuner mechanism for 1.3 GHz niobium cavity has also been developed. A vertical test stand (VTS) has been commissioned.

INFRASTRUCTURE FACILITY FOR DEVELOPMENT OF SCRF CAVITIES

Cavity Fabrication Facility

A dedicated 120 Ton hydraulic press has been installed for forming of cells of SCRF cavity from high RRR niobium sheets. High strength aluminium alloy 7075-T6 is used for fabricating deep drawing die-n-punch, tooling and fixtures for trim machining of cavity halves. The cavity halves are joined together using an electron beam welding (EBW) in high vacuum. An EBW machine of 15 kW beam power has been procured and installed, as shown in Figure 1. The EBW machine has a large size vacuum chamber which is capable of welding from low to high beta SCRF cavities required for the high intensity proton linac.



Figure 1: 15 kW electron beam welding machine.

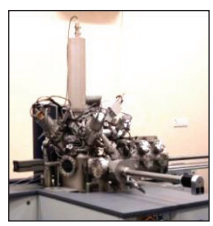


Figure *2*: Secondary ion mass spectrometer.

Material Characterization Facility

A material characterization facility has been set up to support the SCRF cavity development. This includes a 50 kN universal testing machine capable of measuring mechanical properties of samples of cavity materials and stiffness of multi-cell SCRF cavity. A time of flight secondary ion mass spectrometer (TOF-SIMS) has been installed, to analyze the impurity distribution in high purity niobium at different processing steps as shown in Figure 2. A 3-D laser scanning confocal microscope with 1 nm depth resolution, capable of measuring the surface

Copyright © 2014 CC-BY-3.0 and by the respective authors

ISBN 978-3-95450-142-7

EXPERIENCE OF OPERATION OF THE ELECTRON LINEAR ACCELERATOR BASED ON PARALLEL COUPLED ACCELERATING STRUCTURE*

Yu. Chernousov, V. Ivannicov, I. Shebolaev, ICKC, Novosibirsk, RUSSIA
A. Levichev, D. Nikiforov, A. Barnyakov, BINP, Novosibirsk, RUSSIA

Abstract

Electron linear accelerator based on parallel coupled accelerating structure was developed and produced by Budker institute of nuclear physics SB RAS and Institute of Chemical kinetics and combustion SB RAS. There were short and long parallel coupled accelerating structures with frequency 2450 MHz. For easy disassembly the electrical and vacuum connections for the first structure are performed by indium. The second structure is brazed. Now accelerator is working for researching in the field of accelerating and RF technologies. In the report the features of the accelerator working are demonstrated. The test of the long parallel coupled accelerating structure is discussed. The result of dissembled of the short accelerating structure is shown. The RF antenna lead and solid-state key for beam driving of the electron gun with RF control were developed. The design and characteristics of these devices are presented. Now the short parallel coupled accelerating structure is under modernizing to increase the accelerated beam current.

INTRODUCTION

The compact linear electron accelerator produced by Budker Institute of Nuclear Physics of SB RAS and Institute of Chemical Kinetics [1]. It consists of new type parallel coupled accelerating structure and injector based on electron gun with RF control.

Parallel coupled accelerating structure consists of accelerating cavities which are excited from one common cavity. The feature of this design is absence connections between accelerating cavities by electromagnetic field, individual coupling slot for every accelerating cavity and possibility to use magnetic system based on the permanent magnets. All of these lead to more stable working under RF breakdown, more efficient of the particles capture, make the free RF power distribution and so on [1-2]. There were produced two accelerating structure with 5 and 9 accelerating cavities and operating frequency 2450 MHz. For easy disassembly the electrical and vacuum connections for the first structure are performed by indium wire. The second structure is brazed.

The short parallel coupled accelerating structure is successfully working during 3 years for different researchers in the field of accelerating and RF technologies. The last beam parameters were obtained: beam current up to 100 mA with pulse duration 5 μs and the energy was 2.5 MeV with beam capture of 100% [1]; beam current up to 300 mA with pulse duration 2.5 ns and energy of 4 MeV.

The long parallel coupled accelerating structure was brazed, but during testing with high RF power some problems were appeared and the working beam parameters were not achieved.

Besides accelerating structures the linac has injector which allows us working with three regimes: short beam pulses with duration about 3 ns, long pulses with duration more then 0.5 μs and long pulses with RF control. To make the last regime two new devices were developed and produced. These are RF antenna lead and RF coaxial switch based on pin-diodes correspondingly.

In this report some results of linac operating with new devices and ideas are discussed.

TEST OF THE PARALLEL COUPLED ACCELERATING STRUCTURE WITH NINE CELLS

The long parallel coupled accelerating structure consists of 9 cavities, which are brazed with each other. It is shown on the Fig. 1. To match the unrelativistic injected beam with accelerating field the first and second cavities have variable lengths. The sizes of the individual coupling slots between accelerating cavities and exciting cavity were calculated to make increasing electric field distribution for smoothing accelerating.

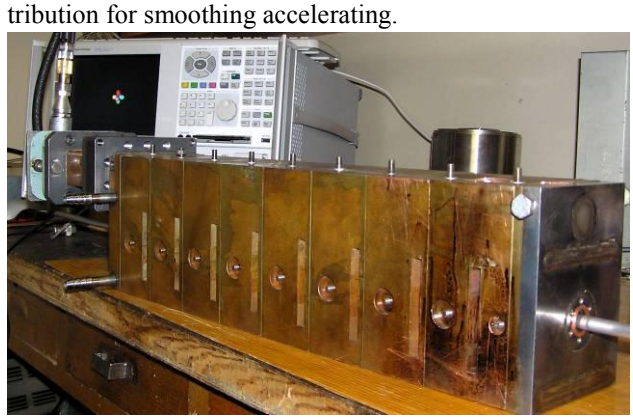


Figure 1: Accelerating structure with 9 accelerating cavities.

After brazing the structure were tuned and measured. According to [4] the coupling factors between exciting and accelerating cavities were obtained and electric field distribution along accelerating cavities was calculated. The histogram of the electric field amplitude with generator power of 2.5 MW is shown on the Fig. 2.

* Work is supported by President grant MK-2129.2014.2

Copyright © 2014 CC-BY-3.0 and by the respective authors

WAKEFIELDS IN THE SUPERCONDUCTING RF CAVITIES OF LCLS-II*

K. Bane#, T. Raubenheimer, SLAC, Menlo Park, CA 94025, USA
A. Romanenko, V. Yakovlev, FNAL, Batavia, IL 60510, USA

INTRODUCTION

The superconducting cavities in the linacs of LCLS-II are designed to operate at 2K, where cooling costs are high. In addition to an unavoidable static load and the dynamic load of the fundamental 1.3 GHz accelerating RF, a further heat source is the higher order mode (HOM) power deposited by the beam. The layout of LCLS-II is sketched in Fig. 1. In L3, the final linac, due to the extremely short bunch length, the beam spectrum extends well above cut-off into the terahertz regime. Ceramic absorbers, at 70K and located between cryomodules (CMs), are meant to absorb much of this power. However, understanding their effectiveness is a challenging research topic.

In this report we primarily calculate the amount of power that the beam radiates in the three linacs of LCLS-II, L1, L2, L3, and in the linearizing, 3rd harmonic (3.9 GHz) cavities. To do this we find the steady-state wakes as well as the transients at the beginning of the three linacs. At the ends of each linac there is a matched pair of 1 cm to 3.5 cm (radius) step transitions, whose effect is also considered. Finally, we estimate—under the pessimistic assumption that all the wake power ends up in the SRF walls—the wall heating and the extent of Cooper pair breaking in L3, where the bunch is most intense. Note that all calculations here are of single bunch effects; resonant interactions are not considered.

In our calculations we assume for LCLS II 1.2 MW of beam power, with charge q = 300 pC and repetition rate f_{rep} = 1 MHz. The bunch shape is nearly Gaussian in L1, L2, and uniform in L3, with rms bunch length σ_z = 1000, 270, 25 μm in the three linacs [1]. Note that the charge represents the maximum charge to be used: nominally q= 100 pC and σ_z = 8 μm (in L3). More details of this report can be found in [2]. A theoretical study of exactly where the HOM power will be absorbed is given in [3].

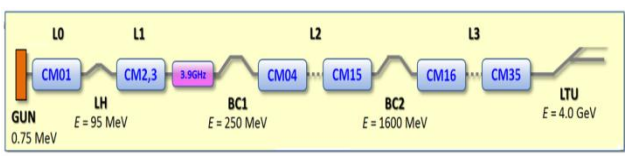


Figure 1: Schematic layout of LCLS II linac which contains the laser gun; acceleration sections L0-L3 having 1.3 GHz TESLA-type CMs (CM01-CM35) and 3.9 GHz CM; laser heater (LH); two bunch compressors (BC1-BC2), and Linac-to-Undulator transfer line (LTU).

WAKEFIELD LOSSES IN CMS

A TESLA CM comprises eight 9-cell cavities, each with active length 1.036 m and iris radius a = 3.5 cm. Between the cavities are bellows that are roughly 6 cm long and have 11 oscillations. When the beam enters the first CM in a linac, it will first encounter transient wakefields that will gradually change to the steady-state wakes. The change occurs over a distance on the order of the catch-up distance, $z_{cu} = a^2/2\sigma_z$. For LCLS-II, the catch-up distance z_{cu} = 0.6, 2.3, 25 m in the 3 three linacs. For all three linacs z_{cu} is small compared to the length of the sequence of CM, meaning that the steady-state results are a good approximation to the average CM wakes. However, the transient wakes excited in the first cavities of each linac are stronger than the steady-state ones, and need to be considered separately.

Steady-State Wakes

The wake power lost by the beam in a CM is given by $P_{wake} = q^2\kappa f_{rep}$, with κ the loss factor per CM. For a sufficiently short bunch, κ—for any cylindrically symmetric, periodic structure with minimum radius a—can be approximated by the asymptotic value (see *e.g.* discussion in [4])

$$\kappa = \frac{Z_0 cL}{2\pi a^2} \qquad (1)$$

with Z_0 = 377 Ω, c the speed of light, and L the structure length. From this formula (taking $L = L_c$ = 8.3 m, a = 3.5 cm) we estimate the steady-state power radiated per CM, P_{asym} = 11 W. We perform a more accurate calculation taking as point charge wake the approximation [5]

$$W(s) = 344.\, e^{-\sqrt{s/s_0}} \quad \left[\frac{V}{pC\cdot CM}\right] \qquad (2)$$

with s_0=1.74 mm, which includes the effects of the cavities, the bellows, and pipes in between. The loss factor for a Gaussian bunch is given by

$$\kappa = \frac{1}{2\sqrt{\pi}\sigma_z}\int_0^\infty W(s) e^{-\frac{(s/\sigma_z)^2}{4}} ds \qquad (3)$$

Performing the integral (3) using this wake (2), we find that κ= 86, 119, 154 V/pC, or P_{wake} = 7.7, 10.7, 13.8 W, in L1, L2 and L3. Note that for a uniform bunch distribution, as is found in L3, if we take σ_z to represent the rms length, the loss factor will differ, but only by a small amount.

Transient Wakes

When a short bunch enters the first cell of the first cavity in a linac, the wake induced will be well approximated by the diffraction model [6], and in subsequent cells and cavities the wake will gradually reach its steady-state form. Let us begin by considering the bunch at its shortest, in L3, where σ_z = 25 μm. According to the diffraction model, the loss factor for a

*Work supported by US DoE contract DE-AC02-76F00515
kbane@slac.stanford

Copyright © 2014 CC-BY-3.0 and by the respective authors

SUPER-COMPACT SLED SYSTEM USED IN THE LCLS DIAGNOSTIC SYSTEM*

J. W. Wang#, S.G. Tantawi, X. Chen, SLAC, Menlo Park, CA 94025, USA

Abstract

At SLAC, we have designed and installed an X-band radio-frequency transverse deflector system at the LCLS for measurement of the time-resolved lasing effects on the electron beam and extraction of the temporal profile of the pulses in routine operations.

We have designed an X-Band SLED system capable to augment the available klystron power and to double the kick.

INTRODUCTION

As shown in Figure 1, Radiofrequency (RF) transverse deflectors are used in conjunction with an electron beam energy spectrometer to measure the electron beam longitudinal (time-energy) phase space downstream of the FEL undulators. Since the lasing process in an FEL induces both electron energy loss and energy spread growth, the output electron longitudinal phase space will include a 'footprint' left by the emitted X-rays [1].
Enabled by well-developed RF technology, this diagnostic method is simple, single shot and non-invasive to FEL operation. Furthermore, it covers a wide dynamic range and works for both soft and hard X-ray energies without requiring any configuration change.

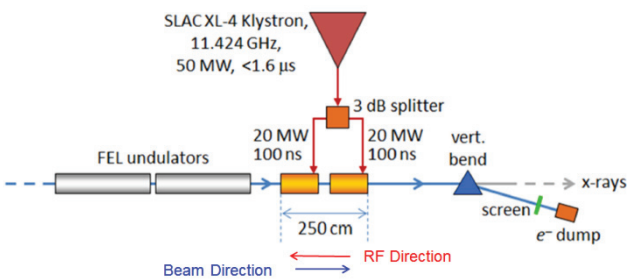


Figure 1: Layout of deflector RF system downstream of the LCLS undulators.

The kick for a 1m Section is 5.46 $(P_{in})^{1/2}$ MV, where P_{in} is the Peak RF Power in MW. The maximum kick of little more than 40 MV was obtained from an old Klystron with peak power of only 35 MW. In order to reach higher resolution, we have been designing a brand new SLED system to double the kick to more than 80MV. This paper describes its principle and technical advances and challenges.

SLED ENERGY GAIN

In June 1974, forty years ago, a clever invention named "SLED" was announced at SLAC [2]. The increase of the peak RF power is in exchange for the RF pulse length reduction by a passive technique called "pulse compression". As shown in Figure 2, the first part of klystron pulse was stored in two low-loss cylindrical tuned cavities installed downstream of the klystron. For the remaining part of the pulse (usually to be the filling time of the feeding accelerator structure), the phase of the klystron was reversed by 180 electrical degrees, and the sum of the power now being discharged by the cavities plus the direct klystron power resulted in a net power gain. The key components of a SLED system include a 3db coupler with two 90° apart divided power ports and high Q energy storage cavities.

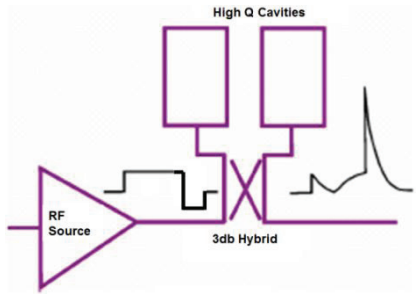


Figure 2: Basic SLED working scheme.

Our system can be described as followings: over-coupling coefficient $\beta=Q_0/Q_e$, where $Q_o=10^5$ is unloaded Q and Q_e and Q_L are external and loaded Q respectively. The cavity filling time Tc is $2Q_L/\omega=2Q_0/\omega(1+\beta)$, the coupling coefficient β will be optimized later. The deflector is 1.0 m long, constant impedance structure with transverse impedance of 41.9 MΩ/m, filling time T_f=106 ns (group velocity of -3.165 % speed of light) and attenuation factor τ=0.62 Neper. Let us assume the total RF pulse is 1.5 μs and last 106 ns has been flipped phase with 180°. Figure 3 shows loaded voltage waveform after SLED.

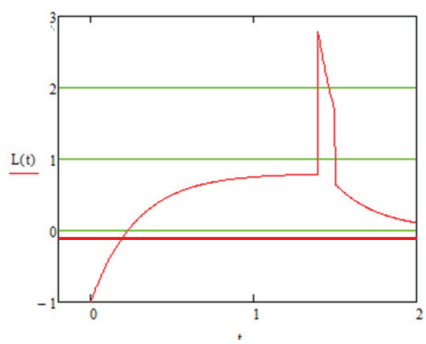


Figure 3: Loaded SLED voltage waveform with horizontal coordinate of time in μs and vertical coordinate in none SLEDed input voltage as unit.

* Work supported by Department of Energy contract DE–AC03–76SF00515.
# jywap@slac.stanford.edu

Copyright © 2014 CC-BY-3.0 and by the respective authors

ISBN 978-3-95450-142-7

DESIGN OF THE HIGH REPETITION RATE PHOTOCATHODE GUN FOR THE CLARA PROJECT*

B.L. Militsyn#, L.S. Cowie, P.A. Goudket, T.J. Jones, J.W. McKenzie, A.E. Wheelhouse,
STFC Daresbury Laboratory, Warrington, WA4 4AD, United Kingdom
V.V. Paramonov, A.K. Skasyrskaya, INR, Moscow, Russian Federation
G.C. Burt, Lancaster University and Cockcroft Institute, Lancaster, LA1 4YW, United Kingdom

Abstract

The CLARA (Compact Linear Accelerator for Research and Applications) injector is required to deliver ultrashort single electron pulses with a charge of 250 pC at a repetition rate of 100 and/or 400 Hz. It should also provide 2 μs trains of twenty 25 pC pulses at a repetition rate of 100 Hz. To meet this challenge, a 1.5 cell S-band photocathode gun with a field of up to 120 MV/m and coaxial coupling has been chosen. The relative length of the first cell of 0.5 is decided on the basis of beam dynamic simulation with the goal to obtain optimal beam for CLARA parameters. In order to improve the amplitude and phase stability of the RF field, the gun is equipped with an RF probe which will provide feedback. The gun and coupler were designed to accept up to 10 MW peak and 10 kW average RF powers. Cooling will be achieved by 9 water channels cut into the bulk of the copper cavity. The coupler will be transitioned from waveguide to coax using an innovative H-shaped dual feed system.

INTRODUCTION

A 1.5 cell, 2998.5 MHz (S-band) photocathode RF gun with a coaxial coupler, shown in Fig. 1, has been designed at STFC Daresbury Laboratory in collaboration with Institute for Nuclear Research, Moscow, to deliver high brightness electron beams for the CLARA FEL test facility [1]. The main specification of the gun is summarised in [2] and the conceptual design described in [3]. In this paper we will give more detail of the gun cavity RF design and its thermal regime and practical cooling system solution.

RF CAVITY DESIGN

Cavity Shape Optimisation

The cavity shape was optimised using the Superfish [4] code. The first cell length was defined using ASTRA [5] beam dynamics simulations [3]. Cavity shape parameters were varied using a Mathematica [6] front-end, which was used to optimise both the frequency and field flatness of the cavity by varying the cell radii for each value of the changing parameter. It was found that the transverse emittance requirements were met for wide range of the first cell length, and a final value of 0.5 of the half-wavelength was therefore chosen where longitudinal beam properties are optimal [3].

The next step was optimisation of the cell to cell coupling iris. It was found that an iris ellipticity of 1.75 at an iris thickness of 16 mm was sufficient to reduce the maximum surface electric field on the iris to the same level as the surface field elsewhere in the cavity, a value of 113 MV/m. This is just 94% of the cathode field, and an acceptable value.

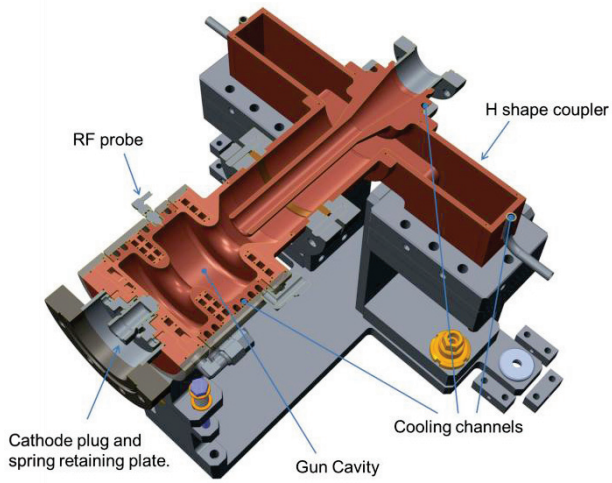


Figure 1: Overview of the gun cavity design.

The geometric shunt impedance R/Q of the cavity was then maximised whilst keeping the mode separation above a conservative value of 20 MHz. It was found that at an iris radius of 13.4 mm R/Q reaches its maximum value keeping the mode separation to 20 MHz.

The edges of the cells were rounded to maximise overall quality factor of the cavity. A study found that whilst increasing the radius of curvature of the rounding does decrease the integrated magnetic field on the surface, the effect is not large. The rounding radii on the first cell were chosen to be 3 mm, and those on the second cell 4 mm, dictated mainly by mechanical and thermal constraints.

RF Probe Considerations

The CLARA gun design requires provision for a RF probe allowing RF feedback to be used. The only realistic position of the probe in this gun is on the equator of the second cell, due to the need for cooling channels accommodation in the copper. In order to ensure that the probe could couple to the cavity electric field, it was offset from the centre of the cell. The position of the probe was

*boris.militsyn@stfc.ac.uk

Copyright © 2014 CC-BY-3.0 and by the respective authors

THE STATUS OF THE CONSTRUCTION OF MICE STEP IV*

S. Ricciardi,† STFC, Rutherford Appleton Laboratory, Chilton, Didcot, Oxfordshire, OX11 0QX, UK

Abstract

The International Muon Ionization Cooling Experiment will provide the demononstration of ionization cooling. The experiment is being built in a series of Steps. Step IV, which consists of a tracking spectrometer upstream and downstream of an absorber/focus-coil module will be completed in early 2015. In this configuration, the emittance of the muon beam upstream and downstream of the absorber will be measured precisely allowing the emittance reduction and the factors that determine the ionization-cooling effect to be studied in detail. Each tracking spectrometer consists of a scintillating-fibre tracker placed within a 4 T field provided by the superconducting spectrometer solenoid. The muon beam is transported to the absorber/focus-coil module: a 22 liter volume of liquid hydrogen placed inside a superconducting focusing coil. The properties of lithium hydride, and possibly other absorber materials, will also be studied. All the components of Step IV have been manufactured and integration of the experiment in the MICE Hall at the Rutherford Appleton Laboratory is underway. The construction and performance of Step IV will be described. A full study of ionization cooling will be carried out with Step V of the experiment which will include a short 201 MHz linac module in which beam transport is achieved with a superconducting "coupling-coil". The status of the preparation of the components of Step V of the experiment will be described briefly.

INTRODUCTION

The Muon Ionization Cooling Experiment (MICE) [1] is under construction at the UK's Rutherford Appleton Laboratory (RAL). It will demonstrate for the first time the feasibility of ionization cooling of muons [2]. The MICE apparatus (Fig. 1) comprises two absorbers and a linac module sandwiched by the input and output spectrometers and particle identification and timing detectors that will be used to characterize the cooling process experimentally.

Ionization cooling is achieved in MICE by placing the absorbing material in the beam line. The absorbing material reduces beam momentum, which is replaced only in the longitudinal direction by acceleration in RF cavities, resulting in a net reduction of emittance. Overall, transverse emittance is reduced while longitudinal emittance stays the same or increases slightly due to stochastic processes in the energy loss. The process can beneficially continue until an equilibrium is reached between the cooling effect of ionization and the heating effect of multiple scattering. Ionization cooling works optimally for momenta near the ionization minimum, hence MICE is designed for the momentum range 140 to 240 MeV/c.

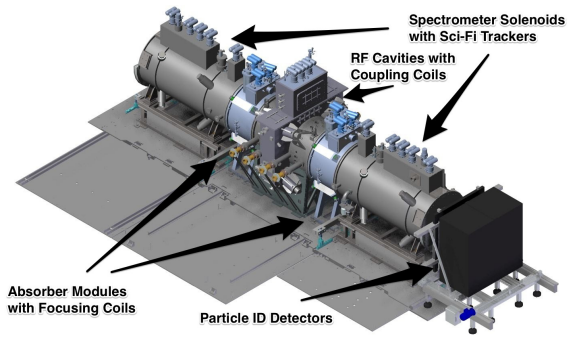


Figure 1: Engineering drawing of MICE Step V apparatus: two precision scintillating–fiber solenoidal spectrometers surround a cooling cell.

Once all the components are in place, a reduction in emittance will be measured with a relative precision of 1%. The beam line and the particle identification detectors were commissioned, and the results of analysis of the data presented [3, 4]. Full results are expected by 2018, with analyses of some configurations available starting in 2015. Early results will include important validations of the models used in ionization-cooling simulation codes, as well as the first experimental test of muon transverse–longitudinal emittance exchange (needed for six-dimensional cooling, e.g., for a muon collider) in a wedge absorber.

MICE STEPS

MICE was originally envisioned to be built in a series of six "Steps," but due to technical considerations the abbreviated sequence was adopted shown in Fig. 2. Step I comprises of the pion-production target, pion-to-muon beam line, particle ID and time-of-flight detectors. Step I has already taken place, and the results are published. The last piece of equipment completing the list of detectors—the electron-muon–ranger (EMR)—was delivered to RAL in 2013, and tested with the muon beam.

MICE STEP IV

MICE Step IV will measure the factors that determine the ionization cooling effect, with results expected starting in 2015. In addition to the Step I components, Step IV requires the two scintillating fiber trackers mounted inside spectrometer solenoids (SS) and one absorber focus coil (AFC) module. The trackers have been completed for some time and tested with cosmic rays.

* On behalf of the Muon Ionization Cooling Experiment collaboration
† stefania.ricciardi@stfc.ac.uk

Copyright © 2014 CC-BY-3.0 and by the respective authors

CARBON FIELD EMISSION STRIP CATHODE ELECTRON SOURCE

T.V. Bondarenko[1], A.I. Botyachkova[1, 3], O. Heid[2], A. Geisler[2], G.G. Karpinsky[1, 3], S.A. Polikhov[1], G.B. Sharkov[1]
[1] Siemens Research Center, Moscow, Russia
[2] Siemens AG, Erlangen, Germany
[3] National Research Nuclear University (MEPhI), Moscow, Russia

Abstract

Over the recent years carbon nanostructure cathodes have become promising high brightness field emission electron sources with large working area. Results of a carbon based field emission strip-shaped cathode simulations and the design of set-up for its investigation are presented in the article. Experimental setup has been designed for cathode emitting properties measurement and determination of emitted electrons initial parameters used as input data for electron beam computer simulation. The setup consists of the high-voltage triode electrode system and allows to investigate the voltage-current characteristics of the cathode and to estimate the electron distribution of the beam on the anode surface. Evaluation of electrons distribution on the anode will be processed by measurement of the emitted X-ray focal spot on the anode using CCD camera. Verification of the electron beam dynamics simulations will be based on the experimentally acquired data.

INTRODUCTION

The carbon nanostructure cathodes nowadays are manufactured using a large number of different techniques providing all kinds of carbon morphologies: single-walled and multi-walled nanotubes, nanowalls and so on [1]. Most of them are also known under different names. A number of works were dedicated to description of the cathodes volt-ampere characteristics investigations and structure growth methods, especially concerning carbon nanotubes [2]. At the same time generation of electron beams for X-ray devices - one of the main aspects of the carbon nanostructure cathodes applications – was inspected not so detailed. Designed set-up discussed here incorporates the electron source and is focused on investigation of the carbon nanostructure cathode operation in terms of X-ray source applications.

Two main process characteristics will be measured using the presented unit: VI-characteristics and electron beam dynamics in the system. The first characteristic is traditionally measured by the volt-meters and ampere-meters. The second can be measured using the faraday cups or other elements implying the electron beam profile measurements. But taking into account the fact that the cathode will be used as an electron source for X-ray generation devices, it is more relevant to perform the measurement of the anode X-ray focal spot because this particular size will characterize the efficiency of the X-ray generator.

Strip shape of the cathode was chosen to get more information about the initial parameters of the electrons emitted from the cathode surface. While along a narrow cathode side the focusing electrical field is applied to electrons, along the broad side there is no transverse electrical field presented.

The system is designed to provide 2 A/cm^2 emitted current density with 100 keV final electrons energy (on the anode) and 50 μm anode beam spot in the narrow direction. In the broad direction anode beam spot should have the distorted edges not larger than 5% from the whole spot size to observe uniform beam distribution. The 50 μm narrow size of the anode spot is dictated by the focal spot size requirements for next generation of high power microfocus X-ray sources.

COMPUTER SIMULATION

The first step for building the unit was to design the triode system that can generate electron beam of high current density and form the corresponding electron spot on anode. Design of the triode unit is shown on the figure 1. The system was designed to provide current density as high as 2 A/cm^2 for 8 V/μm cathode extracting field (for 20 kV extracting electrode potential) typical for investigated type of the carbon cathode material. In vertical direction the electrode system can generate the focusing electrical field that reduces the beam size in ~1:2 proportion vs. the cathode size. Due to this fact the cathode vertical size was chosen to be 100 μm. For such system the vertical 2·σ size of the cathode electrons distribution is 60.4 μm and the anode 2·σ equals 27.5 μm.

High value of the extracting E field on the cathode surface leads to even higher fields on the surface of the electrodes due to blending radii and lower distances and can lead to breakdown issues. The electrode shape was optimized to provide maximum electrodes surface electrical field on the level of 18.5 V/μm for 8 V/μm on the cathode surface. This demand accounts for a drawback of only 2 times of beam transverse size reduction, even more reduction could be obtained for higher surface field values.

The electron beam dynamics was investigated for the case of 0.2 eV mean initial beam energy with 100% energy spread and ±45° angular spread. The energy values

Copyright © 2014 CC-BY-3.0 and by the respective authors

ISBN 978-3-95450-142-7

DEVELOPMENT OF FPGA-BASED PREDISTORTION-TYPE LINEARIZATION ALGORITHMS FOR KLYSTRONS WITHIN DIGITAL LLRF CONTROL SYSTEMS FOR ILC-LIKE ELECTRON ACCELERATORS

M. Omet*, SOKENDAI, Hayama, Japan
S. Michizono, T. Matsumoto, T. Miura, F. Qiu, KEK/SOKENDAI, Tsukuba, Japan
B. Chase, P. Varghese, FNAL, Batavia, USA

Abstract

Two different kinds of predistortion-type linearization algorithms have been implemented and compared on an FPGA within the digital LLRF control system the Advanced Superconducting Test Facility (ASTA) at the Fermi National Accelerator Laboratory (FNAL). The algorithms are based on 2nd order polynomial functions and lookup tables with interpolation by which complex correction factors are obtained. The algorithms were tested in an actual setup including a 5 MW klystron and a superconducting 9-cell TESLA-type cavity at ASTA. By this a proof of concept was demonstrated.

INTRODUCTION

At the International Linear Collider (ILC) [1] the superconducting cavities of the main linacs will be controlled using digital low level radio frequency (LLRF) techniques [2]. Figure 1 shows a schmematic of a typical LLRF control loop. The from the cavity picked up radio frequency (RF) is down converted in frequency by mixing with the local oscillator (LO) signal. The resulting signal, the intermediate frequency (IF), is digitized using a analog-to-digital converter (ADC). The digital signal is processed on an FPGA, which contains beside others the controller. The processed signal is converted from digital to analog. The analog signal is fed beside an RF signal to an IQ modulator for up conversion in frequency. The resulting RF signal is amplified by a klystron, which drives the cavity. In case of ILC groups of 39 cavities will be driven by single 10 MW multi-beam klystrons.

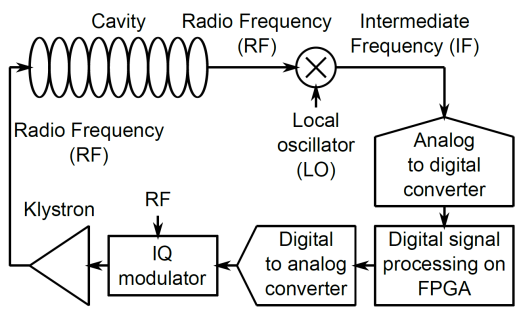


Figure 1: Schematic of a typical digital LLRF control loop.

Typically the input-to-output characteristics of a klystron in both amplitude and phase are not linear. A schematic of a typical input-to-output characteristics is shown in Figure 2 in black. In order to operate the klystrons at ILC most cost effectively, it is intended to operate them 7% in power below the point of saturation. At this point the slope of the input-power-to-output-power characteristics is only about $\frac{1}{10}$ compared to the slope at the linear region. Since the control gain is proportional to this slope, it also degrades close to the point of saturation. In order to keep the feedback effective, it is required to keep the amplitude slope constant and the phase rotation at 0° until the point of saturation. The desired klystron output is shown in Figure 2 in red. This can be accomplished by using a klystron linearization. The linearization algorithms described in the following are predistortion-type linearizations, implemented in the firmware of the field programmable gate array (FPGA), on which beside others the digital LLRF controller is located. The predistortion characteristics are inverse to the non-linear characteristics of the klystron. The predistorer is typically located after the controller and the addition of feedforward tables and before transmitting the signals to the digital-to-analog converters (DACs). The predistortion is generated in dependency of the signal amplitude. In the past linearization concepts were already implemented [3, 4]. The studies described in the following are based on those.

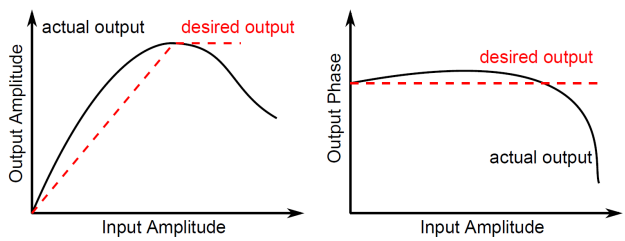


Figure 2: Schematic of the klystron amplitude and phase output characteristics.

KLYSTRON LINEARIZATION ALGORITHM IMPLEMENTATION

At FNAL ASTA [5] is under construction. Since it is beside an user machine also an ILC R&D accelerator, the digital LLRF control system was designed with ILC in mind.

In the presented study two kinds of predistortion-type amplitude dependent klystron linearization algorithms were implemented and tested. The target hardware was an Altera Cyclone II FPGA on the multi-cavity field control (MFC)

* momet@post.kek.jp

Copyright © 2014 CC-BY-3.0 and by the respective authors

SERIES SUPERCONDUCTING CAVITY PRODUCTION FOR THE HIE-ISOLDE PROJECT AT CERN

M. Therasse, L. Alberty, K. Artoos, S. Calatroni, O. Capatina, A. D'Elia, N. Jecklin, Y. Kadi, I. Mondino, K. Schirm, A. Sublet, W. Venturini Delsolaro, P. Zhang, CERN, Geneva, Switzerland

Abstract

In the context of the HIE-ISOLDE linac at CERN, the phase 1 is planned to boost the energy of the machine from 3 MeV/u to 5 MeV/u. For this purpose, it is planned to install 2 cryomodules based on quarter wave resonators (QWRs) made by niobium sputtered on copper. This paper presents the different steps of the cavity series production from the reception from industry to the cavity storage before cryomodule assembly. We will describe the cavity preparation including the resonance frequency measurement, the chemical treatment, the cavity rinsing, the niobium coating and the RF test at 4.5 K.

INTRODUCITON

The HIE-ISOLDE project is the energy upgrade of the existing Isolde facility at CERN. The goal is to boost the beam energy from 3 MeV/u to 10 MeV/u for A/q=4.5 [1]. The superconducting linac will be based on quarter wave resonators (QWR), high-β and low-β, made by niobium (Nb) sputtered on copper (Cu) substrates. In phase 1, it is planned to install 2 cryomodules of 5 high-β cavities each to increase the energy of the machine from 3 MeV/u to 5 MeV/u. The QWR will have to work at 4.5 K in common vacuum (cavity vacuum and insulation vacuum are the same) at the resonant frequency of 101.28 MHz, and with a maximum of 10 W power dissipation at 6 MV/m. This paper presents the different steps of the cavity series production since the reception from the industry to the storage before cryomodule assembly.

CAVITY PRODUCTION WORKFLOW

In order to start the high-β series cavities production and to ensure the traceability and the reproducibility of the production cycle, a quality assurance plan has been implemented. The process flow is represented in Figure 1. For each step a procedure is written and all parameters are logged in a lot traveller following each cavity. The series QWR nomenclature chosen is QSX.Y, with X the cavity serial number and Y the Nb coating number.

CAVITY RECEPTION

The high-β series QWRs are produced by Research Instrument GmbH (RI) and Nb coated at CERN. The first step is the acceptance test of the copper substrate. Dimensional controls are done by RI and by the metrology service at CERN. A leak detection is done on the inner conductor, a leak rate less than 10^{-9} mbar l/s is requested. Then an optical inspection is done on the internal surface of the cavity and on all welds in order to detect any defect or material projections that can be harmful for the Nb coating. The resonant frequency is measured in standard conditions (at 20 °C, 50% humidity) before the cavity tuning.

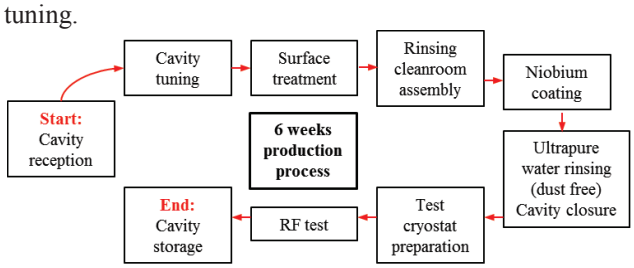


Figure 1: Summary of the 6 weeks cavity production workflow since the copper substrate reception to storage before cryomodule assembly.

CAVITY TUNING

In order to reach the operating frequency 101.28 MHz at 4.5 K under vacuum, the frequency (unperturbed) required has to be close to 100.900 MHz at 20 °C with 50% of humidity. The tip gap of the QWR is reduced by taking in account the different contributions of cavity treatments leading to a frequency shift. All contributions are presented in table 1.

Such operation is carried out in a CNC milling centre, with the QWR in horizontal position. The revolution axis is recreated by supporting the QWR by two circular slots machined close to the extremities of the outer body. This method allows achieving a perpendicularity accuracy in the order of 0.1 mm and a neat finish (Ra<1 µm). A second measurement of the frequency is done after tuning.

Table 1: Frequency Shift Contributions

Parameters	Frequency Shift (kHz)
295 K to 4.5 K and Air to vacuum (10^{-8} mbar)	+371 +/- 5
Chemical etch 40'	-27 +/- 3
Nb coating	-7 +/- 5
Tuning plate range	+/- 20

SURFACE TREATMENT

This step is done to remove the cutting fluids and the surface damaged layers before the final chemical polishing of the copper substrate. The cavity is preliminary degreased in NGL 1740 bath during 15 hours, sanded and pickled respectively with HCl solution at 50% (3 min) and H_2CrO_4 (3min) solution. The cavity is rinsed between each bath. Then two chemical etchings of 40 min are done using a mixture of sulfamic acid (H_3NO_3S, 5 g/l), hydrogen

Copyright © 2014 CC-BY-3.0 and by the respective authors

ISBN 978-3-95450-142-7

WARMING RATE REDUCTION OF THE SARAF RF COUPLERS BY APPLICATION OF A HIGH VOLTAGE DC BIAS

B. Kaizer*, I. Fishman, Y. Ben-Aliz, J. Rodnizki and L. Weissman, Soreq NRC, Yavne, Israel

Abstract

Warming up of the coupler region of the SARAF Half Wave Resonator (HWR) cavities was one of the main limiting factors for long operation at high RF field values. The warming effect is, most likely, associated with multipacting in the coupler region. We have tried to suppress the multipacting discharge in the couplers by application a DC bias to their inner conductors. A bias-T, element that conducts up to 4 kW of 176 MHz RF power and provides DC insulation of the coupler inner conductor, was designed and built for this purpose. First on-line operation showed that the DC bias indeed reduces dramatically the warming rates of most of the cavities by an order of magnitude. Today, coupler warming is no longer the main factor hindering accelerator operation.

THE RF COUPLERS WARMING

During operation of the superconducting 176 MHz HWR cavities in the SARAF Prototype Superconducting Module (PSM) [1], the capacitive RF couplers were warming up. Cooling copper strip lines between the couplers cold windows and the 50 K thermal shield proved not to be adequate [2]. Thus, we were compelled to reduce the field in the 2nd, 3rd and 6th cavities in order to keep the external coupler's temperature below 120 K during long operation (Fig.1). It is noteworthy that only moderate warming is observed at the 5th cavity coupler.

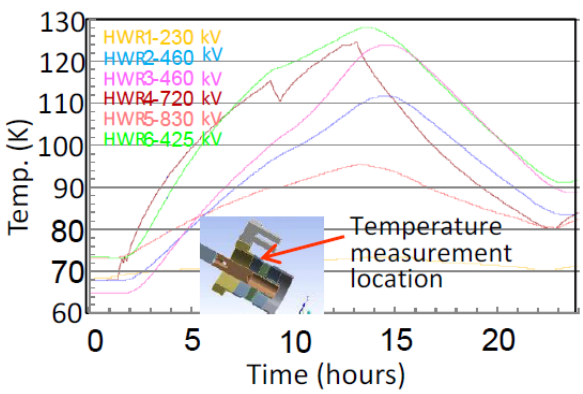


Figure 1: The couplers temperatures during operation of a 1 mA 3.6 MeV proton beam. The cavities voltages are indicated. The location where the temperature is measured is shown in the insert.

It is also worth to note that the warming rates varied on a daily basis. The coupler temperatures taken during two weeks of daily operation are shown in Fig. 2. Two different accelerator setups, involving operation of six and three cavities, were used during this period [3]. This daily variation of the warming rates prompted us to conclude that the origin of the problem is multipacting.

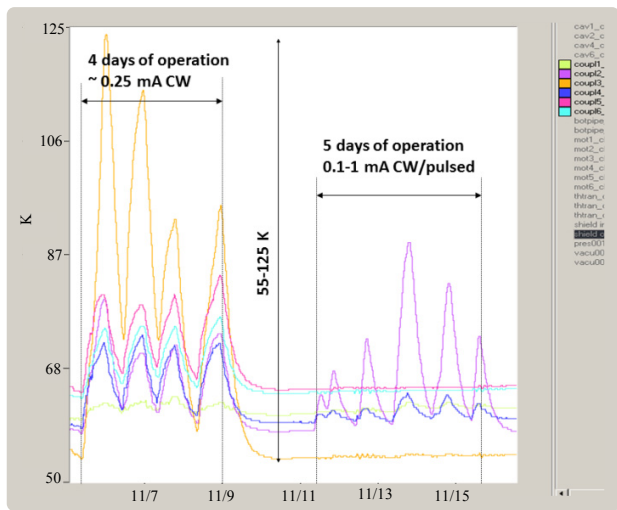


Figure 2: Daily variation of the warming rates during operation at the same field values. The couplers warmed up during day time operation and cooled overnight.

It is known from the literature [4, 5] that application of a DC bias to the coupler inner conductor should suppress multipacting discharge. We therefore decided to test this idea at the SARAF couplers.

DEVELOPMENT OF A BIAS-T

A three port network bias-T adaptor was designed and built in order to apply a high voltage DC bias on the inner conductor without disturbing other components, such as the RF amplifiers.

Conceptually, the bias-T can be viewed as a simple network which includes: 1. an ideal capacitor that allows AC current through but blocks the DC bias and 2. an ideal inductor that blocks AC but allows DC (Fig. 3). The low frequency port is used to set the bias; the high frequency port passes the radio frequency signals but blocks the DC bias.

The combined port is connected to the coupler.

*bozaka@soreq.gov.il

Copyright © 2014 CC-BY-3.0 and by the respective authors

ISBN 978-3-95450-142-7

LLRF SYSTEM FOR THE CEBAF SEPARATOR UPGRADE*

T. Plawski, R. Bachimanchi, C. Hovater, D. Seidman, M. Wissmann
Jefferson Lab, Newport News, VA 23606, USA

Abstract

The Continuous Electron Beam Accelerator Facility (CEBAF) energy upgrade from 6 GeV to 12 GeV includes the installation of four new 748.5 MHz normal conducting deflecting cavities in the 5th pass extraction region. This system will work together with the existing 499 MHz RF Separator in order to allow simultaneous delivery of the beam to four CEBAF experimental halls. The RF system employs two digital LLRF systems controlling four cavities in a vector sum. Cavity tune information of the individual cavities is also obtained using a multiplexing scheme of the forward and reflected RF signals. In this paper we will present detailed LLRF design and the current status of the CEBAF 748.5/499 MHz beam extraction system.

INTRODUCTION

The original beam extraction configuration, allowing simultaneous beam delivery to three experimental halls A, B and C, was designed over 20 years ago. The CEBAF photo-cathode injector produces three interleaving bunches at 499 MHz, hence the operating frequency of the linacs is 1497 MHz. Such a configuration allows extraction of a single bunch out of the three bunches at the end of each pass and directs it to one of the three halls or separates all three bunches at the highest pass [1]

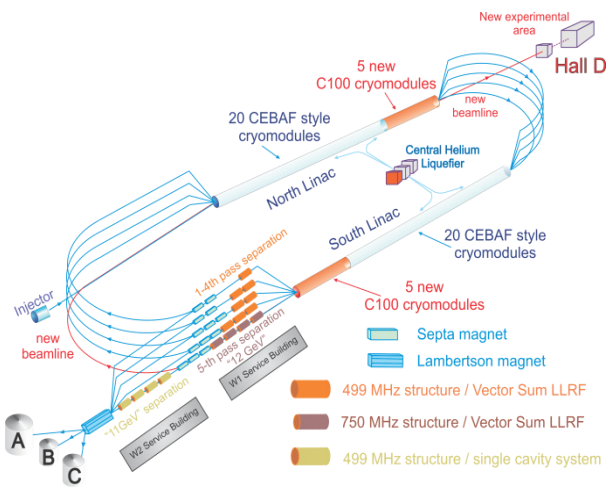


Figure 1: Layout of the 12 GeV CEBAF accelerator

As a part of the 12 GeV Upgrade project, a new experimental hall "D" has been added along with new arc beam line (see Figure 1). This hall will receive the highest energy beam, which comes from the 5th pass separation [2]. Because the existing 499 MHz extraction system only allows bunches to three halls, a new 5th pass extraction system and consequently a new bunch pattern was conceived in order to deliver simultaneous beam to all four halls [3]. A major change in the new separation system is the 5th pass extraction running at 748.5 MHz instead of 499 MHz. The trade-off will be a lower bunch repetition rate because the 5th pass beams for all halls have to operate at 249.5 MHz.

The new beam extraction system requires a number of additional 499 MHz and 748.5 MHz separator cavities to be installed along with new high power RF amplifiers and LLRF systems [4]. To support both 499 MHz and 748.5 MHz LLRF operation a new Separator MO (Master Oscillator) has also been built and installed.

As shown in Figure 1, sixteen deflecting cavities are installed. The first pass has one 499 MHz cavity and one RF system while pass 2, 3 and 4 will use multiple cavities with one RF system, utilizing vector sum control to stabilize the electromagnetic field. Pass 5 has four 748.5 MHz cavities installed and will be driven by one high power amplifier. An additional four 499 MHz cavities have recently been installed on the so called "11 GeV" beam line in order to separate beam among original halls A, B and C. This part of the beam extraction system applies one cavity/one RF source system topology. The separator master oscillator, installed in the W1 service building provides 429 MHz and 678.5 MHz LO signals for RF front-end heterodyning and 70 MHz for the clock reference.

11 GeV SEPARATION SYSTEM

The 5th pass (12 GeV) separation does not separate beams for halls A, B and C. Therefore it was necessary to add a new deflection system on the 11 GeV beam line. It consists of four 499 MHz normal conducting cavities, identical to existing ones. Each cavity has its own high power, solid state amplifier capable delivering up to 10 kW (saturated) of RF power and controlled by a single field control chassis (see Figure 2). These cavities are expected to provide a 499 MHz transverse deflection to the electron bunch train. The requirement is to have the beams to hall A, B and C vertically separated by +17, 0 and -17 mm respectively at the input to the Lamberstson style magnet located 42 m

*Notice: Authored by Jefferson Science Associates, LLC under U.S. DOE Contract No. DE-AC05-06OR23177. The U.S. Government retains a non-exclusive, paid-up, irrevocable, world-wide license to publish or reproduce this manuscript for U.S. Government purposes

Copyright © 2014 CC-BY-3.0 and by the respective authors

ISBN 978-3-95450-142-7

RECENT IMPROVEMENTS TO SOFTWARE USED FOR OPTIMIZATION OF SRF LINACS*

T. Powers, Thomas Jefferson National Accelerator Facility, Newport News, VA, 23606 USA

Abstract

This work describes a software tool that allows one to vary parameters and understand the effects on the optimized costs of construction plus 10 year operations of an SRF linac, where operation costs includes the cost of the electrical utilities but not the labor or other costs. The program includes estimates for the associated cryogenic facility, and controls hardware. The software interface provides the ability to vary the cost of the different aspects of the machine as well as to change the cryomodule and cavity types. Additionally, this work will describe the recent improvements to the software that allow one to estimate the costs of energy-recovery based linacs and to enter arbitrary values of the low field Q_0 and Q_0 slope. The initial goal when developing the software was to convert a spreadsheet format to a graphical interface and to allow the ability to sweep different parameter sets. The tools also allow one to compare the cost of the different facets of the machine design and operations so as to better understand tradeoffs. An example of how it was used to independently investigate cost optimization tradeoffs for the LCLS-II linac will also be presented.

SOFTWARE DESCRIPTION

The software allows one to vary the input costs and operating parameters in order to meet requirements of the machine and regionally driven cost metrics. It is described more fully in references [1] and [2]. There are three variations of the program. The first two allow one to sweep the RF frequency for a selected gradient and beam current. In one variation the cryomodules are not causal in that the calculations use a fractional number of cavities and keep the active length per cryomodule constant. The second variation maintains a relatively constant active length per cryomodule by increasing the number of cells per cavity and cavities per cryomodule with user selectable break points. The third model allows the user to select from a number of different cryomodule types or to provide their own cryomodule parameters (number of cavities, frequency, active length per cavity, shunt impedance, etc.). In all cases the program is meant to give trends, cost minimums, etc. but not to provide an absolute cost for developing and building a linac, as a detailed estimate must take into account matters such as detailed design tradeoffs, local costs, schedules, etc.

Input – Output Parameters

The majority of the input parameters are shown in Figure 1. There are two general terms for cryogenic losses. The first is static losses associated with each of the SRF cryomodules, transfer lines, its associated valve box, and per kilometer transfer line losses. These are user inputs to the program. The second is RF driven, or dynamic, losses which are determined on a cavity by cavity basis. Q_0 losses include the electromagnetic field losses in the cavity walls, RF induced 2 K heat load in the fundamental power couplers, higher order mode couplers, bellows, etc. There are three different approaches for determination of Q_0. Q_0 losses are determined based on the cavity geometry, operating temperature, material type and processing techniques which are all input variables to the program. This information can be used to calculate Q_0 losses based on a statistical analyses of vertical test results performed at Jefferson Lab over the past 20 years[3]. Alternately, once one has selected a frequency and cavity type, one can enter a baseline Q_0 value and slope into the program. The third method which is fully described in reference [4] is based on the field-dependent BCS RF surface resistance model of Xiao with the electron mean free path set to 50 nm. Care must be taken when considering Q_0 calculations based on these methods as there are degradations between vertical tests and cryomodule tests, as well as long term degradation of the Q_0 under operational conditions.

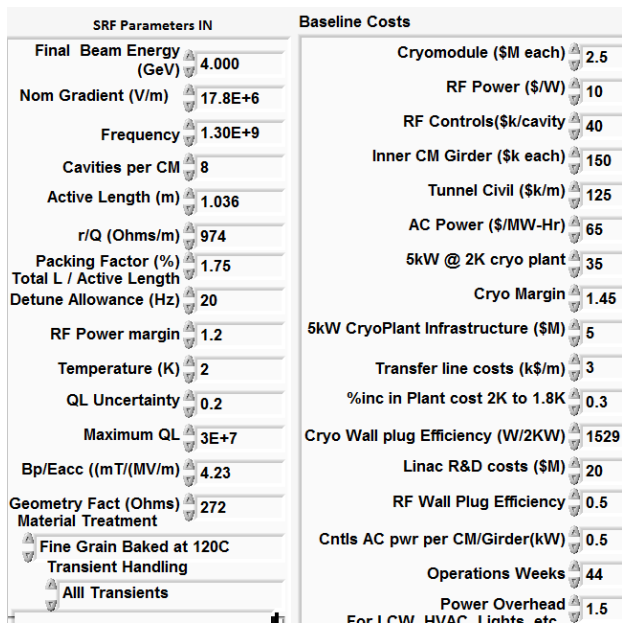


Figure 1: User input screen for input variables.

The output parameters include items such as the total construction costs, operating costs, and SRF parameters.

* Authored by Jefferson Science Associates, LLC under U.S. DOE Contract No. DE-AC05-06OR23177. The U.S. Government retains a non-exclusive, paid-up, irrevocable, world-wide license to publish or reproduce this manuscript for U.S. Government purposes.

Copyright © 2014 CC-BY-3.0 and by the respective authors

STUDY OF FEMTOSECOND ELECTRON BUNCH GENERATION AT T-ACTS, TOHOKU UNIVERSITY

S. Kashiwagi#, F. Hinode, T. Muto, Y. Shibasaki, K. Nanbu, K. Takahashi, I. Nagasawa,
S. Nagasawa, C. Tokoku, A. Lueangaramwong, H. Hama,
Electron Light Science Centre, Tohoku University, Sendai, Japan
Nuan-Ya Huang, National Synchrotron Radiation Research Center, Hsinchu, Taiwan

Abstract

We are conducting a beam experiment of sub-picosecond electron bunch generation at t-ACTS (test accelerator as a coherent terahertz source), Tohoku University. In the t-ACTS, the intense coherent terahertz radiation will be generated from an undulator and an isochronous accumulator ring via producing sub-picosecond bunches. The accelerator is composed of a thermionic cathode RF gun, an alpha magnet and a 3 m-long accelerating structure. Velocity bunching scheme in accelerating structure is applied to generate the short electron bunch. The thermionic RF gun consists of two independent cavities has been developed, which is capable of manipulating the beam longitudinal phase space. To produced femtosecond electron bunch, the longitudinal phase space distribution of the beam entering the accelerating structure is optimized by changing the RF gun parameters. The bunch length is measured by observing an optical tradition radiation using a streak camera. In the study of femtosecond electron bunch generation, a relation between the RF gun parameters and the bunch length after compression was investigated. The preliminary results of experiments are described in this report (Fig. 1).

INTRODUCTION

The intense coherent THz source is a powerful tool for many scientific fields such as biophysics and molecular science. The t-ACTS has been proposed as a test accelerator complex towards intense THz source at Electron Light Science Centre, Tohoku University. The t-ACTS accelerator consists of a compact linear accelerator with a thermionic RF-gun, an isochronous accumulator and undulator [1]. A wide band THz coherent synchrotron radiation (CSR) is emitted from circulated electron beam in the isochronous accumulator ring [2] and a narrow-band one from the undulator has been considered [3, 4]. The t-ACTS project employs the velocity bunching scheme [5] in its compact linear accelerator to produce the femstosecond electron bunches for generating THz CSR [6]. The injector adopts a thermionic cathode RF gun deliberately chosen for stable multi-bunch operation and for cost efficiency. The compressed beam is much shorter than the wavelength of THz radiation, and has a sufficient large form factor for coherent enhancement of radiation power.

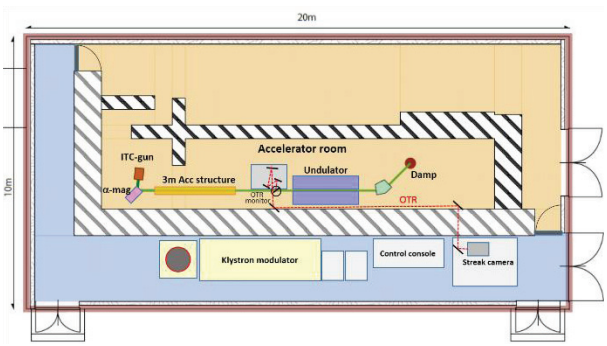


Figure 1: Accelerator-based light source house (t-ACTS).

SHORT BUNCH GENERATION

Velocity Bunching

In the velocity bunching, the non-relativistic electron bunch is injected into zero-cross phase ($\psi = 0$) of an accelerating structure. Since the phase velocity of the accelerating structure is equal to the speed of light, the non-relativistic electron bunch slips backward to the direction of crest phase and starts to accelerate as rotating its longitudinal phase space as shown in Fig. 2. Injected electron bunch moves along the equi-potential line in the longitudinal phase space. Ideally, the compression factor becomes maximum when the injected electron distribution is exactly on the same equi-potential line. Since nonlinearity of the equi-potential line at higher injection energy is stronger, a lower energy beam with

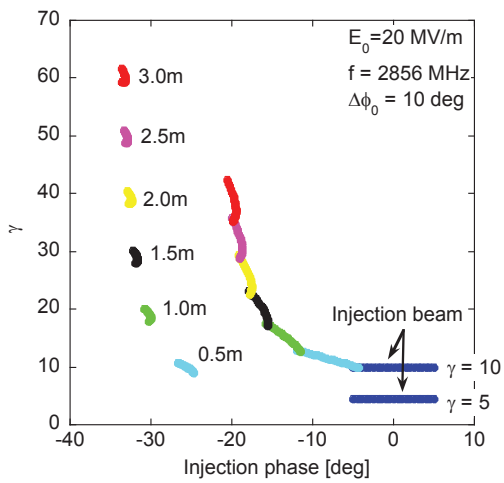


Figure 2: Equi-potential lines for the peak accelerating field E_0 = 20MV/m. Evolutions of electron distributions injected at 0 degree are plotted with colored lines.

kashiwagi@lns.tohoku.ac.jp

Copyright © 2014 CC-BY-3.0 and by the respective authors

ISBN 978-3-95450-142-7

PRESENT STATUS OF THE 3 MeV PROTON LINAC AT TSINGHUA UNIVERSITY*

Q.Z. Xing#, C. Cheng, C.T. Du, L. Du, T.B. Du, X.L. Guan, C. Jiang, C.X. Tang, X.W. Wang, H.Y. Zhang, S.X. Zheng, Key Laboratory of Particle & Radiation Imaging (Tsinghua University), Ministry of Education, Beijing 100084, China
B.C. Wang, Northwest Institue of Nuclear Technology, Xian, China
W.Q. Guan, Y. He, J. Li, NUCTECH Co. Ltd., Beijing 100084, China

Abstract

We present, in this paper, the present status of the 3 MeV high current proton Linac for the Compact Pulsed Hadron Source (CPHS) at Tsinghua University. The ECR ion source produces 50 keV proton beam which is accelerated to 3 MeV by the downstream RFQ accelerator. The RFQ accelerator has been conditioned to 50 Hz/500 μs with the input power of 442 kW. Proton beam with the peak current of 30 mA, pulse length of 100 μs and repetition rate of 50 Hz has been delivered to the Beryllium target to produce the neutron since July 2013. The status of the development of the Drift Tube Linac is also presented in this paper. The beam energy will be enhanced to 13 MeV after the DTL is ready in 2015.

INTRODUCTION

The CPHS (Compact Pulsed Hadron Source) linac at Tsinghua University, which began its construction in the year of 2009 [1], has achieved its mid-term objective: delivering the 3 MeV proton beam to bombard the Beryllium target [2]. Figure 1 shows the CPHS linac facility at Tsinghua University, which contains the ECR Ion Source (IS), Low Energy Beam Transport line (LEBT), a 4-vane Radio Frequency Quadrupole (RFQ) accelerator, and High Energy Beam Transport line (HEBT).

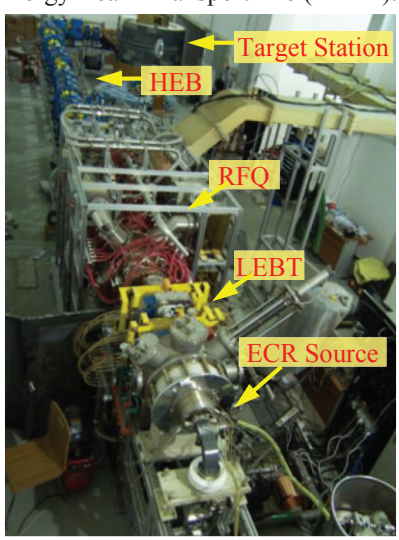


Figure 1: CPHS linac facility and the target station.

Table 1 shows the main designed and achieved parameters of the CPHS linac. The beam current of 23 mA is measured at the entrance of the target station after the 90-degree bending of the beam. The detailed information on the high power test and beam commissioning of the RFQ accelerator, and the characteristics of the 3MeV proton beam can be referred to [3] and [4]. In this paper, the development status of the beam measurement and the Drift Tube Linac (DTL) are mainly presented.

Table 1: Main Parameters of the CPHS Linac

Parameter	Designed	Achieved
Beam Energy	13 MeV	3 MeV
Beam Current	50 mA	23 mA
Pulse Length	500 μs	100 μs
Repetition Rate	50 Hz	50 Hz

OPERATION STATUS

Figure 2 presents the operation status of the CPHS linac in 2014. A stable beam current of 22 mA can be obtained before the target station (after bending). The RFQ suffers from a degradation of the transmission rate from its original 88% (with input peak current of 50mA at 50 μs/ 50 Hz). The reason may come from the unmatched beam from the LEBT, or the deformation of the RFQ cavity. In this year the field distribution of the RFQ is planned to be inspected and the beam emittance at the entrance of the RFQ will be measured.

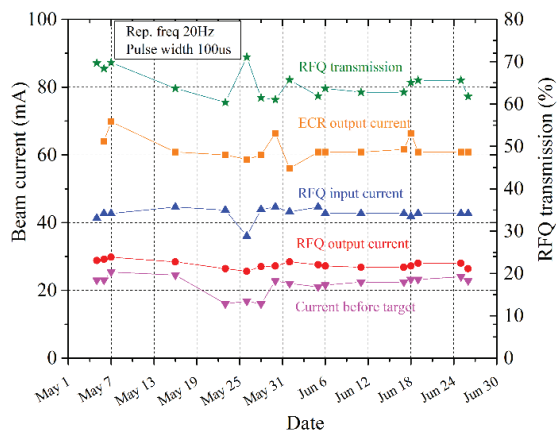


Figure 2: Operation history of the 3 MeV linac in 2014.

*Work supported by National Natural Science Foundation of China (Major Research Plan Grant No. 91126003 and 11175096)
#xqz@tsinghua.edu.cn

Copyright © 2014 CC-BY-3.0 and by the respective authors

MEASUREMENTS OF BEAM CURRENT AND ENERGY-DISPERSION FOR ION BEAM WITH MULTI-COMPONENTS*

A. L. Zhang[1, 2], S. X. Peng[# 1], H.T. Ren [1], Y. Xu[1], J. Zhao [1], T. Zhang [1], Z. Y. Guo[1], J. E. Chen[1,2]
[1]State Key Laboratory of Nuclear Physics and Technology & Institute of Heavy Ion Physics, School of Physics, Peking University Beijing 100871, China;
[2]University of Chinese Academy of Sciences, Beijing 100049, China

Abstract

The multi-component ion beam is very common in nuclear physics, materials physics and most kind of ion source. But the diagnosis of multi-component ion beam [1] can be difficult because of its complex composition and irregular energy-dispersion. We need an effective way to analyze the multi-component ion beam. There is a multi-component ion beam whose total beam current varies from 1 mA to 50mA and the beam energy can be 20keV to 150keV. In this paper, four methods to analyzing this multi-component ion beam are described, which are Faraday cup array, fluorescent screen with Faraday cup, movable aperture with conductive fluorescent screen, and current calibration method, respectively. The distributions and currents of the separated ion beams are obtained by means of the four methods, and the current and energy-dispersion of each component might be measured at the same time. This is of special interest for beams with multi-components. Detailed description and comparison of the four methods are discussed in this paper.

INTRODUCTION

The multi-ion beam is widely used in nuclear physics experiments and material modification. In most of cases, the beams extracted from the ion source are multi-component because there always have some impurities and different ionization state. The composition and energy-dispersion of the beam extracted from the ion source are kernel parameter of an ion source, and it also has a great influence on the beam transportation. It's necessary to develop an effective way to analyzing the multi-component ion beam. Not just for nuclear physics and materials physics, this might have special interest for all kind of ion source.

There is a multi-component beam coming from ion source whose total current varies from 1mA to 50mA and the beam energy can be 20keV to 150keV. The beam contains more or less six kinds of particles and the energy can be 20keV to 150kev. In order to research the composition of the multi-component ion beam, an orthogonal magnetic and electric fields is used to separating the ions with different charge-mass ratio. With numerical simulation, we expect that after the beam crossed the orthogonal magnetic and electric fields the separated ions may have five groups of distribution which was showed in figure 1.

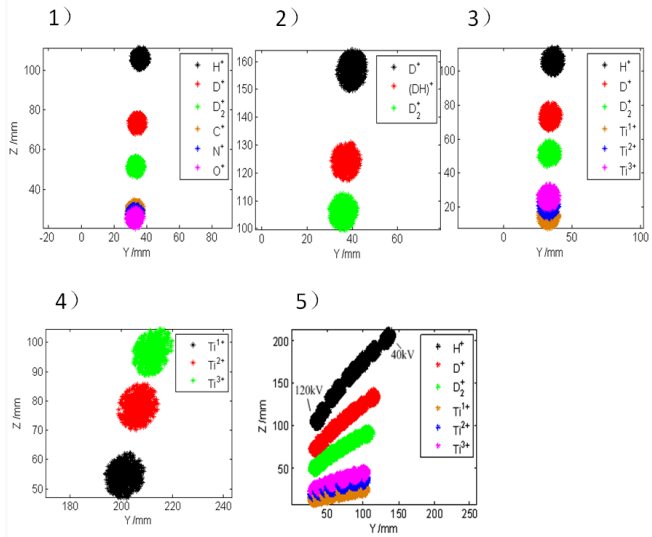


Figure 1: 5 possible distributions of the separated ions

FOUR METHODS TO ANALYZING THE MUTI-ION BEAM

In order to research the composition of this multi-ion beam, four methods are presented in this paper

Method 1: Faraday Cup Array

We use independent faraday cups to install in array and use appropriate acquisition circuit connect each faraday cup to the computer [2]. The faraday cups must to be isolated with each other. It difficult to make the faraday cups smaller than 3mm because of the Install difficulty. The sketch of this device is showed in figure2. In this way we can get the distribution and the current in the same time.

This may be very simple for the operating and we can complete the measurement in just one pulse. Each of the independent faraday cups needs an amplifying circuit. The smaller of the faraday cups the higher of the measurement accuracy. But the smaller of faraday cups result in each faraday cup got smaller current, which means needs more and better amplifying circuit, means higher cost. On the other hand, it's very difficult to install small faraday cups as a detect matrix and isolated with each other. So the accuracy of the distribution measurement can be hardly smaller than 3mm.

*Work supported by the National Science Foundation of China（Grant Nos. 91126004).
#sxpeng@pku.edu.cn

Copyright © 2014 CC-BY-3.0 and by the respective authors

800 MeV LINEAR ACCELERATOR DEVELOPMENT FOR HLS UPGRADE*

K. Jin, S. C. Zhang, G. R. Huang, D. C. Jia, Y. L. Hong
National Synchrotron Radiation Laboratory, NSRL USTC,
P.O. Box 6022, Hefei Anhui 230029, China

Abstract

Hefei Light Source (HLS) was mainly composed of an 800 MeV electron storage ring and a 200 MeV constant-impedance Linac functioning as its injector in NSRL Phase Ⅰ. A new Linac has been developed successfully in view of the Full Energy Injection and the Top-up Injection scheme will be adopted in the HLS upgrade. In this paper, an 800MeV linear accelerating system construction, the constant-gradient structure with the symmetry couplers will be described in detail. The microwave system, the manufacture technology, the RF measurement, the high power testing and the accelerating system operation with beam currents are presented.

INTRODUCTION

In order to ensure the low-emittance focusing parameters steady operation in the HLS Storage Ring, it's necessary to increase the injector energy to 800MeV. After realize Full Energy Injection, each system of Storage Ring can keep single operation state, the light source stability will be improved eminently. A new Linac is developed in view of the Full Energy Injection and the Top-up Injection scheme will be adopted in the HLS upgrade. An 800MeV Linac layout is shown in Fig.1.

The LINAC is a traveling-wave type, operating at 2856MHz and utilizes 8 klystron amplifiers. It consists of pre-bunch, fundamental mode bunch and 16 three-meter long constant-gradient accelerating sections. The total length of the LINAC is about 71.5 meters. The project has been developed successfully. In this paper, the main parameters of the 800MeV linear accelerating system are presented. Specially, the microwave system layout and the constant-gradient accelerating structure with the symmetry couplers design, fabrication, RF measurement and the high power test will be described in detail.

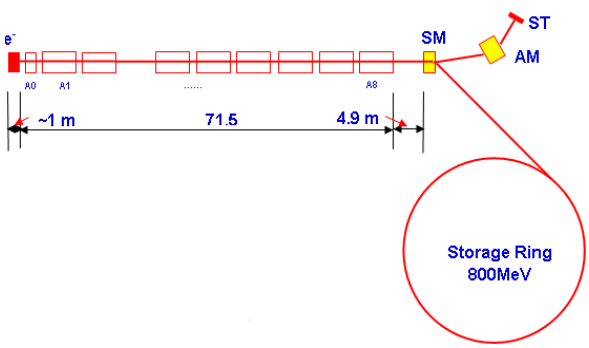


Figure1: HLS 800 MeV Linac and the electron storage ring layout

THE MAIN PARAMETERS OF THE LINAC

The electron gun is thermal emission electron gun, which can produce up to 1.5A (Max.) with 100kV injection energy in 1ns pulse beams. The beam current at the end of the LINAC is supposed to be 1.0A. And there is a switch magnet at the end of the LINAC, by which the electron beams can be switched to the storage ring, the nuclear experiment hall, the energy analysis magnet or the beam dump according to what is needed. Table 1 lists the main parameters of the LINAC.

Table 1: The main parameters of the HLS LINAC

Parameters	HLS Linac
Electron energy	800 MeV
Beam pulse charge	1 nC
Beam pulse width	~10 ps
Energy spread	0.5 %
Beam normalization emittance	<60 mm·mrad
Electron gun voltage	-100kV
Repetition rate	1～10 Hz
RF frequency	2856 MHz
RF power per klystron	50 MWx6，80 MWx2
Number of klystron	8
Temperature of cooling water	42℃
Vacuum (with beam)	$<1\times10^{-6}$ Pa

800 MeV LINAC DEVELOPMENT

HLS accelerating system consists of a pre-buncher, a buncher and eight units of constant-gradient accelerating structures (6m accelerator unit). Total length is about 73meter. The electron beam energy can be achieved to 800MeV~1GeV. In general, seven such as units is in operation condition and another one is in standby state so that to assure storage-ring stability running (Fig.2).

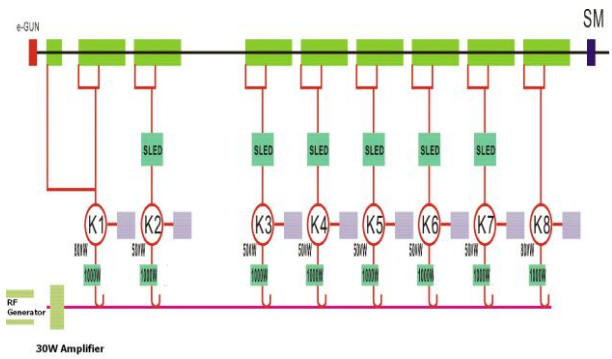


Figure2: 800 MeV electron Linac energy, phase and microwave System Layout

Copyright © 2014 CC-BY-3.0 and by the respective authors

ISBN 978-3-95450-142-7

HIGH TRANSPARENT MATCHED WINDOW FOR STANDING WAVE LINEAR ACCELERATORS

Alberto Leggieri[1,2], Franco di Paolo[1], Davide Passi[1],
Alessia Ciccotelli[2] and Giuseppe Felici[2]
[1]Università degli Studi di Roma "Tor Vergata", Dipartimento di Ingegneria Elettronica, Roma, Italy
[2]S.I.T. Sordina IORT Technologies S.p.A., Aprilia, Italy

Abstract

This paper proposes a particular Dielectric Window (DW) for Standing Wave (SW) Linear Accelerators (LINAC's). This study investigates the in-frequency return loss behaviour of the LINAC, in order to improve matching and transmitting conditions while maintaining the optimum coupling between LINAC and High Power Microwave (HPMW) source. Device design considers the DW input interface as an Input Matching Network (IMN) at the LINAC Normal Mode (NM) working frequency. Thus, design formulas are provided and Computer Aided Design (CAD) techniques are proposed.

A prototype has been made and tested by performing cold S-parameter and Percentage Depth Dose (PDD) measurements of a LINAC with the proposed DW and with a traditional DW.

The proposed device offers more energy transport attitude over the traditional DW, as shown by a return loss increase of 167 % and an output electron energy increase of 5.5% while maintaining the same LINAC input power settings. This solution can offer a decrease of power line size, weight and cost. An after brazing global improvement of the accelerator figures of merit is also possible, as this study have demonstrated...

INTRODUCTION

Vacuum Tubes and LINAC employees Dielectric Windows (DW) to separate the Ultra High Vacuum (UHV) atmosphere to the normal atmosphere in the transport waveguide (which connects the device to the HPMW source), ensuring the microwave power transmission. These windows are made by a waveguide section, in which a solid dielectric medium is inserted.

The most common kind of window is the pill-box type. This window is a double Rectangular Waveguide (RWg) to Circular Waveguide (CWg) transition containing in the centre a dielectric cylindrical plate, typically made of typically alumina ceramic [1]. The internal profile of a Pill-box window is depicted in Fig. 1. Several technological solutions can be adopted, as for example SF6 filled for high-power transmission [1], long pill-box type windows, with a very long longitudinal size [2], or with oversized diameter in order to reduce the RF field strength on the ceramic surface for very high power transfer [3]. Due to complexity of the Electromagnetic field distribution, DW design is by then supported by Computer Aided Design (CAD) techniques [4].

This paper shows the design of a Dielectric Window, according to [5], for a Standing Wave LINAC to be employed in a medical mobile electron LINAC, dedicated to Intra Operative Radiation Therapy (IORT). The whole Medical Device is required to be as small and light as possible: therefore, oversized and long structures are preferably avoided.

After the manufacturing process, every LINAC may present a degradation of its electromagnetic characteristics, and often an increase of the reflection coefficient. By connecting to the LINAC input port a DW made with a high Insertion Loss (IL), these reflections reduces, but transmission efficiency decrease. Choosing a low IL one, the transmission increases but multipath reflections through the LINAC remains unchanged, respect to the same using a high IL medium.

At the end of the complete LINAC fabrication, the matching input characteristics of the system are been inevitably modified. The proposed strategy for improving LINAC Matching is the association of a low IL DW and a waveguide based Input Matching Network (IMN). The assembly of these two devices has been defined as High Transparent Matched Window (HTMW).

Since the IMN is placed in the low pressure section and it can be inserted by screws without vacuum loss and further Matching degradations, it can be sized basing on the effective measured input parameters of the finally brazed LINAC at its frequency of resonance.

A prototype is described with cold measurements of scattering parameters and hot measurements of the electron energy reached by a LINAC which employees this technology.

PILL BOX WINDOW DESIGN

The DW inserts a discontinuity in the power transmission line. Since the CWg is partially filled with alumina ceramic, this may be treated as equivalent to the CWg filled uniformly with a dielectric having effective relative permittivity ε_r' [4]. This assumption simplifies the problem providing initial values that must be optimized.

Since the power transport system is based on RWg, we can consider the wavelength of the fundamental mode in the rectangular waveguide as a known value λ_{gR}.

The CWg radius which ensures the local transparency of the line discontinuity inserted by the DW, can be found by applying the (1) [5]:

Copyright © 2014 CC-BY-3.0 and by the respective authors

ISBN 978-3-95450-142-7

AWAKE: ADVANCED PROTON DRIVEN PLASMA WAKEFIELD ACCELERATION EXPERIMENT AT CERN

E. Gschwendtner, CERN, Geneva, Switzerland
for the AWAKE Collaboration

Abstract

Plasma wakefield acceleration is a promising alternative reaching accelerating fields a magnitude of up to 3 higher (GV/m) when compared to conventional RF acceleration. AWAKE, world's first proton-driven plasma wakefield experiment, was launched at CERN to verify this concept. In this experiment proton bunches at 400 GeV/c will be extracted from the CERN SPS and sent to the plasma cell, where the proton beam drives the plasma wakefields and creates a large accelerating field. This large gradient of ~GV/m can be achieved by relying on the self-modulation instability (SMI) of the proton beam; when seeded by ionization through a short laser pulse, a train of micro-bunches with a period on the order of the plasma wavelength (~mm) develops, which can drive such a large amplitude wake from a long proton bunch (~12 cm). An electron beam will be injected into the plasma to probe the accelerating wakefield.

The AWAKE experiment is being installed at CERN in the former CNGS facility, which must be modified to match the AWAKE requirements. First proton beam to the plasma cell is expected by end 2016.

INTRODUCTION

Motivation

In order to search for new physics, as well as to complement the results from the LHC at CERN, one option for a next energy-frontier accelerator could be a linear collider of electrons and positrons at the TeV energy scale. The accelerating field of today's RF cavities or microwave technology is limited to ~100 MV/m, therefore the length of future linear colliders would be several tens of kilometres. However, plasma can sustain much higher gradients [1], so plasma-based accelerators are of great interest. Three orders of magnitude higher acceleration gradient than in RF cavities have been demonstrated: with laser excitation, electrons have been accelerated to 1 GeV in 3 cm, with a gradient of 33 GV/m [2]. In [3] an electron bunch was used as driver, the energy of particles in the tail of a bunch was doubled from 42 GeV to 85 GeV in 85 cm-corresponding to a gradient of 52 GV/m.

However, the energy gain is limited by the energy carried by the laser or electron drive beam (<100 J) and the propagation length of the driver in the plasma (<1 m). Hence, staging of a large number of acceleration sections would be required to reach the interesting region of 1TeV. Proton beams, as those routinely produced at the CERN SPS, carry much higher energy (19 kJ with 3 10^{11} protons/bunch at 400 GeV/c), which makes it possible to drive wakefields over much longer plasma lengths and potentially take a witness beam to the TeV scale in a single plasma stage. Simulations have shown that an LHC-type proton bunch (1 TeV, 10^{11} protons) with an rms bunch length of 100 μm can accelerate an incoming 10 GeV electron bunch to more than 500 GeV in around 500 m of plasma with an average gradient ≥ 1 GV/m [4].

Self-Modulation Instability

To reach accelerating gradients at the GV/m level the plasma density must be on the order of $n_e = 10^{15}$ electrons/cm^3. With $\lambda_{pe} \approx (10^{15}/n_e)^{-1/2}$, the plasma wavelength is about 1 mm. In order to excite large amplitude wakefields, the proton bunch length σ_z has to be comparable with the plasma wavelength λ_{pe}. The nominal SPS bunch length at top energy (450 GeV) is σ_z ~ 12 cm. However, it was shown in [5] that a long proton beam propagating in plasma undergoes a transverse self-modulation instability (SMI) that modulates the bunch radius and density and drives the wakefields to large amplitudes – opening the path for an immediate experimental investigation of large gradient plasma wakefields with the existing proton bunches at CERN.

At saturation, the initially long and smooth beam is split into a train of micro-bunches naturally spaced at ~λ_{pe} and that resonantly excites the strong plasma wave. When seeded, the self-modulation instability saturates after 4 m of plasma with a density of (1-10) 10^{14} electrons/cm^3. In addition, the injection of the witness electron beam can be controlled with seeding.

THE AWAKE EXPERIMENT

AWAKE, under construction at CERN, will be the first proof-of-principle accelerator R&D experiment addressing the challenges of proton driven plasma wakefield acceleration and is under construction at CERN [6,7].

The measurement program of AWAKE includes benchmark experiments using proton bunches from the CERN SPS at 400 GeV/c to drive the wakefields and to understand the physics of the proton self-modulation instability process in the plasma. It will also probe the accelerating wakefields with externally injected electrons, study the injection dynamics and production of multi-Giga-electron-Volt electron bunches, and develop long, scalable and uniform plasma cells, and schemes for the production and acceleration of short proton bunches.

Baseline Design

For the AWAKE experiment at CERN, an LHC-type proton bunch of 400GeV/c (but with higher intensity of 3 10^{11} protons/bunch) will be extracted from the CERN SPS and sent towards a plasma cell. The proton beam will

Copyright © 2014 CC-BY-3.0 and by the respective authors

POSITIVE TRENDS IN RADIATION RISK ASSESSMENT AND CONSEQUENT OPPORTUNITIES FOR LINAC APPLICATIONS

Y. Socol, Falcon Analytics, Hanevel Str. 13/1 Karney Shomron, 4485500 Israel

Abstract

Ionizing radiation, an unavoidable by-product of high-energy LINACs, makes them subject to strict regulation and severe public concerns. During the last two decades the attitude to ionizing radiation hazards has been becoming more balanced, as opposed to the historical "radiophobia". The linear no-threshold hypothesis (LNTH), based on the assumption that every radiation dose increment constitutes increased cancer risk for humans, is more and more debated. In particular, the recent memorandum of the International Commission on Radiological Protection (ICRP) admits that the LNTH predictions at low doses (that ICRP itself has used and continues to use) are "speculative, unproven, undetectable and "phantom'." Moreover, numerous experimental, ecological, and epidemiological studies show that low doses of ionizing radiation may be beneficial to human health. While these advances in scientific understanding have not yet given fruit regarding radiation regulation and policy, we are hopeful these may happen in near to middle term. The presentation reviews the present status of the low-dose radiation-hazard debate. It also outlines anticipated opportunities for wider LINAC applications, especially in the prospective field of low-dose radiation therapy.

CONTROVERSY OVER THE LINEAR NO-THRESHOLD HYPOTHESIS

The linear no-threshold (LNT) hypothesis (LNTH) of radiation-induced cancers implies that every dose of ionizing radiation, no matter how small, constitutes increased (linear with the dose) cancer risk. This hypothesis, which became well-established for use in radiation safety during the Cold War era increasing fears of nuclear apocalypses in background, is presently used for low-dose radiation cancer risk assessment by advisory bodies, and as such it is the basis for current radiation safety regulations. The LNTH is also widely accepted by the general public. However, the scientific validity of this hypothesis has been questioned and debated for many decades without resolution. The disagreement on this issue in the scientific community has always been acknowledged by relevant professional bodies, including the US Congress Office of Technology Assessment [1].

Two recent examples below demonstrate how mistreatments of experimental data continue to lend support to the LNTH.

A-bomb Survivors

The results of the atomic bomb survivors follow-up are often claimed to support the LNTH [2]. However, this claim is baseless. The cancer mortality of the survivors is equally or better described by an s-shaped dependence on radiation exposure [3] with a threshold of about 0.3 Sievert (Sv) and saturation level at about 1.5 Sv (Fig. 1, left). Moreover, Monte-Carlo simulation of possible outcomes demonstrates that, given the weak statistical power, the follow-up cannot provide support for LNTH. The data that were generated according to s-shaped (a priori) distribution (with variance $Var = 1$), could be well-described (a posteriori) by a straight line (average $Var \approx 1.5$), as shown at Fig. 1, right. E.g., if we use fit variance $Var > 2.0$ as a cut value to exclude LNTH, we have to reject the correct s-shaped description in about 0.5% of cases (7 out of 1000 in this simulation); still we have to accept LNTH in nearly 90% of cases (877 out of 1000 in this simulation).

CT Scans and Childhood Cancer

CT scans are of high clinical usefulness as a valuable diagnostic technique, and new applications continue to be identified. However, the increasing use of CT scans is being challenged by emerging concerns regarding carcinogenesis from the ionizing radiation. Pearce et al. [4] made a significant contribution to the above concerns by claiming, probably for the first time, evidence for direct association of the radiation from CT scans with cancer. However, data points on cancer relative risk vs. CT-dose in their publication fit LNTH straight lines suspiciously-well, taking into account relatively large statistical errors (Fig. 2). The chi-square goodness-of-fit test demonstrates quantitatively that the data are likely "too good to be true". For leukaemia, there are six dose groups (squares in Fig 2, left). The first data group is used for risk normalization, and there is one parameter – LNT slope s. The number of degrees of freedom is 4=5–1, corresponding to 5 independent dose groups and 1 parameter. For brain tumours (eight dose groups), the number of degrees of freedom is 6=8–2. The expected (average) values $<\chi^2>$ are therefore 4.0 and 6.0 for leukaemia and for brain tumors, while the actual fitted χ^2 values are 1.19 and 2.91 correspondingly. The corresponding p-values are 0.12 and 0.18. Here the p-value is the probability that χ^2 will be equal or less than the obtained value, i.e. that the fit will be that good or better. Since the two data sets are expected to be independent, the resulting probability of both fits being that good or better simultaneously is $0.12 \times 0.18 \approx 0.02$. This is below the generally-assumed threshold of $p_{thr} = 0.05$, so the data are statistically *inconsistent* with the LNTH. The credibility of the data is therefore compromised. Most probably, some kind of data manipulation was performed, possibly unknowingly, by the authors of [4].

Copyright © 2014 CC-BY-3.0 and by the respective authors

ISBN 978-3-95450-142-7

PROTON AND CARBON LINACS FOR HADRON THERAPY

U. Amaldi, TERA Foundation, Novara, Italy
A. Degiovanni, CERN, Geneva, Switzerland

Abstract

Beams of 200 MeV protons and 400 MeV/u fully stripped carbon ions are used for the treatment of solid tumours seated at a maximum depth of 27 cm. More than 100'000 patients have been treated with proton beams and more than 10'000 with carbon ions. Very low proton currents - of the order of 1 nA - are enough to deliver the typical dose of 2 Gy/l in one minute. In the case of carbon ions the currents are of the order of 0.1-0.2 nA. For this reason 3 GHz linacs are well suited in spite of the small apertures and low duty cycle. The main advantage of linacs, pulsing at 200-400 Hz, is that the output energy can be continuously varied pulse-by-pulse and in 2-3 min a moving tumour target can be covered about 10 times by deposing the dose in many thousands of 'spots'.

High frequency hadron therapy linacs have been studied in the last 20 years and are now being built as hearts of proton therapy centres, while carbon ion linacs are still in the designing stage. At present the main challenges are the reduction of the footprint of compact 'single-room' proton machines and the power efficiency of dual proton and carbon ions 'multi-room' facilities.

INTRODUCTION

In developed countries more than 2'000 patients every 1 million inhabitants are subject to radiation therapy every year [1]. In more than 95% of cases, the treatment of the tumour disease consists in irradiation with X-rays. Hadron therapy has developed in the last 60 years as an advanced technique in radiation therapy that allows a not invasive and precise irradiation of solid tumours with the advantage of sparing the surrounding healthy tissues. The proposal, published in 1946 by 'Bob' Wilson [2], was based on the presence of the Bragg peak in the depth-dose profile of charged hadrons.

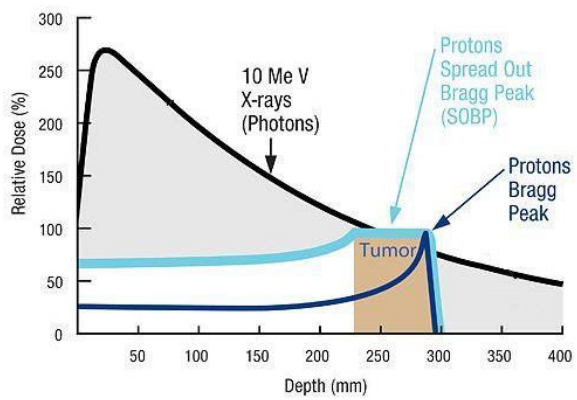


Figure 1: Comparison of depth-dose profile for X-rays (black) and charged hadrons (blue).

The energy released by a beam of mono-energetic charged hadrons is concentrated at the end of the range in matter. Since by changing the beam energy one can adjust the depth of the Bragg peak, the overlapping of many Bragg peaks produces a flat dose distribution in the tumour region, as seen in Fig. 1. The same figure shows that most of the energy deposited by an X-ray beam is outside of the tumour target so that, even with many crossed beams, in an X-ray-treatment, healthy normal tissues are in a 'bath' of radiation, while the total energy delivered to normal tissues with charged hadrons is typically a factor 3-4 smaller than with X-rays.

The use of linacs for hadron therapy has been proposed in the late eighties. Since 1993, TERA Foundation, in parallel with the study of a synchrotron based dual facility for the Italian hadrontherapy project - concluded with the construction of CNAO in Pavia [3] - initiated the study of high frequency linacs for hadron therapy applications. In 2009 a review of the subject was published by Reviews of Accelerator Science and Technology [4].

THE BEGINNINGS

Conventional X-ray Therapy

In the world more than 20'000 electron linacs are used by radiation oncologists daily; they represent 50% of all the existing accelerators having energy larger than 1 MeV [5]. Most of the linacs are based on normal conducting structures at 3 GHz; they are powered by a single magnetron or klystron and are mounted on a rotating support (gantry). The electron beam energy is in the typical range 6-20 MeV.

The Linac Approach to Proton Therapy

The use of linac for protons has first been proposed in 1991 [6]. The system was made up of an RFQ–DTL operating at 499.5 MHz, followed by a 3 GHz Cell Coupled Linac (CCL) that accelerated protons from 70 to 250 MeV (Fig. 2). The energy modulation could be achieved by switching off the modules and by using degrading absorbers.

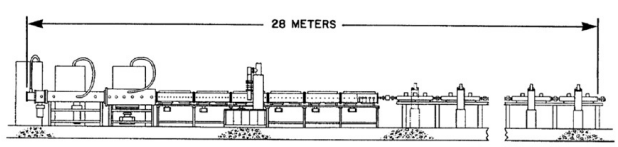


Figure 2: Schematic layout of the model PL-250 proton therapy linac designed by R. Hamm, K. Crandall and J. Potter [6].

Copyright © 2014 CC-BY-3.0 and by the respective authors

ISBN 978-3-95450-142-7

PROSPECTS FOR ACCELERATOR-DRIVEN THORIUM SYSTEMS

Jean-Pierre Revol, Centro Fermi, Rome, Italy & international Thorium Energy Committee (iThEC), Geneva, Switzerland

Abstract

To meet the tremendous world energy needs, systematic R&D has to be pursued to replace fossil fuels. Nuclear energy, which produces no green house gases and no air pollution, should be a leading candidate. How nuclear energy, based on thorium rather than uranium, could be an acceptable solution is discussed. Thorium can be used both to produce energy or to destroy nuclear waste. The thorium conference, organized by iThEC at CERN in October 2013, has shown that thorium is seriously considered by developing countries as a key element of their energy strategy. However, developed countries do not seem to move in that direction, while global cooperation is highly desirable in this domain. As thorium is not fissile, an elegant option is to use a proton accelerator to drive an "Accelerator Driven System (ADS)", as suggested by Nobel Prize laureate Carlo Rubbia. Therefore, the accelerator community has an important challenge to meet: provide the required proton beam for ADS.

BURNING FOSSIL FUEL TILL THE END?

If, by the end of the 21st century, people in developing countries are allowed to live as well as people do in Europe today, the world power consumption will have to increase by a factor 3 or more. Today, fossil fuels represent 87% of world primary energy consumption [1], and their consumption is still increasing, while resources are finite. Even in countries broadly developing renewable energies, fossil fuel consumption remains high, as fossil fuels are used as backup when there is no wind or no sun.

There are at least three good reasons to replace fossil fuels for energy production:

- Their impact on global warming – the atmospheric CO_2 level is higher than ever in the past 15 million years, and increasing faster than ever before. The IPCC reported in March 2014 that by 2100, a global temperature increase larger than 2˚C is more likely than one of less than 2˚C [2];
- Burning fossil fuel is having a severe impact on air pollution. Burning coal cost Europe alone 42.8 billion Euros in annual health care expenses [3]. The ambient air pollution caused the premature death of more than 400 000 Chinese in 2013. WHO reported that in 2012, around 7 million people died – 1 in 8 of total global deaths – as a result of air pollution exposure [4];
- At the present rate fossil fuel will run out relatively quickly on the human time scale, with present reserves of 53, 56 and 110 years [1], respectively for oil, gas and coal, while the current tendency is to increase fossil fuel consumption.

ENERGY R&D

Politicians will not invent the solution; it has to come from innovation. Innovation implies investment in both applied research and fundamental research. Without fundamental research there is no innovation.

Relying entirely on wind and solar energy would imply that, by the end of the century, their contribution to the world energy production would have to increase by a factor 130 or more. This is not realistic; at least not until the issue of the storage of electricity is resolved. In addition, the dispersed and fluctuating nature of these natural energy sources implies an important extension of the electric grid (50 000 km of new power lines in Europe).

Energy R&D has to be systematic, without prejudice. Nuclear fission energy, in particular, must not be left out. It produces no CO_2, no air pollution such as NOx, SOx, etc., and it has the potential to provide abundant, base load type of electric energy for many centuries. Furthermore, nuclear fission technology exists and is well understood.

The question that should be asked is: How should nuclear energy be exploited to be acceptable to Society? Where "acceptable" means that shortcomings of the present generation of critical reactors based on uranium, should be avoided: (a) accidents such as at Chernobyl, Three Mile Island, or Fukushima; (b) waste management (storage up to one million years is the only option developed so far); (c) proliferation of nuclear weapons (the uranium fuel cycle was developed for military purpose); (d) sustainability (uranium reserves for Pressurized Water Reactors (PWR) will last less than 100 years at the present rate).

THORIUM

Thorium is an abundant natural element: 1.2×10^{14} tons in the Earth's crust. It is as abundant as lead, and three to four times more abundant than uranium. Recovering only one part per million would provide the present world power consumption of 15 TW, for 18 000 years. "Thorium is a source of energy essentially sustainable on the human time scale", said Carlo Rubbia at ThEC13 [5].

Isotopically pure, natural thorium (^{232}Th) has an α-decay with a half-life of 14 billion years (almost stable). Thorium occurs in several minerals including thorite, thorianite and monazite and is often a by-product of mining for rare earths.

Known and estimated recoverable resources are between 6.6 and 7.4 million tons according to IAEA [6],

Copyright © 2014 CC-BY-3.0 and by the respective authors

ISBN 978-3-95450-142-7